

“Small Molecule Activation through Radical Formation by Visible Light Photoredox Catalysis”

Dissertation

Zur Erlangung des Doktorgrades der Naturwissenschaften

Dr. rer. nat.

am Institut für Anorganische und Angewandte Chemie der
Universität Hamburg



Vorgelegt von

Luana Cardinale

aus Ariano Irpino (Italien)

Hamburg, September 2021

The experimental part of this work was performed from November 2018 to September 2021 at the Institute of Inorganic and Applied Chemistry, University of Hamburg. This work was supervised by Prof. Dr. Axel Jacobi von Wangelin.

Date of thesis submission: 15.09.2021

Board of examiners: Prof. Dr. Axel Jacobi von Wangelin
Prof. Dr.-Ing. Jakob Albert

Date of thesis defense: 19.11.2021

Board of examiners: Prof. Dr. Axel Jacobi von Wangelin
Prof. Dr. Christian B. W. Stark
Prof. Dr. Wolfgang Maison

*There are the rushing waves
mountains of molecules
each stupidly minding its own business
trillions apart
yet forming white surf in unison.*

*Ages on ages
before any eyes could see
year after year
thunderously pounding the shore as now.
For whom, for what?
On a dead planet
with no life to entertain.*

*Never at rest
tortured by energy
wasted prodigiously by the sun
poured into space
A mite makes the sea roar.*

*Deep in the sea
all molecules repeat
the patterns of one another
till complex new ones are formed.
They make others like themselves
and a new dance starts.*

*Growing in size and complexity
living things
masses of atoms
DNA, protein
dancing a pattern ever more intricate.*

*Out of the cradle
onto dry land
here it is
standing:
atoms with consciousness;
matter with curiosity.*

*Stands at the sea,
wonders at wondering: I
a universe of atoms
an atom in the universe.*

Richard P. Feynman (1918-1988)

Table of Contents

Chapter 1: Photoredox Catalysis	1
1.1 Introduction	2
1.2 Fundamentals of photocatalysis	2
1.2.1 Electron transfer	3
1.2.2 Energy transfer.....	4
1.2.3 Hydrogen atom transfer.....	5
1.3 Photoredox catalysts	6
1.4 References.....	8
2 Chapter 2: Aryl Pyrazoles from Photocatalytic Cycloadditions of Arenediazonium.....	9
2.1 Introduction	10
2.2 Results and discussion.....	11
2.3 Conclusion	16
2.4 Experimental section.....	16
2.4.1 Materials and methods	16
2.4.2 General Procedures	17
2.4.3 Mechanistic experiments.....	28
2.4.4 NMR of compounds.....	38
2.5 References.....	70
3 Chapter 3: Catalyst-Free <i>N</i> -Deoxygenation by Photoexcitation of Hantzsch Ester	71
3.1 Introduction	72
3.2 Results and discussion.....	73
3.3 Conclusions.....	76
3.4 Experimental section.....	76
3.4.1 Materials and methods	76
3.4.2 General procedures.....	77
3.4.3 Characterization of reaction products from Scheme 2	78
3.4.4 NMR of compounds.....	99
3.5 References.....	108
4 Chapter 4: Photoredox-Catalyzed Addition of Carbamoyl Radicals to Olefins: A 1,4-Dihydropyridine Approach	111
4.1 Introduction	112
4.2 Results and discussion.....	113
4.3 Conclusion	117
4.4 Experimental section.....	117
4.4.1 Material and methods.....	117

4.4.2	Extended optimization studies.....	118
4.4.3	General procedures.....	119
4.4.4	Mechanistic experiments.....	134
4.4.5	NMR of compounds.....	143
4.5	References.....	192
5	Chapter 5: Photoredox-Catalyzed Synthesis of α -Amino Acid Amides by Imine Carbamoylation.....	195
5.1	Introduction.....	196
5.2	Results and discussion.....	196
5.3	Conclusion.....	199
5.4	Experimental section.....	200
5.4.1	Materials and methods.....	200
5.4.2	Optimization studies.....	201
5.4.3	General procedures.....	202
5.4.4	Chiral experiments.....	225
5.4.5	Mechanistic investigations.....	227
5.4.6	NMR spectra of all compounds.....	230
5.5	References.....	275
6	Chapter 6: Cobalt (II) Halide – Amine Enabled Cyclotrimerization of Terminal Alkynes 277	
6.1	Introduction.....	278
6.2	Results and discussion.....	279
6.3	Conclusion.....	285
6.4	Experimental section.....	285
6.4.1	Materials and methods.....	285
6.4.2	General procedures.....	286
6.4.3	Extended optimization studies.....	294
6.4.4	Mechanistic experiments.....	298
	Reaction Quench with O ₂	313
	Screening of Solvent Mixtures and Different Nitriles.....	313
	Attempt to Detect or Exclude the Presence of Amine Oxidation Byproducts.....	315
6.4.5	NMR of compounds.....	327
6.5	References.....	342
7	Chapter 7: Appendix.....	343
7.1	List of abbreviations.....	343
7.2	List of used chemicals.....	345
7.3	Summary.....	353

7.4	Zusammenfassung.....	354
7.5	Acknowledgements	355
7.6	Curriculum vitae	356
7.7	Eidesstattliche Erklärung.....	359

Chapter 1: Photoredox Catalysis



1.1 Introduction

Photoredox mediated processes have become a powerful tool in organic synthesis over the last decade.¹ The generation of highly reactive molecules (excited state) with light and the ability to handle them has allowed to tackle several synthetic problems in a totally different way. Moreover, pairing photoredox strategies with other catalysis like electrocatalysis and transition metal catalysis is expanding the limits of accessible redox potentials and possible functionalizations. Despite the advances in the field being recent, photocatalysis has its roots in the earliest days of Earth where sunlight played a pivotal role as driving force for evolution. Photosynthesis, in plants, uses sunlight to convert raw materials (CO₂ and H₂O) into chemical energy (carbohydrates). Sunlight is also the energy source that chemists used in the early days of photocatalysis. Venerable name reactions from the 19th and 20th century such as Paternò-Büchi, Norrish-fragmentation, Schenck-ene, to cite some examples, were all discovered with the use of sunlight irradiation. With the technology advancement and commercialization of LEDs (light emitting diodes) in the 1960-70 a control of the irradiation source was possible in terms of wavelength (UV versus Visible light) and reproducibility. Nowadays, chemists in laboratories from all over the world can easily afford LEDs in different colors and choose between a variety of photocatalyst from common chemical suppliers.

1.2 Fundamentals of photocatalysis

A photochemical reaction is a reaction initiated by the absorption of a photon and involves, at least in one of the reaction steps, an electronically excited state. Simplified state energy diagrams as the one depicted in Figure 1 are usually used for the understanding of how photocatalysts work. After the absorption (10^{-15} s) of a photon by the molecule in the ground state (S_0) within femtoseconds its excited state ($*S_1$) is reached. The fate of $*S_1$ and its way back to ground state S_0 depends on both radiative processes as fluorescence ($10^{-9} - 10^{-6}$ s), through emission of a photon, or non radiative processes as internal conversion (IC, $10^{-7} - 10^{-5}$ s), through loss of heat. Fluorescence and IC are both spin-allowed processes which obey the selection rule $\Delta S = 0$. $*S_1$ can also undergo spin-forbidden processes as the non-radiative intersystem crossing (ISC, $10^{-10} - 10^{-8}$ s) to reach the excited triplet state ($*T_1$). Since the return to ground state S_0 from $*T_1$ is also a spin-forbidden transition (phosphorescence, $10^{-3} - 1000$ s) usually the triplet excited state is the longest-lived species with lifetimes ranging from nanoseconds to milliseconds, depending on the specific excited molecule. A long lifetime of the excited states, both $*S_1$ and $*T_1$, are fundamental for chemical reactions since are the most likely to participate in bimolecular reactions (i.e., reaction with a substrate).²

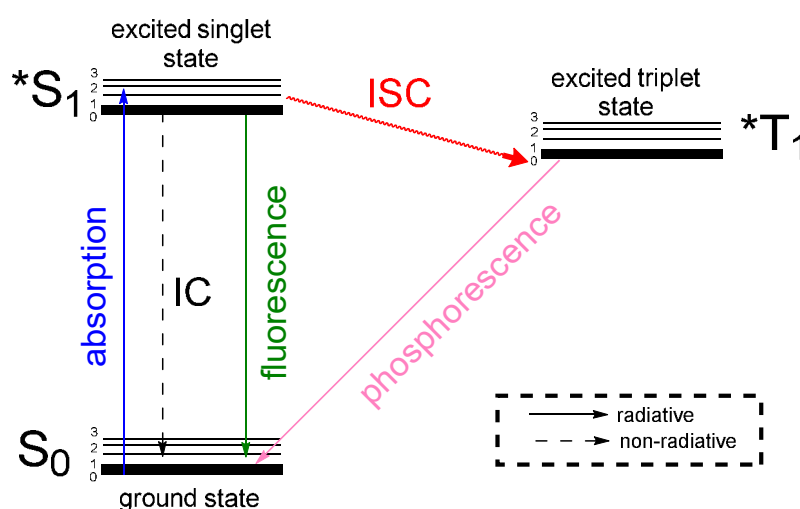


Figure 1. Simplified Jablonski diagram.

There are different possible bimolecular reactions that an excited state molecule can undergo with a substrate, namely: electron transfer, energy transfer (ET) and direct hydrogen atom transfer (HAT) which are going to be discussed below.

1.2.1 Electron transfer

Excitation of a light absorbing molecule, we will call it a photocatalyst (PC), generates an excited state photocatalyst (PC*) that can be described as a whole new chemical species with a totally new reactivity. This is a direct consequence of the promotion of an electron from the ground state to an excited one, as a result the PC* is going to have new redox properties and it will be a better oxidant in case of a reductive quenching cycle with a donor molecule or a better reductant in an oxidative quenching cycle with an acceptor molecule (Figure 2). From another point of view the process can be described as an electron and hole transfer. After the quenching of the excited state PC* in either processes, oxidative or reductive quenching, the oxidized (PC^{•+}) or reduced (PC^{•-}) ground state catalyst is available for one more oxidation or reduction respectively and close the catalytic cycle to form a neutral PC ground state.

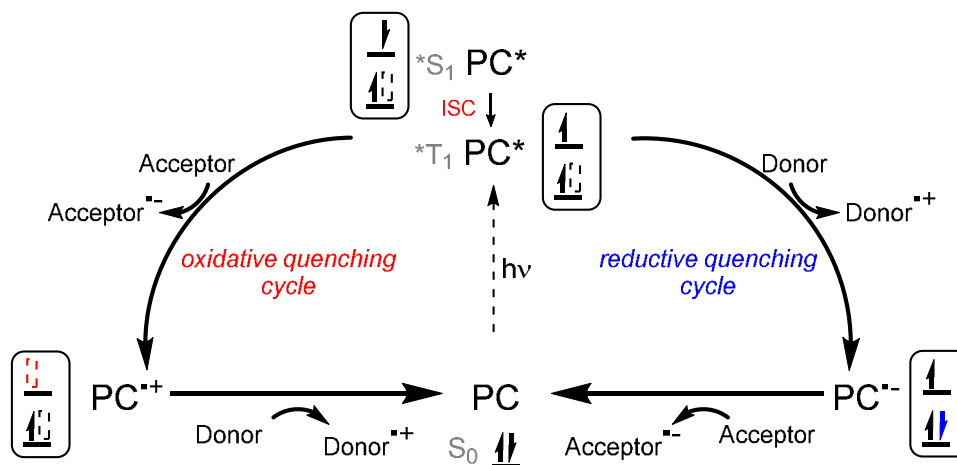


Figure 2. Oxidative and reductive quenching cycles in photoinduced electron transfer.

The thermodynamics of a photoinduced electron transfer (PET) are thus defined by the redox potentials of the photocatalyst in its excited state and redox potentials of the substrates. The general formula to obtain the free energy of a photoinduced electron transfer is illustrated in equation (1):

$$\Delta G_{PET}^0 = F[E_{1/2}(D^{\bullet+}/D) - E_{1/2}(A/A^{\bullet-})] - w - E_{0,0} \quad (1)$$

whereas F is the Farady constant ($23.061 \text{ kcal V}^{-1} \text{ mol}^{-1}$), $E_{1/2}$ (V) is the redox potential for the half reactions of donor oxidation ($D^{\bullet+}/D$) and acceptor reduction ($A/A^{\bullet-}$), w (J) is a work term that accounts for the coulombic interactions in substrates and products due to the presence of charged species. $E_{0,0}$ (kcal mol^{-1}) is the excited state energy of the photocatalyst. As can be seen from equation (1), the redox potentials of the involved species play a major role for the free energy determination. For this reason, determination of such potentials through electrochemical studies (cyclic voltammetry) is fundamental for the planning and execution of photoredox mediated reactions.

On the other hand, for what concerns the kinetics of PET major contributions were made by Marcus.^{3,4} For reactions involving the formation and breaking of bonds the activation energy is characterized by the energy of the transition state. This is not the case for electron transfer processes where the reaction partner are less bound to each other and is more the change in the surroundings (solvent molecules) that rearrange to create a geometrically favoured situation *prior* to the electron transfer. The energy employed in the rearrangement of solvent molecules represents the main part of the activation barrier to the electron transfer.

1.2.2 Energy transfer

Energy transfer is defined as the photophysical process in which an excited state of one molecular entity (the donor D) is deactivated to a lower-lying state by transferring energy to a second molecular entity (the acceptor A), which is thereby raised to a higher energy state with no change in the charge of the involved species.



In this scenario the photocatalyst acts as the donor, excited by the direct absorption of visible light, towards the substrate. Examples such as methylene blue, rose bengal, and benzophenone possess relatively high triplet energy and long triplet lifetimes and are perhaps better known as triplet sensitizers than they are as PET catalysts. One of the most common applications of triplet energy transfer is in the generation of singlet dioxygen (1O_2) by photo-sensitization of the ground state triplet dioxygen (3O_2). The main pathways behind an energy transfer are two non-radiative processes known as Förster and Dexter mechanism. The Förster resonance energy transfer (FRET) proceeds through dipole-dipole (coulumbic) interactions, where energy can be transferred via a transmitter-antenna mechanism. Spectral overlap of the donor's fluorescence and acceptor's absorption is required for the energy transfer. This kind of mechanism plays an important role in natural photosynthesis as well as fluorescence labeling and bioimaging but rarely describes the situation of a photocatalyst in solution. The second type of mechanism, the Dexter energy transfer, accounts for a simultaneous exchange of ground state electrons and excited state electrons. Orbital overlap of donor and acceptor is required for this kind of energy transfer. A general photosensitized organic reaction in solution is better represented with a Dexter mechanism.

In case of an energy transfer mechanism the feasibility of the process is now determined not on redox potentials as in the electron transfer but rather on the comparison between the energy of the triplet state of donor and acceptor. For a general exergonic energy transfer ($\Delta E < 0$) the triplet energy of the donor must be higher than the triplet energy of the acceptor. The triplet energy of a molecule can be experimentally determined through spectroscopic techniques or calculated by DFT. Thanks to the many studies conducted on the topic, triplet energy of common chemicals are tabulated in literature (Figure 3) and can be directly used for the investigation on energy transfers.⁵

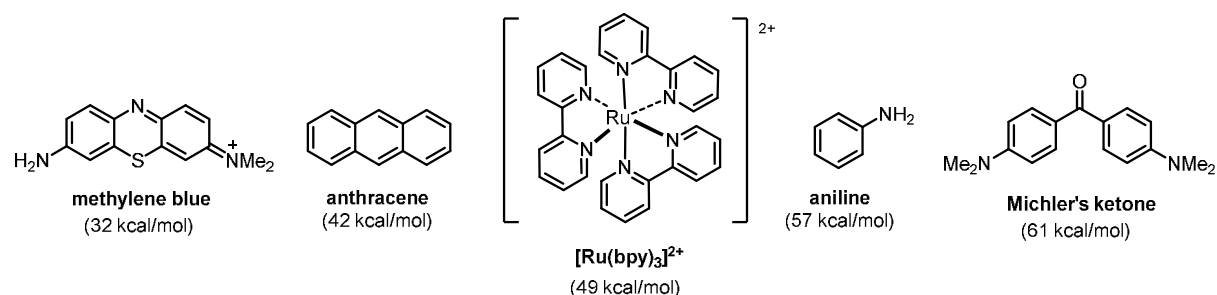


Figure 3. Common chemicals and respective triplet energy.

1.2.3 Hydrogen atom transfer

Hydrogen atom transfer (HAT) consists of the concerted transfer of a proton and an electron in a single step from a hydrogen donor to a hydrogen acceptor (Figure 4). The driving force of the HAT is the gain in energy due to the formation of a stronger bond (A-H) in the acceptor than in the donor (D-H).



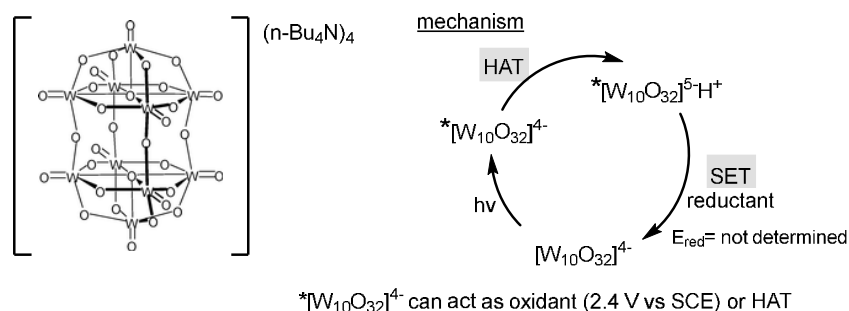
Figure 4. General scheme of a hydrogen atom transfer.

As in the PET, HAT causes the oxidation or reduction of the substrate. As already mentioned, the HAT is thermodynamically dependent on the bond dissociation energy (BDE) of donor (D-H) and acceptor (A-H). HAT represents a key step in many biological reactions (several metalloenzymes are known to operate through HAT). Moreover, in molecular chemistry opens the possibility for the activation of strong C-H bonds as the one present in aliphatic substrates.

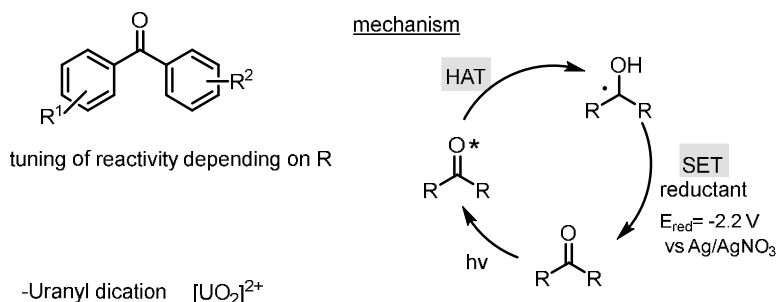
A photocatalyst in its excited state can promote the HAT in two different ways: directly and indirectly. The direct HAT, as the name suggests, takes place right between the excited state of the photocatalyst and the substrate; the catalytic cycle is closed by a back-HAT to one of the reaction intermediates (Figure 5). The number of photocatalysts that are able to perform direct HAT is quite limited, major examples are some aromatic ketones, uranyl cations and polyoxometalates (such as decatungstate anion $W_{10}O_{32}^{4-}$).

direct HAT photocatalysts (i.e. good H abstractor after excitation)

-TBDAT (tetrabutylammonium decatungstate)



-Benzophenone (and Xanthone) derivatives



-Uranyl dication $[UO_2]^{2+}$

Figure 5. Direct HAT photocatalysts and mechanism of action.

The limited number of photocatalysts able to perform direct HAT upon excitation has paved the way for the development of indirect strategies, in which a purposely added species generates a thermal hydrogen abstractor upon activation by the excited photocatalyst. General compounds used in the indirect HAT are: thiols, amines and alkyl-X (X= halogen).⁶

1.3 Photoredox catalysts

Photocatalysts play a central role in photoredox catalysis since they are the light absorbing species and the electron shuttles in the reaction medium. Before discussing in the next chapters, the utilization of photocatalysts in synthetic protocols, the well studied case of $\text{Ru}(\text{bpy})_3^{2+}$ is illustrated. $\text{Ru}(\text{II})$ polypyridine complexes are studied since a long time, dating back to 1936 with the first synthesis of $\text{Ru}(\text{bpy})_3\text{Cl}_2$.⁷ $\text{Ru}(\text{bpy})_3^{2+}$ due to a large ligand field splitting is a low-spin d^6 complex with an octahedral geometry and an intense red color. Upon irradiation in the visible region (455 nm, blue light) a photon is absorbed and one electron from the metal centered t_{2g} orbitals is excited to a π^* orbital of the bipyridine ligand. This transition is known as a metal to ligand charge transfer (MLCT) and corresponds to a situation where the metal has been oxidized to $\text{Ru}(\text{III})$ and the ligand has been reduced to a radical anion.

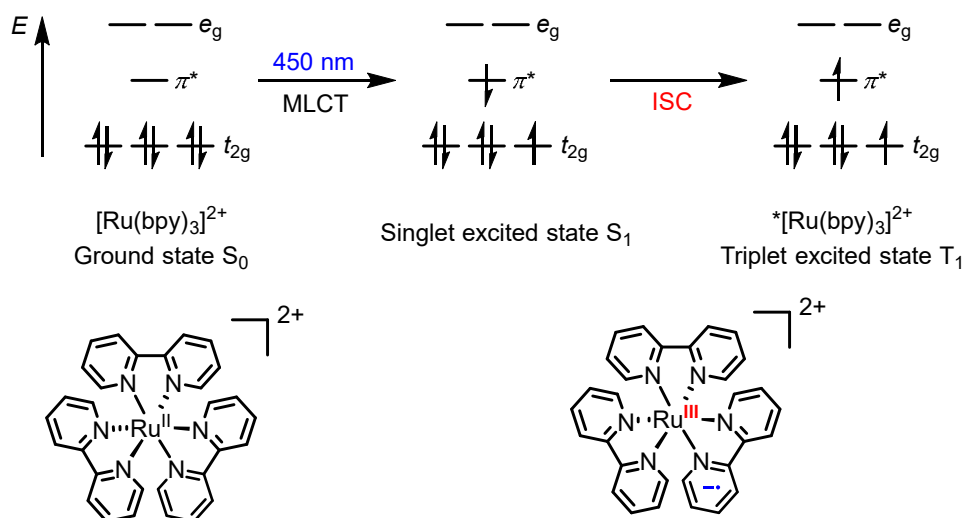


Figure 6. Photochemistry of $\text{Ru}(\text{bpy})_3^{2+}$.

The so generated singlet excited state *S_1 rapidly undergoes intersystem crossing (ISC) to give the long living triplet state *T_1 . The photoexcited species is now a better reductant and oxidant of the ground state. This is directly quantified in terms of redox potentials (Figure 7).⁸

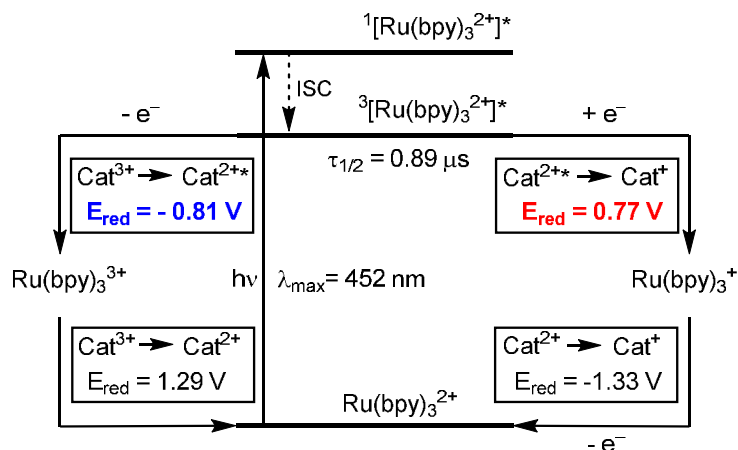


Figure 7. Redox potentials of excited state $^*\text{Ru}(\text{bpy})_3^{2+}$, potentials are reported vs SCE.

As we will see, this allows to selectively generate radical species on substrate molecules that possess the proper redox potentials. The number of available photocatalysts is rapidly increasing: some examples and their respective redox properties are reported in Figure 8. The tuning of the molecular scaffold has generated photocatalysts with wide and different range of reduction potentials going from very strong oxidants to strong reductants all along the electrochemical series.^{9,10}

Excited state Oxidations

Excited state Reductions

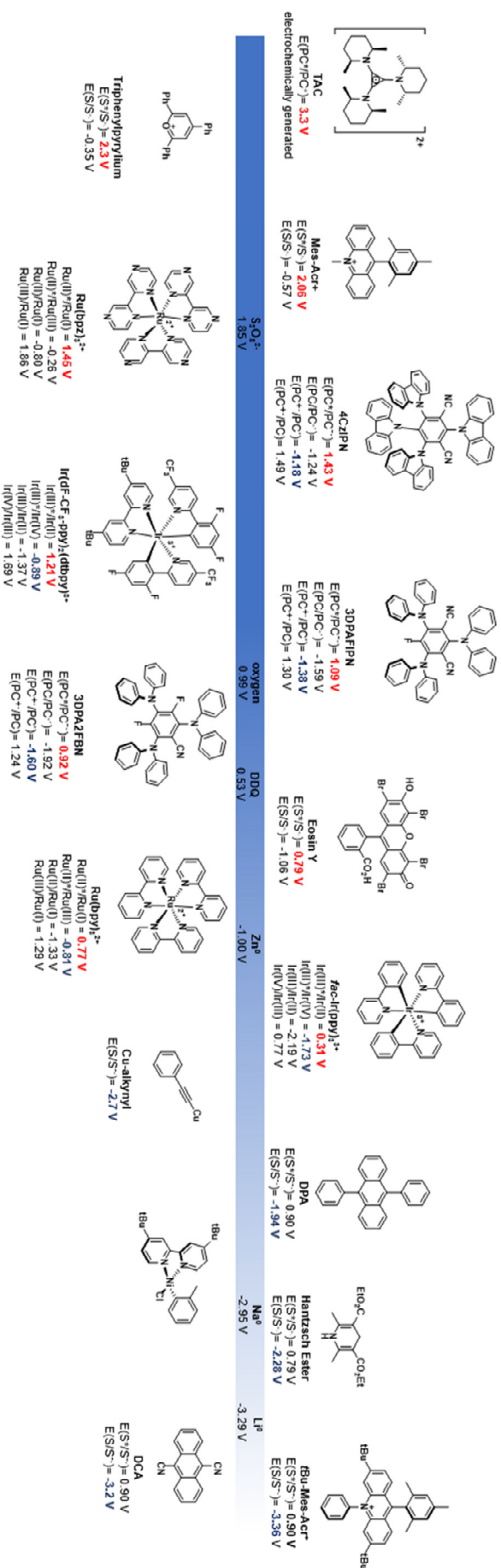
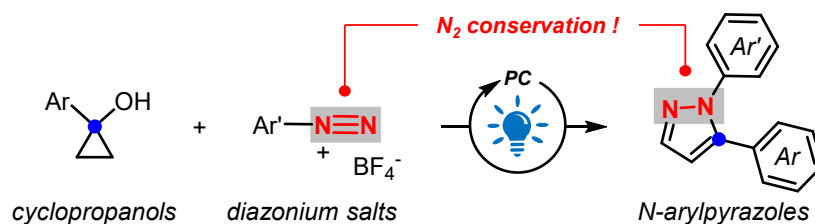


Figure 8. Overview of different photocatalysts and their redox properties.

1.4 References

1. a) Albini, A. *Photochemistry – Past, Present and Future*. Springer Berlin Heidelberg **2016**; b) König, B. *Chemical Photocatalysis*, 2nd edition. De Gruyter GmbH, Berlin/Boston **2020**.
2. a) Turro, N. J.; Ramamurthy, V.; Scaiano, J. C. *Modern molecular photochemistry of organic molecules*. Sausalito: University Science Books **2010**; b) Balzani, v.; Ceroni, P.; Juris, A. *Photochemistry and photophysics*. Weinheim: Wiley-VCH, **2014**; c) Romero, N. A.; Nicewicz, D. A. *Chem. Rev.* **2016**, *116*, 10075–10166.
3. Marcus, R. A. *J. Chem. Phys.* **1956**, *24*, 966.
4. Marcus, R. A. *J. Chem. Phys.* **1956**, *24*, 979.
5. a) Strieth-Kalthoff, F.; James, M.; Teders, M.; Pitzer, L.; Glorius F. *Chem. Soc. Rev.* **2018**, *47*, 7190–7202; b) Zhou, Q.; Zou, Y.; Lu, L.; Xiao, W. *Angew. Chem. Int. Ed.* **2019**, *58*, 1586–1604.
6. Capaldo, L.; Ravelli, D. *Eur. J. Org. Chem.* **2017**, 2056–2071.
7. Burstall, F. H. *J. Chem. Soc.* **1936**, 173–175.
8. a) McCusker, J. K. *Acc. Chem. Res.* **2003**, *36*, 876–887; Tucker, J. W.; Stephenson, C. R. J. *J. Org. Chem.* **2012**, *77*, 1617–1622.
9. A pdf chart of common photocatalysts and their redox properties is available from Merck webpage: https://www.google.com/url?sa=t&rct=j&q=&esrc=s&source=web&cd=&cad=rja&uact=8&ved=2ahUKewi64_iquu_yAhXESvEDHdXiCzUQjBB6BAgREAE&url=http%3A%2F%2Fchemlabs.princeton.edu%2Fmacmillan%2Fwp-content%2Fuploads%2Fsites%2F6%2FMerck-Photocatalysis-Chart.pdf&usq=AOvVawOfMnv5Rgn-GOa-fxwkTRqm
10. For a review on photocatalysts and their molecular tuning: Vega-Peñaloza, A.; Mateos, J.; Companyó, X.; Escudero-Casao, M.; Dell'Amico, L. *Angew. Chem. Int. Ed.* **2021**, *60*, 1082–1097.

2 Chapter 2: Aryl Pyrazoles from Photocatalytic Cycloadditions of Arenediazonium



Abstract: A photocatalytic synthesis of 1,5-diaryl pyrazoles from arenediazoniums and arylcyclopropanols is reported. The reaction proceeded at mild conditions (r.t., 20 min) with catalytic [Ru(bpy)₃]²⁺ under blue-light irradiation and exhibited compatibility with several functional groups (e.g. I, SF₅, SO₂NH₂, N₃, CN) and perfect levels of regiocontrol. Mechanistic studies (luminescence spectroscopy, CV, DFT, radical trapping, quantum yield determination) documented an initial oxidative quenching of the excited photocatalyst and the operation of a radical chain mechanism.

This chapter has been published:

Cardinale L., Neumeier M., Májek M., Jacobi von Wangelin A. *Org. Lett.* **2020**, 22, 18, 7219–7224.

Author contributions:

MN synthesized some of the substrate scope; MM performed quantum yield determination and DFT calculations; LC did the rest of the synthetic and analytical work, and wrote the manuscript.

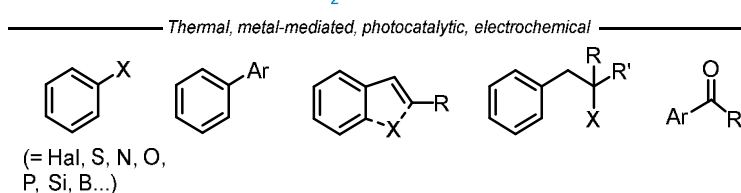
2.1 Introduction

Arenediazonium salts constitute synthetically versatile building blocks for aromatic substitutions by virtue of their easy availability as stable crystalline solids, the high thermodynamic driving force to form reactive aryl radical, aryl cation, or aryl-metal species by loss of N_2 , and the wide variety of onward reactions with many reagents.¹ Numerous protocols involving thermal, metal-catalyzed, electrochemical, and photo-redox conditions were reported that enable facile formations of C-C and C-Het bonds (X = Hal, S, O, N, P, Si, B, and many more, see Scheme 1) as illustrated by the many name reactions based on diazonium salts.²

Synthesis and utility of arenediazonium salts



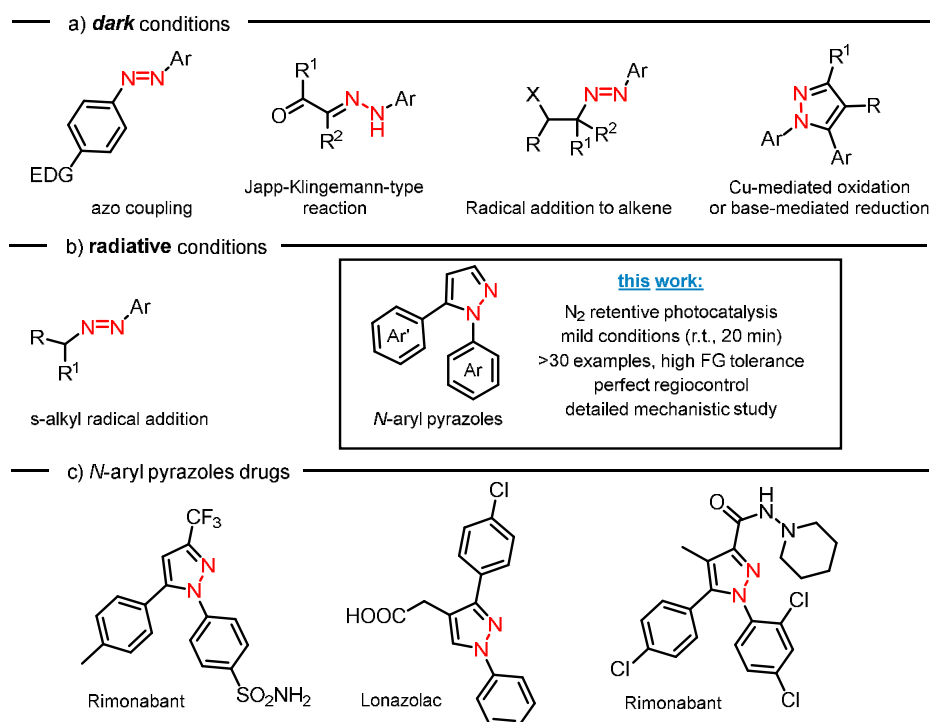
Aromatic substitutions with loss of N_2



Scheme 1. General reactivity of arenediazonium salts via nucleophilic aromatic substitution.

On the other hand, the arsenal of addition reaction mechanisms that conserve the N_2 function into the product structure is much less diverse. Examples include azo-couplings with electron-rich benzenes,³ cyclo-additions,⁴ radical trappings,⁵ and Japp-Klingemann-type reactions.⁶ These protocols proceed through thermal, oxidative or metal-catalyzed reaction mechanisms (Scheme 2, a). Photocatalytic reaction pathways of arene-diazonium salts that operate with retention of N_2 are very rare due to the facile reductive mesolysis of arenediazonium salts at very low redox potentials of ~ 0 V (vs. SCE).⁷

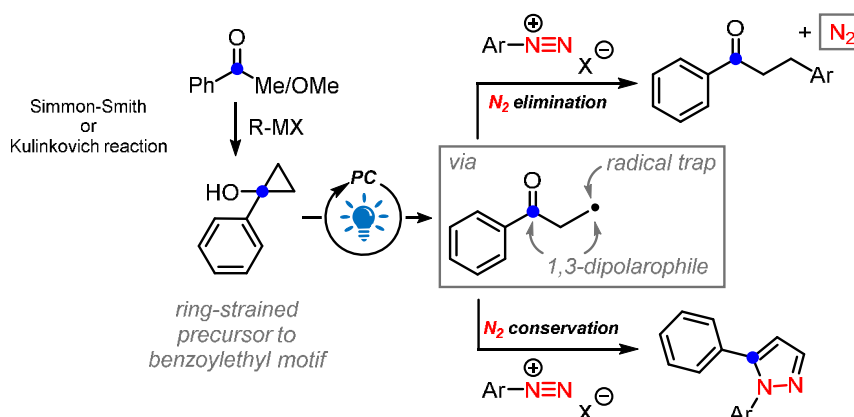
Addition reactions with retention of N_2



Scheme 2. Dark and photocatalytic reactions of diazonium salts with N_2 retention.

There are only three literature reports of photocatalytic arenediazonium reactions which all include the trapping of alkyl radicals to give acyclic azo-compounds.⁸ Minimal mechanistic insight has been provided, especially with regard to the inertness of arenediazonium to 1e-reduction in the presence of sufficiently strong photo-reductants. This work reports an unprecedented photocatalytic cycloaddition of arenediazonium with cyclopropanol to form 1,5-diaryl pyrazoles with perfect regiocontrol. A detailed analysis of the underlying mechanism by preparative, spectroscopic, and theoretical methods is given. This method provides a straightforward access to *N*-aryl pyrazoles,⁹ which constitute key motifs of pharmaceutical blockbusters such as celecoxib, lonazolac, and rimonabant (Scheme 2, c), agrochemicals, and ligands of metal-catalyzed cross-coupling reactions¹⁰.

We envisioned to utilize 1-aryl-1-cyclopropanols as C₃-building blocks that can easily be prepared by organometallic addition to benzoyl derivatives in a Simmons-Smith¹¹ or Kulinkovich reaction.¹²



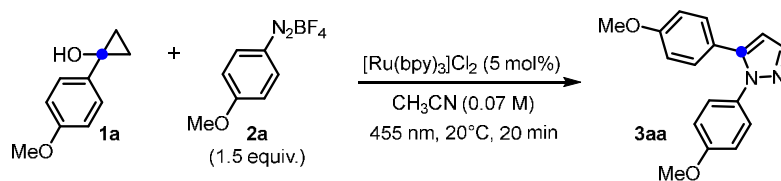
Scheme 3. Postulated reactions of arylcyclopropanol with arenediazonium to give γ -aryl phenones (via N₂-elimination) or 1,5-diaryl pyrazoles (via N₂-conservation).

1-Aryl-1-cyclopropanols could engage in photocatalytic ring-opening to provide a benzoylethyl motif exhibiting 1,3-dipolarophilic reactivity. This kind of reactivity has been known to be promoted both under oxidative and photoredox conditions.¹³ In the presence of arenediazonium, radical trapping would result in the formation of γ -aryl propiophenones via N₂-elimination¹⁴ or diaryl pyrazoles via N₂-retentive formal cycloaddition (Scheme 3).

2.2 Results and discussion

Optimization and substrate scope

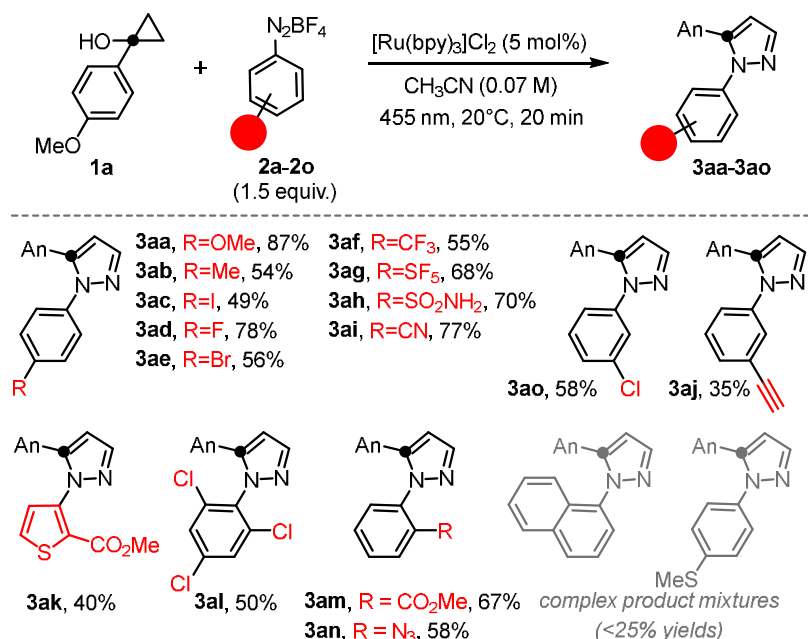
Our initial investigations of the model reaction between 1-anisyl-1-cyclopropanol **1a** and 4-methoxybenzenediazonium tetrafluoroborate **2a** with the organic photocatalyst eosin Y indeed afforded the pyrazole **3aa** in 42% yield as the sole product (Table 1, entry 7). The product yield could be increased to 87% after 20 min reaction time when using [Ru(bpy)₃]Cl₂·6H₂O as photocatalyst and the appropriate irradiation wavelength. Further decrease of the catalyst loading (<5 mol%) or reaction time gave inferior yields. The observed reactivity is noteworthy as the photocatalytic conditions with virtually all common molecular photocatalysts (incl. eosin Y, Ru(bpy)₃Cl₂·6H₂O, Ir(ppy)₃) provide sufficient reduction ability to mesolyze arenediazonium salts irreversibly via a SET.¹⁵

Table 1: Optimization of reaction conditions

Entry	Deviations from standard conditions	Yield % 3aa
1	none	87
2	2.5 mol% cat. loading	79
3	18h reaction time	85
4	15 min reaction time	81
5	No light	0
6	No cat.	0
7^a	2.5 mol% eosin Y	45
8	20 mol% DIPEA as additive	56
9^c	CH_3COOH 20 mol% as additive	49
10	1 equiv. 1a instead of 1.5 equiv.	55

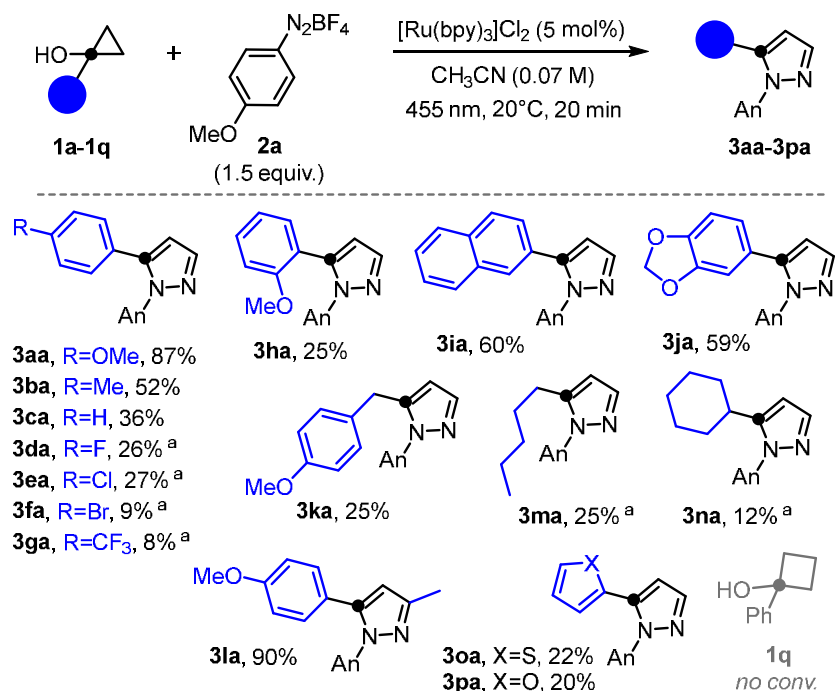
Reaction conditions: cyclopropanol **1a** (0.37 mmol, 1equiv.), diazonium salt **2a** (0.56 mmol, 1.5 equiv.), $\text{Ru}(\text{bpy})_3\text{Cl}_2 \cdot 6\text{H}_2\text{O}$ (as indicated), RT, blue LED irradiation ($\lambda_{\text{max}} = 455 \text{ nm}$), flushed with nitrogen. ^aeosin Y was used instead of $\text{Ru}(\text{bpy})_3\text{Cl}_2 \cdot 6\text{H}_2\text{O}$, green LED irradiation instead of blue. T, 0 °C to RT, 4 ml of THF per mmol of substrate.

The resultant 1,5-diaryl pyrazole is a common structural motif of fine chemicals and pharmaceuticals that is conventionally assembled from aryl 1,3-dicarbonyl derivatives and aryl hydrazines, with the latter substrates being prepared by copper-catalyzed amination reactions of aryl halides.¹⁶ Only one example of a Cu-mediated oxidative cyclization to *N*-aryl pyrazoles was reported⁹ⁱ, whereas a stoichiometric amount of Cu (II) salt is required to achieve the designed pyrazoles through a dark PCET mechanism in opposition with our photoredox oxidation discussed in the following. Control experiments in the absence of photocatalyst and light, respectively, did not afford any products.^{17,18} The optimal conditions involved reaction of the arenediazonium salt **1a** (1.5 equiv.) with the arylcyclopropanol **2a** in acetonitrile at room temperature for 20 min under blue light irradiation (455 nm) in the presence of catalytic $\text{Ru}(\text{bpy})_3\text{Cl}_2 \cdot 6\text{H}_2\text{O}$. The substrate scope was explored upon variation of both starting materials. Arenediazonium salts bearing electron-withdrawing and electron-donating substituents in *o*-, *m*-, and *p*-positions were equally reactive (Scheme 4). Generally, no significant electronic effect on the reactivity of the diazonium salts was observed (**3aa-3ao**). However, naphthalenediazonium tetrafluoroborate and 4-(methylthio)benzenediazonium tetrafluoroborate gave complex product mixtures and only low yields of the corresponding pyrazoles (<25 %), possibly by unwanted radical attack on the naphthalene and thioether moieties.¹⁹



Scheme 4. Substrate scope of arenediazonium salts.

Variations of the cyclopropanol derivative revealed a significant influence of their individual electronic properties (Scheme 5): Electron-donating substituents enabled high yields of the diaryl pyrazoles (**3aa-3ca**, **3ha-3ja**); electron-withdrawing substituents showed poor conversions under the reaction conditions (**3da-3ga**).



Scheme 5. Substrate scope of cyclopropanols.

Increased steric hindrance on the cyclopropane did not lead to decreased yields (**3la**). Alkyl- and benzyl-substituted cyclopropanols gave low yields (**3ka**, **3ma**, **3na**). The higher homolog 1-phenyl-1-cyclobutanol (**1q**) gave no ring-opening or heterocycle formation. In an effort to elucidate the mechanism of this photo-catalytic pyrazole synthesis, we conducted a series of preparative, spectroscopic, and theoretical studies. The preservation of the N₂ moiety within the product structure is a very rare feature of reactions with arenediazonium salts.^{5a,8,9d} Under photocatalytic conditions, this is even less likely due

to the very facile $1e^-$ reduction of arenediazonium salts (at ~ 0 V vs. SCE) followed by irreversible mesolysis and N_2 evolution.⁵

Fluorescence quenching

Consequently, we probed whether the photocatalytic mechanism involved any reduction event of the arenediazonium at all or rather oxidation of the cyclopropanol by the photocatalyst. On this purpose a fluorescence quenching of the employed photocatalyst was performed. A Stern-Volmer study, however, documented that efficient luminescence quenching of the excited state of $[Ru(bpy)_3]Cl_2$ ($[Ru^{2+}]^*$) was indeed operative with the diazonium salt **2a** (see the experimental part for details). Consistently, no quenching was observed with the electron-poor and electron-rich cyclopropanols **1g** and **1a**, respectively (Figure 1).

The non-linearity of the plot for **2a** is a direct consequence of the kinetic salt effect²⁰ of increased ionic strength of the solution by addition of the diazonium salt. Quencher and catalyst are charged species, so the ionic strength affects the rate of their reaction with each other. According to the Debye-Hückel

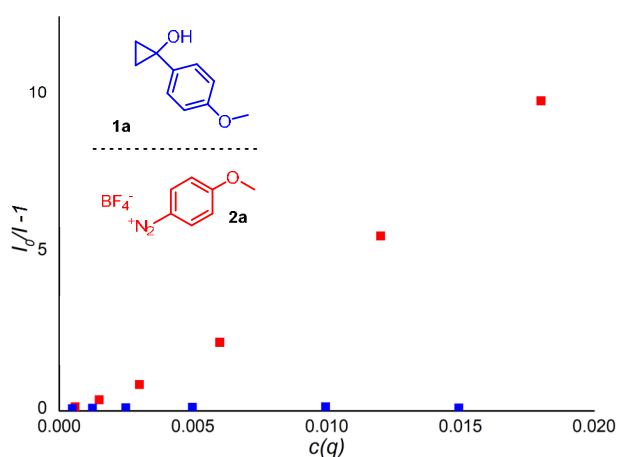


Figure 1. Luminescence quenching of $Ru(bpy)_3^{2+}$ with substrates **1a** and **2a**. $c(q)$: quencher concentration (mol/l).

theory, the Stern-Volmer quenching constants K_{SV0} - extrapolated to zero ionic strength - were calculated. K_{SV0} increased with lower electronic density of the arenediazonium: $K_{SV0}(\mathbf{2a}) = 88$ dm³/mol; $K_{SV0}(\mathbf{2e}) = 490$ dm³/mol; $K_{SV0}(\mathbf{2i}) = 1500$ dm³/mol. These data are indicative of an oxidative quenching of the excited photocatalyst $[Ru^{2+}]^*$ by the diazonium salt. This is further supported by the observed gas evolution during the reaction. The reductive mesolysis of the arenediazonium salt is also in full accord with the detection of an aryl-TEMPO adduct and the inhibition of product formation by addition of 2,2,6,6-tetramethylpiperidin-1-oxyl (TEMPO, see experimental section).

Cyclic voltammetry

Further insight into the operating redox events was provided by the analysis of redox potentials (Figure 2). Cyclic voltammetry (CV) confirmed that facile reduction of arenediazonium salts is thermodynamically feasible with the excited state photocatalyst: $E_{red}(\mathbf{2a}) = -0.18$ V; $E_{red}(\mathbf{2e}) = 0.00$ V; $E_{red}(\mathbf{2i}) = +0.03$ V; $E_{red}([Ru^{2+}]^*) = -0.81$ V (vs. SCE).²¹ The difference in redox potentials of this series explains the observed trend in the quenching constants K_{SV0} above where easily reduced compounds quench $[Ru^{2+}]^*$ faster. On the other hand, $[Ru^{2+}]^*$ ($E_{red} = +0.77$ V) is not a sufficiently strong oxidant for the $1e^-$ oxidation of any of the cyclopropanols ($E_{red} > +1$ V). These data support the notion of an initiating oxidative quenching of $[Ru^{2+}]^*$. The resultant ground-state $[Ru^{3+}]$ is sufficiently oxidizing ($E_{red} = +1.29$ V) to convert electron-rich cyclopropanols ($E_{red}(\mathbf{1a}) = +1.08$ V), while $1e^-$ oxidations of electron-poor cyclopropanols are thermodynamically unfavoured and only feasible when coupled with efficient follow-up reactions ($E_{red}(\mathbf{1g}) = +1.40$ V; $E_{red}(\mathbf{1k}) = +1.54$ V; *i.e.* <250 mV uphill).²² Unstrained cycloalkanols have reduction potentials ($E_{red}(\mathbf{1q}) = +1.72$ V) that are prohibitive for oxidations with $[Ru^{3+}]$ whereas the

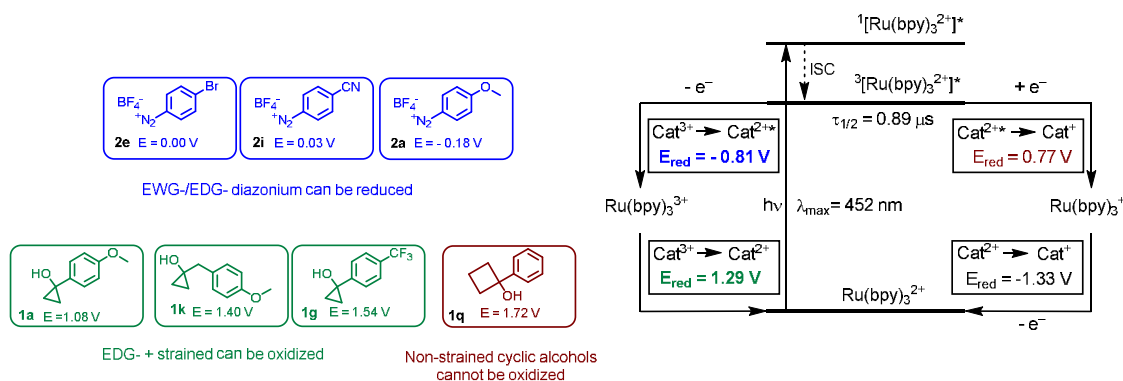


Figure 2. Reduction potentials E_{red} of substrates and photocatalyst (vs. SCE).

substitution with more strongly oxidizing photosensitizers as acridinium salts in combination with PCET (proton coupled electron transfer) strategy, as recent reports have shown,²³ could overcome this limit (Figure 2).

The fate of the oxidized cyclopropanols was another puzzle piece of the operating reaction mechanism. One-electron oxidations of cyclopropanols have been known to result in labile radical cations that undergo rapid ring-opening to β -keto radicals.^{14a} The feasibility of trapping of the intermediate benzoylethyl radicals $1^{+\bullet}$ with arenediazonium **2** was probed by a CV experiment (Figure 3): The cyclopropanol **1a** (blue line) displayed an irreversible oxidation wave ($E_{red} = +1.08 \text{ V}$), the diazonium salt **2f** (red line) an irreversible reduction wave ($E_{red} = +0.00 \text{ V}$). However, subjecting of an equimolar mixture of both substrates to such CV electrolysis (black line; increasing potentials from 0.5 V), an unchanged oxidation peak of **1a** was observed while the reduction peak of **2e** disappeared. This is indicating that the oxidized alcohol $1a^{+\bullet}$ underwent chemical reaction with the diazonium salt prior to reduction of the latter. The resultant adduct of $1^{+\bullet}$ and **2** (*i.e.* **4**⁺) engages in $1e^-$ reduction to a neutral compound that cyclizes to a pyrazole.

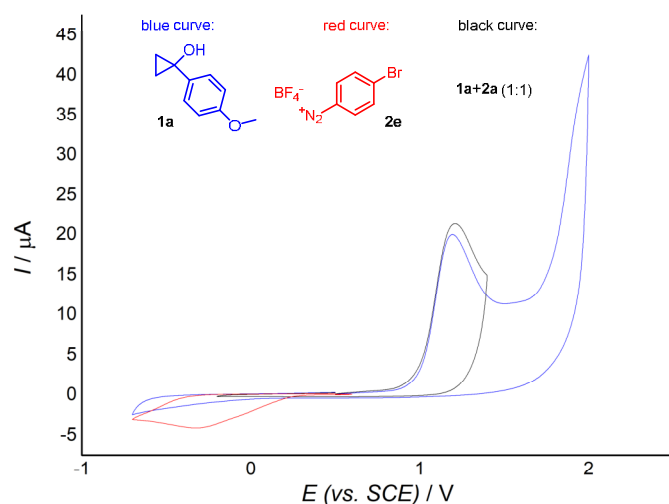


Figure 3. Cyclic voltammetry spectra of **1a**, **2e**, and an equimolar mixture.

Further insight was derived from the quantum yield of $\Phi = 4.2$ for the formation of **3aa**. This value indicates the presence of an efficient radical chain propagation, which most likely is the oxidation of cyclopropanol **1** with the radical adduct **4**⁺ (Figure 4a). To probe its feasibility, we utilized the model compound 2-ethyl-1-phenyl-diazene (**5**) which should exhibit similar redox properties as **4** but undergo no onward cyclization reaction. CV spectra showed irreversible oxidation of **5** at +1.55 V. This value is likely to include over-potential, so we also obtained a DFT-derived theoretical reduction potential of **5**

(+1.40 V, see experimental section). In comparison with the reduction potentials of the cyclopropanols (1.08-1.54 V), these support the operation of radical chain propagation by reactions of the cyclopropanols **1** with the radical adduct intermediates **4**^{•+} (Figure 4a). Based on the collected mechanistic data, we propose the reaction mechanism shown in Figure 4b. The reaction is initiated by oxidative quenching of [Ru²⁺]^{*} with the arenediazonium salt **2**. The resultant [Ru³⁺] oxidizes the strained alcohol **1** to give **1**^{•+} which undergoes rapid ring-opening and radical trapping with the arenediazonium salt. The radical cation adduct **4**^{•+} can engage in a radical chain process by oxidizing another molecule of **1** or quench the excited catalyst to close the photocatalytic cycle. As the radical chain process is dominant ($\Phi = 4.2$), co-catalytic amounts of the arenediazonium **2** are required to produce the key oxidant [Ru(bpy)₃]³⁺ salt must be used to activate the catalyst – which is also evident from the optimal reaction conditions involving a slight excess of **2**. The adduct **4** undergoes cyclization and dehydration to give the pyrazole **3**.

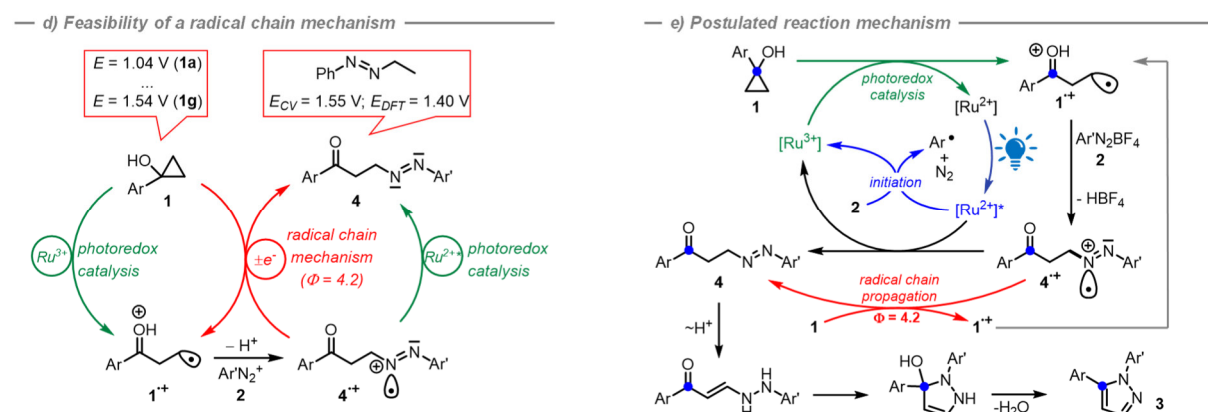


Figure 4. a) Postulated trapping of intermediate **1**^{•+} and the feasibility of radical chain propagation. b) Proposed mechanism based on preparative, spectroscopic, and theoretical studies.

2.3 Conclusion

In conclusion, this protocol enables a rare photocatalytic reaction of arenediazonium that proceeds with retention of the diazo function. In the presence of arylcyclopropanols, *N*-aryl-pyrazoles are obtained within 20 min under blue light irradiation in good yields. The reaction displayed high regiocontrol (only 1,5-diaryl pyrazoles formed) and high functional group tolerance (F, Cl, N₃, CO₂Me, CN, CF₃, SF₅, thiophene, alkyne). Combined synthetic, spectroscopic, and theoretical studies supported the notion of a radical chain mechanism, which involves photocatalytic initiation by oxidative photocatalyst quenching with the arenediazonium, oxidation of the arylcyclopropanol with ground-state [Ru³⁺]^{*}, and radical chain propagation between the arylcyclopropanol and the radical cationic adduct of both starting materials.

2.4 Experimental section

2.4.1 Materials and methods

All reagents and solvents were purchased from commercial suppliers (Acros, Alfa Aesar, Fisher, Fluka, Merck, Sigma Aldrich, Sojuz-Chimexport and TCI) and used as received. Diazonium salts were prepared by synthetic routes (vide infra), with the respective aniline precursors used without further purification as obtained from the vendors. The reactions were carried out in Rotilabo®-sample vials (6mL, Ø22mm, Roth) sealed with Rotilabo®-aluminum caps with septum (Ø20mm, Roth). Irradiation was performed with a blue high-power LED (Luxeon Rebel, Canada, P = 3.8 W, λ_{max} = 450nm). TLC was performed on the commercial SiO₂-coated aluminum plates (DC60 F254, Merck). Visualization was done by UV light (254 nm). Product yields were determined as isolated yields after flash column chromatography on silica gel (Acros Organics, mesh 35-70, 60 Å pore size).

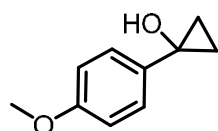
Purity and structure confirmation of literature-known compounds was performed by ^1H NMR, ^{13}C NMR, ^{19}F NMR and MS. NMR spectral data were collected on a Bruker Avance 300 (300 MHz for ^1H ; 75 MHz for ^{13}C , 282 MHz for ^{19}F) spectrometer, Bruker Avance 400 (400 MHz for ^1H ; 100 MHz for ^{13}C) spectrometer and a Bruker Avance 500 (500 MHz for ^1H ; 125 MHz for ^{13}C) spectrometer at 25 °C. Chemical shifts are reported in δ /ppm, coupling constants J are given in Hertz. Solvent residual peaks were used as internal standard for all NMR measurements. The quantification of ^1H cores was obtained from integrations of appropriate resonance signals. Abbreviations used in NMR spectra: s –singlet, d –doublet, t –triplet, q –quartet, m –multiplet, bs –broad singlet, dd –doublet of doublet, ddd –doublet of doublet of doublet. Low-resolution mass spectrometry (LRMS) was carried out on an Agilent6890N GC-System with 5975 MS mass detector and H_2 as carrier gas. High resolution mass spectrometry (HRMS) was carried out by the Central Analytics at the department of chemistry, University of Hamburg. Abbreviations used in MS spectra: M –molar mass of target compound, EI –electron impact.

2.4.2 General Procedures

General procedure A: Simmons-Smith reaction

A dried 100 mL round bottomed Schlenk flask was equipped with a stir bar. The flask was evacuated, heated, flushed with nitrogen three times and sealed with a rubber septum. In a dry nitrogen atmosphere THF (20 mL, dry) and $(i\text{Pr})_2\text{NH}$ (1.5 mL, 11.0 mmol, 1.1 eq.) were added. At 0 °C $n\text{BuLi}$ (7.0 mL, 1.6 mol L $^{-1}$ in hexanes, 11.0 mmol, 1.1 eq.) was added to the stirring mixture dropwise via syringe. The mixture was warmed to room temperature and stirred for 1 h. To this mixture at 0 °C the parent ketone (10.0 mmol, 1.0 eq.) was added by syringe followed by TMSCl (1.4 mL, 11.0 mmol, 1.1 eq.). After the mixture was stirred for 2 h at room temperature, it was quenched by addition of NaHCO_3 solution (30 mL, sat.). The layers were separated and the aqueous layer was extracted with EtOAc (3 \times 30 mL). The combined organic layers were washed with a NaHCO_3 and brine solution (3 \times 20 mL) and dried with Na_2SO_4 followed by filtration. The solvent was removed in vacuum. The crude enol ether was used without further purification. A dried 100 mL round bottomed Schlenk flask was equipped with a stir bar. The flask was evacuated, heated, flushed with nitrogen three times and sealed with a rubber septum. The crude enol ether was solved in DCM (20 mL, dry) and was transferred to the prepared Schlenk flask. To the stirring mixture DCM (1.2 mL, 15.0 mmol, 1.5 eq.) was added followed by Et_2Zn (15 mL, 1 mol L $^{-1}$ in Et_2O , 15 mmol, 1.5 eq.) at 0 °C. The mixture was stirred overnight at room temperature. The reaction mixture was quenched with NH_4Cl solution (30 mL, sat.). The layers were separated and the aqueous layer was extracted with DCM (3 \times 30 mL). The combined organic layers were washed with NaCl solution (3 \times 30 mL, sat.) and dried with Na_2SO_4 followed by filtration. The solvent was removed in vacuum. A dried 100 mL round bottomed Schlenk flask was equipped with a stir bar. The flask was evacuated, heated, flushed with nitrogen three times and sealed with a rubber septum. The crude cyclopropanol ether was solved in MeOH dry (20 mL) and transferred to the prepared Schlenk flask. To the stirring mixture TMSCl (one drop) was added via syringe at 0 °C. The reaction was monitored by GC-MS. After completion the solvent was removed in vacuum and the residue was purified by column chromatography (silica gel, 1:9 EtOAc/pentane) to obtain pure product. The following cyclopropanol products were synthesized using the procedure described above:

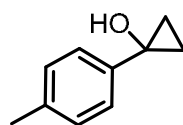
1-(4-methoxyphenyl)cyclopropan-1-ol (1a)



^1H NMR (400 MHz, CDCl_3 , ppm): δ 7.20-7.16 (m, 2H), 6.79-6.76 (m, 2H), 3.71 (s, 3H), 2.46 (bs, 1H), 1.20-1.18 (m, 2H), 0.91-0.85 (m, 2H).

Spectral data were consistent with literature²⁴

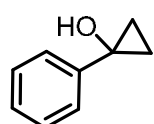
1-(*p*-tolyl)cyclopropan-1-ol (1b)



^1H NMR (300 MHz, CDCl_3 , ppm): δ 7.29-7.20 (m, 4H), 2.86 (bs, 1H), 2.42 (s, 3H), 1.31-1.27 (m, 2H), 1.09-1.04 (m, 2H).

Spectral data were consistent with literature²⁴

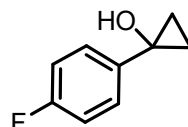
1-phenylcyclopropan-1-ol (1c)



$^1\text{H NMR}$ (400 MHz, CDCl_3 , ppm): δ 7.39-7.19 (m, 5H), 2.68 (bs, 1H), 1.30-1.24 (m, 2H), 1.08-1.02 (m, 2H).

Spectral data were consistent with literature²⁴

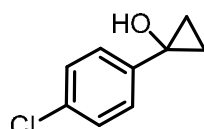
1-(4-fluorophenyl)cyclopropan-1-ol (1d)



$^1\text{H NMR}$ (300 MHz, CDCl_3 , ppm): δ 7.25-7.18 (m, 2H), 6.98-6.90 (m, 2H), 2.25 (s, 1H), 1.19-1.15 (m, 2H), 0.95-0.90 (m, 2H).

Spectral data were consistent with literature²⁵

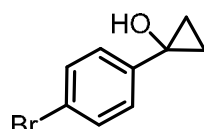
1-(4-chlorophenyl)cyclopropan-1-ol (1e)



$^1\text{H NMR}$ (300 MHz, CDCl_3 , ppm): δ 7.24-7.12 (m, 4H), 2.29 (s, 1H), 1.22-1.18 (m, 2H), 0.97-0.92 (m, 2H).

Spectral data were consistent with literature²⁴

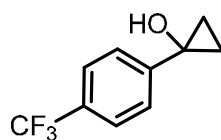
1-(4-bromophenyl)cyclopropan-1-ol (1f)



$^1\text{H NMR}$ (300 MHz, CDCl_3 , ppm): δ 7.39-7.34 (m, 2H), 7.12-7.07 (m, 2H), 2.25 (s, 1H), 1.23-1.18 (m, 2H), 0.97-0.93 (m, 2H).

Spectral data were consistent with literature²⁵

1-(4-(trifluoromethyl)phenyl)cyclopropan-1-ol (1g)

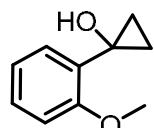


$^1\text{H NMR}$ (300 MHz, CDCl_3 , ppm): δ 7.59-7.55 (m, 2H), 7.39-7.36 (m, 2H), 2.44 (s, 1H), 1.38-1.34 (m, 2H), 1.13-1.08 (m, 2H).

$^{19}\text{F NMR}$ (376 MHz, CDCl_3): -62.37.

Spectral data were consistent with literature²⁴

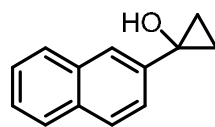
1-(2-methoxyphenyl)cyclopropan-1-ol (1h)



$^1\text{H NMR}$ (300 MHz, CDCl_3 , ppm): δ 7.30-7.19 (m, 2H), 6.94-6.88 (m, 2H), 3.94 (s, 3H), 3.59 (bs, 1H), 1.13-1.09 (m, 2H), 0.94-0.89 (m, 2H).

Spectral data were consistent with literature²⁴

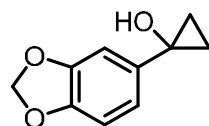
1-(naphthalen-2-yl)cyclopropan-1-ol (1i)



$^1\text{H NMR}$ (300 MHz, CDCl_3 , ppm): δ 7.87-7.77 (m, 4H), 7.52-7.42 (m, 2H), 7.32-7.26 (m, 1H), 2.51 (s, 1H), 1.34 (dd, $J = 4.2, 3.2$ Hz, 2H), 1.17 (dd, $J = 4.2, 3.2$ Hz, 2H).

Spectral data were consistent with literature²⁴

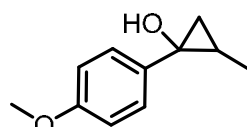
1-(benzo[d][1,3]dioxol-5-yl)cyclopropan-1-ol (1j)



$^1\text{H NMR}$ (300 MHz, CDCl_3 , ppm): δ 6.80-6.72 (m, 3H), 5.92 (s, 2H), 1.19-1.14 (m, 2H), 0.95-0.96 (m, 2H).

Spectral data were consistent with literature²⁶

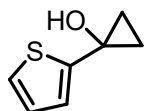
1-(4-methoxyphenyl)-2-methylcyclopropan-1-ol (1l)



$^1\text{H NMR}$ (300 MHz, CDCl_3 , ppm): δ 7.23-7.20 (m, 2H), 6.87-6.84 (m, 2H), 3.79 (s, 3H), 2.49 (bs, 1H), 1.32-1.39 (m, 3H), 1.18-1.10 (m, 2H), 0.76-0.72 (m, 1H).

Spectral data were consistent with literature²⁷

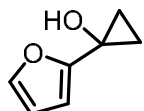
1-(thiophen-2-yl)cyclopropan-1-ol (1o)



¹H NMR (300 MHz, CDCl₃, ppm): δ 7.18 (dd, *J* = 5.1, 1.3 Hz, 1H), 6.94 (dd, *J* = 5.1, 3.5 Hz, 1H), 6.88 (dd, *J* = 3.6, 1.3 Hz, 1H), 2.61 (s, 1H), 1.32-1.28 (m, 2H), 1.09-1.05 (m, 2H).

Spectral data were consistent with literature²⁴

1-(furan-2-yl)cyclopropan-1-ol (1p)



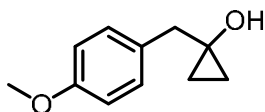
¹H NMR (300 MHz, CDCl₃, ppm): δ 7.29-7.26 (m, 1H), 6.30-6.28 (m, 1H), 6.20-6.18 (m, 1H), 3.23 (s, 1H), 1.12-1.09 (m, 2H), 1.06-1.03 (m, 2H).

Spectral data were consistent with literature²⁵

General Procedure B: Kulinkovich reaction

To an oven-dried round bottom flask (100 mL) equipped with a magnetic stir bar, the ester (10.0 mmol) was dissolved in dry diethyl ether (30 mL). Ti(*i*-PrO)₄ (14.0 mmol, 1.4 equiv) was added to the solution and stirred for 2 min. Then ethylmagnesium bromide (28.0 mmol, 28 mL, 1.0 M in THF) was added dropwise to the solution over 2-3 h. The solution generally turned dark green. After stirring at room temperature for additional 30 min the reaction mixture was cooled with an ice bath and hydrolyzed by slow addition of cold 10% H₂SO₄ solution (50 mL) and then extracted with ether (3 x 40 mL). The combined organic layers were washed with saturated NaHCO₃ solution, brine and dried (Mg₂SO₄). After evaporation of solvent under reduced pressure the cyclopropanol products can be purified using distillation or column chromatography on silica gel. However, in most cases they are pure enough to be used directly in the next step. The following cyclopropanol products were synthesized using the procedure described above:

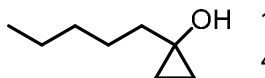
1-(4-methoxybenzyl)cyclopropan-1-ol (1k)



¹H NMR (300 MHz, CDCl₃, ppm): δ 7.24-7.19 (m, 2H), 6.90-6.85 (m, 2H), 3.80 (s, 3H), 2.83 (s, 2H), 2.00 (s, 2H), 0.82-0.78 (m, 2H), 0.64-0.60 (m, 2H).

Spectral data were consistent with literature²⁵

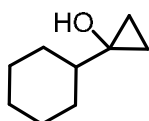
1-pentylcyclopropan-1-ol (1m)



¹H NMR (300 MHz, CDCl₃, ppm): δ 2.18 (s, 1H), 1.52-1.50 (m, 4H), 1.32-1.29 (m, 4H), 0.91-0.86 (m, 3H), 0.72-0.68 (m, 2H), 0.43-0.39 (m, 2H).

Spectral data were consistent with literature²⁸

1-cyclohexylcyclopropan-1-ol (1n)



¹H NMR (300 MHz, CDCl₃, ppm): δ 1.85-1.66 (m, 6H), 1.27-1.16 (m, 5H), 0.87 (m, 1H), 0.67 (m, 2H), 0.42 (m, 2H).

Spectral data were consistent with literature²⁵

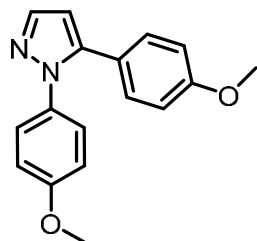
General Procedure C: synthesis of arenediazoniums

The parent aniline (30 mmol) was dissolved in 32% aqueous tetrafluoroboric acid (12mL) at room temperature. Afterwards, an aqueous solution of sodium nitrite (30 mmol) in water (4 mL) was added dropwise at 0 °C over 5 min. The resulting mixture was stirred for 40 min and the precipitate was collected by filtration and re-dissolved in minimum amount of acetone. Then, diethyl ether was added until precipitation of diazonium tetrafluoroborate, which is filtered, washed several times with diethyl ether and dried in the air.

General Procedure D: photocatalytic synthesis of 1,5-diarylpyrazoles

A vial was charged with Ru(bpy)₃Cl₂·6H₂O (18.5 μmol, 5 mol%), the corresponding cyclopropane-1-ol (0.37 mmol, 1 eq.) and the parent diazonium salt (0.56 mmol, 1.5 eq.). The vial was sealed and subsequently MeCN (5 mL) was added, and the reaction mixture was degassed, by purging with nitrogen over 10 min in dark. Light was switched on, and the reaction mixture was stirred at r.t. over 20 min. The reaction mixture was quenched with water (3 mL) and extracted with ethyl acetate (3 x 3 mL). The organic phase was separated and dried over Mg₂SO₄. Solids were filtered off and the volatiles were removed under reduced pressure to afford a viscous oil containing product. The crude product was further purified by column chromatography on silica gel using ethyl acetate/pentane (1:4) as eluent to afford the pure product.

1, 5-bis(4-methoxyphenyl)-1*H*-pyrazole (**3aa**)

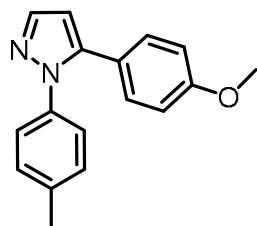


Following the general procedure D, **3aa** was isolated by flash chromatography on silica (gradient: pentane/EtOAc, from 9:1 to 8:2) as a white solid (90.2 mg, 87% yield). ¹H NMR (400 MHz, CDCl₃, ppm): δ 7.67 (d, *J* = 1.6 Hz, 1H), 7.11-7.25 (m, 4H), 6.79-6.89 (m, 4H), 6.43 (d, *J* = 1.9 Hz, 1H), 3.80 (s, 3H), 3.79 (s, 3H). ¹³C NMR (100 MHz, CDCl₃, ppm): δ 159.4, 158.7, 142.8, 139.8, 133.4, 130.0, 126.6, 123.0, 114.0, 113.9, 106.8, 55.5, 55.3.

GC-MS (EI) *m/z* (relative intensity): 280 (100) [M⁺], 281 (73), 265 (36).

Spectral data were consistent with literature²⁹

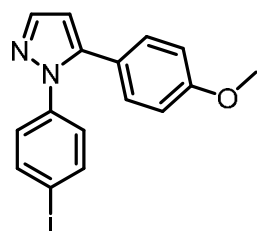
5-(4-methoxyphenyl)-1-(*p*-tolyl)-1*H*-pyrazole (**3ab**)



Following the general procedure D, **3ab** was isolated by flash chromatography on silica (gradient: pentane/EtOAc, from 9:1 to 8:2) as a white solid (52.8 mg, 54% yield). ¹H NMR (400 MHz, CDCl₃, ppm): δ 7.68 (d, *J* = 1.8 Hz, 1H), 7.20-7.11 (m, 6H), 6.85-6.80 (m, 2H), 6.43 (d, *J* = 1.9 Hz, 1H), 3.79 (s, 3H), 2.35 (s, 3H).

Spectral data were consistent with literature³⁰

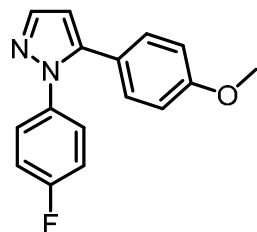
1-(4-iodophenyl)-5-(4-methoxyphenyl)-1*H*-pyrazole (**3ac**)



Following the general procedure D, **3ac** was isolated by flash chromatography on silica (gradient: pentane/EtOAc, from 9:1 to 8:2) as a yellowish solid (68.2 mg, 49% yield). ¹H NMR (300 MHz, CDCl₃, ppm): δ = 7.70 (d, *J* = 1.8 Hz, 1H), 7.65 (d, *J* = 8.8 Hz, 2H), 7.15 (d, *J* = 8.8 Hz, 2H), 7.06 (d, *J* = 8.8 Hz, 2H), 6.86 (d, *J* = 8.8 Hz, 2H), 6.44 (d, *J* = 1.8 Hz, 1H), 3.82 (s, 3H). ¹³C NMR (75 MHz, CDCl₃, ppm): δ = 159.8, 143.1, 140.7, 139.9, 138.1, 130.2, 126.8, 122.7, 114.2, 108.0, 92.4, 55.4.

HRMS (EI): *m/z* = calcd. for C₁₆H₁₃IN₂O⁺: 376.0067, found: 376.0075.

1-(4-fluorophenyl)-5-(4-methoxyphenyl)-1*H*-pyrazole (**3ad**)

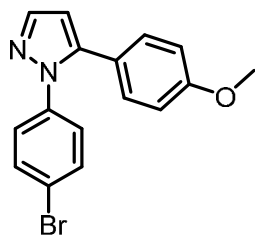


Following the general procedure D, **3ad** was isolated by flash chromatography on silica (gradient: pentane/EtOAc, from 9:1 to 8:2) as a yellowish solid (77.3 mg, 78% yield). ¹H NMR (400 MHz, CDCl₃, ppm): δ 7.68 (d, *J* = 1.8 Hz, 1H), 7.26-7.30 (m, 2H), 7.13 (d, *J* = 8.6 Hz, 2H), 7.02 (t, *J* = 8.6 Hz, 2H), 6.83 (d, *J* = 8.8 Hz, 2H), 6.44 (d, *J* = 1.8 Hz, 1H), 3.80 (s, 3H). ¹³C NMR (100 MHz, CDCl₃, ppm): δ 161.8 (d, *J* = 247.5 Hz), 159.7, 143.0, 140.3, 136.4 (d, *J* = 2.9 Hz), 130.1, 126.9 (d, *J* = 8.6 Hz), 122.7, 115.8 (d, *J* = 23.5 Hz), 114.0, 107.3, 55.4.

¹⁹F NMR (376 MHz, CDCl₃, ppm) δ -114.2 (s, 1F).

Spectral data were consistent with literature²⁹

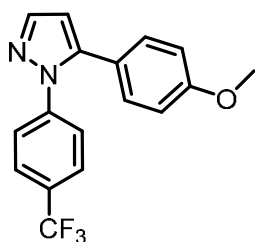
1-(4-bromophenyl)-5-(4-methoxyphenyl)-1H-pyrazole (3ae)



Following the general procedure D, **3ae** was isolated by flash chromatography on silica (gradient: pentane/EtOAc, from 9:1 to 8:2) as a yellow solid (68.1 mg, 56% yield). ¹H NMR (400 MHz, CDCl₃, ppm): δ 7.70 (d, *J* = 1.8 Hz, 1H), 7.45 (d, *J* = 8.8 Hz, 2H), 7.18 (d, *J* = 8.8 Hz, 2H), 7.14 (d, *J* = 8.9 Hz, 2H), 6.86 (d, *J* = 8.8 Hz, 2H), 6.44 (d, *J* = 1.8 Hz, 1H), 3.81 (s, 3H). ¹³C NMR (100 MHz, CDCl₃, ppm): δ 159.7, 143.0, 140.6, 139.2, 132.0, 130.1, 126.6, 122.7, 121.0, 114.1, 107.8, 55.4.

GC-MS (EI) *m/z* (relative intensity): 330 (28) [M⁺], 328 (46), 205 (21), 157 (23), 102 (75), 89 (62), 76 (95), 75 (100), 64 (83), 50 (78).

5-(4-methoxyphenyl)-1-(4-(trifluoromethyl) phenyl)-1H-pyrazole (3af)

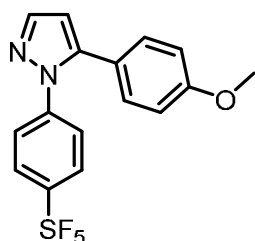


Following the general procedure D, **3af** was isolated by flash chromatography on silica (gradient: pentane/EtOAc, from 9:1 to 8:2) as a yellowish solid (64.7 mg, 55% yield). ¹H NMR (400 MHz, CDCl₃, ppm): δ 7.73 (d, *J* = 1.8 Hz, 1H), 7.58 (d, *J* = 8.8 Hz, 2H), 7.43 (d, *J* = 8.8 Hz, 2H), 7.15 (d, *J* = 8.6 Hz, 2H), 6.87 (d, *J* = 8.8 Hz, 2H), 6.47 (d, *J* = 1.9 Hz, 1H), 3.82 (s, 3H). ¹³C NMR (100 MHz, CDCl₃, ppm): δ 159.9, 143.2, 142.9, 141.1, 130.2, 129.0, 126.1, 124.8, 123.9, 122.5, 114.2, 108.4, 55.4. ¹⁹F NMR (376 MHz, CDCl₃, ppm) δ -62.9 (s, 3F).

GC-MS (EI) *m/z* (relative intensity): 318 (48) [M⁺], 145 (45), 102 (38), 69 (100), 63 (39).

Spectral data were consistent with literature³¹

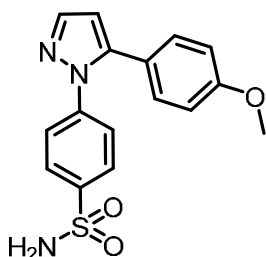
5-(4-Methoxyphenyl)-1-(4-(pentafluoro-sulfaneyl)phenyl)-1H-pyrazole (3ag)



Following the general procedure D, **3ag** was isolated by flash chromatography on silica (gradient: pentane/EtOAc, from 95:5 to 9:1) as a yellow solid (94.5 mg, 68% yield). ¹H NMR (400 MHz, CDCl₃, ppm): δ = 7.74 (d, *J* = 1.8 Hz, 1H), 7.71 (d, *J* = 9.0 Hz, 2H), 7.41 (d, *J* = 9.0 Hz, 2H), 7.17 (d, *J* = 8.8 Hz, 2H), 6.90 (d, *J* = 8.8 Hz, 2H), 6.48 (d, *J* = 1.8 Hz, 1H), 3.84 (s, 3H). ¹³C NMR (100 MHz, CDCl₃, ppm): δ = 160.1, 151.9, 143.4, 142.5, 141.4, 130.3, 126.9, 124.4, 122.5, 114.4, 108.8, 55.5. ¹⁹F NMR (282 MHz, CDCl₃, ppm): δ = 83.7 (quintet, *J* = 149.2 Hz, 1F), 62.8 (d, *J* = 149.2 Hz).

HRMS (EI): *m/z* = calcd. for C₁₆H₁₃F₅N₂OS⁺: 376.0663, found: 376.0661.

4-(5-(4-methoxyphenyl)-1H-pyrazol-1-yl)benzenesulfonamide (3ah)

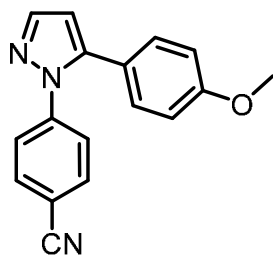


Following the general procedure D, **3ah** was isolated by flash chromatography on silica (gradient: pentane/EtOAc, from 8:2 to 6:4) as a white solid (85.3 mg, 70% yield). ¹H NMR (300 MHz, MeOD, ppm) δ: 7.97-7.86 (m, 2H), 7.77 (d, *J* = 1.8 Hz, 1H), 7.48-7.40 (m, 2H), 7.23-7.15 (m, 2H), 6.95-6.87 (m, 2H), 6.57 (d, *J* = 1.8 Hz, 1H), 3.81 (s, 3H). ¹³C NMR (75 MHz, MeOD, ppm): δ = 160.2, 143.8, 142.7, 142.6, 140.7, 129.9, 126.8, 125.3, 122.4, 113.9, 107.7, 54.4.

HRMS (ESI): *m/z* = calcd. for C₁₆H₁₂Cl₃N₂O [M-H]⁺: 330.0912, found: 330.0913.

m.p.: 185-190 °C

4-(5-(4-methoxyphenyl)-1H-pyrazol-1-yl)benzonitrile (**3ai**)

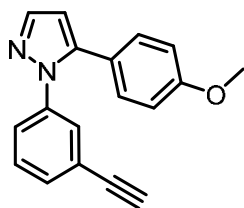


Following the general procedure D, **3ai** was isolated by flash chromatography on silica (gradient: pentane/EtOAc, from 9:1 to 8:2) as a yellow-orange solid (78.3 mg, 77% yield). ¹H NMR (300 MHz, CDCl₃, ppm): δ = 7.74 (d, J = 1.74 Hz, 1H), 7.60 (m, 2H), 7.42 (m, 2H), 7.14 (m, 2H), 6.87 (m, 2H), 6.46 (d, J = 1.77 Hz, 1H), 3.82 (s, 3H). ¹³C NMR (75 MHz, CDCl₃, ppm): δ = 160.0, 143.11, 143.3, 141.5, 132.9, 130.1, 124.9, 122.3, 118.3, 114.3, 110.4, 108.9, 55.4.

HRMS (ESI): m/z = calcd. for C₁₇H₁₄N₃O [M-H]⁺: 276.1131, found: 276.1123.

m.p.: 81-87 °C

1-(3-ethynylphenyl)-5-(4-methoxyphenyl)-1H-pyrazole (**3aj**)

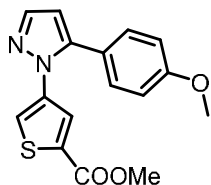


Following the general procedure D, **3aj** was isolated by flash chromatography on silica (gradient: pentane/EtOAc, from 9:1 to 8:2) as a yellow oil (35.5 mg, 35% yield). ¹H NMR (300 MHz, CDCl₃, ppm): δ = 7.62 (d, J = 1.8 Hz, 1H), 7.47 (t, J = 1.9 Hz, 1H), 7.34 (dt, J = 7.4, 1.6 Hz, 1H), 7.21–7.05 (m, 5 H), 6.80–6.75 (m, 2H), 6.37 (d, J = 1.8 Hz, 1H), 3.73 (s, 3H), 2.99 (s, 1H). ¹³C NMR (100 MHz, CDCl₃, ppm): δ = 159.8, 143.1, 140.7, 140.4, 131.1, 130.2, 128.9, 128.8, 125.8,

123.2, 122.8, 114.2, 107.7, 82.7, 78.2, 55.43.

HRMS (ESI): m/z = calcd. for C₁₈H₁₅N₂O [M-H]⁺: 275.1184, found: 275.1174.

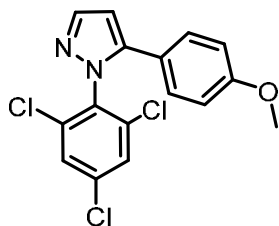
Methyl 3-(5-(4-methoxyphenyl)-1H-pyrazol-1-yl) thiophene-2-carboxylate (**3ak**)



Following the general procedure D, **3ak** was isolated by flash chromatography on silica (gradient: pentane/EtOAc, from 9:1 to 8:2) as a yellowish solid (46.5 mg, 40% yield). ¹H NMR (300 MHz, CDCl₃, ppm): δ = 7.74 (d, J = 1.9 Hz, 1H), 7.53 (d, J = 5.2 Hz, 1H), 7.15 (d, J = 5.2 Hz, 1H), 7.11 (d, J = 8.9 Hz, 2H), 6.79 (d, J = 8.9 Hz, 2H), 6.47 (d, J = 1.9 Hz, 1H), 3.78 (s, 3H), 3.61 (s, 3H). ¹³C NMR (75 MHz, CDCl₃, ppm): δ = 160.5, 159.7, 145.3, 141.6, 140.7, 130.3, 129.4, 128.4, 126.9, 122.6, 113.9, 106.0, 55.4, 52.3.

HRMS (ESI): m/z = calcd. for C₁₆H₁₄N₂O₃S⁺: 314.0720, found: 314.0716.

5-(4-methoxyphenyl)-1-(2,4,6-trichlorophenyl)-1H-pyrazole (**3al**)

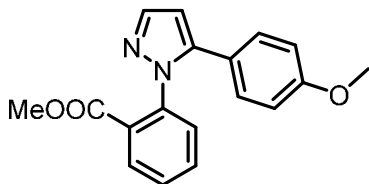


Following the general procedure D, **3al** was isolated by flash chromatography on silica (gradient: pentane/EtOAc, from 9:1 to 8:2) as an orange gum (65.4 mg, 50% yield). ¹H NMR (300 MHz, CDCl₃, ppm): δ = 7.81 (d, J = 1.83 Hz, 1H), 7.40 (s, 2H), 7.16 (m, 2H), 6.82 (m, 2H), 6.50 (d, J = 1.86 Hz, 1H), 3.78 (s, 3H).

¹³C NMR (75 MHz, CDCl₃, ppm): δ = 159.6, 145.47, 141.5, 135.9, 135.8, 129.1, 128.7, 121.9, 114.3, 105.9, 55.2.

HRMS (ESI): m/z = calcd. for C₁₆H₁₂Cl₃N₂O [M-H]⁺: 353.0015, found: 353.0025.

Methyl-2-(5-(4-methoxyphenyl)-1H-pyrazol-1-yl) benzoate (**3am**)



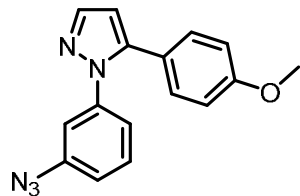
Following the general procedure D, **3am** was isolated by flash chromatography on silica (gradient: pentane/EtOAc, from 9:1 to 8:2) as a yellow gum (76.5 mg, 67% yield). ¹H NMR (400 MHz, CDCl₃, ppm): δ 7.85 (dd, J = 7.7, 1.6 Hz, 1H), 7.70 (d, J = 1.8 Hz, 1H), 7.50 (dt, J = 7.7, 1.7 Hz, 1H), 7.43 (dt, J = 7.6, 1.3 Hz, 1H), 7.30 (dd, J = 7.8, 1.2 Hz, 1H), 7.10 (d, J = 8.7 Hz, 2H), 6.77 (d, J = 8.7 Hz, 2H),

6.45 (d, J = 1.9 Hz, 1H), 3.76 (s, 3H), 3.63 (s, 3H).

¹³C NMR (100 MHz, CDCl₃, ppm): δ 166.1, 159.5, 144.1, 140.2, 139.6, 132.2, 130.7, 132.6, 130.7, 129.8, 128.7, 128.4, 122.5, 113.9, 106.2, 55.4, 52.2.

HRMS (ESI): m/z = calcd. for $C_{18}H_{17}N_2O_3$ $[M-H]^+$: 309.1234, found: 309.1234.

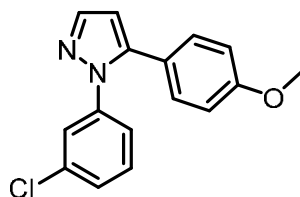
1-(2-Azidophenyl)-5-(4-methoxyphenyl)-1H-pyrazole (3an)



Following the general procedure D, **3an** was isolated by flash chromatography on silica (gradient: pentane/EtOAc, from 9:1 to 8:2) as a white solid (62.3 mg, 58% yield). **¹H NMR** (300 MHz, $CDCl_3$, ppm): δ = 7.75 (d, J = 1.9 Hz, 1H), 7.42 (dt, J = 7.7, 1.6 Hz, 1H), 7.36-7.30 (m, 1H), 7.21-7.14 (m, 2H), 7.13 (d, J = 8.9 Hz, 2H), 6.79 (d, J = 8.9 Hz, 2H), 6.50 (d, J = 1.9 Hz, 1H), 3.84 (s, 3H). **¹³C NMR** (75 MHz, $CDCl_3$, ppm): δ = 159.6, 145.0, 140.8, 137.2, 131.7, 130.3, 129.9, 129.4, 125.3, 122.6, 119.8, 114.0, 106.0, 55.4.

HRMS (ESI): m/z = calcd. for $C_{16}H_{14}N_5O$ $[M-H]^+$: 292.1198, found: 292.1209.

1-(3-chlorophenyl)-5-(4-methoxyphenyl)-1H-pyrazole (3ao)

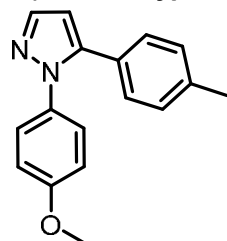


Following the general procedure D, **3ao** was isolated by flash chromatography on silica (gradient: pentane/EtOAc, from 9:1 to 8:2) as a yellow solid (61.1 mg, 58% yield). **¹H NMR** (400 MHz, $CDCl_3$, ppm): δ = 7.70 (d, J = 1.8 Hz, 1H), 7.43 (t, J = 1.8 Hz, 1H), 7.08-7.28 (m, 4H), 6.85 (d, J = 8.9 Hz, 2H), 6.44 (d, J = 1.8 Hz, 1H), 3.81 (s, 3H), 2.35 (s, 3H).

¹³C NMR (100 MHz, $CDCl_3$, ppm): δ = 159.8, 143.1, 141.1, 140.6, 134.6, 130.1, 129.8, 127.5, 125.3, 123.2, 122.5, 114.1, 107.9, 55.3.

GC-MS (EI) m/z (relative intensity): 284 (53) $[M^+]$, 111 (53), 102 (45), 89 (40), 76 (41), 75 (100), 62 (55), 51 (30).

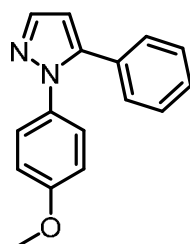
1-(4-methoxyphenyl)-5-(*p*-tolyl)-1H-pyrazole (3ba)



Following the general procedure D, **3ba** was isolated by flash chromatography on silica (gradient: pentane/EtOAc, from 9:1 to 8:2) as a white solid (50.7 mg, 52% yield). **¹H NMR** (300 MHz, $CDCl_3$, ppm) δ : 7.68 (d, J = 1.8 Hz, 1H), 7.23-7.22 (m, 2H), 7.11-7.10 (m, 4H), 6.86-6.84 (m, 2H), 6.46 (d, J = 1.8 Hz, 1H), 3.81 (s, 3H), 2.34 (s, 3H).

Spectral data were consistent with literature²⁹

1-(4-methoxyphenyl)-5-phenyl-1H-pyrazole (3ca)

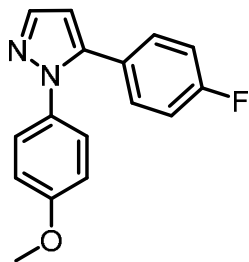


Following the general procedure D, **3ca** was isolated by flash chromatography on silica (gradient: pentane/EtOAc, from 9:1 to 8:2) as a white solid (33.1 mg, 36% yield). **¹H NMR** (300 MHz, $CDCl_3$, ppm) δ : 7.61 (d, J = 1.8 Hz, 1H), 7.24-7.21 (m, 7H), 6.80-6.76 (m, 2H), 6.42 (d, J = 1.9 Hz, 1H), 3.73 (s, 3H).

¹³C NMR (100 MHz, $CDCl_3$, ppm) δ : 158.9, 143.0, 140.0, 133.6, 130.8, 128.8, 128.5, 128.2, 126.7, 114.2, 107.4, 55.6.

Spectral data were consistent with literature²⁹

5-(4-fluorophenyl)-1-(4-methoxyphenyl)-1H-pyrazole (**3da**)

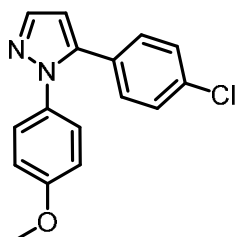


Following the general procedure D, **3da** was isolated by flash chromatography on silica (gradient: pentane/EtOAc, from 9:1 to 8:2) as a yellowish solid (25.6 mg, 26% yield). **¹H NMR** (300 MHz, CDCl₃, ppm) δ: 7.68 (d, *J* = 1.9 Hz, 1H), 7.26–7.16 (m, 4H), 7.02–6.95 (m, 2H), 6.88–6.83 (m, 2H), 6.46 (d, *J* = 1.9 Hz, 1H), 3.81 (s, 3H). **¹³C NMR** (100 MHz, CDCl₃, ppm): δ = 162.5 (d, *J* = 241.5 Hz), 158.9, 141.9, 139.9, 133.2, 130.5 (d, *J* = 8.7 Hz), 126.8 (d, *J* = 3.4 Hz), 126.7, 115.7 (d, *J* = 22.1 Hz), 114.1, 107.2, 55.5. **¹⁹F NMR** (376.5 MHz, CDCl₃, ppm) δ: -113.12 (m, 1F)

HRMS (ESI): *m/z* = calcd. for C₁₆H₁₄FN₂O [M-H]⁺: 269.1090, found: 269.1110.

m.p.: 78-80 °C

5-(4-chlorophenyl)-1-(4-methoxyphenyl)-1H-pyrazole (**3ea**)



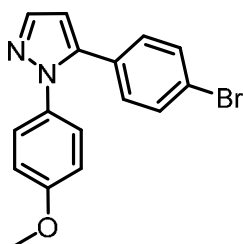
Following the general procedure D, **3ea** was isolated by flash chromatography on silica (gradient: pentane/EtOAc, from 9:1 to 8:2) as a yellow solid (28.5 mg, 27% yield). **¹H NMR** (300 MHz, CDCl₃, ppm) δ: 7.61 (d, *J* = 1.9 Hz, 1H), 7.21–7.06 (m, 6H), 6.79 (d, *J* = 8.9 Hz, 2H), 6.41 (d, *J* = 1.9 Hz, 1H), 3.74 (s, 3H).

¹³C NMR (100 MHz, CDCl₃, ppm) δ: 159.1, 141.9, 140.1, 134.3, 133.2, 130.0, 129.2, 128.8, 126.8, 114.3, 107.5, 60.5, 55.6.

HRMS (ESI): *m/z* = calcd. for C₁₆H₁₄ClN₂O [M-H]⁺: 285.0789, found: 285.0775.

m.p.: 103-105 °C

5-(4-bromophenyl)-1-(4-methoxyphenyl)-1H-pyrazole (**3fa**)

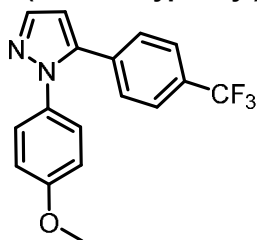


Following the general procedure D, **3fa** was isolated by flash chromatography on silica (gradient: pentane/EtOAc, from 9:1 to 8:2) as a yellow solid (11.0 mg, 9% yield). **¹H NMR** (300 MHz, CDCl₃, ppm) δ: 7.68 (d, *J* = 1.9 Hz, 1H), 7.45–7.40 (m, 2H), 7.22–7.17 (m, 2H), 7.11–7.07 (m, 2H), 6.90–6.84 (m, 2H), 6.49 (d, *J* = 1.9 Hz, 1H), 3.82 (s, 3H). **¹³C NMR** (100 MHz, CDCl₃, ppm) δ: 159.1, 141.9, 140.2, 131.8, 130.3, 129.7, 126.8, 122.5, 114.4, 107.5, 55.6.

HRMS (ESI): *m/z* = calcd. for C₁₆H₁₄BrN₂O [M-H]⁺: 329.0290, found: 329.0291.

m.p.: 107-110 °C

1-(4-methoxyphenyl)-5-(4-(trifluoromethyl) phenyl)-1H-pyrazole (**3ga**)



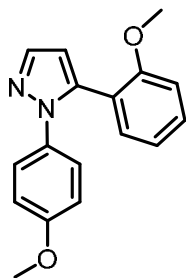
Following the general procedure D, **3ga** was isolated by flash chromatography on silica (gradient: pentane/EtOAc, from 9:1 to 8:2) as a yellow solid (9.5 mg, 8% yield). **¹H NMR** (300 MHz, CDCl₃, ppm): δ = 7.71 (d, *J* = 1.8 Hz, 1H), 7.57–7.54 (m, 2H), 7.39–7.32 (m, 2H), 7.23–7.18 (m, 2H), 6.91–6.85 (m, 2H), 6.55 (d, *J* = 1.8 Hz, 1H), 3.83 (s, 3H).

¹³C NMR (75 MHz, CDCl₃, ppm): δ = 160.0, 143.1, 143.3, 141.5, 132.9, 130.1, 124.9, 122.3, 118.3, 114.3, 110.4, 108.9, 55.4. **HRMS (ESI):** *m/z* = calcd. for

C₁₇H₁₄F₃N₂O [M-H]⁺: 319.1058, found: 319.1061.

Spectral data were consistent with literature²⁹

5-(2-methoxyphenyl)-1-(4-methoxyphenyl)-1H-pyrazole (3ha)

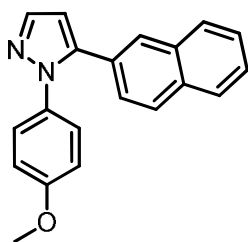


Following the general procedure D, **3ha** was isolated by flash chromatography on silica (gradient: pentane/EtOAc, from 9:1 to 8:2) as a white solid (26.0 mg, 25% yield). ¹H NMR (300 MHz, CDCl₃, ppm) δ: 7.63 (d, *J* = 1.8 Hz, 1H), 7.28–7.22 (m, 1H), 7.19–7.16 (m, 1H), 7.13–7.08 (m, 2H), 6.88 (td, *J* = 7.5, 1.1 Hz, 1H), 6.75–6.70 (m, 3H), 6.37 (d, *J* = 1.8 Hz, 1H), 3.70 (s, 3H), 3.38 (s, 3H). ¹³C NMR (75 MHz, CDCl₃, ppm) δ: 158.4, 156.7, 139.6, 134.5, 131.3, 130.2, 125.1, 120.6, 120.2, 113.6, 111.2, 108.3, 55.4, 55.0.

HRMS (ESI): *m/z* = calcd. for C₁₇H₁₇N₂O₂ [M-H]⁺: 281.1285, found: 281.1279.

m.p.: 65-68 °C

1-(4-methoxyphenyl)-5-(naphthalen-2-yl)-1H-pyrazole (3ia)

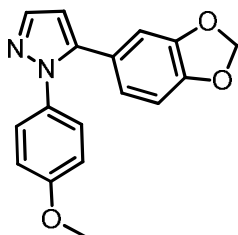


Following the general procedure D, **3ia** was isolated by flash chromatography on silica (gradient: pentane/EtOAc, from 95:5 to 9:1) as a white solid (66.6 mg, 60% yield). ¹H NMR (300 MHz, CDCl₃, ppm): δ = 7.84-7.74 (m, 5H), 7.53-7.49 (m, 2H), 7.30-7.25 (m, 3H), 6.88-6.83 (m, 2H), 6.62 (d, *J* = 1.92 Hz, 1H), 3.81 (s, 3H). ¹³C NMR (75 MHz, CDCl₃, ppm): δ = 158.8, 142.9, 140.1, 133.5, 133.1, 132.7, 128.2, 128.1, 128.0, 127.9, 127.7, 126.6, 126.5, 126.3, 114.1, 107.7, 55.5.

HRMS (ESI): *m/z* = calcd. for C₂₀H₁₇N₂O [M-H]⁺: 301.1341, found: 301.1333.

m.p.: 111-114 °C

5-(benzo[d][1,3]dioxol-5-yl)-1-(4-methoxyphenyl)-1H-pyrazole (3ja)

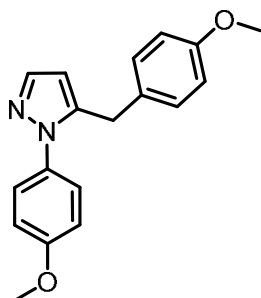


Following the general procedure D, **3ja** was isolated by flash chromatography on silica (gradient: pentane/EtOAc, from 9:1 to 8:2) as a white solid (64.2 mg, 59% yield). ¹H NMR (300 MHz, CDCl₃, ppm): δ = 7.65 (d, *J* = 1.94 Hz, 1H), 7.24-7.21 (m, 2H), 6.88-6.85 (m, 2H), 6.76-6.68 (m, 3H), 6.41 (d, *J* = 1.92 Hz, 1H), 5.96 (s, 2H), 3.82 (s, 3H). ¹³C NMR (75 MHz, CDCl₃, ppm): δ = 158.8, 142.9, 140.1, 133.5, 133.1, 132.7, 128.2, 128.1, 128.0, 127.9, 127.7, 126.6, 126.5, 126.3, 114.1, 107.7, 55.5.

HRMS (ESI): *m/z* = calcd. for C₁₇H₁₅N₂O₃ [M-H]⁺: 295.1083, found: 295.1074.

m.p.: 85-88 °C

5-(4-methoxybenzyl)-1-(4-methoxyphenyl)-1H-pyrazole (3ka)

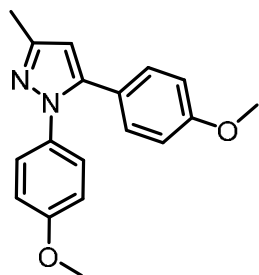


Following the general procedure D, **3ka** was isolated by flash chromatography on silica (gradient: pentane/EtOAc, from 9:1 to 8:2) as an orange gum (27.4 mg, 25% yield). ¹H NMR (300 MHz, CDCl₃, ppm) δ: 7.49 (d, *J* = 1.8 Hz, 1H), 7.20–7.17 (m, 2H), 6.95–6.90 (m, 2H), 6.87–6.82 (m, 2H), 6.75–6.70 (m, 2H), 3.82 (s, 2H), 3.76 (s, 3H), 3.70 (s, 3H).

¹³C NMR (100 MHz, CDCl₃, ppm) δ: 159.2, 158.3, 142.5, 139.5, 132.9, 130.3, 129.5, 126.9, 114.1, 113.9, 106.5, 55.5, 55.3.

HRMS (ESI): *m/z* = calcd. for C₁₈H₁₉N₂O₂ [M-H]⁺: 295.1447, found: 295.1444.

1,5-bis(4-methoxyphenyl)-3-methyl-1H-pyrazole (3la)

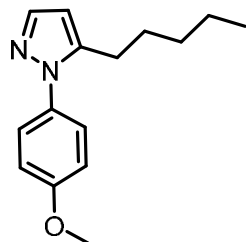


Following the general procedure D, **3la** was isolated by flash chromatography on silica (gradient: pentane/EtOAc, from 9:1 to 8:2) as a white solid (98.1 mg, 90% yield). ¹H NMR (300 MHz, CDCl₃, ppm): δ = 7.20-7.11 (m, 4H), 6.84-6.79 (m, 4H), 6.22 (s, 1H), 3.79 (s, 3H), 3.77 (s, 3H), 2.36 (s, 3H). ¹³C NMR (75 MHz, CDCl₃, ppm): δ = 159.3, 158.5, 148.9, 143.5, 133.6, 129.8, 126.6, 123.2, 114.0, 113.8, 106.6, 55.4, 55.2, 13.6.

HRMS (ESI): m/z = calcd. for C₁₈H₁₉N₂O₂ [M-H]⁺: 295.1441, found: 295.1449.

m.p.: 85-89°C

1-(4-methoxyphenyl)-5-pentyl-1H-pyrazole (3ma)

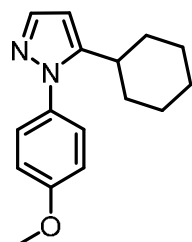


Following the general procedure D, **3ma** was isolated by flash chromatography on silica (gradient: pentane/EtOAc, from 9:1 to 8:2) as a yellowish oil (22.7 mg, 25% yield). ¹H NMR (300 MHz, CDCl₃, ppm) δ: 7.55(d, J = 1.8 Hz, 1H), 7.35-7.28 (m, 2H), 7.01-6.93 (m, 2H), 6.17 (d, J = 1.8 Hz, 1H), 3.85 (s, 3H), 2.61-2.55 (m, 2H), 1.59-1.54 (m, 2H), 1.30-1.22 (m, 4H), 0.87-0.83 (m, 3H).

¹³C NMR (75 MHz, CDCl₃, ppm): δ = 159.1, 143.9, 139.4, 133.5, 126.9, 114.2, 104.8, 55.5, 31.4, 29.7, 28.5, 26.1, 22.3, 13.9.

HRMS (ESI): m/z = calcd. for C₁₅H₂₀N₂O [M-H]⁺: 245.1654, found: 245.1662.

1-(4-methoxyphenyl)-5-cyclohexyl-1H-pyrazole (3na)

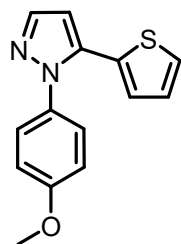


Following the general procedure D, **3na** was isolated by flash chromatography on silica (gradient: pentane/EtOAc, from 9:1 to 8:2) as a white solid (11.5 mg, 12% yield). ¹H NMR (300 MHz, CDCl₃, ppm) δ: 7.55 (d, J = 1.9 Hz, 1H), 7.33-7.26 (m, 2H), 7.00-6.95 (m, 2H), 6.17 (d, J = 1.9 Hz, 1H), 3.86 (s, 3H), 2.59 (tt, J = 11.7, 3.4 Hz, 1H), 1.94-1.65 (m, 7H), 1.42-1.17 (m, 10H), 0.90-0.83 (m, 1H). ¹³C NMR (100 MHz, CDCl₃, ppm) δ: 159.4, 149.6, 139.6, 133.2, 127.3, 114.3, 103.0, 55.7, 35.3, 33.6, 29.9, 26.4, 26.0.

HRMS (ESI): m/z = calcd. for C₁₆H₂₁N₂O [M-H]⁺: 257.1654, found: 257.1654.

m.p.: 53-55°C

1-(4-methoxyphenyl)-5-(thiophen-2-yl)-1H-pyrazole (3oa)

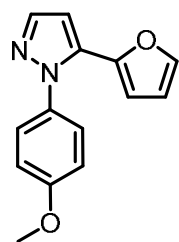


Following the general procedure D, **3oa** was isolated by flash chromatography on silica (gradient: pentane/EtOAc, from 9:1 to 8:2) as a dark yellow solid (20.9 mg, 22% yield). ¹H NMR (300 MHz, CDCl₃, ppm) δ: 7.65 (d, J = 1.9 Hz, 1H), 7.33-7.28 (m, 2H), 7.25 (dd, J = 5.1, 1.2 Hz, 1H), 6.95-6.93 (m, 2H), 6.92-6.90 (m, 1H), 6.83 (dd, J = 3.6 Hz, 1.2 Hz, 1H), 6.55 (d, J = 1.9 Hz, 1H), 3.95 (s, 3H). ¹³C NMR (100 MHz, CDCl₃, ppm) δ: 159.7, 139.9, 137.1, 132.9, 131.6, 127.7, 127.5, 127.3, 126.9, 126.3, 123.6, 114.2, 106.9, 55.5.

HRMS (ESI): m/z = calcd. for C₁₄H₁₃N₂OS [M-H]⁺: 257.0749, found: 257.0753.

m.p.: 81-87 °C

5-(furan-2-yl)-1-(4-methoxyphenyl)-1H-pyrazole (3pa)

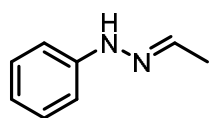


Following the general procedure D, **3pa** was isolated by flash chromatography on silica (gradient: pentane/EtOAc, from 9:1 to 8:2) as a yellow gum (17.9 mg, 20% yield).

¹H NMR (300 MHz, CDCl₃, ppm): δ = 7.65 (d, J = 1.8 Hz, 1H), 7.38 (dd, J = 1.8, 0.7 Hz, 1H), 7.34-7.30 (m, 2H), 6.97-6.93 (m, 2H), 6.65 (d, J = 1.8 Hz, 1H), 6.31 (dd, J = 3.4, 1.8 Hz, 1H), 5.88 (dd, J = 3.5, 0.7 Hz, 1H), 3.86 (s, 3H).

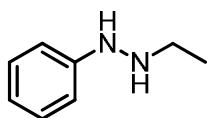
¹³C NMR (75 MHz, CDCl₃, ppm): δ = 159.6, 144.7, 142.4, 139.9, 134.6, 133.3, 127.4, 114.2, 111.2, 108.4, 105.4, 55.6. **HRMS (ESI)**: m/z = calcd. for C₁₄H₁₃N₂O₂ [M-H]⁺: 241.0972, found: 241.0974.

Acetaldehyde phenylhydrazone (S1)



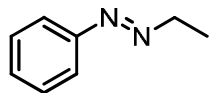
Acetaldehyde (7.6 mL, 6.0 g, 0.14 mol) was dissolved in aqueous ethanol, prepared by mixing ethanol (24 mL) and water (4 mL), and the reaction mixture was placed in ice-water cooling bath. Phenylhydrazine (10.9 mL, 12.0 g, 0.11 mol) was added in portions. Evolution of heat was observed after addition of each portion, and reaction mixture was let to cool before adding further phenylhydrazine to the reaction. After addition was finished, crystallization of product occurred, and after stirring the reaction mixture for further 1 h, crystals were filtered off and washed with small amount of aqueous ethanol. Product was obtained as oil, which solidified on standing at room temperature (8.6 g, 58%), that was according to NMR analysis a mixture of *E*- and *Z*- isomers. Solid was used without further separation in the next step.

2-ethyl-1-phenylhydrazine (S2)



Dry, argon flushed, flask was charged with lithium aluminum hydride (1.14 g, 30 mmol), to which dry THF (20 mL) was added, and the reaction mixture was stirred for 10 min under argon. Reaction mixture was then cooled to 5 °C by an ice-water cooling bath, and the solution of acetaldehyde phenylhydrazone (mixture of isomers, 4.03 g, 30 mmol) in dry THF (10 mL) was added dropwise to the well-stirred reaction mixture. After the addition was complete, the reaction was stirred for further 20 min at 5 °C, after which the cooling bath was removed. Reaction mixture was then heated up to reflux, stirred for 40 min, and then let to cool to room temperature. Flask with the reaction mixture was then placed in an ice-water cooling bath, and diethylether saturated with water (15 mL) was carefully added. The white aluminum salts were filtered off on frit and washed several times with diethylether. Combined organic fractions were concentrated on rotary evaporator, and the residue was subjected to vacuum distillation. Fraction containing the product distilled off between 74 °C – 77 °C at 3 mbar. Product was collected as colorless oil (1.4 g, 34%), that was unstable on air, and progressively darkened when stored at room temperature. **¹H NMR** (300 MHz, CDCl₃, ppm): δ 1.05 (t, *J* = 7.3 Hz, 3H), 2.83 (q, *J* = 7.1 Hz, 2H), 4.97 (bs, 2H), 6.78 (tt, *J* = 7.4 Hz, *J* = 1.1 Hz, 1H), 6.78-6.81 (m, 2H), 7.10-7.16 (m, 2 H). Spectral data were consistent with literature³²

2-ethyl-1-phenyldiazene (5)



2-ethyl-1-phenylhydrazine (108 mg, 0.78 mmol) was dissolved in 1 M aqueous sulfuric acid (3 mL) at room temperature. Iron (III) sulfate hydrate (400 mg) was added in single portion, and the reaction mixture was stirred under argon for 30 min. Iron salts dissolved over this period. The reaction mixture was extracted with diethylether (10 mL), and the organic fraction was washed with saturated aqueous sodium bicarbonate (10 mL), water (10 mL) and brine (10 mL), before it was dried over sodium sulfate. Solids were filtered off and solvent was evaporated in vacuo to obtain product (97 mg, 93%) as quickly yellowing oil. Sample was used immediately to measure cyclic voltammetry. Compound quickly deteriorates at ambient conditions, with main decomposition product being the acetaldehyde phenylhydrazone, which could be seen on the ¹H NMR spectra measured within 1 h of the synthesis of the diazene compound.

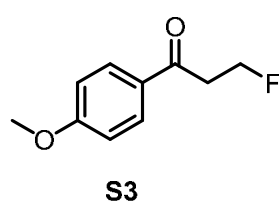
¹H NMR (300 MHz, CDCl₃, ppm): δ 1.46 (t, *J* = 7.4 Hz, 3H), 4.11 (q, *J* = 7.4 Hz, 2H), 4.97 (bs, 2H), 7.41-7.50 (m, 3H), 7.65-7.70 (m, 2 H). Spectral data were consistent with literature³⁴

2.4.3 Mechanistic experiments

Radical scavenger



A vial was charged with Ru(bpy)₃Cl₂·6H₂O (18.5 μmol, 5 mol%), 1-(4-methoxyphenyl)cyclopropane-1-ol (0.37 mmol, 1 eq.) the parent diazonium salt (0.56 mmol, 1.5 eq.), and the radical scavenger (Selectfluor, 1.85 mmol, 5.0 equiv.). The vial was sealed and subsequently MeCN (5 mL) was added, and the reaction mixture was degassed, by purging with nitrogen over 10 min in dark. Light was switched on, and the reaction mixture was stirred at r.t. over 20 min. The reaction mixture was quenched with water (3 mL) and extracted with ethyl acetate (3 x 3 mL). The organic phase was separated and dried over MgSO₄. Solids were filtered off and the volatiles were removed under reduced pressure to afford a viscous oil containing product. The crude product was purified by column chromatography on silica gel. The conversion of 1a was 56%, the yield of 3aa and S3 were respectively of 35% (35.9 mg) and 22% (15 mg). ¹H NMR (300 MHz, CDCl₃, ppm): δ 7.98-7.91 (m, 2H), 6.97-6.92 (m, 2H), 4.95 (t, *J* = 6.1 Hz, 1H), 4.83 (t, *J* = 6.1 Hz, 1H), 3.87 (s, 3H), 3.36 (t, *J* = 6.1 Hz, 1H), 3.30 (t, *J* = 6.1 Hz, 1H); ¹⁹F NMR (376 MHz, CDCl₃, ppm): δ -220.76 /-221.16 (m, 1F).³³



-220.8983
-220.9358
-220.9789
-221.0595
-221.1020
-221.1415

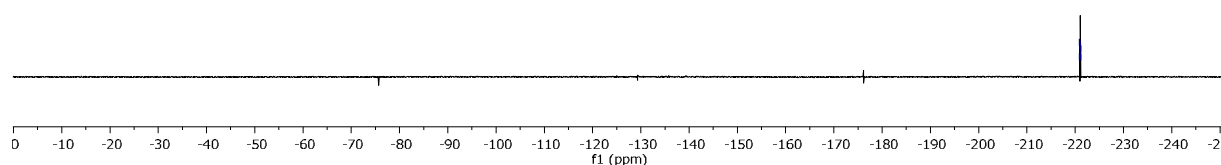
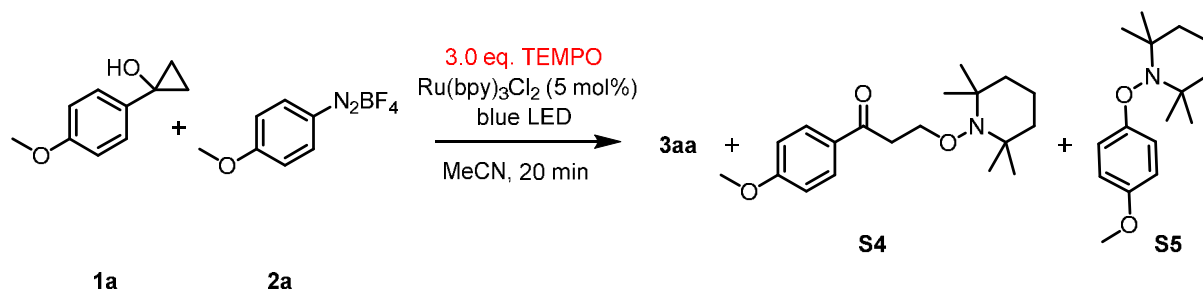
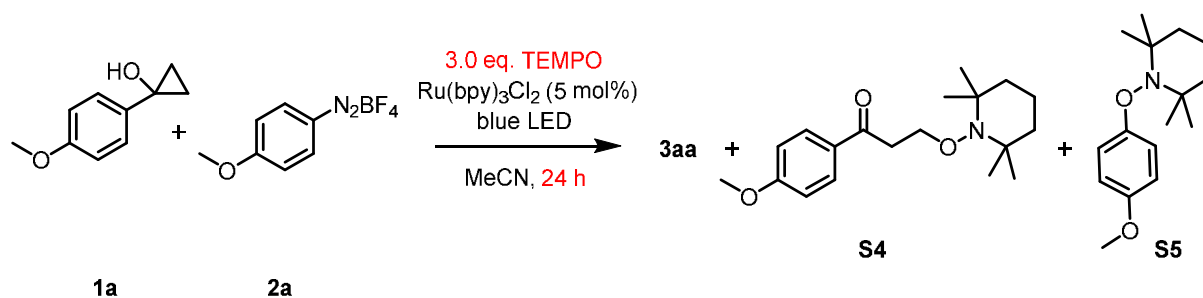


Figure 5. ¹⁹F NMR (376 MHz, CDCl₃, ppm): of 3-fluoro-1-(4-methoxyphenyl)propan-1-one isolated from the reaction with Selectfluor.



Following the same procedure as above except 2,2,6,6-tetramethylpiperidin-1-yl)oxy (TEMPO) (174.3 mg, 1.11 mmol, 3.0 eq.) was added instead of Selectfluor, the reaction afforded **3aa** < 10%, the products **S4** and **S5** were not detected by GC/MS.



Following the same procedure as above except 2,2,6,6-tetramethylpiperidin-1-yl)oxy (TEMPO) (174.3 mg, 1.11 mmol, 3.0 eq.) was added and the reaction time was extended to 24 h, the reaction afforded **3aa** < 10%, the product **S4** was not detected and **S5** was detected by GC/MS.

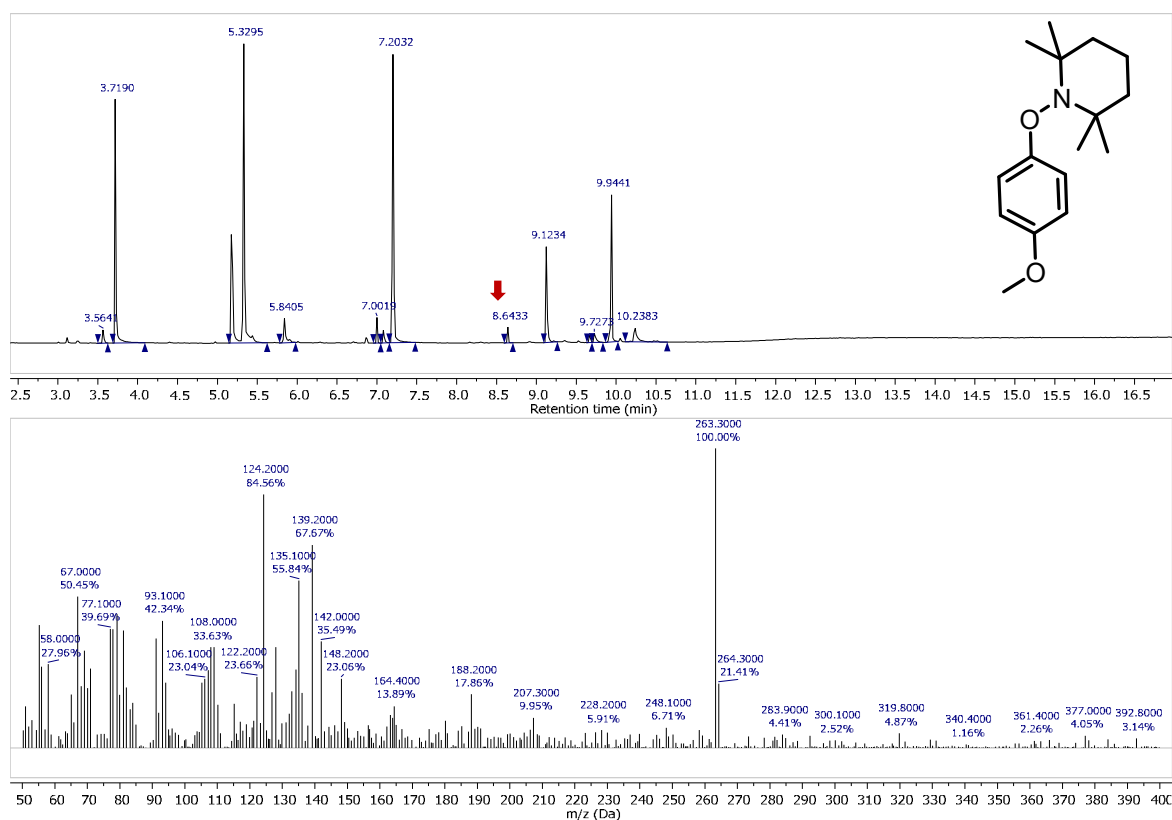


Figure 6. GC-MS of crude reaction mixture after 24 h in presence of 3.0 eq. TEMPO.

Cyclic Voltammetry

The experiments were carried out in a conventional three electrode cell using a Parstat 4000 (Ametek, Berwin, USA). A glassy carbon disc (diameter: 1.6 mm) served as the working electrode and a platinum wire as counter electrode. The glassy carbon disc was polished using polishing alumina (0.05 μm) prior to each experiment. As reference a Ag/AgNO₃ electrode (silver wire in 0.1 M NBu₄ClO₄/CH₃CN solution; c(AgNO₃) = 0.01 M; $E^0 = -87$ mV vs the ferrocene redox couple) was used and this compartment was separated from the rest of the cell with a Vycor frit. As a solvent, anhydrous acetonitrile (Sigma-Aldrich) stored over molecular sieves was used. Tetrabutylammonium hexafluorophosphate was used as a conductive salt to obtain final electrolyte concentration of 100 mmol/L. Analyzed samples were dissolved in electrolyte solution in concentrations of 1-5 mmol/l. Electrochemical cell was dried in oven prior to each experiment, flushed with argon and charged with 4 ml of electrolyte/analyte solution. The electrolyte solution containing analyte was then degassed with a stream of argon for at least five minutes prior to recording. Measurements were performed at scan rate of 100 mV/s. Thermodynamic redox potentials were approximated as the half-wave experimental potential. Redox properties of the photocatalyst in acetonitrile were taken from literature.³⁵

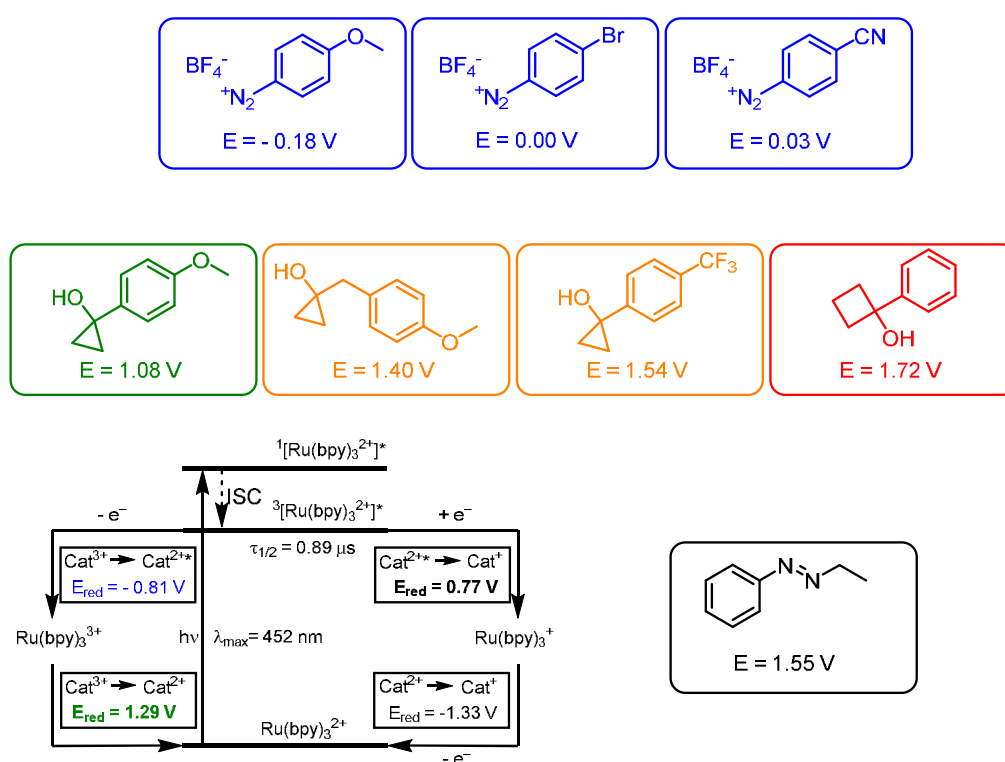
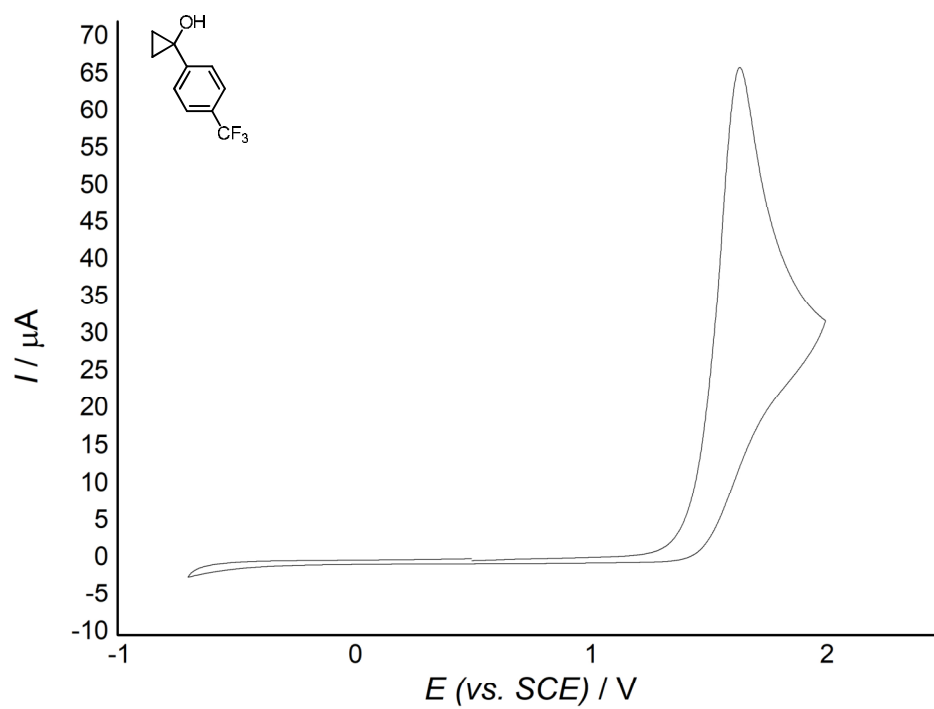
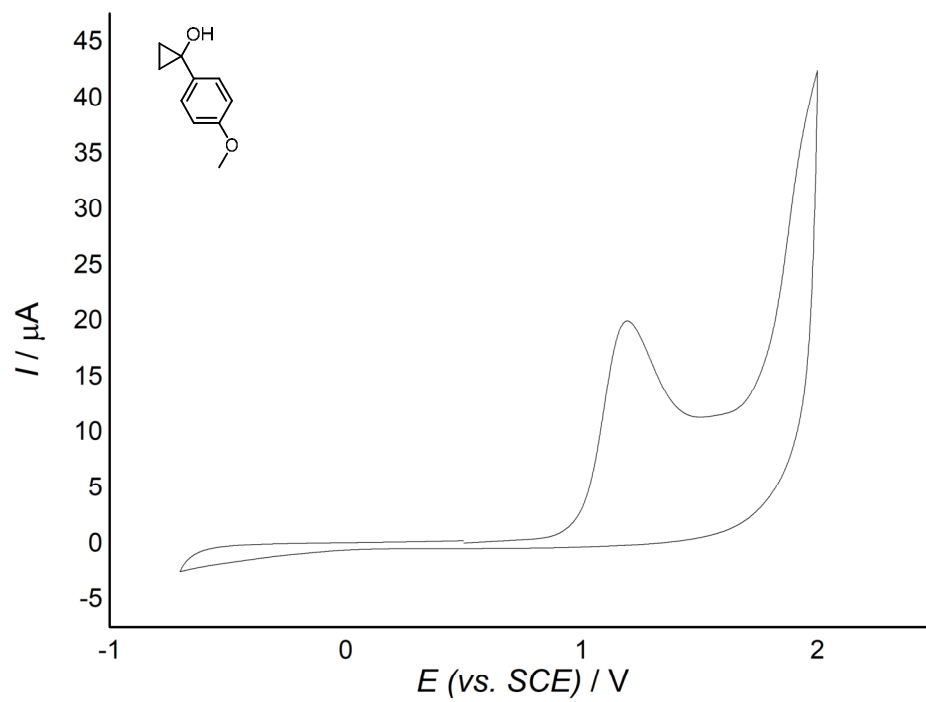
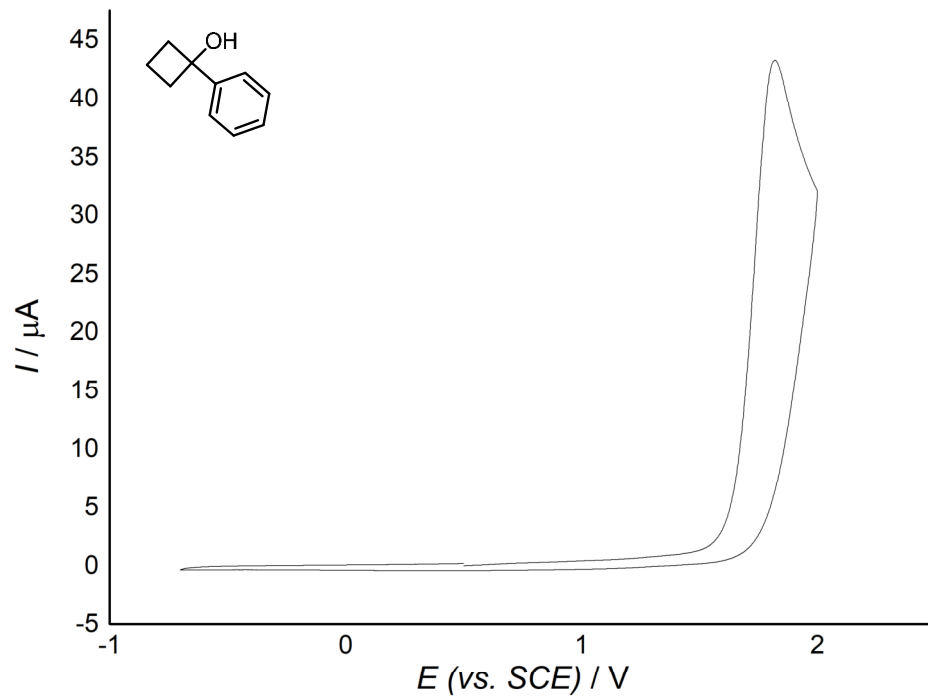
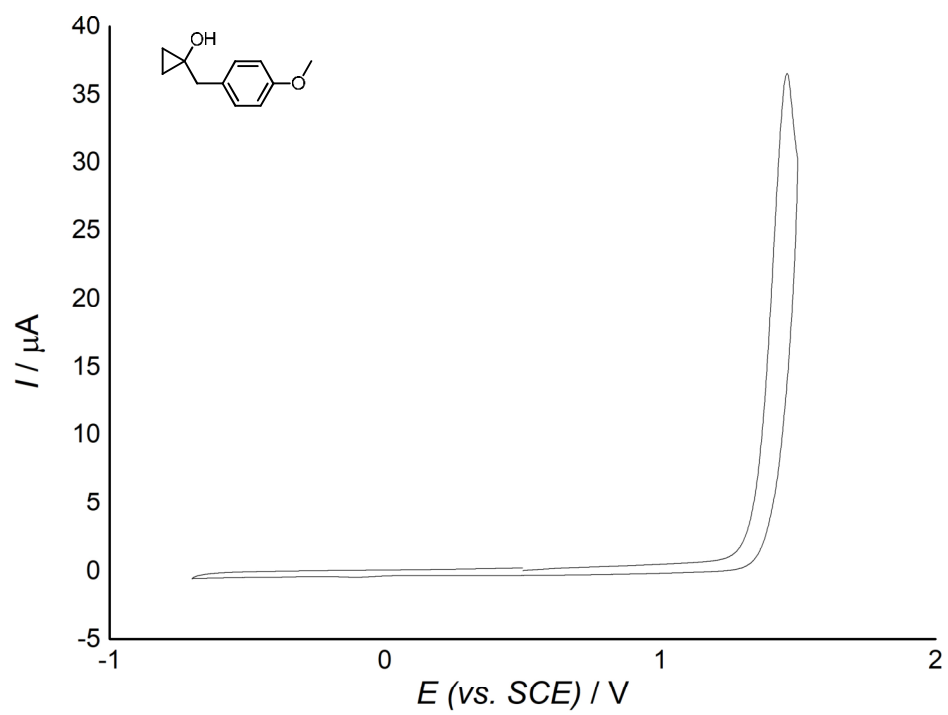
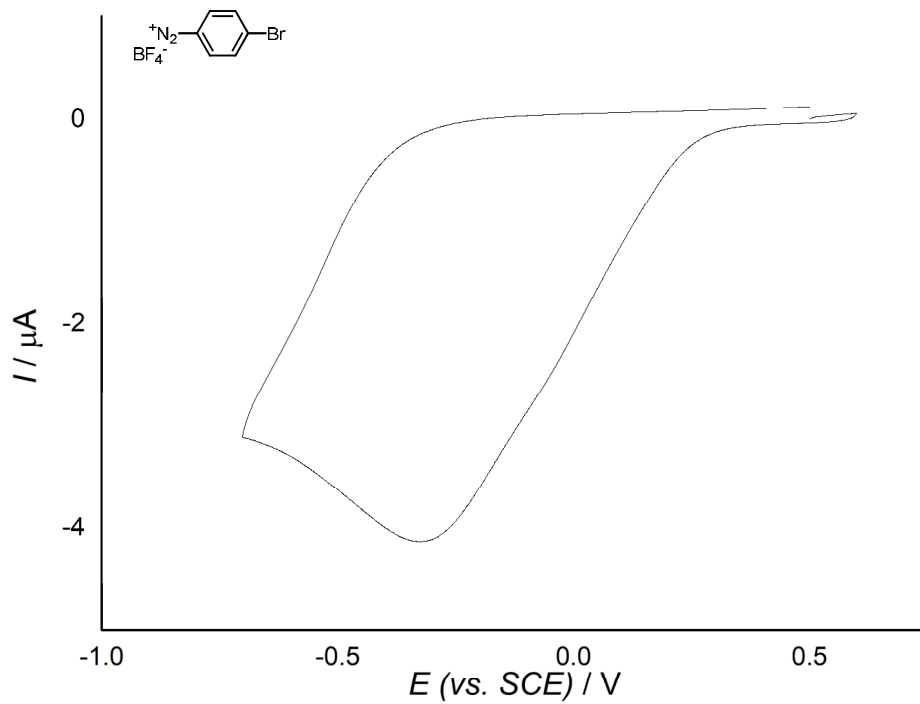
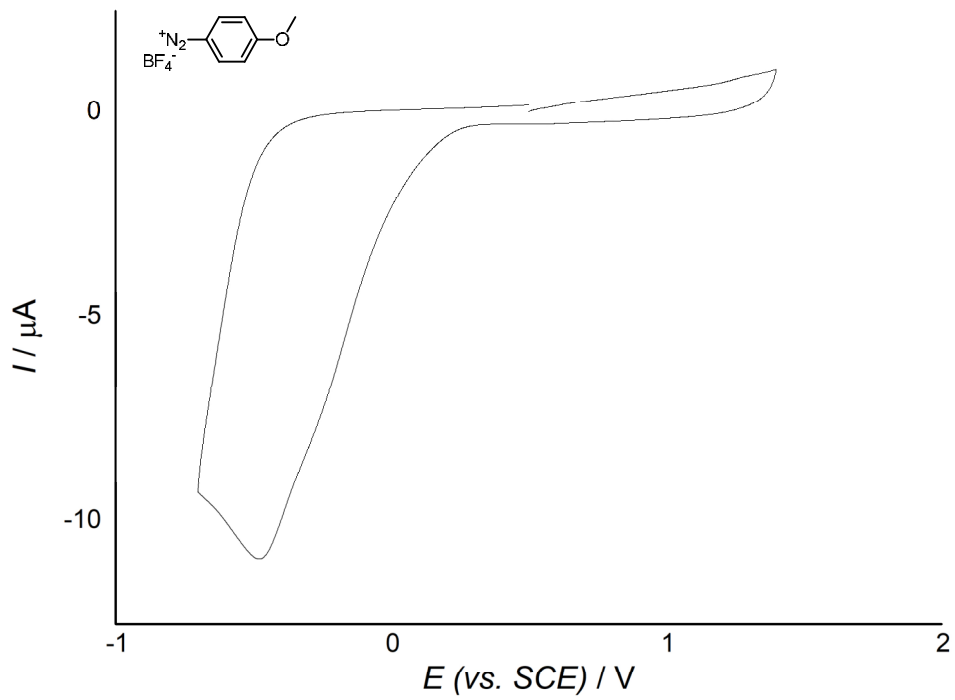


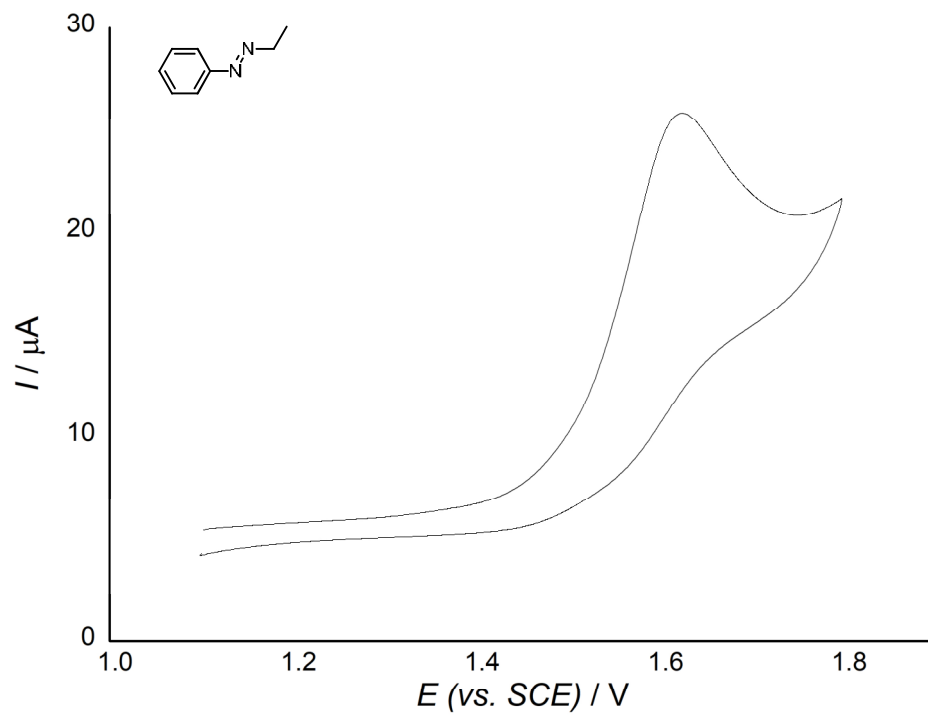
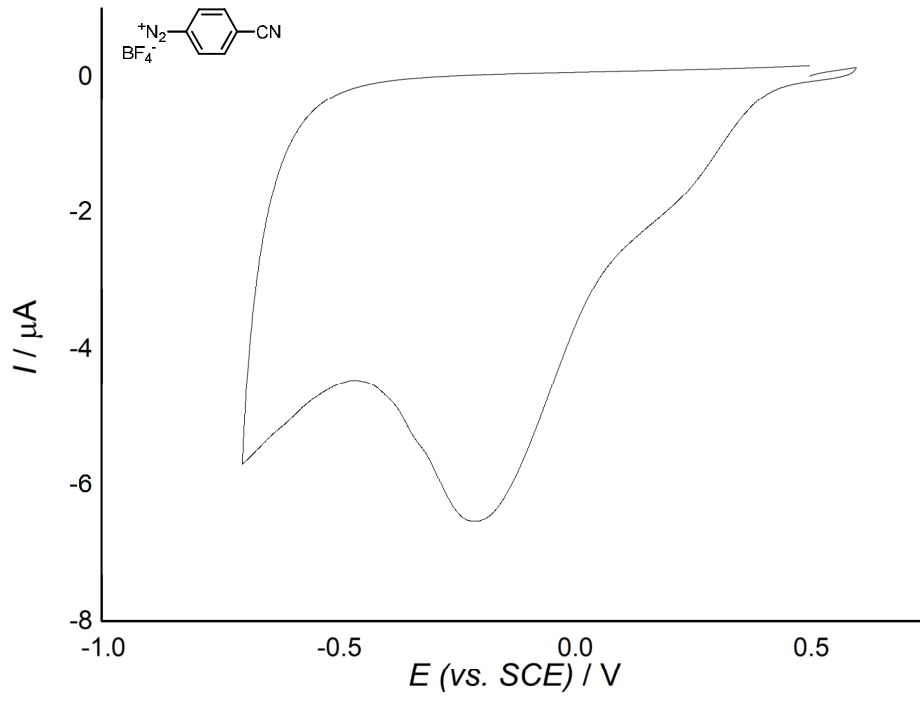
Figure 7. Reduction potentials of starting materials obtained from cyclic voltammetry, and their comparison with the redox properties of the ruthenium photocatalyst.³⁵

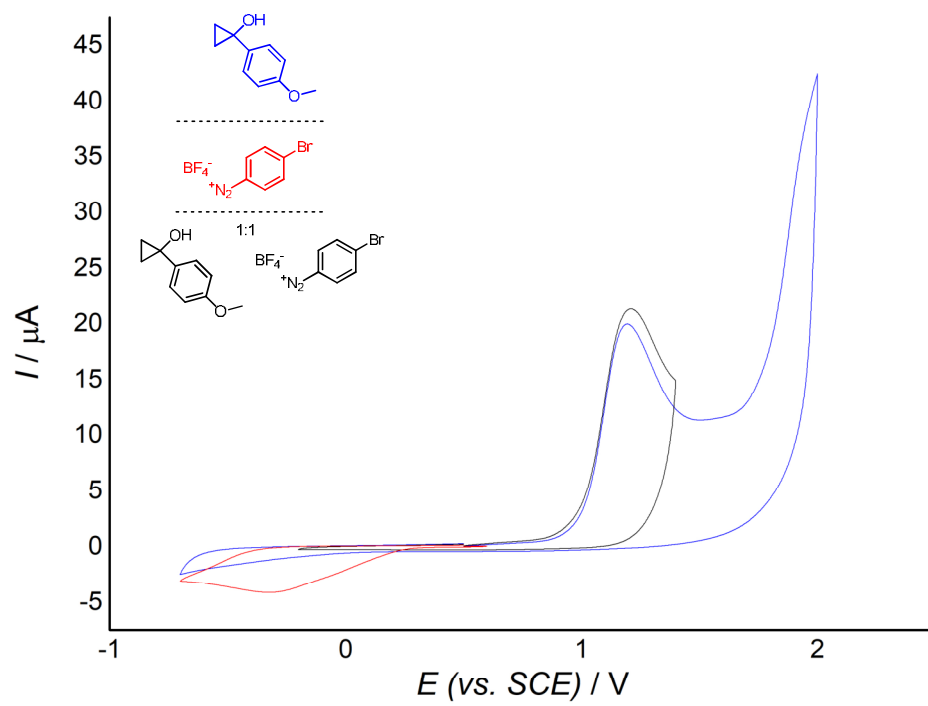
Results of the cyclic voltammetry measurements











Stern Volmer Quenching

UV/Vis absorption and fluorescence spectra were measured with a Specord 50 UV/Vis spectrophotometer (Analytic Jena) and a FluoroMax4 spectrofluorimeter (Horiba Scientific), respectively. Concentration of Ru(bpy)₃Cl₂ was chosen such, that the absorbance at the excitation wavelength, 450 nm, did not exceed 0.1 absorbance units. Both excitation as well as emission slits were 5 nm wide. Emission spectra were recorded in the region 480 nm – 860 nm. Emission values were corrected taking into account the wavelength dependence of detector, and the internal filter effect of the quencher, where applicable. Corrected emission spectra were integrated, and the integral values were used to estimate the quenching constant K_{SV} using the Stern-Volmer equation³⁶:

$$\frac{I_0}{I} - 1 = K_{SV} \cdot c(Q)$$

where I_0 and I is the total intensity of the fluorescence in the absence of quencher, and in the presence of quencher in concentration $c(Q)$, respectively. It should be noted, that constant K_{SV} is derived from the life-time of the quenched excited species τ and from the rate constant of the bimolecular quenching k ³⁶:

$$K_{SV} = \tau \cdot k$$

When both quencher and the quenched excited species are charged, reaction rate is no longer constant with respect to quencher, as it is dependent on the total ionic strength of the solution, behavior known as kinetic salt effect.³⁷ To take this into account, we can use the Brønsted-Bjerrum equation³⁸ derived from the Debye-Hückel extended theory:

$$\ln(k) = \ln(k_0) + \frac{e^3 \cdot \sqrt{N_A}}{4 \cdot \pi \cdot \sqrt{2 \cdot (\epsilon_r \cdot \epsilon_0 \cdot k_B \cdot T)^3}} \cdot \sqrt{1000} \cdot z_a \cdot z_b \cdot \frac{2 \cdot \sqrt{I}}{1 + B \cdot \sqrt{I}} = \ln(k_0) + A \cdot z_a \cdot z_b \cdot \frac{2 \cdot \sqrt{I}}{1 + B \cdot \sqrt{I}}$$

where e is the elementary charge; N_A is the Avogadro's number; ϵ_r is the relative permittivity of the solvent; ϵ_0 is the permittivity of vacuum; k_B is the Boltzmann's constant; T is the thermodynamic temperature; z_A and z_B are the charges of the quencher and the quenched molecule and I is the ionic strength (using mol/dm³ units). Factor $\sqrt{1000}$ comes from the unit conversion of ionic strength (from mol/m³ to the usual mol/dm³). k_0 and k are quenching rates at ionic strengths of zero and I , respectively. Constant B is dependent on the size of the interacting species, but can be approximated in most cases as unity without any significant error.³⁸ For acetonitrile we can calculate, that $A = 3.351$ at 300 K. Using this equation, we can write the following for Stern-Volmer quenching:

$$\ln(K_{SV}) = \ln(\tau) + \ln(k) = \ln(\tau) + \ln(k_0) + A \cdot z_a \cdot z_b \cdot \frac{2 \cdot \sqrt{I}}{1 + B \cdot \sqrt{I}} = \ln(K_{SV0}) + A \cdot z_a \cdot z_b \cdot \frac{2 \cdot \sqrt{I}}{1 + B \cdot \sqrt{I}}$$

where K_{SV0} is the Stern-Volmer quenching constant at zero ionic strength. Furthermore:

$$\ln\left(\frac{I_0}{I} - 1\right) = \ln(K_{SV}) + \ln[c(Q)] = \ln[c(Q)] + \ln(K_{SV0}) + A \cdot z_a \cdot z_b \cdot \frac{2 \cdot \sqrt{I}}{1 + B \cdot \sqrt{I}}$$

$$Q = \ln\left(\frac{I_0}{I} - 1\right) - A \cdot z_a \cdot z_b \cdot \frac{2 \cdot \sqrt{I}}{1 + B \cdot \sqrt{I}} = \ln[c(Q)] + \ln(K_{SV0})$$

By plotting quantity Q (vide supra) against natural logarithm of quencher concentration, we can obtain K_{SV0} – the Stern-Volmer quenching constant at zero ionic strength even for charged pair quencher-luminescent dye, which occurs in our case – diazonium salts and Ru(bpy)₃²⁺.

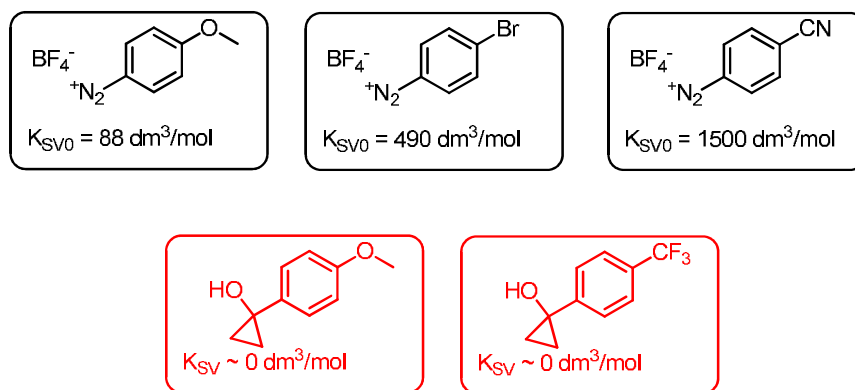


Figure 8. Stern-Volmer quenching constants of excited $\text{Ru}(\text{bpy})_3^{2+}$ with substrates.

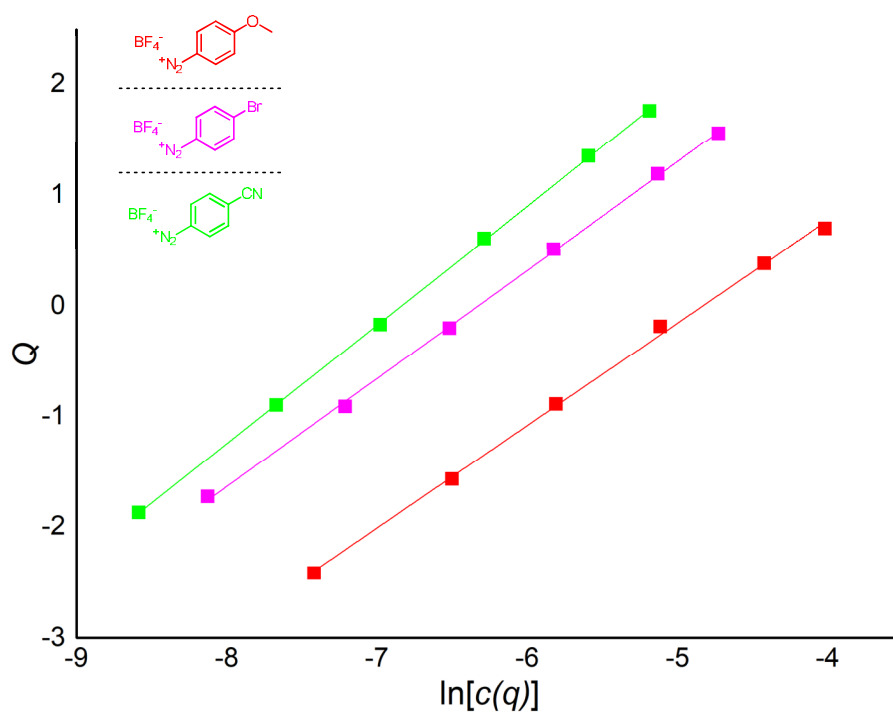
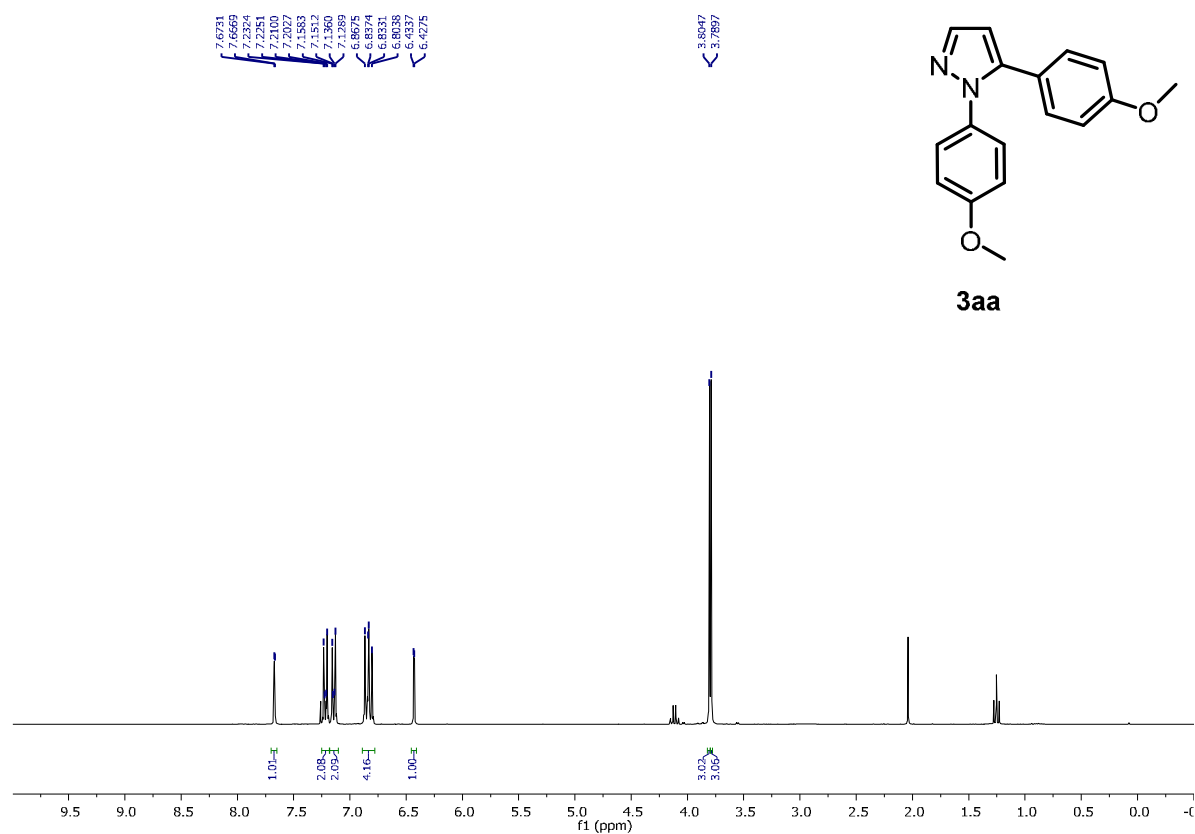
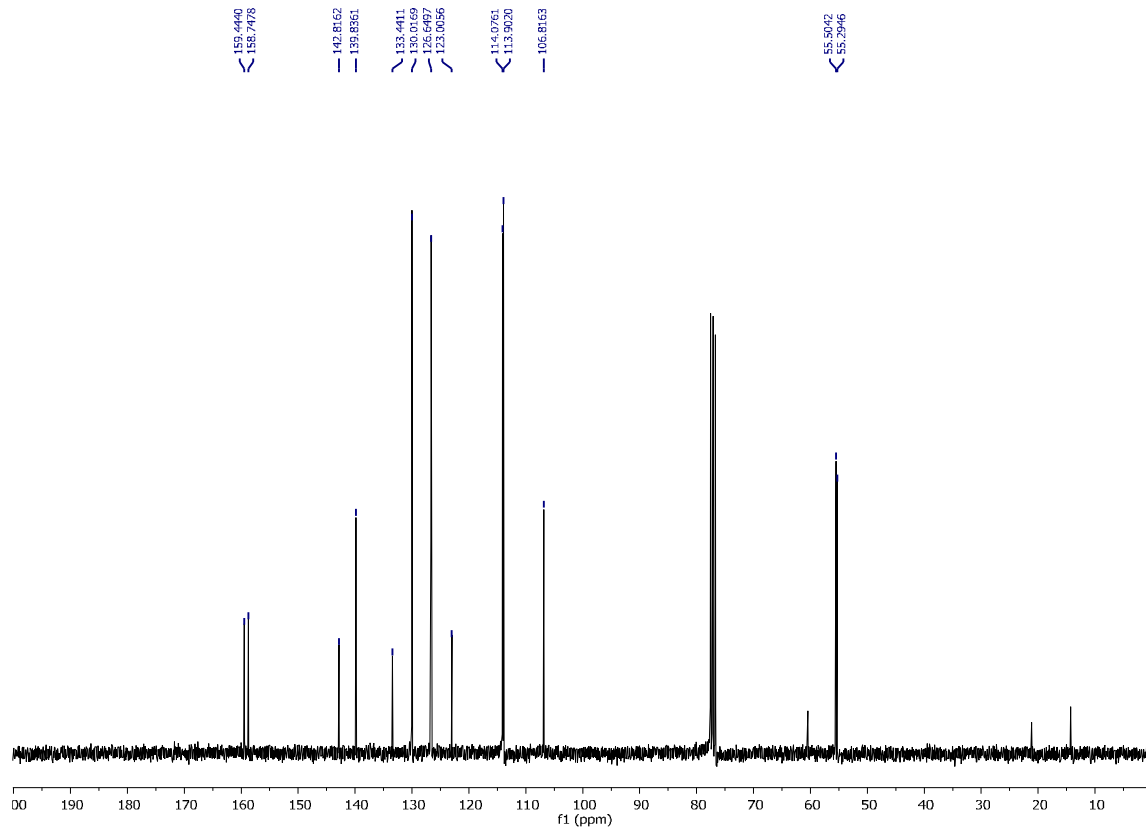


Figure 9. Modified Stern-Volmer plot of diazonium salt quenching of $\text{Ru}(\text{bpy})_3^{2+}$ luminescence.

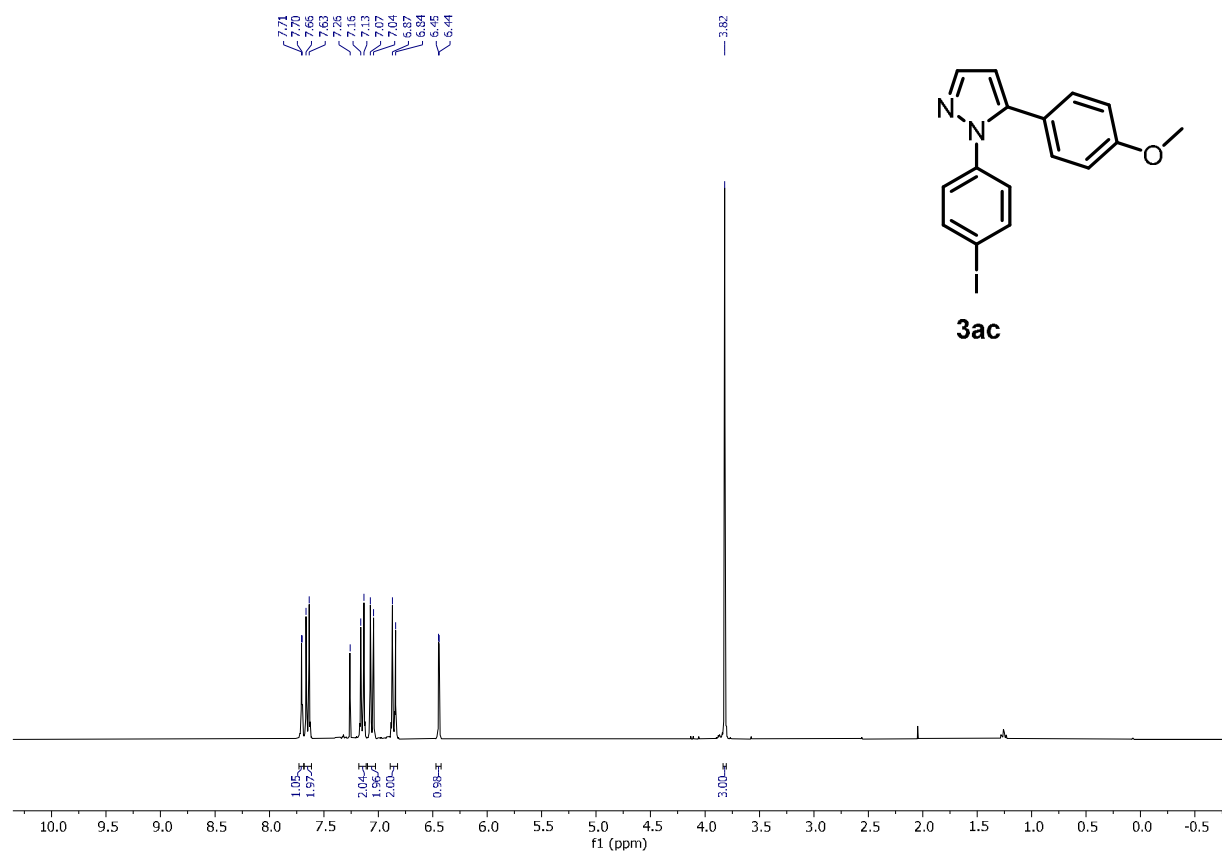
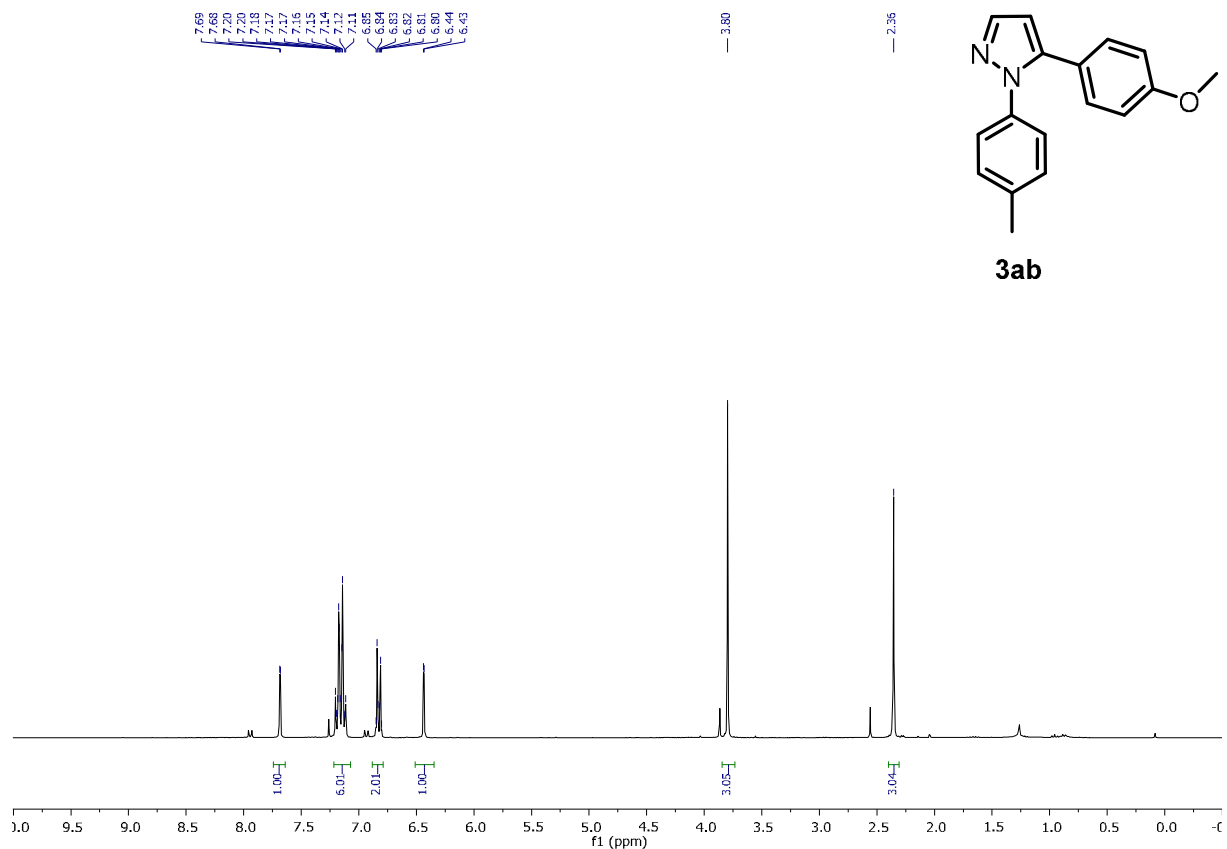
2.4.4 NMR of compounds



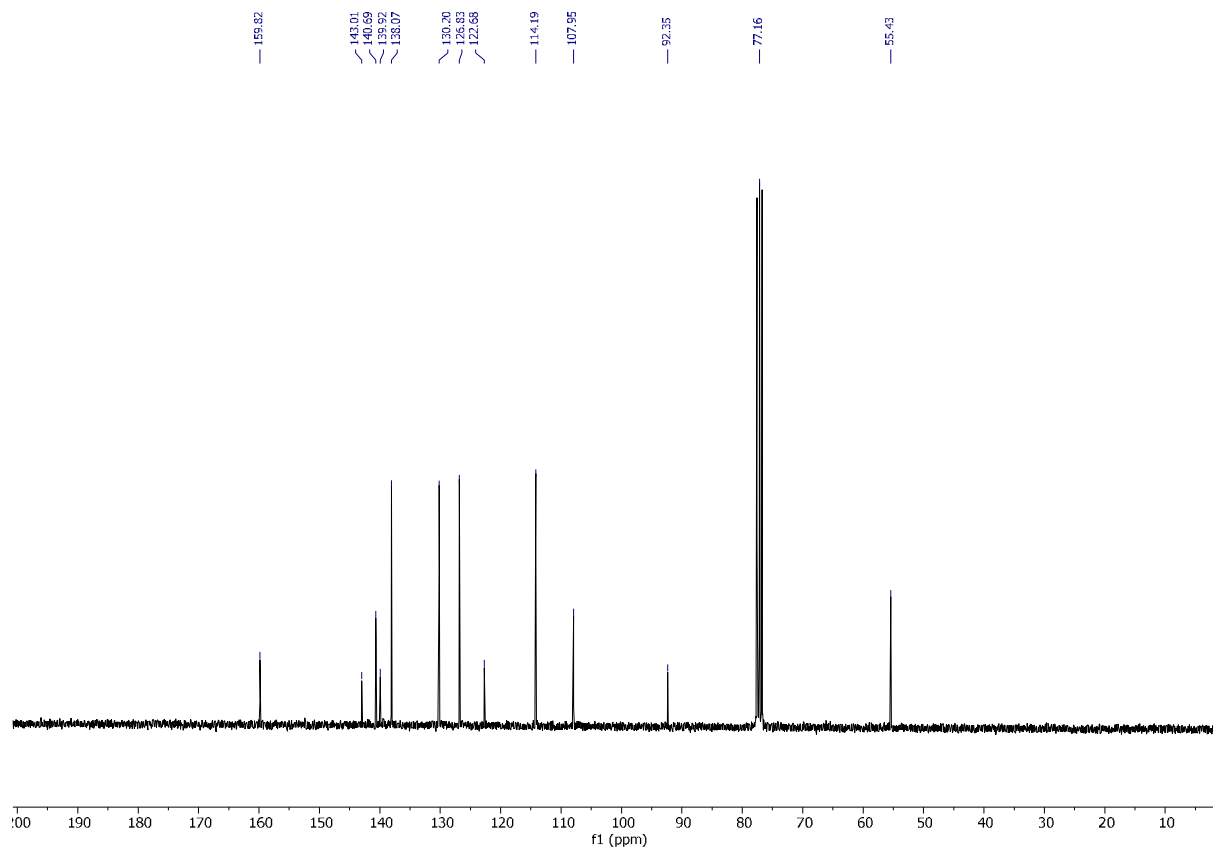
¹H NMR (400 MHz, CDCl₃) of 1,5-bis(4-methoxyphenyl)-1H-pyrazole



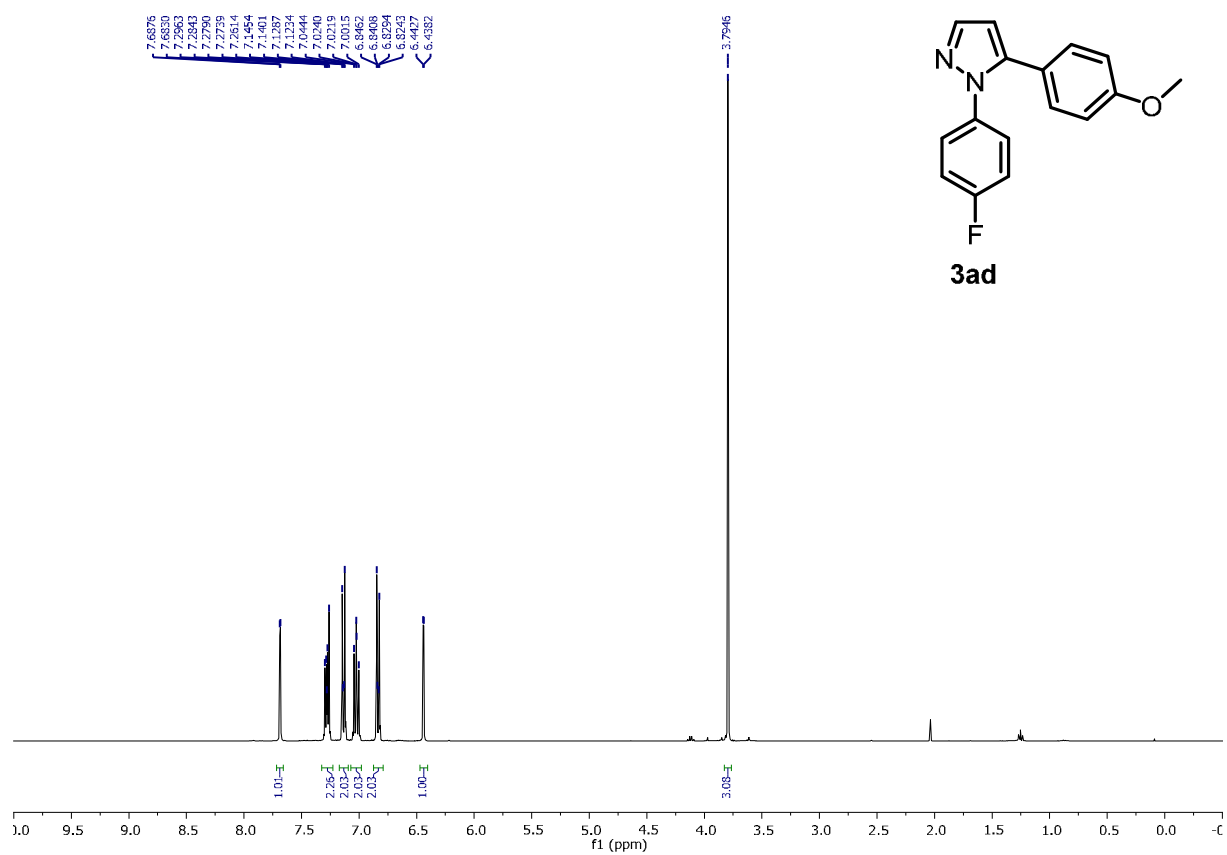
¹³C NMR (100 MHz, CDCl₃) of 1,5-bis(4-methoxyphenyl)-1H-pyrazole



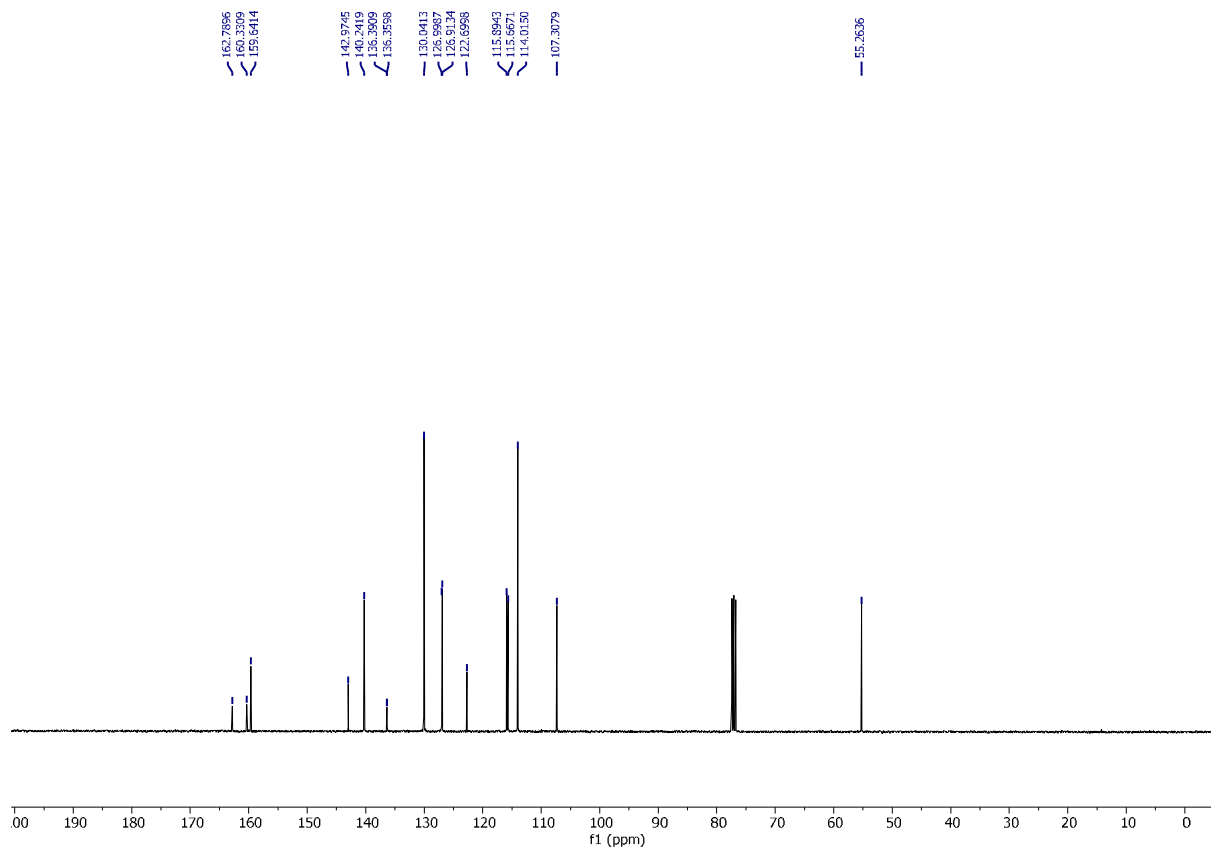
¹H NMR (300 MHz, CDCl₃) of 1-(4-iodophenyl)-5-(4-methoxyphenyl)-1*H*-pyrazole



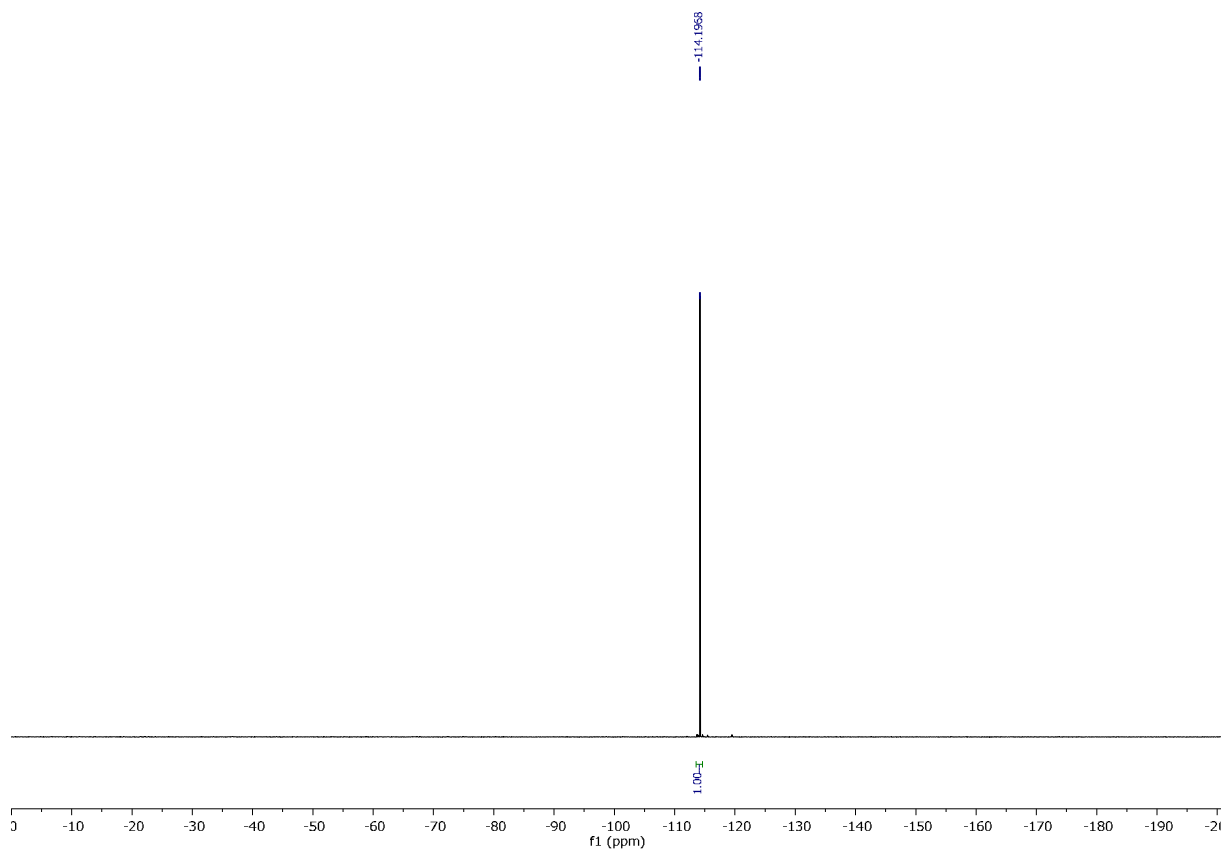
13C NMR (75 MHz, CDCl₃) of 1-(4-iodophenyl)-5-(4-methoxyphenyl)-1H-pyrazole



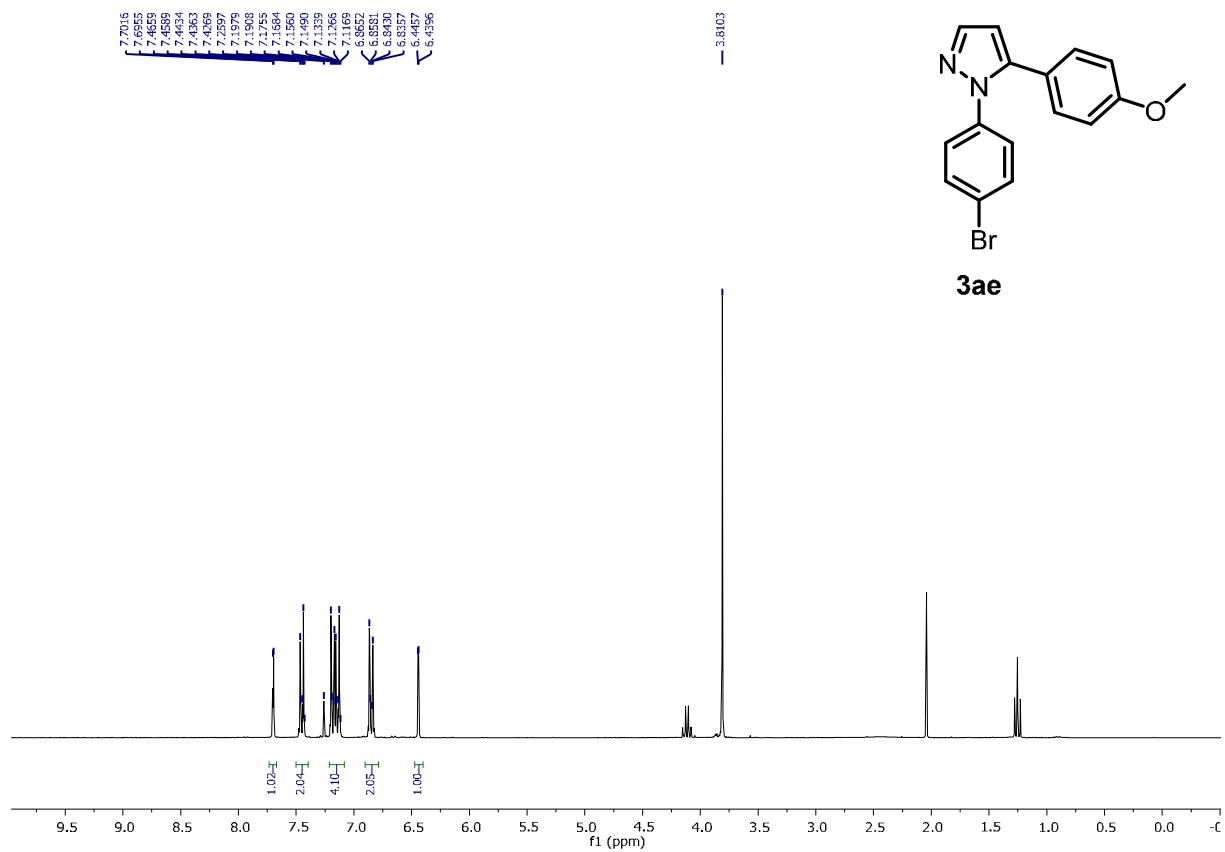
1H NMR (400 MHz, CDCl₃) of 1-(4-fluorophenyl)-5-(4-methoxyphenyl)-1H-pyrazole



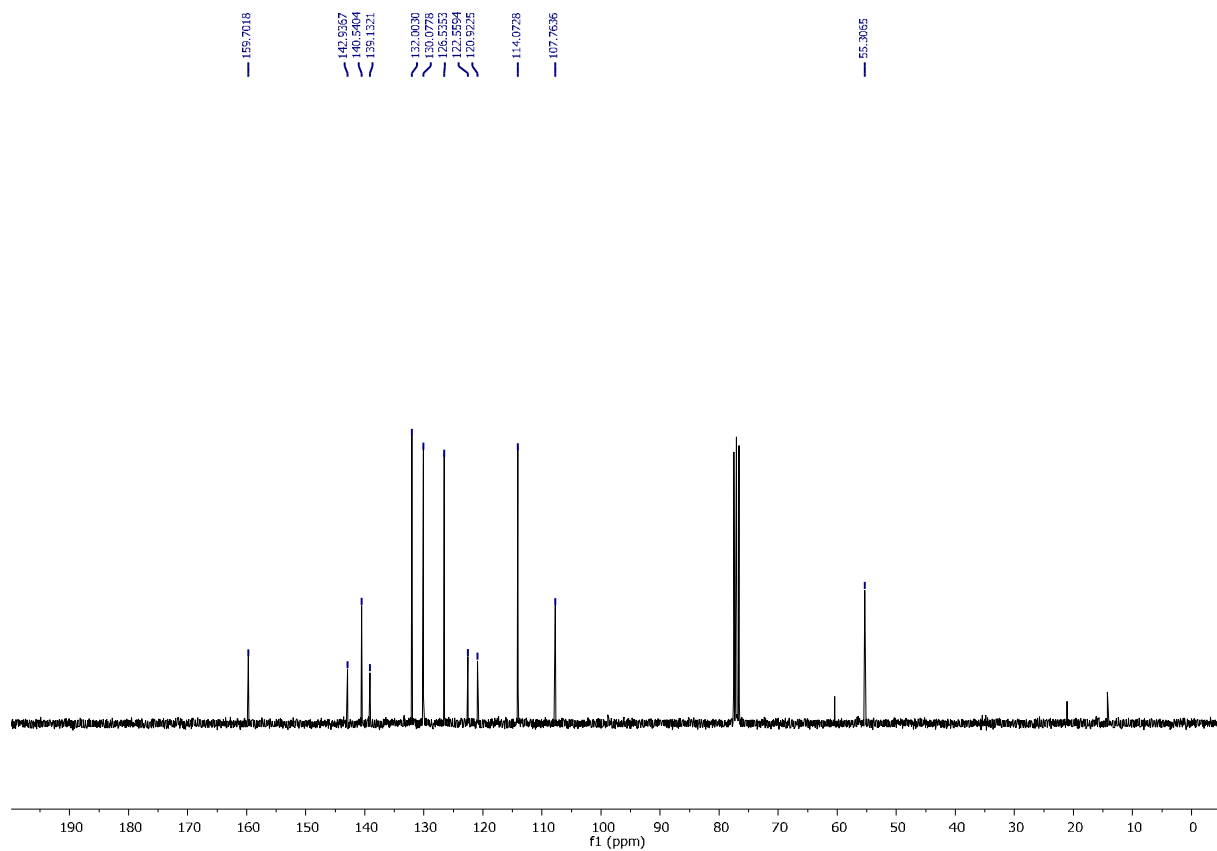
¹³C NMR (100 MHz, CDCl₃) of 1-(4-fluorophenyl)-5-(4-methoxyphenyl)-1H-pyrazole



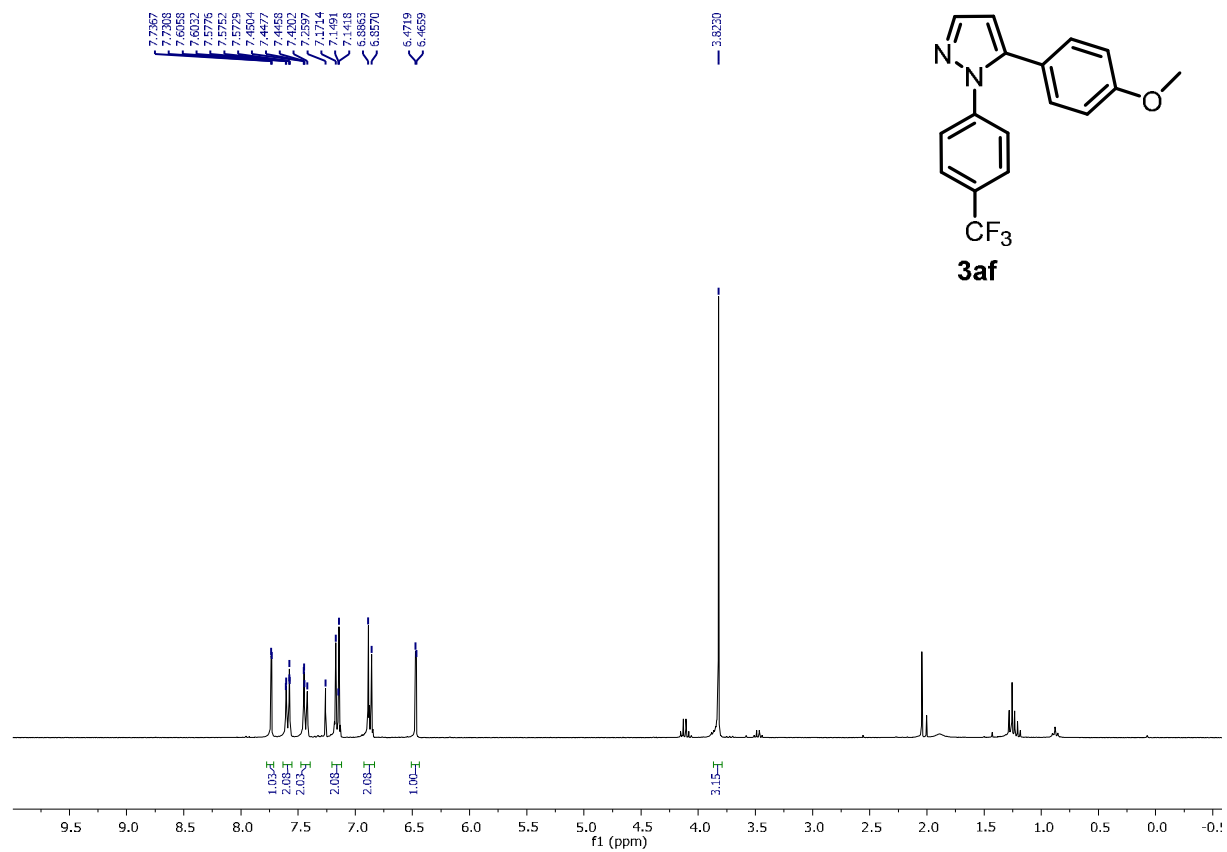
¹⁹F NMR (376 MHz, CDCl₃) of 1-(4-fluorophenyl)-5-(4-methoxyphenyl)-1H-pyrazole



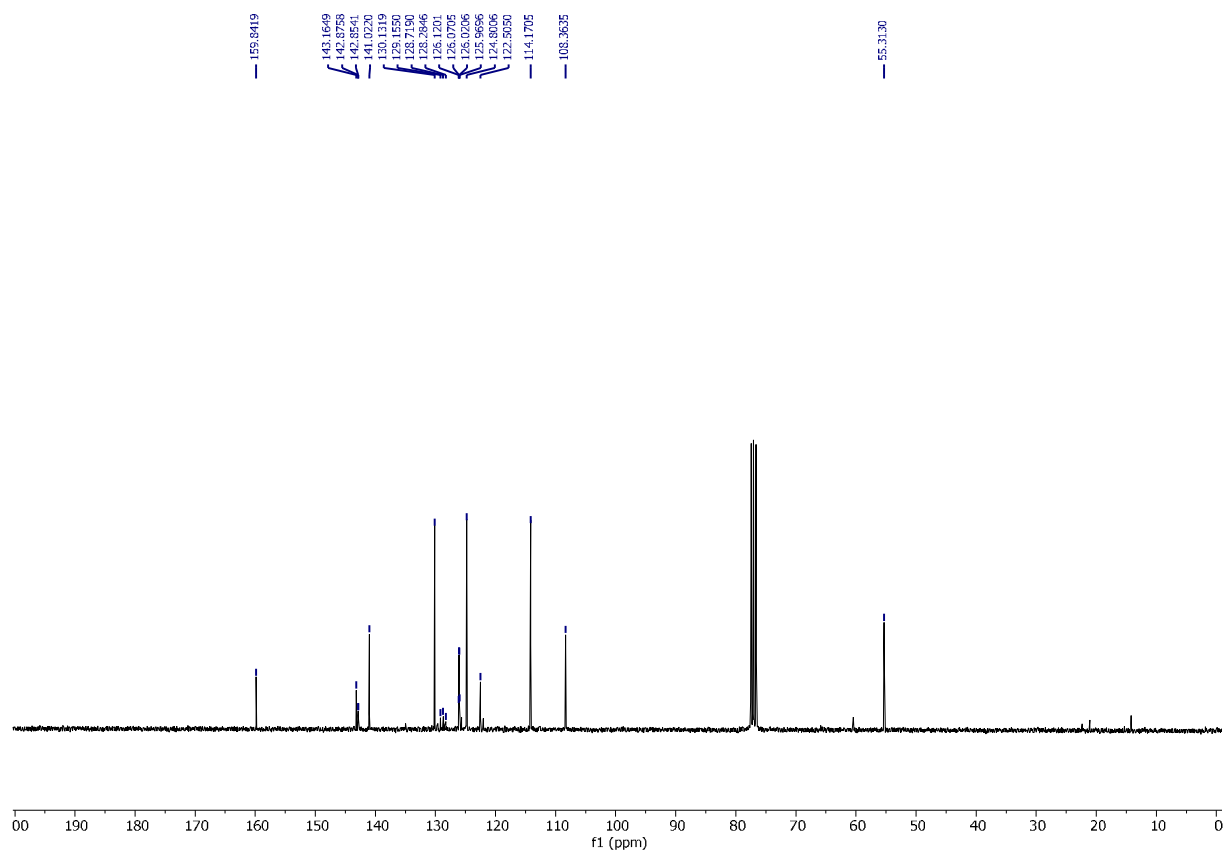
¹H NMR (400 MHz, CDCl₃) of 1-(4-bromophenyl)-5-(4-methoxyphenyl)-1H-pyrazole



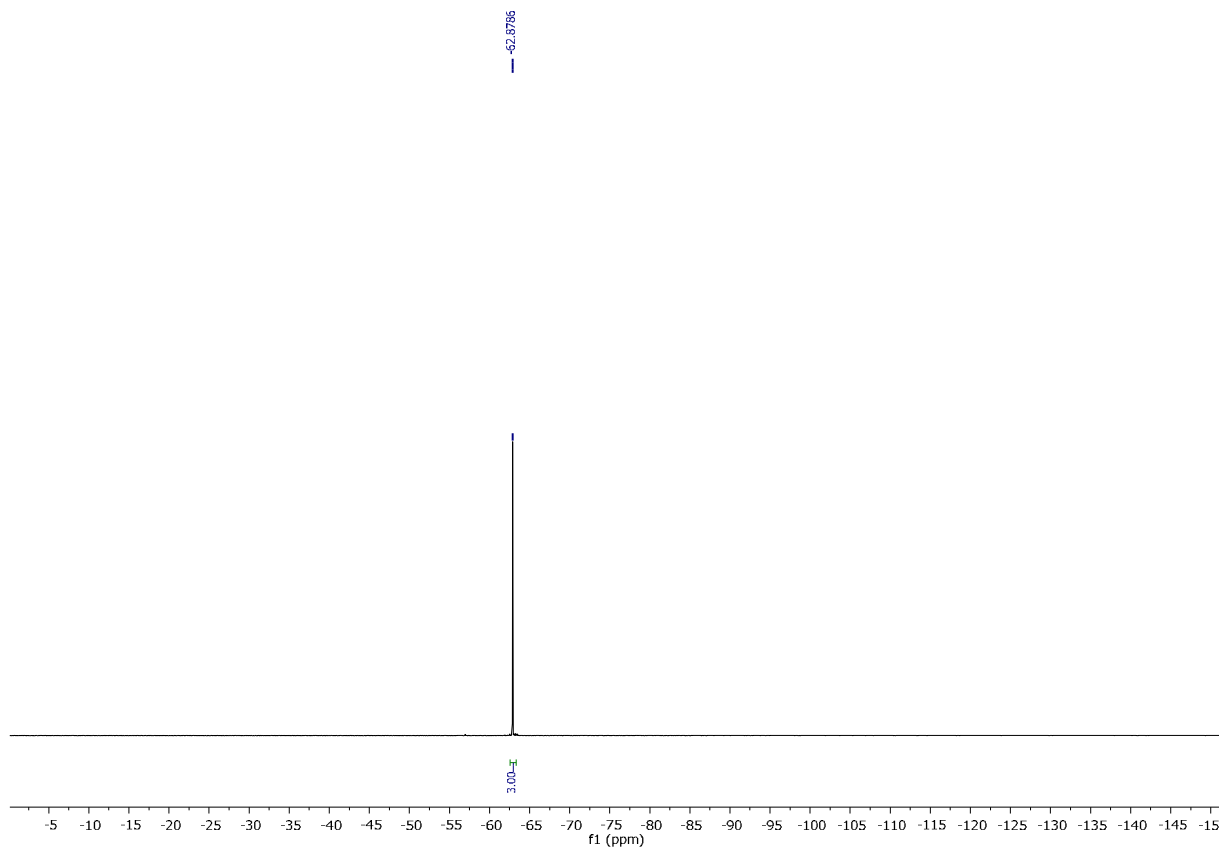
¹³C NMR (100 MHz, CDCl₃) of 1-(4-bromophenyl)-5-(4-methoxyphenyl)-1H-pyrazole



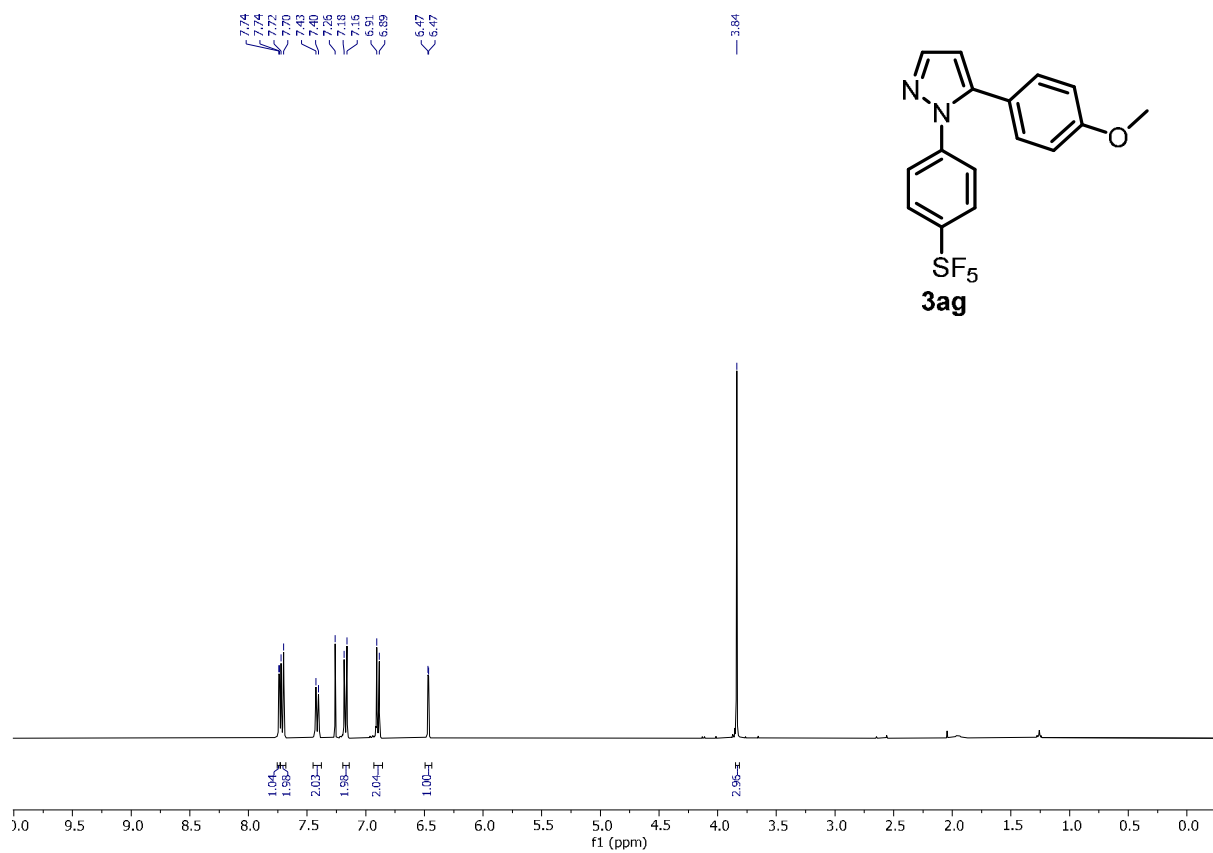
¹H NMR (400 MHz, CDCl₃) of 5-(4-methoxyphenyl)-1-(4-(trifluoromethyl) phenyl)-1H-pyrazole



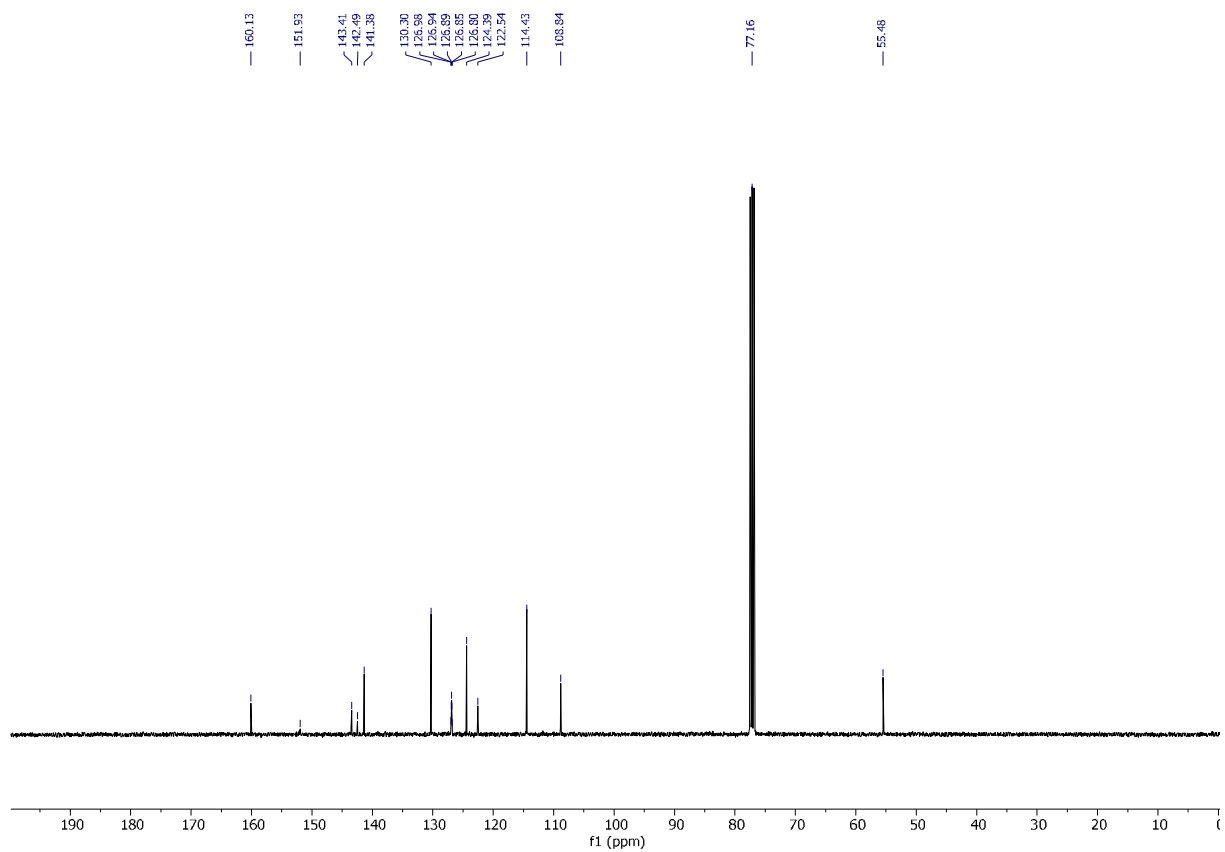
¹³C NMR (100 MHz, CDCl₃) of 5-(4-methoxyphenyl)-1-(4-(trifluoromethyl) phenyl)-1H-pyrazole



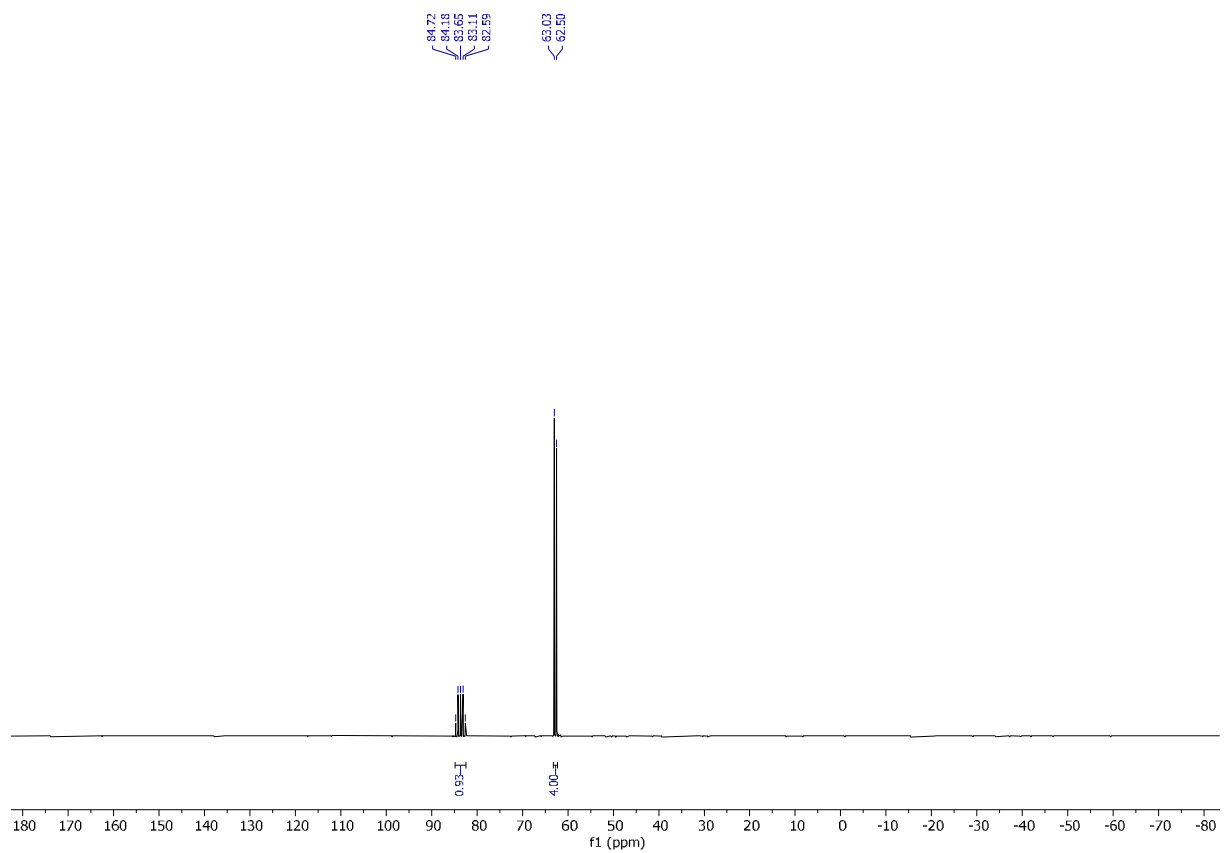
^{19}F NMR (376 MHz, CDCl_3) of 5-(4-methoxyphenyl)-1-(4-(trifluoromethyl)phenyl)-1H-pyrazole



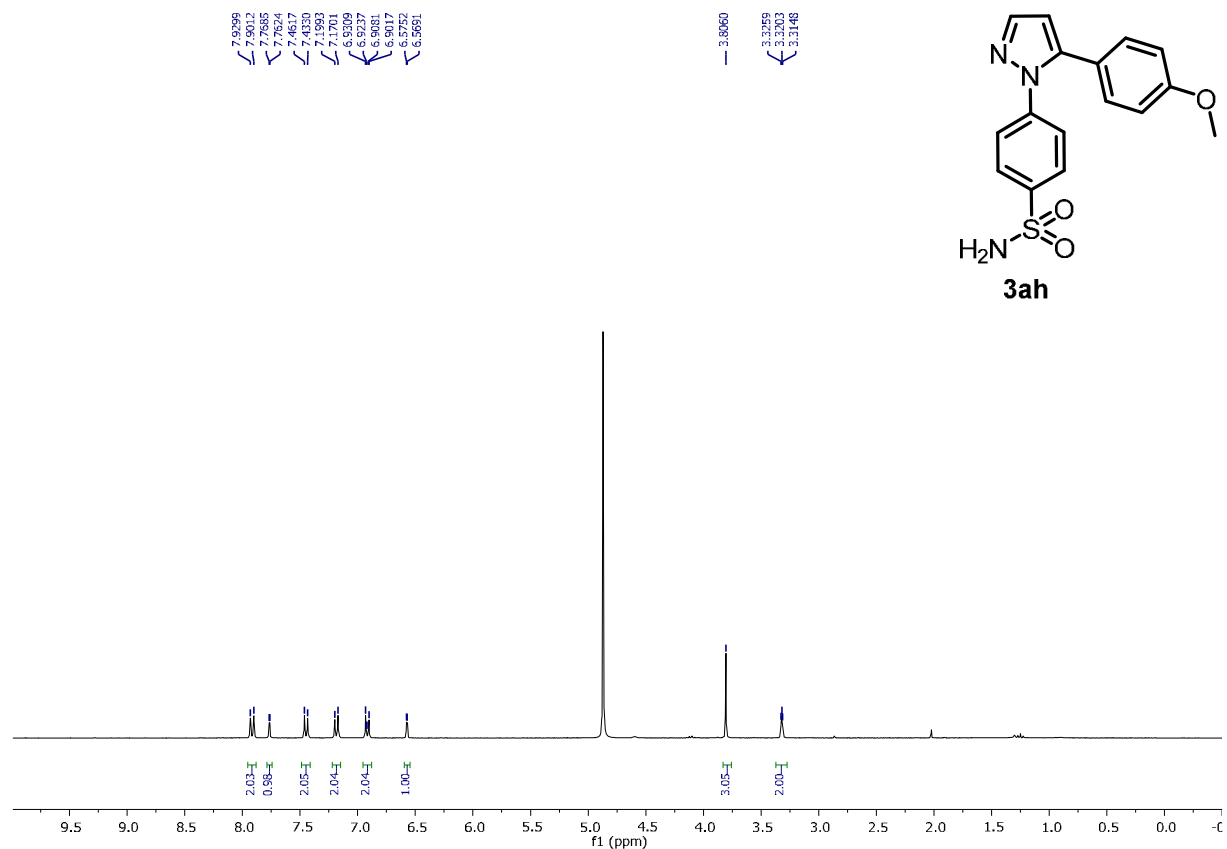
^1H NMR (400 MHz, CDCl_3) of 5-(4-Methoxyphenyl)-1-(4-(pentafluoro-sulfanyl)phenyl)-1H-pyrazole



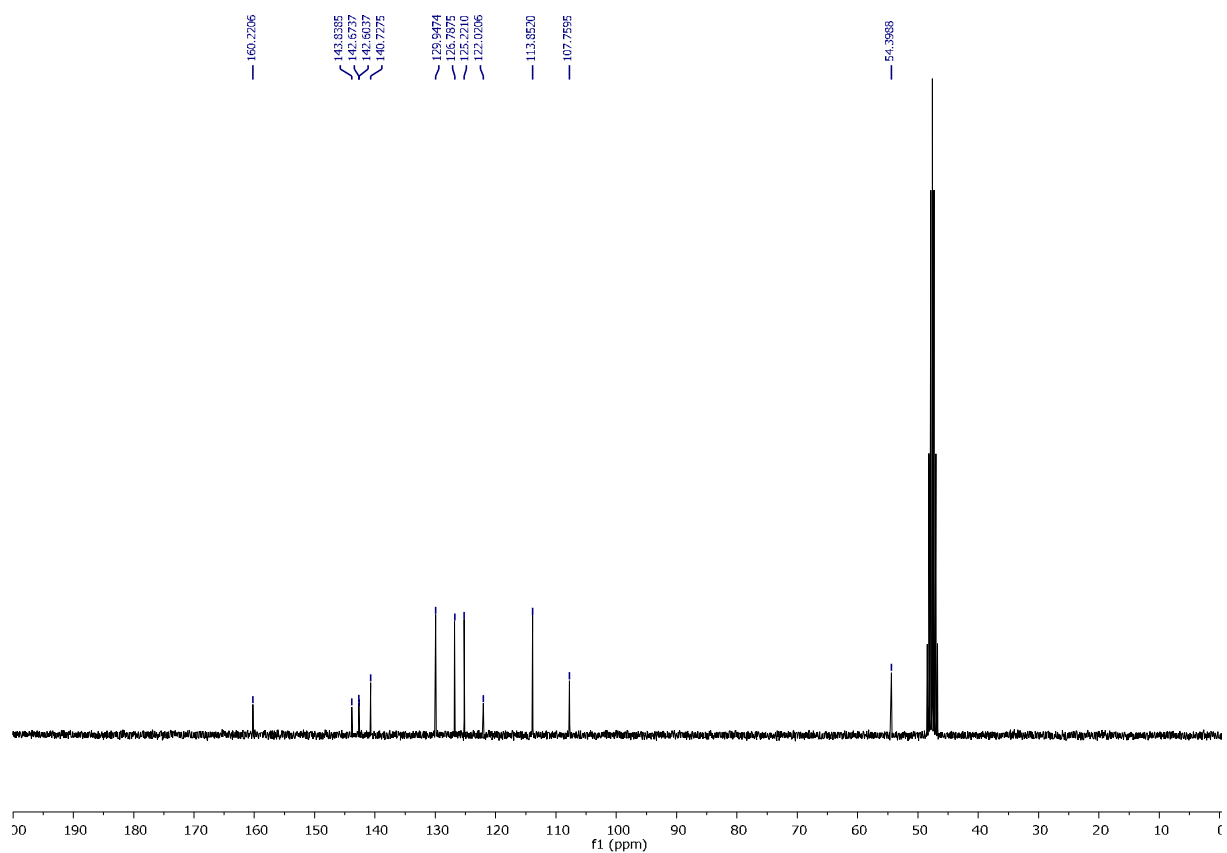
¹³C NMR (100 MHz, CDCl₃) of 5-(4-Methoxyphenyl)-1-(4-(pentafluoro-sulfanyl)phenyl)-1H-pyrazole



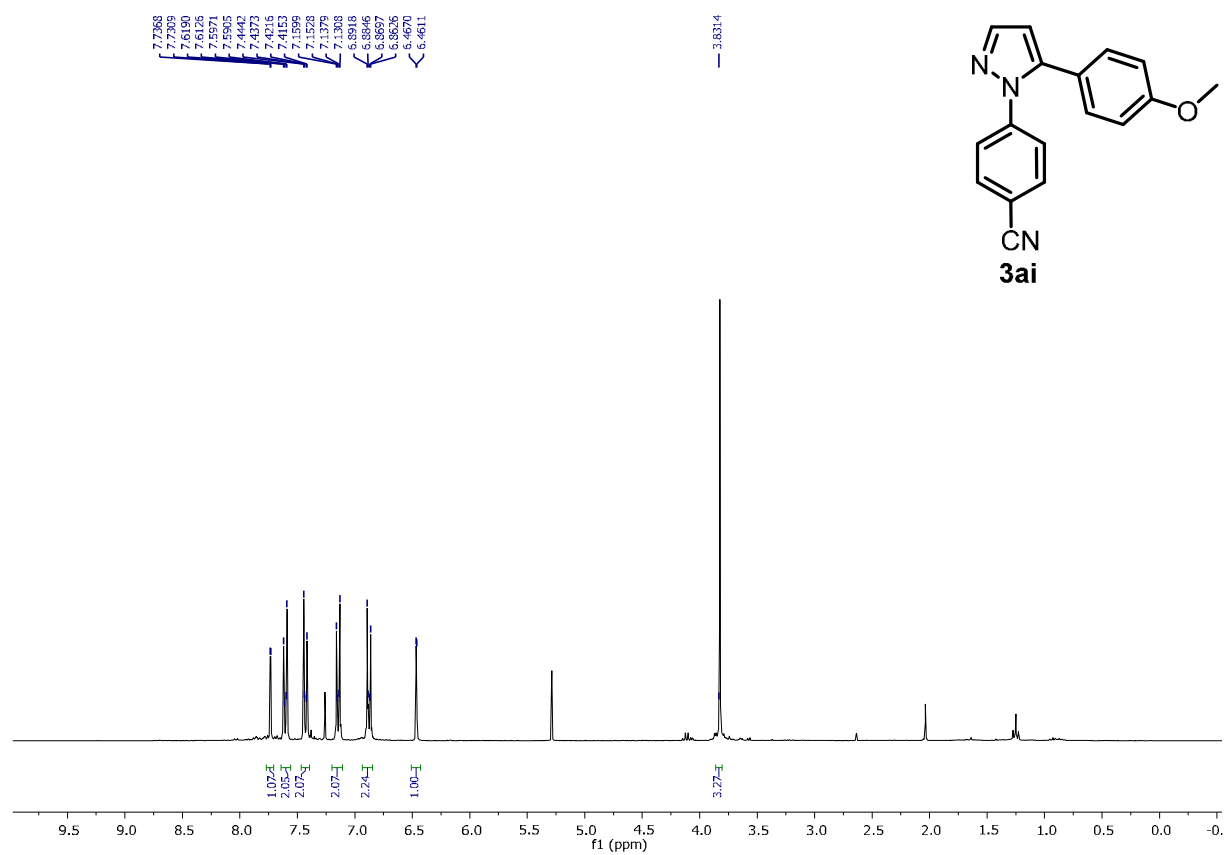
¹⁹F NMR (282 MHz, CDCl₃) of 5-(4-Methoxyphenyl)-1-(4-(pentafluoro-sulfanyl)phenyl)-1H-pyrazole



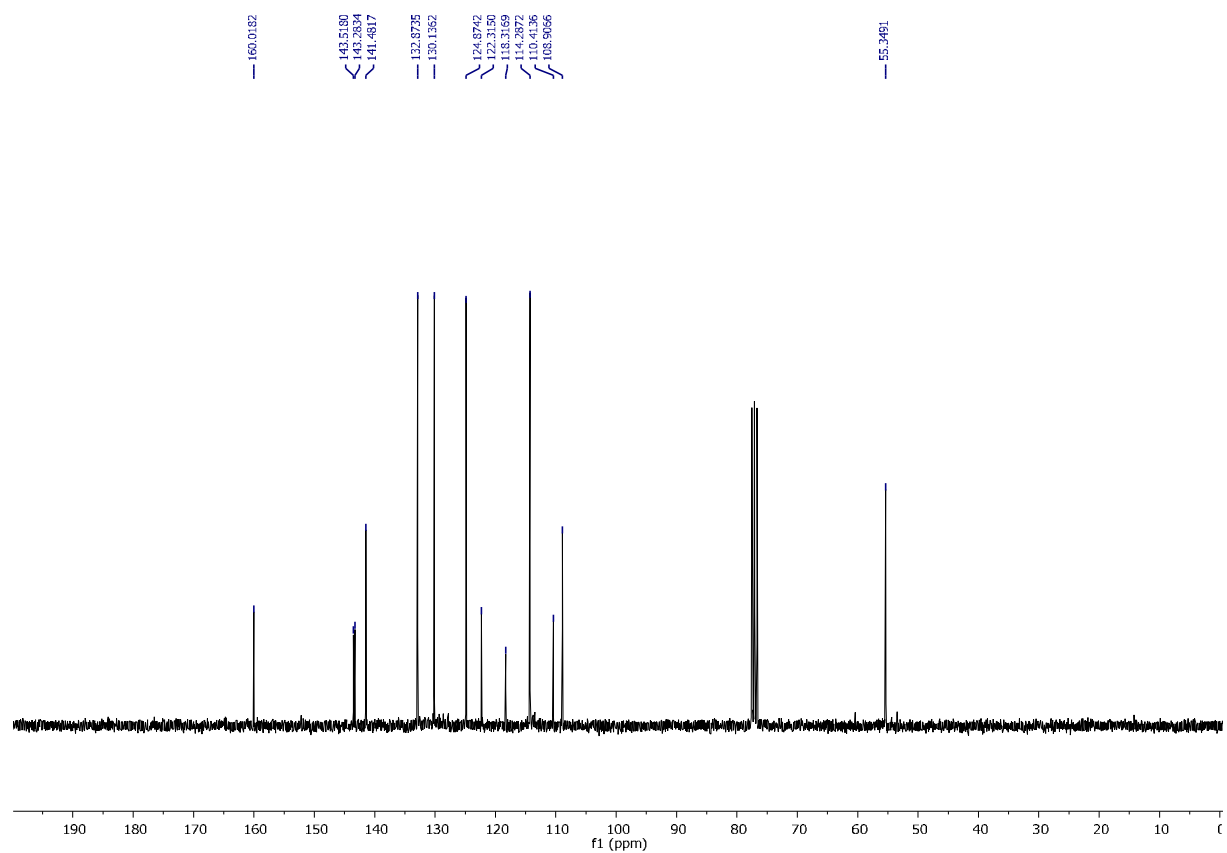
¹H NMR (300 MHz, MeOD) of 4-(5-(4-methoxyphenyl)-1H-pyrazol-1-yl)benzenesulfonamide



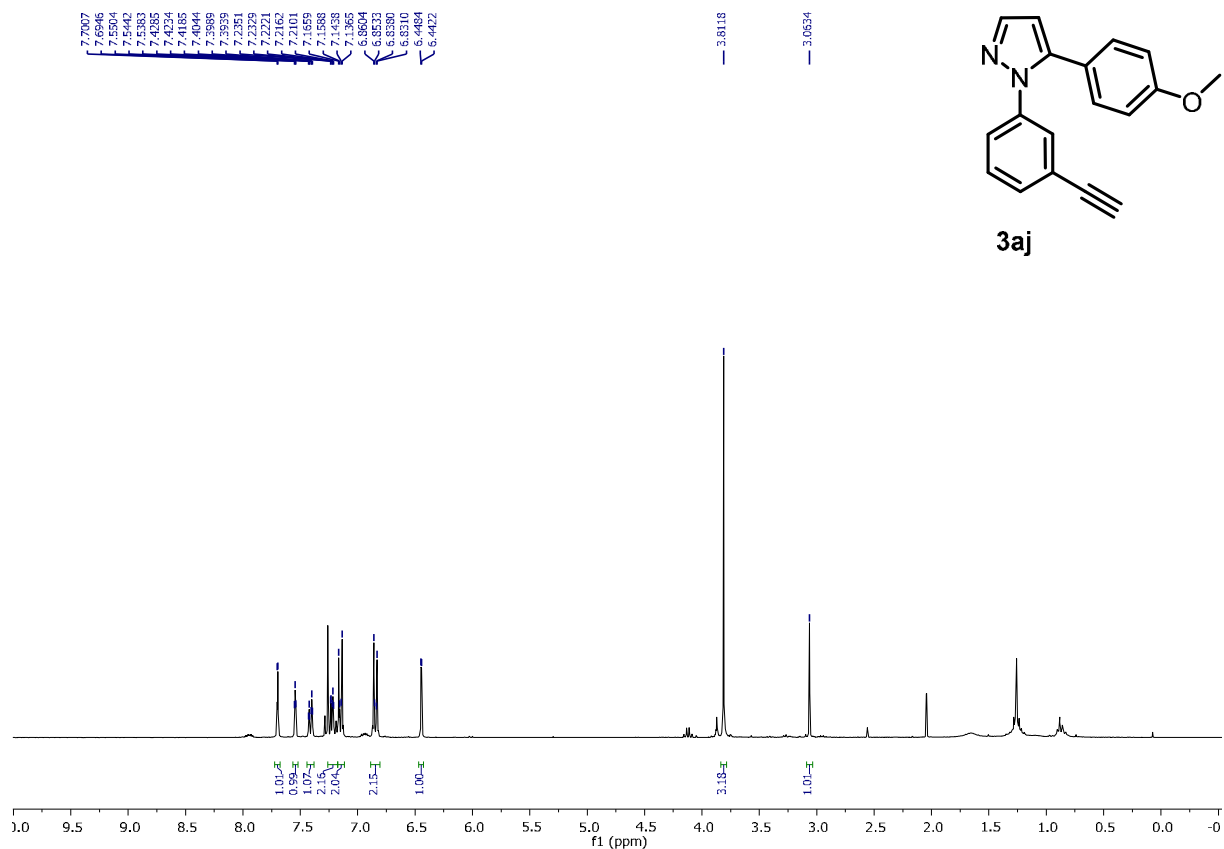
¹³C NMR (75 MHz, MeOD) of 4-(5-(4-methoxyphenyl)-1H-pyrazol-1-yl)benzenesulfonamide



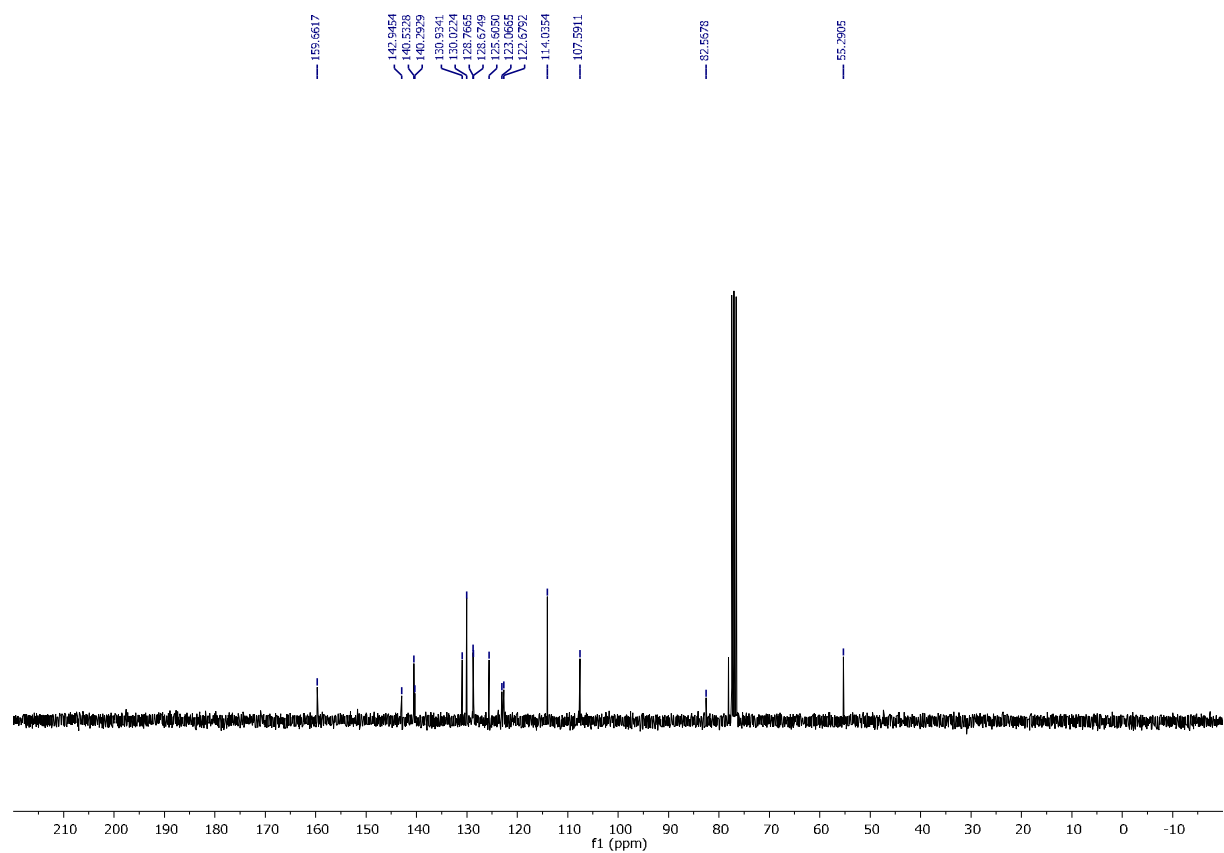
¹H NMR (300 MHz, CDCl₃) of 4-(5-(4-methoxyphenyl)-1H-pyrazol-1-yl)benzonitrile



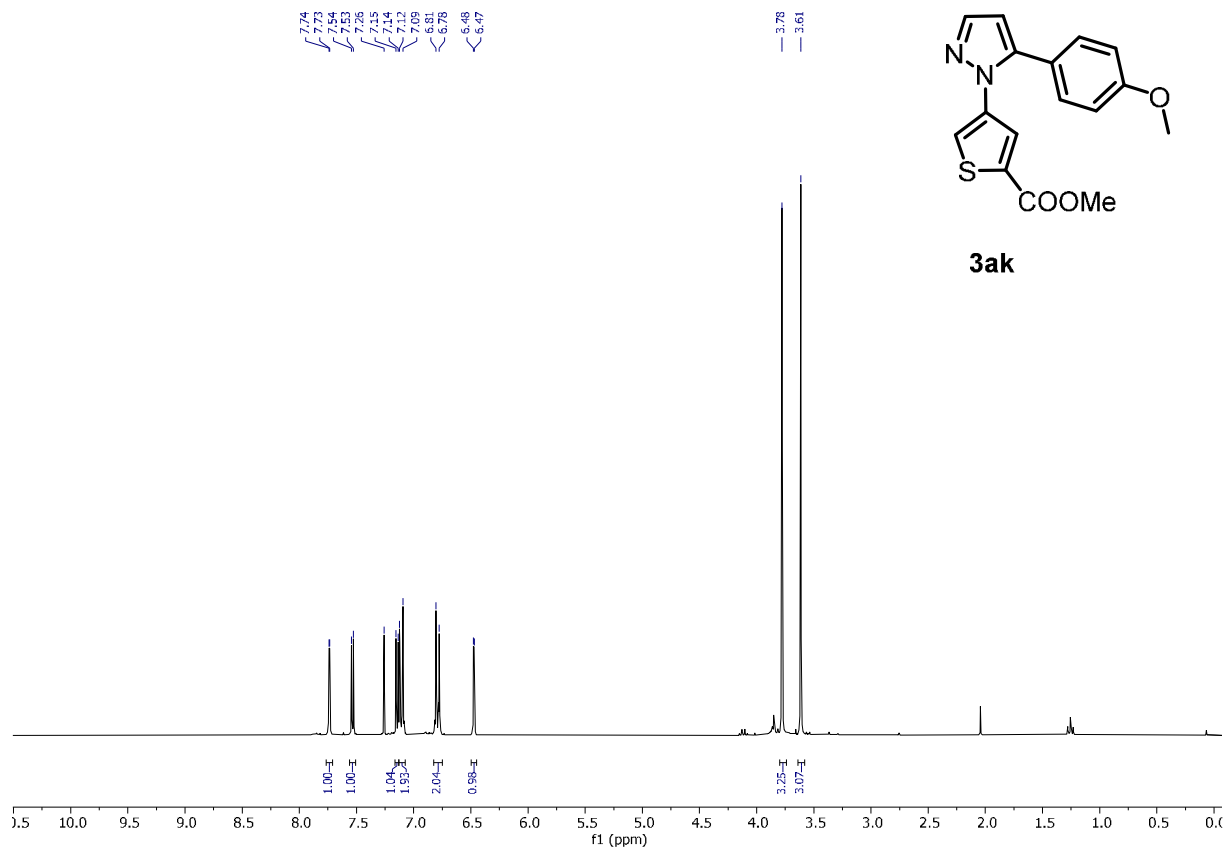
¹³C NMR (75 MHz, CDCl₃) of 4-(5-(4-methoxyphenyl)-1H-pyrazol-1-yl)benzonitrile



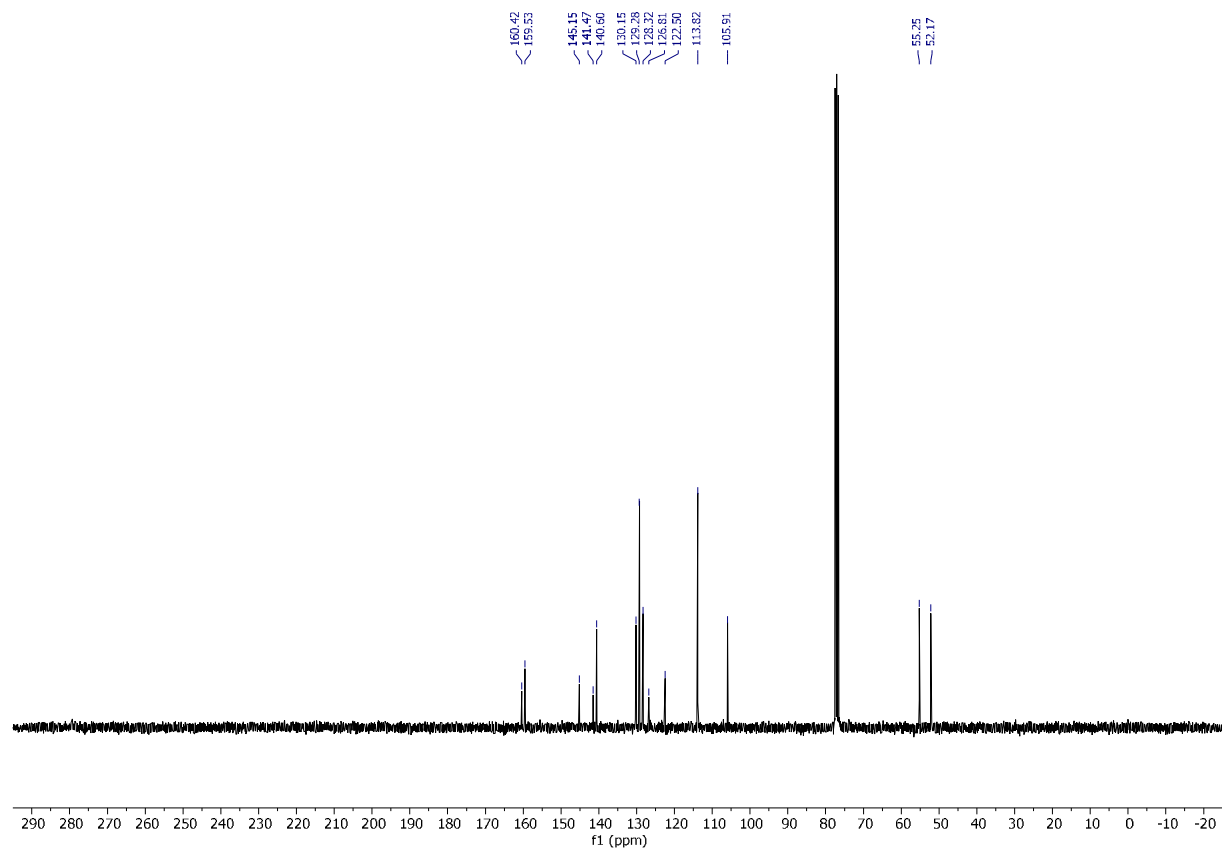
¹H NMR (300 MHz, CDCl₃) of 1-(3-ethynylphenyl)-5-(4-methoxyphenyl)-1H-pyrazole



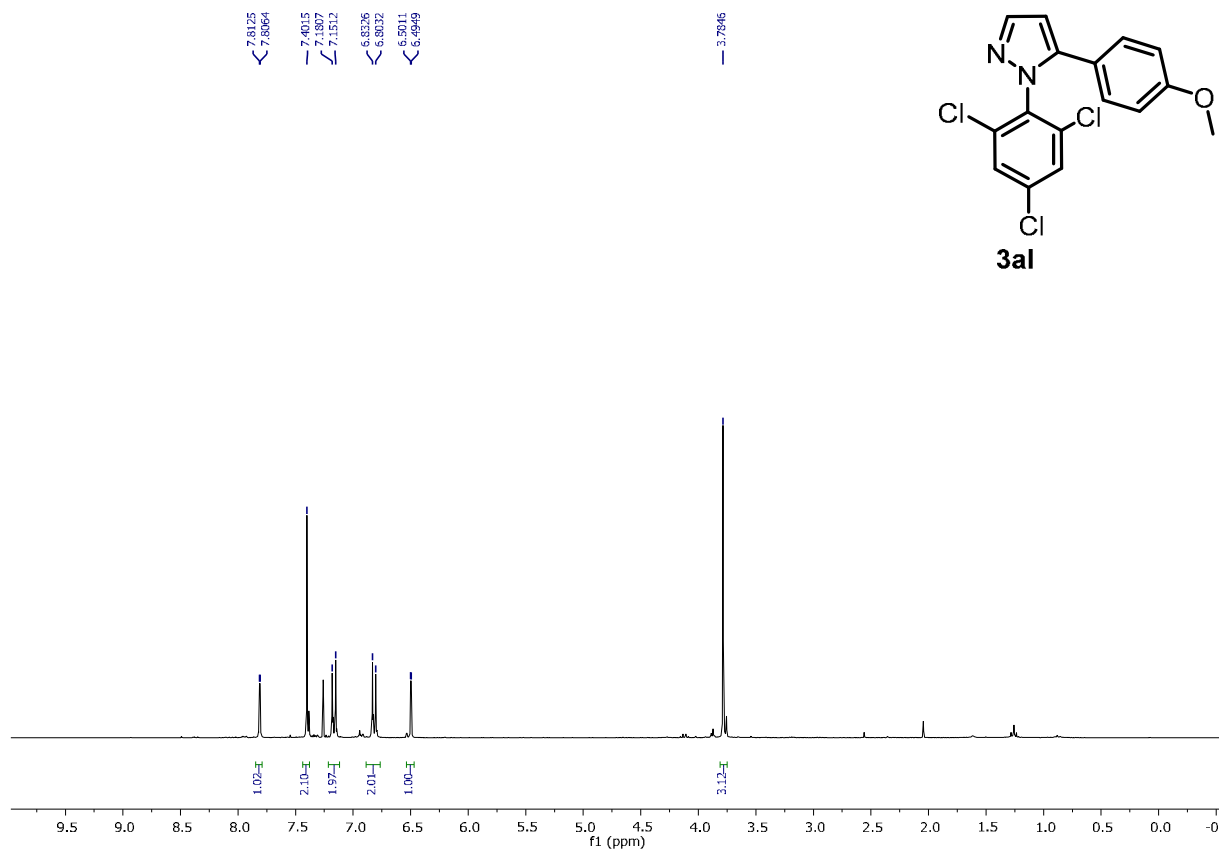
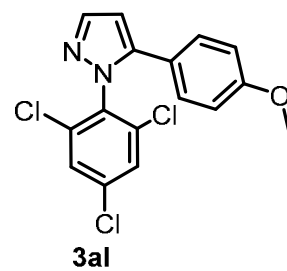
¹³C NMR (100 MHz, CDCl₃) of 1-(3-ethynylphenyl)-5-(4-methoxyphenyl)-1H-pyrazole



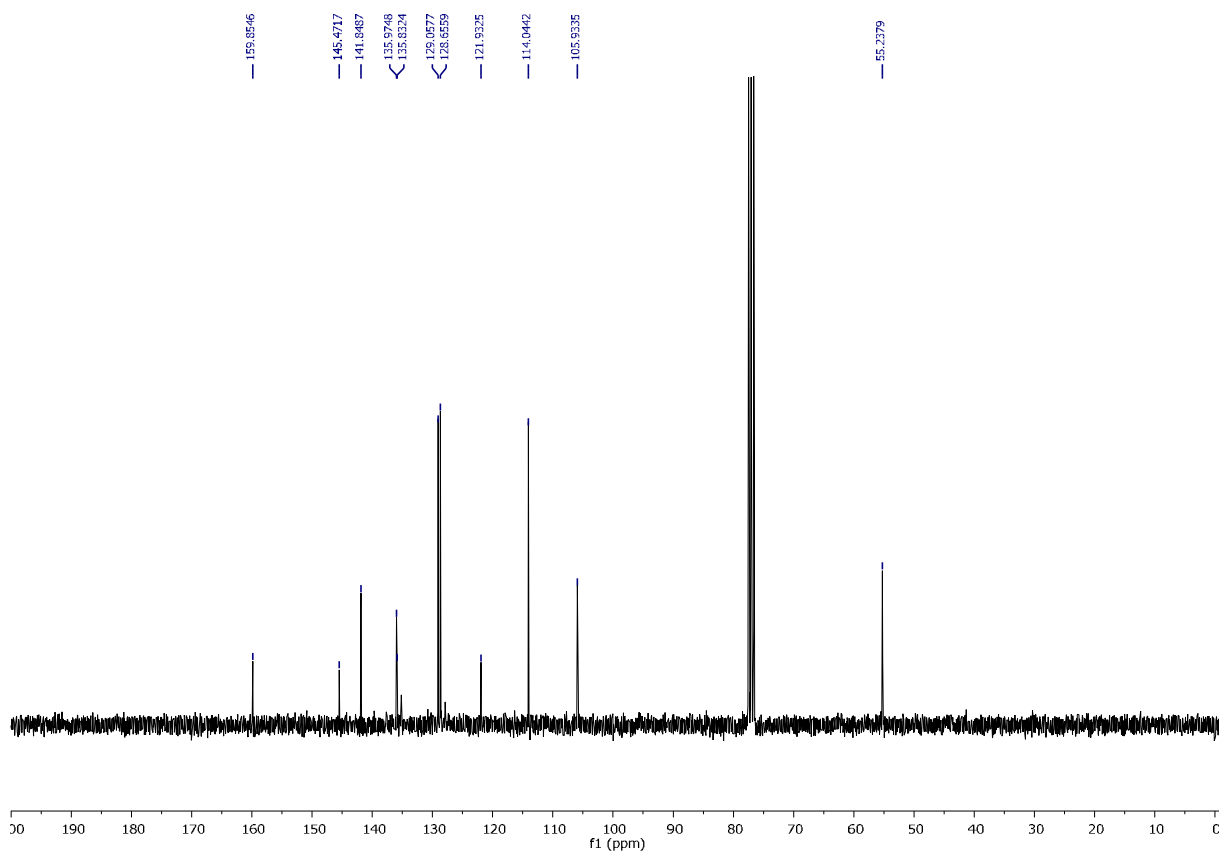
¹H NMR (300 MHz, CDCl₃) of Methyl 3-(5-(4-methoxyphenyl)-1*H*-pyrazol-1-yl) thiophene-2-carboxylate



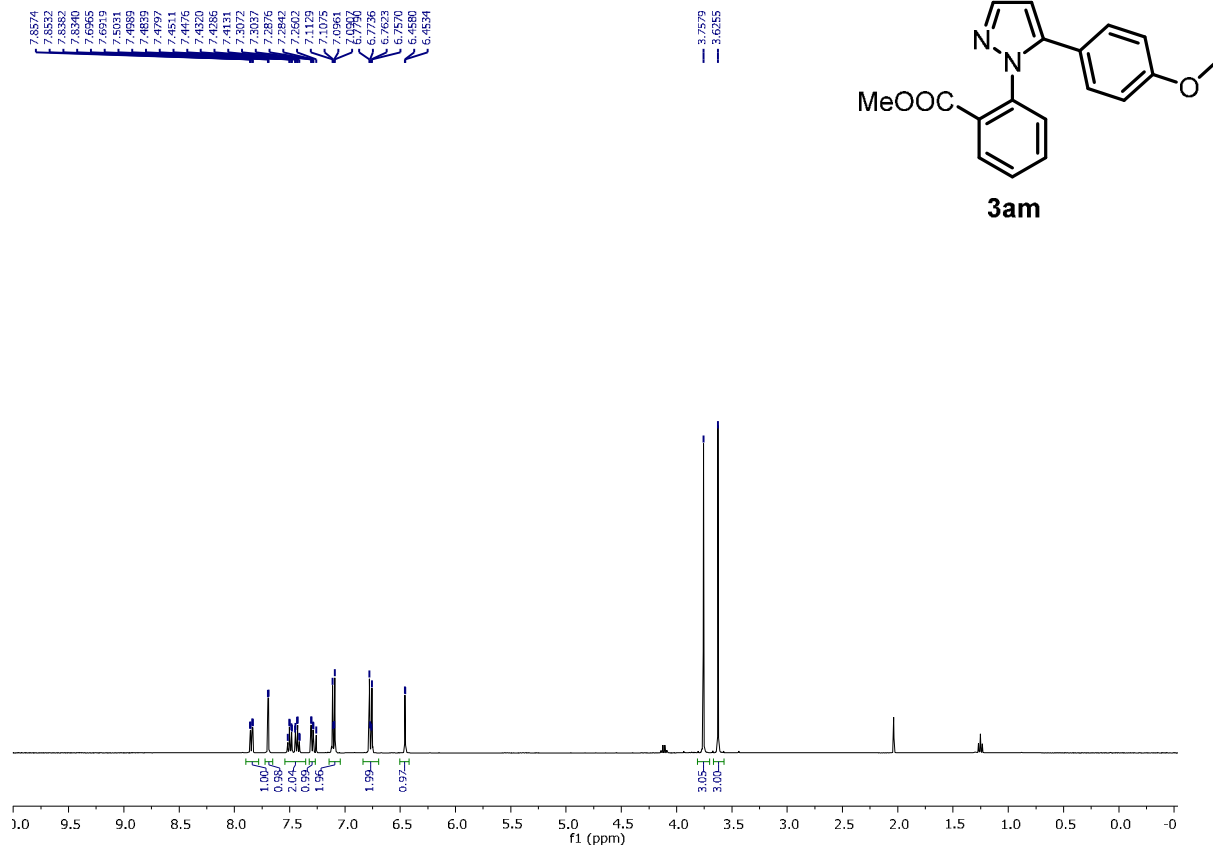
¹³C NMR (75 MHz, CDCl₃) of Methyl 3-(5-(4-methoxyphenyl)-1*H*-pyrazol-1-yl) thiophene-2-carboxylate



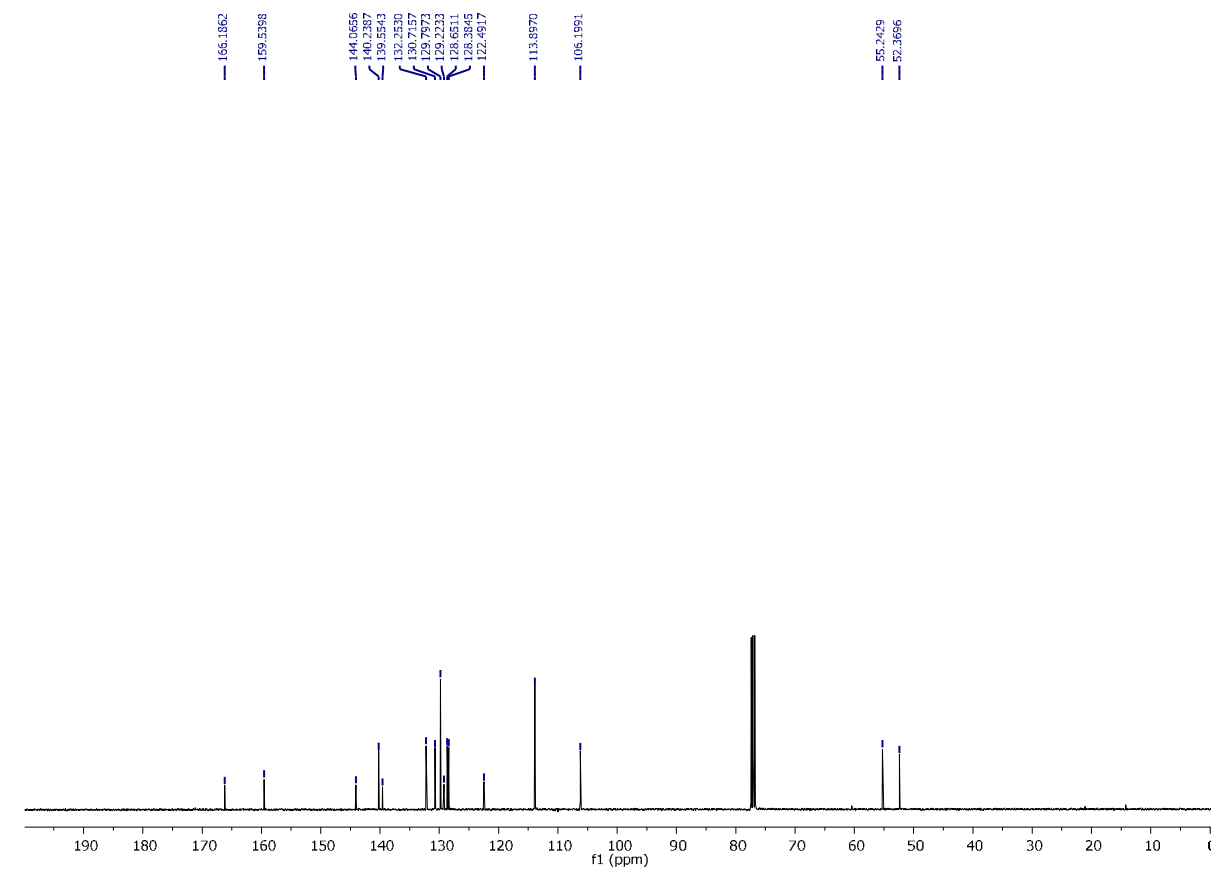
¹H NMR (300 MHz, CDCl₃) of 5-(4-methoxyphenyl)-1-(2,4,6-trichlorophenyl)-1H-pyrazole

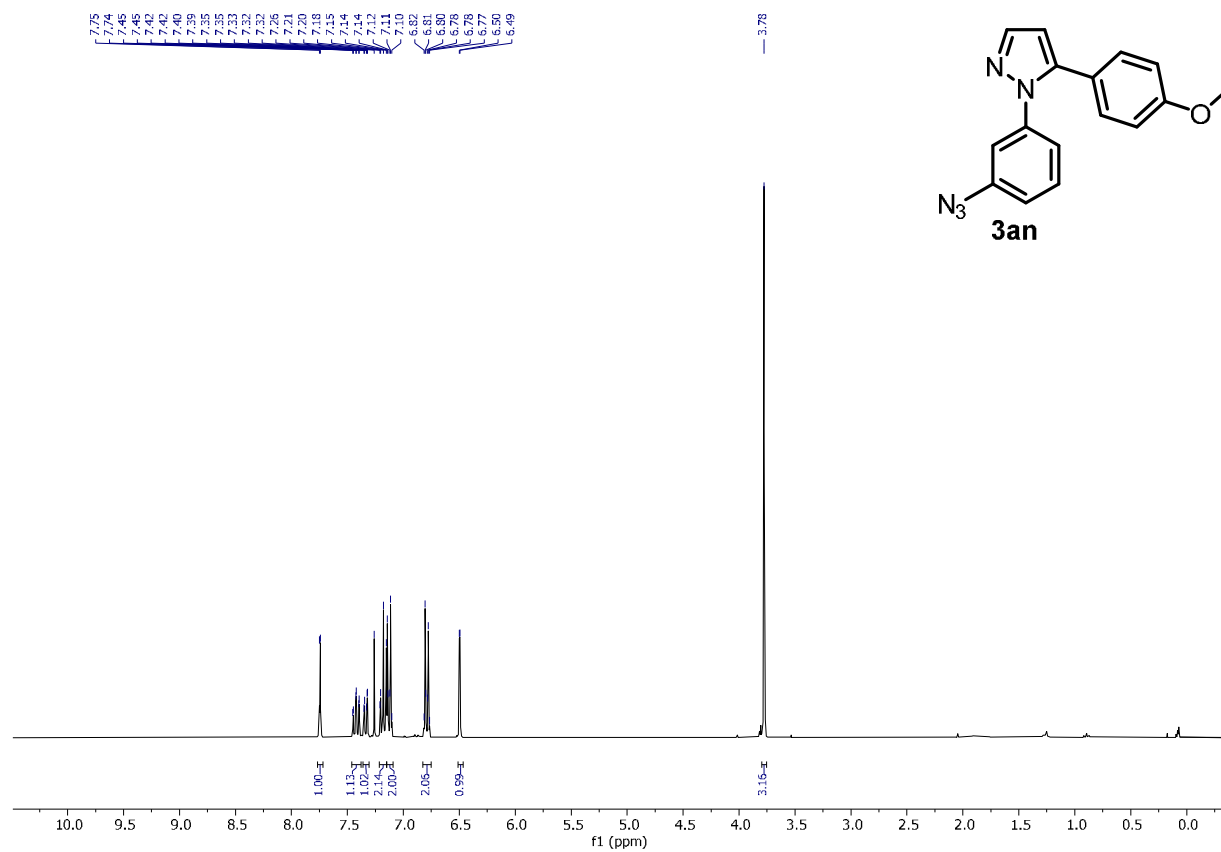


¹³C NMR (75 MHz, CDCl₃) of 5-(4-methoxyphenyl)-1-(2,4,6-trichlorophenyl)-1H-pyrazole

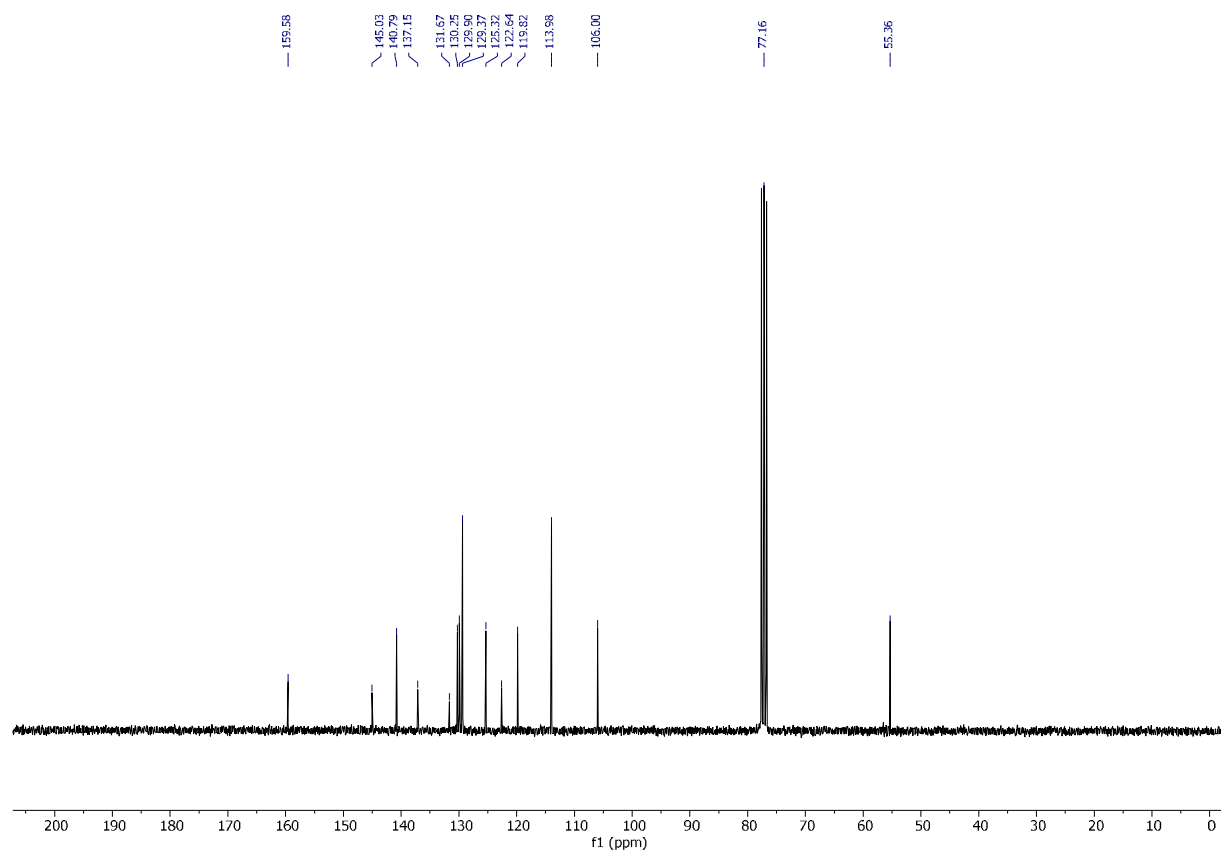


¹H NMR (400 MHz, CDCl₃) of Methyl-2-(5-(4-methoxyphenyl)-1H-pyrazol-1-yl) benzoate

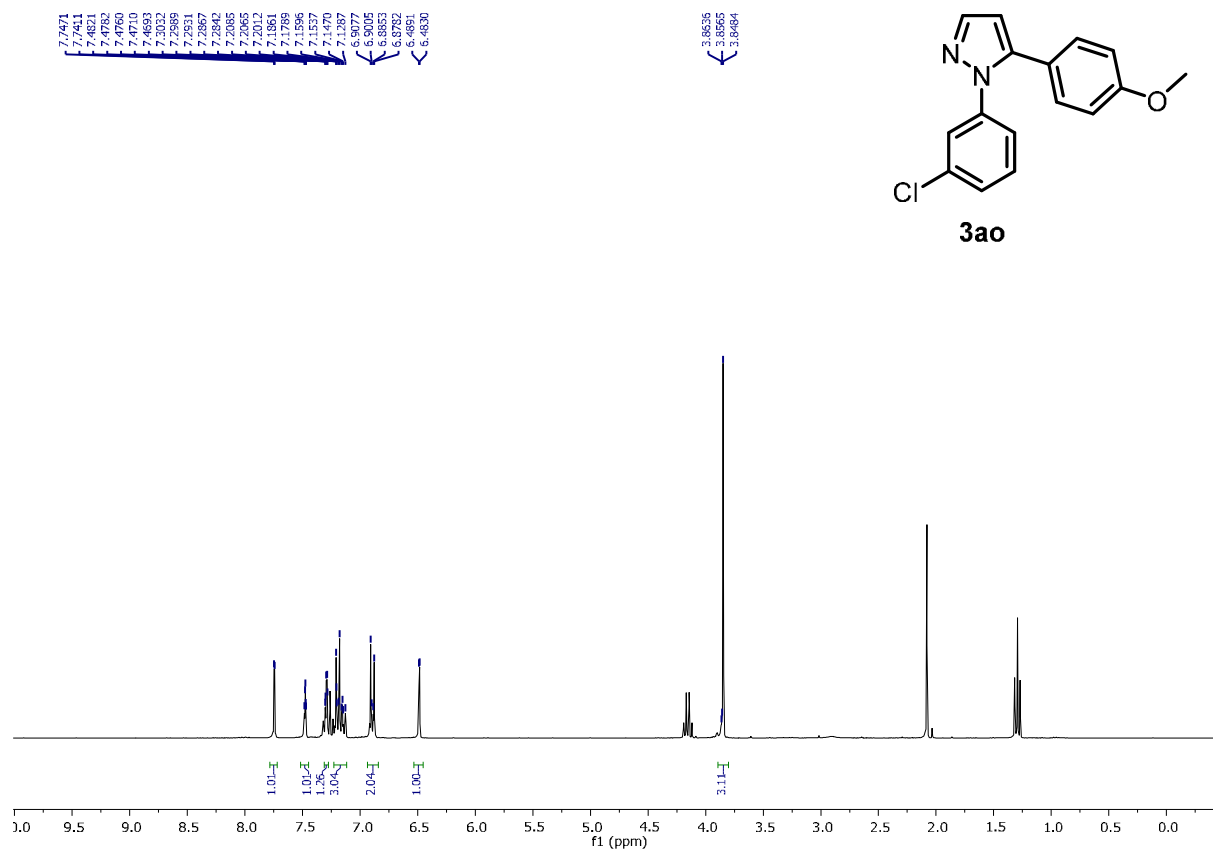




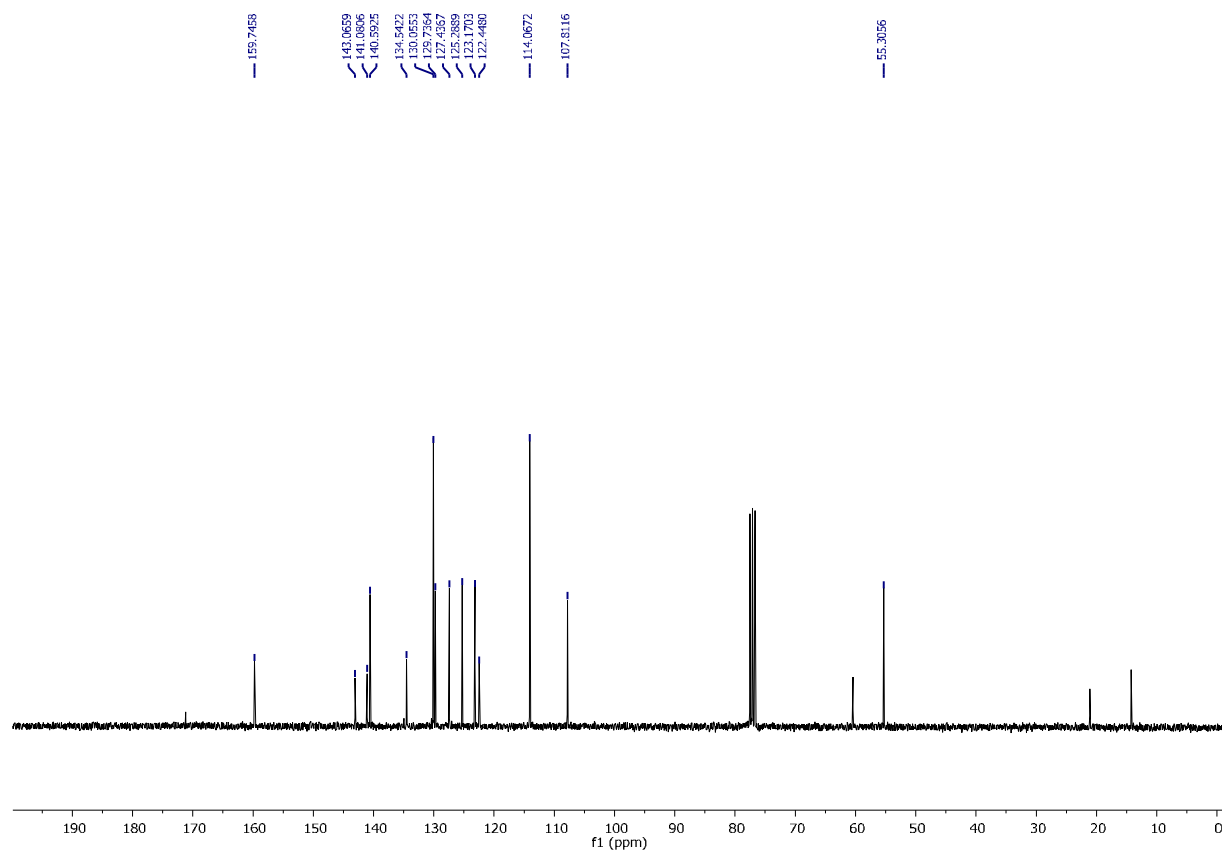
$^1\text{H NMR}$ (300 MHz, CDCl_3) of 1-(2-Azidophenyl)-5-(4-methoxyphenyl)-1H-pyrazole



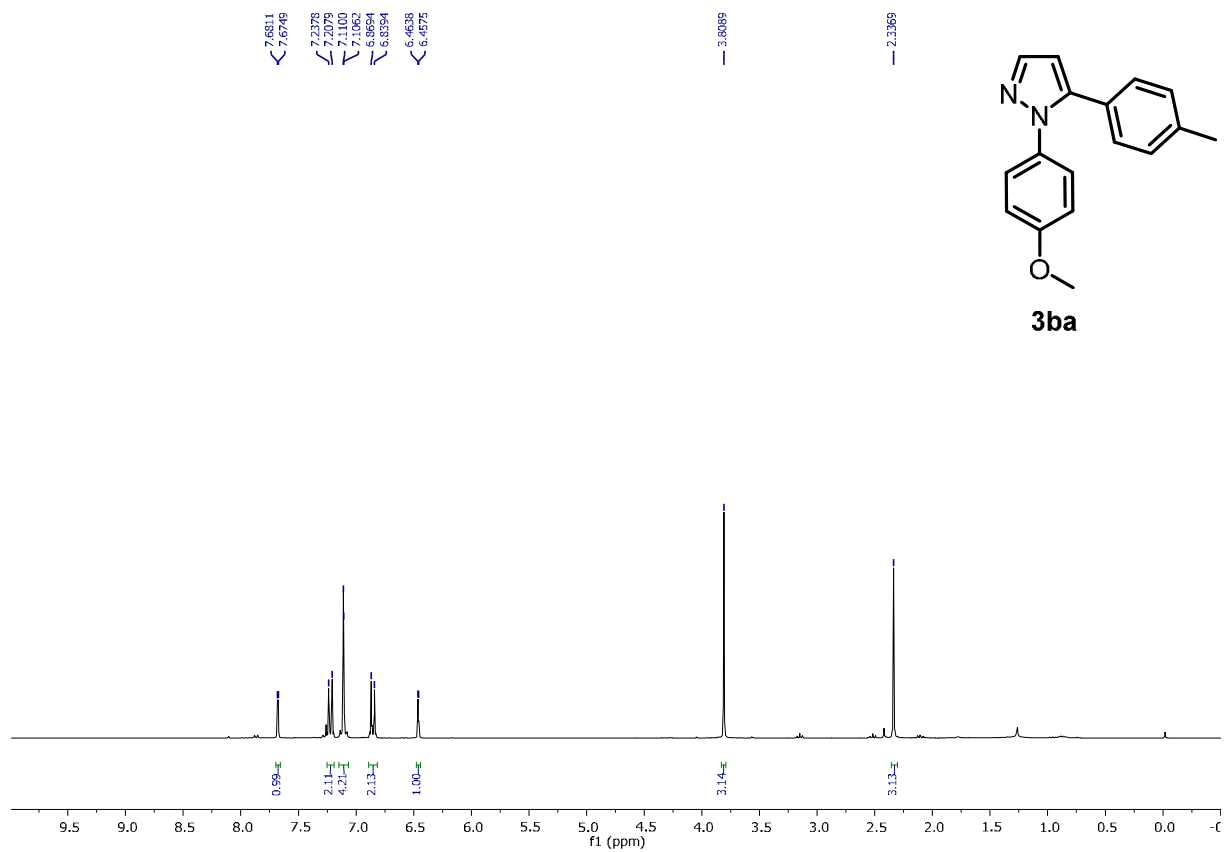
$^{13}\text{C NMR}$ (75 MHz, CDCl_3) of 1-(2-Azidophenyl)-5-(4-methoxyphenyl)-1H-pyrazole



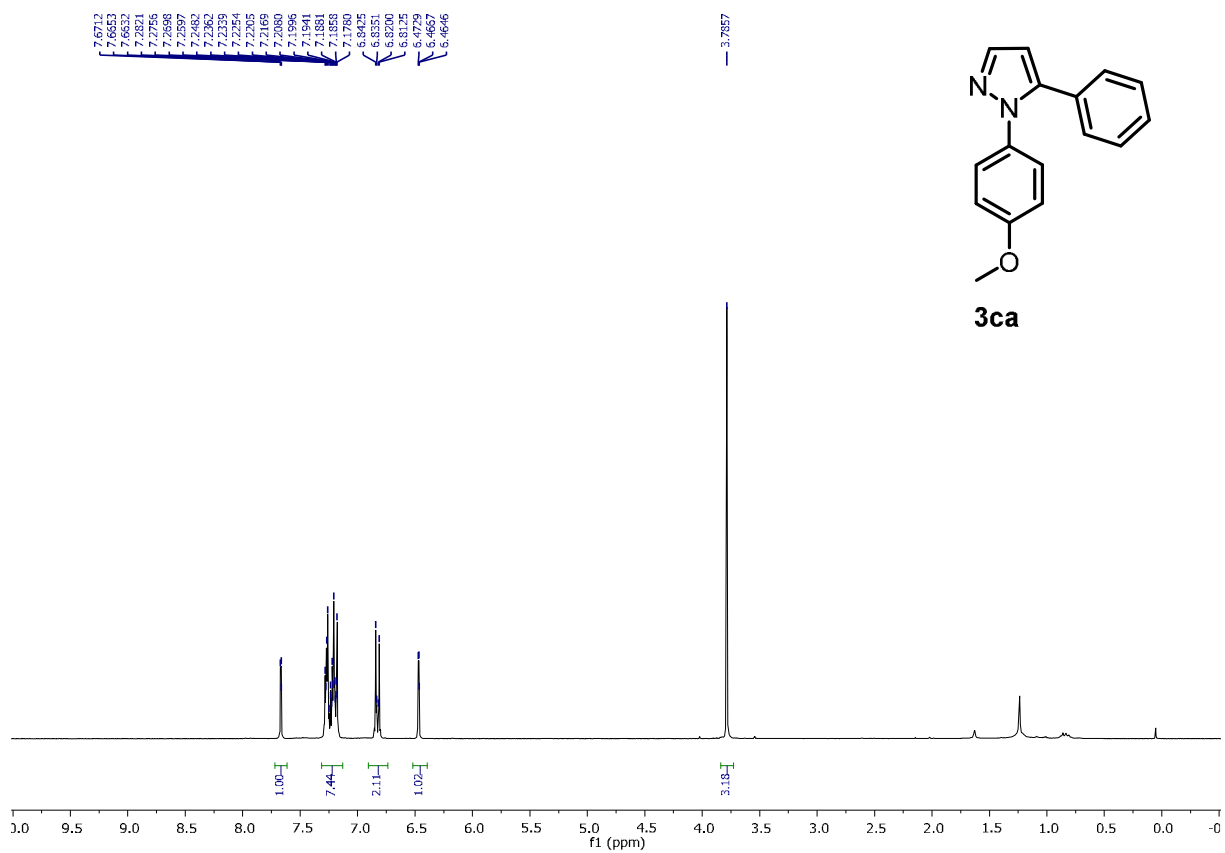
¹H NMR (400 MHz, CDCl₃) of 1-(3-chlorophenyl)-5-(4-methoxyphenyl)-1H-pyrazole



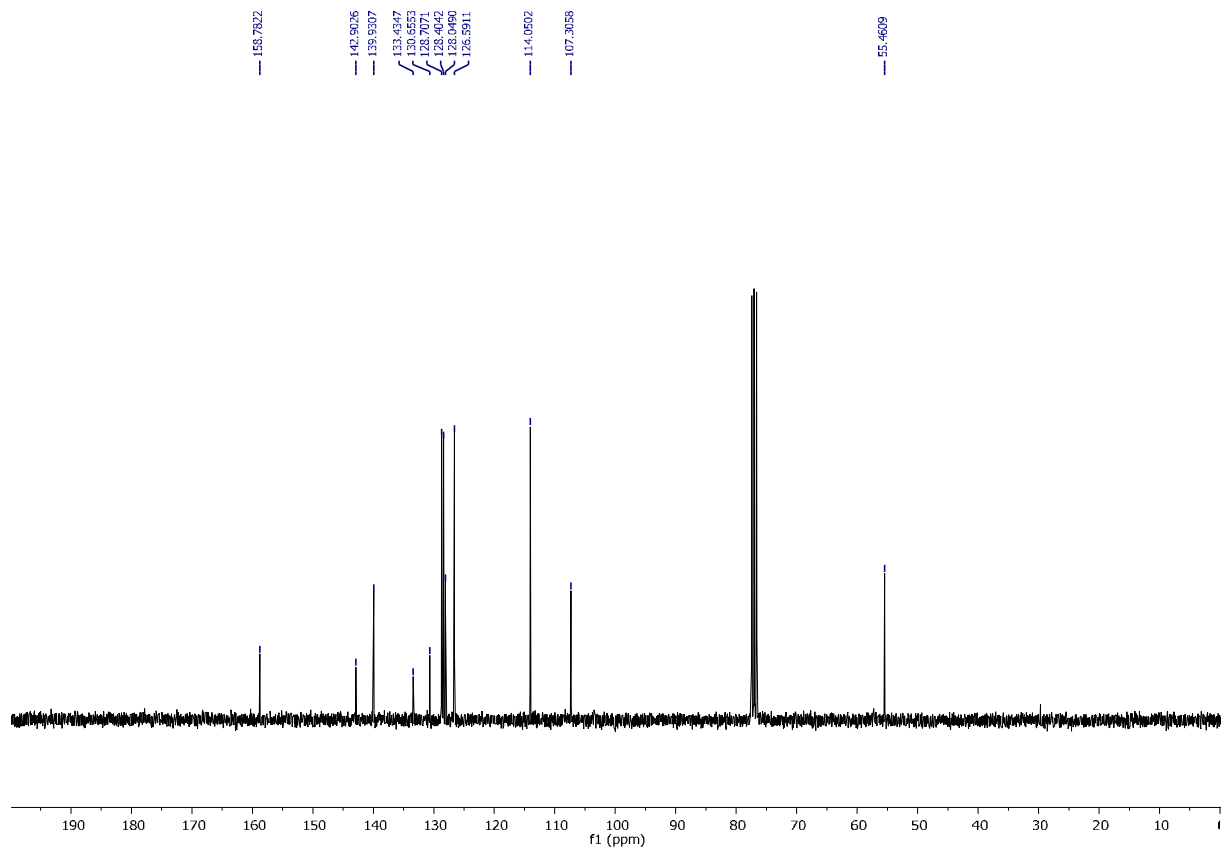
¹³C NMR (100 MHz, CDCl₃) of 1-(3-chlorophenyl)-5-(4-methoxyphenyl)-1H-pyrazole



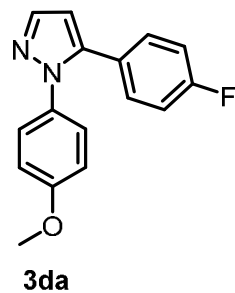
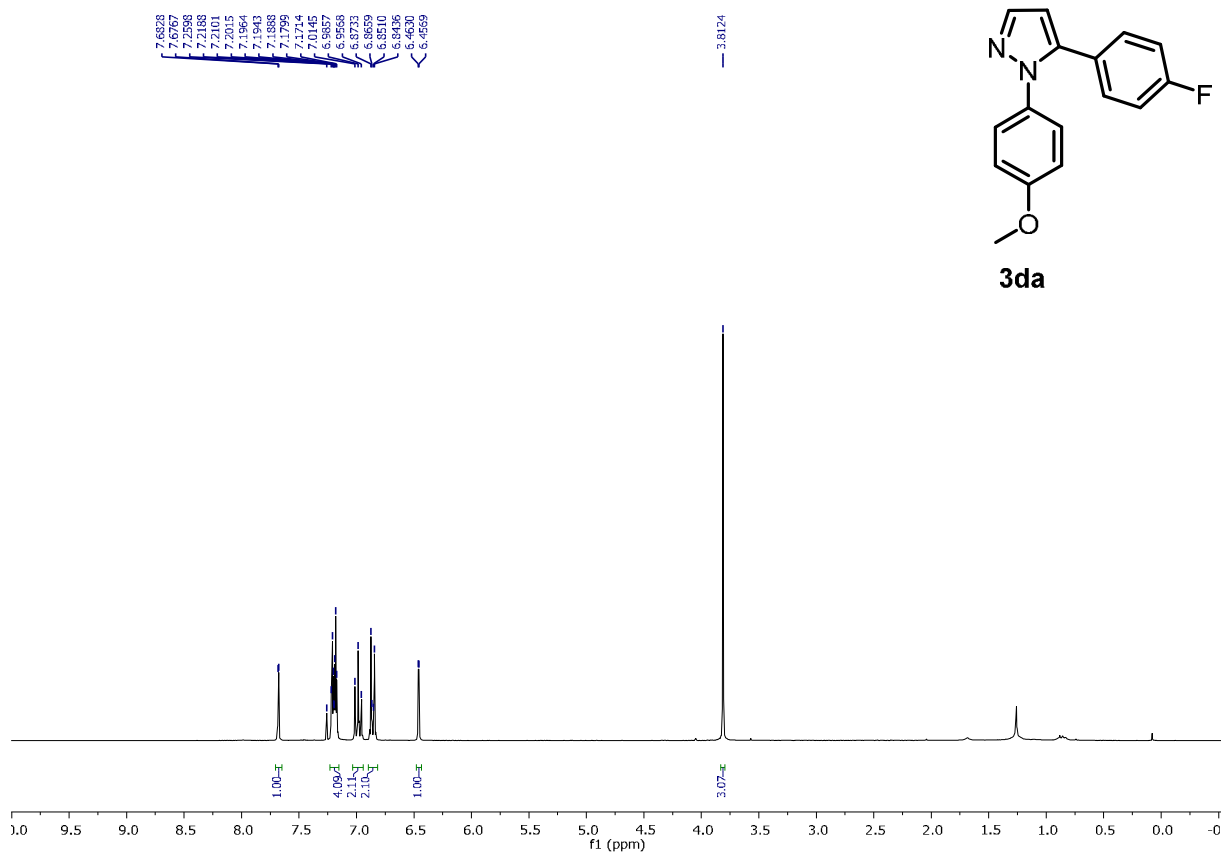
¹H NMR (300 MHz, CDCl₃) of 1-(4-methoxyphenyl)-5-(p-tolyl)-1H-pyrazole



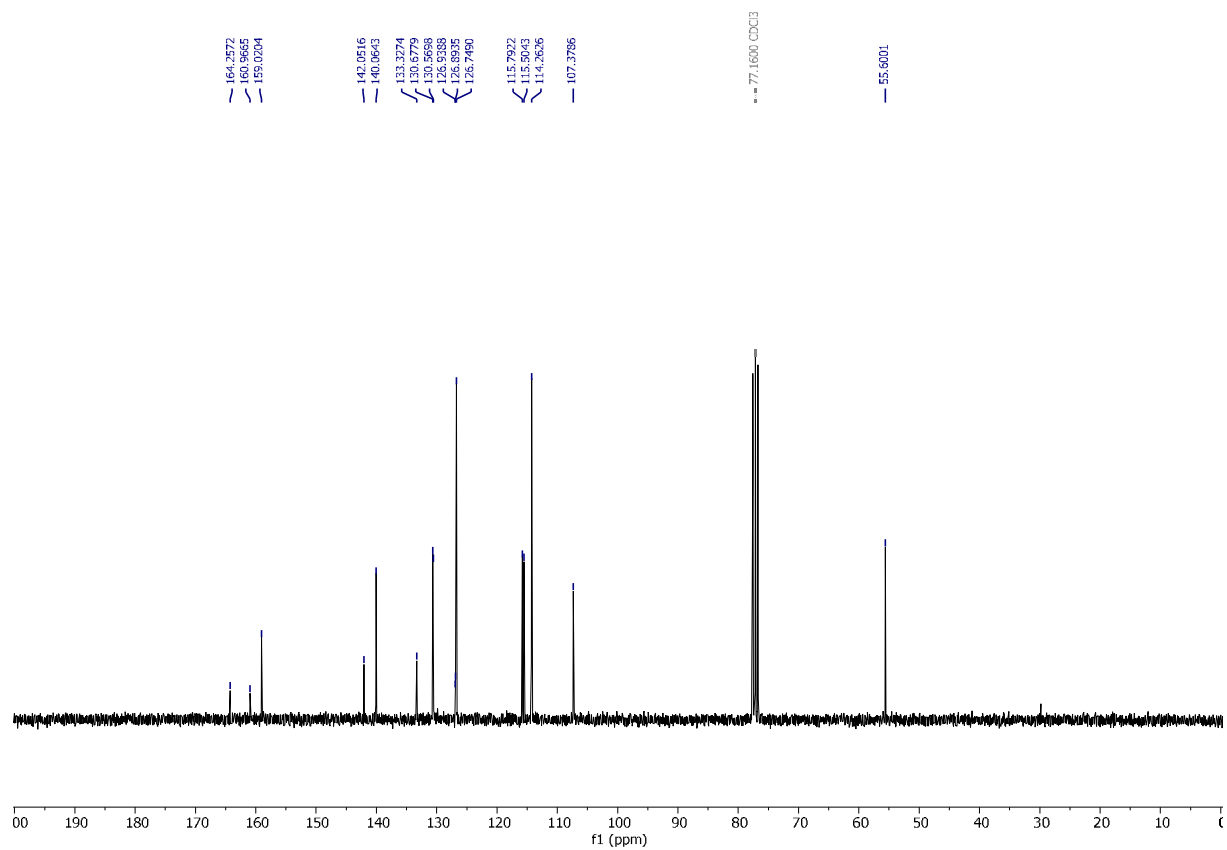
¹H NMR (300 MHz, CDCl₃) of 1-(4-methoxyphenyl)-5-phenyl-1H-pyrazole



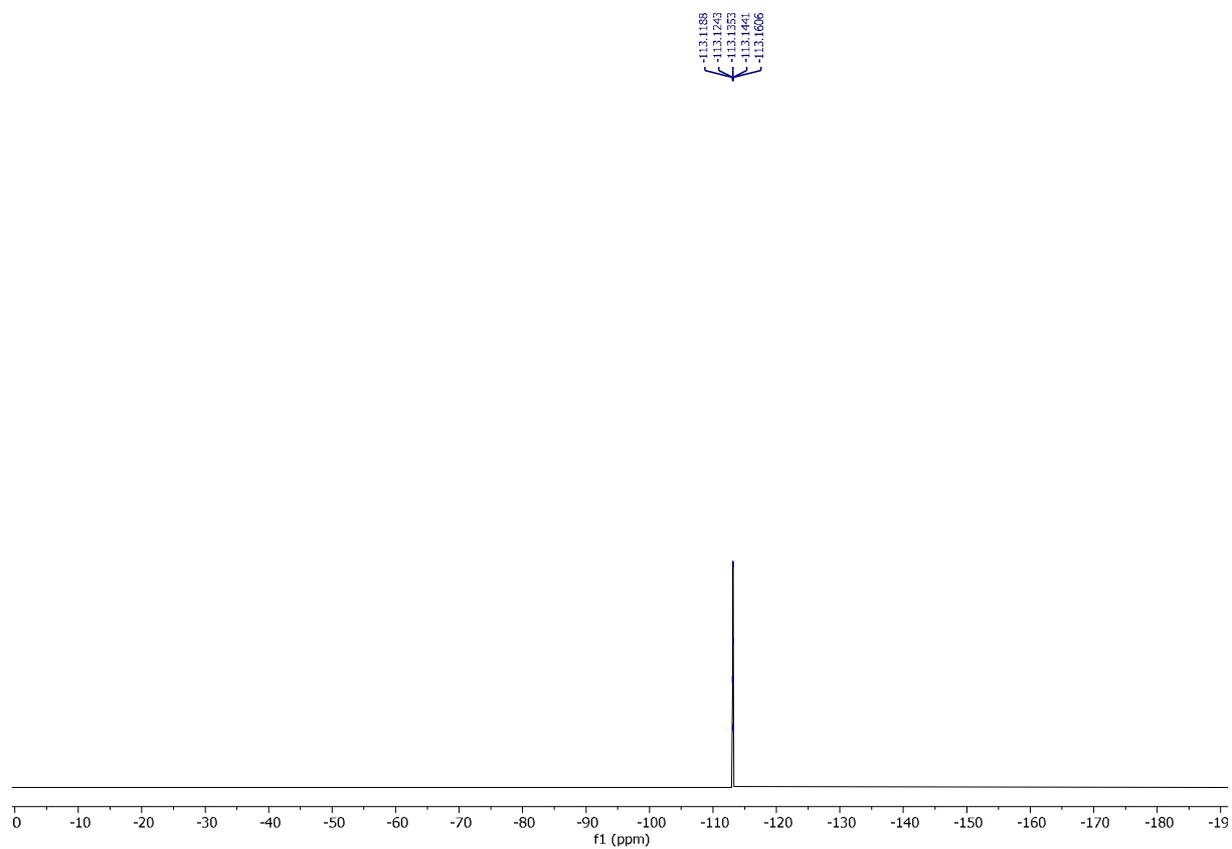
¹³C NMR (100 MHz, CDCl₃) of 1-(4-methoxyphenyl)-5-phenyl-1H-pyrazole



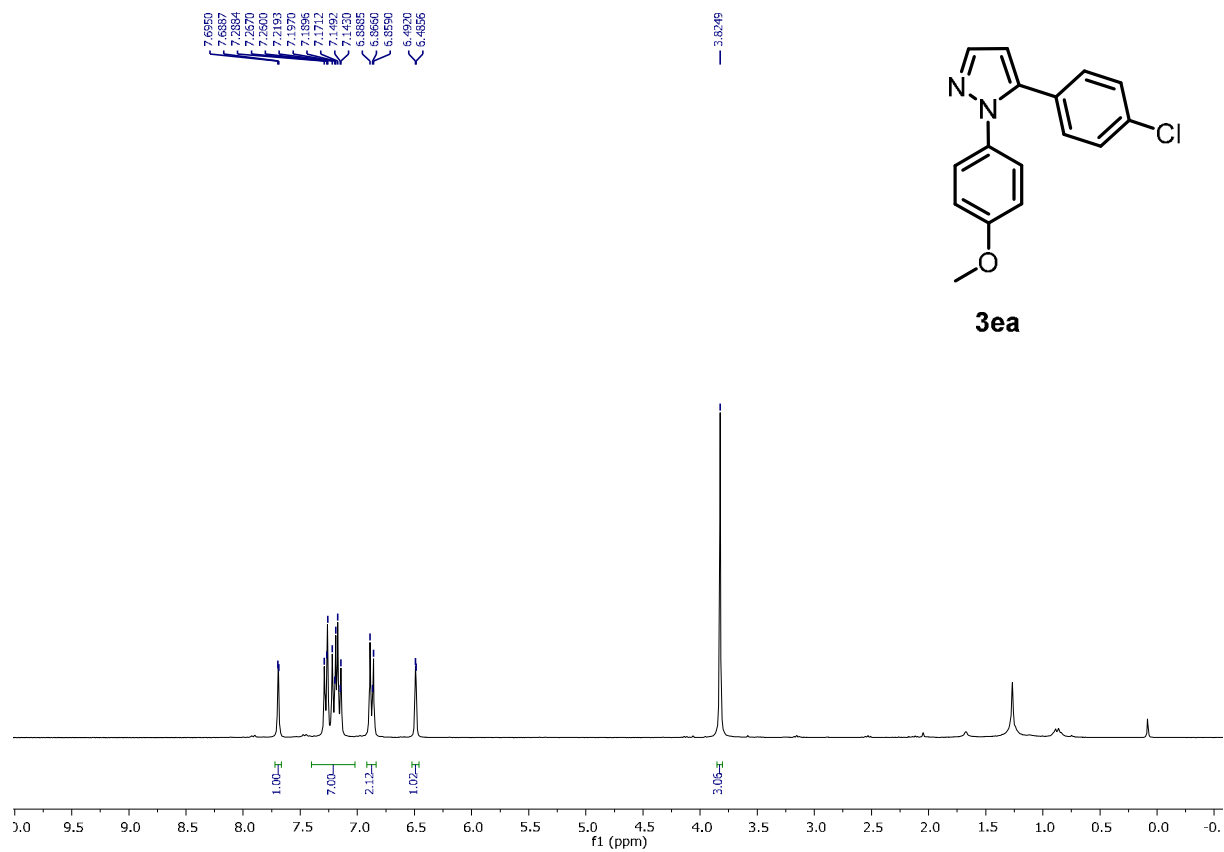
¹H NMR (300 MHz, CDCl₃) of 5-(4-fluorophenyl)-1-(4-methoxyphenyl)-1H-pyrazole



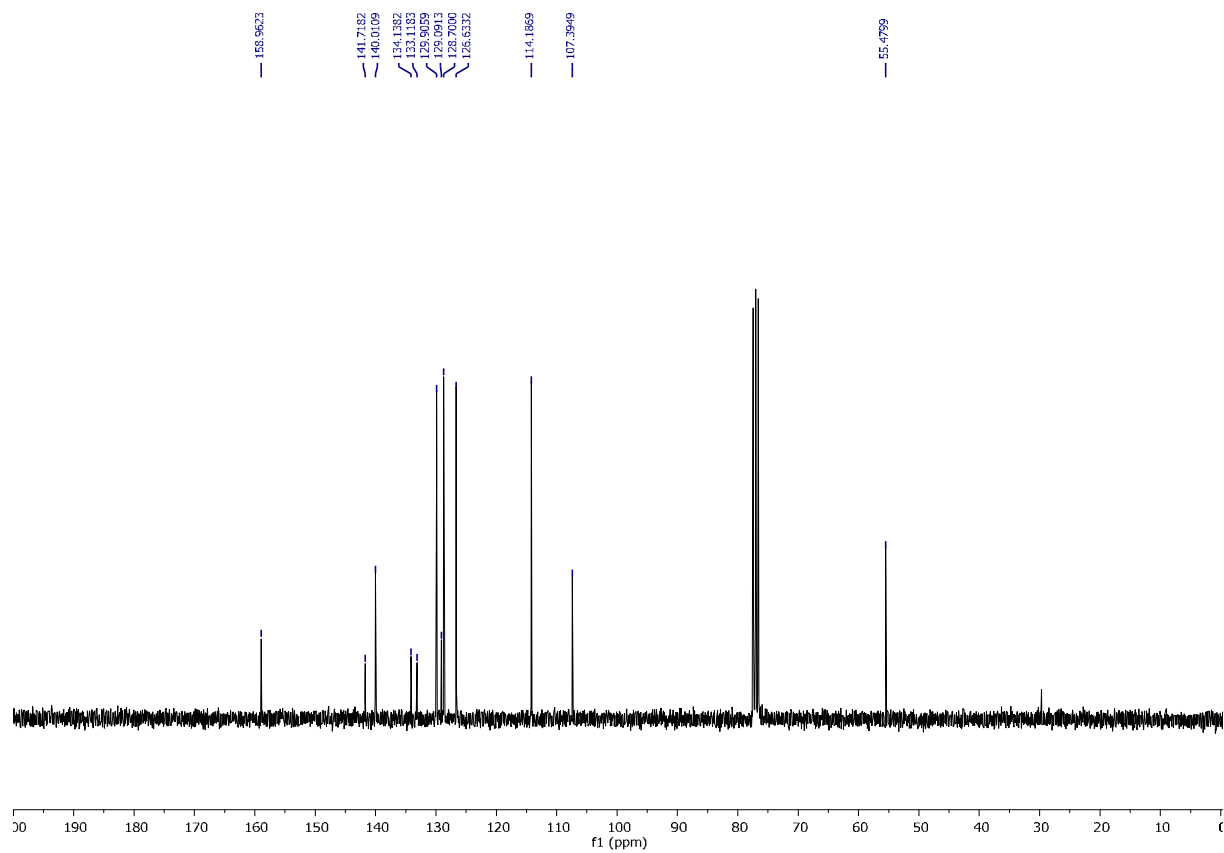
¹³C NMR (100 MHz, CDCl₃) of 5-(4-fluorophenyl)-1-(4-methoxyphenyl)-1H-pyrazole



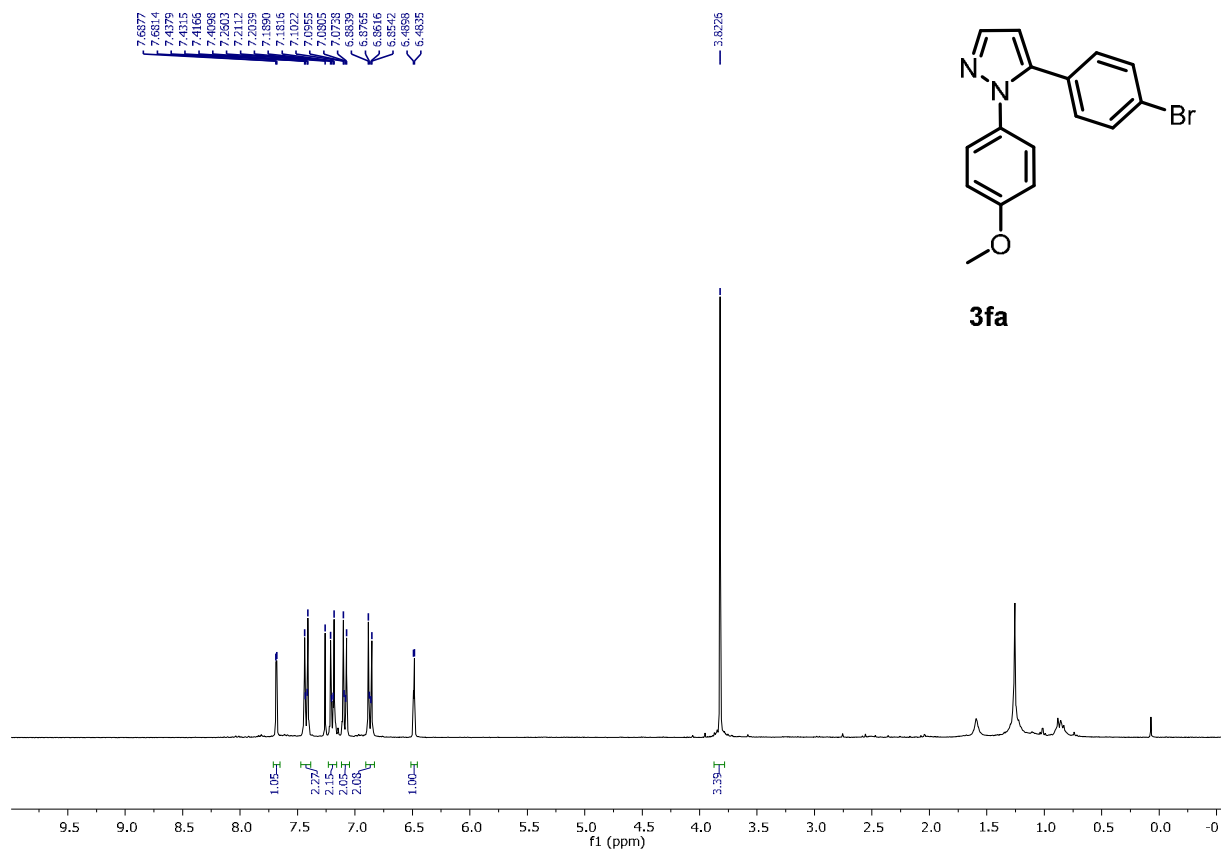
¹⁹F NMR (376.5 MHz, CDCl₃) of 5-(4-fluorophenyl)-1-(4-methoxyphenyl)-1H-pyrazole



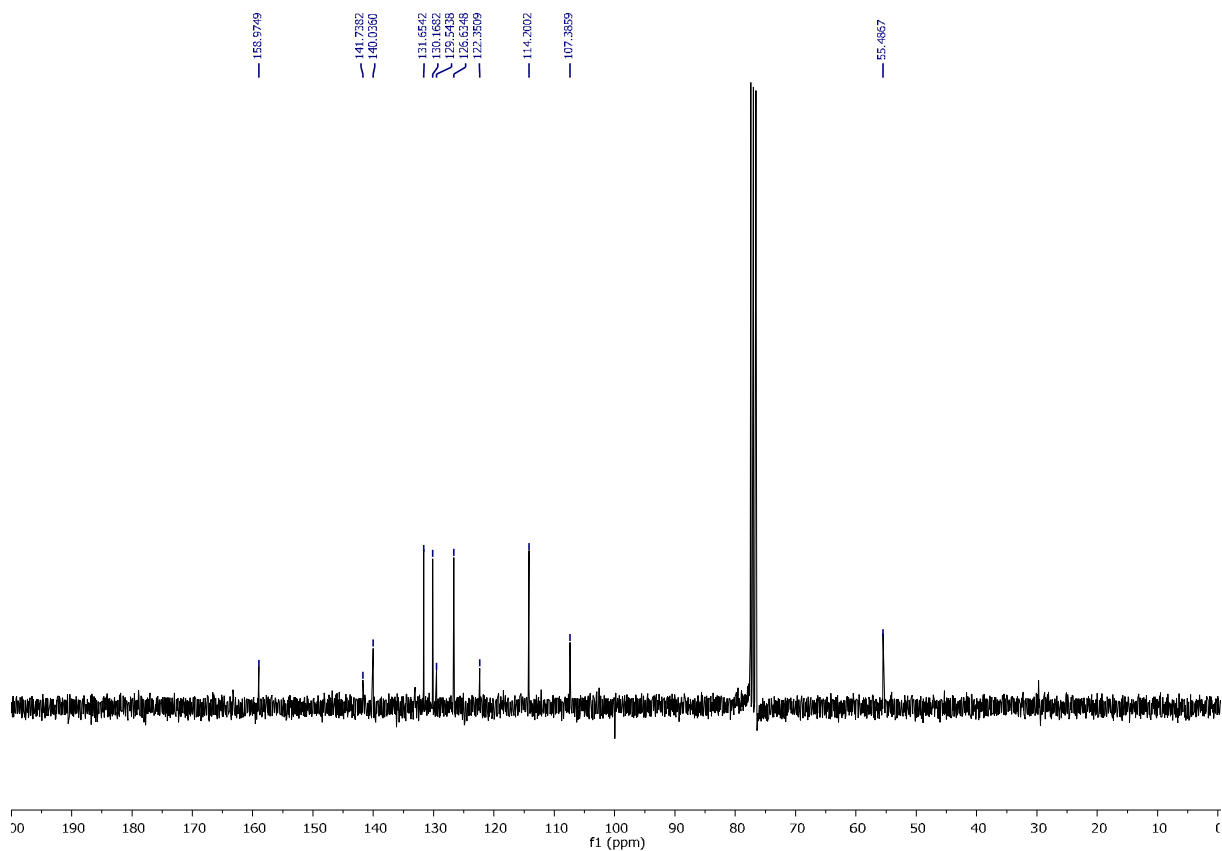
¹H NMR (300 MHz, CDCl₃) of 5-(4-chlorophenyl)-1-(4-methoxyphenyl)-1H-pyrazole



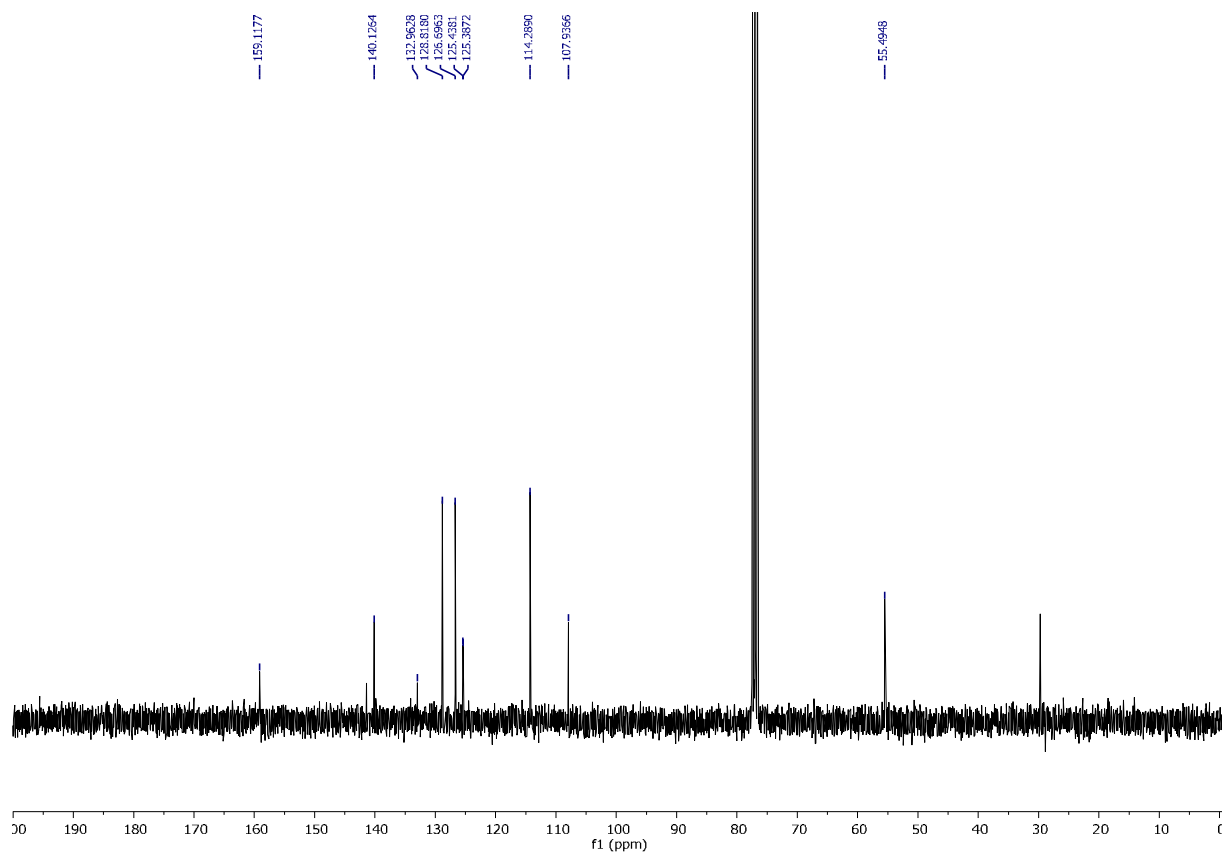
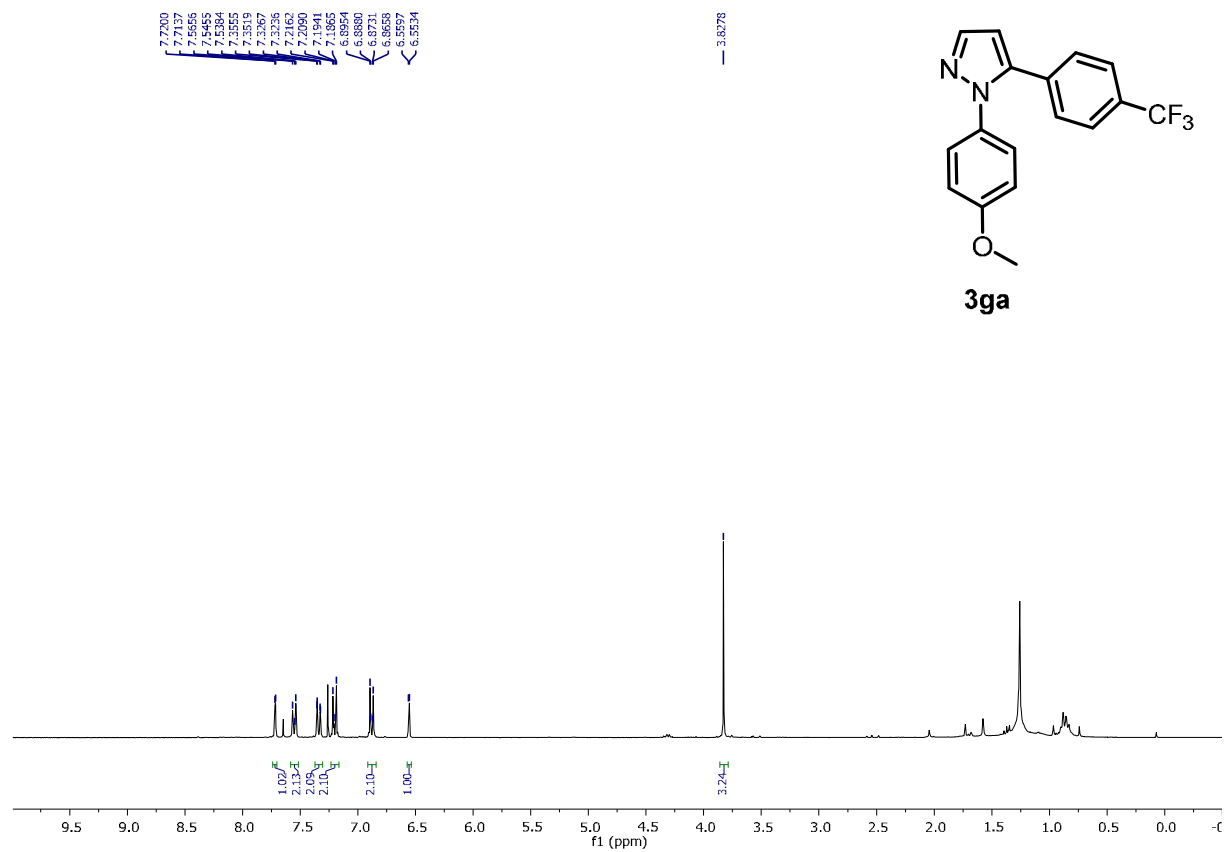
¹³C NMR (100 MHz, CDCl₃) of 5-(4-chlorophenyl)-1-(4-methoxyphenyl)-1H-pyrazole

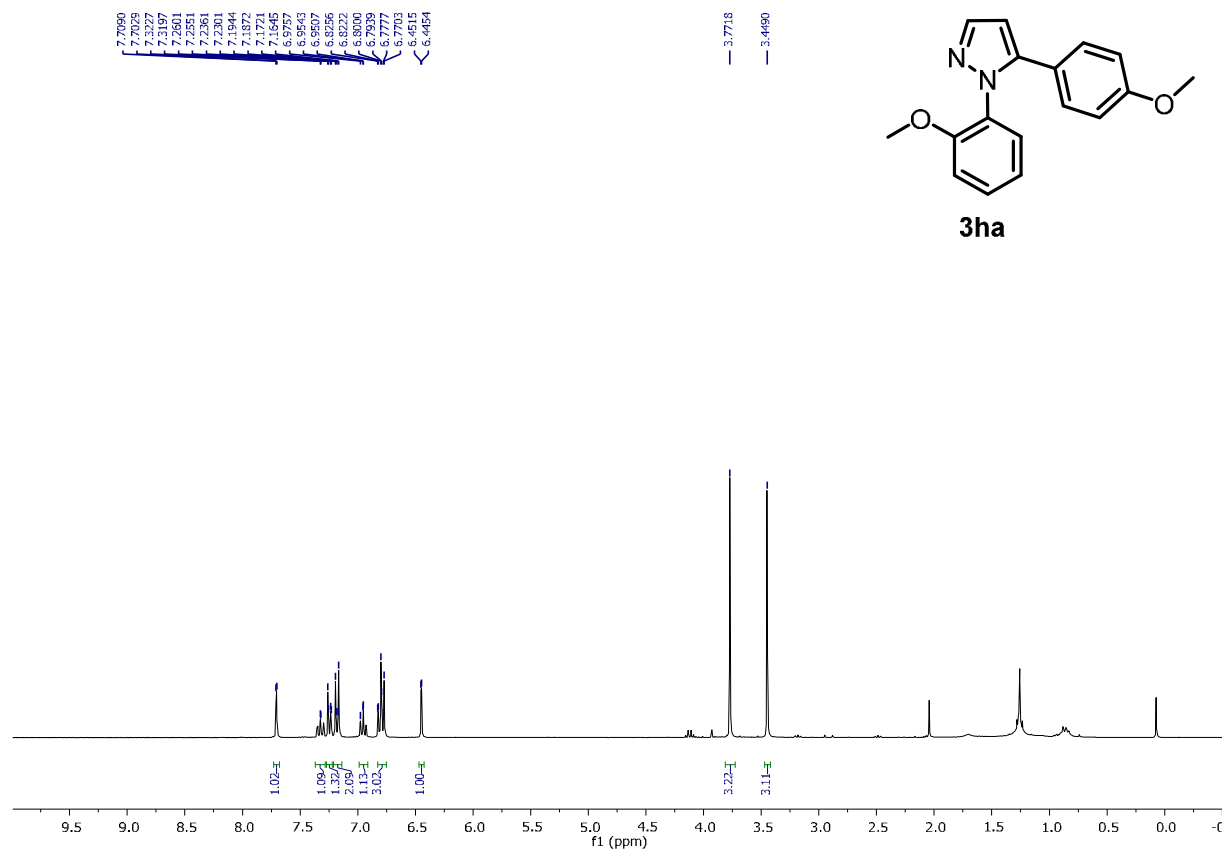


¹H NMR (300 MHz, CDCl₃) of 5-(4-bromophenyl)-1-(4-methoxyphenyl)-1H-pyrazole

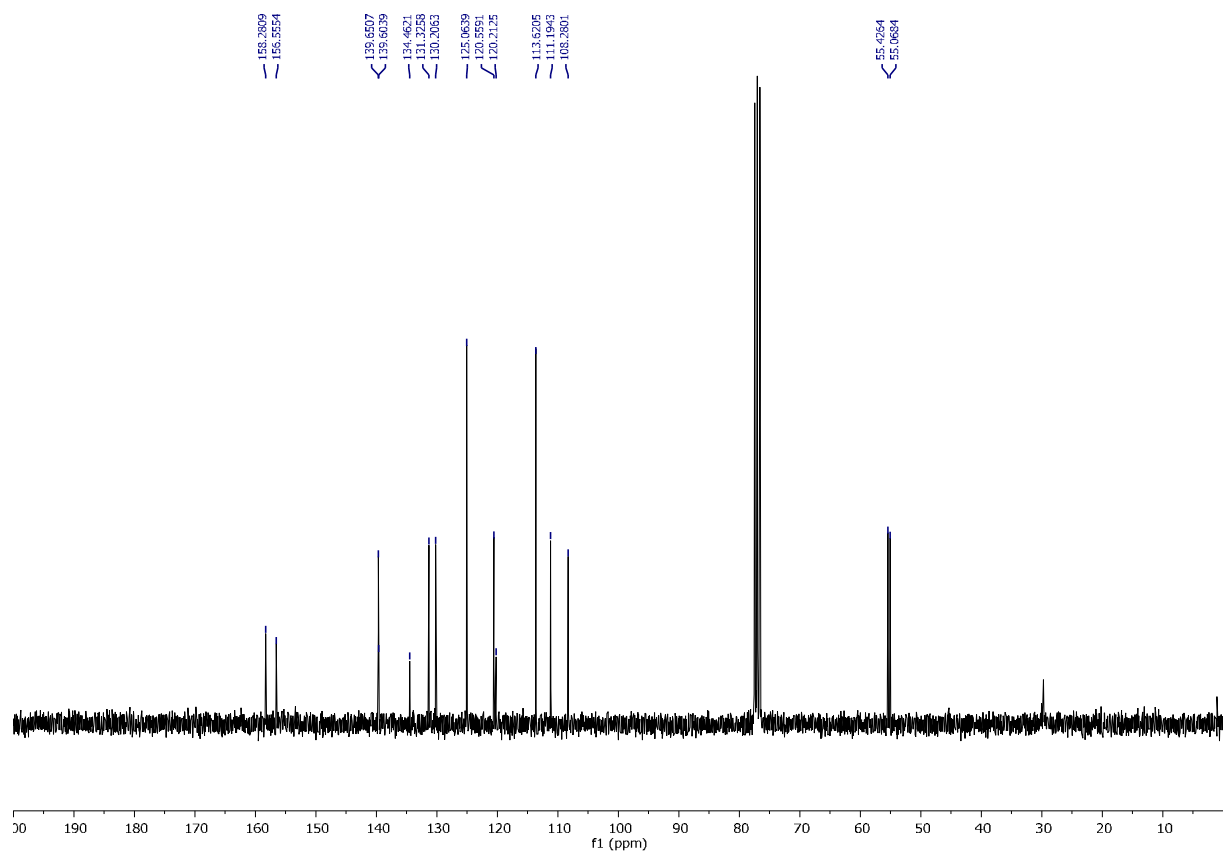


¹³C NMR (100 MHz, CDCl₃) of 5-(4-bromophenyl)-1-(4-methoxyphenyl)-1H-pyrazole

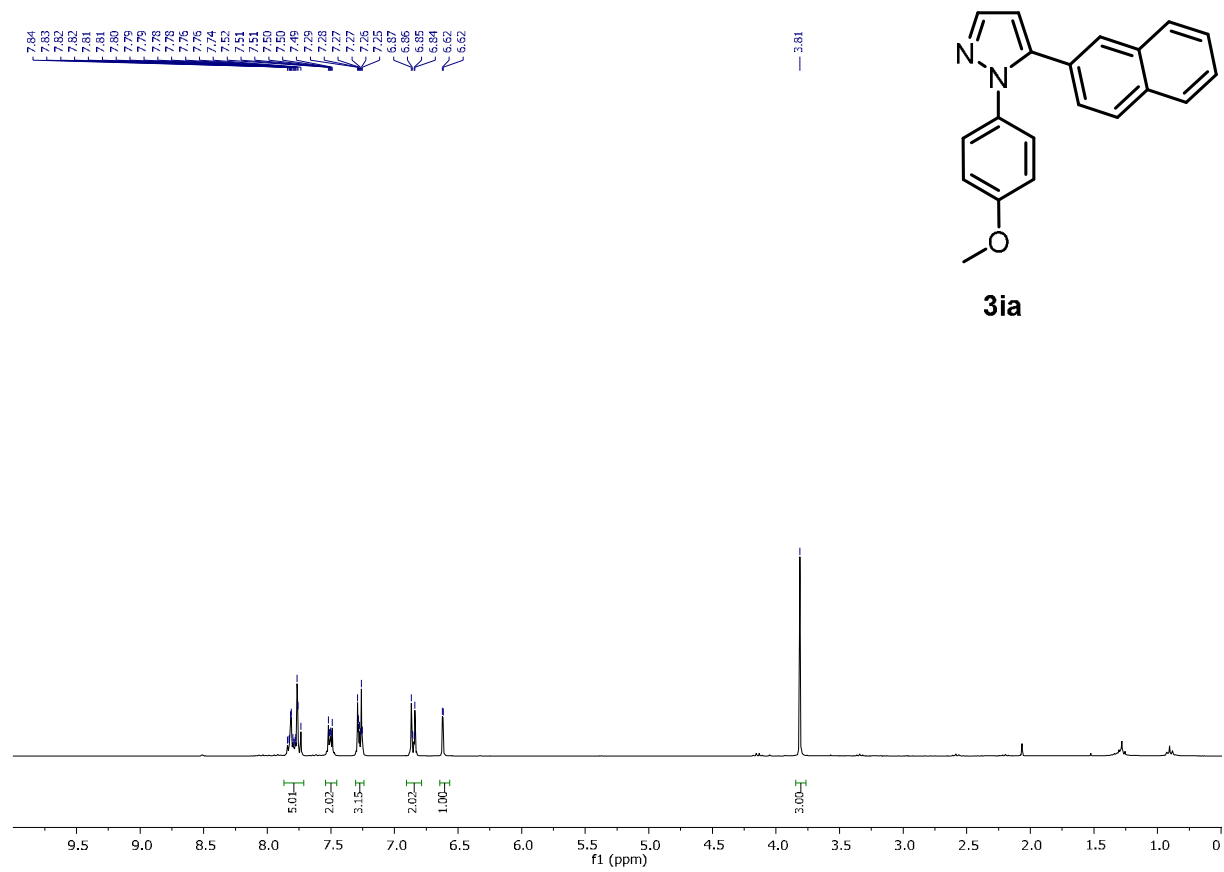




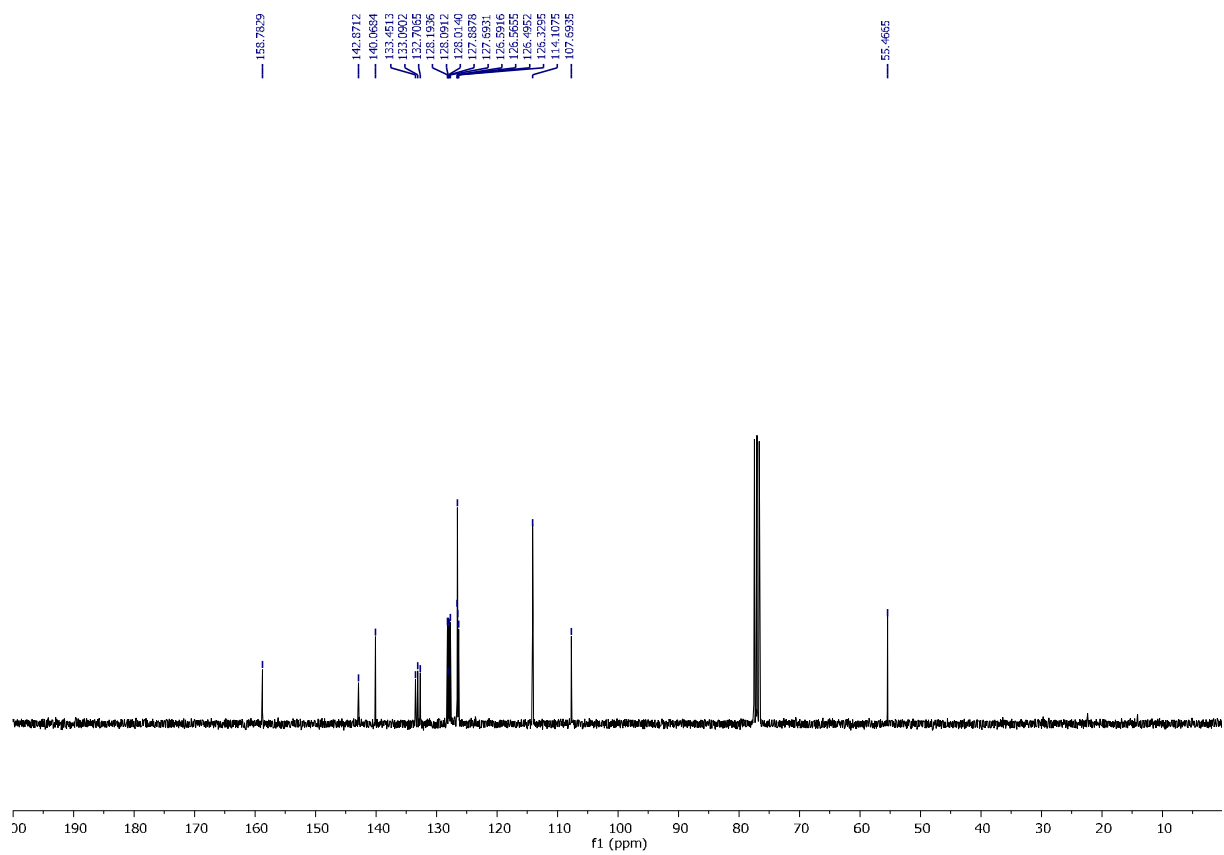
¹H NMR (300 MHz, CDCl₃) of 1-(4-methoxyphenyl)-5-(2-methoxyphenyl)-1H-pyrazole



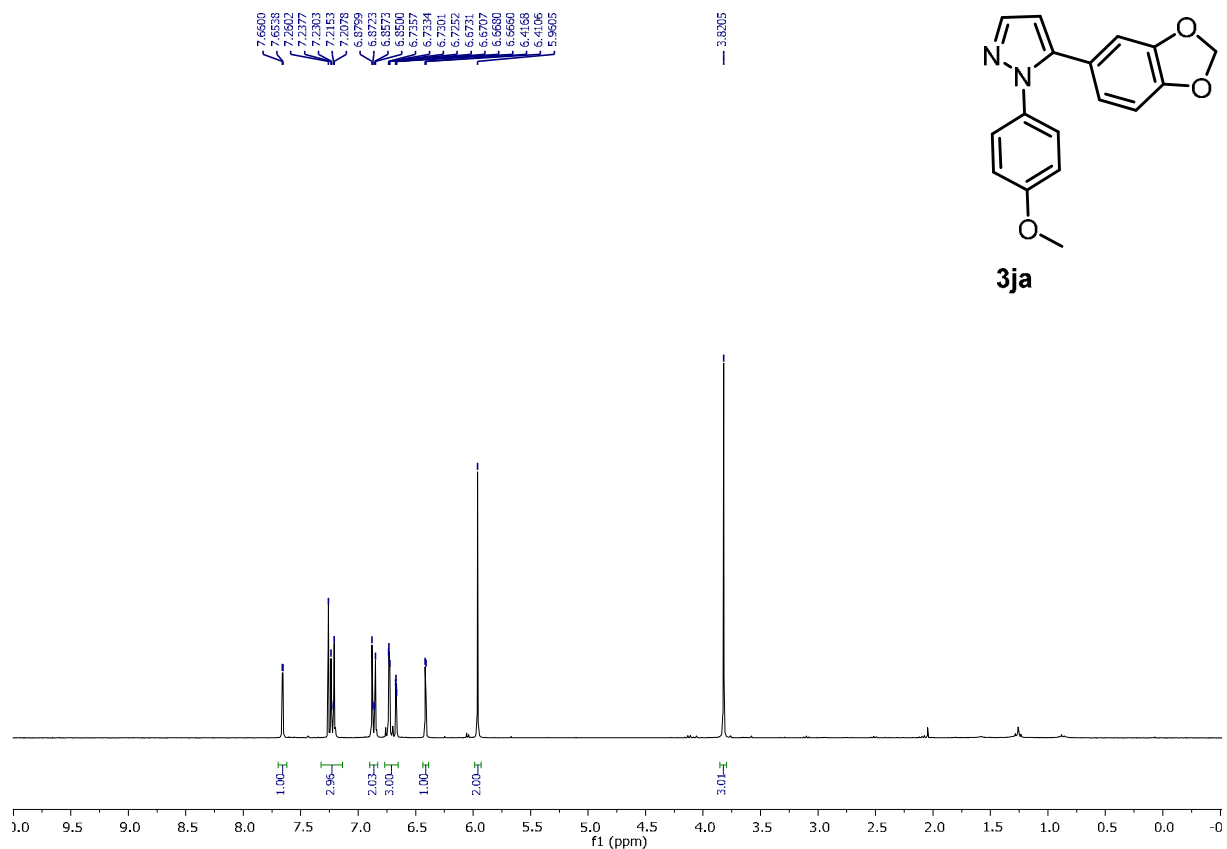
¹³C NMR (75 MHz, CDCl₃) of 1-(4-methoxyphenyl)-5-(2-methoxyphenyl)-1H-pyrazole



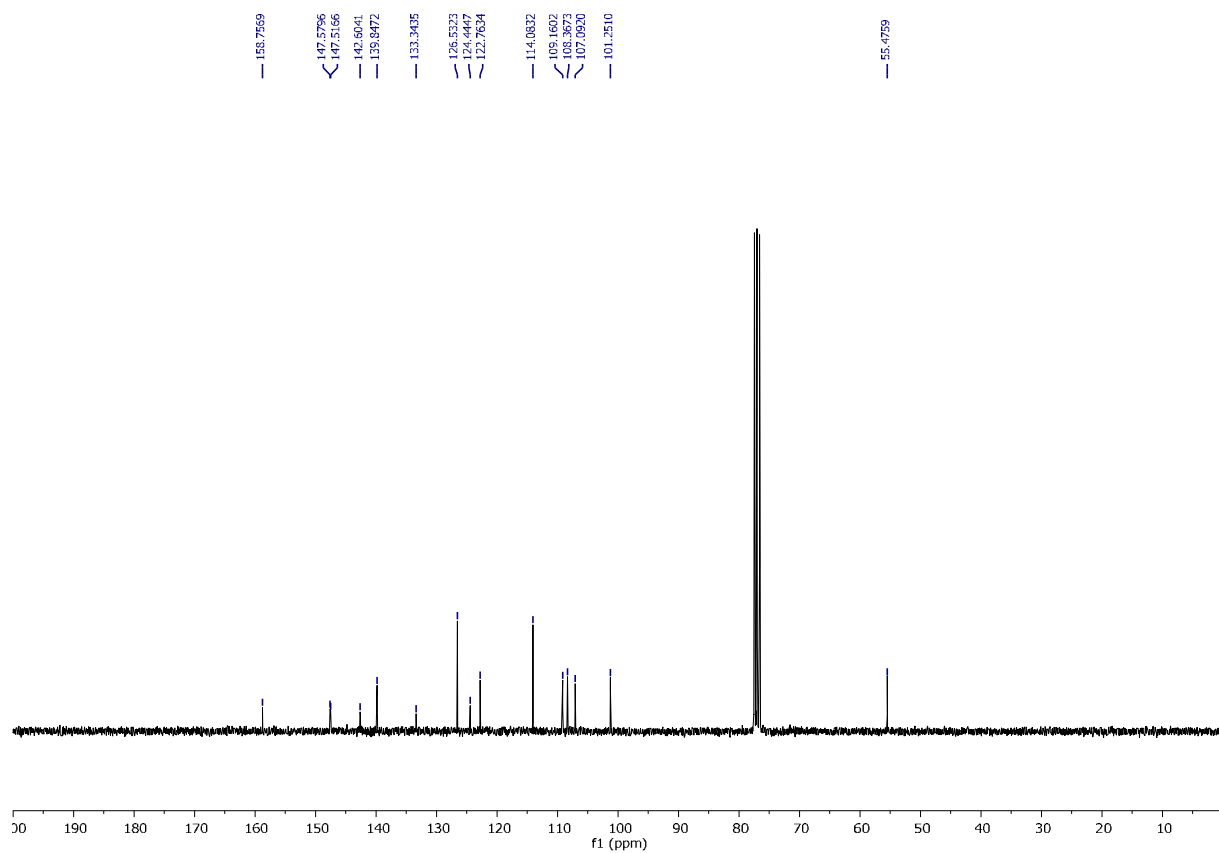
¹H NMR (300 MHz, CDCl₃) of 1-(4-methoxyphenyl)-5-(naphthalen-2-yl)-1H-pyrazole



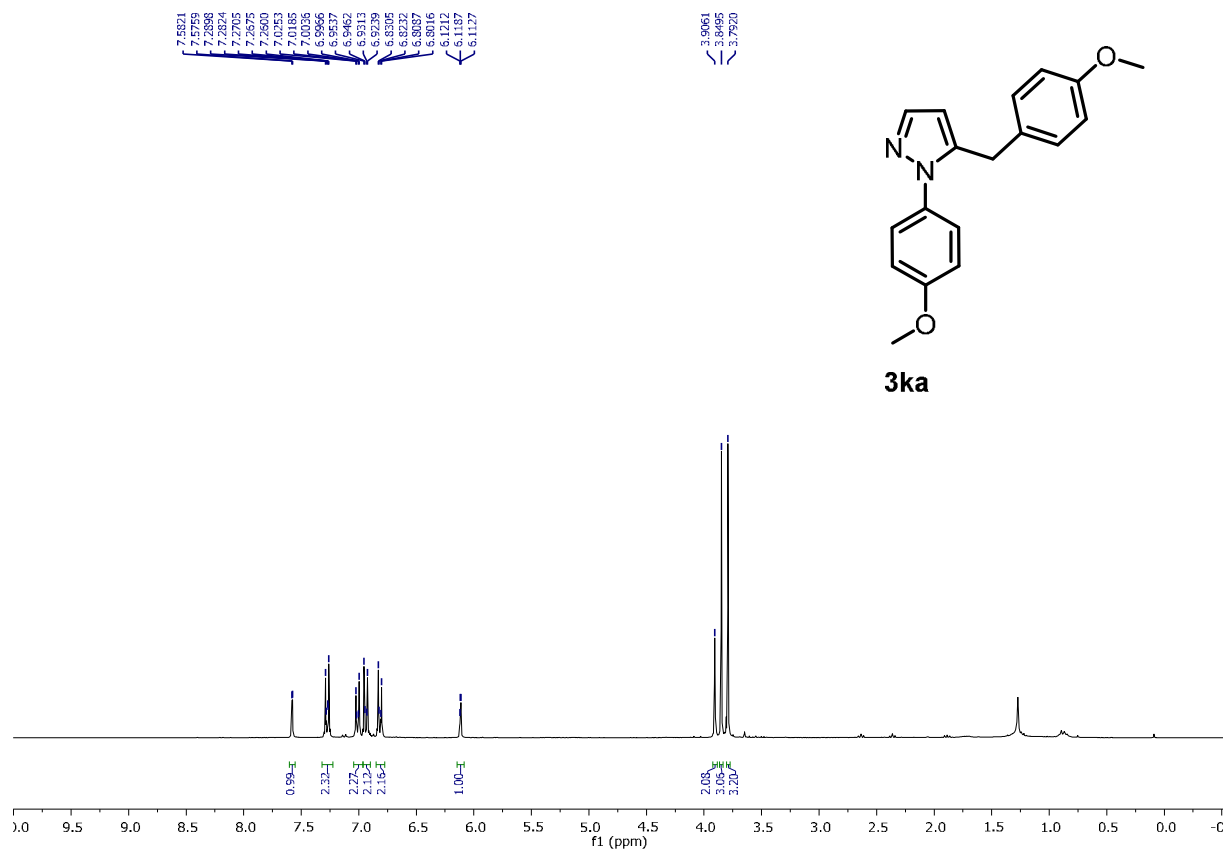
¹³C NMR (75 MHz, CDCl₃) of 1-(4-methoxyphenyl)-5-(naphthalen-2-yl)-1H-pyrazole



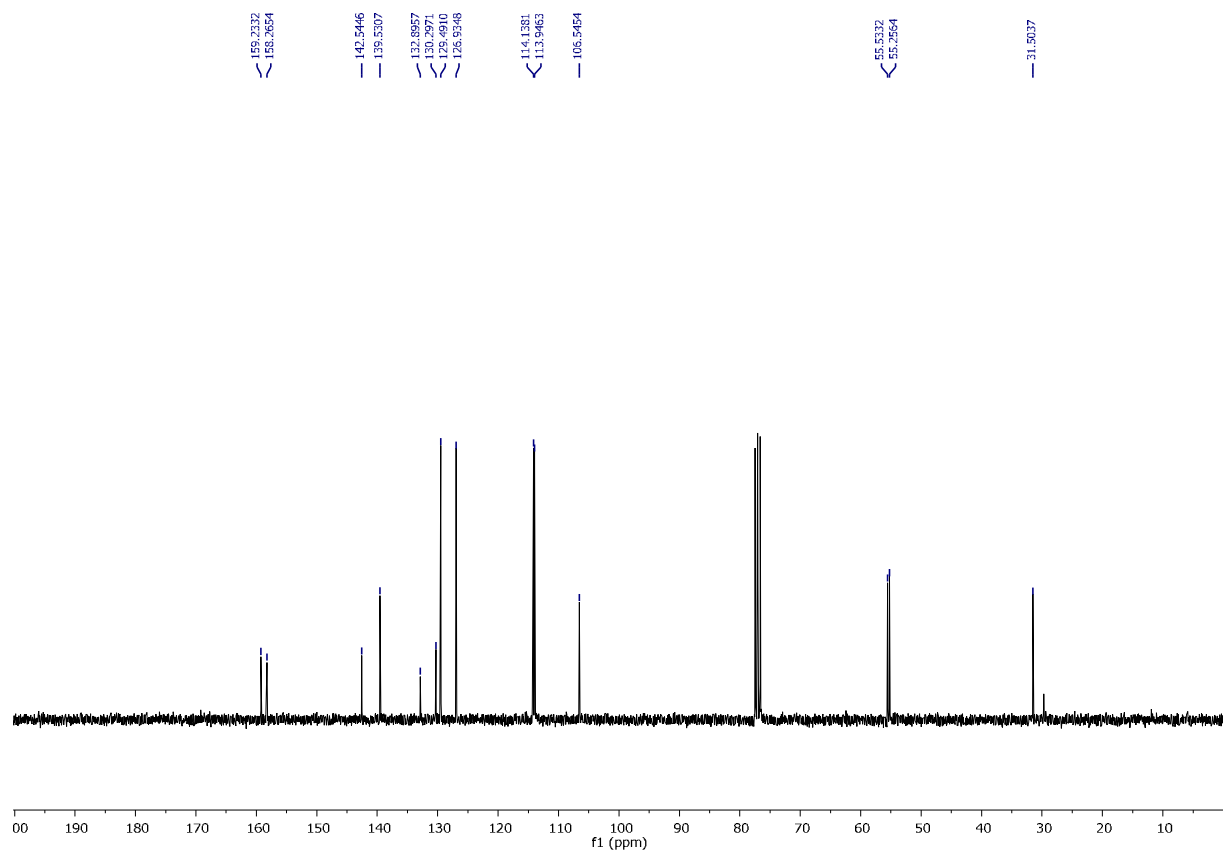
¹H NMR (300 MHz, CDCl₃) of 5-(benzo[d][1,3]dioxol-5-yl)-1-(4-methoxyphenyl)-1H-pyrazole



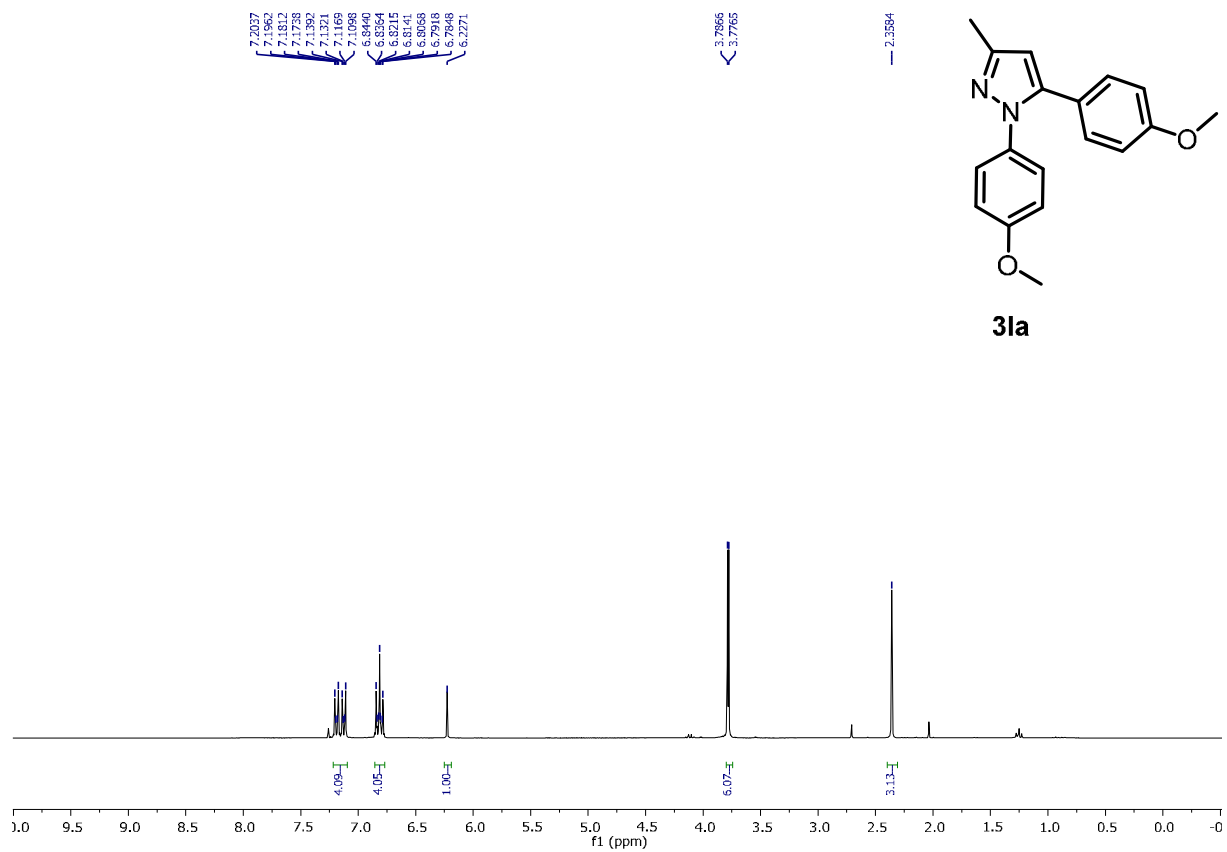
¹³C NMR (75 MHz, CDCl₃) of 5-(benzo[d][1,3]dioxol-5-yl)-1-(4-methoxyphenyl)-1H-pyrazole



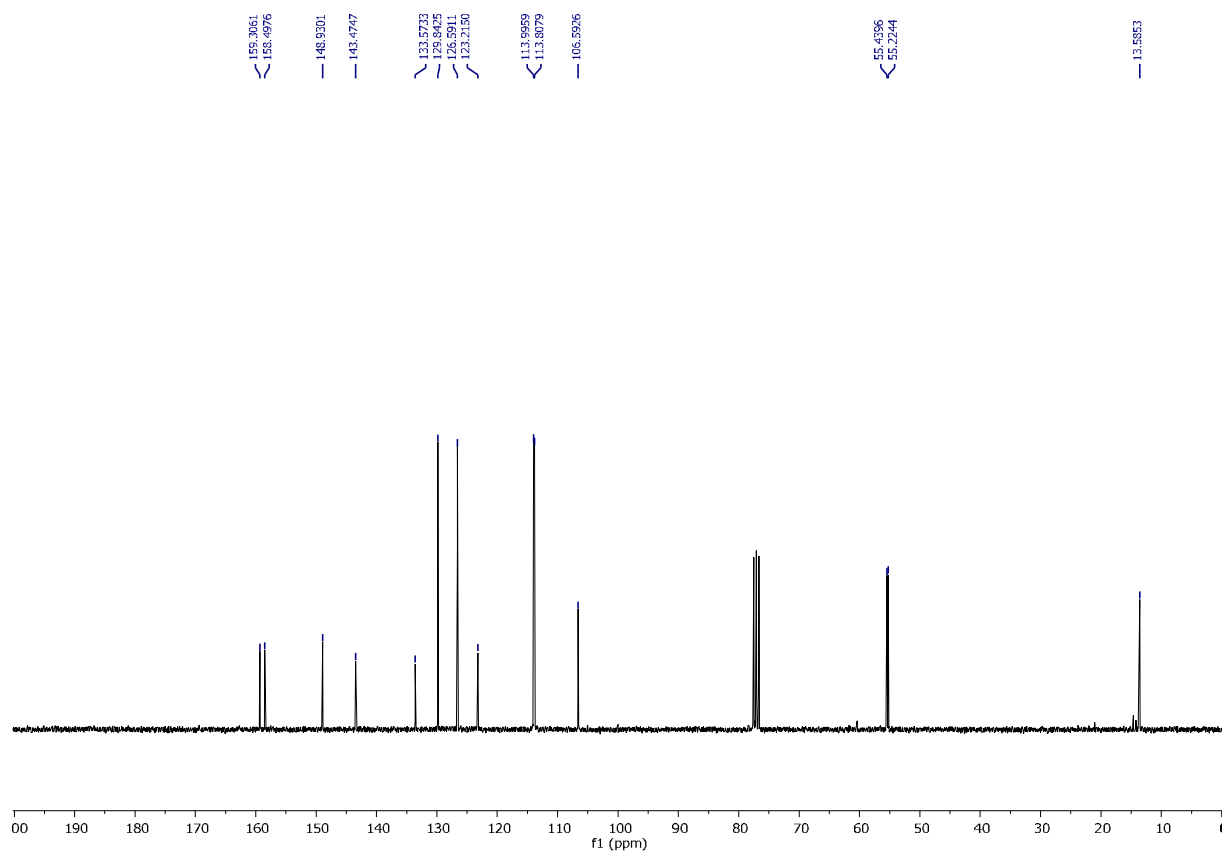
¹H NMR (300 MHz, CDCl₃) of 5-(4-methoxybenzyl)-1-(4-methoxyphenyl)-1H-pyrazole



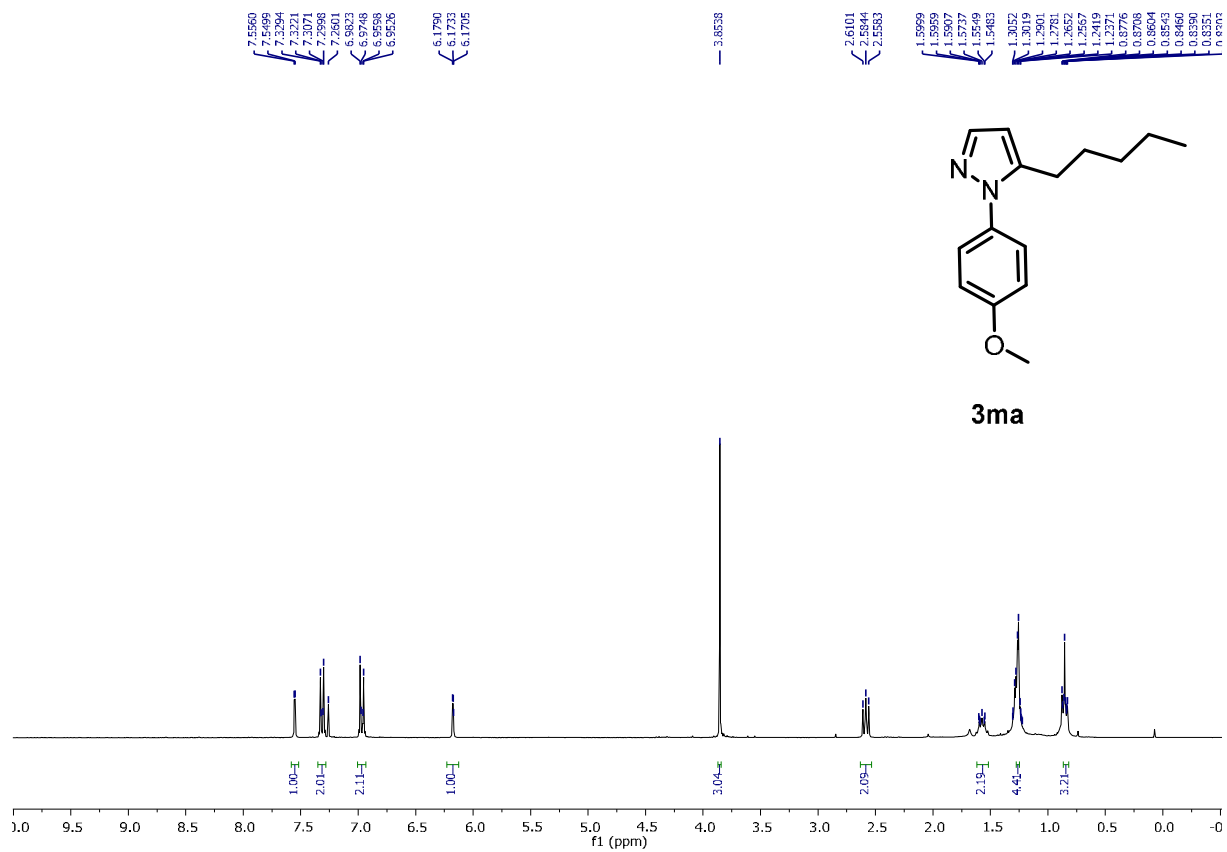
¹³C NMR (100 MHz, CDCl₃) of 5-(4-methoxybenzyl)-1-(4-methoxyphenyl)-1H-pyrazole



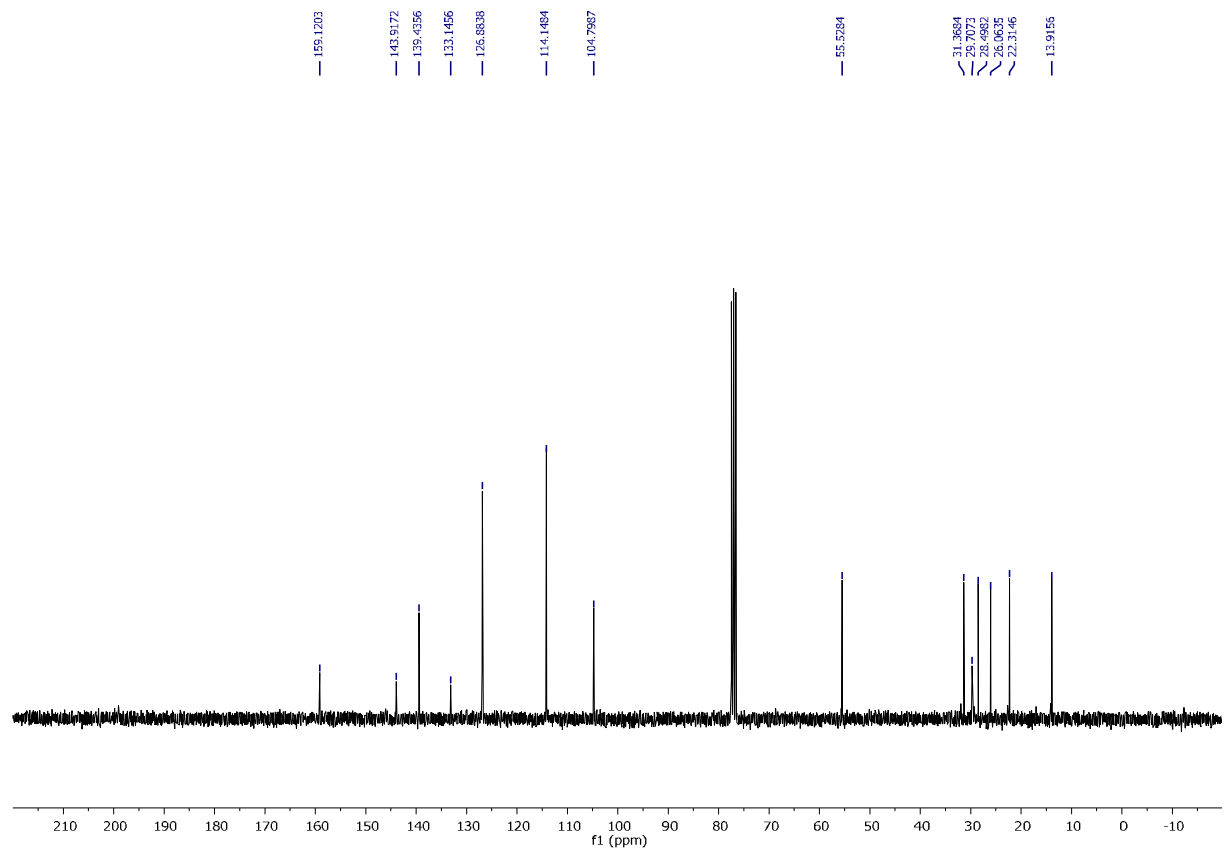
1H NMR (300 MHz, CDCl₃) of 1,5-bis(4-methoxyphenyl)-3-methyl-1H-pyrazole



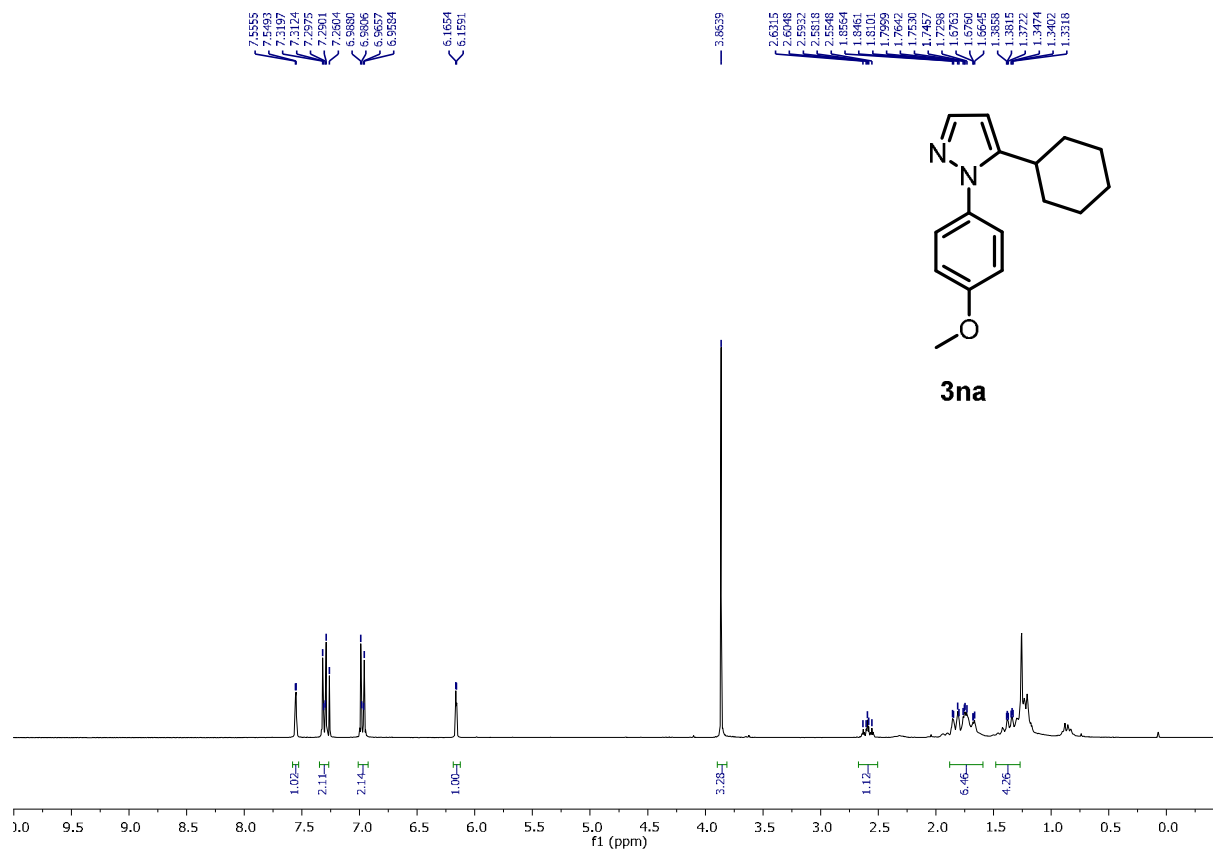
13C NMR (75 MHz, CDCl₃) of 1,5-bis(4-methoxyphenyl)-3-methyl-1H-pyrazole



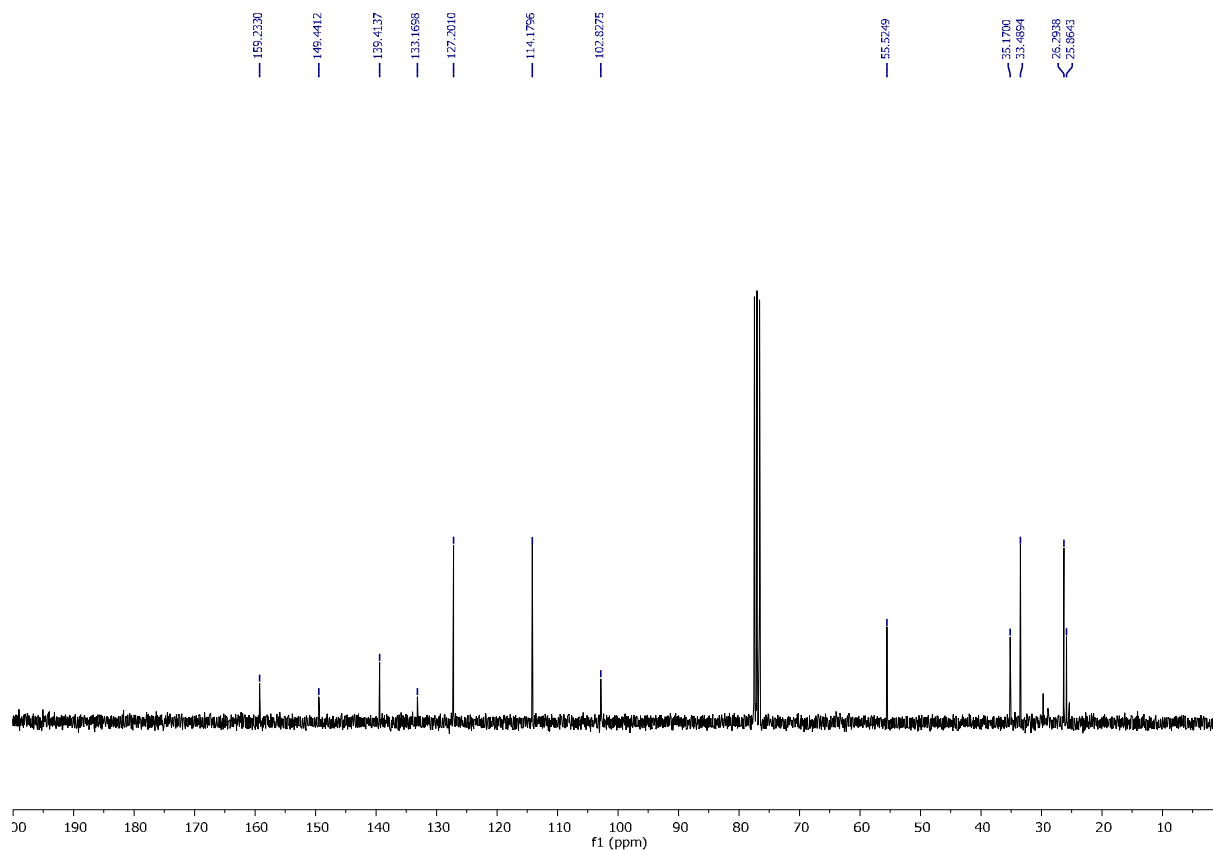
¹H NMR (300 MHz, CDCl₃) of 1-(4-methoxyphenyl)-5-pentyl-1H-pyrazole



¹³C NMR (75 MHz, CDCl₃) of 1-(4-methoxyphenyl)-5-pentyl-1H-pyrazole



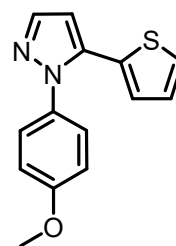
¹H NMR (300 MHz, CDCl₃) of 1-(4-methoxyphenyl)-5-cyclohexyl-1H-pyrazole



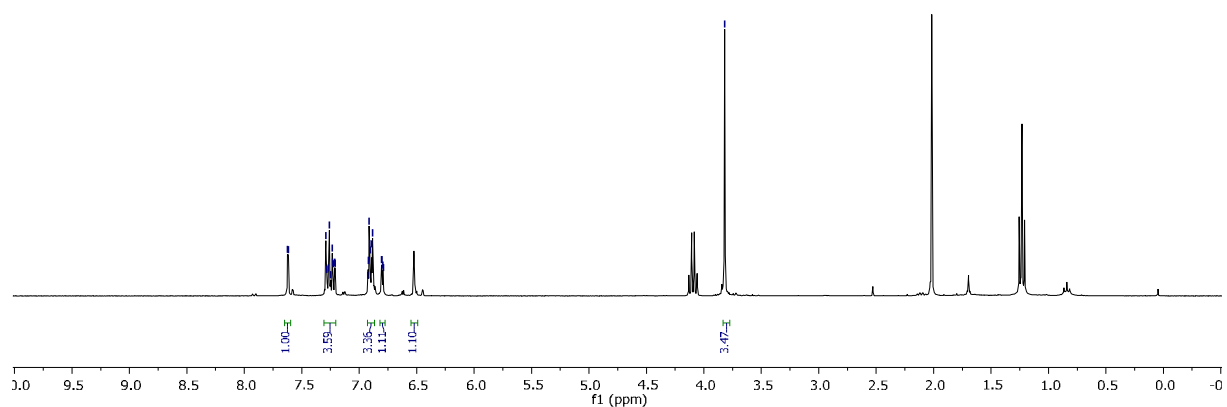
¹³C NMR (100 MHz, CDCl₃) of 1-(4-methoxyphenyl)-5-cyclohexyl-1H-pyrazole

7.6325
7.6171
7.2900
7.2827
7.2676
7.2602
7.2493
7.2352
7.2203
7.2064
7.2137
7.2093
6.9740
6.9709
6.9128
6.9086
6.8875
6.8916
6.8939
6.8958
6.8918
6.7937
6.7896

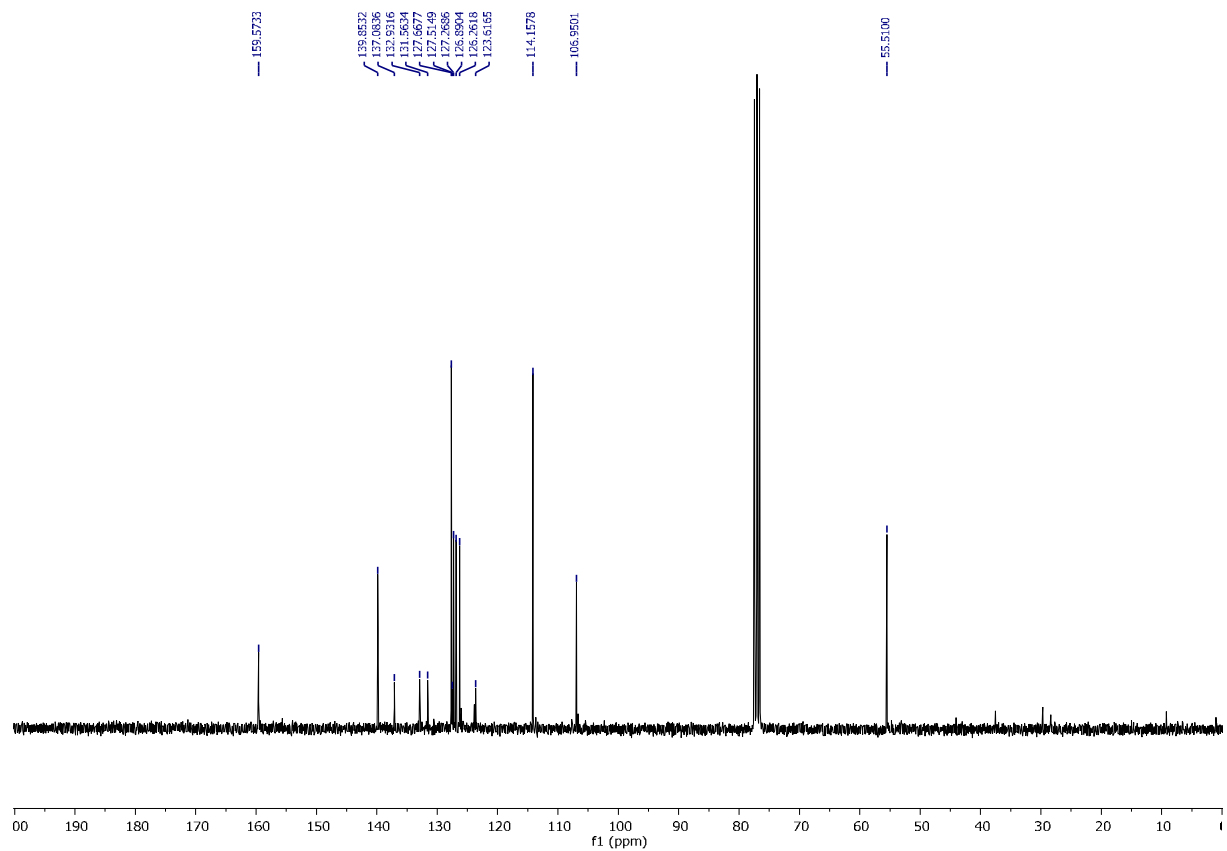
3.8194



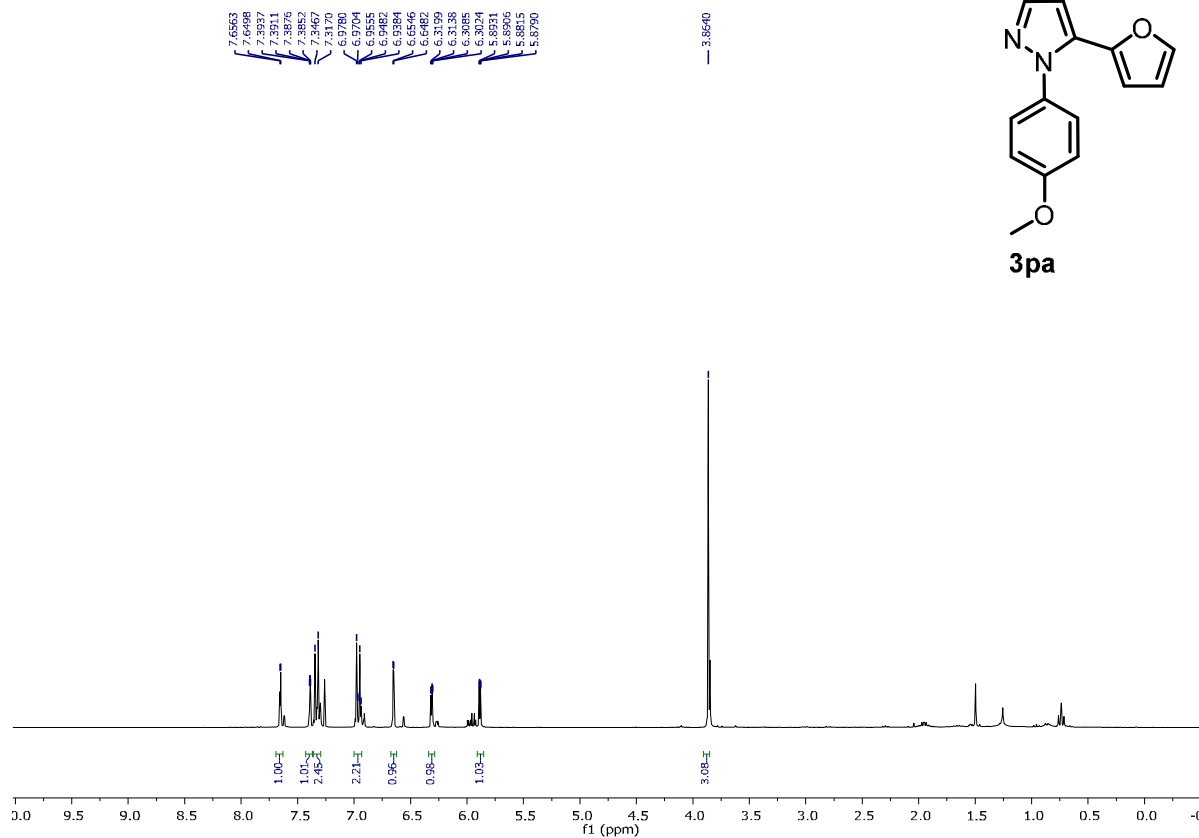
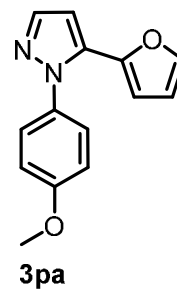
30a



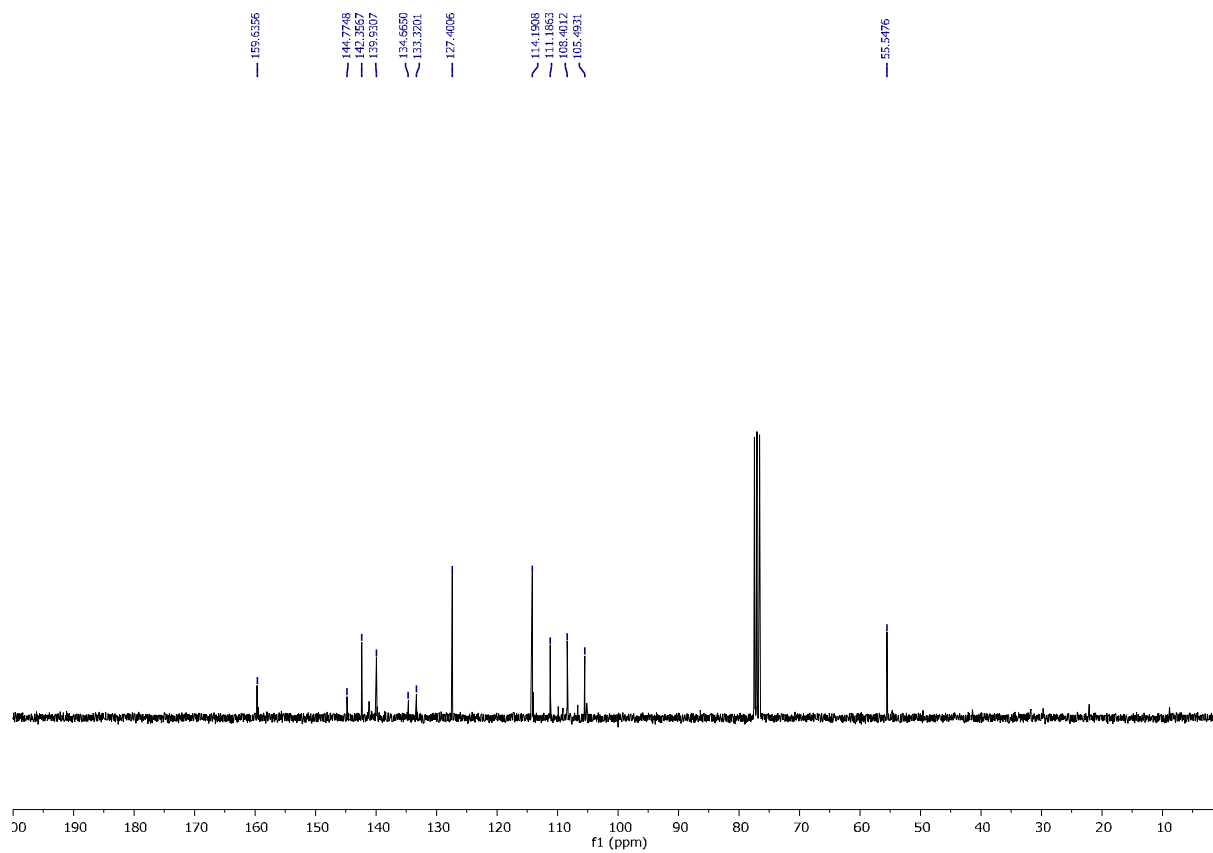
¹H NMR (300 MHz, CDCl₃) of 1-(4-methoxyphenyl)-5-(thiophen-2-yl)-1H-pyrazole



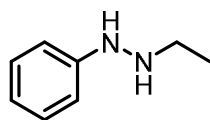
¹³C NMR (100 MHz, CDCl₃) of 1-(4-methoxyphenyl)-5-(thiophen-2-yl)-1H-pyrazole



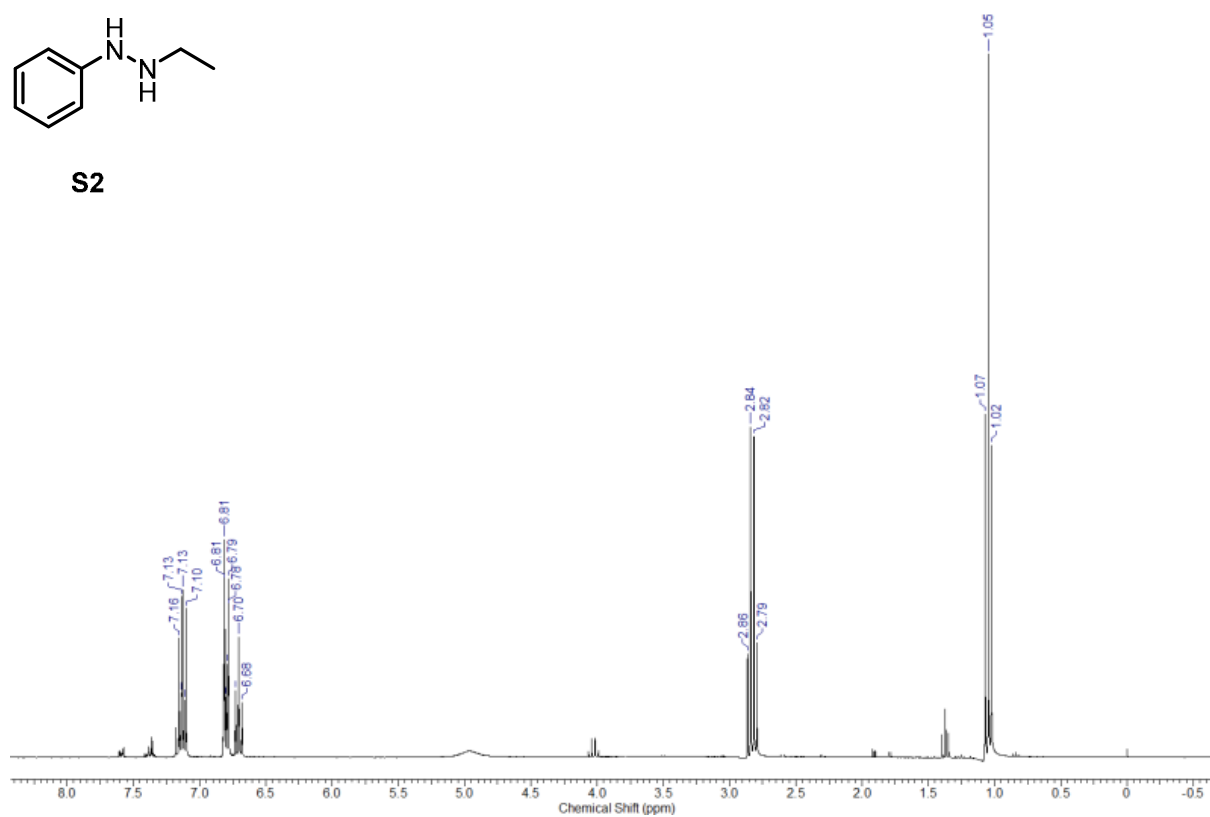
^1H NMR (300 MHz, CDCl_3) of 5-(furan-2-yl)-1-(4-methoxyphenyl)-1H-pyrazole



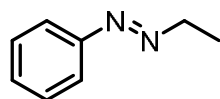
^{13}C NMR (75 MHz, CDCl_3) of 5-(furan-2-yl)-1-(4-methoxyphenyl)-1H-pyrazole



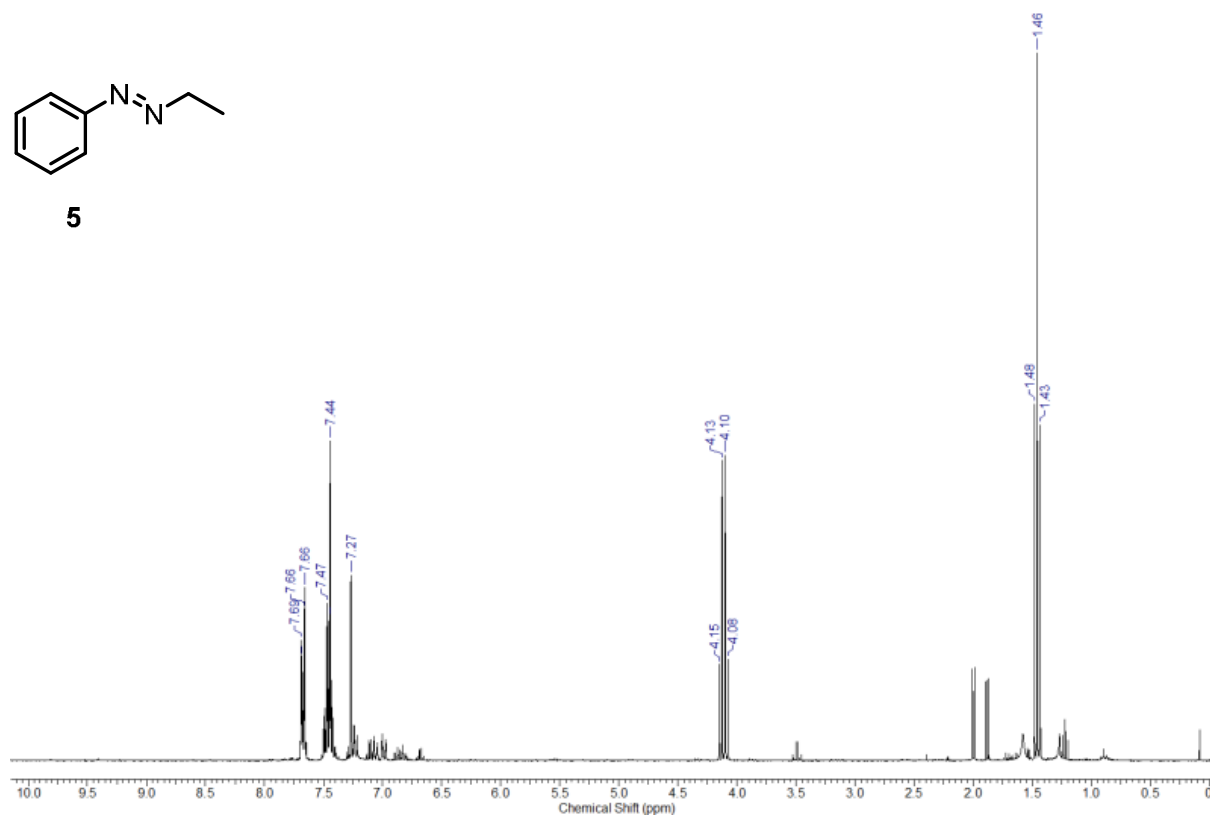
S2



¹H NMR of 2-ethyl-1-phenylhydrazine



5

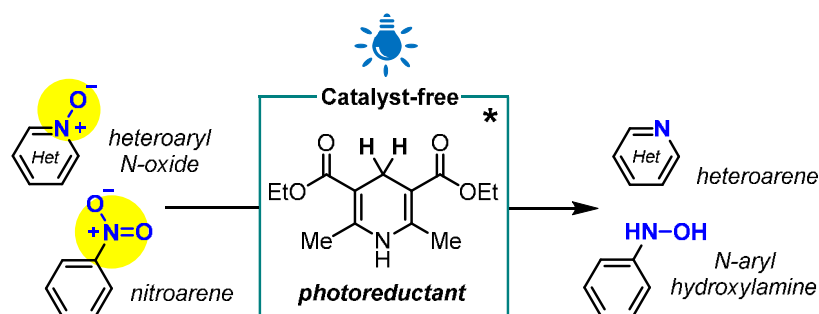


¹H NMR of 2-ethyl-1-phenyldiazene

2.5 References

1. a) Griess, J. P. *Philos. Trans. R. Soc. London* **1864**, 164, 693. b) Griess, J. P. *Justus Liebigs Ann. Chem.* **1866**, 137, 39–91.
2. N₂-releasing reactions of diazonium salts: Mo, F.; Dong, G.; Zhang, Y.; Wang, J. *Org. Biomol. Chem.* **2013**, 11, 1582–1593. b) Koziakov, D.; Wu, G.; Jacobi von Wangelin, A. *Org. Biomol. Chem.* **2018**, 16, 4942–4953.
3. Wang, M.; Funabiki, K.; Matsui, M. *Dyes and Pigments*. **2003**, 57, 77–86.
4. a) Deng, G.-B.; Li, H.-B.; Yang, X.-H.; Song, R.-J.; Hu, M.; Li, J.-H. *Org. Lett.* **2016**, 18, 2012–2015. b) Shao, Y.; Zheng, H.; Qian, J.; Wan, X. *Org. Lett.* **2018**, 20, 2412–2415.
5. a) Matcha, K.; Antonchick, A. P. *Angew. Chem. Int. Ed.* **2014**, 53, 11960–11964; b) Kindt, S.; Wicht, K.; Heinrich, M. *Org. Lett.* **2015**, 17, 6122–6125.
6. a) Frank, R. L.; Phillips, R. R. Pyridines. V. *J. Am. Chem. Soc.* **1949**, 71, 2804–2806. b) Yao, H. C.; Resnick, P. J. *Am. Chem. Soc.* **1962**, 84, 3514–3517.
7. Redox potentials were determined from CV studies (see experimental section).
8. a) Yu, X.-L.; Chen, J.-R.; Chena, D.-Z.; Xiao, W.-J. *Chem. Commun.* **2016**, 52, 8275–8278. b) Abrams, R.; Lefebvre, Q.; Clayden, J. *Angew. Chem. Int. Ed.* **2018**, 57, 13587–13591. c) Angnes, R. A.; Potnis, C.; Liang, S.; Correia, C. R. D.; Hammond, G. B. *J. Org. Chem.* **2020**, 85, 4153–4164.
9. Photocatalyzed syntheses of pyrazoles: a) Yadav, S.; Rai, P.; Srivastava, M.; Singh, J.; Tiwari, K. P.; Singh, J. *Tetrahedron Lett.* **2015**, 56, 5831–5835. b) Chen, J. R.; Hu, X. Q.; Lu, L. Q.; Xiao, W. J. *Acc. Chem. Res.* **2016**, 49, 1911–1923. c) Fan, X. W.; Lei, T.; Zhou, C.; Meng, Q. Y.; Chen, B.; Tung, C. H.; Wu, L. Z. *J. Org. Chem.* **2016**, 81, 7127–7133. d) Ding, Y.; Zhang, T.; Chen, Q.-Y.; Zhu, C. *Org. Lett.* **2016**, 18, 4206–4209. e) Sagir, H.; Rai, P.; Ibad, A.; Ibad, F.; Siddiqui, I. R. *Catal. Commun.* **2017**, 153–156. f) Cheng, J.; Li, W.; Duan, Y.; Cheng, Y.; Yu, S.; Zhu, C. *Org. Lett.* **2017**, 19, 214–217. g) Meng, Y.; Zhang, T.; Gong, X.; Zhang, M.; Zhu, C. *Tetrahedron Lett.* **2019**, 60, 171–174.
10. Diazonium salts in the synthesis of pyrazoles under dark conditions: h) Wang, M.; Tang, B.-C.; Xiang, J.-C.; Chen, X.-L.; Ma, J.-T.; Wu, Y.-D.; Wu, A.-X. *Org. Lett.* **2019**, 21, 8934–8937. i) Liu, J.; Xu, E.; Jiang, J.; Huang, Z.; Zheng, L.; Liu, Z. Q. *Chem. Commun.* **2020**, 56, 2202–2205.
11. a) Singer, R. A.; Caron, S.; McDermott, R. E.; Arpin, P.; Do, N. M. *Synthesis* **2003**, 1727–1731. b) Singer, R. A.; Dore, M.; Sieser, J. E.; Berliner, M. A. *Tetrahedron Lett.* **2006**, 47, 3727–3731.
12. Simmons, H. E.; Smith, R. D. *J. Am. Chem. Soc.* **1959**, 81, 4256–4264.
13. a) Jia, K.; Zhang, F.; Huang, H.; Chen, Y. *J. Am. Chem. Soc.* **2016**, 138, 1514–1517. b) Ji, M.; Wu, Z.; Zhu, C. *Chem. Commun.* **2019**, 55, 2368–2371. c) Bloom, S.; Bume, D. D.; Pitts, C. R.; Lectka, T. *Chem. Eur. J.* **2015**, 21, 8060–8063.
14. Radical β -functionalization of cyclopropanols under dark conditions: a) Jiao, J.; Nguyen, L. X.; Patterson, D. R.; Flowers, R. A. *Org. Lett.* **2007**, 9, 1323–1326. b) He, X.-P.; Shu, Y.-J.; Dai, J.-J.; Zhang, W.-M.; Feng, Y.-S.; Xu, H.-J. *Org. Biomol. Chem.* **2015**, 13, 7159–7163. c) Mills, L. R.; Zhou, C.; Fung, E.; Rousseaux, S. A. L. *Org. Lett.* **2019**, 21, 8805–8809. d) Chen, D.; Fu, Y.; Cao, X.; Luo, J.; Wang, F.; Huang, S. *Org. Lett.* **2019**, 21, 5600–5605. e) Ramar, T.; Subbaiah, M. A. M.; Ilangovan, A. *J. Org. Chem.* **2020**, 85, 7711–7727.
15. Aryl radical generation from diazonium salts under photoredox conditions: a) Cano-Yelo, H.; Deronzier, A. J. *Photochem.* **1987**, 37, 315–321. b) Kalyani, D.; McMurtrey, K. B.; Neufeldt, S. R.; Sanford, M. S. *J. Am. Chem. Soc.* **2011**, 133, 18566–18569. c) Hari, D. P.; Schroll, P.; König, B. *J. Am. Chem. Soc.* **2012**, 134, 2958–2961.
16. Makino, K.; Kim, H. S.; Kurasawa, Y. *J. Heterocycl. Chem.* **1998**, 35, 489–497.
17. Majek, M.; Filace, F.; Jacobi von Wangelin, A. *Beilstein J. Org. Chem.* **2014**, 10, 981–989.
18. Bockman, T. M.; Kosynkin, D.; Kochi, J. K. *J. Org. Chem.* **1997**, 62, 5811–5820.
19. Majek, M.; Jacobi von Wangelin, A. *Chem. Commun.* **2013**, 49, 5507–5509.
20. Logan, S. R. *Trans. Faraday Soc.* **1967**, 63, 3004–3008.
21. Rillema, D. P.; Allen, G.; Meyer, T. J.; Conrad, D. *Inorg. Chem.* **1983**, 22, 1617–1622.
22. a) Zhang, N.; Zeng, C.; Lam, C. M.; Gbur, R. K.; Little, R. D. *J. Org. Chem.* **2013**, 78, 2104–2110; b) Francke, R.; Little, R. D. *Chem. Rev.* **2014**, 43, 2492–2521.
23. Huang, L.; Tengfei, J.; Lam, Rueping, M. Remote Nickel-Catalyzed Cross-Coupling Arylation via Proton-Coupled Electron Transfer-Enabled C–C Bond Cleavage. *J. Am. Chem. Soc.* **2020**, 142 (7), 3532–3539.
24. He, X.-P.; Shu, Y.-J.; Dai, J. J.; Zhang, W.-M.; Feng, Y. S.; Xu, H. J. *Org. Biomol. Chem.*, **2015**, 13, 7159.
25. Jia, K.; Zhang, F.; Huang, H.; Chen, Y. *J. Am. Chem. Soc.*, **2016**, 138 (5), 1514–1517.
26. Sum, T. H.; Sum, T. J.; Stokes, J. E.; Galloway, W. R. G. D.; Spring, D. R. *Tetrahedron*, **2015**, 71, 4557–4564.
27. Nomura, K.; Matsubara, S. *Chem. Lett.*, **2007**, 36, 164–165.
28. Konik, Y. A.; Elek, G. Z.; Kabela, S.; Järving, I.; Lopp, M.; Kananovich, D. *Org. Biomol. Chem.*, **2017**, 15, 8334–8340.
29. Fuse, S.; Morita, T.; Johmoto, K.; Uekusa, H.; Tanaka, H. *Chem. Eur. J.*, **2015**, 21, 14370.
30. Zhang, Z.; Kang, J.; Niu, P.; Wu, J.; Chang, J. *J. Org. Chem.* **2014**, 79, 10170.
31. Zora, M.; Kivrak, A. *J. Org. Chem.*, **2011**, 76, 9379.
32. Baruenga, J.; Merino, I.; Vina, S.; Palacios, F. *Synthesis* **1990**, 398–400.
33. Bume, D. D.; Pitts, C. R.; Lectka, T. *Eur. J. Org. Chem.* **2016**, 26–30.
34. Sun, H.-L.; McNamara, B.; Anselme, J.P. *Bull. Soc. Chim. Belg.* **1992**, 101, 791–794.
35. Rillema, D. P.; Allen, G.; Meyer, T. J.; Conrad, D. *Inorg. Chem.* **1983**, 22, 1617–1622.
36. Klán, P.; Wirtz, J. Photochemistry of Organic Compounds, *John Wiley and Sons*, Chichester, **2009**.
37. Scandola, M. A. R.; Scandola, F.; Indelli, A. *J. Chem. Soc., Faraday Trans. 1* **1985**, 81, 2967–2974.
38. Carstensen, J. T. *J. Pharm. Sci.* **1970**, 59, 1140–1143.

3 Chapter 3: Catalyst-Free *N*-Deoxygenation by Photoexcitation of Hantzsch Ester



Abstract: A mild and operationally simple protocol for the deoxygenation of a variety of heteroaryl *N*-oxides and nitroarenes has been developed. A mixture of substrate and Hantzsch ester is proposed to result in an electron donor-acceptor complex, which upon blue-light irradiation undergoes photo-induced electron transfer between the two reactants to afford the products. *N*-oxide deoxygenation is demonstrated with 22 examples of functionally diverse substrates and chemoselective reduction of nitroarenes to the corresponding hydroxylamines is also shown. Spectroscopic experiments support the formation of an EDA complex between the reactants and suggest a 1:1 stoichiometry of Hantzsch ester and *N*-oxide.

This chapter has been published:

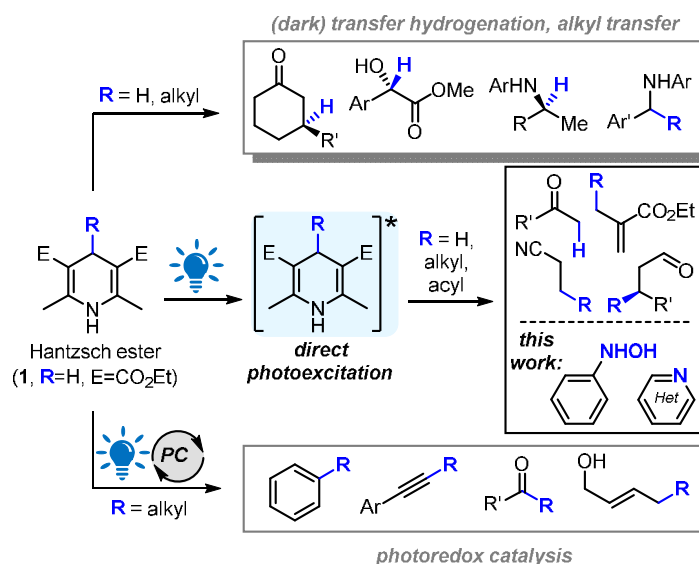
Konev M., Cardinale L., Jacobi von Wangelin A. *Org. Lett.* **2020**, 22, 1316–1320.

Author contributions:

MK led the project, LC synthesized part of the substrate scope and contributed to the mechanistic experiments.

3.1 Introduction

Hantzsch esters, versatile reagents in the fields of synthetic chemistry and reaction development, have only recently become part of a rapidly growing collection of literature of photo-mediated reaction platforms.¹ While their ground-state reactivity has been investigated for the better part of a century,² Hantzsch esters have traditionally been used as hydride donors, playing the role of NADH analogues for transfer hydrogenation reactions,^{3,4} alkyl-group transfer,⁵ and related reactions under thermal and oxidative conditions (Scheme 1, top).^{6,7} In recent years, the chemistry of these 1,4-dihydropyridine derivatives has expanded to photo-mediated transformations, likely as a result of the increased interest in photoredox catalysis.⁸ Hantzsch esters behave as competent single-electron donors in the ground state ($E_{\text{ox}} = +0.79$ V vs. SCE in DMF) and have been used to initiate reductive quenching cycles of photocatalysts or as a terminal hydrogen atom source.⁹ More recently, 4-alkyl substituted derivatives were shown to behave in a similar manner, by serving as alkyl radical precursors. Nishibayashi pioneered the use of these systems, wherein the single-electron oxidation of 4-alkyl Hantzsch esters facilitates the expulsion of an alkyl radical by aromatization-driven fragmentation. The resulting radicals can then engage in C–C bond forming reactions with electron-deficient cyanoarenes.¹⁰ Building upon this platform, a plethora of related reactions for the coupling of various radical species via photoredox catalysis have been reported (Scheme 1, bottom).¹¹



Scheme 1. Use of Hantzsch esters in organic synthesis.

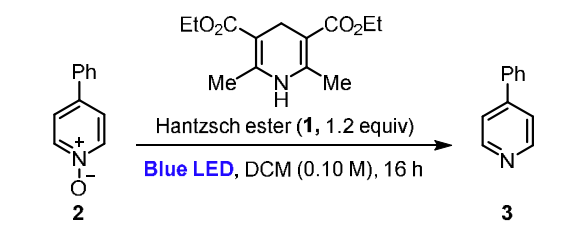
In addition to the modes of reactivity mentioned above, the excitation of Hantzsch esters with visible light results in a highly potent single-electron reductant ($E_{\text{ox}} = -2.28$ V vs. SCE in DMF).¹² While this reactivity was first reported in the late 1970s,¹³ only recently was it applied in the context of synthetic organic chemistry.¹⁴ Furthermore, 1,4-dihydropyridine derivatives have also been employed in a rapidly developing field of electron-donor-acceptor (EDA) complex photochemistry.¹⁵ For example, several recent reports have demonstrated the capability of Hantzsch ester to facilitate cleavage of redox-active auxiliaries and its propensity to promote reductive fragmentation (Scheme 1, middle).¹⁶ To this end, we set forth to examine the feasibility of this strongly reducing excited state intermediate for the deoxygenation of pyridine *N*-oxides to pyridines, a ubiquitous moiety in organic chemistry.¹⁷

While several photoredox-mediated procedures for the deoxygenation of pyridine *N*-oxides and their derivatives have been developed,¹⁸ certain limitations are evident. These protocols tend to rely on the use of a large excess of sacrificial electron donors (from 5 equivalents to solvent quantities) to generate the reducing photocatalyst under inert conditions. Furthermore, the necessity of expensive photocatalysts additionally discourages the use of these reactions. To address these shortcomings, we sought the use of photoexcited Hantzsch ester to perform the desired reduction, using an operationally simple setup.

3.2 Results and discussion

We began our investigation using 4-phenylpyridine *N*-oxide **2** as the model substrate. Upon irradiation of a mixture of the *N*-oxide and Hantzsch ester in acetonitrile, we observed significant product formation (Table 1, entry 2). Optimization began with the investigation of a variety of solvents. Dichloromethane (DCM) and dimethylformamide (DMF) were found to be the top performers (entries 1 and 4), leading to nearly complete conversion in 16 hours. Due to convenience, DCM was the preferred choice for most cases going forward. While a 1:1 ratio of *N*-oxide to Hantzsch ester was sufficient to afford good yields of product (entry 6), a slight excess of reductant was used to facilitate shorter reaction times. Control reactions were performed and confirmed that blue-light irradiation is essential for efficient reduction to occur (entries 7 and 8).¹⁹ Furthermore, the presence of oxygen only marginally compromises reaction efficiency and, as expected, degassing with nitrogen was shown to improve the yield (entry 1 vs. 9).²⁰

Table 1. Evaluation of reaction conditions.

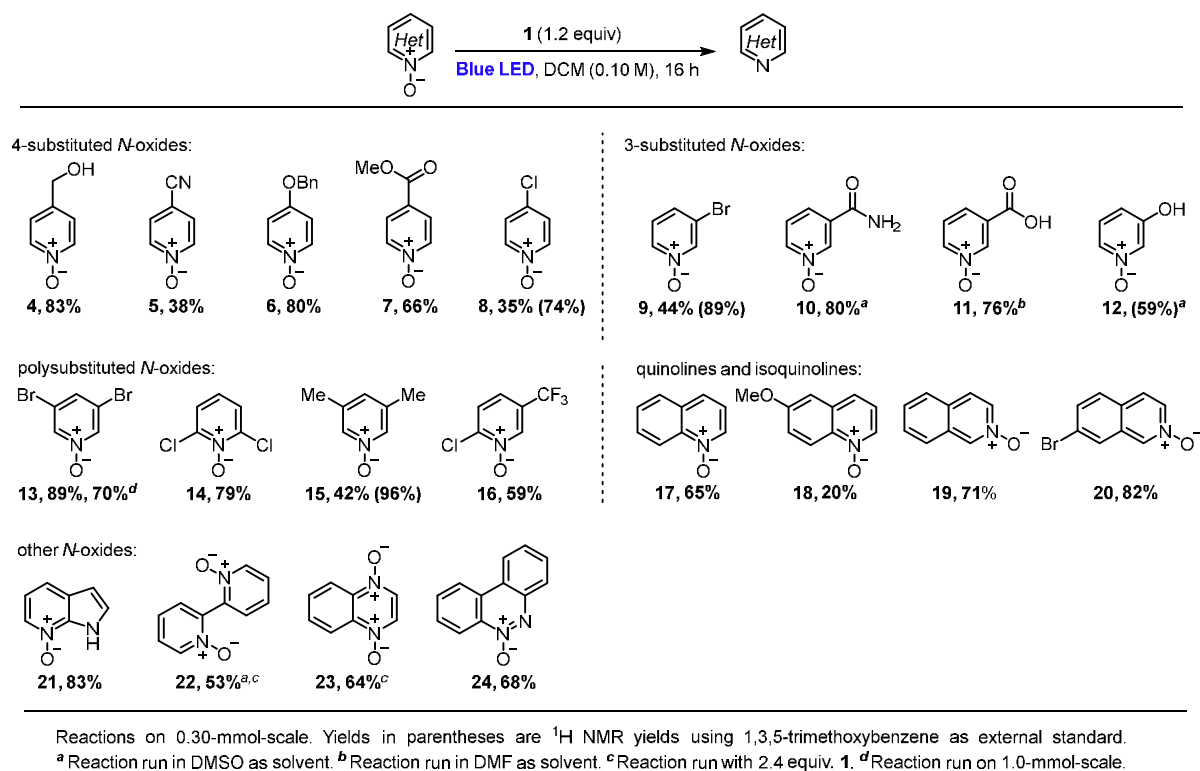


entry	variation from standard conditions	yield (%)
1	none	86
2	MeCN as solvent	41
3	DMSO as solvent	65
4	DMF as solvent	80
5	1.0 equiv 1	82
6	without 1	0
7	run in dark at 35 °C	17
8	run in dark at 65 °C	45
9	sparged with N ₂ for 5 min.	94
10	410 nm irradiation instead of 458 nm	97 ^a

Yields determined by ¹H NMR using 1,3,5-trimethoxybenzene as external standard. Run on 0.10 mmol-scale.

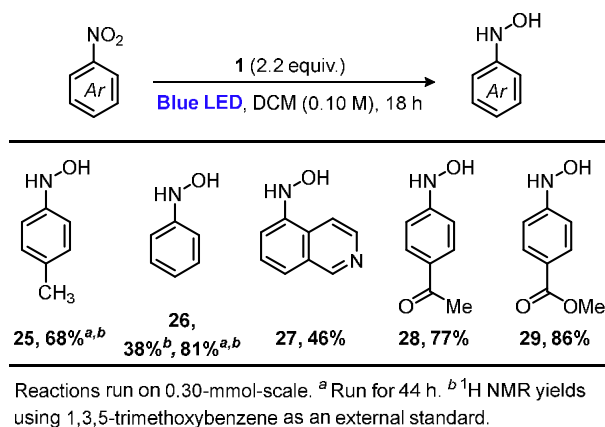
^a Reaction run for 6 h on 0.30 mmol-scale.

Having optimized the reaction conditions, we then examined a variety of functionalized pyridine *N*-oxides and other heteroaryl *N*-oxides to evaluate the scope of the transformation (Scheme 2). A variety of electronically diverse mono- and poly-substituted pyridine *N*-oxides were well tolerated without any observed reduction of the pendant functionalities, including the electron-withdrawing cyano group (5), methyl ester (7), primary amide (10), and free carboxylic acid (11). For substrates that were insoluble in DCM, more polar solvents were employed without diminishing yields (entries 10, 11, and 22). More electron-rich substituents such as 4-carbinol (4), 4-benzyloxy (6), 3-hydroxy (12), and 3,5-dimethyl (15) pyridines were also compatible. Furthermore, this method does not result in cleavage of benzyl ethers of the pyridine under the photo-reductive conditions.²¹ Heteroaromatics containing halogens at any position were tolerated without any observable hydrodehalogenation (entries 8, 9, 13, 14, 20). Oxides of quinolines and isoquinolines also performed well under the reaction conditions, affording their corresponding reduced products in modest yields (entries 17–20). Finally, several other heteroarene *N*-oxides were successfully deoxygenated in good yields, including azaindole, bipyridine, benzopyrazine, and benzo[*c*]cinnoline (entries 21–24). Attempts at using 4-alkyl substituted Hantzsch esters to affect the sequential radical alkylation and deoxygenation did not result in much success and only trace product was observed.²²



Scheme 2. Substrate scope for the photoreduction of heteroaryl *N*-oxides.

Next, we explored the feasibility of our system for the photoreduction of nitroaromatic compounds. Interestingly, upon irradiation of a 1:3 mixture of 4-nitrotoluene and Hantzsch ester in DCM, only the corresponding hydroxylamine was obtained. No further reduction was observed upon either addition of excess of Hantzsch ester or heating to 45 °C. As with the *N*-oxide deoxygenation above, the reduction of nitroarenes also featured good functional group compatibility, selectively producing a variety of substituted hydroxylamines (Scheme 3). Substrates bearing electron-donating groups required extended reactions times, whereas those with electron-withdrawing groups underwent deoxygenation more rapidly.



Scheme 3. Photoreduction of nitroarenes

Mechanistic studies

In order to understand the reaction mechanism, we conducted several spectroscopic experiments to determine whether Hantzsch ester **1** was undergoing photoexcitation without preorganization, or whether an EDA complex was formed between **1** and either substrate, which could help facilitate electron transfer between them. We first analyzed **1** using UV-Vis spectroscopy and found that it alone does absorb within the emission range of our LEDs, suggesting that it can undergo direct photoexcitation to generate the highly reducing excited-state species (Figure 1 a).¹² However, in the presence of either

4-phenyl pyridine *N*-oxide **2**, or methyl 4-nitrobenzoate, a bathochromic shift was observed, supporting the formation of an EDA complex between the reactants (Figure 1 a, b).^{16h,i} ¹H NMR experiments were also performed and further corroborate this hypothesis. Upon mixing of either neutral, electron-rich, or electron-deficient pyridine *N*-oxides with Hantzsch ester results in a shift of all ¹H NMR resonances compared to each substrate alone (Figure 1 c. See SI for details). A Job plot was also constructed which indicated a 1:1 ratio of donor and acceptor were involved in the EDA complex of **1** and **2** (Figure 1 d).²³ While these data suggest the formation of an EDA complex between the reactants, the mode of interaction is not readily discernable.

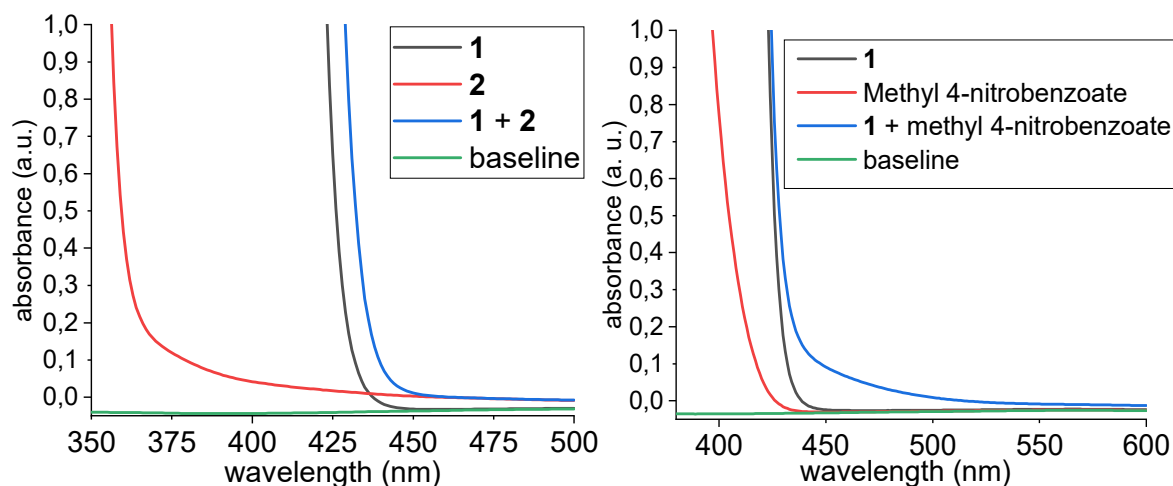


Figure 1. UV-Vis spectra of a) 4-phenylpyridine *N*-oxide **2** (red line, 0.050 M in DCM), Hantzsch ester **1** (black line, 0.050 M in DCM), and an equimolar mixture of **2** and **1** (0.050 M in DCM). b) Methyl 4-nitrobenzoate (red line, 0.050 M in DCM), **1** (black line, 0.050 M in DCM), and an equimolar mixture of methyl 4-nitrobenzoate and **1** (0.050 M in DCM).

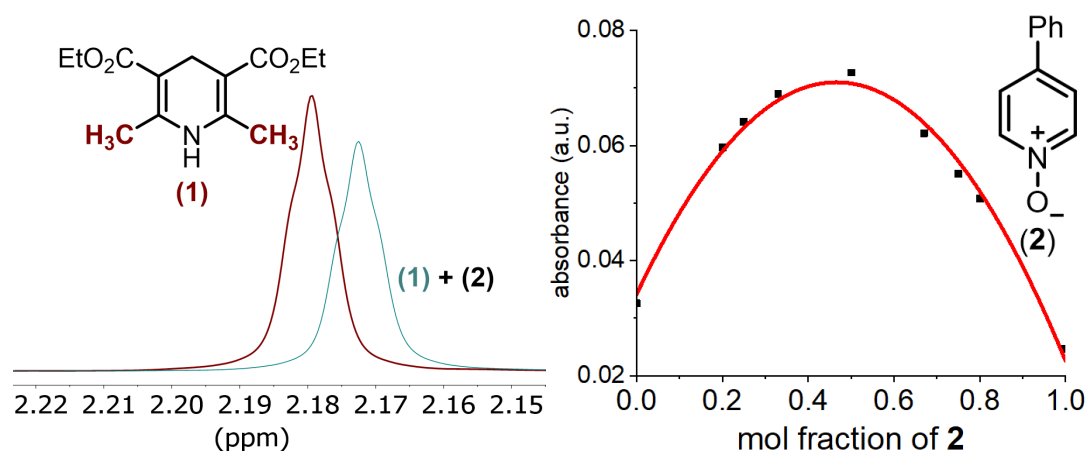
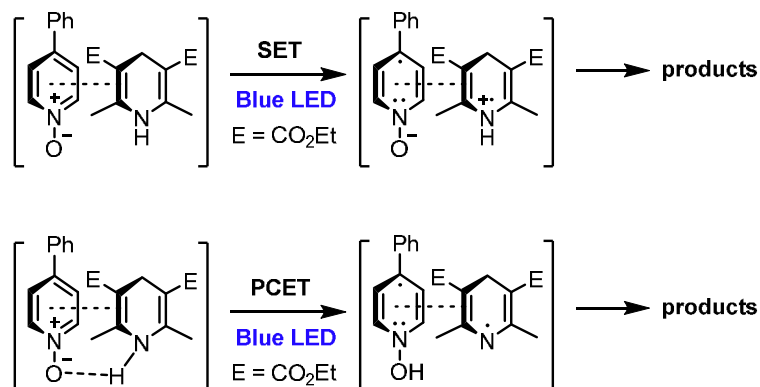


Figure 2. a) Shift of methyl resonance of **1** in the presence of equimolar **2** (0.10 M in CDCl₃). b) Job plot of **1** and **2** (0.050 M in CH₂Cl₂) at 435 nm.

One possibility is π -stacking between **1** and pyridine *N*-oxide (Scheme 4, top), which has been previously proposed to occur between **1** and *N*-alkyl pyridinium salts.¹⁶ⁱ The alternative pathway may involve Hantzsch ester as a hydrogen-atom donor with the *N*-oxide as an acceptor (Scheme 4, bottom).²⁴ Finally, in further support of our findings, a similar photoreduction of pyridine *N*-oxide by 1-benzyl-1,4-dihydro-nicotinamide under UV irradiation was previously reported, wherein the authors demonstrate that the *N*-oxide was quenching the singlet excited state of the dihydropyridine and afforded the de-oxygenated product.²⁵



Scheme 4. Proposed EDA complexes between **1** and **2**

3.3 Conclusions

In conclusion, a reductive deoxygenation of heteroaryl *N*-oxides was developed and the reduction of nitroarenes to the corresponding hydroxylamines via visible-light photoexcitation of Hantzsch ester. These reactions are operationally simple, can be performed under ambient conditions without the exclusion of moisture or air, proceed smoothly in the presence of a variety of functional groups, and do not require the use of an expensive photocatalyst. Finally, spectroscopic studies support the formation of an EDA complex between Hantzsch ester and pyridine *N*-oxides or nitroarenes.

3.4 Experimental section

3.4.1 Materials and methods

Reagents were purchased from commercial sources and were used as received unless otherwise stated. All solvents were used without distillation. All reactions were performed using LABSOLUTE 4 mL Screw Neck Vials, 45 x 14.7 mm, clear glass, 1st hydrolytic class unless otherwise stated. Column chromatography was performed on 35-70 mesh silica gel (Acros Organics). LEDs were purchased from CREE and reactions were run using the blue LED ($\lambda_{\text{max}} = 458 \text{ nm}$). (Cree® XLamp® XM-L Color LEDs, the emission spectrum of the blue LED can be found on the third page of the following link: https://www.cree.com/led-components/media/documents/XLampXML_Color.pdf) ¹H, ¹³C, ¹⁹F spectra were recorded on a Bruker Advance 300 or Advance 600 Kryo spectrometer and were internally referenced to residual protio-solvent signals (CDCl₃ referenced at 7.26 and 77.0 ppm respectively, CD₃OD referenced at 3.30 ppm, SO(CD₃)₂ referenced at 2.50 and 39.5 ppm respectively). Data for ¹H NMR are reported as follows: chemical shift (δ ppm), multiplicity (s = singlet, d = doublet, dd = doublet of doublets, ddd = doublet of doublet of doublets, t = triplet, q = quartet, m = multiplet, b = broad), coupling constant (Hz), and integration (H). Data for ¹³C{¹H} NMR are reported in terms of chemical shift and no special nomenclature is used for equivalent carbons. High Resolution Mass Spectrometry (HRMS) were recorded on Finnigan MAT 900s.

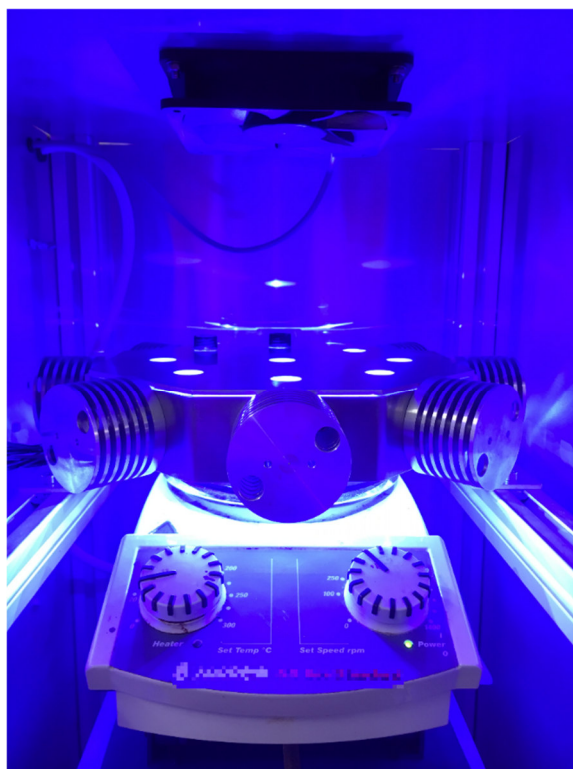
3.4.2 General procedures

General procedure A. Photoreduction of heteroaryl *N*-oxides:

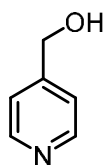
To a 4 mL screw cap vial was added heteroaryl *N*-oxide (0.30 mmol, 1.0 equiv), diethyl 2,6-dimethyl-1,4-dihydropyridine-3,5-dicarboxylate (Hantzsch ester, 91.2 mg, 0.360 mmol, 1.2 equiv), and solvent (3.0 mL). The vial was then sealed with a plastic screw cap and placed in a home-made reactor (see below) on a stir plate and irradiated for 16 hours with a 3 W blue LED (10 mm from the vial). The temperature was maintained at 31 °C by an internal fan. After the elapsed time, the mixture was concentrated under reduced pressure and purified by flash column chromatography on silica gel to afford the title compound.

General procedure B. Photoreduction of nitroarenes:

To a 4 mL screw cap vial was added nitroarene (0.30 mmol, 1.0 equiv), diethyl 2,6-dimethyl-1,4-dihydropyridine-3,5-dicarboxylate (Hantzsch ester, 167 mg, 0.660 mmol, 2.2 equiv), and solvent (3.0 mL). The vial was then sealed with a plastic screw cap and placed in a home-made reactor (see below) on a stir plate and irradiated for 18 hours with a 3 W blue LED (10 mm from the vial). The temperature was maintained at 31 °C by an internal fan. After the elapsed time, the mixture was concentrated under reduced pressure and purified by flash column chromatography on silica gel to afford the title compound.

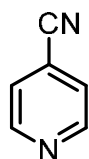


3.4.3 Characterization of reaction products from Scheme 2



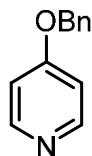
4-Hydroxymethyl-pyridine (SI-1) Starting from 4-hydroxymethylpyridine *N*-oxide and following the general procedure A, **SI-1** was isolated by flash chromatography on silica (eluent: pentane/EtOAc, 1:1) as a white solid (27.2 mg, 86% yield). **¹H NMR** (300 MHz, CDCl₃, ppm): δ 8.44–8.42 (m, 2H), 7.29–7.27 (m, 2H), 4.72 (s, 2H).

¹H NMR is consistent with previously published data²⁶



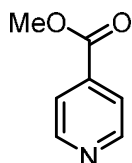
Isonicotinonitrile (SI-2). Starting from isonicotinonitrile *N*-oxide and following the general procedure A, **SI-2** was isolated by flash chromatography on silica (eluent: pentane/EtOAc, 80:20) yield as pale-yellow crystals (12.0 mg, 38%). **¹H NMR** (300 MHz, CDCl₃, ppm): δ 8.83–8.80 (m, 2H), 7.54–7.52 (m, 2H).

¹H NMR is consistent with previously published data²⁷



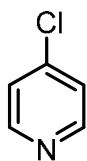
4-(Benzyloxy)pyridine (SI-3). Starting from 4-(benzyloxy)pyridine *N*-oxide and following the general procedure A, **SI-3** was isolated by flash chromatography on silica (eluent: pentane/EtOAc, 50:50) as a yellow solid (44.5 mg, 80% yield). **¹H NMR** (300 MHz, CDCl₃, ppm): δ 8.44 (d, *J* = 5.6 Hz, 2H), 7.42–7.35 (m, 5H), 6.89–6.87 (m, 2H), 5.11 (s, 2H).

¹H NMR is consistent with previously published data²⁸



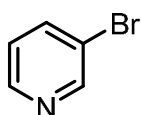
4-(Methoxycarbonyl)pyridine (SI-4). Starting from 4-(methoxycarbonyl)pyridine *N*-oxide and following the general procedure A, **SI-4** was isolated by flash chromatography on silica (gradient: pentane/EtOAc, 90:10 to 70:30) as a pale-yellow oil (27.1 mg, 66% yield). **¹H NMR** (300 MHz, CDCl₃, ppm) δ 8.78 (apparent dd, *J* = 4.5, 1.6 Hz, 2H), 7.85 (apparent dd, *J* = 4.4, 1.6 Hz, 2H), 3.96 (s, 3H).

¹H NMR is consistent with previously published data²⁹



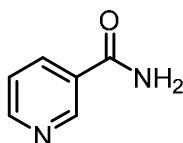
4-Chloropyridine (SI-5) Starting from 4-chloropyridine *N*-oxide and following the general procedure A, **SI-5** was isolated by flash chromatography on silica (eluent: pentane/EtOAc, 80:20) as a yellow oil (12.0 mg, 35% yield). **¹H NMR** (300 MHz, CDCl₃, ppm): δ 8.50–8.48 (m, 2H), 7.30–7.28 (m, 2H).

¹H NMR is consistent with previously published data³⁰



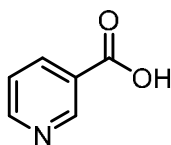
3-Bromopyridine (SI-6). Starting from 3-bromopyridine *N*-oxide and following the general procedure A, **SI-6** was isolated by flash chromatography on silica (eluent: pentane/EtOAc, 95:5) as a pale-yellow oil (25.0 mg, 44% yield). **¹H NMR** (300 MHz, CDCl₃, ppm): δ 8.69 (s, 1H), 8.53 (d, *J* = 4.7 Hz, 1H), 7.82 (dt, *J* = 8.2, 1.2 Hz, 1H), 7.20 (dd, *J* = 8.2, 4.8 Hz, 1H).

¹H NMR is consistent with previously published data³¹



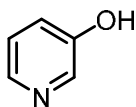
Nicotinamide (SI-7) Starting from nicotinamide *N*-oxide and following the general procedure A in DMSO instead of DCM, **SI-7** was isolated by flash chromatography on silica (EtOAc 100%) as a pale-yellow solid (29.3 mg, 80% yield). **¹H NMR** (300 MHz, DMSO-*d*₆, ppm): δ 9.03 (dd, *J* = 2.03, 0.9 Hz, 1H), 8.69 (dd, *J* = 4.8, 1.7 Hz, 1H), 8.22–8.17 (m, 2H), 7.61 (s, 1H), 7.49 (ddd, *J* = 8.0, 4.8, 0.9 Hz, 1H).

¹H NMR is consistent with previously published data³¹



Nicotinic acid (SI-8) Starting from nicotinic acid *N*-oxide and following the general procedure A in DMF instead of DCM, **SI-8** was isolated by flash chromatography on silica (EtOAc 100%) as a white solid (28.1 mg, 76% yield). **¹H NMR** (300 MHz, DMSO-*d*₆, ppm): δ 9.07 (dd, *J* = 2.2, 0.9 Hz, 1H), 8.78 (dd, *J* = 4.8, 1.7 Hz, 1H), 8.26 (dt, *J* = 8.0, 2.0 Hz, 1H), 7.54 (ddd, *J* = 7.9, 4.8, 0.9 Hz, 1H).

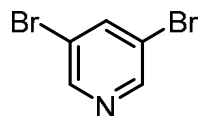
¹H NMR is consistent with previously published data²⁸



3-Hydroxypyridine (SI-9) Starting from 3-hydroxypyridine *N*-oxide and following the general procedure A in DMSO-*d*₆ instead of DCM, the yield of **SI-12** was obtained by adding 10.3 mg 1,3,5-trimethoxybenzene as an external standard to the yellow powder crude reaction mixture. **¹H NMR**

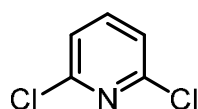
(300 MHz, DMSO- d_6 , ppm): δ 9.83 (broad s, 1H), 8.12 (apparent d, J = 2.8 Hz, 1H), 8.01 (dd, J = 4.4, 1.6 Hz, 1H), 7.24–7.16 (m, 1H).

^1H NMR is consistent with previously published data³²



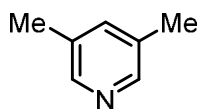
3,5-Dibromopyridine (SI-10). Starting from 3,5-dibromopyridine *N*-oxide and following the general procedure A, **SI-10** was isolated by flash chromatography on silica (eluent: pentane/EtOAc, 95:5) as a white solid (63.2 mg, 89% yield). ^1H NMR (300 MHz, CDCl_3 , ppm): δ 8.61 (d, J = 2.0 Hz, 2H), 8.01 (t, J = 2.0 Hz, 1H).

^1H NMR is consistent with previously published data³³



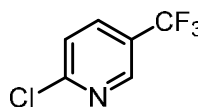
2,6-Dichloropyridine (SI-11). Starting from 2,6-dichloropyridine *N*-oxide and following the general procedure A, **SI-11** was isolated by flash chromatography on silica (eluent: pentane/EtOAc, 97:3) as a white solid (35.0 mg, 79% yield). ^1H NMR (300 MHz, CDCl_3 , ppm): δ 7.64 (t, J = 7.9 Hz, 1H), 7.30 (d, J = 7.9 Hz, 2H).

^1H NMR is consistent with previously published data³¹



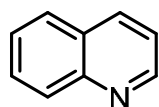
3,5-Dimethylpyridine (SI-12) Starting from 3,5-dimethylpyridine *N*-oxide and following the general procedure A, **SI-12** was isolated by flash chromatography on silica (eluent: pentane/EtOAc, 95:5) as a colorless oil (13.5 mg, 42% yield). ^1H NMR (300 MHz, CDCl_3 , ppm): δ 8.27–8.26 (m, 2H), 7.32–7.30 (m, 1H), 2.30 (s, 6H).

^1H NMR is consistent with previously published data²⁶



2-Chloro-5-(trifluoromethyl)pyridine (SI-13) Starting from 2-chloro-5-(trifluoromethyl)pyridine *N*-oxide and following the general procedure A, **SI-13** was isolated by flash chromatography on silica (eluent: pentane/EtOAc, 98:2) as a white solid (32.1 mg, 59% yield). ^1H NMR (300 MHz, CDCl_3 , ppm): δ 8.68–8.67 (m, 1H), 7.88 (dd, J = 8.4, 2.5 Hz, 1H), 7.47 (d, J = 8.3 Hz, 1H).

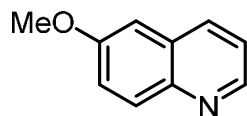
^1H NMR is consistent with previously published data³⁴



Quinoline (SI-14). Starting from quinoline *N*-oxide and following the general procedure A, **SI-14** was isolated by flash chromatography on silica (eluent: pentane/EtOAc, 90:10) as a pale-yellow oil (25.0 mg,

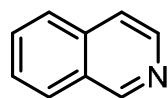
65% yield). $^1\text{H NMR}$ (300 MHz, CDCl_3 , ppm): δ 8.92 (dd, $J = 4.2, 1.7$ Hz, 1H), 8.17–8.09 (m, 2H), 7.83–7.80 (m, 1H), 7.74–7.69 (m, 1H), 7.57–7.51 (m, 1H), 7.41–7.36 (dd, $J = 8.2, 4.3$ Hz, 1H).

$^1\text{H NMR}$ is consistent with previously published data³⁵



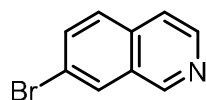
6-Methoxyquinoline (SI-15). Starting from 6-methoxyquinoline *N*-oxide and following the general procedure A, **SI-15** was isolated by flash chromatography on silica (eluent: pentane/EtOAc, 80:20) as a yellow solid (10.0 mg, 20% yield). $^1\text{H NMR}$ (300 MHz, CDCl_3 , ppm): δ 8.70 (dd, $J = 4.3, 1.7$ Hz, 1H), 8.00–7.99 (m, 1H), 7.93 (d, $J = 9.2$ Hz, 1H), 7.29 (ddd, $J = 8.3, 6.5, 3.5$ Hz, 2H), 7.00 (d, $J = 2.8$ Hz, 1H), 3.86 (s, 3H).

$^1\text{H NMR}$ is consistent with previously published data³⁵



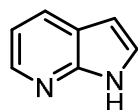
Isoquinoline (SI-16). Starting from isoquinoline *N*-oxide and following the general procedure A, **SI-16** was isolated by flash chromatography on silica (eluent: pentane/EtOAc, 90:10) as a pale-yellow oil (28.0 mg, 71% yield). $^1\text{H NMR}$ (300 MHz, CDCl_3 , ppm): δ 9.26 (s, 1H), 8.53 (d, $J = 5.8$ Hz, 1H), 8.00–7.96 (m, 1H), 7.84–7.81 (m, 1H), 7.73–7.58 (m, 3H).

$^1\text{H NMR}$ is consistent with previously published data³⁵



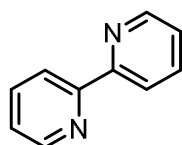
7-Bromoisoquinoline (SI-17). Starting from 7-bromoisoquinoline *N*-oxide and following the general procedure A, **SI-17** was isolated by flash chromatography on silica (gradient: pentane/EtOAc, 80:20) as a pale-yellow solid (51.2 mg, 82% yield). $^1\text{H NMR}$ (300 MHz, CDCl_3 , ppm) δ 9.18 (s, 1H), 8.56 (d, $J = 5.9$ Hz, 1H), 8.15–8.11 (m, 1H), 7.76 (dd, $J = 8.8, 1.9$ Hz, 1H), 7.70 (apparent d, $J = 8.8$ Hz, 1H), 7.62 (apparent d, $J = 5.8$ Hz, 1H).

$^1\text{H NMR}$ is consistent with previously published data³⁶



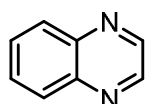
7-Azaindole (SI-18) Starting from 7-azaindole *N*-oxide and following the general procedure A, **SI-18** was isolated by flash chromatography on silica (gradient: pentane/EtOAc, 30:70) as a beige solid (31.5 mg, 83% yield). $^1\text{H NMR}$ (300 MHz, CDCl_3 , ppm): δ 11.39 (s, 1H), 8.35 (dd, $J = 4.8, 1.6$ Hz, 1H), 7.98 (dd, $J = 7.8, 1.6$ Hz, 1H), 7.40 (d, $J = 3.5$ Hz, 1H), 7.11 (dd, $J = 7.8, 4.8$ Hz, 1H), 6.52 (d, $J = 3.5$ Hz, 1H).

$^1\text{H NMR}$ is consistent with previously published data³⁵



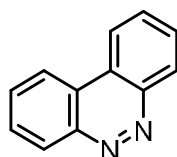
2,2'-Bipyridine (SI-19) Starting from 2,2'-bipyridyl-*N,N'*-dioxide and following the general procedure A in DMSO instead of DCM and with 2.4 equiv Hantzsch ester, **SI-19** was isolated by flash chromatography on silica (eluent: pentane/EtOAc, 80:20) as a white solid (24.8 mg, 53% yield). **¹H NMR** (300 MHz, CDCl₃, ppm): δ 8.69–8.66 (m, 2H), 8.41–8.37 (m, 2H), 7.80 (td, *J* = 7.7, 1.8 Hz, 2H), 7.30 (ddd, *J* = 7.5, 4.8, 1.2 Hz, 2H).

¹H NMR is consistent with previously published data²⁸



Quinoxaline (SI-20) Starting from quinoxaline 1,4-di-*N*-oxide and following the general procedure A with 2.4 equiv Hantzsch ester, **SI-20** was isolated by flash chromatography on silica (eluent: pentane/EtOAc, 90:10) as a white solid (25.0 mg, 64% yield). **¹H NMR** (300 MHz, CDCl₃, ppm): δ 8.85 (s, 2H), 8.12 (dd, *J* = 6.4, 3.5 Hz, 2H), 8.78 (dd, *J* = 6.4, 3.5 Hz, 2H).

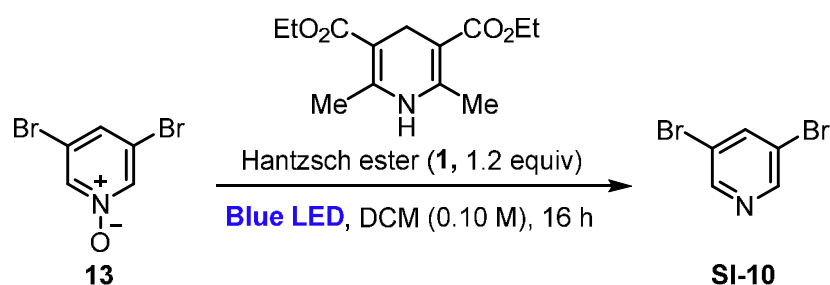
¹H NMR is consistent with previously published data³²



Benzo[c]cinnoline (SI-21). Starting from benzo[c]cinnoline *N*-oxide and following the general procedure A, **SI-21** was isolated by flash chromatography on silica (gradient: pentane/EtOAc, 90:10 to 70:30) as a yellow solid (36.6 mg, 68% yield). **¹H NMR** (300 MHz, CDCl₃, ppm) δ 8.80–8.72 (m, 2H), 8.63–8.54 (m, 2H), 7.97–7.86 (m, 4H).

¹H NMR is consistent with previously published data³⁷

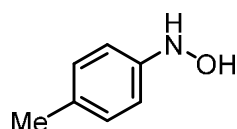
Scale-up Experiment



On the benchtop, 3,5-dibromopyridine *N*-oxide (253 mg, 1.00 mmol, 1 equiv), diethyl 1,4-dihydro-2,6-dimethyl-3,5-pyridinedicarboxylate (Hantzsch ester, 304 mg, 1.20 mmol, 1.2 equiv) and DCM (10 mL) were added to a 10 mL round-bottom flask equipped with a stir bar and was fitted with a glass stopper. The flask was then placed into the photoreactor (after removing the vial holder) and placed 5 mm away from an LED. The mixture was irradiated and stirred for 16 hours. After the elapsed time, the reaction mixture was concentrated under reduced pressure and the crude product was purified by flash column chromatography on silica gel (eluent: pentane/EtOAc, 95:5). The title compound was obtained as white flaky crystals (165 mg, 70% yield).

¹H NMR analysis was consistent with the above reported values.

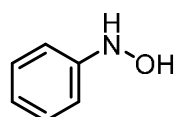
Characterization of products in Scheme 3



25. Starting from 4-nitrotoluene and following the general procedure B, the yield of **25** was obtained by adding 11.6 mg 1,3,5-trimethoxybenzene as an external standard to the concentrated (*in vacuo*) yellow powder crude reaction mixture. **¹H NMR** (300 MHz, SO(CD₃)₂) δ 8.21 (bs, 1H), 8.07 (bs, 1H), 6.96 (apparent d, *J* = 8.2 Hz, 2H), 6.74 (apparent d, *J* = 8.4 Hz, 2H), 2.18 (s, 3H).

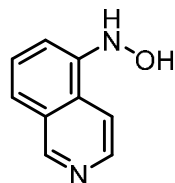
¹H NMR is consistent with previously published data³⁸

Note: Product is unstable under air and readily decomposes.



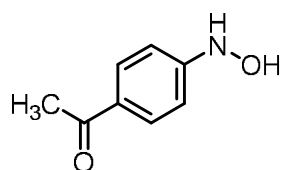
26. Starting from nitrobenzene and following the general procedure B, the yield of **26** was obtained by adding 9.1 mg 1,3,5-trimethoxybenzene as an external standard to the concentrated (*in vacuo*) yellow powder crude reaction mixture. **¹H NMR** (300 MHz, SO(CD₃)₂) δ 8.28 (s, 1H), 8.23 (s, 1H), 7.15 (apparent t, *J* = 8.0 Hz, 2H), 6.83 (apparent d, *J* = 8.9 Hz, 2H), 6.72 (apparent t, *J* = 7.4 Hz, 1H).

¹H NMR is consistent with previously published data³⁸



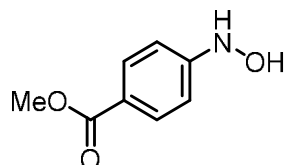
27. Starting from 5-nitroisoquinoline and following the general procedure B, **27** was isolated by flash chromatography on silica (pentane/EtOAc, 70:30) as a dark yellow solid (20.0 mg, 46% yield). **¹H NMR** (300 MHz, SO(CD₃)₂, ppm) δ 9.20–9.14 (m, 2H), 8.60 (d, *J* = 1.7 Hz, 1H), 8.40 (d, *J* = 6.0 Hz, 1H), 7.81–7.76 (m, 1H), 7.57–7.43 (m, 2H), 7.29 (dd, *J* = 7.3, 1.1 Hz, 1H).

¹H NMR is consistent with previously published data³⁹



28. Starting from 4'-nitroacetophenone and following the general procedure B, **28** was isolated by flash chromatography on silica (gradient: pentane/EtOAc, 90:10 to 70:30) as a pale-yellow solid (34.9 mg, 77% yield). **¹H NMR** (300 MHz, SO(CD₃)₂, ppm) δ 9.00 (s, 1H), 8.67 (s, 1H), 7.79 (d, *J* = 5.9 Hz, 1H), 8.15–8.11 (m, 1H), 7.76 (d, *J* = 8.4 Hz, 2H), 6.81 (d, *J* = 8.4 Hz, 2H), 2.44 (s, 3H).

¹H NMR is consistent with previously published data³⁸



29. Starting from methyl 4-nitrobenzoate and following the general procedure B, **29** was isolated by flash chromatography on silica (gradient: pentane/EtOAc, 90:10 to 70:30) as a pale-yellow solid (43.1 mg,

86% yield). $^1\text{H NMR}$ (300 MHz, $\text{SO}(\text{CD}_3)_2$, ppm) δ 8.96 (s, 1H), 8.65 (d, $J = 1.5$ Hz, 1H), 7.77 (apparent d, $J = 8.7$ Hz, 2H), 6.83 (apparent d, $J = 8.7$ Hz, 2H), 3.76 (s, 3H).

$^1\text{H NMR}$ is consistent with previously published data³⁸

3.4.4 Mechanistic experiments

UV-Vis and $^1\text{H NMR}$ spectra from Figure 1

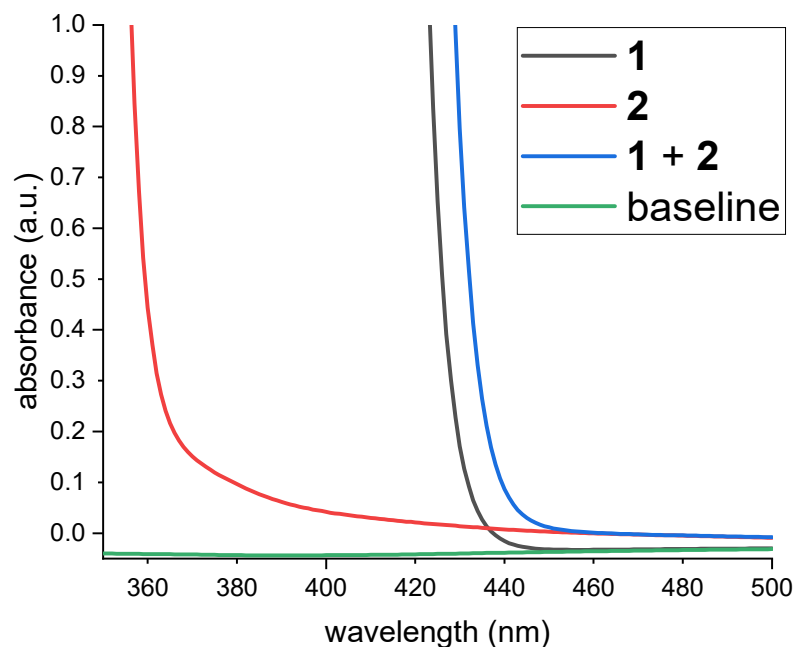


Figure 1a. UV-Vis spectra of a) 4-phenylpyridine *N*-oxide **2** (red line, 0.050 M in DCM), Hantzsch ester **1** (black line, 0.050 M in DCM), and an equimolar mixture of **2** and **1** (0.050 M in DCM).

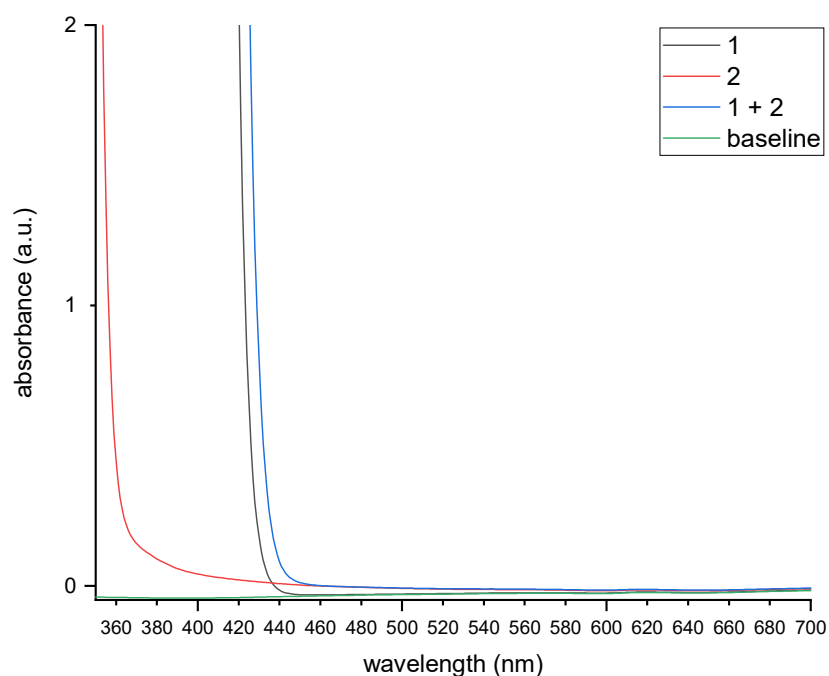


Figure 1a'. Zoomed-out UV-Vis spectra of a) 4-phenylpyridine *N*-oxide **2** (red line, 0.050 M in DCM), Hantzsch ester **1** (black line, 0.050 M in DCM), and an equimolar mixture of **2** and **1** (0.050 M in DCM).

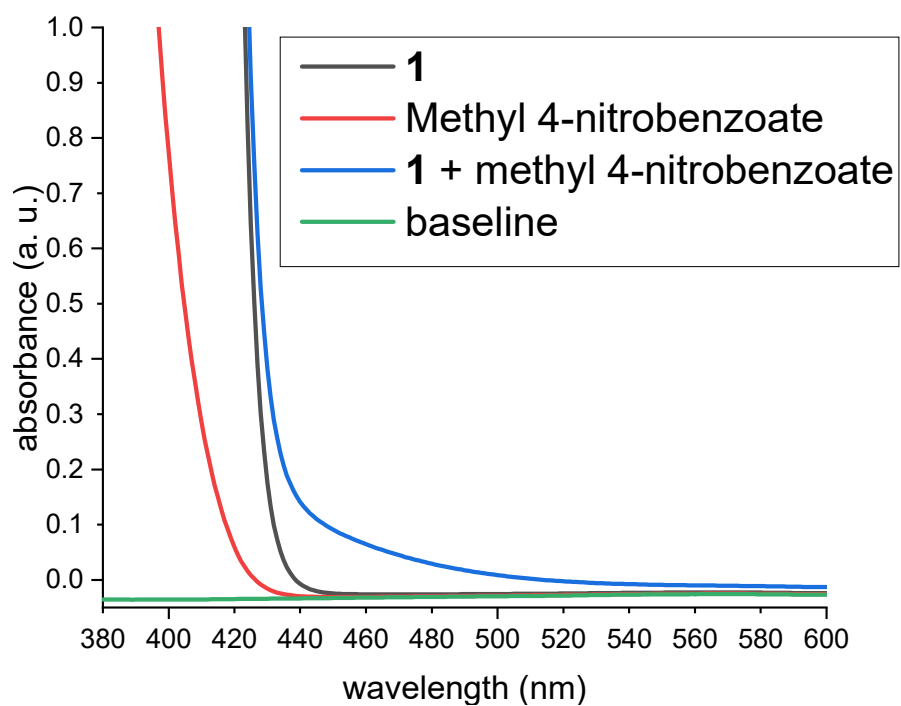


Figure 1b. UV-Vis spectra of methyl 4-nitrobenzoate (red line, 0.050 M in DCM), **1** (black line, 0.050 M in DCM), and an equimolar mixture of methyl 4-nitrobenzoate and **1** (0.050 M in DCM).

Table 2: Absorbance values for various ratios of Hantzsch ester **1** to 4-phenyl pyridine *N*-oxide **2** measured at 435 nm.

Ratio of 1:2	% HEH	1 (M)	2 (M)	Abs _{EDA}	mol fraction 2
5:0	100	0.0500	0.0000	0.032554	0.00
4:1	80	0.0400	0.0100	0.059680	0.20
3:1	75	0.0375	0.0125	0.064125	0.25
2:1	67	0.0335	0.0165	0.068938	0.33
1:1	50	0.0250	0.0250	0.072690	0.50
1:2	33	0.0165	0.0335	0.062129	0.67
1:3	25	0.0125	0.0375	0.055140	0.75
1:4	20	0.0100	0.0400	0.050786	0.80
1:5	0	0.0000	0.0500	0.024672	1.00

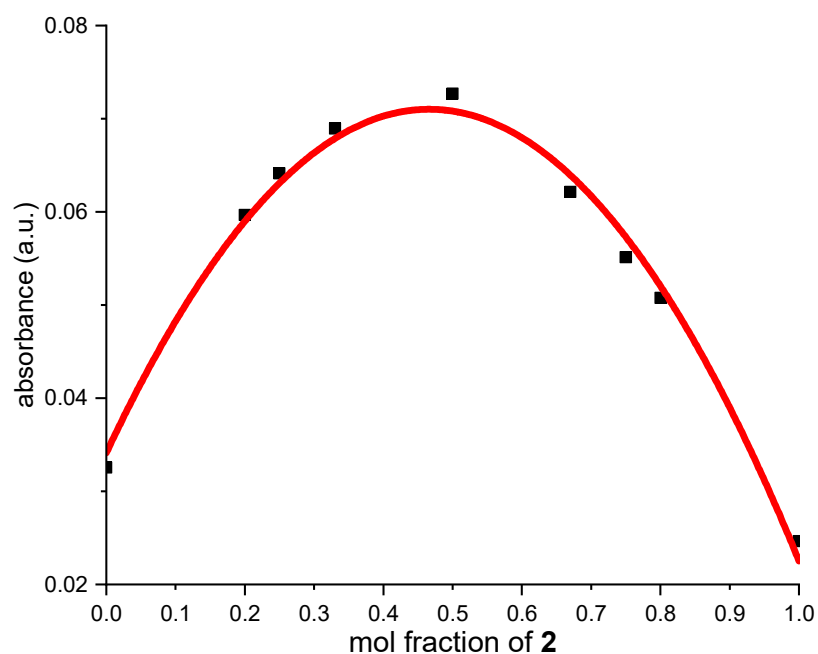


Figure 3. Job plot of **1** and **2** (0.050 M in CH₂Cl₂) at 435 nm with a maximum absorption for a 1:1 ratio of substrates.

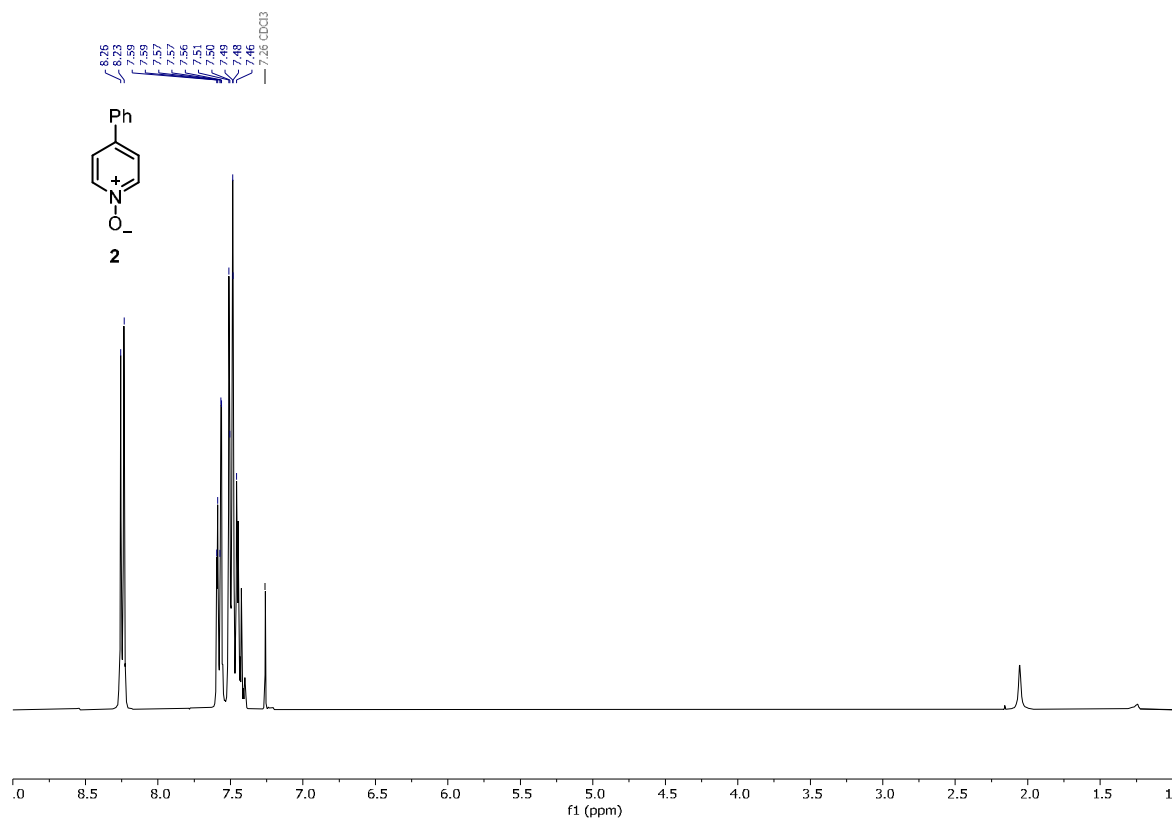


Figure 4. ¹H NMR spectrum of 4-phenyl-pyridine N-oxide **2** (0.10 M in CDCl₃).

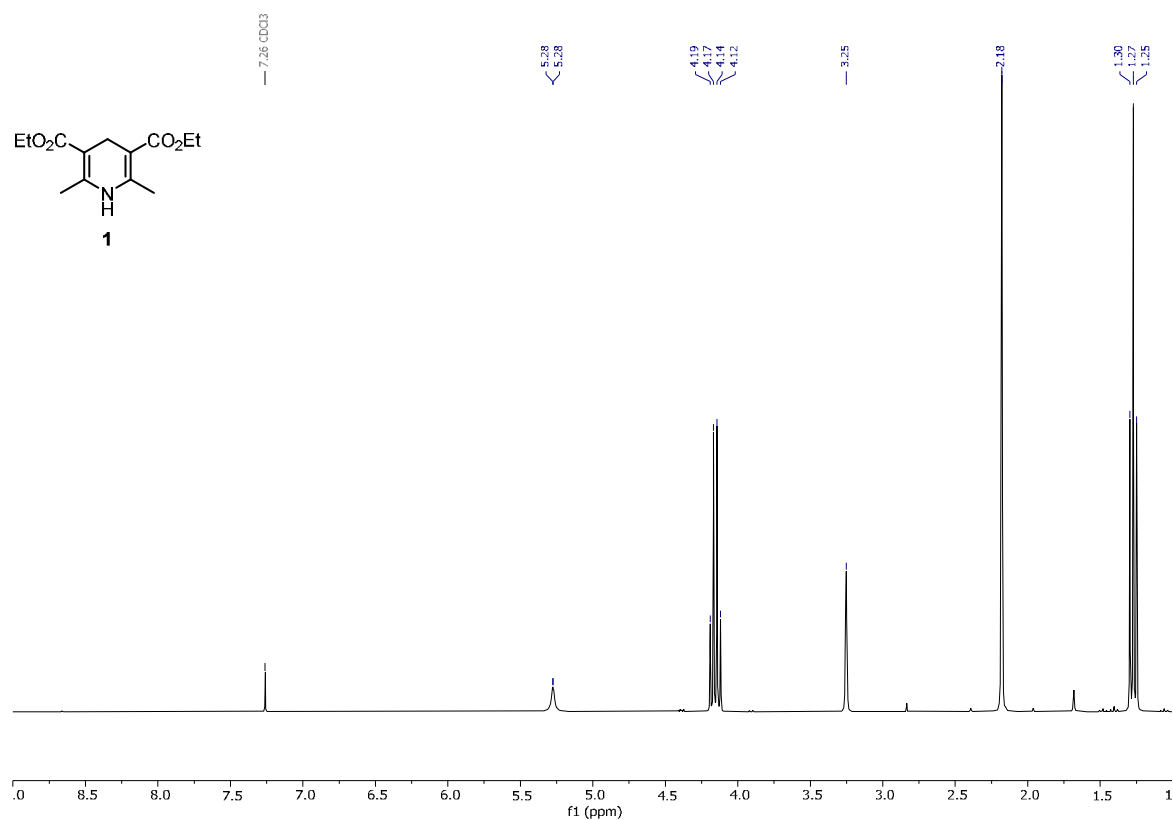


Figure 5. ¹H NMR spectrum of Hantzsch ester **1** (0.10 M in CDCl₃). (0.10 mmol in 1.0 mL CDCl₃).

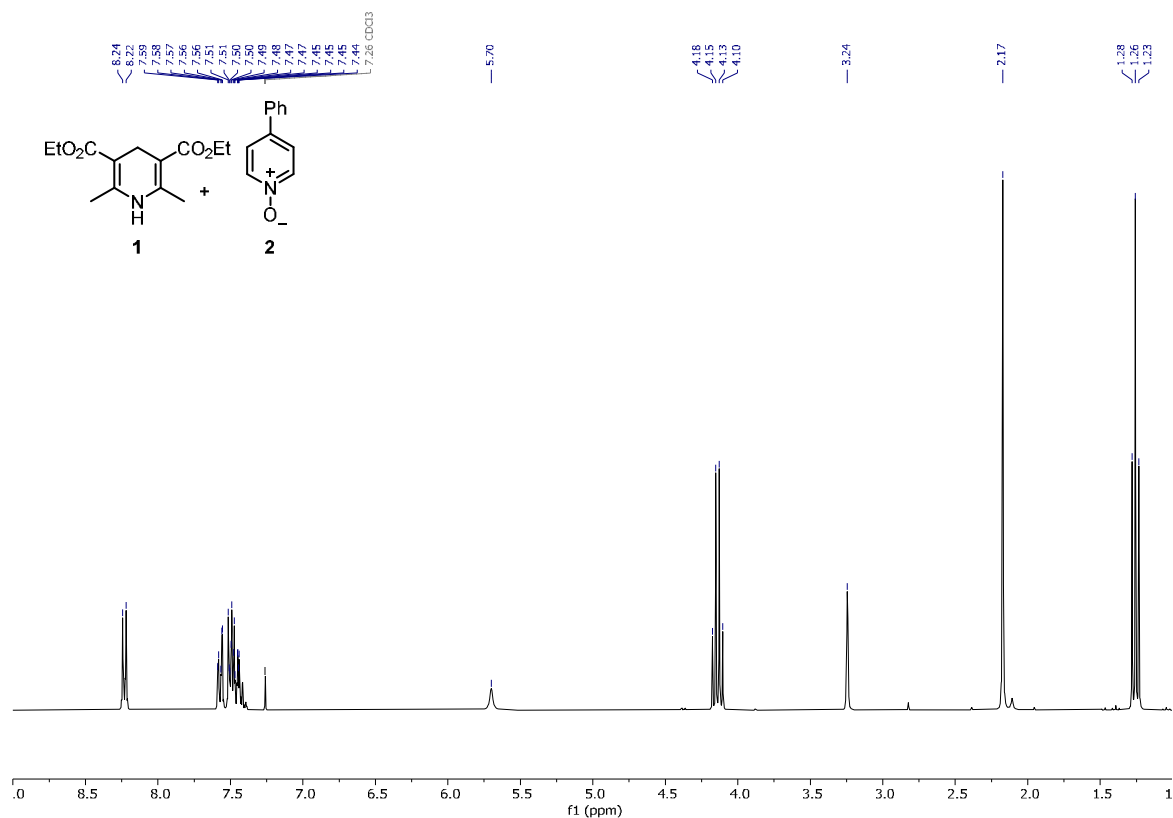


Figure 6. ^1H NMR spectrum of **1** (0.10 M in CDCl_3) and **2** (0.10 M in CDCl_3).

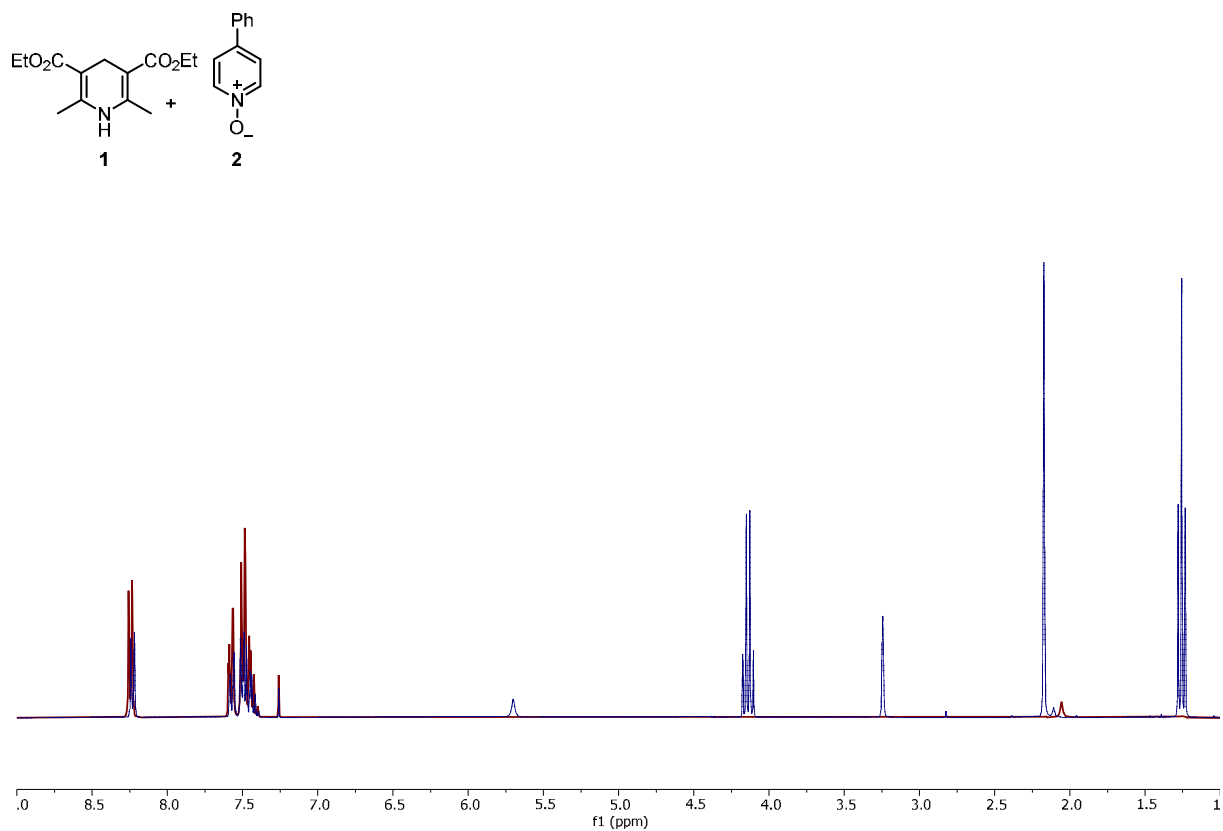


Figure 7. ^1H NMR spectrum overlay of **Figure 4** (red), **Figure 5** (green), and **Figure 6** (blue).

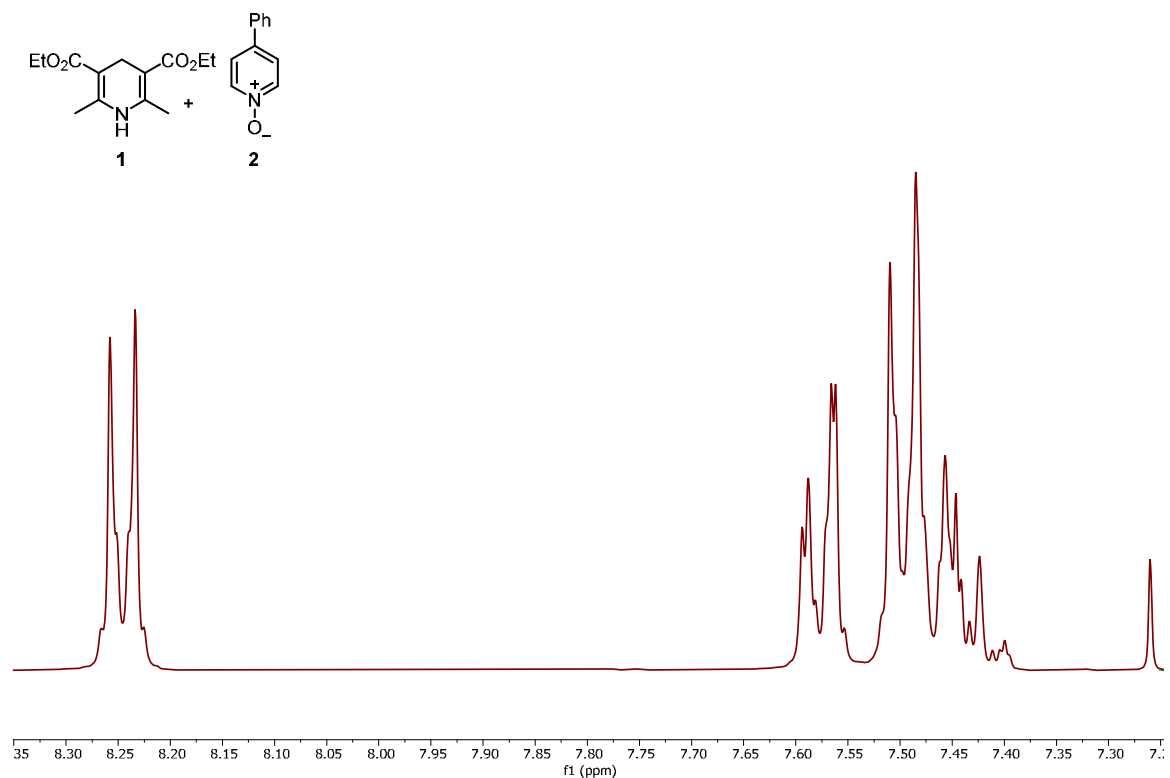


Figure 8. Zoom of Figure 7 between 8.35–7.25 ppm.

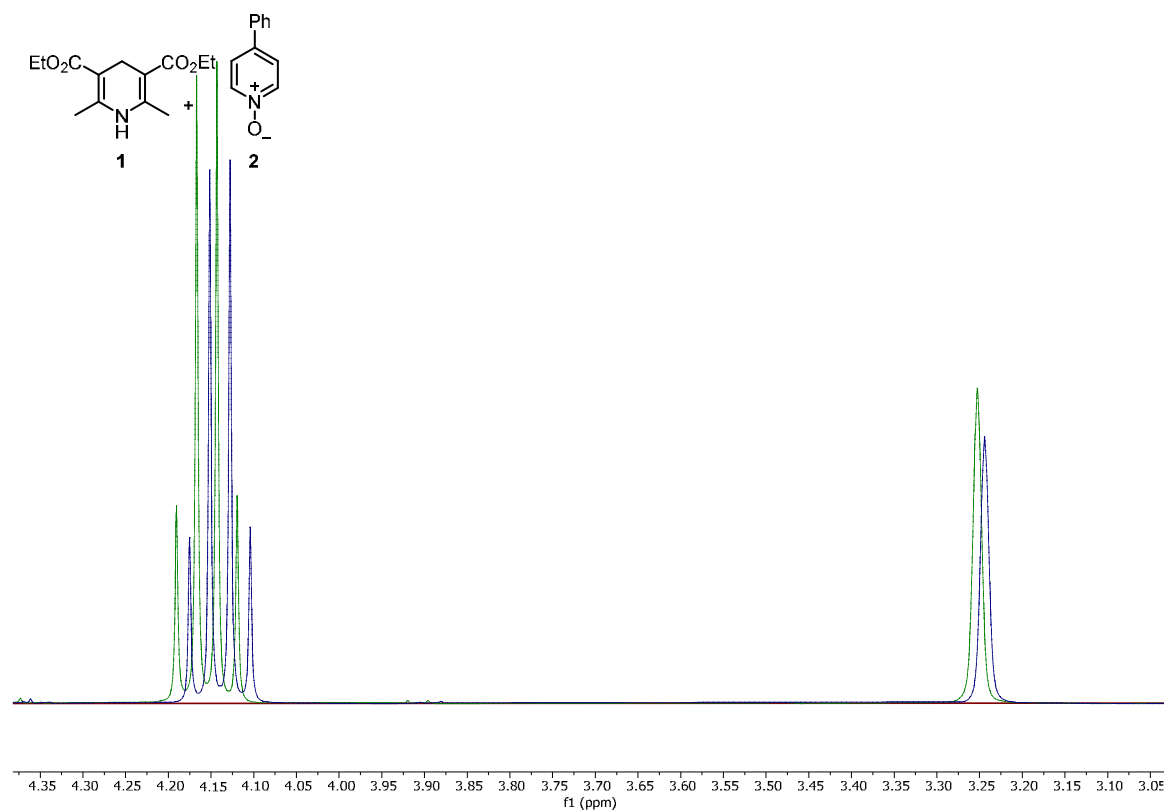


Figure 9. Zoom of Figure 7 between 4.35–3.00 ppm.

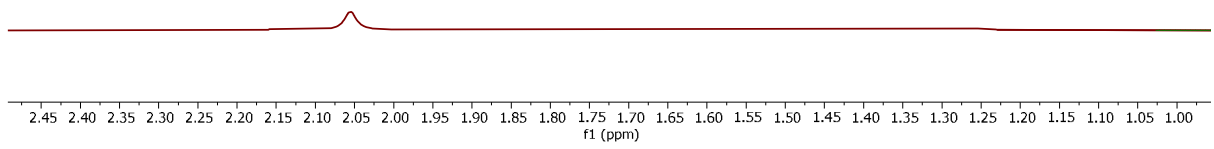
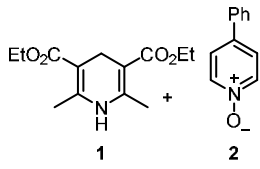
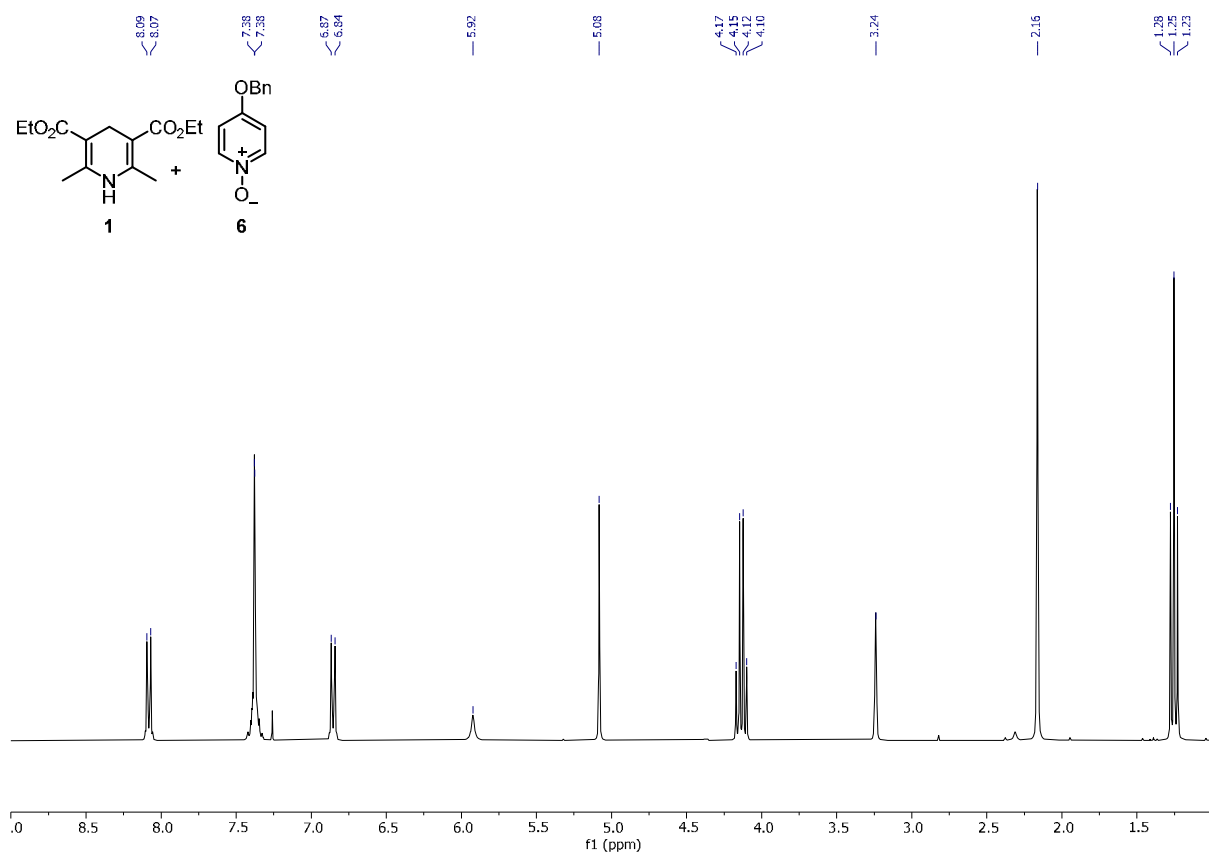
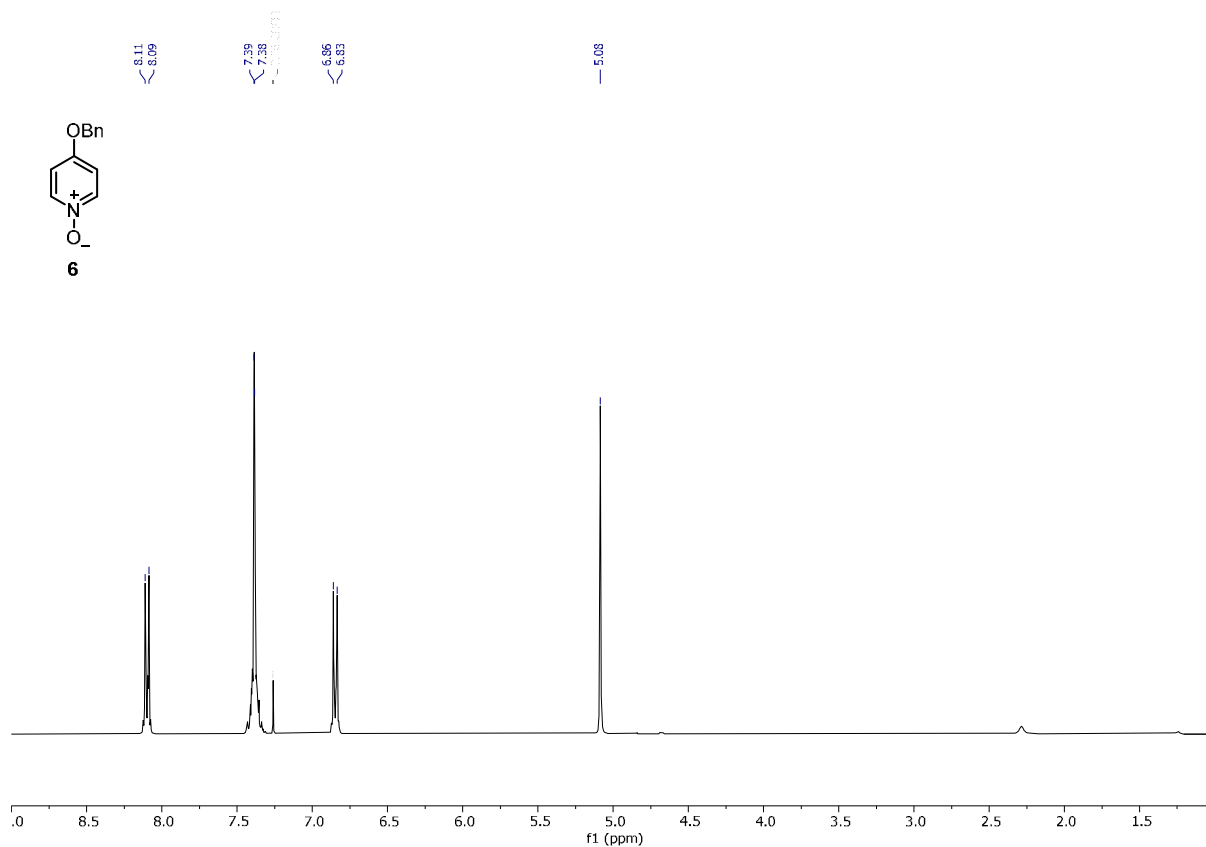


Figure 10. Zoom of Figure 7 between 2.50–0.95 ppm.



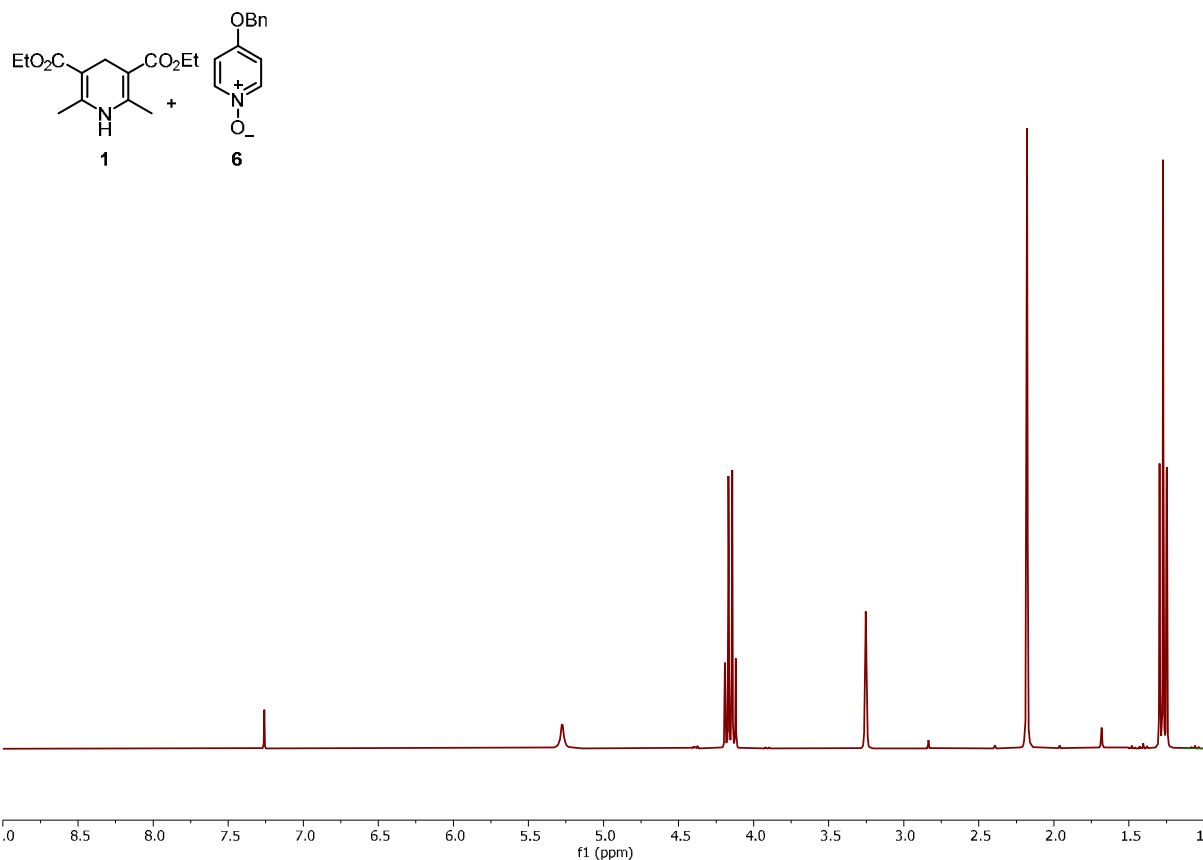


Figure 13. ¹H NMR spectrum overlay of Figure 9 (green), Figure 3 (red), and Figure 10 (blue).

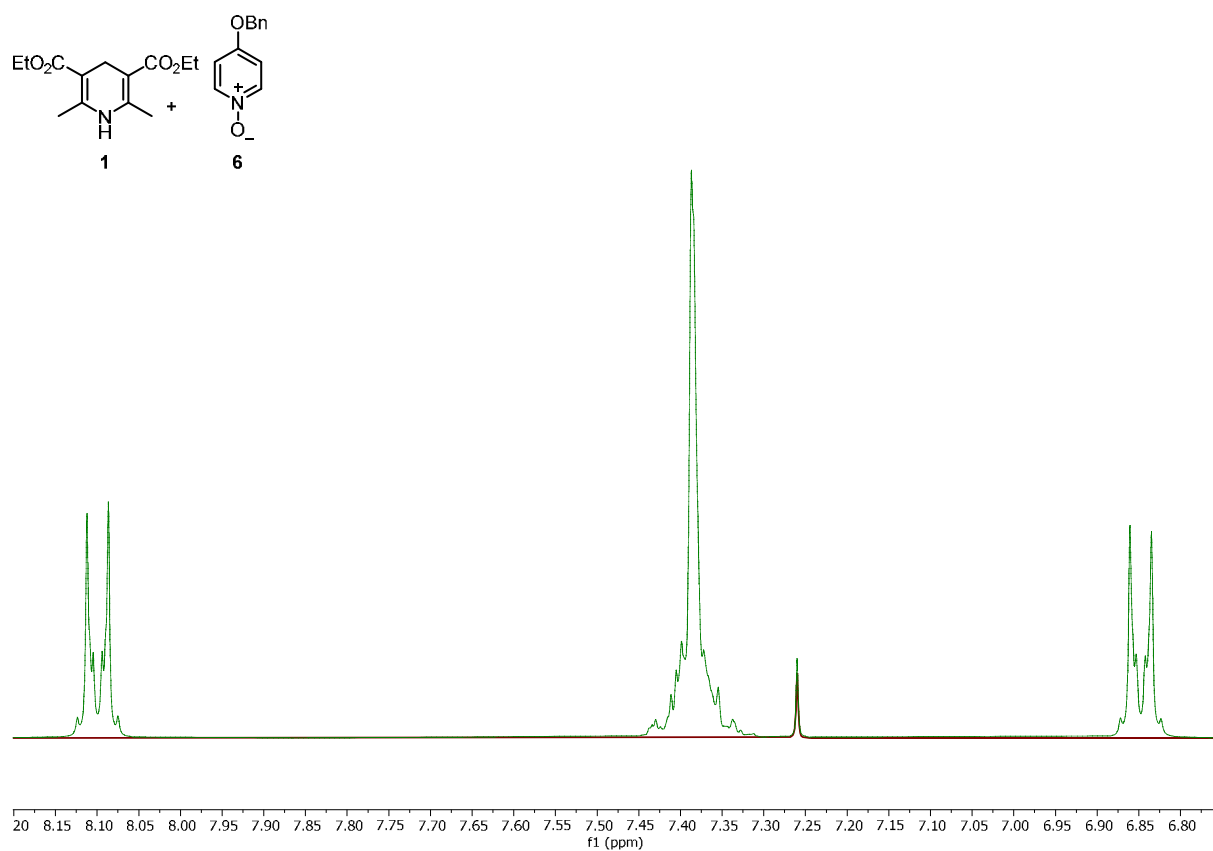


Figure 14. Zoom of Figure 11 between 8.20–6.75 ppm.

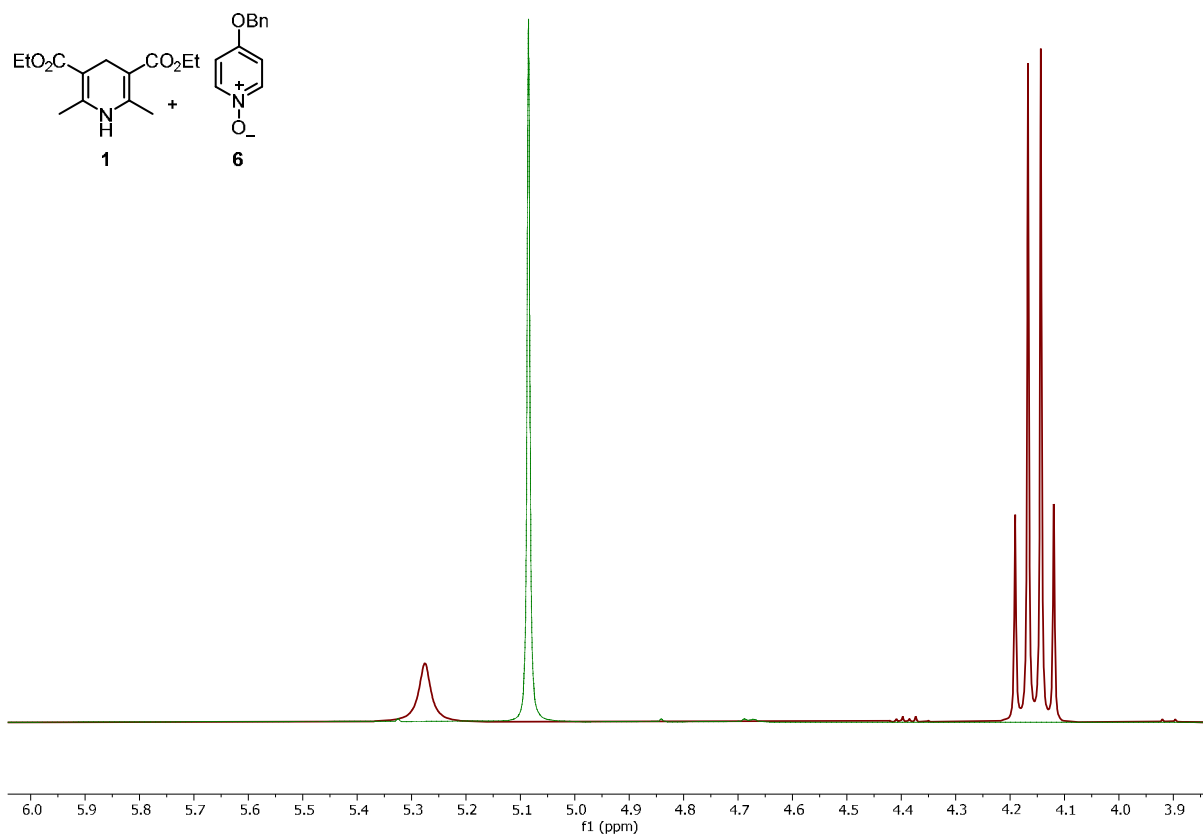


Figure 15. Zoom of Figure 11 between 6.05–3.85 ppm.

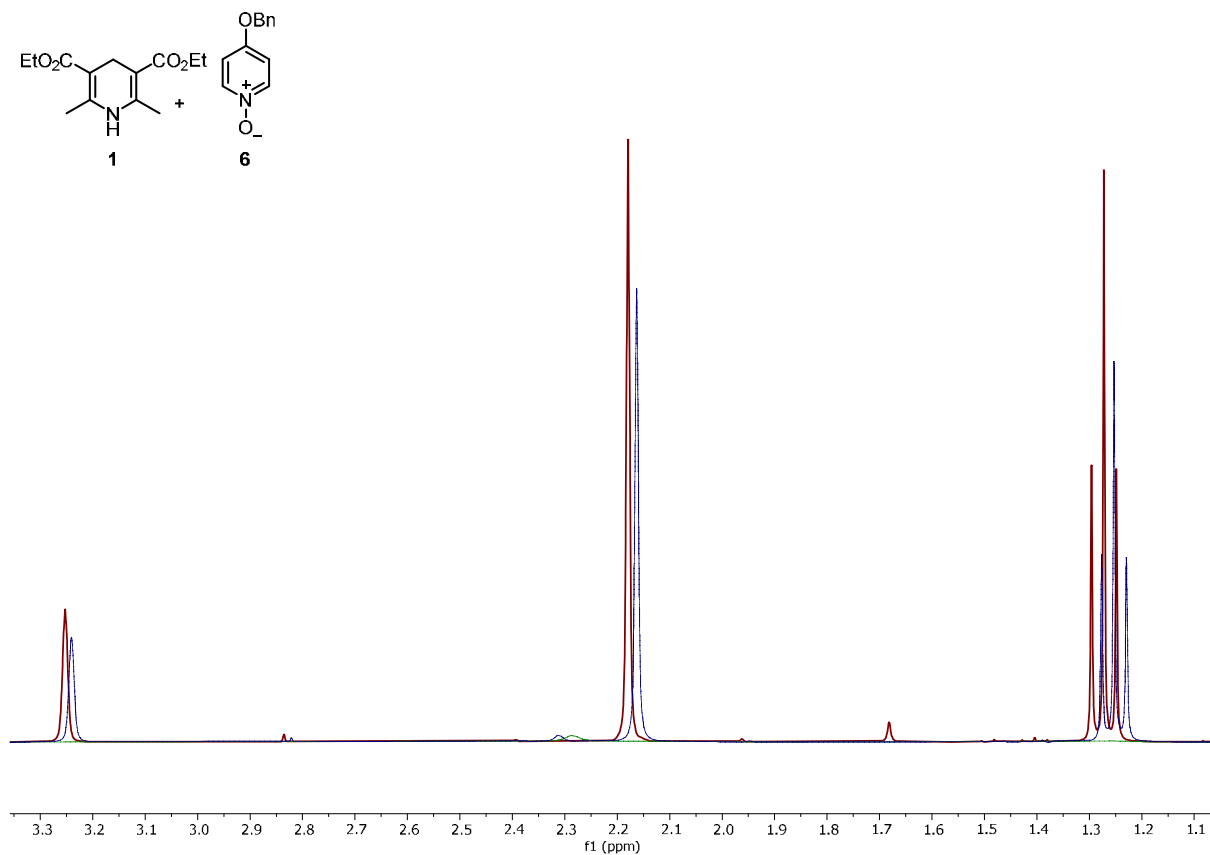


Figure 16. Zoom of Figure 11 between 3.25–1.05 ppm.

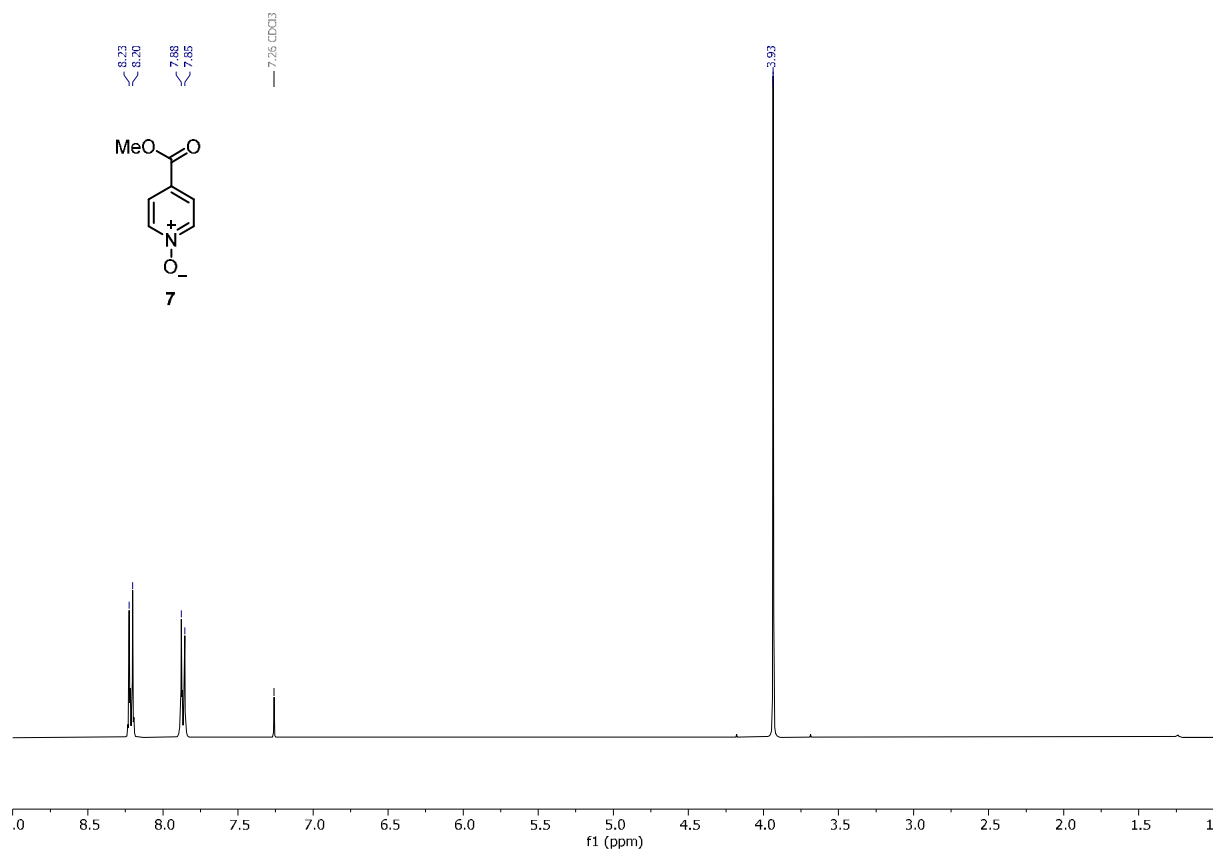


Figure 17. ¹H NMR spectrum of 4-(methoxycarbonyl)pyridine *N*-oxide **7** (0.10 M in CDCl₃).

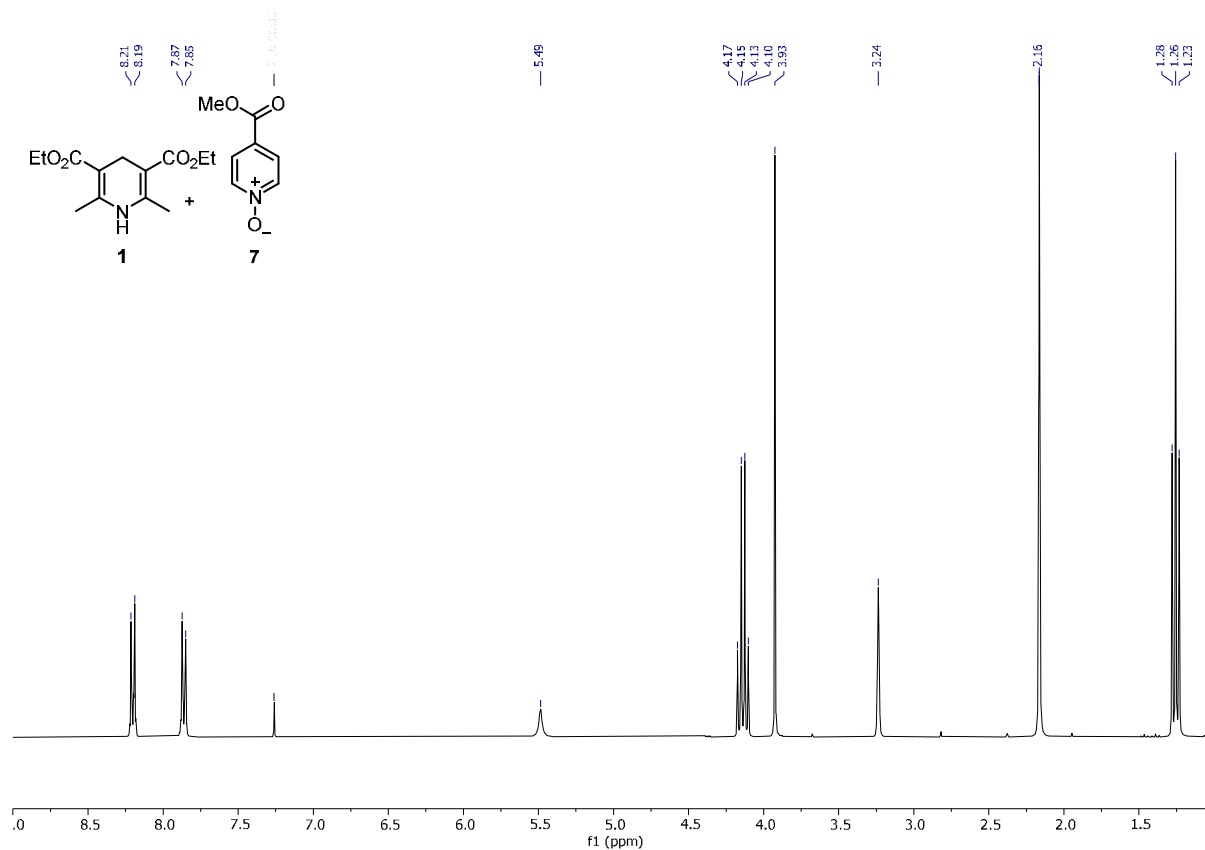


Figure 18. ¹H NMR spectrum of **1** (0.10 M in CDCl₃) and **7** (0.10 M in CDCl₃).

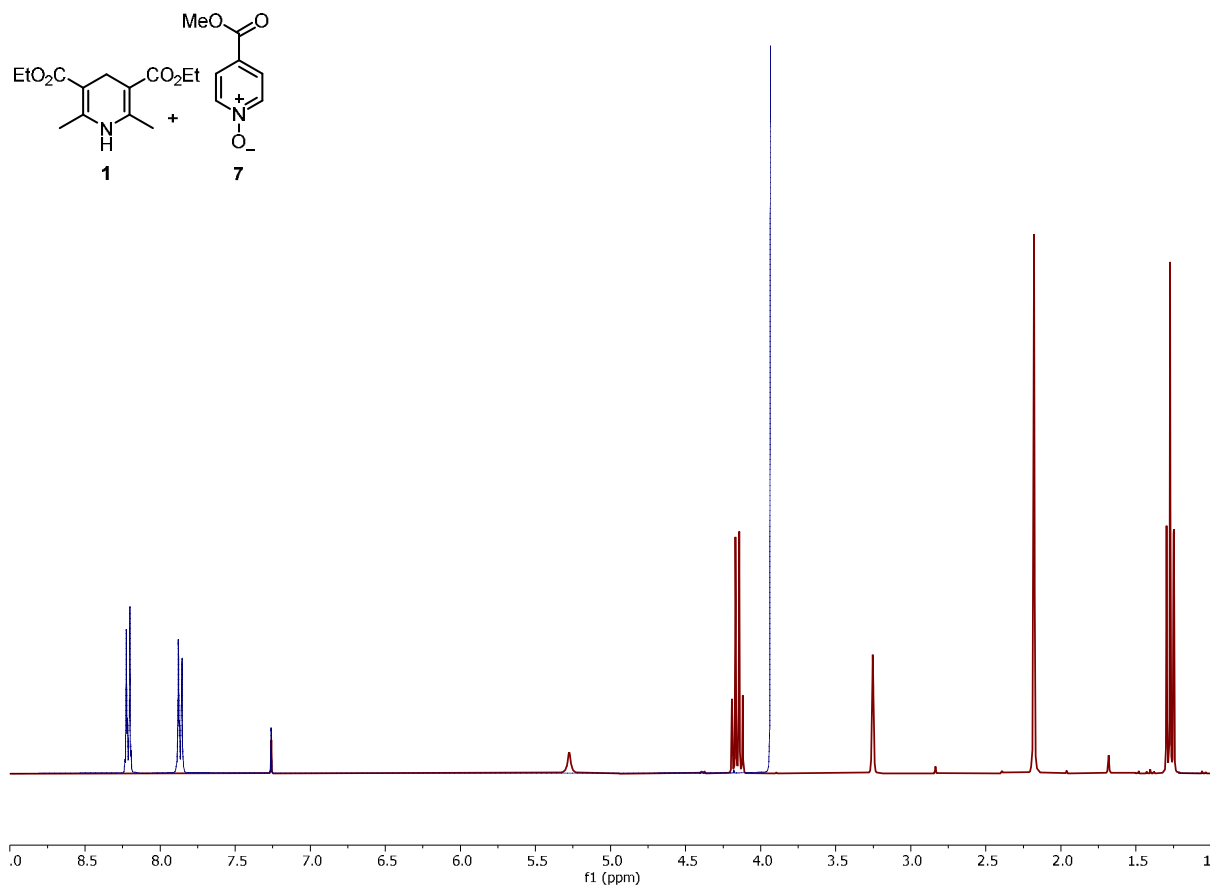


Figure 19. ^1H NMR spectrum overlay of **Figure 15** (blue), **Figure 3** (red), and **Figure 16** (green).

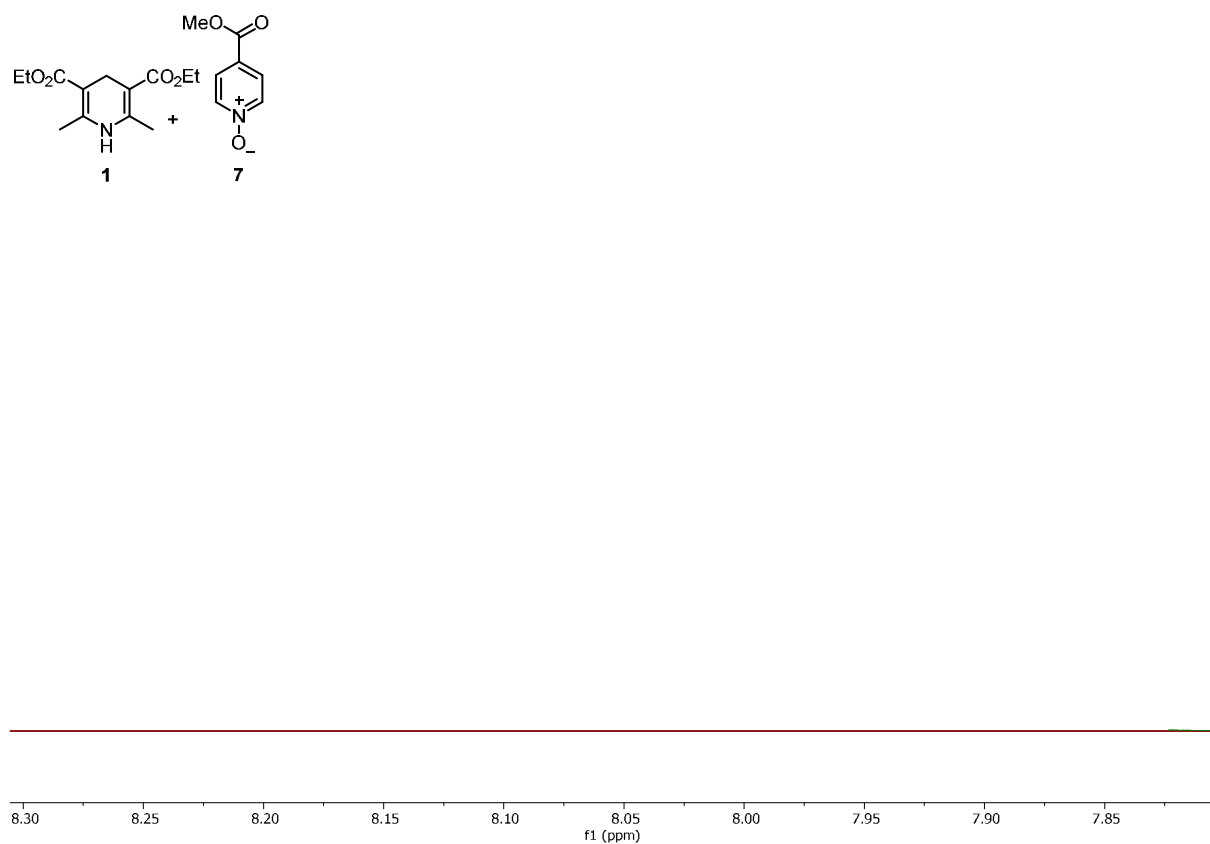


Figure 20. Zoom of **Figure 17** between 8.30-7.80 ppm.

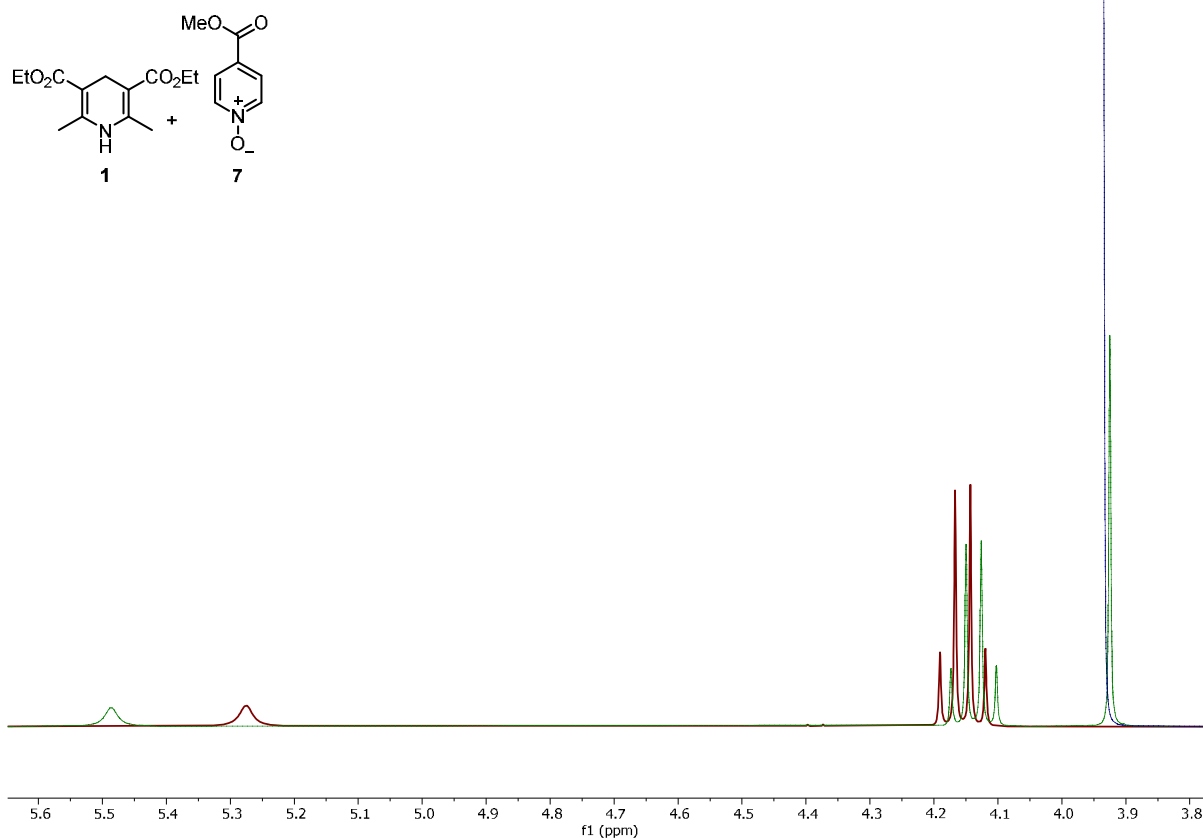


Figure 21. Zoom of Figure 17 between 5.65–3.75 ppm.

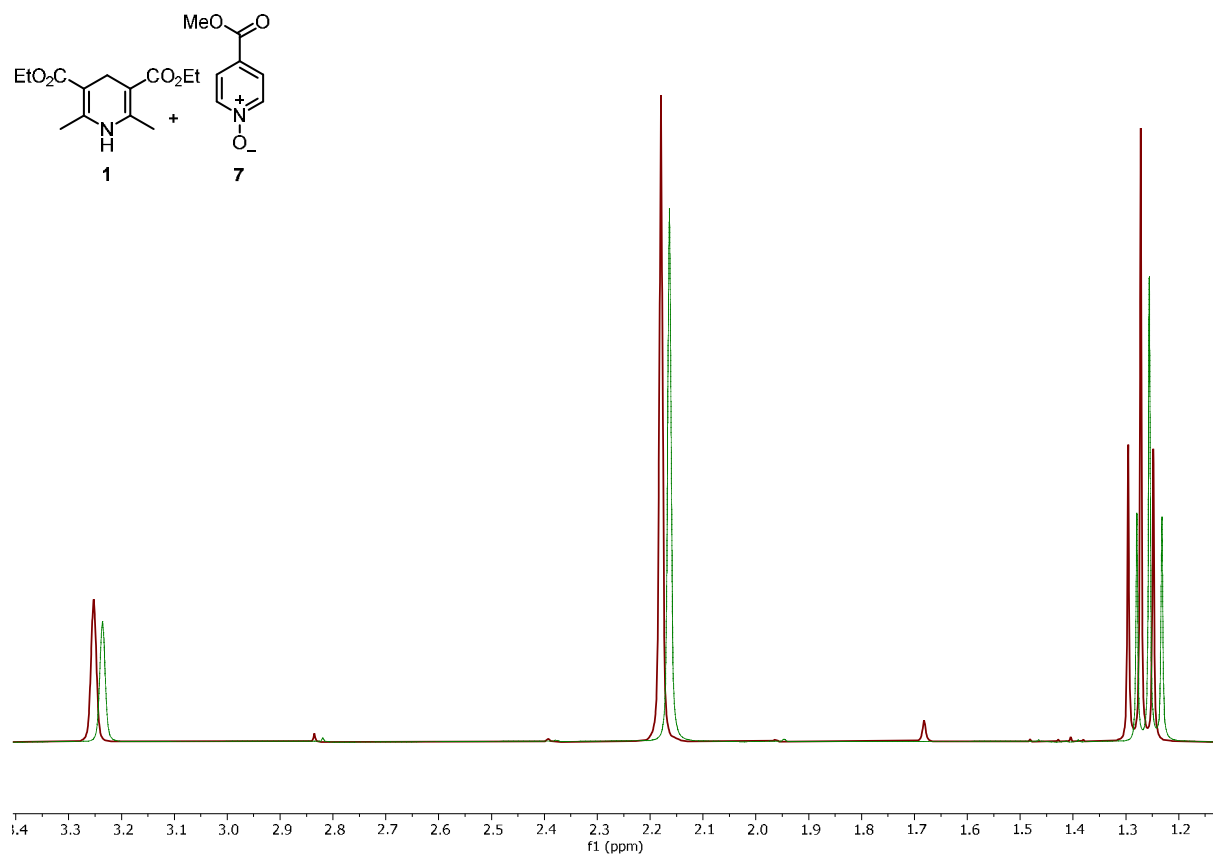
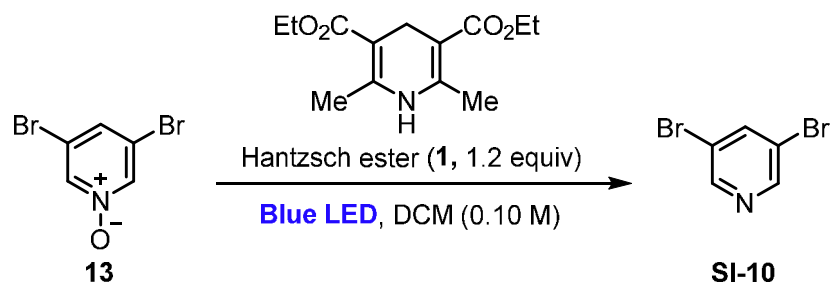


Figure 22. Zoom of Figure 17 between 3.40–1.15 ppm.

On/Off Experiment

To rule out a radical chain process for the deoxygenation, we conducted an “on/off” experiment described below. The results suggest no long-lived radical-chain processes; however, we cannot rule out short-lived radical-chain processes.



A typical experiment using 3,5-dibromopyridine *N*-oxide **13** was setup according to the general procedure A on 0.40 mmol-scale. Upon addition of all reagents, the reaction was irradiated for an hour (“on”) and after the elapsed time, 100 μ L were taken out of the reaction mixture and combined with 100 μ L of a stock solution of 1,3,5-trimethoxybenzene (0.10 M in DCM) as an external standard. This mixture was concentrated under reduced pressure and taken up in CDCl_3 for ^1H NMR analysis to determine the yield of product. Meanwhile, the reaction mixture was allowed to stir in the dark (“off”) for an additional hour, and the ^1H NMR analysis protocol was repeated. This procedure was conducted for three “on” and two “off” cycles as shown below.

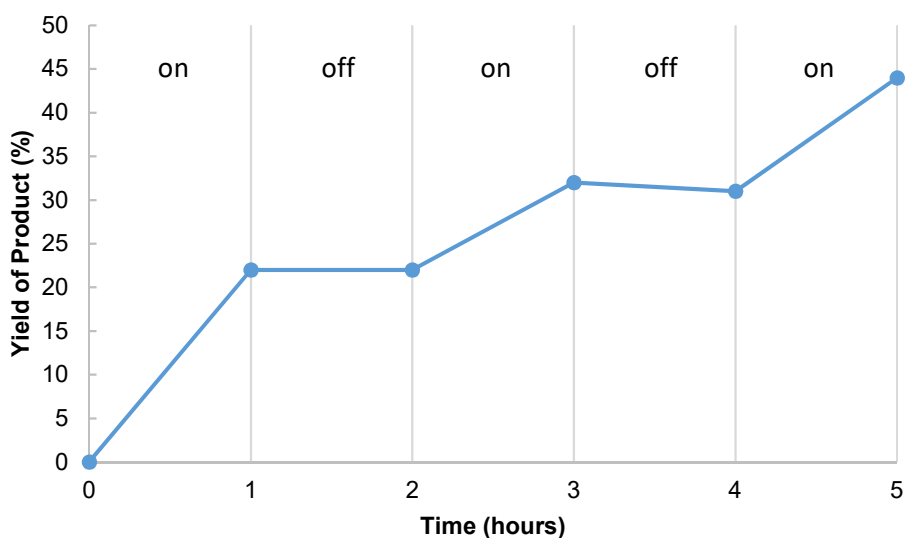


Figure 23. On/Off experiment results indicating deoxygenation occurs only upon irradiation on an hour time scale.

Emission Quenching Experiments

Fluorescence measurements were acquired at room temperature using an Agilent Technologies Cary Eclipse Fluorescence Spectrophotometer with excitation slits open at 5 nm and emission slit open at 10 nm. Emission quenching of Hantzsch ester (0.33 mM) by 4-phenylpyridine-*N*-oxide was done in quartz cuvettes (Precision cell SUPRASIL, Art. No. 117100F-10-40, Hellma Analytics) with argon-purged DMSO. The quencher solution of 4-phenylpyridine-*N*-oxide (50 mM) and Hantzsch ester (0.33 mM) was degassed for 8 minutes and added using 1 mL gas tight syringe through a rubber septum fitted with an argon balloon. The balloon remained inserted in between quencher additions to prevent oxygen from entering the cuvette and quenching the Hantzsch ester emission. An excitation wavelength of 380 nm was used. Fluorescence intensity was integrated from 400 nm to 600 nm.

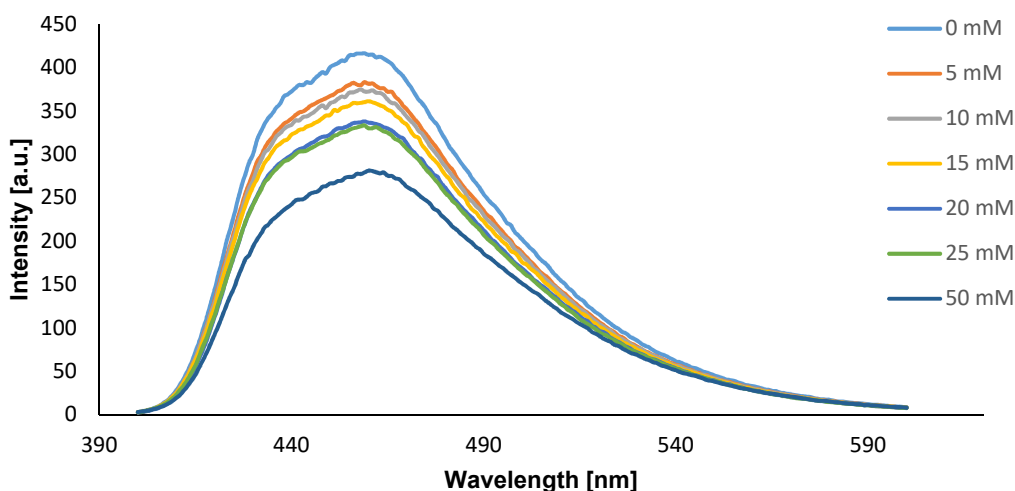


Figure 24. Emission of a Hantzsch ester solution (top blue line, DMSO, 0.33 mM) recorded in presence of increasing amounts of 4-phenylpyridine-*N*-oxide with a $\lambda_{\text{ex}} = 380$ nm.

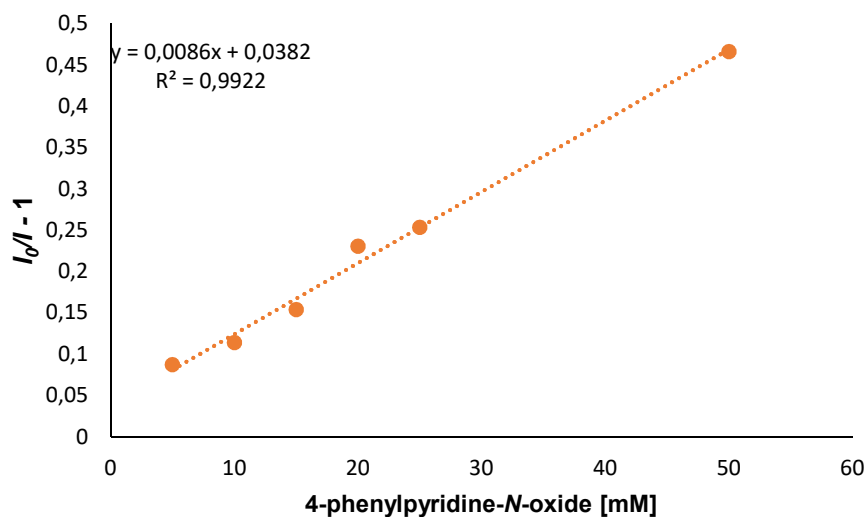
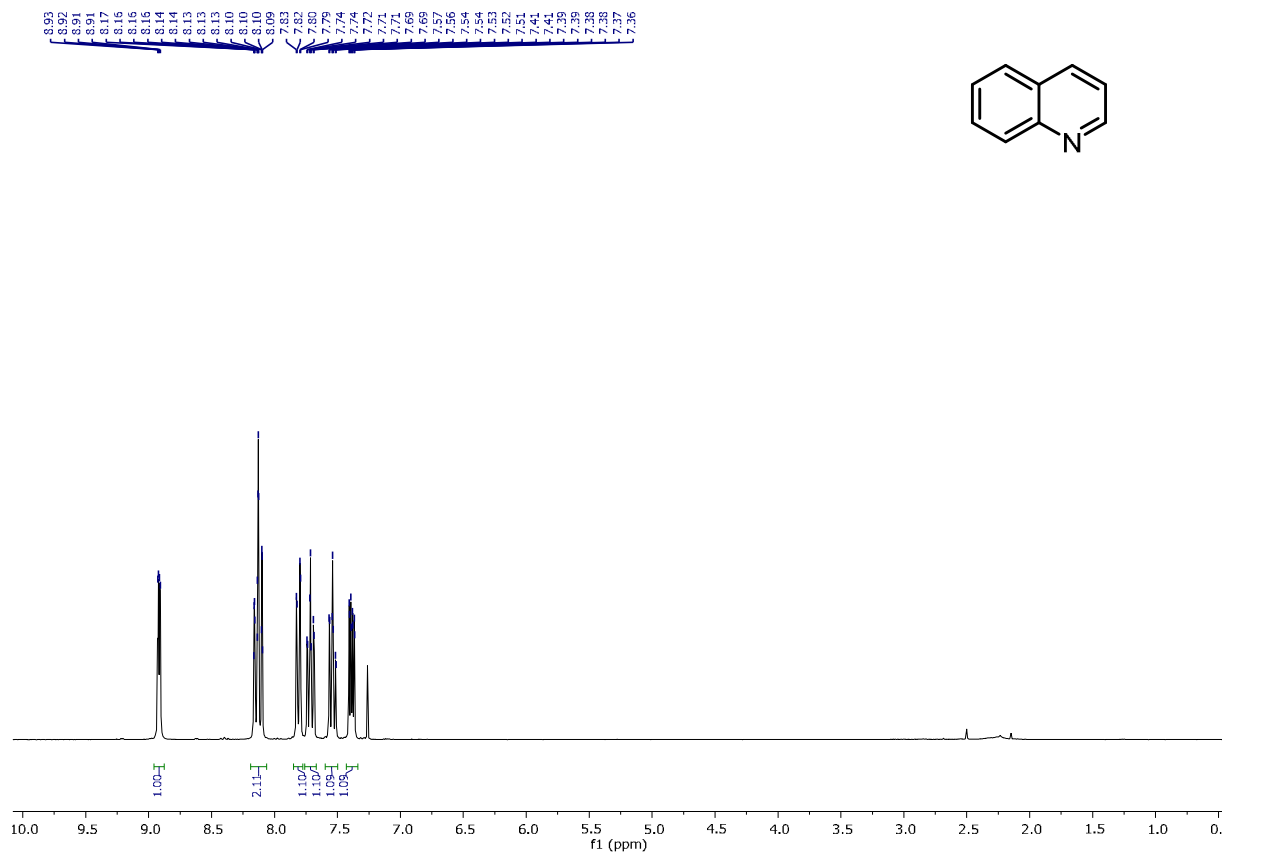
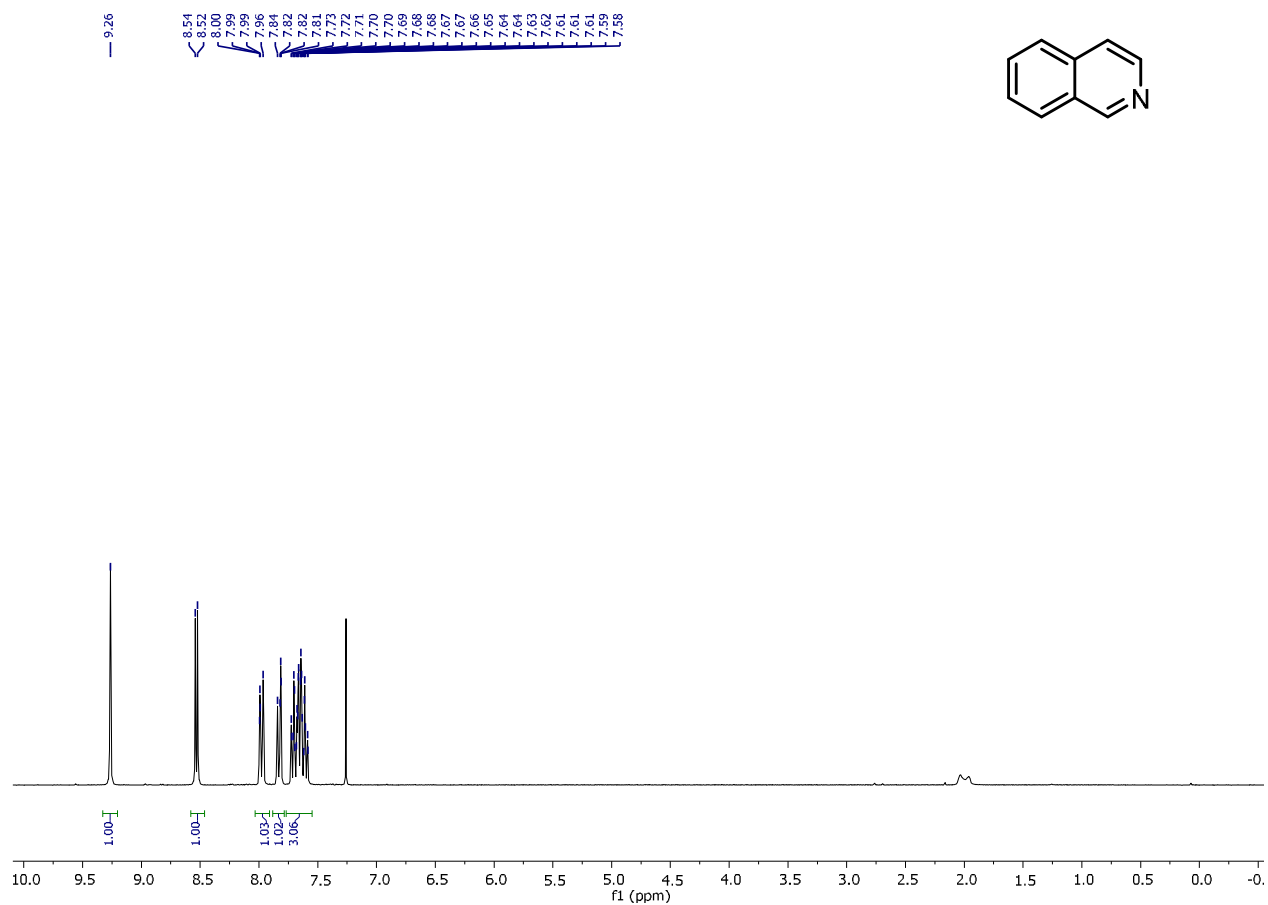
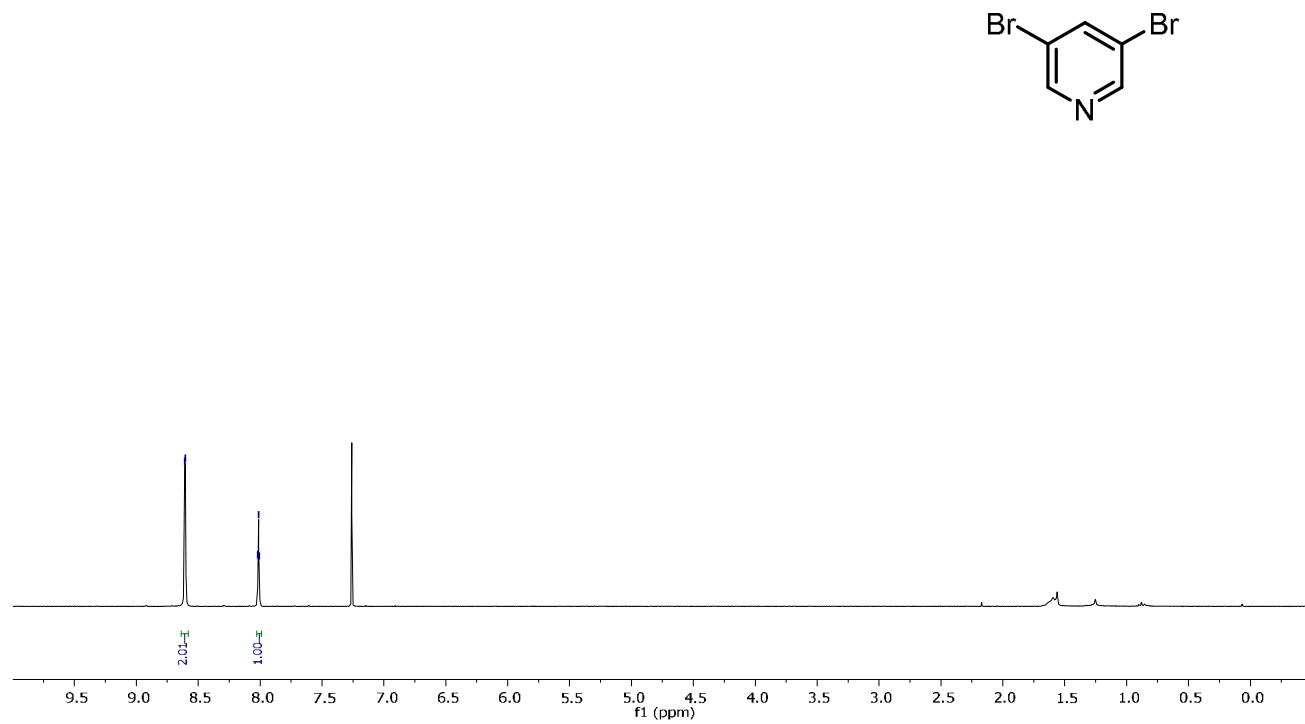
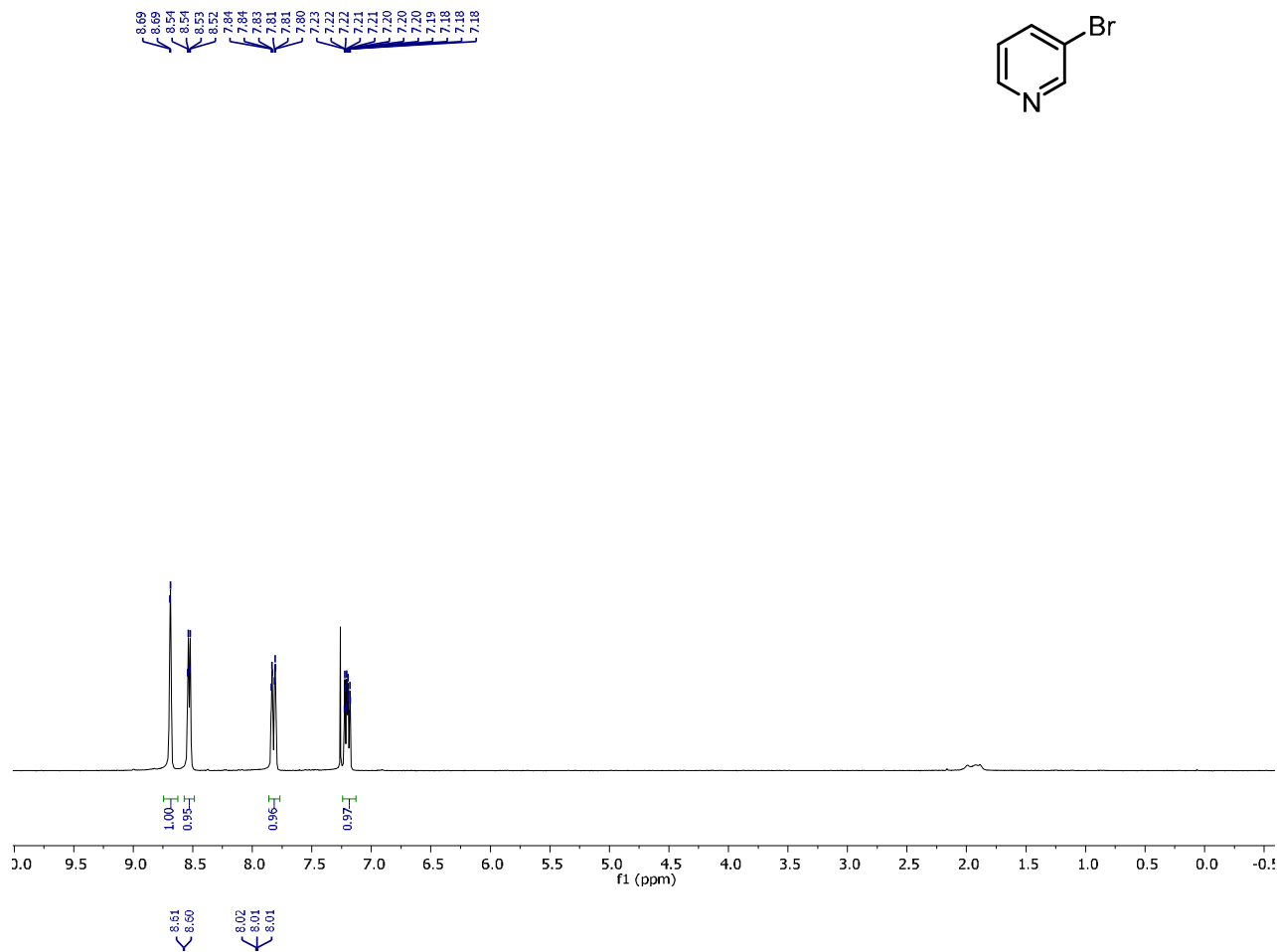
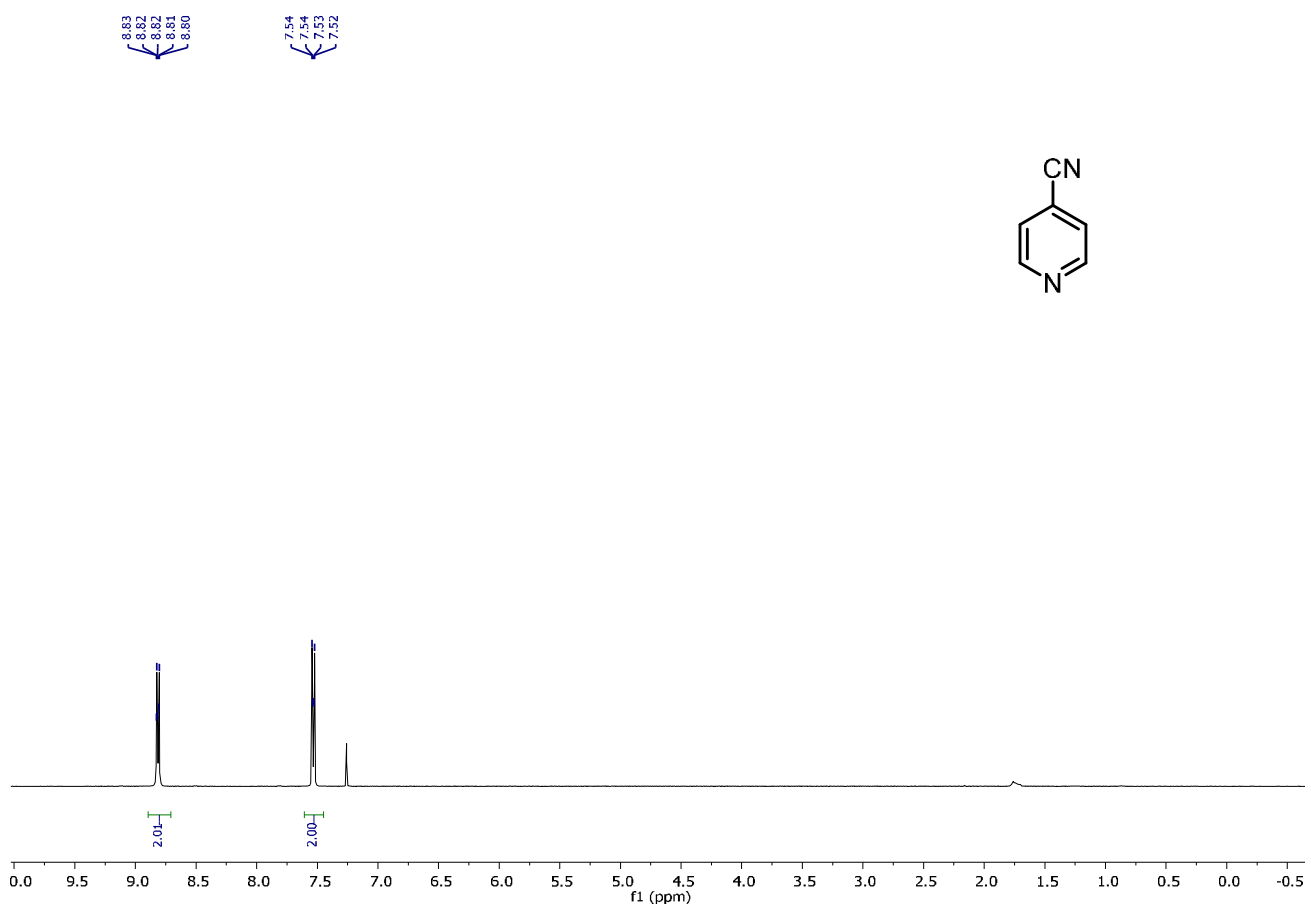
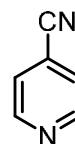
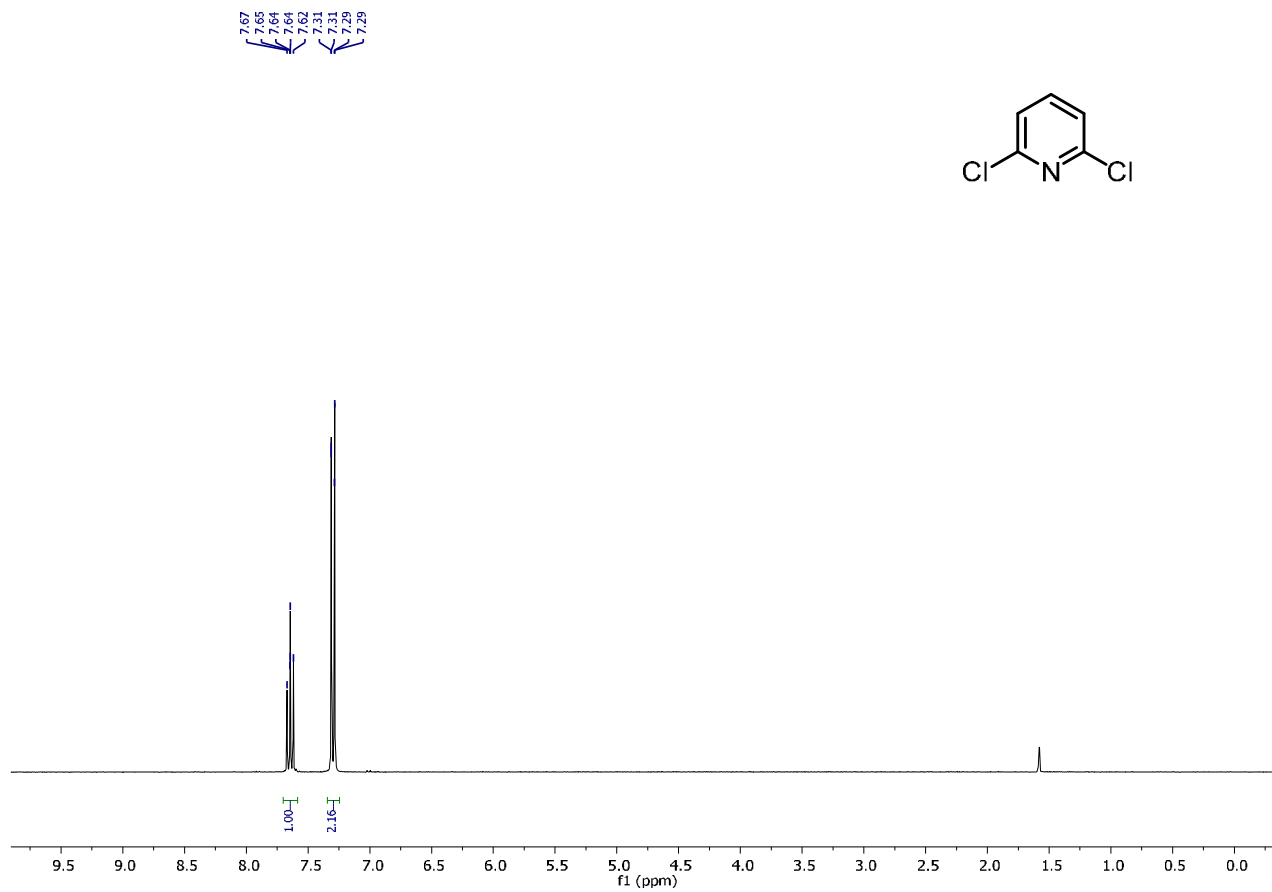
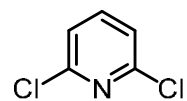


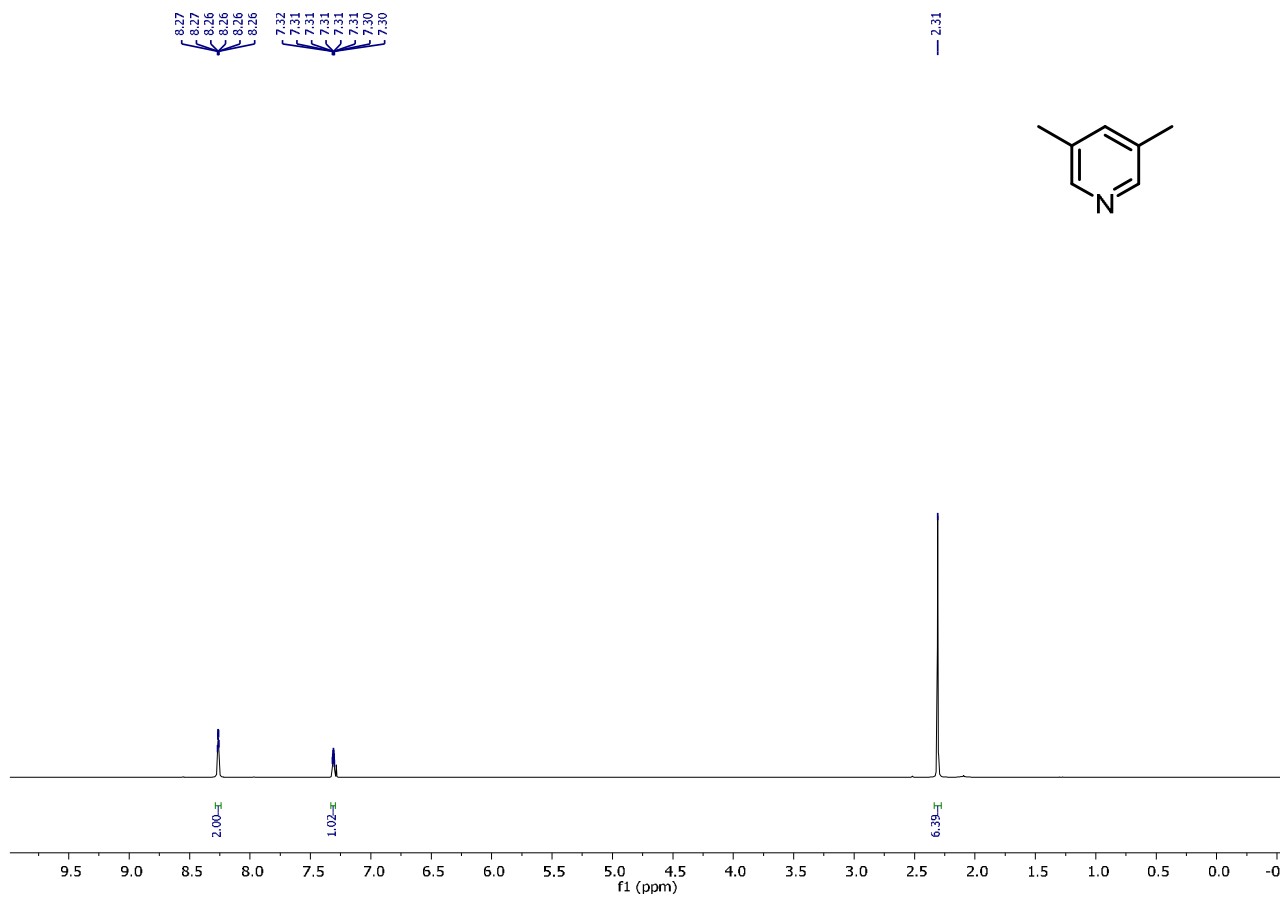
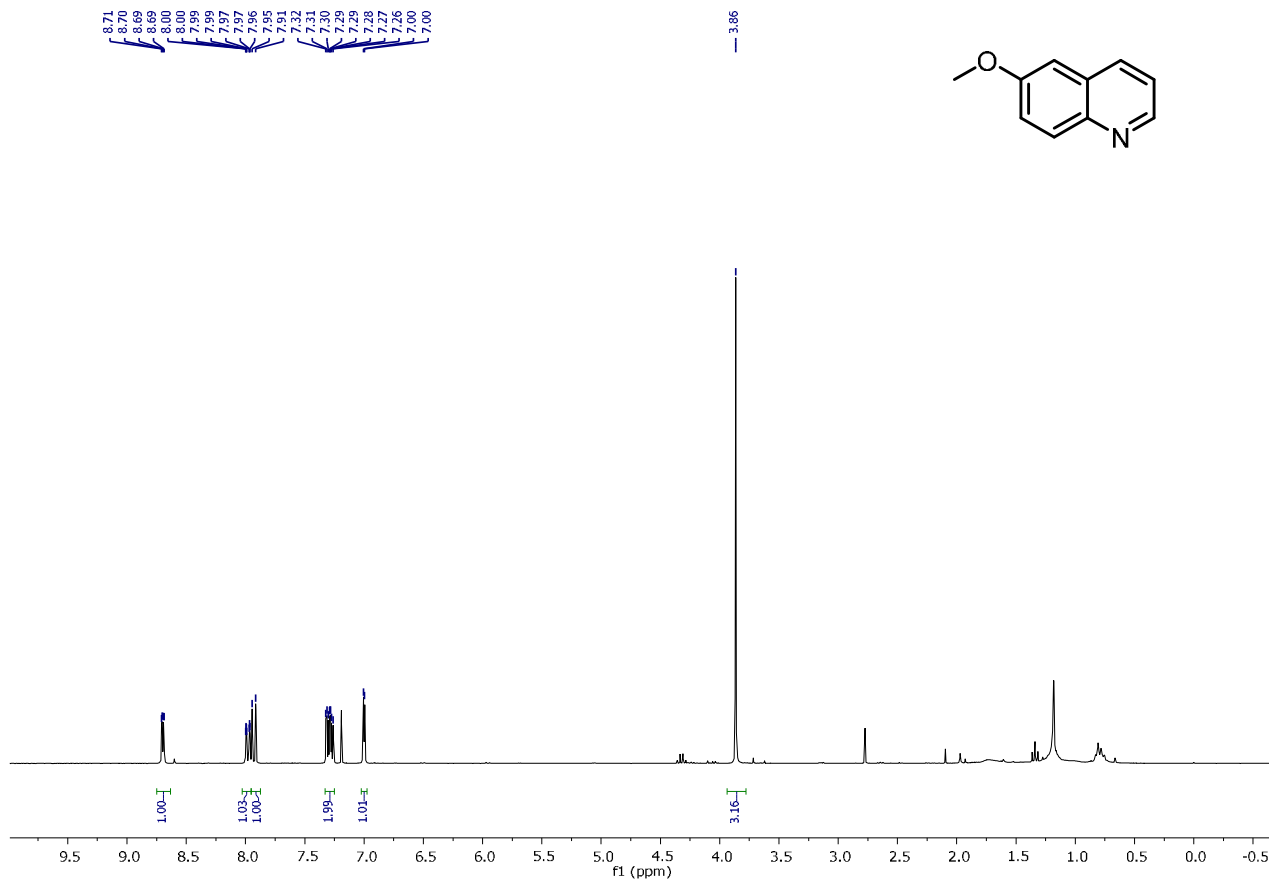
Figure 25. Stern-Volmer plot analysis derived from the data extracted from Figure 24.

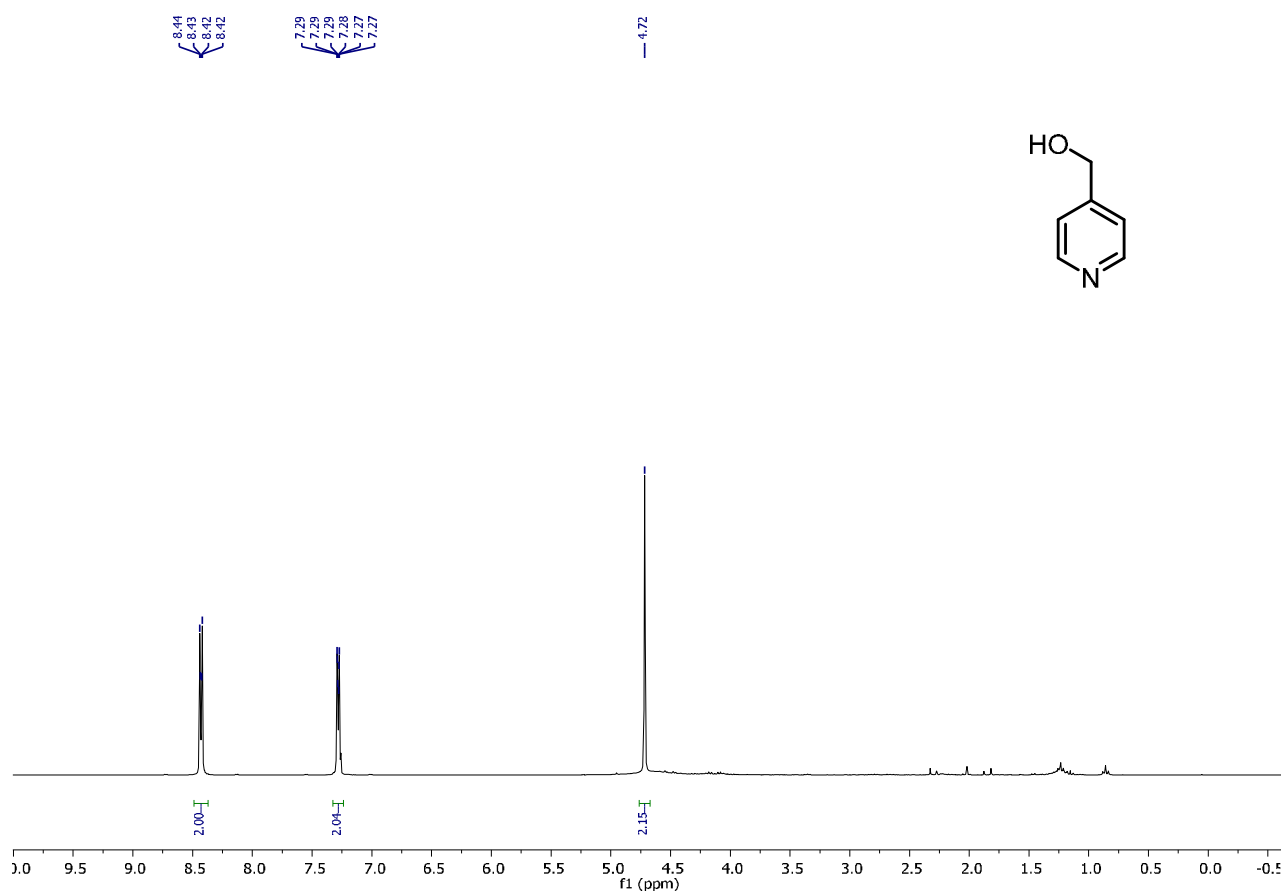
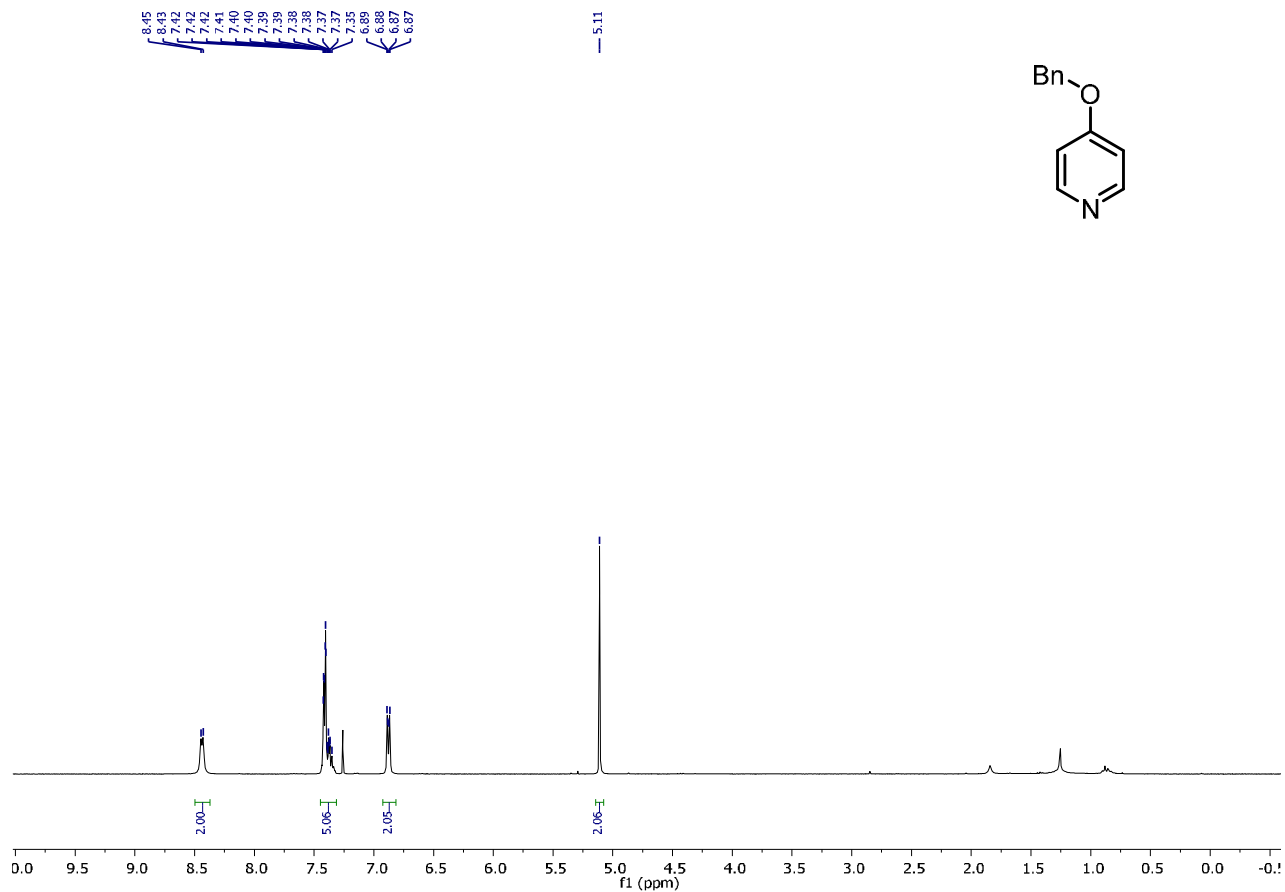
3.4.4 NMR of compounds

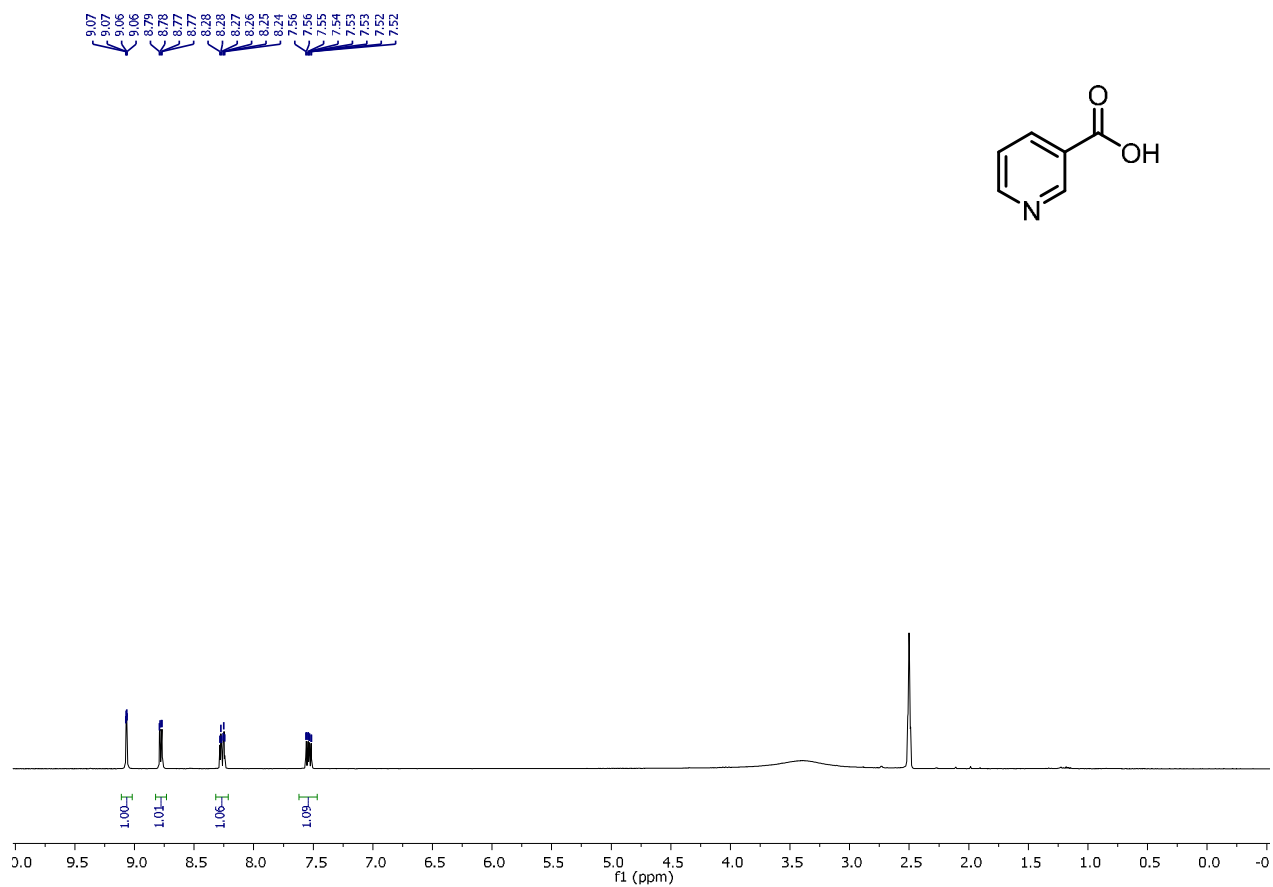
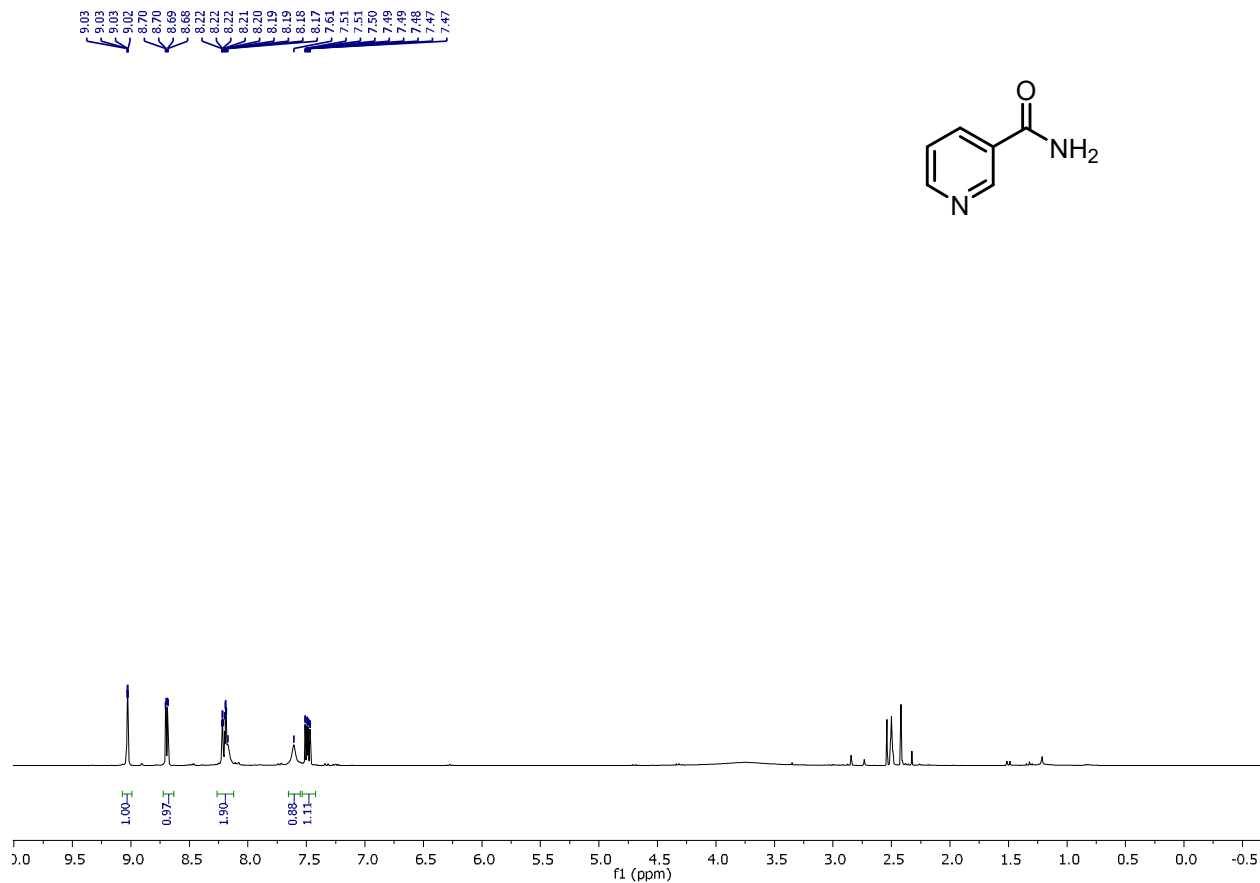


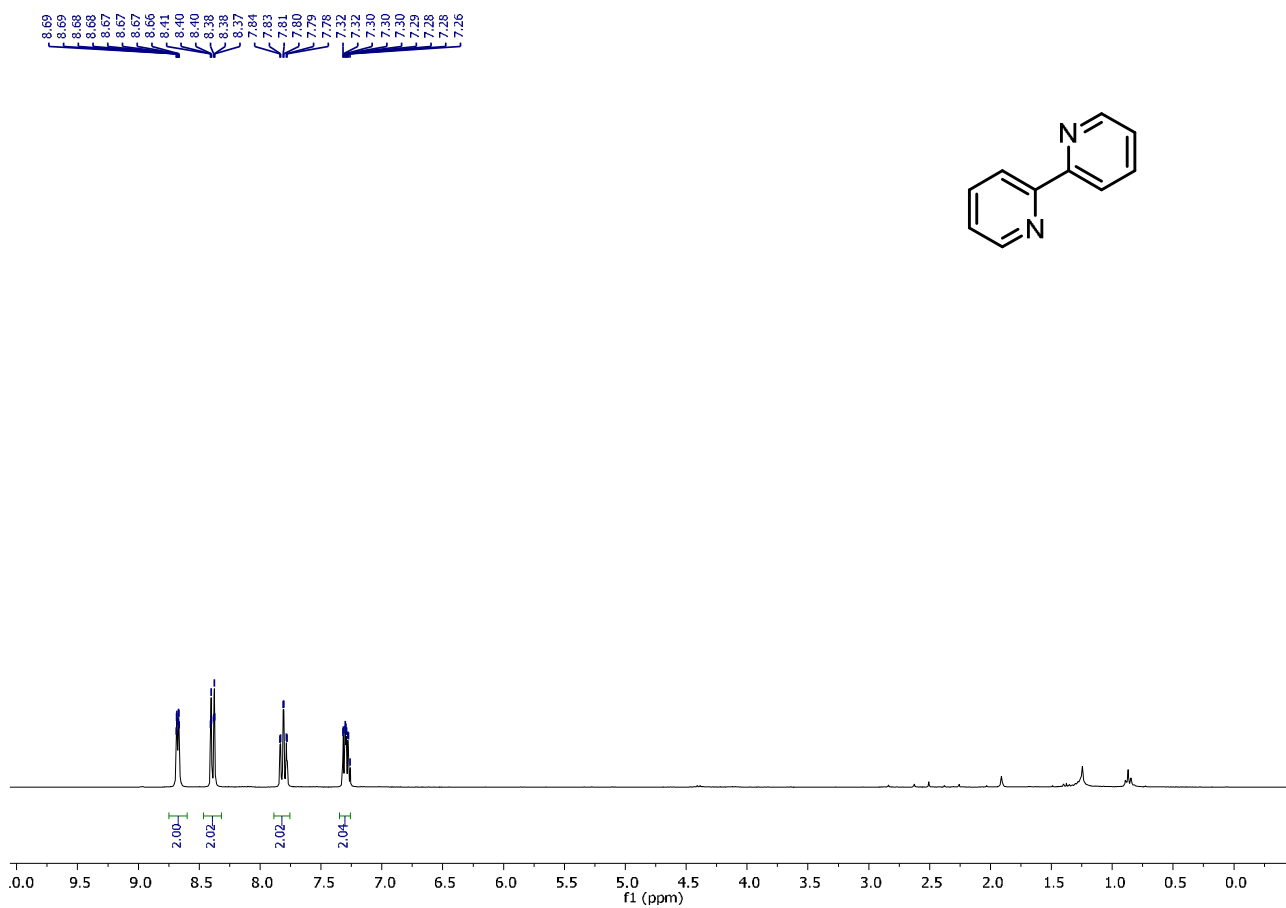
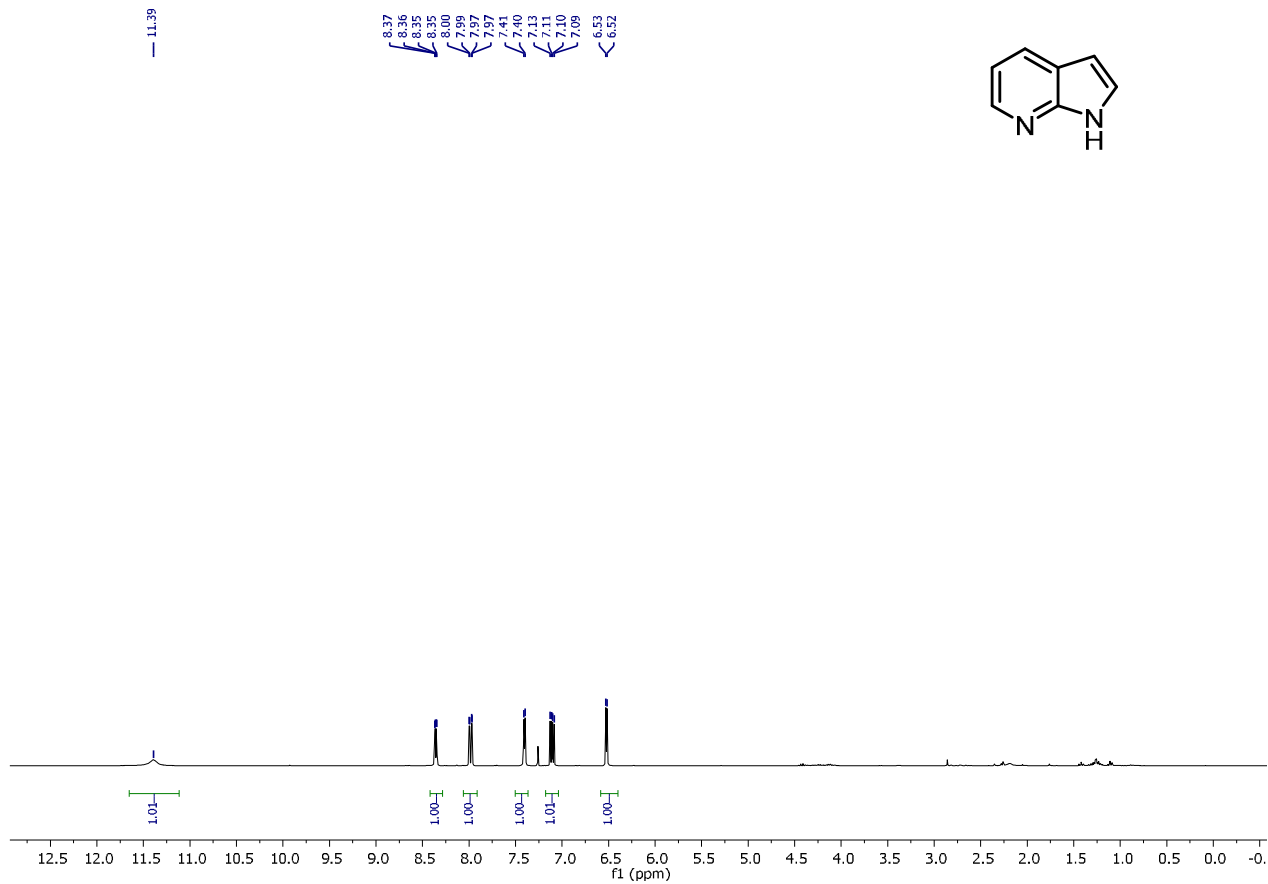


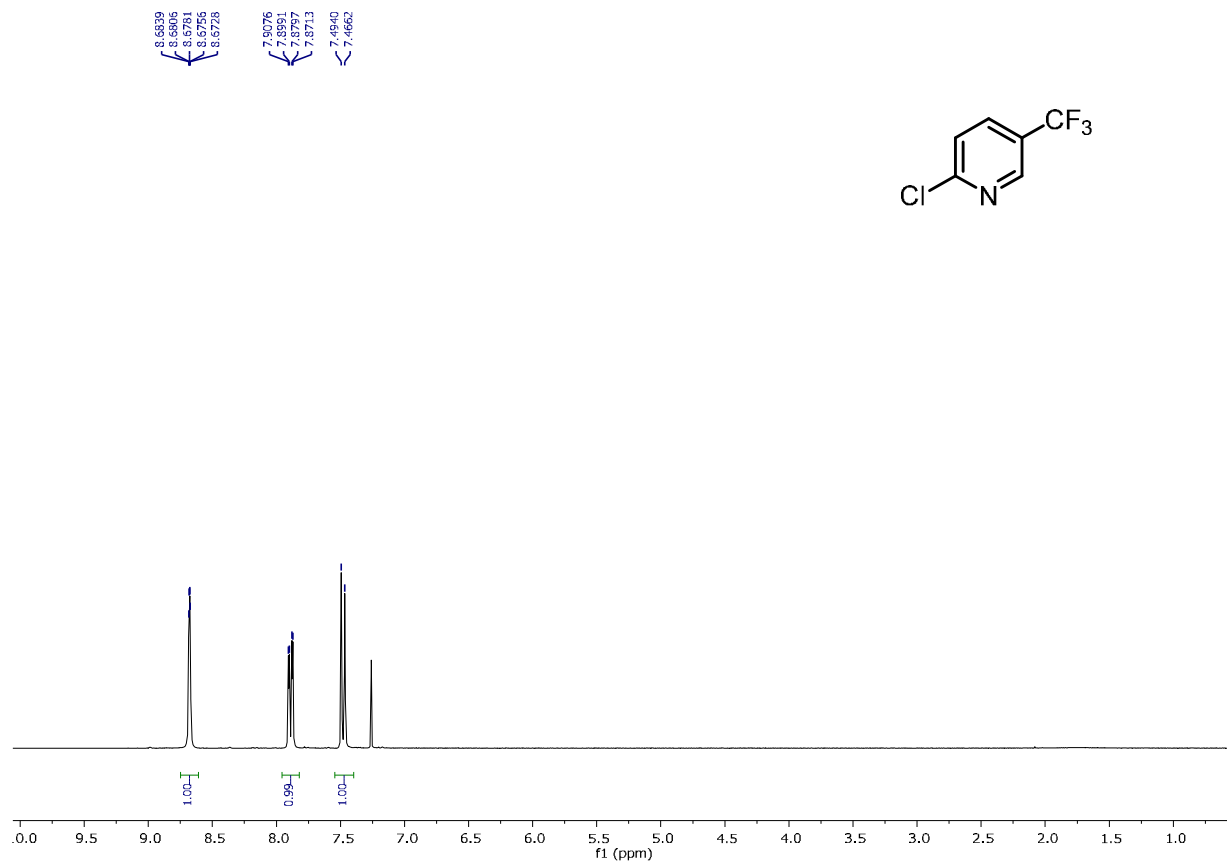
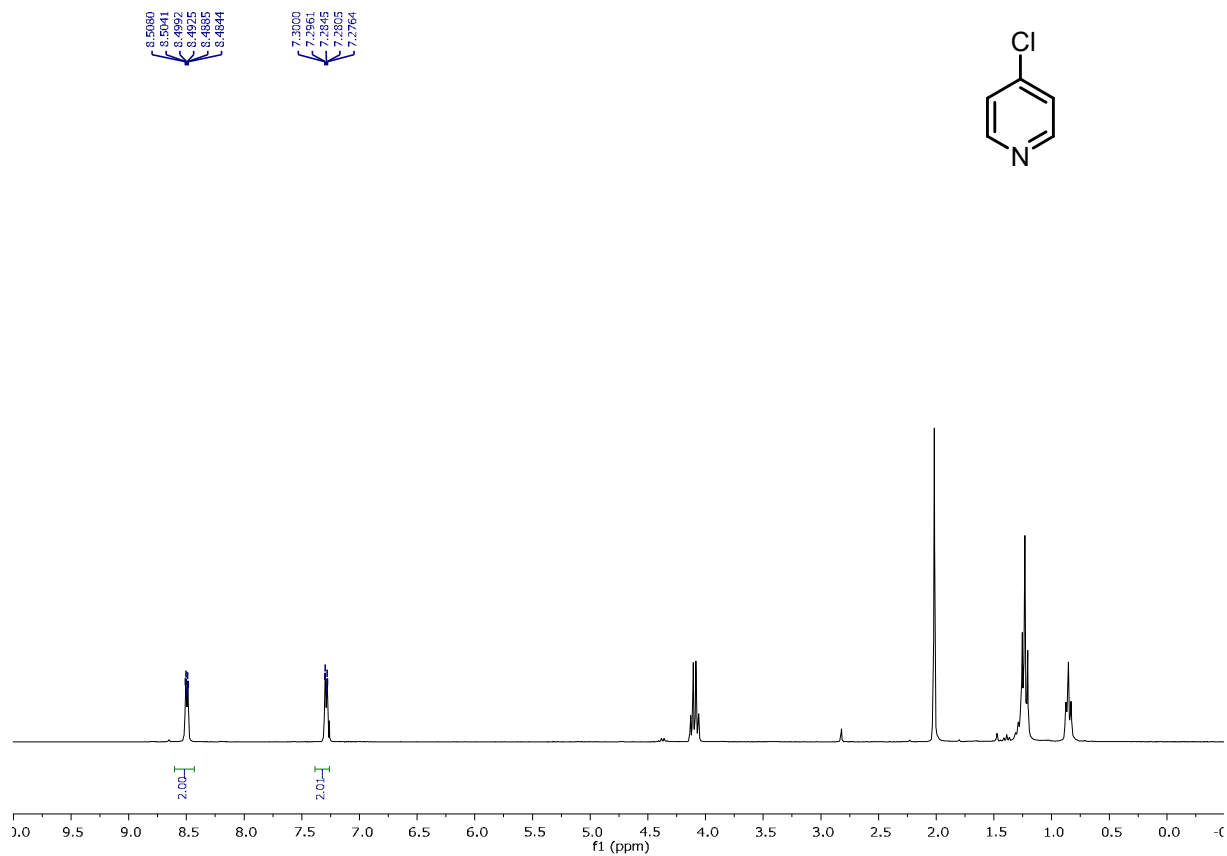


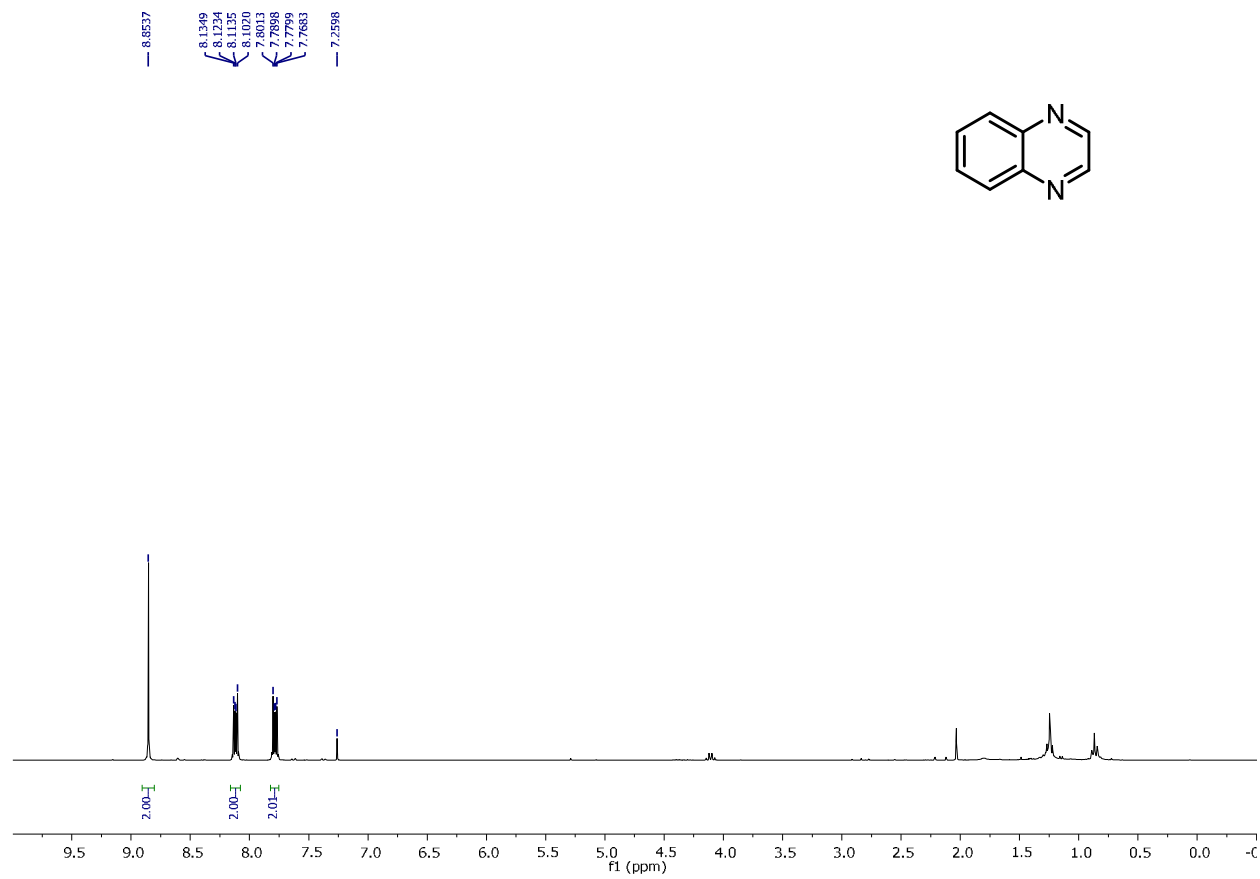










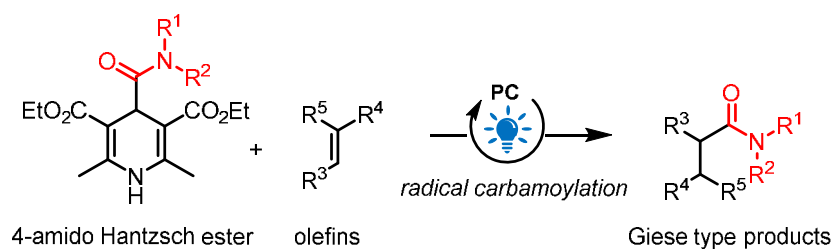


3.5 References

1. Wang, P.-Z.; Chen, J.-R.; Xiao, W.-J. *Org. Biomol. Chem.*, **2019**, *17*, 6936–6951.
2. Eisner, U.; Kuthan, J. *Chem. Rev.* **1972**, *72*, 1–42.
3. You, S.-L. *Chem. Asian J.* **2007**, *2*, 820–827.
4. Zheng, S.-L. You, *Chem. Soc. Rev.* **2012**, *41*, 2498–2518.
5. a) Li, G.; Chen, R.; Wu, L.; Fu, Q.; Zhang, X.; Tang, Z. *Angew. Chem., Int. Ed.* **2013**, *52*, 8432–8436. b) Nakajima, K.; Zhang, Y.; Nishibayashi, Y. *Org. Lett.* **2019**, *21*, 4642–4645.
6. T. He, R. Shi, Y. Gong, G. Jiang, M. Liu, S. Qian and Z. Wang. *Synlett*, **2016**, *27*, 1864–1869.
7. Gutiérrez-Bonet, Á.; Remeur, C.; Matsui, J. K.; Molander, G. A. *J. Am. Chem. Soc.* **2017**, *139*, 12251–12258.
8. For selected reviews see: a) Prier, C. K.; Rankic, D. A.; MacMillan, D. W. C. *Chem. Rev.* **2013**, *113*, 5322–5363. b) Zhou, Q.-Q.; Zou, Y.-Q.; Lu, L.-Q.; Xiao, W.-J. *Angew. Chem., Int. Ed.* **2019**, *58*, 1586–1604. c) Strieth-Kalthoff, F.; James, M. J.; Teders, M.; Pitzer, L.; Glorius, F. *Chem. Soc. Rev.* **2018**, *47*, 7190–7202. d) Fukuzumi, S.; Ohkubo, K. *Chem. Sci.*, **2013**, *4*, 561–574. e) Romero, N. A.; Nicewicz, D. A. *Chem. Rev.* **2016**, *116*, 10075–10166. f) Marzo, L.; Pagire, S. K.; Reiser, O.; König, B. *Angew. Chem., Int. Ed.* **2018**, *57*, 10034–10072 and references therein.
9. For selected examples see: a) Lee, K. N.; Lei, Z.; Ngai, M.-Y. *J. Am. Chem. Soc.* **2017**, *139*, 5003–5006. b) Lackner, G. L.; Quasdorf, K. W.; Overman, L. E. *J. Am. Chem. Soc.* **2013**, *135*, 15342–15345. c) Park, G.; Yi, S. Y.; Jung, J.; Cho, E. J.; You, Y. *Chem. Eur. J.* **2016**, *22*, 17790–17799. d) Konev, M. O.; McTeague, T. A.; Johannes, J. W. *ACS Catal.* **2018**, *8*, 9120–9124.
10. Nakajima, K.; Nojima, S.; Sakata, K.; Nishibayashi, Y. *ChemCatChem* **2016**, *8*, 1028–1032.
11. a) Gutiérrez-Bonet, Á.; Tellis, J. C.; Matsui, J. K.; Vara, B. A.; Molander, G. A. *ACS Catal.* **2016**, *6*, 8004–8008. b) Nakajima, K.; Nojima, S.; Nishibayashi, Y. *Angew. Chem. Int. Ed.* **2016**, *55*, 14106–14110. c) Milligan, J. A.; Phelan, J. P.; Badir, S. O.; Molander, G. A. *Angew. Chem., Int. Ed.* **2019**, *58*, 6152–6163.
12. Jung, J.; Kim, J.; Park, G.; You, Y.; Cho, E. J. *Adv. Synth. Catal.* **2016**, *358*, 74–80.
13. Hedstrand, D. M.; Kruizinga, W. M.; Kellogg, R. M. *Tetrahedron Lett.* **1978**, *19*, 1255–1258.
14. For early examples see: a) Jin, M.-Z.; Yang, L.; Wu, L.-M.; Liu, Y.-C.; Liu, Z.-L. *Chem. Commun.* **1998**, 2451–2452. b) Zhang, J.; Jin, M.-Z.; Zhang, W.; Yang, L.; Liu, Z.-L. *Tetrahedron Lett.* **2002**, *43*, 9687–9689.
15. For recent reviews see: a) Lima, C. G. S.; Lima, T. M.; Lima, T.; Duarte, M.; Jurberg, I. D.; Paixão, M. W. *ACS Catal.* **2016**, *6*, 1389–1407. b) Wei, Y.; Zhou, Q.-Q.; Tan, F.; Lu, L.-Q.; Xiao, W.-J. *Synthesis*, **2019**, *51*, 3021–3054. For a classic review, see: c) Mulliken, R. S. *J. Phys. Chem.*, **1952**, *56*, 801–822.
16. a) Chen, W.; Tao, H.; Huang, W.; Wang, G.; Li, S.; Cheng, X.; Li, G. *Chem. Eur. J.* **2016**, *22*, 9546–9550. b) Zhang, J.; Li, Y.; Xu, R.; Chen, Y. *Angew. Chem. Int. Ed.* **2017**, *56*, 12619–12623. c) Chen, D.; Xu, L.; Long, T.; Zhu, S.; Yang, J.; Chu, L. *Chem. Sci.* **2018**, *9*, 9012–9017. d) Buzzetti, L.; Prieto, A.; Roy, S. R.; Melchiorre, P. *Angew. Chem., Int. Ed.* **2017**, *56*, 15039–15043. e) van Leeuwen, T.; Buzzetti, L.; Perego, L. A.; Melchiorre, P. *Angew. Chem., Int. Ed.*, **2019**, *58*, 4953–4957. f) Verrier, C.; Alandini, N.; Pezzetta, C.; Moliterno, M.; Buzzetti, L.; Hepburn, H. B.; Vega-Peñaloza, A.; Silvi, M.; Melchiorre, P. *ACS Catal.*, **2018**, *8*, 1062–1066. g) Goti, G.; Bieszcza, B.; Vega-Peñaloza, A.; Melchiorre, P.; *Angew. Chem., Int. Ed.*, **2019**, *58*, 1213–1217. h) Zheng, C.; Wang, G.-Z.; Shang, R. *Adv. Synth. Catal.* **2019**, *361*, 4500–4505. i) Wu, J.; Grant, P. S.; Li, X.; Noble, A.; Aggarwal, V. K. *Angew. Chem., Int. Ed.* **2019**, *58*, 5697–5701. j) Huang, X.; Luo, S.; Burghaus, O.; Webster, R. D.; Harms, K.; Meggers, E. *Chem. Sci.* **2017**, *8*, 7126–7131.
17. Eicher, T.; Hauptmann, S. *The Chemistry of Heterocycles: Structures, Reactions, Synthesis and Applications*, 2nd ed.; Wiley-VCH: Weinheim, Germany, **2003**.
18. a) Kim, K. D.; Lee, J. H. *Org. Lett.* **2018**, *20*, 7712–7716. b) Todorov, A. R.; Aikonen, S.; Muuronen, M.; Helaja, J. *Org. Lett.* **2019**, *21*, 3764–3768. c) Jeong, J.; Suzuki, K.; Hibino, M.; Yamaguchi, K.; Mizuno, N. *Chem. Select* **2016**, *1*, 5042–5048. d) Jeong, J.; Suzuki, K.; Yamaguchi, K.; Mizuno, N. *New J. Chem.* **2017**, *41*, 13226–13229. e) Maki, Y.; Sako, M. *J. Synth. Org. Chem. Jpn.* **1994**, *52*, 149–160. f) Petrosyan, A.; Hauptmann, R.; Pospesch, J. *Eur. J. Org. Chem.* **2018**, 5237–5252.
19. Deoxygenation of heteroaryl *N*-oxides with Hantzsch ester and its derivatives has been reported to occur under thermal conditions when heated to >160 °C: a) Kurbatova, A. S.; Kurbatov, Yu. V.; Niyazova, D. A. *Khimiya Geterotsiklicheskikh Soedinenii*, **1977**, *12*, 1651–1653. b) Kurbatova, A. S.; Kurbatov, Yu. Y. *Khimiya Geterotsiklicheskikh Soedinenii*, **1989**, *5*, 652.
20. Wang, D.; Liu, Q.; Chen, B.; Zhang, L.; Tung, C.; Wu, L. *Chin. Sci. Bull.* **2010**, *55*, 2855–2858.
21. Todorov, A. R.; Wirtanen, T.; Helaja, J. *J. Org. Chem.* **2017**, *82*, 13756–13767.
22. Zhang, W.-M.; Dai, J.-J.; Xu, J.; Xu, H.-J. *J. Org. Chem.* **2017**, *824*, 2059.
23. a) Job, P. *Ann. Chim.* **1928**, *9*, 113–203. b) Renny, J. S.; Tomasevich, L. L.; Tallmadge, E. H.; Collum, D. B. *Angew. Chem. Int. Ed.* **2013**, *52*, 11998–12013.
24. Schneider, J. F.; Lauber, M. B.; Muhr, V.; Kratzer, D.; Paradies, J. *Org. Biomol. Chem.*, **2011**, *9*, 4323–4327.
25. Nakanishi, I.; Nishizawa, C.; Ohkubo, K.; Takeshita, K.; Suzuki, K. T.; Ozawa, T.; Hecht, S. M.; Tanno, M.; Sueyoshi, S.; Miyata, N.; Okuda, H.; Fukuzumi, S.; Ikota, N.; Fukuhara, K. *Org. Biomol. Chem.* **2005**, *3*, 3263–3265.
26. Toganoh, M.; Fujino, K.; Ikeda, S.; Furuta, H. *Tetrahedron Lett.*, **2008**, *49*, 1488–1491.
27. Xu, P.; Xu, H.-C. *Synlett*. **2019**, *30*, 1219–1221.
28. Rubio-Presa, R.; Fernández-Rodríguez, M.-A.; Pedrosa, M.-R.; Arnáiz, F.-J.; Sanz, R. *Adv. Synth. Catal.*, **2017**, *359*, 1752–1757.
29. Kiran, Y. B.; Ikeda, R.; Sakai, N.; Konakahara, T. *Synthesis*. **2010**, 276–280.
30. Marsais, F.; Trecourt, F.; Breant, P.; Queguiner, G. *J. Heterocyclic Chem.* **1988**, *25*, 81–87.
31. Raghuvanshi, D. S.; Verma, N.; Gupta, A. *Chemistry Select*. **2019**, *4*, 2075–2078.
32. ACD-A: Sigma-Aldrich (Spectral data were obtained from Advanced Chemistry Development, Inc.)
33. Greulich, T.-W.; Yamaguchi, E.; Doerenkamp, C.; Lübbsmeyer, M.; Daniliuc, C.-G.; Fukazawa, A.; Eckert, H.; Yamaguchi, S.; Studer, A. *Chem. Eur. J.*, **2017**, *23*, 6029–6023.
34. Oishi, M.; Kondo, H.; Amii, H. *Chem. Commun.* **2009**, 1909–1911.
35. Jaiswal, G.; Subramanian, M.; Sahoo, M.-K.; Balaraman, E. *Chem. Cat. Chem.* **2019**, *11*, 2449–2457.

36. Shi, J.; Manolikakes, G.; Yeh, C.-H.; Guerrero, C. A.; Shenvi, R. A.; Shigehisa, H.; Baran, P. S. *J. Am. Chem. Soc.* **2011**, *133*, 8014–8027.
37. Bhattacharjee, A.; Hosoya, H.; Ikeda, H.; Nishi, K.; Tsurugi, H.; Mashima, K. *Chem. - Eur. J.* **2018**, *24*, 11278–1128.
38. Hojczyk, K. N.; Feng, P.; Zhan, C.; Ngai, M.-Y. *Angew. Chem., Int. Ed.* **2014**, *53*, 14559–14563.
39. Shil, A. K.; Das, P. *Green Chem.* **2013**, *15*, 3421–3428.

4 Chapter 4: Photoredox-Catalyzed Addition of Carbamoyl Radicals to Olefins: A 1,4-Dihydropyridine Approach



Abstract: Functionalization with C₁-building blocks are key synthetic methods in organic synthesis. The low reactivity of the most abundant C₁-molecule, carbon dioxide, makes alternative carboxylation reactions with CO₂-surrogates especially important. We report a photoredox-catalyzed protocol for alkene carbamoylations. Readily accessible 4-carboxamido-Hantzsch esters serve as convenient starting materials that generate carbamoyl radicals upon visible light-mediated single-electron transfer. Addition to various alkenes proceeded with high levels of regio- and chemoselectivity.

This chapter has been published:

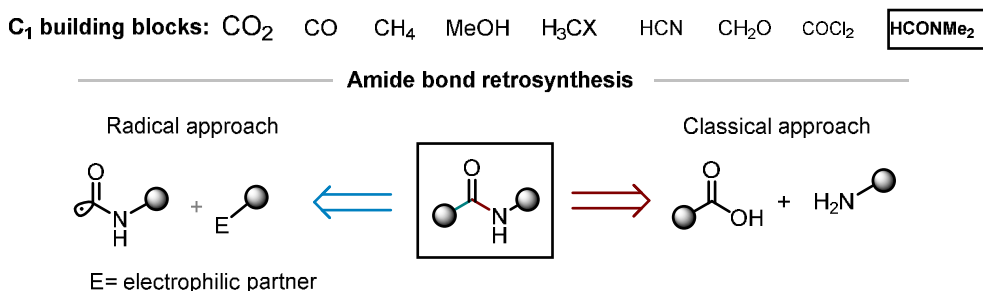
Cardinale L., Konev M., Jacobi von Wangelin A. *Chem. Eur.J.* **2020**, 26, 8239–8243.

Author contributions:

MK initiated the project and contributed to the synthesis of the substrate scope, LC did the rest of the analytical and synthetic work, and wrote the manuscript.

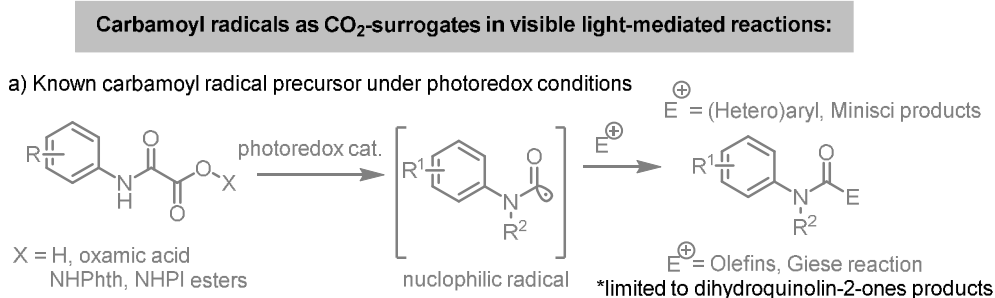
4.1 Introduction

C₁-building blocks are among the most abundant and available chemicals (e.g. CO₁₋₂, COCl₂, Me-H/OH/Hal, HCN). However, the range of diverse C₁-building blocks is rather limited, hence the access to a wide variety of methods is crucial to their implementation into various chemical syntheses. The use of nucleophilic carbamoyl radicals, as a one electron reduced CO₂ surrogates, are amongst the most valuable carboxyl derivatives: amides. Amide containing products are seen across every corner of chemical constituents, from proteins and pharmaceuticals, to polymers and agrochemicals, to cite a few examples. Classic condensation-based protocols are readily contrasted with modern and non-obvious retrosynthetic approaches as the less explored radical strategies (Scheme 1). As such, the addition of organic radicals to electron-deficient olefins (Giese reaction) has become a versatile tool for the construction of C–C bonds in organic synthesis.^{1a-c} Since its discovery, a variety of free radical species (alkyl,^{2a} acyl,^{2b} carbamoyl^{2c}) have been employed as nucleophiles to furnish their corresponding homologues (alkanes, ketones, amides, respectively). While conventional Giese-type protocols rely on harsh conditions for the initiation of the reaction (incl. toxic tin reagents, elevated temperatures, or high-energy light), the advent of modern photoredox catalysis has provided milder routes of radical generation.³ Significant progress has been made towards photoredox-alkylations and acylations, whereas the formation and utilization of free carbamoyl radicals has remained elusive and limited, in most of the cases, to the addition into (hetero)aryl substrates in a Minisci fashion reaction⁴



Scheme 1. Common C₁-building block and amide bond retrosynthesis.

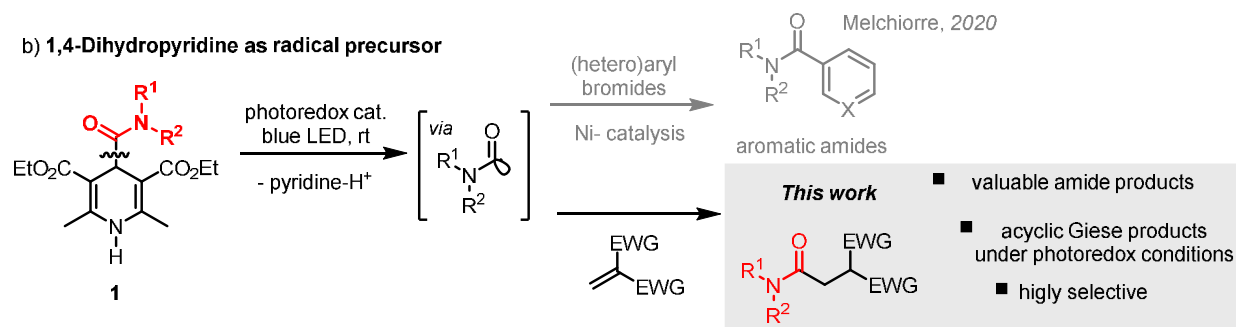
The first light-mediated radical carbamoylation of olefins was reported by Elad and Rokach in 1964 via H-atom abstraction of formamide to give low yields and low selectivity of the desired products.⁵ Photoredox-catalyzed carbamoylations were recently reported by Donald⁶ via reductive decarboxylation of *N*-oxyphthalimido oxamides and by Feng⁷ via oxidative decarboxylation of oxamic acids (Scheme 2). Both protocols involve noble-metal containing photocatalysts and further reaction of the intermediate alkyl radicals onto arene substituents leading to dihydroquinolin-2-one class of products. Hantzsch ester derivatives have recently been discovered as convenient precursors to alkyl,⁸ acyl,⁹ and - during the course of our study- carbamoyl¹⁰ radicals via photoredox-catalysis or direct photoexcitation.



Scheme 2. General route to carbamoyl radicals under photoredox conditions.

We surmised that the easily accessible 4-carboxamido-substituted Hantzsch esters (**1**) could be utilized for an unprecedented photocatalytic approach into mild Giese-type additions to furnish functionalized

carboxyl derivatives (Scheme 3) complementing and expanding the explored reactivity by Melchiorre's work.



Scheme 3. Carbamoyl radicals as CO₂-surrogates in the synthesis of carboxylate derivatives by a Giese radical addition to alkenes.

4.2 Results and discussion

Optimization and substrate scope

We commenced our study with the model reaction between the 4-substituted Hantzsch ester derivative **1a** and benzylidene malonitrile **2a** under visible light irradiation (Table 1).

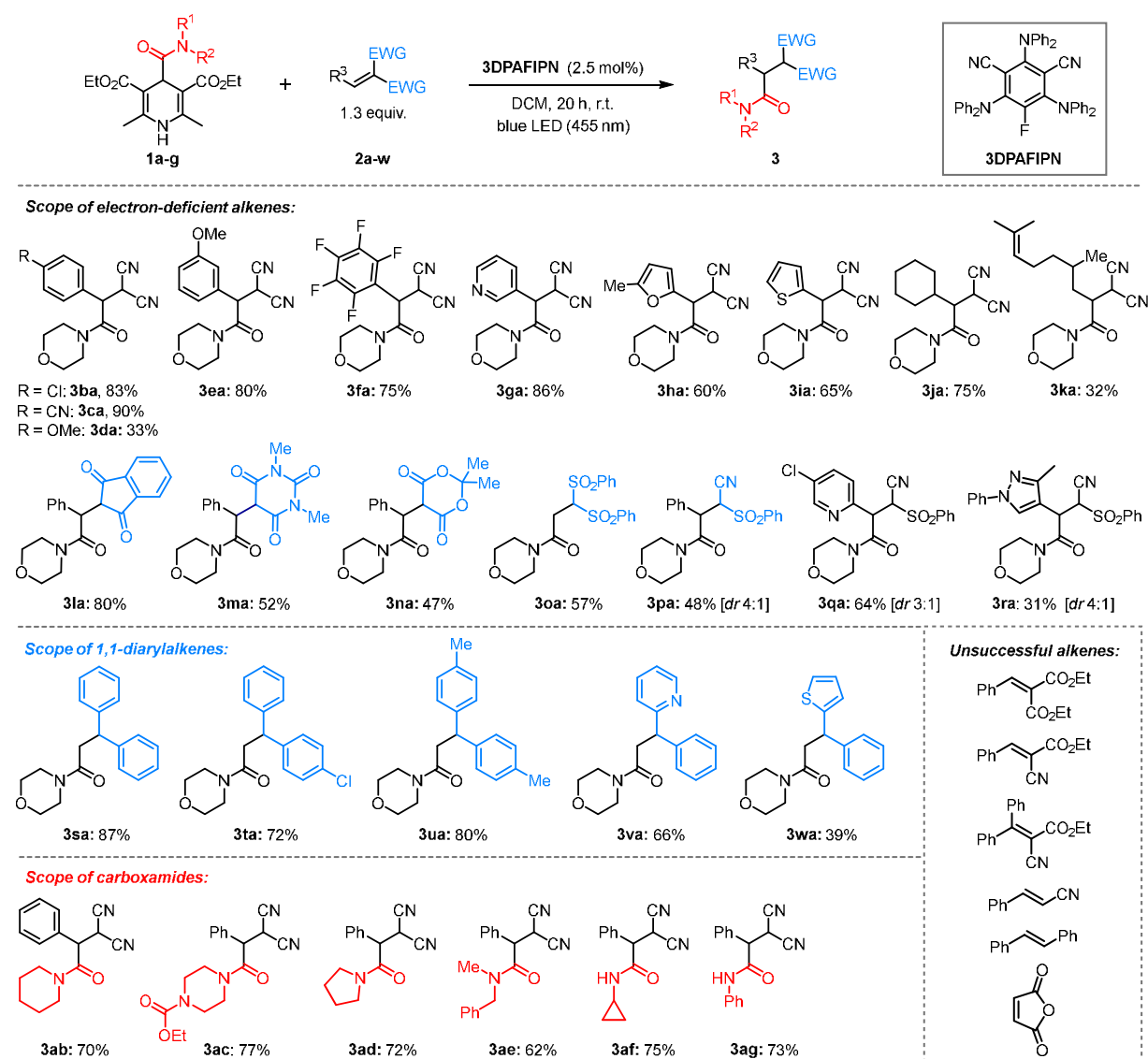
Table 1. Selected optimization and control experiments.^[a]

Entry	Deviations from standard conditions	Yield of 3aa [%] ^[b]
1	none	80
2	3DPA2FBN instead of 3DPAFIPN	78
3	Mes-Acr ⁺ instead of 3DPAFIPN	65
4	CH ₃ CN instead of CH ₂ Cl ₂	65
5	405 nm, no 3DPAFIPN	60
6	sparged with N ₂	80
7	1 mol% 3DPAFIPN	67
8	addition of 20 mol% 1,4-dicyanobenzene	89
9	no irradiation	0
10	no 3DPAFIPN	8
11	0.3 mmol scale, 20 h	73

[a] 0.1 mmol **1a** (0.1 M in DCM), **2a** (1.3 equiv.), 16 h, at r.t. under irradiation of blue LED (455 nm). [b] ¹H NMR yields vs. external 1,3,5-trimethoxybenzene.

We chose the organic dye 3DPAFIPN as photocatalyst based on its oxidation capability ($E_{1/2}(\text{PC}^+/\text{PC}^\cdot) = +1.09 \text{ V vs. SCE, CH}_3\text{CN}$)¹¹ which may enable single-electron transfer (SET) from **1a** ($E_{\text{pa}} = +1.17 \text{ V vs. SCE, CH}_3\text{CN}$) to deliver the carbamoyl radical. Indeed, irradiation of a solution of **1a** and **2a** (1.3 equiv.) with 2.5 mol% 3DPAFIPN in CH_2Cl_2 with blue light ($\lambda_{\text{max}} = 455 \text{ nm}$) resulted in the formation of the desired dicyanopropionamide **3a** in 80% yield (Table 1, entry 1). Alternative organic photocatalysts such as the more reducing 3DPA2FBN ($E_{1/2}(\text{PC}^+/\text{PC}^\cdot) = -1.60 \text{ V vs. SCE, CH}_3\text{CN}$)¹¹ and the more oxidizing Mes-Acr⁺ ($E_{\text{red}} = +1.88 \text{ V vs. SCE, CH}_3\text{CN}$)¹² afforded lower yields (entries 2 and 3). The choice of solvent was crucial to the outcome of the reaction (entry 4, see ESI for further details). Acetonitrile, dimethylformamide, and chlorinated solvents gave lower yields. The influence of electron mediators (e.g. 1,4-dicyanobenzene, $[\text{Ni}(\text{bipy})_3](\text{BF}_4)_2$, methyl viologen) was tested (entry 8). Slightly enhanced reactivity was observed in the presence of 1,4-dicyanobenzene. Control experiments established the necessity of photocatalyst and light (entries 9 and 10).

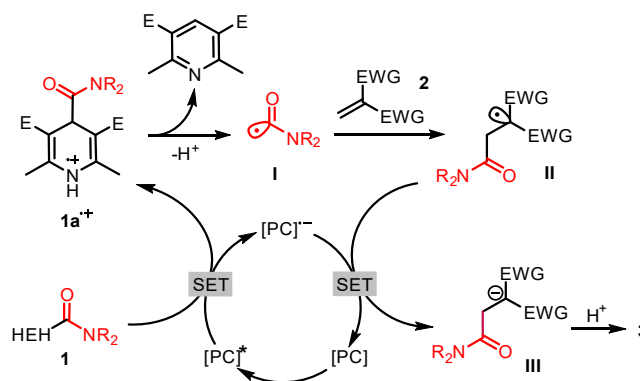
With the optimized conditions, we explored the scope of the photo-catalyzed carbamoyl-Giese reaction (Scheme 4). A diverse set of benzylidene malononitriles gave high yields of the adducts (**3ba-3fa**). Electron-rich aryl substituents lowered the yield significantly. Heteroaryl motifs, such as pyridine (**3ga**), thiophene (**3ha**), and furan (**3ia**), and alkylidene malononitriles (**3ja, 3ka**) were well tolerated.



Scheme 4. Scope of the photoredox-catalyzed carbamoylation of alkenes. Isolated yields are given (0.3 mmol scales, 0.1 M in DCM).

The reaction was also applied to alternative alkenes with good reactivity including Meldrum's acid, 1,3-indandione, and 1,3-dimethyl barbiturates (**3la-3na**). 1,1-Diaryl-ethylene derivatives were also competent radical acceptors (**3sa-3wa**). The scope of 4-carboxamido substituents within the Hantzsch esters included acyclic and cyclic *sec*- and *tert*-amides (**3ab-3af**).

We performed key experiments in an effort to probe the mechanism of this photo-catalyzed carbamoyl addition reaction. The UV-Vis spectrum of the 4-carboxamido-Hantzsch ester derivative **1a** exhibited an absorption maximum at 350 nm. This excludes direct excitation and photolytic reactivity under irradiation with a blue LED ($\lambda_{\text{max}} = 455 \text{ nm}$) where only the photocatalyst shows high absorption. Cyclic voltammetry experiments supported the thermodynamic feasibility of the reaction as the oxidation potential of **1a** ($E_{\text{pa}} = +1.17 \text{ V vs. SCE, CH}_3\text{CN}$) matches that of the excited photocatalyst 3DPAFIPN* ($E_{1/2}(\text{PC}^*/\text{PC}^{\cdot-}) = +1.09 \text{ V vs. SCE, CH}_3\text{CN}$).¹¹ Fluorescence quenching studies and Stern-Volmer analysis documented that the rate of single-electron transfer between **1a** and the photocatalyst operates at the diffusion limit ($K_{\text{q}} = 9.22 \cdot 10^{10} \text{ M}^{-1}\text{s}^{-1}$), while the quenching with the benzylidene malononitrile **2a** is significantly less effective ($K_{\text{q}} = 2.26 \cdot 10^9 \text{ M}^{-1}\text{s}^{-1}$). The standard reaction was completely inhibited in the presence of 1 equiv. of the radical scavenger (2,2,6,6-tetra-methylpiperidin-1-yl)oxyl (TEMPO, see experimental part). Based on our synthetic and spectroscopic observations and literature data, we propose the following reaction mechanism (Scheme 5): Excitation of the organic dye 3DPAFIPN by blue light ($\lambda_{\text{max}} = 455 \text{ nm}$) affords the strongly oxidizing species 3DPAFIPN* that undergoes single-electron transfer (SET) from the electron-rich Hantzsch ester derivative **1a**.



Scheme 5. Mechanistic proposal.

The resultant radical cation **1a**^{•+} eliminates the carbamoyl radical **I** upon aromatization-driven fragmentation. Addition of the nucleophilic radical species **I** to the electron-deficient alkene **2** furnishes an electrophilic radical that can engage in a single-electron reduction with the reduced photocatalyst $\text{PC}^{\cdot-}$ ($E_{1/2}(\text{PC}/\text{PC}^{\cdot-}) = -1.59 \text{ V vs. SCE, CH}_3\text{CN}$).¹³ The stabilized anion **III** is protonated to give the hydrocarboxamidation adduct **3**. The operation of long radical chains was excluded by a light-on/off experiment. Over a period of 7 h, steady conversion was recorded under irradiation while no turnover was detected in the dark (Figure 1).

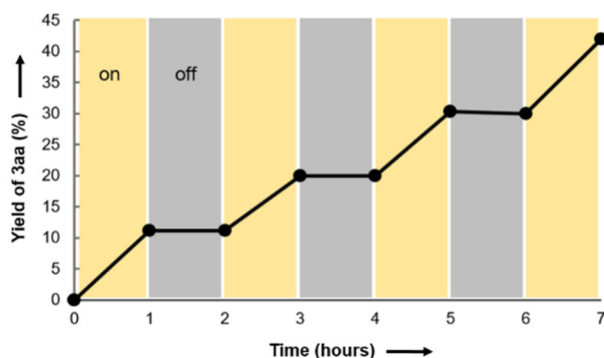


Figure 1. Alternating on (■)-off (■) experiments under standard conditions.

Hantzsch ester derivatives have been demonstrated to undergo direct photoexcitation in the absence of photocatalysts. The resultant highly reducing excited state species¹⁴ are capable of engaging in SET with a variety of π -electrophiles to afford products of formal hydrogenation,¹⁵ alkylation or acylation.¹⁶ Such reactivity may be harnessed in catalyst-free Giese reactions between suitable Hantzsch esters and alkenes, which was already observed in Table 1 (entries 5 and 10). We recorded the UV-Vis spectra of **1a**, **2a**, and of their equimolar combination (Figure 2a). The formation of an electron donor-acceptor (EDA) complex became obvious from the bathochromic shift observed when combining both reactants¹⁷ that exhibits considerable absorbance at 455 nm. From the UV/Vis absorption and emission spectra and electrochemical data (see experimental part) we determined the redox potential $E_{ox}(1a^+/1a^*)$ of the excited state **1a**^{*} to be -1.9 V vs. SCE according to the Rehm-Weller approximation.¹⁸ This observation together with the fluorescence quenching experiments corroborated our hypothesis of effective SET between **1a**^{*} and **2a** within the EDA complex (Figure 2b).^{19a} Consequently, reactions under irradiation at 405 nm (for better match with the absorption as the 455 nm irradiation led to only 8% of yield) afforded good reactivity after short reaction times (Table 1, entry 5). A brief substrate scope evaluation showed that electron-deficient alkenes fared better and afforded comparable yields to the photocatalytic conditions above (Scheme 6). However, the more electron-rich 1,1-diphenylethylene remained unreacted.^{19b}

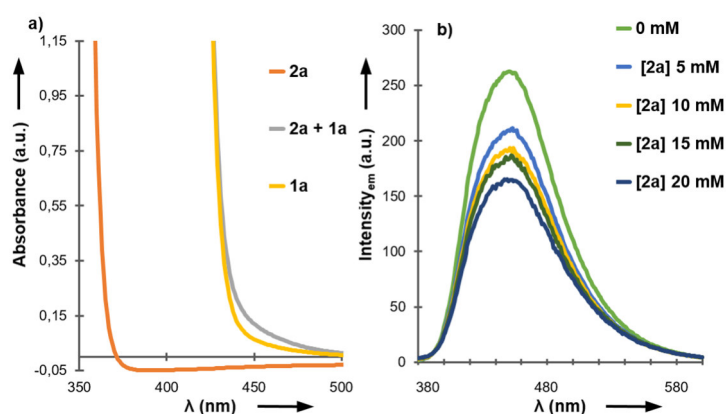
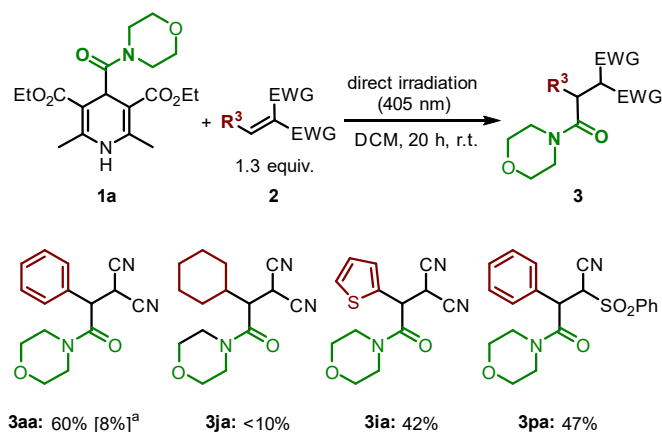


Figure 2. a) UV-Vis spectra of **2a** (orange line, 0.05 M in DCM), **1a** (yellow line, 0.05 M in DCM) and a 1:1 mixture of **1a** and **2a** (grey line, 0.05 M in DCM). b) Fluorescence quenching of **1a** in the presence of increasing amounts of **2a**.



Scheme 6. Catalyst-free Giese reaction. 0.3 mmol **1a**; ¹H NMR yields vs. external 1,3,5-trimethoxybenzene. [a] Yield obtained under 455 nm irradiation (Table 1, entry 10).

4.3 Conclusion

In conclusion, we have reported a novel photoredox-protocol that enables the facile generation of carbamoyl radicals from 4-carboxamido-1,4-dihydropyridines and their rapid addition to various electron-deficient and 1,1-disubstituted alkenes. Notably, this synthetic strategy relies on the use of easily accessible and bench-stable Hantzsch ester derivatives, the use of an inexpensive organic photocatalyst, and the operation under mild conditions at room temperature with visible light. Mechanistic studies supported the notion of a rapid photo-induced SET between the excited photocatalyst and the Hantzsch ester. Finally, mechanistic studies were conducted to support the proposed reaction mechanism. Suitable combinations of Hantzsch esters and alkenes can be reacted via catalyst-free direct excitation.

4.4 Experimental section

4.4.1 Material and methods

Chemicals and solvents: All reagents ($\geq 96\%$ purity) and solvents ($\geq 99\%$ purity) were purchased from commercial suppliers (Acros, Alfa Aesar, Fisher, Fluka, Merck, Sigma Aldrich, TCI, Th. Geyer) and used as received unless otherwise indicated.

Reaction setup: All reactions were carried out in LABSOLUTE 4 mL Screw Neck Vials, 45 x 14.7 mm, clear glass, 1st hydrolytic class unless otherwise stated. Irradiation was performed with EvoluChemTM PhotoRedOx reactor fitted with a 455 nm high-power single LED or 405 nm as specified.

Nuclear magnetic resonance (NMR) spectroscopy: ^1H NMR, ^{13}C NMR and ^{19}F NMR were used for purity and structure determination of products. NMR spectral data were collected on a Bruker Avance 300 (300 MHz for ^1H ; 75 MHz for ^{13}C , 282 MHz for ^{19}F) spectrometer, a Bruker Avance 400 (400 MHz for ^1H ; 100 MHz for ^{13}C) spectrometer or a Bruker Avance III 600 (600 MHz for ^1H ; 585 MHz for ^{19}F) spectrometer at 25 °C. Chemical shifts are reported in δ/ppm , coupling constants J are given in Hertz. Solvent residual peaks were used as internal standard for all NMR measurements. The quantification of ^1H cores was obtained from integrations of appropriate resonance signals. Abbreviations used in NMR spectra: s – singlet, d – doublet, t – triplet, q – quartet, m – multiplet, bs – broad singlet, dd – doublet of doublet.

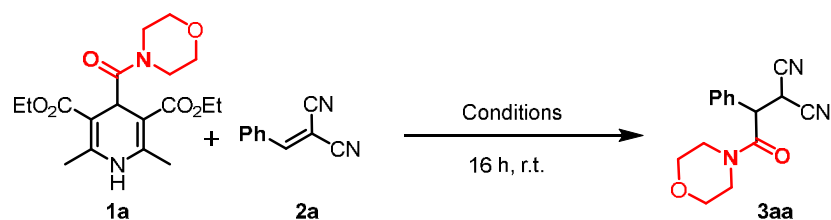
High resolution mass spectrometry (HRMS): HRMS was carried out by the Central Analytics at the department of chemistry, University of Hamburg. Abbreviations used in MS spectra: M – molar mass of target compound, ESI – electrospray ionization.

Column chromatography: TLC was performed on the commercial SiO_2 -coated aluminum plates (DC60 F254, Merck). Visualization was done by UV light (254 nm). Product yields were determined as isolated yields after flash column chromatography on silica gel (Acros Organics, mesh 35-70, 60 Å pore size).

UV/VIS absorption spectroscopy: UV/Vis absorption spectroscopy was performed at room temperature on an Agilent Cary 5000 UV/VIS NIR double beam spectrometer with a 10 mm quartz cuvette.

Cyclic voltammetry: CV measurements were performed with a potentiostat galvanostat PGSTAT101 from Metrohm Autolab using a glassy carbon working electrode, a platinum wire counter electrode, a silver/silver(I)chloride reference electrode and $\text{N}(n\text{-Bu})_4\text{PF}_6$ (0.1 M) as supporting electrolyte. The potentials were achieved relative to the Fc/Fc^+ redox couple with ferrocene as external standard.

4.4.2 Extended optimization studies

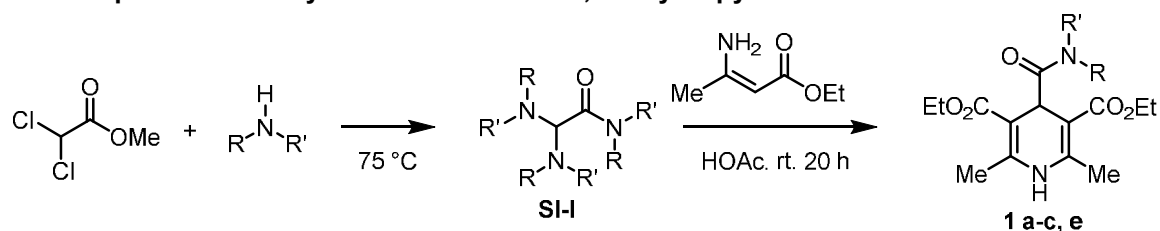


Entry	Solvent	PC (mol %)	mmol ratio	Conc. (M)	hv (nm)	Additive	Yield %
1	DCM	2.5	1:1.3	0.1	455	none	80
2	DCM	2.5	1:1.3	0.1	410	none	77
3	DCM	-	1:1.3	0.1	405	none	60
4	CH ₃ CN	2.5	1:1.3	0.1	455	none	65
5	DCM degas	2.5	1:1.3	0.1	455	none	80
6	DCM:H ₂ O (1:1)	2.5	1:1.3	0.1	455	none	65
7	DCM:hexafluoro Propanol 2:1	2.5	1:1.3	0.1	455	none	52
8	DCM dry	2.5	1:1.3	0.1	455	none	71
9	EtOAc	2.5	1:1.3	0.1	455	none	14
10	DCE	2.5	1:1.3	0.1	455	none	50
11	CHCl ₃	2.5	1:1.3	0.1	455	none	14
12	DMF	2.5	1:1.3	0.1	455	none	50
13	DMA	2.5	1:1.3	0.1	455	none	60
14	DCM	1.0	1:1.3	0.1	455	none	67
15	DCM	Mes-Acr 2.5	1:1.3	0.1	455	none	65
16	DCM	3DPA2FBN 2.5	1:1.3	0.1	455	none	78
17	DCM	2.5	1:1.3	0.06	455	none	76
18	DCM	2.5	1:1.3	0.2	455	none	76
19	DCM	2.5	1:1.3	0.5	455	none	73
20	DCM	2.5	1:2	0.1	455	none	78
21	DCM	2.5	1.5:1	0.1	455	none	73
22	DCM	2.5	1:1	0.1	455	none	72
23	DCM	2.5	1:1.3	0.1	455	Benzophenone 20 mol%	51
24	DCM	2.5	1:1.3	0.1	455	1,4-dicyanobenzene 20 mol%	89
25	DCM	-	1:1.3	0.1	455	1,4-dicyanobenzene 20 mol%	7
26	DCM	2.5	1:1.3	0.1	455	Ni(bpy) ₃ (BF ₄) ₂	36
27	DCM	2.5	1:1.3	0.1	455	K ₂ HPO ₄	46
28	DCM	2.5	1:1.3	0.1	455	Thiophenol 20 mol%	8
29	DCM	2.5	1:1.3	0.1	455	TFA	49
30	DCM	2.5	1:1.3	0.1	455	DMAP 20 mol%	20

Table 2. Optimization studies. Reaction run on 0.1 mmol scale following the general procedure D using the dihydropyridine **1a** and benzylidenemalononitrile **2a** as model substrates in the presence of 3DPAFIPN as photocatalyst. Deviations from standard conditions are highlighted in blue. The yield of **3aa** was determined using 1,3,5-trimethoxybenzene as the external standard.

4.4.3 General procedures

General procedure A: Synthesis of 4-Amido-1,4-Dihydropyridines

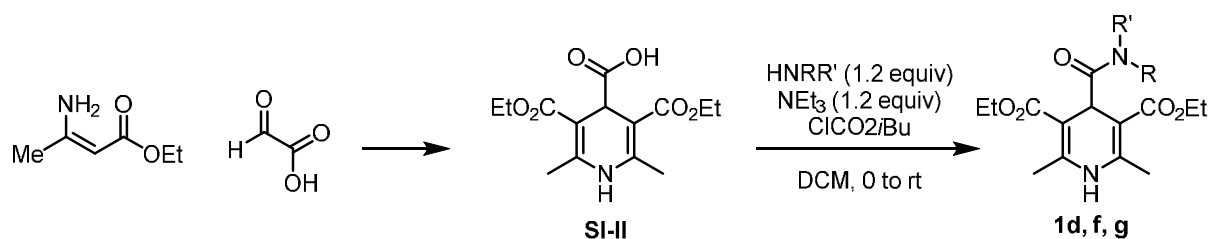


Scheme 7. Synthesis of 4-carbamoyl-1,4-dihydropyridines **1a-c, e**.

This procedure was adapted from one reported by Dubur and Uldriks.²⁰

A mixture of methyl dichloroacetate (0.72 g, 5.0 mmol) and amine (25 mmol) was heated at 75 °C for 30 minutes in an oil bath, during which the reaction mixture crystallized. The reaction product was a mixture of **SI-I** and amine hydrochloride that was subsequently used without purification. Ethyl 3-aminocrotonate (1.3 g, 10 mmol) and **SI-I** (5.0 mmol) were dissolved in glacial acetic acid (10 mL), and the mixture was allowed to stir at room temperature for 20 h. The resultant suspension was diluted with water, the precipitate was removed by filtration, and washed with water to give the corresponding 4-amido-1,4-dihydropyridine.

General Procedure B: Synthesis of 4-Amido-1,4-Dihydropyridines



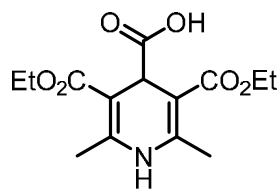
Scheme 8. Synthesis of 4-carbamoyl-1,4-dihydropyridines **1d, f, g**.

This procedure was adapted from two separate reports by Dubur and Uldriks and by Duburs.²¹

A 100 mL round bottom flask equipped with a magnetic stir bar was charged with 3-ethyl aminocrotonate (14.9 g, 115 mmol) in glacial acetic acid (5 mL) and the mixture was cooled to 0 °C. A solution of glyoxylic acid (4.6 g, 62 mmol) in glacial acetic acid (20 mL) was then added dropwise to the mixture. The mixture was allowed to warm up to room temperature and stirred overnight. The resulting suspension was then filtered and washed with acetic acid until the yellow color of the washings no longer persisted. The precipitate was collected and 4-carboxy-1-4-dihydropyridine was obtained (4.0 g, 14 mmol, 22% yield).

A 25 mL round bottom flask equipped with a magnetic stir bar was charged with carboxylic acid (1.0 equiv.) **SI-II** and DCM (0.20 M). Triethylamine (1.2 equiv) was added dropwise to the mixture and the yellow solution was cooled to 0 °C. Isobutylchloroformate (1.2 equiv.) was then added dropwise. After 10 minutes, the mixture was warmed to room temperature and was stirred for 20 minutes upon which the amine was added, and the mixture was stirred overnight. The mixture was then concentrated under reduced pressure and purified by flash column chromatography (eluent: pentane/acetone 70/30).

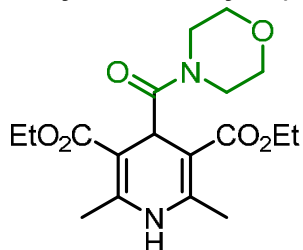
3,5-bis(ethoxycarbonyl)-2,6-dimethyl-1,4-dihydropyridine-4-carboxylic acid (SI-II)



$^1\text{H NMR}$ (300 MHz, DMSO- d_6 , ppm): 11.81 (s, 1H), 8.84 (s, 1H), 4.58 (s, 1H), 4.16 – 4.00 (m, 4H), 2.22 (s, 6H), 1.19 (t, $J = 7.1$ Hz, 6H).

$^1\text{H NMR}$ is consistent with previously published data.²²

diethyl 2,6-dimethyl-4-(morpholine-4-carbonyl)-1,4-dihydropyridine-3,5-dicarboxylate (1a)

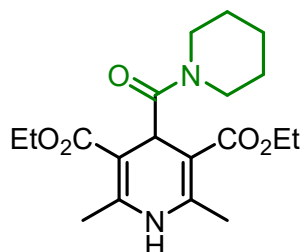


Starting from methyl dichloroacetate (0.72 g), morpholine (2.2 g), ethyl 3-aminocrotonate (1.3 g) and following the general procedure A, **1a** was isolated by filtration as a pale-yellow powder (0.82 g, 45% yield).

$^1\text{H NMR}$ (300 MHz, CDCl_3 , ppm): 7.17 (s, 1H), 5.01 (s, 1H), 4.27 – 4.07 (m, 4H), 3.97–3.87 (m, 2H), 3.79–3.70 (m, 2H), 3.70–3.55 (m, 4H), 2.24 (s, 6H), 1.28 (t, $J = 7.1$ Hz, 6H).

$^1\text{H NMR}$ is consistent with previously published data.²³

diethyl 2,6-dimethyl-4-(piperidine-1-carbonyl)-1,4-dihydropyridine-3,5-dicarboxylate (1b)

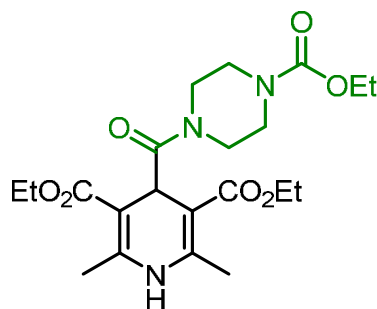


Starting from methyl dichloroacetate (0.72 g), piperidine (2.1 g), ethyl 3-aminocrotonate (1.3 g) and following the general procedure A, **1b** was isolated by filtration as a pale-yellow powder (0.92 g, 50% yield).

$^1\text{H NMR}$ (300 MHz, CDCl_3 , ppm): 7.76 (s, 1H), 5.10 (s, 1H), 4.27 – 4.05 (m, 4H), 3.88–3.75 (m, 2H), 3.60–3.43 (m, 2H), 3.70–3.55 (m, 4H), 2.22 (s, 6H), 1.88–1.70 (m, 2H), 1.70–1.44 (m, 4H), 1.27 (t, $J = 7.1$ Hz, 6H).

$^1\text{H NMR}$ is consistent with previously published data²³

diethyl 4-(4-(ethoxycarbonyl)piperazine-1-carbonyl)-2,6-dimethyl-1,4-dihydropyridine-3,5-dicarboxylate (1c)

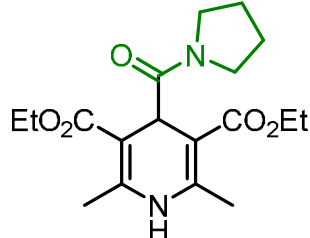


Starting from methyl dichloroacetate (0.72 g), ethyl 1-piperazinecarboxylate (4.0 g), ethyl 3-aminocrotonate (1.3 g) and following the general procedure A, **1c** was isolated by filtration as a pale-yellow powder (0.71 g, 32% yield).

$^1\text{H NMR}$ (300 MHz, CDCl_3 , ppm): 7.66 (s, 1H), 5.03 (s, 1H), 4.29 – 4.03 (m, 6H), 3.99–3.78 (m, 2H), 3.74–3.34 (m, 6H), 2.21 (s, 6H), 1.26 (apparent t, $J = 7.2$ Hz, 9H). $^{13}\text{C NMR}$ (75 MHz, CDCl_3 , ppm): δ 174.6, 167.5, 155.5, 147.6, 98.9, 61.6, 60.0, 46.6, 42.1, 36.7, 19.5, 14.7, 14.6. **HRMS** (ESI): $m/z = \text{calcd. for } \text{C}_{21}\text{H}_{31}\text{ClN}_3\text{O}^+ [\text{M-H}]^+$: 438.2235,

found: 438.2246.

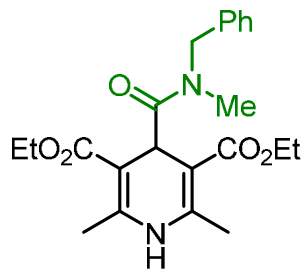
diethyl 2,6-dimethyl-4-(pyrrolidine-1-carbonyl)-1,4-dihydropyridine-3,5-dicarboxylate (1d)



Starting from 4-carboxy-1,4-dihydropyridine (0.600 g), NEt_3 (340 μL), pyrrolidine (250 μL), isobutylchloroformate (320 μL) in DCM and following the general procedure B, **1d** was isolated by column chromatography on silica (eluent: pentane/acetone, 70:30) as a yellow powder (0.272 g, 54% yield). $^1\text{H NMR}$ (300 MHz, CDCl_3 , ppm): 8.39 (s, 1H), 4.81 (s, 1H), 4.16 (q, $J = 7.3$ Hz, 4H), 4.01 (t, $J = 6.7$ Hz, 2H), 3.40 (t, $J = 6.9$ Hz, 2H), 2.21 (s, 6H), 1.88 (m, 4H), 1.27 (t, $J = 7.1$ Hz, 6H).

$^1\text{H NMR}$ is consistent with previously published data²³

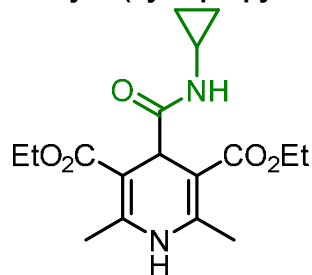
diethyl 4-(benzyl(methyl)carbamoyl)-2,6-dimethyl-1,4-dihydropyridine-3,5-dicarboxylate (**1e**)



Starting from methyl dichloroacetate (0.72 g), *N*-benzylmethylamine (3.0 g), ethyl 3-aminocrotonate (1.3 g) and following the general procedure A, **1e** was isolated by column chromatography on silica (eluent: pentane/acetone, 60:40) as a yellow powder (0.19 g, 10% yield). ¹H NMR (300 MHz, CDCl₃, ppm): δ 7.76 (s, 1H), 7.32 – 7.13 (m, 5H), 5.07 (s, 1H), 4.59 (s, 2H), 4.25–4.02 (m, 4H), 3.29 (s, 3H), 2.24 (s, 6H), 1.21 (t, *J* = 7.1 Hz, 6H)

¹H NMR is consistent with previously published data²³

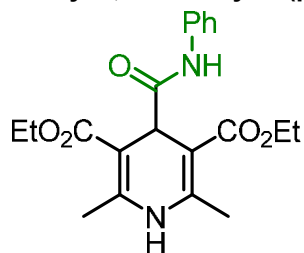
diethyl 4-(cyclopropylcarbamoyl)-2,6-dimethyl-1,4-dihydropyridine-3,5-dicarboxylate (**1f**)



Starting from 4-carboxy-1,4-dihydropyridine (0.446 g), NEt₃ (250 μL), cyclopropylamine (130 μL), isobutylchloroformate (230 μL) in DCM and following the general procedure B, **1f** was isolated by column chromatography on silica (eluent: pentane/acetone, 70:30) as a pale-yellow powder (0.272 g, 54% yield). ¹H NMR (300 MHz, CDCl₃, ppm): δ 8.05 (s, 1H), 6.82 (d, *J* = 3.3 Hz, 1H), 4.49 (s, 1H), 4.17 (qd, *J* = 7.2, 0.9 Hz, 4H), 2.67 (tq, *J* = 7.4, 3.7 Hz, 1H), 2.21 (s, 6H), 1.27 (t, *J* = 7.1 Hz, 6H), 0.76–0.68 (m, 2H), 0.47 – 0.39 (m, 2H) ppm.

¹H NMR is consistent with previously published data²³

diethyl 2,6-dimethyl-4-(phenylcarbamoyl)-1,4-dihydropyridine-3,5-dicarboxylate (**1g**)



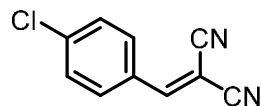
Starting from 4-carboxy-1,4-dihydropyridine (0.315 g), NEt₃ (300 μL), aniline (300 mg), isobutylchloroformate (170 mg) in DCM and following the general procedure B, **1g** was isolated by column chromatography on silica (eluent: pentane/acetone, 70:30) as a pale-yellow powder (0.168 g, 43% yield). ¹H NMR (300 MHz, CDCl₃, ppm): δ 8.86 (s, 1H), 7.59–7.52 (m, 2H), 7.45 (s, 1H), 7.33–7.35 (m, 2H), 7.10 – 7.03 (m, 1H), 4.73 (s, 1H), 4.20 (q, *J* = 7.1 Hz, 4H), 2.24 (s, 6H), 1.28 (t, *J* = 7.1 Hz, 6H).

¹H NMR is consistent with previously published data.²³

General procedure C: Synthesis of electron poor olefins

The (electron-poor olefins) **2(b-j)** used in the present work were prepared following a procedure reported in literature.²⁴ To a 5 mL round bottom flask the desired aldehyde (1.0 equiv, 3.0 mmol) and the activated methylene (1.0 equiv, 3.0 mmol) were added and suspended in 3 mL of H₂O. DABCO (10 mol%) was added in one portion to the suspension. Reaction was monitored by TLC. The product precipitated upon formation, the obtained solid was filtered and recrystallized from hot ethanol.

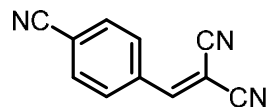
2-(4-chlorobenzylidene)malononitrile (**2b**)



Starting from 4-chlorobenzaldehyde and following the general procedure C, **2b** was obtained as a white powder (450 mg, 80% yield). ¹H NMR (300 MHz, CDCl₃) δ 7.91 – 7.80 (m, 2H), 7.73 (s, 1H), 7.58 – 7.48 (m, 2H).

¹H NMR is consistent with previously published data²⁴

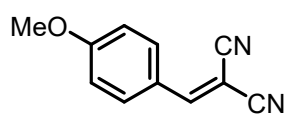
2-(4-cyanobenzylidene)malononitrile (**2c**)



Starting from 4-cyanobenzaldehyde and following the general procedure C, **2c** was obtained as a white powder (484 mg, 90% yield). ¹H NMR (300 MHz, CDCl₃) δ 8.03 – 7.95 (m, 2H), 7.90 – 7.75 (m, 3H).

¹H NMR is consistent with previously published data²⁵

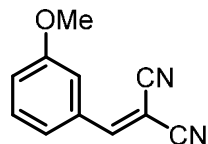
2-(4-methoxybenzylidene)malononitrile (**2d**)



Starting from 4-methoxybenzaldehyde and following the general procedure C, **2d** was obtained as a white powder (431 mg, 78% yield). ¹H NMR (300 MHz, CDCl₃) δ 7.96 – 7.86 (m, 2H), 7.65 (s, 1H), 7.06 – 6.95 (m, 2H), 3.92 (s, 3H).

¹H NMR is consistent with previously published data²⁵

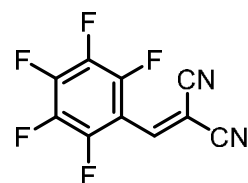
2-(3-methoxybenzylidene)malononitrile (**2e**)



Starting from 3-methoxybenzaldehyde and following the general procedure C, **2e** was obtained as a white powder (387 mg, 70% yield). ¹H NMR (300 MHz, CDCl₃) δ 7.75 (s, 1H), 7.53 – 7.38 (m, 3H), 7.17 (dt, *J* = 7.2, 2.4 Hz, 1H), 3.87 (s, 3H).

¹H NMR is consistent with previously published data²⁵

2-(pentafluorobenzylidene)malononitrile (**2f**)

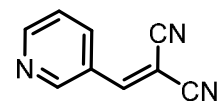


Starting from pentafluorobenzaldehyde and following the general procedure C, **2f** was obtained as a white powder (658 mg, 90% yield). ¹H NMR (300 MHz, CDCl₃) δ 7.75 (q, *J* = 1.2 Hz, 1H).

¹⁹F NMR (565 MHz, CDCl₃) δ -132.33 (dt, *J* = 19.0, 5.8 Hz,), -143.34 (dd, *J* = 20.9, 5.6 Hz), -157.79 – -158.77 (m).

¹H NMR data are consistent with previously published data²⁶

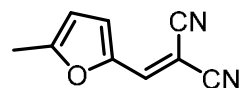
2-(pyridin-3-ylmethylene)malononitrile (**2g**)



Starting from 3-pyridincarboxaldehyde and following the general procedure C, **2g** was obtained as a white powder (349 mg, 75% yield). ¹H NMR (300 MHz, CDCl₃, ppm): δ 8.82 (d, *J* = 2.4 Hz, 1H), 8.76 (dd, *J* = 4.8, 1.6 Hz, 1H), 8.43–8.39 (m, 1H), 7.75 (s, 1H), 7.45 (dd, *J* = 8.2, 4.8 Hz, 1H).

¹H NMR is consistent with previously published data²⁷

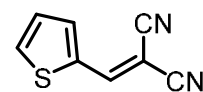
2-[(5-methylfuran-2-yl)methylene]malononitrile (**2h**)



Starting from 5-methylfurfural and following the general procedure C, **2h** was obtained as a yellow powder (261, 55% yield). ¹H NMR (300 MHz, CDCl₃, ppm): δ 7.37 (s, 1H), 7.26 (s, 1H), 6.36–6.35 (m, 1H), 2.46 (s, 3H).

¹H NMR is consistent with previously published data²⁸

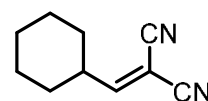
2-(thiophen-2-ylmethylene malononitrile (**2i**)



Starting from thiophene-2-carboxaldehyde and following the general procedure C, **2i** was obtained as a yellow powder (311 mg, 65% yield). ¹H NMR (300 MHz, CDCl₃, ppm): δ 7.90–7.87 (m, 2H), 7.82–7.80 (m, 1H), 7.28–7.27 (m, 1H).

¹H NMR is consistent with previously published data²⁵

2-(cyclohexylmethylene)malononitrile (**2j**)

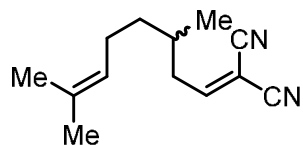


Starting from cyclohexylcarboxaldehyde and following the general procedure C, **2j** was obtained as a colorless oil (335 mg, 70% yield). ¹H NMR (300 MHz, CDCl₃) δ 7.15 (d, *J* = 10.5 Hz, 1H), 2.80 – 2.60 (m, 1H), 1.83 – 1.67 (m, 5H), 1.37 – 1.19 (m, 5H).

¹H NMR is consistent with previously published data²⁴

The following compounds were obtained following literature procedures:

2-(3,7-dimethyloct-6-en-1-ylidene)malononitrile (**2k**)

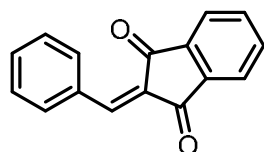


Starting from citronellal (0.90 mL, 5.0 mmol) and malononitrile (360 mg, 5.5 mmol) and following the literature procedure²⁹ **2k** was obtained as a colorless oil (0.80 mg, 76% yield).

¹H NMR (300 MHz, CDCl₃, ppm): δ 7.37 (t, *J* = 8.0 Hz, 1H), 5.08 (dddd, *J* = 7.1, 5.7, 2.9, 1.5 Hz, 1H), 2.62 (ddd, *J* = 14.7, 7.7, 5.8 Hz, 1H), 2.49 (ddd, *J* = 14.7, 8.4, 7.5 Hz, 1H), 2.04 (m, 2H), 1.88 – 1.77 (m, 1H), 1.72 (s, 3H), 1.63 (s, 3H), 1.42 – 1.30 (m, 2H), 1.00 (d, *J* = 6.7 Hz, 3H).

¹H NMR is consistent with previously published data³⁰

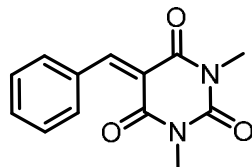
2-benzylidene-1*H*-indene-1,3(2*H*)-dione (**2l**)



Starting from indandione (440 mg, 3.0 mmol) and benzaldehyde (0.31 mL, 3.0 mmol) and following the literature procedure³¹ **2l** was obtained as a beige powder (540 mg, 77% yield). ¹H NMR (300 MHz, CDCl₃) δ 8.50 – 8.43 (m, 2H), 8.06 – 7.98 (m, 2H), 7.92 (s, 1H), 7.86 – 7.77 (m, 2H), 7.59 – 7.48 (m, 3H).

¹H NMR is consistent with previously published data³¹

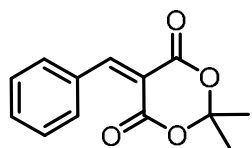
5-benzylidene-1,3-dimethylpyrimidine-2,4,6-(1*H*,3*H*,5*H*)-trione (**2m**)



Starting from barbituric acid (1.0 g, 6.5 mmol) and benzaldehyde (0.70 mL, 6.5 mmol) and following the literature procedure³¹ **2m** was obtained as a yellow powder (1.3 g, 83% yield). ¹H NMR (300 MHz, CDCl₃, ppm): δ 8.58 (s, 1H), 8.07–8.03 (m, 2H), 7.53–7.44 (m, 3H), 3.42 (s, 3H), 3.39 (s, 3H).

¹H NMR is consistent with previously published data³²

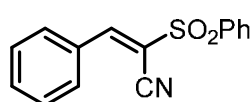
5-benzylidene-2,2-dimethyl-1,3-dioxane-4,6-dione (**2n**)



Starting from Meldrum's acid (1.0 g, 7.0 mmol) and benzaldehyde (0.70 mL, 7.0 mmol) and following the literature procedure³¹ **2n** was obtained as a yellow solid (0.89 mg, 55% yield). ¹H NMR (300 MHz, CDCl₃, ppm): δ 8.42 (s, 1H), 8.06–8.02 (m, 2H), 7.56–7.45 (m, 3H), 1.81 (s, 6H).

¹H NMR is consistent with previously published data³³

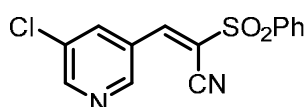
(*E*)-3-phenyl-2-(phenylsulphonyl)acrylonitrile (**2p**)



Starting from (*E*)-3-phenyl-2-(phenylsulfonyl)acrylonitrile (270 mg, 1.5 mmol) and benzaldehyde (0.15 mL, 1.5 mmol) and following the literature³⁴ procedure **2p** was obtained as a white powder (300 mg, 74% yield). ¹H NMR (300 MHz, CDCl₃, ppm): δ 8.24 (s, 1H), 8.07 – 7.99 (m, 2H), 7.97 – 7.89 (m, 2H), 7.77 – 7.67 (m, 1H), 7.67 – 7.55 (m, 3H), 7.53 – 7.48 (m, 2H).

¹H NMR is consistent with previously published data³⁴

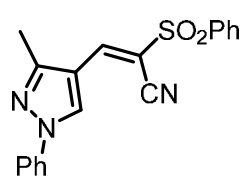
(*E*)-3-(5-chloropyridin-3-yl)-2-(phenylsulphonyl)acrylonitrile (**2q**)



Starting from (*E*)-3-phenyl-2-(phenylsulfonyl)acrylonitrile (270 mg, 1.5 mmol) and 5-Chloro-pyridine-3-carbaldehyde (210 mg, 1.5 mmol) and adapting a literature procedure³⁴ **2q** was obtained as a white powder (410 mg, 87% yield). ¹H NMR (300 MHz, CDCl₃, ppm): δ 8.72 (dd, *J* = 2.4, 0.6 Hz, 1H), 8.21 (s, 1H), 8.09 – 7.99 (m, 2H), 7.82 (dd, *J* = 8.3, 2.5 Hz, 1H), 7.75 – 7.56 (m, 4H). ¹³C NMR (75 MHz, CDCl₃, ppm): δ 149.88, 147.67, 146.70, 137.12, 136.82, 135.72, 134.96, 129.75, 129.05, 127.85, 119.43, 112.34.

HRMS (ESI): *m/z* = calcd. for C₁₄H₁₀ClN₂O₂S⁺ [M-H]⁺: 305.0146, found: 305.0133.

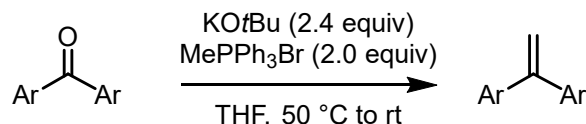
(E)-3-(3-methyl-1-phenyl-1H-pyrazol-4-yl)-2-(phenylsulfonyl)acrylonitrile (**2r**)



Starting from (*E*)-3-phenyl-2-(phenylsulfonyl)acrylonitrile (270 mg, 1.5 mmol) and 3-Methyl-1-phenyl-1*H*-pyrazole-4-carboxaldehyde (280 mg, 1.5 mmol) and adapting a literature procedure³⁴ **2r** was obtained as a yellow powder (497 mg, 94% yield). ¹H NMR (300 MHz, CDCl₃, ppm): δ 8.80 (s, 1H), 8.11 (d, *J* = 0.6 Hz, 1H), 8.05 – 7.98 (m, 2H), 7.71 – 7.55 (m, 5H), 7.47 (ddd, *J* = 8.0, 7.0, 1.3 Hz, 2H), 7.40 – 7.32 (m, 1H), 2.50 (s, 3H). ¹³C NMR (75 MHz, CDCl₃, ppm): δ 153.8, 142.4, 138.7, 138.6, 134.4, 129.7, 129.7, 128.7, 128.3, 128.2, 119.8, 114.6, 114.2, 109.9, 11.8.

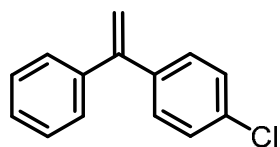
HRMS (ESI): *m/z* = calcd. for C₁₉H₁₆N₃O₂S⁺ [M-H]⁺: 350.0958, found: 350.0961.

General procedure D: Synthesis of 1,1-Diarylalkenes



This procedure was adapted from one reported by Zhang.³⁵ A dry 100 mL round bottom flask equipped with a magnetic stir bar was charged with methyl triphenylphosphonium bromide (3.6 g, 10 mmol, 2.0 equiv) and KOtBu (1.3 g, 12 mmol, 1.2 equiv) followed by THF (20 mL). The resulting yellow suspension was stirred at room temperature for 1 hour. A solution of 1,1-diarylethanone (5.0 mmol, 1.0 equiv) in THF (10 mL) was added dropwise and the resulting mixture was stirred at 50 °C for 1 hour and allowed to cool down overnight. Next, a saturated solution of NH₄Cl (25 mL) followed by distilled water (25 mL) were added and the resulting mixture was extracted with EtOAc (3 x 50 mL). The organic phases were combined and dried with anhydrous Na₂SO₄. The solvent was removed under reduced pressure and the residue was further purified by flash chromatography on silica gel to afford the corresponding alkenes.

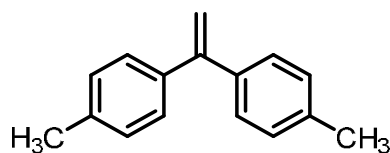
1-chloro-4-(1-phenylvinyl)benzene (**2t**)



Starting from 4-chlorobenzophenone (1.08 g) and following the general procedure D, **2t** was isolated by flash chromatography on silica (eluent: pentane/EtOAc, 98:2) as a colorless oil (0.80 g, 75% yield). ¹H NMR (300 MHz, CDCl₃, ppm) δ 7.36 – 7.31 (m, 9H), 5.50 (bs, 1H), 5.48 (bs, 1H).

¹H NMR is consistent with previously published data³⁶

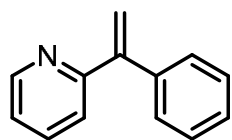
4,4'-(ethene-1,1-diyl)bis(methylbenzene) (**2u**)



Starting from 4,4'-dimethylbenzophenone (1.05 g) and following the general procedure D, **2u** was isolated by flash chromatography on silica (eluent: pentane/EtOAc, 98:2) as a white solid (0.83 g, 80% yield). ¹H NMR (300 MHz, CDCl₃, ppm): δ 7.26 (apparent d, *J* = 8.1 Hz, 4H), 7.15 (apparent d, *J* = 8.0 Hz, 4H), 5.40 (s, 2H), 2.38 (s, 6H).

¹H NMR is consistent with previously published data³⁶

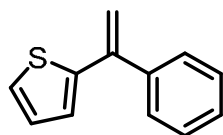
2-(1-phenylvinyl)pyridine (**2v**)



Starting from 2-benzoylpyridine (0.92 g) and following the general procedure D, **2v** was isolated by flash chromatography on silica (eluent: pentane/EtOAc, 95:5) as a yellow oil (0.90 g, 99% yield). ¹H NMR (300 MHz, CDCl₃, ppm): δ 8.56 (ddd, *J* = 4.8, 1.8, 0.9 Hz, 1H), 7.54 (td, *J* = 7.8, 1.9 Hz, 1H), 7.31–7.21 (m, 5H), 7.81 (td, *J* = 7.9, 1.1 Hz, 1H), 7.12 (ddd, *J* = 7.5, 4.8, 1.1 Hz, 1H), 5.91 (d, *J* = 1.5 Hz, 1H), 5.52 (d, *J* = 1.5 Hz, 1H).

¹H NMR is consistent with previously published data³⁶

2-(1-phenylvinyl)thiophene (**2w**)



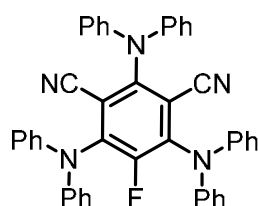
Starting from 2-benzoylthiophene (0.70 g) and following the general procedure D on 3.7 mmol scale, **2w** was isolated by flash chromatography on silica (eluent: pentane/EtOAc, 98:2) as a colorless oil (0.44 g, 63% yield). **¹H NMR** (300 MHz, CDCl₃, ppm): δ 7.50–7.33 (m, 5H), 7.25 (dd, *J* = 5.1, 1.1 Hz, 1H), 6.99 (dd, *J* = 5.1, 3.7 Hz, 1H), 6.92 (dd, *J* = 3.6, 1.1 Hz, 1H), 5.60 (s, 1H), 5.26 (s, 1H).

¹H NMR is consistent with previously published data³⁶

Synthesis of Photocatalysts **3DPAFIPN** and **3DPA2FBN**

The organic photocatalysts **3DPAFIPN** and **3DPA2FBN** used in this work were synthesized following a literature procedure³⁷ on 1.0 mmol scale.

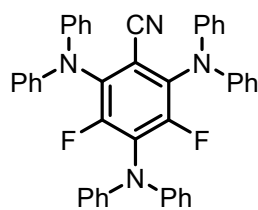
2,4,6-Tris(diphenylamino)-5-fluoroisophthalonitrile (**3DPAFIPN**)



¹H NMR (300 MHz, CDCl₃, ppm): δ 7.28–7.23 (m, 14H), 7.08–7.05 (m, 6H), 7.00–6.96 (m, 12H). **¹⁹F NMR** (377 MHz, CDCl₃, ppm): δ –121.31 (s, 1F).

Spectroscopic data are consistent with previously published data³⁷

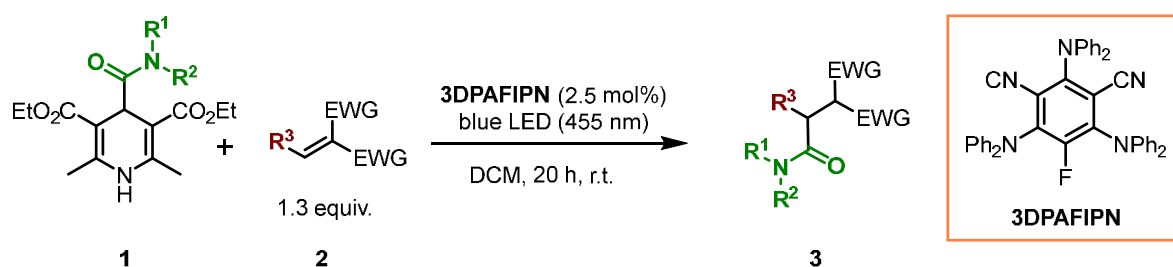
2,4,6-Tris(diphenylamino)-3,5-difluorobenzonitrile (**3DPA2FBN**)



¹H NMR (300 MHz, CDCl₃, ppm): δ 7.27–7.22 (m, 13 H), 7.04–6.95 (m, 17H). **¹⁹F NMR** (377 MHz, CDCl₃, ppm): δ –120.22 (s, 1F).

Spectroscopic data are consistent with previously published data³⁷

General Procedure E. Carbamoylation Reaction of Olefins



Scheme 9. Photoredox-mediated carbamoylation of olefins.

To a 4 mL screw cap vial equipped with a stir bar was added dihydropyridines **1** (0.30 mmol, 1.0 equiv), the desired olefin **2** (0.39 mmol, 1.3 equiv), the photocatalyst 3DPAFIPN (2.5 mol%) and DCM as solvent (3.0 mL, 0.10 M). The vial was then sealed with a plastic screw cap and placed in an EvoluChemTMPhotoRedOx reactor fitted with a 455 nm high-power single LED ($\lambda_{\text{max}}= 455 \text{ nm}$) with an irradiance of 55 mW/cm² (the set-up is detailed in Figure S1). After 20 hours of irradiation, the mixture was concentrated under reduced pressure and purified by flash column chromatography on silica gel to afford the title compound.

General procedure F. Carbamoylation reaction of olefins

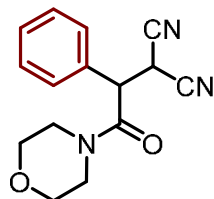
To a 4 mL screw cap vial equipped with a stir bar was added dihydropyridines **1** (0.30 mmol, 1.0 equiv), the desired olefin **2** (0.39 mmol, 1.3 equiv), and DCM as solvent (3.0 mL, 0.10 M). The vial was then sealed with a plastic screw cap and placed in an EvoluChemTMPhotoRedOx reactor fitted with a 405 nm high-power single LED ($\lambda_{\text{max}}= 405 \text{ nm}$) with an irradiance of 28 mW/cm² (the set-up is detailed in Figure S1). After 20 hours of irradiation, the mixture was concentrated under reduced pressure. The yield of product was determined by ¹H NMR analysis using 1,3,5-trimethoxybenzene as the external standard.



Figure 3. EvoluChemTMPhotoRedOx reactor fitted with a 455 nm high-power single LED.

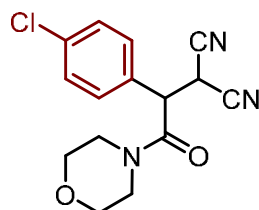
Characterization of Products

2-(2-morpholino-2-oxo-1-phenylethyl)malononitrile (**3aa**)



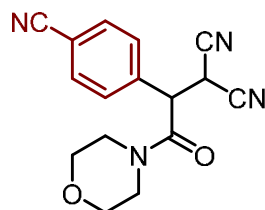
Starting from benzylidenemalononitrile **2a** (60.1 mg, 0.390 mmol) and dihydropyridine **1a** (109 mg, 0.300 mmol) following the general procedure E, **3aa** was isolated by flash chromatography on silica (gradient: pentane/EtOAc, from 7:3 to 4:6) as a white solid (59.2 mg, 73% yield). **¹H NMR** (300 MHz, CDCl₃, ppm): δ 7.48–7.43 (m, 3H), 7.37–7.33 (m, 2H), 4.50 (d, *J* = 8.6 Hz, 1H), 4.30 (d, *J* = 8.6 Hz, 1H), 3.84–3.67 (m, 2H), 3.58–3.46 (m, 3H), 3.33 (ddd, *J* = 13.3, 7.5, 3.1 Hz, 1H) 3.15 (ddd, *J* = 13.4, 5.7, 3.0 Hz, 1H), 3.01 (ddd, *J* = 11.6, 7.5, 3.0 Hz, 1H). **¹³C NMR** (75 MHz, CDCl₃, ppm): δ 165.8, 132.0, 130.0, 128.2, 112.4, 111.7, 66.5, 65.8, 50.7, 46.0, 42.9, 27.8. **HRMS** (ESI): *m/z* = calcd. for C₁₅H₁₆N₃O₂⁺ [M-H]⁺: 270.1243, found: 270.1236.

2-(1-(4-chlorophenyl)-2-morpholino-2-oxoethyl)malononitrile (**3ba**)



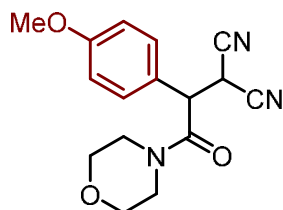
Starting from 2-(4-chlorobenzylidene)malononitrile **2b** (118 mg, 0.390 mmol) and dihydropyridine **1a** (109 mg, 0.300 mmol) following the general procedure E, **3ba** was isolated by flash chromatography on silica (gradient: pentane/EtOAc, from 7:3 to 4:6) as a white solid (75.0 mg, 83% yield). **¹H NMR** (300 MHz, CDCl₃, ppm): δ 7.46–7.43 (m, 2H), 7.32–7.29 (m, 2H), 4.48 (d, *J* = 8.4 Hz, 1H), 4.28 (d, *J* = 8.4 Hz, 1H), 3.82–3.66 (m, 2H), 3.63–3.44 (m, 3H), 3.40–3.30 (m, 1H), 3.12 (td, *J* = 10.6, 10.1, 3.1 Hz, 1H). **¹³C NMR** (75 MHz, CDCl₃, ppm): δ 165.4, 136.3, 130.4, 130.3, 129.6, 112.1, 111.4, 66.5, 65.9, 49.9, 46.1, 43.0, 27.8. **HRMS** (ESI): *m/z* = calcd. for C₁₅H₁₅ClN₃O₂⁺ [M-H]⁺: 304.0853, found: 304.0850.

2-(1-(4-cyanophenyl)-2-morpholino-2-oxoethyl)malononitrile (**3ca**)



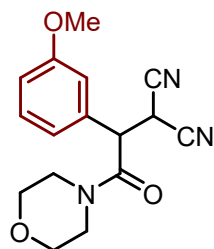
Starting from 2-(4-cyanobenzylidene)malononitrile **2c** (115 mg, 0.390 mmol) and dihydropyridine **1a** (109 mg, 0.300 mmol) following the general procedure E, **3ca** was isolated by flash chromatography on silica (gradient: pentane/EtOAc, from 7:3 to 4:6) as a white solid (89.0 mg, 90% yield). **¹H NMR** (300 MHz, CDCl₃, ppm): δ 7.80–7.77 (m, 2H), 7.54–7.51 (m, 2H), 4.53 (d, *J* = 8.2 Hz, 1H), 4.38 (d, *J* = 8.3 Hz, 1H), 3.74–3.54 (m, 5H), 3.39–3.32 (m, 1H), 3.18–3.05 (m, 2H). **¹³C NMR** (75 MHz, CDCl₃, ppm): δ 164.7, 136.8, 133.7, 129.2, 117.5, 114.4, 111.7, 111.1, 66.5, 65.9, 50.2, 46.1, 43.1, 27.6. **HRMS** (ESI): *m/z* = calcd. for C₁₆H₁₅N₄O₂⁺ [M-H]⁺: 295.1190, found: 295.1170.

2-(1-(4-methoxyphenyl)-2-morpholino-2-oxoethyl)malononitrile (**3da**)



Starting from 2-(4-methoxybenzylidene)malononitrile **2d** (117 mg, 0.390 mmol) and dihydropyridine **1a** (109 mg, 0.300 mmol) following the general procedure E, **3da** was isolated by flash chromatography on silica (gradient: pentane/EtOAc, from 7:3 to 4:6) as a colorless gum (30.6 mg, 33% yield). **¹H NMR** (300 MHz, CDCl₃, ppm): δ 7.27–7.24 (m, 2H), 9.96–6.93 (m, 2H), 4.46 (d, *J* = 8.3 Hz, 1H), 4.26 (d, *J* = 8.3 Hz, 1H), 3.82 (s, 3H), 3.80–3.67 (m, 2H), 3.56–3.47 (m, 3H), 3.32–3.28 (m, 1H), 3.18–3.12 (m, 1H), 3.09–3.01 (m, 1H). **¹³C NMR** (75 MHz, CDCl₃, ppm): δ 166.0, 160.6, 129.5, 123.7, 115.3, 112.5, 111.8, 66.5, 65.9, 55.4, 50.1, 46.1, 42.9, 28.0. **HRMS** (ESI): *m/z* = calcd. for C₁₆H₁₈N₃O₃⁺ [M-H]⁺: 300.1343, found: 300.1325.

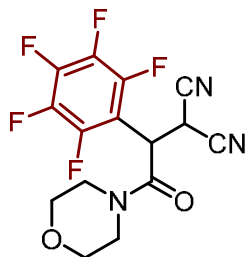
2-(1-(3-methoxyphenyl)-2-morpholino-2-oxoethyl)malononitrile (**3ea**)



Starting from 2-(3-methoxybenzylidene)malononitrile **2e** (117 mg, 0.390 mmol) and dihydropyridine **1a** (109 mg, 0.300 mmol) following the general procedure E, **3ea** was isolated by flash chromatography on silica (gradient: pentane/EtOAc, from 7:3 to 4:6) as a white solid (59.2 mg, 80% yield). **¹H NMR** (300 MHz, CDCl₃, ppm): δ 7.39–7.34 (m, 1H), 6.97–6.85 (m, 3H), 4.50 (d, *J* = 8.3 Hz, 1H), 4.27 (*J* = 8.3 Hz, 1H), 3.81 (s, 3H), 3.73–3.68 (m, 2H), 3.56–3.52 (m, 3H), 3.34–3.30 (m, 1H), 3.22–3.14 (m, 1H), 3.11–3.03 (m, 1H). **¹³C NMR** (75 MHz, CDCl₃, ppm): δ 165.6, 160.5,

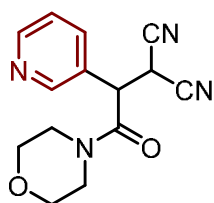
113.3, 131.1, 120.4, 115.1, 113.9, 112.4, 111.6, 66.5, 65.9, 55.5, 50.7, 46.1, 43.0, 27.8. **HRMS** (ESI): m/z = calcd. for $C_{16}H_{18}N_3O_3^+$ $[M-H]^+$: 300.1343, found: 300.1357.

2-(2-morpholino-2-oxo-1-(perfluorophenyl)ethyl)malononitrile (3fa)



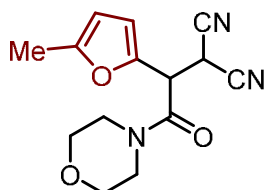
Starting from 2-(pentafluorobenzylidene)malononitrile **2f** (141 mg, 0.390 mmol) and dihydropyridine **1a** (109 mg, 0.300 mmol) following the general procedure E, **3fa** was isolated by flash chromatography on silica (gradient: pentane/EtOAc, from 7:3 to 4:6) as an orange solid (80.7 mg, 75% yield). **¹H NMR** (300 MHz, $CDCl_3$, ppm): δ 4.80 (d, J = 8.3 Hz, 1H), 4.71 (d, J = 8.3 Hz, 1H), 3.86–3.78 (m, 1H), 3.71–3.51 (m, 4H), 3.45–3.29 (m, 2H), 3.09–3.04 (m, 1H). **¹³C NMR** (75 MHz, $CDCl_3$, ppm): δ 162.6, 111.3, 110.7, 66.5, 65.9, 45.9, 43.5, 40.5, 24.9. **¹⁹F NMR** (565 MHz, $CDCl_3$, ppm) δ -137.62 – -139.80 (m), -147.70 (t, J = 21.5 Hz), -156.53 – -158.24 (m). **HRMS** (ESI): m/z = calcd. for $C_{15}H_{11}F_5N_3O_2^+$ $[M-H]^+$: 360.0766, found: 360.0754.

2-(2-morpholino-2-oxo-1-(pyridin-3-yl)ethyl)malononitrile (3ga)



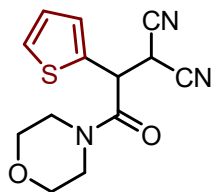
Starting from 2-(pyridin-3-ylmethylene)malononitrile **2g** (105 mg, 0.390 mmol) and dihydropyridine **1a** (109 mg, 0.300 mmol) following the general procedure E, **3ga** was isolated by flash chromatography on silica (gradient: pentane/EtOAc, from 7:3 to 4:6) as a pink solid (70.5 mg, 86% yield). **¹H NMR** (300 MHz, $CDCl_3$, ppm): δ 8.73 (dd, J = 4.8, 1.6 Hz, 1H), 8.68–8.61 (m, 1H), 7.79–7.68 (m, 1H), 7.49–7.38 (m, 1H), 4.54 (d, J = 8.3 Hz, 1H), 4.38 (d, J = 8.3 Hz, 1H), 3.81–3.49 (m, 5H), 3.37–3.34 (m, 1H), 3.14 (m, 1H). **¹³C NMR** (75 MHz, $CDCl_3$, ppm): δ 164.9, 151.5, 149.7, 135.5, 128.1, 124.5, 66.5, 65.9, 47.9, 46.1, 43.1, 27.7. **HRMS** (ESI): m/z = calcd. for $C_{14}H_{15}N_4O_2^+$ $[M-H]^+$: 271.1190, found: 271.1252.

2-(1-(5-methylfuran-2-yl)-2-morpholino-2-oxoethyl)malononitrile (3ha)



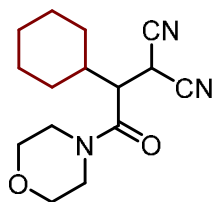
Starting from 2-[(5-methylfuran-2-yl)methylene]malononitrile **2h** (61.7 mg, 0.390 mmol) and dihydropyridine **1a** (109 mg, 0.300 mmol) following the general procedure E, **3ha** was isolated by flash chromatography on silica (gradient: pentane/EtOAc, from 7:3 to 5:5) as a brown gum (49.3 mg, 60% yield). **¹H NMR** (300 MHz, $CDCl_3$, ppm): δ 6.35 (d, J = 3.2 Hz, 1H), 6.04–5.96 (m, 1H), 4.57 (d, J = 8.2 Hz, 1H), 4.48 (d, J = 8.2 Hz, 1H), 3.86–3.68 (m, 2H), 3.65–3.51 (m, 3H), 3.43–3.25 (m, 3H), 2.29 (s, 3H). **¹³C NMR** (75 MHz, $CDCl_3$, ppm): δ 163.6, 154.4, 142.8, 112.1, 111.8, 111.5, 107.4, 66.6, 66.1, 46.1, 44.8, 43.1, 26.1, 13.6. **HRMS** (ESI): m/z = calcd. for $C_{14}H_{16}N_3O_3^+$ $[M-H]^+$: 274.1186, found: 274.1207.

2-(2-morpholino-2-oxo-1-(thiophen-2-yl)ethyl)malononitrile (3ia)



Starting from 2-(thiophen-2-ylmethylene)malononitrile **2i** (62.5 mg, 0.390 mmol) and dihydropyridine **1a** (109 mg, 0.300 mmol) following the general procedure E, **3ia** was isolated by flash chromatography on silica (gradient: pentane/EtOAc, from 7:3 to 5:5) as a yellow solid (54.0 mg, 65% yield). **¹H NMR** (300 MHz, $CDCl_3$, ppm): δ 7.40 (dd, J = 5.2, 1.2 Hz, 1H), 7.16 (dd, J = 3.2, 1.2 Hz, 1H), 7.07 (dd, J = 5.2, 3.2 Hz, 1H), 4.67 (d, J = 8.4 Hz, 1H), 4.56 (d, J = 8.4 Hz, 1H), 3.85–3.68 (m, 2H), 3.62–3.52 (m, 3H), 3.47–3.37 (m, 1H), 3.33–3.27 (m, 1H), 3.22–3.14 (m, 1H). **¹³C NMR** (75 MHz, $CDCl_3$, ppm): δ 165.1, 133.1, 128.9, 128.0, 127.9, 112.1, 111.5, 66.4, 65.9, 46.3, 45.6, 43.2, 28.5. **HRMS** (ESI): m/z = calcd. for $C_{13}H_{14}N_3O_2S^+$ $[M-H]^+$: 276.0801, found: 276.0547.

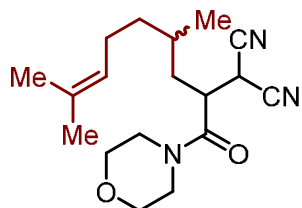
2-(1-cyclohexyl-2-morpholino-2-oxoethyl)malononitrile (3ja)



Starting from 2-(cyclohexylmethylene)malononitrile **2j** (107 mg, 0.390 mmol) and dihydropyridine **1a** (109 mg, 0.300 mmol) following the general procedure E, **3ja** was isolated by flash chromatography on silica (gradient: pentane/EtOAc, from 7:3 to 4:6) as a yellowish solid (62.2 mg, 75% yield). **¹H NMR** (300 MHz, $CDCl_3$, ppm): δ 4.26 (d, J = 9.0 Hz, 1H), 3.96–3.88 (m, 1H), 3.75–3.50 (m, 7H), 3.23 (dd, J = 9.0, 6.2 Hz, 1H), 1.99–1.89 (m, 1H), 1.81–1.62 (m, 4H), 1.31–1.07 (m, 6H). **¹³C NMR**

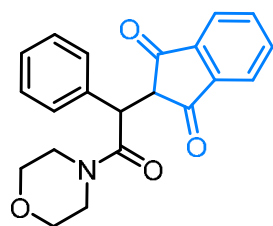
(75 MHz, CDCl₃, ppm): δ 167.2, 112.1, 67.0, 66.0, 47.2, 46.7, 42.9, 39.4, 30.9, 28.8, 26.1, 25.9, 25.7, 24.1. **HRMS** (ESI): m/z = calcd. for C₁₅H₂₂N₃O₂⁺ [M-H]⁺: 276.1707, found: 276.1608.

2-[(4*R*)-4,8-dimethyl-1-morpholino-1-oxonon-7-en-2-yl]malononitrile (**3ka**)



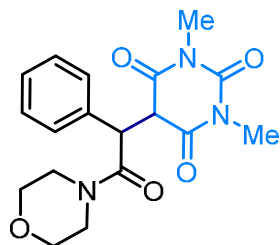
Starting from 2-(3,7-dimethyloct-6-en-1-ylidene)malononitrile **2k** (78.9 mg, 0.390 mmol) and dihydropyridine **1a** (109 mg, 0.300 mmol) following the general procedure E, **3ka** was isolated by flash chromatography on silica (gradient: pentane/EtOAc, from 7:3 to 4:6) as a yellowish oil (30.0 mg, 32% yield). **¹H NMR** (300 MHz, CDCl₃, ppm): δ 5.04 (dt, J = 6.9, 1.5 Hz, 1H), 4.08 (dd, J = 9.0, 4.2 Hz, 1H), 3.87 – 3.83 (m, 1H), 3.76 – 3.49 (m, 6H), 3.40 (td, J = 6.4, 2.8 Hz, 1H), 2.00 – 1.80 (m, 2H), 1.68 (s, 3H), 1.60 (s, 3H), 1.40 – 1.13 (m, 6H), 0.95 (d, J = 6.5 Hz, 3H). **¹³C NMR** (75 MHz, CDCl₃, ppm): δ 168.4, 132.3, 123.7, 112.0, 66.8, 66.5, 46.8, 43.0, 40.5, 38.7, 37.1, 29.8, 26.1, 25.1, 19.7, 19.5, 17.7. **HRMS** (ESI): m/z = calcd. for C₁₈H₂₈N₃O₂⁺ [M-H]⁺: 318.2176, found: 318.2165.

2-(2-morpholino-2-oxo-1-phenylethyl)-1*H*-indene-1,3(2*H*)-dione (**3la**)



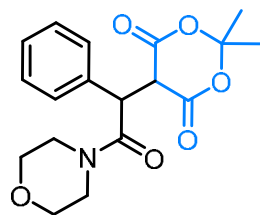
Starting from 2-benzylidene-1*H*-indene-1,3(2*H*)-dione **2l** (136 mg, 0.390 mmol) and dihydropyridine **1a** (109 mg, 0.300 mmol) following the general procedure E, **3la** was isolated by flash chromatography on silica (gradient: pentane/EtOAc, from 7:3 to 5:5) as an orange solid (89.5 mg, 80% yield). **¹H NMR** (300 MHz, CDCl₃, ppm): δ 7.97 – 7.92 (m, 2H), 7.84 – 7.71 (m, 2H), 7.45 – 7.28 (m, 5H), 4.85 (d, J = 3.4 Hz, 1H), 3.65 – 3.54 (m, 2H), 3.54 – 3.30 (m, 3H), 3.28 – 3.18 (m, 1H), 3.15 (d, J = 3.4 Hz, 1H), 3.13 – 3.04 (m, 2H). **¹³C NMR** (75 MHz, CDCl₃, ppm): δ 199.7, 197.7, 169.2, 143.3, 140.7, 136.1, 135.5, 134.6, 129.0, 128.9, 127.8, 123.1, 122.9, 66.6, 66.0, 55.7, 51.2, 46.5, 42.6. **HRMS** (ESI): m/z = calcd. for C₂₁H₂₀NO₄⁺ [M-H]⁺: 350.1387, found: 350.1441.

1,3-dimethyl-5-(2-morpholino-2-oxo-1-phenylethyl)pyrimidine-2,4,6-(1*H*,3*H*,5*H*)-trione (**3ma**)



Starting from 5-benzylidene-1,3-dimethylpyrimidine-2,4,6-(1*H*,3*H*,5*H*)-trione **2m** (140 mg, 0.390 mmol) and dihydropyridine **1a** (109 mg, 0.300 mmol) following the general procedure E, **3ma** was isolated by flash chromatography on silica (gradient: pentane/EtOAc, from 7:3 to 2:8) as a yellow solid (56.1 mg, 52% yield). **¹H NMR** (300 MHz, CDCl₃, ppm): δ 7.41 – 7.39 (m, 3H), 7.30 – 7.28 (m, 2H), 4.66 (bs, 1H), 3.66 – 3.61 (m, 2H), 3.58 – 3.35 (m, 5H), 3.31 (s, 3H), 3.26 (s, 3H), 3.07 – 3.03 (m, 2H). **¹³C NMR** (75 MHz, CDCl₃, ppm): δ 169.3, 169.1, 168.5, 150.9, 131.9, 130.3, 129.2, 128.9, 74.1, 66.6, 66.1, 59.1, 46.6, 42.5, 29.3, 28.9. **HRMS** (ESI): m/z = calcd. for C₁₈H₂₂N₃O₆⁺ [M-OH]⁺: 376.1503, found: 376.1503.

2,2-dimethyl-5-(2-morpholino-2-oxo-1-phenylethyl)-1,3-dioxane-4,6-dione (**3na**)



Starting from 5-benzylidene-2,2-dimethyl-1,3-dioxane-4,6-dione **2n** (135 mg, 0.390 mmol) and dihydropyridine **1a** (109 mg, 0.300 mmol) following the general procedure E, **3na** was isolated by flash chromatography on silica (gradient: pentane/EtOAc, from 7:3 to 2:8) as a yellowish solid (48.7 mg, 47% yield). **¹H NMR** (300 MHz, CDCl₃, ppm): δ 7.31-7.29 (m, 5H), 4.88 (d, J = 4.2 Hz, 1H), 3.75 (d, J = 4.2 Hz, 1H), 3.65-3.52 (m, 5H), 3.45-3.38 (m, 1H), 3.21-3.03 (m, 2H), 1.74 (s, 3H), 1.70 (s, 3H). **¹³C NMR** (75 MHz, CDCl₃, ppm): δ 168.4, 165.5, 164.1, 135.7, 129.4, 128.7, 127.9, 104.9, 66.7, 66.0, 50.0, 49.6, 46.5, 42.8, 28.2, 27.4. **HRMS** (ESI): m/z = calcd. for C₁₈H₂₃NO₇⁺ [M-H₂O]⁺: 365.1475, found: 365.1334.

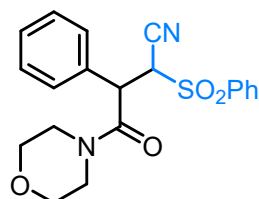
1-morpholino-3,3-bis(phenylsulfonyl)propan-1-one (**3oa**)



Starting from 1,1-bis(phenylsulfonyl)ethylene (121 mg, 0.390 mmol) and dihydropyridine **1a** (109 mg, 0.300 mmol) following the general procedure A, **3oa** was isolated by flash chromatography on silica (gradient: pentane/EtOAc, from 5:5 to 2:8) as a yellow solid (73.0 mg, 57% yield). **¹H NMR** (300 MHz, CDCl₃, ppm): δ 7.92 – 7.77 (m, 4H), 7.69 – 7.60 (m, 2H), 7.52 – 7.47 (m, 4H),

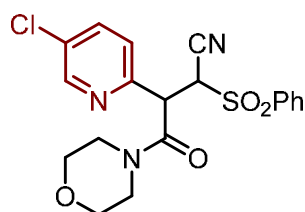
5.68 (t, $J = 5.7$ Hz, 1H), 3.75 – 3.48 (m, 8H), 3.25 (d, $J = 5.7$ Hz, 2H). ^{13}C NMR (75 MHz, 300 MHz, CDCl_3 , ppm) δ 165.7, 138.3, 134.7, 129.4, 129.3, 66.7, 66.5, 46.1, 43.0, 28.5. HRMS (ESI): $m/z = \text{calcd. for } \text{C}_{19}\text{H}_{22}\text{NO}_6\text{S}_2^+ [\text{M}-\text{H}]^+$: 424.0883, found: 424.0878.

4-morpholino-4-oxo-3-phenyl-2-(phenylsulphonyl)butanenitrile (3pa)



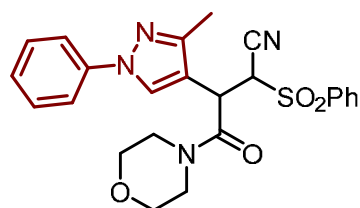
Starting from (*E*)-3-phenyl-2-(phenylsulphonyl)acrylonitrile **2p** (105 mg, 0.390 mmol) and dihydropyridine **1a** (109 mg, 0.300 mmol) following the general procedure E, **3pa** was isolated by flash chromatography on silica (gradient: pentane/EtOAc, from 7:3 to 4:6) as a white solid (55.4 mg, 48% yield). ^1H NMR (300 MHz, CDCl_3 , ppm): δ 8.05–8.02 (m, 2H), 7.76–7.73 (m, 1H), 7.66–7.61 (m, 2H), 7.39–7.35 (m, 5H), 5.43 (d, $J = 8.0$ Hz, 1H), 4.68 (d, $J = 8.0$ Hz, 1H), 3.74–3.49 (m, 6H), 3.39–3.28 (m, 1H), 3.23–3.11 (m, 1H). ^{13}C NMR (75 MHz, CDCl_3 , ppm): δ 166.8, 136.7, 135.3, 133.1, 129.7, 129.6, 129.4, 129.3, 128.6, 112.7, 66.5, 66.0, 60.3, 46.3, 45.6, 43.3. HRMS (ESI): $m/z = \text{calcd. for } \text{C}_{20}\text{H}_{21}\text{N}_2\text{O}_4^+ [\text{M}-\text{H}]^+$: 385.1217, found: 385.1179.

3-(5-chloropyridin-2-yl)-4-morpholino-4-oxo-2-(phenylsulphonyl)butanenitrile (3qa)



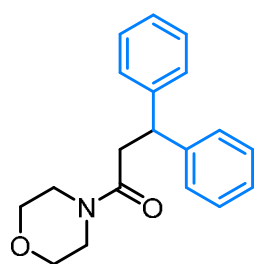
Starting from (*E*)-3-(5-chloropyridin-3-yl)-2-(phenylsulphonyl)acrylonitrile **2q** (119 mg, 0.390 mmol) and dihydropyridine **1a** (109 mg, 0.300 mmol) following the general procedure E, **3qa** was isolated by flash chromatography on silica (gradient: pentane/EtOAc, from 7:3 to 4:6) as a brown solid (80.2 mg, 64% yield). ^1H NMR (300 MHz, CDCl_3 , ppm): δ 8.54–8.53 (m, 1H, major), 8.51–8.50 (m, 1H, minor), 8.04–8.01 (m, 2H, major), 7.96–7.93 (m, 2H, minor), 7.66–7.60 (m, 4H major + 4H minor), 7.41 (dd, $J = 8.4, 0.7$ Hz, 1H minor), 7.36 (dd, $J = 8.4, 0.7$ Hz, 1H major), 5.46 (d, $J = 8.4$ Hz, 1H major), 4.98 (d, $J = 8.4$ Hz, 1H major), 4.97 (d, $J = 8.3$ Hz, 1H minor), 4.91 (d, $J = 8.3$ Hz, 1H minor), 3.72–3.26 (m, 8H major + 8H minor). ^{13}C NMR (75 MHz, CDCl_3 , ppm): δ 165.8 (major), 165.3 (minor), 151.6 (major), 150.8 (minor), 149.2 (major), 148.9 (minor), 137.4 (major), 137.3 (minor), 136.4 (major), 136.0 (minor), 135.5 (major), 135.4 (minor), 132.6 (major), 132.3 (minor), 129.7 (major), 129.6 (minor), 129.5 (minor), 129.4 (major), 123.9 (major), 123.8 (minor), 113.3 (minor), 112.7 (major), 66.5 (minor), 66.4 (major), 66.3 (minor), 66.2 (major), 59.6 (minor), 59.0 (major), 48.0 (minor), 47.2 (major), 46.5 (minor), 46.4 (major), 43.5 (major), 43.0 (minor). HRMS (ESI): $m/z = \text{calcd. for } \text{C}_{19}\text{H}_{19}\text{ClN}_3\text{O}_4\text{S}^+ [\text{M}-\text{H}]^+$: 420.0779, found: 420.0717.

3-(3-methyl-1-phenyl-1H-pyrazol-4-yl)-4-morpholino-4-oxo-2-(phenylsulfonyl)butanenitrile (3ra)



Starting from (*E*)-3-(3-methyl-1-phenyl-1H-pyrazol-4-yl)-2-(phenylsulfonyl)acrylonitrile **2r** (136 mg, 0.390 mmol) and dihydropyridine **1a** (109 mg, 0.300 mmol) following the general procedure E, **3ra** was isolated by flash chromatography on silica (gradient: pentane/EtOAc, from 6:4 to 2:8) as a yellow solid (45.3 mg, 31% yield). ^1H NMR (300 MHz, CDCl_3 , ppm): δ 8.07 – 7.98 (m, 2H), 7.88 (s, 1H), 7.79 – 7.73 (m, 1H), 7.69 – 7.57 (m, 4H), 7.41 (dd, $J = 8.7, 7.1$ Hz, 2H), 7.26 – 7.24 (m, 1H), 5.27 (d, $J = 7.7$ Hz, 1H), 4.71 (d, $J = 7.6$ Hz, 1H), 3.80 – 3.52 (m, 7H), 3.49 – 3.30 (m, 1H), 2.42 (s, 3H). ^{13}C NMR (75 MHz, CDCl_3 , ppm): δ 167.5, 148.7, 139.5, 136.4, 135.5, 129.8, 129.5, 129.4, 126.7, 118.8, 113.6, 66.5, 66.2, 46.4, 43.3, 35.9, 23.9, 14.2. HRMS (ESI): $m/z = \text{calcd. for } \text{C}_{24}\text{H}_{25}\text{N}_4\text{O}_4\text{S}^+ [\text{M}-\text{H}]^+$: 465.1591, found: 465.1591.

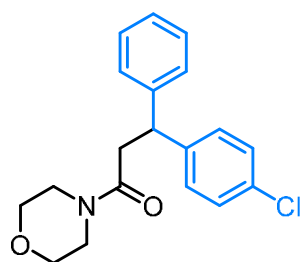
1-morpholino-3,3-diphenylpropan-1-one (3sa)



Starting from 1,1-diphenylethylene **2s** (70.3 mg, 0.390 mmol) and dihydropyridine **1a** (109 mg, 0.300 mmol) following the general procedure E, **3sa** was isolated by flash chromatography on silica (eluent: pentane/EtOAc, 70:30) as a pale-yellow solid (77.3 mg, 87% yield). ^1H NMR (300 MHz, CDCl_3 , ppm): δ 7.73–7.16 (m, 10H), 4.67 (t, $J = 7.6$ Hz, 1H), 3.54 (m, 4H), 3.31 (m, 4H), 3.05 (d, $J = 7.6$ Hz, 2H).

^1H NMR is consistent with previously published data³⁸

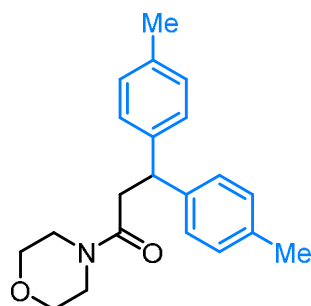
3-(4-chlorophenyl)-1-morpholino-3-phenylpropan-1-one (3ta)



$C_{19}H_{20}ClN_3O_2^+$ [M-H]⁺: 330.1255, found: 330.1254.

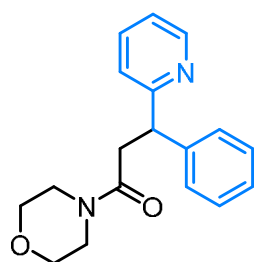
Starting from 1-chloro-4-(1-phenylvinyl)benzene **2t** (83.7 mg, 0.390 mmol) and dihydropyridine **1a** (109 mg, 0.300 mmol) following the general procedure E, **3ta** was isolated by flash chromatography on silica (eluent: pentane/EtOAc, 70:30) as a pale-yellow solid (82.5 mg, 83% yield). ¹H NMR (300 MHz, CDCl₃, ppm): δ 7.35–7.16 (m, 9H), 4.67 (t, *J* = 7.5 Hz, 1H), 3.67–3.30 (m, 8H), 3.03 (d, *J* = 7.5 Hz, 2H), 2.29 (s, 6H). ¹³C NMR (75 MHz, CDCl₃, ppm): δ 169.6, 143.5, 142.5, 132.3, 129.2, 128.70, 128.67, 127.8, 126.8, 66.8, 66.4, 46.9, 46.2, 42.1, 38.5. HRMS (ESI): *m/z* = calcd. for

1-morpholino-3,3-di-p-tolylpropan-1-one (3ua)



Starting from 4,4'-(ethene-1,1-diyl)bis(methylbenzene) **2u** (83.7 mg, 0.390 mmol) and dihydropyridine **1a** (109 mg, 0.300 mmol) following the general procedure E, **3ua** was isolated by flash chromatography on silica (eluent: pentane/EtOAc, 70:30) as a white solid (82.5 mg, 83% yield). ¹H NMR (300 MHz, CDCl₃, ppm): δ 7.18–7.02 (m, 8H), 4.57 (t, *J* = 7.6 Hz, 1H), 3.66–3.44 (m, 4H), 3.42–3.22 (m, 4H), 3.01 (d, *J* = 7.6 Hz, 2H), 2.29 (s, 6H). ¹³C NMR (75 MHz, CDCl₃, ppm): δ 170.1, 141.2, 136.0, 129.2, 127.7, 66.8, 66.4, 46.7, 46.2, 42.0, 38.7, 21.0. HRMS (ESI): *m/z* = calcd. for C₂₁H₂₅NO₂⁺ [M-H]⁺: 324.1958, found: 324.1973.

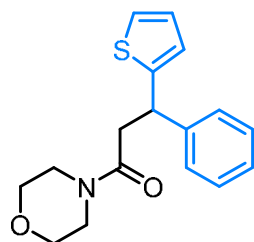
1-morpholino-3-phenyl-3-(pyridin-2-yl)propan-1-one (3va)



[M-H]⁺: 297.1598, found: 297.1633.

Starting from 2-(1-phenylvinyl)pyridine **2v** (70.7 mg, 0.390 mmol) and dihydropyridine **1a** (109 mg, 0.300 mmol) following the general procedure E, **3va** was isolated by flash chromatography on silica (gradient: pentane/EtOAc, 70:30 to 100% EtOAc) as an orange solid (59.0 mg, 66% yield). ¹H NMR (300 MHz, CDCl₃, ppm): δ 8.56–8.50 (m, 1H), 7.54 (td, *J* = 7.7, 1.8 Hz, 1H), 7.36–7.14 (m, 6H), 7.09 (ddd, *J* = 7.4, 4.9, 1.0 Hz, 1H), 4.75 (dd, *J* = 8.5, 6.1 Hz, 1H), 3.63–3.34 (m, 9H), 2.90 (dd, *J* = 15.3, 6.1 Hz, 1H). ¹³C NMR (75 MHz, CDCl₃, ppm): δ 170.4, 162.2, 148.8, 143.5, 136.5, 128.6, 128.1, 126.7, 124.1, 121.5, 66.9, 66.6, 49.3, 46.2, 42.0, 37.8. HRMS (ESI): *m/z* = calcd. for C₁₈H₂₀N₂O₂⁺ [M-

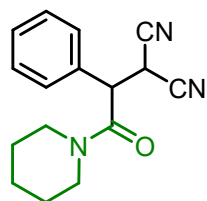
1-morpholino-3-phenyl-3-(thiophen-2-yl)propan-1-one (3wa)



for C₁₇H₁₉N₂O₂S⁺ [M-H]⁺: 302.1209, found: 302.1221.

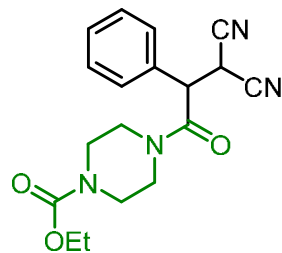
Starting from 2-(1-phenylvinyl)thiophene **2w** (72.6 mg, 0.390 mmol) and dihydropyridine **1a** (109 mg, 0.300 mmol) following the general procedure E, **3wa** was isolated by flash chromatography on silica (eluent: pentane/EtOAc, 80:20) as a white solid (35.2 mg, 39% yield). ¹H NMR (300 MHz, CDCl₃, ppm): δ 7.33–7.19 (m, 5H), 7.15 (dd, *J* = 1.2 Hz, 1H), 6.92 (dd, *J* = 5.1, 3.5 Hz, 1H), 6.84 (dt, *J* = 3.5, 1.0 Hz, 2H), 4.90 (t, *J* = 7.4 Hz, 1H), 3.65–3.24 (m, 8H), 3.06 (m, 2H). ¹³C NMR (75 MHz, CDCl₃, ppm): δ 169.3, 148.0, 143.6, 128.7, 127.7, 127.0, 126.7, 124.4, 123.9, 66.8, 66.4, 46.2, 43.2, 42.1, 40.2. HRMS (ESI): *m/z* = calcd.

2-[2-oxo-1-phenyl-2-(piperidin-1-yl)ethyl]malononitrile (3ab)



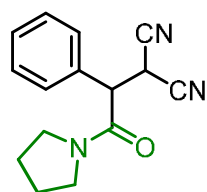
Starting from benzylidenemalononitrile **2a** (60.1 mg, 0.390 mmol) and dihydropyridine **1b** (109 mg, 0.300 mmol) following the general procedure E, **3ab** was isolated by flash chromatography on silica (gradient: pentane/EtOAc, from 7:3 to 5:5) as a yellowish gum (55.6 mg, 70% yield). **¹H NMR** (300 MHz, CDCl₃, ppm): δ 7.44–7.36 (m, 5H), 4.52 (d, *J* = 8.5 Hz, 1H), 4.34 (d, *J* = 8.4 Hz, 1H), 3.85–3.79 (m, 1H), 3.38–3.32 (m, 1H), 3.22–3.18 (m, 2H), 1.55–1.31 (m, 5H), 0.83 (dq, *J* = 12.7, 6.1 Hz, 1H). **¹³C NMR** (75 MHz, CDCl₃, ppm): δ 165.2, 132.6, 129.7, 129.6, 128.3, 112.7, 112.0, 50.7, 46.8, 43.8, 28.0, 25.5, 24.1. **HRMS** (ESI): *m/z* = calcd. for C₁₆H₁₈N₃O⁺ [M-H]⁺: 268.1444, found: 268.1456.

Ethyl 4-(3,3-dicyano-2-phenylpropanoyl)piperazine-1-carboxylate (3ac)



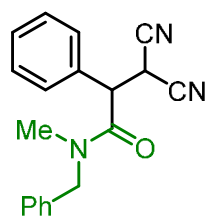
Starting from benzylidenemalononitrile **2a** (60.1 mg, 0.390 mmol) and dihydropyridine **1c** (131 mg, 0.300 mmol) following the general procedure E, **3ac** was isolated by flash chromatography on silica (gradient: pentane/EtOAc, from 7:3 to 2:8) as a yellowish solid (78.5 mg, 77% yield). **¹H NMR** (300 MHz, CDCl₃, ppm): δ 7.47–7.44 (m, 3H), 7.37–7.38 (m, 2H), 4.50 (d, *J* = 7.9 Hz, 1H), 4.33 (d, *J* = 7.9 Hz, 1H), 4.11 (q, *J* = 6.8 Hz, 2H), 3.93–3.87 (m, 1H), 3.66–3.62 (m, 1H), 3.44–3.41 (m, 1H), 3.25–3.22 (m, 1H), 2.59 (ddd, *J* = 13.2, 7.6, 4.1 Hz, 1H), 1.22 (t, *J* = 7.1 Hz, 3H). **¹³C NMR** (75 MHz, CDCl₃, ppm): δ 165.9, 156.1, 132.0, 130.0, 128.2, 112.4, 111.6, 61.8, 50.8, 45.5, 42.5, 27.9, 14.6. **HRMS** (ESI): *m/z* = calcd. for C₁₈H₂₁N₄O₃⁺ [M-H]⁺: 341.1608, found: 341.1615.

2-[2-oxo-1-phenyl-2-(pyrrolidin-1-yl)ethyl]malononitrile (3ad)



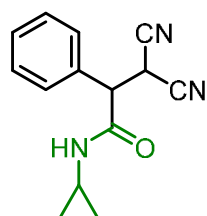
Starting from benzylidenemalononitrile **2a** (60.1 mg, 0.39 mmol) and dihydropyridine **1d** (76.0 mg, 0.300 mmol) following the general procedure E, **3ad** was isolated by flash chromatography on silica (gradient: pentane/EtOAc, from 8:2 to 6:4) as a yellowish solid (54.5 mg, 72% yield). **¹H NMR** (300 MHz, CDCl₃, ppm): 7.54–7.29 (m, 5H), 4.55 (d, *J* = 8.8 Hz, 1H), 4.19 (d, *J* = 8.8 Hz, 1H), 3.67–3.35 (m, 3H), 3.02–2.87 (m, 1H), 2.01–1.67 (m, 4H). **¹³C NMR** (75 MHz, CDCl₃, ppm): δ 165.4, 132.0, 129.72, 129.70, 128.5, 112.6, 111.8, 51.9, 46.7, 46.3, 27.6, 25.9, 24.0. **HRMS** (ESI): *m/z* = calcd. for C₁₅H₁₆N₃O⁺ [M-H]⁺: 254.1288, found: 254.1286.

N-benzyl-3,3-dicyano-*N*-methyl-2-phenylpropanamide (3ae)



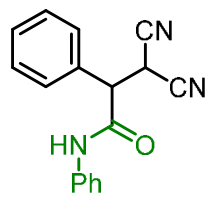
Starting from benzylidenemalononitrile **2a** (60.1 mg, 0.390 mmol) and dihydropyridine **1e** (121 mg, 0.300 mmol) following the general procedure E, **3ae** was isolated by flash chromatography on silica (gradient: pentane/EtOAc, from 7:3 to 5:5) as a yellowish solid (56.5 mg, 62% yield). **¹H NMR** (300 MHz, CDCl₃, ppm): δ 7.45 – 7.26 (m, 9H), 7.17 – 7.14 (m, 1H), 4.63 (s, 2H), 4.36 (d, *J* = 8.2 Hz, 1H), 4.27 (d, *J* = 8.2 Hz, 1H), 2.75 (s, 3H). **¹³C NMR** (75 MHz, CDCl₃, ppm): δ 167.4, 136.0, 131.8, 129.8, 128.8, 128.4, 127.9, 126.1, 112.6, 111.8, 52.8, 51.7, 51.0, 34.7, 34.6, 28.0. **HRMS** (ESI): *m/z* = calcd. for C₁₉H₁₈N₃O⁺ [M-H]⁺: 304.1444, found: 304.1449.

3,3-dicyano-*N*-cyclopropyl-2-phenylpropanamide (3af)



Starting from benzylidenemalononitrile **2a** (60.1 mg, 0.390 mmol) and dihydropyridine **1f** (71.8 mg, 0.300 mmol) following the general procedure E, **3af** was isolated by flash chromatography on silica (gradient: pentane/EtOAc, from 7:3 to 4:6) as a white solid (76.0 mg, 75% yield). **¹H NMR** (300 MHz, CDCl₃, ppm): δ 7.46–7.35 (m, 5H), 5.81 (s, 1H), 4.60 (d, *J* = 7.9 Hz, 1H), 3.97 (d, *J* = 7.9 Hz, 1H), 2.70 (tq, *J* = 7.1, 3.6 Hz, 1H), 0.83–0.67 (m, 2H), 0.53–0.37 (m, 2H). **¹³C NMR** (75 MHz, CDCl₃, ppm): δ 168.7, 132.3, 130.0, 129.8, 129.7, 128.6, 112.1, 111.5, 52.7, 26.8, 23.2, 6.8, 6.6. **HRMS** (ESI): *m/z* = calcd. for C₁₄H₁₄N₃O⁺ [M-H]⁺: 240.1131, found: 240.1152.

3,3-dicyano-N,2-diphenylpropanamide (3ag)



Starting from benzylidenemalononitrile **2a** (60.1 mg, 0.390 mmol) and dihydropyridine **1g** (112 mg, 0.300 mmol) following the general procedure E, **3ag** was isolated by flash chromatography on silica (gradient: pentane/EtOAc, from 8:2 to 6:4) as a white solid (60.3 mg, 73% yield). **¹H NMR** (300 MHz, DMSO-*d*₆, ppm): δ 10.42 (s, 1H), 7.57–7.54 (m, 2H), 7.48–7.42 (m, 5H), 7.34–7.29 (m, 2H), 7.11–7.08 (m, 1H), 5.48 (d, *J* = 7.8 Hz, 1H), 4.57 (d, *J* = 7.8 Hz, 1H). **¹³C NMR** (75 MHz, DMSO-*d*₆, ppm): δ 166.1, 138.7, 134.4, 129.5, 129.4, 128.9, 124.5, 119.9, 114.0, 113.9, 51.5, 27.0. **HRMS** (ESI): *m/z* = calcd. for C₁₇H₁₄N₃O [M-H]⁺: 276.1137, found: 276.0851.

Unsuccessful Substrates

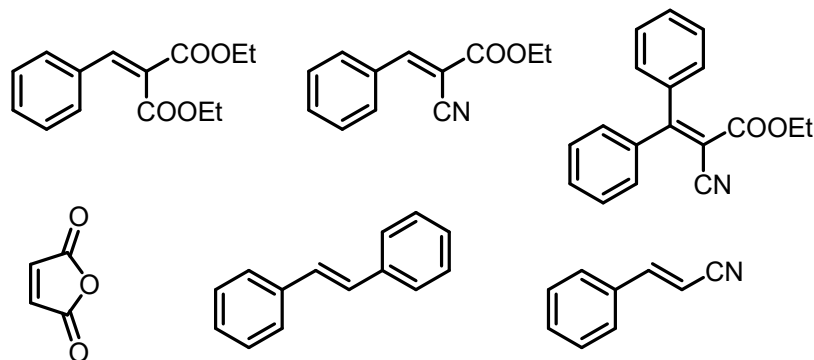


Figure 4. Unsuccessful substrates under reaction conditions.

4.4.4 Mechanistic experiments

Cyclic voltammetry

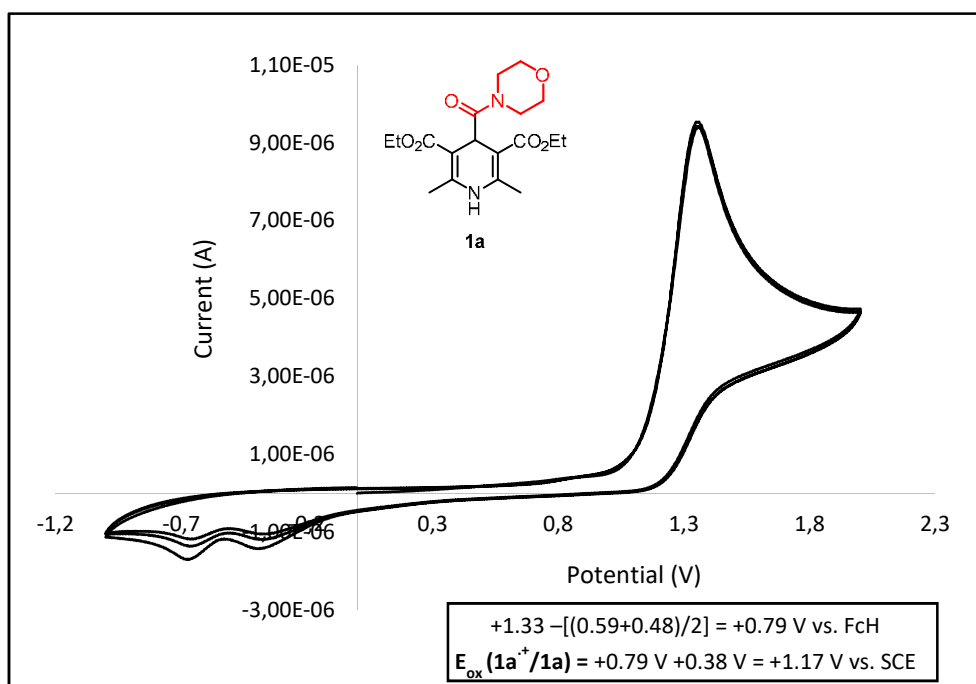


Figure 5. Cyclic voltammogram of **1a** [0.5 mM] in [0.1 M] TBAPF₆ in CH₃CN. Scan rate 100 mV s⁻¹.

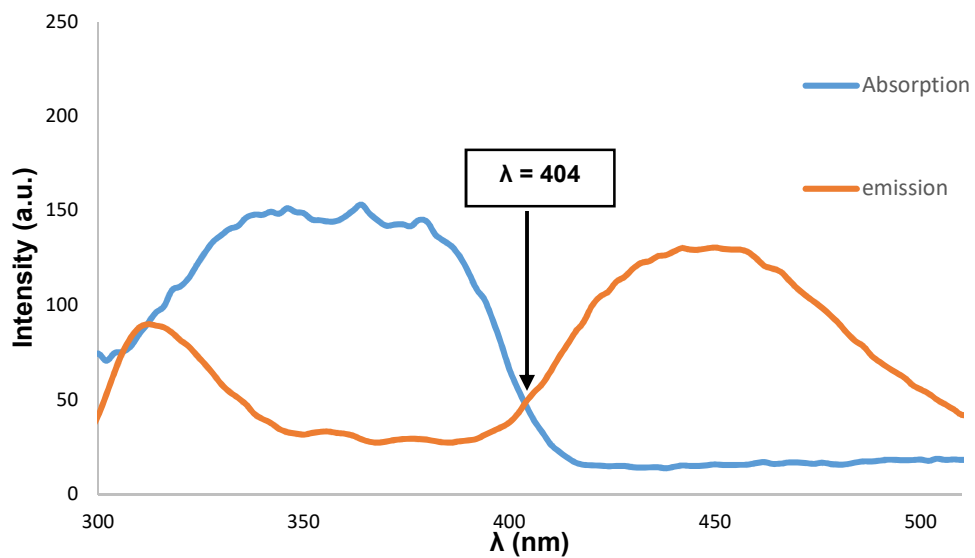


Figure 6. Absorption and emission spectra of a solution of **1a** (CH₃CN, 0.15 mM).

Evaluation of the Excited State Potential of 1a

Using the data collected from the cyclic voltammetry studies (Figure 5) and from the absorption/emission spectra (Figure 6) of **1a**, the redox potential of the excited state **1a** was determined as follow:

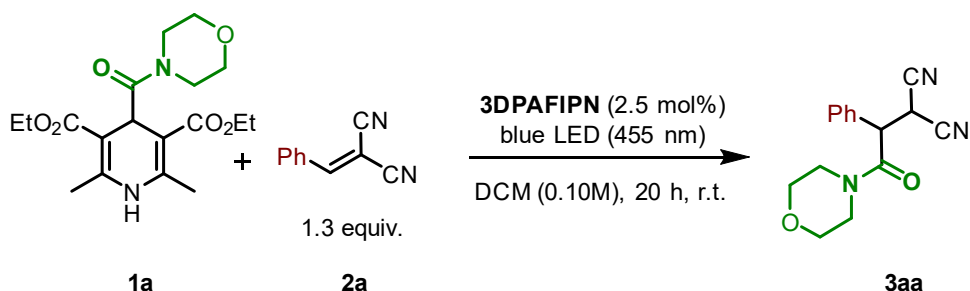
$$E(1a^+/1a^*) = E(1a^+/1a) - E_{0-0}(1a^*/1a) \quad [\text{Eq. 1}]$$

The irreversible peak potential E_{pa} was used for (1a⁺/1a) (Figure 5). The zero-zero vibrational state excitation energy E_{0-0} was estimated by the corresponding energy of

the wavelength at which emission and absorption overlap that corresponds to 404 nm (Figure 6) which translates into an $E_{0-0}(1a^*/1a)$ of 3.07 eV.

$$E(1a^+/1a^*) = +1.17 \text{ V} - 3.07 \text{ V} = -1.90 \text{ V (vs SCE)}.$$

On/Off Experiments.



Following the general procedure E, the reaction between dihydropyridine **1a** and benzylidenemalononitrile **2a** was performed on 0.3 mmol scale. Upon addition of all reagents, the reaction was irradiated alternating intervals of 1 hour irradiation (light on) with 1 hour dark (light off), during a total of 7 hours. Aliquots (100 μ L) of the reaction were collected after every hour, combined with 100 μ L of a stock solution of 1,3,5-trimethoxybenzene (0.1 mmol, 0.1 M in DCM) as the external standard and analysed by ¹H NMR to obtain the corresponding yields. As shown in the Figure 7 the reaction proceeds only during the irradiation time excluding a possible long-lived radical-chain process.

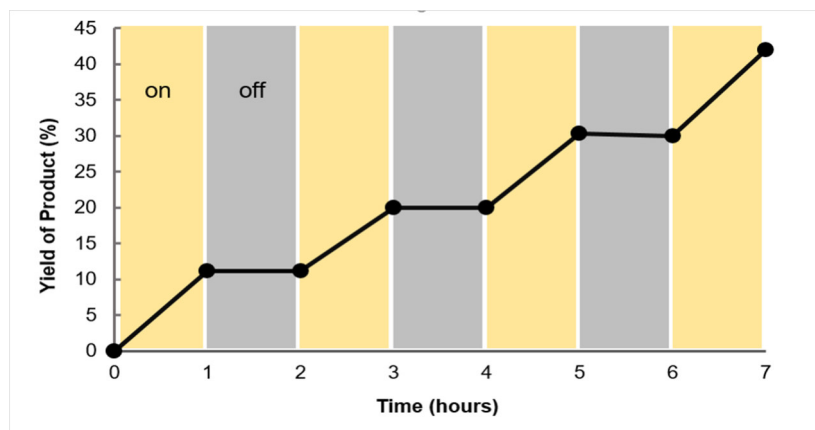
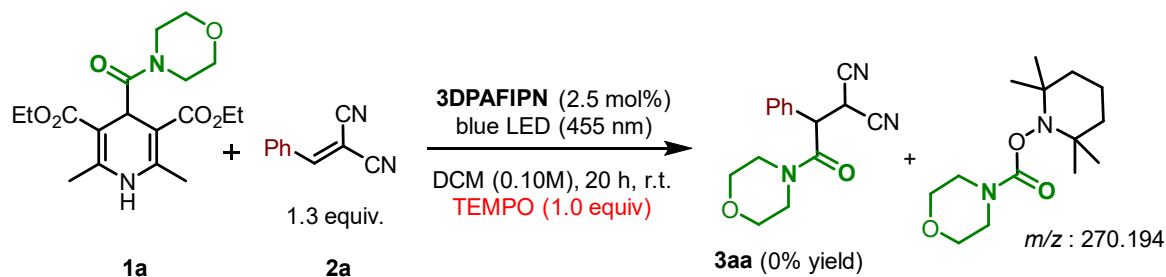


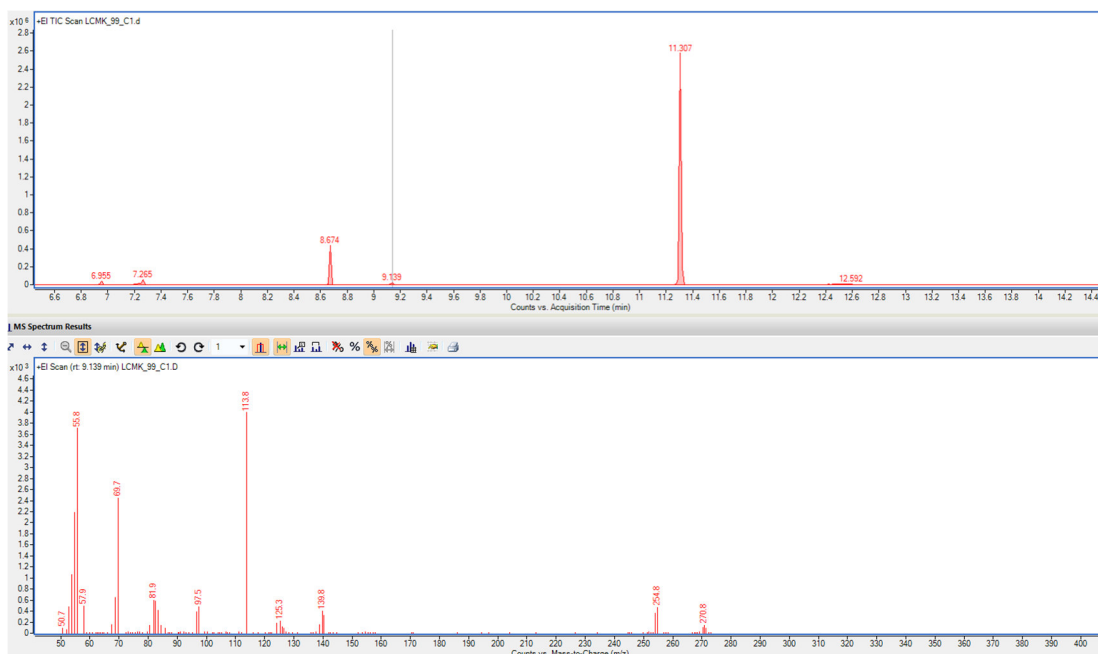
Figure 7. Light On/Off experiment.

Radical trapping

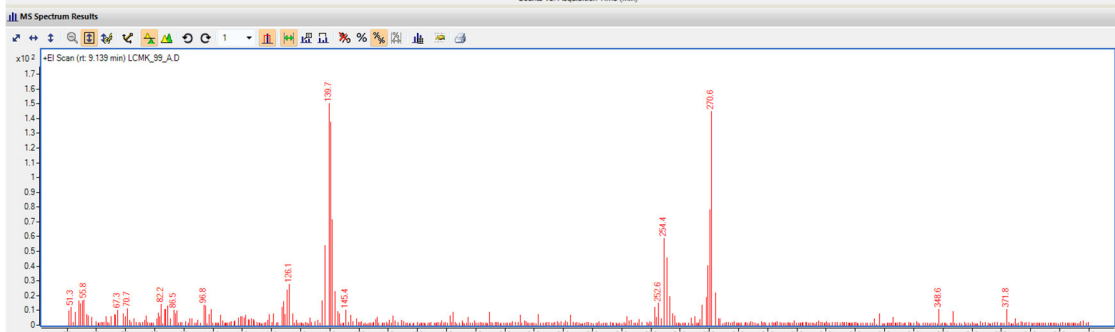
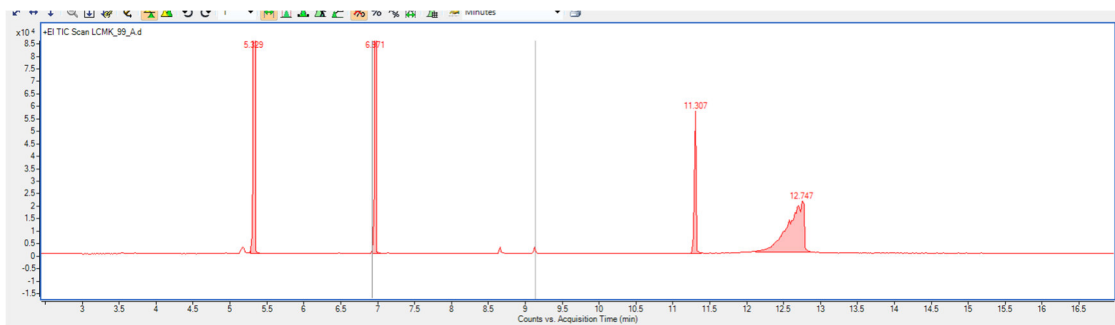
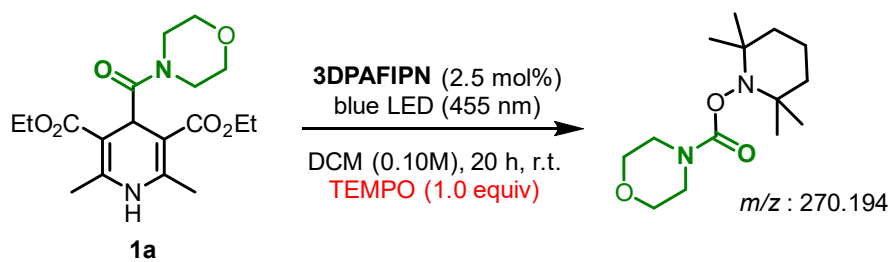
a)



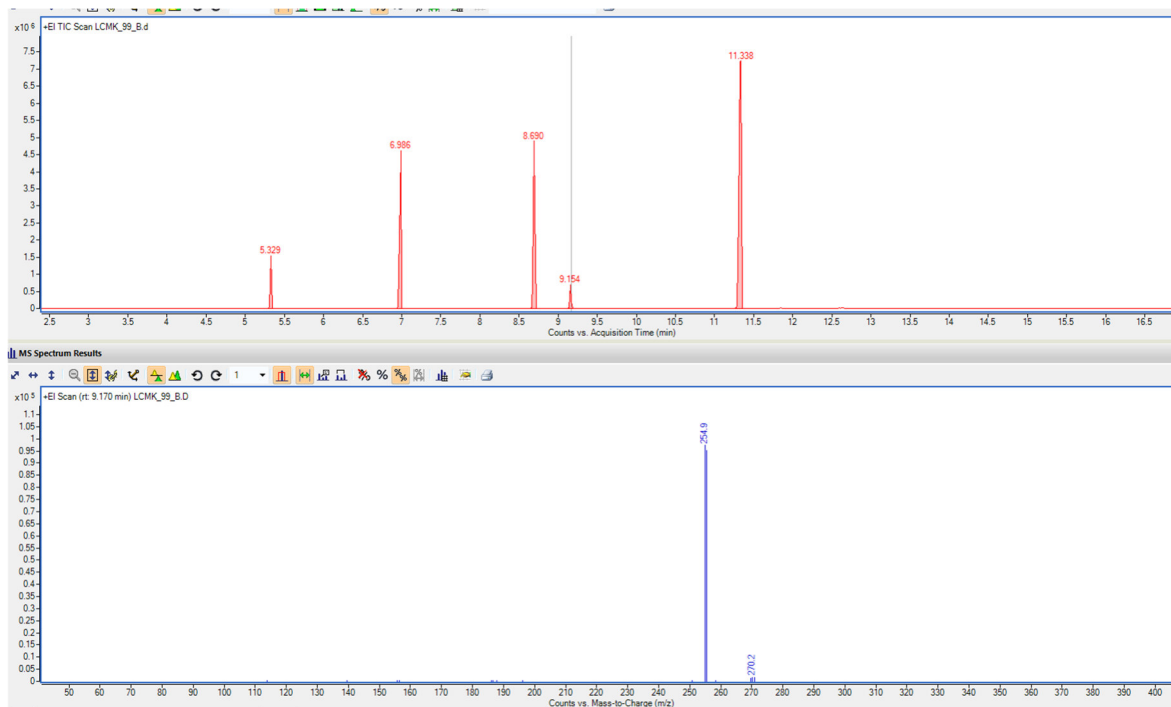
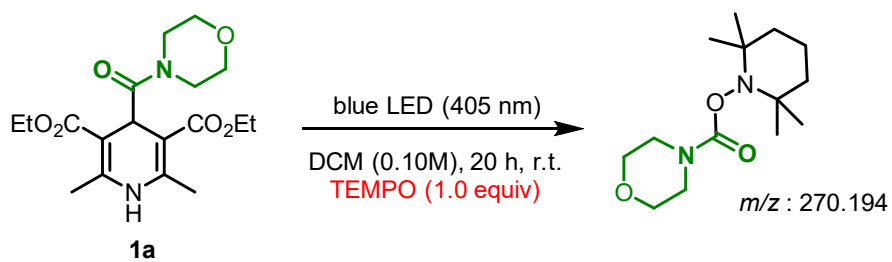
Following the general procedure E, a reaction of dihydropyridine **1a** and benzylidenemalononitrile **2a** on a 0.1 mmol scale in the presence of the radical trapping agent TEMPO (0.1 mmol, 1.0 equiv) was setup. The reaction mixture was sparged with nitrogen and irradiated for 16 h. ^1H NMR analysis, after the addition of 1,3,5-trimethoxybenzene as the external standard, showed no product formation. The presence of the carbamoyl-TEMPO adduct was confirmed by GC-MS analysis: peak at 9.1 min in the chromatogram. MS: m/z : 270.8, 254.8, 139.8, 125.3, 113.8, 97.5, 81.9, 69.7, 55.8, 50.7.



b)



c)



Fluorescence Quenching Experiments.

Fluorescence measurements were acquired at room temperature using an Agilent Technologies Cary Eclipse Fluorescence Spectrophotometer with excitation slits open at 5 nm and emission slit open at 5 nm. Emission quenching of the different samples were done using quartz cuvettes (Precision cell SUPRASIL, Art. No. 117100F-10-40, Hellma Analytics) with argon-purged solvent (DMSO or CH₃CN). All the prepared solutions were degassed for 8 minutes and successively added to the cuvette using 1 mL gas tight syringe through a rubber septum fitted with an argon balloon. The balloon remained inserted in between quencher additions to prevent oxygen from entering the cuvette.

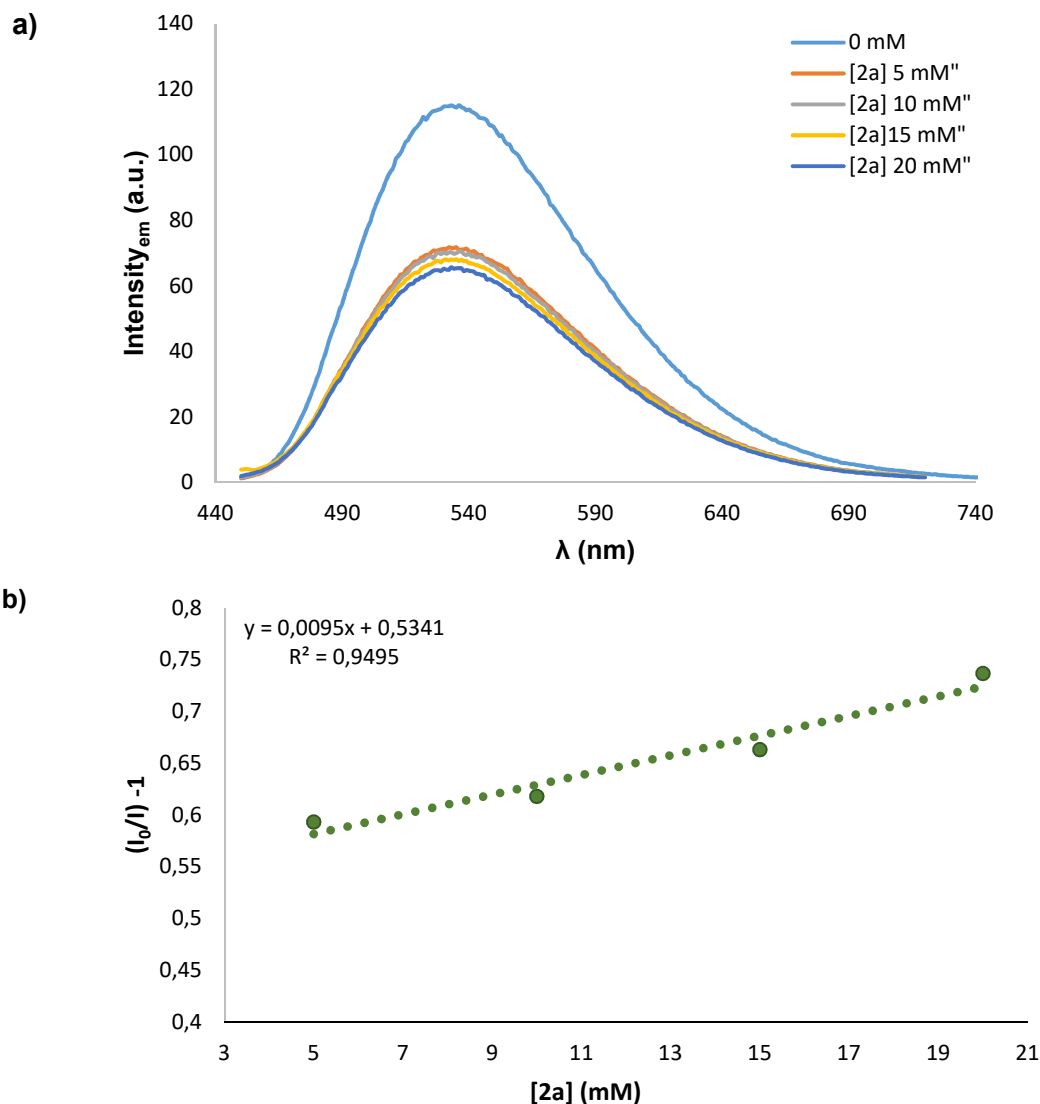


Figure 8. a) Emission of a 3DPAFIPN solution (top blue line, DMSO, 0.09 mM) recorded in presence of increasing amounts of benzylidenemalononitrile **2a** as quencher with a $\lambda_{ex} = 380$ nm. Fluorescence intensity was integrated from 450 nm to 700 nm b) Stern-Volmer plot analysis derived from the data extracted from Figure 8a. The K_q was determined from Stern-Volmer equation [$K_{sv} = K_q \tau$] using a lifetime of $\tau = 4.2$ ns for 3DPAFIPN¹⁸. The resulting K_q for benzylidenemalononitrile **2a** was of $2.26 \cdot 10^9$ L mol⁻¹ s⁻¹.

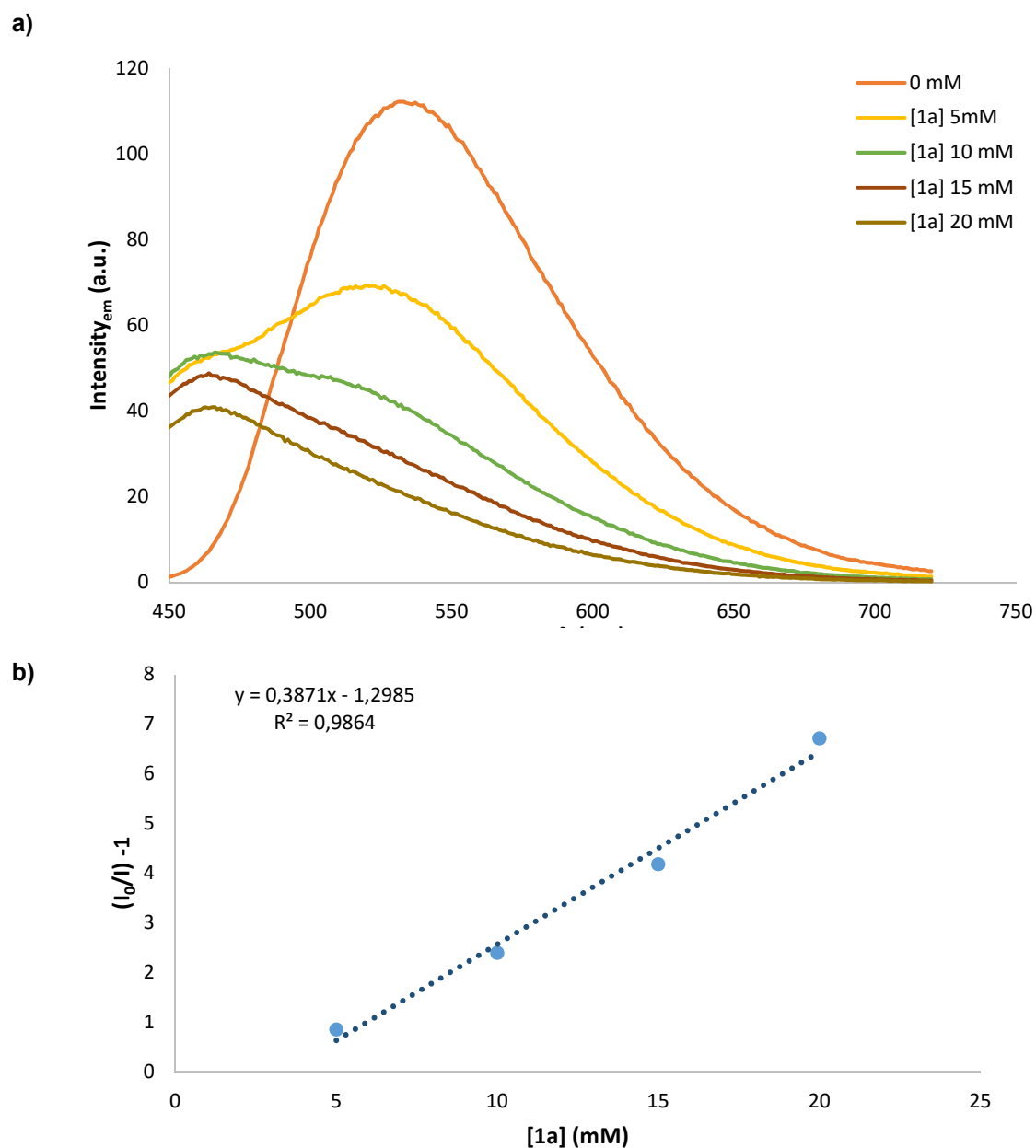
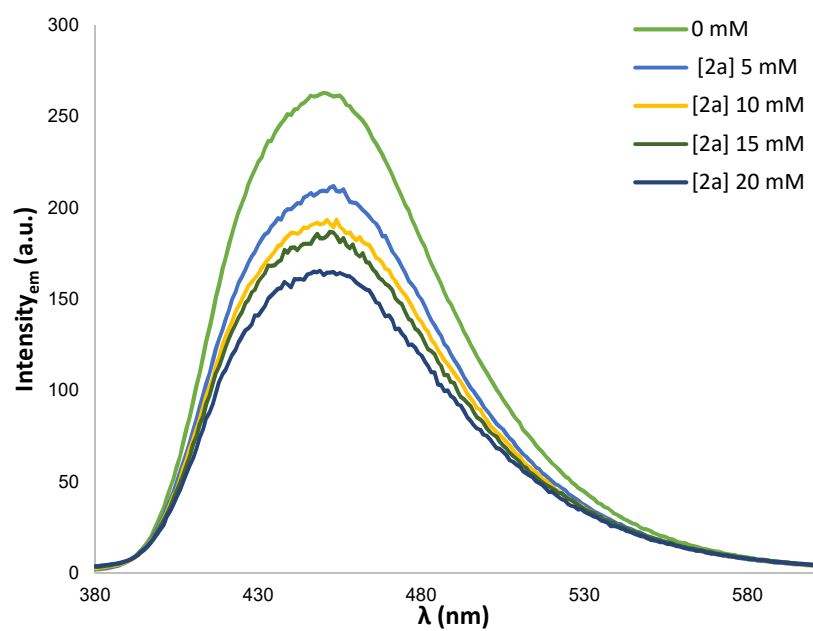


Figure 9. a) Emission of a 3DPAFIPN solution (top orange line, DMSO, 0.09 mM) recorded in presence of increasing amounts of dihydropyridine **1a** as quencher with a $\lambda_{\text{ex}} = 410$ nm. Fluorescence intensity was integrated from 550 nm to 720 nm due to the overlapping with the emission of dihydropyridine **1a**. b) Stern-Volmer plot analysis derived from the data extracted from Figure 9a. The K_q was determined from Stern-Volmer equation and using a lifetime of $\tau = 4.2$ ns for 3DPAFIPN¹⁸. The resulting K_q for dihydropyridine **1a** was of $9.22 \cdot 10^{10} \text{ L mol}^{-1} \text{ s}^{-1}$.

a)



b)

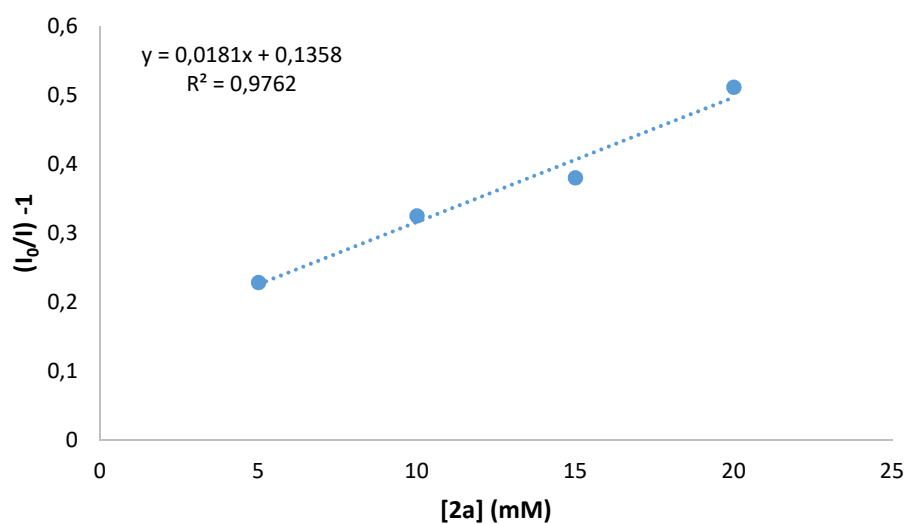


Figure 10. a) Emission of a dihydropyridine **1a** solution (top green line, CH_3CN , 0.15 mM) recorded in presence of increasing amounts of benzylidenemalononitrile **2a** as quencher with a $\lambda_{\text{ex}} = 365$ nm. Fluorescence intensity was integrated from 380 nm to 600 nm. b) Stern-Volmer plot analysis derived from the data extracted from Figure 10a.

UV-Vis Experiments

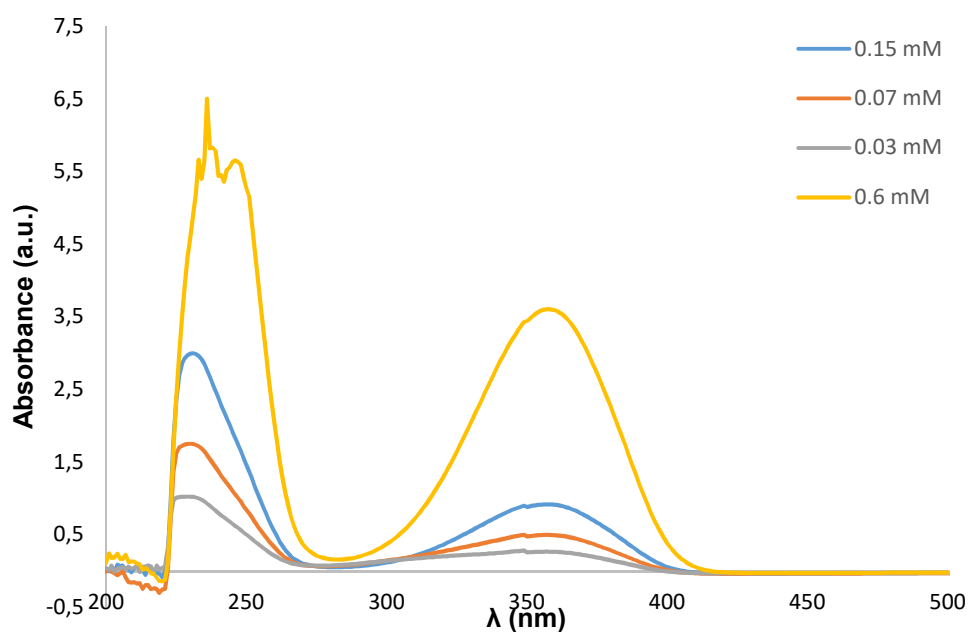


Figure 11. Absorption spectra of **1a** at different concentrations in CH₃CN.

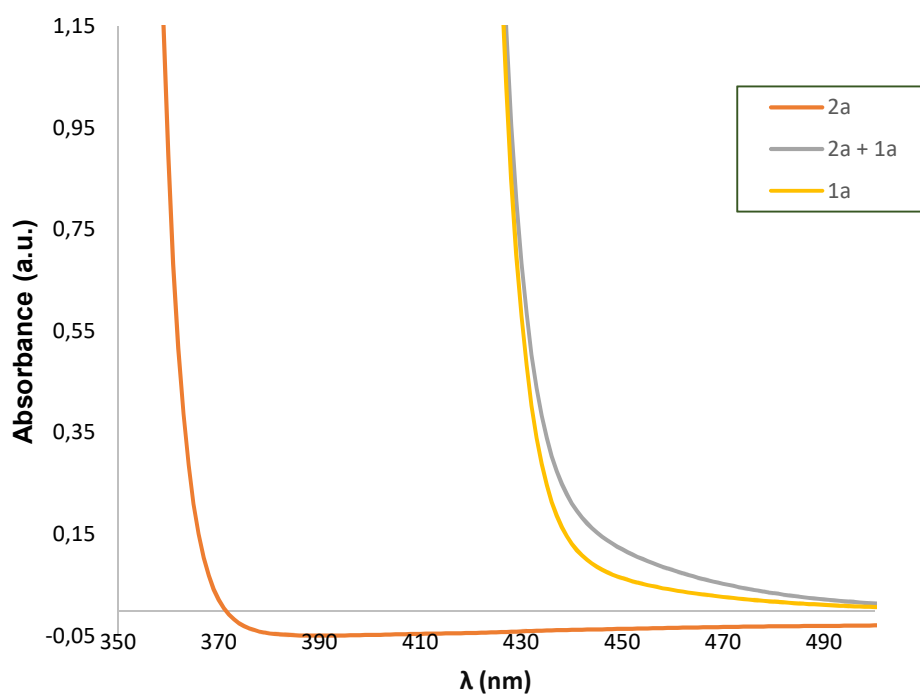
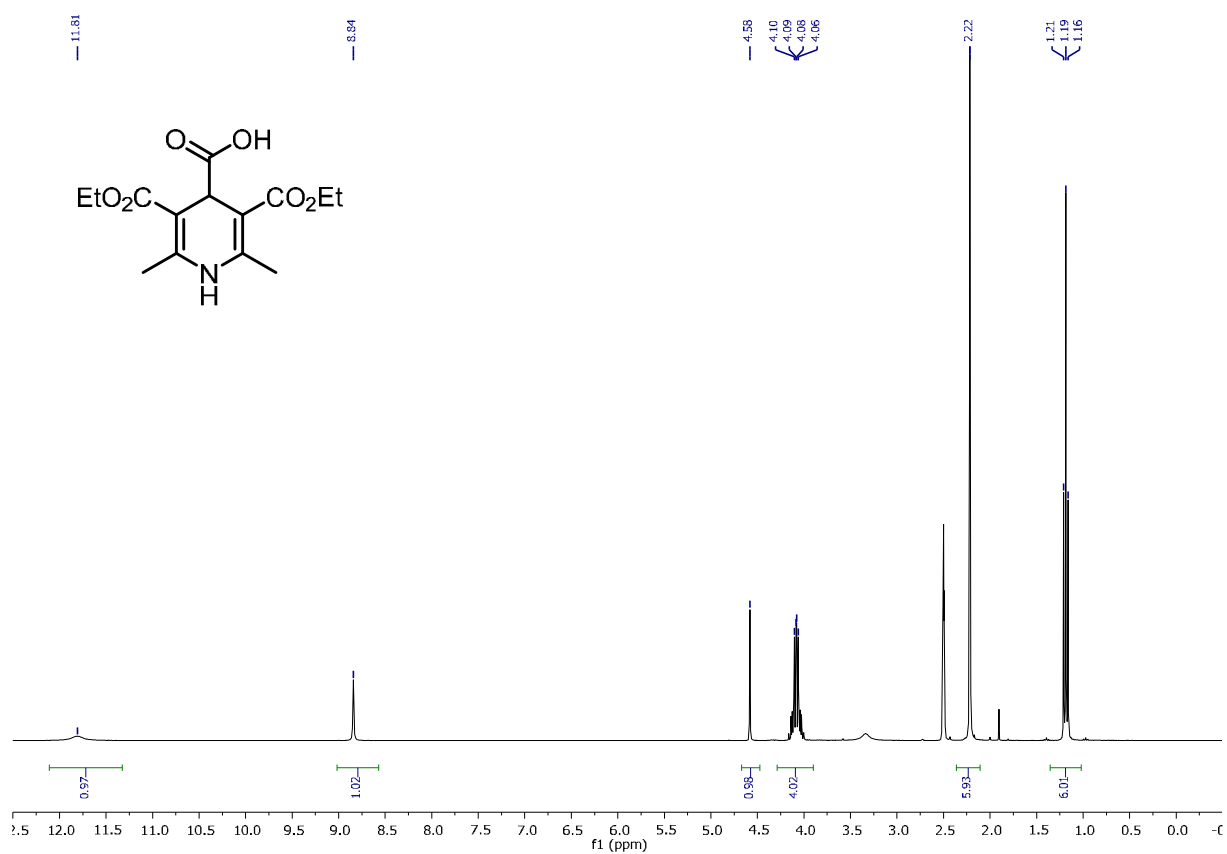
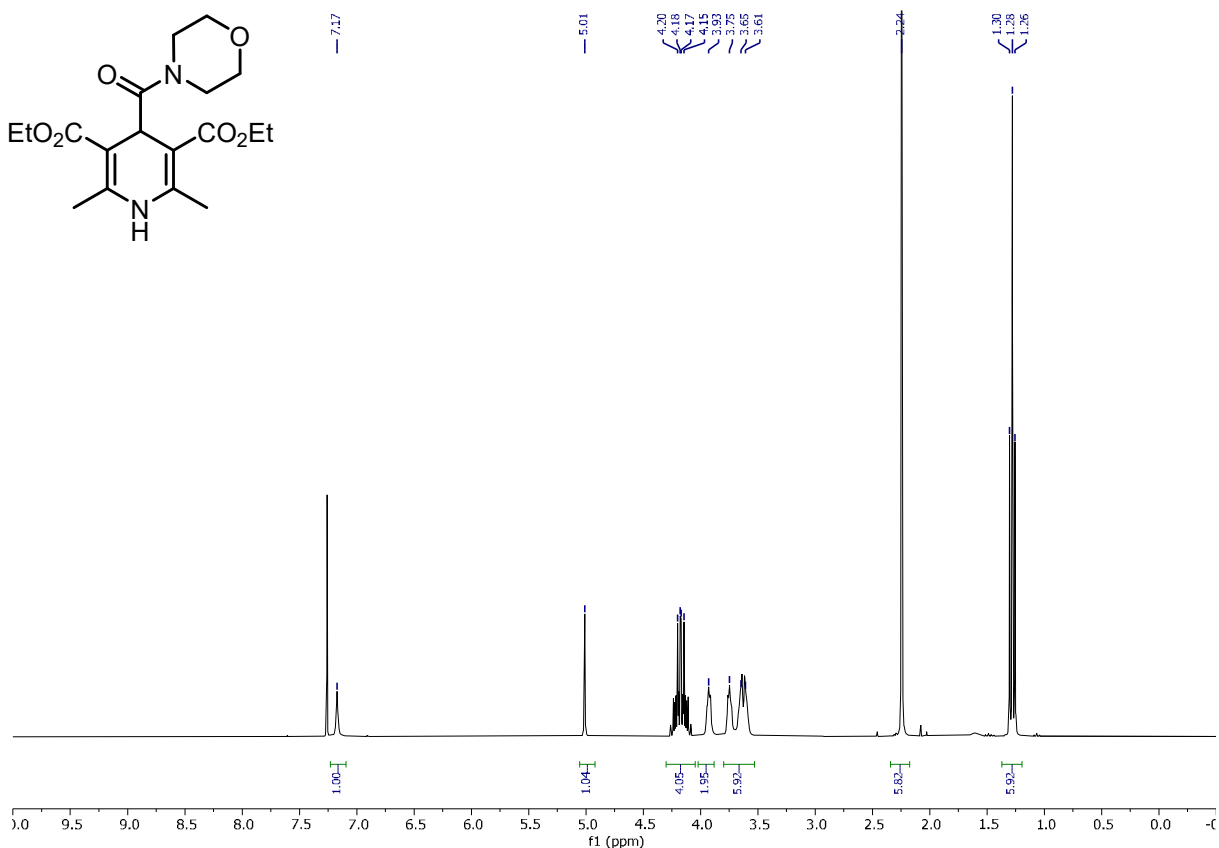


Figure 12. UV-Vis spectra of benzylidenemalononitrile **2a** (orange line, 0.050 M in DCM), dihydropyridine **1a** (yellow line, 0.050 M in DCM), and an equimolar mixture of **2a** and **1a** (grey line, 0.050 M in DCM).

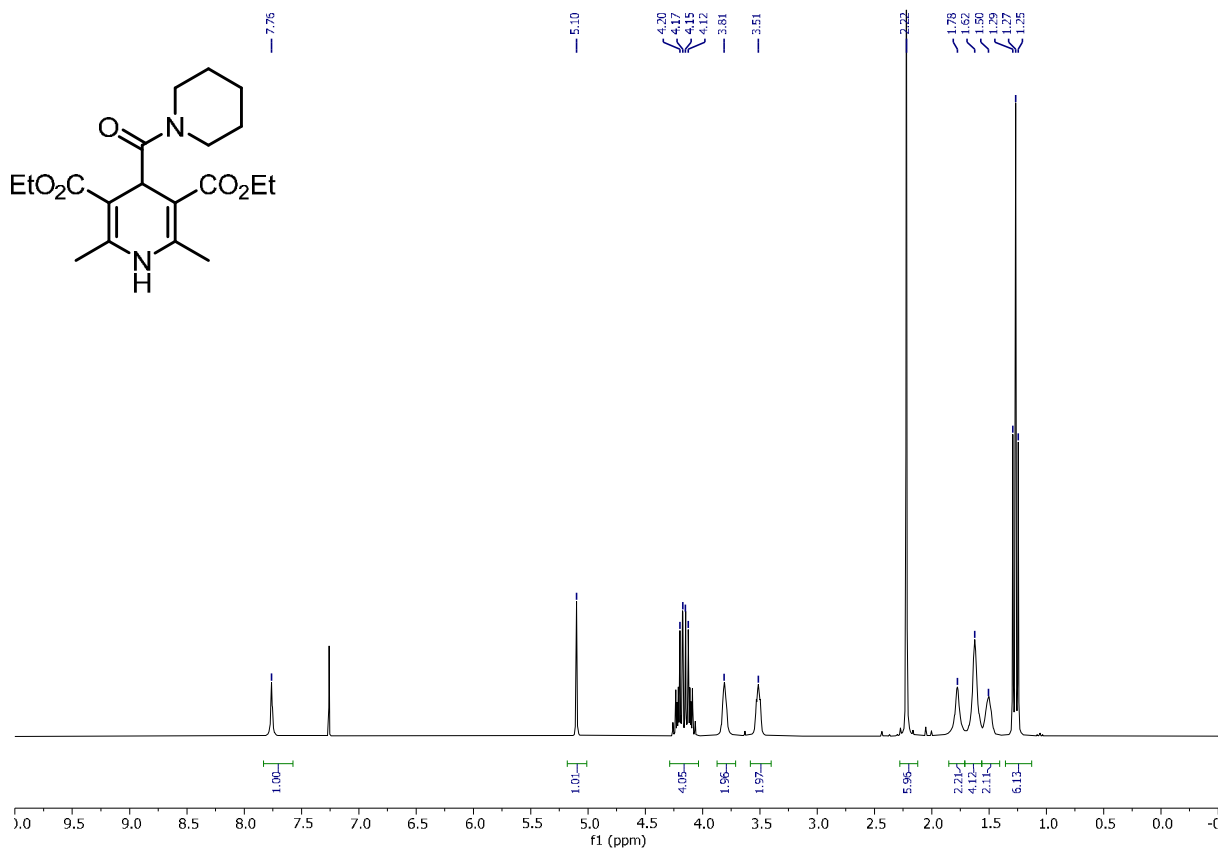
4.4.5 NMR of compounds



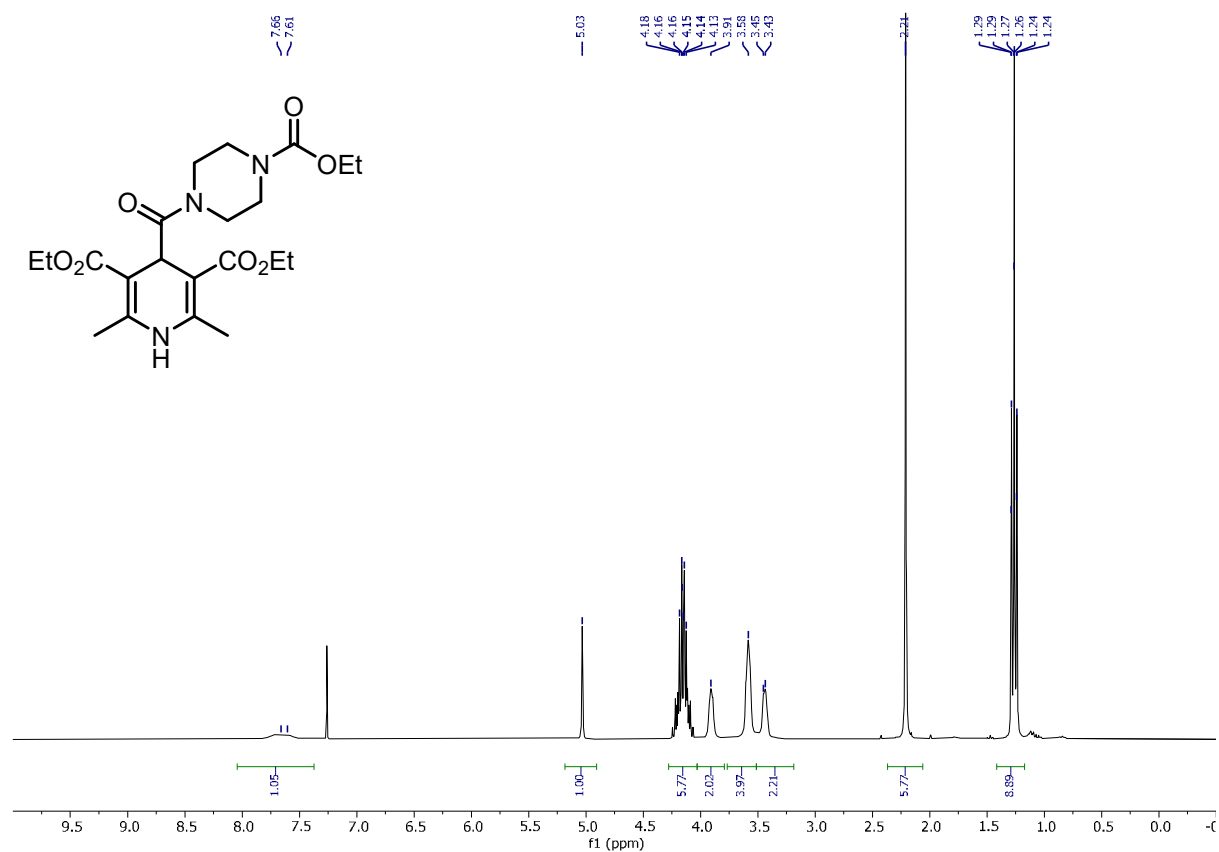
¹H NMR of 3,5-bis(ethoxycarbonyl)-2,6-dimethyl-1,4-dihydropyridine-4-carboxylic acid (SI-II)



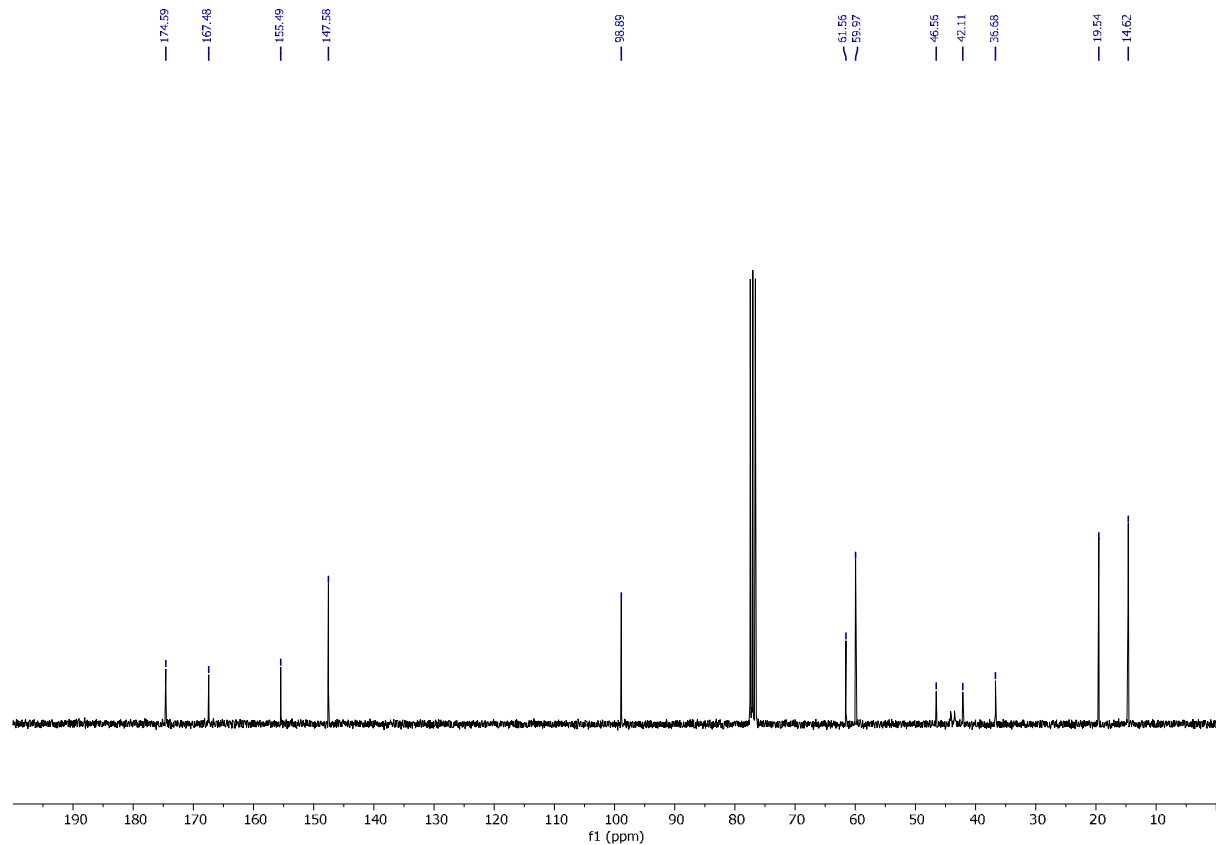
¹H NMR of diethyl 2,6-dimethyl-4-(morpholine-4-carbonyl)-1,4-dihydropyridine-3,5-dicarboxylate (1a)



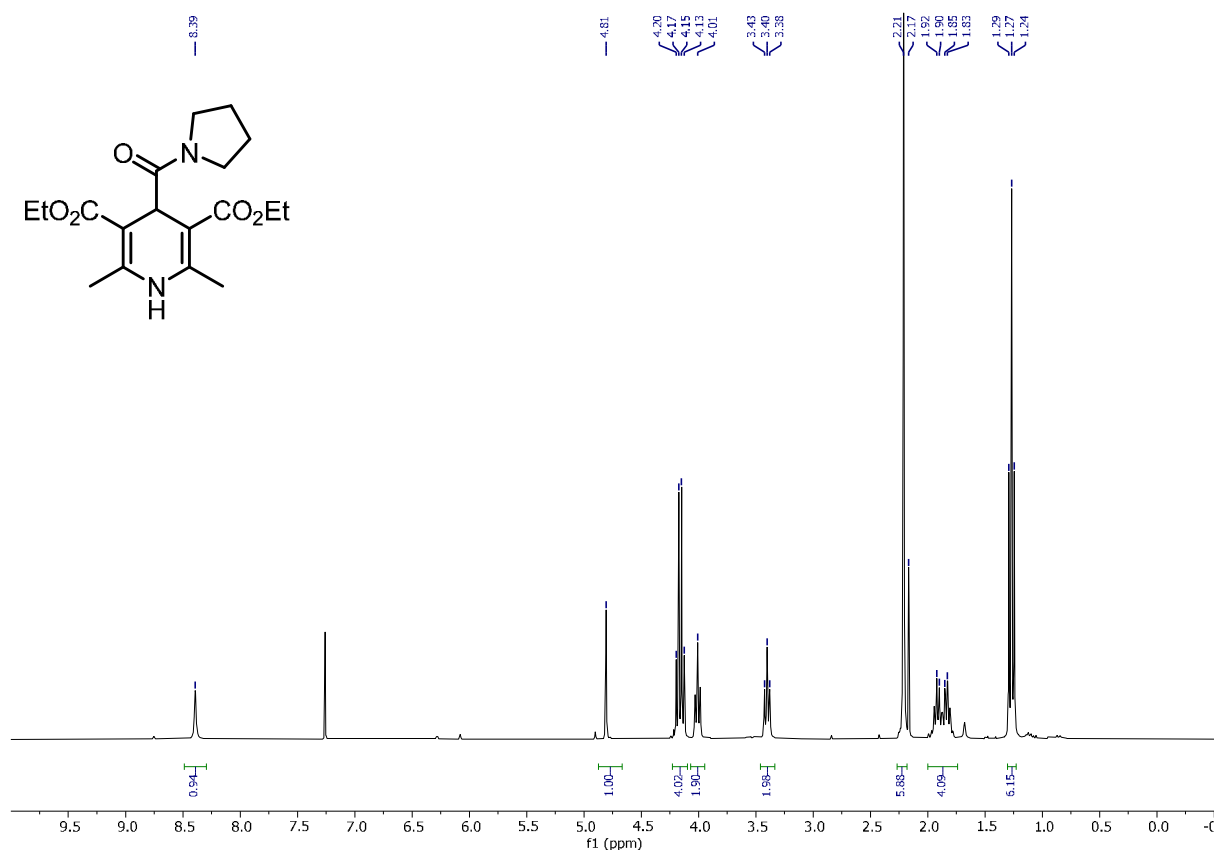
¹H NMR of diethyl 2,6-dimethyl-4-(piperidine-1-carbonyl)-1,4-dihydropyridine-3,5-dicarboxylate (**1b**)



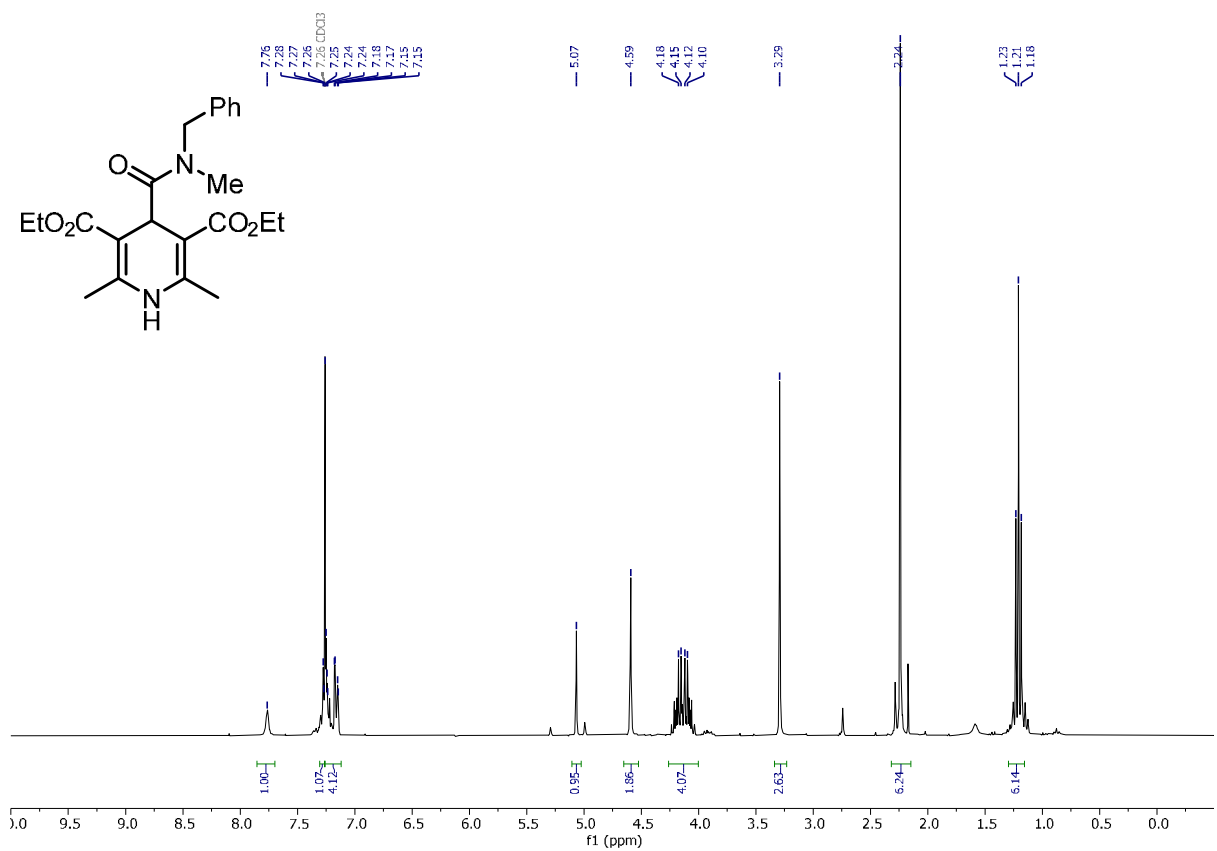
¹H NMR of diethyl 4-(4-(ethoxycarbonyl)piperazine-1-carbonyl)-2,6-dimethyl-1,4-dihydropyridine-3,5-dicarboxylate (**1c**)



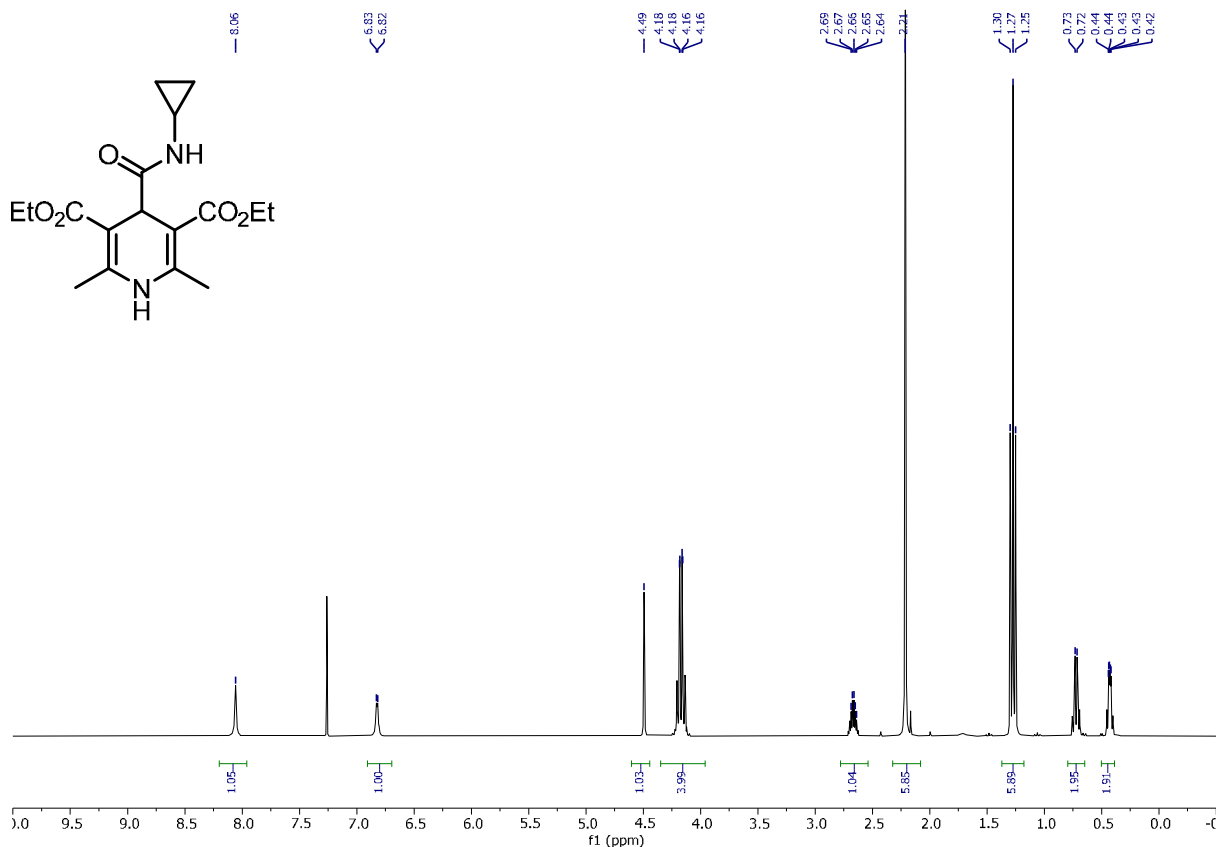
¹³C NMR of diethyl 4-(4-(ethoxycarbonyl)piperazine-1-carbonyl)-2,6-dimethyl-1,4-dihydropyridine-3,5-dicarboxylate (**1c**)



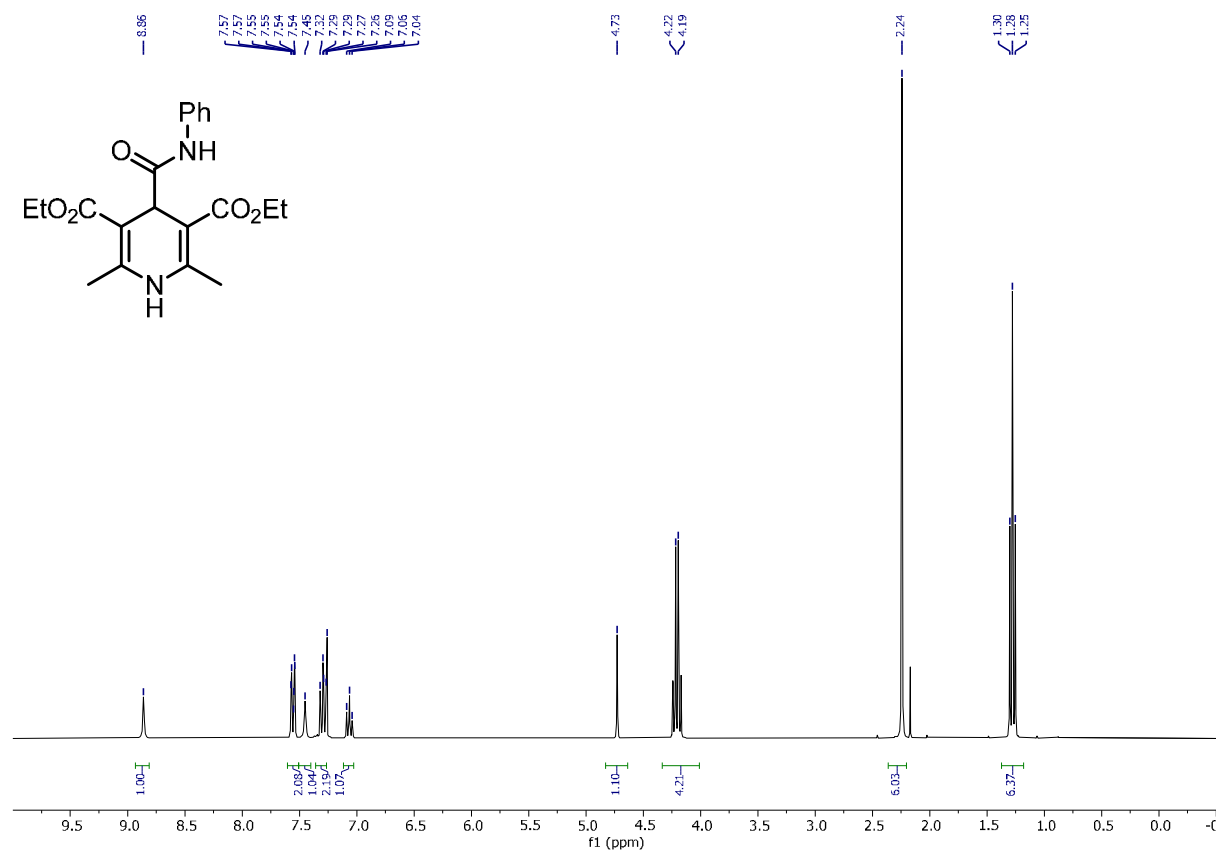
¹H NMR of diethyl 2,6-dimethyl-4-(pyrrolidine-1-carbonyl)-1,4-dihydropyridine-3,5-dicarboxylate (1d)



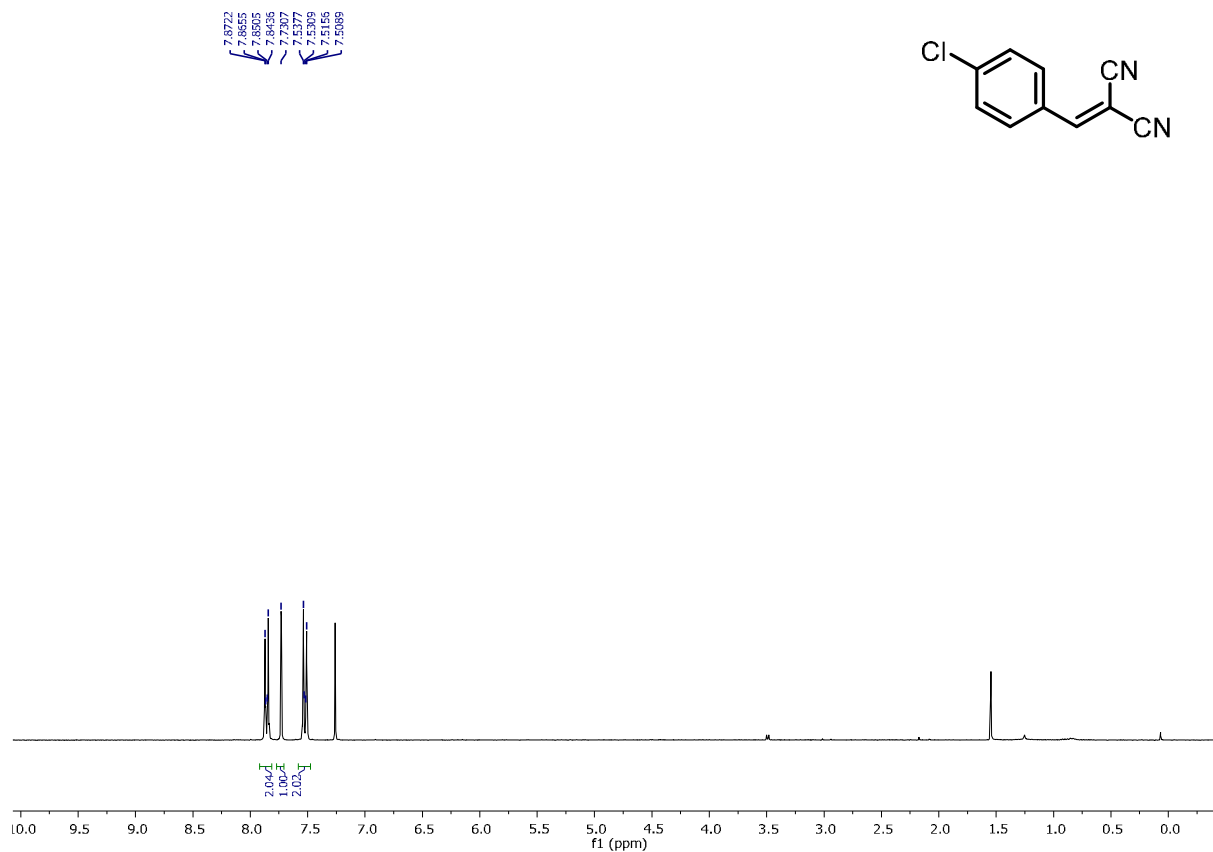
¹H NMR of diethyl 4-(benzyl(methyl)carbamoyl)-2,6-dimethyl-1,4-dihydropyridine-3,5-dicarboxylate (1e)



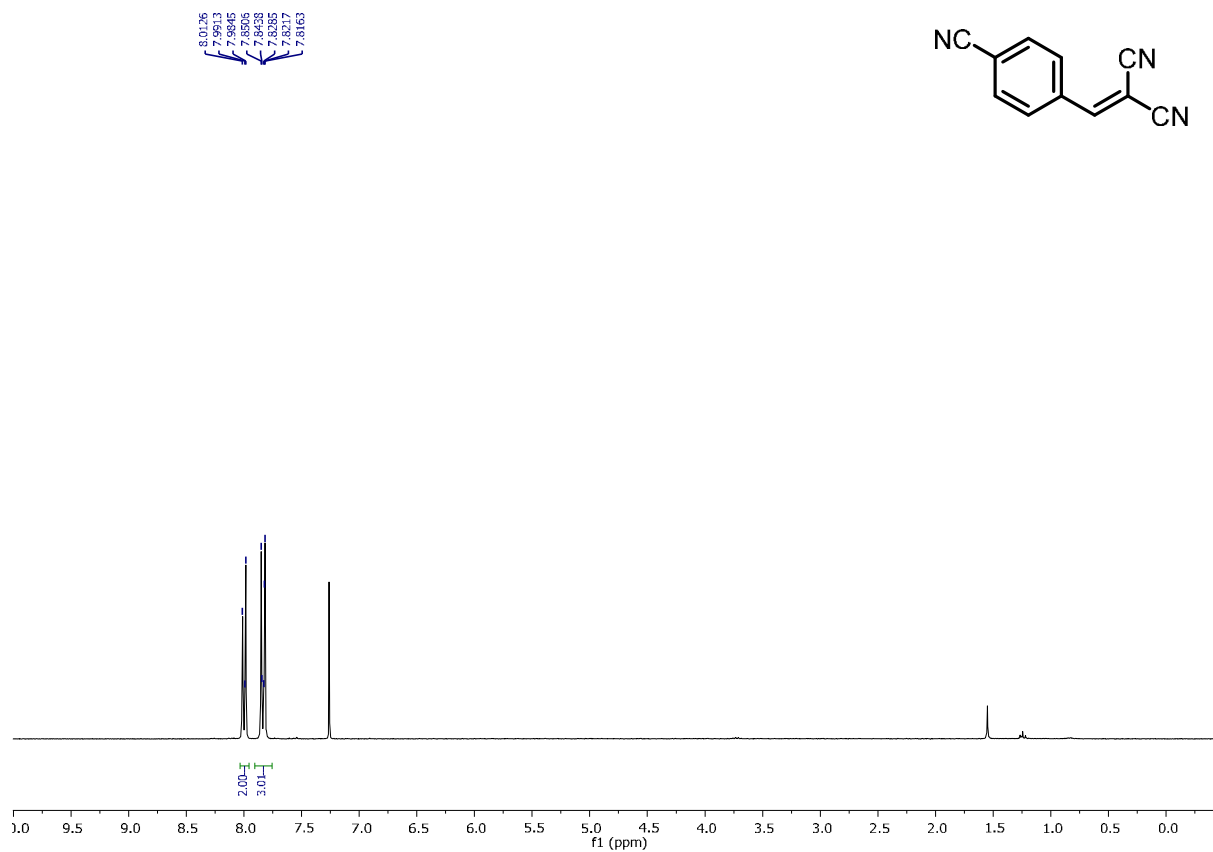
¹H NMR of diethyl 4-(cyclopropylcarbamoyl)-2,6-dimethyl-1,4-dihydropyridine-3,5-dicarboxylate (1f)



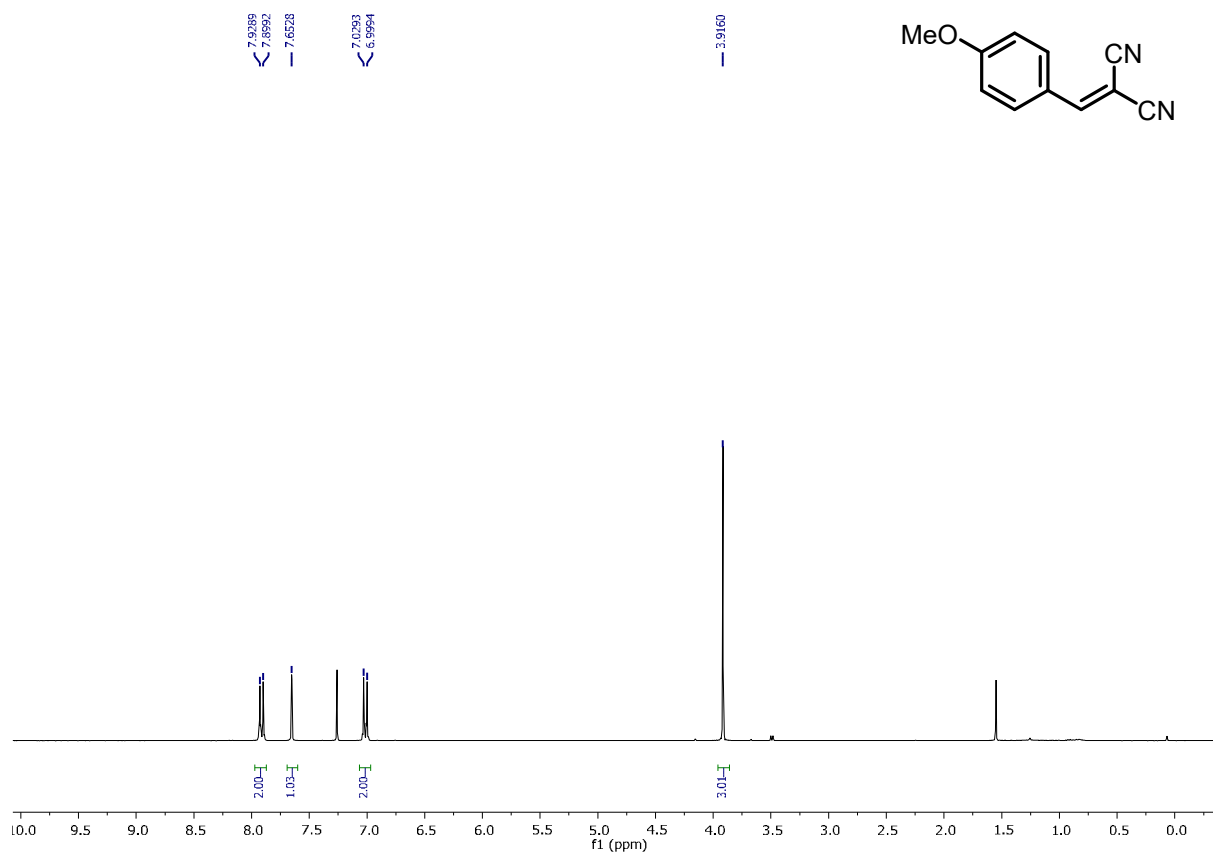
¹H NMR of diethyl 2,6-dimethyl-4-(phenylcarbamoyl)-1,4-dihydropyridine-3,5-dicarboxylate (1g)



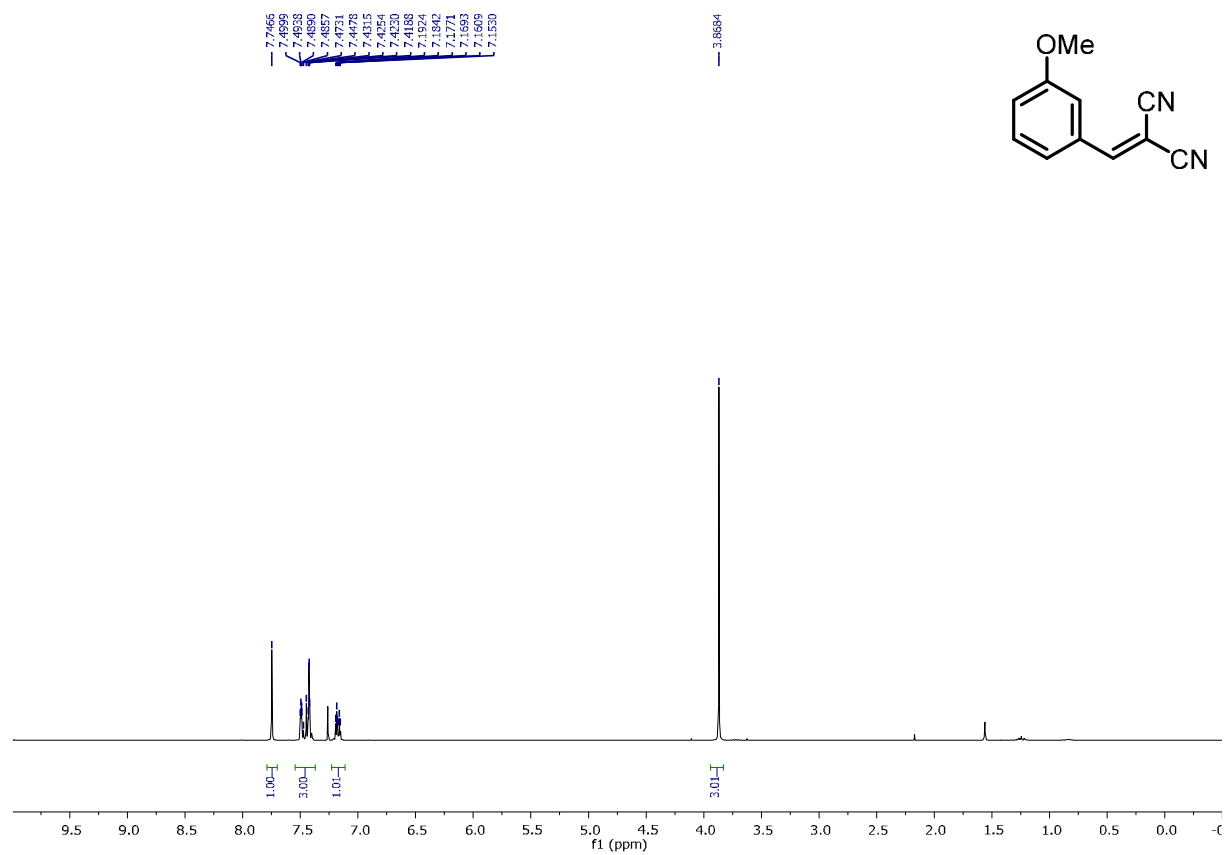
¹H NMR of 2-(4-chlorobenzylidene)malononitrile (2b)



¹H NMR of 2-(4-cyanobenzylidene)malononitrile (2c)

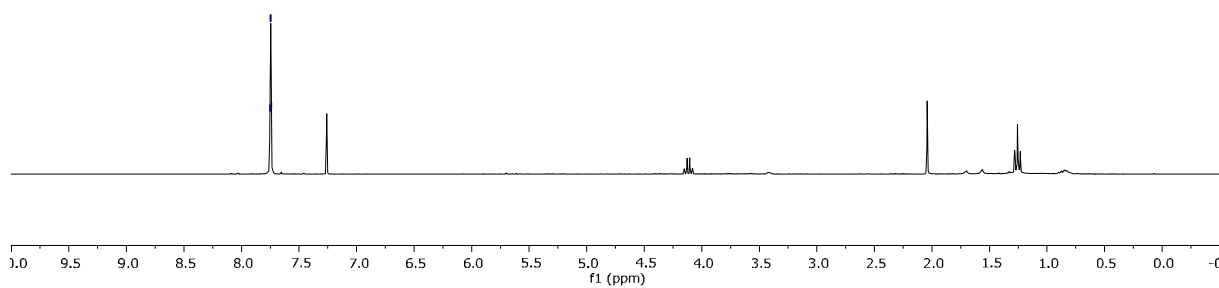
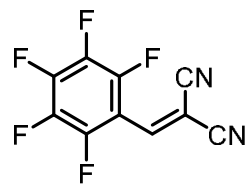


¹H NMR of 2-(4-methoxybenzylidene)malononitrile (2d)



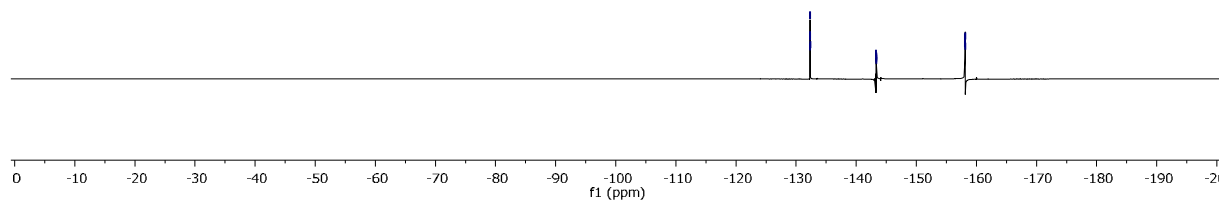
¹H NMR of 2-(3-methoxybenzylidene)malononitrile (2e)

7.7527
7.7487
7.7447
7.7409

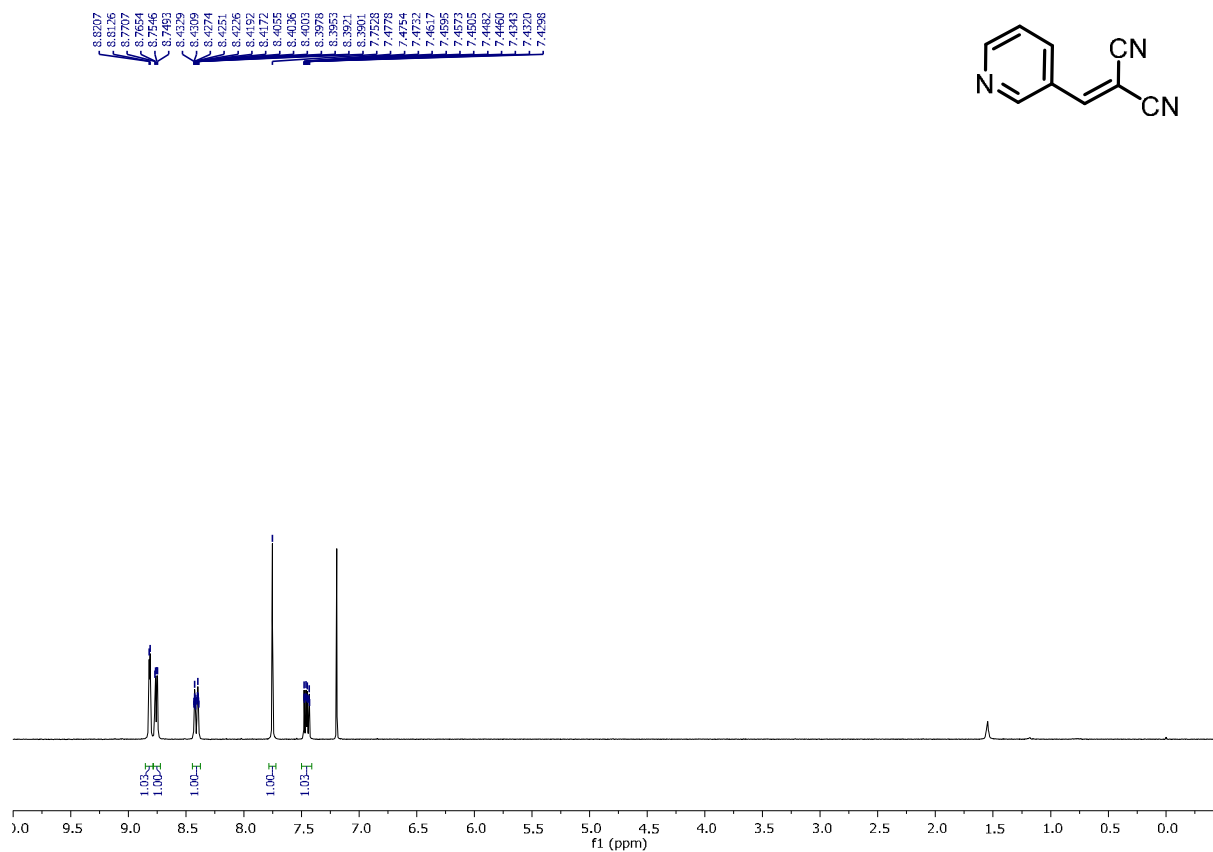


¹H NMR of 2-(pentafluorobenzylidene)malononitrile (2f)

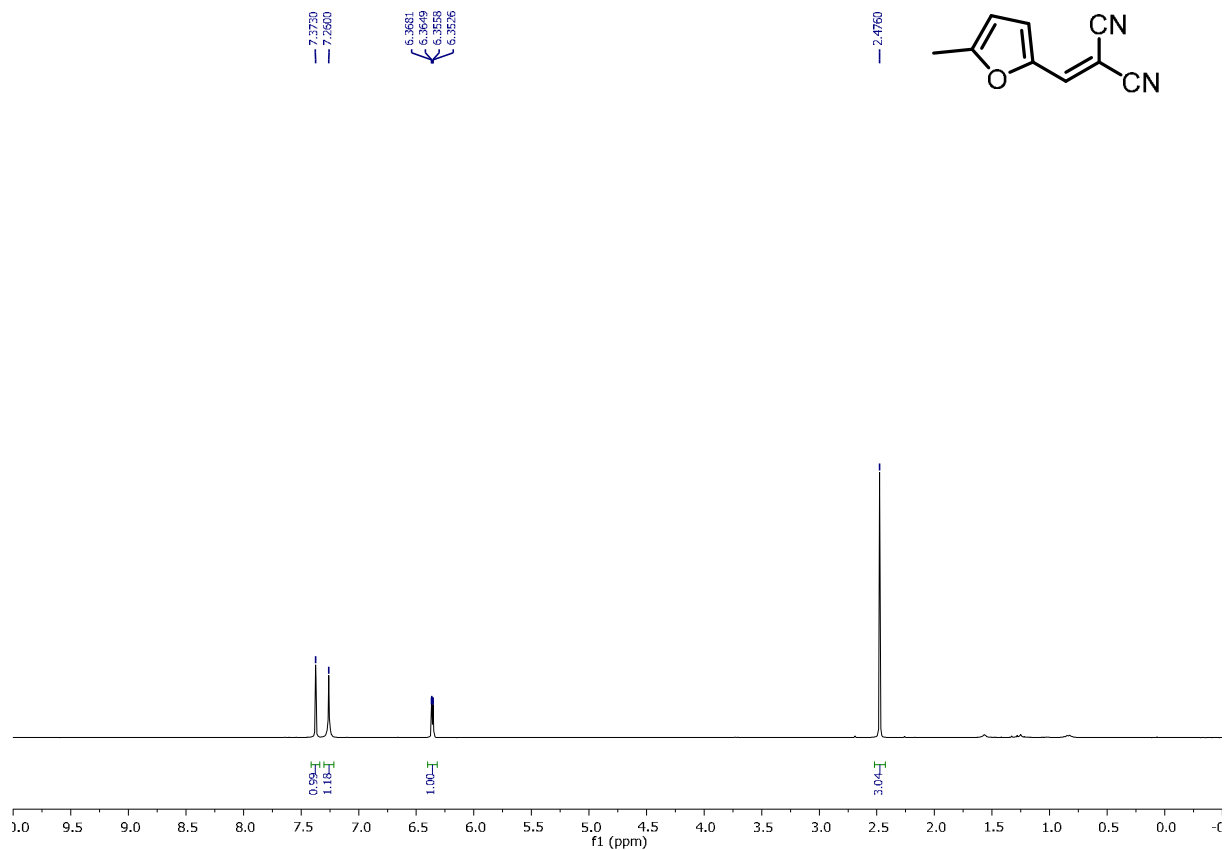
132.2995
132.3101
132.3196
132.3238
132.3494
132.3577
143.3232
143.3230
143.3602
143.3600
156.1001
156.1093
156.1327
156.1705



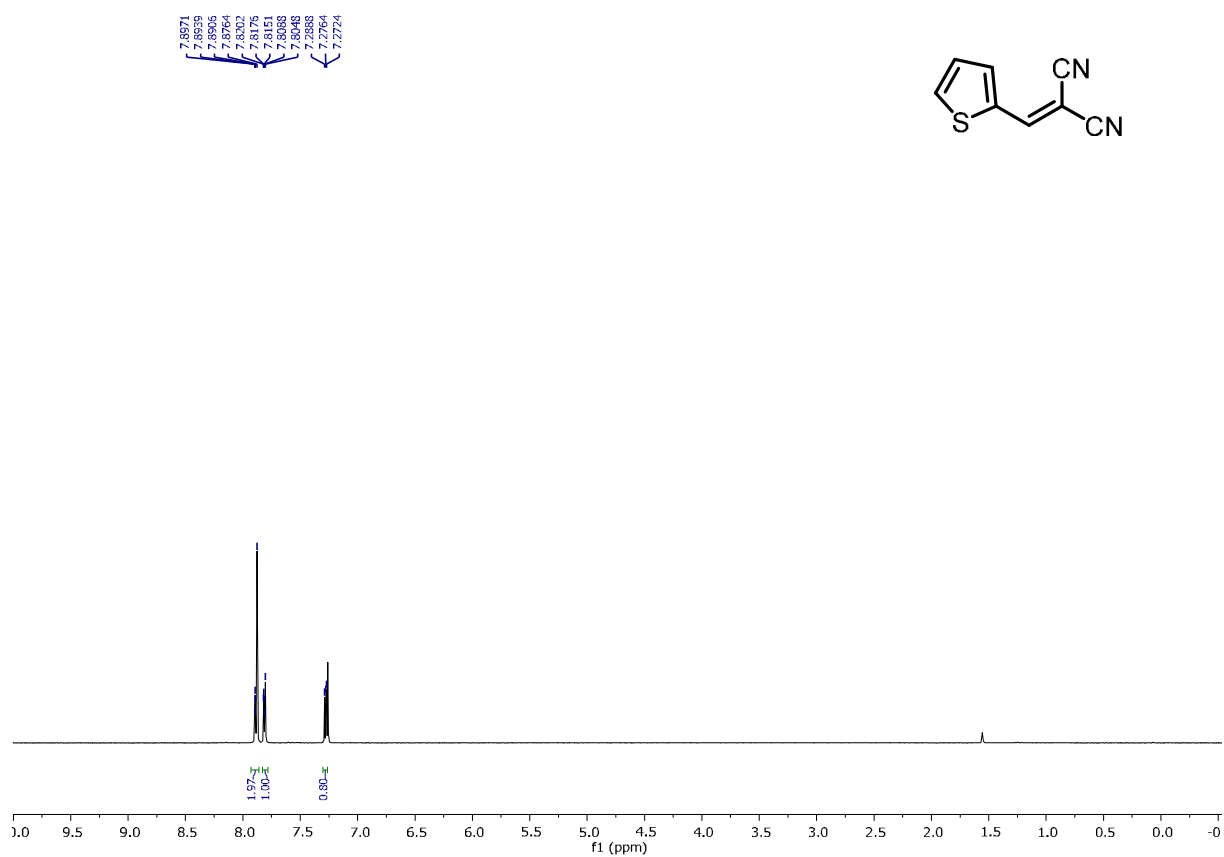
¹⁹F NMR of 2-(pentafluorobenzylidene)malononitrile (2f)



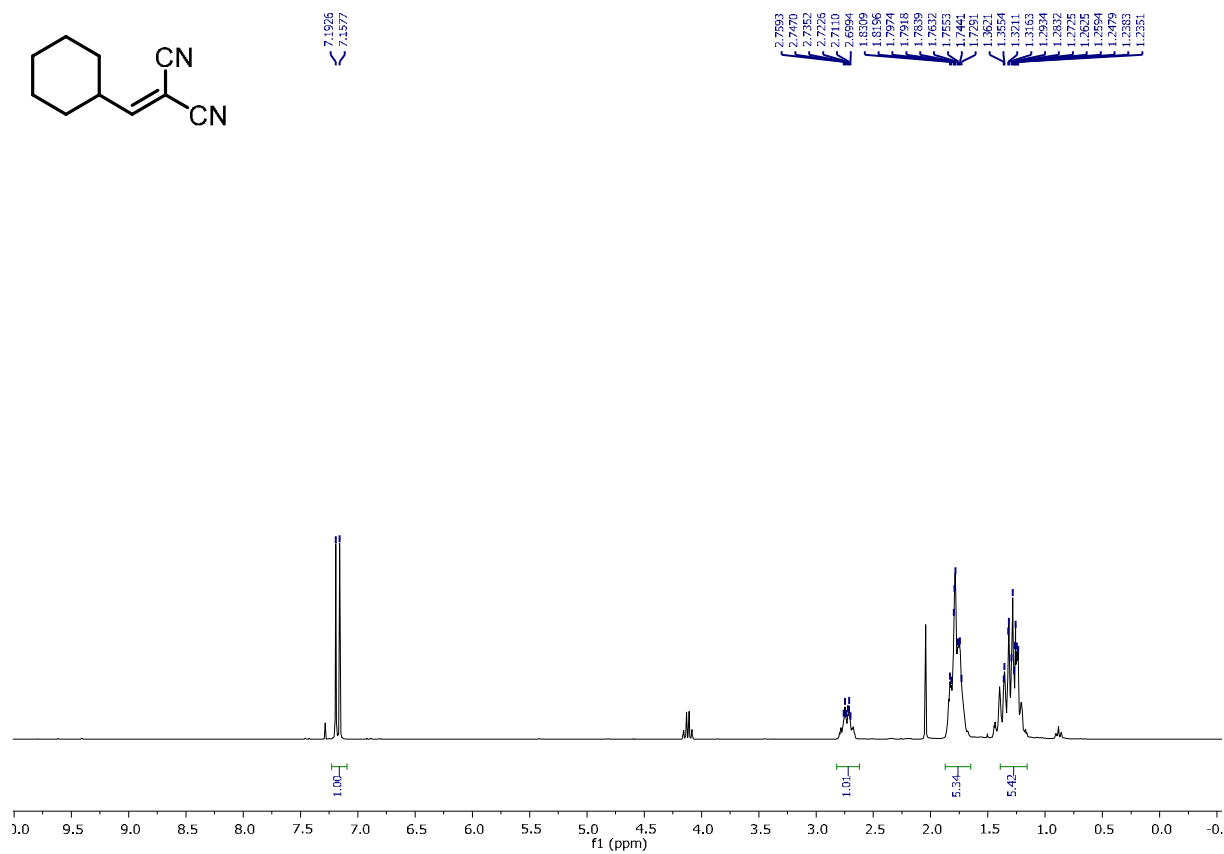
¹H NMR of 2-(pyridin-3-ylmethylene)malononitrile (2g)



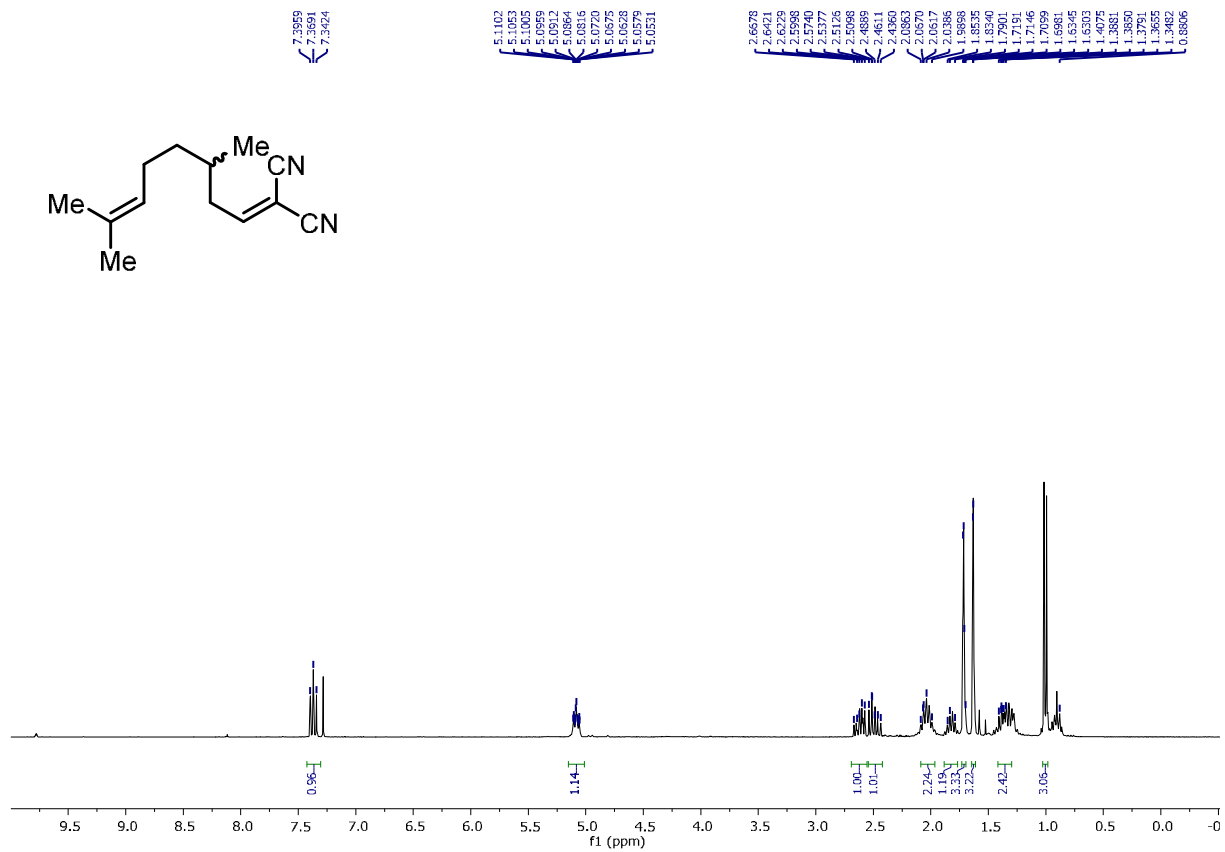
¹H NMR of 2-[(5-methylfuran-2-yl)methylene]malononitrile (2h)



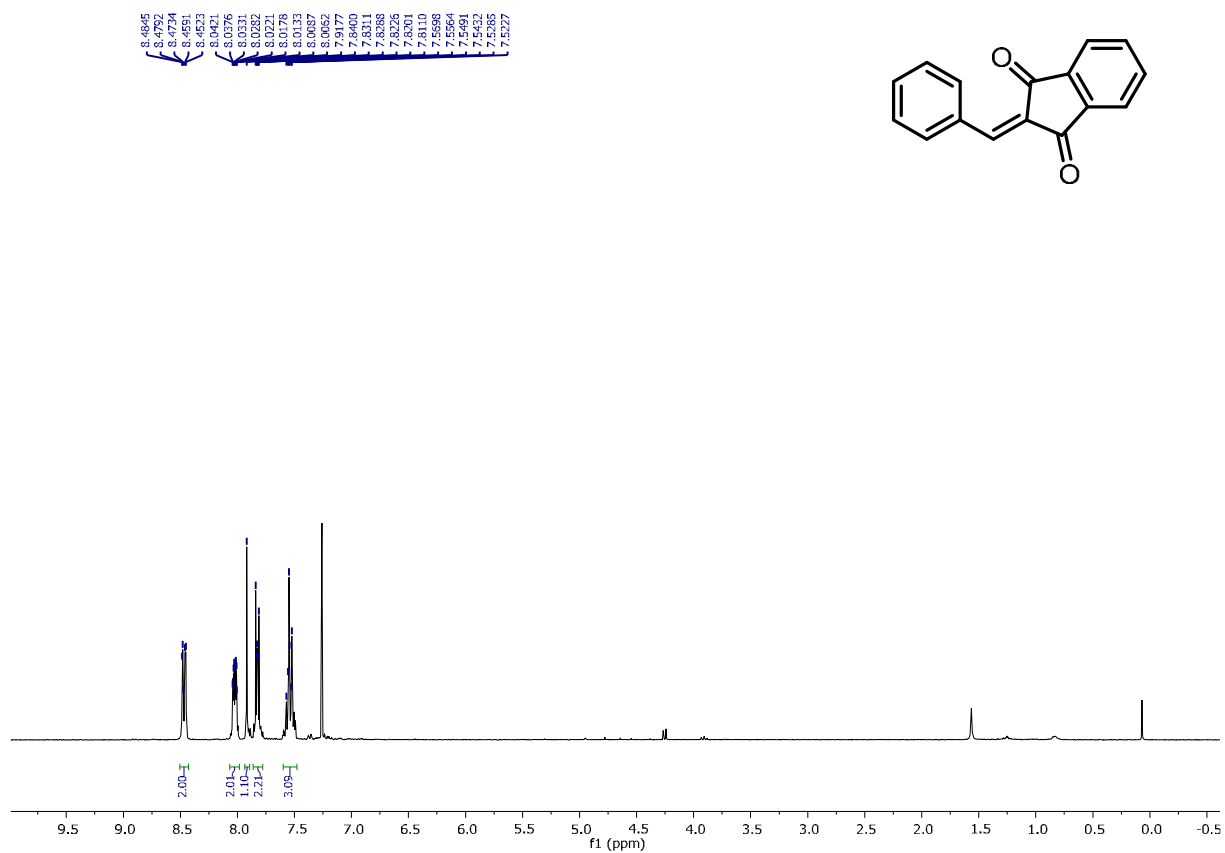
¹H NMR of 2-(thiophen-2-ylmethylene)malononitrile (2i)



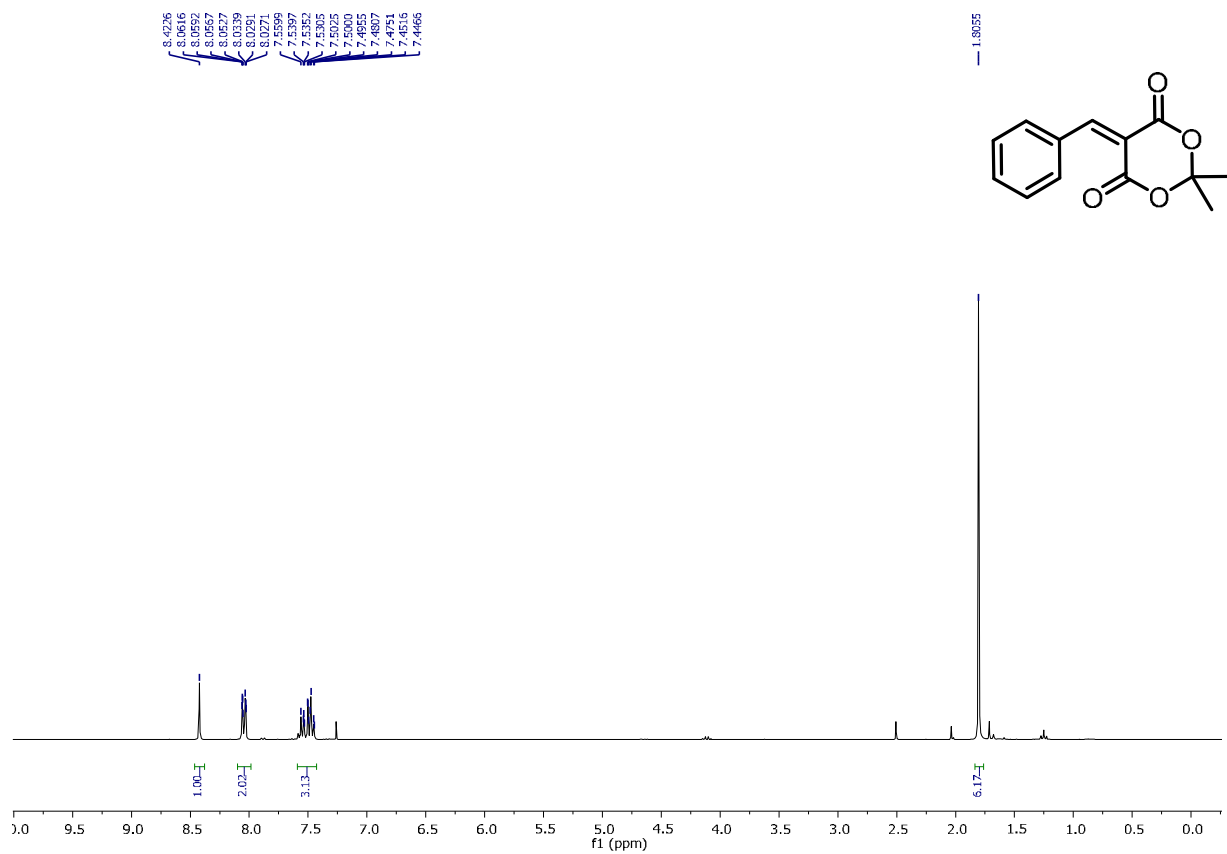
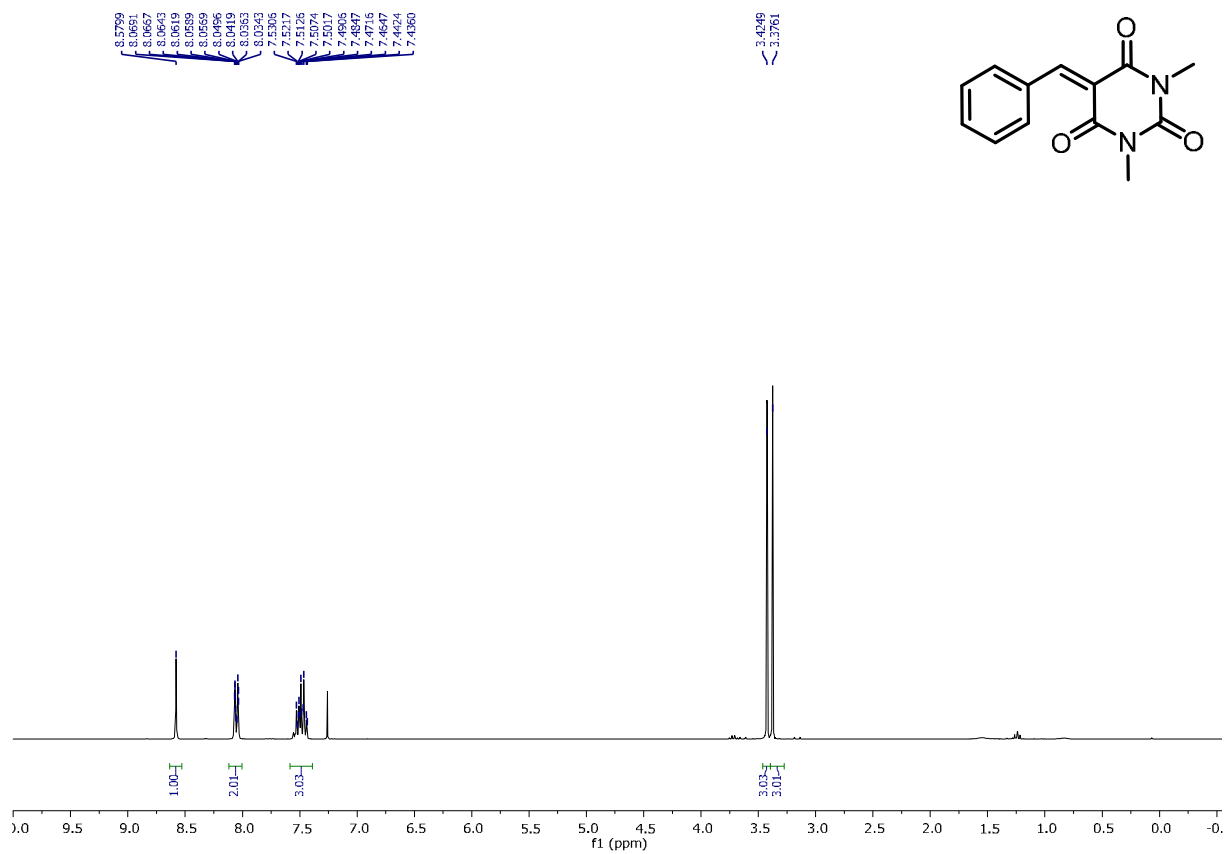
¹H NMR of 2-(cyclohexylmethylene)malononitrile (2j)

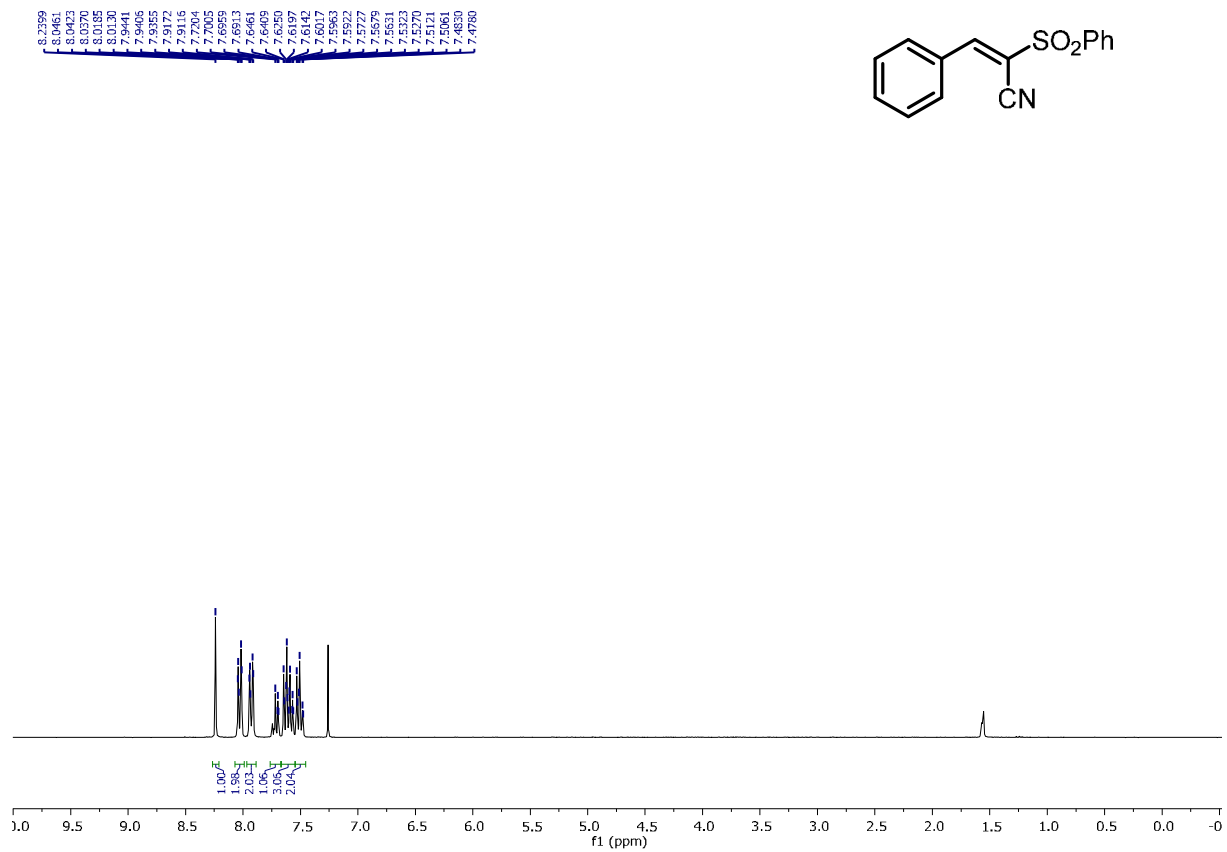


¹HNM of 2-(3,7-dimethyloct-6-en-1-ylidene)malononitrile (2k)

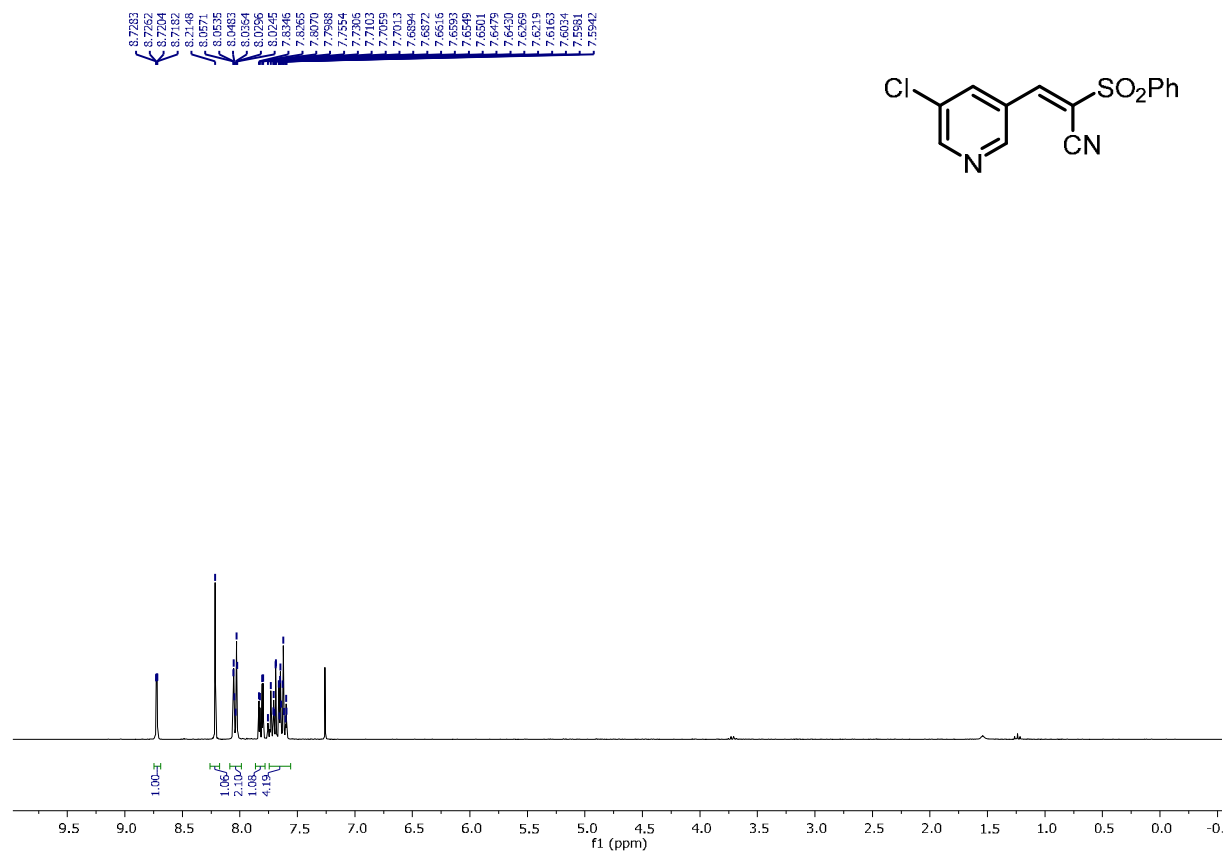


¹HNM of 2-benzylidene-1H-indene-1,3(2H)-dione (2l)

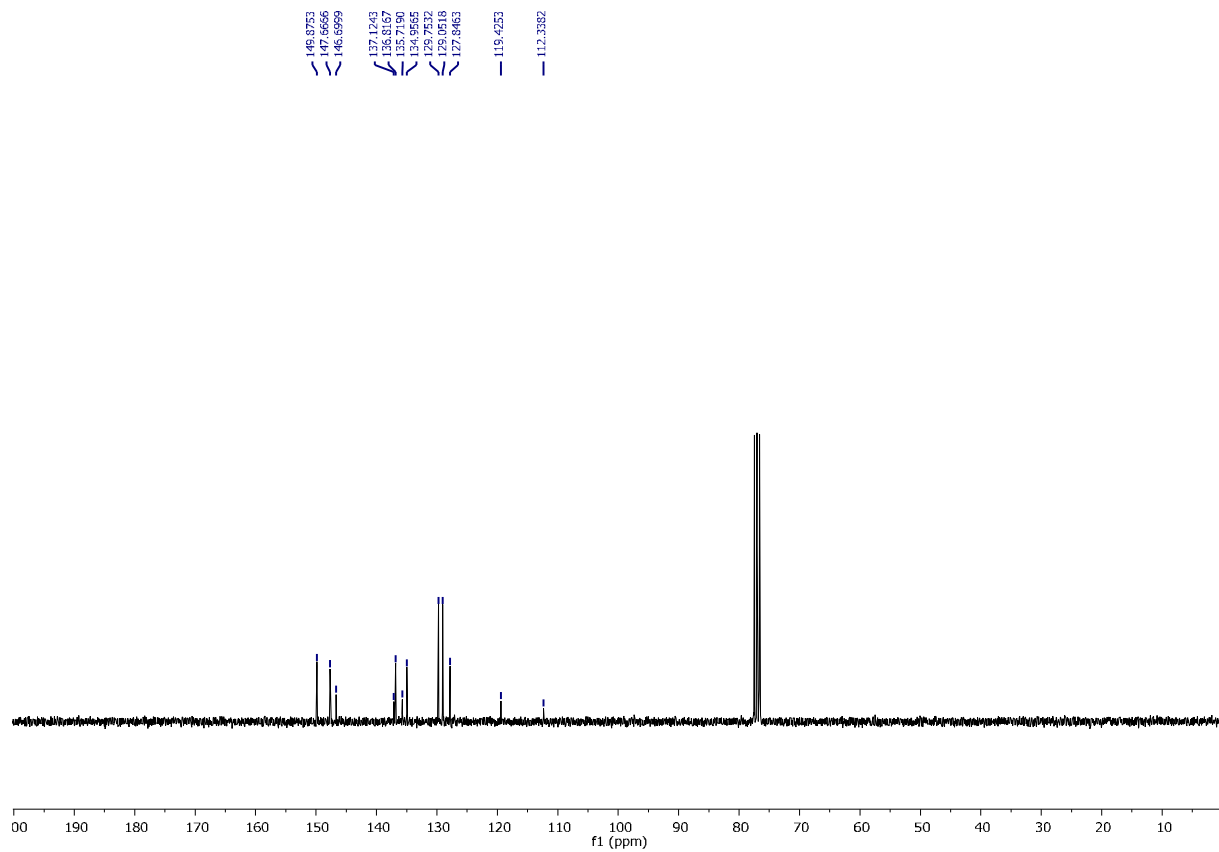




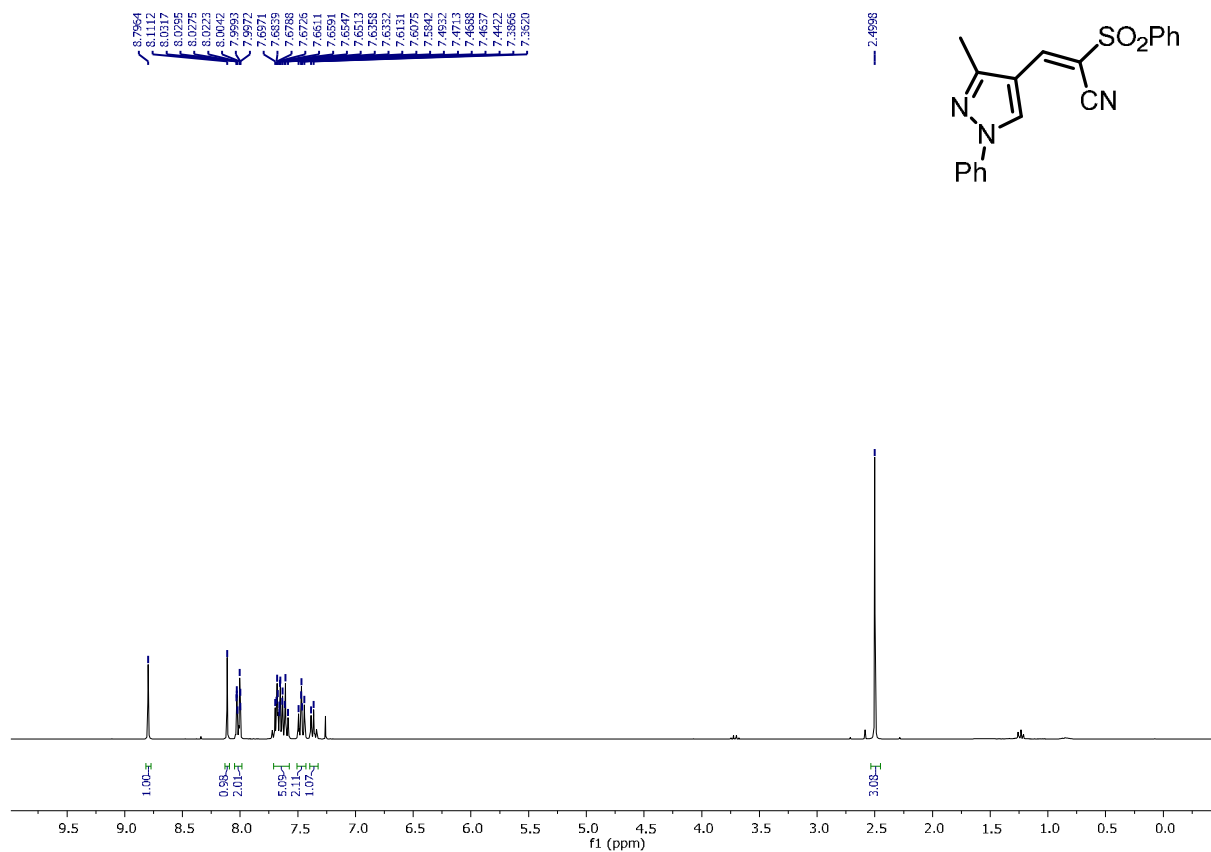
¹H NMR of (E)-3-(5-chloropyridin-3-yl)-2-(phenylsulphonyl)acrylonitrile (2p)



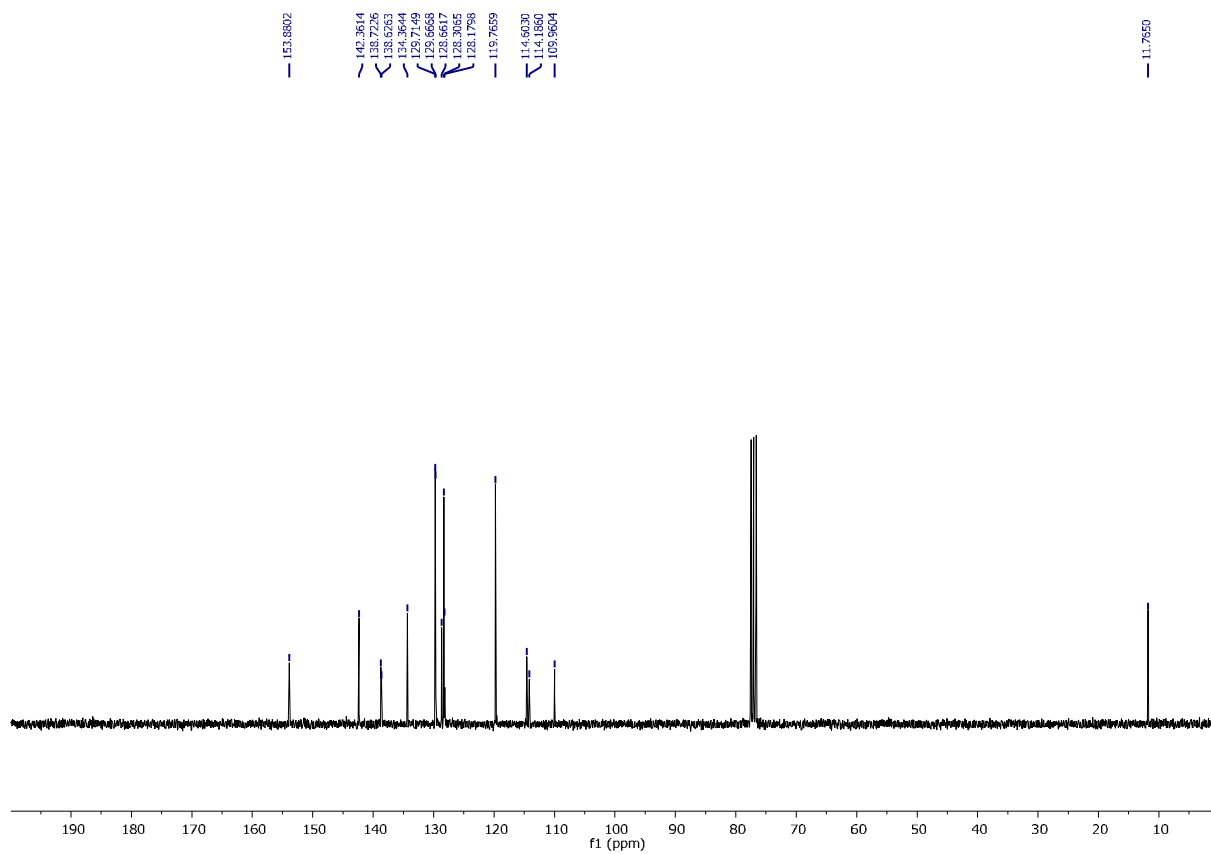
¹H NMR of (E)-3-(5-chloropyridin-3-yl)-2-(phenylsulphonyl)acrylonitrile (2q)



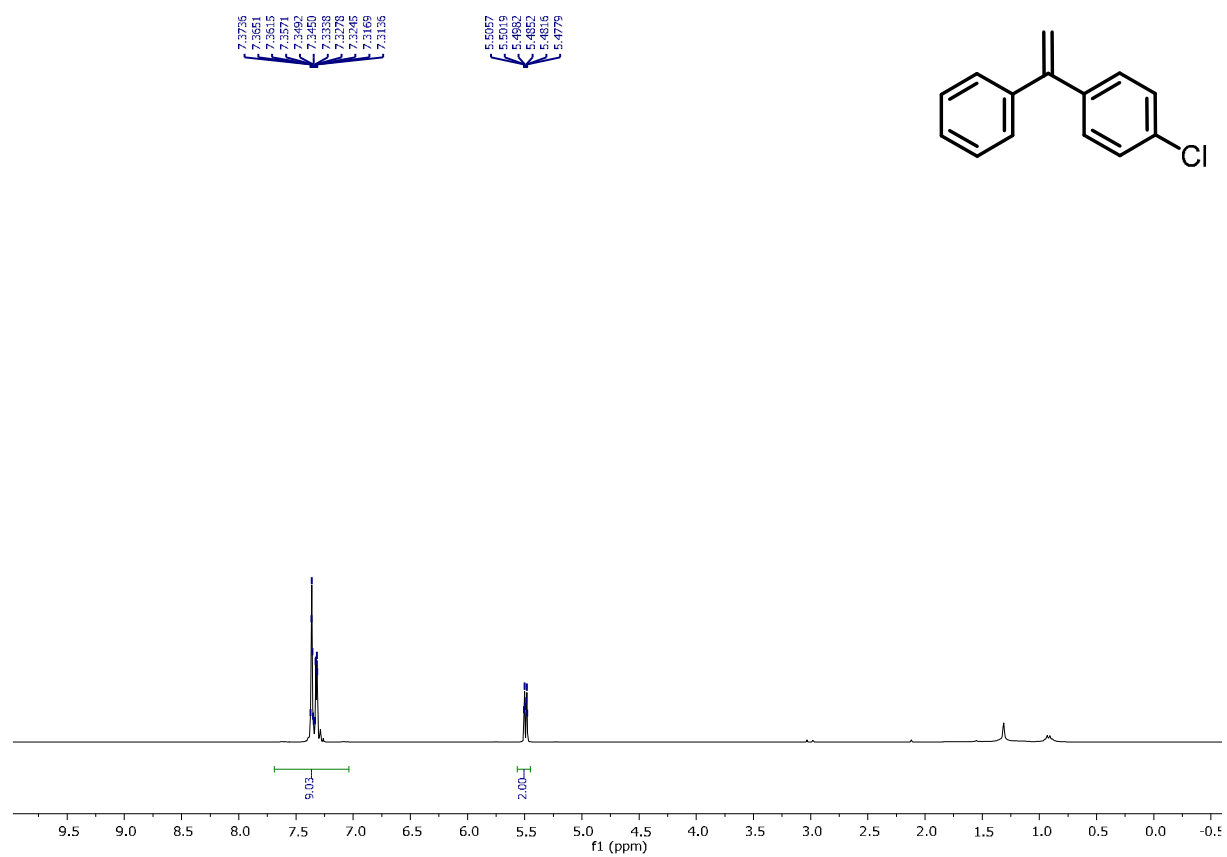
¹³C NMR of (E)-3-(5-chloropyridin-3-yl)-2-(phenylsulphonyl)acrylonitrile (2q)



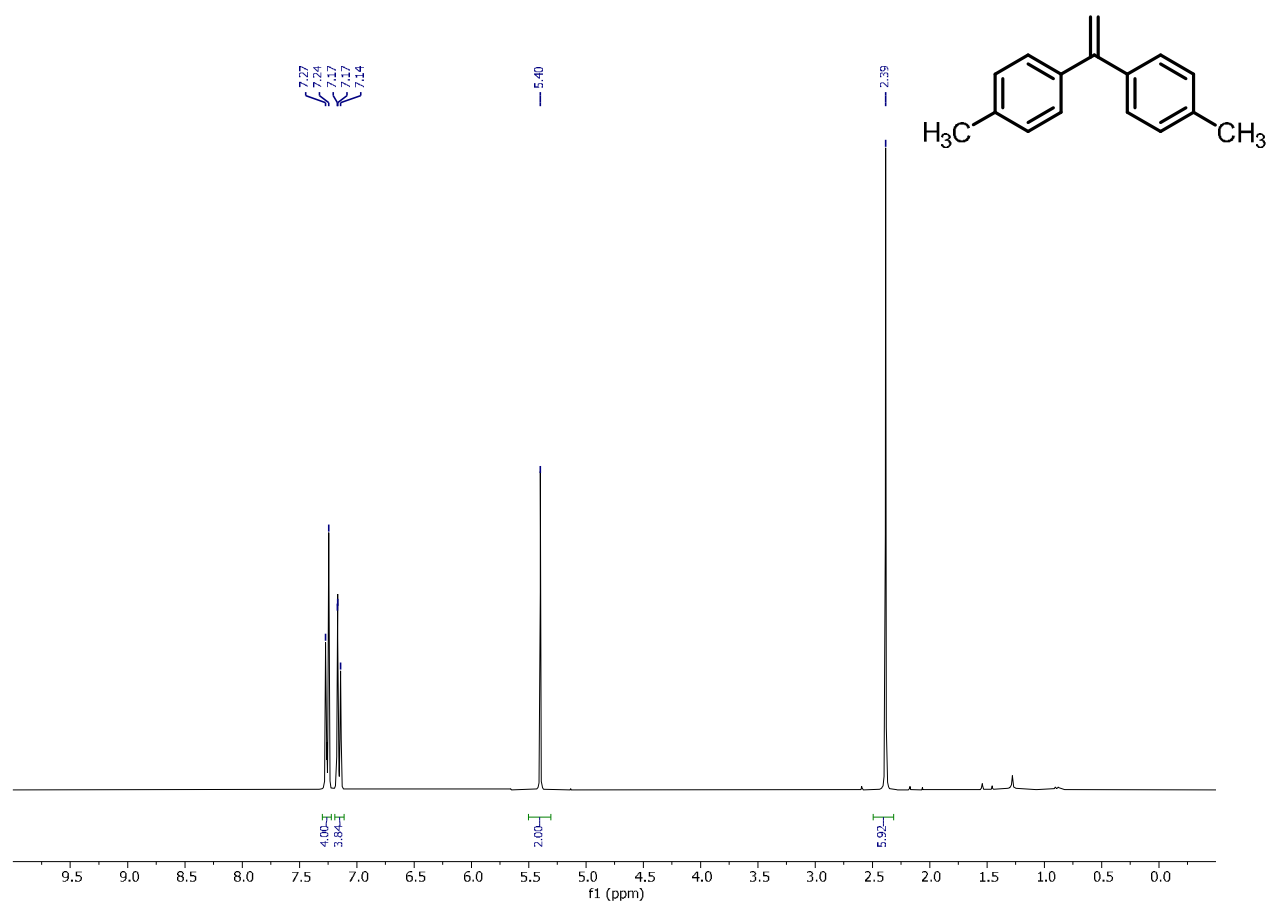
¹H NMR of (*E*)-3-(3-methyl-1-phenyl-1H-pyrazol-4-yl)-2-(phenylsulfonyl)acrylonitrile (**2r**)



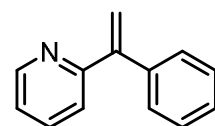
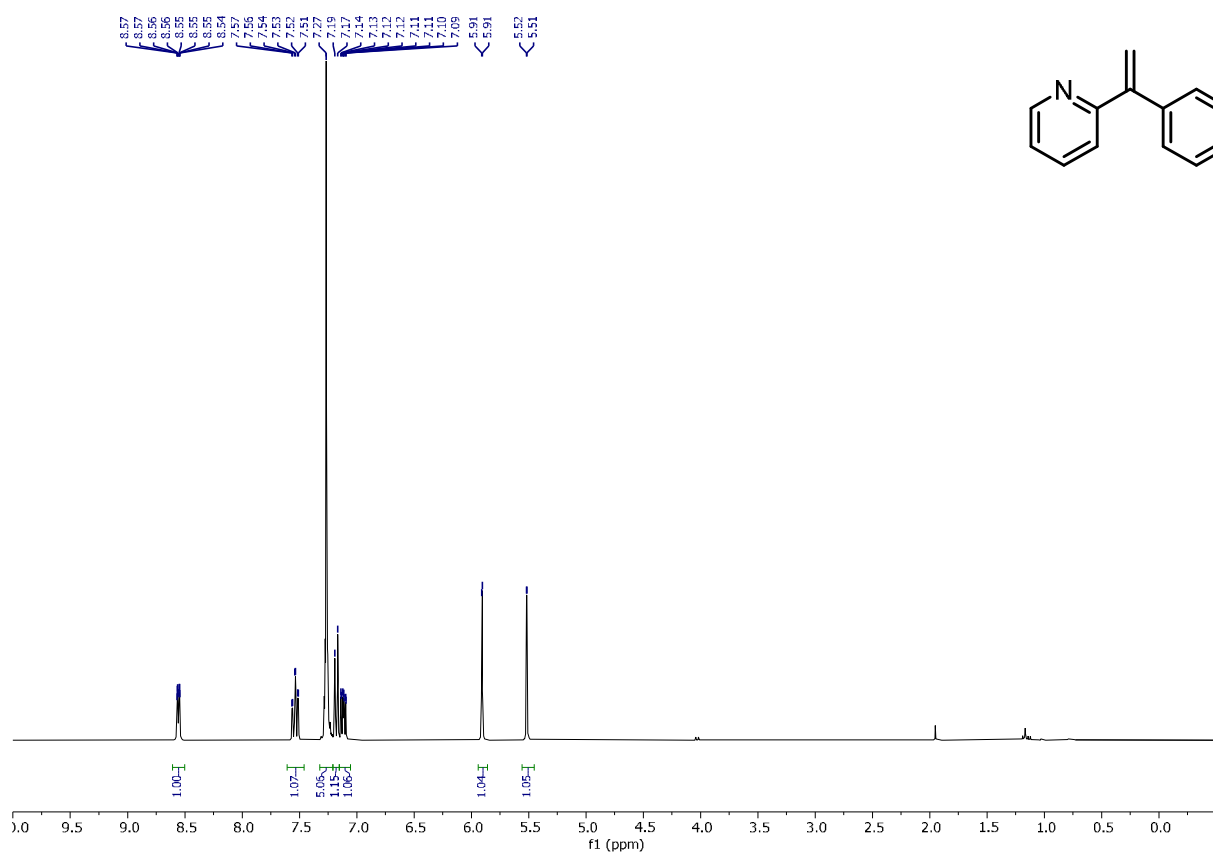
¹³C NMR of (*E*)-3-(3-methyl-1-phenyl-1H-pyrazol-4-yl)-2-(phenylsulfonyl)acrylonitrile (**2r**)



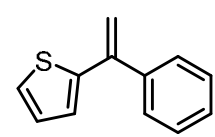
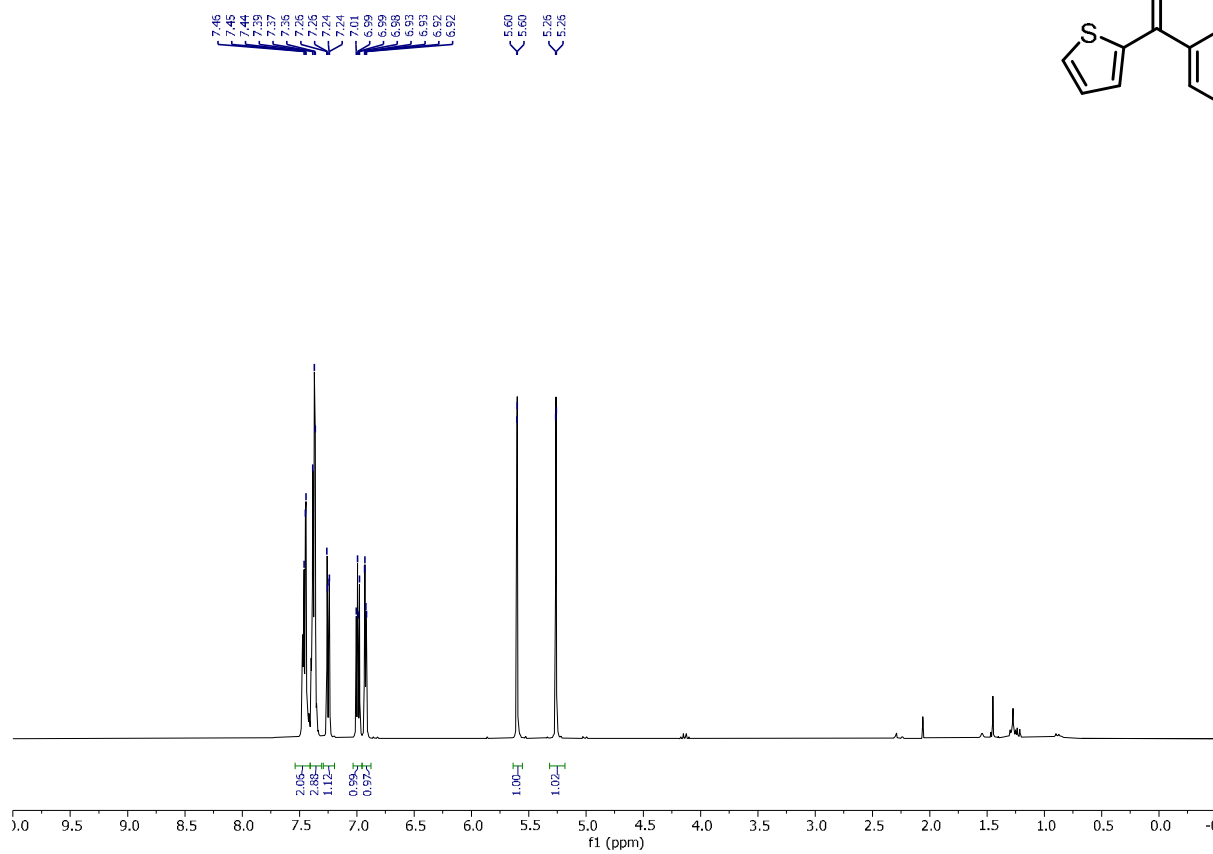
¹H NMR of 1-chloro-4-(1-phenylvinyl)benzene (**2t**)



¹H NMR of 4,4'-(ethene-1,1-diyl)bis(methylbenzene) (**2u**)

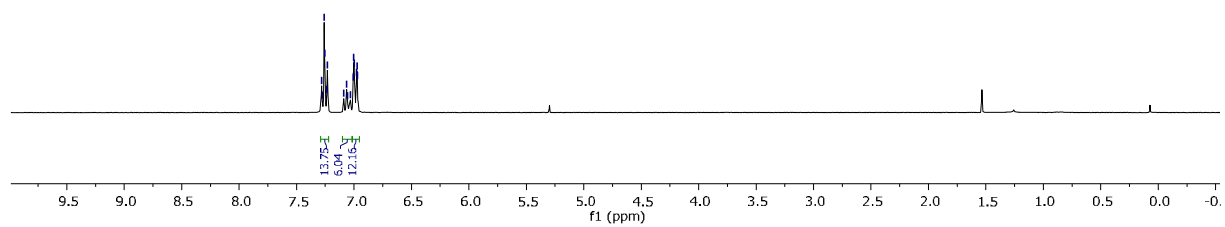
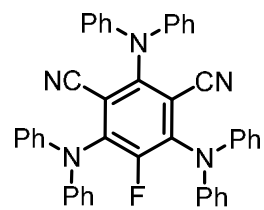


¹H NMR of 2-(1-phenylvinyl)pyridine (2v)



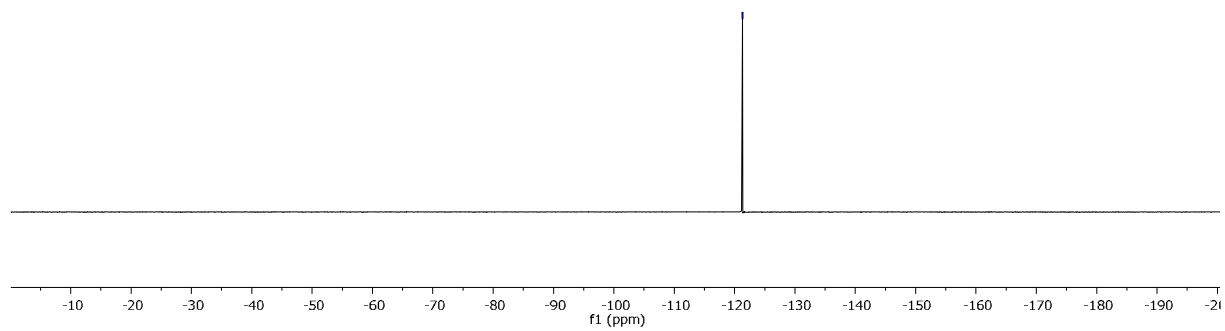
¹H NMR of 2-(1-phenylvinyl)thiophene (2w)

7.2832
7.2766
7.2650
7.2551
7.2367
7.2208
7.0892
7.0649
7.0577
7.0316
7.0073
7.0021
6.9969
6.9778
6.9731
6.9586



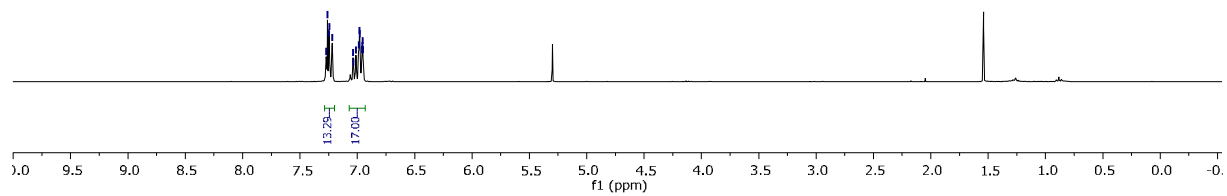
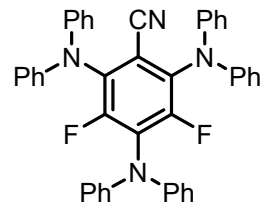
¹H NMR of 3DPAFIPN

-121.3071



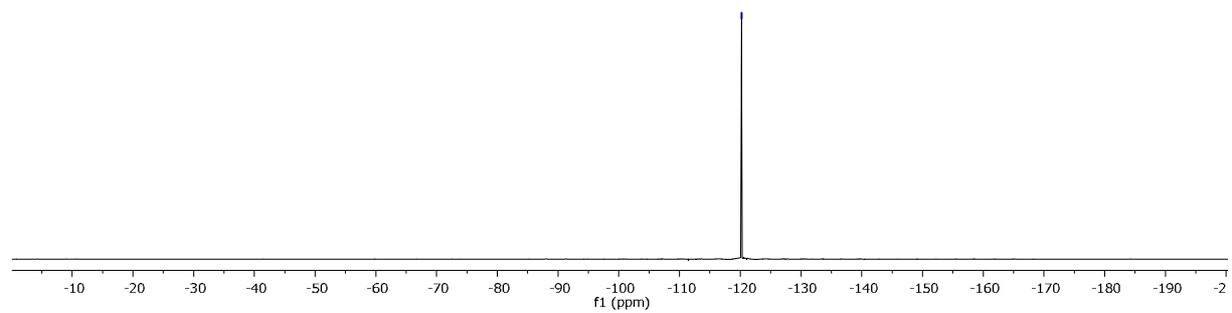
¹⁹F NMR of 3DPAFIPN

7.2723
7.2600
7.2483
7.2366
7.2248
7.2131
7.2014
7.0124
6.9800
6.9682
6.9564
6.9446
6.9328
6.9210
6.9092
6.8974

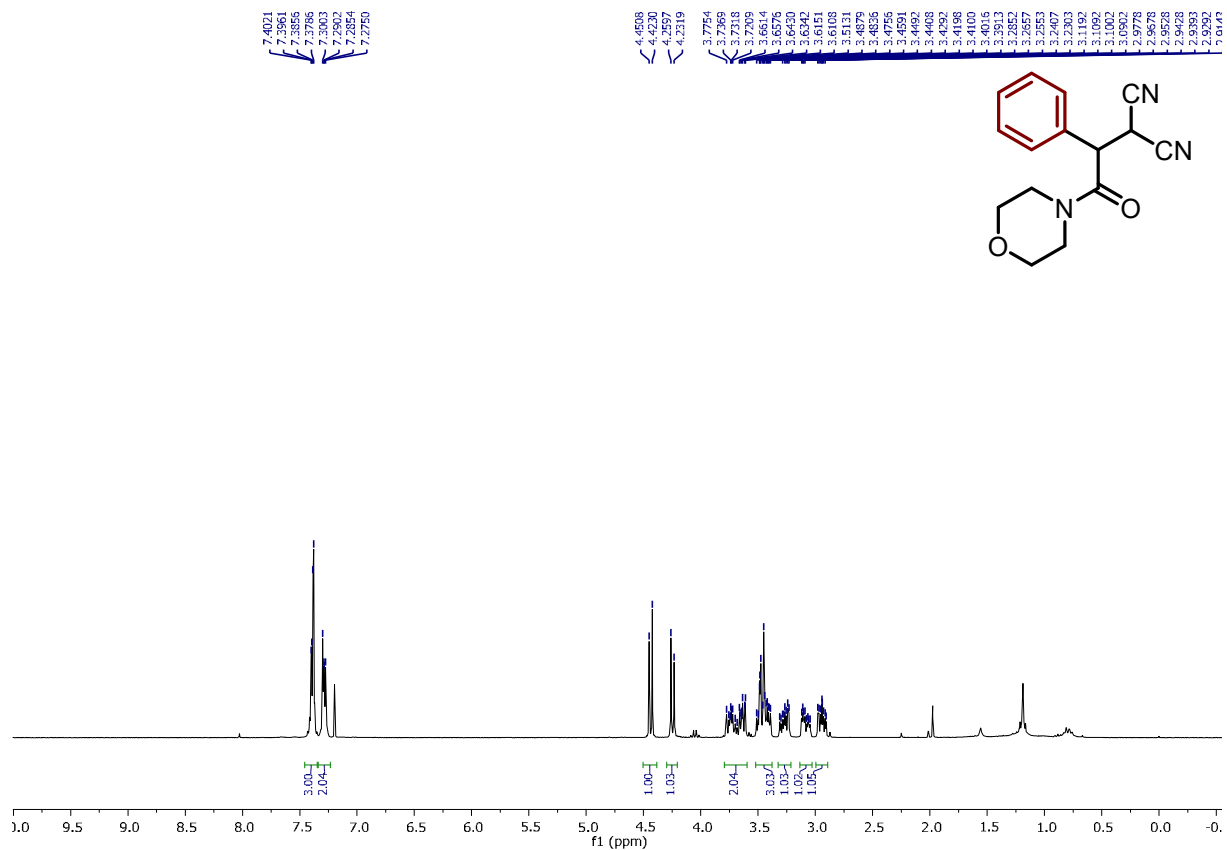


¹H NMR of 3DPA2FBN

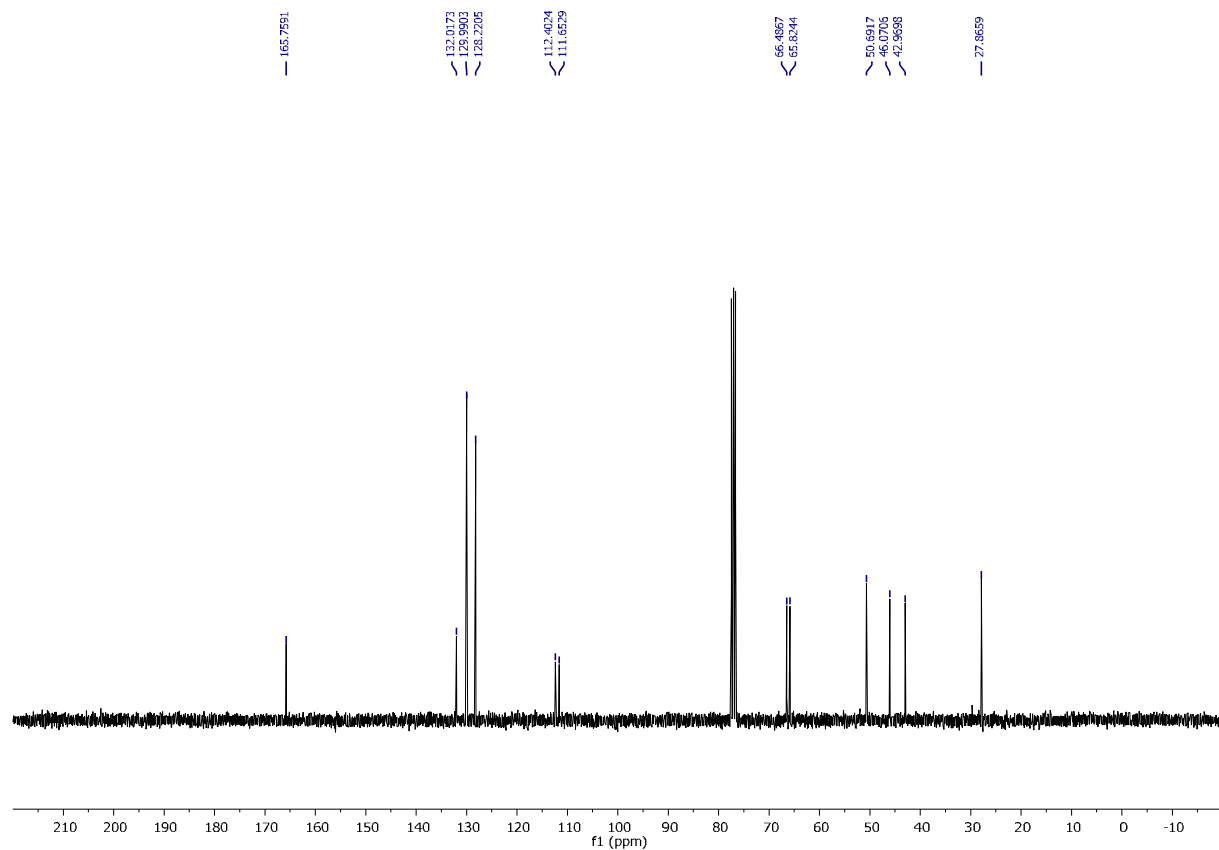
-120.2222



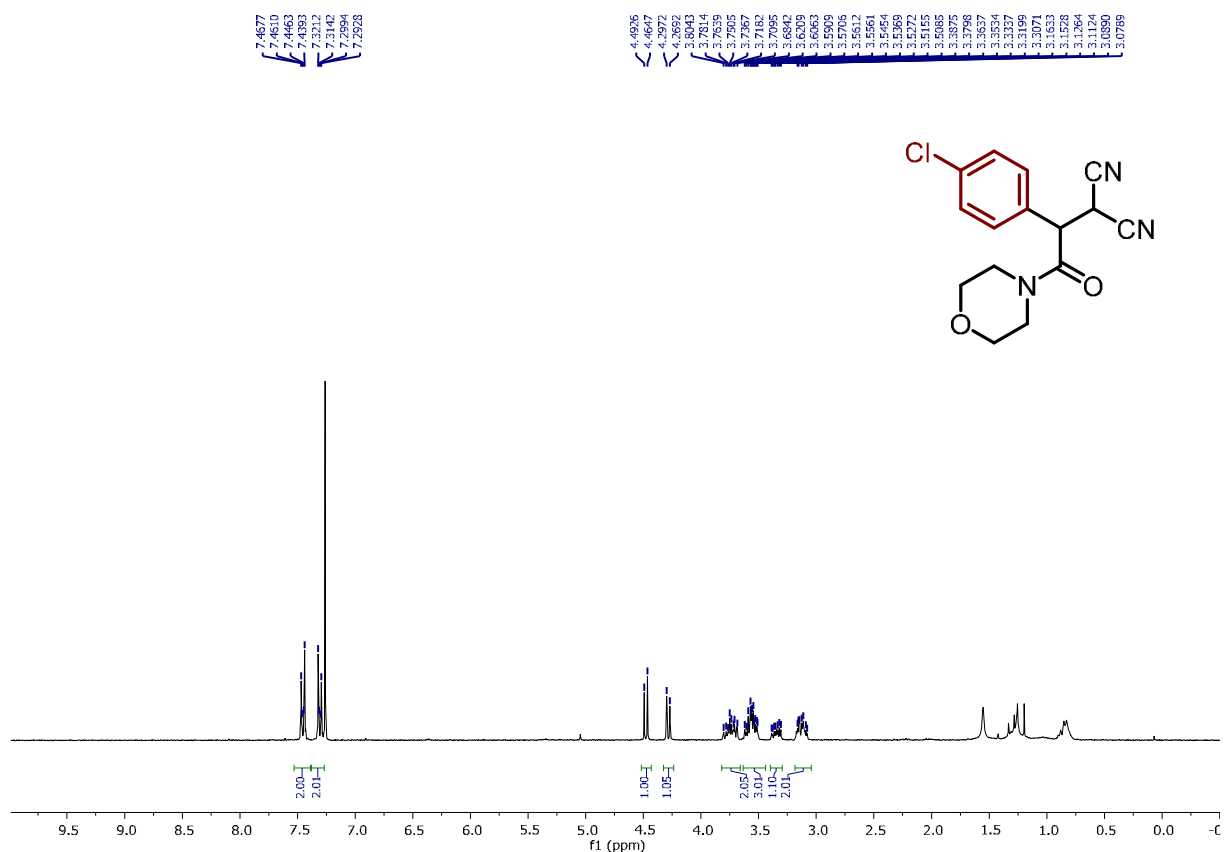
¹⁹F NMR of 3DPA2FBN



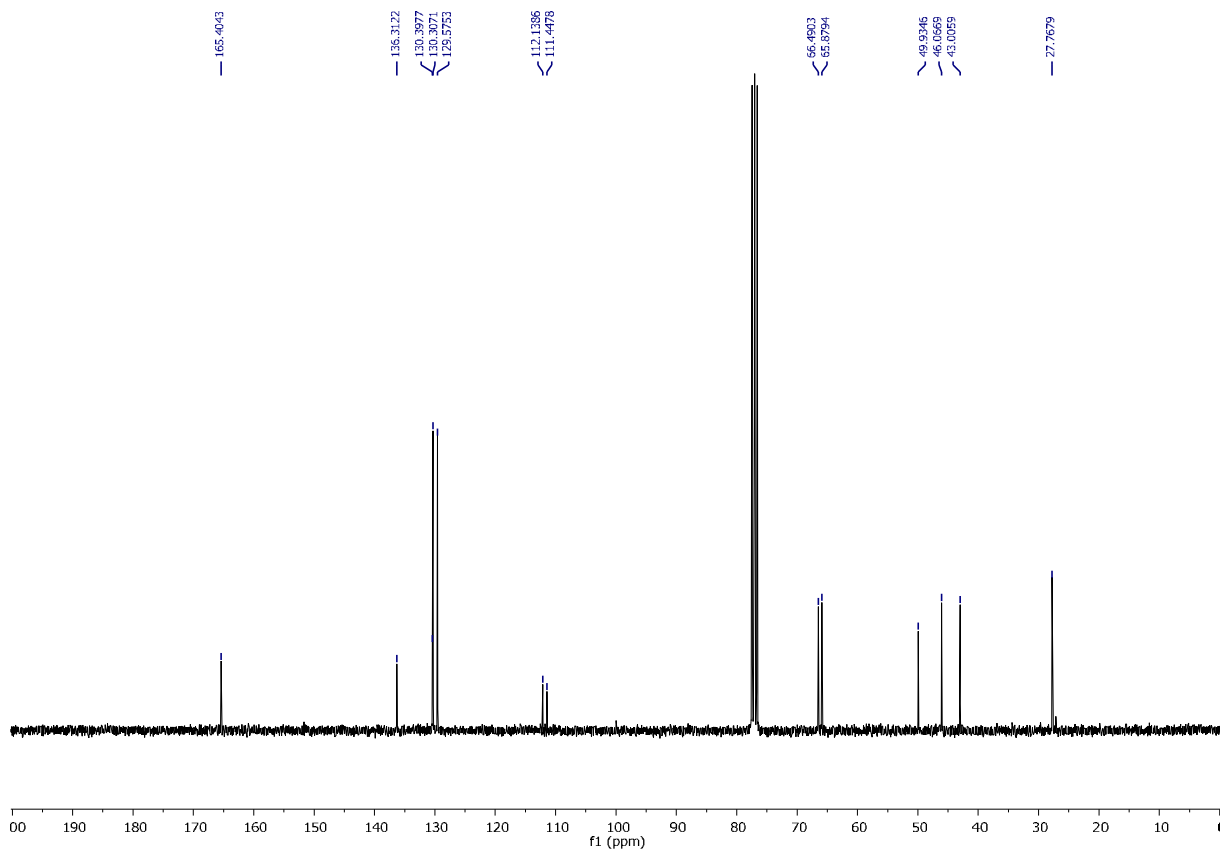
¹H NMR of 2-(2-morpholino-2-oxo-1-phenylethyl)malononitrile (3aa)



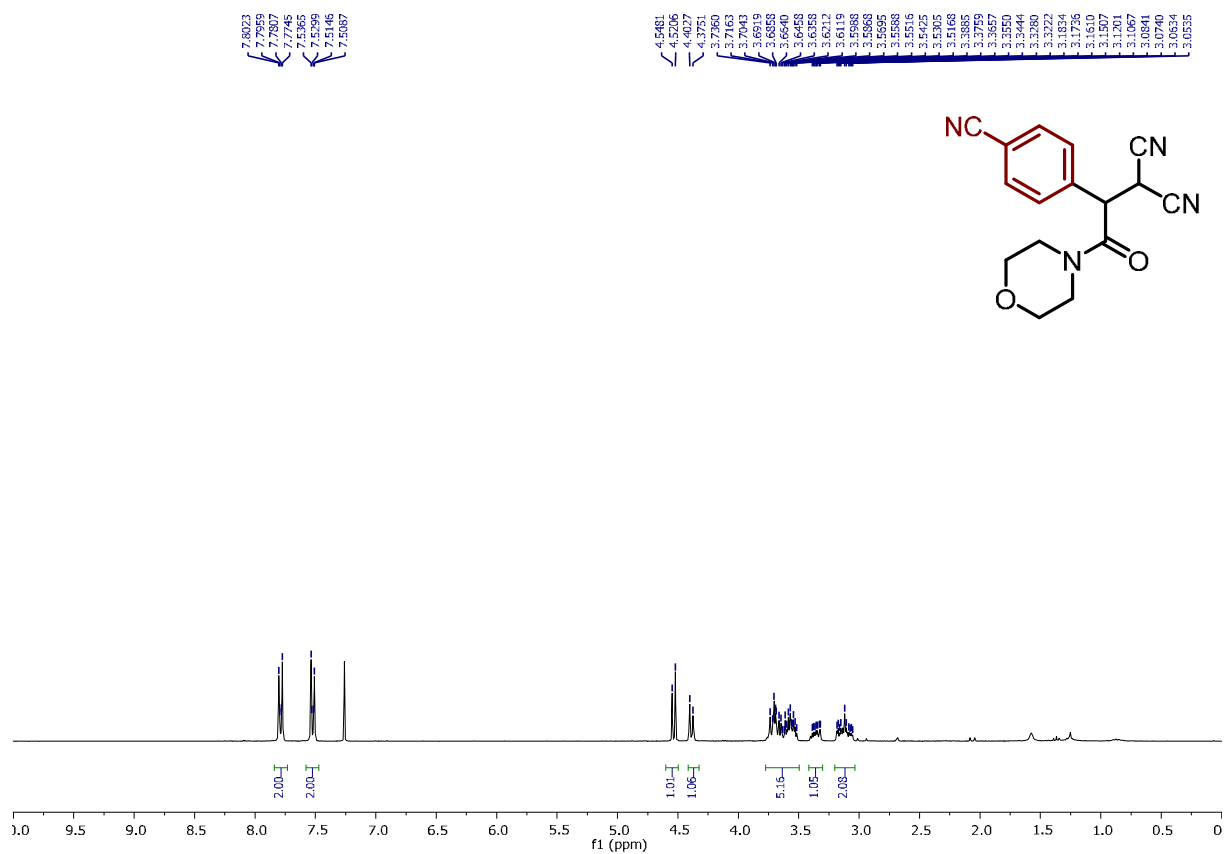
¹³C NMR of 2-(2-morpholino-2-oxo-1-phenylethyl)malononitrile (3aa)



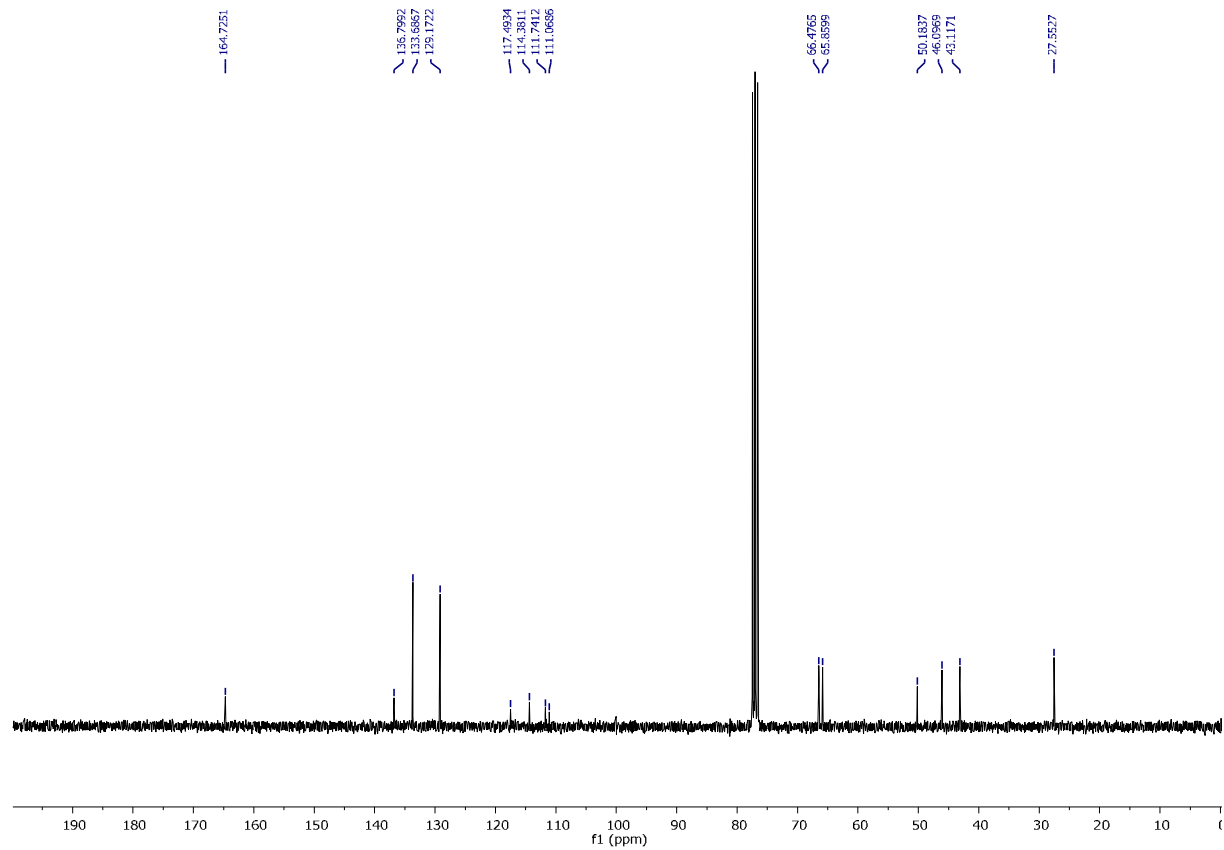
¹H NMR of 2-(1-(4-chlorophenyl)-2-morpholino-2-oxoethyl)malononitrile (3ba)



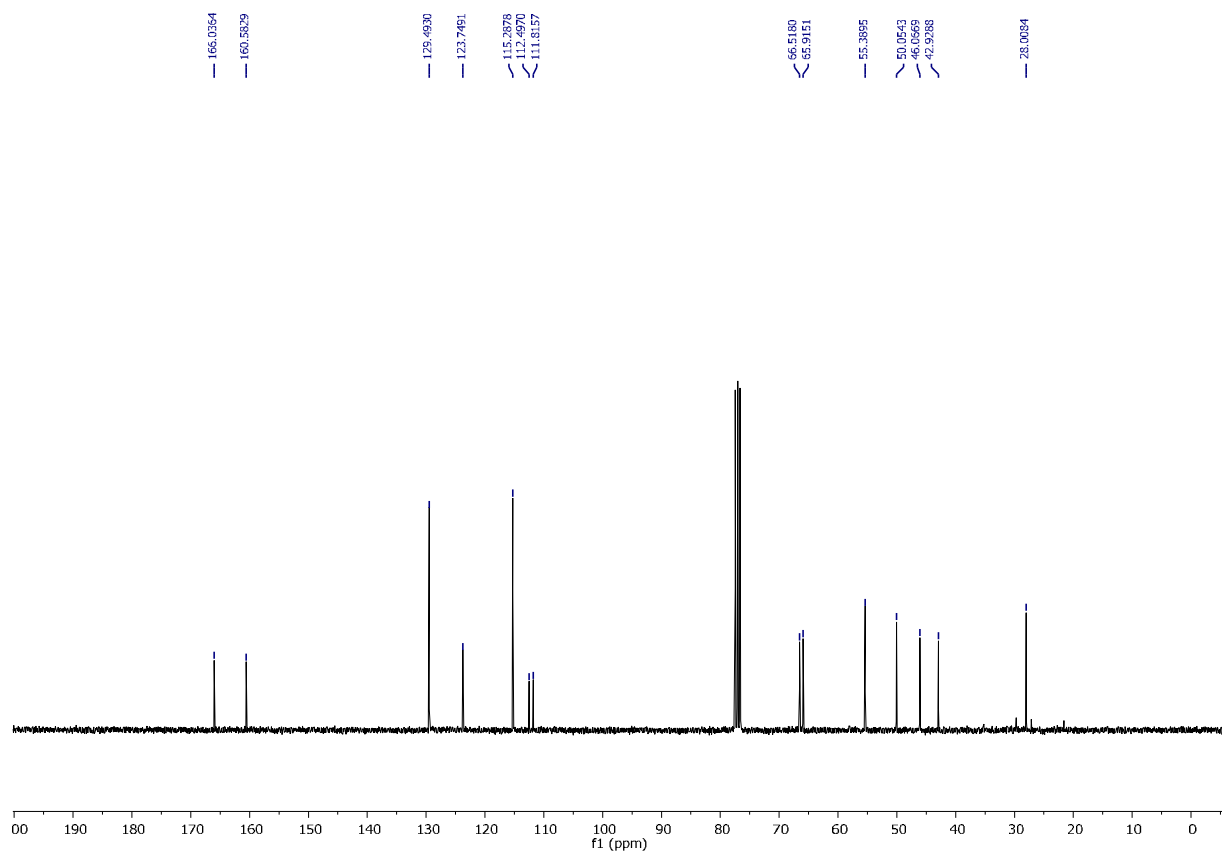
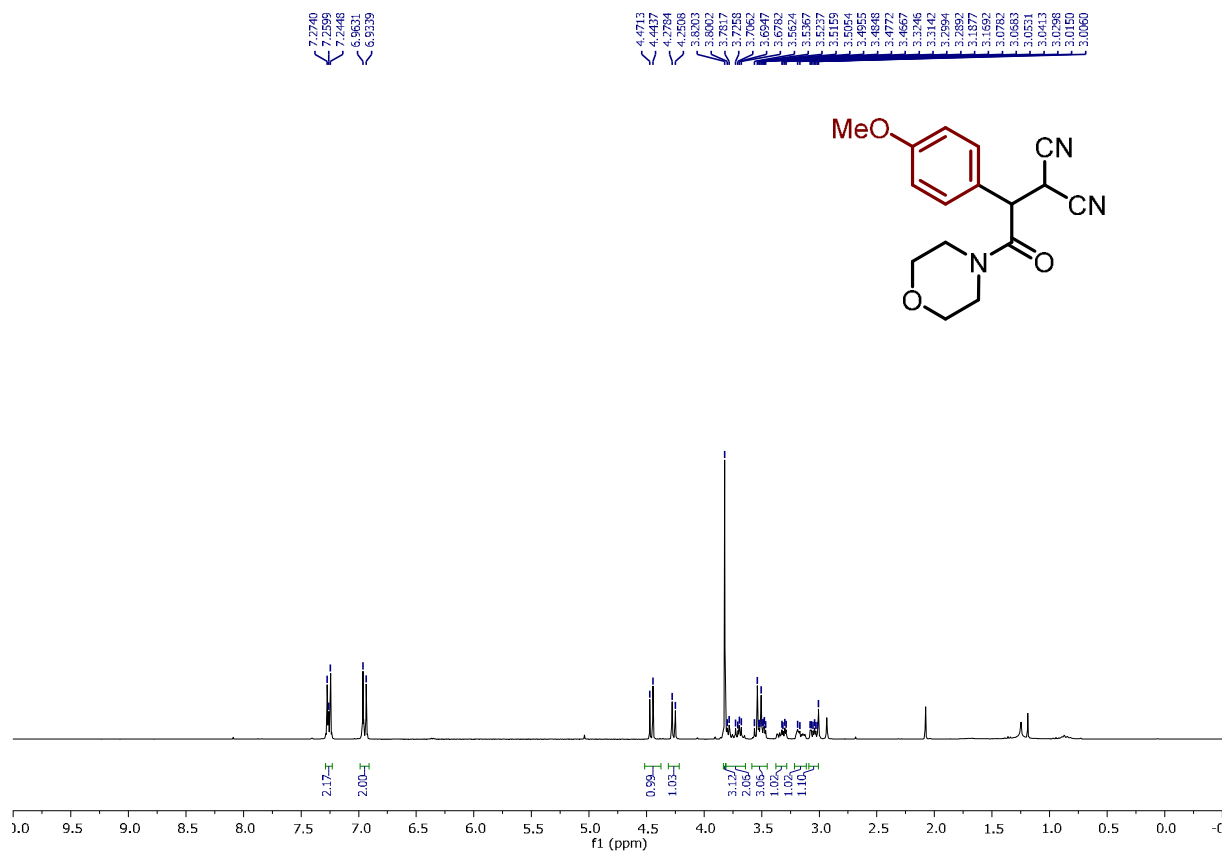
¹³C NMR of 2-(1-(4-chlorophenyl)-2-morpholino-2-oxoethyl)malononitrile (3ba)

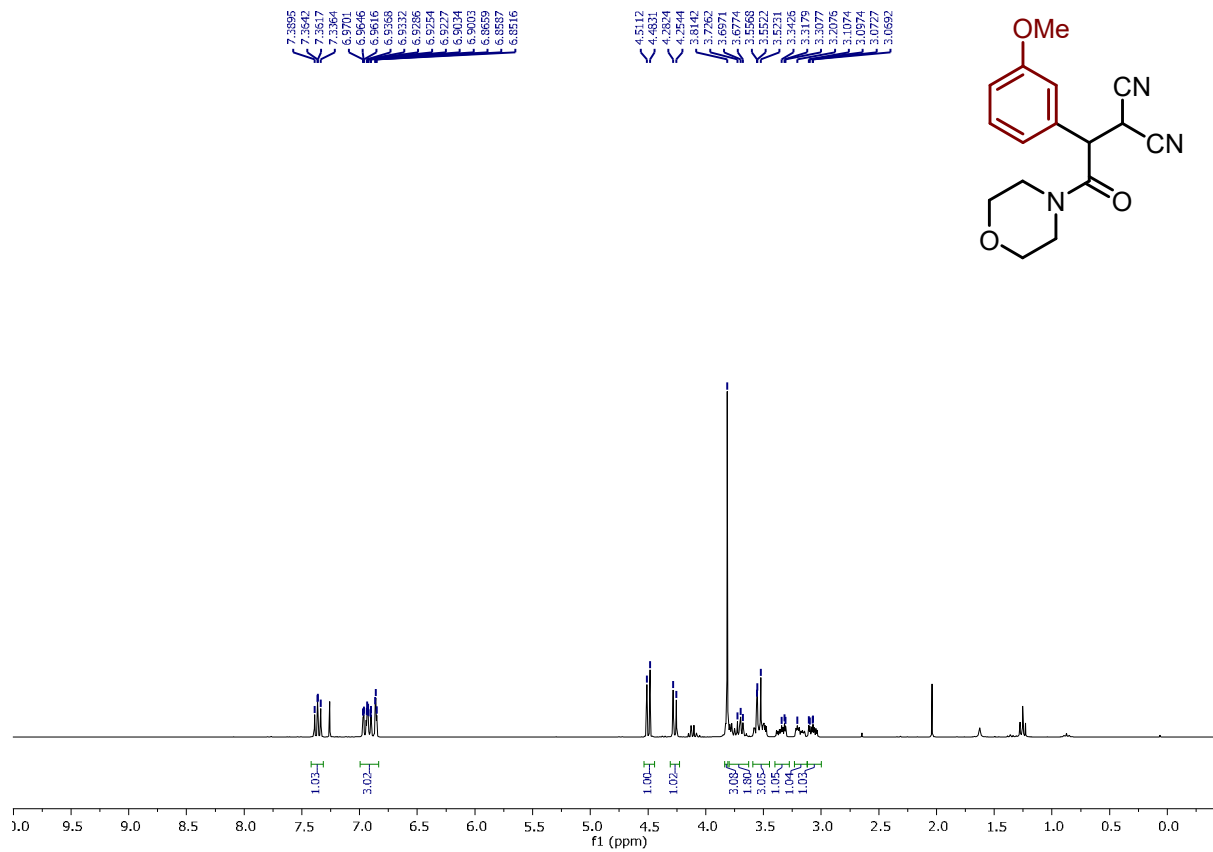


¹H NMR of 2-(1-(4-cyanophenyl)-2-morpholino-2-oxoethyl)malononitrile (3ca)

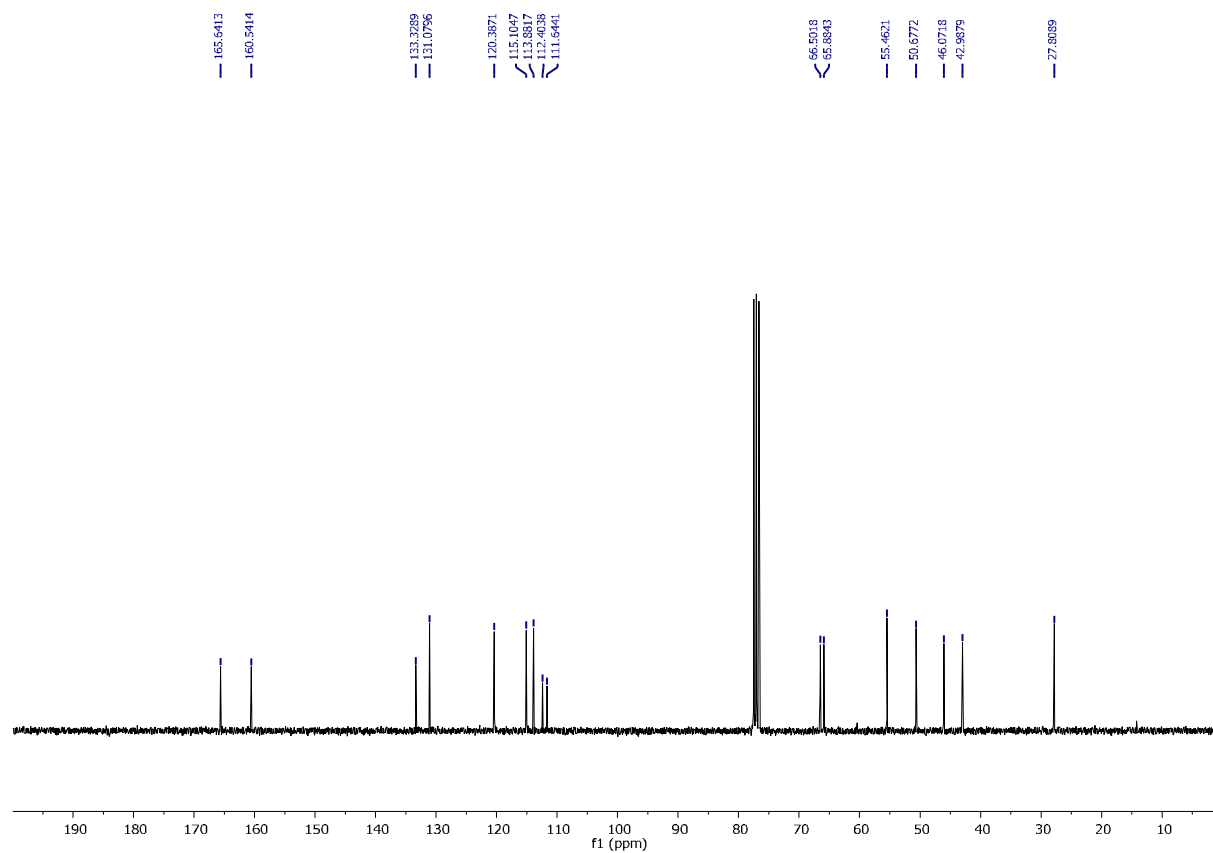


¹³C NMR of 2-(1-(4-cyanophenyl)-2-morpholino-2-oxoethyl)malononitrile (3ca)

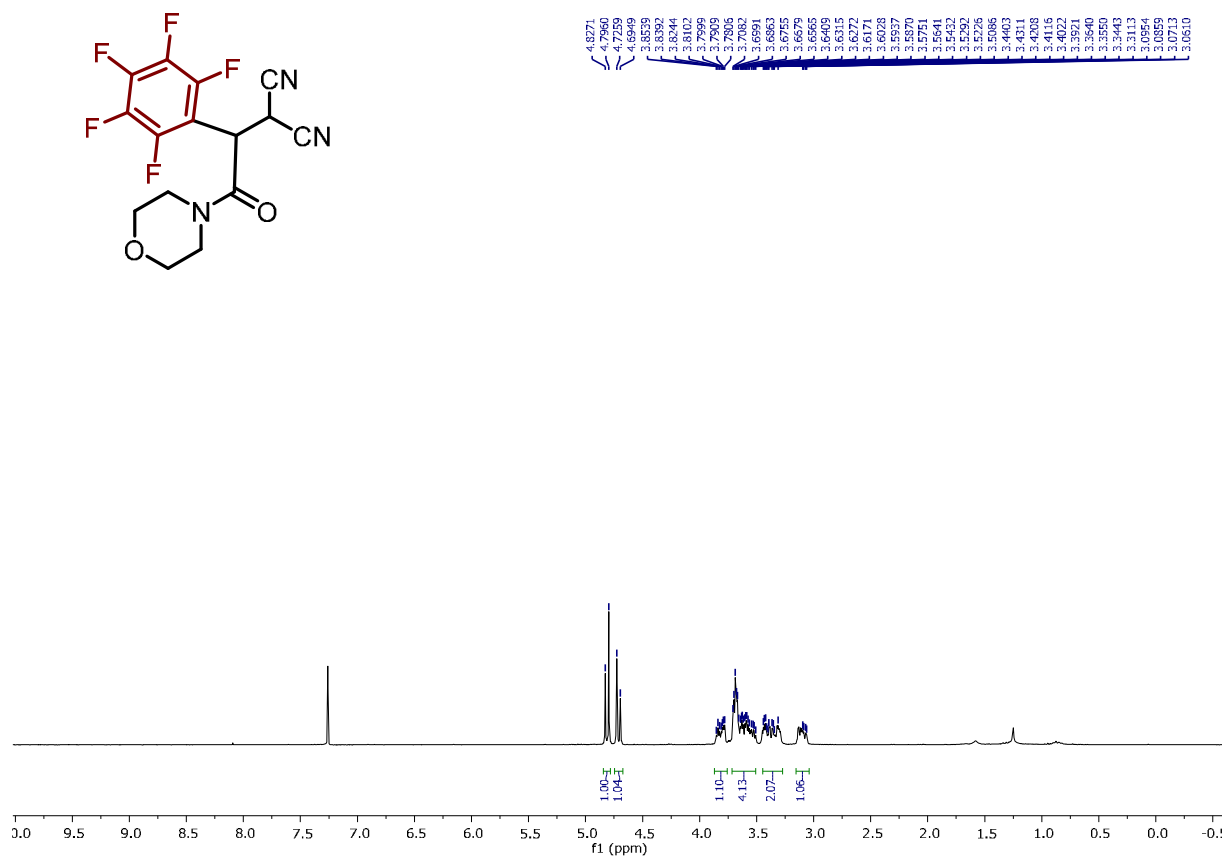




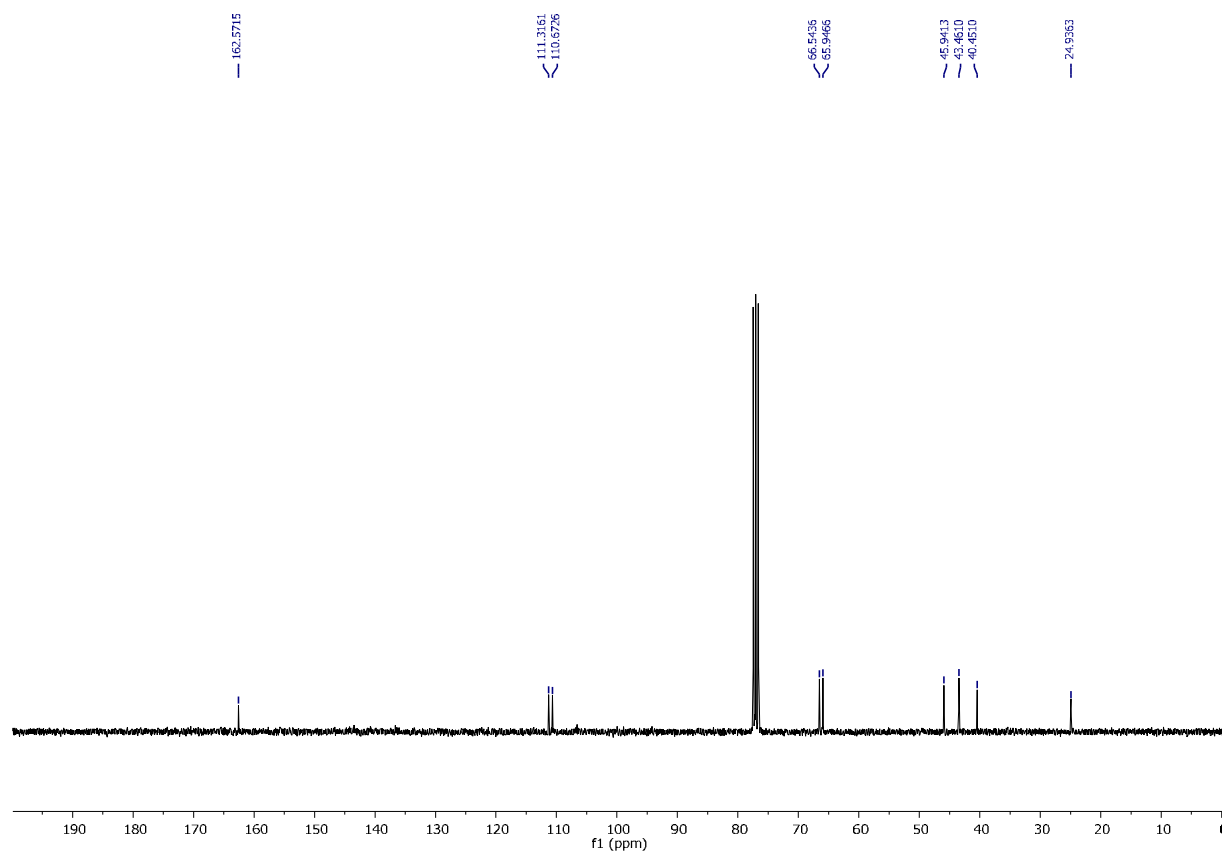
¹H NMR of 2-(1-(3-methoxyphenyl)-2-morpholino-2-oxoethyl)malononitrile (3ea)



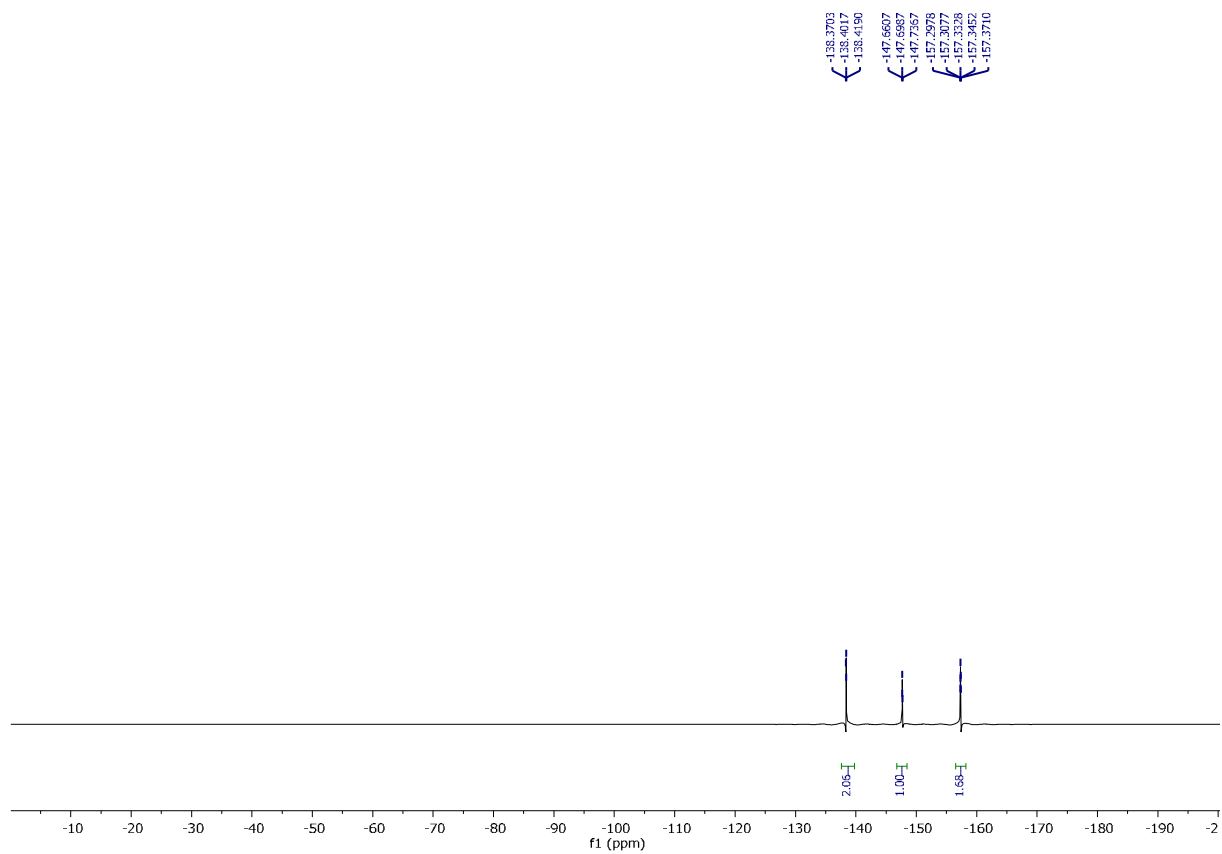
¹³C NMR of 2-(1-(3-methoxyphenyl)-2-morpholino-2-oxoethyl)malononitrile (3ea)



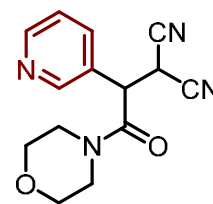
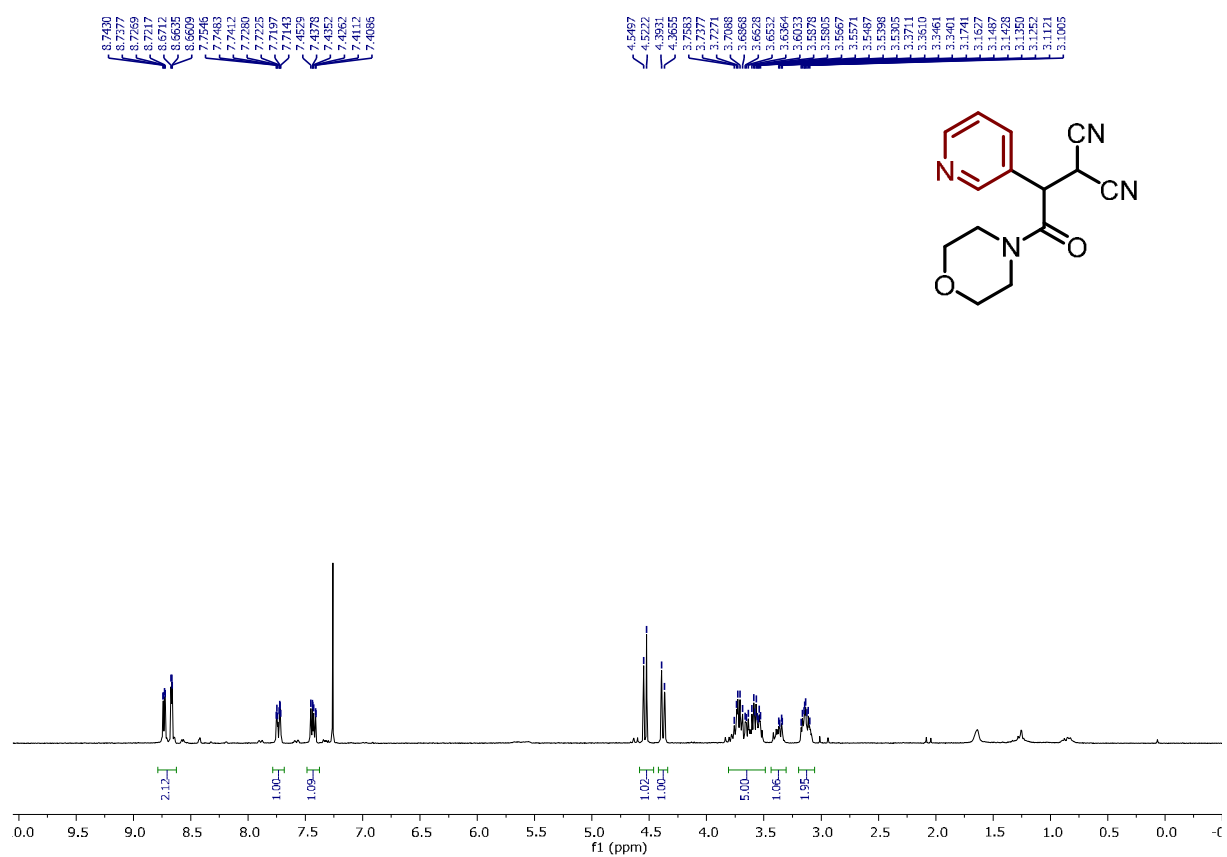
¹H NMR of 2-(2-morpholino-2-oxo-1-(perfluorophenyl)ethyl)malononitrile (3fa)



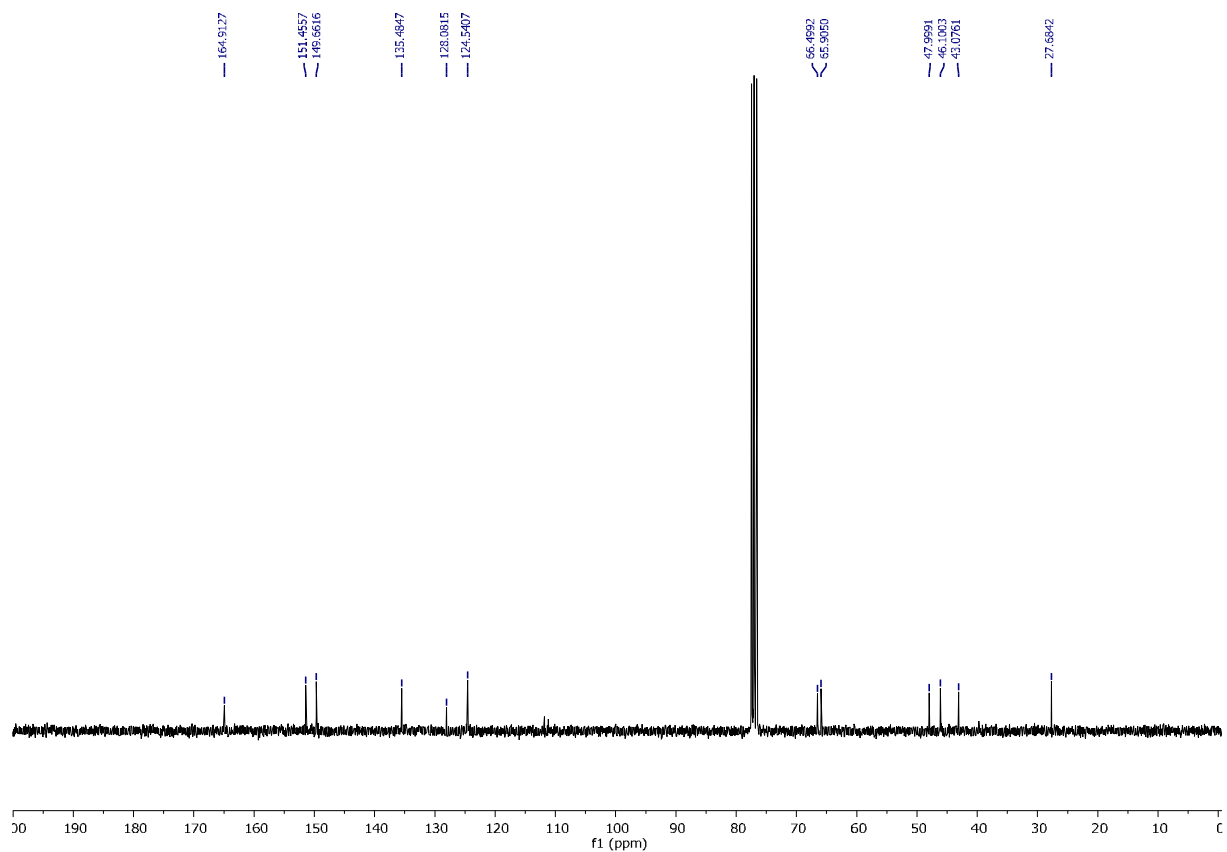
¹³C NMR of 2-(2-morpholino-2-oxo-1-(perfluorophenyl)ethyl)malononitrile (3fa)



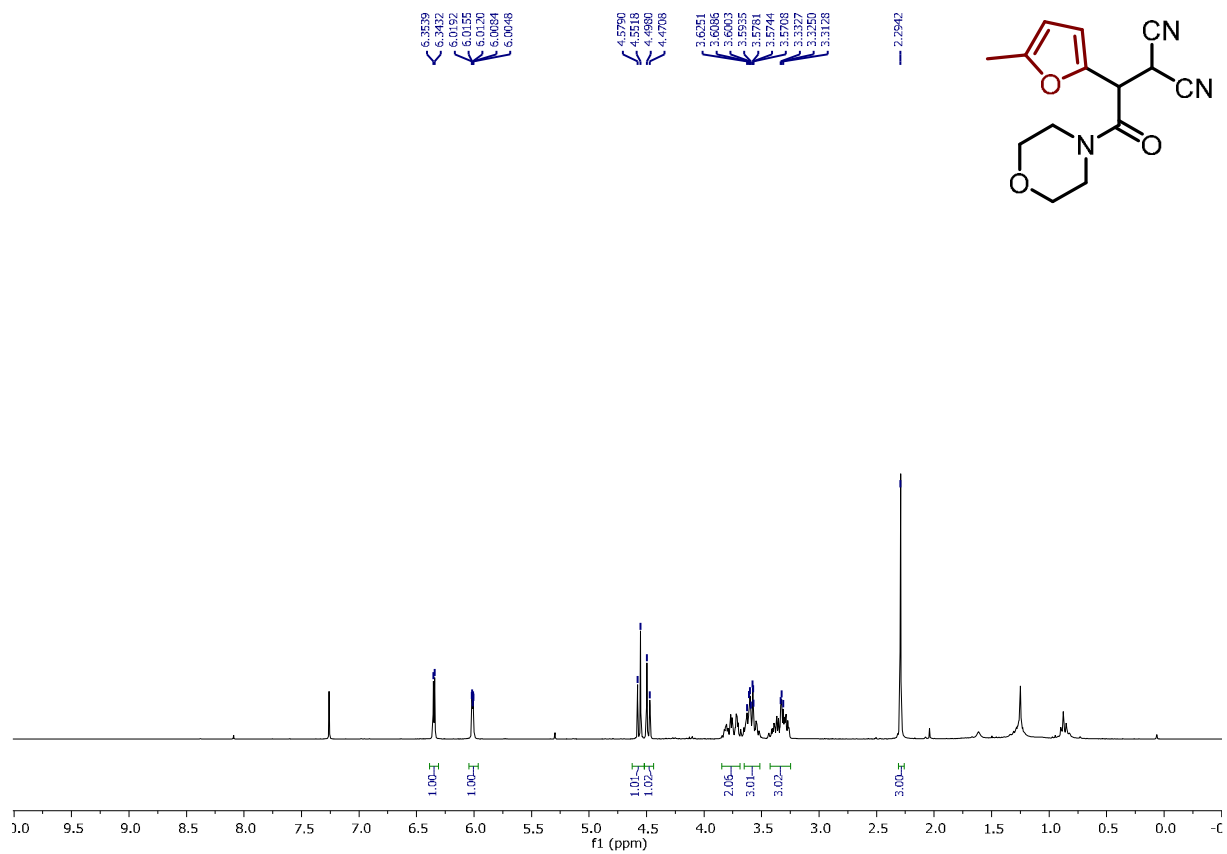
¹⁹F NMR of 2-(2-morpholino-2-oxo-1-(perfluorophenyl)ethyl)malononitrile (3fa)



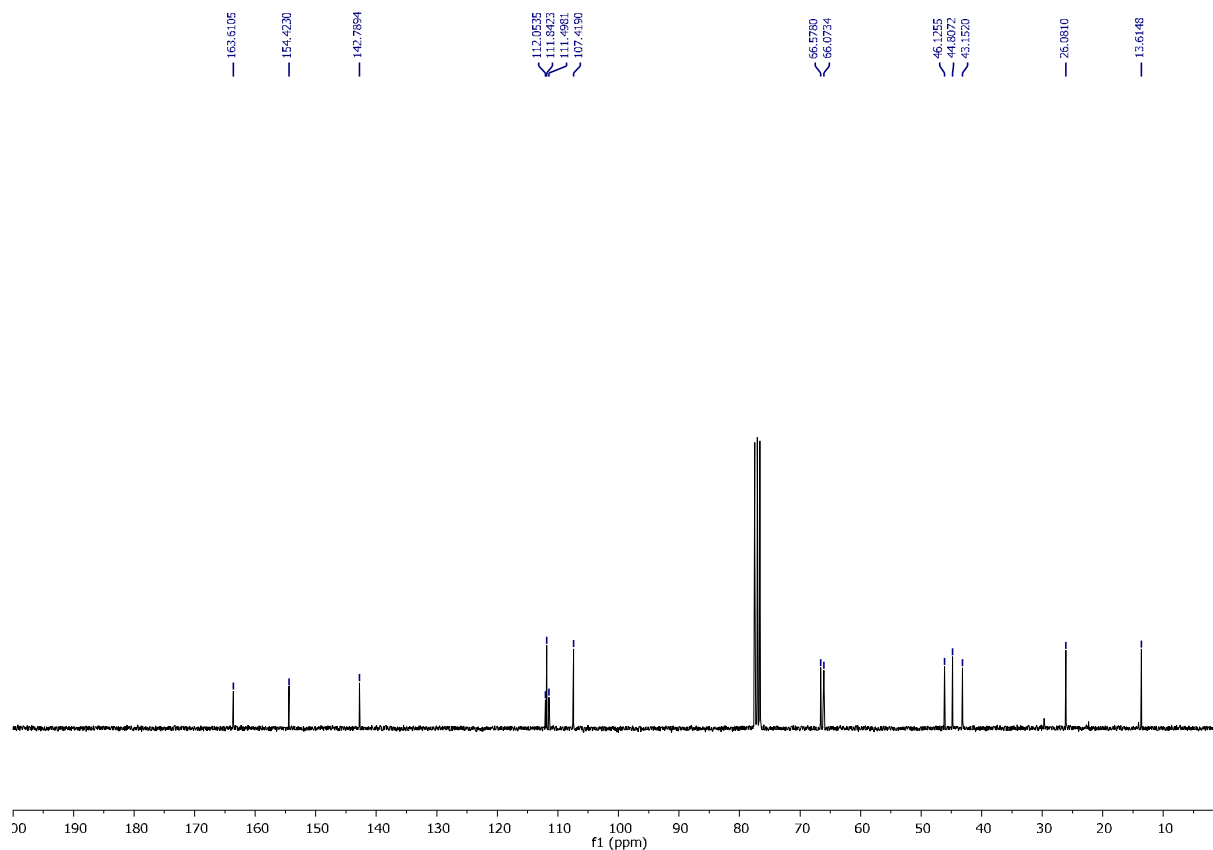
¹H NMR of 2-(2-morpholino-2-oxo-1-(pyridin-3-yl)ethyl)malononitrile (3ga)



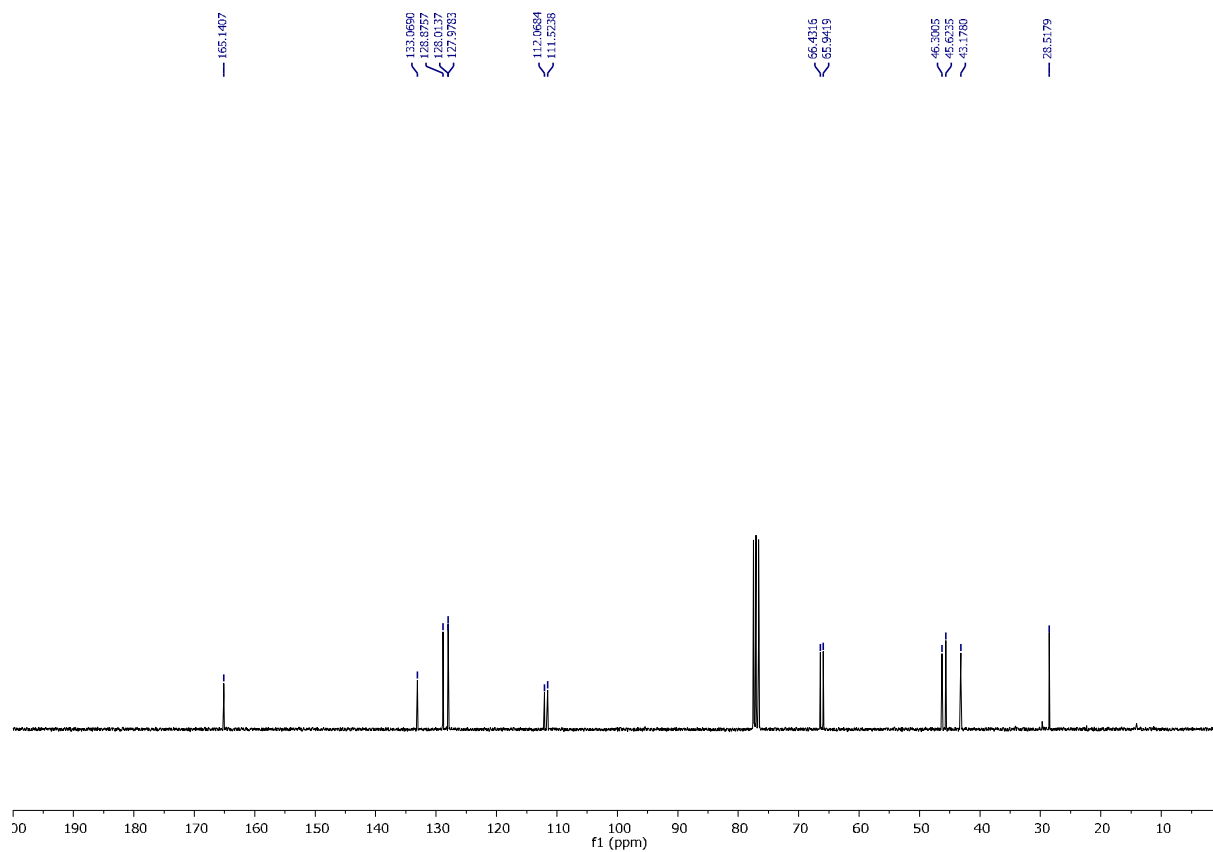
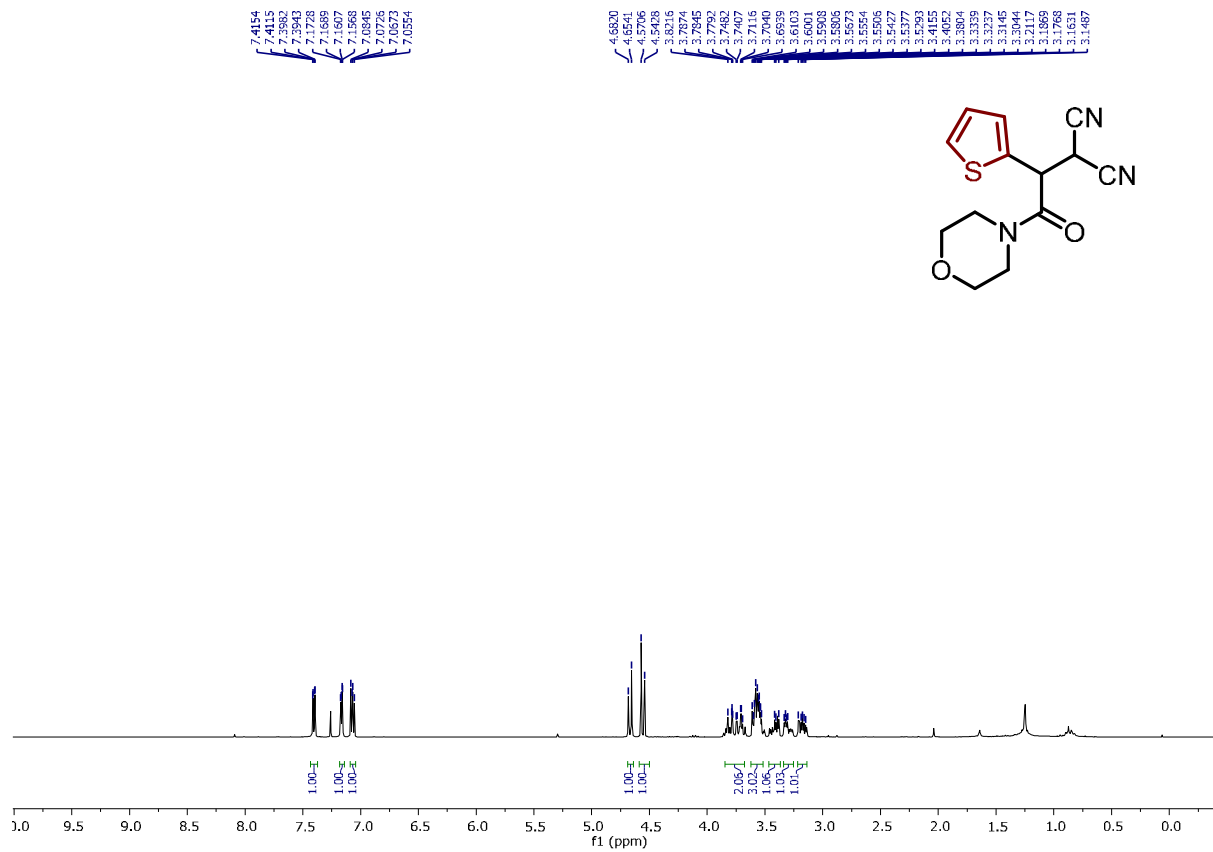
¹³C NMR of 2-(2-morpholino-2-oxo-1-(pyridin-3-yl)ethyl)malononitrile (3ga)

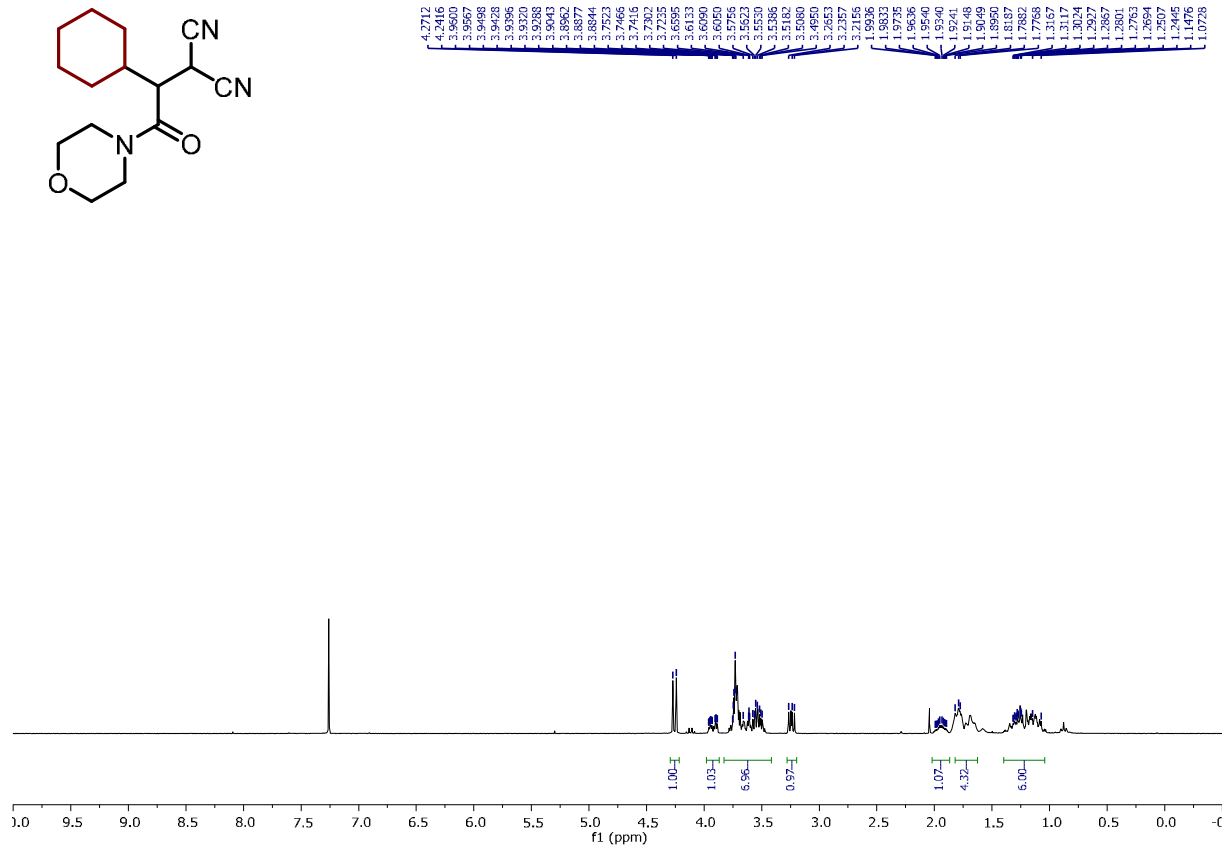
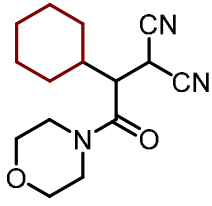


¹H NMR of 2-(1-(5-methylfuran-2-yl)-2-morpholino-2-oxoethyl)malononitrile (3ha)

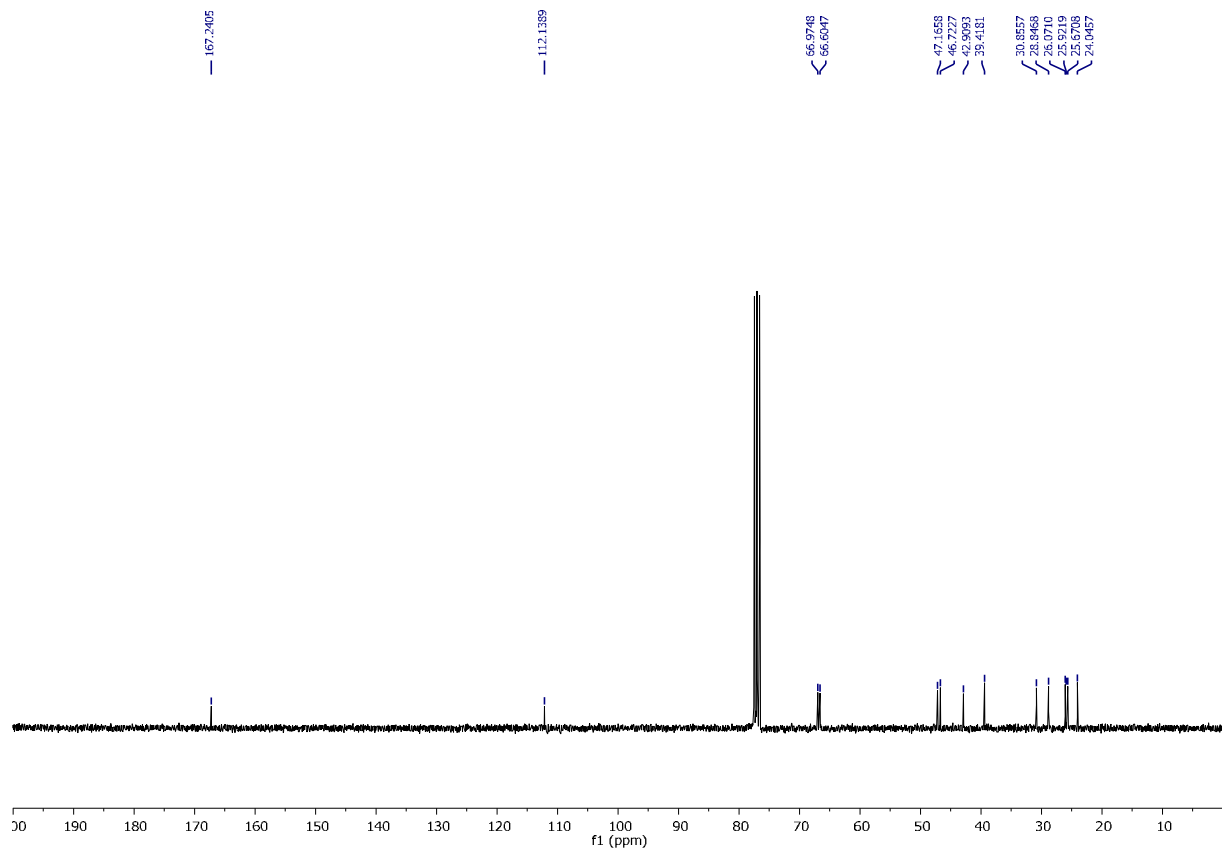


¹³C NMR of 2-(1-(5-methylfuran-2-yl)-2-morpholino-2-oxoethyl)malononitrile (3ha)

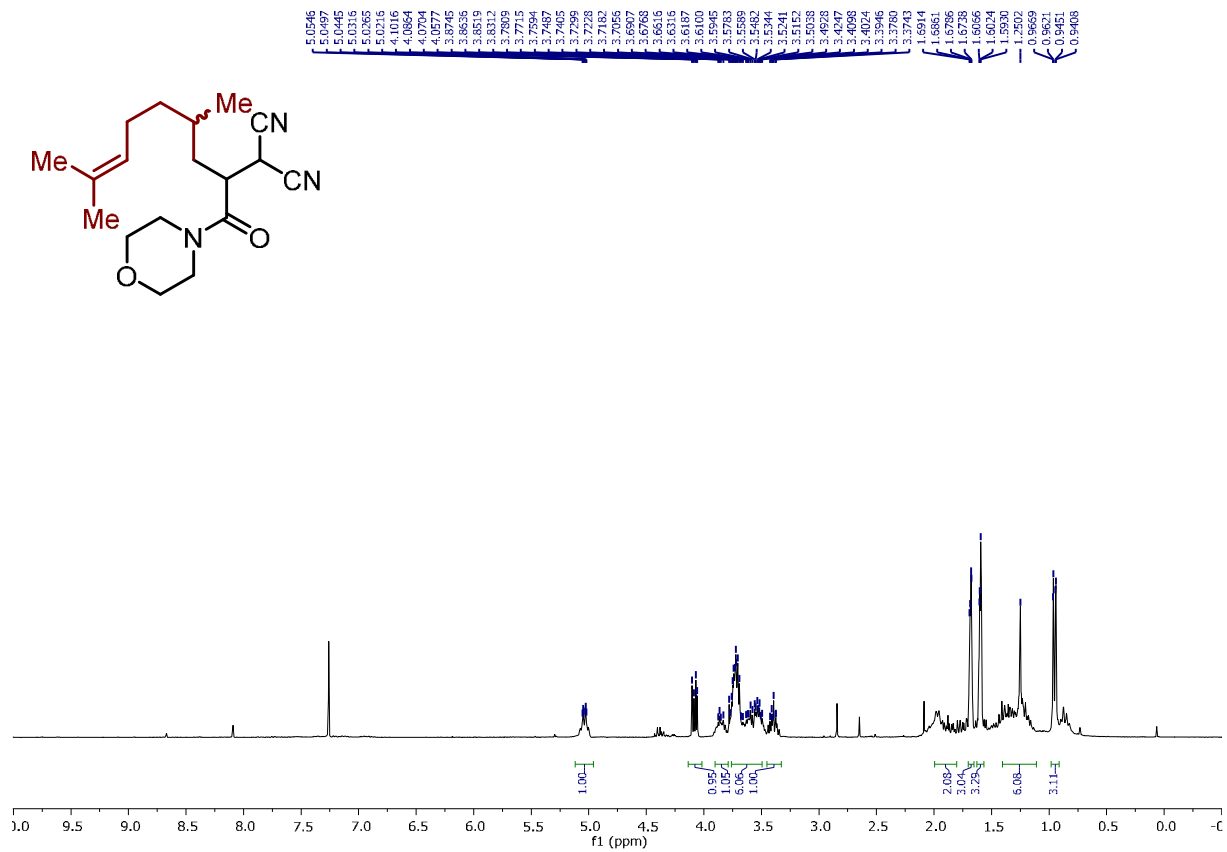




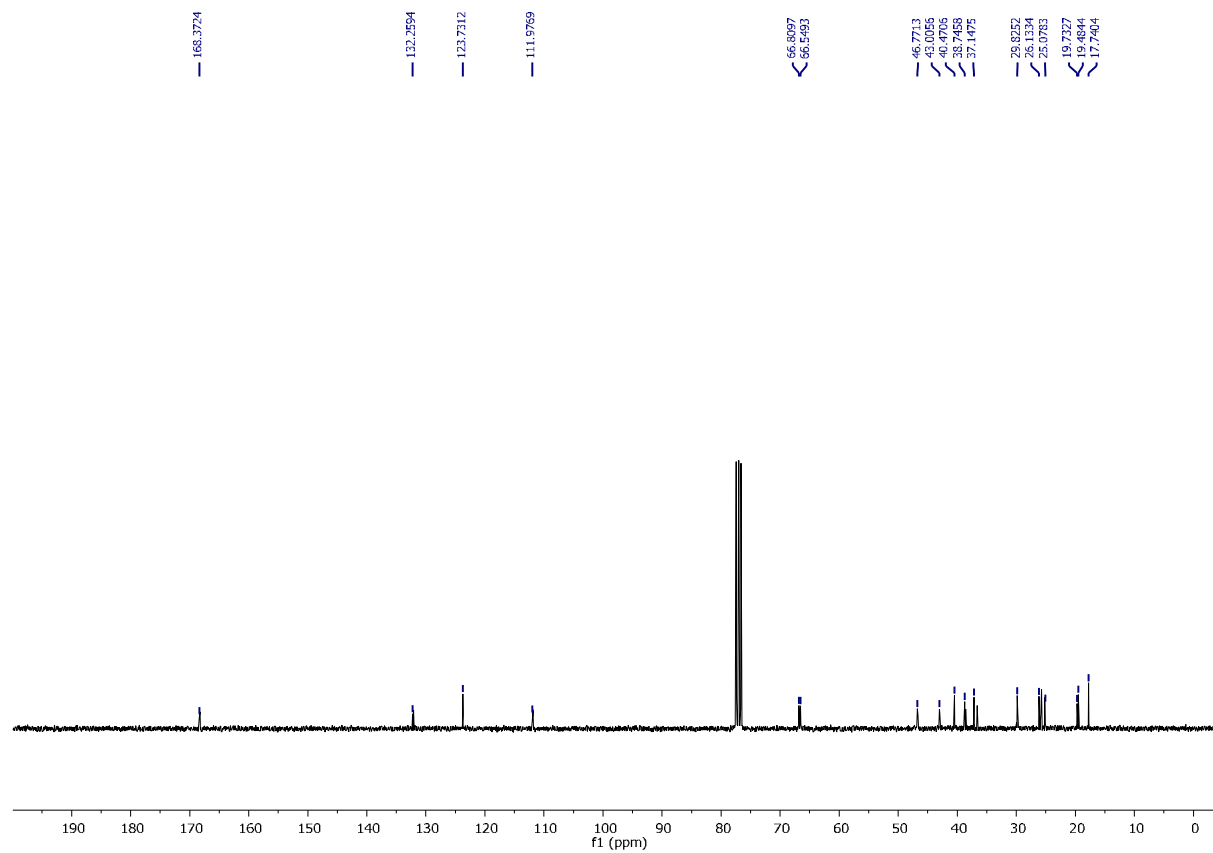
¹H NMR of 2-(1-cyclohexyl-2-morpholino-2-oxoethyl)malononitrile (**3ja**)



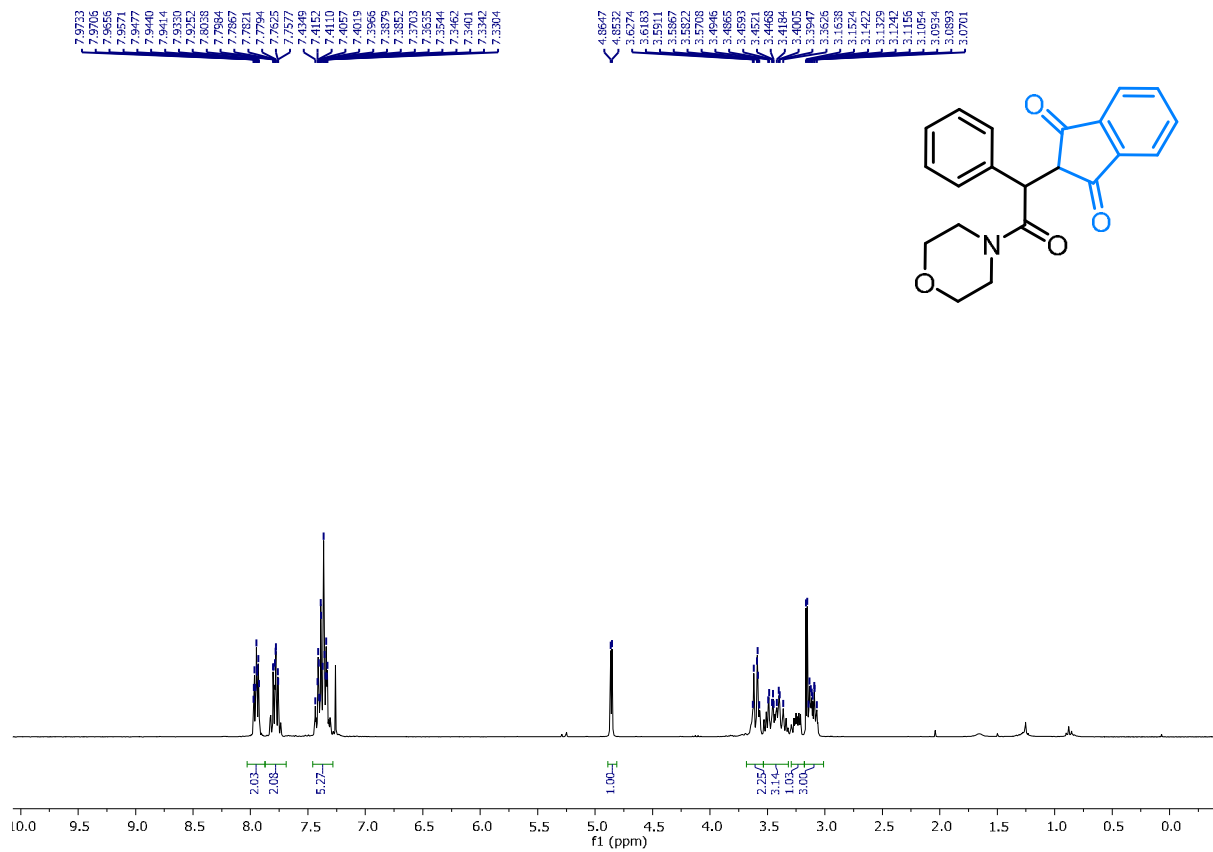
¹³C NMR of 2-(1-cyclohexyl-2-morpholino-2-oxoethyl)malononitrile (**3ja**)



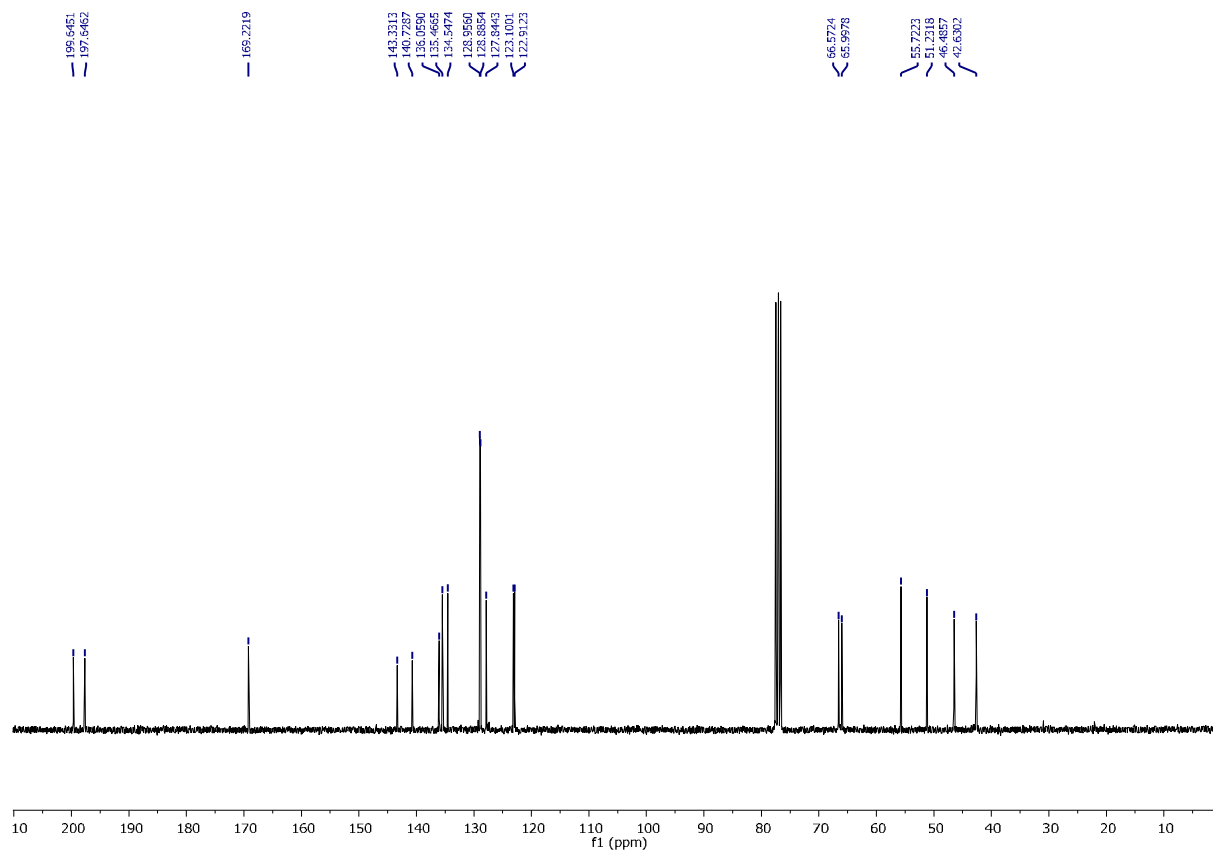
¹H NMR of 2-[(4R)-4,8-dimethyl-1-morpholino-1-oxonon-7-en-2-yl]malononitrile (3ka)



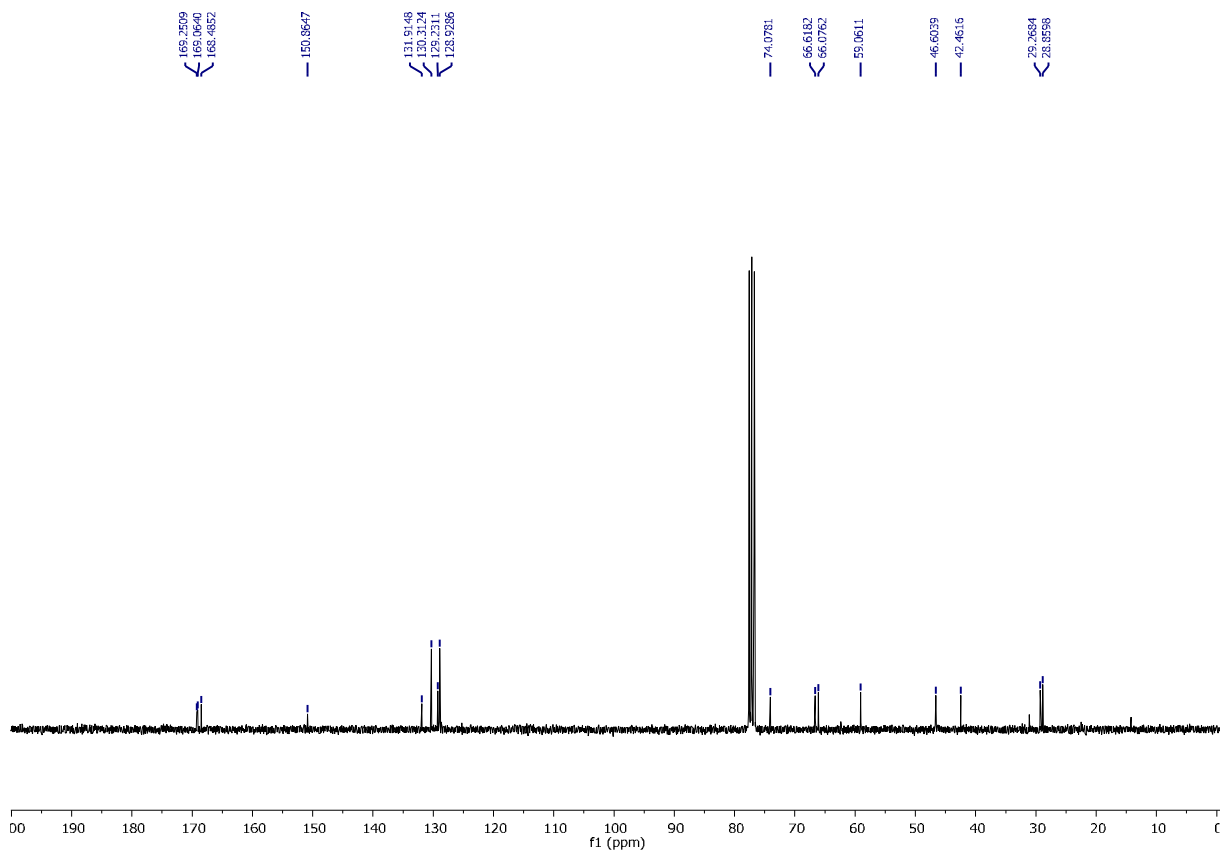
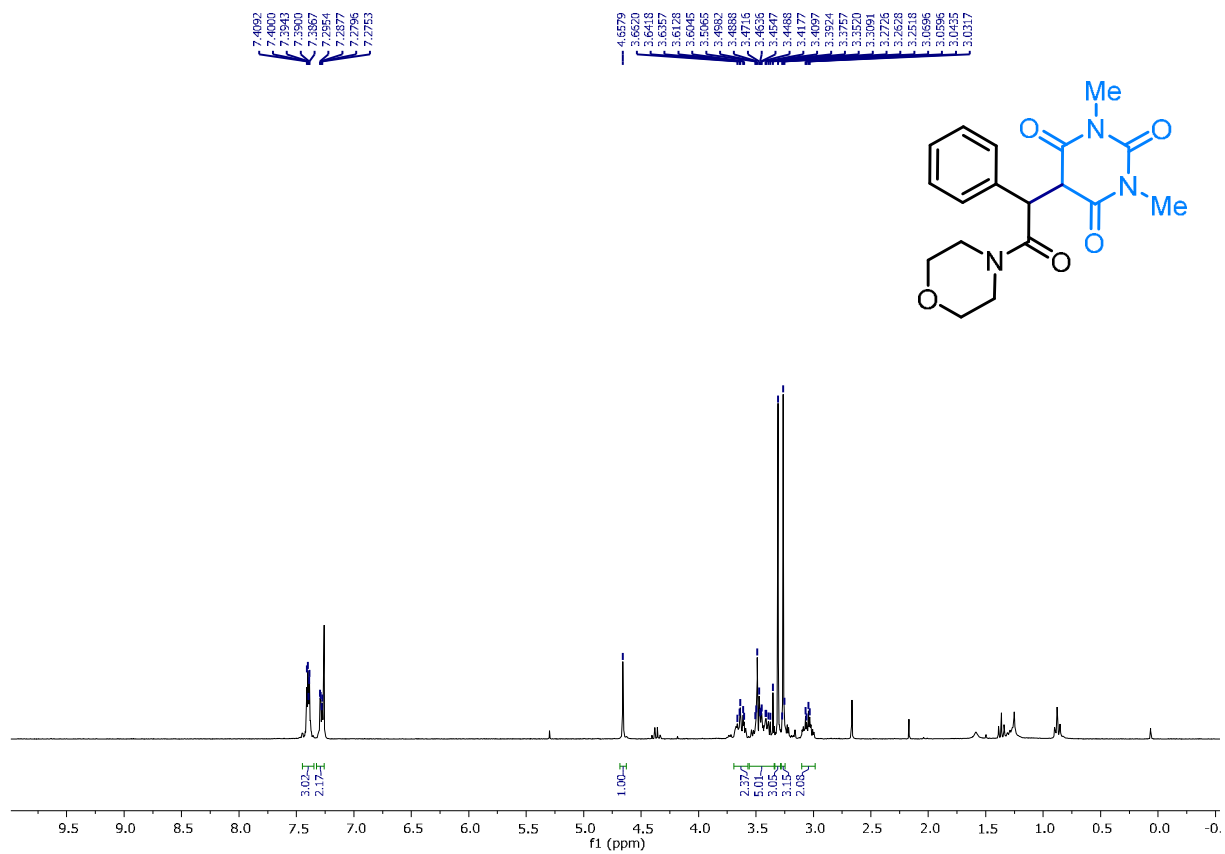
¹³C NMR of 2-[(4R)-4,8-dimethyl-1-morpholino-1-oxonon-7-en-2-yl]malononitrile (3ka)

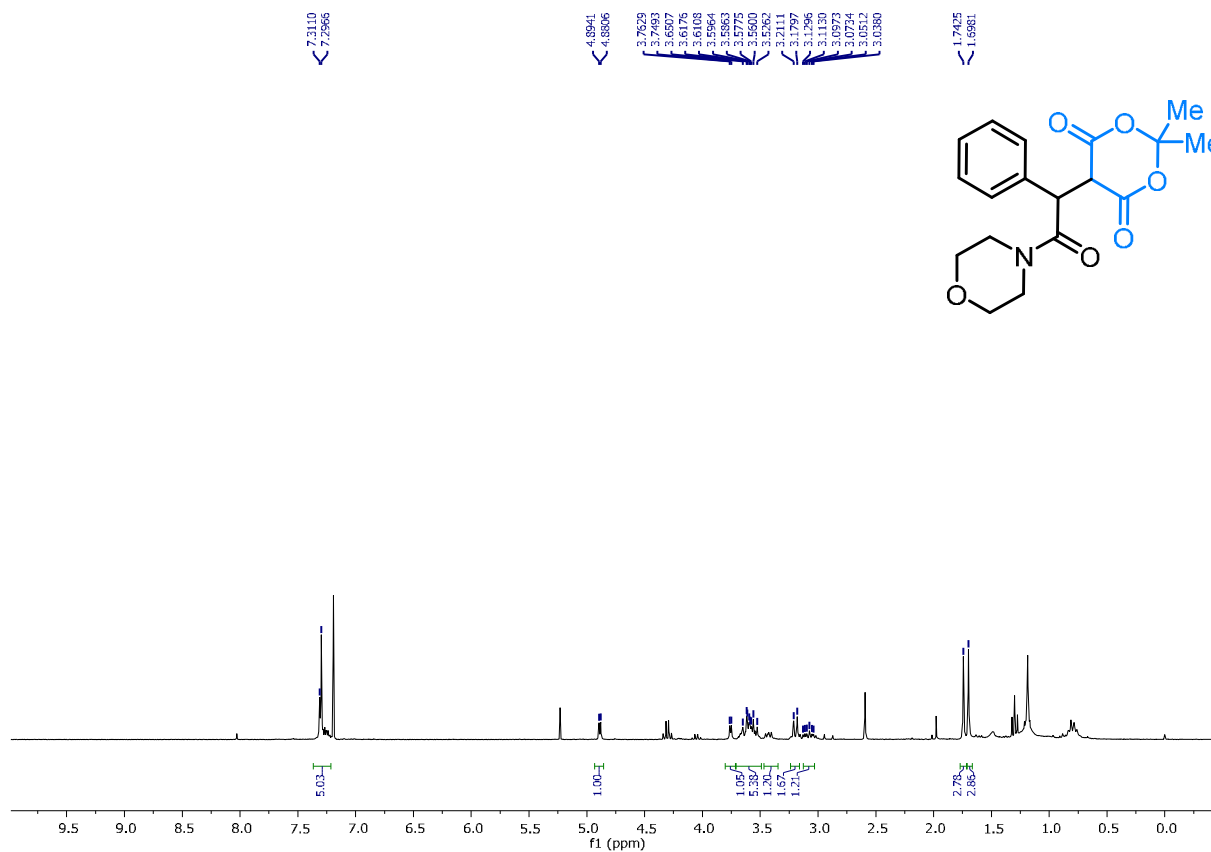


¹H NMR of 2-(2-morpholino-2-oxo-1-phenylethyl)-1*H*-indene-1,3(2*H*)-dione (3la)

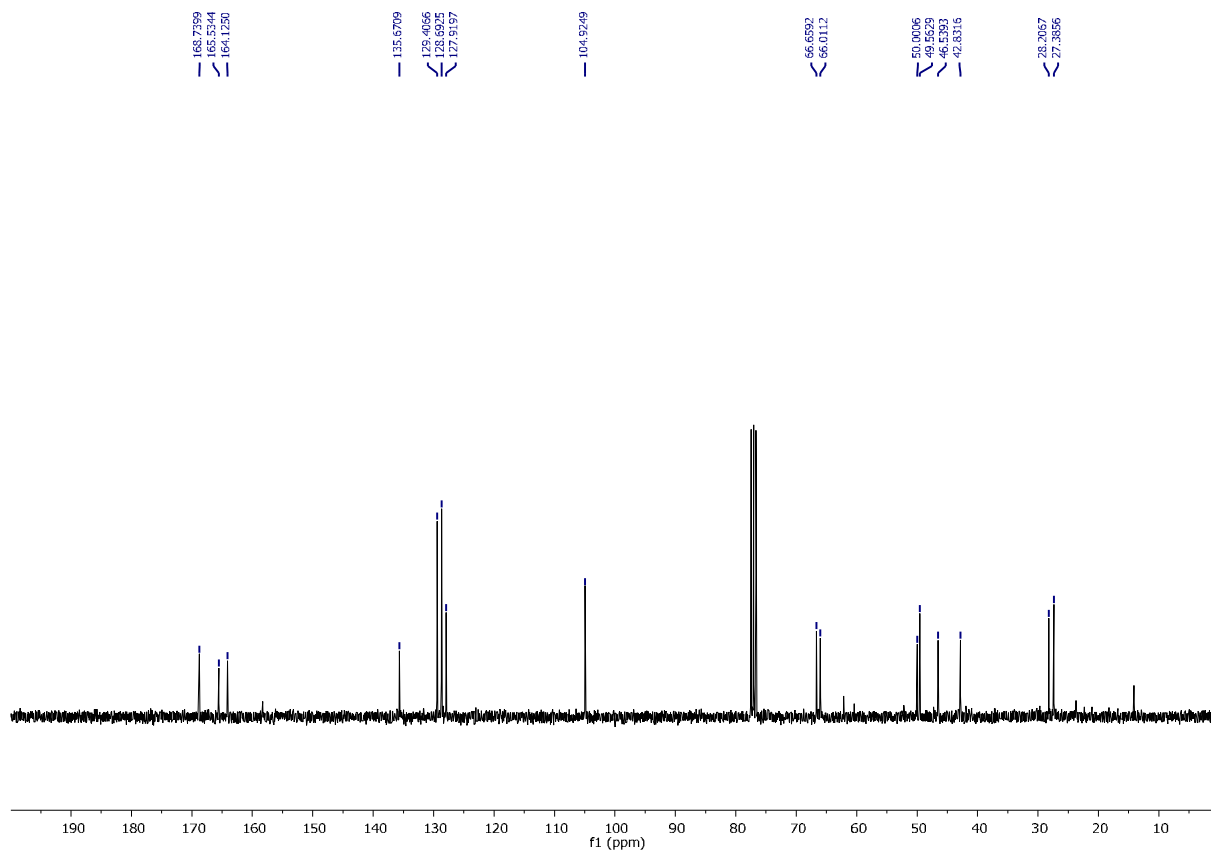


¹³C NMR of 2-(2-morpholino-2-oxo-1-phenylethyl)-1*H*-indene-1,3(2*H*)-dione (3la)

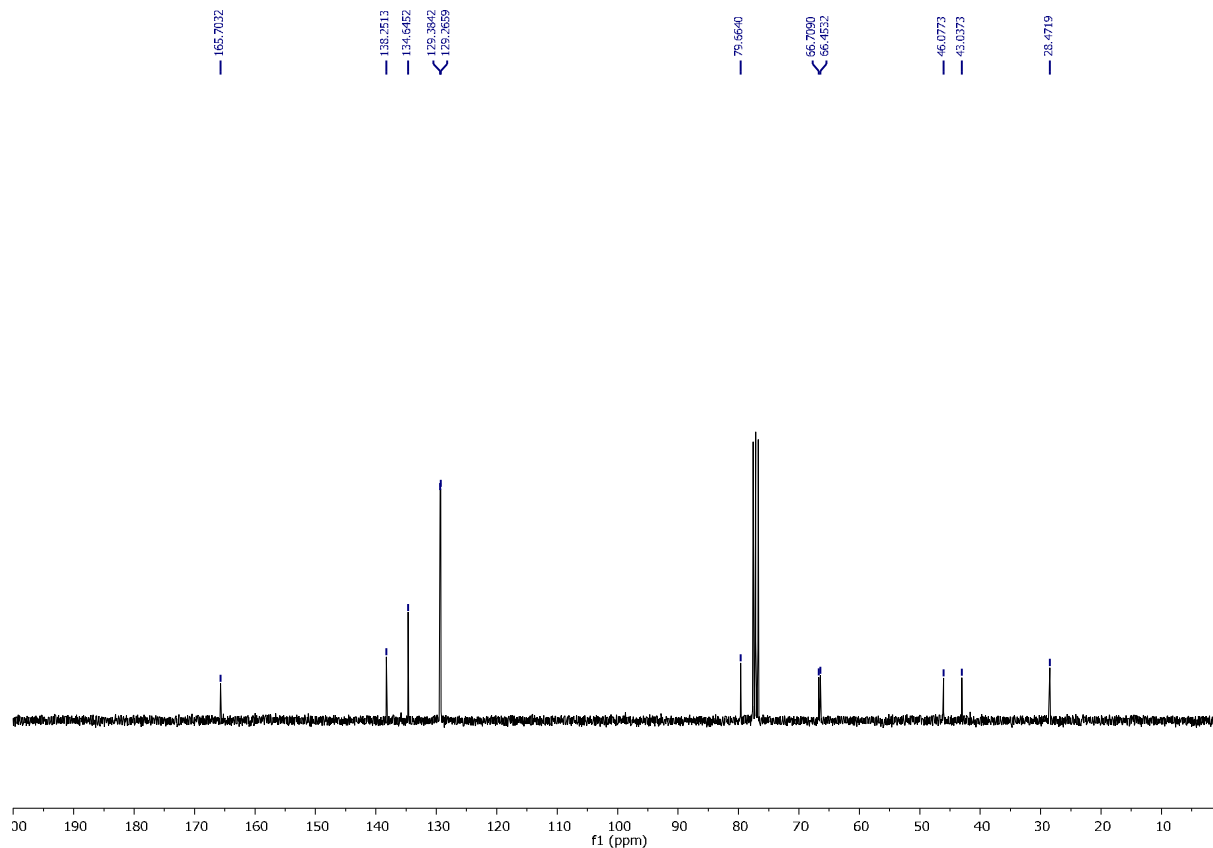
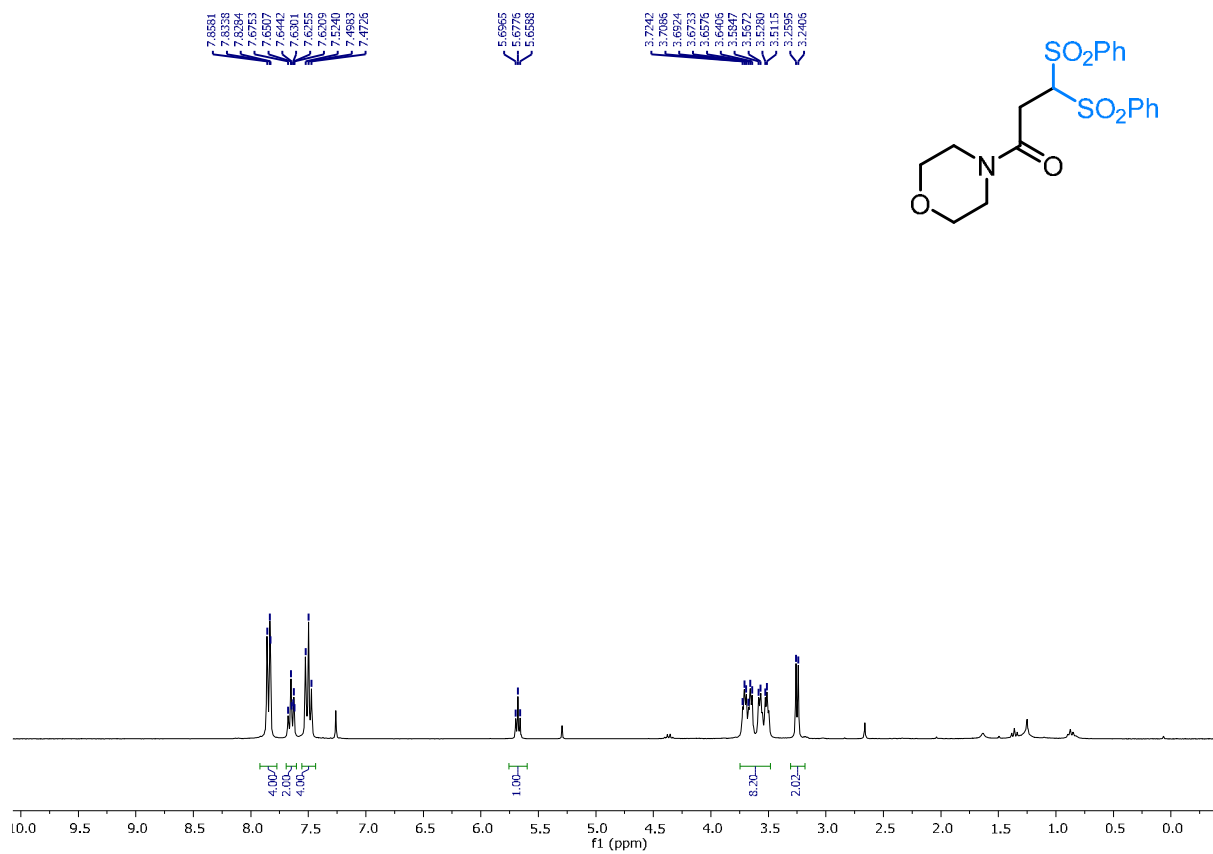


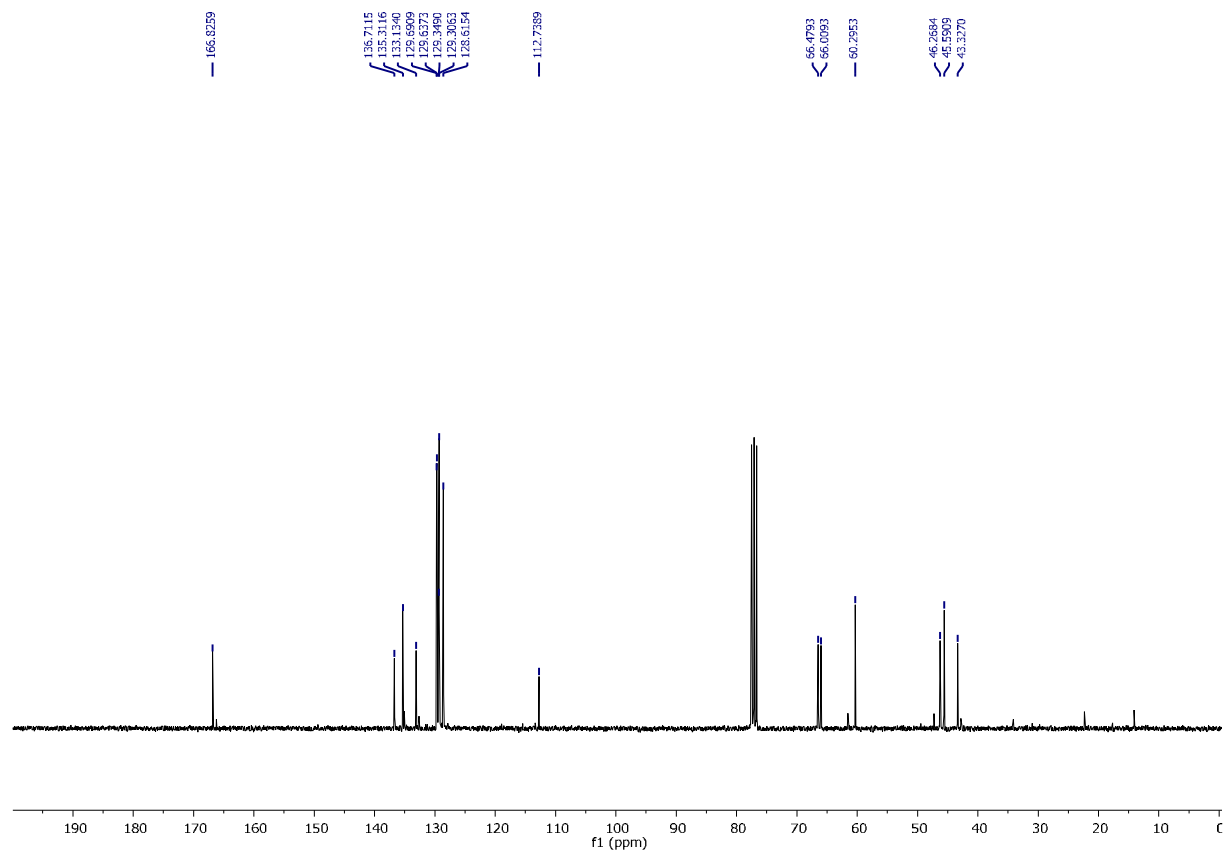
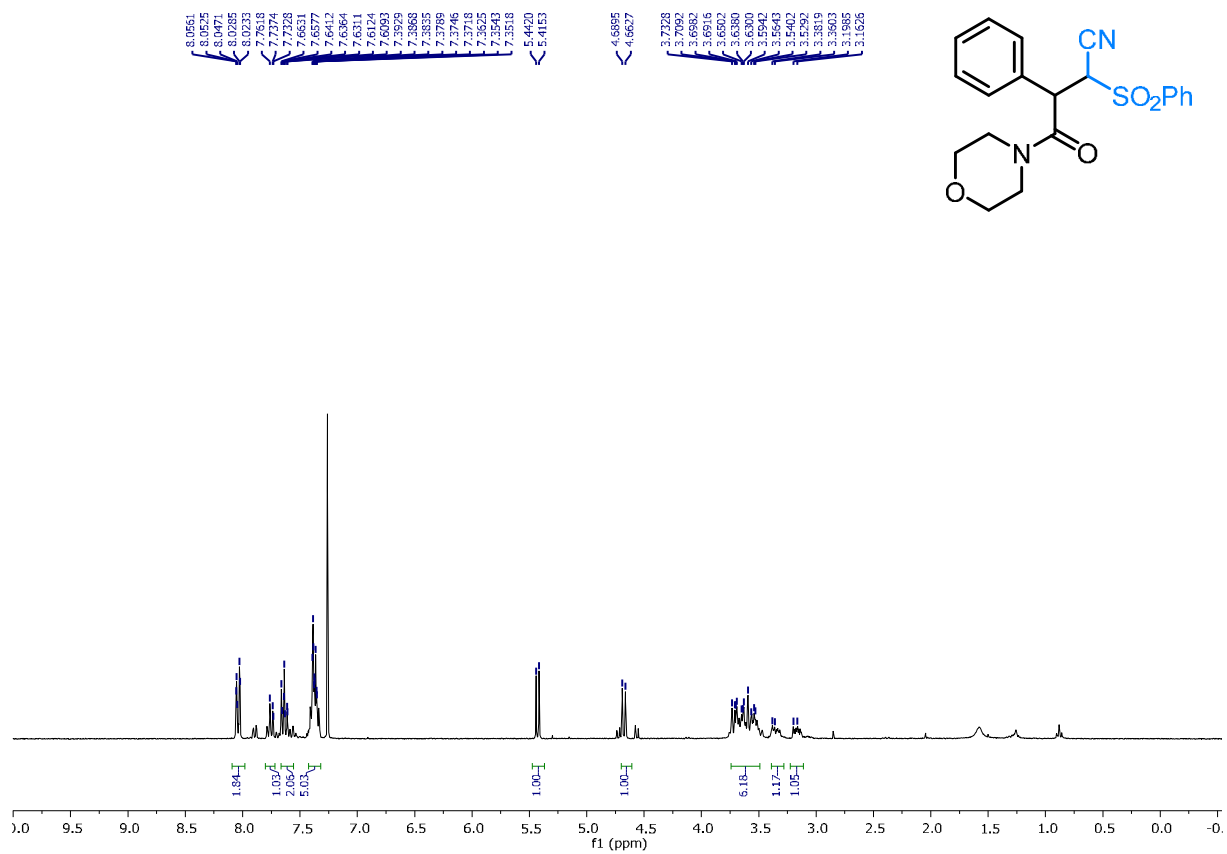


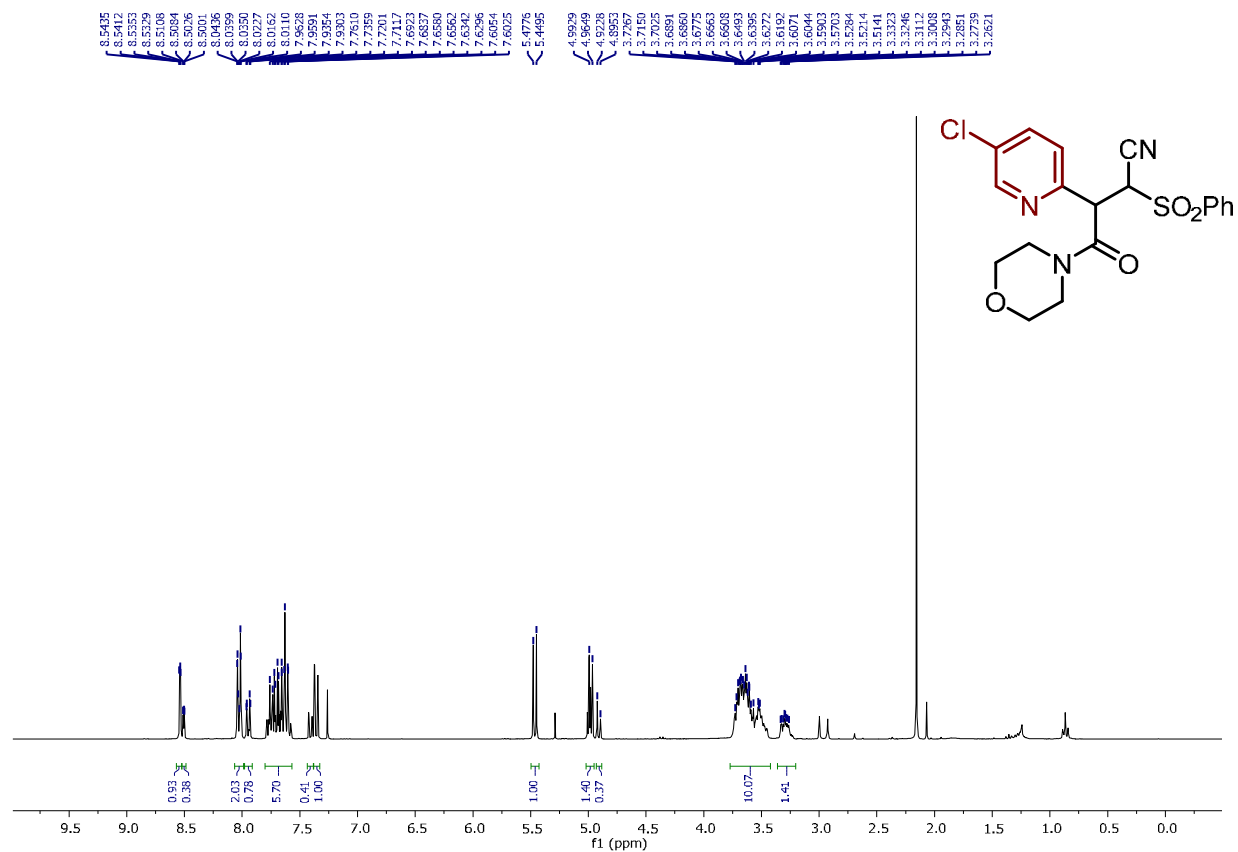
¹H NMR of 2,2-dimethyl-5-(2-morpholino-2-oxo-1-phenylethyl)-1,3-dioxane-4,6-dione (**3na**)



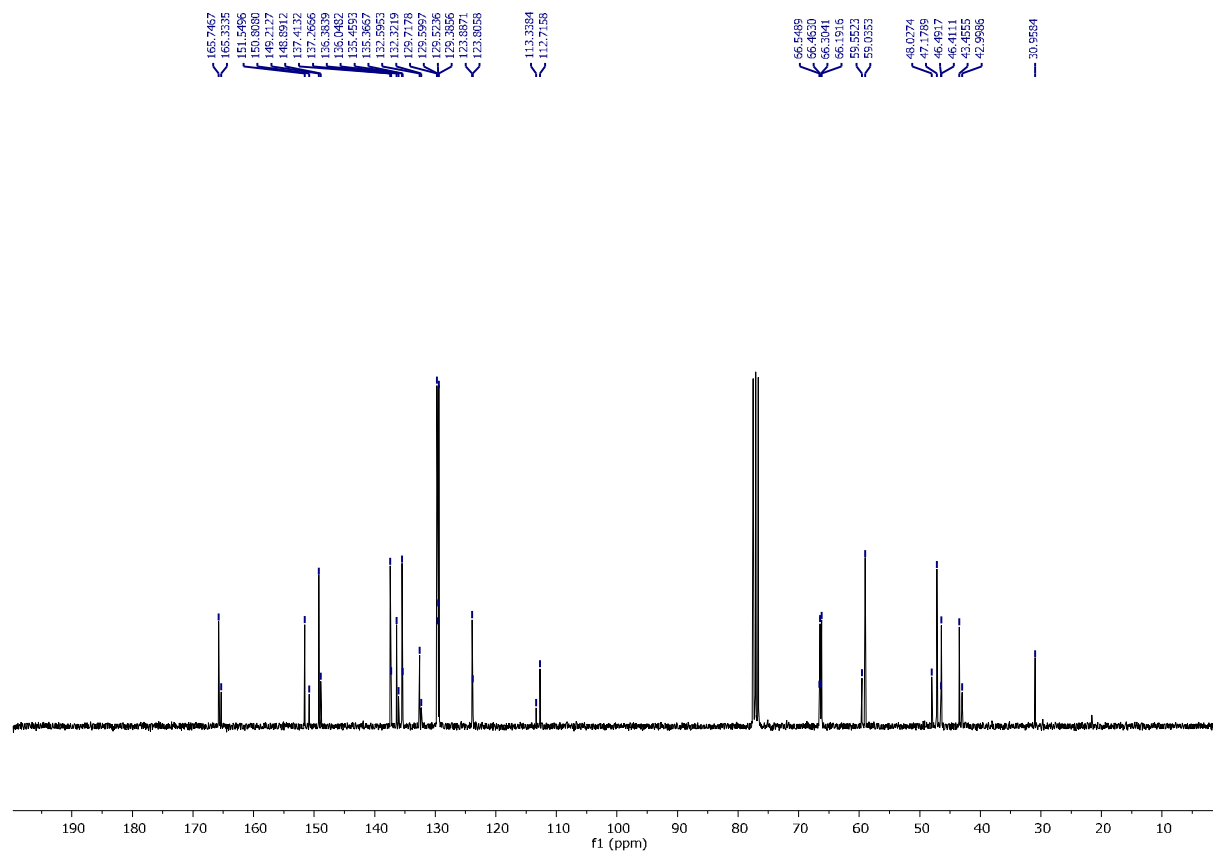
¹³C NMR of 2,2-dimethyl-5-(2-morpholino-2-oxo-1-phenylethyl)-1,3-dioxane-4,6-dione (**3na**)



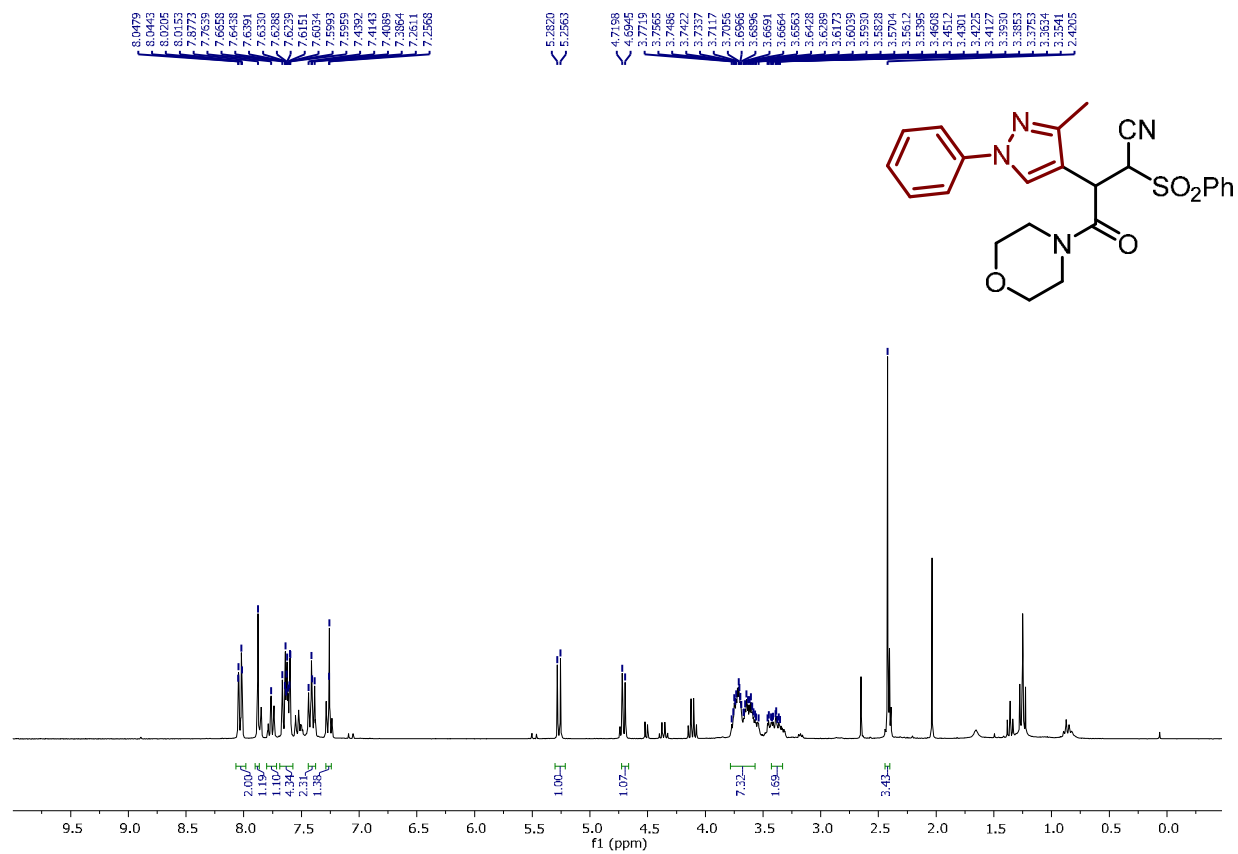




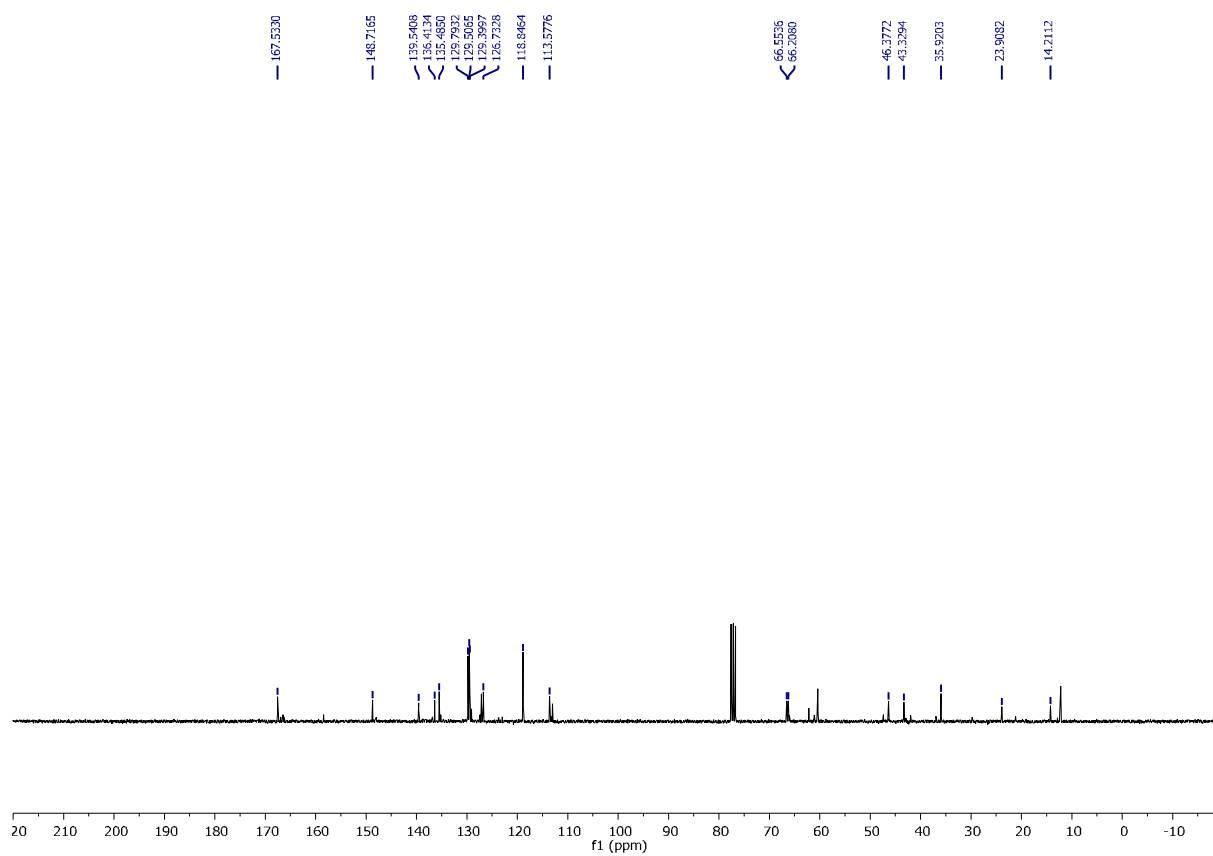
¹H NMR of 3-(5-chloropyridin-2-yl)-4-morpholino-4-oxo-2-(phenylsulfonyl)butanenitrile (3qa)

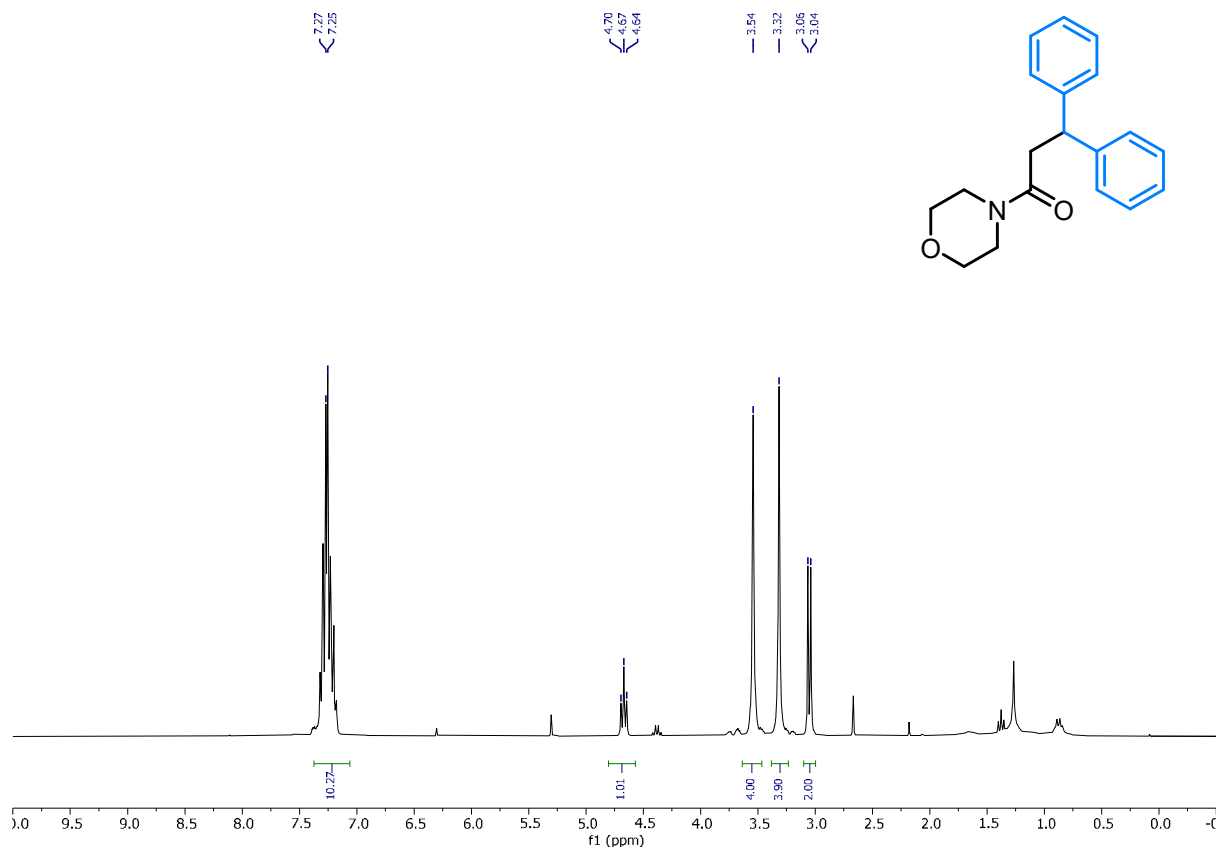


¹³C NMR of 3-(5-chloropyridin-2-yl)-4-morpholino-4-oxo-2-(phenylsulfonyl)butanenitrile (3qa)

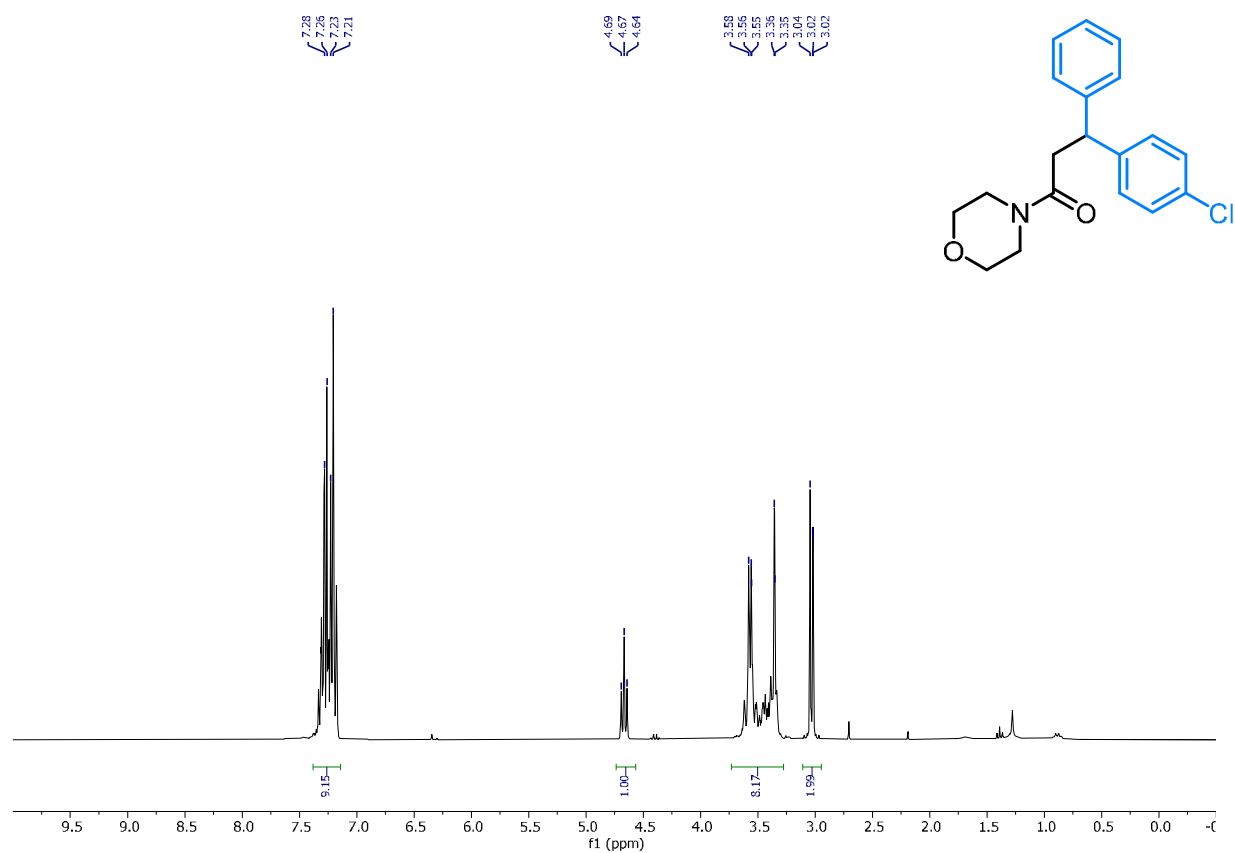


¹H NMR of 3-(3-methyl-1-phenyl-1H-pyrazol-4-yl)-4-morpholino-4-oxo-2-(phenylsulfonyl)butanenitrile (**3ra**)

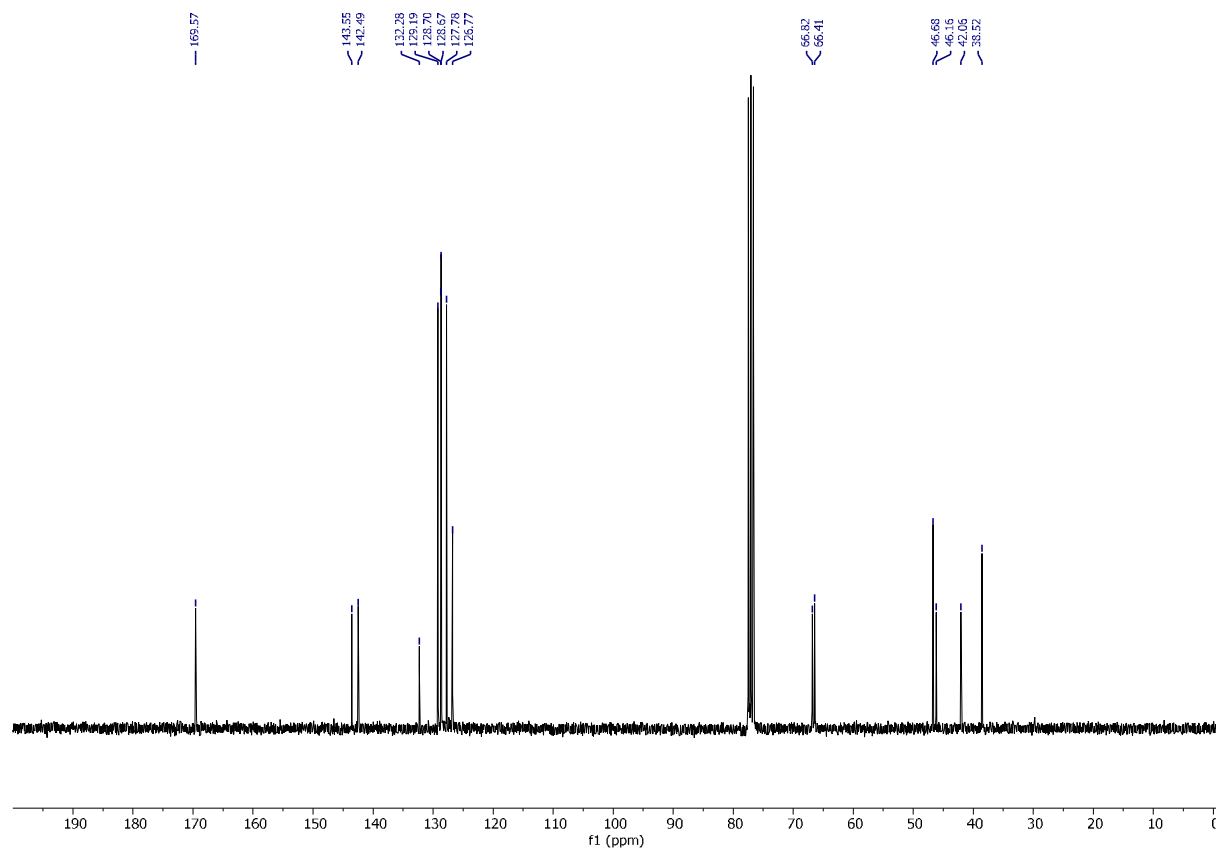




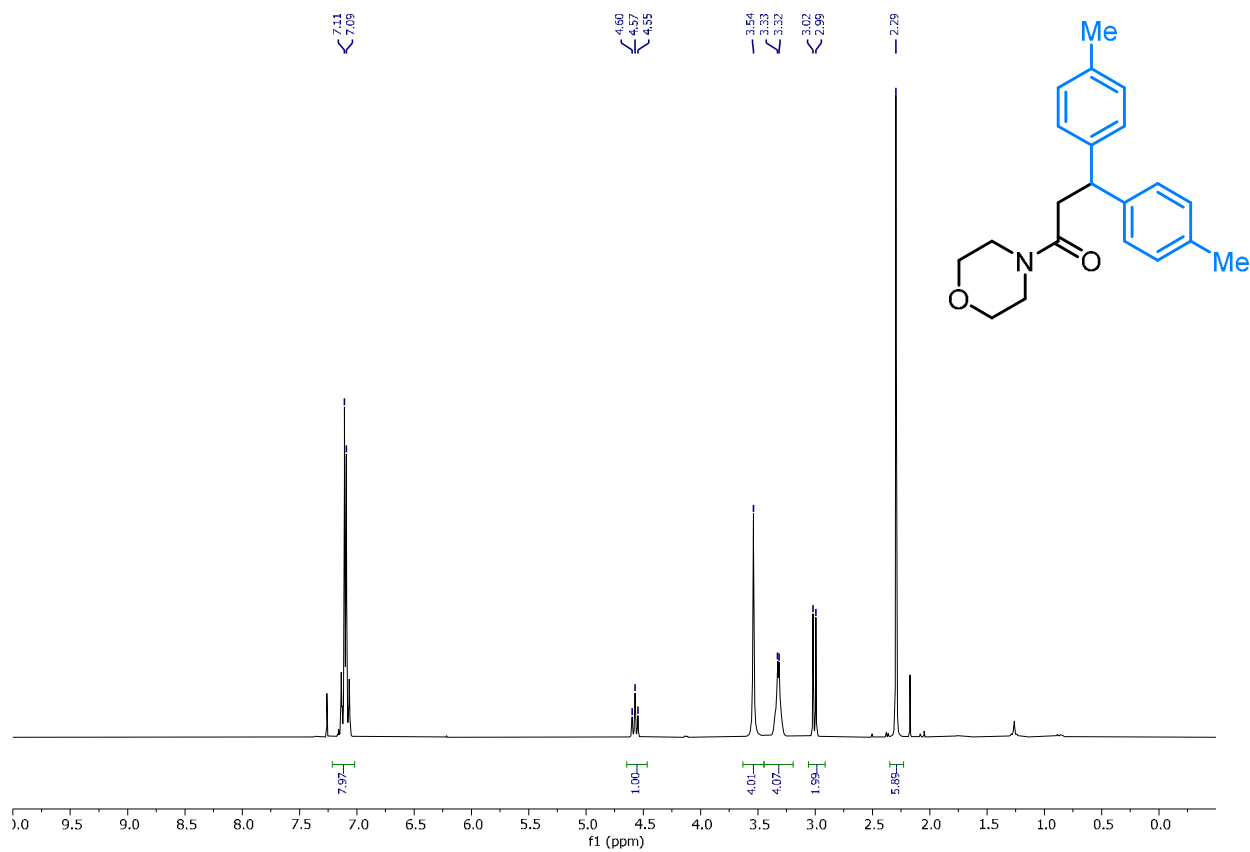
¹H NMR of 1-morpholino-3,3-diphenylpropan-1-one (3sa)



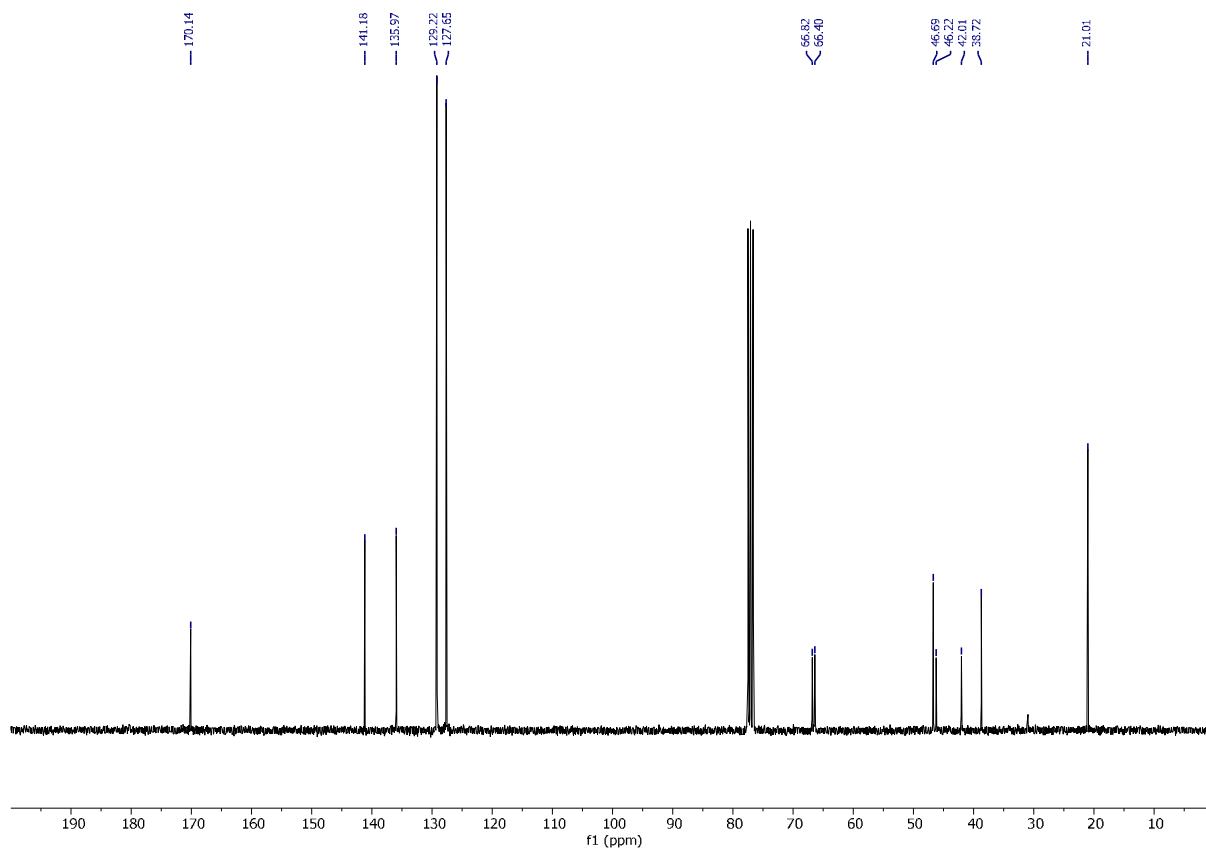
¹H NMR of 3-(4-chlorophenyl)-1-morpholino-3-phenylpropan-1-one (3ta)



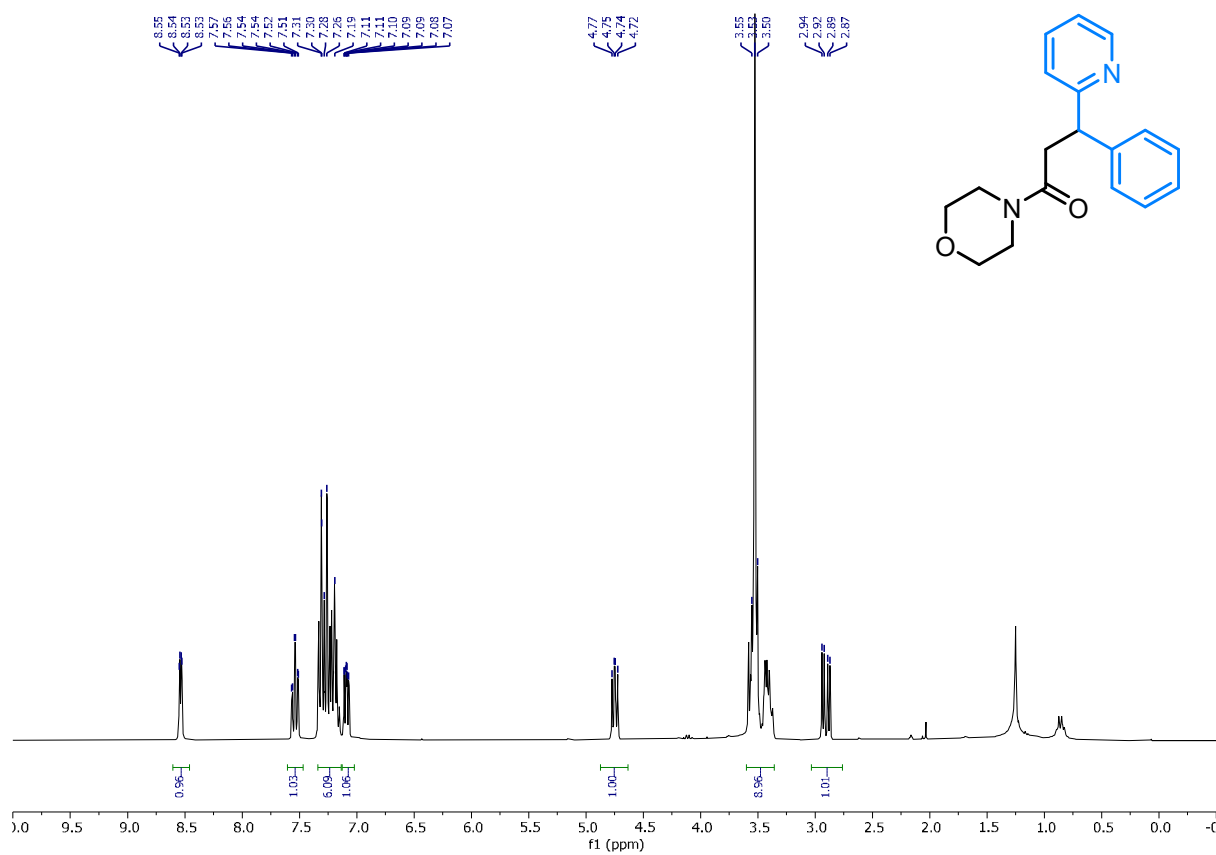
¹³C NMR of 3-(4-chlorophenyl)-1-morpholino-3-phenylpropan-1-one (**3ta**)



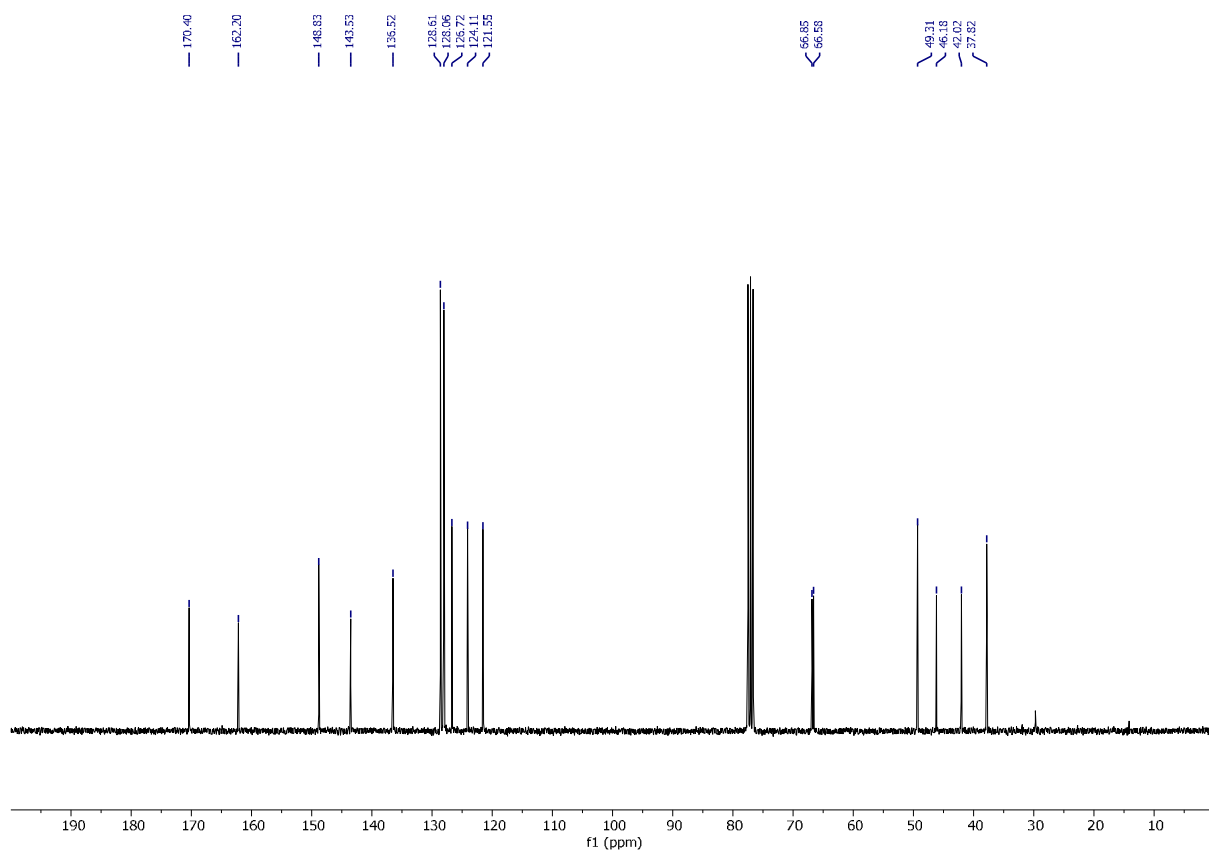
¹H NMR of 1-morpholino-3,3-di-p-tolylpropan-1-one (**3ua**)



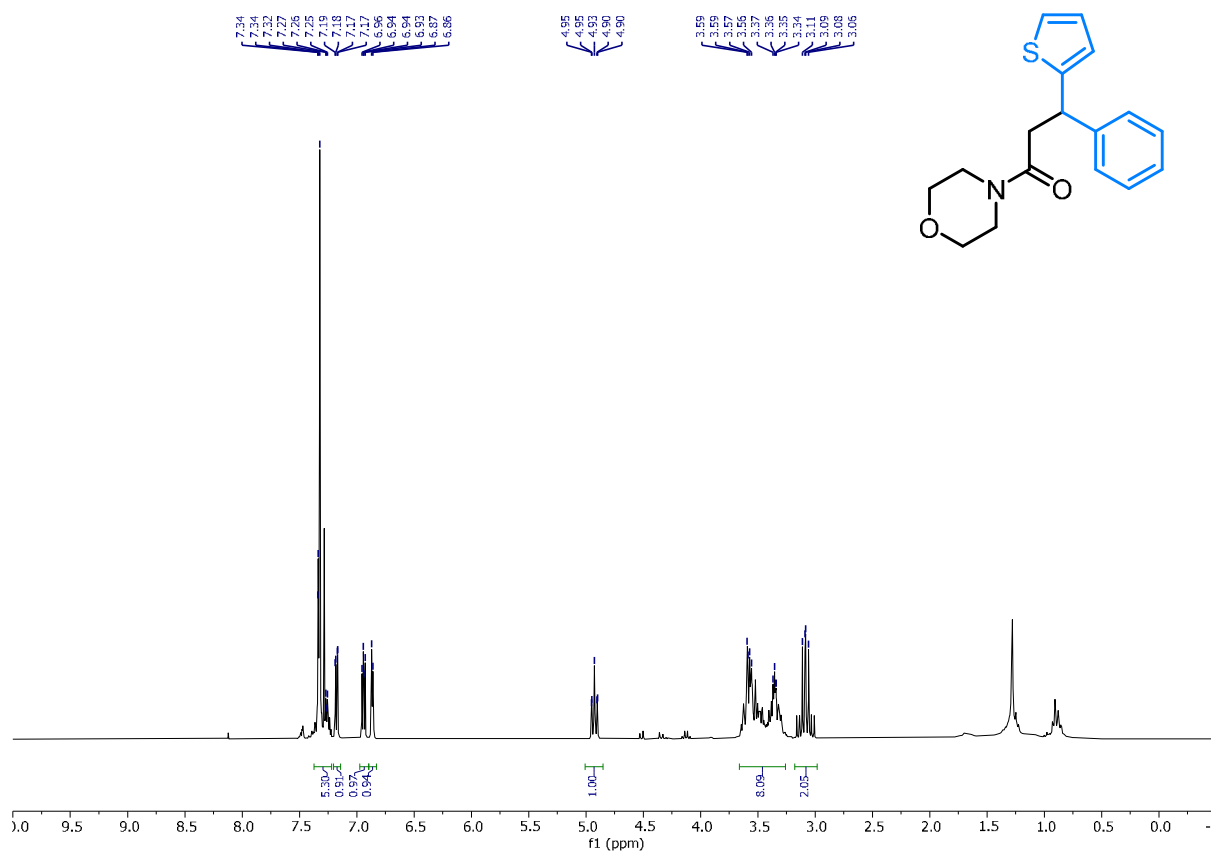
¹³C NMR of 1-morpholino-3,3-di-p-tolylpropan-1-one (3ua)



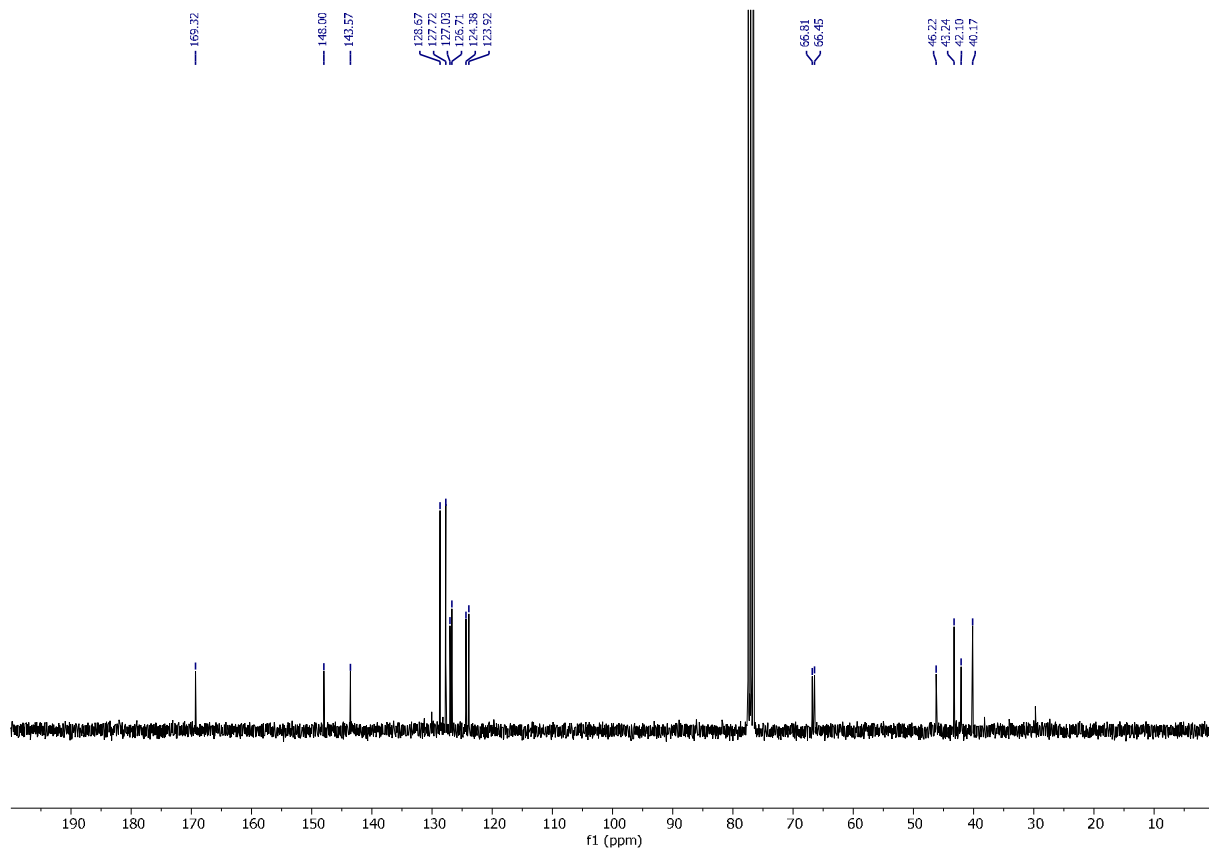
¹H NMR of 1-morpholino-3-phenyl-3-(pyridin-2-yl)propan-1-one (3va)



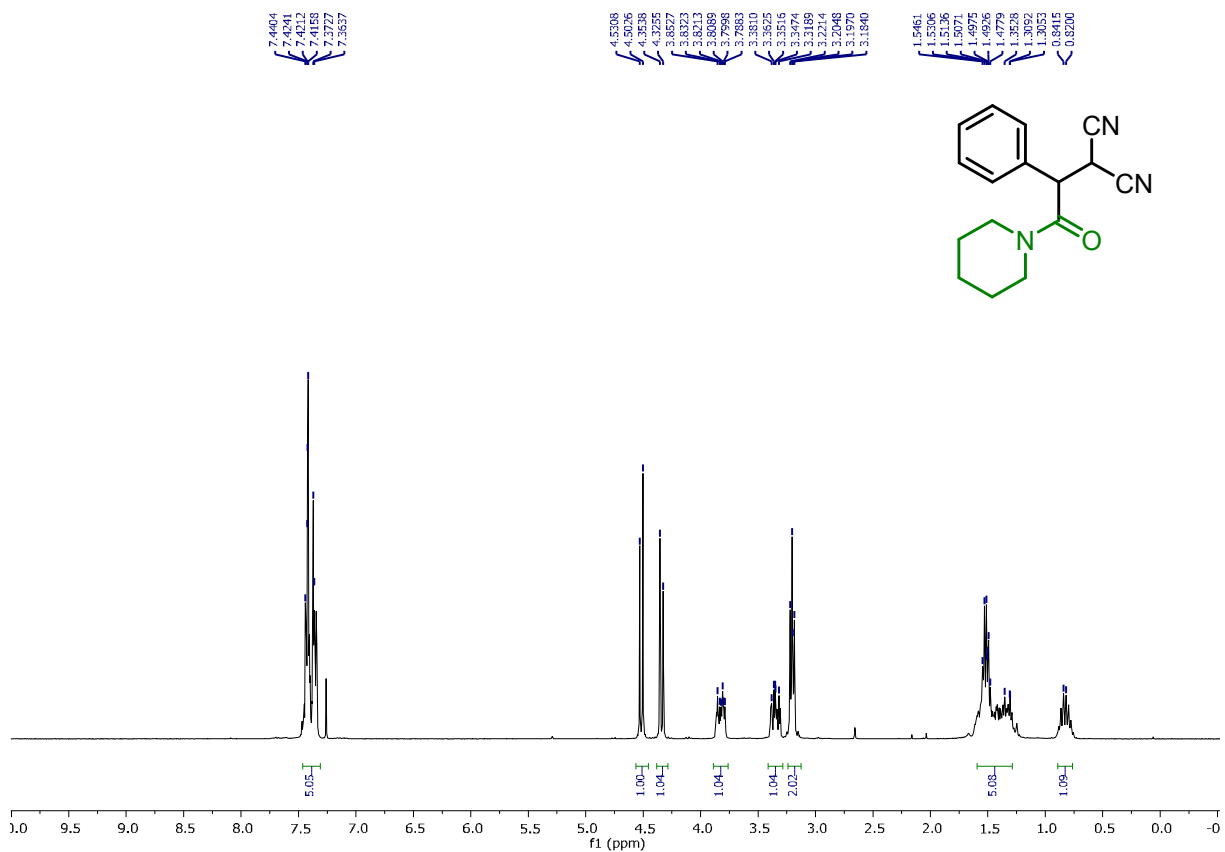
^{13}C NMR of 1-morpholino-3-phenyl-3-(pyridin-2-yl)propan-1-one (**3va**)



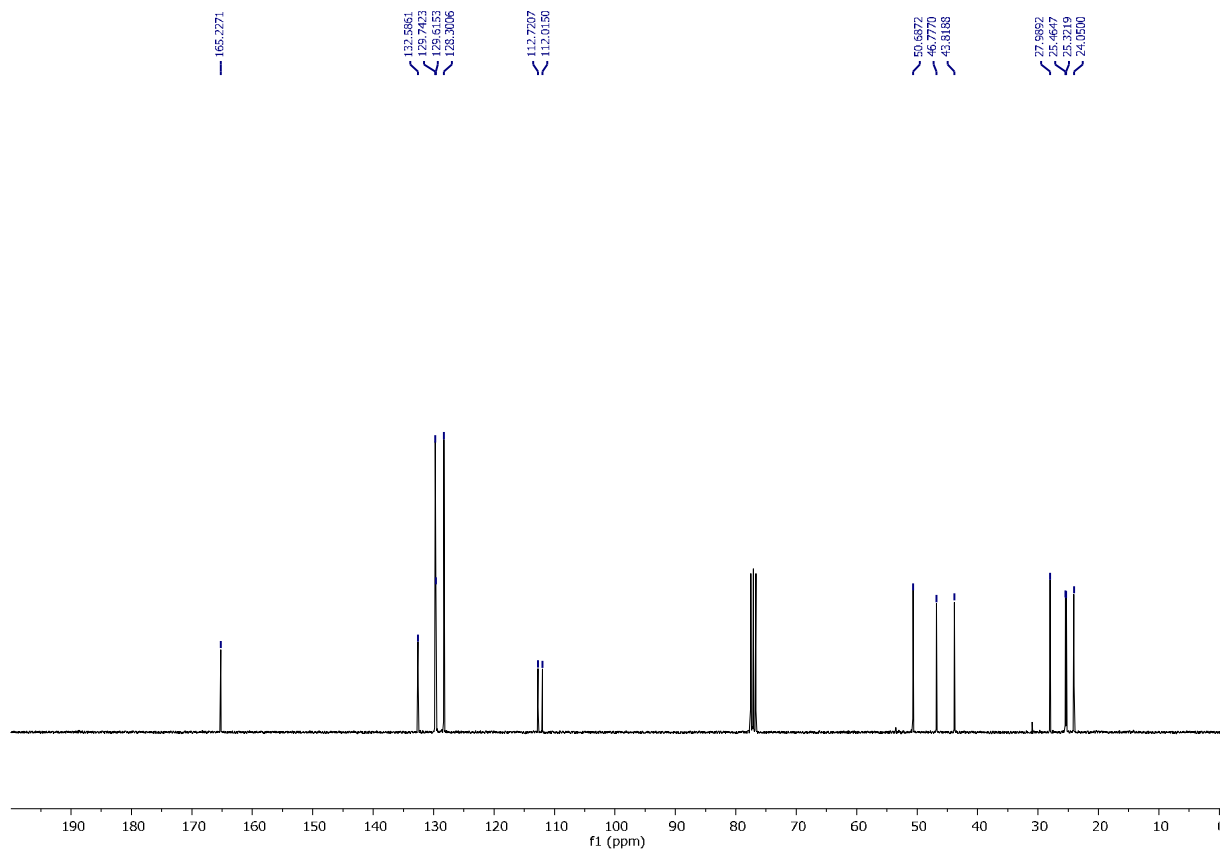
^1H NMR of 1-morpholino-3-phenyl-3-(thiophen-2-yl)propan-1-one (**3wa**)



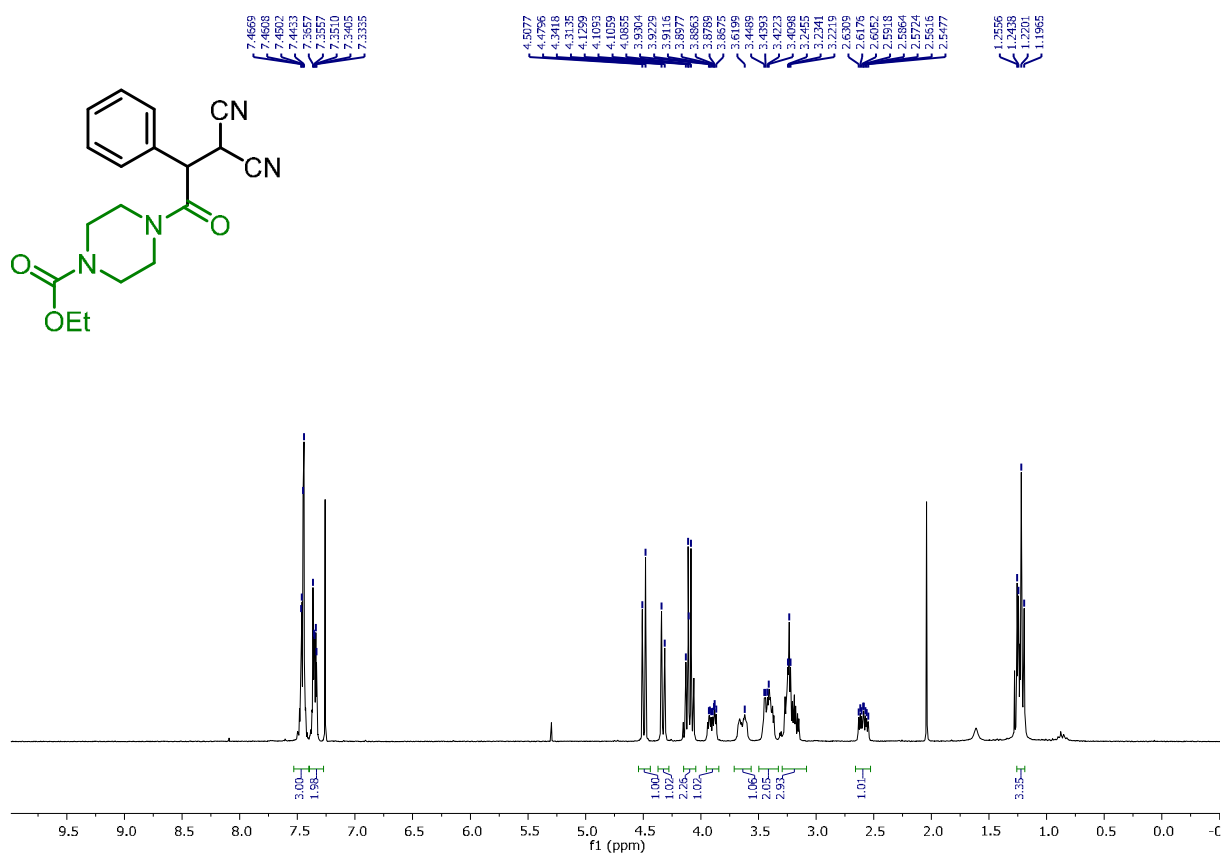
¹³C NMR of 1-morpholino-3-phenyl-3-(thiophen-2-yl)propan-1-one (**3wa**)



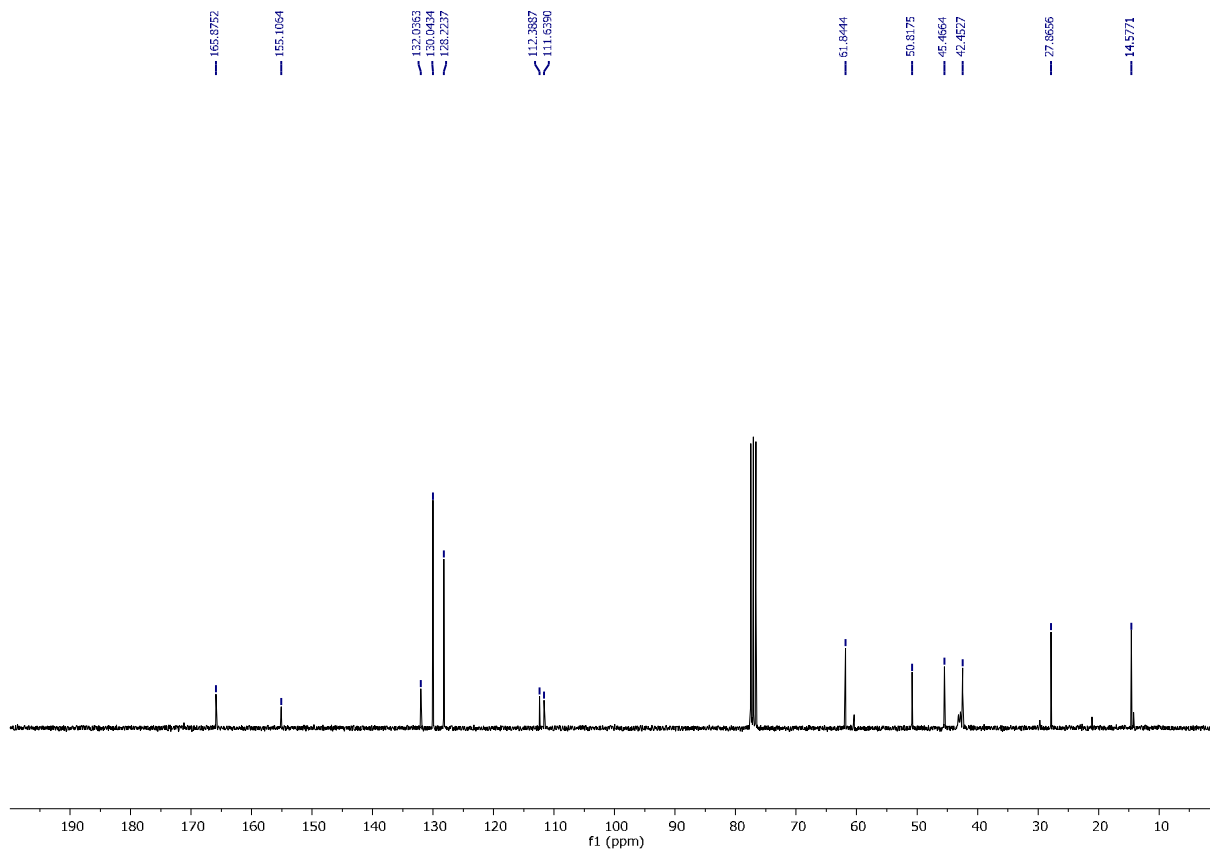
¹H NMR of 2-[2-oxo-1-phenyl-2-(piperidin-1-yl)ethyl]malononitrile (**3ab**)



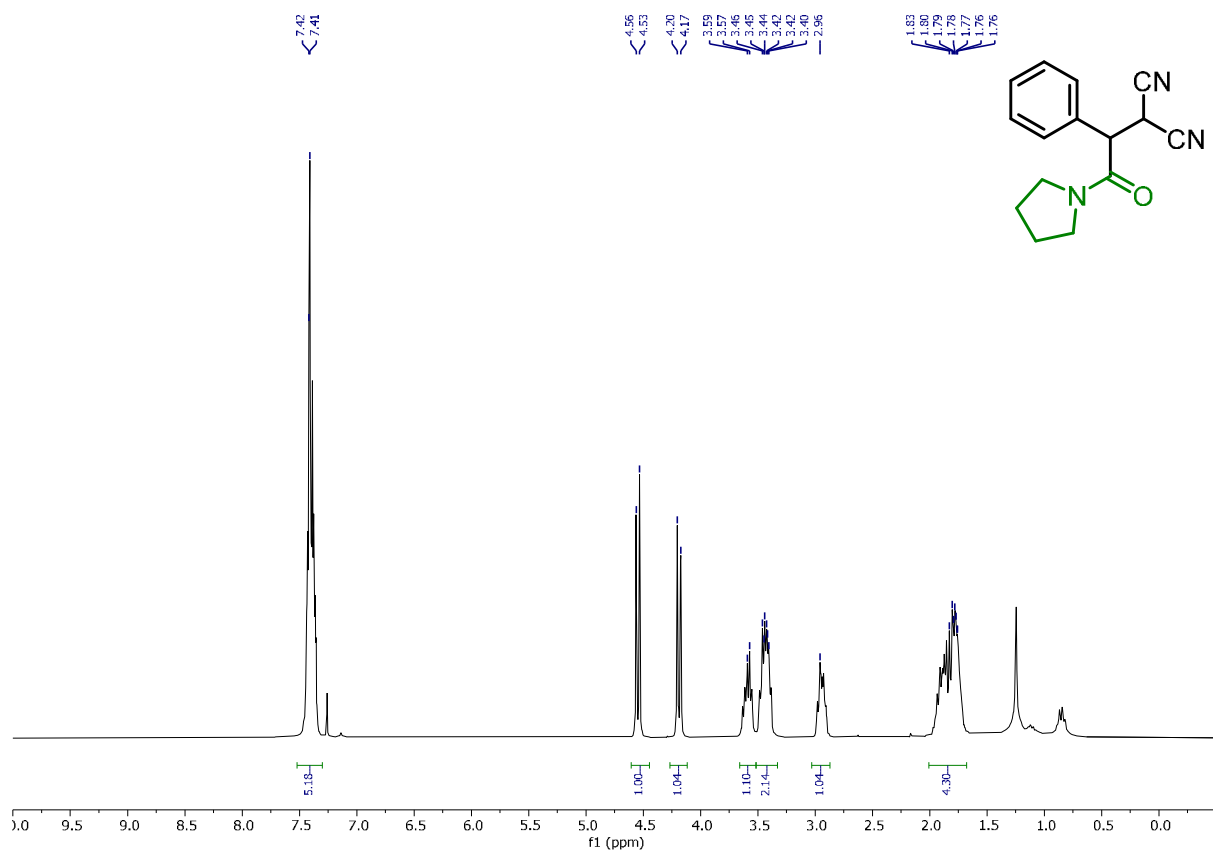
¹³C NMR of 2-[2-oxo-1-phenyl-2-(piperidin-1-yl)ethyl]malononitrile (**3ab**)



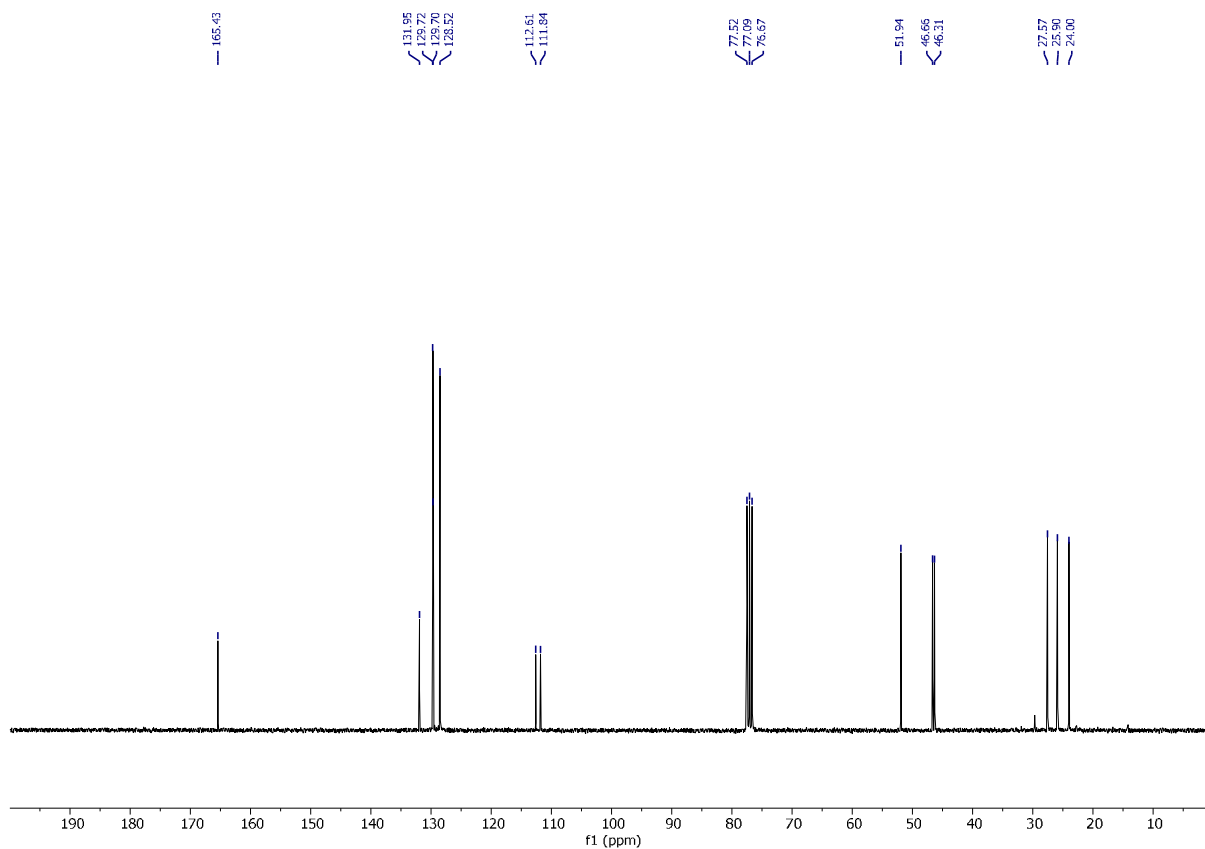
¹H NMR of ethyl 4-(3,3-dicyano-2-phenylpropanoyl)piperazine-1-carboxylate (**3ac**)



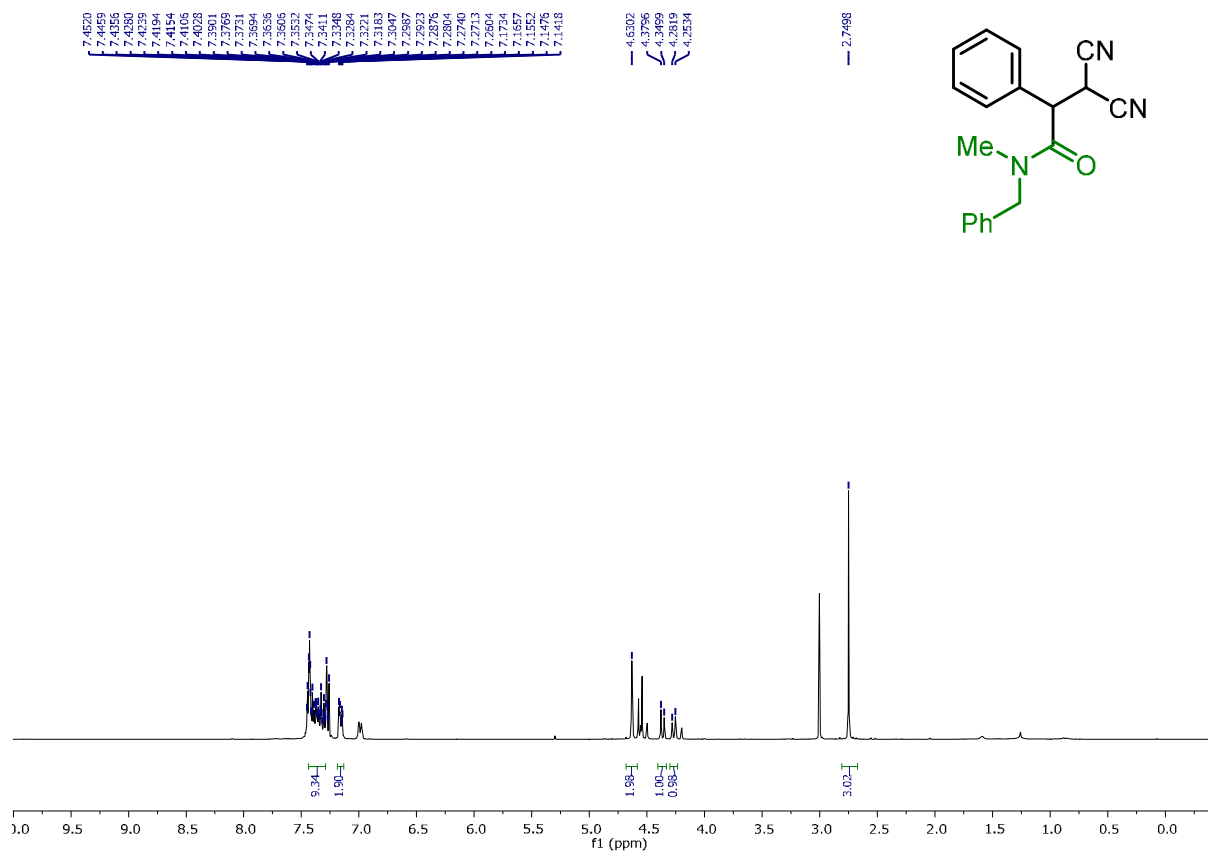
¹³C NMR of ethyl 4-(3,3-dicyano-2-phenylpropanoyl)piperazine-1-carboxylate (**3ac**)



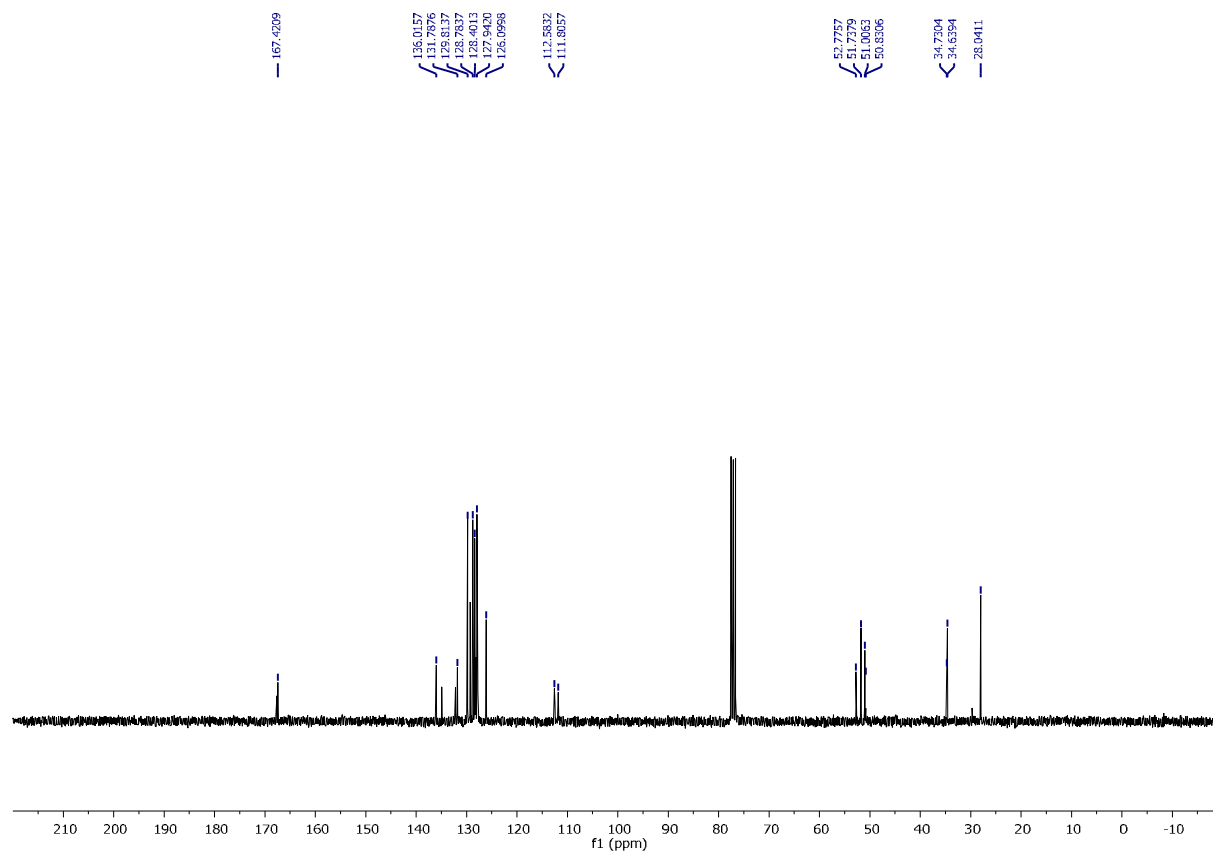
¹H NMR of 2-[2-oxo-1-phenyl-2-(pyrrolidin-1-yl)ethyl]malononitrile (**3ad**)



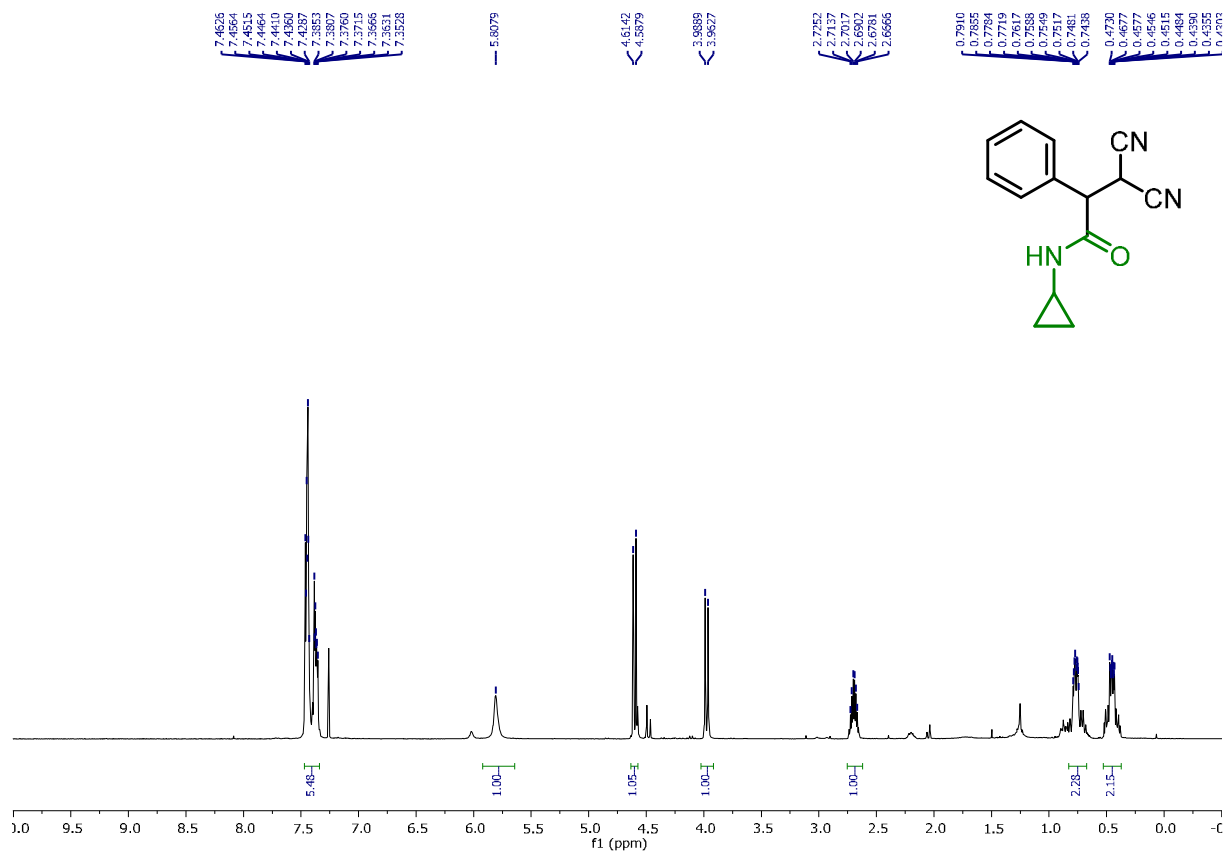
¹³C NMR of 2-[2-oxo-1-phenyl-2-(pyrrolidin-1-yl)ethyl]malononitrile (**3ad**)



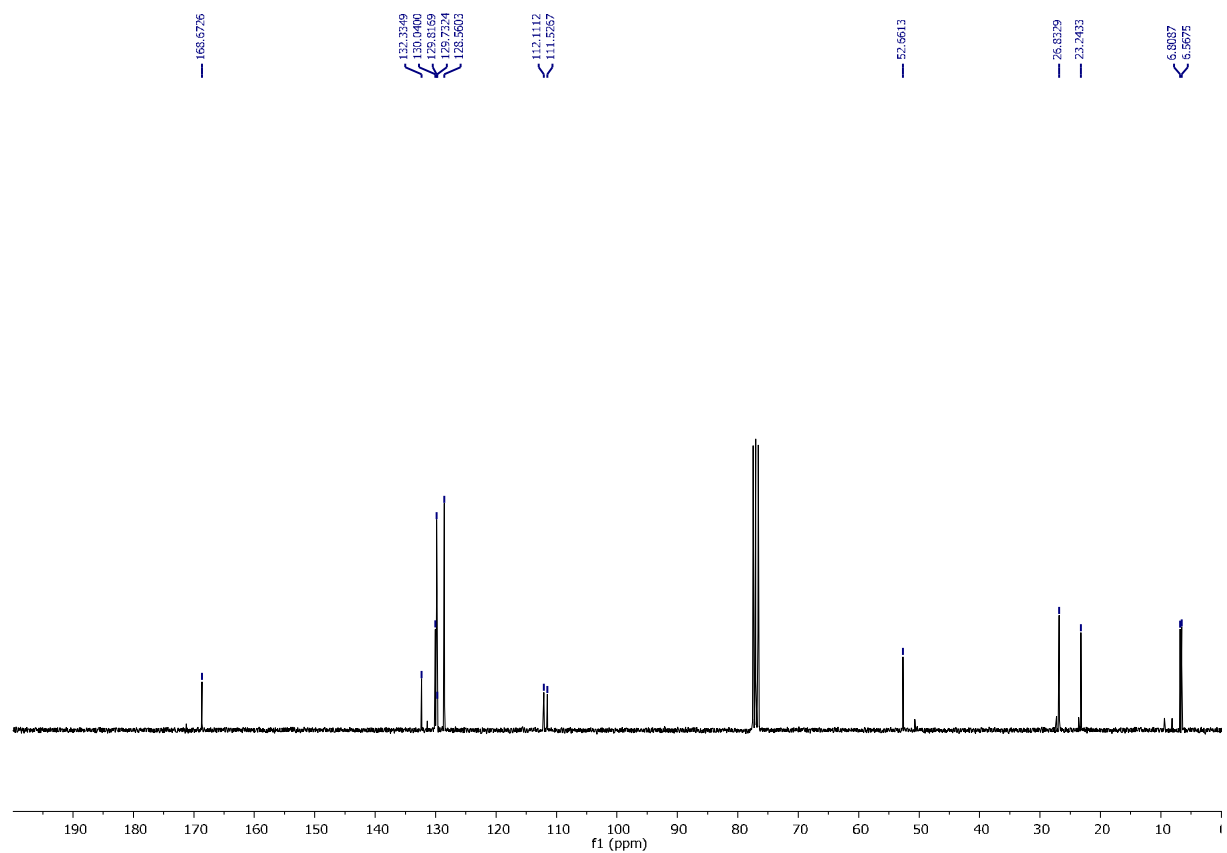
¹H NMR of *N*-benzyl-3,3-dicyano-*N*-methyl-2-phenylpropanamide (**3ae**)



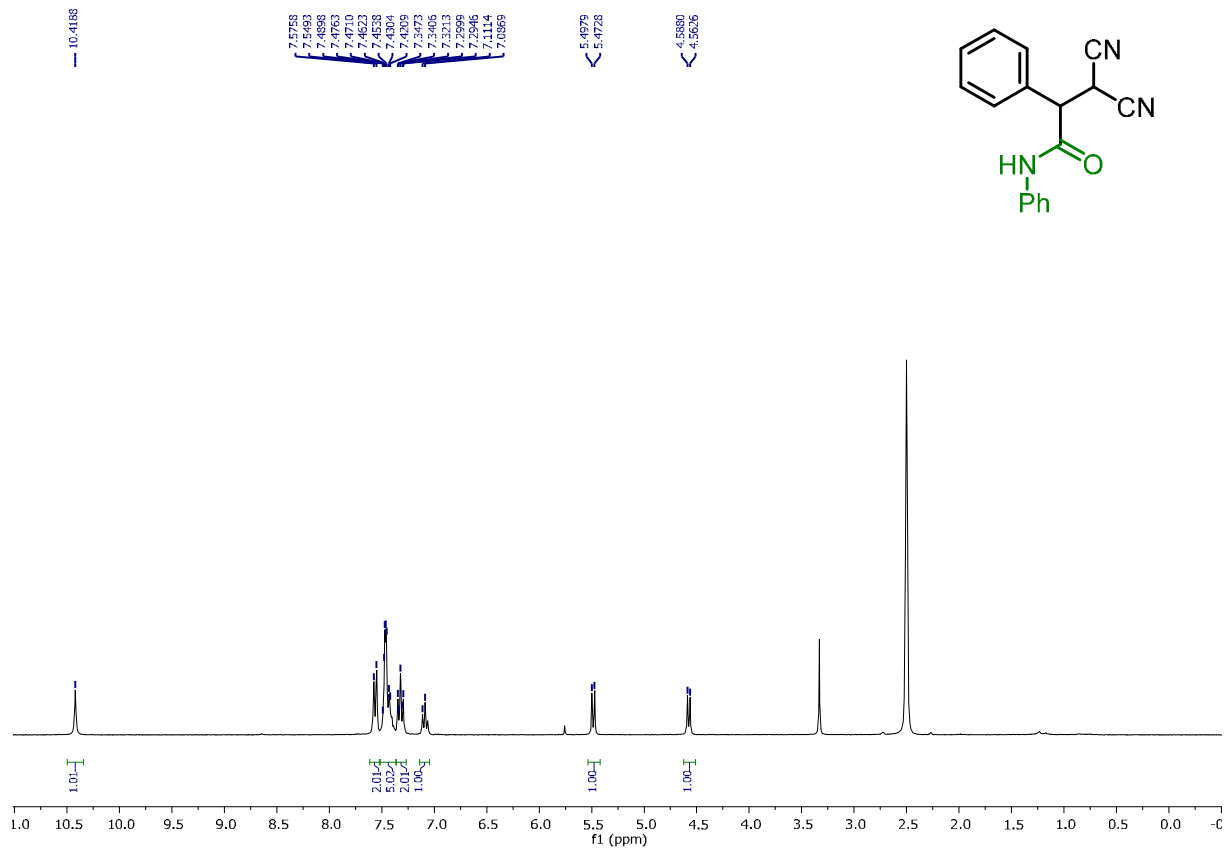
¹³C NMR of *N*-benzyl-3,3-dicyano-*N*-methyl-2-phenylpropanamide (**3ae**)



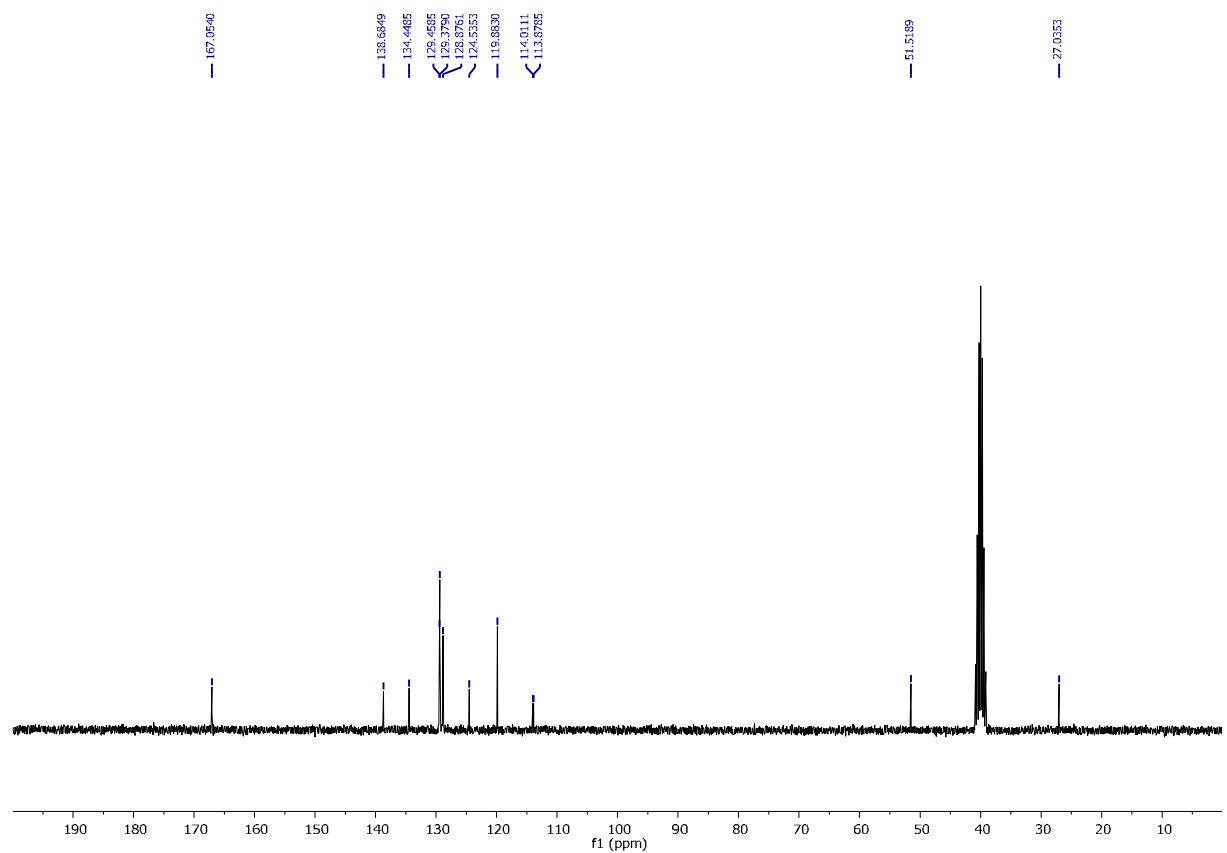
¹H NMR of 3,3-dicyano-*N*-cyclopropyl-2-phenylpropanamide (3af)



¹³C NMR of 3,3-dicyano-*N*-cyclopropyl-2-phenylpropanamide (3af)



¹H NMR of 3,3-dicyano-N,2-diphenylpropanamide (3ag)



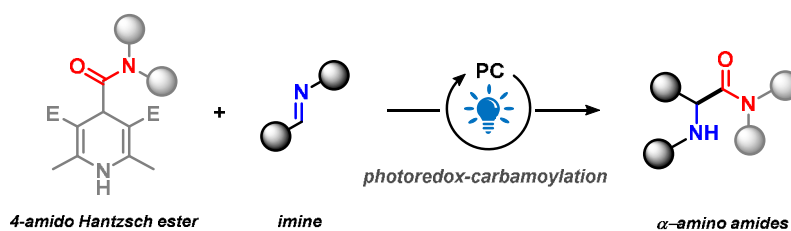
¹³C NMR of 3,3-dicyano-N,2-diphenylpropanamide (3ag)

4.5 References

- [1] a) B. Giese, *Angew. Chem. Int. Ed.* **1983**, *22*, 753-764; General reviews: b) W. Zhang, *Tetrahedron* **2001**, *57*, 7237-7262; c) G. S. C. Srikanth, S. L. Castle, *Tetrahedron* **2005**, *61*, 10377-10441; d) G. J. Rowlands, *Tetrahedron* **2009**, *65*, 8603-8655; e) C. P. O. Jasperese, D. P. Curran, T. L. Fevig, *Chem. Rev.* **1991**, *91*, 1237-1286.
- [2] a) B. Giese, J. A. Gonzalez-Gomez, T. Witzel, *Angew. Chem. Int. Ed.* **1984**, *23*, 69-70; b) C. Chatgililoglu, D. Crich, M. Komatsu, I. Ryu, *Chem. Rev.* **1999**, *99*, 1991-2069; c) G. Bryon Gill, G. Pattenden, S. J. Reynolds, *J. Chem. Soc., Perkin Trans. 1* **1994**, 369-378.
- [3] a) C. Raviola, S. Protti, D. Ravelli, M. Fagnoni, *Green Chem.* **2019**, *21*, 748-764. For recent selected examples of photoredox-mediated Giese reactions: b) A. Millet, Q. Lefevre, M. Rueping, *Chem. Eur. J.* **2016**, *22*, 13464-13468; c) N. P. Ramirez, J. C. Gonzalez-Gomez, *Eur. J. Org. Chem.* **2017**, 2154-2163; d) A. El Marrouni, C. B. Ritts, J. Balsells, *Chem. Sci.* **2018**, *9*, 6639-6646; e) B. Abadie, D. Jardel, G. Pozzi, P. Toullec, J.-M. Vincent, *Chem. Eur. J.* **2019**, *25*, 16120-16127.
- [4] a) F. Coppa, F. Fontana, E. Lazzarini, F. Minisci, *Heterocycles* **1993**, *36*, 2687; b) M. Jouffroy, J. Kong, *Chem. Eur. J.* **2019**, *25*, 2217-2221; c) A. H. Jatoi, G. G. Pawar, F. Robert, Y. Landais, *Chem. Commun.* **2019**, 55, 466-469.
- [5] D. Elad, J. Rokach, *J. Org. Chem.* **1964**, *29*, 7, 1855-1859.
- [6] W. F. Petersen, R. J. K. Taylor, J. R. Donald, *Org. Biomol. Chem.* **2017**, *15*, 5831-5845.
- [7] A. Q.-F. Bai, C. Jin, J.-Y. He, G. Feng, *Org. Lett.* **2018**, *20*, 2172-2175.
- [8] P.-Z. Wang, J.-R. Chen, W.-J. Xiao, *Org. Biomol. Chem.* **2019**, *17*, 6936-6951.
- [9] a) G. Goti, B. Bieszcza, A. Vega-Peñalosa, P. Melchiorre, *Angew. Chem. Int. Ed.* **2019**, *58*, 1213-1217; b) B. Bieszcza, L. A. Perego, P. Melchiorre, *Angew. Chem. Int. Ed.* **2019**, *58*, 16878-16883.
- [10] N. Alandini, L. Buzzetti, G. Favi, T. Schulte, L. Candish, K. D. Collins, P. Melchiorre, *Angew. Chem. Int. Ed.* **2020**, *59*, 2-8.
- [11] E. Speckmeier, T. G. Fischer, K. Zeitler, *J. Am. Chem. Soc.* **2018**, *140*, 15353-15365.
- [12] S. Fukuzumi, H. Kotani, K. Ohkubo, S. Ogo, N. V. Tkachenko, H. Lemmetyinen, *J. Am. Chem. Soc.* **2004**, *126*, 1600-1601.
- [13] L. Capaldo, D. Merli, M. Fagnoni, D. Ravelli, *ACS Catal.* **2019**, *9*, 3054-3058.
- [14] J. Jung, J. Kim, G. Park, Y. You, E. J. Cho, *Adv. Synth. Catal.* **2016**, *358*, 74-80.
- [15] a) D. M. Hedstrand, W. M. Kruizinga, R. M. Kellogg, *Tetrahedron Lett.* **1978**, *19*, 1255-1258; b) J. Zhang, M.-Z. Jin, W. Zhang, L. Yang, Z.-L. Liu, *Tetrahedron Lett.* **2002**, *43*, 9687-9689; c) J. Jung, J. Kim, G. Park, Y. You, E. J. Cho, *Adv. Synth. Catal.* **2016**, *358*, 74-80; d) M. O. Konev, L. Cardinale, A. Jacobi von Wangelin *Org. Lett.* **2020**, *22*, 1316-1320.
- [16] a) J. Zhang, Y. Li, R. Xu, Y. Chen, *Angew. Chem. Int. Ed.* **2017**, *56*, 12619-12623; b) L. Buzzetti, A. Prieto, S. R. Roy, P. Melchiorre, *Angew. Chem. Int. Ed.* **2017**, *56*, 15039-15043; c) T. van Leeuwen, L. Buzzetti, L. A. Perego, P. Melchiorre, *Angew. Chem. Int. Ed.* **2019**, *58*, 4953-4957; d) C. Zheng, G.-Z. Wang, R. Shang, *Adv. Synth. Catal.* **2019**, *361*, 4500-4505; e) J. Wu, P. S. Grant, X. Li, A. Noble, V. K. Aggarwal, *Angew. Chem. Int. Ed.*, **2019**, *58*, 5697-5701.
- [17] a) R. S. Mulliken, *J. Phys. Chem.* **1952**, *56*, 801-822; b) R. Foster, *J. Phys. Chem.* **1980**, *84*, 2135-2141.
- [18] D. Rehm, A. Weller, *Isr. J. Chem.* **1970**, *8*, 259-271.
- [19] a) Redox potentials of alkylidene malononitriles: L. Capaldo, D. Merli, M. Fagnoni, D. Ravelli, *ACS Catal.* **2019**, *9*, 3054-3058. Redox potentials of styrenes: b) F. Corvaisier, Y. Schuurman, A. Fecant, C. Thomazeau, P. Raybaud, H. Toulhoat, D. Farrusseng, *J. Catal.* **2013**, *307*, 352-361; c) A. Dahlén, Å. Nilsson, G. Hilmersson, *J. Org. Chem.* **2006**, *71*, 1576-1580.
- [20] Dubur, G. Ya.; Uldrikis, Ya. R. Synthesis and oxidation of 1,4-dihydroisonicotinic acid derivatives. *Chem. Heterocycl. Compd.* **1972**, *5*, 321-323.
- [21] a) Dubur, G. Ya.; Uldrikis, Ya. R. Preparation of 3,5-diethoxycarbonyl-2,6-dimethyl-1,4-dihydroisonicotinic acid and 3,5-diacetyl-2,6-dimethyl-1,4-dihydroisonicotinic acid and their salts. *Chem. Heterocycl. Compd.* **1972**, *5*, 762-763. b) Poikans, J.; Tiritis, G.; Bisenieks, E.; Uldrikis, J.; Gurevich, V. S.; Mikhailova, I. A.; Duburs, G. *Eur. J. Med. Chem.* **1994**, *29*, 325.
- [22] Wu, D.-H.; Hu, L. 3,5-Bis(ethoxycarbonyl)-2,6-dimethyl-1,4-dihydropyridine-4-carboxylic acid *Acta Cryst.* **2009**, E65, o1748.
- [23] Alandini, N.; Buzzetti, L.; Favi, G.; Schulte, T.; Candish, L.; Collins, K. D.; Melchiorre, P. Amide Synthesis by Nickel/Photoredox-Catalyzed Direct Carbamoylation of (Hetero)Aryl Bromides *Angew. Chem. Int. Ed.* **2020**, *59*, 2-8.
- [24] Yu, Y.-Q.; Wang, Z.-L. A Simple, Efficient and Green Procedure for Knoevenagel Condensation in Water or under Solvent-free Conditions *J. Chin. Chem. Soc.* **2013**, *60*, 288-292.
- [25] Mona, H.-S.; Hashem, S.; Samane, E. Solvent-free Knoevenagel Condensations over TiO₂. *Chin. J. Chem.* **2007**, *25*, 1563-1567.
- [26] Berryman, O.B.; Sather, A.C.; Lledó, A.; Rebek Jr., J. Switchable Catalysis with a Light-Responsive Cavitand. *Angew. Chem. Int. Ed.* **2011**, *50*, 9400-9403.
- [27] Jimenez, D.-Q.; Ferreira, I.-M.; Birolli, W.-G.; Fonseca, L.-P.; Porto, A.-M. Synthesis and Biocatalytic Ene-Reduction of Knoevenagel Condensation Compounds by the Marine-Derived Fungus *Penicillium Citrinum* CBMAI 1186. *Tetrahedron.* **2016**, *72*, 7317-7322.
- [28] Altundas, A.; Ayvaz, S.; Logoglu, E. Synthesis and Evaluation of a Series of Aminocyanopyridines as Antimicrobial Agents. *Med Chem Res.* **2011**, *20*, 1-8.
- [29] L.F. Tietze, U. Beifuss, M. Ruther *J. Org. Chem.* **1989**, *54*, 3120.
- [30] Volchoa, K.P.; Kurbakovaa, S.Yu.; Korchaginaa, D.V.; Suslova, E.V.; Salakhutdinova, N.F.; Toktarevb, A.V.; Echevskii, G.V.; Barkhash, V.A. Competing Michael and Knoevenagel Reactions of Terpenoids with Malononitrile on Basic Cs-beta Zeolite. *J. M. Catal. A: Chem.* **2003**, *195*, 263-274.

- [31] He, G.; Wu, C.; Zhou, J.; Yang, Q.; Zhang, C.; Zhou, Y.; Zhang, H.; Liub, H. A Method for Synthesis of 3-hydroxy-1-indanones via Cu-Catalyzed Intramolecular Annulation Reactions. *J. Org. Chem.* **2018**, *83*, 13356–13362.
- [32] Rezende, M.-C.; Almodovar, I. Substituent Electrophilicities in the NMR Spectra of Barbituric Derivatives. *Magn. Reson. Chem.* **2012**, *50*, 266–270.
- [33] Ferreira, J.M.G.O.; de Resende Filho, J.B.M.; Batista, P.K.; Teotonio, E.E.S.; Vale, J.A. Rapid and Efficient Uncatalyzed Knoevenagel Condensations from Binary Mixture of Ethanol and Water. *J. Braz. Chem. Soc.* **2018**, *29* (7), 1382-1387.
- [34] Pandit, K.S.; Kupwade, R.V.; Chavan, P.V.; Desai, U.V.; Wadgaonkar, P.P.; Kodam, K.M. Problem Solving and Environmentally Benign Approach toward Diversity Oriented Synthesis of Novel 2-Amino-3-phenyl (or Alkyl)Sulfonyl-4H-chromenes at Ambient Temperature. *ACS Sustainable Chem. Eng.* **2016**, *4*, 3450–3464.
- [35] Yang, H.; Wang, E.; Yang, P.; Lv, H.; Zhang, X. Pyridine-Directed Asymmetric Hydrogenation of 1,1-Diarylalkenes. *Org. Lett.* **2017**, *19*, 5062.
- [36] Zhang, H.-R.; Xiao, C.; Zhang, S.-L.; Zhang, X. Radical C–H Bond Trifluoromethylation of Alkenes by High-Valent Copper(III) Trifluoromethyl Compounds. *Adv. Synth. Catal.* **2019**, *361*, 5305.
- [37] Speckmeier, E.; Fischer, T.G.; Zeitler, K. A Toolbox Approach To Construct Broadly Applicable Metal-Free Catalysts for Photoredox Chemistry: Deliberate Tuning of Redox Potentials and Importance of Halogens in Donor–Acceptor Cyanoarenes *J. Am. Chem. Soc.* **2018**, *140*, 15353–15365.
- [38] Koltunov, K.-Y.; Walspurger, S.; Sommer, J. Superacidic Activation of α,β -Unsaturated Amides and their Electrophilic Reactions. *Eur. J. Org. Chem.* **2004**, 4039-4047.

5 Chapter 5: Photoredox-Catalyzed Synthesis of α -Amino Acid Amides by Imine Carbamoylation

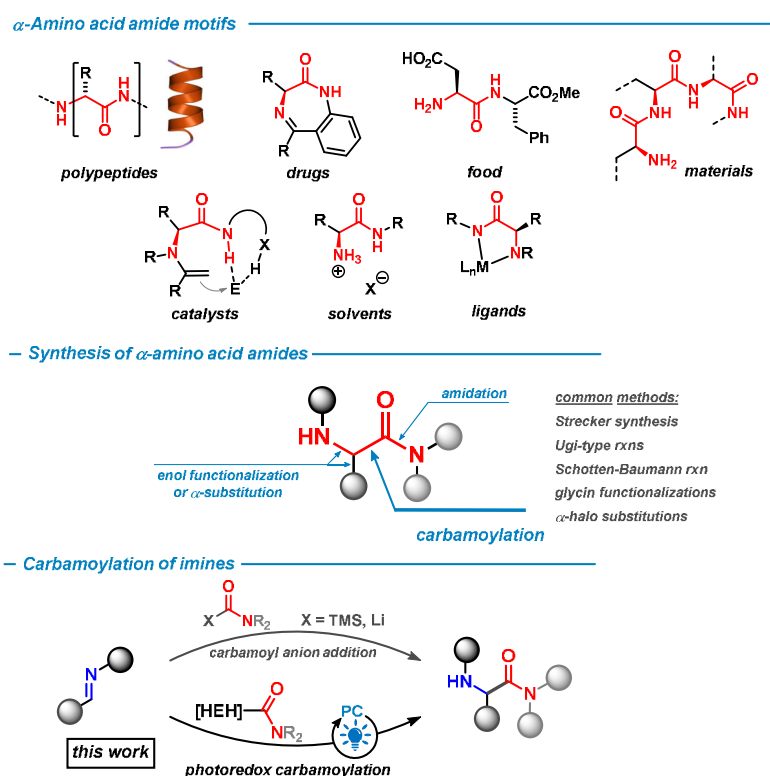


Abstract: An operationally simple protocol for the photocatalytic carbamoylation of imines is reported. The easily synthesizable, bench-stable 4-amido Hantzsch esters are explored as carbamoyl radical precursors to afford α -amino amides from over twenty substrates. The reaction proceeds under blue light irradiation of the fluoroisophthalonitrile derivative (3DPAFIPN) as photocatalyst (16 h, r.t.), with tolerance of different functional groups (e.g. halides, (thio)ethers, esters, alcohols or pyridines). Mechanistic experiments (radical trapping and Stern-Volmer experiments) are reported for elucidation of the reaction pathway.

This chapter has been submitted.

5.1 Introduction

Amino acid derivatives undoubtedly are among the most abundant, most versatile, and most studied functional molecules.¹ They form the molecular basis of biological life and find diverse applications as pharmaceuticals, food, materials, fine chemicals, and catalysts. α -Amino acid amides are the formal monomeric entities of polypeptides and a recurrent structural motif in numerous natural and synthetic molecules (Scheme 1, top). This molecular skeleton displays high density of functionalization (*i.e.* amine, proton, carbonyl, amide, and substituents) and high thermodynamic stability. Numerous syntheses have been developed to access α -amino acid amides with most methodologies involving peripheral manipulations of pre-functionalized core structures (*e.g.* Schotten-Baumann, α -carbonyl substitutions).² The *de novo* construction of the amino acid amide motif by construction of the central C-C bond by a formal addition to imines displays high modularity and enables high product diversity. The most prominent methods include Strecker reactions, Ugi reactions, and aminocarbonylations.^{3,4,5} Direct carbamoyl-ations of imines have remained very rare due to the limited availability of reactive carbamoyl precursors and low functional group compatibility. Nucleophilic additions of carbamoylmetal reagents (Li, Si) were reported.^{6,7} Photoredox catalysis has recently emerged as a powerful tool to access functionalized radical species from stable and available synthetic precursors under mild conditions. Successful applications to photoredox-carbamoylations furnished new syntheses of carboxamides and anilides.⁸ 4-Amido-substituted Hantzsch esters were demonstrated to serve as convenient precursors to various acyl radicals under photoredox conditions, including carbamoyl radicals.⁹ Here, we report on the development of mild conditions that enable the visible light-mediated carbamoylation of imines with Hantzsch ester derivatives (HEH-CONR₂) and the implementation of such synthetic strategy to the synthesis of a diverse set of α -amino acid amides (Scheme 1, bottom).



Scheme 1. The α -amino acid amide motif: General occurrence, general synthetic methods, and carbamoylations of imines.

5.2 Results and discussion

We commenced our investigations with the model reaction between 4-morpholinocarbonyl-substituted Hantzsch ester (**1a**) and benzylidene aniline (**2a**) in the presence of 3DPAFIPN (Table 1). This organic

photocatalyst is commercially available and displays oxidative and reductive reactivity under visible light irradiation, so that either mechanistic scenario may be operative with the employed combination of an electrophilic (imine) and nucleophilic (Hantzsch ester) starting material.¹⁰ The addition of Brønsted or Lewis acids proved beneficial, most likely due to higher reducibility (imine: $E = -2.0$ V; iminium ion: $E = -1.0$ V, vs. SCE) or higher electrophilicity.^{11,12} No reaction operates in the dark (entry 7). Direct irradiation of a catalyst-free reaction afforded low yields (entry 8, see ESI for UV/Vis spectra of the presumably formed EDA complex).

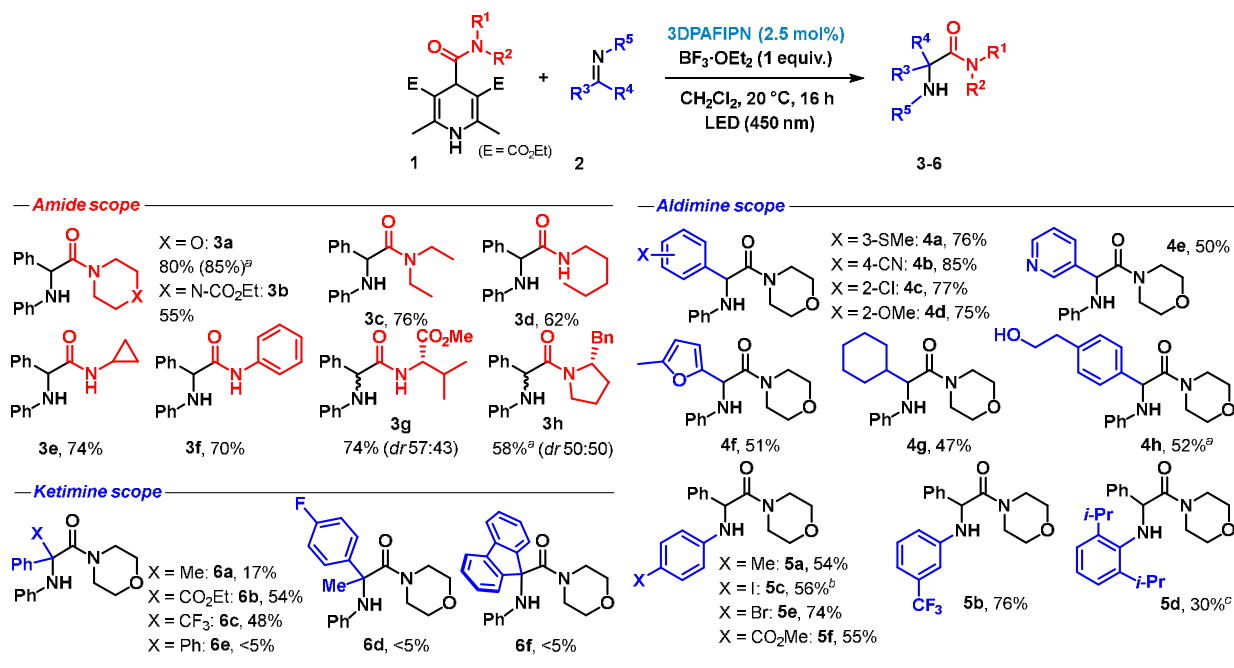
Table 1. Key experiments of method development and redox properties of the photocatalyst.

entry	deviation from standard conditions	yield (%) ^a	photocatalyst
1	none	85	<p>3DPAFIPN</p> <p>$E(\text{PC}^{\bullet+}/\text{PC}^{\bullet}) = -1.38$ V $E(\text{PC}^{\bullet}/\text{PC}^{\bullet-}) = +1.09$ V $E(\text{PC}^{\bullet+}/\text{PC}) = +1.30$ V $E(\text{PC}/\text{PC}^{\bullet-}) = -1.59$ V</p>
2	no $\text{BF}_3 \cdot \text{OEt}_2$	10	
3	$\text{BF}_3 \cdot \text{OEt}_2$ (20 mol%)	54	
4	TFA instead of $\text{BF}_3 \cdot \text{OEt}_2$	77	
5	$\text{Sc}(\text{OTf})_3$ instead of $\text{BF}_3 \cdot \text{OEt}_2$	51	
6	PhCO_2H instead of $\text{BF}_3 \cdot \text{OEt}_2$	24	
7	in the dark	0	
8	no 3DPAFIPN, 365 nm or 450 nm	~20	

^a Yields determined by ¹H NMR vs. 1,3,5-trimethoxybenzene.

0.10 mmol scale reactions, 0.1 M in DCM, 1.3 equiv. **1a**, under N₂ in dry solvents.

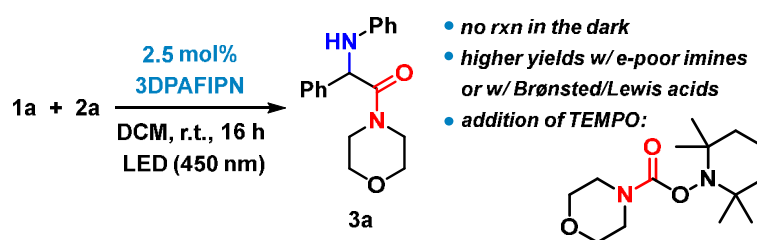
A diverse set of carboxamido-Hantzsch esters, aldimines, and ketimines was subjected to the optimized conditions (Scheme 2). Tertiary and secondary carboxamides bearing aryl and (cyclo)alkyl substituents were cleanly installed into the amino acid derivatives (**3a–h**). Electron-deficient aldimines afforded good yields (e.g. **4b**) which is in accord with an electrophilic or oxidizing reactivity of the imine. Reactions of aliphatic imines, due to their instability at room temperature and their tendency to undergo further condensation, were exemplarily shown with the *N*-cyclohexylcarboxamide **4g**. Variations of the *N*-substituents of the imines were limited to aryl groups. Tosyl, benzyl, *n*-alkyl, and *t*-alkyl substituents at the imine-nitrogen afforded no products. Hydrazones and oximes were also not tolerated. The reactivity of ketimines showed higher sensitivity to stereoelectronic properties. Generally lower yields were observed (**6a–f**), with electron-deficient ketimines still affording moderate yields (**6b**, **6c**). The mild reaction conditions tolerated halides (F, Cl, Br and I), electron-rich and electron-deficient heteroarenes, free alcohols, and esters, and nitriles. This documents high chemoselectivity of a presumably operating reductive electron transfer event within the reaction mechanism.¹³ Only in the case of the 4-iodoaniline derivative (**5c**), minor amounts of deiodinated product were observed (~9% of **3a**).



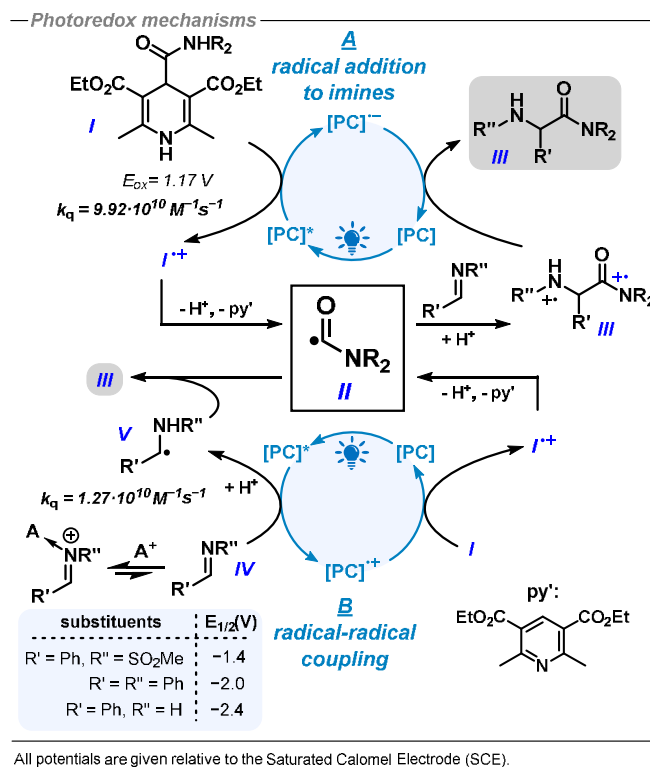
0.30 mmol scale reactions, 0.1 M in CH₂Cl₂, 1.3 equiv. **1**. Isolated yields are given. ^aNMR yields vs. 1,3,5-trimethoxybenzene. ^bIsolated as mixture with 9% **3a** (HPLC). ^c 72 h.

Scheme 2. Substrate scope.

During the development of optimal conditions for the photo-carbamoylation of imines, key mechanistic data were already collected (Scheme 3): The reaction does not proceed in the dark. Higher yields were obtained from electron-deficient imines. The presence of Brønsted or Lewis acids effected faster reactions and significantly higher yields also when used in excess. These observations rule out a free carbamoyl anion mechanism.¹⁴ When adding 1 equiv. of the radical scavenger TEMPO (2,2,6,6-tetramethylpiperidine-*N*-oxyl) to the standard reaction, the reaction was completely inhibited and the carbamoyl-TEMPO adduct was detected. The visible light-mediated reaction with the organic catalyst (PC) 3DPAFIPN may operate via two distinct photoredox mechanisms that both involve the intermediacy of a carbamoyl radical species. The first scenario (Scheme 4, A) proceeds through reductive photocatalyst quenching by the Hantzsch ester (**I**) followed by aromatization-driven fragmentation to give the carbamoyl radical **II**.¹⁵ Addition of this nucleophilic radical to the imine (or better the more electrophilic iminium ion) and a successive SET reduction of the presumably formed amino amide radical cation **III**⁺ furnish the desired α -amino amide **III**.



Scheme 3. Mechanistic observations.



Scheme 4. Mechanistic proposal.

The second scenario (Scheme 4, B) may involve initial oxidative catalyst quenching by the imine/iminium (IV) to give the persistent but electrophilic α -amino radical V.¹⁶ Product formation results from radical-radical coupling with the carbamoyl radical (II), which was generated by SET oxidation of I with the radical cation PC^{•+}. Both mechanistic scenarios align well with the redox potentials of the photocatalyst states.^{10,16c} Stern-Volmer studies of the individual quenching events of the excited state of photocatalyst with the imine and the Hantzsch ester amide (in the absence of acid additives), respectively, documented that both SET events are very rapid and in the same order of magnitude (see experimental section for full details): $k_q = 1.27 \cdot 10^{10} \text{ M}^{-1}\text{s}^{-1}$ (Hantzsch ester); $k_q = 9.22 \cdot 10^{10} \text{ M}^{-1}\text{s}^{-1}$ (imine).^{9b} It is very likely that the oxidative PC quenching by the imine may experience a dramatic acceleration by acid additives, so that mechanism B may be dominant under such conditions.

The presence of Brønsted/Lewis acid additives in the photo-carbamoylation of imines could be potentially exploited for stereoselective reactions.¹⁷ We envisioned three possible approaches: *i*) the use of chiral *N*-alkyl imines (not explored due to the incompatibility of the reaction with *N*-alkyl substituents),¹⁸ *ii*) the use of chiral acids (Brønsted or Lewis), and *iii*) the use of chiral Hantzsch ester amides. Our efforts to employ chiral Lewis acids ((+)-(Ipc)BCl₂, Sc(OTf)₃ or Yb(OTf)₃ with BOX and PyBOX ligands; see ESI) afforded low to moderate yields of essentially racemic product mixtures. A low stereocontrol of ~10% *e.e.* was obtained from a chiral BINOL-derived phosphoric acid (see ESI for details). This result also suggests that mechanistic proposal A (Scheme 3) is present, as chiral induction by a chiral counter-anion could only be realized when the imine is protonated upon attack of the carbamoyl radical. Diastereoselective reactions were attempted with chiral Hantzsch ester amides: A tethered Evans auxiliary did not undergo photoredox fragmentation. The (*L*)-valine derivative gave low stereoinduction (**3g**, *dr* 57:43); (*S*)-2-benzylpyrrolidine derivative (**3h**, *dr* 50:50; Scheme 2).

5.3 Conclusion

In conclusion, we have developed a photoredox-mediated approach for the synthesis of α -amino amides starting from imines and 4-amido Hantzsch esters as carbamoyl radical sources. The simple protocol proceeds in presence of several functional groups and allows the simultaneous introduction of four different substituents depending on the chosen starting material. Mechanistic studies such as radical

trapping and fluorescence quenching were conducted for elucidation. Lastly, stereoselective strategies were tested.

5.4 Experimental section

5.4.1 Materials and methods

Chemicals and solvents: All reagents (≥ 95 % purity) and solvents ($\geq 99\%$ purity) were purchased from commercial suppliers (Acros, Alfa Aesar, Fisher, Fluka, Grüssing, Merck, Sigma-Aldrich, TCI, Th. Geyer) and used as received unless otherwise indicated.

Reaction setup: All reactions were carried out in LABSOLUTE 4 mL Screw Neck Vials, 45 x 14.7 mm, clear glass, 1st hydrolytic class unless otherwise stated. Irradiation was performed in an air-cooled EvoluChem™ PhotoRedOx Box fitted with a blue (450 nm) EvoluChem™ 450DX LED (55 mW/cm²).

Nuclear magnetic resonance (NMR) spectroscopy: ¹H-NMR, ¹³C-NMR and ¹⁹F-NMR were used for purity and structure determination of products. NMR spectral data were collected on a Bruker Avance 300 (300 MHz for ¹H, 75 MHz for ¹³C, 282 MHz for ¹⁹F) spectrometer, a Bruker Avance 400 (400 MHz for ¹H, 100 MHz for ¹³C) spectrometer or a Bruker Avance III 600 (600 MHz for ¹H, 565 MHz for ¹⁹F) spectrometer at 25 °C. Chemical shifts are reported in δ /ppm, coupling constants *J* are given in Hertz. Solvent residual peaks were used as internal standard for all NMR measurements. The quantification of ¹H nuclei was performed by integration of appropriate resonance signals. Abbreviations used in NMR spectra: s – singlet, d – doublet, t – triplet, q – quartet, pent – pentet, sept – septet, m – multiplet, br. s – broad singlet.

High-resolution mass spectrometry (HRMS): HRMS was carried out by the Central Analytics at the department of chemistry, Universität Hamburg. Abbreviations used in MS spectra: *m/z* – mass-to-charge ratio, ESI – electrospray ionization.

Thin-layer chromatography (TLC) and column chromatography: TLC was performed on commercial SiO₂-coated aluminum plates (DC60 F254, Merck). The spots were visualized by UV light (365 nm and/or 254 nm) or alkaline potassium permanganate solution. Column chromatography was performed using SiO₂ (Acros Organics, 35-70 mesh, 60 Å pore size).

UV/Vis absorption spectroscopy: UV/Vis absorption spectroscopy was performed at room temperature on an Agilent Cary 5000 UV/Vis-NIR double beam spectrometer with a 10 mm quartz cuvette.

Fluorescence spectroscopy: The fluorescence spectra were recorded at room temperature using an Agilent Cary Eclipse Fluorescence Spectrophotometer in quartz cuvettes fitted with a rubber septum. The excitation slit was opened to 5 nm and the emission slit to 10 nm.

Polarimetry: Specific rotations were obtained using an A. KRÜSS Optronic P8000 at 20 °C using the sodium D-line (589.3 nm) and a cuvette with a length of 1 dm. Concentrations *c* are given in g/100 mL.

Analytical chiral HPLC: The ratio of enantiomers in chiral experiments was determined *via* HPLC using a CHIRALPAK® IB (250 x 4.6 mm, 5 μ m) column after isolation of the mixture of enantiomers using column chromatography as indicated.

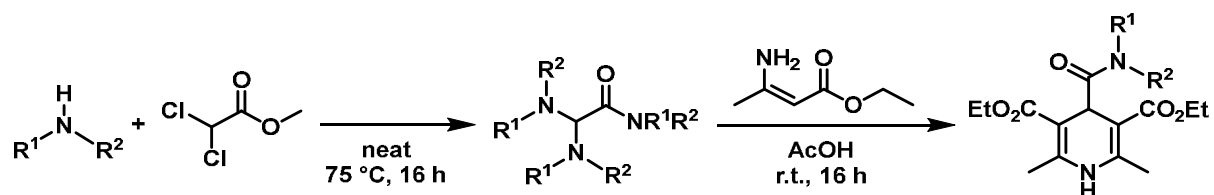
5.4.2 Optimization studies

Solvent (M)	Photocatalyst (mol%)	Additives (equiv.)	Yield of 3a ^a [%]
DCM (0.2)	3DPAFIPN (2.5)	–	10
DMA (0.2)	3DPAFIPN (2.5)	–	22
Acetone (0.2)	3DPAFIPN (2.5)	–	26
DCM (0.2)	3DPA2FBN (2.5)	–	10
DCM (0.2)	4CziPN (2.5)	–	31
DCM (0.1)	3DPAFIPN (2.5)	TFA (1)	77
DCM (0.1)	3DPAFIPN (2.5)	TFA (1)	59 ^b
DCM (0.1)	3DPAFIPN (2.5)	TFA (2)	71
DCM (0.2)	3DPAFIPN (2.5)	TFA (10)	96
DCM (0.1)	3DPAFIPN (2.5)	MgCl ₂ (1)	26
DCM (0.1)	3DPAFIPN (2.5)	Sc(OTf) ₃ (1)	51
DCM (0.5)	3DPAFIPN (2.5)	TFA (1)	60
Toluene (0.1)	3DPAFIPN (2.5)	TFA (1)	61
DCM (0.2)	3DPAFIPN (2.5)	PhCOOH (1)	24
DCM (0.1)	3DPAFIPN (2.5)	BF₃·OEt₂ (1)	85
DCM (0.1)	3DPAFIPN (2.5)	BF ₃ ·OEt ₂ (0.2)	54
DCM (0.1)	3DPAFIPN (2.5)	BF ₃ ·OEt ₂ (1.5)	81
DCM (0.2)	4CziPN (2.5)	TFA (1)	36
DCM (0.2)	3DPA2FBN (2.5)	TFA (1)	42
MeCN/MeOH 4:1 (0.2)	3DPAFIPN (2.5)	TFA (1)	14
DCM (0.2)	3DPAFIPN (2.5)	ZnCl ₂ (0.2)	46
DCM (0.1)	–	BF ₃ ·OEt ₂ (1)	18
DCM (0.2)	–	TFA (1)	13 ^c
DCM (0.1)	–	BF ₃ ·OEt ₂ (1)	20 ^c
DCM (0.2)	3DPAFIPN (2.5)	TFA (1)	0 ^d
DCM (0.1)	3DPAFIPN (2.5)	BF ₃ ·OEt ₂ (1)	0 ^d

^a ¹H-NMR yield using 1,3,5-Trimethoxybenzene as an external standard. ^b Under non-inert conditions. ^c Irradiation at 365 nm. ^d In the dark.

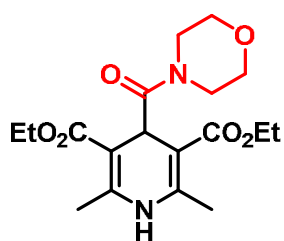
5.4.3 General procedures

General procedure 1.A: Synthesis of 4-amido-1,4-dihydropyridines



Methyl dichloroacetate (1.0 equiv.) and the corresponding amine (5.0 equiv.) were mixed and heated to 75 °C overnight, during which the mixture crystallized to form an orange, waxy solid. The solid was broken up using a glass rod and dissolved in glacial acetic acid (0.5 M with regard to methyl dichloroacetate). Ethyl 3-aminocrotonate (2.0 equiv.) was added and the mixture was stirred at room temperature overnight. The resultant suspension was diluted with water and the precipitate was removed by filtration, washed with water and dried *in vacuo* to yield the Hantzsch esters **1a–1b**.

Diethyl 2,6-dimethyl-4-(morpholine-4-carbonyl)-1,4-dihydropyridine-3,5-dicarboxylate (**1a**)

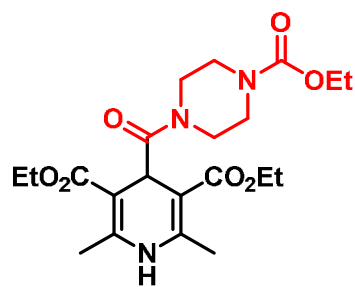


Starting from methyl dichloroacetate (718 mg, 520 μ L, 5.00 mmol), morpholine (2.18 g, 219 μ L, 25.0 mmol), ethyl 3-aminocrotonate (1.29 g, 1.26 mL, 10.0 mmol) and following the general procedure 1.A, **1a** was obtained as a light beige powder (831 mg, 45 %).

$^1\text{H NMR}$ (600 MHz, CDCl_3): δ [ppm] = 7.35 (s, 1H), 5.01 (s, 1H), 4.20 (dq, J = 10.9, 7.1 Hz, 2H), 4.14 (dq, J = 10.9, 7.1 Hz, 2H), 3.93 (t, J = 4.8 Hz, 2H), 3.75 (t, J = 4.7 Hz, 2H), 3.65 (t, J = 4.8 Hz, 2H), 3.60 (t, J = 4.7 Hz, 2H), 2.24 (s, 6H), 1.28 (*pseudo*-t, J = 7.1 Hz, 6H).

L. Cardinale, M. O. Konev, A. Jacobi von Wangelin, *Chem. Eur. J.* **2020**, 26, 8239–8243.

Diethyl 4-(4-(ethoxycarbonyl)piperazine-1-carbonyl)-2,6-dimethyl-1,4-dihydro-pyridine-3,5-dicarboxylate (**1b**)



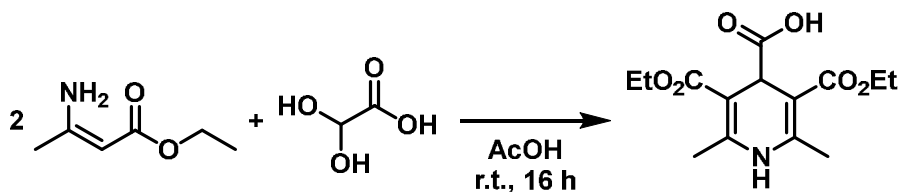
Starting from methyl dichloroacetate (0.72 g, 0.52 mL, 5.0 mmol), ethyl 1-piperazinecarboxylate (4.0 g, 3.7 mL, 25 mmol), ethyl 3-aminocrotonate (1.3 g, 1.3 mL, 10 mmol) and following the general procedure 1.A, **1b** was obtained as a pale-yellow powder (710 mg, 32 %).

$^1\text{H NMR}$ (300 MHz, CDCl_3): δ [ppm] = 7.66 (br. s, 1H), 5.03 (s, 1H), 4.25 – 4.06 (m, 6H), 3.95 – 3.86 (m, 2H), 3.64 – 3.53 (m, 4H), 3.49 – 3.39 (m, 2H), 2.21 (s, 6H), 1.26 (*pseudo*-t, J = 7.1, 1.0 Hz, 9H).

L. Cardinale, M. O. Konev, A. Jacobi von Wangelin, *Chem. Eur. J.* **2020**, 26, 8239–8243.

General procedure 1.B: Synthesis of 4-amido-1,4-dihydropyridines

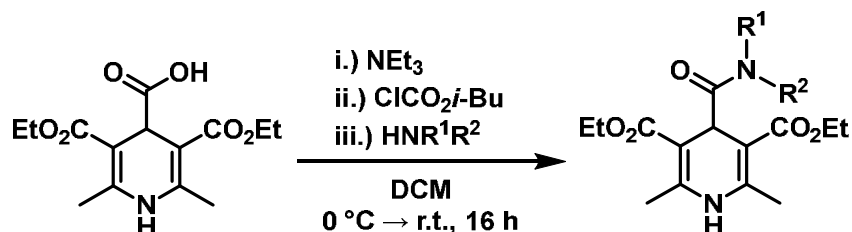
Synthesis of **I** (HE-COOH):



Ethyl 3-aminocrotonate (14.9 g, 115 mmol, 2.3 equiv.) was dissolved in glacial acetic acid (5 mL) and the solution was cooled to 0 °C. A solution of glyoxylic acid monohydrate (4.6 g, 50 mmol, 1.0 equiv.) in glacial acetic acid (30 mL)^a was added dropwise, leading to a yellow suspension. The mixture was warmed to room temperature and stirred overnight. The resultant suspension was diluted with water and the precipitate was removed by filtration and washed with acetic acid. The solid was dried *in vacuo* to yield the Hantzsch ester carboxylic acid **I** (HE-COOH) as a colorless to pale-yellow powder (2.99 g, 10 mmol, 20 %

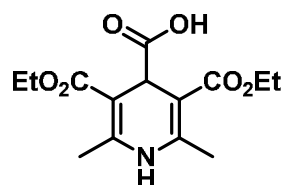
^a Dissolution of the glyoxylic acid monohydrate in the glacial acetic acid may take as long as 10–20 minutes and may require manual breaking of the crystal chunks into smaller pieces.

Synthesis of 1a–1g:



The Hantzsch ester carboxylic acid **I** was suspended in DCM (0.20 M) and triethylamine (1.2–2.0 equiv.) was added dropwise, leading to dissolution of **I**. The solution was cooled to $0\text{ }^\circ\text{C}$ and isobutyl chloroformate (1.2 equiv.) was added dropwise. After 10 minutes of stirring at $0\text{ }^\circ\text{C}$, the mixture was warmed to room temperature and stirred for additional 20 minutes. Subsequently, the amine (1.2–3.0 equiv.) was added and the mixture was stirred for 1 hour (primary amines) or overnight (secondary amines). The mixture was concentrated *in vacuo* and the residue purified by silica column chromatography (pentane/acetone or pentane/ethyl acetate) to yield the Hantzsch esters **1c–1g**.

3,5-Bis(ethoxycarbonyl)-2,6-dimethyl-1,4-dihydropyridine-4-carboxylic acid (**I**)

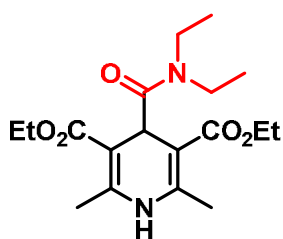


Colorless to pale-yellow powder.

$^1\text{H NMR}$ (300 MHz, $\text{DMSO}-d_6$): δ [ppm] = 11.81 (s, 1H), 8.84 (s, 1H), 4.58 (s, 1H), 4.16 – 4.00 (m, 4H), 2.22 (s, 6H), 1.19 (t, $J = 7.1, 6\text{H}$).

L. Cardinale, M. O. Konev, A. Jacobi von Wangelin, *Chem. Eur. J.* **2020**, *26*, 8239–8243.

Diethyl (4-diethylcarbamoyl)-2,6-dimethyl-1,4-dihydropyridine-3,5-dicarboxylate (**1c**)

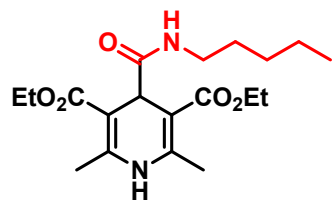


Starting from HE-COOH **I** (500 mg, 1.68 mmol), triethylamine (203 mg, 280 μL , 2.01 mmol), diethylamine (247 mg, 350 μL , 3.38 mmol), isobutyl chloroformate (274 mg, 260 μL , 2.00 mmol) and following the general procedure 1.B, **1d** was obtained as a pale-yellow powder (100 mg, 14 %).

$^1\text{H NMR}$ (300 MHz, CDCl_3): δ [ppm] = 8.44 (br. s, 1H), 5.08 (s, 1H), 4.17 (qq, $J = 10.9, 7.1\text{ Hz}$, 4H), 3.77 (q, $J = 7.1\text{ Hz}$, 2H), 3.34 (q, $J = 7.0\text{ Hz}$, 2H), 2.20 (s, 6H), 1.27 (t, $J = 7.1\text{ Hz}$, 8H), 1.03 (t, $J = 7.0\text{ Hz}$, 3H).

N. Alandini, L. Buzzetti, G. Favi, T. Schulte, L. Candish, K. D. Collins, P. Melchiorre, *Angew. Chem. Int. Ed.* **2020**, *59*, 5248–5253, *Angew. Chem.* **2020**, *132*, 5286–5291.

Diethyl 2,6-dimethyl-4-(pentylcarbamoyl)-1,4-dihydropyridine-3,5-dicarboxylate (**1d**)



Starting from HE-COOH **I** (297 mg, 1.0 mmol), triethylamine (123 mg, 170 μL , 1.22 mmol), pentylamine (174 mg, 230 μL , 2.00 mmol), isobutyl chloroformate (158 mg, 150 μL , 1.16 mmol) and following the general procedure 1.B, **1d** was obtained as a pale-yellow powder (140 mg, 0.382 mmol, 38 %). Instead of column chromatography, **1d** was purified by recrystallization from diethyl ether (hot filtration required).

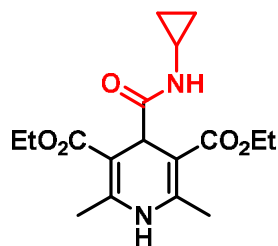
m.p. = $146\text{--}148\text{ }^\circ\text{C}$

$^1\text{H NMR}$ (500 MHz, CDCl_3): δ [ppm] = 7.89 (s, 1H), 6.67 (t, $J = 5.8\text{ Hz}$, 1H), 4.55 (s, 1H), 4.18 (q, $J = 7.1\text{ Hz}$, 4H), 3.18 (td, $J = 6.9, 5.7\text{ Hz}$, 2H), 2.21 (s, 6H), 1.61 (s, 2H), 1.46 (pent, $J = 7.1\text{ Hz}$, 2H), 1.28 (t, $J = 7.1\text{ Hz}$, 8H), 0.88 (t, $J = 7.0\text{ Hz}$, 3H).

$^{13}\text{C}\{-^1\text{H}\}$ -NMR (75 MHz, CDCl_3): δ [ppm] = 174.9, 168.2, 147.7, 97.9, 60.2, 41.8, 39.6, 29.4, 29.1, 22.5, 19.0, 14.5, 14.1.

HRMS (ESI): m/z = calcd. for $\text{C}_{19}\text{H}_{31}\text{N}_2\text{O}_5^+$: 367.2227, found: 367.2220.

Diethyl (4-cyclopropylcarbamoyl)-2,6-dimethyl-1,4-dihydropyridine-3,5-dicarboxylate (**1e**)

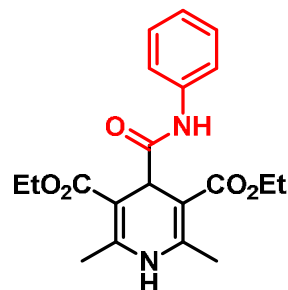


Starting from HE-COOH **I** (446 mg, 1.50 mmol), triethylamine (182 mg, 250 μL , 1.84 mmol), cyclopropylamine (107 mg, 130 μL , 1.87 mmol), isobutyl chloroformate (242 mg, 230 μL , 1.77 mmol) and following the general procedure 1.B, **1e** was obtained as a pale-yellow powder (272 mg, 0.809 mmol, 54 %).

^1H NMR (300 MHz, CDCl_3): δ [ppm] = 8.05 (s, 1H), 6.82 (d, J = 3.3 Hz, 1H), 4.49 (s, 1H), 4.17 (qd, J = 7.2, 0.9 Hz, 4H), 2.67 (tq, J = 7.4, 3.7 Hz, 1H), 2.21 (s, 6H), 1.27 (t, J = 7.1 Hz, 6H), 0.76–0.68 (m, 2H), 0.47 – 0.39 (m, 2H).

L. Cardinale, M. O. Konev, A. Jacobi von Wangelin, *Chem. Eur. J.* **2020**, *26*, 8239–8243.

Diethyl 2,6-dimethyl-4-(phenylcarbamoyl)-1,4-dihydropyridine-3,5-dicarboxylate (**1f**)

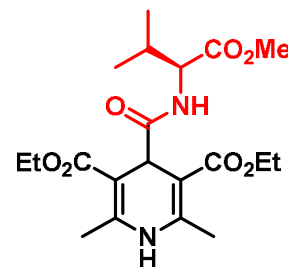


Starting from HE-COOH **I** (1.02 g, 3.43 mmol), triethylamine (682 mg, 940 μL , 6.78 mmol), aniline (949 mg, 930 μL , 5.04 mmol), isobutyl chloroformate (558 mg, 530 μL , 10.2 mmol) and following the general procedure 1.B, **1f** was obtained as a pale-yellow powder (760 mg, 2.04 mmol, 58 %).

^1H NMR (300 MHz, CDCl_3): δ [ppm] = 8.81 (s, 1H), 7.61 – 7.50 (m, 2H), 7.35 – 7.24 (m, 2H), 7.11 – 7.00 (m, 1H), 4.72 (s, 1H), 4.21 (q, J = 7.1 Hz, 4H), 2.27 (s, 4H), 1.58 – 1.56 (m, 1H), 1.28 (t, J = 7.1 Hz, 6H).

N. Alandini, L. Buzzetti, G. Favi, T. Schulte, L. Candish, K. D. Collins, P. Melchiorre, *Angew. Chem. Int. Ed.* **2020**, *59*, 5248–5253, *Angew. Chem.* **2020**, *132*, 5286–5291.

Diethyl 2,6-dimethyl-4-((S)-valine-N-carbonyl)-1,4-dihydropyridine-3,5-dicarboxylate (**1g**)

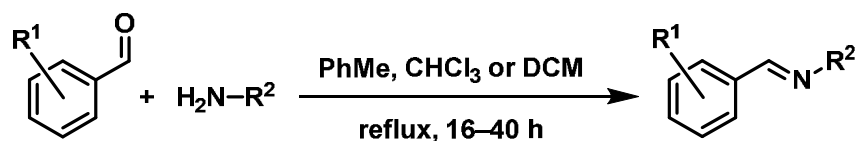


Starting from HE-COOH **I** (297 mg, 1.00 mmol), triethylamine (203 mg, 280 μL , 2.00 mmol), (S)-valine methyl ester hydrochloride (201 mg, 1.20 mmol), isobutyl chloroformate (158 mg, 150 μL , 1.16 mmol) and following the general procedure 1.B, **1g** was obtained as yellow solid (290 mg, 0.707 mmol, 71%).

^1H NMR (300 MHz, CDCl_3): δ [ppm] = 8.10 (br. s, 1H), 7.12 (d, J = 9.0 Hz, 1H), 4.67 (br. s, 1H), 4.44 – 4.39 (m, 1H), 4.18 – 4.13 (m, 4H), 3.67 (s, 3H), 2.17 (s, 3H), 2.10 (s, 3H), 1.29 – 1.23 (m, 6H), 0.91 – 0.88 (m, 6H).

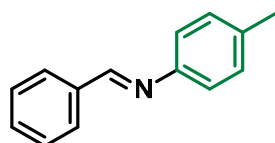
N. Alandini, L. Buzzetti, G. Favi, T. Schulte, L. Candish, K. D. Collins, P. Melchiorre, *Angew. Chem. Int. Ed.* **2020**, *59*, 5248–5253, *Angew. Chem.* **2020**, *132*, 5286–5291.

General procedure 2: Synthesis of aldimines



In a Soxhlet apparatus with anhydrous calcium chloride in the extraction thimble, the aldehyde (10 mmol) and the amine (10 mmol) were refluxed in 50 mL of toluene, chloroform or dichloromethane for 16–40 hours until complete conversion of the starting material was observed (determined *via* GC-MS). The solvent was removed *in vacuo* and the imines **2b–2k** were obtained. In some cases, further purification was necessary.

Benzylidene(4-methylphenyl)amine (2b)

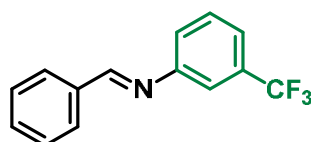


Starting from benzaldehyde (1.06 g) and *p*-toluidine (1.07 g), was obtained as a beige solid after 16 hours of reflux in toluene (1.34 g, 69 %).

$^1\text{H NMR}$ (300 MHz, CDCl_3): δ [ppm] = 8.49 (s, 1H), 7.96 – 7.88 (m, 2H), 7.53 – 7.45 (m, 3H), 7.27 – 7.13 (m, 4H), 2.40 (s, 3H).

X. Hong, H. Wang, B. Liu, B. Xu, *Chem. Comm.* **2014**, 50, 14129–14132.

Benzylidene(3-(trifluoromethyl)phenyl)amine (2c)



Starting from benzaldehyde (1.06 g) and 3-(trifluoromethyl)-aniline (1.61 g), the crude product was obtained after 16 hours of reflux in chloroform. Recrystallization from hexane yielded pure **2c** as colorless crystals (1.95 g, 78 %).

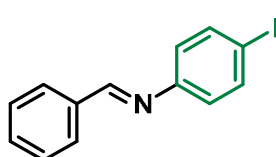
m.p. = 66–67 °C

$^1\text{H NMR}$ (600 MHz, CDCl_3): δ [ppm] = 8.46 (s, 1H), 7.95 – 7.89 (m, 2H), 7.56 – 7.48 (m, 5H), 7.48 – 7.45 (m, 1H), 7.40 – 7.35 (m, 1H)

$^{19}\text{F NMR}$ (565 MHz, CDCl_3): δ [ppm] = –62.61.

L. J. Silverberg, C. Pacheco, D. Sahu, P. Scholl, H. F. Sobhi, J. T. Bachert, K. Bandholz, R. V. Bendinsky, H. G. Bradley, B. K. Colburn, D. J. Coyle, J. R. Dahl, M. Felty, R. F. Fox, K. M. Gonzalez, J. M. Islam, S. E. Koperna, Q. J. Moyer, D. J. Noble, M. E. Ramirez, Z. Yang, *J. Heterocyclic Chem.* **2020**, 57, 1797–1805.

Benzylidene(4-iodophenyl)amine (2d)

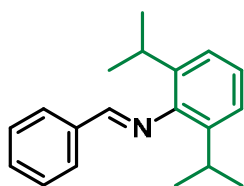


Starting from benzaldehyde (1.06 g) and 4-iodoaniline (2.19 g), **2d** was obtained as a grey solid after 16 hours of reflux in toluene (2.90 g, 94 %).

$^1\text{H NMR}$ (300 MHz, CDCl_3): δ [ppm] = 8.42 (s, 1H), 7.93 – 7.86 (m, 2H), 7.74 – 7.67 (m, 2H), 7.53 – 7.44 (m, 3H), 7.00 – 6.94 (m, 2H).

J. Bhattacharjee, M. Sachdeva, T. K. Panda, *Z. Anorg. Allg. Chem.* **2016**, 17, 937–940.

Benzylidene(2,6-diisopropylphenyl)amine (2e)

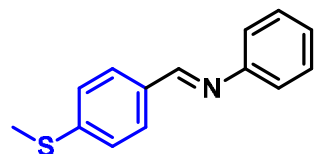


Starting from benzaldehyde (1.06 g) and 2,6-diisopropylaniline (1.77 g), the crude product was obtained after 40 hours of reflux in toluene. Crystallisation from hexane at –20 °C yielded pure **2e** as yellow crystals (1.32 g, 50 %).

$^1\text{H NMR}$ (300 MHz, CDCl_3): δ [ppm] = 8.20 (s, 1H), 7.97 – 7.87 (m, 2H), 7.59 – 7.45 (m, 3H), 7.21 – 7.03 (m, 3H), 2.98 (sept, J = 6.8 Hz, 2H), 1.17 (d, J = 6.9 Hz, 12H).

G. Verardo, A. G. Giumanini, P. Strazzolini, M. Poiana, *Synthesis* **1993**, 1, 121–125.

N-Phenyl-1-(3-methylthio)methanimine (2f)

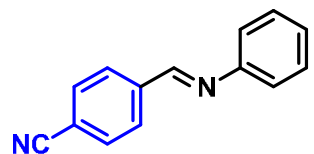


Starting from 3-(methylthio)benzaldehyde (1.52 g) and aniline (931 mg), **2f** was obtained as a bright orange solid after 16 hours of reflux in toluene (2.30 g, 100 %).

$^1\text{H NMR}$ (300 MHz, CDCl_3): δ [ppm] = 8.40 (s, 1H), 7.84 – 7.81 (m, 2H), 7.39 – 7.33 (m, 2H), 7.30–7.26 (m, 2H), 7.23 – 7.20 (m, 3H), 2.54 (s, 3H).

R. D. Chakravarthy, V. Ramkumar, D. K. Chand, *Green Chem.* **2014**, 16, 2190–2196.

N-Phenyl-1-(4-cyanophenyl)methanimine (2g)

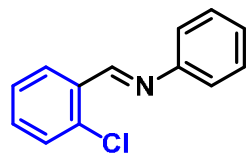


Starting from 4-cyanobenzaldehyde (1.31 g) and aniline (931 mg), the crude product was obtained after 16 hours of reflux in chloroform. Recrystallization from dry methanol yielded pure **2g** as large yellow crystals (1.46 g, 71 %).

$^1\text{H NMR}$ (400 MHz, CDCl_3): δ [ppm] = 8.50 (s, 1H), 8.05 – 7.98 (m, 2H), 7.80 – 7.73 (m, 2H), 7.47 – 7.38 (m, 2H), 7.32–7.27 (m, 1H), 7.27 – 7.21 (m, 2H).

D. J. Dibble, R. Kurakake, A. G. Wardrip, A. Bartlett, R. Lopez, J. A. Linares, M. Firstman, A. M. Schmidt, M. J. Umerani, A. A. Gorodetsky, *Org. Lett.* **2018**, 20, 3, 502–505.

N-Phenyl-1-(2-chlorophenyl)methanimine (2h)

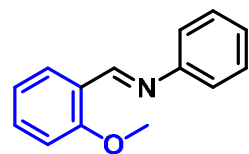


Starting from 2-chlorobenzaldehyde (1.41 g) and aniline (931 mg) **2h** was obtained as a pale-brown oil after 16 hours of reflux in toluene (1.90 g, 88 %).

$^1\text{H NMR}$ (300 MHz, CDCl_3): δ [ppm] = 8.92 (s, 1H), 8.29 – 8.22 (m, 1H), 7.44 – 7.34 (m, 5H), 7.29 – 7.22 (m, 3H).

E. Zhang, H. Tian, S. Xu, X. Yu, Q. Xu, *Org. Lett.* **2013**, 15, 2704–2707.

N-Phenyl-1-(2-methoxyphenyl)methanimine (2i)

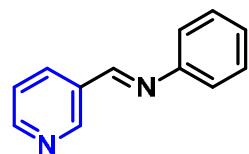


Starting from 2-methoxybenzaldehyde (1.36 g) and aniline (931 mg) **2i** was obtained after 16 hours of reflux in chloroform as a pale-yellow solid (2.10 g, 100 %).

$^1\text{H NMR}$ (300 MHz, CDCl_3): δ [ppm] = 9.00 (s, 1H), 8.25 – 8.21 (m, 1H), 7.54 – 7.43 (m, 3H), 7.32 – 7.26 (m, 3H), 7.14 – 7.09 (m, 1H), 7.04 – 7.00 (m, 1H), 3.96 (s, 3H).

L. Han, P. Xing, B. Jiang, *Org. Lett.* **2014**, 16, 3428–3431.

N-Phenyl-1-(3-pyridinyl)methanimine (2j)

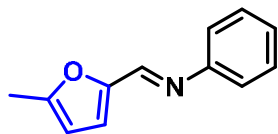


Starting from 3-formylpyridine (1.07 g) and aniline (931 mg), **2j** was obtained as a yellow oil after 16 hours of reflux in chloroform (1.51 g, 83 %).

$^1\text{H NMR}$ (300 MHz, CDCl_3): δ [ppm] = 8.97 (d, J = 2.1 Hz, 1H), 8.65 (dd, J = 4.8, 1.7 Hz, 1H), 8.42 (s, 1H), 8.22 (dt, J = 7.9, 1.9 Hz, 1H), 7.40 – 7.29 (m, 3H), 7.25 – 7.15 (m, 3H).

R. R. Donthiri, R. D. Patil, S. Adimurthy, *Eur. J. Org. Chem.* **2012**, 24, 4457–4460.

N-Phenyl-1-(5-methylfuran-2-yl)methanimine (2k)



Starting from 5-methylfurfural (1.10 g) and aniline (931 mg), the crude product was obtained as a dark brown oil after 16 hours of reflux in toluene. Vacuum Kugelrohr distillation yielded pure **2k** as a yellow oil (1.33 g, 72 %).

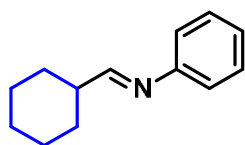
b.p. = 220–225 °C / 9 Torr

¹H NMR (400 MHz, CDCl₃): δ [ppm] = 8.18 (s, 1H), 7.39 – 7.35 (m, 2H), 7.24 – 7.19 (m, 3H), 6.39 (d, *J* = 3.3 Hz, 1H), 6.17 (dq, *J* = 3.2, 1.0 Hz, 1H), 2.44 – 2.43 (m, 3H).

I. Sasaki, T. Ikeda, T. Amou, J. Taguchi, H. Ito, T. Ishiyama, *Synlett*, **2016**, 27, 1582–1586.

Syntheses of ketimines and aldimines by other procedures

N-Phenyl-1-(cyclohexyl)methanimine (2l)



A mixture of cyclohexanecarboxaldehyde (927 mg, 1.00 mL, 8.26 mmol) and anhydrous Na₂SO₄ (11.7 g, 82.6 mmol) in acetonitrile (4.25 mL) was cooled to –40 °C using a cryostat. A solution of aniline (769 mg, 0.75 mL, 8.26 mmol) in acetonitrile (6.25 mL) was added dropwise and the mixture was subsequently stirred for 45 minutes at –40 °C. The cooling bath was removed and the mixture

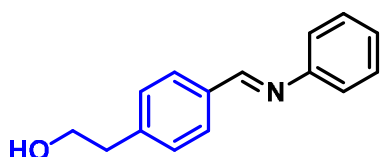
stirred for further 30 minutes while slowly warming to room temperature. The mixture was filtered and concentrated *in vacuo* to yield a yellow, viscous oil, which was vacuum-distilled to give pure **2l** as a pale-yellow liquid (758 mg, 51 %).

b.p. = 95–105 °C / 0.1 Torr

¹H NMR (300 MHz, CDCl₃): δ [ppm] = 7.71 (d, *J* = 5.0 Hz, 1H), 7.38 – 7.28 (m, 2H), 7.20 – 7.13 (m, 1H), 7.05 – 6.98 (m, 2H), 2.44 – 2.31 (m, 1H), 2.00 – 1.65 (m, 6H), 1.46 – 1.31 (m, 4H).

G. J. T. Kuster, L. W. A. van Berkomp, M. Kalmoua, A. van Loevezijn, L. A. J. M. Sliedregt, B. J. van Steen, C. G. Kruse, F. P. J. T., Rutjes, H. W. Scheeren, *J. Comb. Chem.* **2006**, 8, 85–94.

N-Phenyl-1-(4-(2-hydroxyethyl)phenyl)methanimine (2m)



A mixture of 4-(2-hydroxyethyl)benzaldehyde (see section 3.6) (309 mg, 2.05 mmol) and aniline (191 mg, 190 μL, 2.05 mmol) in DCM (15 mL) was stirred overnight at room temperature over activated 4 Å molecular sieves. The mixture was filtered and concentrated *in vacuo*.

The residue was purified by column chromatography on basic silica (deactivated with NEt₃, pentane/ethyl acetate 1:1) to yield **2m** as a yellow solid, which was dried at 40–50 °C and 10⁻² mbar to remove last traces of the starting materials (202 mg, 0.896 mmol, 44 %). The product may turn orange upon storage.

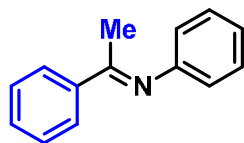
m.p. = 56–57 °C

¹H NMR (300 MHz, CDCl₃): δ [ppm] = 8.44 (s, 1H), 7.91 – 7.84 (m, 2H), 7.43 – 7.33 (m, 4H), 7.27 – 7.20 (m, 3H), 3.91 (t, *J* = 6.5 Hz, 2H), 2.95 (t, *J* = 6.5 Hz, 2H).

¹³C-{¹H}-NMR (75 MHz, CDCl₃): δ [ppm] = 160.3, 152.1, 142.6, 134.7, 129.6, 129.3, 129.2, 126.0, 121.0, 63.5, 39.3.

HRMS (ESI): *m/z* = calcd. for C₁₅H₁₆NO⁺: 226.1226, found: 226.1226.

N,1-Diphenylethan-1-imine (2n)

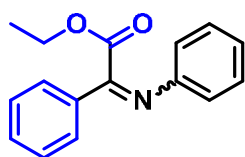


A mixture of acetophenone (1.20 g, 1.17 mL, 10 mmol) and aniline (931 mg, 910 μ L, 10 mmol) was refluxed overnight in toluene (20 mL) over activated 4 Å molecular sieves. The mixture was filtered and concentrated *in vacuo*. The yellow residue was dissolved in a minimal amount of methanol and **2n** was crystallized at -20 °C overnight as a pale-yellow solid (1.04 g, 5.33 mmol, 53 %).

$^1\text{H NMR}$ (300 MHz, CDCl_3): δ [ppm] = 8.02 – 7.96 (m, 2H), 7.51 – 7.43 (m, 3H), 7.40 – 7.32 (m, 2H), 7.13 – 7.06 (m, 1H), 6.86 – 6.77 (m, 2H), 2.25 (s, 3H).

Y. Xie, T. Chen, S. Fu, X.-S. Li, Y. Deng, H. Jiang, W. Zeng, *Chem. Commun.* **2014**, 50, 10699–10702.

2-Phenyl-2-(phenylimino)acetate (2o)



A mixture of ethyl benzoylformate (885 mg, 790 μ L, 4.98 mmol), aniline (459 mg, 450 μ L, 4.98 mmol) and *p*-toluenesulfonic acid monohydrate (95 mg, 0.50 mmol, 10 mol%) in toluene (50 mL) was refluxed for 16 hours in a Soxhlet apparatus with anhydrous calcium chloride in the extraction thimble. The mixture was filtered and concentrated *in vacuo*. The brown residue was purified by column

chromatography on silica (pentane/diethyl ether) to yield a mixture of (*E*)-**2o** and (*Z*)-**2o** as a yellow oil (975 mg, 77 %). The ratio of isomers was determined *via* $^1\text{H-NMR}$ spectroscopy to be 2.5/1, however, the isomers were not assigned.

Major isomer:

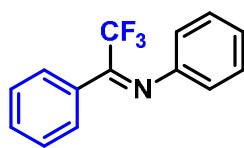
$^1\text{H NMR}$ (300 MHz, CDCl_3): δ [ppm] = 7.92 – 7.86 (m, 2H), 7.53 – 7.43 (m, 3H), 7.36 – 7.29 (m, 2H), 7.17 – 7.09 (m, 1H), 6.99 – 6.93 (m, 2H), 4.13 (q, J = 7.1 Hz, 2H), 0.99 (t, J = 7.1 Hz, 3H).

Minor isomer:

$^1\text{H NMR}$ (300 MHz, CDCl_3): δ [ppm] = 8.05 – 7.98 (m, 2H), 7.70 – 7.63 (m, 1H), 4.46 (q, J = 7.1 Hz, 2H), 1.43 (t, J = 7.1 Hz, 3H), other aromatic signals could not accurately be determined due to overlapping.

D. Enders, A. Rembiak, B. A. Stöckel, *Adv. Synth. Catal.* **2013**, 335, 1937–1942.

2,2,2-Trifluoro-N,1-diphenylethan-1-imine (2p)



In a SOXHLET apparatus with anhydrous calcium chloride in the extraction thimble, a mixture of 2,2,2-trifluoroacetophenone (500 mg, 400 μ L, 2.87 mmol), aniline (267 mg, 260 μ L, 2.85 mmol) and *p*-toluenesulfonic acid monohydrate (27 mg, 0.15 mmol, 5 mol%) in toluene (50 mL) was refluxed for 40 hours. The mixture was filtered, concentrated *in vacuo* and the brown residue was purified by Kugelrohr distillation. The obtained liquid was dried at 70 °C at 5 mbar for one hour using a rotary evaporator to remove traces of the starting materials to yield pure **2p** as a yellow liquid (232 mg, 931 μ L, 32 %).

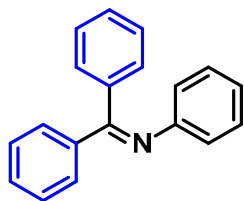
b.p. = 190–200 °C / 7.5 Torr

$^1\text{H NMR}$ (600 MHz, CDCl_3): δ [ppm] = 7.37 – 7.34 (m, 1H), 7.32 – 7.28 (m, 2H), 7.23 – 7.17 (m, 4H), 7.06 – 7.02 (m, 1H), 6.76 – 6.72 (m, 2H).

$^{19}\text{F NMR}$ (565 MHz, CDCl_3): δ [ppm] = -70.00 .

M. Abid, M. Savolainen, S. Landge, J. Hu, G. K. S. Prakash, G. A. Olah, B. Török, *J. Fluor. Chem.* **2007**, 128, 587–594.

***N*,1,1-Triphenylmethanimine (2q)**

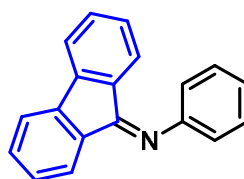


In a Soxhlet apparatus with anhydrous calcium chloride in the extraction thimble, a mixture of benzophenone (1.82 g, 10.0 mmol), aniline (931 mg, 910 μ L, 10.0 mmol) and *p*-toluenesulfonic acid monohydrate (114 mg, 0.60 mmol, 6 mol%) in toluene (50 mL) was refluxed for 40 hours. The mixture was filtered, washed with water (20 mL), dried over Na₂SO₄, filtered and concentrated *in vacuo*. The residual dark yellow solid was recrystallized from diethyl ether to yield **2q** as light-yellow crystal plates (809 mg, 3.14 mmol, 31 %).

¹H NMR (300 MHz, CDCl₃): δ [ppm] = 7.79 – 7.72 (m, 2H), 7.50 – 7.37 (m, 3H), 7.30 – 7.22 (m, 3H), 7.18 – 7.09 (m, 4H), 6.97 – 6.89 (m, 1H), 6.79 – 6.68 (m, 2H).

T. Ogata, J. F. Hartwig, *J. Am. Chem. Soc.* **2008**, *42*, 13848–13849.

***N*-Phenyl-9*H*-fluoren-9-imine (2r)**

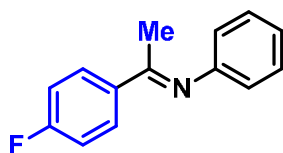


In a Soxhlet apparatus with anhydrous calcium chloride in the extraction thimble, a mixture of fluorenone (1.81 g, 10.0 mmol), aniline (931 mg, 910 μ L, 10.0 mmol) and *p*-toluenesulfonic acid monohydrate (97 mg, 0.51 mmol, 5 mol%) in toluene (50 mL) was refluxed for 40 hours. The mixture was filtered, washed with water (20 mL), dried over Na₂SO₄, filtered and concentrated *in vacuo*. The residual dark-orange solid was recrystallized from diethyl ether to yield **2r** as yellow-orange needles (1.52 g, 5.95 mmol, 60 %).

¹H NMR (300 MHz, CDCl₃): δ [ppm] = 7.98 – 7.88 (m, 1H), 7.63 – 7.57 (m, 2H), 7.51 – 7.29 (m, 5H), 7.25 – 7.18 (m, 1H), 7.04 – 6.97 (m, 2H), 6.93 (td, *J* = 7.6, 1.1 Hz, 1H), 6.57 (dt, *J* = 7.8, 0.9 Hz, 1H).

D. J. van As, T. U. Connell, M. Brzozowski, A. D. Scully, A. Polyzos, *Org. Lett.* **2018**, *20*, 905–908.

1-(4-Fluorophenyl)-*N*-phenylethan-1-imine (2s)



A mixture of 4-fluoroacetophenone (570 mg, 0.50 mL, 4.14 mmol), aniline (388 mg, 0.38 mL, 4.14 mmol) and *p*-toluenesulfonic acid monohydrate (21 mg, 0.207 mmol, 5 mol%) in toluene (10 mL) was stirred overnight at room temperature over activated 4 Å molecular sieves. The mixture was filtered and concentrated *in vacuo*. The residue was recrystallized from ethanol to yield **2s** as white crystal plates (290 mg, 1.36 mmol, 33 %).

¹H NMR (300 MHz, CDCl₃): δ [ppm] = 8.05 – 7.92 (m, 2H), 7.42 – 7.30 (m, 2H), 7.18 – 7.06 (m, 3H), 6.85 – 6.73 (m, 2H), 2.23 (s, 3H).

¹⁹F NMR (565 MHz, CDCl₃): δ [ppm] = –110.35.

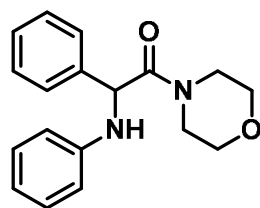
N. Nghia Pham, T. T. Dang, N. T. Ngo, A. Villinger, P. Ehlers, P. Langer, *Org. Biomol. Chem.* **2015**, *13*, 6047–6058.

General procedure 3: Synthesis of α -amino amides

A 4 mL glass vial was charged with a magnetic stir bar, the corresponding imine (0.30 mmol, 1.0 equiv.), the corresponding Hantzsch ester (0.39 mmol, 1.3 equiv.) and 3DPAFIPN (4.9 mg, 7.5 μ mol, 2.5 mol%) and closed with a septum screw cap. The vial was evacuated and flushed with nitrogen three times before adding dry DCM (3 mL, results in a 0.1 M soln. of the imine) and BF₃·OEt₂ (37 μ L, 0.30 mmol, 1.0 equiv.). The vial was shaken and the mixture was stirred for 16 hours at room temperature under blue light irradiation (λ = 450 nm, EvoluChem™ 450DX). The mixture was then washed with water (5 mL), the aqueous phase was extracted with DCM (3 \times 5 mL) and the combined organic phases were dried over MgSO₄ or Na₂SO₄. After filtration and removal of the solvent *in vacuo*, the residue was purified

using silica column chromatography (gradient of pentane/ethyl acetate, generally starting from 9:1) to yield the α -amino amides **3–6**.

1-Morpholino-2-phenyl-2-(phenylamino)ethan-1-one (**3a**)



Starting from benzylideneaniline (54 mg), HE **1a** (143 mg), and following the general procedure 3, **3a** was obtained as a brown solid (70 mg, 80 %).

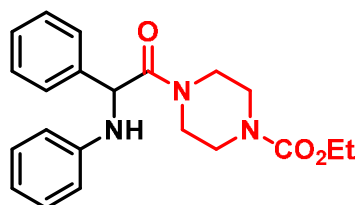
m.p. = 103–104 °C

$^1\text{H NMR}$ (400 MHz, CDCl_3): δ [ppm] = 7.45 – 7.39 (m, 2H), 7.39 – 7.32 (m, 2H), 7.32 – 7.27 (m, 1H), 7.18 – 7.08 (m, 2H), 6.75 – 6.62 (m, 3H), 5.27 (s, 1H), 4.44 (br. s, 1H, NH), 3.78 – 3.43 (m, 7H), 3.29 – 3.13 (m, 1H).

$^{13}\text{C}\{-^1\text{H}\}$ -NMR (75 MHz, CDCl_3): δ [ppm] = 169.5, 146.0, 138.1, 129.4, 129.2, 128.4, 127.8, 118.4, 114.1, 66.8, 66.3, 58.5, 46.1, 43.0.

HRMS (ESI): m/z = calcd. for $\text{C}_{18}\text{H}_{21}\text{N}_2\text{O}^+$: 297.1598, found: 297.1600.

Ethyl 4-(2-phenyl-2-(phenylamino)acetyl)piperazine-1-carboxylate (**3b**)



Starting from benzylideneaniline (54 mg), HE **1b** (171 mg), and following the general procedure 3, **3b** was obtained as a beige solid (61 mg, 55 %).

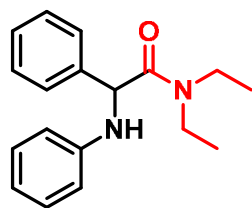
m.p. = 109–111 °C

$^1\text{H NMR}$ (400 MHz, CDCl_3): δ [ppm] = 7.43 – 7.39 (m, 2H), 7.38 – 7.32 (m, 2H), 7.31 – 7.26 (m, 1H), 7.16 – 7.10 (m, 2H), 6.75 – 6.67 (m, 3H), 5.30 (s, 1H), 5.20 (br. s, 1H, NH), 4.11 (q, J = 7.1 Hz, 2H), 3.83 – 3.71 (m, 1H), 3.60 – 3.39 (m, 5H), 3.28 – 3.17 (m, 1H), 2.89 – 2.77 (m, 1H), 1.23 (t, J = 7.1 Hz, 3H).

$^{13}\text{C}\{-^1\text{H}\}$ -NMR (101 MHz, CDCl_3): δ [ppm] = 169.5, 155.4, 145.5, 137.7, 129.6, 129.4, 129.3, 128.6, 127.9, 118.9, 114.5, 61.9, 59.1, 45.3, 43.3, 42.5, 14.7.

HRMS (ESI): m/z = calcd. for $\text{C}_{21}\text{H}_{26}\text{N}_3\text{O}_3^+$: 368.1969, found: 368.1967.

N,N-Diethyl-2-phenyl-2-(phenylamino)acetamide (**3c**)



Starting from benzylideneaniline (54 mg), HE **1c** (138 mg), and following the general procedure 3, **3c** was obtained as a yellow solid (65 mg, 76 %).

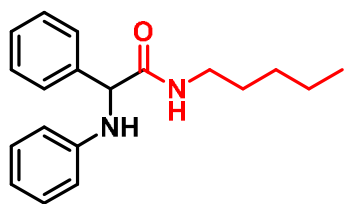
m.p. = 103–105 °C

$^1\text{H NMR}$ (300 MHz, CDCl_3): δ [ppm] = 7.50 – 7.47 (m, 2H), 7.40 – 7.25 (m, 3H), 7.17 – 7.12 (m, 2H), 6.72 – 6.67 (m, 3H), 5.48 (br. s, 1H, NH), 5.25 (s, 1H), 3.48 (dq, J = 14.2, 7.1 Hz, 2H), 3.31 (dq, J = 13.9, 7.0 Hz, 2H), 1.12 (t, J = 7.1 Hz, 3H), 1.02 (t, J = 7.1 Hz, 3H).

$^{13}\text{C}\{-^1\text{H}\}$ -NMR (101 MHz, CDCl_3): δ [ppm] = 169.9, 146.6, 138.9, 129.3, 129.0, 128.0, 127.9, 117.0, 113.8, 58.4, 41.6, 40.8, 14.0, 12.8.

HRMS (ESI): m/z = calcd. for $\text{C}_{18}\text{H}_{23}\text{N}_2\text{O}^+$: 283.1805, found: 283.1798.

N-Pentyl-2-phenyl-2-(phenylamino)acetamide (3d)



Starting from benzylideneaniline (54 mg), HE **1d** (143 mg), and following the general procedure 3, **3d** was obtained as a brown gum (55 mg, 62 %).

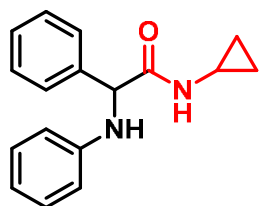
¹H NMR (300 MHz, CDCl₃): δ [ppm] = 7.43 – 7.36 (m, 5H), 7.19 – 7.16 (m, 2H), 6.83 – 6.78 (m, 1H), 6.66 – 6.63 (m, 2H), 4.73 (s, 1H), 4.44 (br. s, 1H), 3.30 – 3.23 (m, 2H), 1.45 – 1.42 (m, 2H), 1.25 – 1.20 (m, 4H),

0.84 (t, 3H, *J* = 7.0 Hz).

¹³C-¹H-NMR (75 MHz, CDCl₃): δ [ppm] = 171.1, 146.8, 139.1, 129.5, 129.3, 128.7, 127.5, 119.3, 114.0, 64.4, 39.6, 29.3, 29.0, 22.4, 14.1.

HRMS (ESI): *m/z* = calcd. for C₁₉H₂₅N₂O⁺: 297.1961, found: 297.1965.

N-Cyclopropyl-2-phenyl-2-(phenylamino)acetamide (3e)



Starting from benzylideneaniline (54 mg), HE **1e** (131 mg), and following the general procedure 3, **3e** was obtained as a yellow solid (65 mg, 74 %).

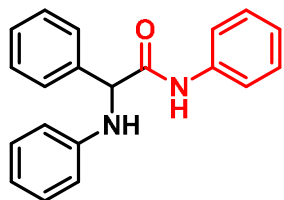
m.p. = 134–136 °C

¹H NMR (300 MHz, CDCl₃): δ [ppm] = 7.41 – 7.35 (m, 4H), 7.21 – 7.16 (m, 2H), 6.87 – 6.77 (m, 2H), 6.63 – 6.59 (m, 2H), 4.72 (s, 1H), 4.59 (br. s, 1H, NH), 2.76 – 2.67 (m, 1H), 0.76 – 0.71 (m, 2H), 0.46 – 0.42 (m, 2H).

¹³C-¹H-NMR (101 MHz, CDCl₃): δ [ppm] = 172.7, 146.7, 138.8, 129.4, 129.2, 128.6, 127.4, 119.1, 113.8, 64.0, 22.7, 6.8, 6.5.

HRMS (ESI): *m/z* = calcd. for C₁₇H₁₉N₂O⁺: 267.1492, found: 267.1499.

N,2-Diphenyl-2-(phenylamino)acetamide (3f)



Starting from benzylideneaniline (54 mg), HE **1c** (145 mg), and following the general procedure 3, **3f** was obtained as a pale-yellow solid (64 mg, 70 %).

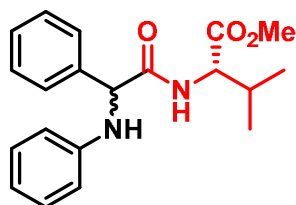
m.p. = 130–135 °C (dec.)

¹H NMR (300 MHz, CDCl₃): δ [ppm] = 8.75 (s, 1H, CONH), 7.59 – 7.50 (m, 4H), 7.48 – 7.38 (m, 3H), 7.38 – 7.22 (m, 4H), 7.18 – 7.10 (m, 1H), 6.94 – 6.85 (m, 1H), 6.79 – 6.72 (m, 2H), 4.86 (s, 1H), 4.52 (s, 1H, NH).

¹³C-¹H-NMR (75 MHz, CDCl₃): δ [ppm] = 169.6, 146.7, 138.6, 137.4, 129.7, 129.5, 129.1, 129.0, 127.6, 124.8, 120.1, 120.0, 114.3, 65.6.

HRMS (ESI): *m/z* = calcd. for C₂₀H₁₉N₂O⁺: 303.1492, found: 303.1495.

Methyl (2-phenyl-2-(phenylamino)acetyl)-(S)-valinate (3g)



Starting from benzylideneaniline (54 mg), HE **1e** (156 mg), and following the general procedure 3, **3g** was obtained as a mixture of the two diastereomers (1:1.3 ratio) as a yellow powder (75 mg, 74 %).

Major diastereomer:

¹H NMR (300 MHz, CDCl₃): δ [ppm] = 7.49 – 7.46 (m, 2H), 7.40 – 7.36 (m, 3H), 7.22 – 7.18 (m, 2H), 6.83 – 6.77 (m, 1H), 6.67 – 6.65 (m, 2H), 4.80 (d, *J* = 3.9 Hz, 1H), 4.58 (dd, *J* = 9.3, 4.5 Hz), 3.73 (s, 3H), 2.26 – 2.06 (m, 1H), 0.79 (d, *J* = 6.7 Hz), 0.67 (d, *J* = 6.8 Hz).

^{13}C - $\{^1\text{H}\}$ -NMR (75 MHz, CDCl_3): δ [ppm] = 172.3, 171.1, 146.5, 138.9, 129.3, 128.7, 127.6, 119.2, 113.9, 64.1, 57.0, 52.3, 31.2, 19.0, 17.3.

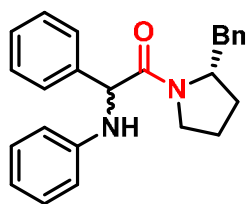
Minor diastereomer:

^1H NMR (300 MHz, CDCl_3): δ [ppm] = 7.49 – 7.46 (m, 2 H), 7.40 – 7.36 (m, 3H), 7.22 – 7.18 (m, 2H), 6.83 – 6.77 (m, 1H), 6.67 – 6.65 (m, 2H), 4.80 (d, J = 3.9 Hz, 1H), 4.53 (dd, J = 8.9, 4.9 Hz, 1H), 3.59 (s, 3H), 0.89 (t, J = 7.2 Hz, 6H).

^{13}C - $\{^1\text{H}\}$ -NMR (75 MHz, CDCl_3): δ [ppm] = 171.7, 171.5, 146.7, 138.7, 129.4, 129.3, 127.4, 119.3, 114.2, 64.5, 57.3, 52.1, 31.3, 19.1, 17.9.

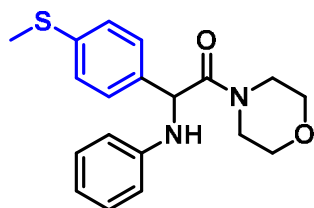
HRMS (ESI): m/z = calcd. for $\text{C}_{20}\text{H}_{25}\text{N}_2\text{O}_3^+$: 341.1860, found: 341.1864.

1-((S)-2-Benzylpyrrolidin-1-yl)-2-phenyl-2-(phenylamino)ethan-1-one (3h)



Starting from benzylideneaniline (54 mg), HE-(Bn-Pyrrolidine) (see section 3.6) (168 mg), and following the general procedure 3, **3h** was obtained as a mixture of the two diastereomers (near 1:1) as a yellow, fluorescent gum (58 %). The yield was determined *via* ^1H -NMR using 1,3,5-trimethoxybenzene as an external standard. Attempts to obtain a pure sample *via* crystallization or preparative HPLC were unsuccessful.

2-(3-(Methylthio)phenyl)-1-morpholino-2-(phenylamino)ethan-1-one (4a)



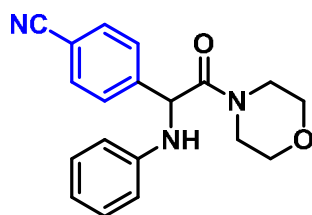
Starting from imine **2f** (65 mg), HE **1a** (143 mg), and following the general procedure 3, **4a** was obtained as a brownish gum (82 mg, 85 %).

^1H NMR (300 MHz, CDCl_3): δ [ppm] = 7.36 – 7.33 (m, 2H), 7.22– 7.20 (m, 2H), 7.15 – 7.10 (m, 2H), 6.71 – 6.61 (m, 3H), 5.22 (s, 1H), 3.65 – 3.48 (m, 7H), 3.29 – 3.25 (m, 1H), 2.45 (s, 3H).

^{13}C - $\{^1\text{H}\}$ -NMR (75 MHz, CDCl_3): δ [ppm] = 169.4, 146.1, 138.8, 134.8, 129.3, 128.1, 126.8, 118.0, 113.7, 66.7, 66.2, 57.5, 45.9, 42.9, 15.5.

HRMS (ESI): m/z = calcd. for $\text{C}_{19}\text{H}_{22}\text{N}_2\text{O}_2\text{S}^+$: 343.1475, found: 343.1477.

2-(4-Cyanophenyl)-1-morpholino-2-(phenylamino)ethan-1-one (**4b**)



Starting from imine **2g** (65 mg), HE **1a** (143 mg), and following the general procedure 3, **4b** was obtained as a pale-yellow solid (82 mg, 85 %).

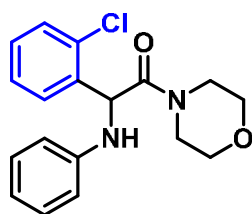
m.p. = 69–70 °C

¹H NMR (500 MHz, CDCl₃): δ [ppm] = 7.68 – 7.62 (m, 2H), 7.59 – 7.54 (m, 2H), 7.16 – 7.09 (m, 2H), 6.75 – 6.68 (m, 1H), 6.61 – 6.56 (m, 2H), 5.39 (d, *J* = 7.2 Hz, 1H), 5.33 (d, *J* = 6.4 Hz, 1H), 3.72 – 3.54 (m, 6H), 3.51 – 3.42 (m, 1H), 3.42 – 3.34 (m, 1H).

¹³C-¹H-NMR (75 MHz, CDCl₃): δ [ppm] = 168.4, 145.2, 143.6, 132.9, 129.4, 128.4, 118.7, 118.3, 113.7, 112.3, 66.6, 66.2, 57.5, 46.1, 43.0.

HRMS: *m/z* = calcd. for C₁₉H₂₀N₃O₂⁺: 322.1550, found: 322.1552.

2-(2-Chlorophenyl)-1-morpholino-2-(phenylamino)ethan-1-one (**4c**)



Starting from imine **2h** (62 mg), HE **1a** (143 mg), and following the general procedure 3, **4c** was obtained as a cream-colored solid (76 mg, 77 %).

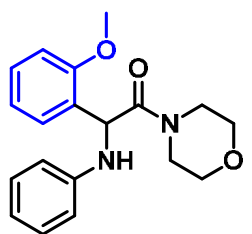
m.p. = 161–162 °C

¹H NMR (300 MHz, CDCl₃): δ [ppm] = 7.55 – 7.48 (m, 1H), 7.43 – 7.36 (m, 1H), 7.31 – 7.21 (m, 2H), 7.20 – 7.11 (m, 2H), 6.77 – 6.69 (m, 3H), 5.71 (s, 1H), 5.16 (br. s, 1H, NH), 3.77 – 3.48 (m, 7H), 3.35 – 3.20 (m, 1H).

¹³C-¹H-NMR (75 MHz, CDCl₃): δ [ppm] = 169.5, 146.2, 136.0, 133.0, 129.9, 129.7, 129.4, 129.2, 128.1, 118.7, 114.2, 66.8, 66.5, 54.6, 45.9, 43.3.

HRMS: *m/z* = calcd. for C₁₈H₂₀ClN₂O₂⁺: 331.1208, found: 331.1209.

2-(2-Methoxyphenyl)-1-morpholino-2-(phenylamino)ethan-1-one (**4d**)



Starting from imine **2i** (62 mg), HE **1a** (143 mg), and following the general procedure 3, **4d** was obtained as a yellow solid (73.2 mg, 75 %).

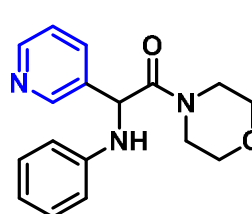
m.p. = 114–116 °C

¹H NMR (300 MHz, CDCl₃): δ [ppm] = 7.44 – 7.41 (m, 1H), 7.35 – 7.21 (m, 1H), 7.16 – 7.11 (m, 2H), 6.98 – 6.92 (m, 2H), 6.72 – 6.68 (m, 3H), 5.76 (s, 1H), 5.45 (br. s, 1H, NH), 4.00 (s, 3H), 3.73 – 3.52 (m, 7H), 3.18 – 3.14 (m, 1H).

¹³C-¹H-NMR (75 MHz, CDCl₃): δ [ppm] = 170.3, 155.7, 146.5, 129.5, 129.2, 128.2, 126.6, 121.9, 117.7, 113.7, 110.7, 66.8, 66.4, 55.7, 50.3, 45.4, 43.1.

HRMS (ESI): *m/z* = calcd. for C₁₉H₂₃N₂O₃⁺: 327.1703, found: 327.1703.

1-Morpholino-2-(phenylamino)-2-(pyridin-3-yl)ethan-1-one (**4e**)



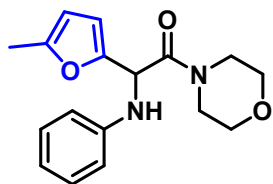
Starting from imine **2j** (55 mg), HE **1a** (143 mg), and following the general procedure 3 (elution: pentane/ethyl acetate 9/1 to 1/9), **4e** was obtained as a yellow gum (45 mg, 50 %).

¹H NMR (300 MHz, DMSO-*d*₆): δ [ppm] = 8.70 (s, 1H), 8.46 (d, *J* = 4.8 Hz, 1H), 7.85 (d, *J* = 7.9 Hz, 1H), 7.36 (dd, *J* = 7.9, 4.8 Hz, 1H), 7.04 (t, *J* = 7.7 Hz, 2H), 6.74 (d, *J* = 7.9 Hz, 2H), 6.54 (t, *J* = 7.3 Hz, 1H), 6.32 (d, *J* = 8.8 Hz, 1H), 5.72 (d, *J* = 8.8 Hz, 1H), 3.86 – 3.68 (m, 1H), 3.68 – 3.40 (m, 7H).

¹³C-¹H-NMR: (75 MHz, DMSO-*d*₆): δ [ppm] = 168.6, 149.3, 148.7, 146.7, 135.3, 134.6, 128.8, 123.6, 116.8, 113.3, 66.0, 65.8, 53.7, 45.6, 42.3.

HRMS: m/z = calcd. for $C_{17}H_{20}N_3O_2^+$: 298.1550, found: 298.1550.

2-(5-Methylfuran-2-yl)-1-morpholino-2-(phenylamino)ethan-1-one (4f)



Starting from imine **2k** (56 mg), HE **1a** (143 mg), and following the general procedure 3, **4f** was obtained as a brown solid (46 mg, 51 %).

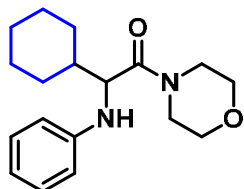
m.p. = 121–123 °C

1H NMR (300 MHz, $CDCl_3$): δ [ppm] = 7.20 – 7.12 (m, 2H), 6.78 – 6.62 (m, 3H), 6.17 (d, J = 3.1 Hz, 1H), 5.90 (dd, J = 3.1, 1.2 Hz, 1H), 5.32 (s, 1H), 5.26 (br. s, 1H, NH), 3.89 – 3.77 (m, 1H), 3.77 – 3.40 (m, 7H), 2.27 (s, 3H).

^{13}C -{ 1H }-NMR (75 MHz, $CDCl_3$): δ [ppm] = 167.7, 152.2, 149.5, 146.4, 129.3, 118.3, 113.8, 108.9, 106.8, 66.8, 66.5, 52.6, 46.2, 43.1, 13.7.

HRMS (ESI): m/z = calcd. for $C_{17}H_{21}N_2O_3^+$: 301.1547, found: 301.1545.

2-Cyclohexyl-1-morpholino-2-(phenylamino)ethan-1-one (4g)



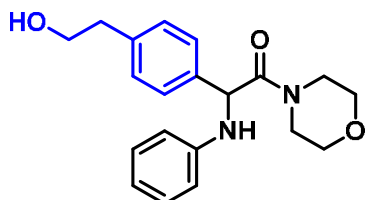
Starting from imine **2l** (57 mg), HE **1a** (143 mg), and following the general procedure 3, **4g** was obtained as a pale-yellow gum (44 mg, 47 %).

1H NMR (300 MHz, $CDCl_3$): δ [ppm] = 7.17 – 7.12 (m, 2H), 6.73 – 6.68 (m, 1H), 6.64 – 6.61 (m, 2H), 4.55 (br. s, NH), 4.10 (d, J = 5.6 Hz, 1H), 3.69 – 3.52 (m, 8H), 1.77 – 1.65 (m, 5H), 1.26 – 1.17 (m, 6H).

^{13}C -{ 1H }-NMR (75 MHz, $CDCl_3$): δ [ppm] = 172.0, 148.2, 129.4, 118.2, 114.0, 67.1, 66.8, 58.5, 46.4, 42.5, 42.1, 30.4, 28.8, 26.4, 26.3, 26.2.

HRMS: m/z = calcd. for $C_{18}H_{27}N_2O_2^+$: 303.2067, found: 303.2066.

2-(4-(2-Hydroxyethyl)phenyl)-1-morpholino-2-(phenylamino)ethan-1-one (4h)



Starting from imine **2m** (67 mg), HE **1a** (143 mg), and following the general procedure 3 using TFA (23 μ L, 1 equiv.) instead of $BF_3 \cdot OEt_2$, **4h** was obtained as a brown solid (52 %). The yield was determined *via* 1H -NMR using 1,3,5-trimethoxybenzene as an external standard. An analytical sample was crystallized from DCM (colorless crystals).

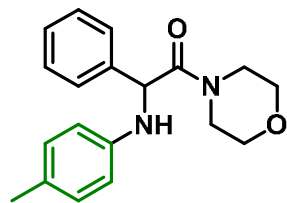
m.p. = 166–167 °C

1H NMR (300 MHz, $CDCl_3$): δ [ppm] = 7.38 – 7.35 (m, 2H), 7.22 – 7.19 (m, 2H), 7.15 – 7.10 (m, 2H), 6.71 – 6.63 (m, 3H), 5.25 (br. s, 1H), 3.82 (t, 2H, J = 6.56 Hz), 3.64 – 3.42 (m, 7H), 3.29 – 2.18 (m, 1H), 2.83 (t, 2H, J = 6.56 Hz).

^{13}C -{ 1H }-NMR (75 MHz, $CDCl_3$): δ [ppm] = 169.6, 146.2, 138.9, 136.3, 129.8, 129.4, 127.9, 118.2, 113.8, 66.8, 66.3, 63.5, 57.9, 46.1, 42.9, 38.9.

HRMS (ESI): m/z = calcd. for $C_{20}H_{25}N_2O_3^+$: 341.1860, found: 341.1863.

1-Morpholino-2-phenyl-2-((4-methylphenyl)amino)ethan-1-one (5a)



Starting from imine **2b** (59 mg), HE **1a** (143 mg), and following the general procedure 3, **5a** was obtained as an orange-brown solid (50 mg, 54 %).

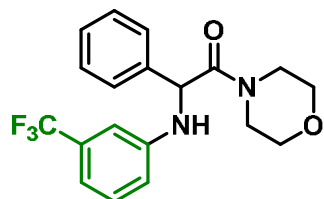
m.p. = 137–138 °C

1H NMR (500 MHz, $CDCl_3$): δ [ppm] = 7.44 – 7.40 (m, 2H), 7.37 – 7.33 (m, 2H), 7.30 – 7.26 (m, 1H), 6.96 – 6.92 (m, 2H), 6.60 – 6.55 (m, 2H), 5.24 (s, 1H), 3.76 – 3.43 (m, 7H), 3.25 – 3.16 (m, 1H), 2.20 (s, 3H).

$^{13}\text{C}\{-^1\text{H}\}$ -NMR (75 MHz, CDCl_3): δ [ppm] = 169.7, 144.1, 138.4, 129.8, 129.2, 128.3, 127.8, 127.4, 114.0, 66.8, 66.3, 58.6, 46.0, 43.0, 20.5.

HRMS (ESI): m/z = calcd. for $\text{C}_{19}\text{H}_{23}\text{N}_2\text{O}_2^+$: 311.1754, found: 311.1756.

1-Morpholino-2-phenyl-2-((3-(trifluoromethyl)phenyl)amino)ethan-1-one (**5b**)



Starting from imine **2c** (63 mg), HE **1a** (143 mg), and following the general procedure 3, **5b** was obtained as a colorless solid (83 mg, 76 %).

m.p. = 110–111 °C

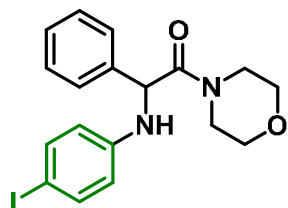
^1H NMR (300 MHz, CDCl_3): δ [ppm] = 7.45 – 7.27 (m, 5H), 7.23 – 7.16 (m, 1H), 6.94 – 6.75 (m, 3H), 5.25 (s, 1H), 3.77 – 3.38 (m, 7H), 3.28 – 3.11 (m, 1H).

$^{13}\text{C}\{-^1\text{H}\}$ -NMR (75 MHz, CDCl_3): δ [ppm] = 168.9, 146.4, 137.6, 131.4 (q, J = 31.7 Hz), 129.7, 129.3, 128.5, 127.7, 124.3 (q, J = 272.7 Hz), 116.6 (q, J = 1.1 Hz), 114.2 (q, J = 3.9 Hz), 109.6 (q, J = 4.0 Hz), 66.7, 66.1, 57.8, 46.0, 43.0.

^{19}F NMR (565 MHz, CDCl_3): δ [ppm] = –62.89.

HRMS (ESI): m/z = calcd. for $\text{C}_{19}\text{H}_{20}\text{F}_3\text{N}_2\text{O}_2^+$: 365.1471, found: 365.1472.

1-Morpholino-2-phenyl-2-((4-iodophenyl)amino)ethan-1-one (**5c**)



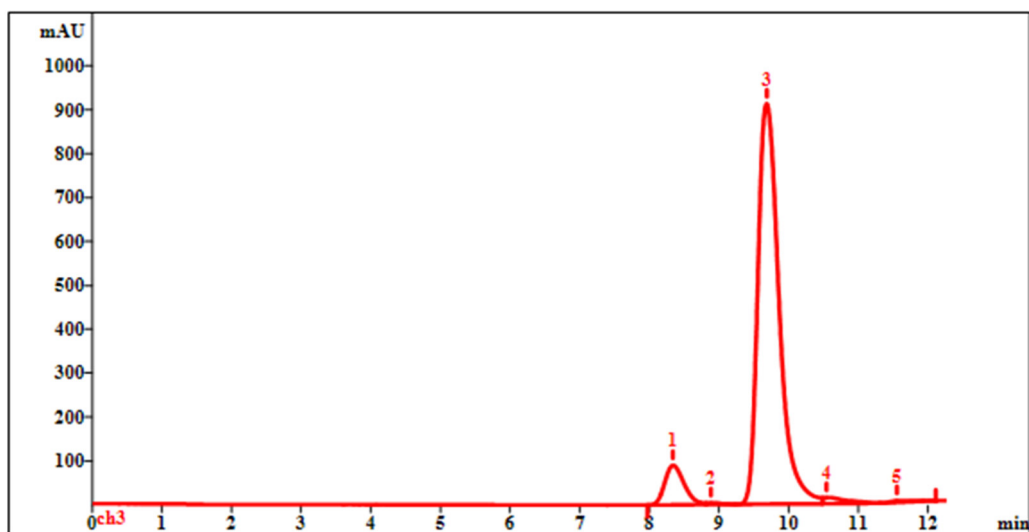
Starting from imine **2d** (92 mg), HE **1a** (143 mg), and following the general procedure 3, a mixture of **5c** and **3a** inseparable by preparative column chromatography was obtained due to deiodination of the product during the photoreaction as a white-brown solid (75 mg). The ratio of **5c** to **3a** was determined as 11/1 *via* HPLC, which corresponds to a yield of 56 % for **5c**.

Due to the large excess of **5c**, it could nonetheless be characterized by NMR spectroscopy and mass spectrometry.

^1H NMR (300 MHz, CDCl_3): δ [ppm] = 7.31 – 7.18 (m, 7H), 6.35 – 6.32 (m, 2H), 5.33 (br. s, 1H, NH), 5.11 (s, 1H), 3.60 – 3.40 (m, 7H), 3.12 – 3.09 (m, 1H).

$^{13}\text{C}\{-^1\text{H}\}$ -NMR (75 MHz, CDCl_3): δ [ppm] = 169.1, 145.7, 137.9, 137.7, 129.3, 128.5, 127.7, 115.9, 78.8, 66.7, 66.2, 57.9, 46.0, 43.0.

HRMS (ESI): m/z = calcd. for $\text{C}_{18}\text{H}_{20}\text{IN}_2\text{O}_2^+$: 423.0564, found: 423.0560.

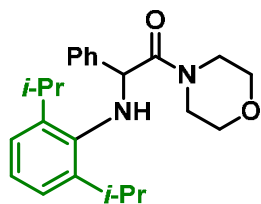


Quantitation method: Custom

Peak	Retention min	Height mAU	Area mAU*sec	Conc.	Component
1	8.34	89.59	1732.232	86.61	
2	8.89	3.63	53.514	2.68	
3	9.68	910.44	19218.891	960.94	
4	10.54	13.89	327.177	16.36	
5	11.55	3.81	89.503	4.48	
5	12.26	1021.36	21421.318	1071.07	

Figure 1. Chromatogram of the mixture of **5c** and **3a** obtained via HPLC (ProntoSIL, C₁₈ column, MeCN 100 %, 5 mL/min).

2-((2,6-Diisopropylphenyl)amino)-1-morpholino-2-phenylethan-1-one (5d)



Starting from imine **2e** (77 mg), HE **1a** (143 mg), and following the general procedure 3, **5d** was obtained as a colorless solid after 40 hours of reaction time (35 mg, 30 %).

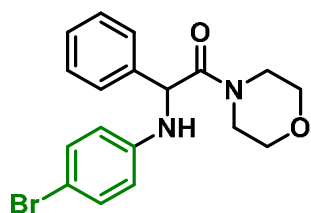
m.p. = 119–121 °C

¹H NMR (300 MHz, CDCl₃): δ [ppm] = 7.31 – 7.24 (m, 3H), 7.19 – 7.12 (m, 2H), 7.04 (s, 3H), 4.92 (s, 1H), 4.63 (br. s, 1H), 3.95 – 3.81 (m, 1H), 3.79 – 3.53 (m, 3H), 3.52 – 3.31 (m, 2H), 3.29 – 3.18 (m, 1H), 3.18 – 3.05 (m, 3H), 1.22 (d, *J* = 7.3 Hz, 6H), 0.99 (d, *J* = 7.3 Hz, 6H).

¹³C-^{{1}H}-NMR (75 MHz, CDCl₃): δ [ppm] = 170.6, 142.8, 140.4, 138.3, 128.9, 128.1, 127.5, 123.9, 123.6, 66.8, 66.2, 63.9, 45.9, 42.7, 27.9, 24.5, 24.1.

HRMS (ESI): *m/z* = calcd. for C₂₄H₃₃N₂O₂⁺: 381.2537, found: 381.2535.

1-Morpholino-2-phenyl-2-((4-bromophenyl)amino)ethan-1-one (5e)



Starting from *N*-Phenyl-1-(4-bromophenyl)methanimine (74 mg), HE **1a** (143 mg), and following the general procedure 3, **5e** was obtained as an off-white powder (83 mg, 74 %).

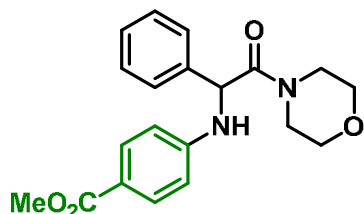
m.p. = 175–176 °C

¹H NMR (300 MHz, CDCl₃): δ [ppm] = 7.34 – 7.16 (m, 5H), 7.13 – 7.06 (m, 2H), 6.45 – 6.37 (m, 2H), 5.35 (d, *J* = 7.2 Hz, 1H), 5.09 (d, *J* = 7.2 Hz, 1H), 3.66 – 3.34 (m, 7H), 3.16 – 3.02 (m, 1H).

¹³C-^{{1}H}-NMR (75 MHz, CDCl₃): δ [ppm] = 169.1, 145.2, 137.7, 131.9, 129.2, 128.4, 127.6, 115.2, 109.5, 66.6, 66.1, 58.0, 45.9, 42.9.

HRMS (ESI): *m/z* = calcd. for C₁₈H₂₀BrN₂O₂⁺: 375.0703, found: 375.0704.

Methyl 4-((2-morpholino-2-oxo-1-phenylethyl)amino)benzoate (5f)



Starting from methyl 4-(benzylideneamino)benzoate (76 mg), HE **1a** (143 mg), and following the general procedure 3, **5f** was obtained as a yellow solid (42 mg, 55 %).

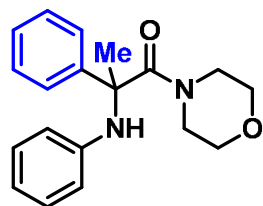
m.p. = 174–176 °C

¹H NMR (300 MHz, CDCl₃): δ [ppm] = 7.85 – 7.77 (m, 2H), 7.47 – 7.26 (m, 5H), 6.64 – 6.56 (m, 2H), 6.00 (s, 1H), 5.29 (s, 1H), 3.82 (s, 3H), 3.78 – 3.42 (m, 7H), 3.26 – 3.10 (m, 1H).

¹³C-^{{1}H}-NMR (75 MHz, CDCl₃): δ [ppm] = 168.8, 167.3, 149.8, 137.6, 131.6, 129.3, 128.6, 127.7, 118.9, 112.3, 66.7, 66.1, 57.3, 51.6, 46.0, 43.1.

HRMS (ESI): *m/z* = calcd. for C₂₀H₂₃N₂O₄⁺: 355.1652, found: 355.1652.

1-Morpholino-2-phenyl-2-(phenylamino)propan-1-one (6a)



Starting from imine **2n** (47 mg, 0.24 mmol), HE **1a** (114 mg, 0.311 mmol), and following the general procedure 3 with adjusted scale, **6a** was obtained as a beige solid (12 mg, 17 %).

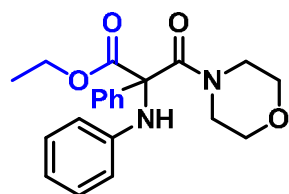
m.p. = 148–150 °C

$^1\text{H NMR}$ (300 MHz, CDCl_3): δ [ppm] = 7.51 – 7.35 (m, 4H), 7.35 – 7.27 (m, 1H), 7.18 – 7.06 (m, 2H), 6.78 – 6.59 (m, 3H), 5.07 (br. s, 1H, NH), 3.77 – 3.05 (m, 8H), 1.86 (s, 3H).

$^{13}\text{C}\{-^1\text{H}\}$ -NMR (75 MHz, CDCl_3): δ [ppm] = 172.2, 144.9, 143.4, 129.3, 129.2, 127.8, 125.3, 118.4, 115.3, 77.6, 77.2, 76.7, 66.4, 63.9, 45.7 (br. s), 25.7.

HRMS: m/z = calcd. for $\text{C}_{19}\text{H}_{23}\text{N}_2\text{O}_2^+$: 311.1754, found: 311.1750.

Ethyl 3-morpholino-3-oxo-2-phenyl-2-(phenylamino)propanoate (6b)



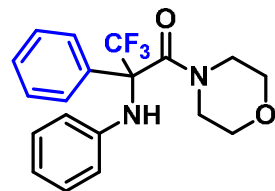
Starting from imine **2o** (76 mg), HE **1a** (143 mg), and following the general procedure 3, **6b** was obtained as a yellow gum (60 mg, 54 %).

$^1\text{H NMR}$ (300 MHz, CDCl_3): δ [ppm] = 7.68 – 7.65 (m, 2H), 7.34 – 7.29 (m, 3H), 7.11 – 7.06 (m, 2H), 6.75 – 6.72 (m, 1H), 6.62 – 6.59 (m, 2H), 4.28 (dq, 2H, J = 7.2, 1.8 Hz), 3.76 – 3.23 (m, 8H), 1.25 (t, J = 7.2 Hz, 3H).

$^{13}\text{C}\{-^1\text{H}\}$ -NMR: (75 MHz, CDCl_3): δ [ppm] = 169.9, 166.2, 143.9, 135.7, 129.6, 129.2, 128.9, 128.2, 127.9, 118.6, 114.6, 70.4, 66.4, 63.1, 14.1.

HRMS (ESI): m/z = calcd. for $\text{C}_{21}\text{H}_{25}\text{N}_2\text{O}_4^+$: 369.1809, found: 369.1803.

1-Morpholino-2-phenyl-2-(phenylamino)-2-(trifluoromethyl)propan-1-one (6c)



Starting from imine **2p** (75 mg), HE **1a** (143 mg), and following the general procedure 3, **6c** was obtained as a pale-yellow solid (52 mg, 48 %).

m.p. = 189–191 °C

$^1\text{H NMR}$ (300 MHz, CDCl_3): δ [ppm]: 7.59 – 7.38 (m, 5H), 7.23– 7.09 (m, 2H), 6.92 – 6.79 (m, 3H), 5.02 (s, 1H), 3.82 – 2.67 (m, 8H).

$^{13}\text{C}\{-^1\text{H}\}$ -NMR (101 MHz, CDCl_3 , -20 °C): δ [ppm] = 164.9, 143.0, 133.1, 129.8, 129.3, 129.2, 126.1, 123.1 (q, J = 288.9 Hz), 120.1, 115.4, 68.8 (q, J = 26.0 Hz), 66.3^a, 65.2^a, 46.6^a, 42.8^a.

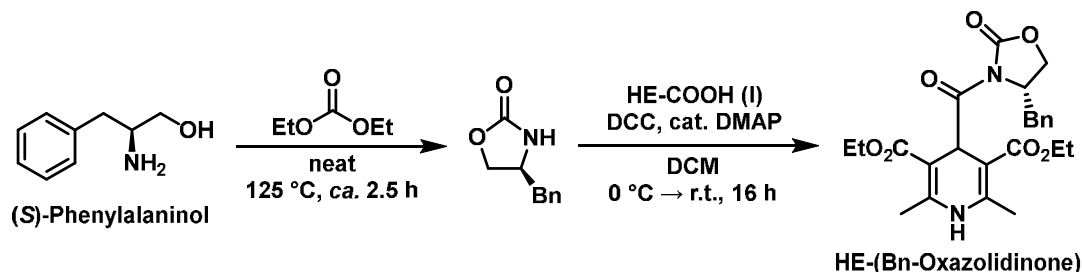
$^{19}\text{F NMR}$ (565 MHz, CDCl_3): δ [ppm]: = -71.02 .

HRMS (ESI): m/z = calcd. for $\text{C}_{19}\text{H}_{20}\text{F}_3\text{N}_2\text{O}_2^+$: 365.1471, found: 365.1478.

^a At room temperature, these signals (corresponding to the carbon atoms of the morpholine moiety) are almost not visible, even when 50 mg of substance is used for the ^{13}C -NMR measurement.

3.6 Syntheses of other starting materials

Diethyl (S)-4-(4-benzyl-2-oxooxazolidine-3-carbonyl)-2,6-dimethyl-1,4-dihydropyridine-3,5-dicarboxylate (HE-(Bn-Oxazolidinone))



(S)-4-Benzyl-2-oxazolidinone

A mixture of (S)-phenylalaninol (1.00 g, 6.61 mmol, 1.0 equiv.), anhydrous potassium carbonate (935 mg, 1.0 equiv.) and diethyl carbonate (1.60 mL, 13.2 mmol, 2.0 equiv.) was heated to 125 °C in a distillation apparatus fitted with a 10 cm Vigreux column until no more ethanol was obtained in the receiving flask (ca. 2.5 hours). The mixture was diluted with DCM (20 mL), washed with water (2× 10 mL) and brine (10 mL), dried over Na₂SO₄ and filtered. The solvent was removed *in vacuo* and the residue purified by flash column chromatography on silica (pentane/ethyl acetate) to yield (S)-4-benzyl-2-oxazolidinone as a colorless solid (876 mg, 4.94 mmol, 75 %).

¹H NMR (300 MHz, CDCl₃): δ [ppm] = 7.38 – 7.23 (m, 3H), 7.21 – 7.14 (m, 2H), 5.53 (s, 1H), 4.46 (t, *J* = 8.1 Hz, 1H), 4.19 – 4.05 (m, 2H), 2.88 (d, *J* = 6.7 Hz, 2H).

X.-Y. Tian, J.-W. Han, Q. Zhao, H. N. C. Wong, *Org. Biomol. Chem.* **2014**, *12*, 3686–3700.

HE-(Bn-Oxazolidinone)

A suspension of (S)-4-benzyl-2-oxazolidinone (494 mg, 2.79 mmol, 1.0 equiv.), HE-COOH I (1.09 g, 3.67 mmol, 1.3 equiv.), and 4-(dimethylamino)-pyridine (51.9 mg, 0.425 mmol, 15 mol%) in dry DCM (10 mL) was cooled to 0 °C and dicyclohexylcarbodiimide (749 mg, 3.63 mmol, 1.3 equiv.) was added in one portion. The mixture was stirred at 0 °C for 10 minutes, after which it was warmed to room temperature and stirred for 16 hours. The bright-yellow suspension was filtered, the filter cake was washed with DCM (10 mL) and the filtrate was washed with sat. aq. NaHCO₃ (10 mL). The organic phase was dried over Na₂SO₄, filtered and concentrated *in vacuo*. The residue was purified by column chromatography on silica (pentane/ethyl acetate 7:3, two columns were necessary) to yield HE-(Bn-Oxazolidinone) as a pale-brown solid (158 mg, 0.346 mmol, 12 %).

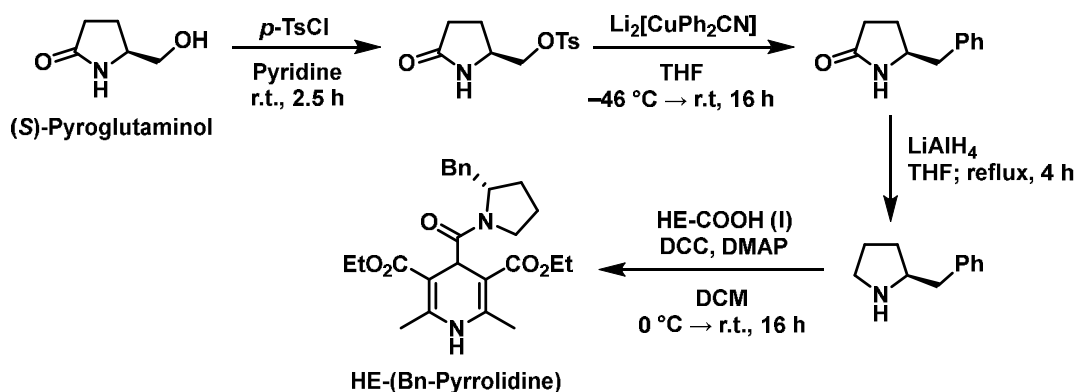
m.p. = 140–141 °C

¹H NMR (300 MHz, CDCl₃): δ [ppm] = 7.30 – 7.24 (m, 5H), 6.06 (br. s, 1H, NH), 6.00 (s, 1H), 4.68 – 4.61 (m, 1H), 4.22 – 4.08 (m, 6H), 3.37 (dd, *J* = 13.1, 3.1 Hz, 1H), 2.62 (dd, *J* = 13.1, 10.7 Hz, 1H), 2.28 (d, *J* = 4.5 Hz, 6H), 1.25 (dt, *J* = 11.9, 7.1, 6H).

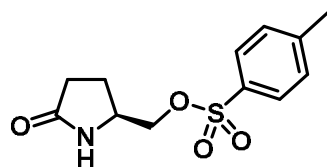
¹³C-¹H-NMR (75 MHz, CDCl₃): δ [ppm] = 166.9, 152.3, 135.9, 129.3, 128.9, 127.1, 65.5, 60.13, 60.07, 56.3, 38.6, 37.9, 19.7, 19.5, 14.3, 14.1.

HRMS (ESI): *m/z* = calcd. for C₂₁H₂₅N₂NaO₄⁺: 479.1789, found: 479.1783.

Diethyl (S)-4-(2-benzylpyrrolidine-1-carbonyl)-2,6-dimethyl-1,4-dihydropyridine-3,5-dicarboxylate (HE-(Bn-Pyrrolidine))



(S)-(5-Oxopyrrolidin-2-yl)methyl 4-toluenesulfonate

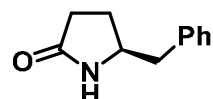


(S)-Pyroglutaminol (600 mg, 5.21 mmol, 1.0 equiv.) was dissolved in pyridine (4.5 mL) and *p*-toluenesulfonyl chloride (1.49 g, 7.82 mmol, 1.5 equiv.) was added. The mixture was stirred for 2.5 hours at room temperature, after which water (3 mL) was added and the mixture stirred for additional 30 minutes. Then aq. HCl (2 M, 20 mL) was added and the organics were extracted with DCM (8 × 30 mL). The combined organic phases were dried over Na₂SO₄, filtered and concentrated *in vacuo*. The solid residue was recrystallized from DCM/Hexane to yield (S)-(5-oxopyrrolidin-2-yl)methyl 4-toluene-sulfonate as a pinkish solid (565 mg, 2.10 mmol, 40 %).

¹H NMR (300 MHz, CDCl₃): δ [ppm] = 7.82 – 7.75 (m, 2H), 7.39 – 7.33 (m, 2H), 6.00 (br. s, NH), 4.05 (dd, *J* = 9.4, 3.3 Hz), 3.94 – 3.83 (m, 2H), 2.46 (s, 3H), 2.38 – 2.20 (m, 3H), 1.80 – 1.75 (m, 1H).

S. Lebrun, A. Couture, E. Deniau, P. Grandclaoudon, *Tetrahedron Asymmetry* **2003**, *14*, 2625–2632.

(S)-5-Benzyl-2-pyrrolidinone

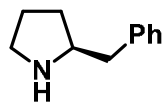


A suspension of cuprous cyanide (dried twice azeotropically with toluene, 505 mg, 5.64 mmol, 2.7 equiv.) in dry THF (5 mL) was cooled to –84 °C using an ethyl acetate/liquid N₂ bath and phenyllithium (1.9 M in dibutyl ether, 5.90 mL, 11.2 mmol, 5.4 equiv.) was added slowly. The mixture was stirred for 5 minutes at –84 °C, after which it was warmed to –46 °C using an acetonitrile/liquid N₂ bath and stirred for further 5 minutes. A suspension of (S)-(5-oxopyrrolidin-2-yl)methyl 4-toluenesulfonate (557 mg, 2.07 mmol, 1.0 equiv.) in dry THF (5 mL) was cannulated to the mixture which was then stirred for 3 hours at –46 °C and then overnight at room temperature. The clear, yellow mixture was poured into NH₄Cl/NH₃ buffer (ca. 20 mL, adjusted to pH 8 by adding dilute aq. NaOH to sat. aq. NH₄Cl) and the organic layer was diluted with ethyl acetate (20 mL) and washed with water (2 × 20 mL). The combined deep blue aqueous layers were extracted with ethyl acetate (2 × 30 mL) and the combined organic phases were dried over Na₂SO₄, filtered and concentrated *in vacuo*. The residue was purified by column chromatography on silica (100% pentane, then 100% ethyl acetate) to yield (S)-5-benzyl-2-pyrrolidinone as a colorless solid (257 mg, 1.47 mmol, 71 %).

¹H NMR (300 MHz, CDCl₃): δ [ppm] = 7.36 – 7.21 (m, 3H), 7.20 – 7.14 (m, 2H), 5.66 (br. s, 1H, NH), 3.94 – 3.83 (m, 1H), 2.86 (dd, *J* = 13.4, 5.3 Hz, 1H), 2.70 (dd, *J* = 13.4, 8.4 Hz, 1H), 2.41 – 2.21 (m, 3H), 1.91 – 1.79 (m, 1H).

S. Lebrun, A. Couture, E. Deniau, P. Grandclaoudon, *Tetrahedron Asymmetry* **2003**, *14*, 2625–2632.

(S)-2-Benzylpyrrolidine

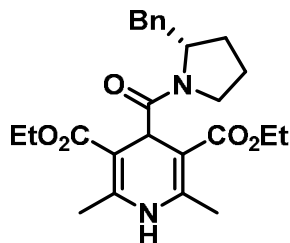


A solution of (S)-5-benzyl-2-pyrrolidinone (251 mg, 1.43 mmol, 1.0 equiv.) in dry THF (5 mL) was cooled to 0 °C and a suspension of lithium aluminium hydride (108 mg, 2.85 mmol, 2.0 equiv.) in dry THF (5 mL) was added dropwise. After stirring for 10 more minutes at 0 °C the mixture was refluxed for 4 hours. The mixture was then cooled to 0 °C and water (0.1 mL), then 15 % aq. NaOH (0.1 mL), then water (0.3 mL) were added under vigorous stirring. The mixture was stirred for 15 minutes at room temperature, then Na₂SO₄ was added and the mixture was stirred for further 15 minutes, upon which it was filtered and concentrated *in vacuo*. The residue was purified by column chromatography on silica (DCM/MeOH 20:1 containing 1 % of NEt₃) to yield (S)-2-benzylpyrrolidine as a yellow liquid (175 mg, 0.997 mmol, 70 %).

¹H NMR (300 MHz, CDCl₃): δ [ppm] = 7.33 – 7.17 (m, 5H), 3.32 – 3.19 (m, 1H), 3.06 (ddd, *J* = 10.3, 7.6, 5.1 Hz, 1H), 2.90 – 2.74 (m, 3H), 2.31 (br. s, 1H, NH), 1.91 – 1.65 (m, 3H), 1.48 – 1.37 (m, 1H).

S. Lebrun, A. Couture, E. Deniau, P. Grandclaoudon, *Tetrahedron Asymmetry* **2003**, *14*, 2625–2632.

HE-(Bn-Pyrrolidine)



A mixture of HE-COOH **I** (288 mg, 0.968 mmol, 1.0 equiv.), (S)-2-benzylpyrrolidine (170 mg, 0.968 mmol, 1.0 equiv.) and 4-(dimethylamino)pyridine (118 mg, 0.968 mmol, 1.0 equiv.) in dry DCM (5 mL) was cooled to 0 °C and dicyclohexylcarbodiimide (200 mg, 0.968 mmol, 1.0 equiv.) was added in one portion. The mixture was stirred at 0 °C for 30 minutes, after which it was slowly warmed to room temperature and stirred overnight. The bright yellow suspension was stored at –20 °C for several hours to precipitate as much dicyclohexylurea as possible, then filtered cold. The filtrate was washed with aq. HCl (1 M, 15 mL) and water (15 mL) and the combined aqueous phases were extracted with DCM (3× 15 mL). The organic phases were combined, dried over Na₂SO₄, filtered, and concentrated *in vacuo*. The solid residue was purified by column chromatography on silica (pentane/ethyl acetate 7:3 to 6:4, each containing 0.5 % of AcOH) to yield HE-(Bn-Pyrrolidine) as a yellow solid (186 mg, 0.422 mmol, 44 %).

m.p. = 117–119 °C

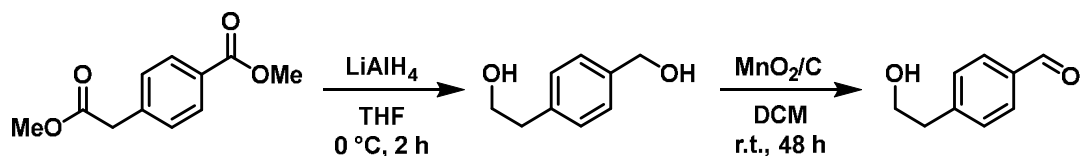
¹H NMR (300 MHz, CDCl₃): δ [ppm] = 8.49 (s, 1H, NH), 7.35 – 7.14 (m, 5H), 4.84 (s, 1H), 4.31 – 4.11 (m, 5H), 4.09 – 3.96 (m, 2H), 3.12 (dd, *J* = 13.0, 3.2 Hz, 1H), 2.49 (dd, *J* = 12.9, 9.4 Hz, 1H), 2.31 (s, 3H), 2.24 (s, 3H), 1.91 – 1.65 (m, 4H), 1.27 (t, *J* = 7.1 Hz, 6H).

¹³C-{¹H}-NMR (75 MHz, CDCl₃): δ [ppm] = 174.1, 167.9, 148.3, 147.9, 139.5, 129.6, 128.4, 126.2, 98.8, 98.7, 77.2, 60.0, 59.9, 59.3, 47.4, 39.8, 38.9, 28.6, 24.1, 19.7, 19.5, 14.73, 14.68.

HRMS (ESI): *m/z* = calcd. for C₂₅H₃₃N₂O₅⁺: 441.2389, found: 441.2387.

[α]_D²⁰ = –26.2° (c = 0.455, CHCl₃).

4-(2-Hydroxyethyl)benzaldehyde



Synthesis of activated MnO_2 on carbon (MnO_2/C):

In a 600 mL beaker, potassium permanganate (20.0 g, 127 mmol, 1.0 equiv.) was dissolved in water (250 mL) and the solution was brought to a boil. Activated carbon (6.25 g, 520 mmol, 4.1 equiv.) was added portionwise under strong stirring and mild gas evolution. The mixture was boiled until the purple color disappeared (*ca.* 20–30 min) and the mixture had turned brown. The beaker was taken off the hot plate and left at room temperature for 10–15 min upon which it was filtered warm. The filter cake was dried at $105\text{ }^\circ\text{C}$ for 18 hours to yield 18.5 g of MnO_2/C as a lightweight black powder.

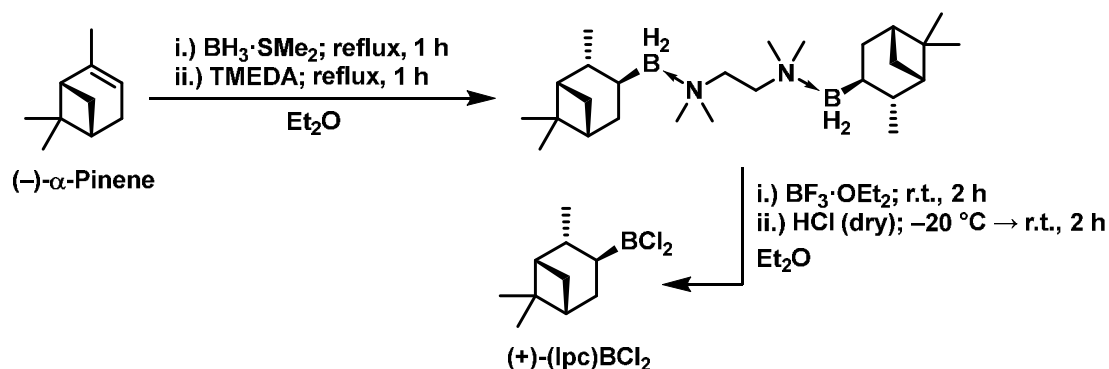
Synthesis of 4-(2-hydroxyethyl)benzyl alcohol:

A solution of dimethyl homoterephthalate (2.00 g, 9.61 mmol, 1.0 equiv.) in dry THF (10 mL) was cooled to $0\text{ }^\circ\text{C}$ and a suspension of LiAlH_4 (567 mg, 14.8 mmol, 1.5 equiv.) in dry THF (15 mL) was added dropwise. After stirring the mixture for 2 hours at $0\text{ }^\circ\text{C}$, water (0.6 mL), then aq. NaOH (15 %, 0.6 mL), then water (1.8 mL) were added at $0\text{ }^\circ\text{C}$ under vigorous stirring. After 15 minutes of stirring at room temperature, MgSO_4 was added and the mixture was stirred for another 15 minutes, followed by filtration. The filtrate was washed with brine (10 mL) and the organic phase was dried over MgSO_4 and filtered. Removal of the solvent *in vacuo* yielded crude 4-(2-hydroxyethyl)benzyl alcohol as a yellow oil, which was used without characterization or further purification (*ca.* 1.40 g).

Synthesis of 4-(2-hydroxyethyl)benzaldehyde:

The oil was dissolved in DCM (50 mL) and MnO_2/C (18.5 g) was added, followed by vigorous stirring at room temperature for 48 hours (monitored by GC-MS). The mixture was filtered and the filter cake was washed thoroughly with DCM and ethyl acetate. Removal of the solvent *in vacuo* yielded 4-(2-hydroxyethyl)benzaldehyde as a yellow oil (*ca.* 502 mg), which was used without further purification in the synthesis of **2m**.

Monoisopinocampheylboron dichloride



Synthesis of the monoisopinocampheylborane TMEDA complex:

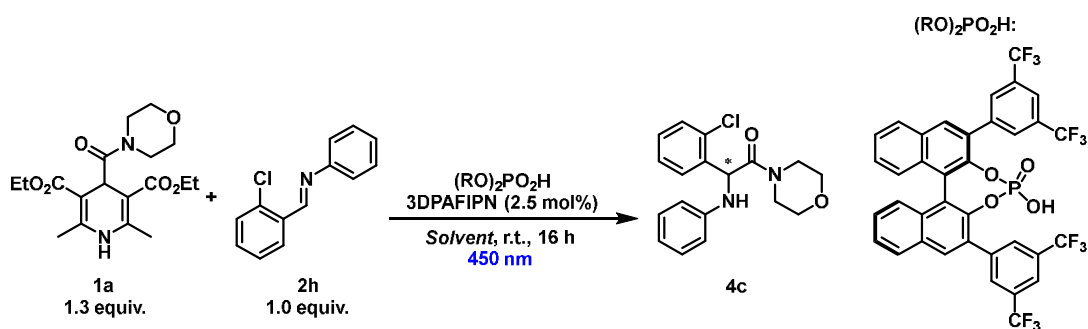
To a solution of borane dimethylsulfide (401 mg, 500 μ L, 5.26 mmol, 1.0 equiv.) in dry diethyl ether (5 mL) was added dropwise (-)- α -pinene (1.65 g, 1.92 mL, 12.0 mmol, 2.3 equiv.) so as to maintain gentle reflux, after which the mixture was refluxed for 1 hour. To the cooled down mixture was added tetramethylethylenediamine (306 mg, 0.39 mL, 2.62 mmol, 0.5 equiv.) and the mixture was subsequently refluxed for 1 hour. After the mixture had cooled to room temperature, a slow stream of nitrogen was passed through the flask to evaporate a small amount of the diethyl ether to generate seed crystals on the inner walls. The mixture was stored in the freezer overnight to induce complete crystallization. The solidified mixture was broken up using a glass rod and washed several times with cold pentane to yield the monoisopinocampheylborane TMEDA complex as a colorless powder which was used in the next step without further purification or characterization (259 mg, 0.621 mmol, 24 %).

Synthesis of monoisopinocampheylboron dichloride:

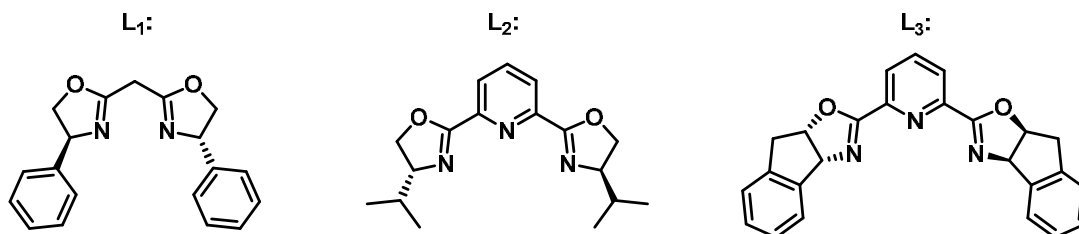
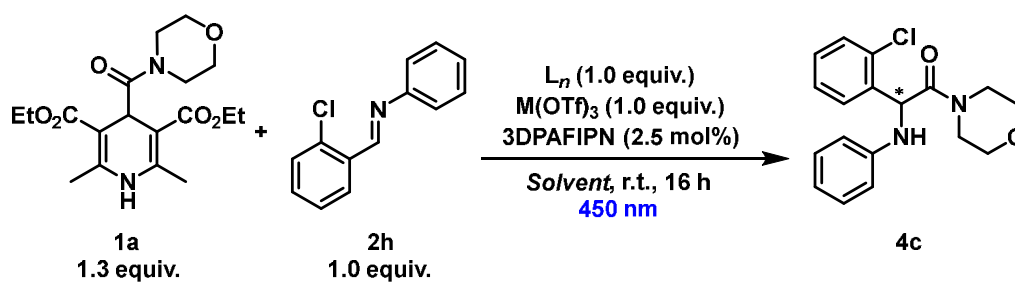
To a solution of the monoisopinocampheylborane TMEDA complex (259 mg, 0.621 mmol, 1.0 equiv.) in dry diethyl ether (5 mL) was added boron trifluoride diethyl etherate (171 mg, 0.15 mL, 1.22 mmol, 1.96 equiv.), after which the mixture was stirred at room temperature for 2 hours, during which a colorless precipitate formed. The suspension was filtered and the filtrate containing the monoisopinocampheylborane was cooled down to -20 °C using an ice/salt bath. A solution of HCl in diethyl ether (1.0 M, 2.48 mL, 2.48 mmol, 4.0 equiv.) was added dropwise under gas evolution. After complete addition, the mixture was stirred for 10 minutes at -20 °C, then for 2 hours at room temperature. The solvent was subsequently removed *in vacuo* at 0 °C to yield ether-free monoisopinocampheylboron dichloride as a viscous oil which was used without further purification (234 mg, 1.07 mmol, 86 %). The identity of the product was confirmed by a signal at 61 ppm in the ¹¹B-NMR spectrum (193 MHz, dry CDCl₃).

H. C. Brown, P. V. Ramachandran, J. Chandrasekharan, *Heteroat. Chem.* **1995**, *6*, 117–131.

5.4.4 Chiral experiments

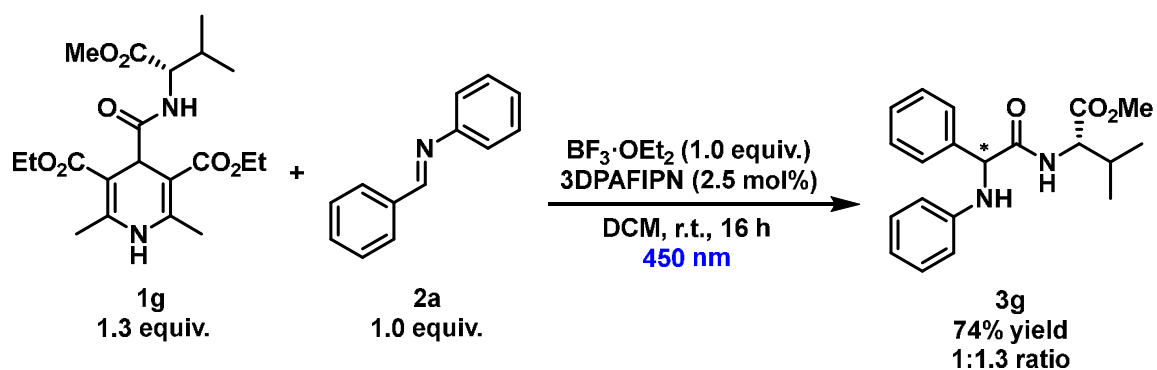
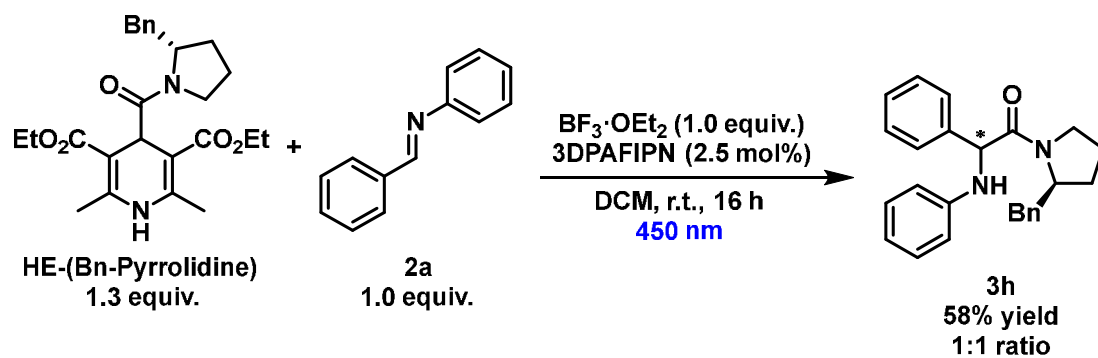
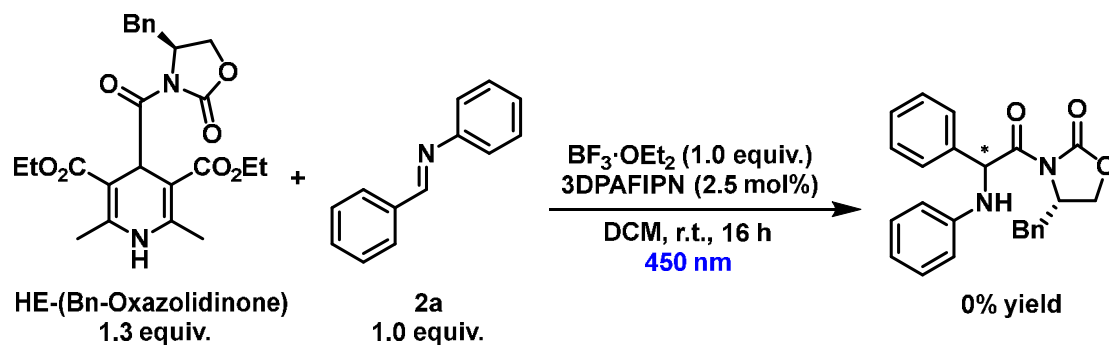
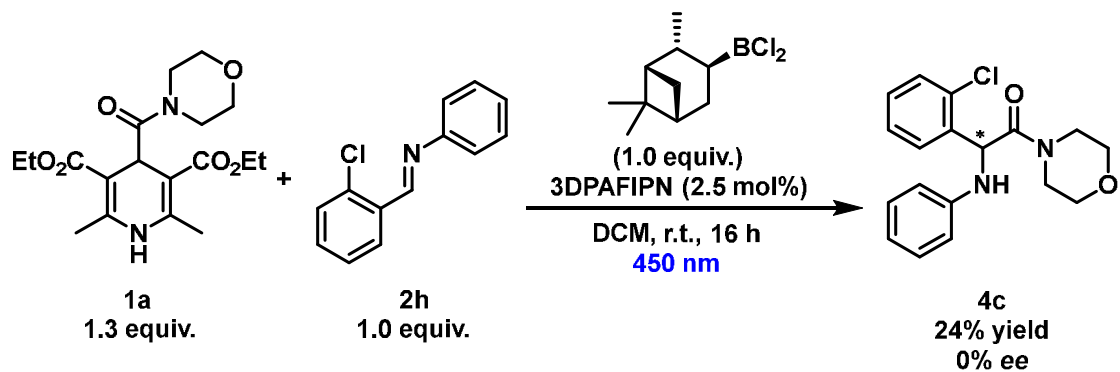


Solvent	Equiv. of $(RO)_2PO_2H$	Yield of 4c [%]	ee [%]
Toluene	1.0	80	10
Toluene	0.2	61	10
DCM	1.0	52	0



Note: $Sc(OTf)_3$ and $Yb(OTf)_3$ are sparingly soluble in aromatic or apolar solvents, also under irradiation.

M	L_n	Solvent	Yield of 4c [%]	ee [%]
Sc	L_1	DCM	39	0
Sc	L_2	MeCN	59	0
Yb	L_3	DCM	34	0
Yb	L_3	<i>o</i> -Xylene	0	—



5.4.5 Mechanistic investigations

Fluorescence-quenching experiments

The stock solutions were prepared by dissolving 0.61 mg of 3DPAFIPN in 100 mL of DMSO (0.01 mM) and by dissolving 90.2 mg of benzylideneaniline **2a** in 25.0 mL of the previously prepared 3DPAFIPN solution (0.02 M of the imine). All stock solutions were degassed for 10 minutes by purging with argon and transferred to the cuvette through the rubber septum fitted with an argon-filled balloon.

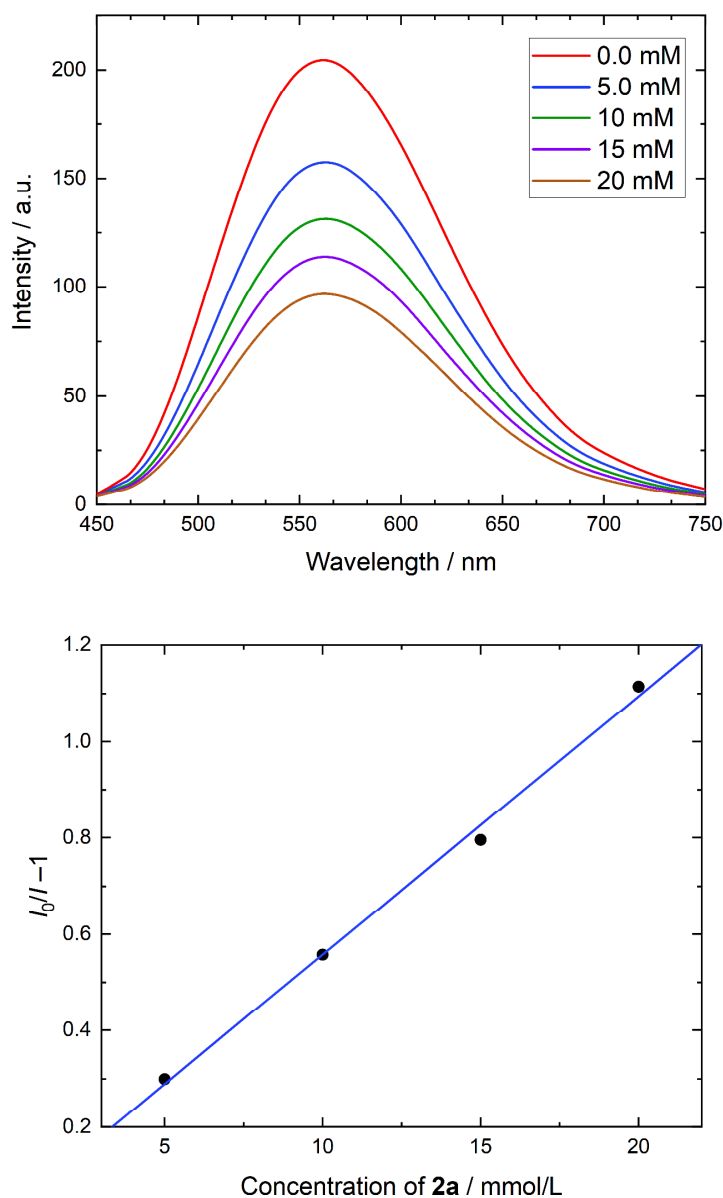
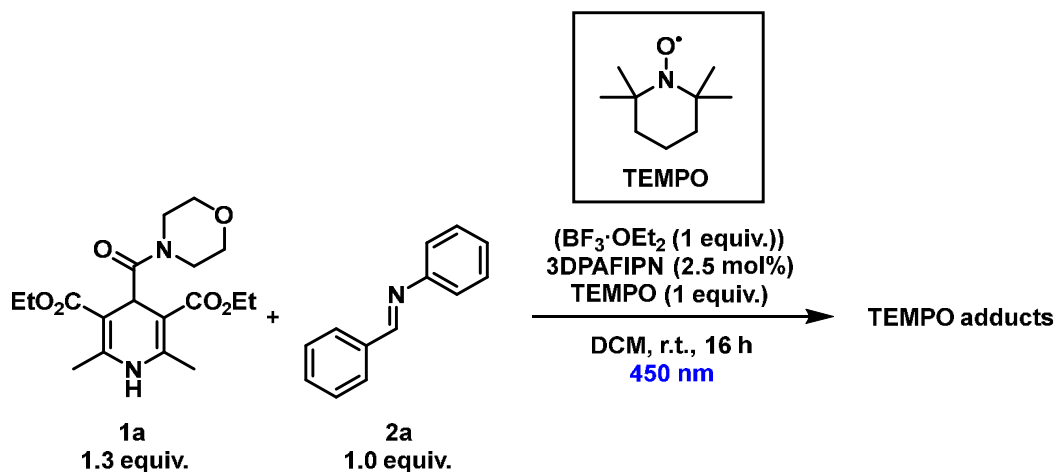


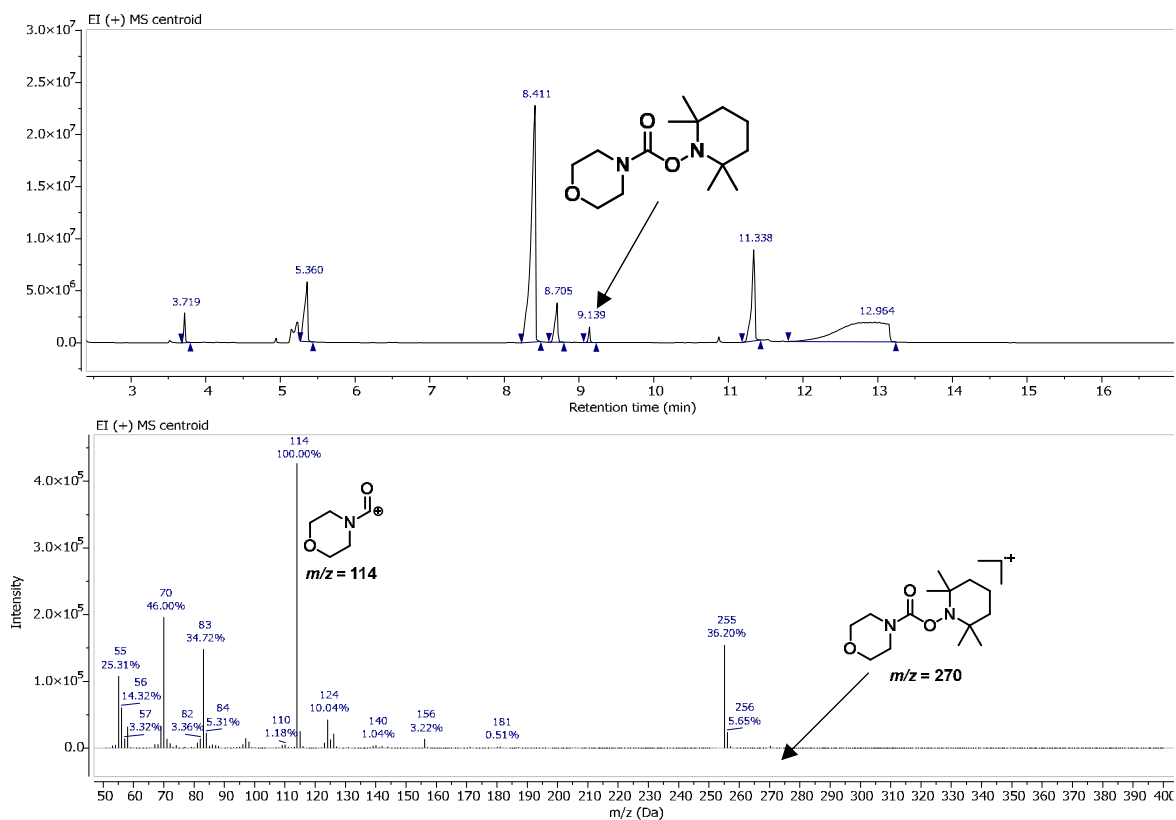
Figure 2. *Top:* The fluorescence intensity of a 3DPAFIPN solution (0.01 mM in DMSO) containing increasing amounts of benzylideneaniline **2a** as the quencher. Excitation wavelength: 400 nm. *Bottom:* STERN-VOLMER plot of the above data ($y = 0.05369 \cdot x + 0.02059$, $R^2 = 0.9960$). The quenching constant k_q was determined using the STERN-VOLMER equation $K_{sv} = k_q \cdot \tau$ and a lifetime of $\tau = 4.2$ ns for 3DPAFIPN as $k_q = 1.27 \cdot 10^{10}$ L \cdot mol $^{-1}$ \cdot s $^{-1}$.

Radical trapping experiments

The radical trapping experiments were conducted analogously to general procedure 3 on a 0.1 mmol scale in the presence of 1 equiv. of TEMPO. Experiments were conducted in the presence and absence of the Hantzsch ester and both in the presence or absence of $\text{BF}_3 \cdot \text{OEt}_2$. The reaction mixtures were analyzed *via* GC-MS after quenching the mixtures containing $\text{BF}_3 \cdot \text{OEt}_2$ as described in general procedure 3.



Scheme 5. The conditions of the TEMPO radical scavenging experiments.



UV/Vis experiments

The samples were prepared by diluting 1.5 mL of a 0.06 M stock solution of the respective substance in DCM with 1.5 mL of DCM in a quartz cuvette. For the mixtures of both substrates, 1.5 mL of both 0.06 M stock solutions were combined. The samples containing BF_3 were prepared in a quartz cuvette fitted with a rubber septum and an argon balloon by adding 1.0 eq of $\text{BF}_3 \cdot \text{OEt}_2$ (11 μL) to the solutions. To all solutions was added 0.1 mL of DMSO to solubilize precipitates, which results in a 0.028 M solution in DCM/DMSO 15/1.

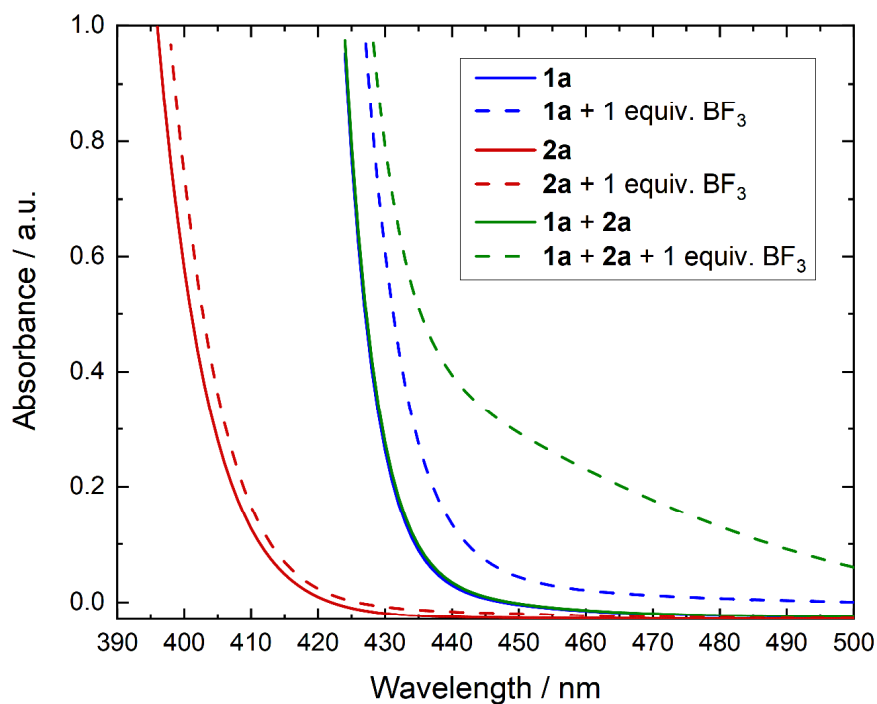
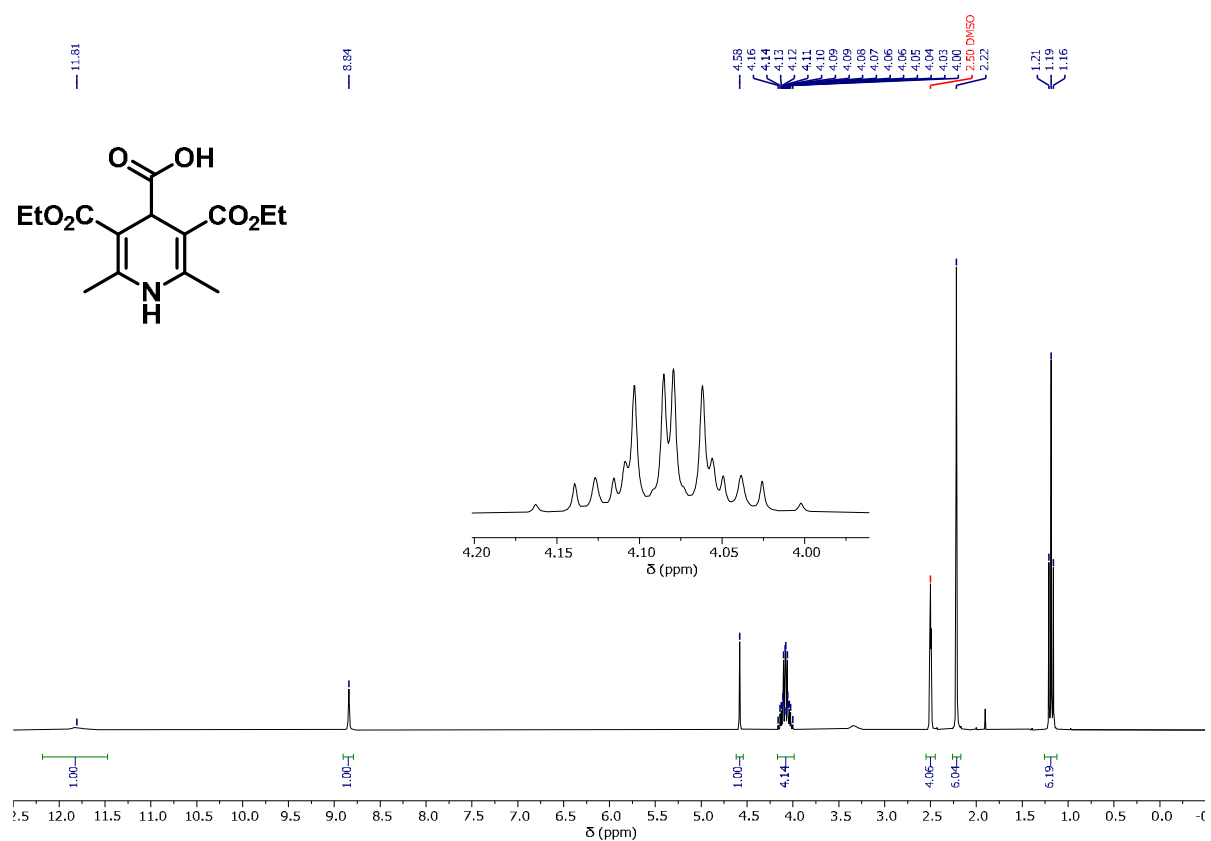
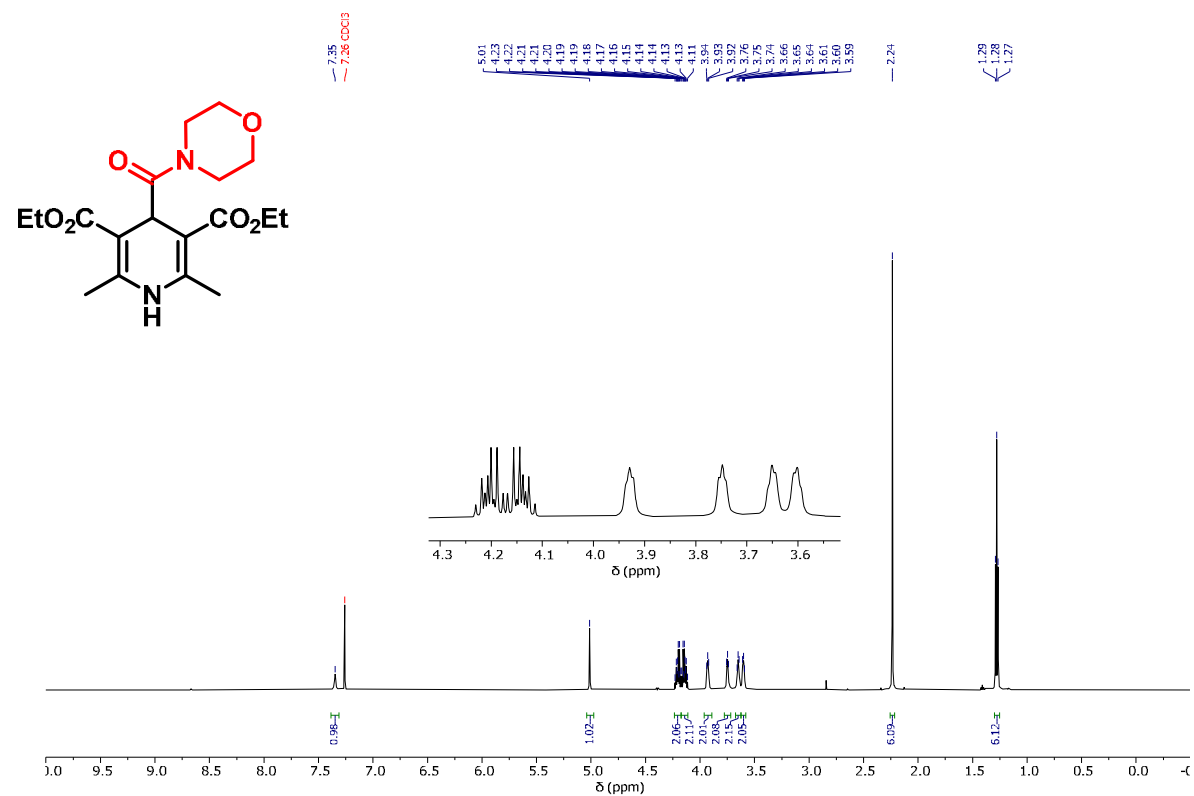


Figure 3. The UV/Vis absorption spectra of HE **1a**, benzylideneaniline **2a** and **1a + 2a** (1:1) without $\text{BF}_3 \cdot \text{OEt}_2$ as well as **1a**, **2a** and **1a + 2a** (1:1) with 1 equivalent of $\text{BF}_3 \cdot \text{OEt}_2$ each, all 0.028 M in DCM/DMSO 15/1, in the range of 390–500 nm.

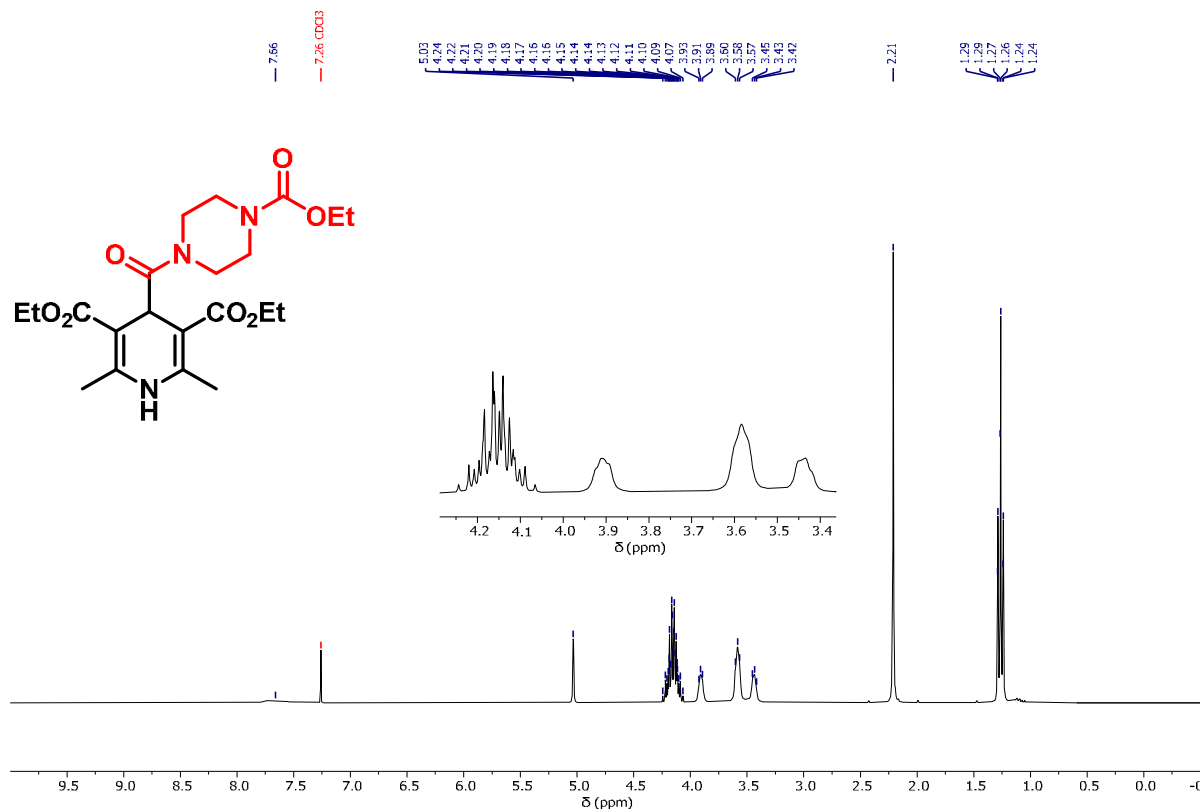
5.4.6 NMR spectra of all compounds



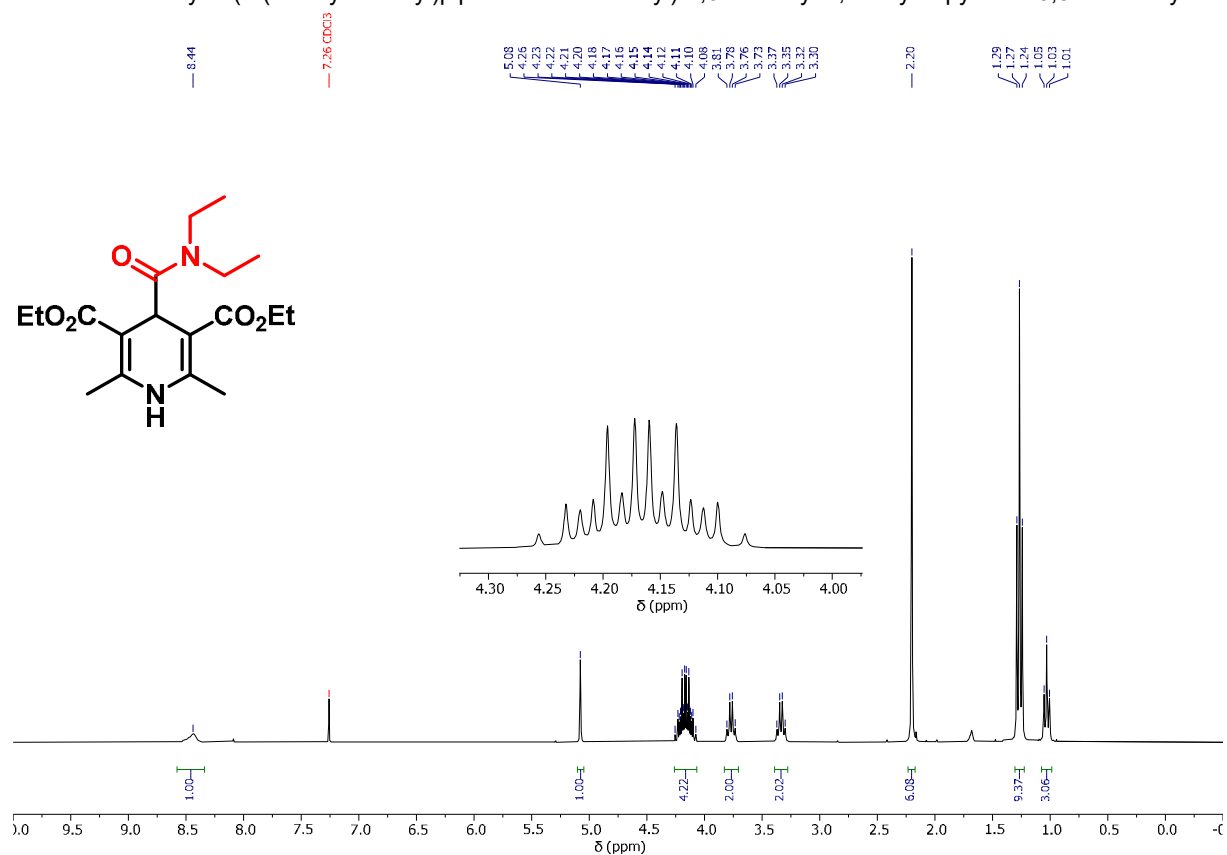
¹H-NMR of 3,5-bis(ethoxycarbonyl)-2,6-dimethyl-1,4-dihydropyridine-4-carboxylic acid (HE-COOH, I).



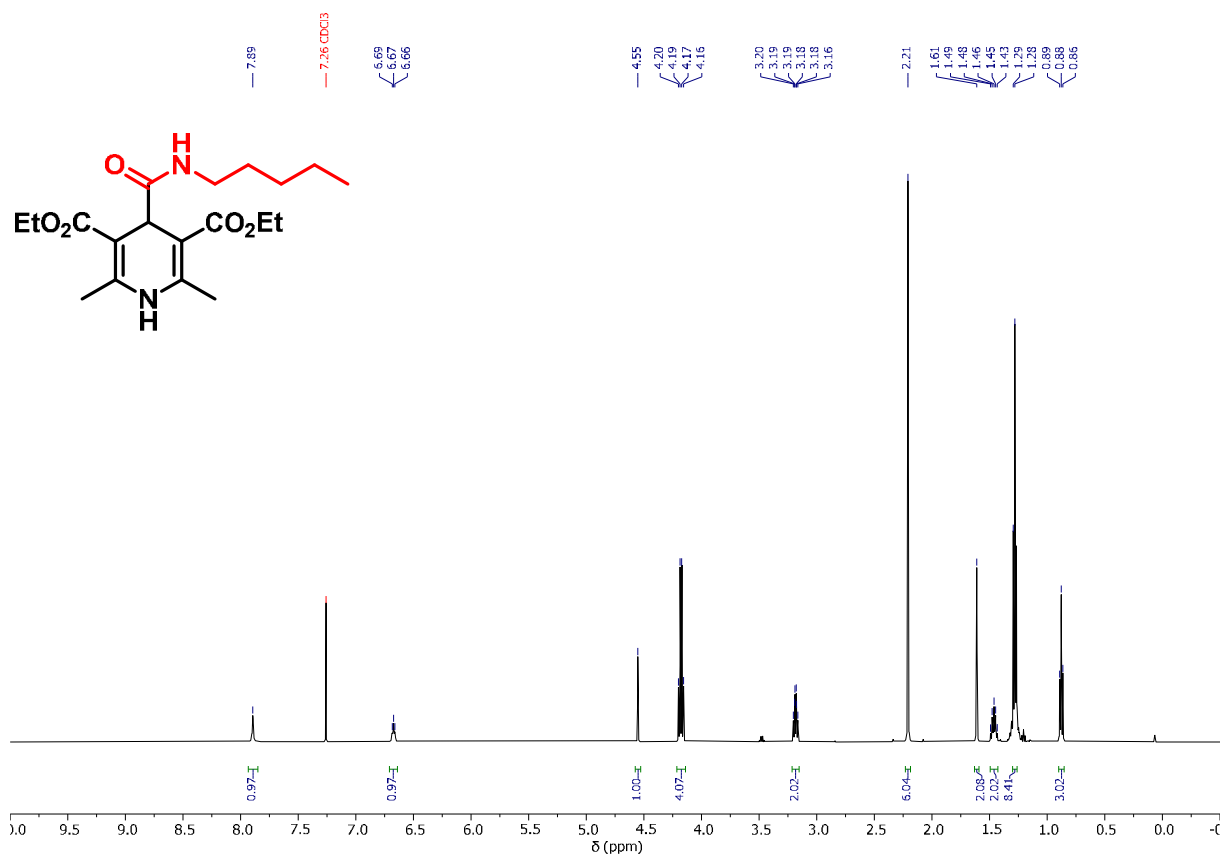
¹H-NMR of diethyl 2,6-dimethyl-4-(morpholine-4-carbonyl)-1,4-dihydropyridine-3,5-dicarboxylate (1a).



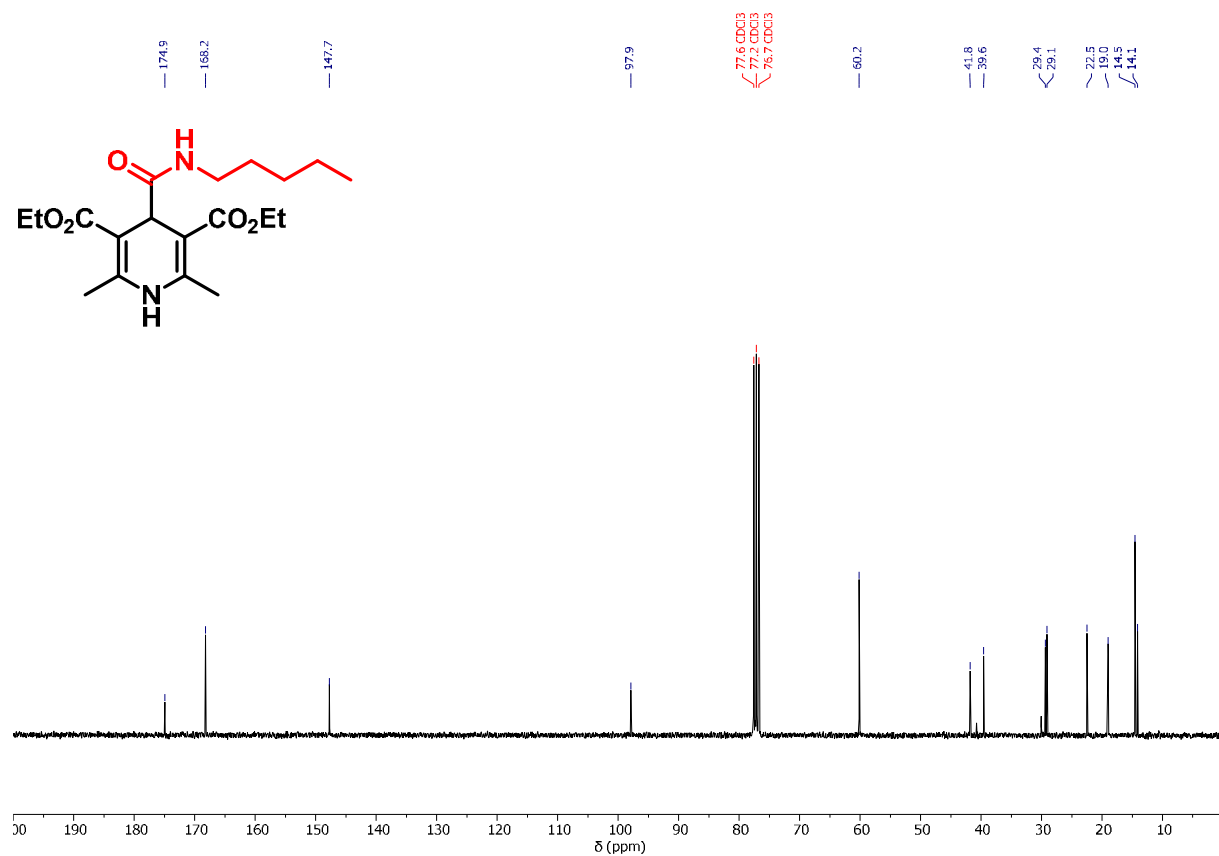
¹H-NMR of diethyl 4-(4-(ethoxycarbonyl)piperazine-1-carbonyl)-2,6-dimethyl-1,4-dihydropyridine-3,5-dicarboxylate (1b).



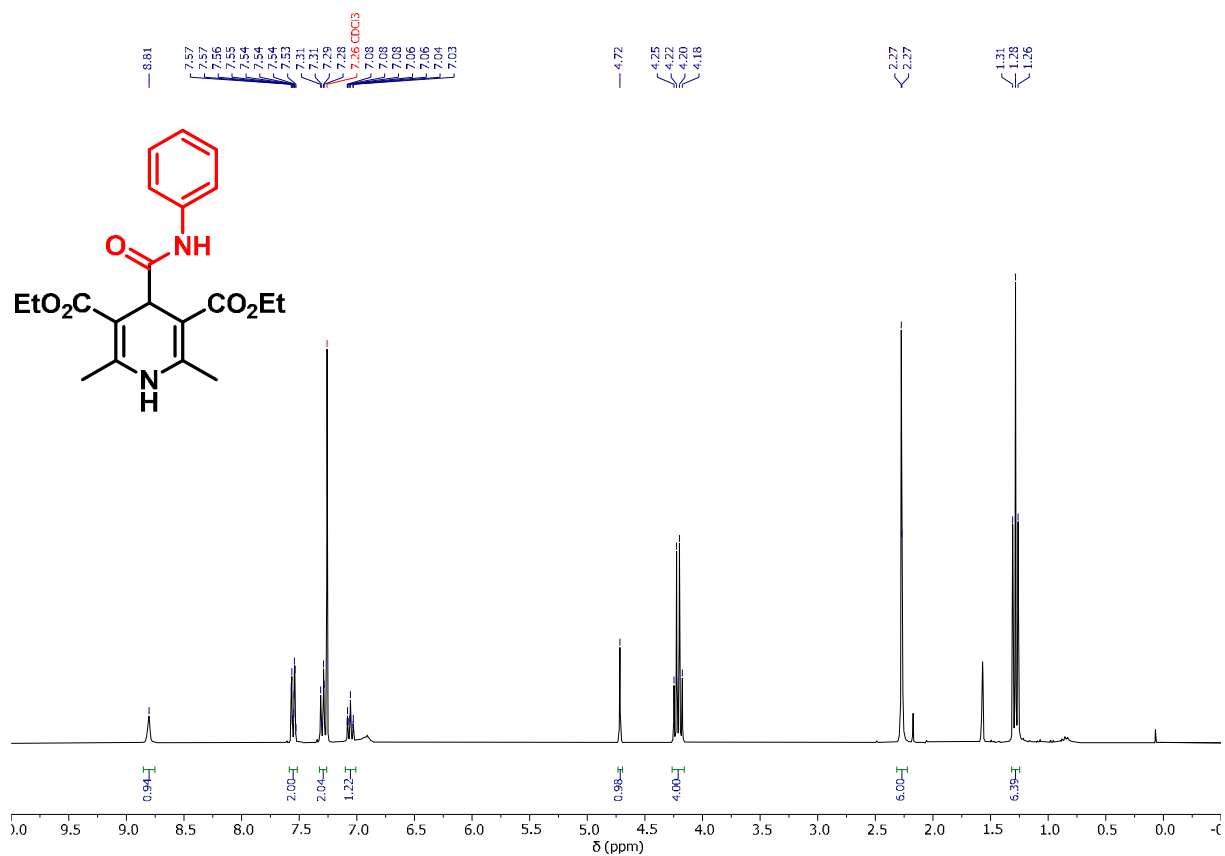
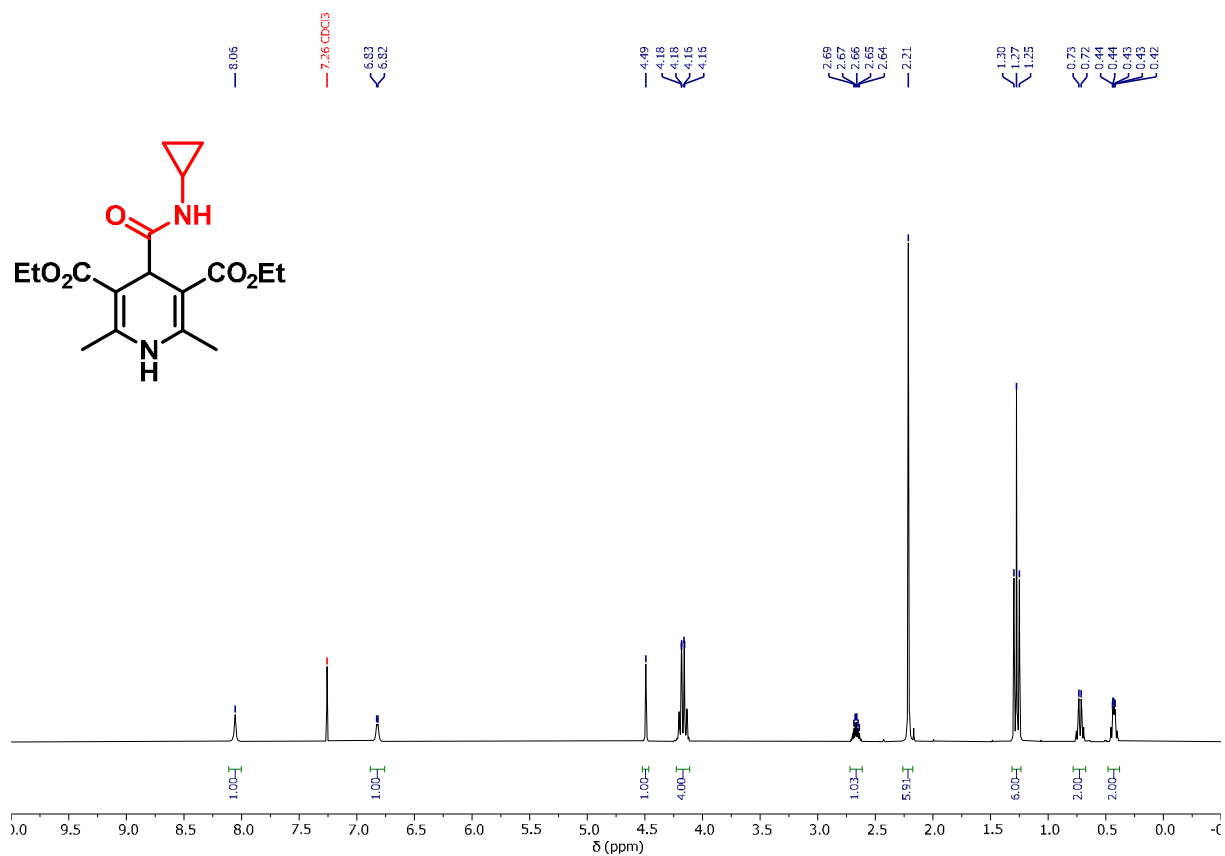
¹H-NMR of diethyl (4-diethylcarbamoyl)-2,6-dimethyl-1,4-dihydropyridine-3,5-dicarboxylate (1c).

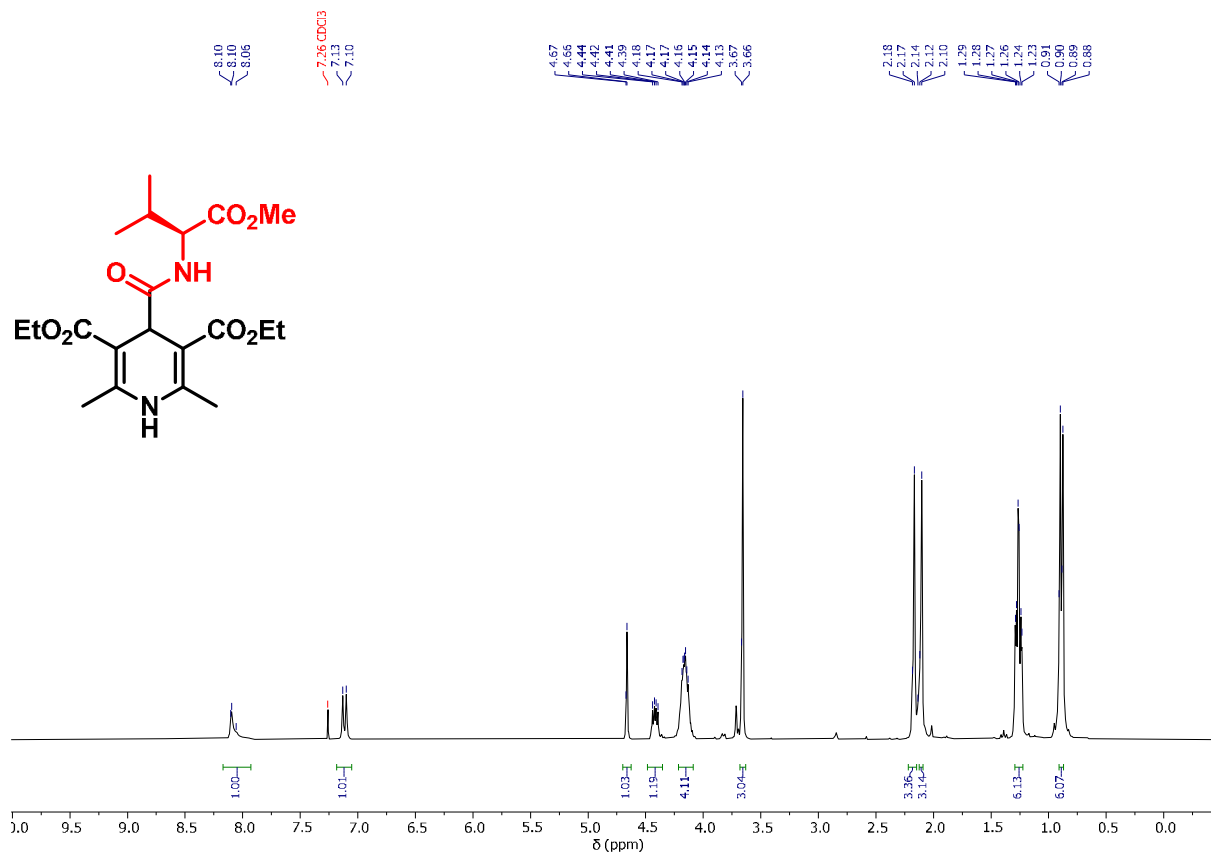


¹H-NMR of diethyl 2,6-dimethyl-4-(pentylcarbamoyl)-1,4-dihydropyridine-3,5-dicarboxylate (1d).

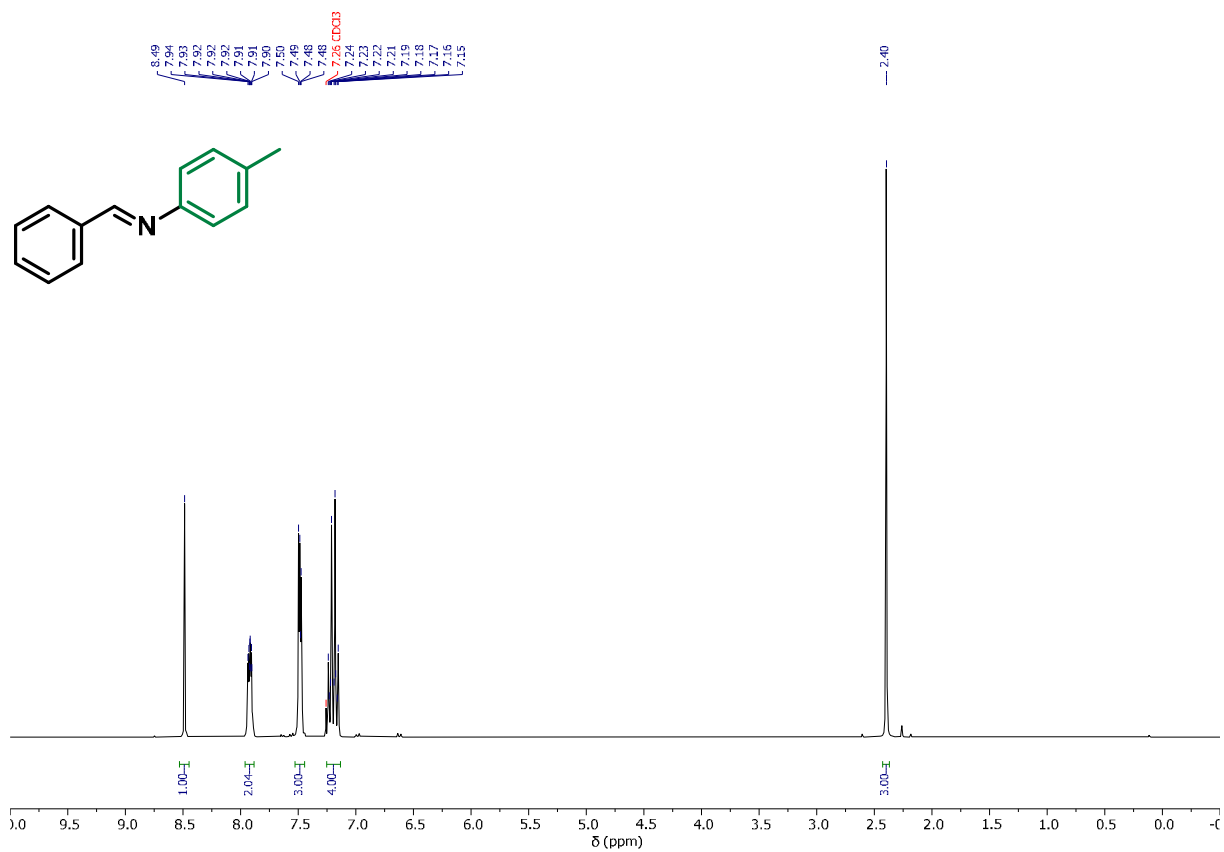


¹³C-{¹H}-NMR of diethyl 2,6-dimethyl-4-(pentylcarbamoyl)-1,4-dihydropyridine-3,5-dicarboxylate (1d).

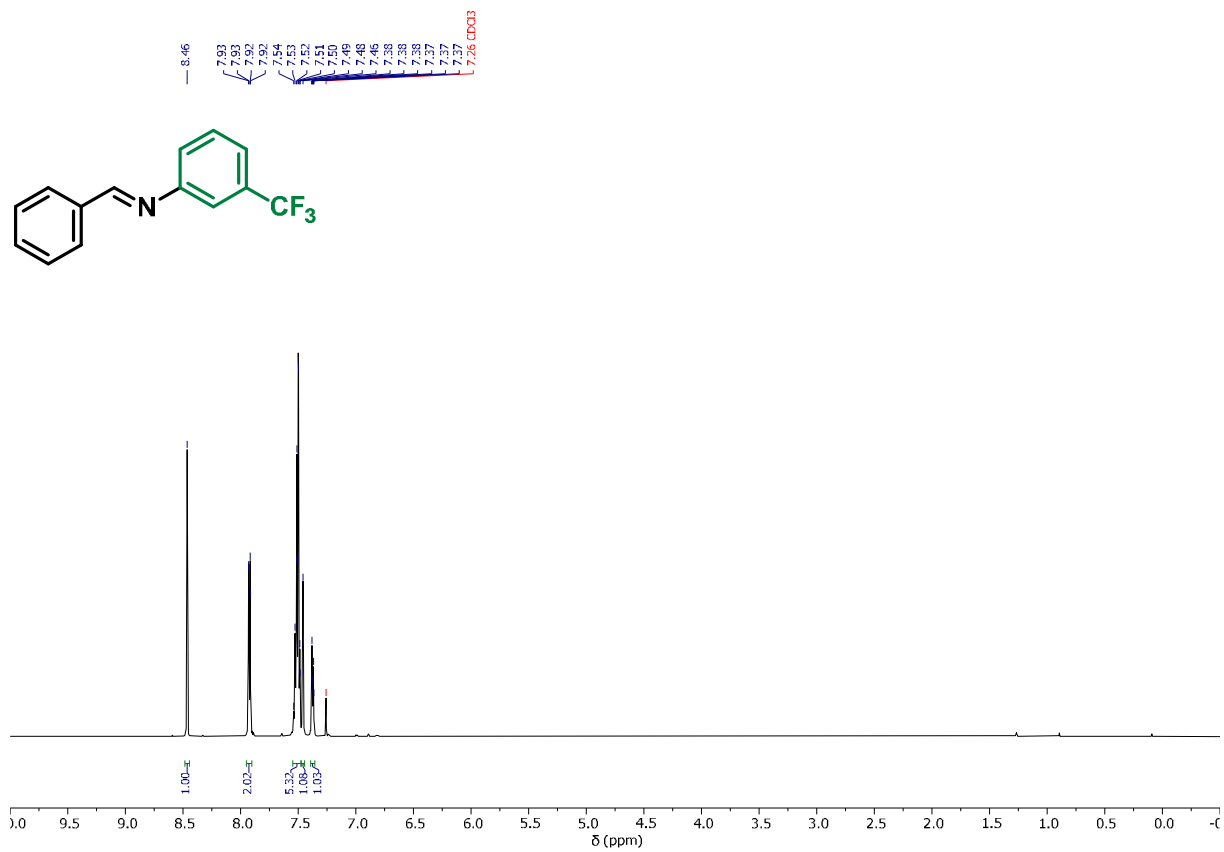




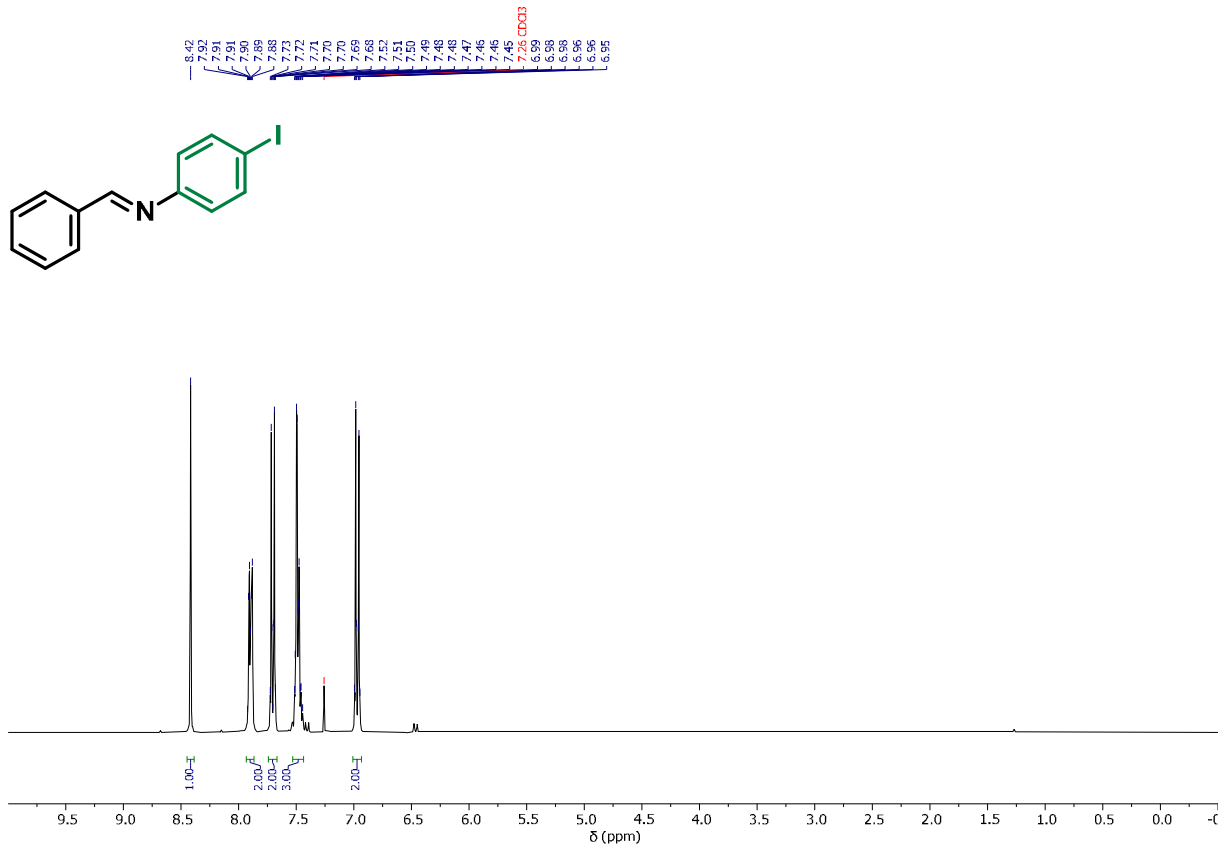
¹H-NMR of Diethyl 2,6-dimethyl-4-((S)-valine-N-carbonyl)-1,4-dihydropyridine-3,5-dicarboxylate (**1g**).



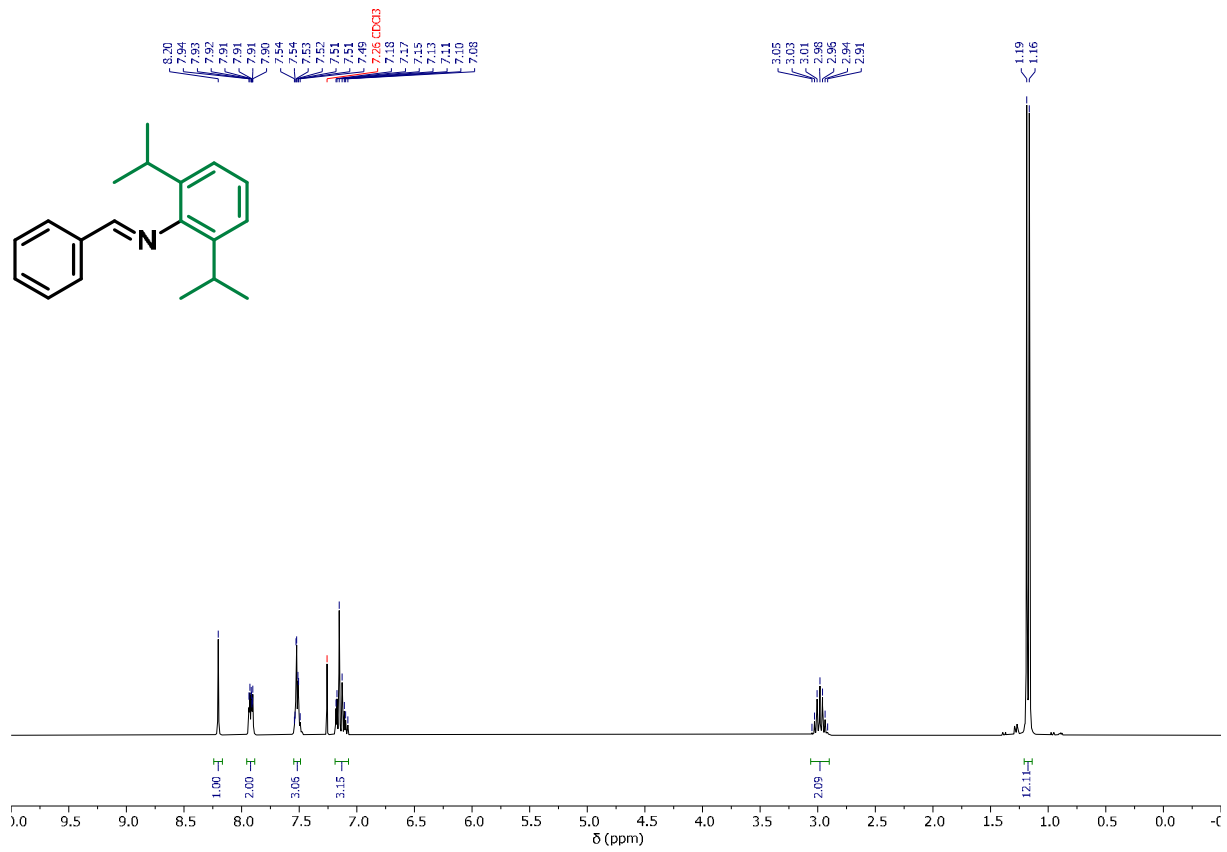
¹H-NMR of benzylidene(4-methylphenyl)amine (**2b**).



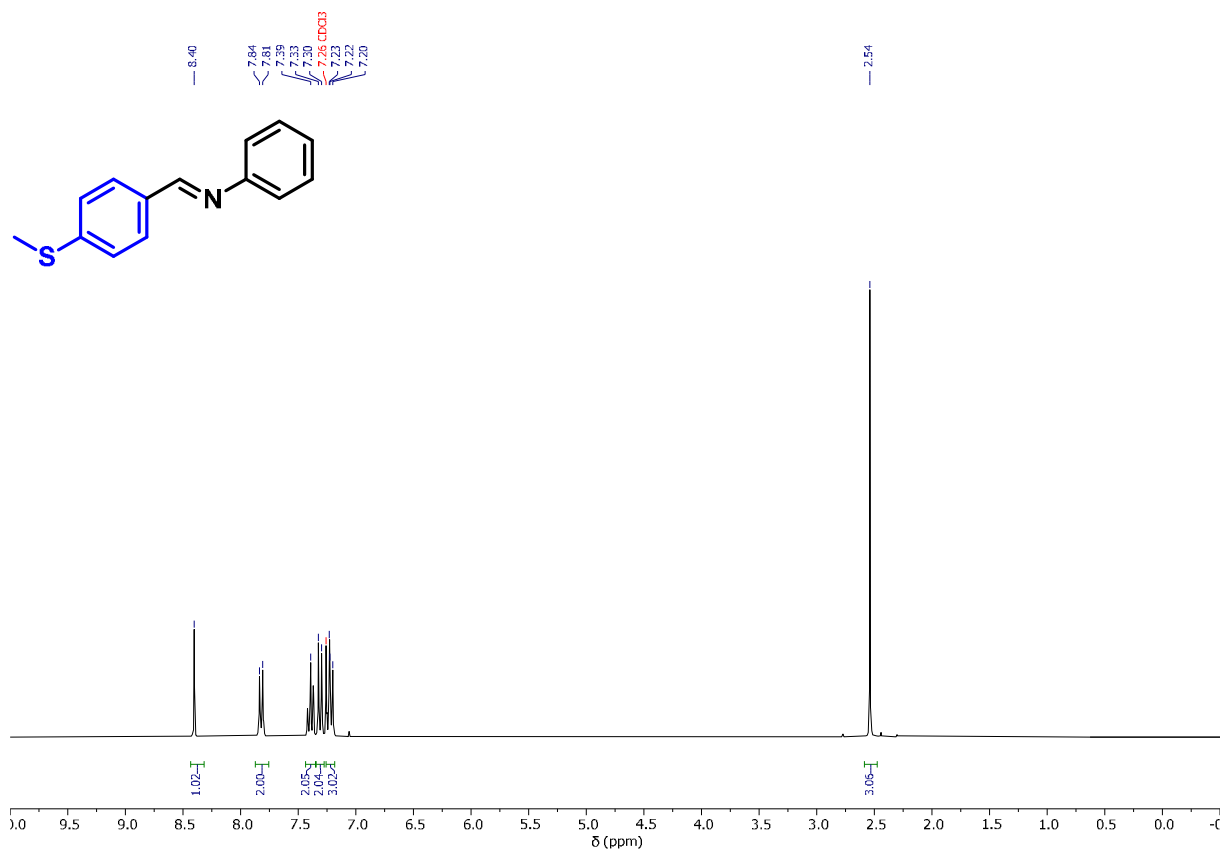
¹H-NMR of benzylidene(3-(trifluoromethyl)phenyl)amine (**2c**).



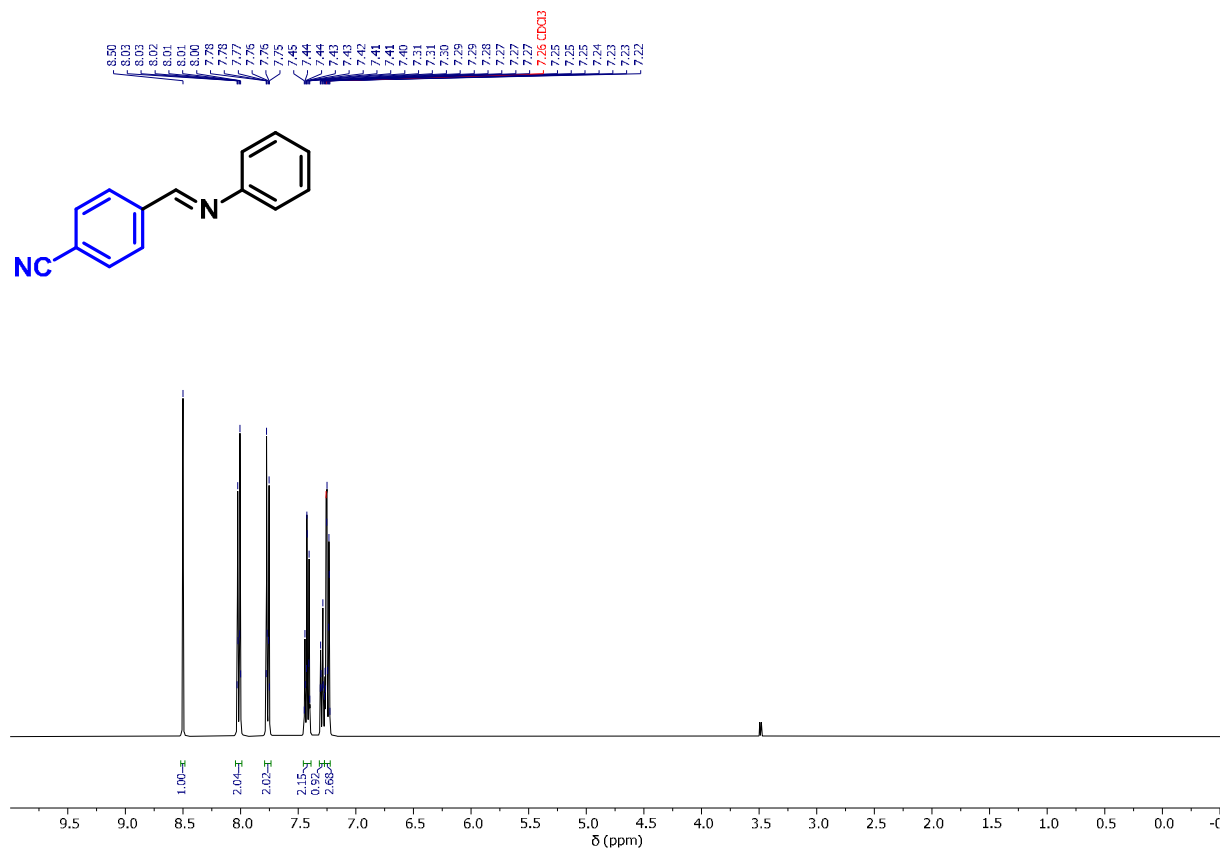
¹H-NMR of benzylidene(4-iodophenyl)amine (**2d**).



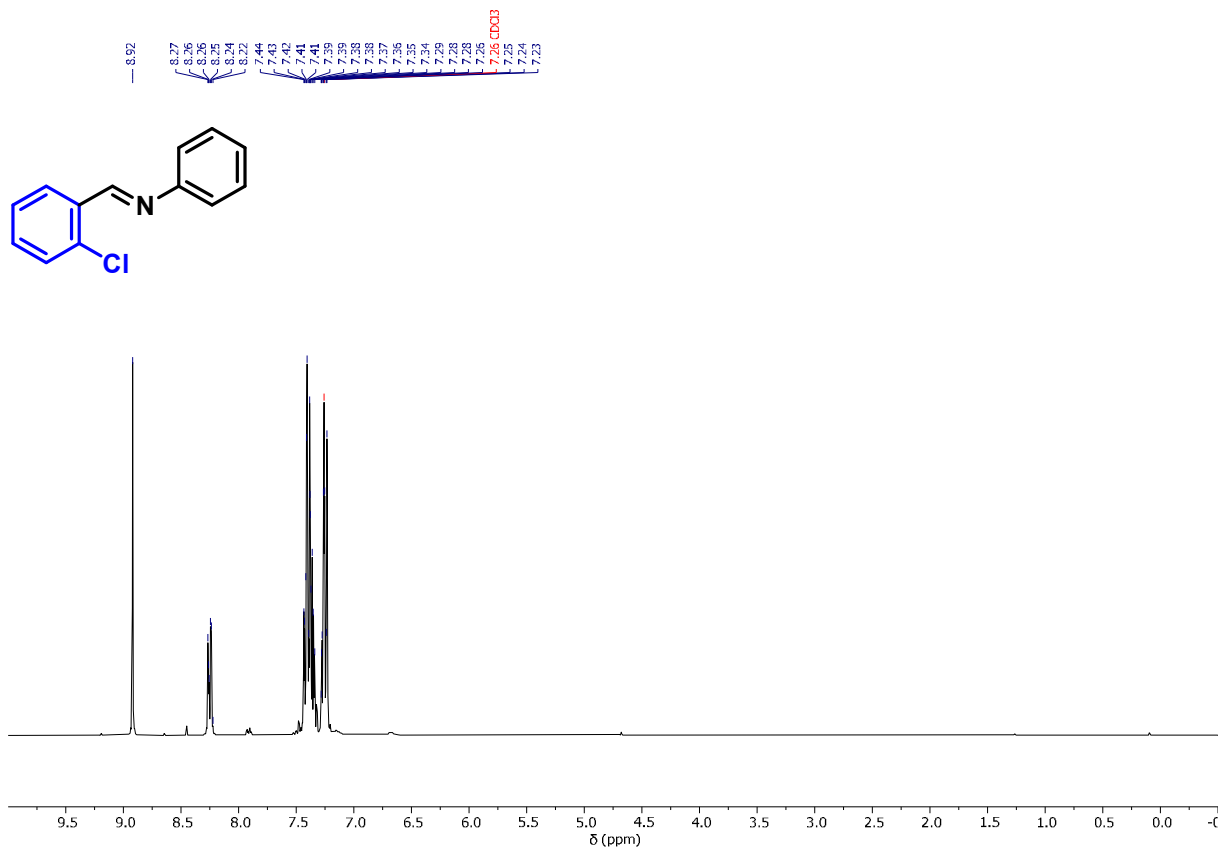
¹H-NMR of benzylidene(2,6-diisopropylphenyl)amine (**2e**).



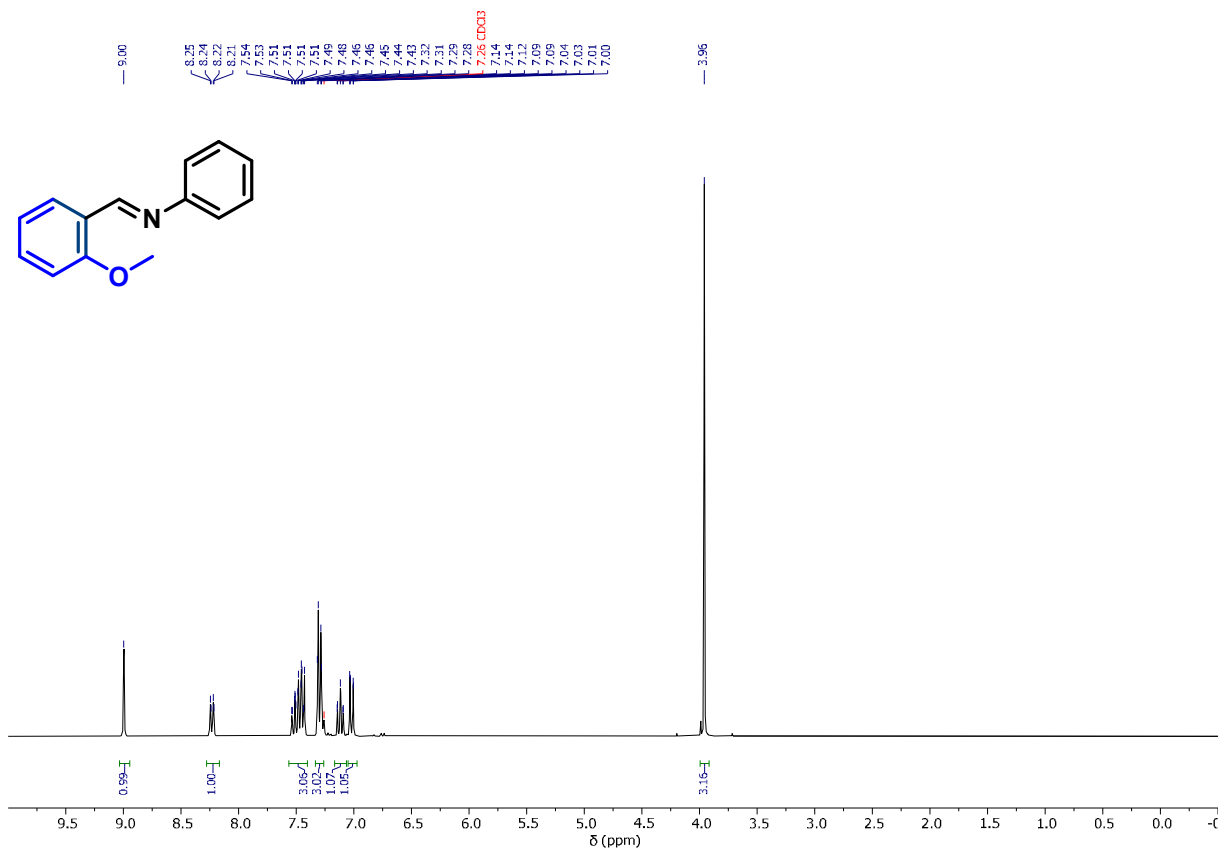
$^1\text{H-NMR}$ of *N*-phenyl-1-(3-methylthio)methanimine (**2f**).



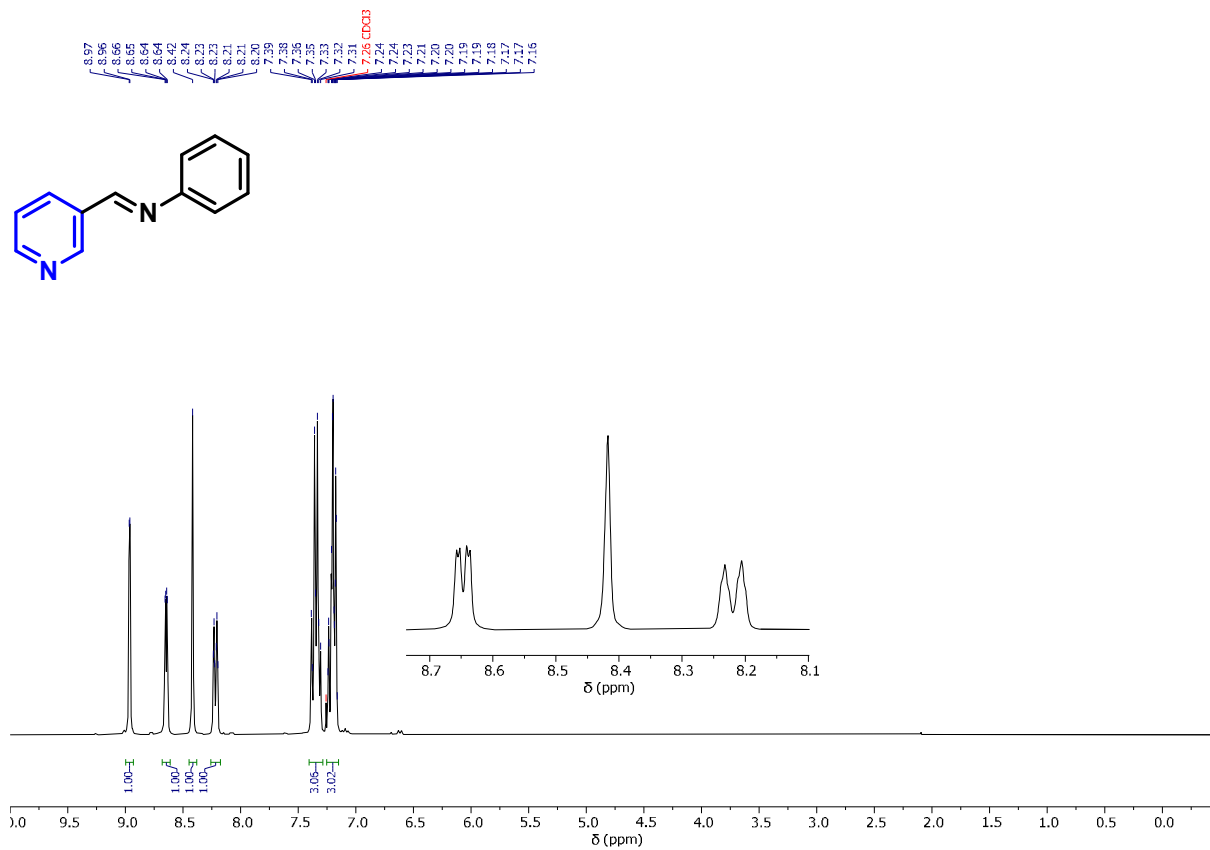
$^1\text{H-NMR}$ of *N*-phenyl-1-(4-cyanophenyl)methanimine (**2g**).



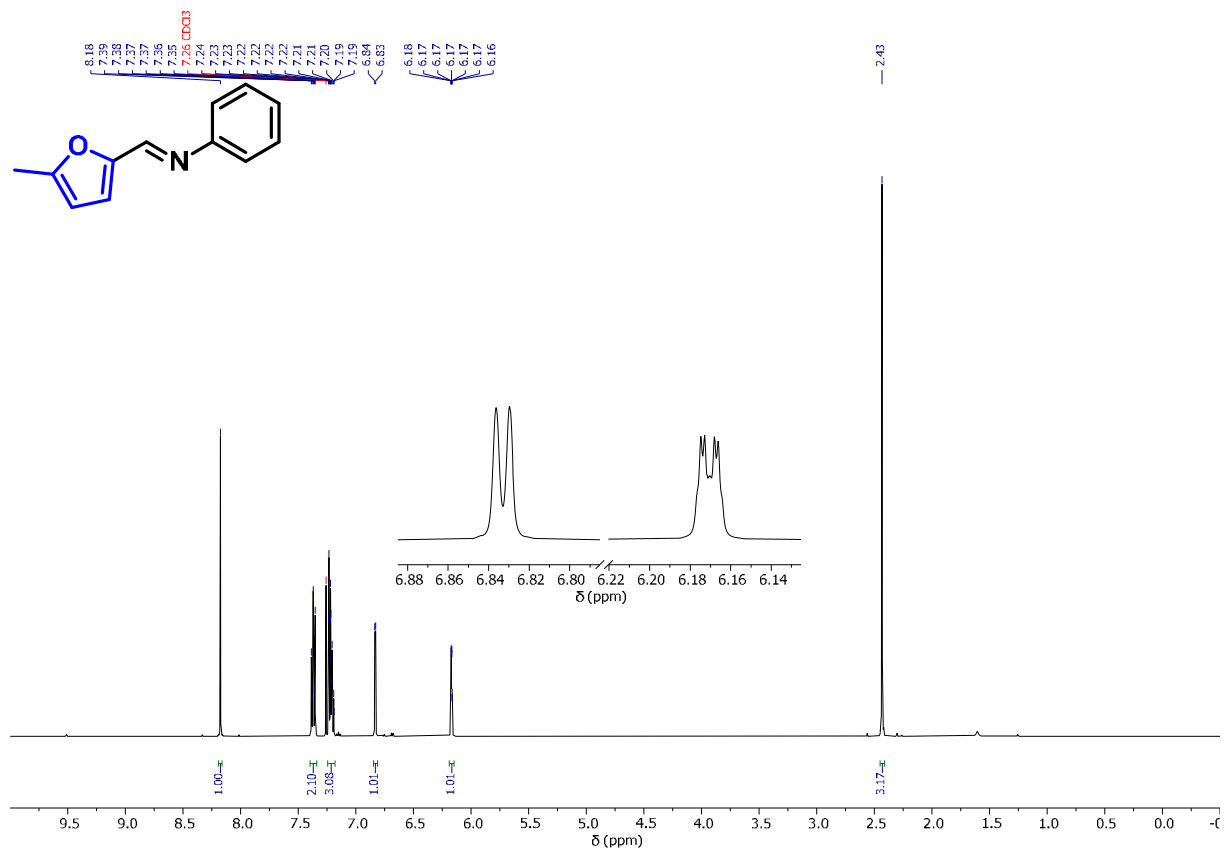
$^1\text{H-NMR}$ of *N*-phenyl-1-(2-chlorophenyl)methanimine (**2h**).



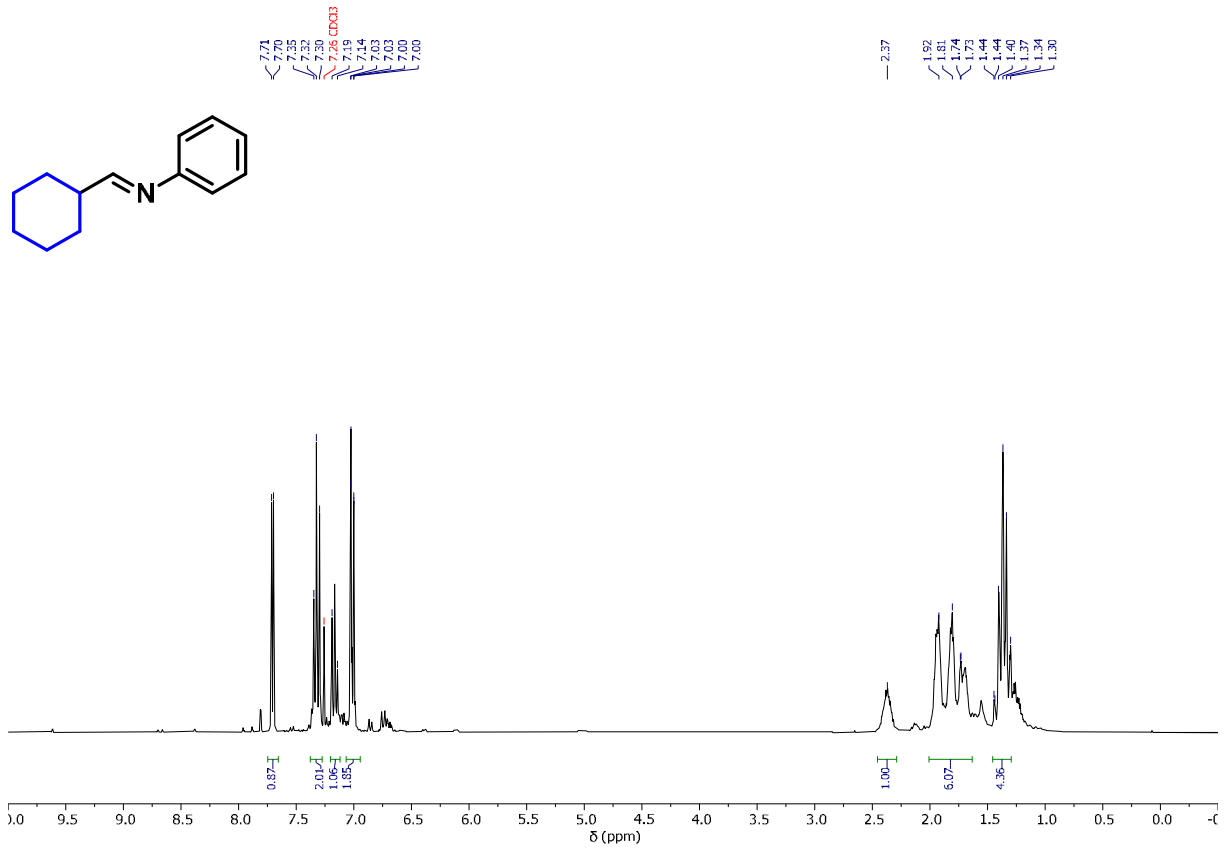
$^1\text{H-NMR}$ of *N*-phenyl-1-(2-methoxyphenyl)methanimine (**2i**).



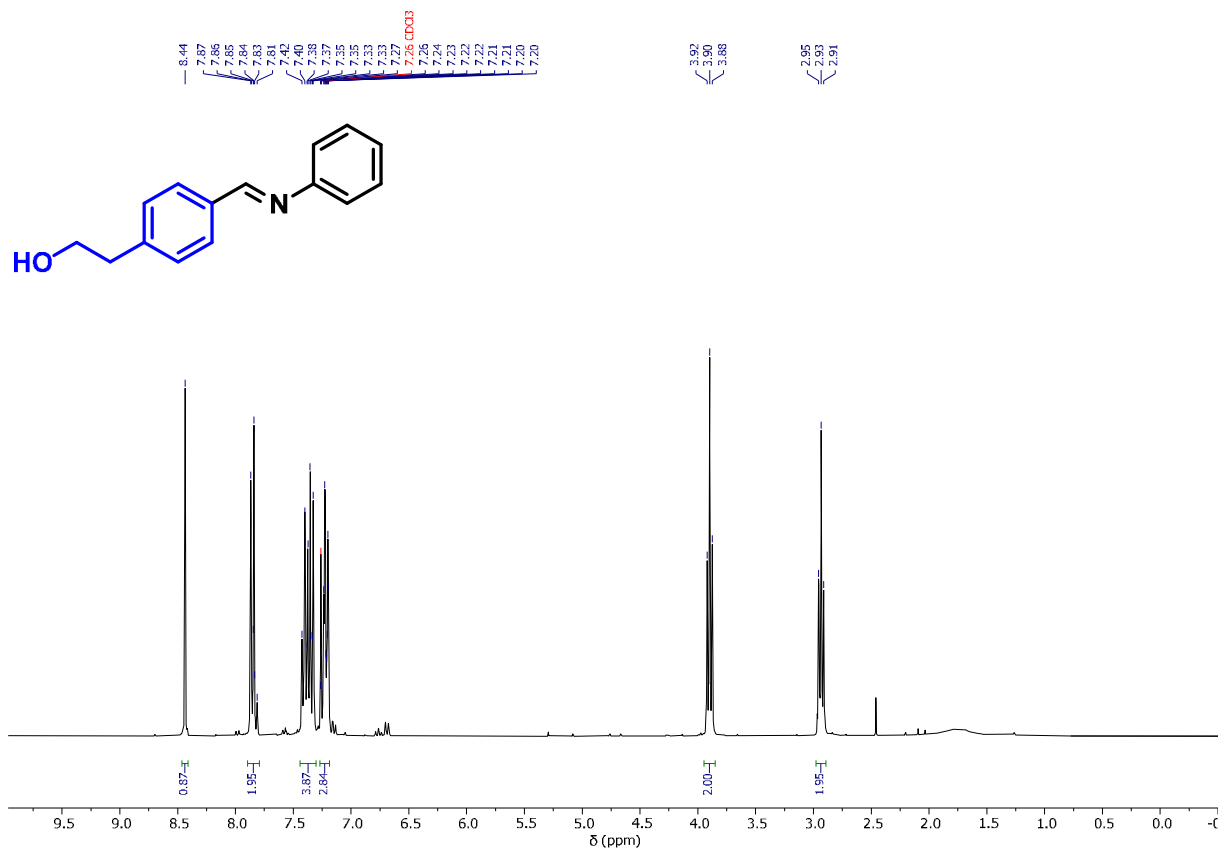
$^1\text{H-NMR}$ of *N*-phenyl-1-(3-pyridinyl)methanimine (**2j**).



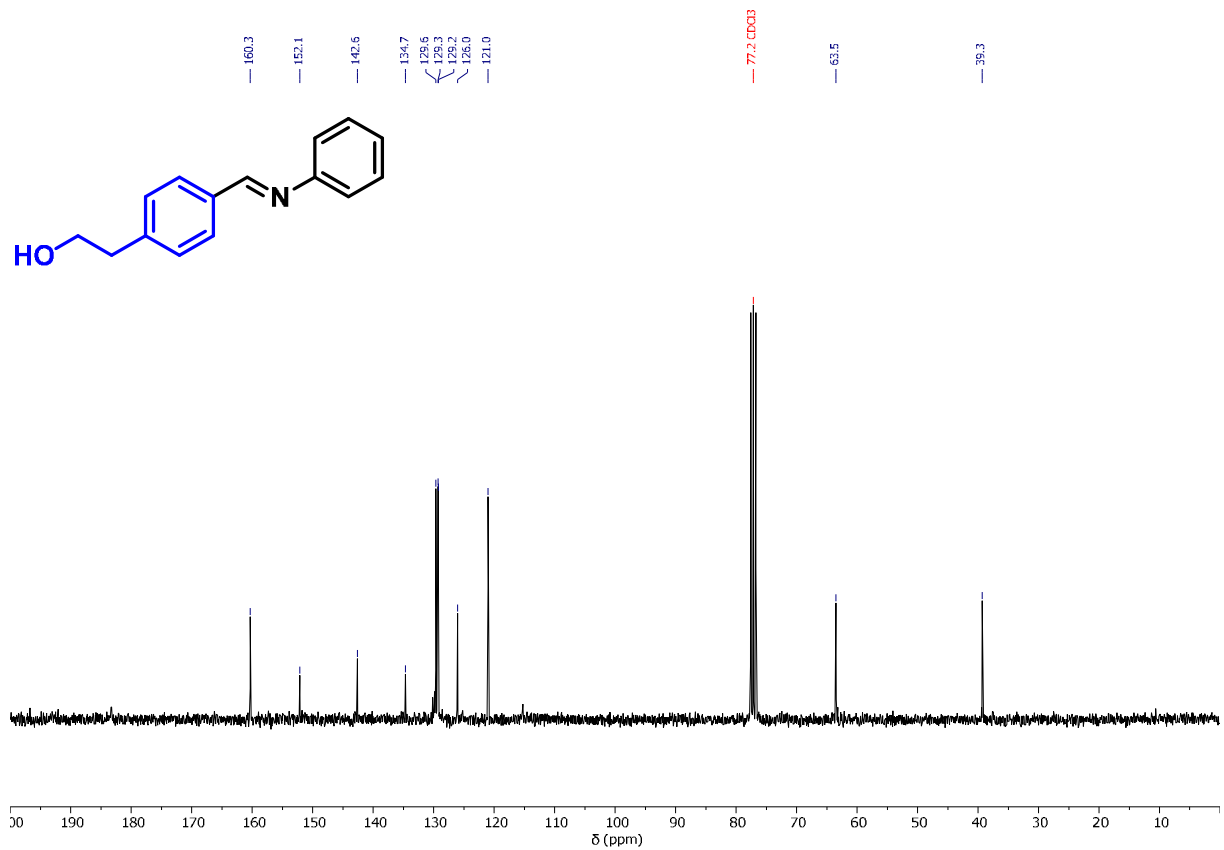
$^1\text{H-NMR}$ of *N*-phenyl-1-(5-methylfuran-2-yl)methanimine (**2k**).



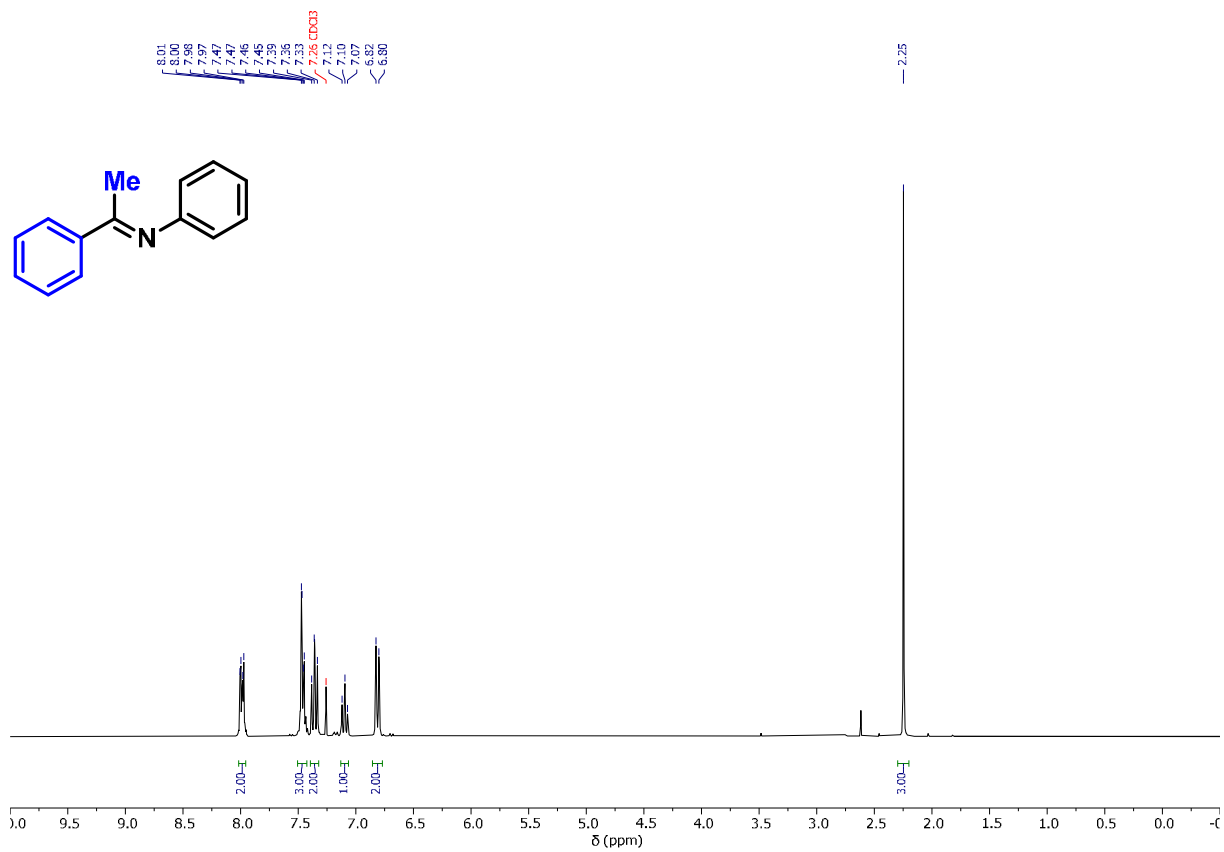
¹H-NMR of *N*-phenyl-1-(cyclohexyl)methanimine (**2l**).



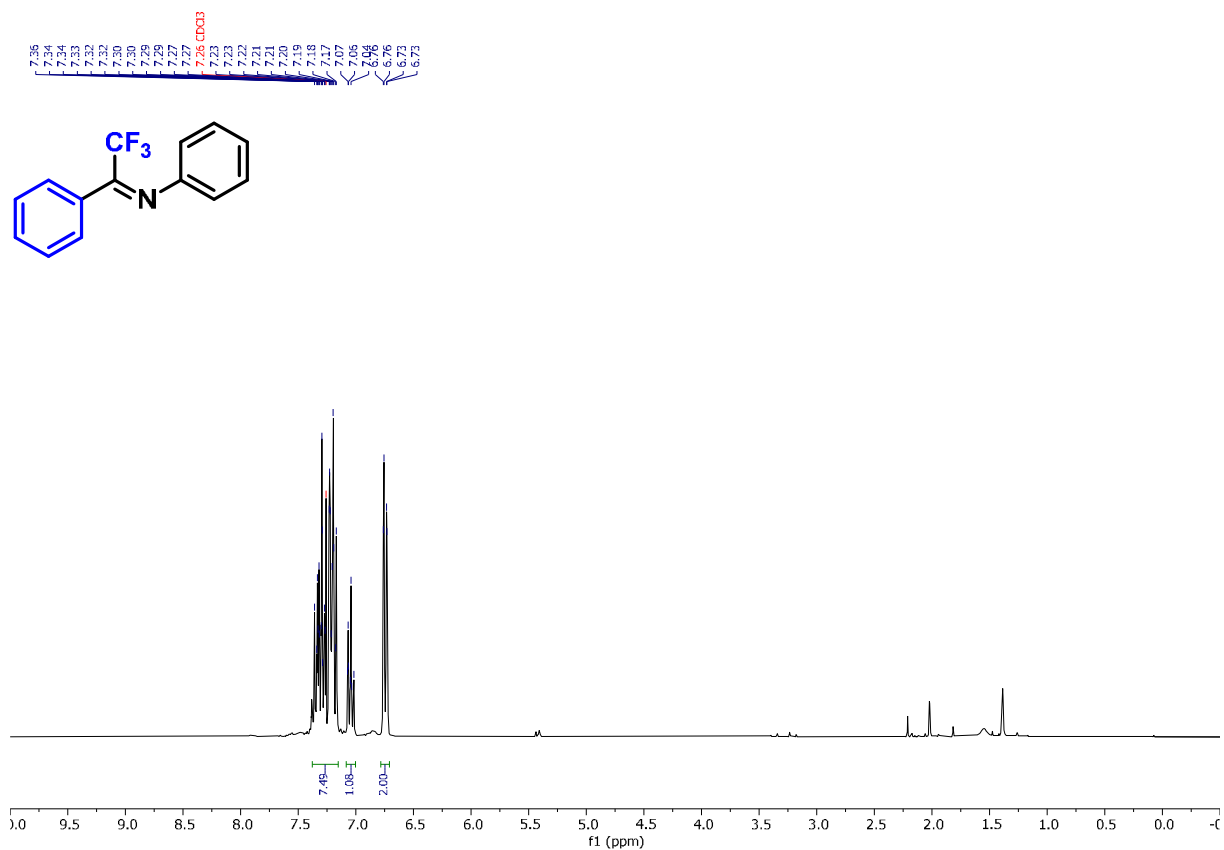
¹H-NMR of *N*-phenyl-1-(4-(2-hydroxyethyl)phenyl)methanimine (**2m**).



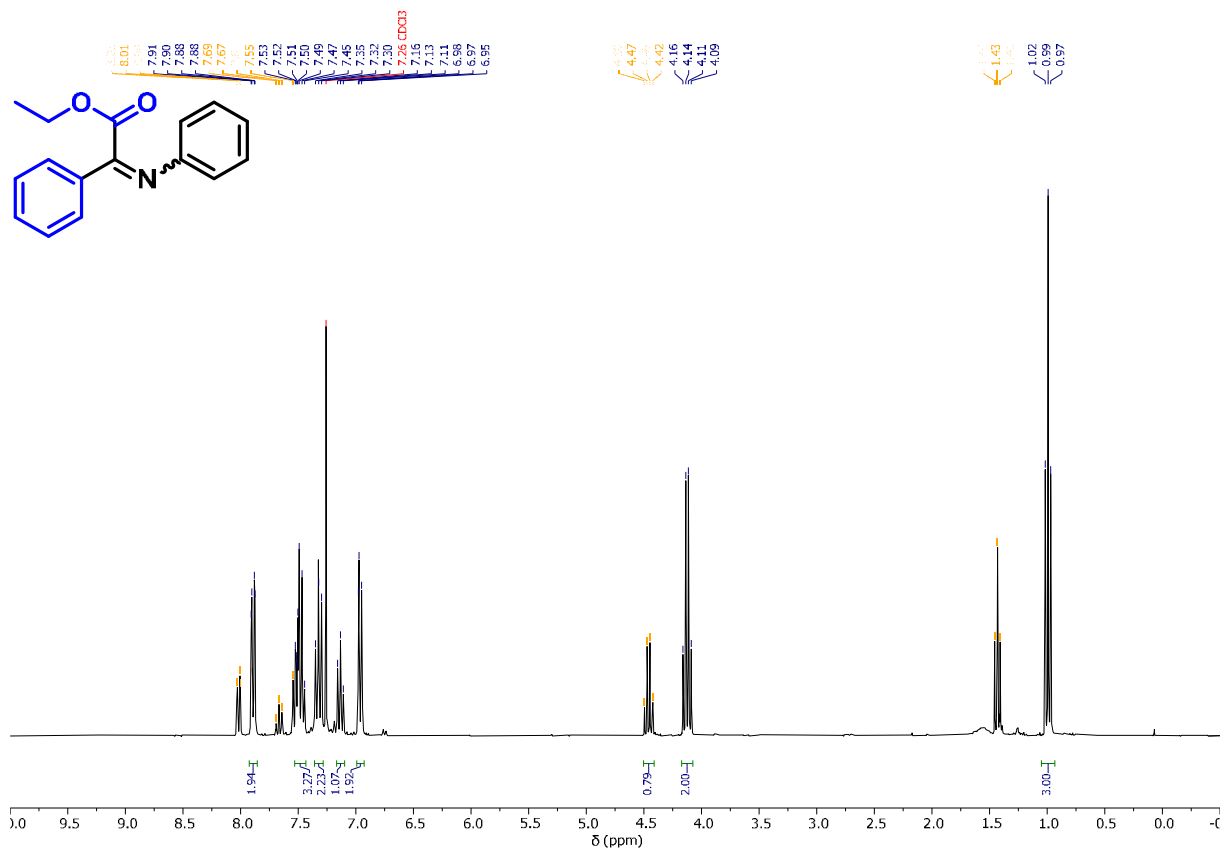
^{13}C - $\{^1\text{H}\}$ -NMR of *N*-phenyl-1-(4-(2-hydroxyethyl)phenyl)methanimine (**2m**).



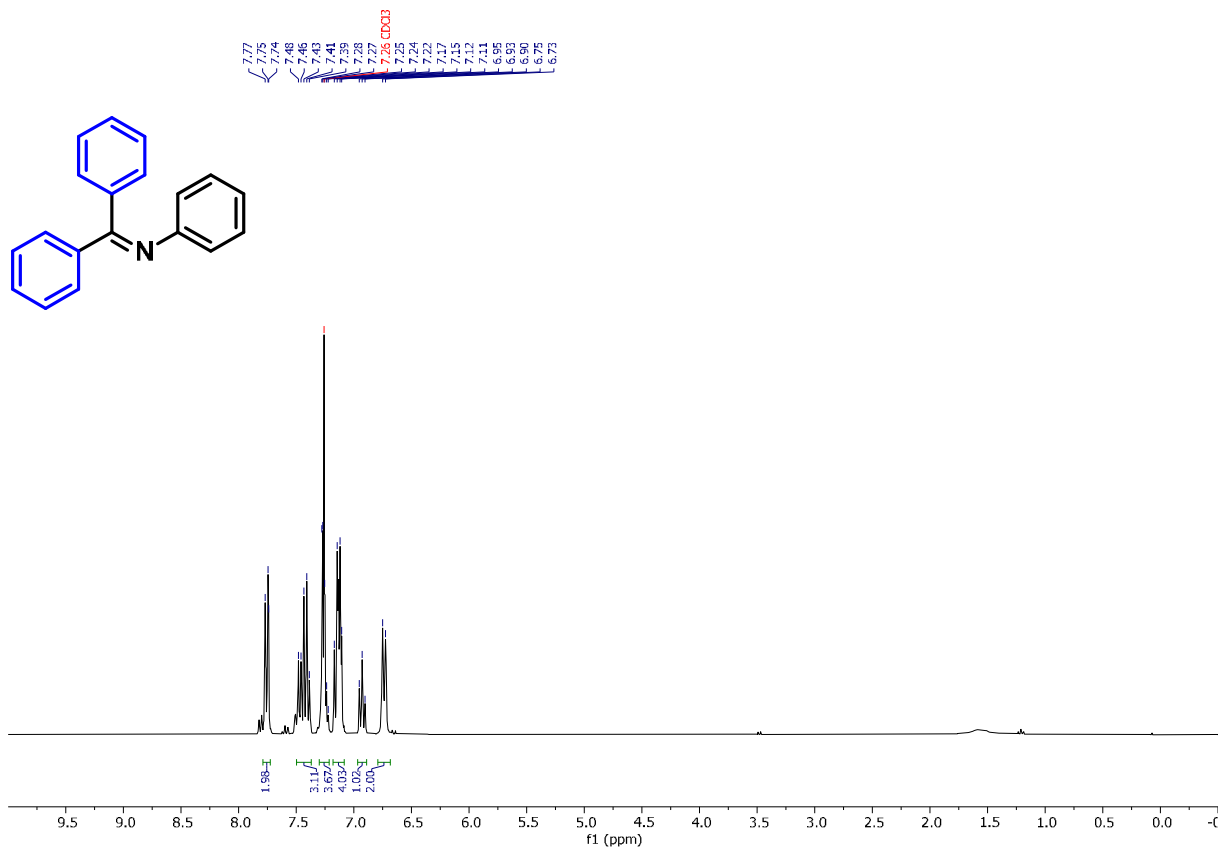
^1H -NMR of *N*,1-diphenylethan-1-imine (**2n**).



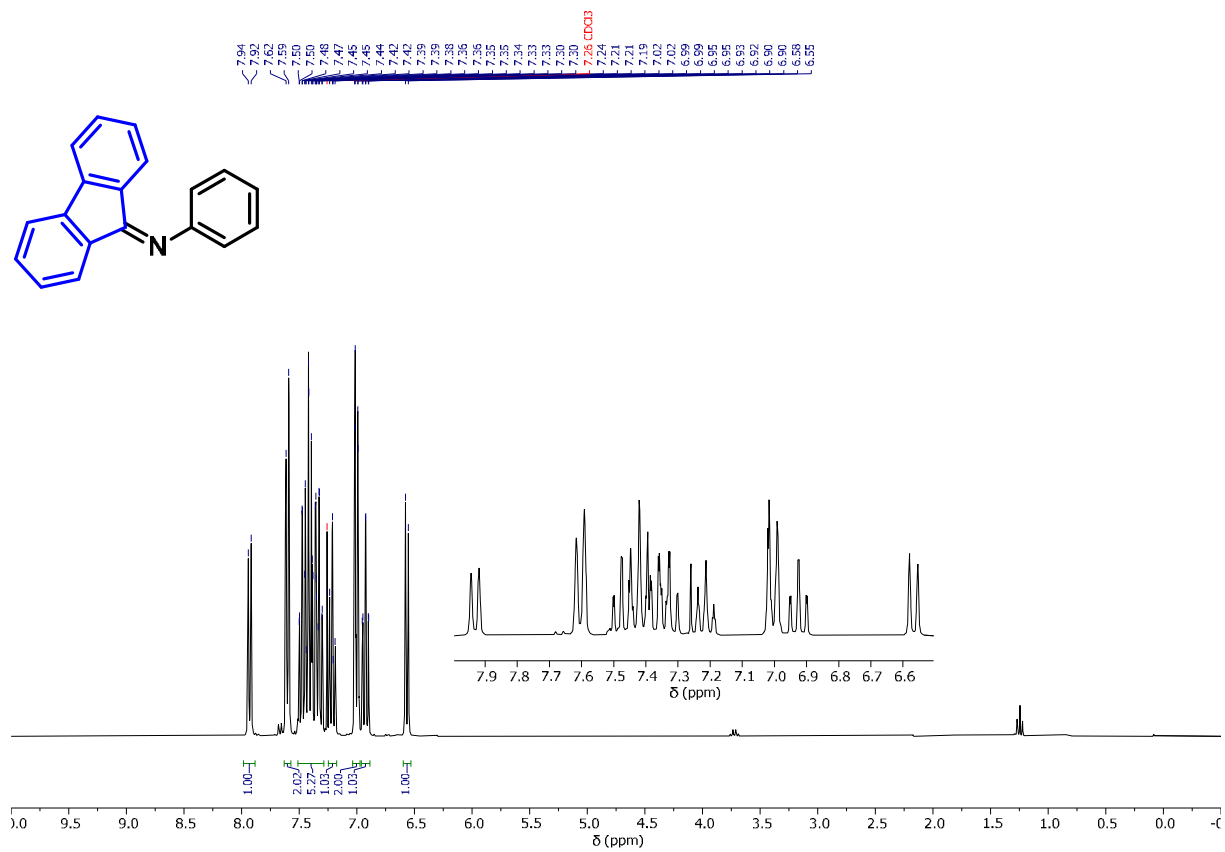
¹H-NMR of 2,2,2-trifluoro-N,1-diphenylethan-1-imine (2p).



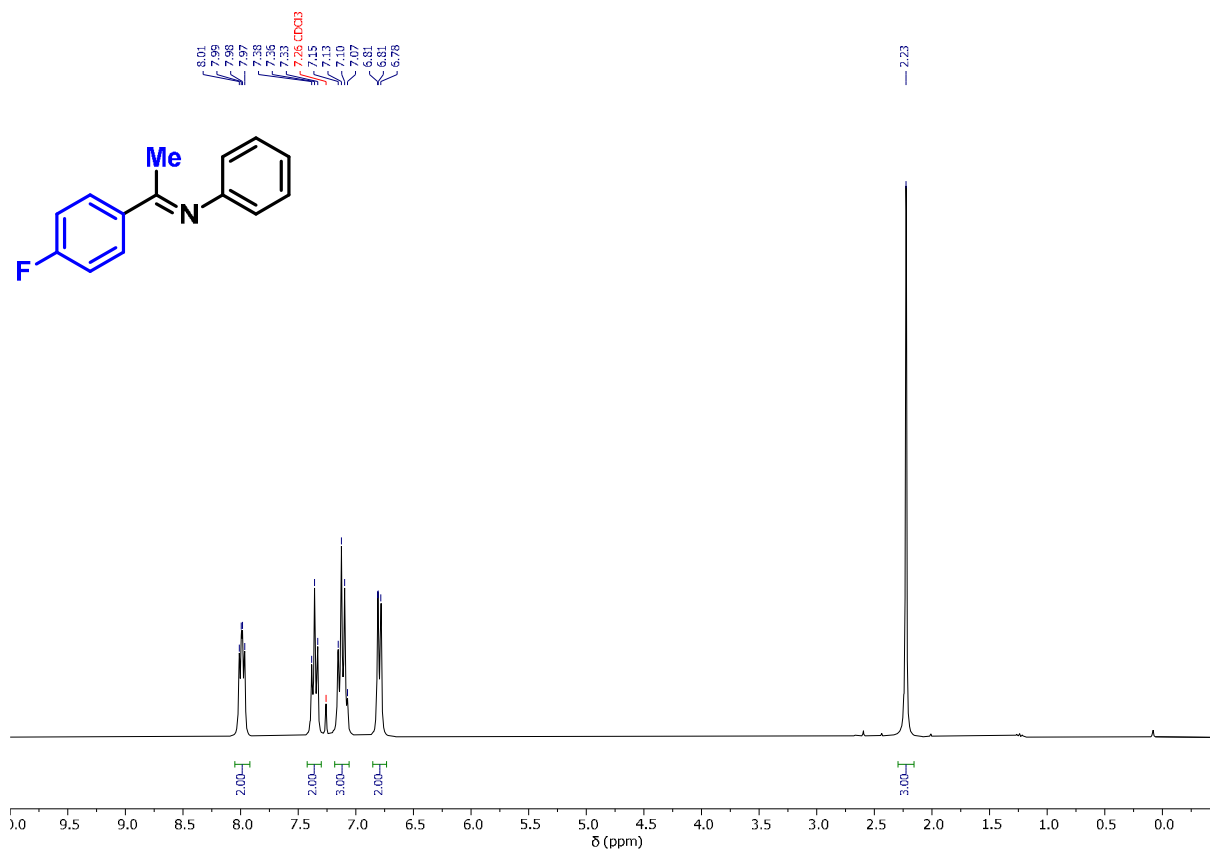
¹H-NMR of (E)-2-phenyl-2-(phenylimino)acetate and (Z)-2-phenyl-2-(phenylimino)acetate (2o).



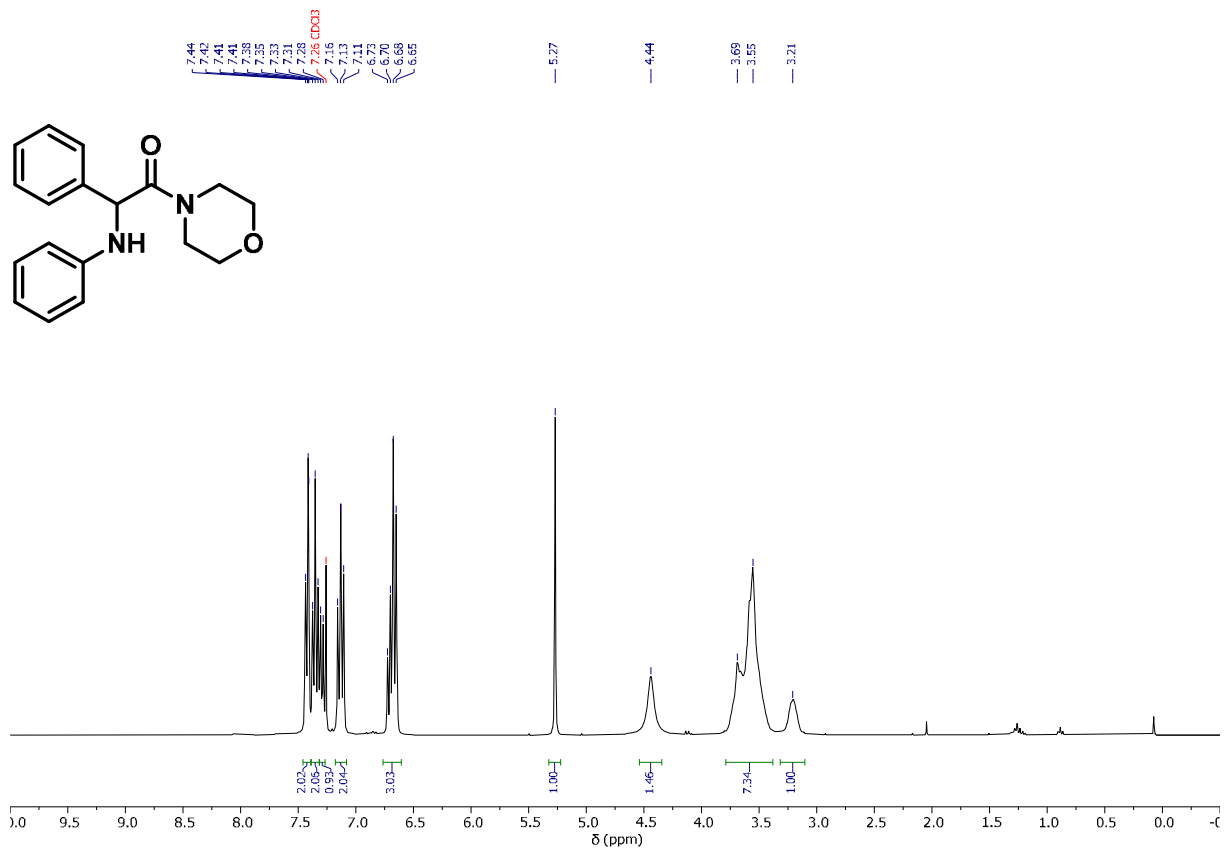
¹H-NMR of *N*,1,1-triphenylmethanimine (2q).



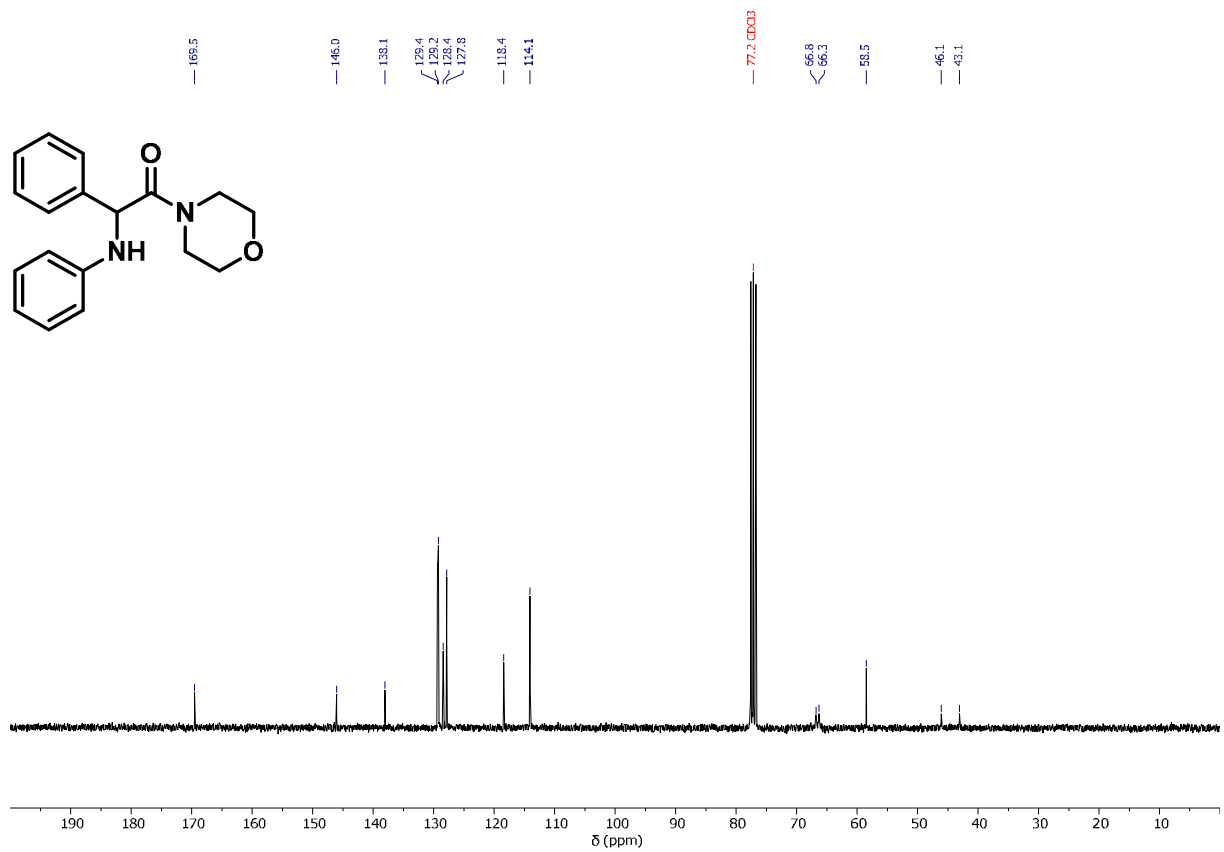
¹H-NMR of *N*-phenyl-9*H*-fluoren-9-imine (2r).



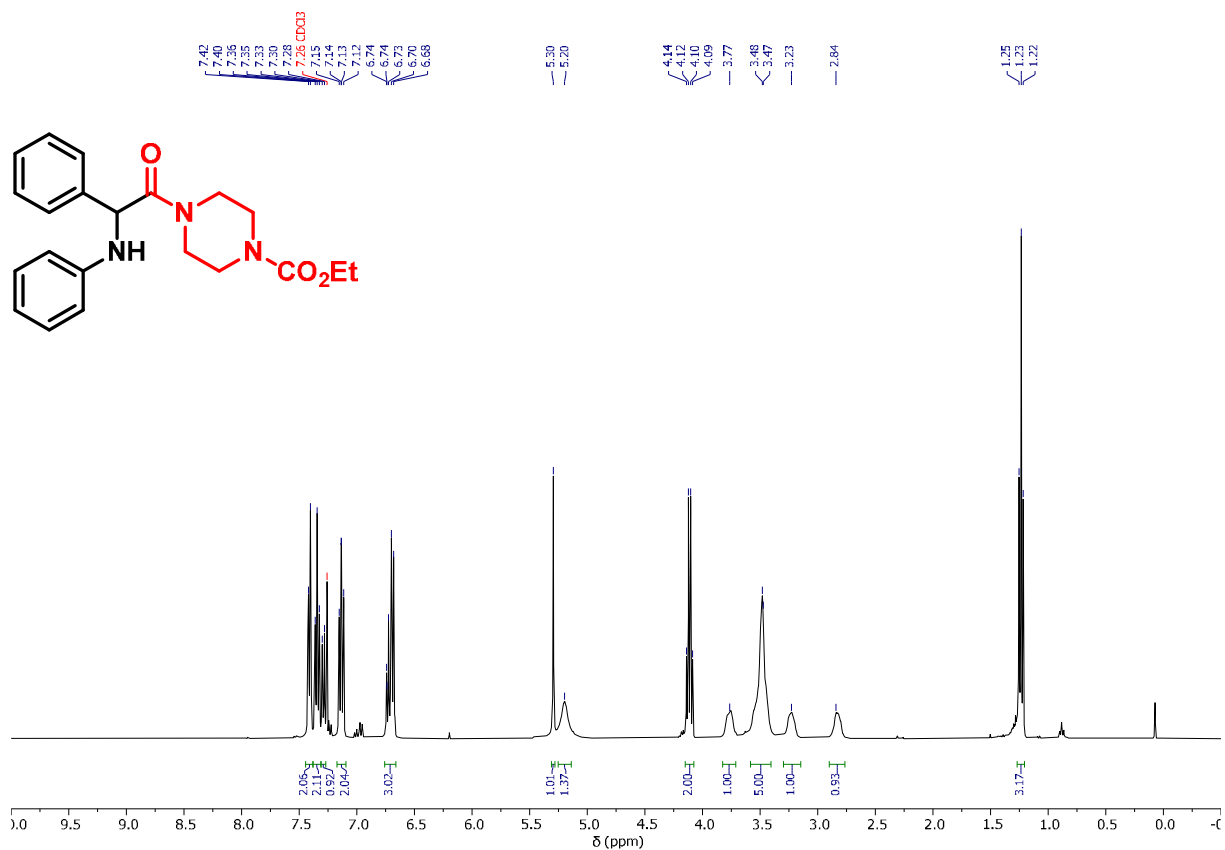
¹H-NMR of 1-(4-fluorophenyl)-*N*-phenylethan-1-imine (**2s**).



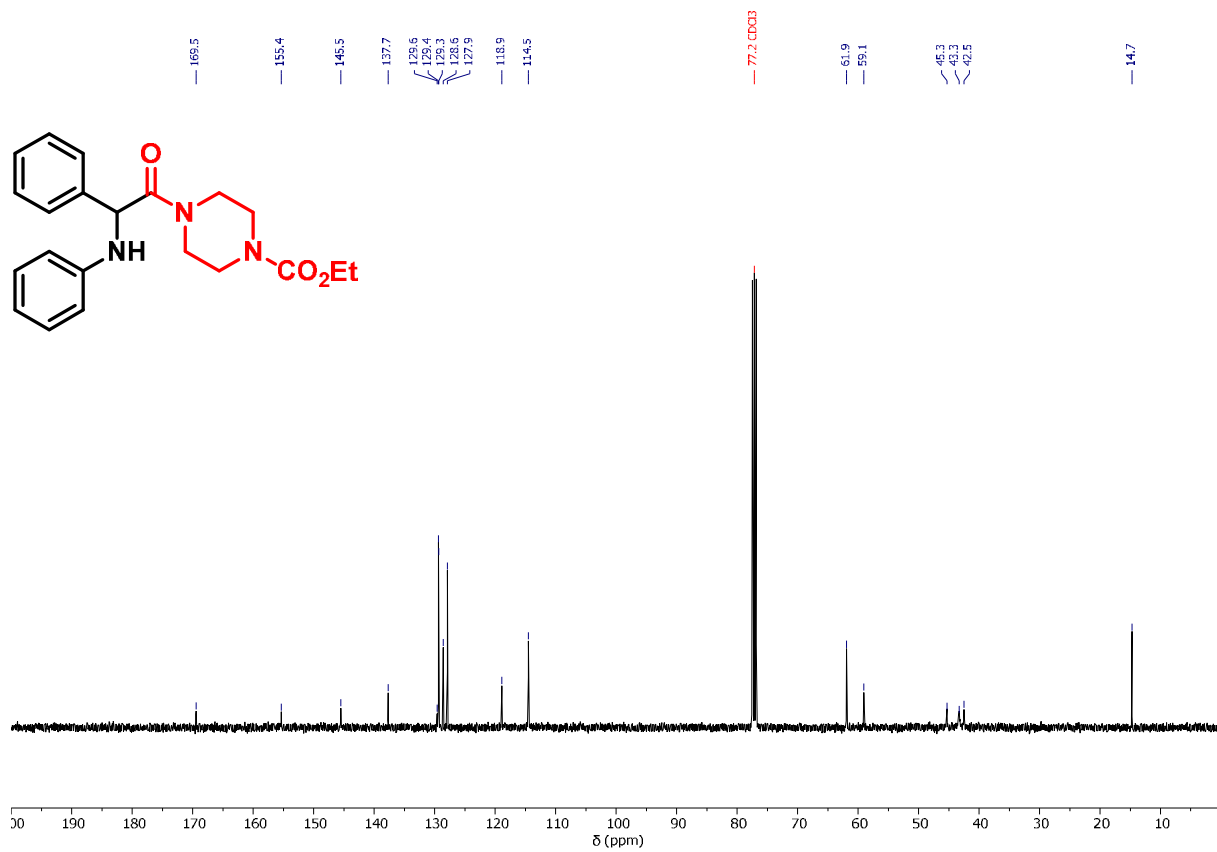
¹H-NMR of 1-morpholino-2-phenyl-2-(phenylamino)ethan-1-one (3a).



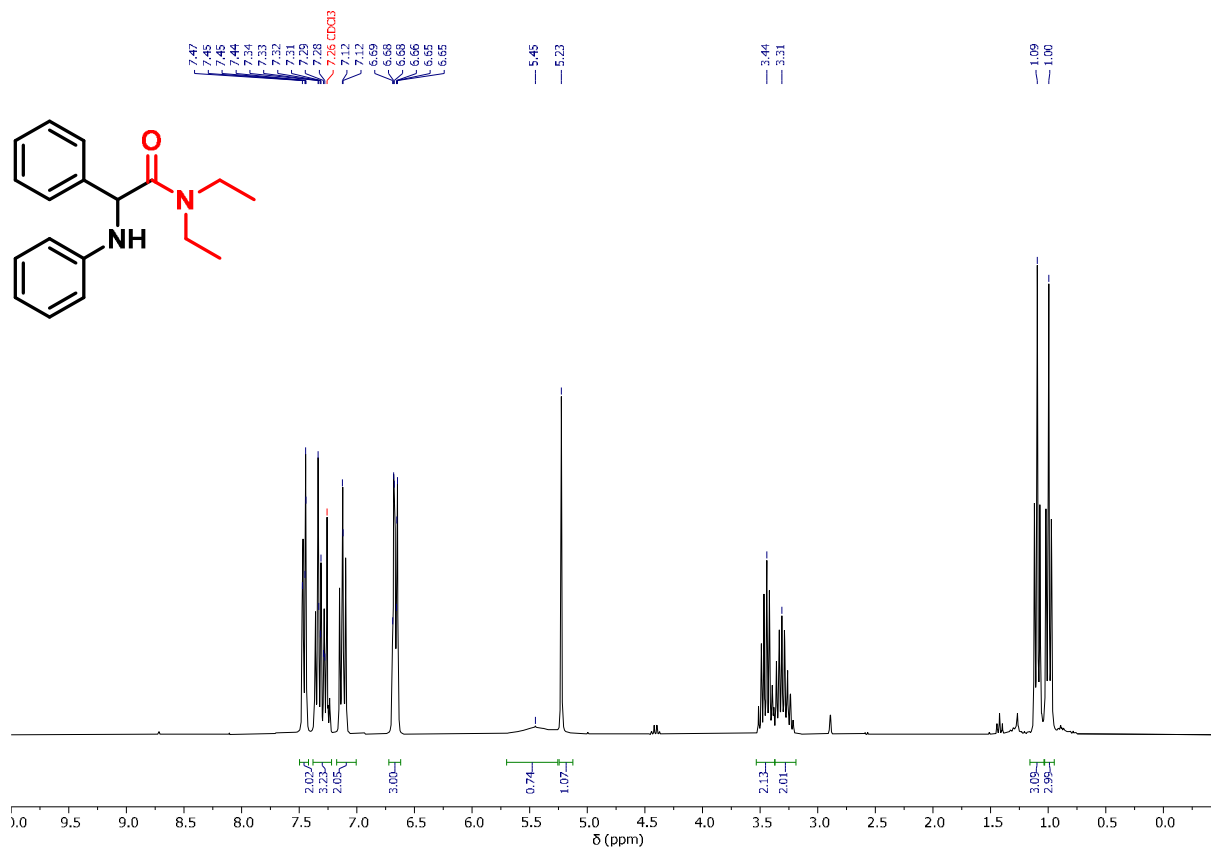
¹³C-NMR of 1-morpholino-2-phenyl-2-(phenylamino)ethan-1-one (3a).



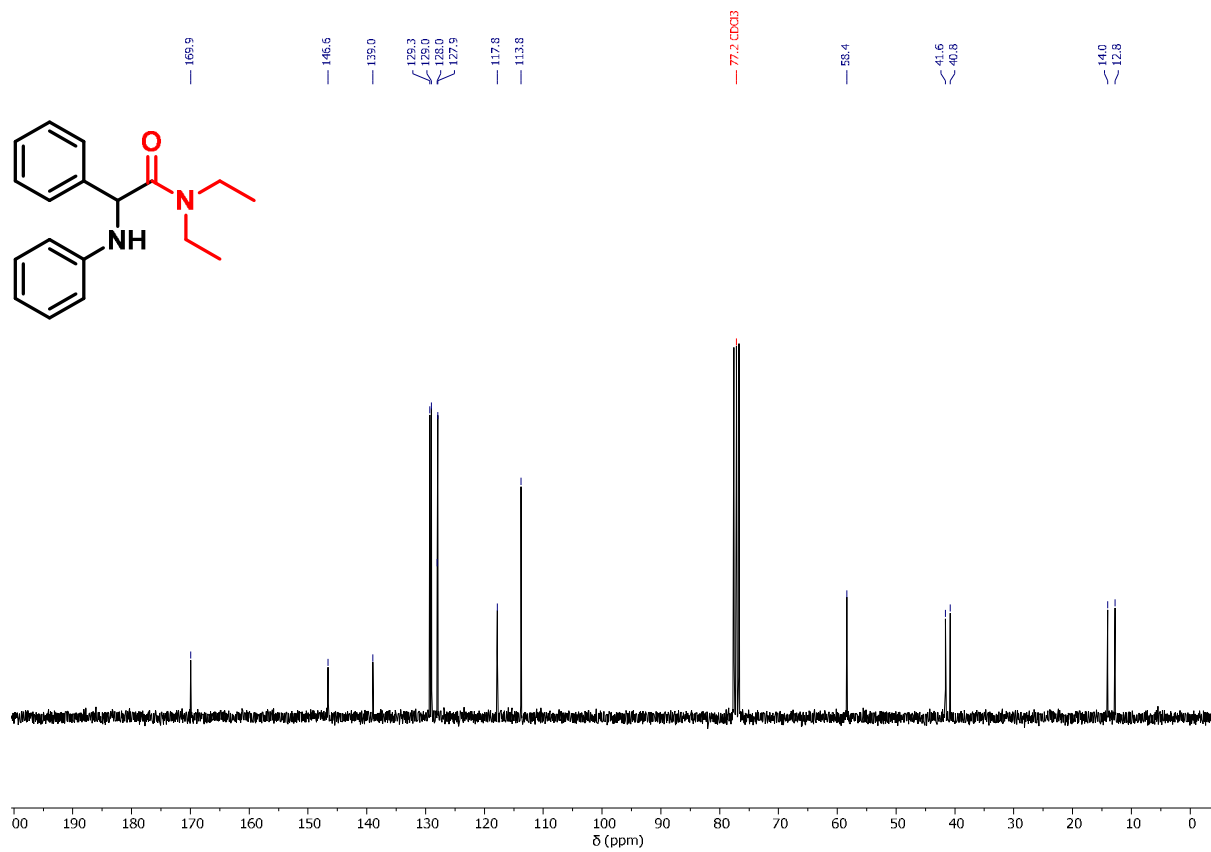
¹H-NMR of ethyl 4-(2-phenyl-2-(phenylamino)acetyl)piperazine-1-carboxylate (3b).



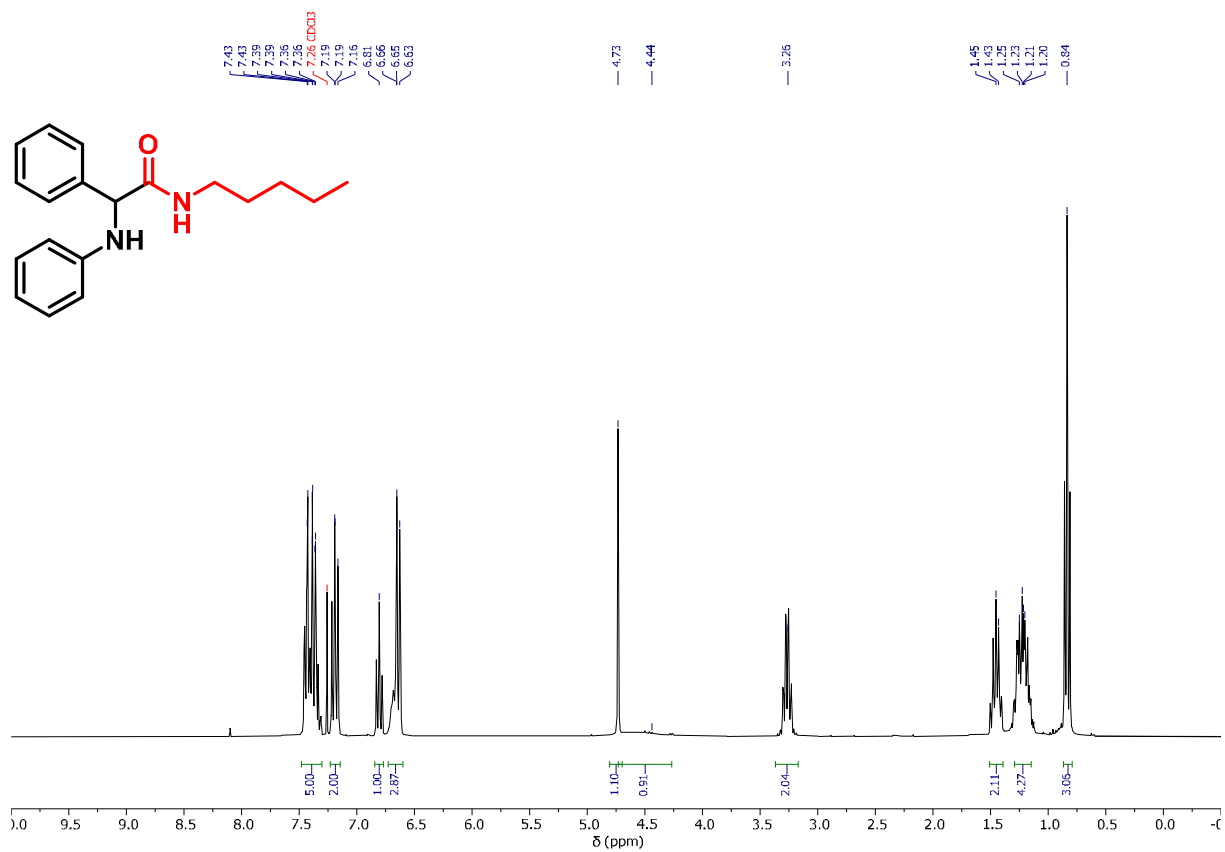
¹³C-NMR of ethyl 4-(2-phenyl-2-(phenylamino)acetyl)piperazine-1-carboxylate (3b).



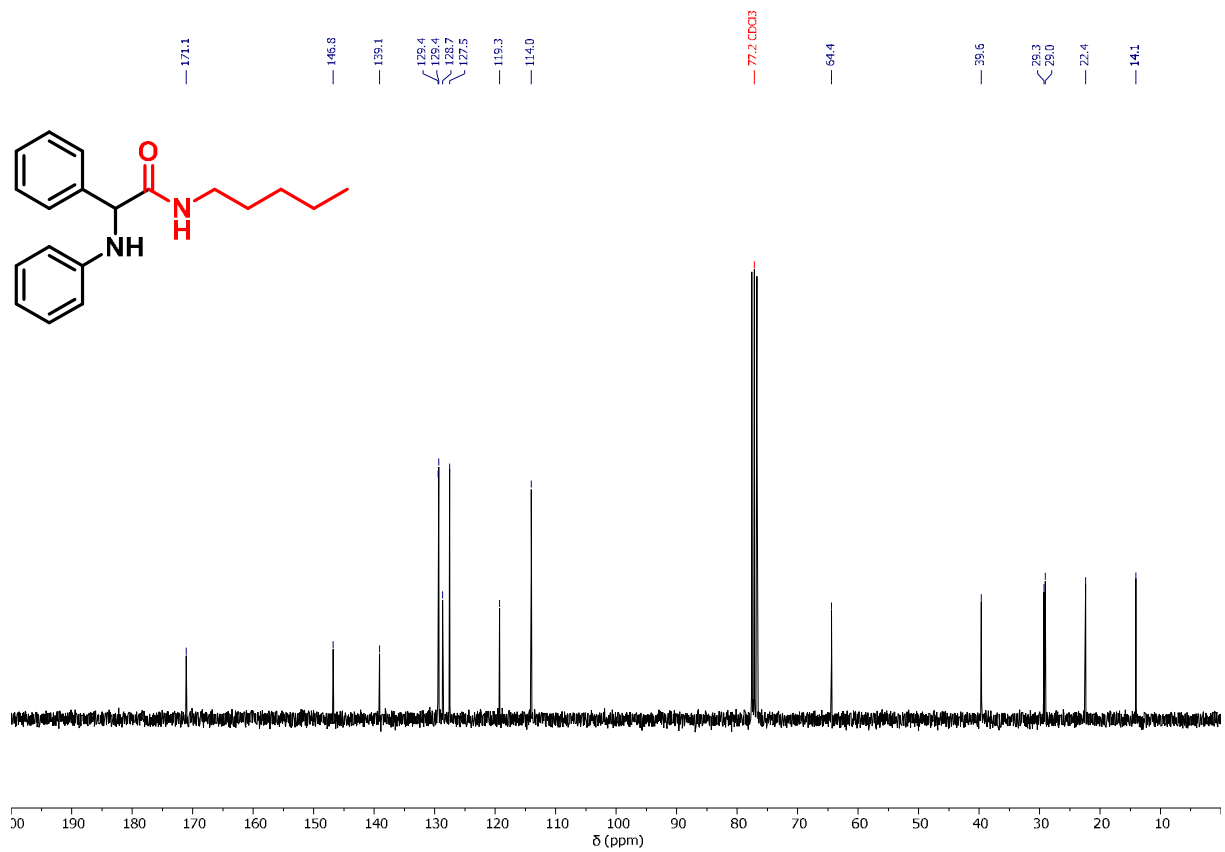
¹H-NMR of *N,N*-diethyl-2-phenyl-2-(phenylamino)acetamide (**3c**).



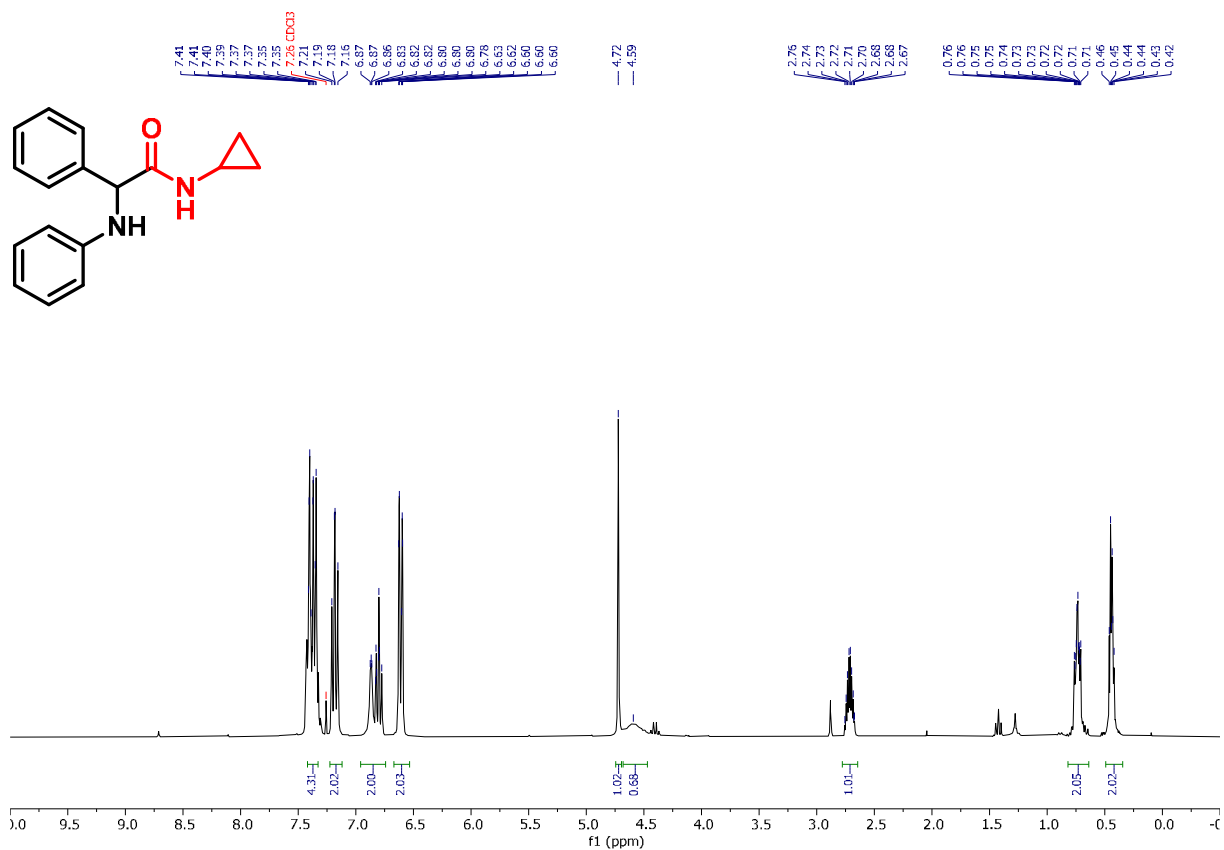
¹³C-{¹H}-NMR of *N,N*-diethyl-2-phenyl-2-(phenylamino)acetamide (**3c**).



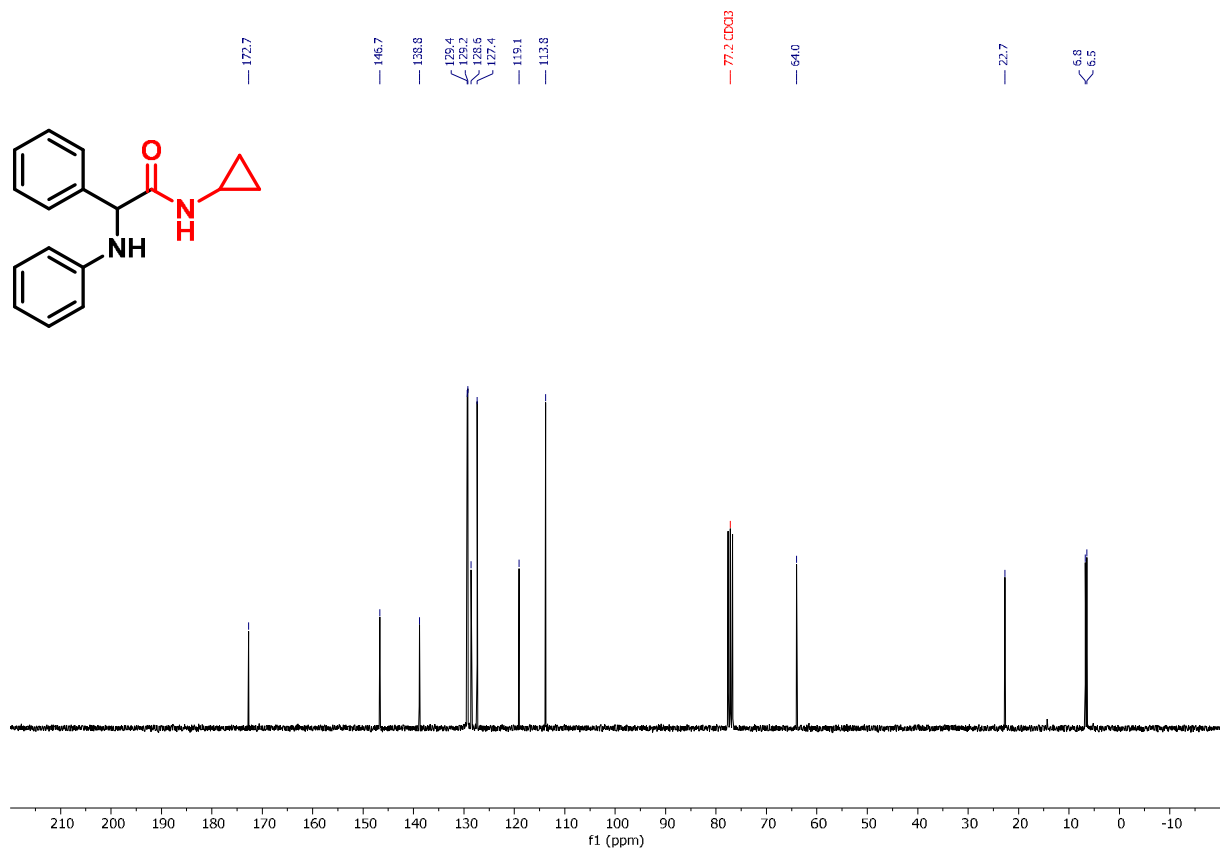
¹H-NMR of *N*-pentyl-2-phenyl-2-(phenylamino)acetamide (3d).



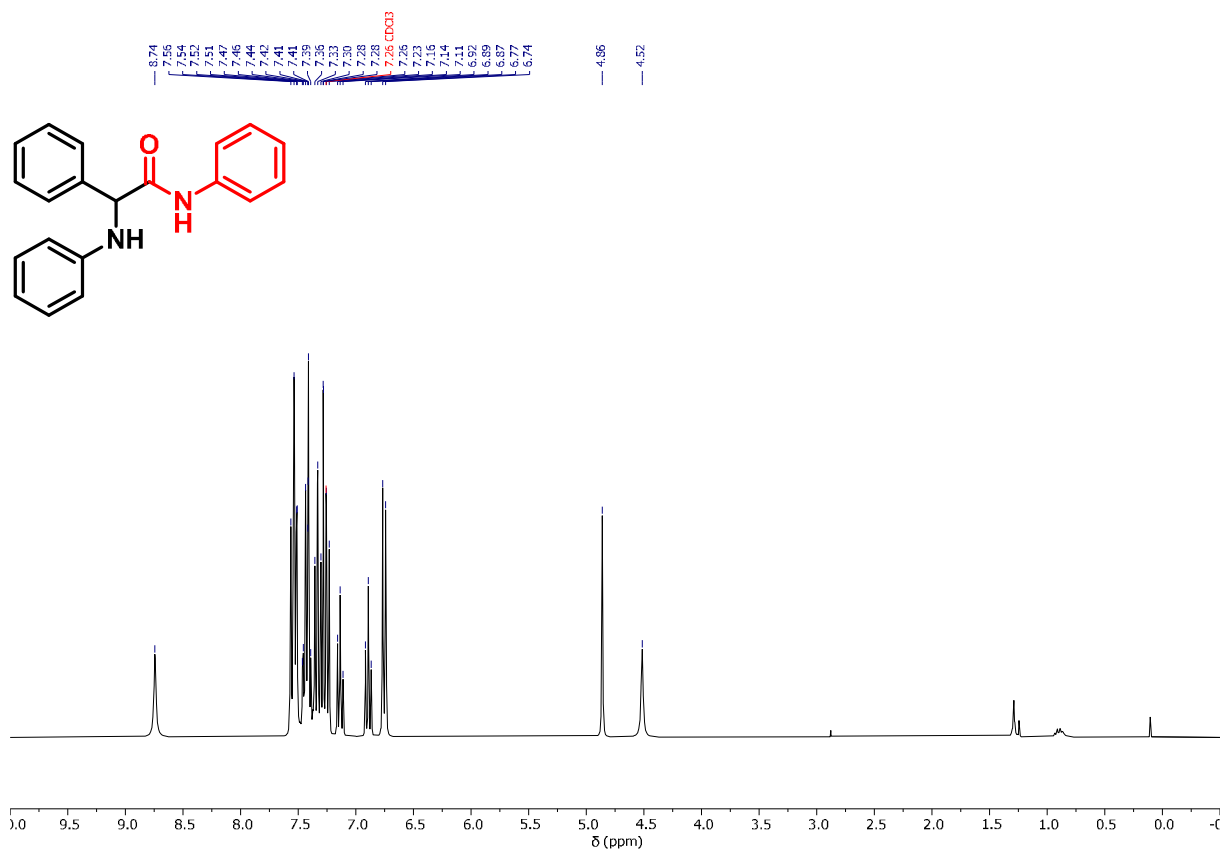
¹³C-¹H-NMR of *N*-pentyl-2-phenyl-2-(phenylamino)acetamide (3d).



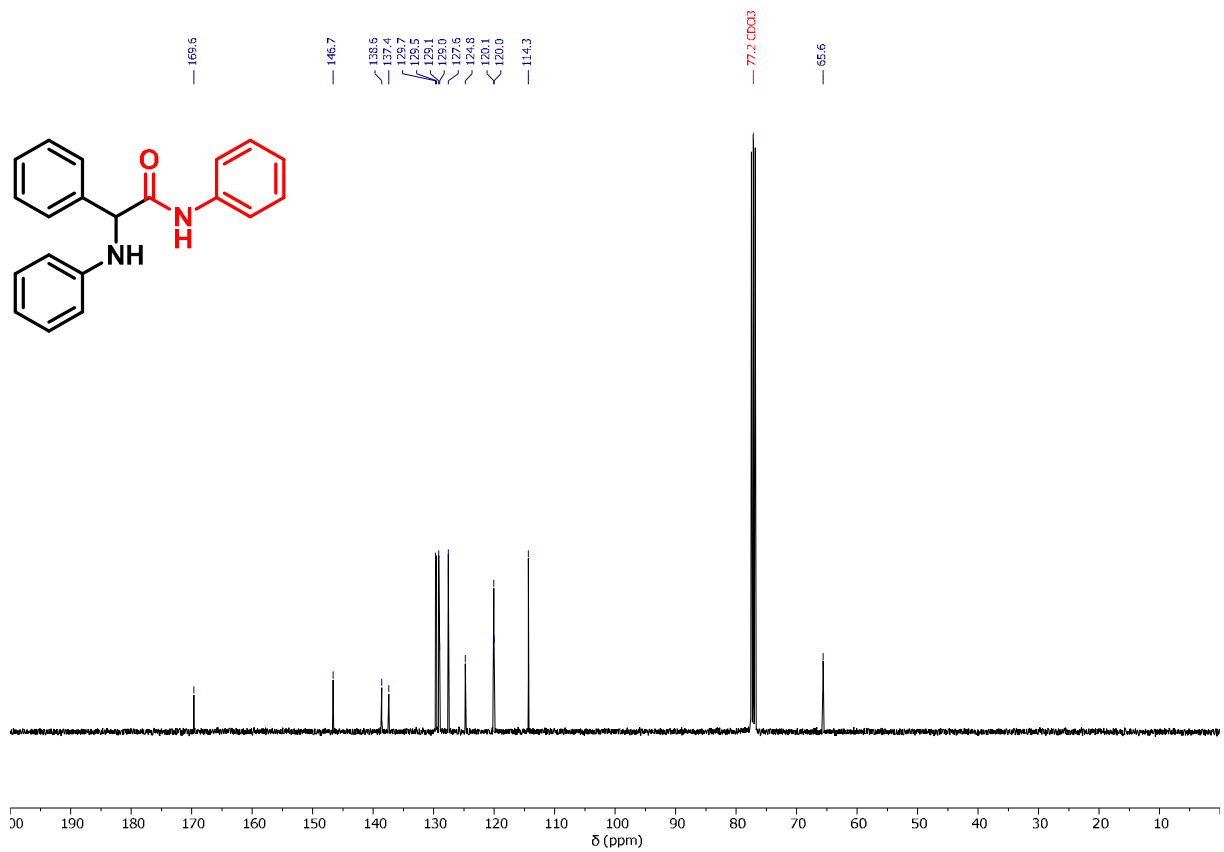
¹H-NMR of *N*-cyclopropyl-2-phenyl-2-(phenylamino)acetamide (3e).



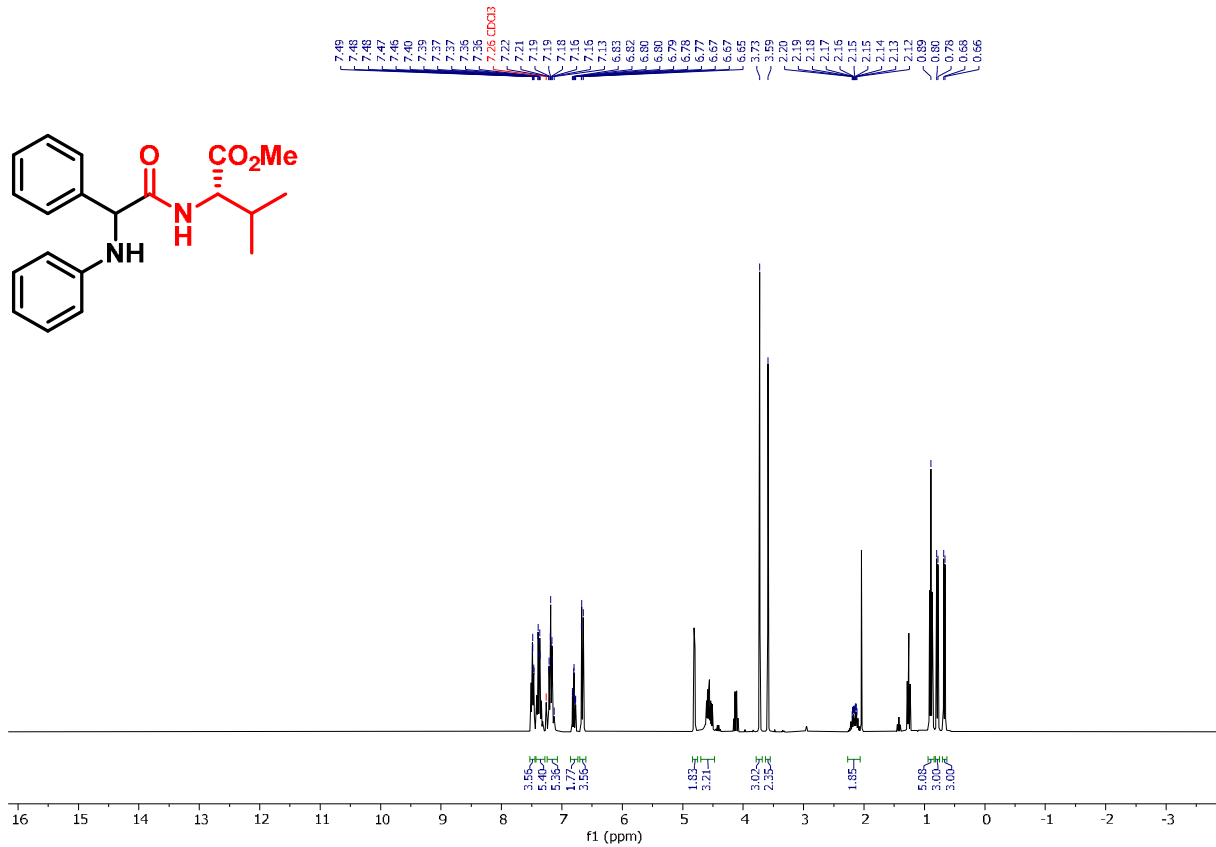
¹³C-{¹H}-NMR of *N*-cyclopropyl-2-phenyl-2-(phenylamino)acetamide (3e).



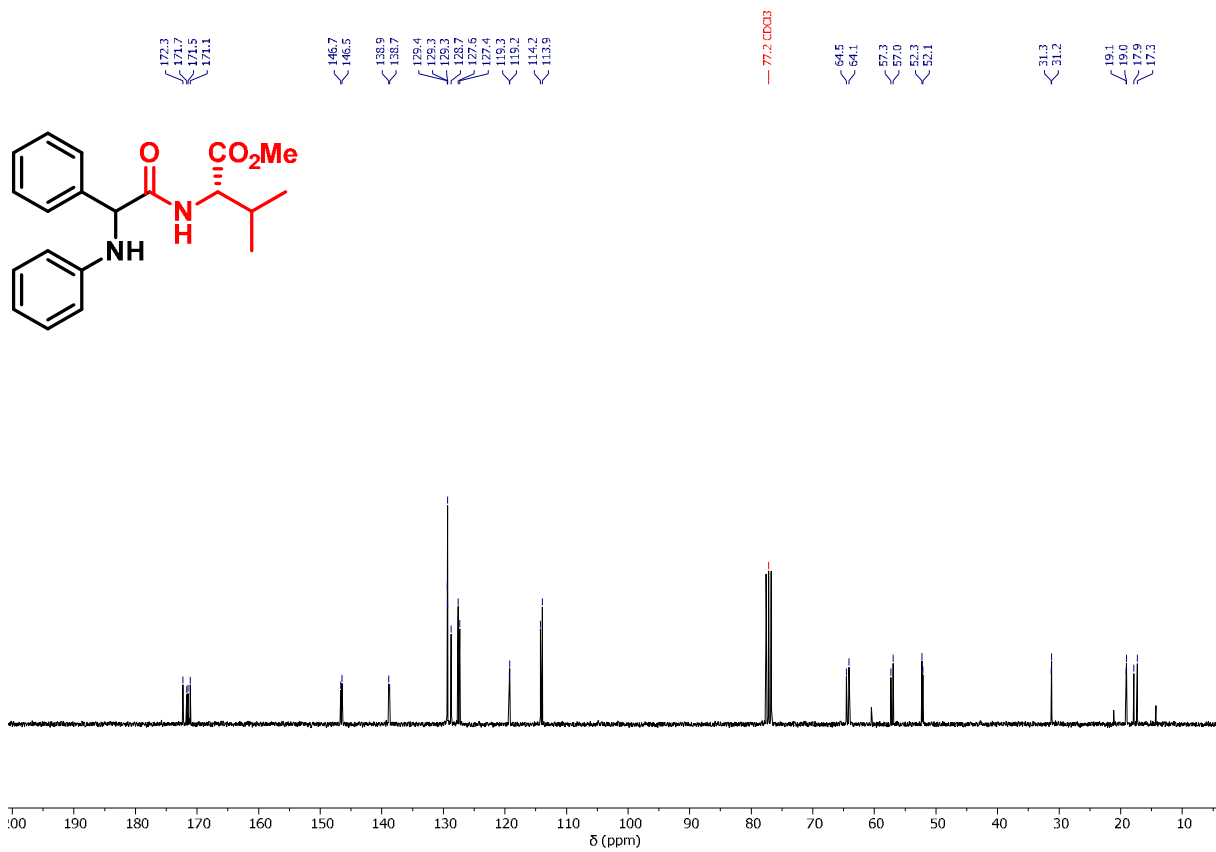
¹H-NMR of *N*,2-diphenyl-2-(phenylamino)acetamide (3f**).**



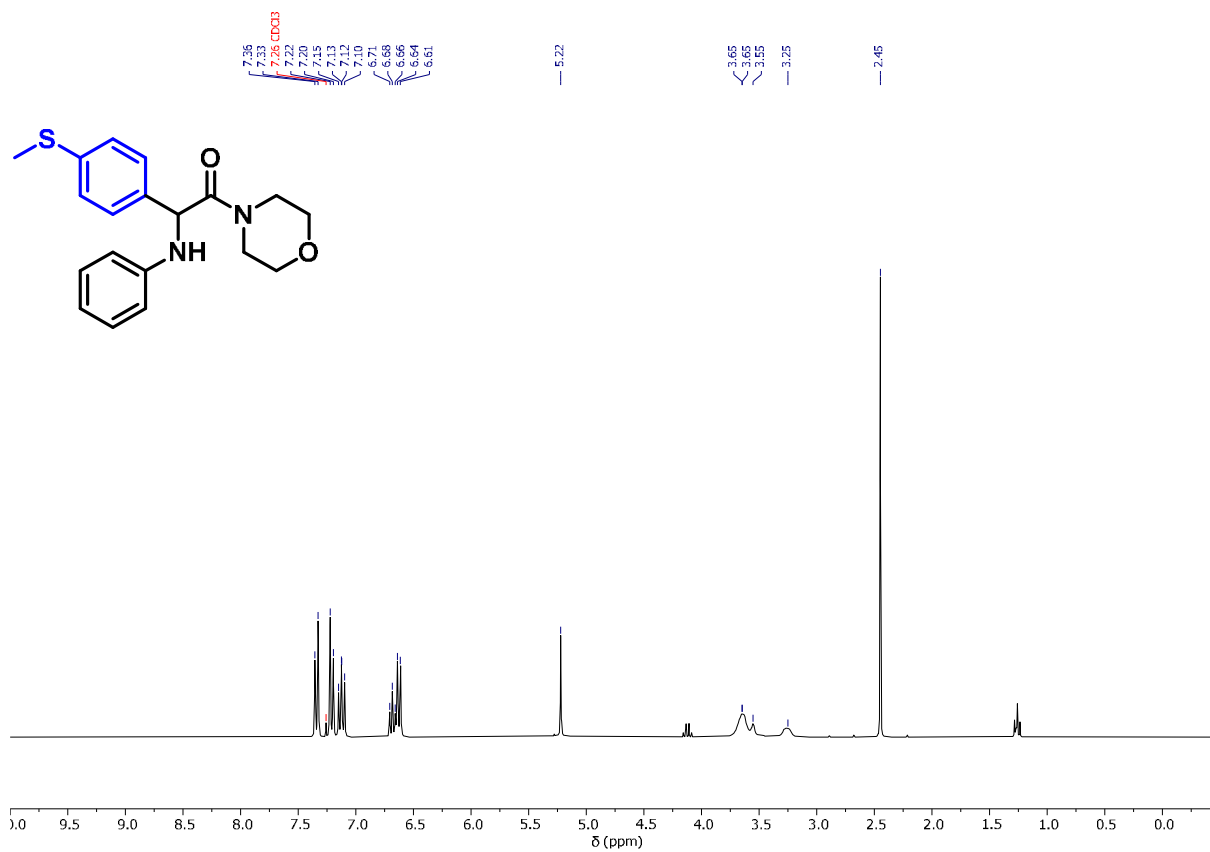
¹³C-¹H-NMR of *N*,2-diphenyl-2-(phenylamino)acetamide (3f**).**



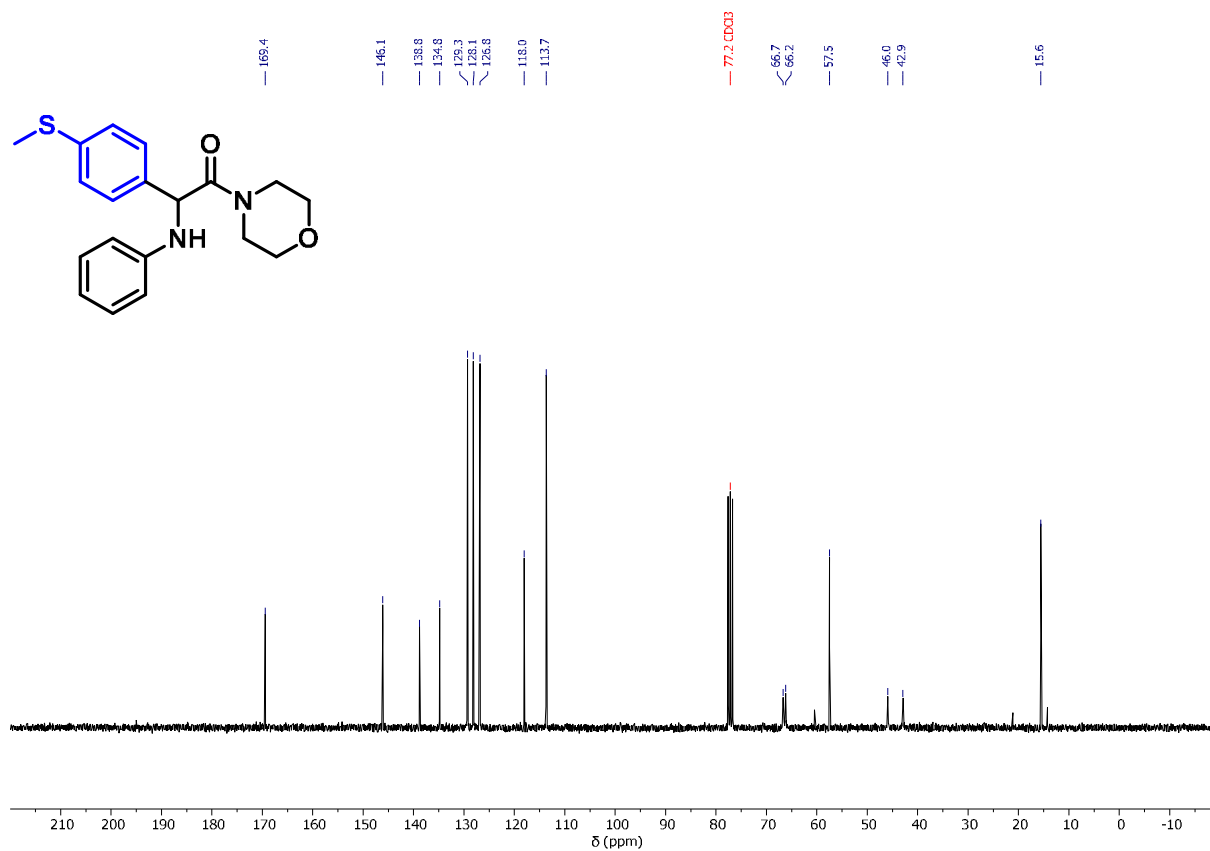
¹H-NMR of methyl (2-phenyl-2-(phenylamino)acetyl)-(S)-valinate (diastereomeric mixture) (**3g**).



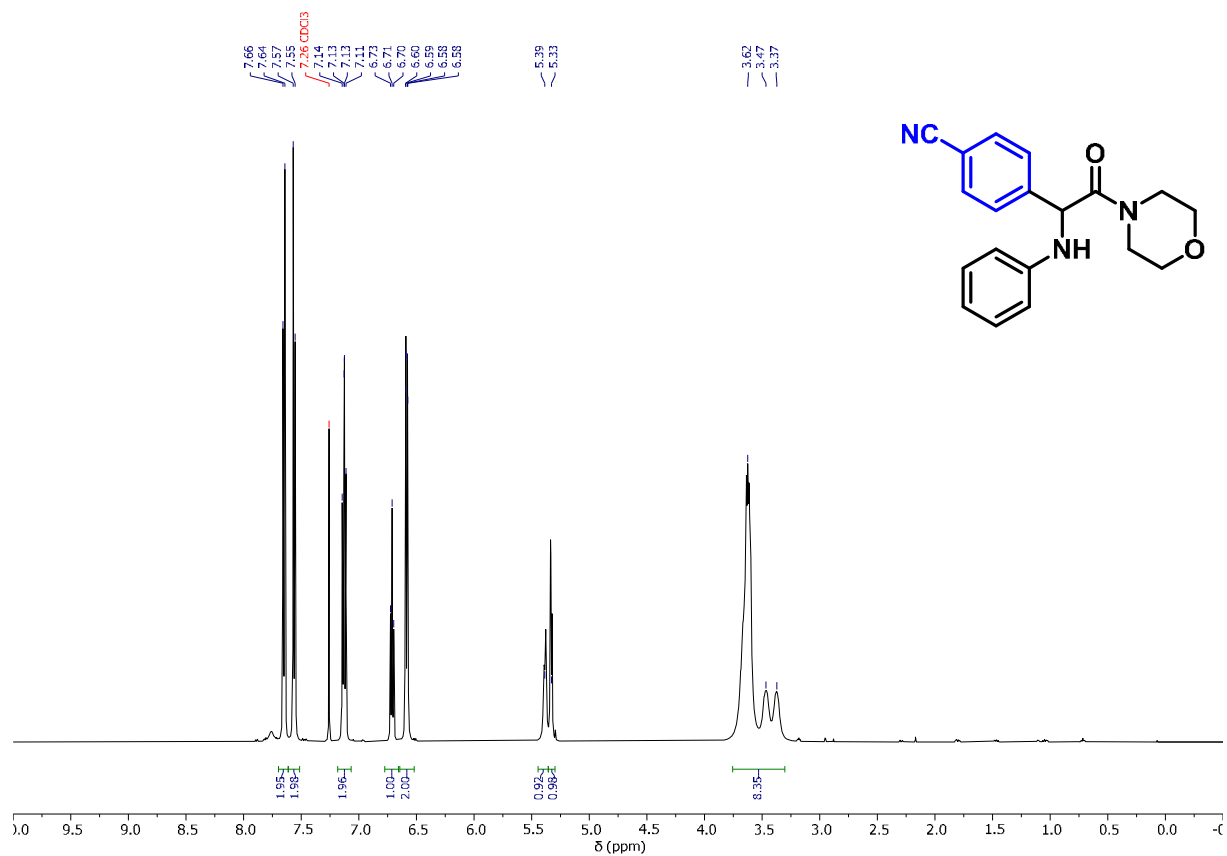
¹³C-{¹H}-NMR of methyl (2-phenyl-2-(phenylamino)acetyl)-(S)-valinate (diastereomeric mixture) (**3g**).



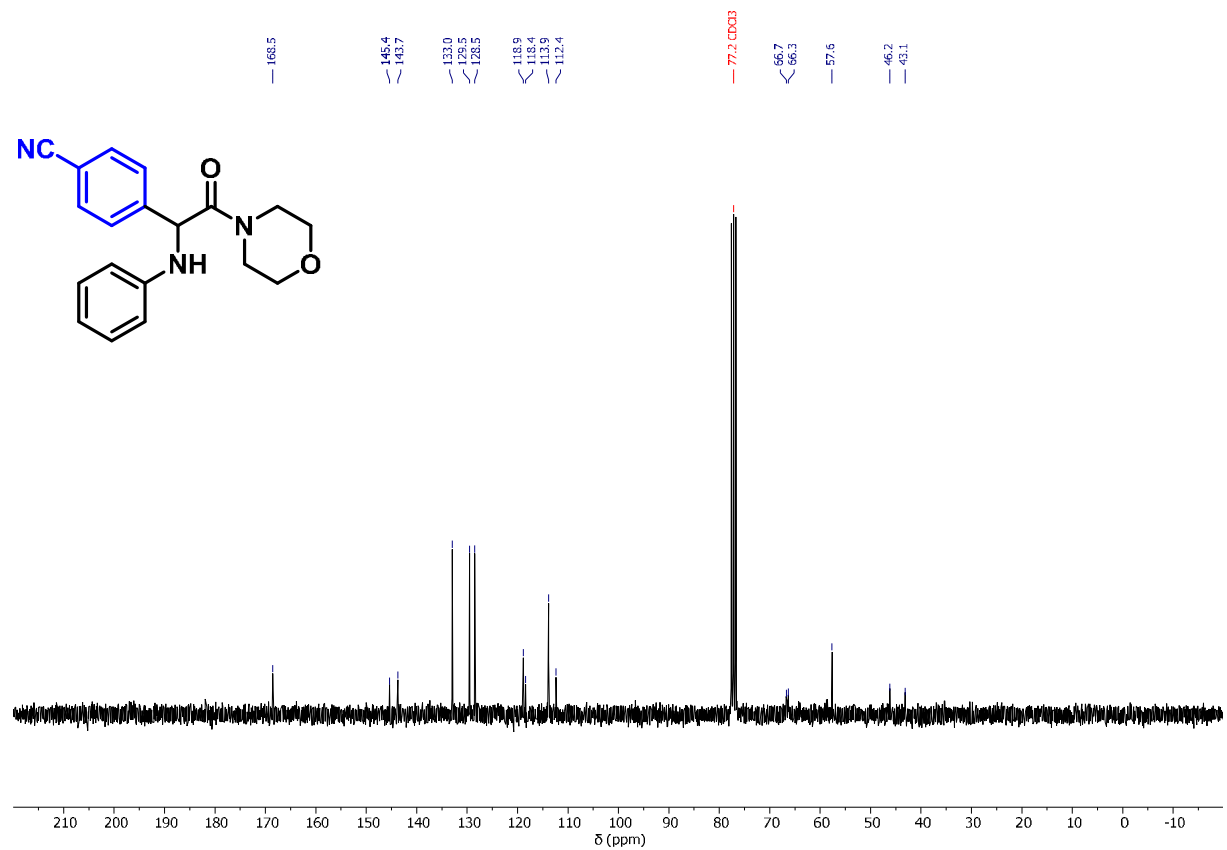
$^1\text{H-NMR}$ of 2-(3-(methylthio)phenyl)-1-morpholino-2-(phenylamino)ethan-1-one (**4a**).



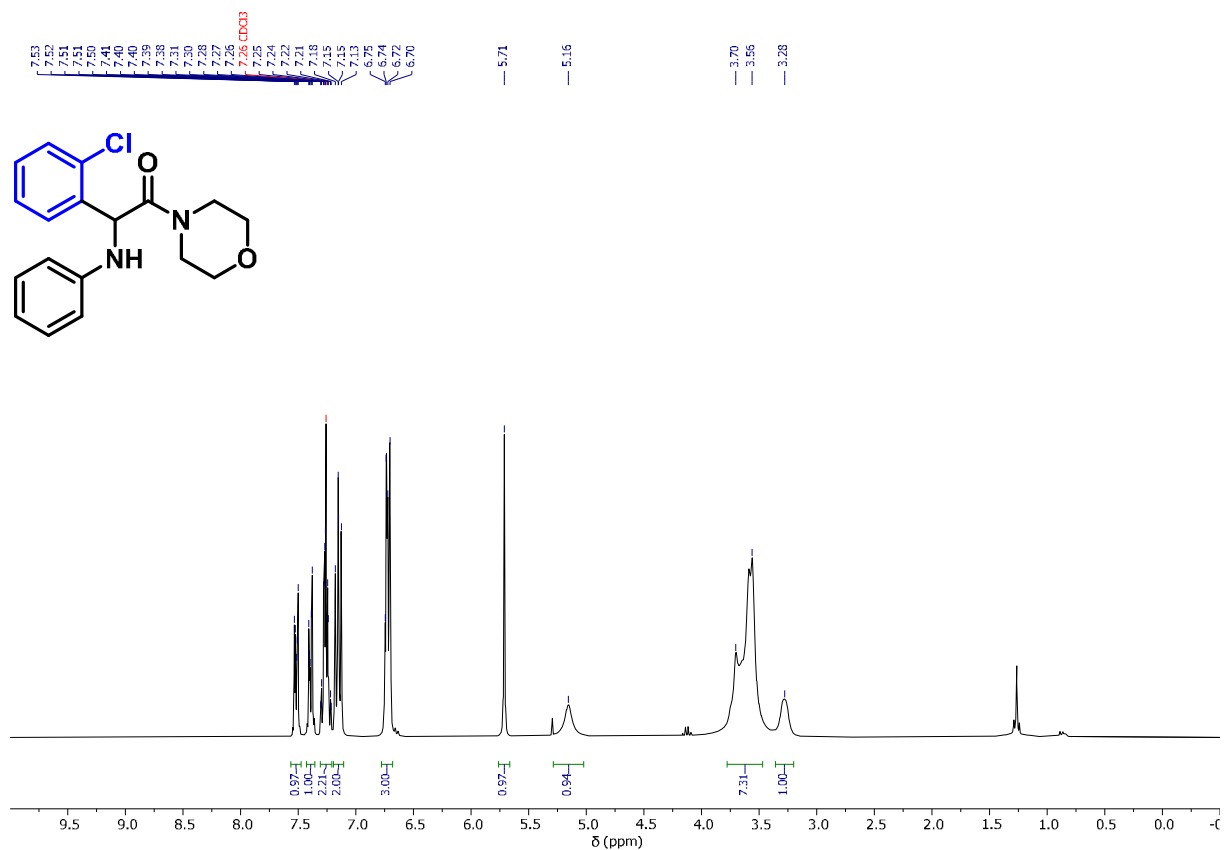
$^{13}\text{C}\{-^1\text{H}\}$ -NMR of 2-(3-(methylthio)phenyl)-1-morpholino-2-(phenylamino)ethan-1-one (**4a**).



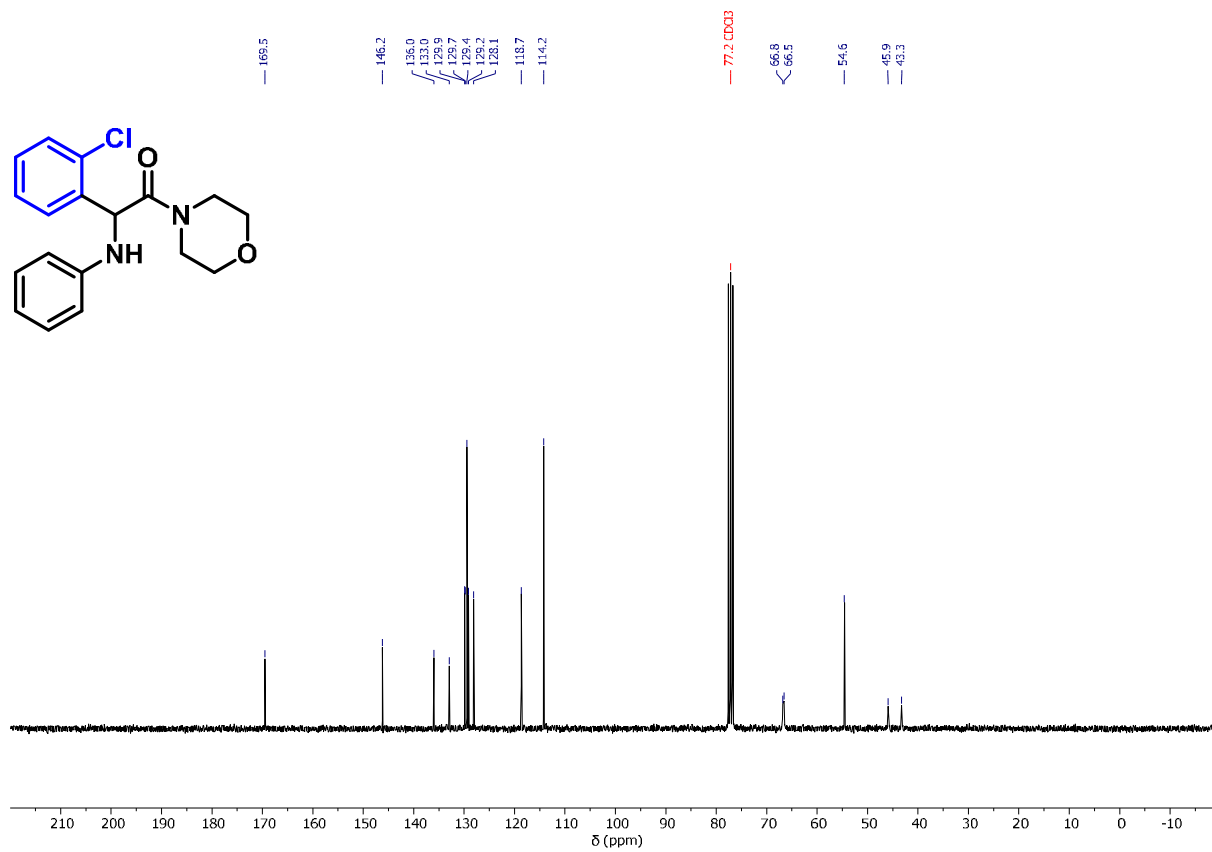
¹H-NMR of 2-(4-cyanophenyl)-1-morpholino-2-(phenylamino)ethan-1-one (4b).



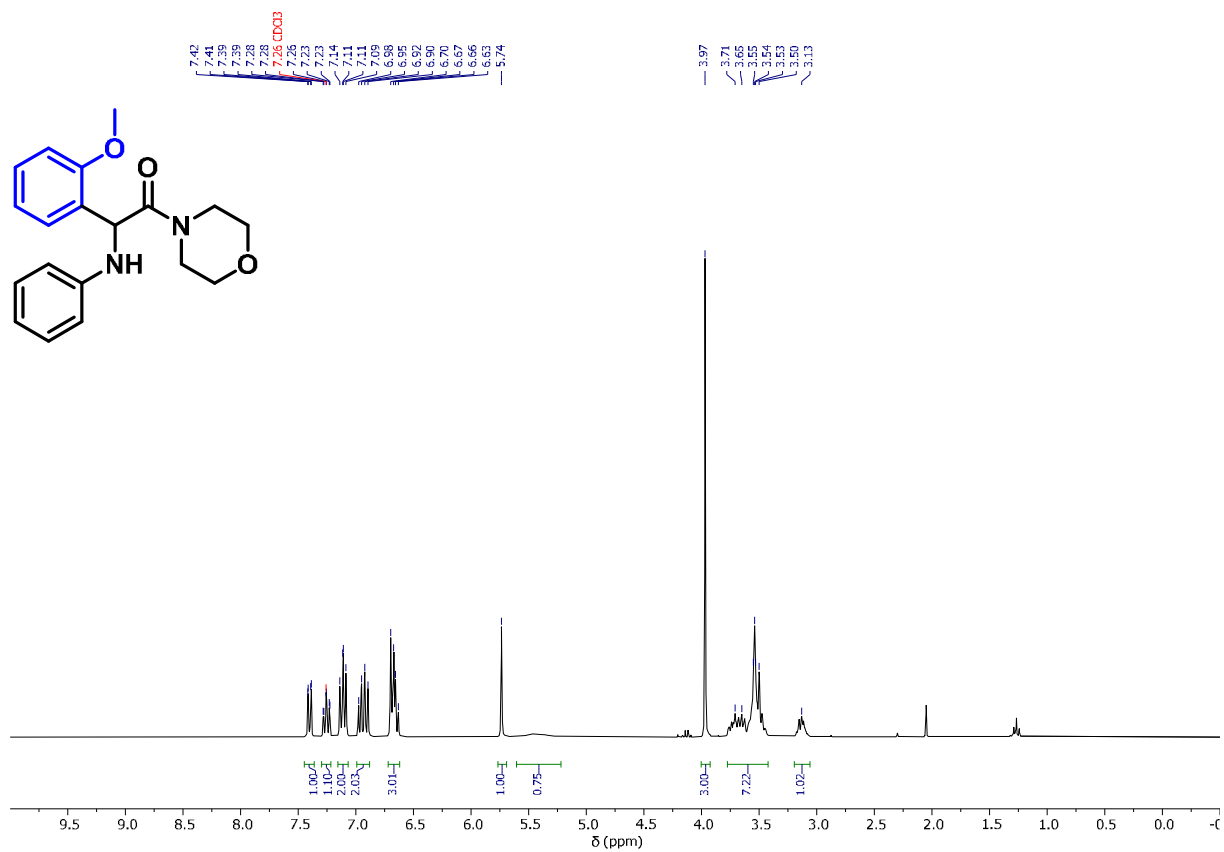
¹³C-{¹H}-NMR of 2-(4-cyanophenyl)-1-morpholino-2-(phenylamino)ethan-1-one (4b).



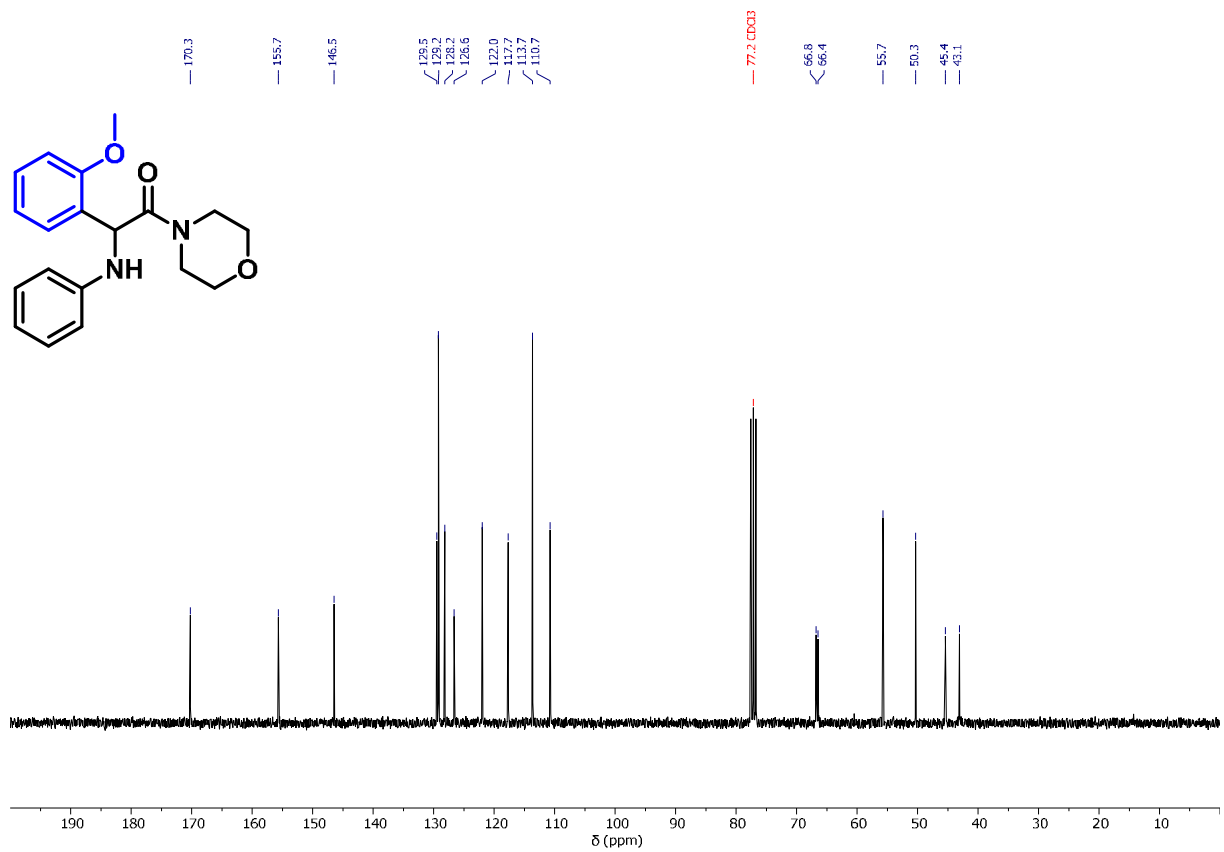
¹H-NMR of 2-(2-chlorophenyl)-1-morpholino-2-(phenylamino)ethan-1-one (4c).



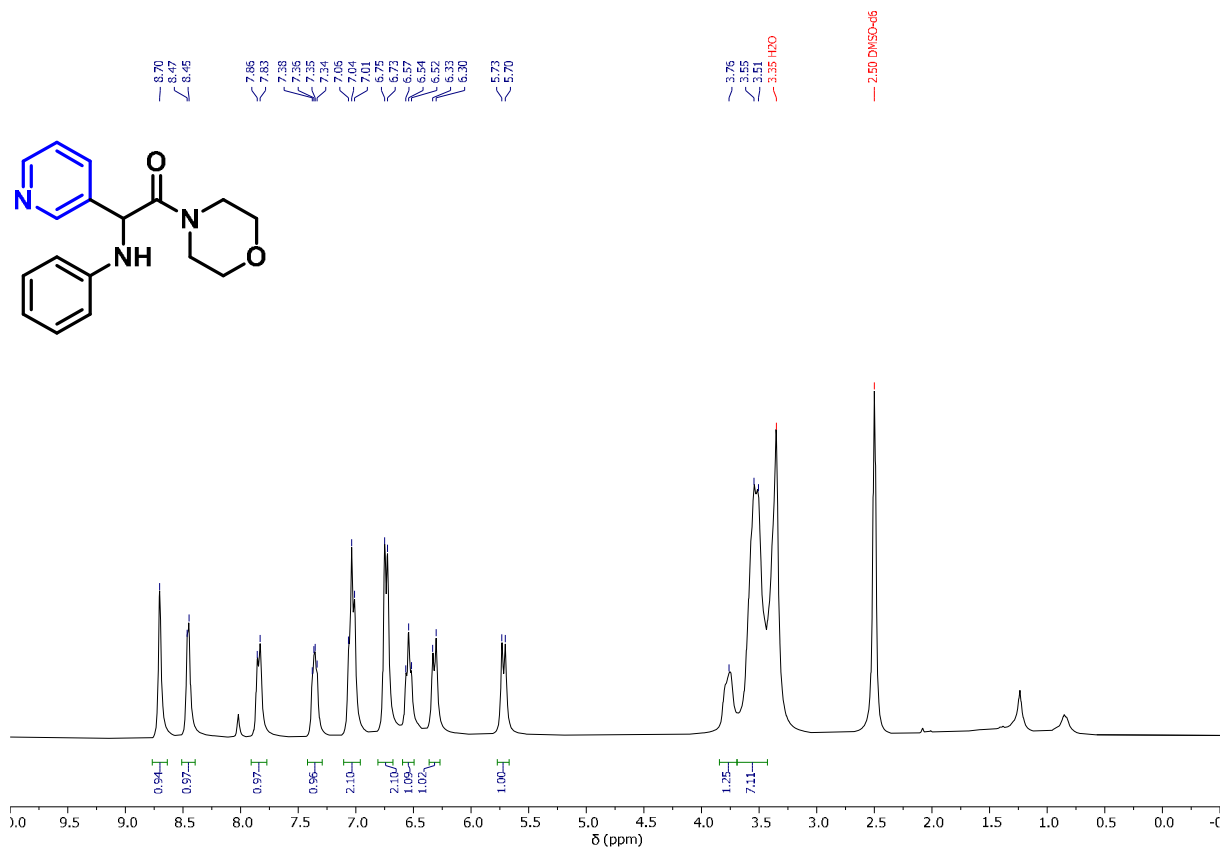
¹³C-NMR of 2-(2-chlorophenyl)-1-morpholino-2-(phenylamino)ethan-1-one (4c).



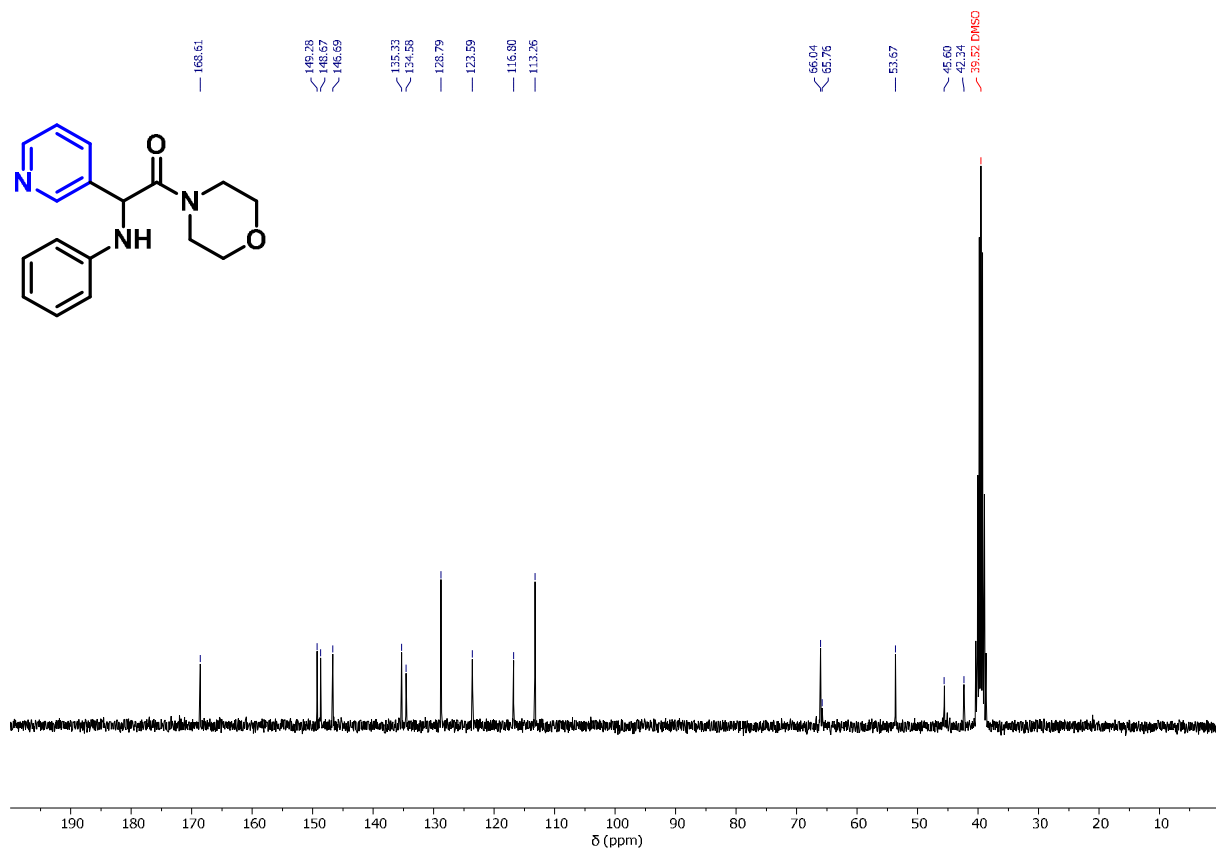
¹H-NMR of 2-(2-methoxyphenyl)-1-morpholino-2-(phenylamino)ethan-1-one (4d).



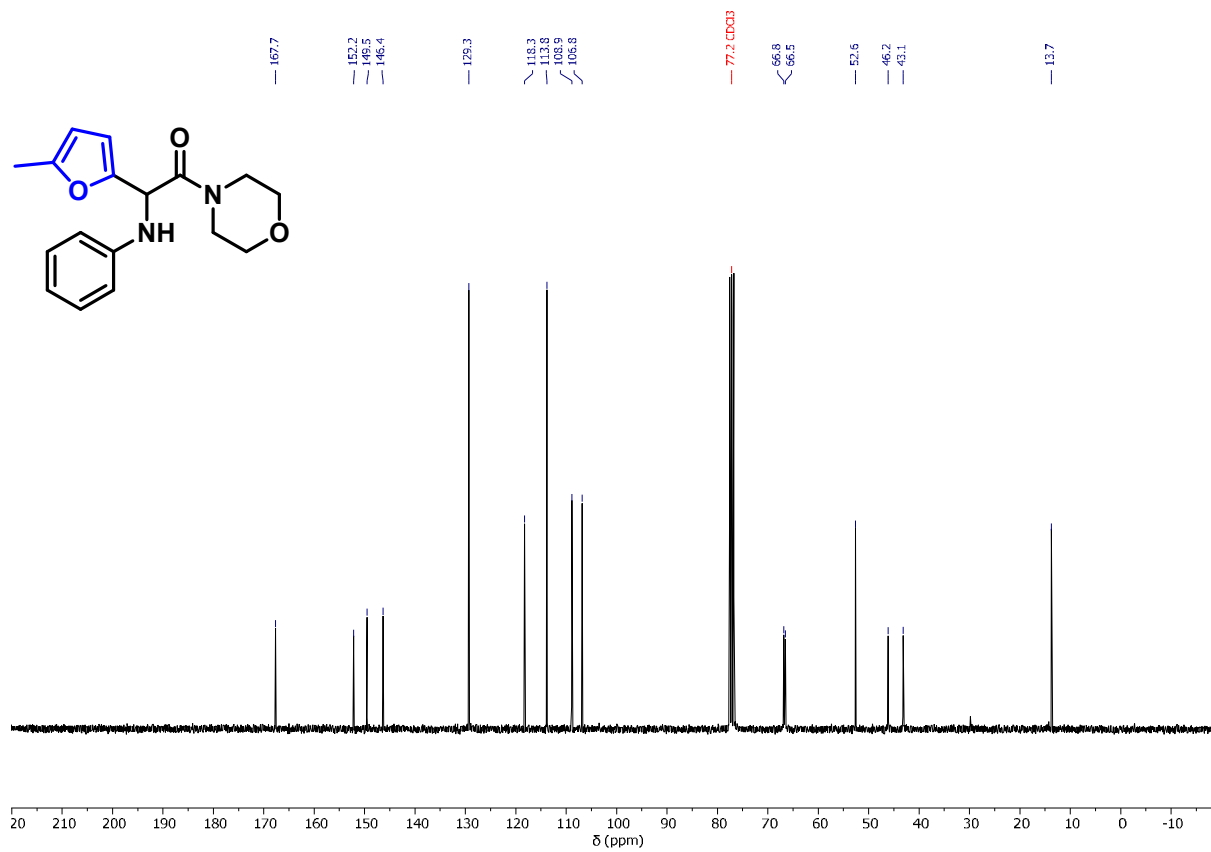
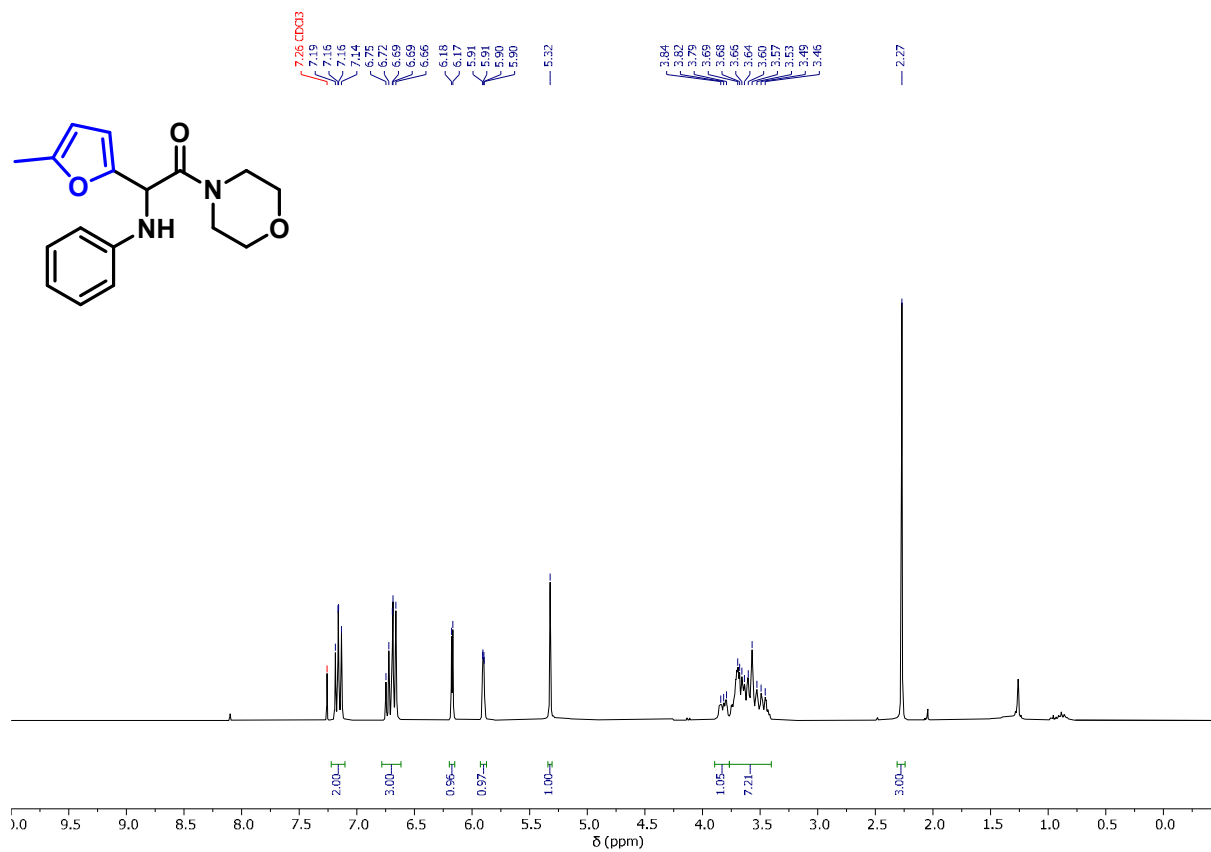
¹³C-NMR of 2-(2-methoxyphenyl)-1-morpholino-2-(phenylamino)ethan-1-one (4d).

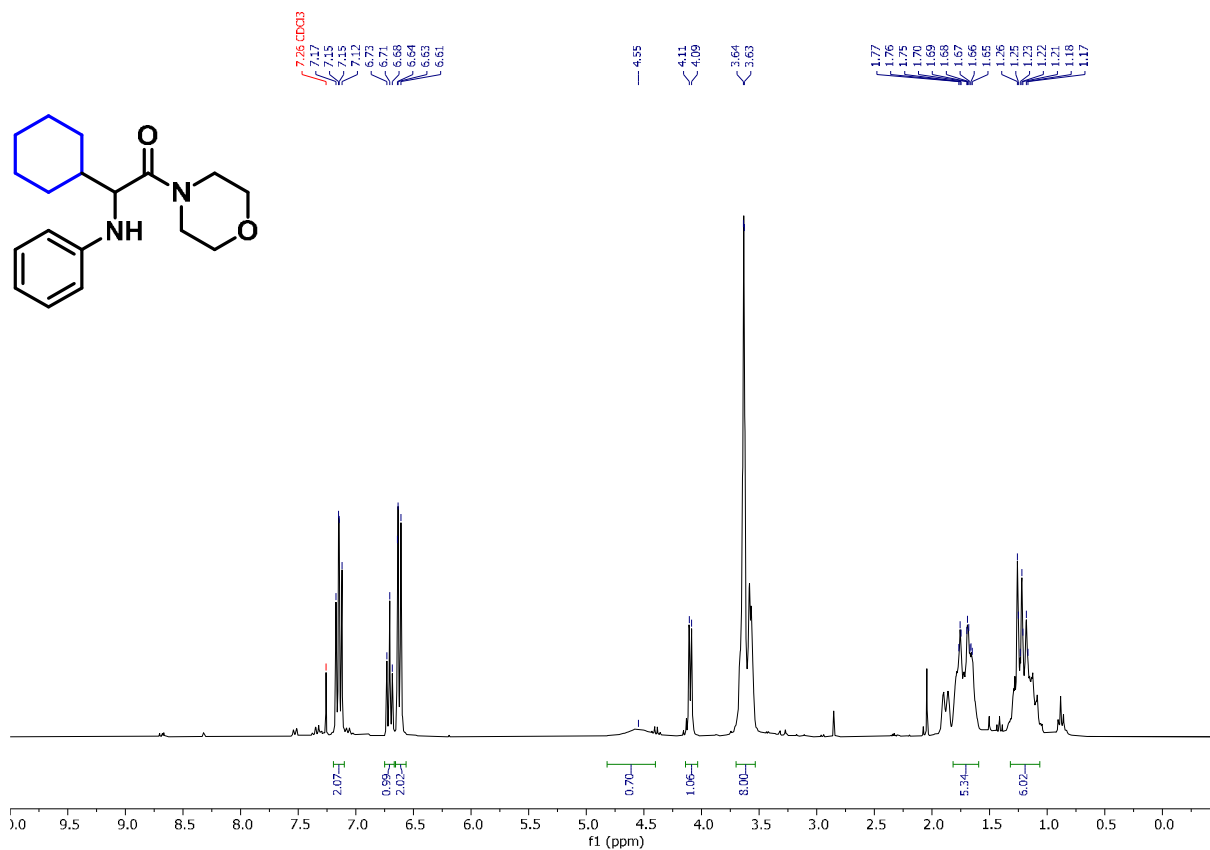


¹H-NMR of 1-morpholino-2-(phenylamino)-2-(pyridin-3-yl)ethan-1-one (4e).

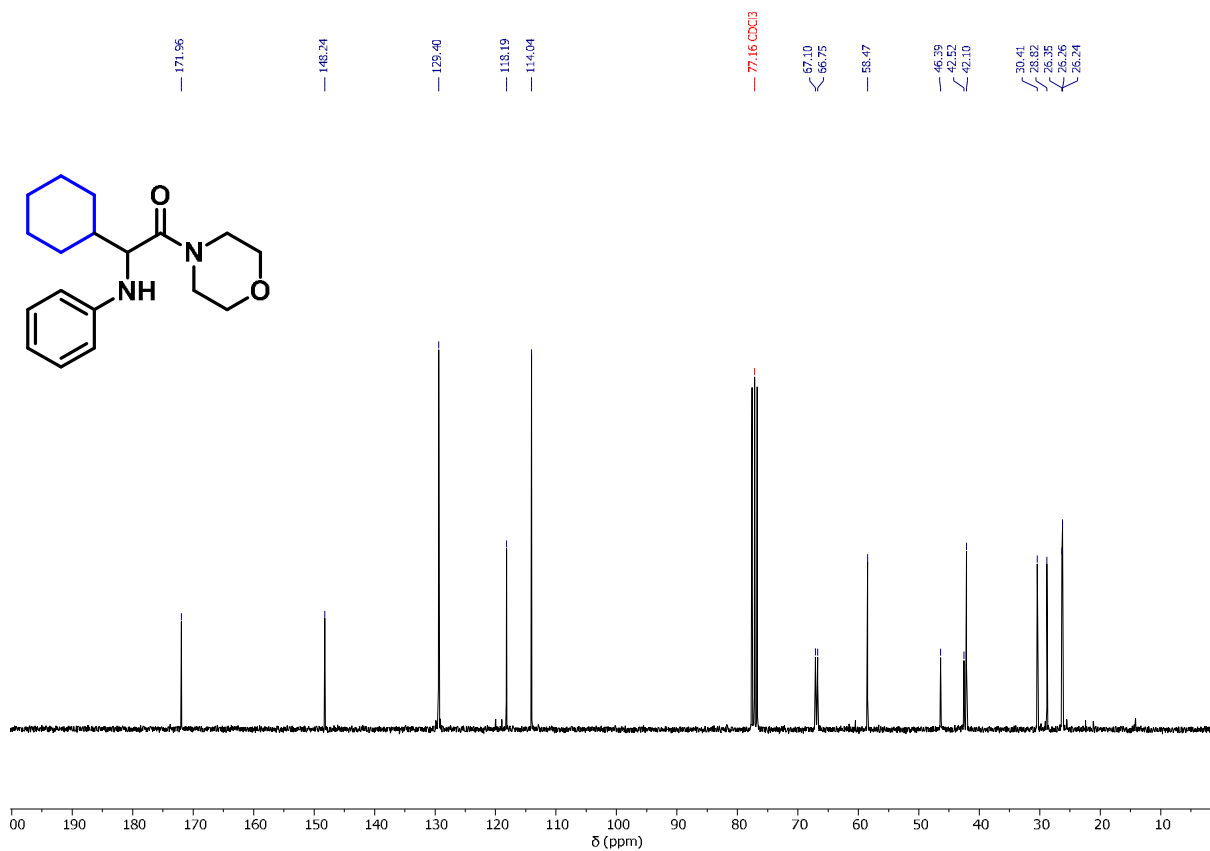


¹³C-{¹H}-NMR of 1-morpholino-2-(phenylamino)-2-(pyridin-3-yl)ethan-1-one (4e).

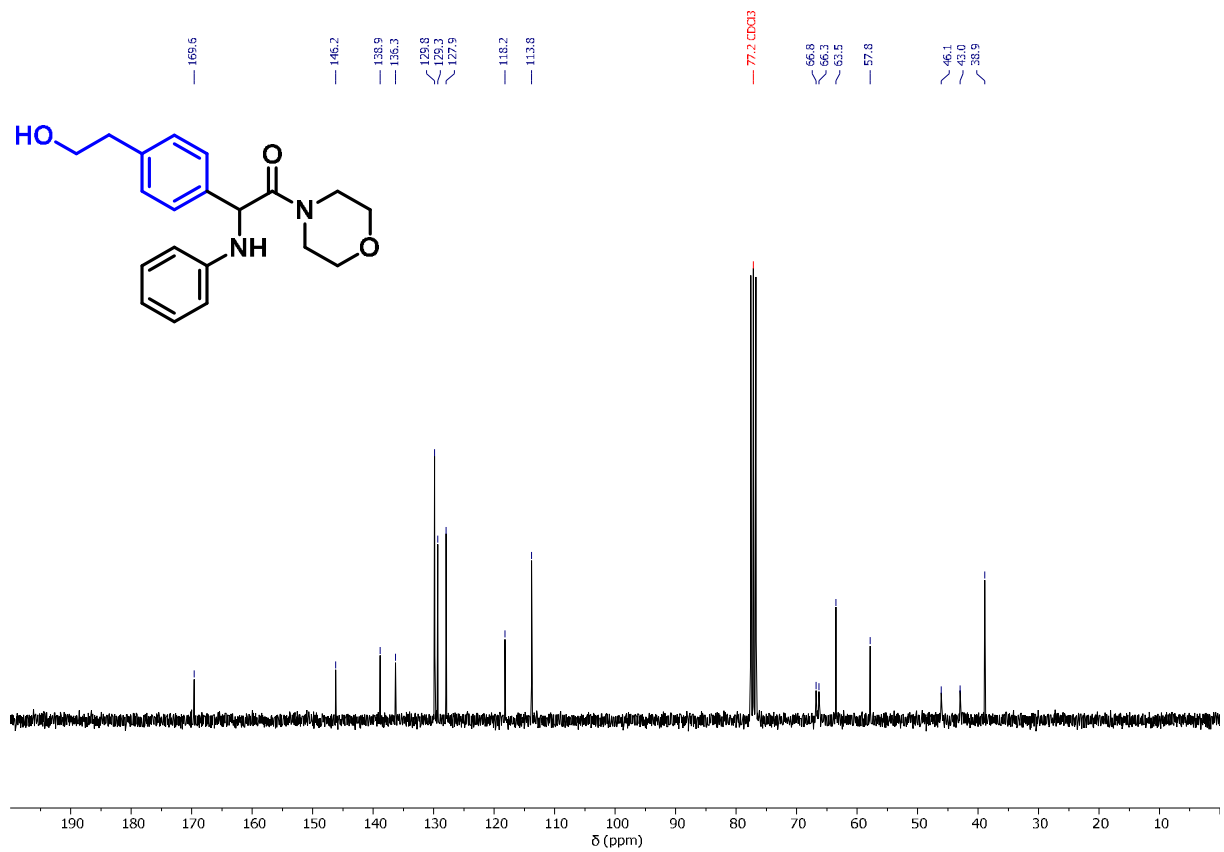
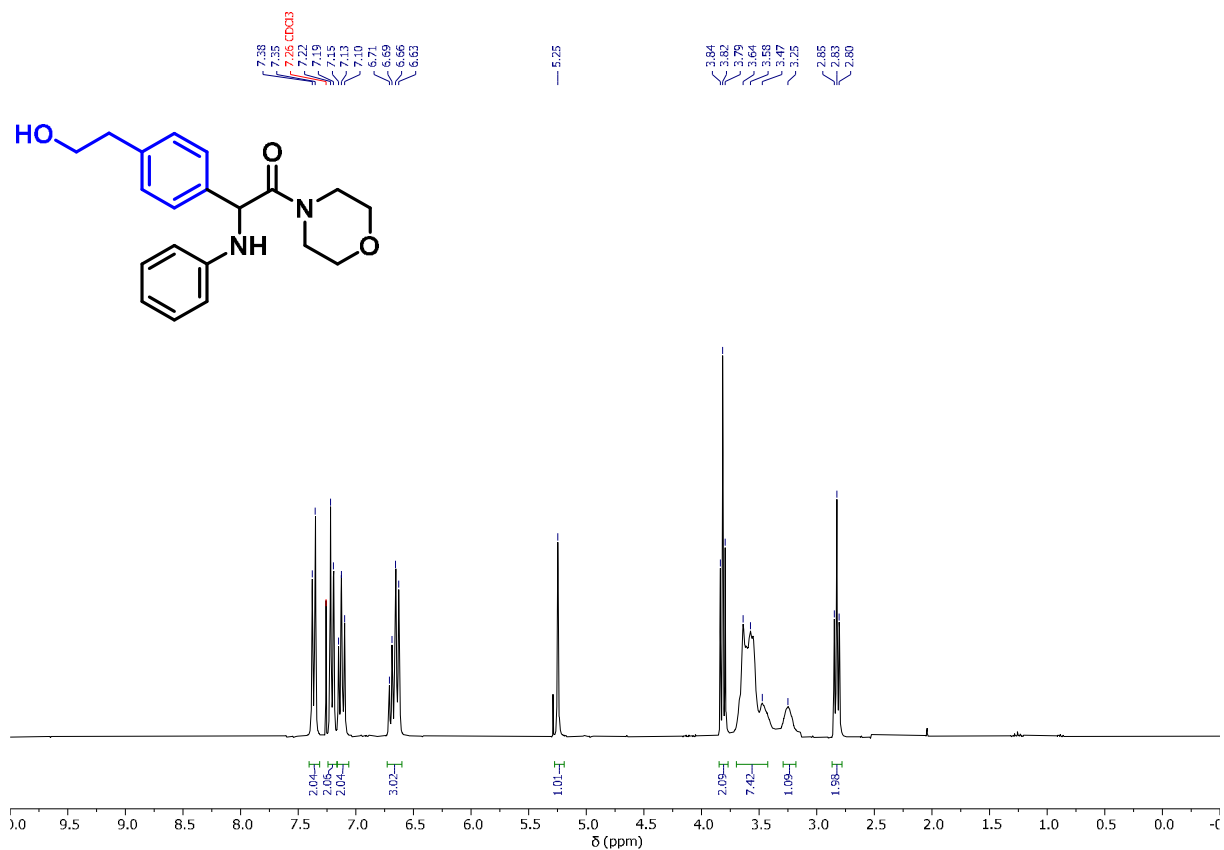




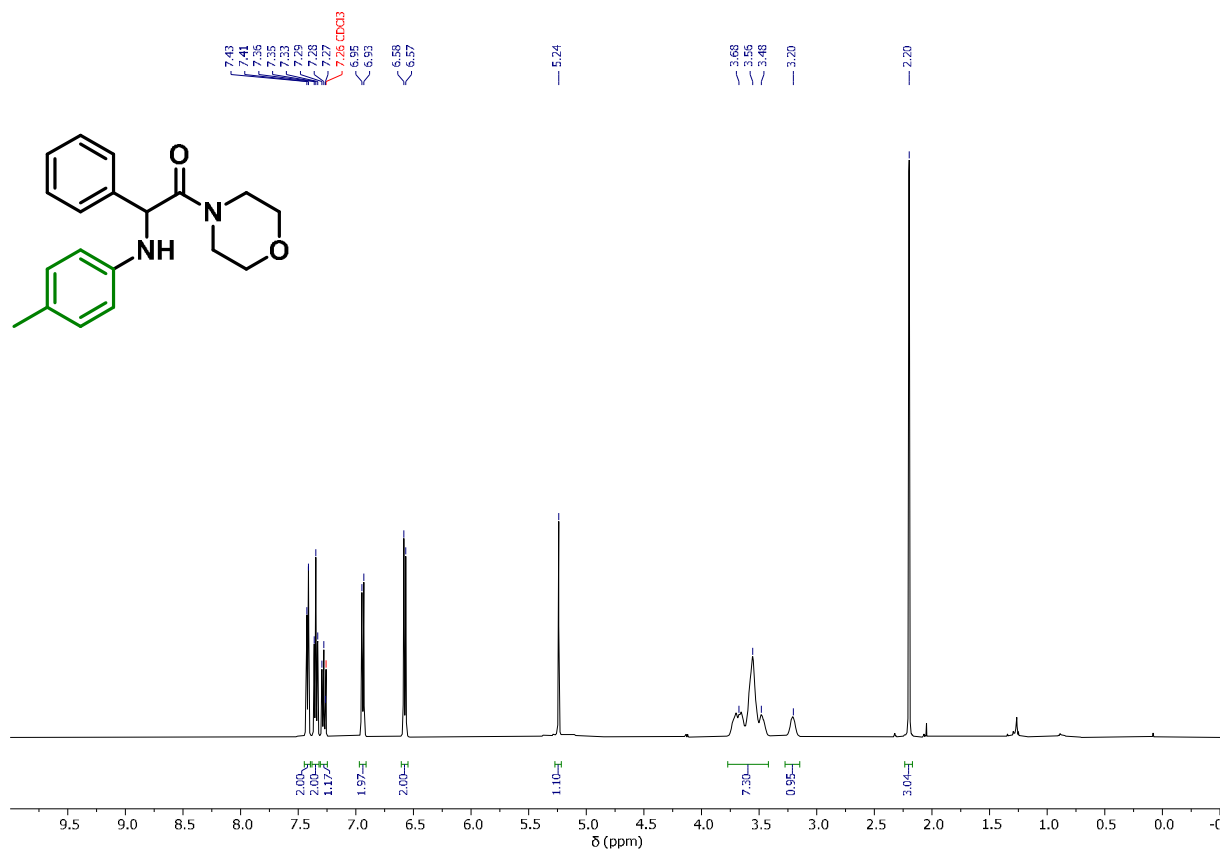
¹H NMR of 2-cyclohexyl-1-morpholino-2-(phenylamino)ethan-1-one (4g)



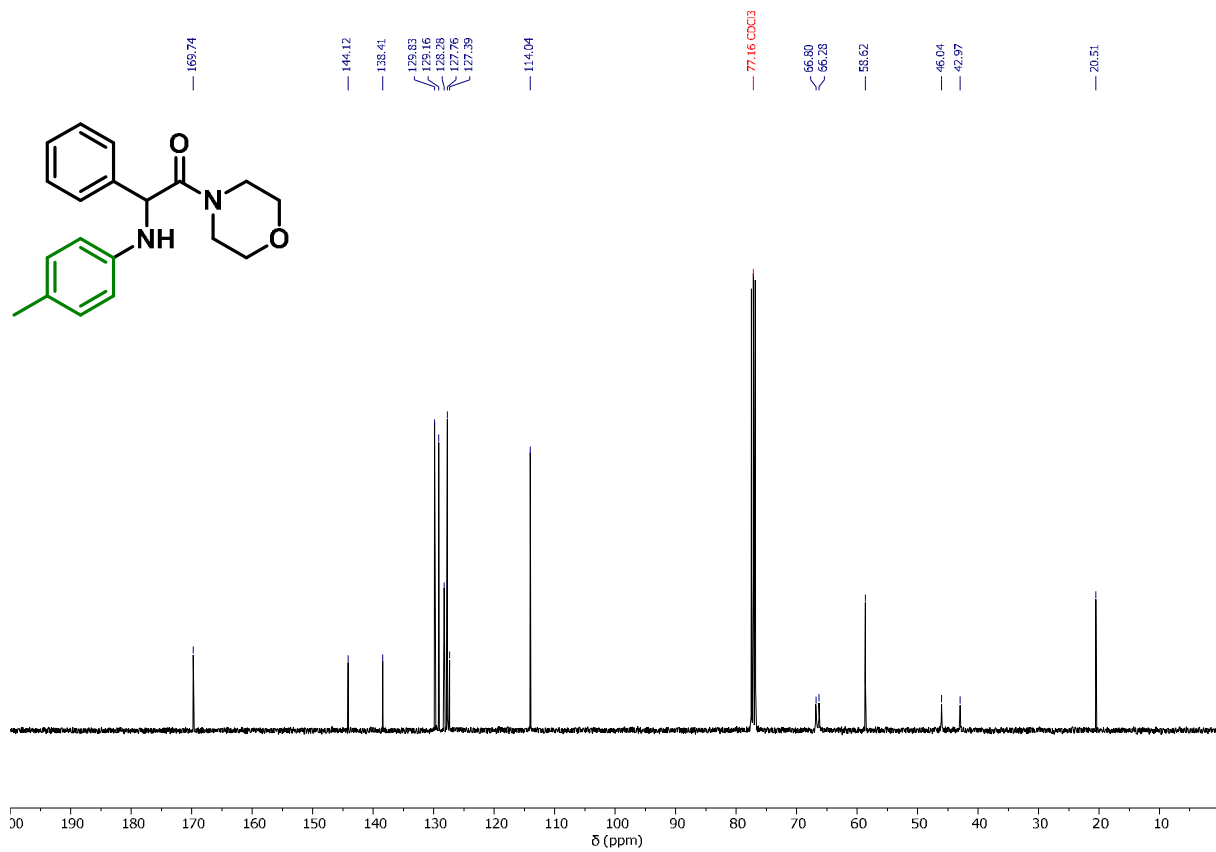
¹³C-{¹H}-NMR of 2-cyclohexyl-1-morpholino-2-(phenylamino)ethan-1-one (4g)



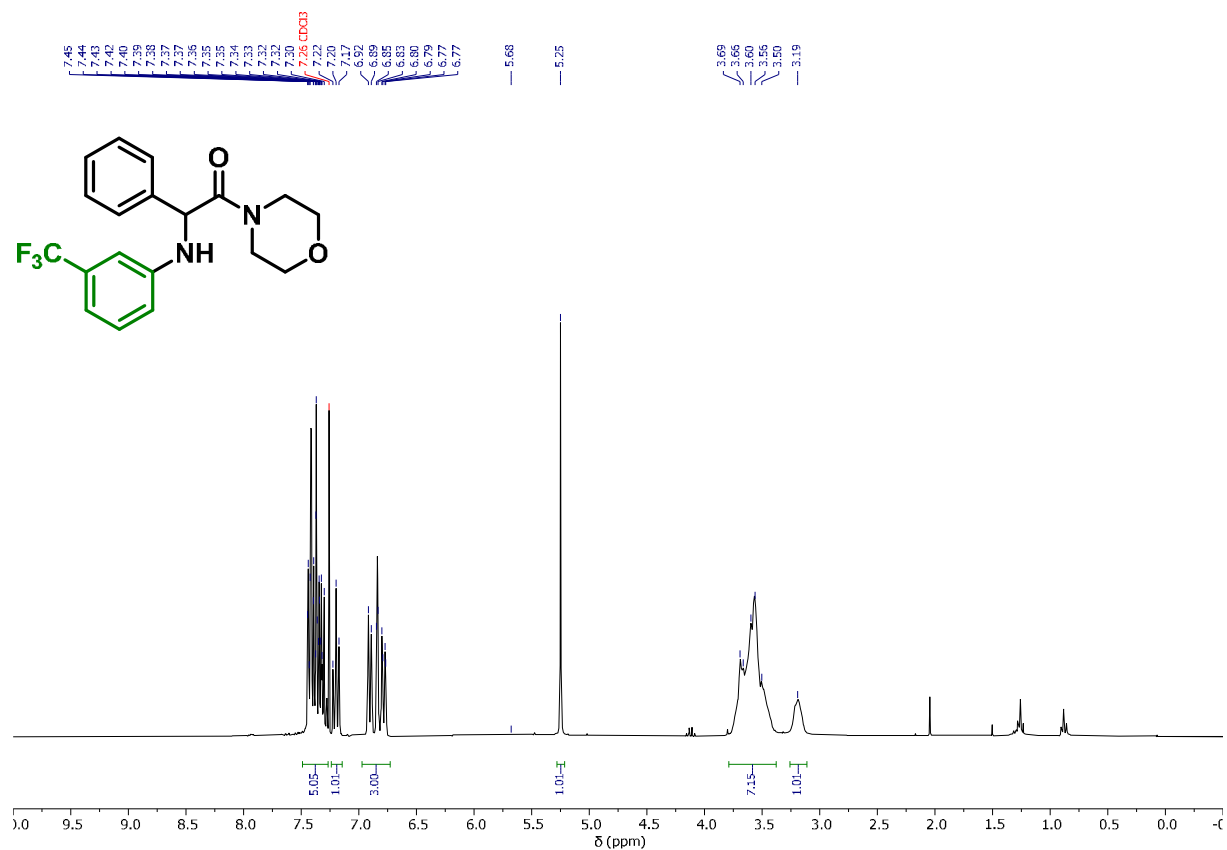
¹³C-¹H-NMR of 2-(4-(2-hydroxyethyl)phenyl)-1-morpholino-2-(phenylamino)ethan-1-one (4h).



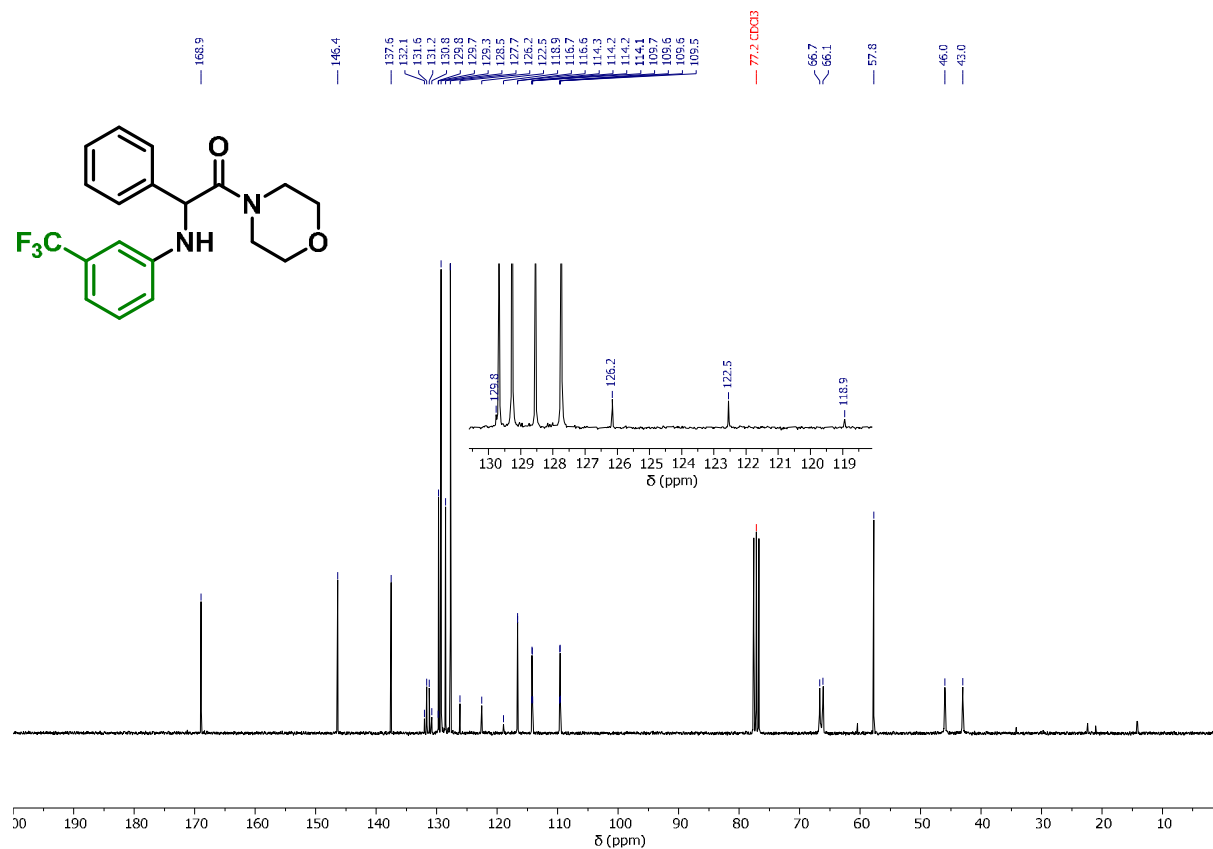
¹H-NMR of 1-morpholino-2-phenyl-2-((4-methylphenyl)amino)ethan-1-one (5a).



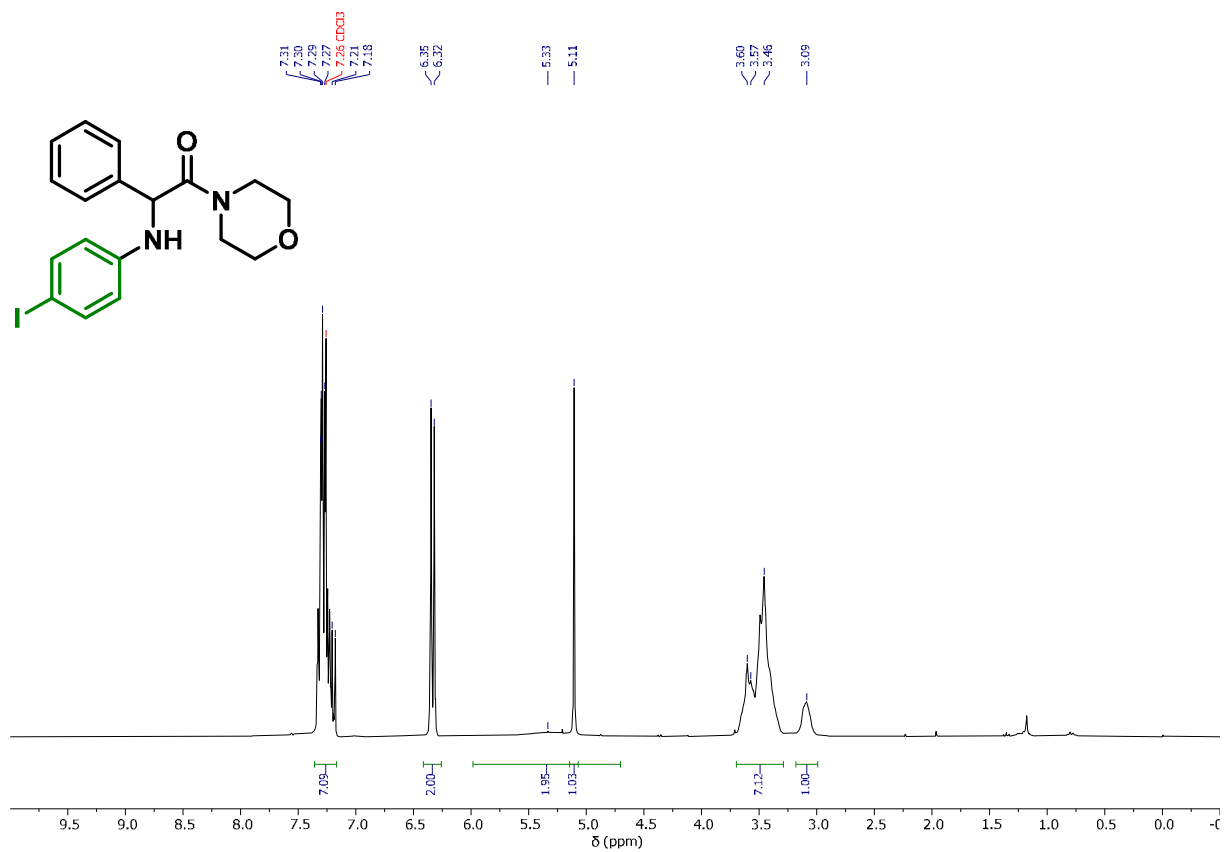
¹³C-{¹H}-NMR of 1-morpholino-2-phenyl-2-((4-methylphenyl)amino)ethan-1-one (5a).



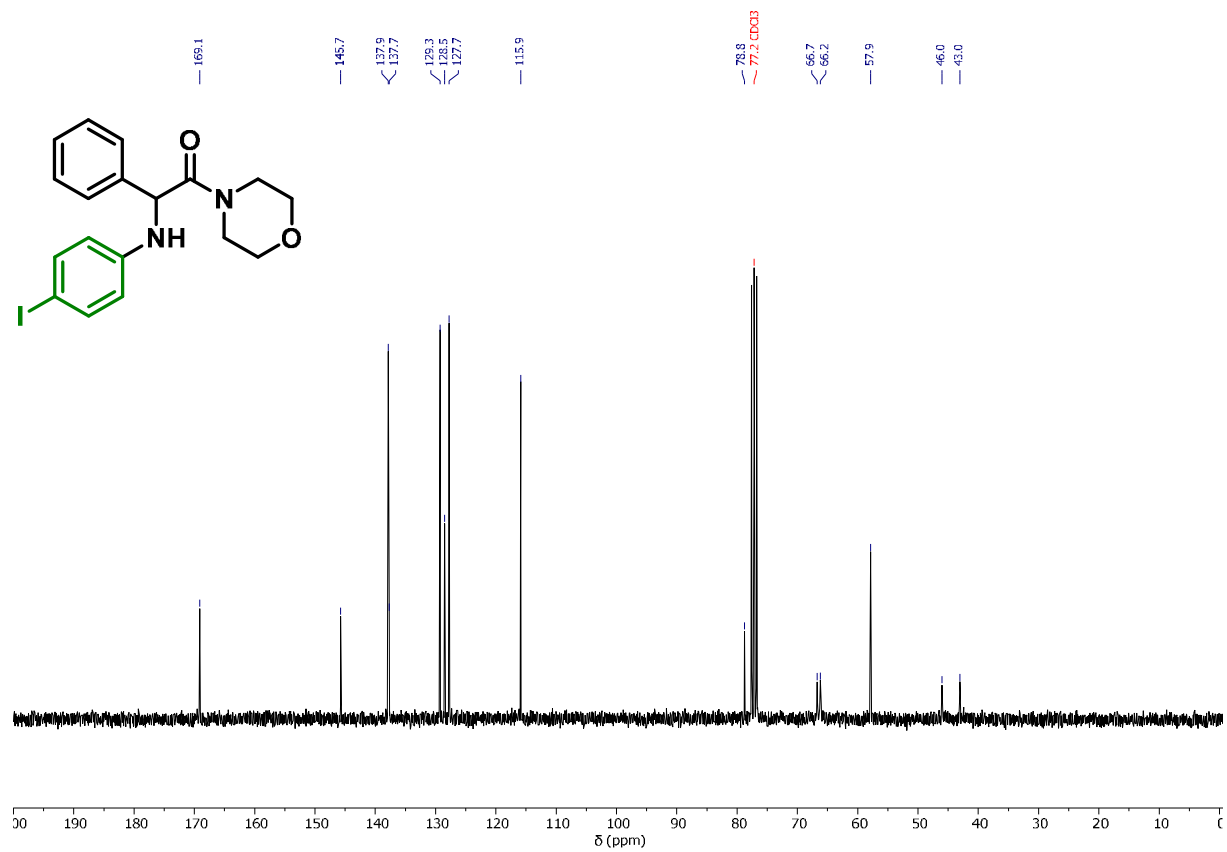
¹H-NMR of 1-morpholino-2-phenyl-2-((3-(trifluoromethyl)phenyl)amino)ethan-1-one (**5b**).



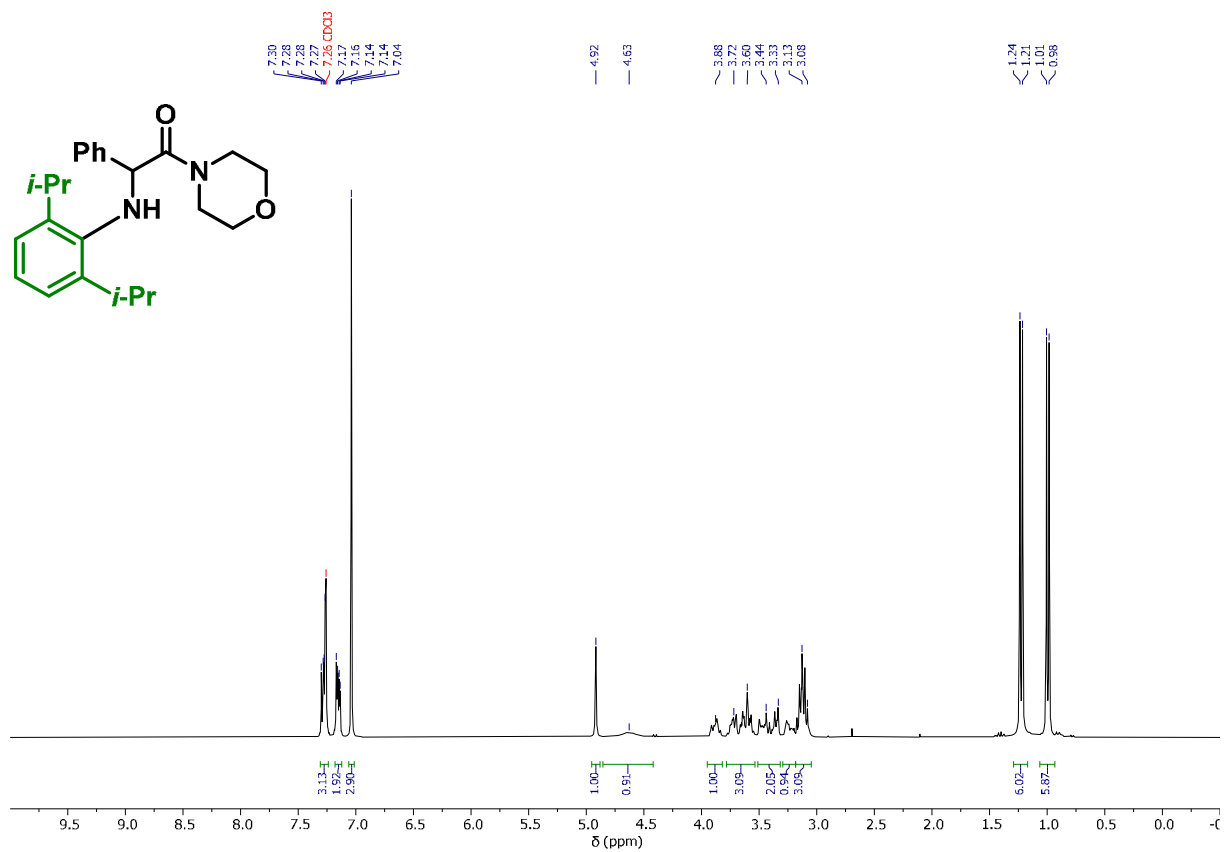
¹³C-¹H-NMR of 1-morpholino-2-phenyl-2-((3-(trifluoromethyl)phenyl)amino)ethan-1-one (**5b**).



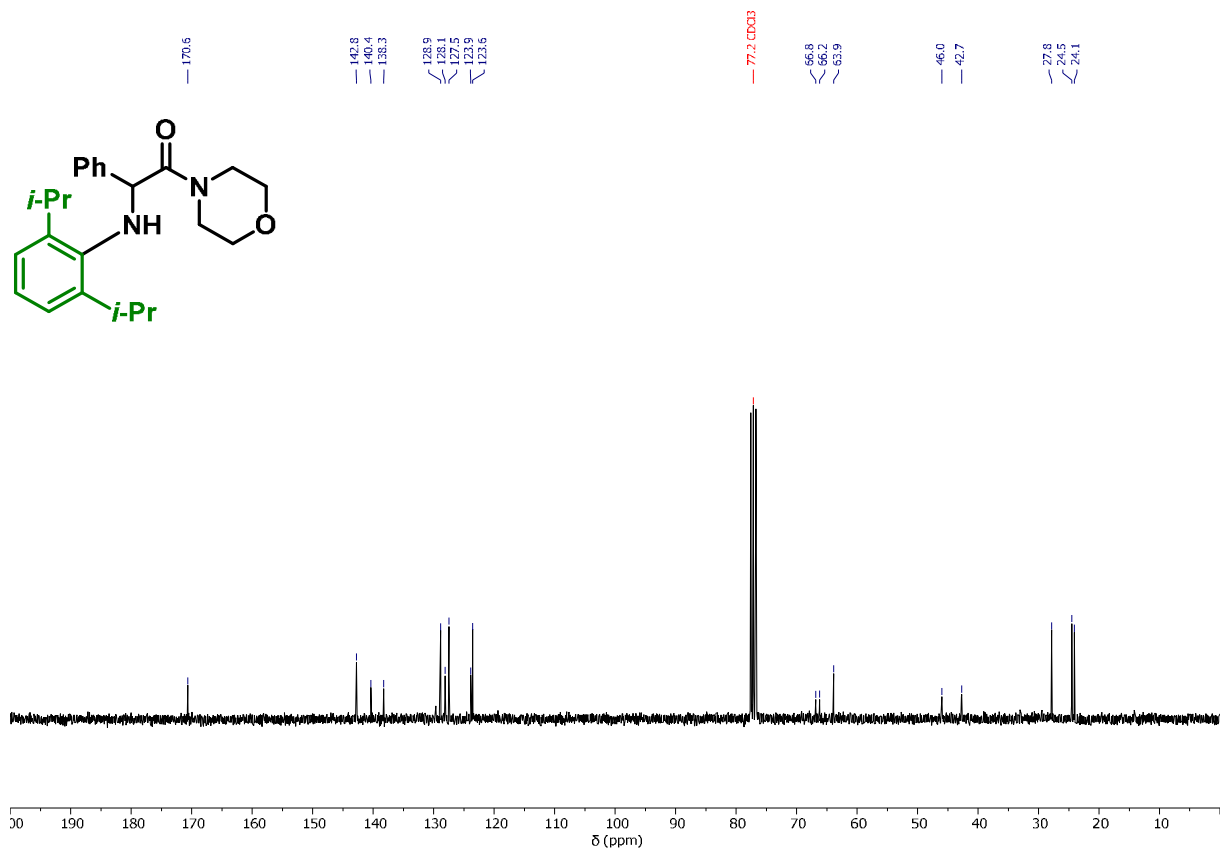
¹H-NMR of 1-morpholino-2-phenyl-2-((4-iodophenyl)amino)ethan-1-one (**5c**).



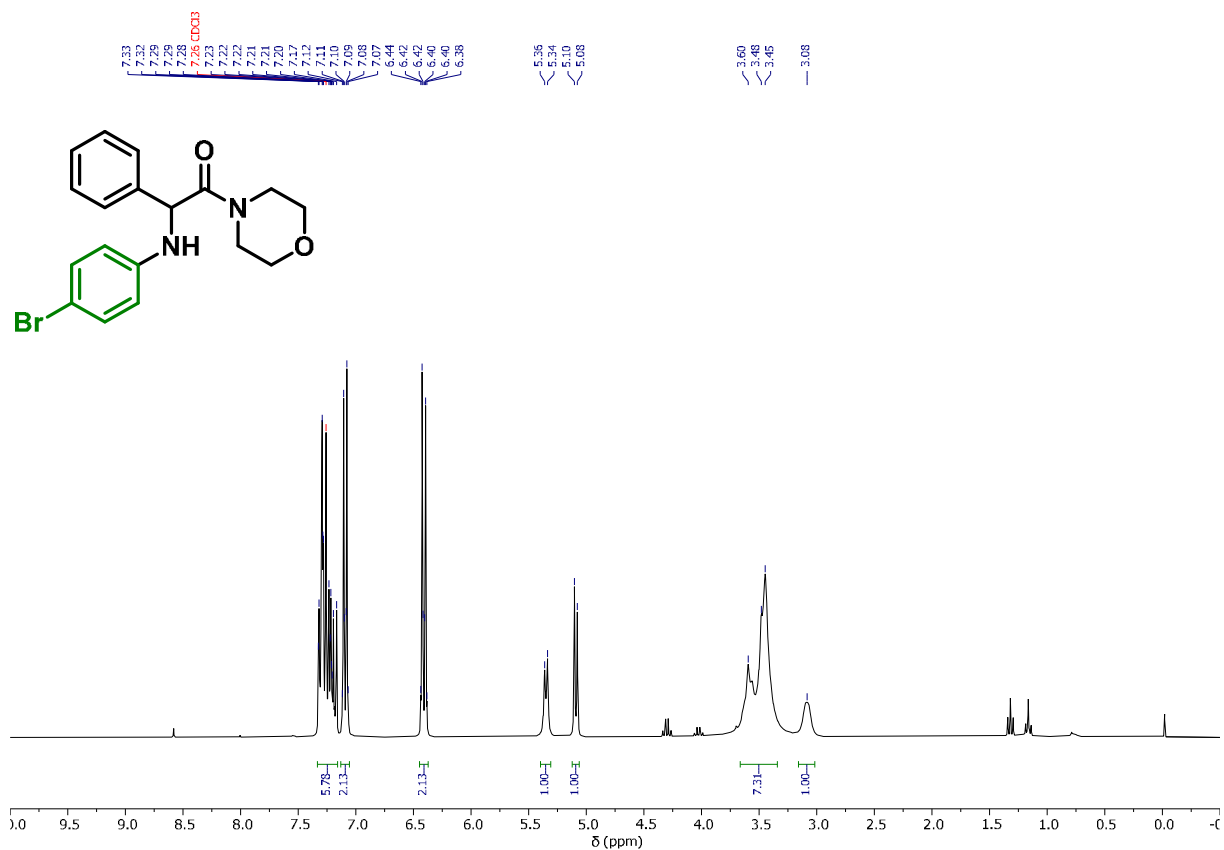
¹³C-{¹H}-NMR of 1-morpholino-2-phenyl-2-((4-iodophenyl)amino)ethan-1-one (**5c**).



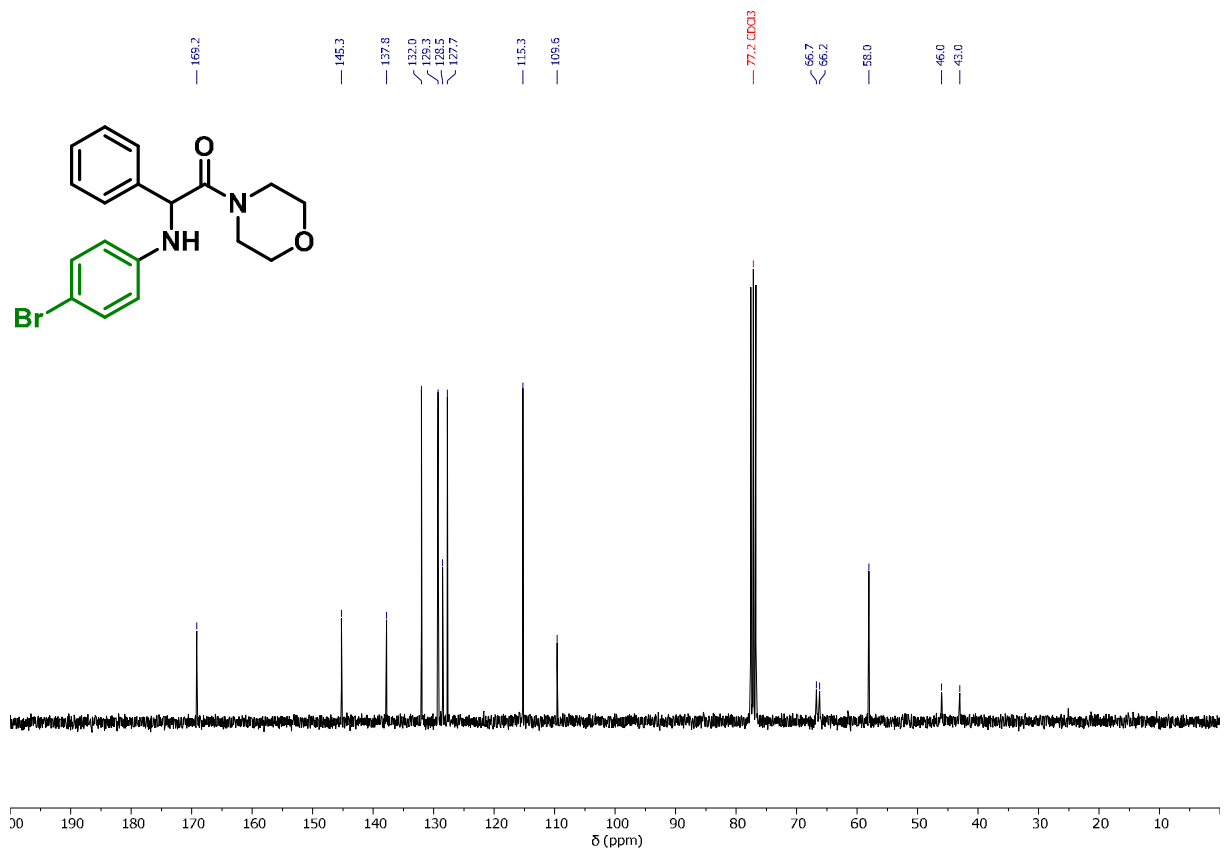
¹H-NMR of 2-((2,6-diisopropylphenyl)amino)-1-morpholino-2-phenylethan-1-one (**5d**).



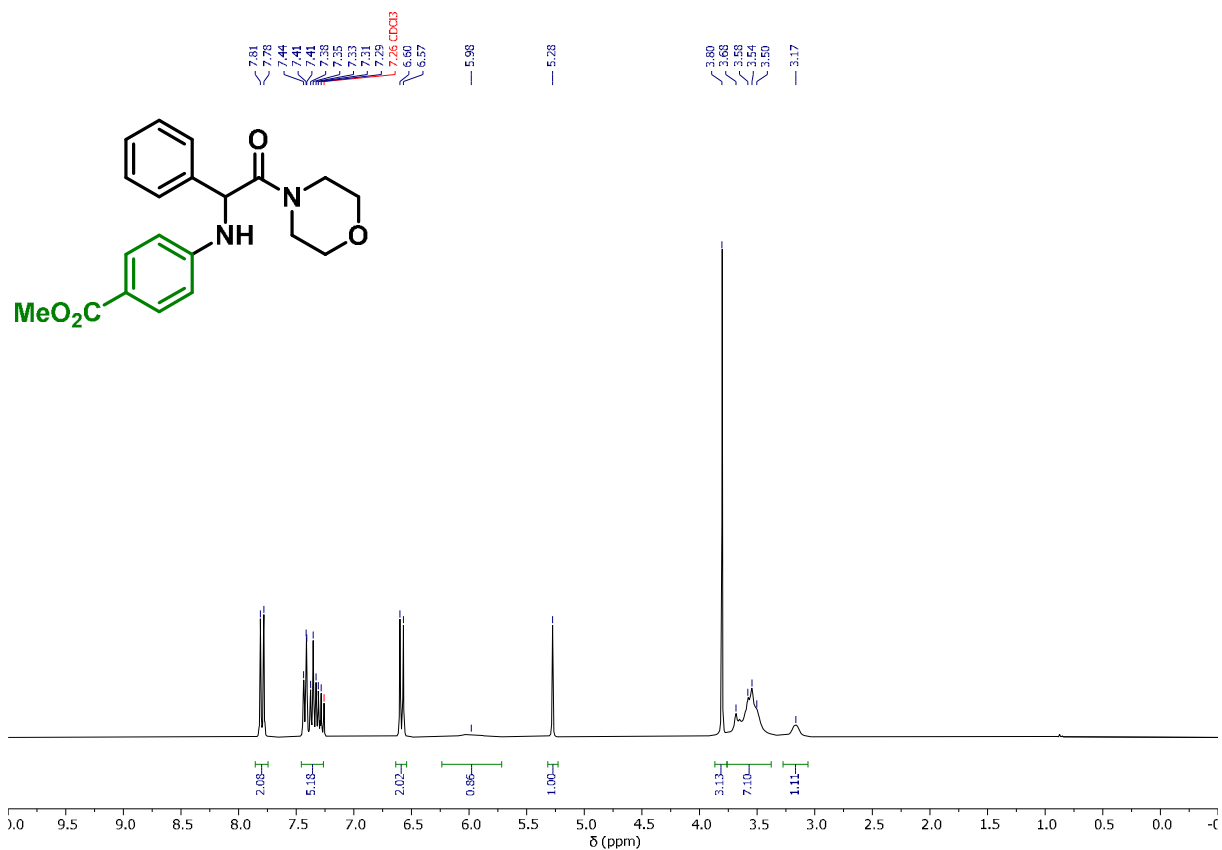
¹³C-{¹H}-NMR of 2-((2,6-diisopropylphenyl)amino)-1-morpholino-2-phenylethan-1-one (**5d**).



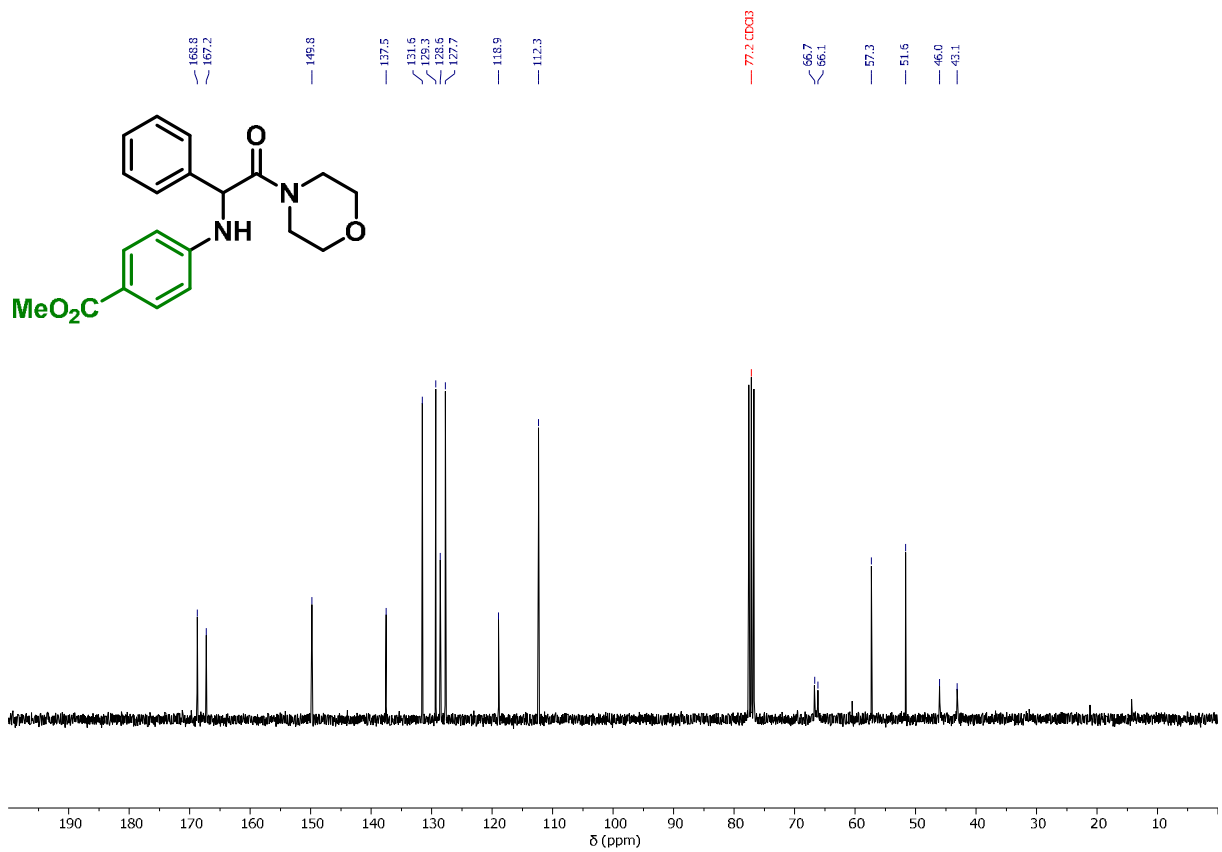
$^1\text{H-NMR}$ of 1-morpholino-2-phenyl-2-((4-bromophenyl)amino)ethan-1-one (**5e**).



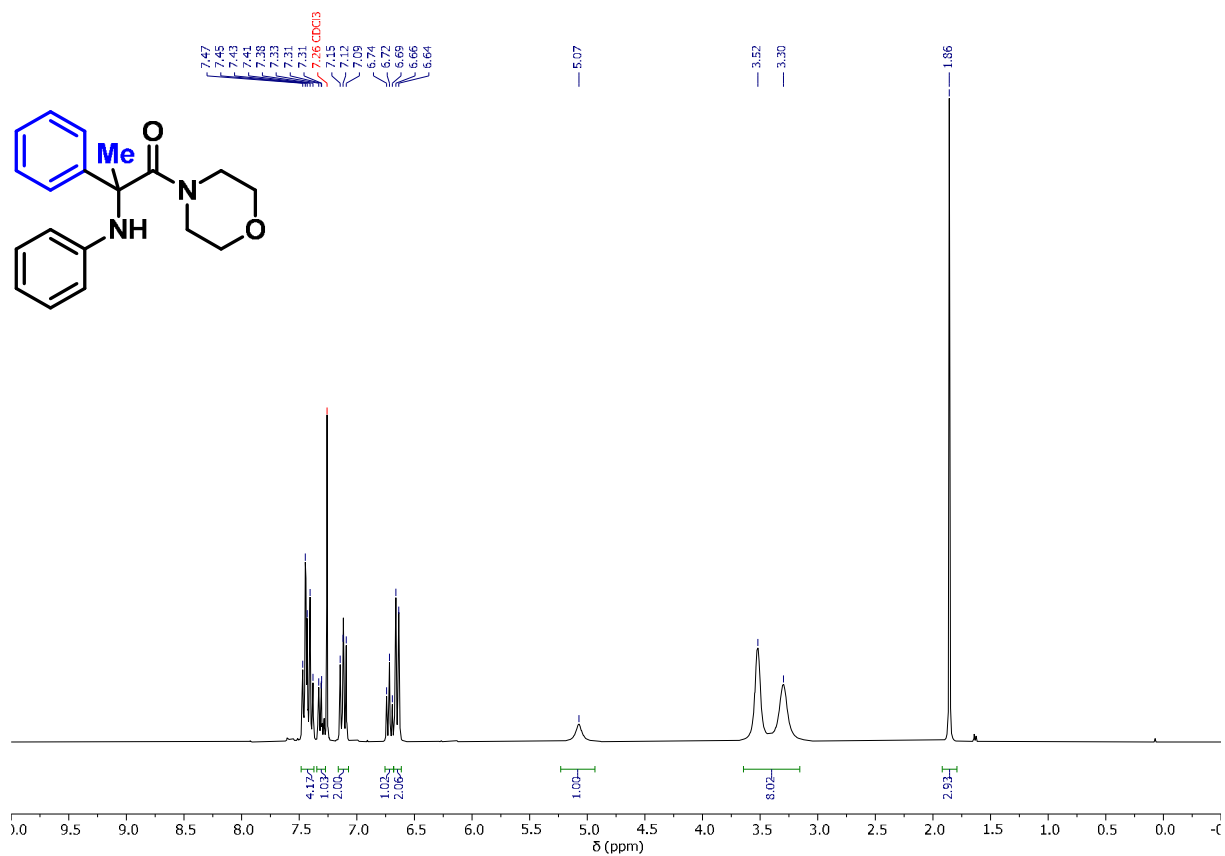
$^{13}\text{C-NMR}$ of 1-morpholino-2-phenyl-2-((4-bromophenyl)amino)ethan-1-one (**5e**).



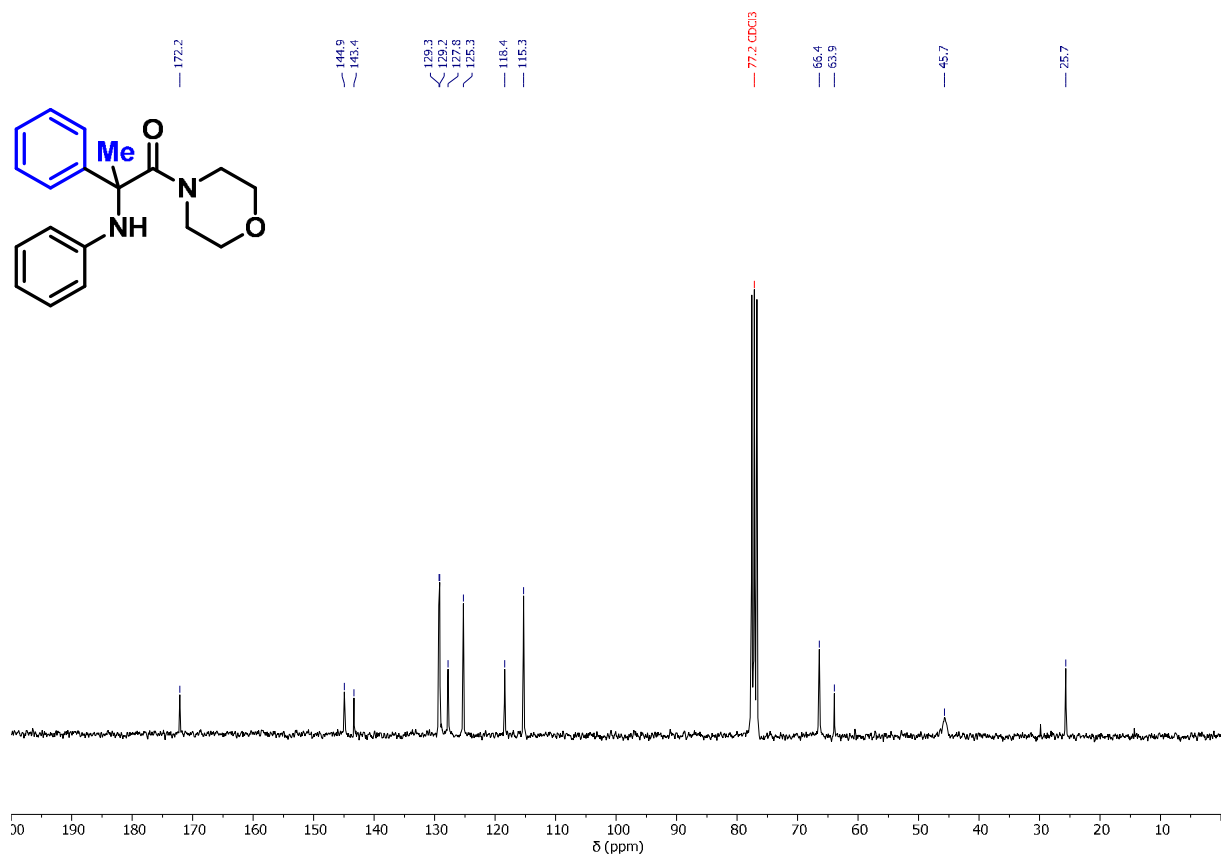
¹H-NMR of methyl 4-((2-morpholino-2-oxo-1-phenylethyl)amino)benzoate (5f).



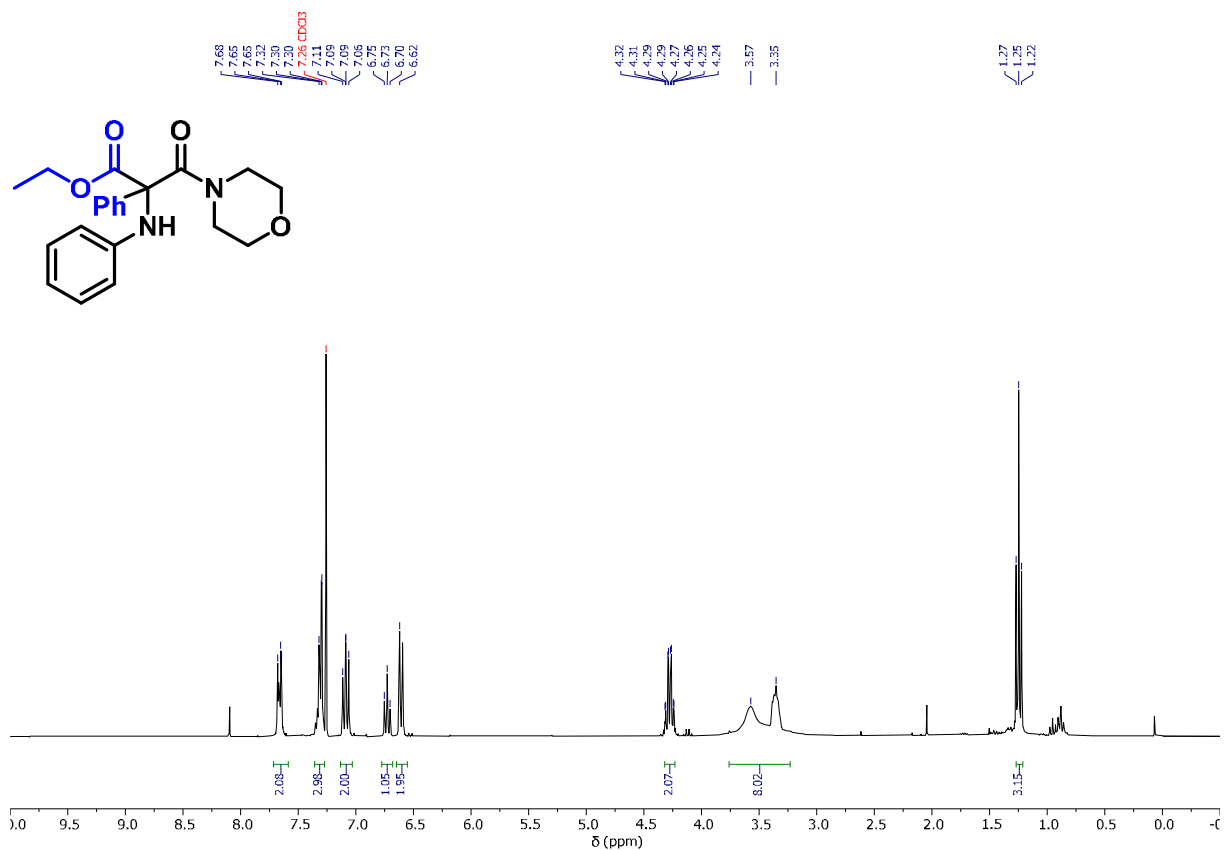
¹³C-{¹H}-NMR of methyl 4-((2-morpholino-2-oxo-1-phenylethyl)amino)benzoate (5f).



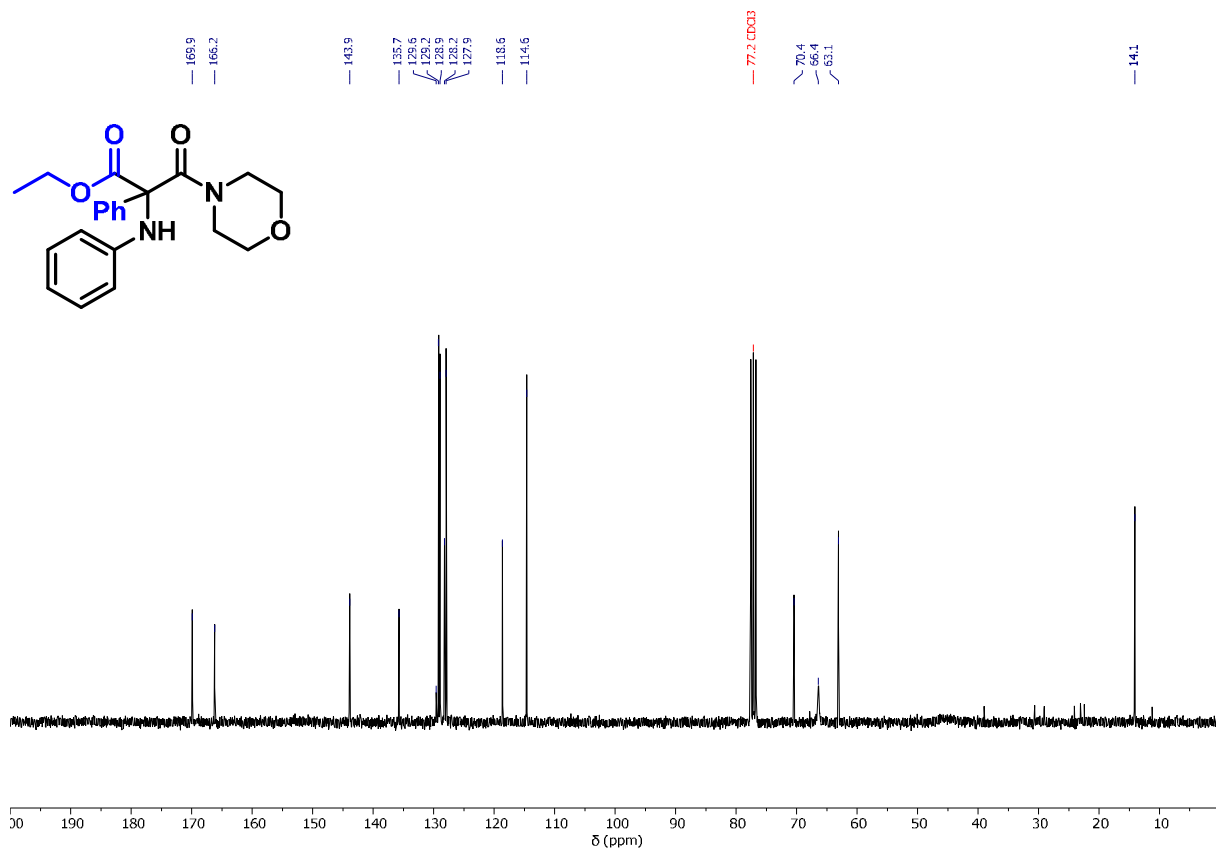
¹H-NMR of 1-morpholino-2-phenyl-2-(phenylamino)propan-1-one (**6a**).



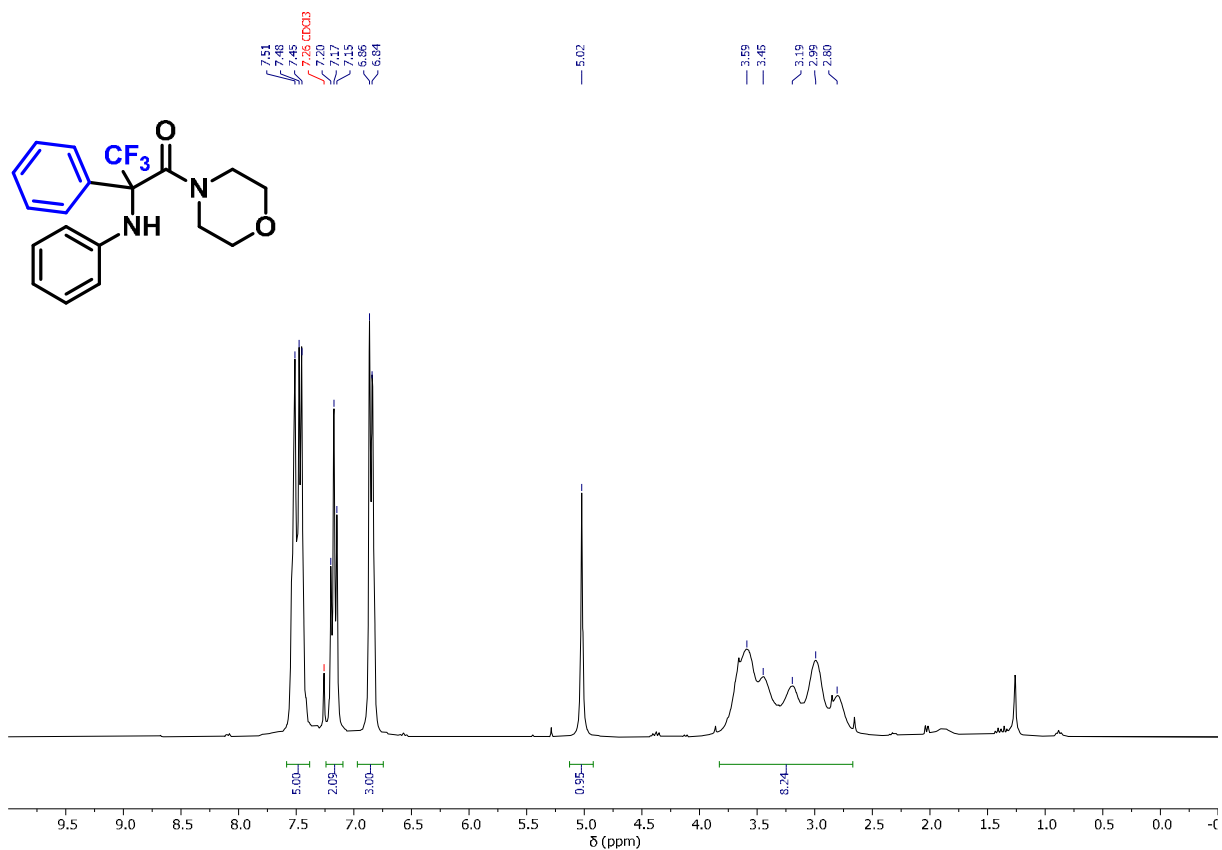
¹³C-¹H-NMR of 1-morpholino-2-phenyl-2-(phenylamino)propan-1-one (**6a**).



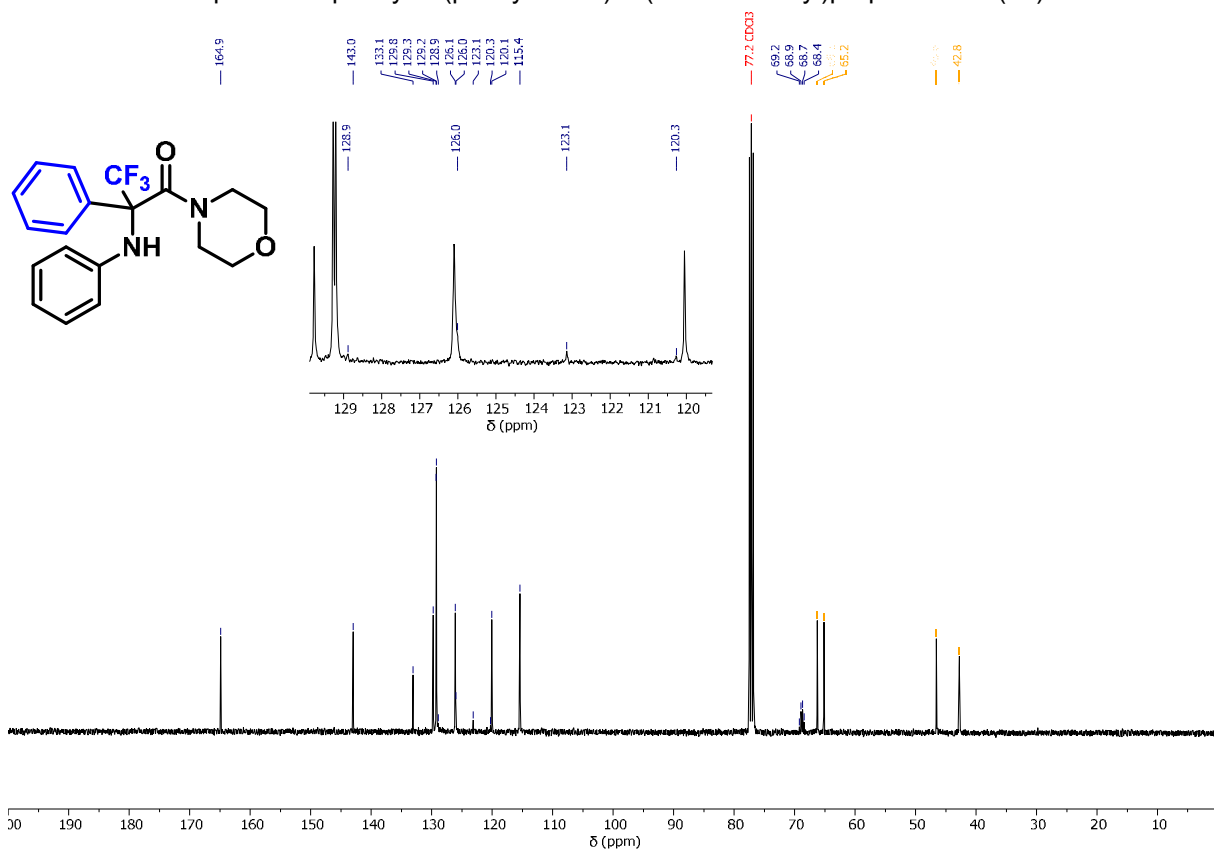
¹H-NMR of ethyl 3-morpholino-3-oxo-2-phenyl-2-(phenylamino)propanoate (6b).



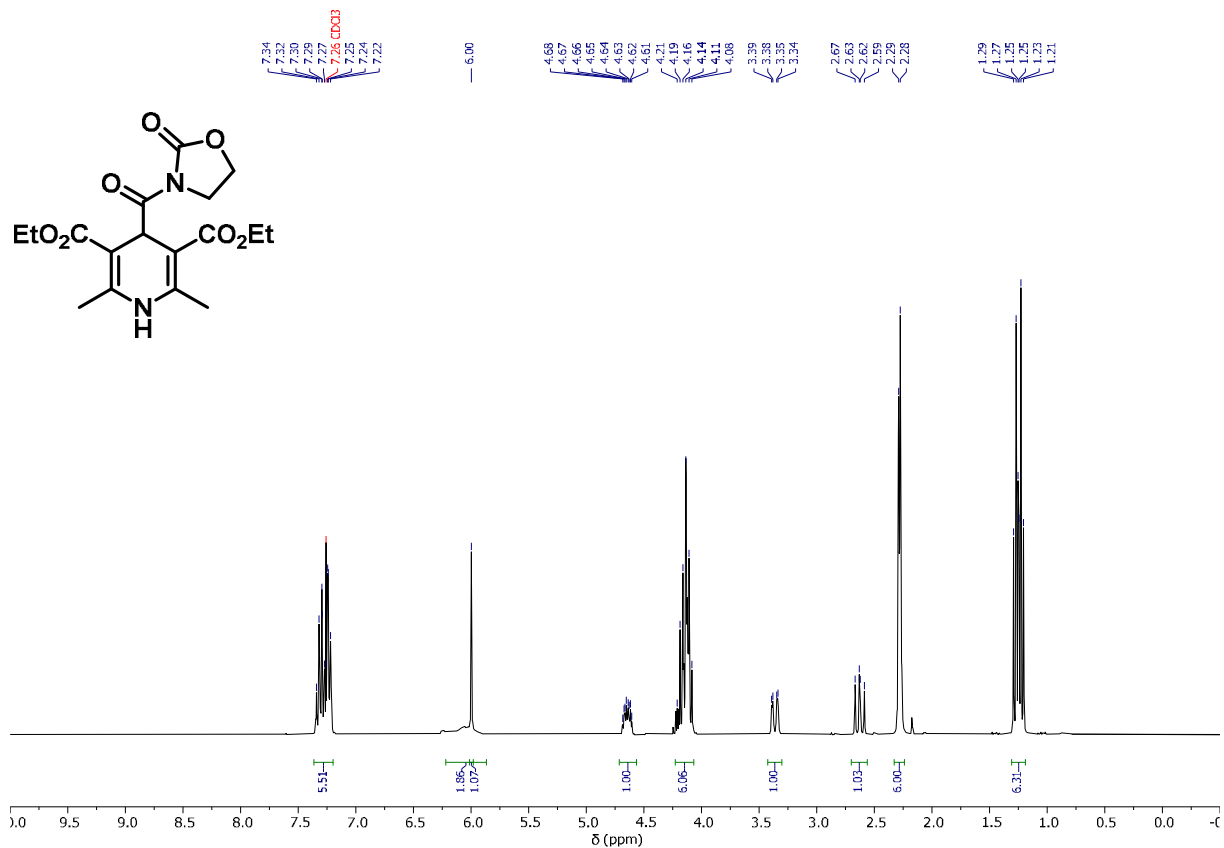
¹³C-{¹H}-NMR of ethyl 3-morpholino-3-oxo-2-phenyl-2-(phenylamino)propanoate (6b).



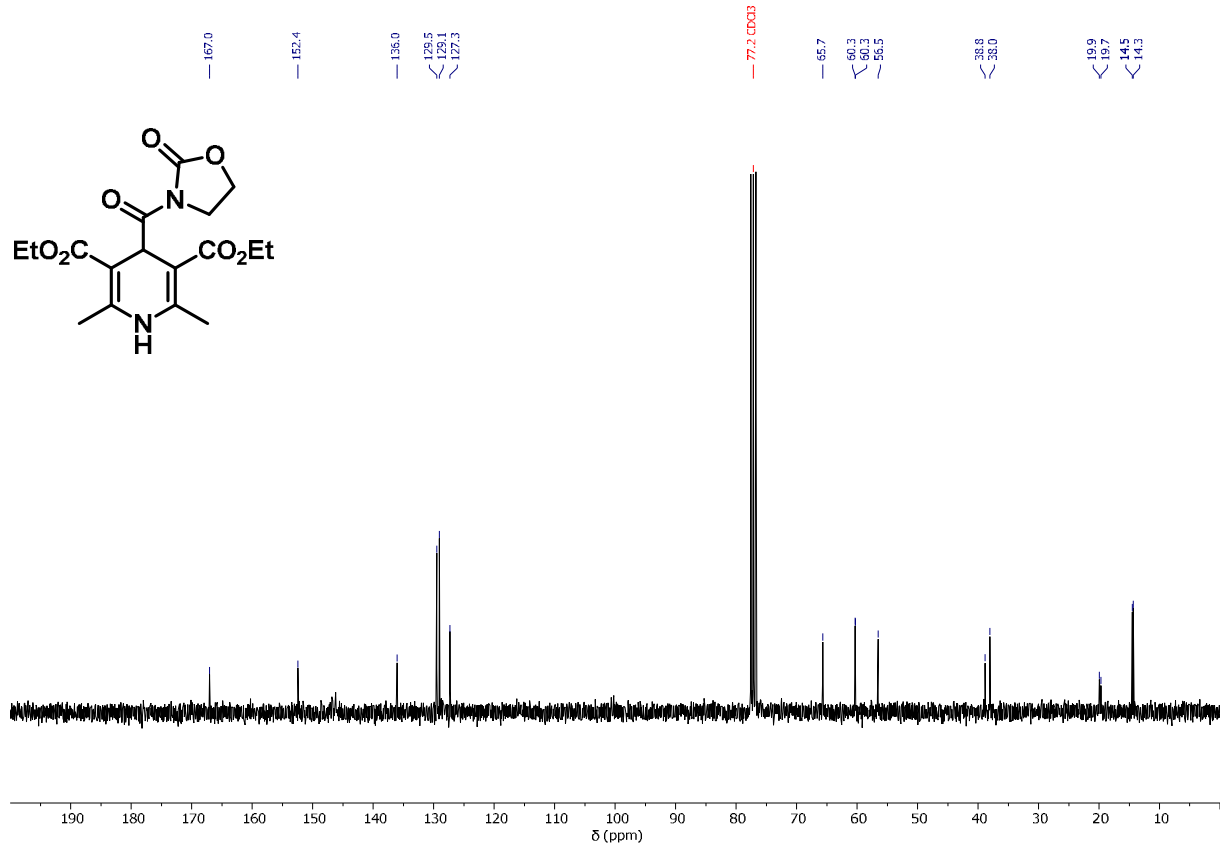
¹H-NMR of 1-morpholino-2-phenyl-2-(phenylamino)-2-(trifluoromethyl)propan-1-one (**6c**).



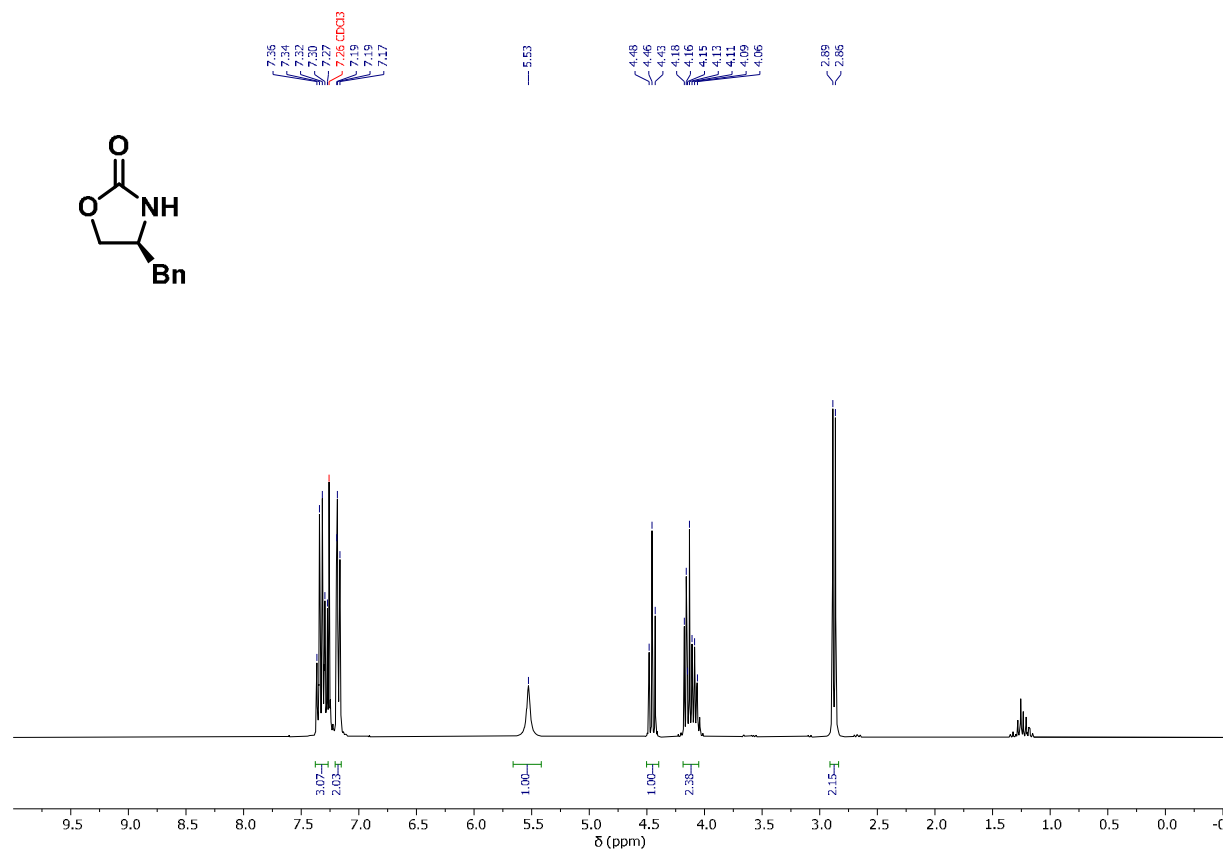
¹³C-¹H-NMR of 1-morpholino-2-phenyl-2-(phenylamino)-2-(trifluoromethyl)propan-1-one (**6c**) at –20 °C. The signals labeled in yellow are not or just barely visible at room temperature.



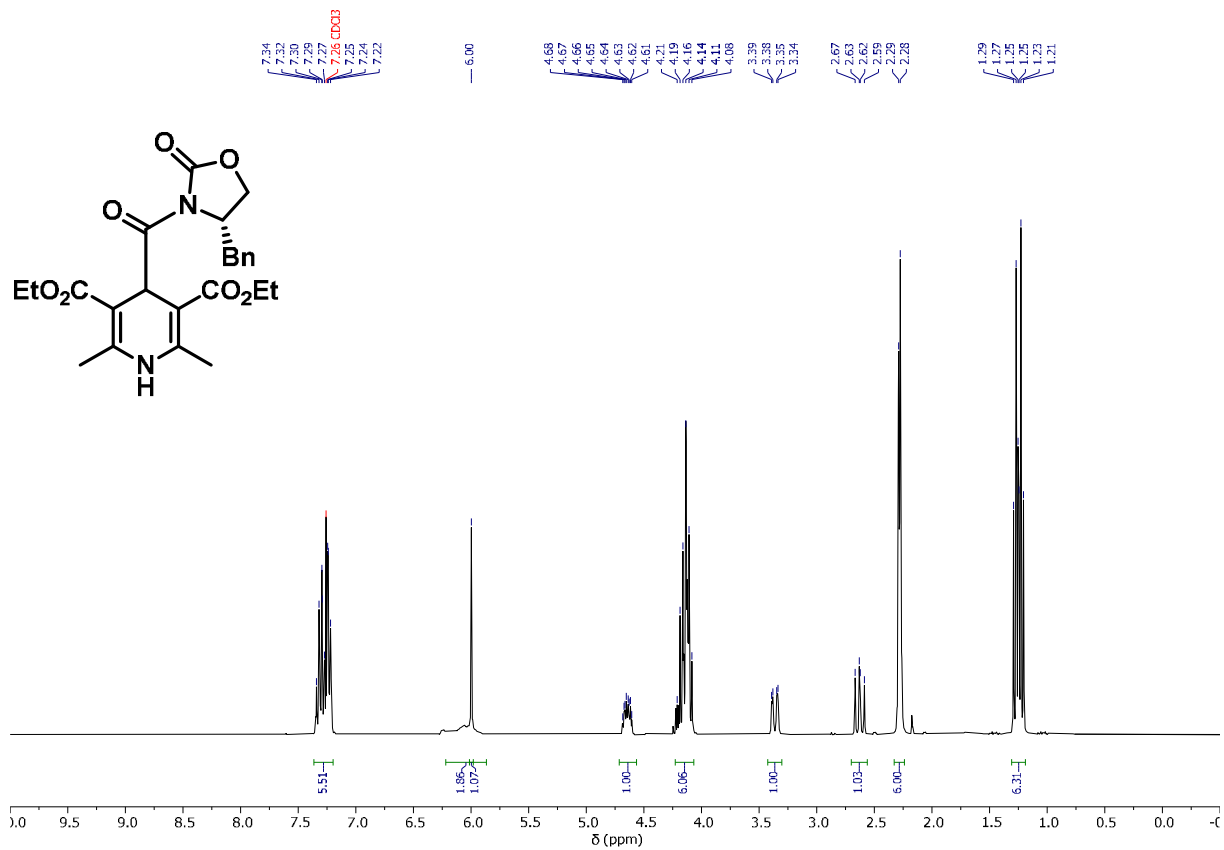
¹H-NMR of diethyl 2,6-dimethyl-4-(2-oxooxazolidine-3-carbonyl)-1,4-dihydropyridine-3,5-dicarboxylate.



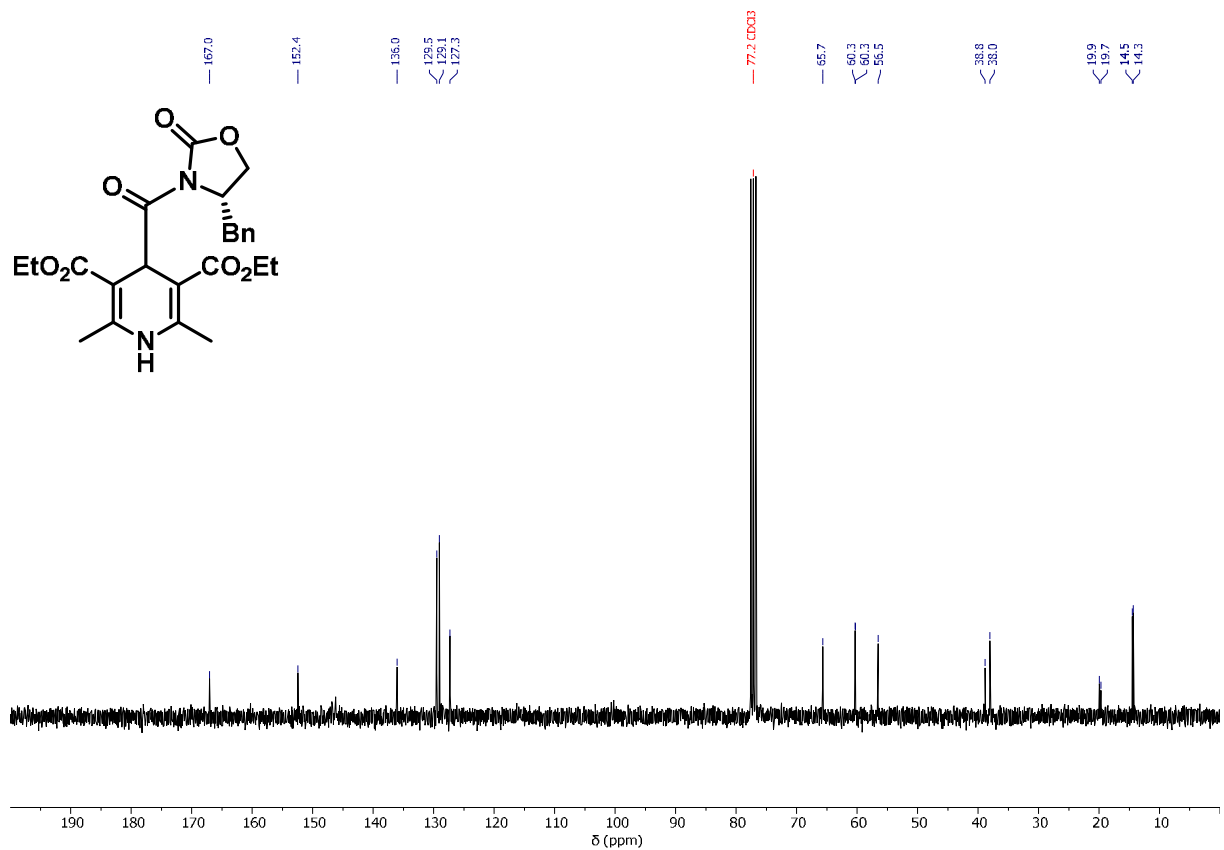
¹³C-NMR of diethyl 2,6-dimethyl-4-(2-oxooxazolidine-3-carbonyl)-1,4-dihydropyridine-3,5-dicarboxylate.



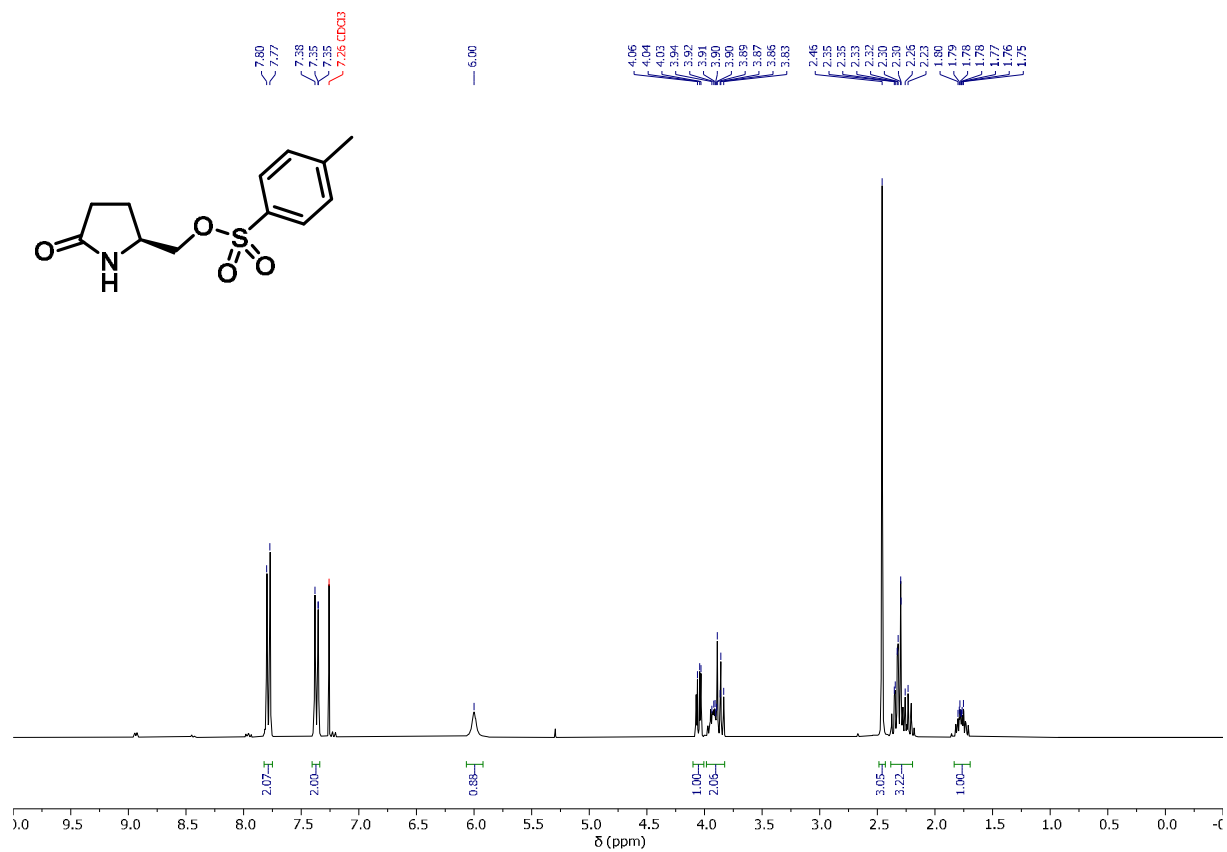
¹H-NMR of (S)-4-benzyl-2-oxazolidinone.



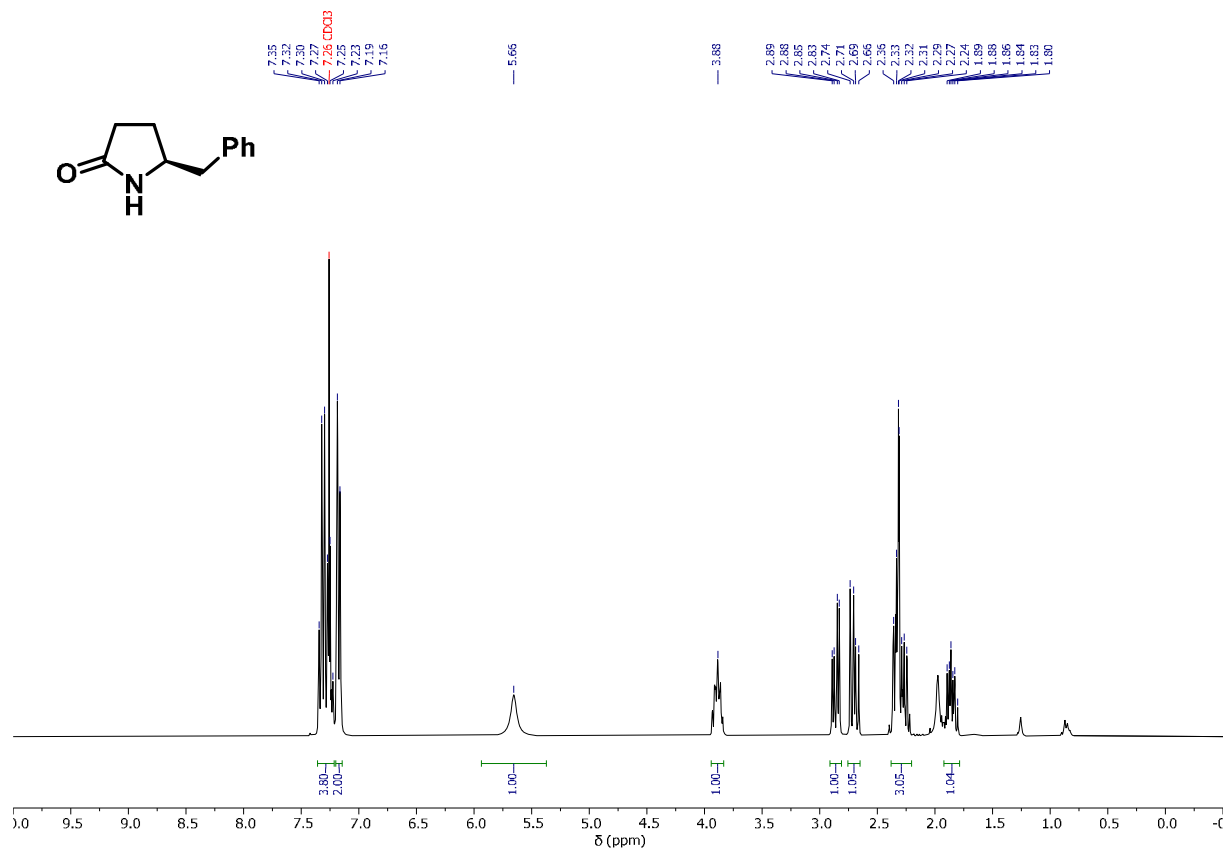
¹H-NMR of diethyl (S)-4-(4-benzyl-2-oxooxazolidine-3-carbonyl)-2,6-dimethyl-1,4-dihydropyridine-3,5-dicarboxylate.



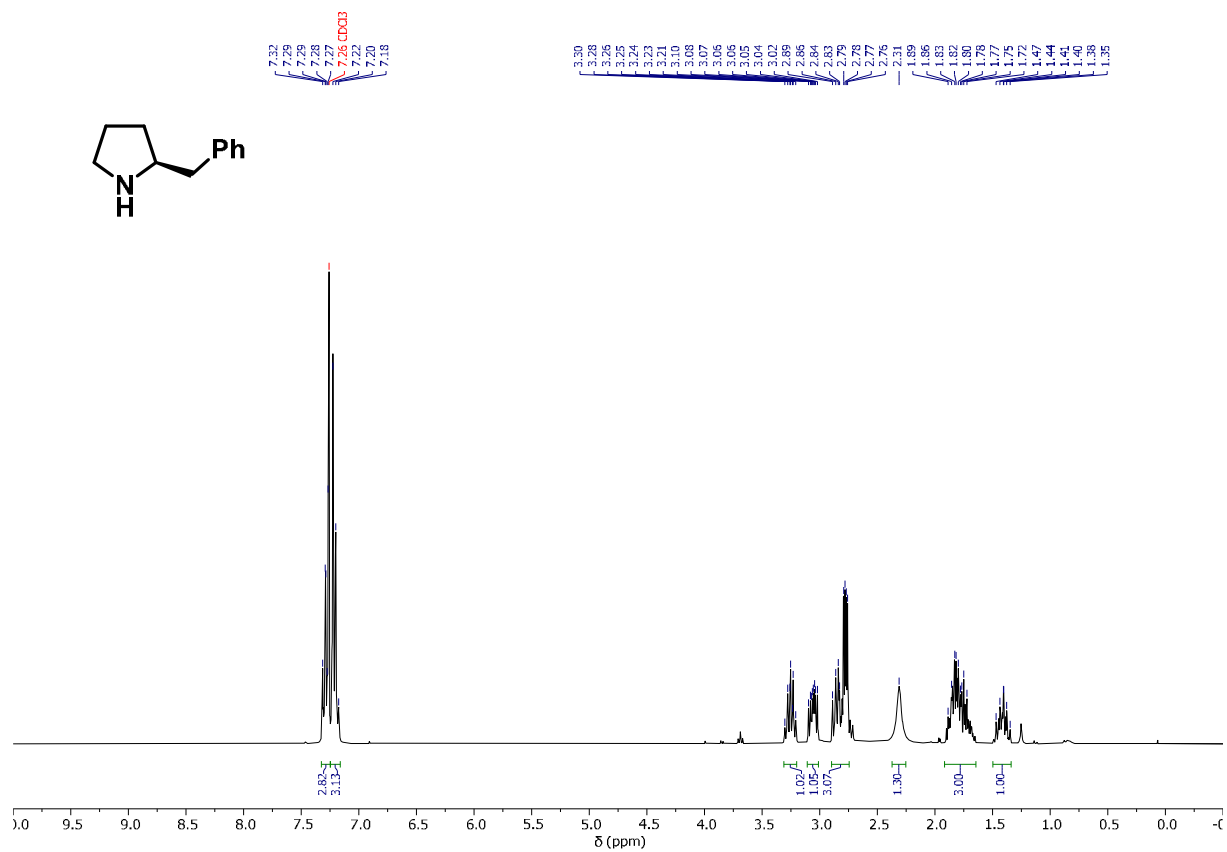
¹³C-¹H-NMR of diethyl (S)-4-(4-benzyl-2-oxooxazolidine-3-carbonyl)-2,6-dimethyl-1,4-dihydropyridine-3,5-dicarboxylate.



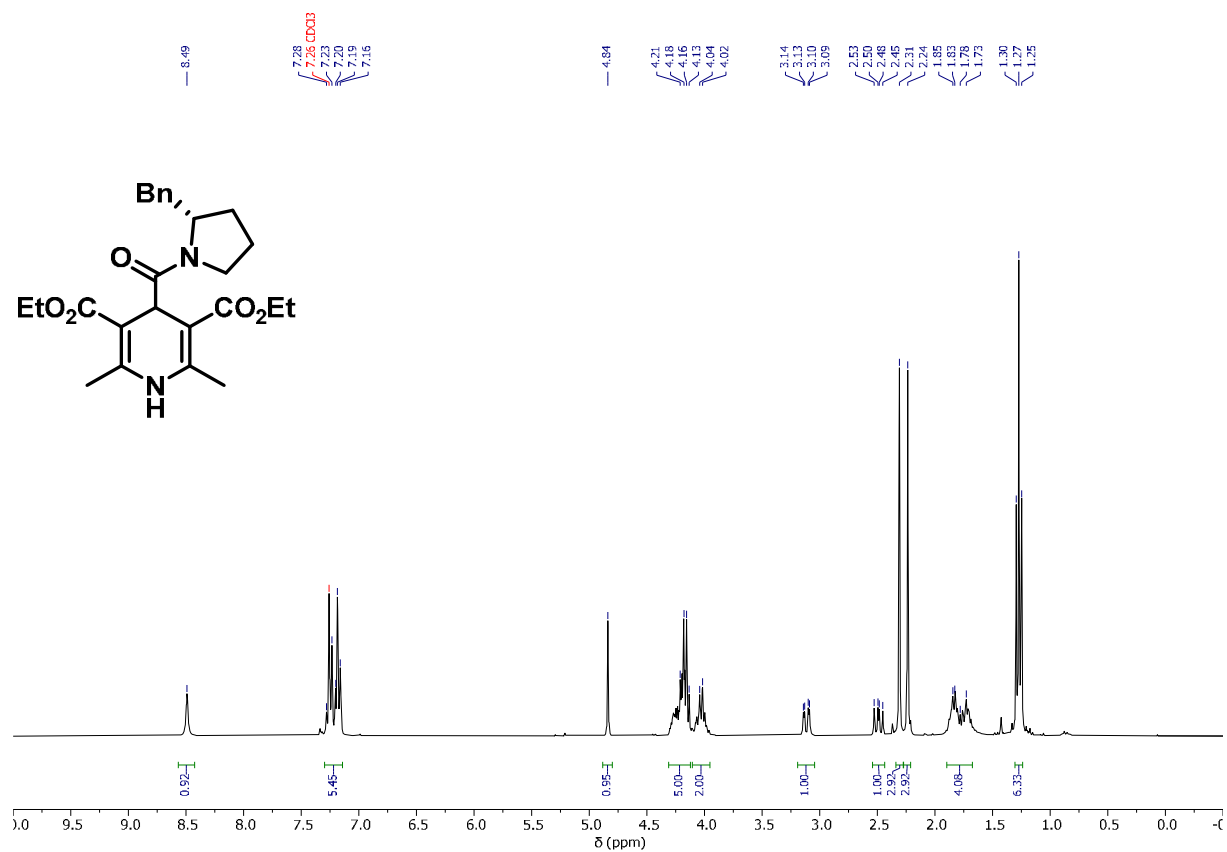
¹H-NMR of (S)-(5-oxopyrrolidin-2-yl)methyl 4-toluenesulfonate.



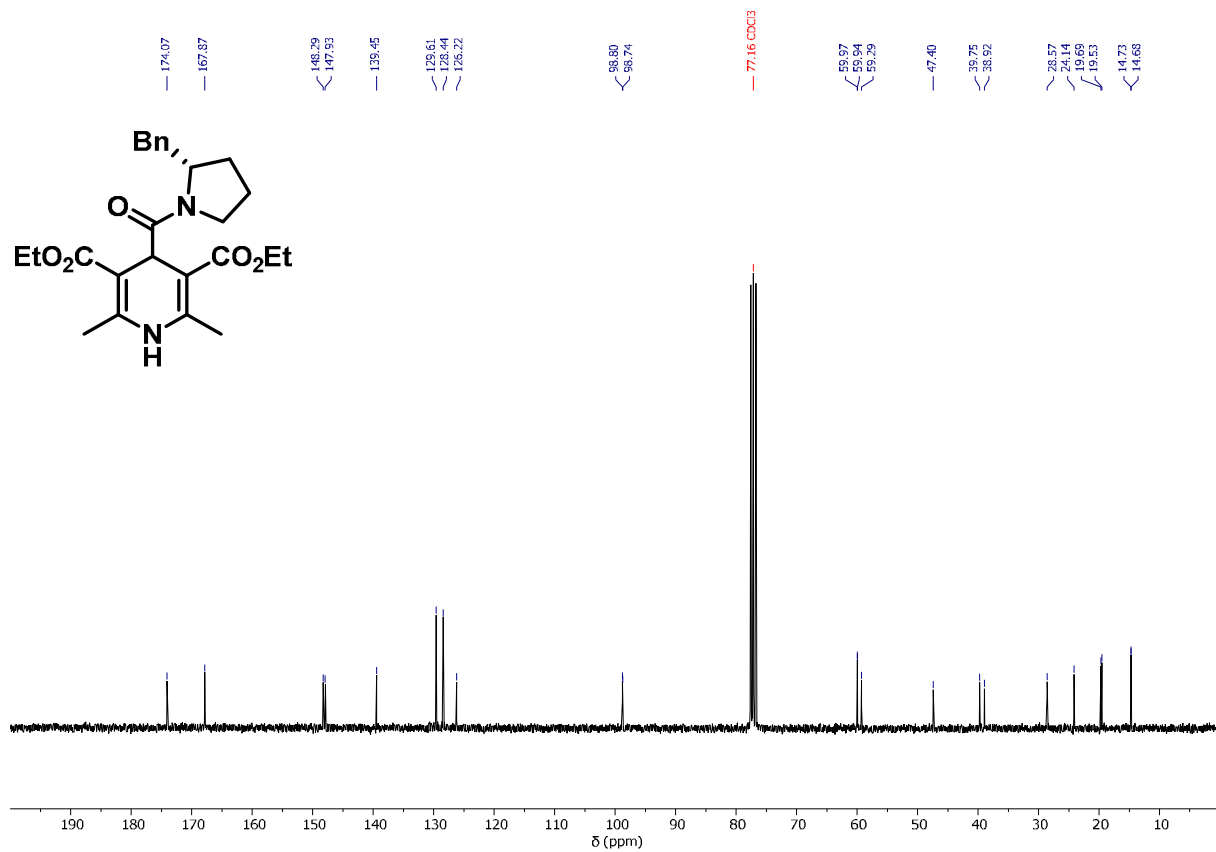
¹H-NMR of (S)-5-benzyl-2-pyrrolidinone.



$^1\text{H-NMR}$ of (S)-2-benzylpyrrolidine.



$^1\text{H-NMR}$ of Diethyl (S)-4-(2-benzylpyrrolidine-1-carbonyl)-2,6-dimethyl-1,4-dihydropyridine-3,5-dicarboxylate.



^{13}C - $\{^1\text{H}\}$ -NMR of Diethyl (S)-4-(2-benzylpyrrolidine-1-carbonyl)-2,6-dimethyl-1,4-dihydropyridine-3,5-dicarboxylate.

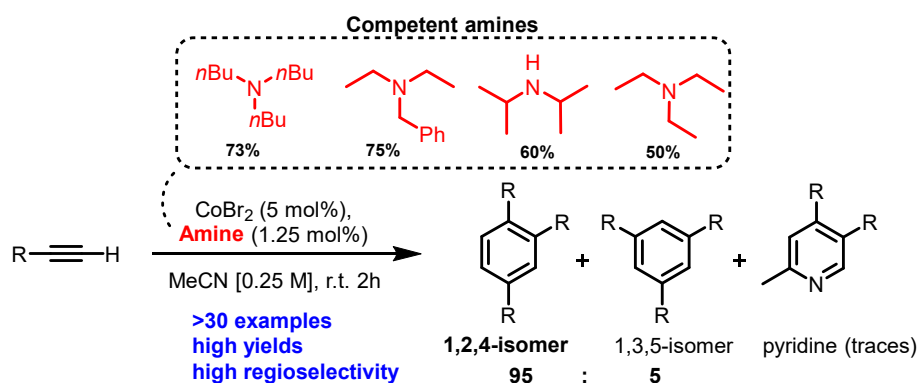
5.5 References

1. a) Greenberg, G. *The Amide Linkage: Selected Structural Aspects in Chemistry, Biochemistry, and Materials Science* (Wiley-Interscience, **2000**); b) Soloshonok, V. A.; Izawa, K. *Asymmetric Synthesis and Application of α -Amino Acids* (Oxford University Press: Washington, DC, **2009**); c) Blaskovich, M. A. *Handbook on Syntheses of Amino Acids: General Routes for the Syntheses of Amino Acids* (Oxford University Press: Oxford; New York, **2010**).
2. a) Krauch, H.; Kunz, H., *Reaktionen der Organischen Chemie*, 6. Aufl.; Hüthig: Heidelberg, (**1997**), S.22–23; b) Rogers, S. A.; Bero, J. D.; Melander, C. *Chemical Synthesis and Biological Screening of 2-Aminoimidazole-Based Bacterial and Fungal Antibiofilm Agents*. *Chem. Bio. Chem.* **2010**, *11*, 396–410; c) Smith, A. M. R.; Hii, K. K. *Transition Metal Catalyzed Enantioselective α -Heterofunctionalization of Carbonyl Compounds*. *Chem. Rev.* **2011**, *111*, 1637–1656; d) Tona, V.; de la Torre, A.; Padmanaban, M.; Ruider, S.; González, L.; Maulide, N. *Chemo- and Stereoselective Transition-Metal-Free Amination of Amides with Azides*. *J. Am. Chem. Soc.* **2016**, *138*, 8348–8351.
3. a) Pattabiraman, V. R.; Bode, J. W. *Rethinking Amide Bond Synthesis*. *Nature* **2011**, *480*, 471–479; b) Marcia de Figueiredo, R.; Suppo, J.-S.; Campagne, J.-M. *Nonclassical Routes for Amide Bond Formation*. *Chem. Rev.* **2016**, *116*, 12029–12122; c) Wang, J.; Liu, X.; Feng, X. *Asymmetric Strecker Reactions*. *Chem. Rev.* **2011**, *111* (11), 6947–6983.
4. a) Ngouansavanh, T.; Zhu, J. P. *IBX-Mediated Oxidative Ugi-Type Multicomponent Reactions: Application to the N and C1 functionalization of Tetrahydroisoquinoline*. *Angew. Chem. Int. Ed.* **2007**, *46*, 5775–5778; b) Jiang, G. X.; Chen, J.; Huang, J. S.; Che, C. M. *Highly Efficient Oxidation of Amines to Imines by Singlet Oxygen and Its Application in Ugi-Type Reactions*. *Org. Lett.* **2009**, *11*, 4568–4571; c) Ye, X.; Xie, C.; Pan, Y.; Han, L.; Xie, T. *Copper-Catalyzed Synthesis of α -Amino Imides from Tertiary Amines: Ugi-Type Three-Component Assemblies Involving Direct Functionalization of sp^3 C-Hs Adjacent to Nitrogen Atoms*. *Org. Lett.* **2010**, *12*, 4240–4243; d) Ye, X.; Xie, C.; Huang, R.; Liu, J. *Direct Synthesis of α -Amino Amides from N-Alkyl Amines by the Copper-Catalyzed Oxidative Ugi-Type Reaction*. *Synlett* **2012**, *23*, 409–412.
5. Lin, Y.-Z.; Alper, H. *A Novel Approach for the One-Pot Preparation of α -Amino Amides by Pd-Catalyzed Double Carbohydroamination*. *Angew. Chem. Int. Ed.* **2001**, *40*, 779–781.
6. J. T. Reeves, Z. Tan, M. A. Herbage, Z. S. Han, M. A. Marsini, Z. Li, G. Li, Y. Xu, K. R. Fandrick, N. C. Gonnella, S. Campbell, S. Ma, N. Grinberg, H. Lee, B. Z. Lu and C. H. Senanayake. *Carbamoyl Anion Addition to N-Sulfinyl Imines: Highly Diastereoselective Synthesis of α -Amino Amides*. *J. Am. Chem. Soc.* **2013**, *135*, 5565–5568.
7. a) Chen, J.; Cunico, R. F. *α -Amino Amides from a Carbamoylsilane and Aldehyde Imines*. *Tetrahedron Lett.* **2003**, *44*, 8025–8027; b) Chen, J.; Pandey, R. K.; Cunico, R.F. *Diastereoselective formation of α -Amino Amides from Carbamoylsilanes and Aldehyde Imines*. *Tetrahedron: Asymm.* **2005**, *16*, 941–947; c) Cunico, R. F.; Pandey, R.K.; Chen, J.; Motta, A. R. *Copper(II) Trifluoromethanesulfonate Catalyzed Addition of a Carbamoylsilane to Aldehyde Imines*. *Synlett* **2005**, 3157–3159.
8. Photoredox-catalyzed carboxamide syntheses have also been realized by an Umpolung approach with imines and isocyanates: a) Rueping, M.; Vila, C. *Visible Light Photoredox-Catalyzed Multicomponent Reactions*. *Org. Lett.* **2013**, *15*, 2092–2095; b) Zhu, J.; Dai, C.; Ma, M.; Yue, Y.; Fan, X. *Visible Light-Mediated Cross-Coupling of Electrophiles: Synthesis of α -Amino Amides from Isocyanates and Ketimines*. *Org. Chem. Front.* **2021**, *8*, 1227–1232.
9. a) Alandini, N.; Buzzetti, L.; Favi, G.; Schulte, T.; Candish, L.; Collins, K. D.; Melchiorre P. *Amide Synthesis by Nickel/Photoredox-Catalyzed Direct Carbamoylation of (Hetero)Aryl Bromides*. *Angew. Chem. Int. Ed.* **2020**, *59*, 5248–5253. b) Cardinale, L.; Konev, M. O.; Jacobi von Wangelin, A. *Photoredox-Catalyzed Addition of Carbamoyl Radicals to Olefins: A 1,4-Dihydropyridine Approach*. *Chem. Eur. J.* **2020**, *26*, 8239–8243.
10. Speckmeier, E.; Fischer, T. G.; Zeitler, K. *A Toolbox Approach to Construct Broadly Applicable Metal-Free Catalysts for Photoredox Chemistry: Deliberate Tuning of Redox Potentials and Importance of Halogens in Donor–Acceptor Cyanoarenes*. *J. Am. Chem. Soc.* **2018**, *140*, 15353–15365.
11. Leitch, J. A.; Rossolini, T.; Rogova, T.; Maitland, J. A. P.; Dixon, D. J. *α -Amino Radicals via Photocatalytic Single-Electron Reduction of Imine Derivatives*. *ACS Catal.* **2020**, *10*, 2009–2025.
12. Rong, J.; Seeberger, P. H.; Gilmore, K. *Chemoselective Photoredox Synthesis of Unprotected Primary Amines Using Ammonia*. *Org. Lett.* **2018**, *20*, 4081–4085; b) Gentry, E. C.; Knowles, R. R. *Synthetic Applications of Proton-Coupled Electron Transfer*. *Acc. Chem. Res.* **2016**, *49*, 1546–1556.
13. Kim, H.; Lee, C. *Visible-Light-Induced Photocatalytic Reductive Transformations of Organohalides*. *Angew. Chem. Int. Ed.* **2012**, *51*, 12303–12306.
14. Li, G.; Chen, R.; Wu, L.; Fu, Q.; Zhang, X.; Tang, Z. *Alkyl Transfer from C–C Cleavage*. *Angew. Chem. Int. Ed.* **2013**, *52*, 8432–8436.
15. Li, Z.; Yang, J.-D.; Cheng, J.-P. *Thermodynamic and Kinetic Studies of Hydride Transfer from Hantzsch Ester under the Promotion of Organic Bases*. *Org. Chem. Front.* **2021**, *8*, 876–882.
16. a) Studer, A. *The Persistent Radical Effect in Organic Synthesis*. *Chem. Eur. J.* **2001**, *7*, 1159–1164; b) Fischer, H. *The Persistent Radical Effect: A Principle for Selective Radical Reactions and Living Radical Polymerizations*. *Chem. Rev.* **2001**, *101*, 3581–3610; c) Patel, N. R.; Kelly, C. B.; Siegenfeld, A. P.; Molander, G. A. *Mild, Redox-Neutral Alkylation of Imines Enabled by an Organic Photocatalyst*. *ACS Catal.* **2017**, *7*, 1766–1770.
17. For enantioselective synthesis of α -amino amides see: a) Hacking, M. A. P. J.; Wegman, M. A.; Rops, J.; van Rantwijk, F.; Sheldon, R. A. *Enantioselective Synthesis of Amino Acid Amides via Enzymatic Ammonolysis of Amino Acid Esters*. *J. Mol. Catal. B Enzym.* **1998**, *5*, 155–157; b) Nanayakkara, P.; Alper, H. *Asymmetric Synthesis of α -Amino Amides by Pd-Catalyzed Double Carbohydroamination*. *Chem. Commun.* **2003**, 2384–2385; c) Wang, J.; Liu, X.; Feng, X.

Asymmetric Strecker Reactions. *Chem. Rev.* **2011**, *111*, 6947; d) Schwieter, K. E.; Johnston, J. N. Enantioselective Synthesis of D- α -Amino Amides from Aliphatic Aldehydes. *Chem. Sci.* **2015**, *6*, 2590–2595.

18. a) Shatskiy, A.; Axelsson, A.; Stepanova, E. V.; Liu, J.-Q.; Temerdashev, A. Z.; Kore, B. P.; Blomkvist, B.; Gardner, J. M.; Dinér, P.; Kärkäs, M. D. Stereoselective Synthesis of Unnatural α -Amino Acid Derivatives through Photoredox Catalysis. *Chem. Sci.* **2021**, *12*, 5430–5437; b) Morton, D.; Stockman, R. A. Chiral non-racemic sulfinimines: versatile reagents for asymmetric synthesis. *Tetrahedron* **2006**, *62*, 8869–8905; c) Robak, M. T.; Herbage, M. A.; Ellman, J. A. Synthesis and Applications of *tert*-Butanesulfinamide, *Chem. Rev.* **2010**, *110*, 3600–3740.

6 Chapter 6: Cobalt (II) Halide – Amine Enabled Cyclotrimerization of Terminal Alkynes



Abstract: Self-sustained Co^{III} cycles are well known for the formation of new C-C bonds in reactions such as the cyclotrimerization of alkynes. Finding new strategies to generate *in situ* the low valent species are essential for the mechanistic understanding and the achievement of easier protocols. This report shows an effective CoBr_2 -amine catalyzed cyclotrimerization of terminal alkynes for the synthesis of substituted benzenes in high regiocontrol in absence of ligands, reductants or light.

This chapter contains unpublished work.

6.1 Introduction

Transition metal catalyzed [2+2+2] cycloadditions of alkynes are a straightforward route to aromatic rings synthesis. This atom economic approach leads in a concerted way to more complex molecules, six-membered rings, otherwise challenging to obtain with alternative synthetic pathways.¹ Despite being feasible, the uncatalyzed cyclotrimerization of alkynes shows very low yields even at temperatures above 400 °C.² On the other hand, in the presence of a transition metal the reaction proceeds smoothly, in high performance even at room temperature. Since its first report by Reppe and Schweckendiek of a Ni⁰ mediated alkynes cyclotrimerization,³ several other transition metals (Co, Ru, Rh, Ir, Pd, Ti and Fe) have been successfully used and tremendous efforts have been done to elucidate the underlying mechanism.⁴ A key step for the reaction initiation is the achievement of an open shell metal core in its low valent state that would allow the coordination and activation of the alkyne molecules through oxidative addition.

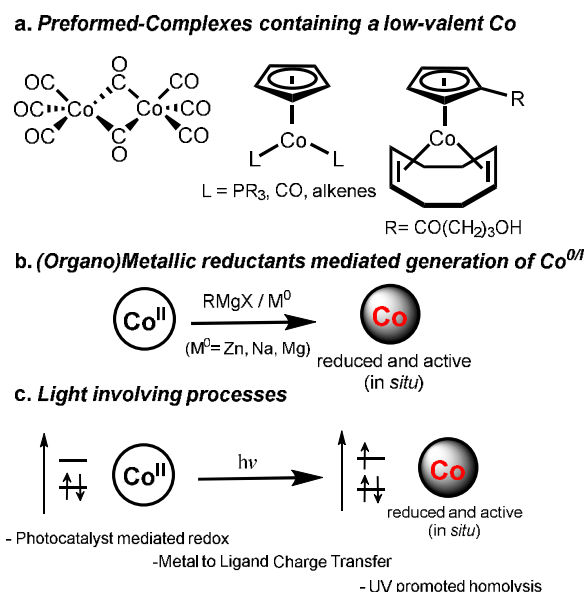


Figure 1. a) Common precatalysts used in Co-catalyzed cyclotrimerization reactions; b, c) Known strategies for the reduction of Co^{II} to low-valent species *in situ*.

Based on recent studies conducted in our laboratory on the generation of low valent iron species, through deprotonation/reductive elimination⁵ and photoredox strategies⁶ in the cyclotrimerization of terminal alkynes, we observed catalytic activity in presence of simple cobaltous salts.

Co⁰ complexes such as Co₂(CO)₈ and CpCo(CO)₂, are historically known to be good precatalysts in these type of transformation under UV or thermal activation (a, Figure 1).⁷ However, several alternatives to the carbonyl-based complexes have been explored as the use of more stable Co^{II} complexes (phosphine or diimine ligands are required, in most of the cases, to stabilize the generated reactive metal center) activated *in situ* to the Co⁰ reactive species. With a reduction potential for the Co^{II}/Co⁰ transition laying between -0.5 and -1.6 V vs SCE, depending on the specific ligands, a quite strong reductant is required (b and c, Figure 1).⁸ Canonical activation modes are the addition of Grignard reagents or the use of metals as single electron reductants (Li, Mg, Na, Zn). It is also known the use of hydride donors (as NaBH₄ or LiAlH₄) for the generation of Co^{II} hydrides readily convertible in Co⁰.⁹ More recently, through light mediated processes as photoredox catalysis^{10a-c} or through direct irradiation and light induced LMCT (ligand to metal charge transfer) (c, Scheme1) the same reactivity was achieved.^{10d}

The use of external reductant, generation of byproducts, expensive photocatalysts and time demanding design of ligands make appealing the study of new activation modes towards simpler systems. We report

the use of Co^{II} halides salts where nor obvious reductant, nor ligand, nor light-involved strategies are required.

6.2 Results and discussion

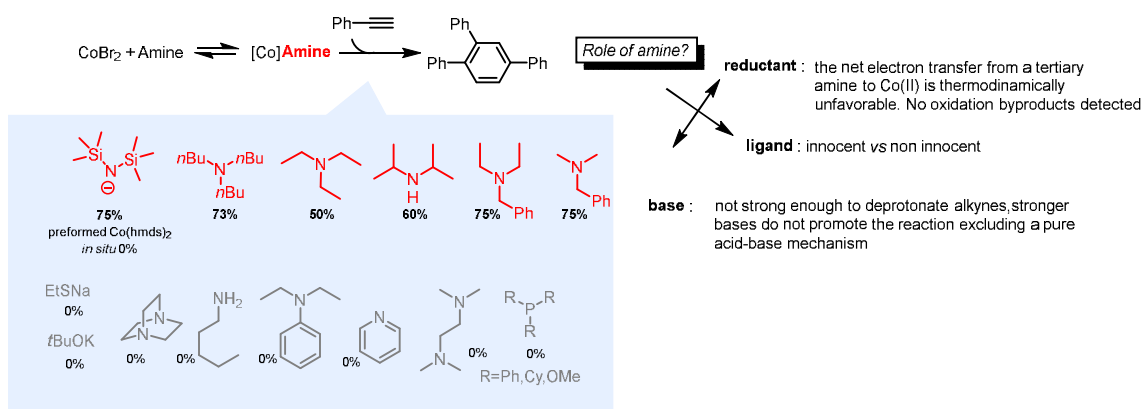
We commenced our studies with the screening of various simple cobaltous salts in the cyclotrimerization of phenylacetylene. CoCl₂, CoBr₂ and Co(OTf)₂ showed to be competent precatalysts in the presence of Hünig's base (DIPEA) while simple salts of other first row transition metals, such as Fe or Ni, gave no or little turnover and full recovery of starting material (Entry 2-3, Table 1). These results might be justified with an increase in redox potentials, towards more negative values, for the series FeBr₂ > NiBr₂ > CoBr₂ for the transition M^(II)/M^(I).¹¹ Screening of solvents showed acetonitrile to be not only the best solvent but necessary for the outcome of the reaction, this might be due to a role played by acetonitrile not only as solvent but also as ligand and stabilizer of the generated low valent Co species (Entry 5, Table 1; experimental part for full overview).¹² Moreover in the presence of 20 equivalents of MeCN the reaction proceeds also in other solvents such as hexanes, pentane, toluene, THF and Et₂O. Solvents as DCE, DMF and NMP were unsuccessful even in mixture with acetonitrile probably due to their high coordination ability and incompatibility with radical processes. Different bases were tested (Scheme 1; see experimental section for a full overview) and the reaction showed to be sensitive to basicity and steric hindrance of the chosen system. Within the bases only aliphatic amines resulted in competent activators and DIPEA resulted the best candidate.

Table 1. Optimization of reaction conditions

Ph-C≡C-C≡C-C≡C + $\xrightarrow[\text{MeCN [0.25 M], r.t., 2h}]{\text{CoBr}_2 (5 \text{ mol\%}), \text{DIPEA} (1.25 \text{ mol\%})}$ 1,3,5-triphenylbenzene + 1,3,5-triphenylbenzene isomer

Entry	Deviations from standard conditions	Yield % ^[a]
1	none	82
2	5 mol% FeBr ₂ or NiCl ₂	5; 0
3	5 mol% CoCl ₂	49
4	No DIPEA, no CoBr ₂ , air	< 5%
5	THF, hexanes, DMF as solvents	0
6	2.5 mol% CoBr ₂	51 ^[b]
7	10 mol% DIPEA	70
8	Warming up to 70 °C	80 ^[c]
9	10 mol% PPh ₃ , PCy ₃ as ligand	0

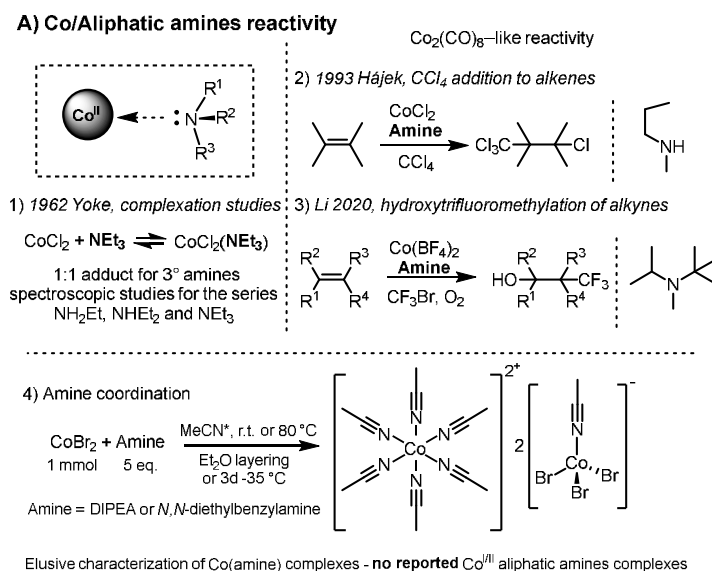
[a] Overall GC yield of both isomers were determined by GC-FID versus internal dodecanenitrile; yield of minor 1,3,5-isomer < 5%; CoBr₂ (> 99.99%) was used. [b] 24h reaction. [c] 1h reaction.



Scheme 1. Example of tested amines in the cyclotrimerization reaction.

Interestingly even very similar amines as *N,N*-diethylaniline and *N,N*-diethylbenzylamine could go from no reactivity to good conversion. In case of not effective amines such as pentylamine or *N,N*-diethylaniline the reactivity could be restored whenever DIPEA was added with no alteration of the outcome. From the screening of different bases, we also excluded a correlation between the basicity of the amines and the reaction promotion.

Aliphatic amines are known for SET (single electron transfer) especially in light involving reactions¹³ and in few cases under dark conditions. Back to 1962 are reported the first studies about Co- aliphatic amines complexation however no defined crystal structures are reported (Scheme 2, 1).¹⁴ In 1993 Hájek et al. reported a CoCl_2 /methylpropylamine catalyzed addition of tetrachloro methane to alkenes, showing the ability of such a system to be competent in a reaction previously reported for dicobalt octacarbonyl complex (Scheme 2, 2).^{15a} In a recent work by Li et al., a stoichiometric mixture of $\text{Co}(\text{BF}_4)_2$ and tertiary amine was used for the hydroxytrifluoromethylation of alkenes (Scheme 2, 3).^{15b} Based on such observations can be deduced that Co(II) not only can create complexes with highly sterically hindered tertiary amines but such complexes can also be used in catalysis, mimicking the reactivity of low valent cobalt species such as dicobaltoctacarbonyl. Must be noted that in none of the mentioned cases a real Co(II) catalytic system (with loading < 30 mol%) could be generated under such conditions and stoichiometric amounts of Co(II) sources were required together with amine.

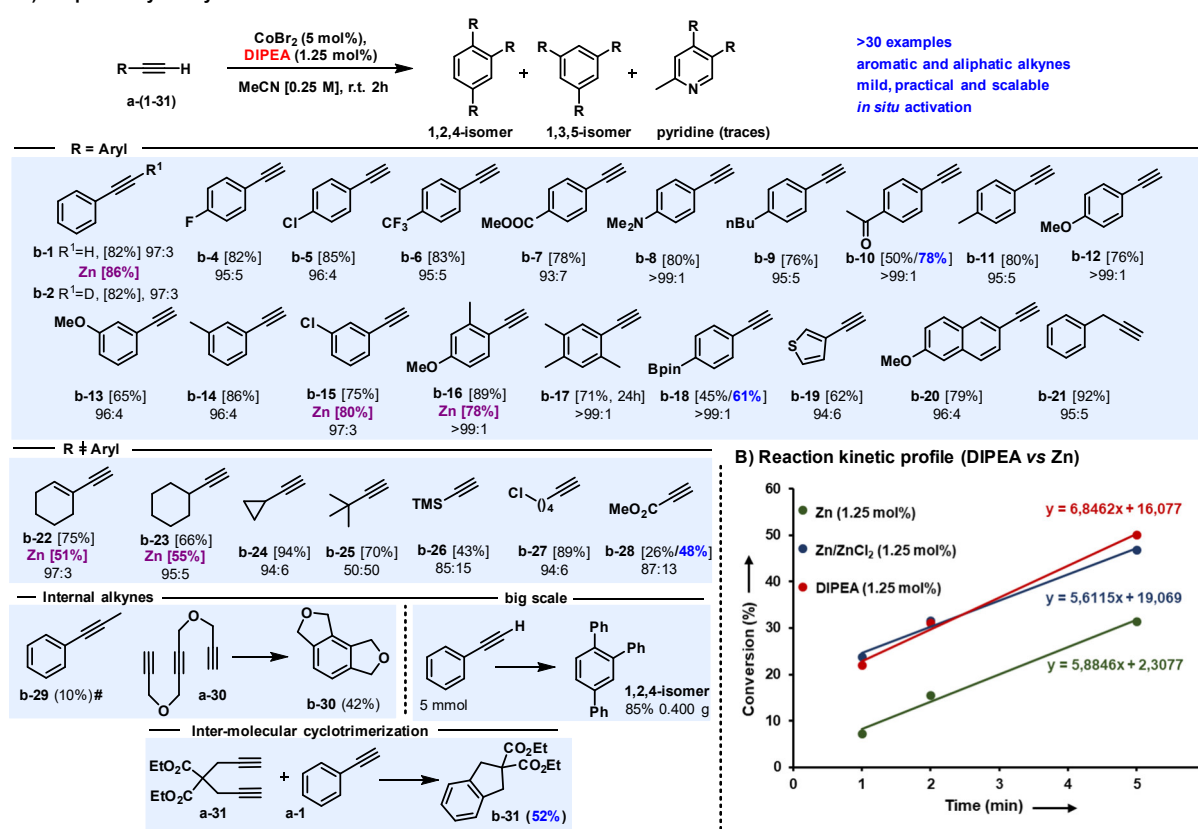


Scheme 2. Overview of Co/aliphatic amines reactivity.

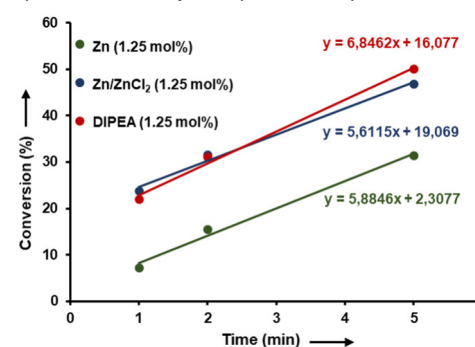
We report, at the best of our knowledge, the first example of cobalt-amine strategy in catalytic fashion for the generation of a self-sustained Co^{III} catalytic cycle, whereas the cyclotrimerization of terminal alkynes is performed in high regiocontrol with only 5 mol% of CoBr_2 and 1.25 mol% of amine.

With the optimized conditions developed we explored the substrate scope on different alkynes (A, Scheme 3). The reaction exhibited a well group tolerance on aromatic and aliphatic terminal alkynes with no marked electronic trends. Under the reaction conditions were tolerated halogens (**b-4**, **b-5**, **b-15**, **b-27**), boronic acid (**b-18**), esters (**b-7**, **b-28**), acetyl (**b-10**) and thiophene (**b-19**). Unsuccessful were the reaction on substrates containing strong coordinating groups as free amines or nitriles probably due to a competition with acetonitrile and/or DIPEA. Full incorporation of all three deuterium atoms into the resultant arene (**b-2**) was observed upon reaction of 2-deutero-phenylacetylene. The conversion of internal alkyne (**b-29**) was not achieved, if not in low yields, even at higher loadings of DIPEA/CoBr₂ or high temperatures. Nevertheless, in case of triene with one internal alkyne (**a-30**) the desired product (**b-30**) was achieved in discrete yields. Finally, it was possible to scale up 10 times the cyclotrimerization of phenylacetylene maintaining good yields and regioselectivity (**b-1**, 85%, 97:3). Mixed systems starting from diyne (**a-31**) and phenylacetylene were obtained (**b-32**). Controlling the solvent (pure CH₃CN vs mixtures), the stoichiometry (excess of **1-a**) and addition order (first **a-31**, then slowly **1-a**) the intramolecular reactivity could be suppressed in favor of the intermolecular product (**b-32**).

A) Scope of alkynes cyclotrimerization

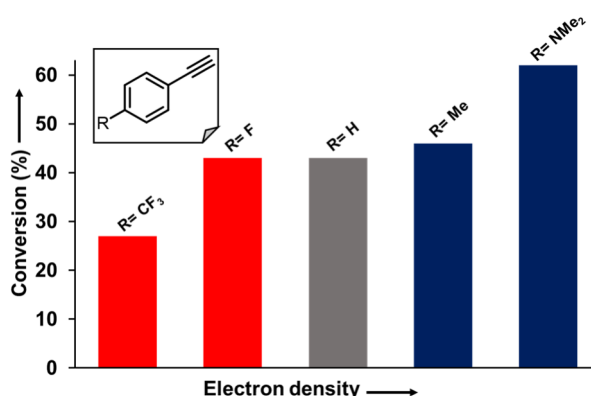


B) Reaction kinetic profile (DIPEA vs Zn)



Scheme 3. A) Scope of the cyclotrimerization reaction, isolated yields are reported in brackets. Regioselectivity is reported as ratio between the two possible regioisomers as determined by ¹H NMR analysis. In blue the isolated yields in case of hexane:MeCN (3:1) as solvents mixture; in violet the yields for reactions run in presence of Zn/ZnCl₂ (1.25 mol%) instead of DIPEA. # denotes NMR yield. B) Reaction kinetic profile of reaction under standard conditions vs reaction run with Zn/ZnCl₂ as reductant.

Within the investigation of substrate scope, we also performed a direct comparison between our protocol and the literature known Zn mediated cyclotrimerization. We found not only that our protocol is comparable with the yields obtained under Zn reductive conditions (substrates **b1**, **b15**, **b18**) but even superior in case of aliphatic or unsaturated substrates (see substrates **b22**, **b23**). We also compared the kinetic reaction profile of our DIPEA-mediated cyclotrimerization and the Zn mediated one. What we found, from the analysis of initial rates, is a faster reaction for the CoBr₂/DIPEA system.



Scheme 4. Evaluation of substituents electrondensity on the cyclotrimerization reaction rate, reactions stopped after 4 minutes.

The effect of the electron density of the chosen starting material on the reaction rate was shortly investigated, using 5 different aromatic alkynes (**b-1**, **b-4**, **b-6**, **b-8**, and **b-11**). We observed, stopping the reactions after 4 minutes, higher conversions in case of electron rich substituents such as NMe₂ and Me compared to F and CF₃ (Scheme 4).

Intrigued from the simplicity of the system many efforts were applied to elucidate the mechanism behind the reaction and the activation of the Co^{II} halide salt. Key observations were that all three components (alkyne, amine, and nitrile) are essential for the outcome of the reaction, in absence of one of them no background reactions were detected. The amine could be replaced by Zn dust showing similar reactivity, suggesting a key role in the Co(II) reduction played by the amine. The reaction was run under light irradiation (365, 410 or 650 nm) or in aluminum foil but no differences could be detected excluding a light promoted SET (see experimental part). The acetonitrile could be replaced by other nitriles as α -methoxy-, benzyl-, and pivalonitrile with good yields. In all cases was also observed the [2+2+2] pyridine byproduct generated from the incorporation of one nitrile molecule (b, Figure 2).

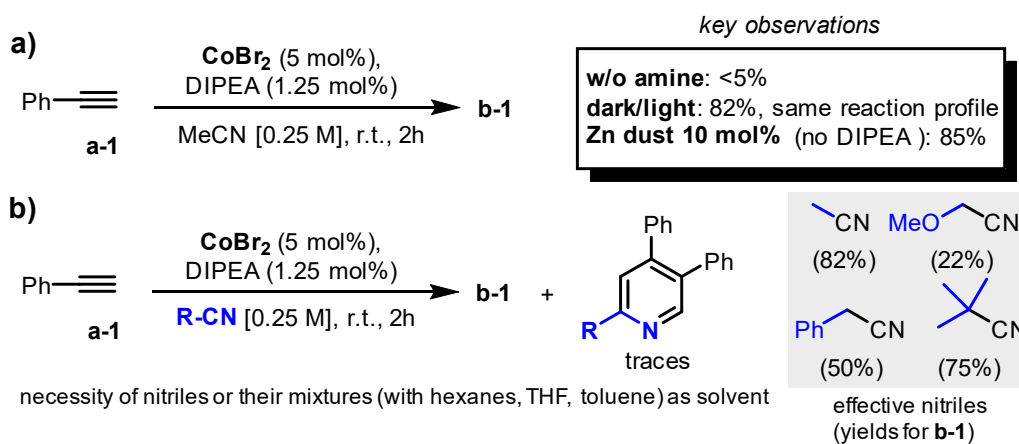


Figure 2. a) Key observations and b) different nitriles used as solvent.

From acetonitrile-amine mixtures (either DIPEA or DEBA) was possible to crystallize the previously reported [Co(MeCN)₆][CoBr₃MeCN]₂ solvated complex¹⁶ but in none of the attempts amine complexation was observed (Scheme 2, 4). We think that due the steric hindrance and the low coordinating ability of tertiary aliphatic amines, crystal structures might be challenging to obtain, nevertheless the coordination in solution of the amine can be supposed based on UV spectroscopy absorption (a, Figure 3)¹⁴ and deshielding of shifts in ¹H-NMR signals of DIPEA upon addition of CoBr₂ (b, Figure 3).

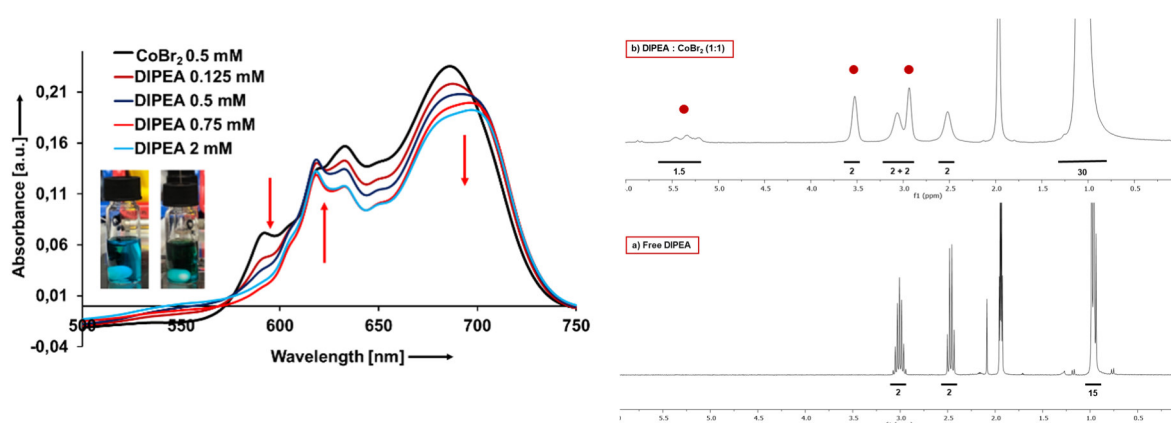
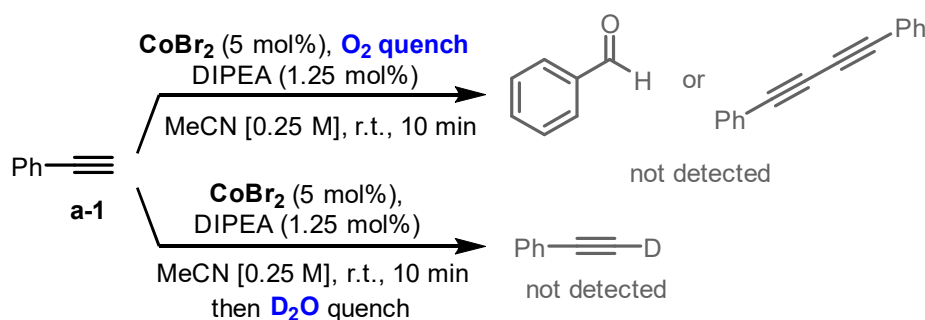


Figure 3. a) UV-Vis spectra of after addition of increasing amounts of DIPEA in MeCN. In the picture: color change from royal blue to green after additions of amine; b) ^1H NMR in CD_3CN of DIPEA compared with b) ^1H NMR in CD_3CN of a mixture of CoBr_2 :DIPEA (1:1 ratio). The red dots show the new peaks formed.

The deprotonation of the alkyne by DIPEA was ruled out based on their pK_a values and the following observations: i) quenching the reaction with O_2 balloon led to no characteristic byproducts of alkyne-activation as benzaldehyde or 1,4-diphenylbutadiyne¹⁷; ii) quench of the reaction with D_2O led to no deuterium incorporation into unreacted phenylacetylene (Figure 4); iii) from IR spectra of reaction mixture no $\nu_{\text{C}\equiv\text{C}}$ bands of a hypothetical σ -alkynylcobalt species were detected (see experimental part)¹⁸, iv) no shift in ^1H -NMR signals were recorded for the $\equiv\text{CH}$ proton upon addition of DIPEA. We focused our attention on DIPEA due its possible role as formal reductant in the reaction. A single electron transfer in dark conditions was excluded based on redox potentials of the species involved. From CV studies a redox potential for CoBr_2 in CH_3CN of 0.6 V (vs Ag/AgCl) ca. was determined and +0.8 V for DIPEA (in CH_3CN , vs Ag/AgCl). Due the big gap in redox potentials it seems thermodynamically unfeasible an electron transfer within the two species. Moreover, in no case, big scale experiment or the in case of larger amines (as DEBA or tributylamine) instead of DIPEA, was observed byproducts formation of amine oxidation.



*reactions were repeated for stoichiometric amounts of Co and amine

Figure 4. Experiments on alkyne deprotonation.

In absence of chemical evidence of a Co(II) reduction we tested several reactions that are known to be catalyzed from Co(I) systems but not Co(II) . The CoBr_2 /DIPEA mixture in presence of α -Br-esters **33** and phenylacetylene **a-1** led to the compound **34**. Under these conditions Co(II) systems should be inert while Co(I) species, for example generated in situ by metallic Zn, would lead to α -Br-esters reduction and consecutive ATRA reaction on alkynes.¹⁹ In our conditions we did not obtained the expected ATRA product **35** but compound **34** where has followed a further debromination and C-C coupling with phenylacetylene The control reaction on the ATRA product **35** led to the same result; most likely under our reaction conditions the same intermediate is generated but further reacts in a Sonogashira-like coupling to give **34** (a-b, Figure 5)²⁰. Another observation comes from one of the reaction substrates **36**, whereas -Cl and -F groups were tolerated the easier reducible -Br led to no conversion of the starting material if not in traces and the cyclotrimerization product **37** partially dibrominated. Also in this case a Co(II) species would be ineffective for the oxidative addition of arylbromides or their single electron

reduction (c, Figure 5). Finally, in presence of a non-reactive alkyne such as **b-29** the electron-poor aryl bromide **38** underwent to debromination furnishing the homocoupling product **39**. Also in this case the biaryl product can be justified only assuming a reduced cobalt species different from Co(II); not being known homocoupling reactions for the latest systems (d, Figure 5).

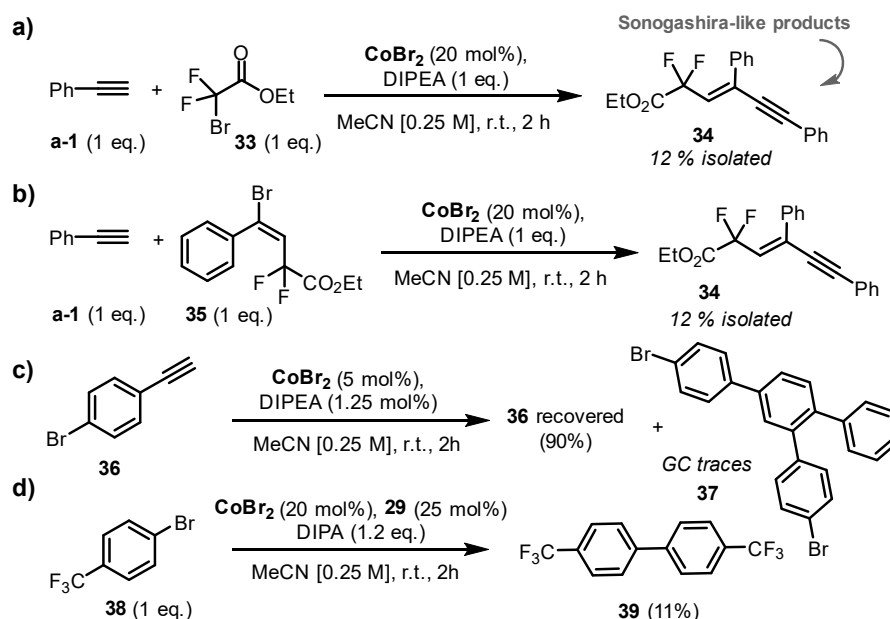


Figure 5. Test of our reaction conditions in Co(I)-reactivity.

Reaction orders were determined for all the reaction components and we found a 1st order in phenylacetylene and 2nd order for the CoBr₂/DIPEA (4:1) catalytic mixture suggesting the presence of 2 cobalt species per substrate molecule in the *rds* (rate determining step). We also evaluated KIE from intermolecular experiments for the single components and we found for the couples phenylacetylene-H/D, CH₃CN/CD₃CN and NEt₃/NEt₃-d₁₅ the following values KIE: 1.20, 1.85, 1.54. A not marked effect could be detected for phenylacetylene confirming a not involvement of the C-H bond in the *rds*.

Poisoning experiments showed a strong reaction inhibition in presence of both phosphines (as PMe₃ and P(OMe)₃) and dibenzo-[a,e]cyclooctatetraene (dct) (Figure 6) Various phosphine not only poisoned the reaction but in their presence, acting as good ligands and competing with amines, no substrate conversion could be achieved (see optimization studies, experimental part).

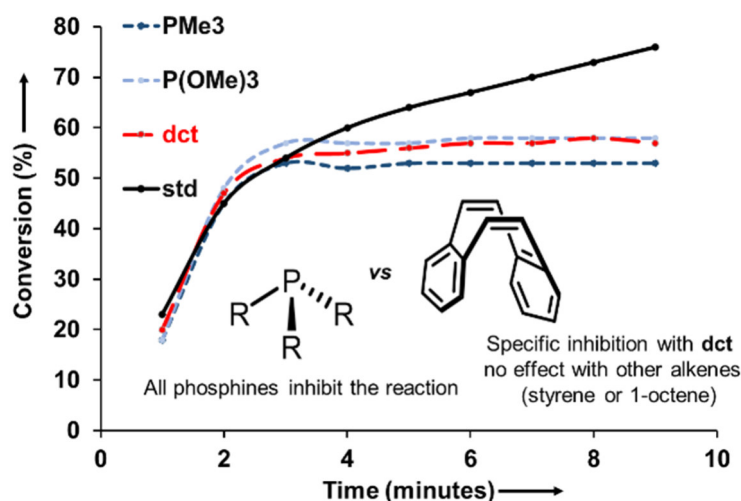


Figure 6. Poisoning experiments. Addition of poisons after 3 minutes.

This might not stand for heterotopic catalyst system but more for an incompatibility between phosphines and cobalt activation in our reaction conditions; probably the Co(II)PL₃ complex results in much more stabilized and no disproportionations or reduction events can take place. On the other hand, dct, a potent poison for homogeneous catalysis, affected the catalyst turnover in a specific way whereas other alkenes such as 1-octene or 2-vinylnaphthalene were ineffective.

6.3 Conclusion

In conclusion we demonstrated the possibility to activate a Co^{II} – halide species, in its high oxidation state, to partially reduced one with a simple tertiary amine system where no light or ligand or reductant is needed. The reduction of the cobalt center resulted in the efficient cycotrimerization reaction of terminal alkynes to substituted benzenes with high regiocontrol and good functional group tolerance under mild conditions. Mechanistic studies followed to elucidate the activation mode behind this simple system. We hope that this report would open the scenario to the use of such a system for Co^{II} – based chemistry.

6.4 Experimental section

6.4.1 Materials and methods

Chemicals and solvents: All reagents ($\geq 96\%$ purity) and solvents ($\geq 99\%$ purity) were purchased from commercial suppliers (Acros, Alfa Aesar, Fisher, Fluka, Merck, Sigma Aldrich, TCI, Th. Geyer) and used as received unless otherwise indicated. Liquid acetylene derivatives as well as Hünig's base were distilled under vacuum prior to use. Dry solvents were obtained by either common drying techniques or directly purchased in extra dry ($>99.9\%+$, over molecular sieves) form. CoBr₂ (99.99%, trace metal pure) beads were ground with mortar and pestle to obtain a homogeneous powder. All reagents and dried solvents were stored in an argon-filled glovebox.

Nuclear magnetic resonance (NMR) spectroscopy: ¹H NMR, ¹³C NMR and ¹⁹F NMR were used for purity and structure determination of products. NMR spectral data were collected on a Bruker Avance 300 (300 MHz for ¹H; 75 MHz for ¹³C, 282 MHz for ¹⁹F) spectrometer, a Bruker Avance 400 (400 MHz for ¹H; 100 MHz for ¹³C) spectrometer or a Bruker Avance III 600 (600 MHz for ¹H; 585 MHz for ¹⁹F) spectrometer at 25 °C. Chemical shifts are reported in δ /ppm, coupling constants *J* are given in Hertz. Solvent residual peaks were used as internal standard for all NMR measurements. The quantification of ¹H cores was obtained from integrations of appropriate resonance signals. Abbreviations used in NMR spectra: s – singlet, d – doublet, t – triplet, q – quartet, m – multiplet, bs – broad singlet, dd – doublet of doublet.

Gas chromatography (GC-FID and GC-MS): GC-FID measurements on an Agilent 7820A GC-system with N₂ as carrier gas were used for quantification purposes in reaction optimization screenings and kinetic experiments. Mesitylene or dodecanenitrile were used as internal standards; the conversion-% and yield-% were calculated from a linear calibration curve that was set up from at least three data points of various concentrations of the respective analytically pure material. GC-MS measurements on an Agilent 7820A GC-system coupled with a 5977B MSD detector (EI ionization source) and H₂ as carrier gas were used for reaction control purposes and structure determination of literature-known products (LMRS).

High resolution mass spectrometry (HRMS): HRMS was carried out by the Central Analytics at the department of chemistry, University of Hamburg. Abbreviations used in MS spectra: M – molar mass of target compound, EI – electron impact ionization, ESI – electrospray ionization.

Column chromatography: Column chromatography was performed using silica gel (Acros Organics, mesh 35-70, 60 Å pore size) as the stationary phase.

UV/VIS absorption spectroscopy: UV-Vis absorption spectroscopy was performed at room temperature on an Agilent Cary 5000 UV/VIS NIR double beam spectrometer with a 10 mm quartz cuvette.

Cyclic voltammetry: CV measurements were performed with a potentiostat galvanostat PGSTAT101 from Metrohm Autolab using a glassy carbon working electrode, a platinum wire counter electrode, a silver/silver(I)chloride reference electrode and $N(n\text{-Bu})_4\text{PF}_6$ (0.1 M) as supporting electrolyte. The potentials were achieved relative to the Fc/Fc^+ redox couple with ferrocene as external standard.

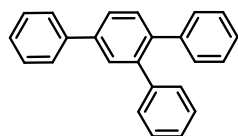
Determination of regioisomeric ratios: The ratios of regioisomers were determined by integration of either GC-FID or $^1\text{H-NMR}$ signals. In case of GC-FID evaluation an equal response factor of both regioisomers was assumed. For regioisomeric ratios greater than 90:10 only the main isomer is depicted in the following NMR characterizations.

6.4.2 General procedures

General procedure A for the scope of [2+2+2] cyclotrimerization:

CoBr_2 (5 mol%, 5.47 mg) was dissolved in acetonitrile (2.0 mL, 0.25 M). DIPEA (1.25 mol%, 1.12 μL) and the respective acetylene derivative (0.50 mmol) were added consecutively. The reaction mixture was stirred at r.t. for two hours (up to 24h for less reactive substrates as specified). After two hours the reaction was quenched by addition of aqueous hydrochloric acid (3mL, 1 M) and extracted with ethyl acetate (3 \times 10mL). The combined organic layers were washed with brine (10 mL), dried over sodium sulfate and filtered. After removing the volatiles in vacuum, the residue was purified by column chromatography. The isolated yields are given as combined yields of both regioisomers. Efforts to separate the 1,2,4-regioisomer from 1,3,5-regioisomer failed due to lacking differences in polarity.

1,2,4-Triphenylbenzene (2)



Following the general procedure A starting from phenylacetylene (0.50 mmol, 51.1 mg, 55.0 μL) the compound **2** was obtained as a white solid (89%, 45.4 mg).

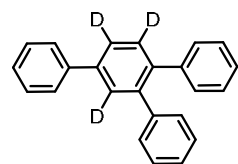
$^1\text{H NMR}$ (300 MHz, CDCl_3 , ppm): δ 7.73-7.64 (m, 4H), 7.57-7.44 (m, 3H), 7.42-7.34 (m, 1H), 7.30-7.15 (m, 10H).

GC-MS(EI): m/z (relative intensity) = 306 (100), 289 (26), 228 (20).

Amount of the 1,3,5-regioisomer (characteristic NMR signal at $\delta = 7.81$ ppm) according to $^1\text{H NMR}$: $(0.10/3)/[(4.00/4)+(0.10/3)] = 3\%$.

The analytical data were in agreement with the literature (D. Brenna, M. Villa, T. N. Gieshoff, F. Fischer, M. Hapke, A. Jacobi von Wangelin, *Angew. Chem., Int. Ed.* **2017**, *56*, 8451-8454).

1,2,4-Triphenyl-3,5,6-trideuterobenzene (3)



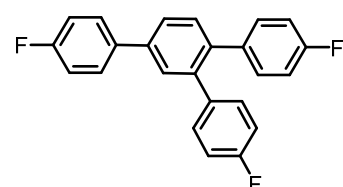
Following the general procedure A starting from phenylacetylene- d (0.50 mmol, 51.6 mg, 54.9 μL) the compound **3** was obtained as a white solid (82%, 42.3 mg). $^1\text{H NMR}$ (400 MHz, CDCl_3): $\delta = 7.73-7.64$ (m, 2H), 7.53-7.43 (m, 2H), 7.42-7.34 (m, 1H), 7.30-7.15 (m, 10H).

GC-MS(EI): m/z (relative intensity) = 309 (100), 292 (17), 231 (10).

Amount of the 1,3,5-regioisomer according to GC-FID analysis: 3%

The analytical data were in agreement with the literature (G. Kalikhman, *Bull. Acad. Sciences of the USSR, Div. Chem. Sci. (Engl. Transl.)* **1969**, 1714).

1,2,4-Tris(4-fluorophenyl)benzene (5)



Following the general procedure A starting from 1-ethynyl-4-fluorobenzene (0.50 mmol, 60.1 mg, 57.3 μL) the compound **5** was obtained as a white solid (82%, 54.1 mg). $^1\text{H NMR}$ (500 MHz, CDCl_3): $\delta = 7.65-7.57$ (m, 4H), 7.49-7.45 (m, 1H), 7.16-7.13 (m, 6H), 7.00-6.92 (m, 4H). Signals of ethyl acetate are excluded.

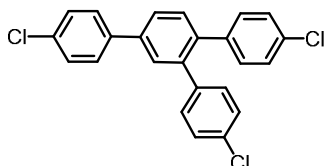
¹⁹F NMR (565 MHz, CDCl₃): δ = -115.16 (m, 1F), -115.63 (m, 1F), -115.75 (m, 1F).

GC-MS (EI): m/z (relative intensity) = 360 (100), 338 (18), 262 (14).

Amount of the 1,3,5-regioisomer (characteristic NMR signal at δ = 7.68 ppm) according to ¹H NMR: (0.16/3)/[(4.00/4)+(0.16/3)] = 5%

The analytical data were in agreement with the literature (Z. Zhu, J. Wang, Z. Zhang, X. Xiang, X. Zhou, *Organometallics* **2007**, *26*, 2499–2500).

1,2,4-Tris(4-chlorophenyl)benzene (6)



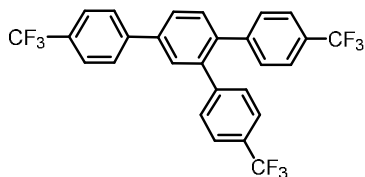
Following the general procedure A starting from 1-chloro-4-ethynylbenzene (0.50 mmol, 54.1 mg, 49.3 μL) the compound **6** was obtained as a yellowish solid (85%, 59.9 mg). ¹H NMR (300 MHz, CDCl₃, ppm): δ 7.65-7.56 (m, 4H), 7.49-7.41 (m, 3H), 7.30-7.20 (m, 4H), 7.17-7.07 (m, 4H).

GC-MS(EI): m/z(relative intensity) = 410 (98), 408 (100), 338 (77), 302 (59), 150 (91).

Amount of the 1,3,5-regioisomer(characteristic NMR signal at δ = 7.71 ppm) according to ¹H NMR: (0.14/3)/[(4.00/4)+(0.14/3)]= 4%

The analytical data were in agreement with the literature (X. Bu, Z. Zhang, X. Zhou, *Organometallics* **2010**, *29*, 3530–3534).

1,2,4-Tris(4-trifluoromethylphenyl)benzene (7)



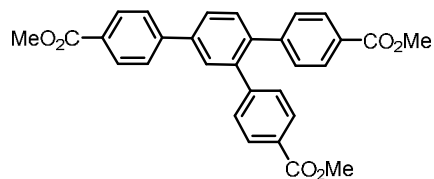
Following the general procedure A starting from 4-ethynyl-α,α,α-trifluorotoluene (0.50 mmol, 85.1 mg, 81.6 μL) the compound **7** was obtained as a white solid (83%, 71.5 mg). ¹H NMR (300 MHz, CDCl₃, ppm): δ 7.82-7.71 (m, 5H), 7.69-7.67 (m, 1H), 7.60-7.49 (m, 5H), 7.35-7.27 (m, 4H).

GC-MS (EI): m/z (relative intensity) = 510 (100), 372 (31), 211 (28).

Amount of the 1,3,5-regioisomer (characteristic NMR signal at δ = 7.83 ppm) according to ¹H NMR: (0.17/3)/[(4.00/1)+(0.17/3)] = 5%.

The analytical data were in agreement with the literature (D. Brenna, M. Villa, T. N. Gieshoff, F. Fischer, M. Hapke, A. Jacobi von Wangelin, *Angew. Chem., Int. Ed.* **2017**, *56*, 8451–8454.)

Trimethyl 1,2,4-benzenetricarboxylate (8)

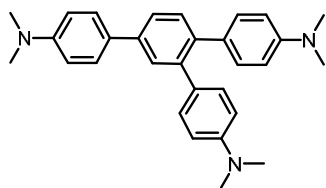


Following the general procedure A starting from 4-ethynylbenzoic acid methyl ester (0.50 mmol, 80.1 mg) the compound **8** was obtained as a white solid (78%, 62.5 mg). ¹H NMR (400 MHz, CDCl₃): δ = 8.16-8.12 (m, 2H), 7.92-7.89 (m, 4H), 7.76-7.68 (m, 4H), 7.55-7.52 (d, J = 6.65 Hz, 1H); 7.24-7.20 (m, 4H overlapping with chloroform peak), 3.95-3.90 (s+s+s, 9H).

Amount of the 1,3,5-regioisomer (characteristic NMR signal at δ = 7.86ppm) according to ¹H NMR: (0.21/3)/[(4.01/4)+(0.21/3)] = 7%

The analytical data were in agreement with the literature (S. K. Rodrigo, I.V. Powell, M. G. Coleman, J. A. Krause; H. Guan, *Org. Biomol. Chem.*, **2013**, *11*, 7653–7657).

1,2,4-Tris(4-dimethylaminophenyl)benzene (9)

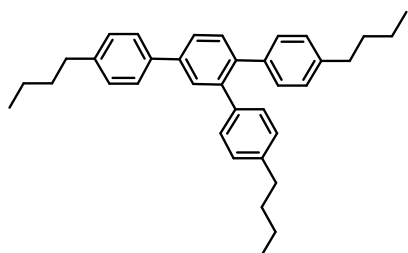


Following the general procedure A starting from 1-ethynyl-4-dimethylaniline (0.50 mmol, 72.6 mg) the compound **9** was obtained as a white solid (80%, 58.1 mg). ¹H NMR (400 MHz, CDCl₃): δ = 7.59-7.49 (m, 4H), 7.41 (d, J = 7.9 Hz, 1H), 7.12 (m, 4H), 6.82 (d, J = 8.7 Hz, 2H), 6.65 (m, 4H), 3.00-2.85 (m, 18H).

Amount of the 1,3,5-regioisomer according to ¹H NMR: no significant signal detected, therefore <1% assumed.

The analytical data were in agreement with the literature (D. Brenna, M. Villa, T. N. Gieshoff, F. Fischer, M. Hapke, A. Jacobi von Wangelin, *Angew. Chem., Int. Ed.* **2017**, *56*, 8451–8454).

1,2,4-Tris(4-n-butylphenyl)benzene (10)



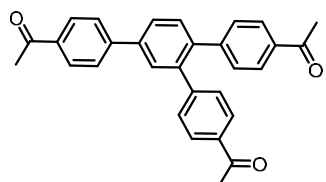
Following the general procedure A starting from 1-butyl-4-ethynylbenzene (0.50 mmol, 79.1 mg, 87.4 μL) the compound **10** was obtained as a white solid (76%, 60.3 mg). ¹H NMR (300 MHz, CDCl₃, ppm): δ = 7.67-7.56 (m, 4H), 7.52-7.45 (m, 1H), 7.30-7.23 (m, 2H), 7.16-6.96 (m, 8H), 2.73-2.63 (m, 6H), 1.73-1.50 (m, 6H), 1.50-1.24 (m, 6H), 1.02-0.88 (m, 9H).

GC-MS(EI): m/z(relative intensity) = 474 (100), 431 (20), 57 (10).

Amount of the 1,3,5-regioisomer (characteristic NMR signal at δ = 7.75 ppm) according to ¹H NMR: (0.15/3)/[(8.00/8)+(0.15/3)] = 5%.

The analytical data were in agreement with the literature (M. Neumeier, U. Chakraborty, D. Schaarschmidt, V. de la Pena O'Shea, R. Perez-Ruiz, A. Jacobi von Wangelin, *Angew. Chem., Int. Ed.* **2020**, *59*, 13473–13478).

1,2,4-Tris(4-acetylphenyl)benzene (11)

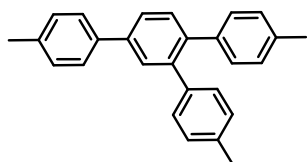


Following the general procedure A starting from 4'-ethynylacetophenone (0.50 mmol, 72.1 mg) the compound **11** was obtained as a white solid (50%, 35.8 mg). ¹H NMR (300 MHz, CDCl₃, ppm): δ 8.11-8.05 (m, 2H), 7.90-7.75 (m, 8H), 7.60-7.58 (m, 1H), 7.35-7.27 (m, 4H), 2.68 (s, 3H), 2.61 (s, 6H).

Amount of the 1,3,5-regioisomer according to ¹H NMR: no significant signal detected, therefore <1% assumed.

The analytical data were in agreement with the literature (Y. Liu, X. Yan, N. Yang, C. Xi, *Catalysis Communications* **2011**, *12*, 489–4929).

1,2,4-Tris(4-methylphenyl)benzene (12)



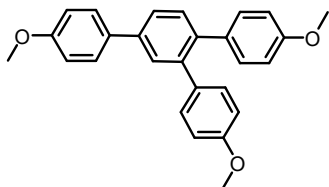
Following the general procedure A starting from 1-ethynyl-4-methylbenzene (0.50 mmol, 58.1 mg, 63.0 μL) the compound **12** was obtained as a white solid (80%, 46.5 mg). ¹H NMR (300 MHz, CDCl₃, ppm): δ = 7.64-7.57 (m, 4H), 7.47-7.42 (m, 1H), 7.34-7.27 (m, 2H), 7.18-7.03 (m, 8H), 2.42 (s, 3H), 2.34 (s, 6H).

GC-MS (EI): m/z (relative intensity) = 348 (100), 318 (15), 151 (13).

Amount of the 1,3,5-regioisomer (characteristic NMR signal at δ = 7.77ppm) according to ¹H NMR: (0.17/3)/[(1.00/1)+(0.14/3)] = 5%.

The analytical data were in agreement with the literature (X. Bu, Z. Zhang, X. Zhou, *Organometallics* **2010**, *29*, 3530–3534).

1,2,4-Tris(4-methoxyphenyl)benzene (13)

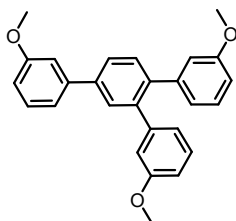


Following the general procedure A starting from 4-ethynylanisole (0.50 mmol, 66.1 mg, 64.9 μL) the compound **13** was obtained as a white solid (76%, 49.9 mg). $^1\text{H NMR}$ (300 MHz, CDCl_3 , ppm): δ 7.63-7.54 (m, 4H), 7.47-7.42 (m, 1H), 7.17-7.07(m, 4H), 7.02-6.96 (m, 2H), 6.84-6.76(m, 4H), 3.87 (s, 3H), 3.80 (2 s, 6H).

Amount of the 1,3,5-regioisomer (characteristic NMR signal at δ = 3.88 ppm) according to $^1\text{H NMR}$: no significant signal detected, therefore <1% assumed.

The analytical data were in agreement with the literature (X. Bu, Z. Zhang, X. Zhou, *Organometallics* **2010**, 29, 3530–3534).

1,2,4-Tris(3-methoxyphenyl)benzene (14)



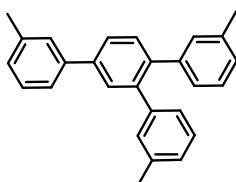
Following the general procedure A starting from 3-ethynylanisole (0.50 mmol, 66.1 mg, 63.5 μL) the compound **14** was obtained as a white solid (65%, 42.8 mg). $^1\text{H NMR}$ (300 MHz, CDCl_3 , ppm): = δ 7.68-7.63 (m, 2H), 7.53-7.51 (m, 1H), 7.41-7.36 (m, 1H), 7.27-7.14 (m, 4H), 6.94-6.91 (m, 1H), 6.85-6.72 (m, 6H), 3.88 (s, 3H), 3.64 (s, 3H), 3.63 (s, 3H).

GC-MS (EI): m/z (relative intensity) = 396 (100), 381 (40), 77 (80).

Amount of the 1,3,5-regioisomer (characteristic NMR signal at δ = 7.84 ppm) according to $^1\text{H NMR}$: $(0.13/3)/[(6.00/6)+(0.13/3)] = 4\%$.

The analytical data were in agreement with the literature (P. Tagliatesta, B. Floris, P. Galloni, A. Leoni, G. D'Arcangelo, *Inorg. Chem.* **2003**, 42, 7701–7703).

1,2,4-Tris(3-methylphenyl)benzene (15)



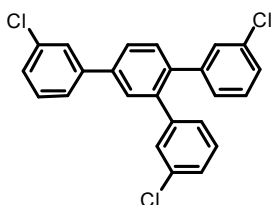
Following the general procedure A starting from 1-ethynyl-3-methylbenzene (0.50 mmol, 58.1 mg, 63.1 μL) the compound **15** was obtained as a white solid (86%, 50.2 mg). $^1\text{H NMR}$ (300 MHz, CDCl_3 , ppm): δ = 7.66-7.62 (m, 2H), 7.51-7.48 (m, 3H), 7.38-7.33 (m, 1H), 7.28-7.18 (m, 1H), 7.13-6.99 (m, 6H), 6.97-6.92 (m, 2H); 2.44 (s, 3H), 2.28 (s, 6H).

GC-MS (EI): m/z (relative intensity): 348 (100), 333 (20), 318 (25).

Amount of the 1,3,5-regioisomer (characteristic NMR signal at δ = 7.82ppm) according to $^1\text{H NMR}$: $(0.14/3)/[(2.00/2)+(0.14/3)] = 4\%$.

The analytical data were in agreement with the literature (M. Neumeier, U. Chakraborty, D. Schaarschmidt, V. de la Pena O'Shea, R. Perez-Ruiz, A. Jacobi von Wangelin, *Angew. Chem., Int. Ed.* **2020**, 59, 13473–13478).

1,2,4-Tris(3-chlorophenyl)benzene (16)



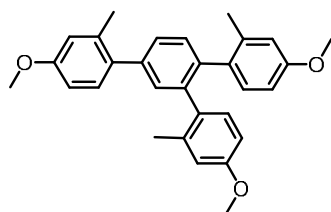
Following the general procedure A starting from 3-chloro-1-ethynylbenzene (0.50 mmol, 68.3 mg, 62.1 μL) the compound **16** was obtained as yellow solid (75%, 51.1 mg). $^1\text{H NMR}$ (300 MHz, CDCl_3 , ppm): δ = 7.64-7.58 (m, 3H), 7.54-7.51 (m, 1H), 7.49-7.46 (m, 1H), 7.25-7.20 (m, 4H), 7.19-7.13 (m, 2H), 7.00-6.94 (m, 2H).

GC-MS (EI): m/z (relative intensity) = 408 (33), 338 (54), 302 (35), 150 (100).

Amount of the 1,3,5-regioisomer (characteristic NMR signal at δ = 7.63 ppm) according to $^1\text{H NMR}$: $(0.11/3)/[(2.00/2)+(0.11/3)] = 3\%$.

The analytical data were in agreement with the literature (M. Neumeier, U. Chakraborty, D. Schaarschmidt, V. de la Pena O'Shea, R. Perez-Ruiz, A. Jacobi von Wangelin, *Angew. Chem., Int. Ed.* **2020**, 59, 13473–13478).

1,2,4-Tris-(2'-methyl-4'-methoxyphenyl)benzene (17)



Following the general procedure A starting from 1-ethynyl-4-methoxy-2-methylbenzene (0.50 mmol, 73.1 mg) the compound **17** was obtained as a white solid (89%, 65.6 mg).

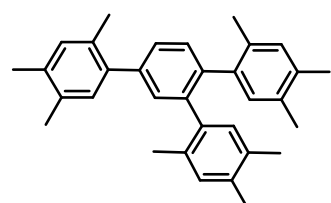
¹H NMR (300 MHz, CDCl₃, ppm): δ 7.26-7.18 (m, 4H), 6.87-8.76 (m, 4H), 6.62-6.53 (m, 4H), 3.81 (s, 3H), 3.72 (s, 3H), 3.71 (s, 3H), 2.34 (s, 3H), 2.04 (bs, 6H).

GC-MS (EI): m/z (relative intensity) = 438 (100), 423 (20), 91 (35), 77 (20).

Amount of the 1,3,5-regioisomer according to ¹H NMR: no significant signal detected, therefore <1% assumed.

The analytical data were in agreement with the literature (M. Neumeier, U. Chakraborty, D. Schaarschmidt, V. de la Pena O'Shea, R. Perez-Ruiz, A. Jacobi von Wangelin, *Angew. Chem., Int. Ed.* **2020**, 59, 13473–13478).

1,2,4-Tris-(2',4',5'-trimethylphenyl)benzene (18)



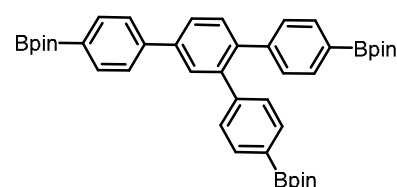
Following the general procedure A starting from 1-ethynyl-2,4,5-trimethylbenzene (0.50 mmol, 72.1 mg, 78.3 μL) the compound **18** was obtained as a white solid (71%, 51.2 mg). **¹H NMR** (400 MHz, CDCl₃): δ = 7.29-7.18 (m, 3H), 7.08 (s, 1H), 7.02 (s, 1H), 6.86-6.71 (m, 4H), 2.28 (s, 3H), 2.25 (s, 3H), 2.23 (s, 3H), 2.14 (s, 3H), 2.12 (s, 3H), 2.07 (s, 3H), 2.05 (s, 3H), 2.00 (s, 6H).

GC-MS (EI): m/z (relative intensity) = 432 (100), 324 (25).

Amount of the 1,3,5-regioisomer according to ¹H NMR: no significant signal detected, therefore <1% assumed.

The analytical data were in agreement with the literature (D. Brenna, M. Villa, T. N. Gieshoff, F. Fischer, M. Hapke, A. Jacobi von Wangelin, *Angew. Chem. Int. Ed.* **2017**, 56, 8451–8454).

1,2,4-Tris(4-(pinacolato)boronylphenyl)benzene (19)

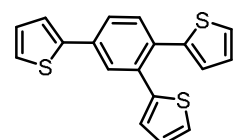


Following the general procedure A starting from 4-ethynylphenylboronic acid pinacol ester (0.50 mmol, 114.1 mg) the compound **19** was obtained as a white solid (45%, 51.8 mg). **¹H NMR** (300 MHz, CDCl₃, ppm): δ = 7.92-7.97 (m, 2H); 7.69-7.63 (m, 8H); 7.51-7.49 (m, 1H); 1.37-1.35 (m, 36 H).

Amount of the 1,3,5-regioisomer according to ¹H NMR: no significant signal detected, therefore <1% assumed.

The analytical data were in agreement with the literature (M. Neumeier, U. Chakraborty, D. Schaarschmidt, V. de la Pena O'Shea, R. Perez-Ruiz, A. Jacobi von Wangelin, *Angew. Chem. Int. Ed.* **2020**, 59, 13473–13478).

2,2',2''-(benzene-1,2,4-triyl)trithiophene (20)



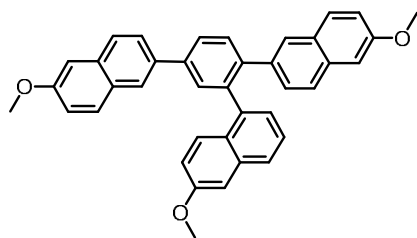
Following the general procedure A starting from 3-ethynylthiophene (0.50 mmol, 54.1 mg, 49.3 μL) the compound **20** was obtained as a yellowish solid (62%, 33.8 mg). **¹H NMR** (300 MHz, CDCl₃, ppm): δ = 7.69 (d, *J* = 1.7 Hz, 1H), 7.60 (dd, *J* = 7.9 Hz, 1.7 Hz, 1H), 7.52-7.48 (m, 2H), 7.43-7.39 (m, 2H), 7.25-7.18 (m, 2H), 7.17-7.13 (m, 1H), 7.12-7.07 (m, 1H), 6.89-6.81 (m, 2H).

GC-MS (EI): m/z (relative intensity) = 324 (100), 290 (28), 279 (18).

Amount of the 1,3,5-regioisomer (characteristic NMR signal at δ = 7.75 ppm) according to ¹H NMR: (0.18/3)/[(2.00/2)+(0.18/3)] = 6%

The analytical data were in agreement with the literature (C. Xi, Z. Sun, Y. Liu, *Dalton Trans.* **2013**, 42, 13327–13330).

1,2,4-Tris-(6-methoxy-2-naphthyl)benzene (**21**)

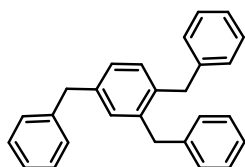


Following the general procedure A starting from 2-ethynyl-6-methoxynaphthalene (0.50 mmol, 91.1 mg) the compound **21** was obtained as a white solid (79%, 72.0 mg). ¹H NMR (300 MHz, CDCl₃, ppm): δ = 8.10 (s, 1H), 8.00–7.74 (m, 7H), 7.73–7.62 (m, 3H), 7.53–7.44 (m, 2H), 7.25–7.04 (m, 8H), 3.96 (s, 3H), 3.90 (s, 6H).

Amount of the 1,3,5-regioisomer (characteristic NMR signal at δ = 8.16 ppm) according to ¹H NMR: (0.14/3)/[(2.01/2)+(0.14/3)] = 4%

The analytical data were in agreement with literature the (D. Brenna, M. Villa, T. N. Gieshoff, F. Fischer, M. Hapke, A. Jacobi von Wangelin, *Angew. Chem. Int. Ed.* **2017**, 56, 8451–8454.

1,2,4-Tri-benzylbenzene (**22**)



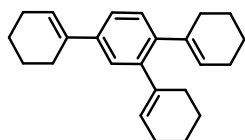
Following the general procedure A starting from 3-phenyl-1-propyne (0.50 mmol, 58.1 mg, 62.3 μL) the compound **22** was obtained as a white solid (92%, 53.5 mg). ¹H NMR (400 MHz, CDCl₃): δ = 7.27–7.16 (m, 12H); 7.06–7.00 (m, 6H); 3.93 (s, 3H); 3.90 (s, 3H); 3.89 (s, 3H).

GC-MS (EI): m/z (relative intensity) = 348 (35), 257 (30), 179 (100), 91 (65).

Amount of the 1,3,5-regioisomer (characteristic NMR signal at δ = 6.87 ppm) according to ¹H NMR: (0.14/3)/[(12.00/12)+(0.14/3)] = 5%

The analytical data were in agreement with the literature (K. Tanaka, K. Toyoda, A. Wada, K. Shirasaka, M. Hirano, *Chem. Eur. J.* **2005**, 11, 1145–1156.)

1,2,4-Tri(cyclohexen-1-yl)benzene (**23**)



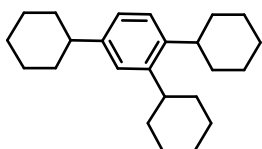
Following the general procedure A starting from 1-ethynylcyclohexene (0.50 mmol, 53.1 mg, 58.8 μL) the compound **23** was obtained as a white solid (75%, 39.8 mg). ¹H NMR (400 MHz, CDCl₃): δ = 7.22–7.17 (m, 1 H); 7.16–7.13 (m, 1H); 7.10 (d, J = 8.1 Hz, 1H); 6.14–6.10 (m, 1H), 5.71–5.64 (m, 2H); 2.43–2.39 (m, 2H); 2.27–2.08 (m, 10 H); 1.77–1.57 (m, 10 H).

GC-MS (EI): m/z (relative intensity) = 318 (100), 275 (75), 81 (36).

Amount of the 1,3,5-regioisomer (characteristic NMR signal at δ = 7.25 ppm) according to ¹H NMR: (0.10/3)/[(1.03/1)+(0.10/3)] = 3%

The analytical data were in agreement with the literature (K. Tanaka, K. Shirasaka, *Org. Lett.* **2003**, 5, 4697–4699).

1,2,4-Tricyclohexylbenzene (**24**)



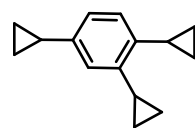
Following the general procedure A starting from ethynylcyclohexane (0.50 mmol, 54.1 mg, 65.3 μL) the compound **24** was obtained as a white solid (66%, 35.6 mg). ¹H NMR (500 MHz, CDCl₃): δ = 7.16 (d, J = 8.0 Hz, 1H), 7.08 (d, J = 1.7 Hz, 1H), 7.00 (dd, J = 8.0 Hz, J = 1.8 Hz, 1H), 2.75–2.75 (m, 2H), 2.56–2.36 (m, 1H), 2.00–1.65 (m, 15H), 1.55–1.15 (m, 15H).

GC-MS (EI): m/z (relative intensity) = 324 (100), 129 (26), 83 (61).

Amount of the 1,3,5-regioisomer (characteristic NMR signal at δ = 6.89 ppm) according to ¹H NMR: (0.15/3)/[(1.00/1)+(0.15/3)] = 5%

The analytical data were in agreement with the literature (X. Bu, Z. Zhang, X. Zhou, *Organometallics* **2010**, *29*, 3530–3534).

1,2,4-Tricyclopropylbenzene (**25**)



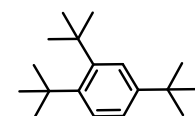
Following the general procedure A starting from ethynylcyclopropane (0.50 mmol, 33.1 mg, 42.3 μ L) the compound **25** was obtained as a white solid (94%, 30.8 mg). $^1\text{H NMR}$ (500 MHz, CDCl_3 , ppm): δ 6.88 (d, $J = 7.9$ Hz, 1H), 6.80 (dd, $J = 7.9$ Hz, 1.8 Hz, 1H), 6.71 (d, $J = 1.8$ Hz, 1H), 2.24–2.14 (m, 2H), 1.85–1.82 (m, 1H), 0.97–0.89 (m, 6H), 0.70–0.64 (m, 6H).

GC-MS (EI): m/z (relative intensity) = 198 (73), 155 (65), 141 (100), 129 (88), 115 (63).

Amount of the 1,3,5-regioisomer (characteristic NMR signal at $\delta = 6.58$ ppm) according to $^1\text{H NMR}$: $(0.20/3)/[(1.00/1)+(0.20/3)] = 6\%$.

The analytical data were in agreement with the literature (S. K. Rodrigo, I. V. Powell, M. G. Coleman, J. A. Krause, H. Guan, *Org. Biomol. Chem.* **2013**, *11*, 7653–7657).

1,3,5- and 1,2,4-Tri-tert-butylbenzene (**26**)



Following the general procedure A (due the high volatility of the substrate, in this case the reaction mixture containing all the other components was cooled down in the fridge before the addition of alkyne) starting from 3,3-Dimethyl-1-butyne (0.50 mmol, 41.1 mg, 61.5 μ L) the compound **26** was obtained as a white solid (70%, 28.3 mg). **1,2,4- $^1\text{H NMR}$** (300 MHz, CDCl_3): $\delta = 7.66$ (d, $J = 2.2$ Hz, 1H), 7.54 (d, $J = 8.4$ Hz, 1H), 7.15 (dd, $J = 8.4$ Hz, 2.2 Hz, 1H), 1.59 (s, 9H), 1.57 (s, 9H), 1.34 (s, 9H).

1,2,4: GC-MS (EI): m/z (relative intensity) = 246 (17), 231 (50), 175 (23), 57 (100).

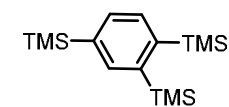
1,3,5- $^1\text{H NMR}$ (300 MHz, CDCl_3): $\delta = 7.29$ (s, 3H), 1.37 (s, 27H).

1,3,5: GC-MS (EI): m/z (relative intensity) = 246 (11), 231 (100), 57 (57).

Amount of the 1,3,5-regioisomer (characteristic NMR signal at $\delta = 7.29$ ppm) according to $^1\text{H NMR}$: $(3.00/3)/[(0.90/1)+(3.00/3)] = 53\%$

The analytical data were in agreement with the literature (H. Künzer, S. Berger, *J. Org. Chem.* **1985**, *50*, 3222–3223; J. A. Murphy, J. Garnier, S. R. Park, F. Schönebeck, S. Zhou, A. T. Turner, *Org. Lett.* **2008**, *10*, 1227–1230).

1,2,4-Tris(trimethylsilyl)benzene (**27**)



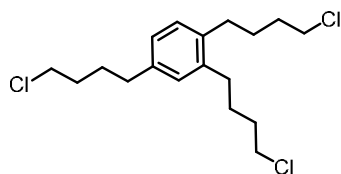
Following the general procedure A starting from ethynyltrimethylsilane (0.50 mmol, 49.1 mg, 70.2 μ L) the compound **27** was obtained as a yellowish solid (43%, 21.3 mg). $^1\text{H NMR}$ (400 MHz, CDCl_3): $\delta = 7.84$ (s, 1H), 7.66 (d, $J = 7.4$ Hz, 1H), 7.50 (d, $J = 7.4$ Hz, 1H), 0.38 (s, 9H), 0.37 (s, 9H), 0.28 (s, 9H); Mixture of both regioisomers: 7.69 (s, 3H); 0.30 (s, 27 H).

GC-MS (EI): m/z (relative intensity) 294 (100), 279 (60), 263 (25), 191 (30), 73 (25).

Amount of the 1,3,5-regioisomer (characteristic NMR signal at $\delta = 7.69$ ppm) according to $^1\text{H NMR}$: $(0.50/3)/[(1.00/1)+(0.50/3)] = 15\%$

The analytical data were in agreement with the literature (K. Geetharani, S. Tussupbayev, J. Borowka, M. C. Holthausen, S. Gosh, *Chem. Eur. J.* **2012**, *18*, 8482–8489).

1,2,4-Tris(4-chlorobutyl)benzene (28)



Following the general procedure A starting from 6-chloro-1-hexyne (0.50 mmol, 72.3 mg, 77.9 μ L) the compound **28** was obtained as a white solid (89%, 52.1 mg). $^1\text{H NMR}$ (300 MHz, CDCl_3 , ppm): δ 7.08-7.05 (m, 1H), 6.98-6.95 (m, 2H), 3.60-3.53 (m, 6H), 2.65-2.57 (m, 6H), 1.90-1.70 (m, 12H).

GC-MS (EI): m/z (relative intensity) 348 (35), 333 (100), 318 (25).

Amount of the 1,3,5-regioisomer (characteristic NMR signal at δ = 6.83ppm) according to $^1\text{H NMR}$: $(0.19/3)/[(1.00/1)+(0.19/3)]=6\%$.

The analytical data were in agreement with the literature (C. C. Eichman, J. P. Bragdon, J. P. Stambuli, *Synlett* **2011**, 8, 1109–1112).

Trimethyl 1,2,4-benzenetricarboxylate and Trimethyl 1,3,5-benzenetricarboxylate (29a + 29b)



Following the general procedure A starting from methyl propiolate (0.50 mmol, 42.0 mg, 44.5 μ L) the compound **29** was obtained as a white solid (26%, 11.2 mg).

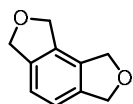
Trimethyl 1,2,4-benzenetricarboxylate $^1\text{H NMR}$ (400 MHz, CDCl_3): δ = 8.42 (d, J = 1.6 Hz, 1H), 8.20 (dd, J = 8.0, 1.7 Hz, 1H), 7.75 (d, J = 8.0 Hz, 1H), 3.96 (s, 3H), 3.94 (s, 6H).

Trimethyl 1,3,5-benzenetricarboxylate $^1\text{H NMR}$ (400 MHz, CDCl_3): δ = 8.86 (s, 3H); 3.98 (s, 9H).

Amount of the 1,3,5-regioisomer (characteristic NMR signal at δ = 8.86 ppm) according to $^1\text{H NMR}$: $(0.45/3)/[(1.00/1)+(0.45/3)]=13\%$.

GC-MS (EI): m/z (relative intensity) = 252 (10), 221 (100), 193 (10), 75 (20). The analytical data were in agreement with the literature (D. Brenna, M. Villa, T. N. Gieshoff, F. Fischer, M. Hapke, A. Jacobi von Wangelin, *Angew. Chem. Int. Ed.* **2017**, 56, 8451–8454).

1,3,6,8-Tetrahydro-2,7-dioxa-as-indacene (30)



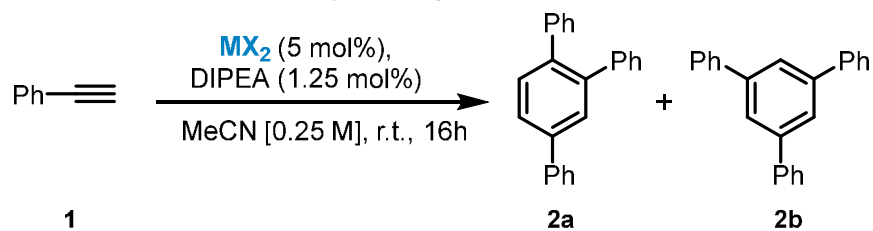
Following the general procedure A starting from 1,4-bis(prop-2-yn-1-yloxy)but-2-yne (0.50 mmol, 81.1 mg) the compound **30** was obtained as a white solid (42%, 33.8 mg). $^1\text{H NMR}$ (300 MHz, CDCl_3 , ppm): δ = 7.15 (s, 2H), 5.13 (s, 4H), 5.03 (s, 4H).

GC-MS (EI): m/z = 162 (100), 133 (30), 104 (15), 77 (40).

The analytical data were in agreement with the literature (A. Geny, N. Agenet, L. Iannazzo, M. Malacria, C. Aubert, V. Gandon, *Angew. Chem. Int. Ed.* **2009**, 48, 1810–1813).

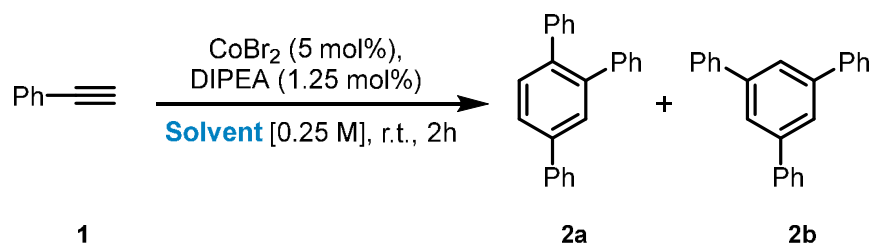
6.4.3 Extended optimization studies

Table 2. Optimization of metal salt and catalyst loading



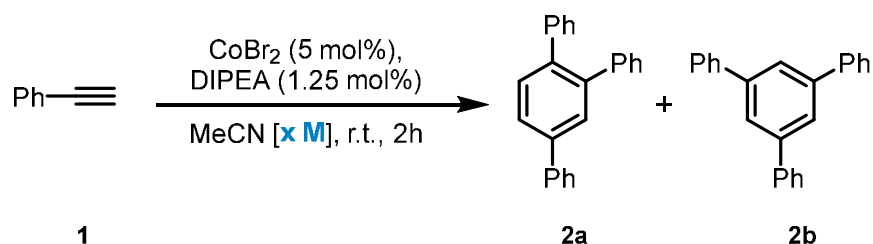
Entry	MX_2	Yield (%) ^(a)	Conversion (%)
1	FeBr_2	5	5
2	NiBr_2	0	0
3	CoCl_2	49	61
4	NiCl_2	0	0
5	FeBr_2 (DME)	5	31
6	CoBr_2	82	100
7	$\text{Co}(\text{OTf})_2$	33	40
8	$\text{Co}(\text{acac})_2$	0	0
9	MnBr_2	10	26
10	$\text{Co}(\text{OAc})_2$	0	0
11	$\text{Co}(\text{hmds})_2$	65 (8:2 products ratio)	100
12	–	0	0
13	CoBr_2 (10 mol%)	75	100
14	CoBr_2 (2.5 mol%)	51	70
15	CoBr_2 (air)	0	0
16	$[\text{Co}(\text{MeCN})_6][\text{CoBr}_3\text{MeCN}]_2$	83	100
17	$[\text{Co}(\text{MeCN})_6][\text{CoBr}_3\text{MeCN}]_2$ without DIPEA	0	5

(a) Determined by GC-FID analysis with dodecanenitrile as internal standard. Yields are given as combined yields of 1,2,4- and 1,3,5-regioisomers. Reaction setup according to general procedure A.

Table 3. Optimization of solvent

Entry	Solvent	Yield (%) ^(a)	Conversion (%)
1	DMF	0	0
2	Toluene	0	0
3	Hexanes	0	0
4	DEE	0	0
5	THF	0	0
6	MeCN	82	100

(a) Determined by GC-FID analysis with dodecanenitrile as internal standard. Yields are given as combined yields of 1,2,4- and 1,3,5-regioisomers. Reaction setup according to general procedure A.

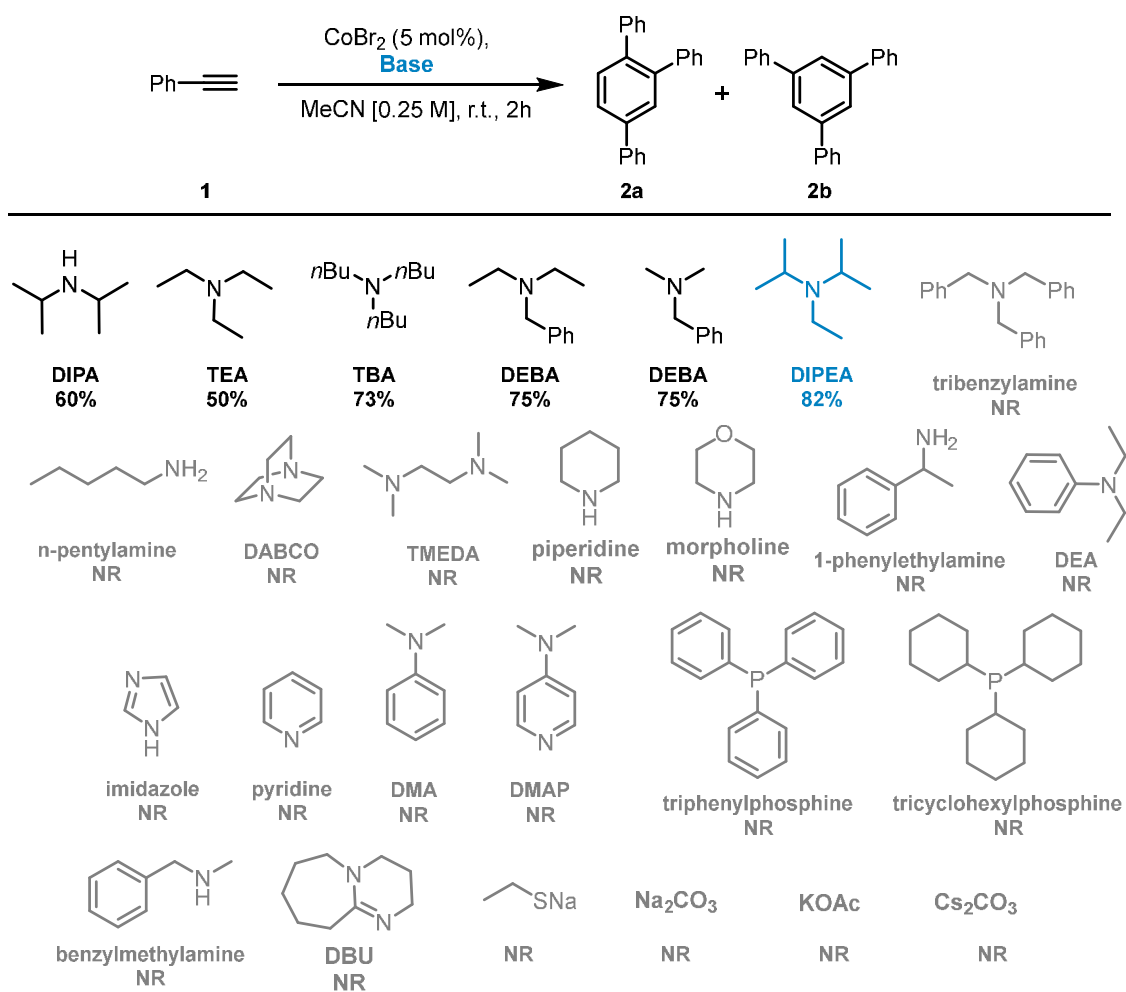
Table 4. Optimization of concentration

Entry	Concentration (M)	Yield (%) ^(a)	Conversion (%)
1	0.25	82	100
2	0.13	70	97
3	0.08	67	90
4	0.5	50	100

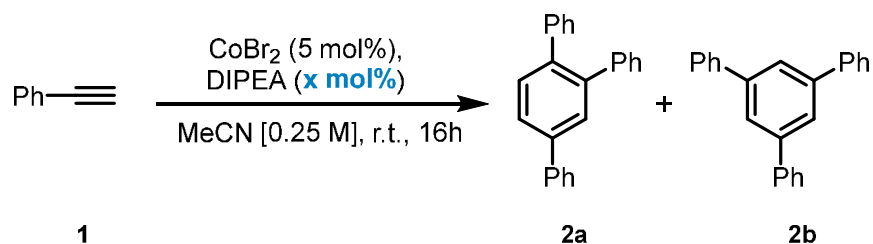
*The reaction time for entries 2 and 3 was prolonged to 6h to obtain a full conversion of s.m.

(a) Determined by GC-FID analysis with dodecanenitrile as internal standard. Yields are given as combined yields of 1,2,4- and 1,3,5-regioisomers. Reaction setup according to general procedure A.

Table 5. Optimization of base/ligand

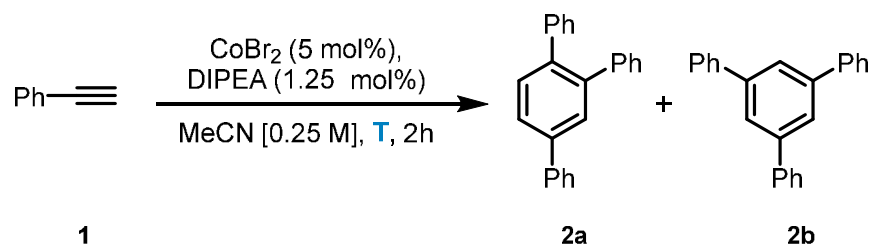


Determined by GC-FID analysis with dodecanenitrile as internal standard. Yields are given as combined yields of 1,2,4- and 1,3,5-regioisomers. Reaction setup according to general procedure A.

Table 6. Optimization of base loading

Entry	DIPEA (mol%)	Yield (%) ^(a)	Conversion (%)
1	10	70	100
2	5	74	100
3	2.5	79	100
4	1.25	82	100
5	–	0	nd

(a) Determined by GC-FID analysis with dodecanenitrile as internal standard. Yields are given as combined yields of 1,2,4- and 1,3,5-regioisomers. Reaction setup according to general procedure A.

Table 7. Optimization of temperature

Entry	T (°C)	Yield (%) ^(a)	Conversion (%)
1	r.t.	82	100
2	0	39	50
3*	70	80	100

*the total conversion was achieved in less than 1h.

(a) Determined by GC-FID analysis with dodecanenitrile as internal standard. Yields are given as combined yields of 1,2,4- and 1,3,5-regioisomers. Reaction setup according to general procedure A.

6.4.4 Mechanistic experiments

Kinetics

CoBr₂ (0.025 mmol, 0.05 equiv.) or [Co(MeCN)₆][CoBr₃MeCN]₂ (0.025mmol, 0.05 equiv.) were dissolved in acetonitrile (2.0 mL). Hünig's base (0.00625 mmol, 0.0125 equiv.), phenylacetylene (0.5 mmol, 1.0 equiv.) and dodecanenitrile (50 μL) were added consecutively. The reaction mixture was stirred in the glovebox at ambient temperature. Aliquots of 50 μL were taken within the given time intervals. These aliquots were directly quenched with *p*-toluenesulfonic acid (ca 5 mg) inside the glovebox. After the completion, workup and GC-FID analysis was performed according to General Method A.

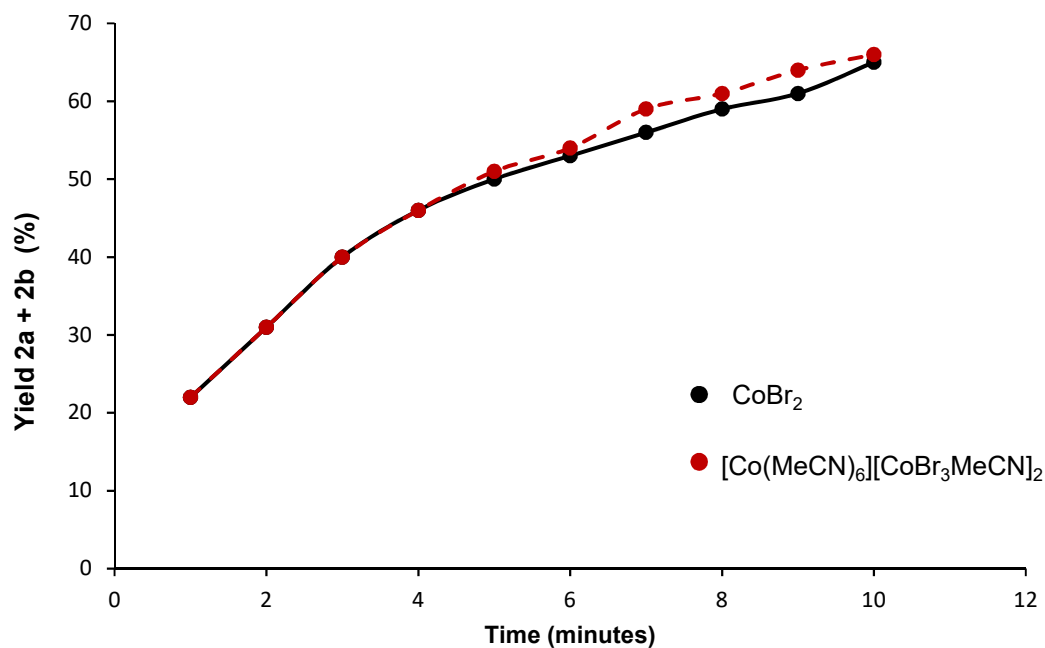


Figure 7—Yield vs. time diagram of the model reaction with different Cobalt sources. Yield was determined by GC-FID analysis with dodecanenitrile as internal standard. The data were normalized to show the similarity between the two systems.

Light irradiation

CoBr₂ (0.025 mmol, 0.05 equiv.) was dissolved in acetonitrile (2.0 mL). Hünig's base (0.00625 mmol, 0.0125 equiv.), phenylacetylene (0.5 mmol, 1.0 equiv.) and dodecanenitrile (50 μ L) were added consecutively. The reaction mixture was stirred in the glovebox at ambient temperature and irradiated with a 410 nm LED. Aliquots of 50 μ L were taken within the given time intervals. These aliquots were directly quenched with *p*-toluenesulfonic acid (ca. 5 mg) inside the glovebox. After the completion, workup and GC-FID analysis was performed according to General Method A.

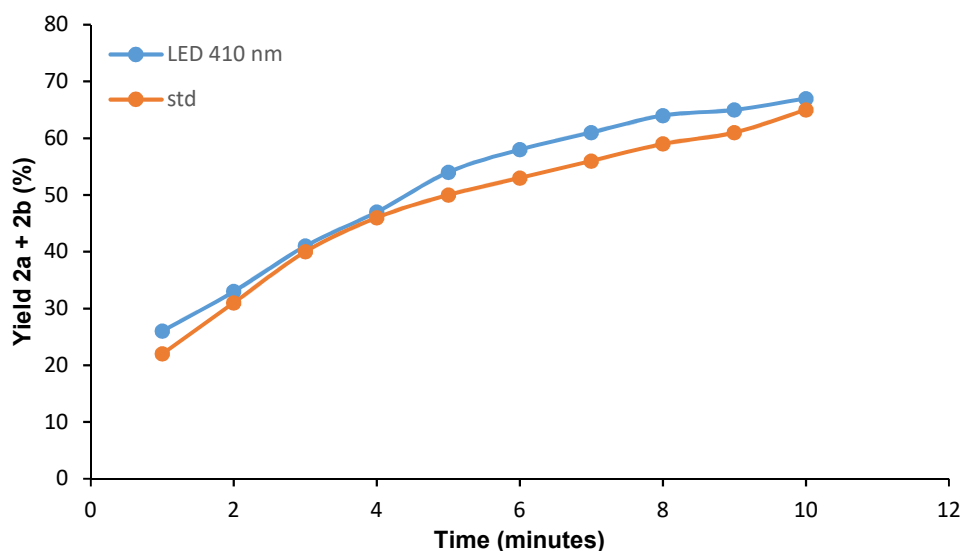


Figure 8—Yield vs. time diagram of the model reaction with and without light irradiation. Yield was determined by GC-FID analysis with dodecanenitrile as internal standard.

Poisoning experiments

CoBr₂ (0.025 mmol, 0.05 equiv.) was dissolved in acetonitrile (2.0 mL). Hünig's base (0.00625 mmol, 0.0125 equiv.), phenylacetylene (0.5 mmol, 1.0 equiv.) and dodecanenitrile (50 μL) were added consecutively. The reaction mixture was stirred in the glovebox at ambient temperature. Aliquots of 50 μL were taken within the given time intervals. These aliquots were directly quenched with *p*-toluenesulfonic acid (ca 5 mg) inside the glovebox. After three minutes from the start of the reaction a stock solution of dct (50 μmol in 100 μL, 0.1 equiv.) or P(OMe)₃ (5 μmol in 100 μL, 0.01 equiv.) or PMe₃ (5 μmol in 100 μL, 0.01 equiv.) was added to the reaction mixture. For the rest of the reaction time aliquots were taken as described before. After the completion of the reaction, workup and GC-FID analysis was performed according to General Method A.

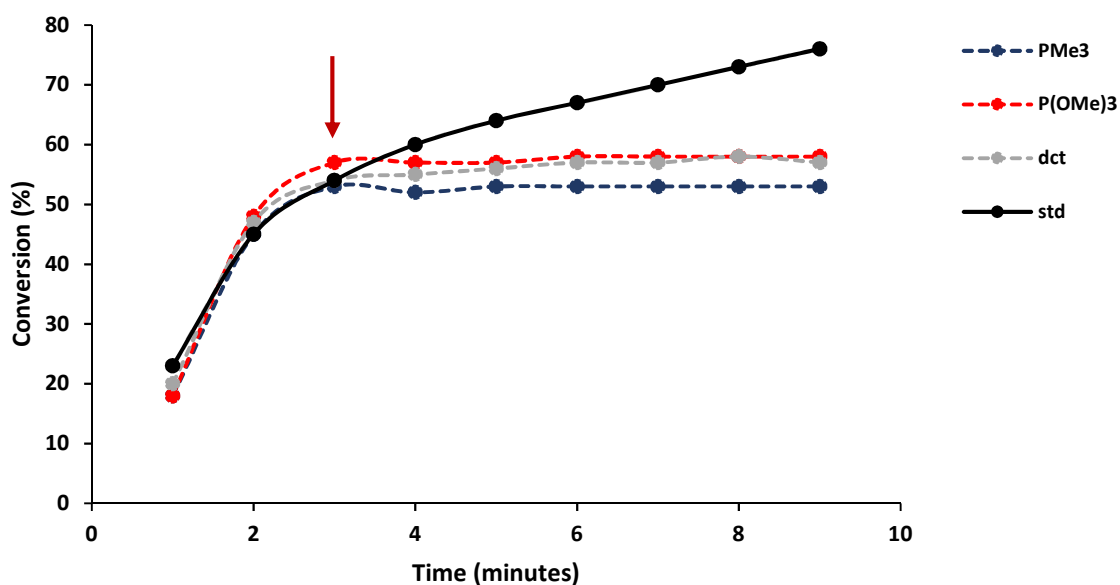


Figure 9– Conversion vs. time diagram of the model reaction with addition of different poisoning agents. The yield was determined by GC-FID analysis with dodecanenitrile as internal standard.

Typical poison agents were chosen to distinguish between homotopic and heterotopic systems.

PMe₃ and P(OMe)₃, strong field ligands, are effectively quenching any reactivity immediately after their addition even in low loadings as 1 mol%. The reaction inhibition in presence of such small poison concentration can be compatible with a heterotopic system whereas the surface active sites are relatively few and a low concentration of poison result in complete inhibition. Nevertheless, our system is totally incompatible with phosphines (also sterically hindered or with different electronics) due to their nature as good ligands for both Co(II) and Co(I) species. For this reason this result should be critically evaluated and can't stand alone as proof of a heterotopic system.

Dct (Dibenzo[a,e]cyclooctatetraene) is recognized as a homotopic poison due to its ability to selectively bind to molecular metal-ligand complexes. An inhibition of reaction is detected after addition of dct (10 mol%). In this case the poison effect is molecule specific whereas other alkenes are tolerated in the reaction mixture without altering the reaction outcome (respectively 2-vinylnaphthalene or 1-octene 10 mol% were tested).

Kinetic isotope effect (KIE)

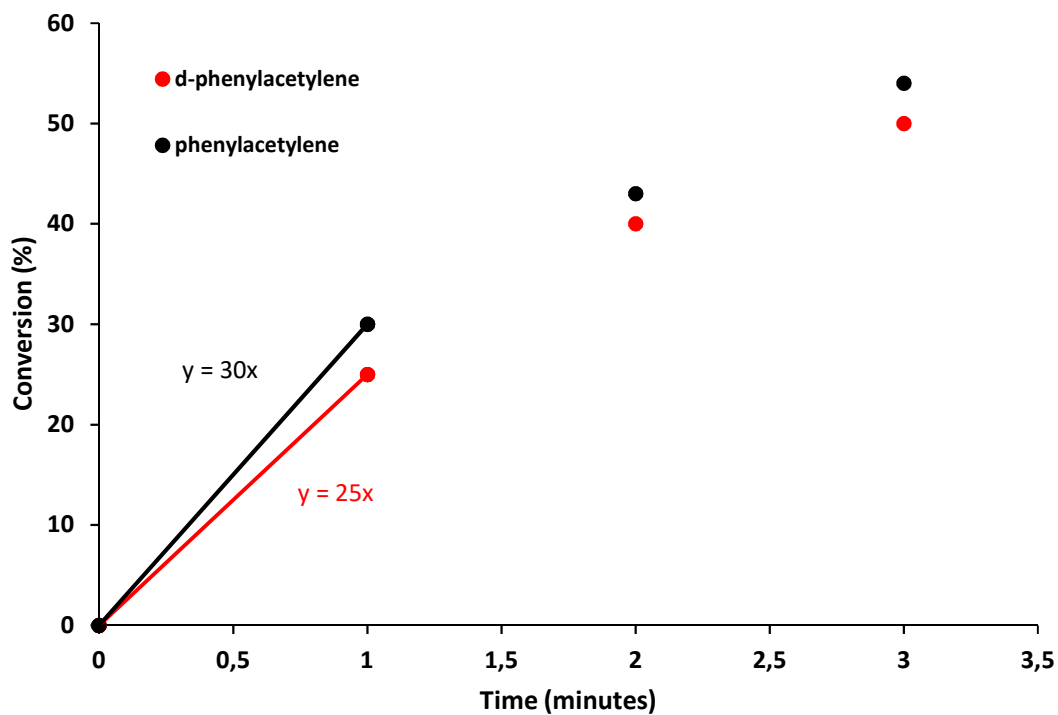


Figure 10. Initial kinetic rate calculated with phenylacetylene and deuterio-phenylacetylene as substrates.

KIE= 1.20

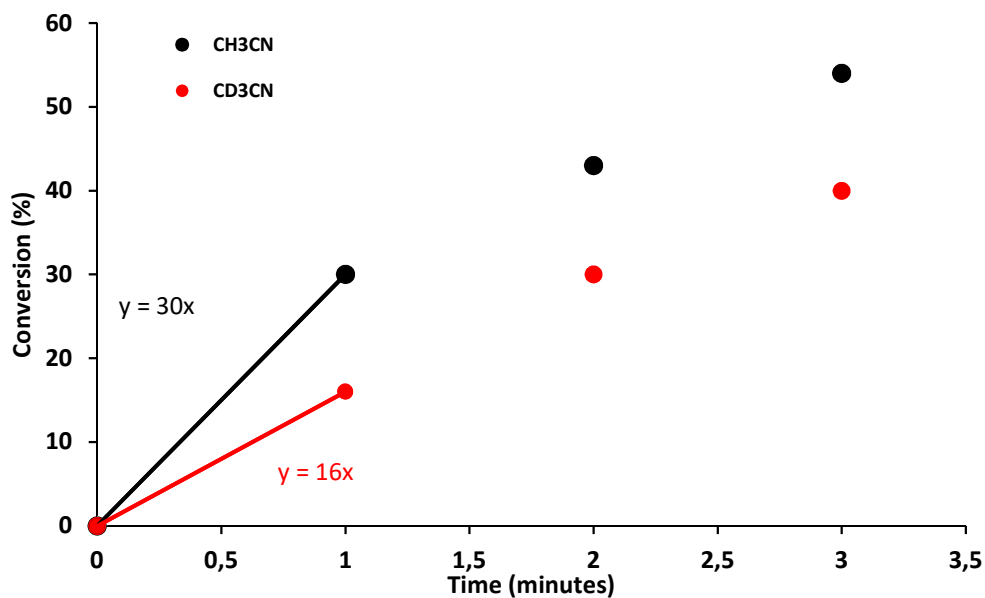


Figure 11. Initial kinetic rate calculated with acetonitrile and deuterated acetonitrile as solvents.

KIE= 1.85

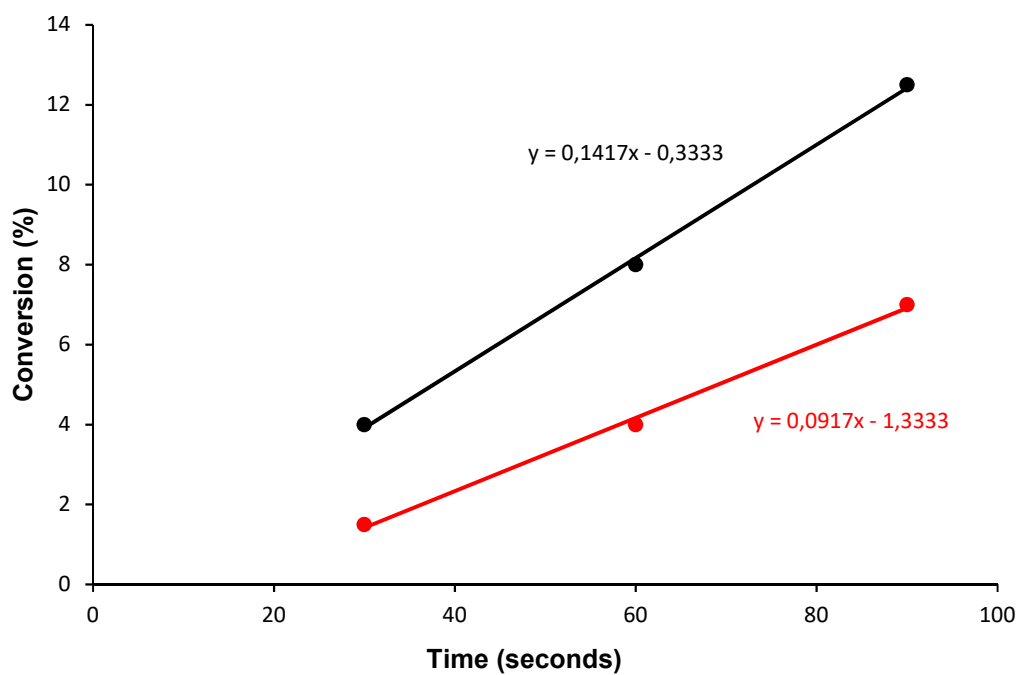


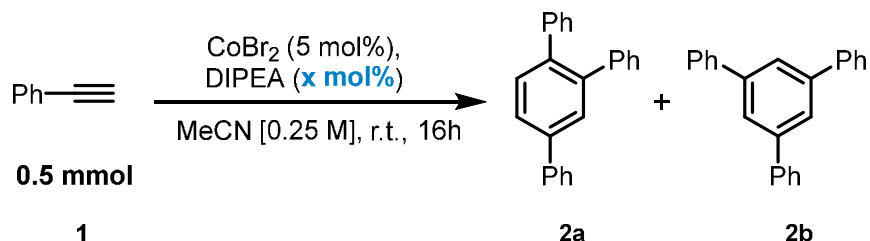
Figure 12. Initial kinetic rate calculated with triethylamine and triethylamine-d₁₅ as bases.

KIE= 1.54 (stock solutions were used for amines instead of directly addition of 1 μ L)

Reaction orders

The reaction velocity (v) was determined at small conversions as the consumption of phenylacetylene per time period in mmol per second.

Table 8. Determination of reaction orders –varying amount of DIPEA.



Amount of DIPEA	c (DIPEA) [mol/L]	log c	v ^(a) (mmol/s)	log v
0.5 mol%	0,00125	-2,90309	0	0
1 mol%	0,0025	-2,60206	0,000617	-3,20971
1.5 mol%	0,00375	-2,42597	0,00131	-2,88273
2 mol%	0,005	-2,30103	0,0015	-2,82391
3 mol%	0,0075	-2,12494	0,00333	-2,47756
5 mol%	0,0125	-1,90309	0,004	-2,39794

(a) Determined by GC-FID analysis with dodecanenitrile internal standard. Reaction setup according to general method A.

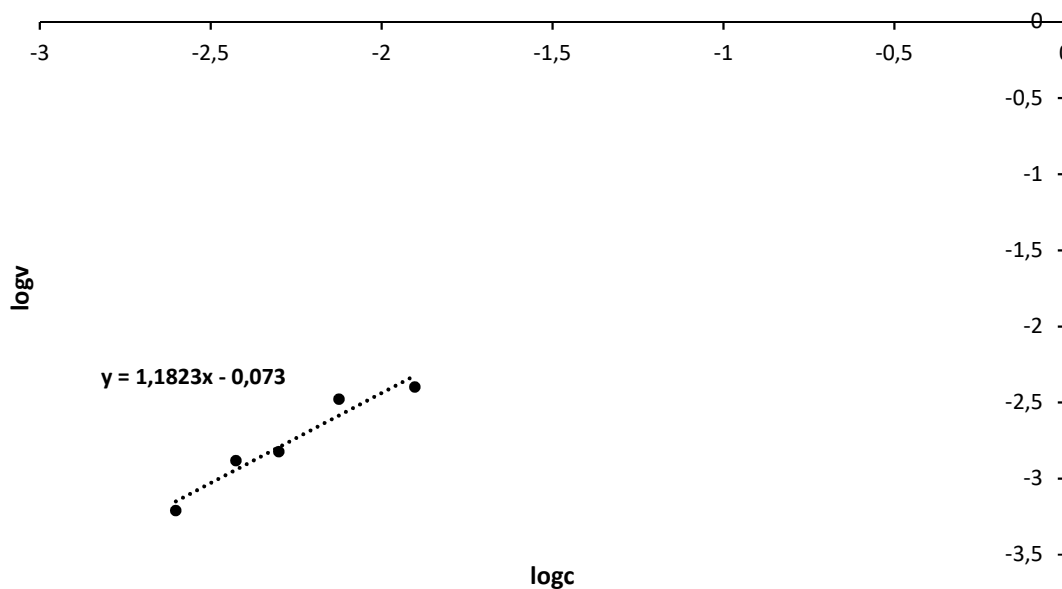
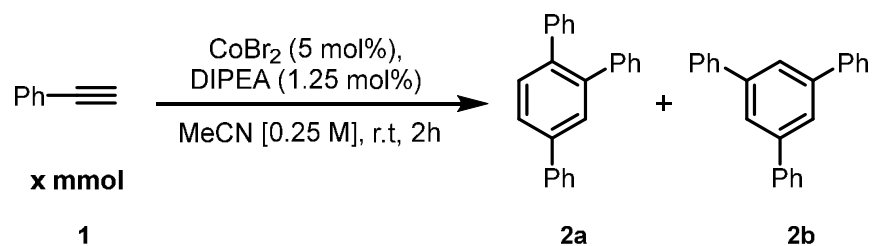
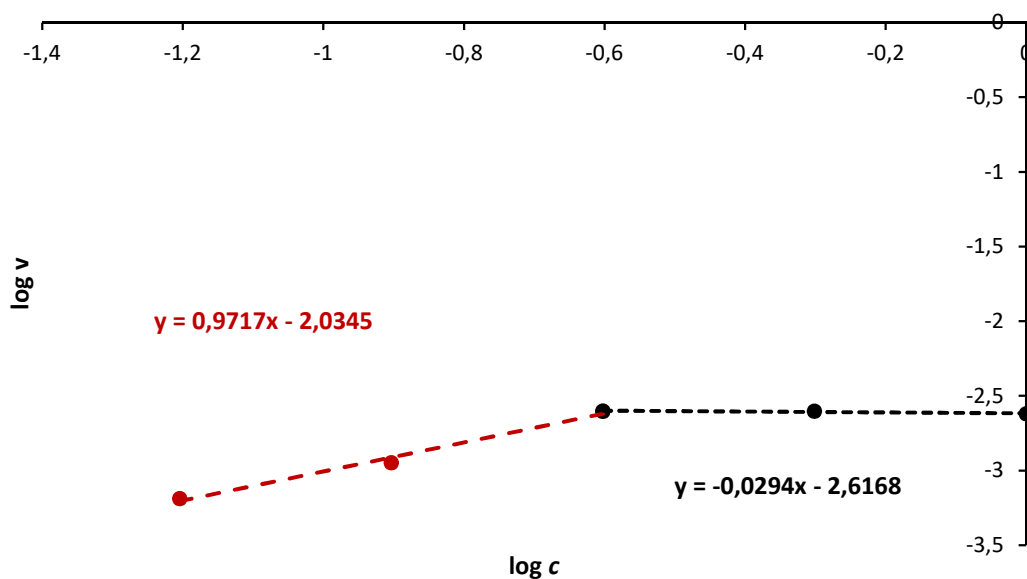


Figure 13. For loadings of DIPEA higher than 5 mol% the reaction order is 0.

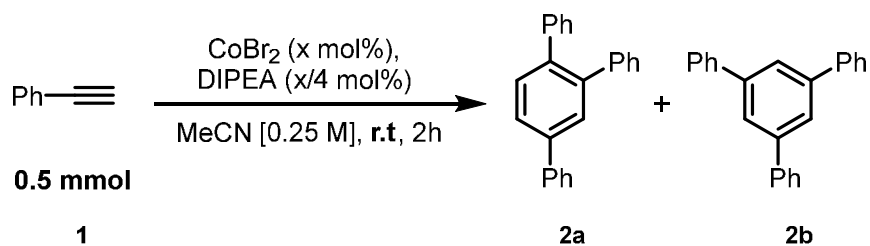
Table 9. Determination of reaction orders –varying amount of Phenylacetylene

Amount of PhCCH	c (PhCCH) [mol/L]	log c	v ^(a) (mmol/s)	log v
0.125 mmol	0,0625	-1,20412	0,00065	-3,82391
0.25 mmol	0,125	-0,90309	0,00113	-3,63827
0.5 mmol	0,25	-0,60206	0,0025	-3,20761
1 mmol	0,5	-0,30103	0,0025	-3,04576
2 mmol	1	0	0,0026	-3,02228

(a) Determined by GC-FID analysis with dodecanenitrile internal standard. Reaction setup according to general method A.

**Figure 14.** Determination of reaction order under varying amounts of phenylacetylene.

The reaction order in phenylacetylene (for concentrations between 0.06 and 0.25 M) is 1st, for higher concentrations of starting material the order is 0 (the conversions are very low, the catalyst is poisoned).

Table 10. Determination of reaction orders –varying amount of CoBr₂

Amount of CoBr ₂	c (CoBr ₂) [mol/L]	log c	v ^(a) (mmol/s)	log v
1.5 mol%	0,00375	-2,42597	0,000167	-3,77728
2 mol%	0,005	-2,30103	0,000167	-3,77728
2.5 mol%	0,00625	-2,20412	0,00033	-3,47756
3.5 mol%	0,00875	-2,05799	0,00058	-3,23411
5 mol%	0,0125	-1,90309	0,00167	-2,77728
7.5 mol%	0,01875	-1,727	0,003167	-2,49935

(a) Determined by GC-FID analysis with dodecanenitrile internal standard. Reaction setup according to general method A.

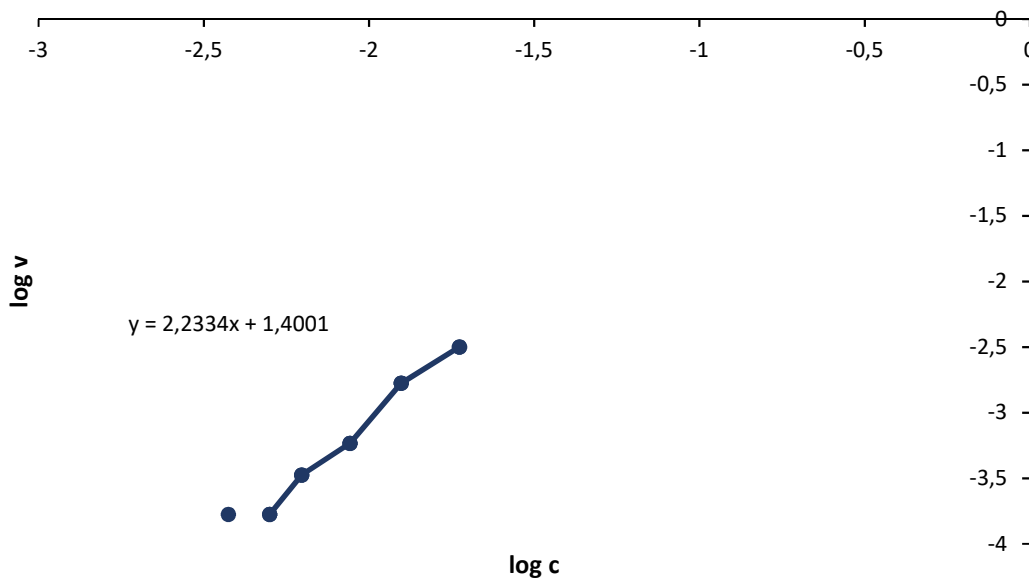
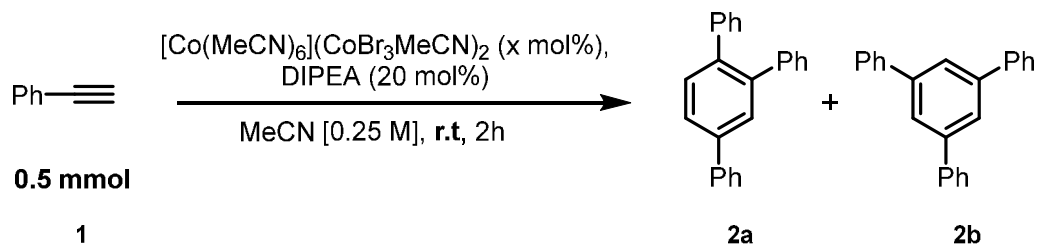
**Figure 15.** Determination of reaction order under varying amounts of CoBr₂ with constant ratio (4:1) between CoBr₂ and DIPEA.

Table 11. Determination of reaction orders –varying amount of $[\text{Co}(\text{MeCN})_6](\text{CoBr}_3\text{MeCN})_2$



Amount of $[\text{Co}(\text{MeCN})_6](\text{CoBr}_3\text{MeCN})_2$	c (Co-complex) [mol/L]	log c	v ^(a) (mmol/s)	log v
1 mol%	0,0025	-2,60206	0,003	-3,10329
2.5 mol%	0,0063	-2,20066	0,0042	-2,91662
5 mol%	0,013	-1,88606	0,0078	-2,80595
7.5 mol%	0,019	-1,72125	0,0083	-2,73593
10 mol%	0,025	-1,60206	0,0083	-2,69108

(a) Determined by GC-FID analysis with dodecanenitrile internal standard. Reaction setup according to general method A.

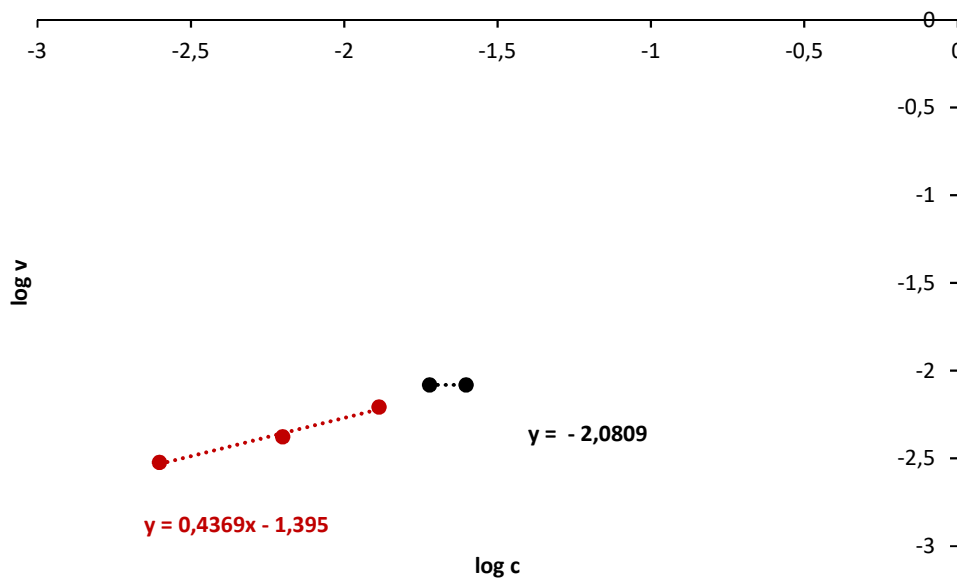


Figure 16. The reaction order in $[\text{Co}(\text{MeCN})_6](\text{CoBr}_3\text{MeCN})_2$ is 0.44 for catalyst loadings between 1-5 mol% and it becomes 0 order for high loadings in co-complex since all the starting material is immediately consumed in 1 min.

UV/VIS Absorption Spectroscopy

The samples were prepared in an argon filled glovebox using a 10 mm quartz cuvette with a screwing cap to keep the inert atmosphere. The spectra were recorded immediately after the preparation using an Agilent Cary 5000 UV/VIS NIR double beam spectrometer.

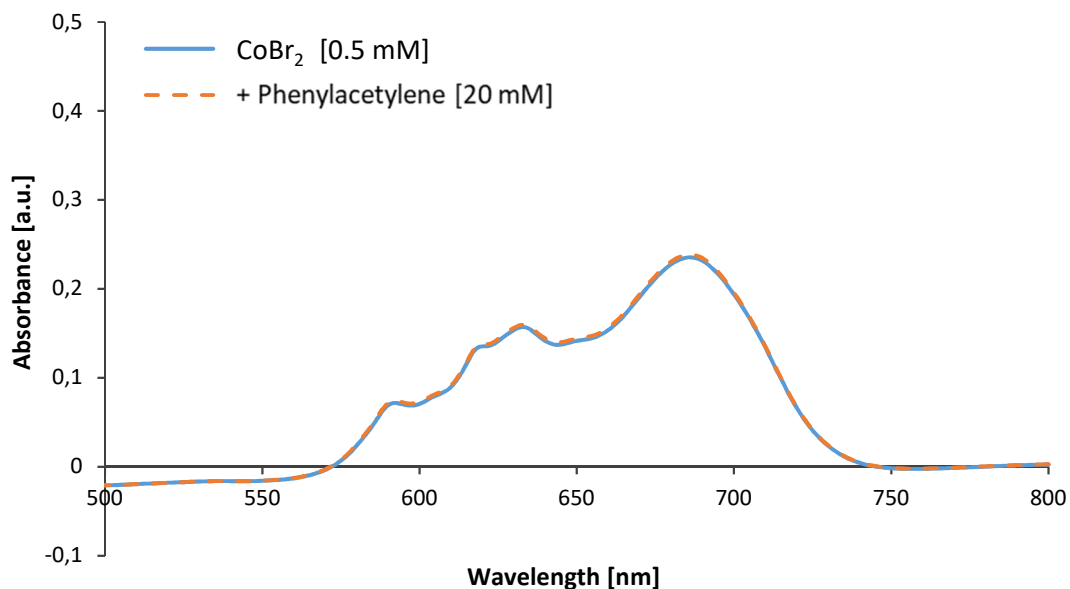


Figure 17. UV-Vis absorption spectrum of a solution of pure CoBr₂ in acetonitrile [0.5 mM, blue line] and the same sample after addition of phenylacetylene [20 mM, orange dotted line].

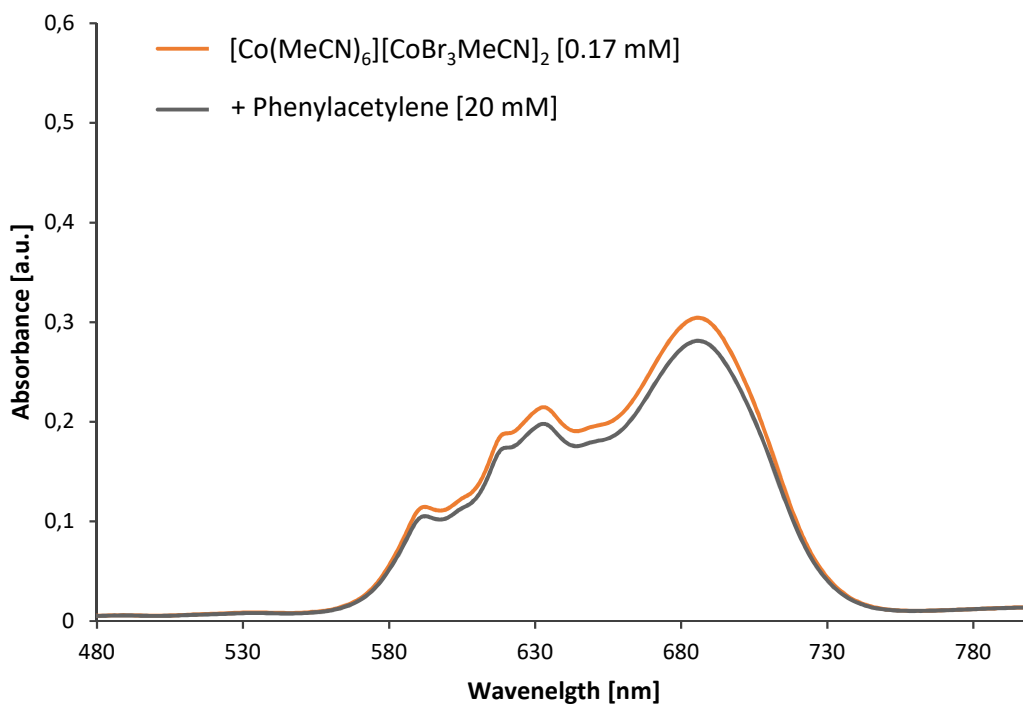


Figure 18. UV-Vis absorption spectrum of a solution of [Co(MeCN)₆][CoBr₃MeCN]₂ in acetonitrile [0.17 mM, orange line] and the same sample after addition of phenylacetylene [20 mM, grey line].

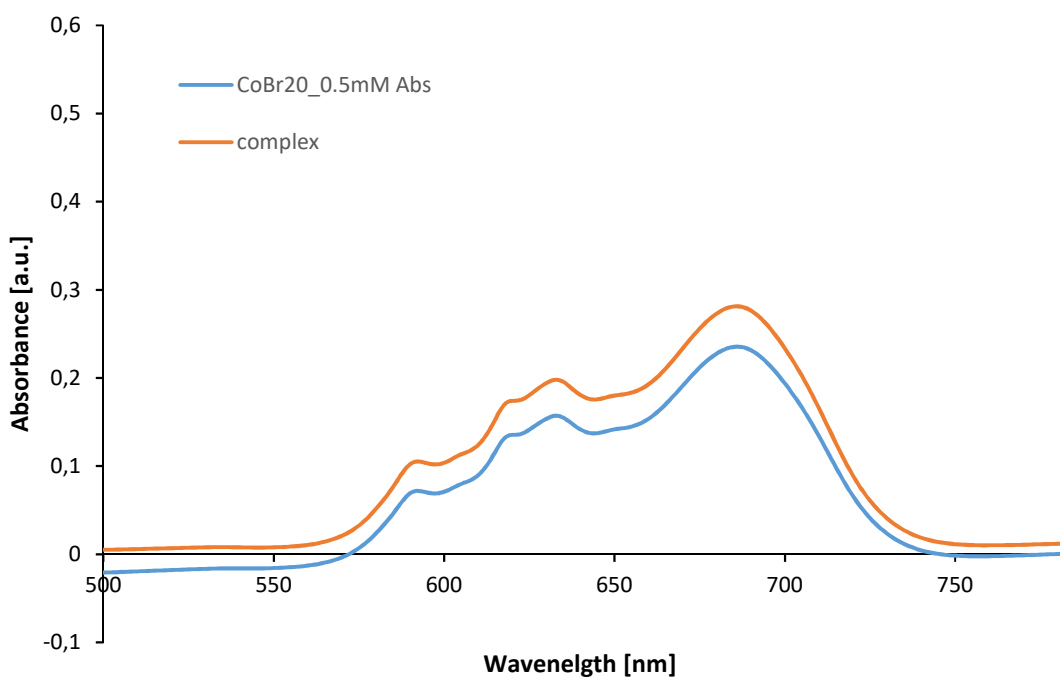


Figure 19. UV-Vis absorption spectrum of a solution of $[\text{Co}(\text{MeCN})_6][\text{CoBr}_3\text{MeCN}]_2$ in acetonitrile [0.17 mM, orange line] and pure CoBr_2 in acetonitrile [0.5 mM, blue line].

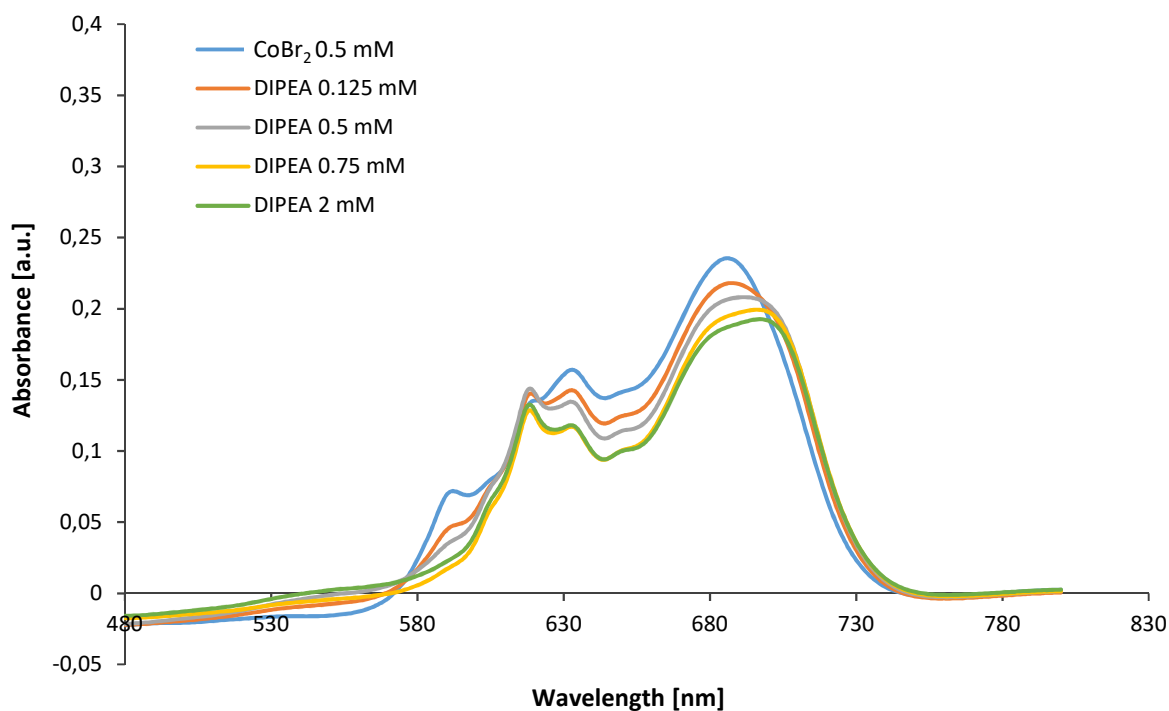


Figure 20. UV-Vis absorption spectrum of a solution of CoBr_2 in acetonitrile [0.17 mM, blue line] and after addition of increasing amounts of DIPEA.

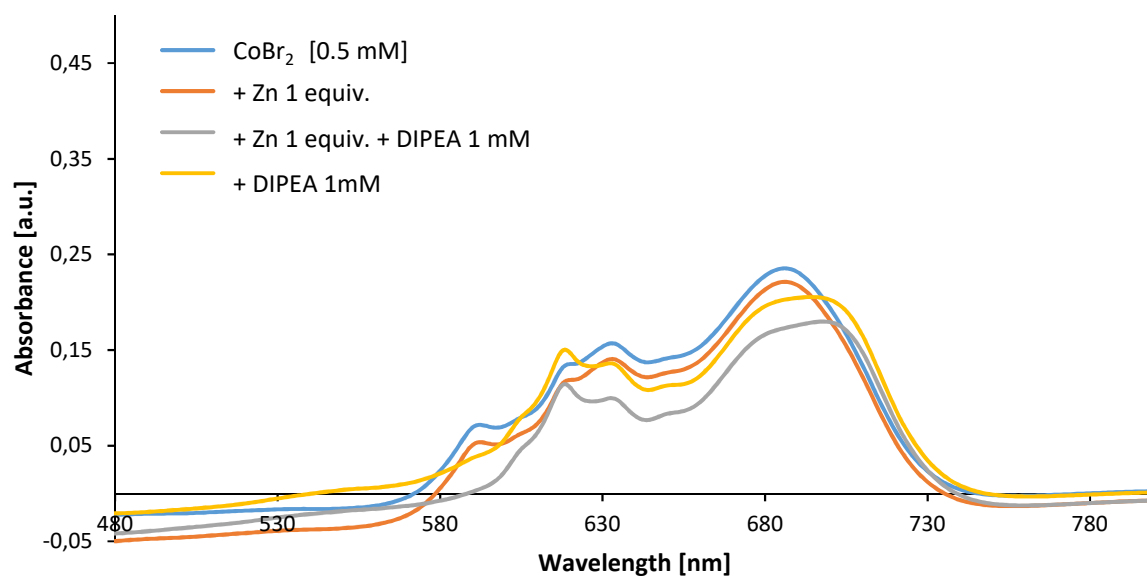


Figure 21. UV-Vis absorption spectrum of a solution of CoBr₂ in acetonitrile [0.17 mM, blue line]; after addition of 1 equiv. of Zn dust (the solution was stirred for 20 minutes in the glovebox and then filtered with a syringe filter before the acquisition, orange line), after addition of 1 equiv. of Zn dust and DIPEA 1 mM (grey line) and in presence of only DIPEA (1 mM, yellow line).

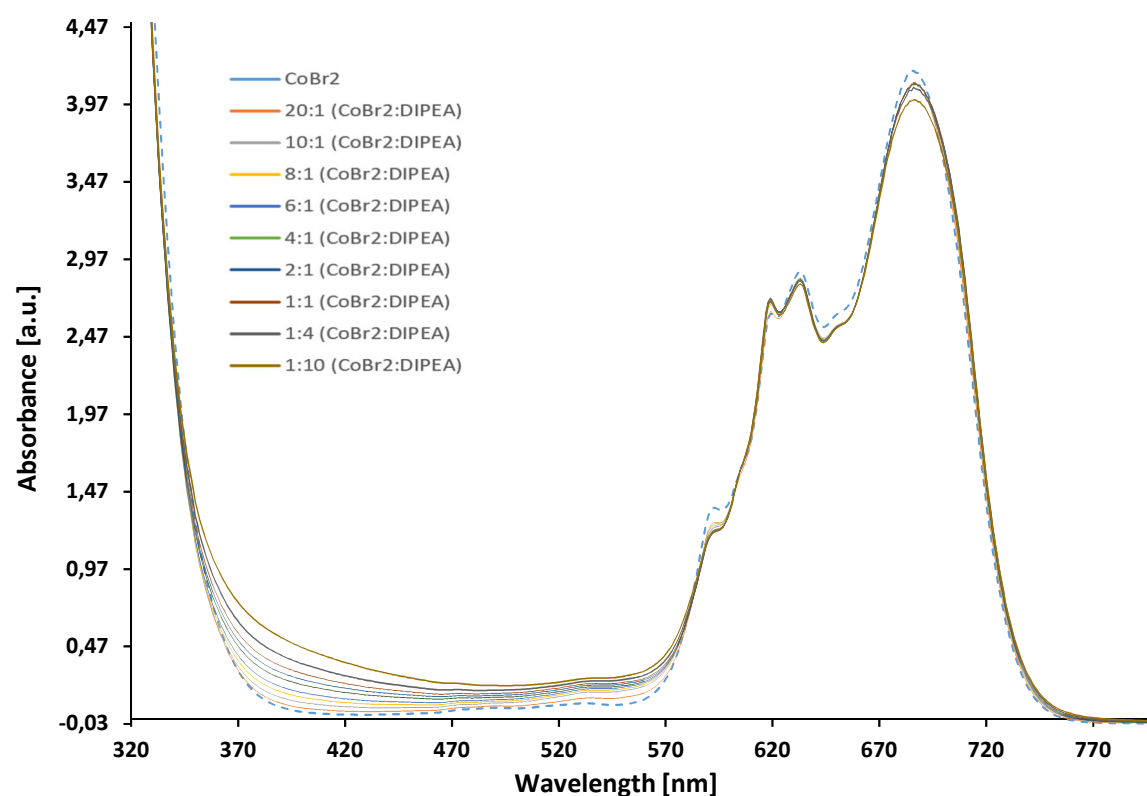


Figure 22. UV-Vis: A solution of CoBr₂ in acetonitrile [6.6 mM, 0.02 mmol] was transferred to a modified quartz cuvette with a screw cap in the glovebox. Spectra were recorded in sequence immediately after the addition of increasing amount of DIPEA [from 1 μ mol to 0.2 mmol].

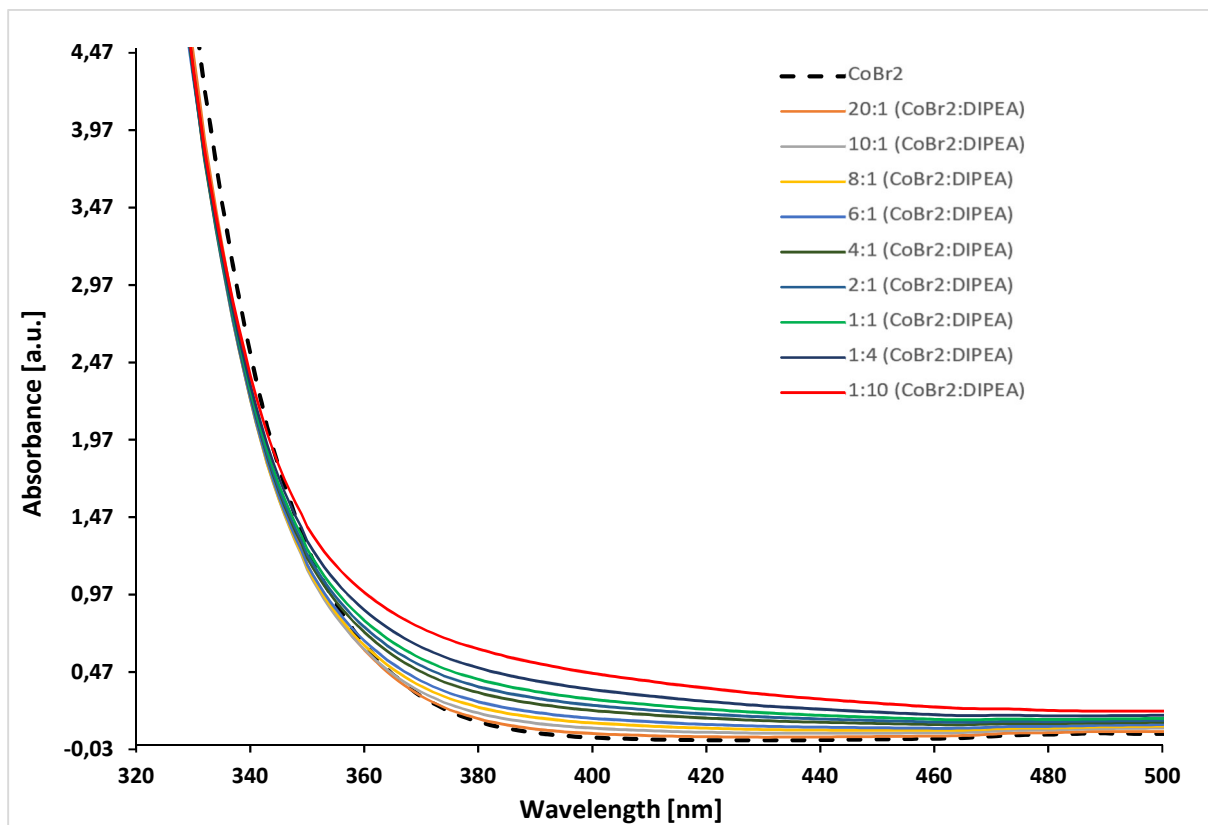


Figure 23. Zoom of the first isosbestic point (ca. 350 nm) in the region 320 - 500 nm.

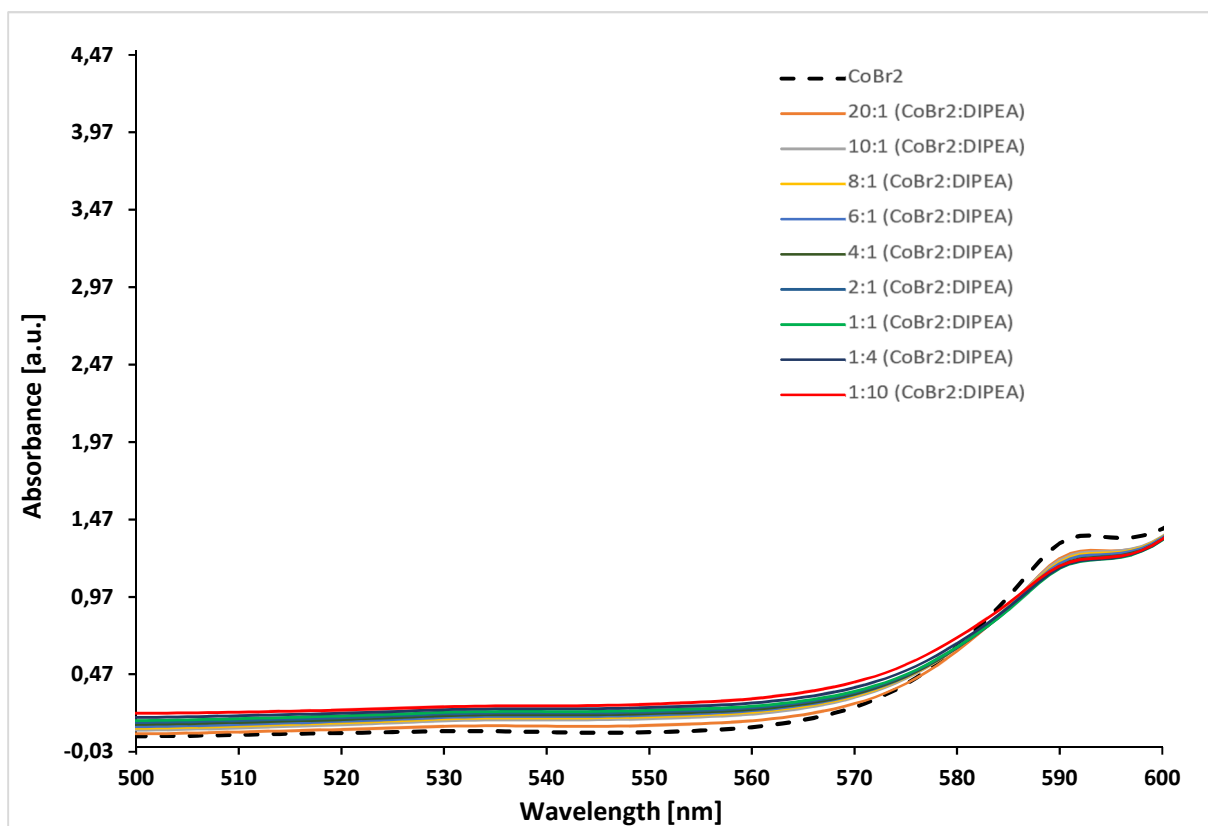


Figure 24. Zoom of the second isosbestic point (ca. 580 nm) in the region 500 - 600 nm.

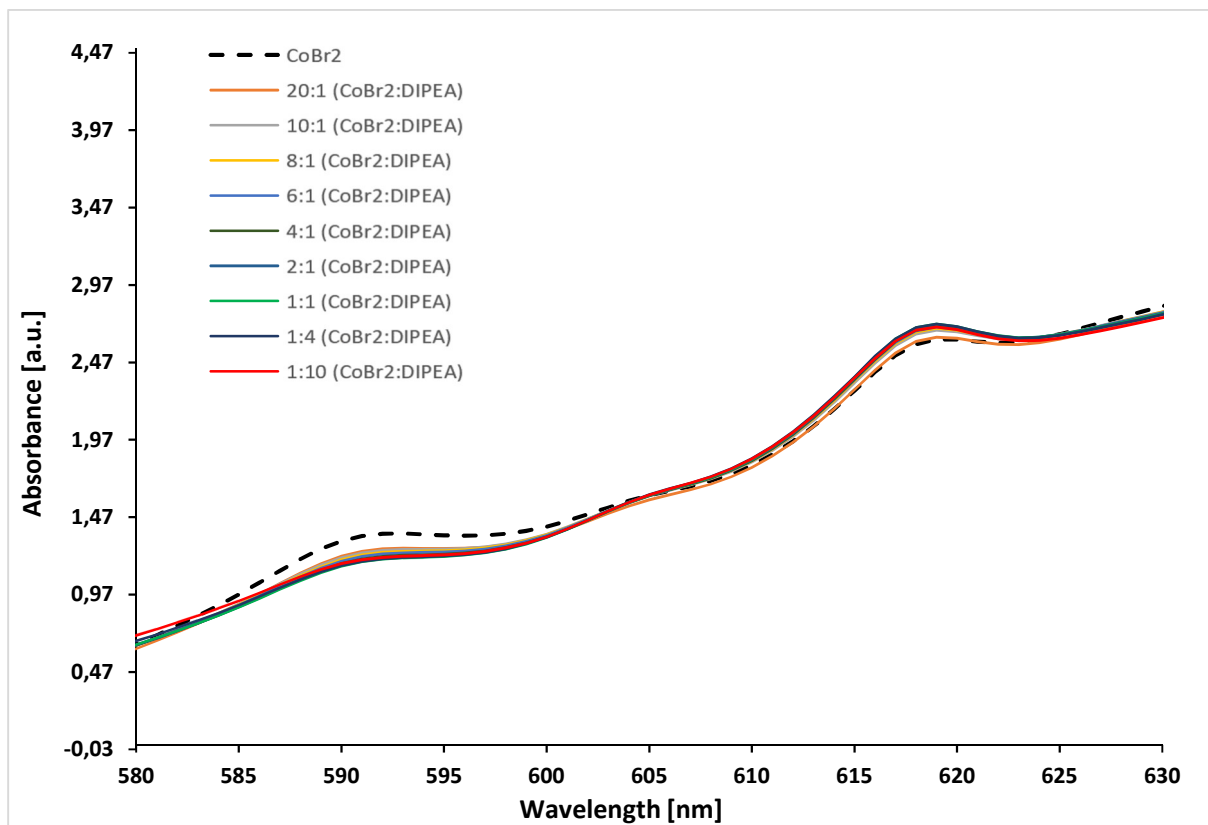


Figure 25. Zoom of the third and fourth isosbestic points (ca 609 and 625 nm) in the region 580 - 630 nm.

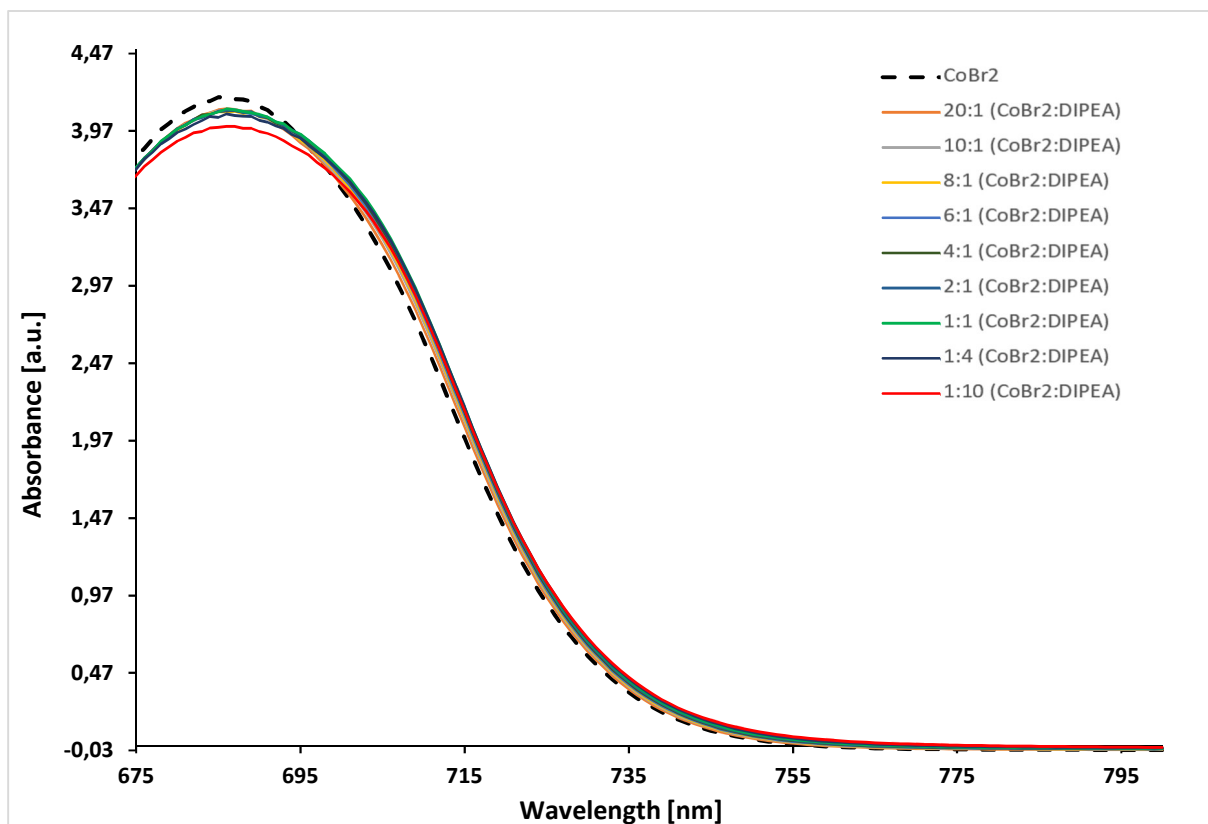
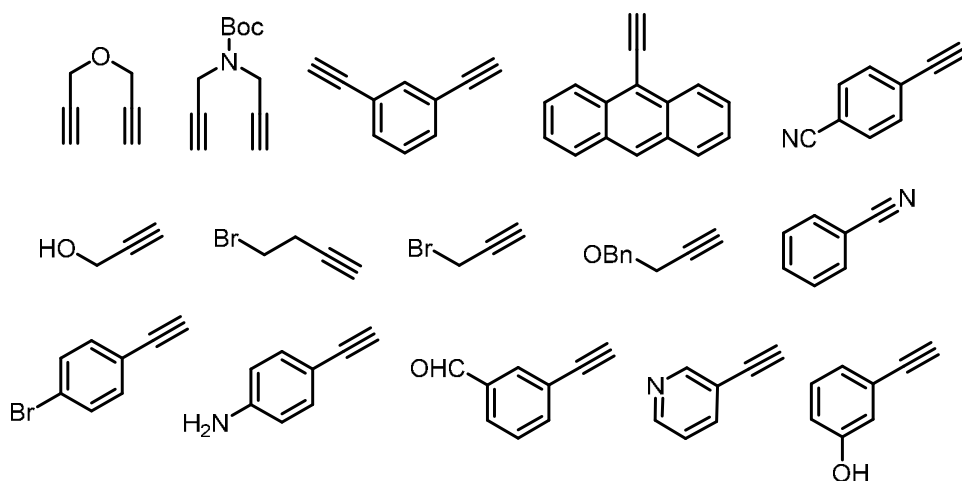
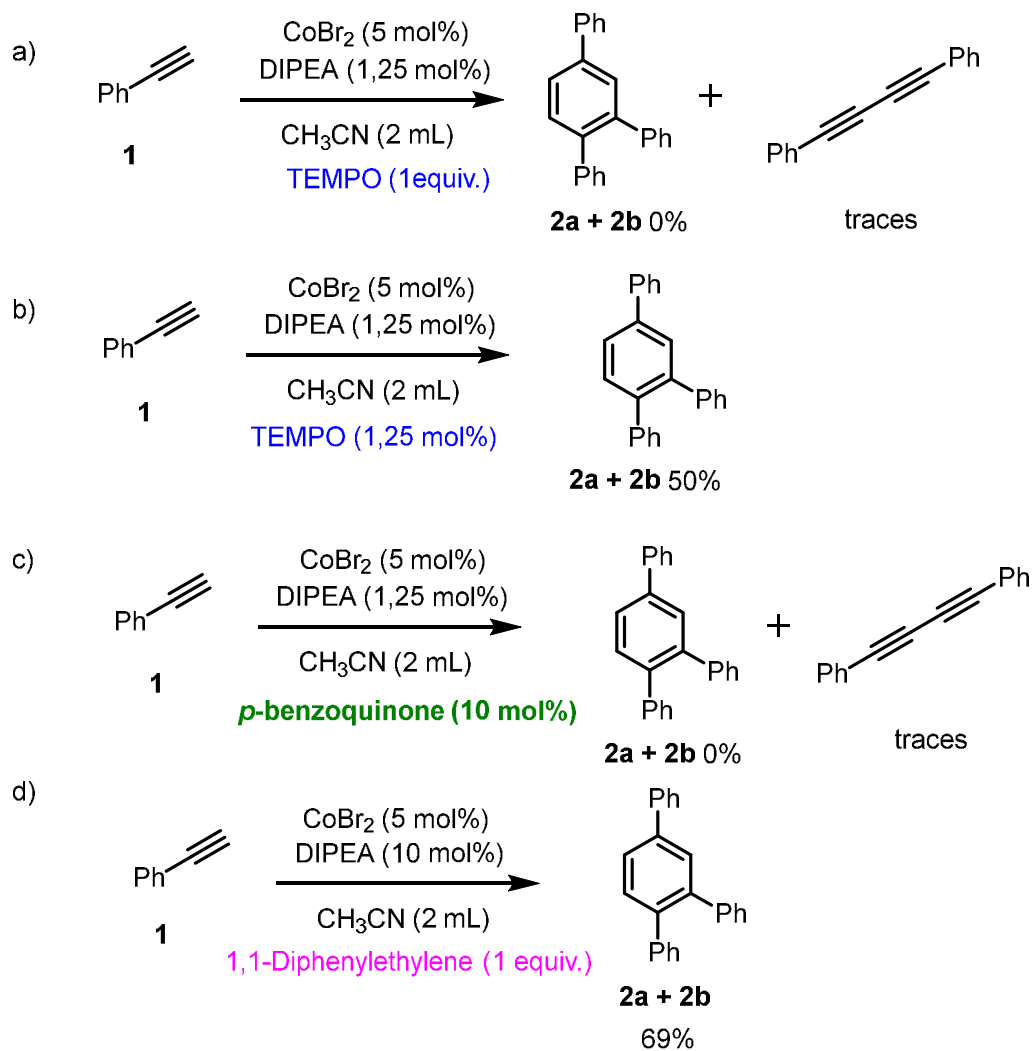


Figure 26. Zoom of the fifth isosbestic point (ca 700 nm) in the region 675 - 800 nm.

Unsuccessful Substrates



Experiments with Radical Trapping Agents



*TEMPO was added from the beginning together with CoBr₂.

Reaction Quench with O₂

Following the general procedure A the reaction was quenched with O₂ gas after 1, 2 or 10 minutes respectively. The crude of reaction was filtered over silica and analyzed by GC/MS. In all the cases no oxidation products were observed, in particular no benzaldehyde (from a possible vinylidene intermediate) was detected.

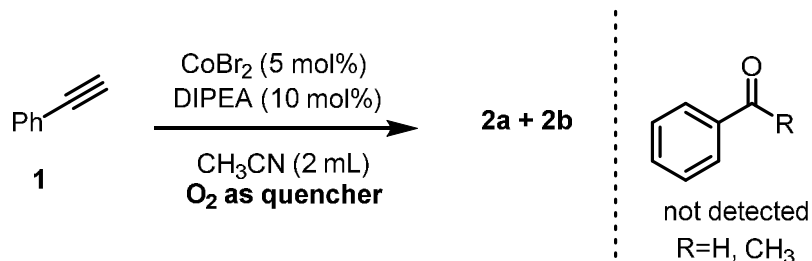
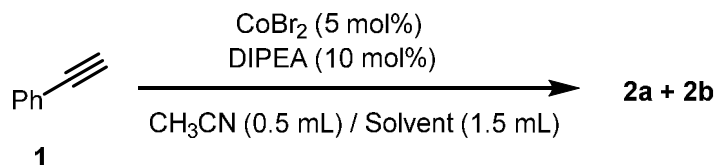


Figure 27. Quench of a standard reaction with O₂.

Screening of Solvent Mixtures and Different Nitriles

Following the general procedure A the reaction was performed in presence of solvent mixtures or nitriles, different from acetonitrile, as solvents.



Solvent:

-Hexanes: 93% yield, 100% conversion

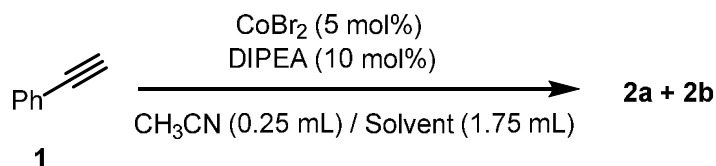
-THF 36% yield, 38% conversion

-DCE: no conversion

-NMP, no conversion

-Toluene: 80% yield, 100% conversion

-Pentane: 98%yield, 100%conversion



Solvent:

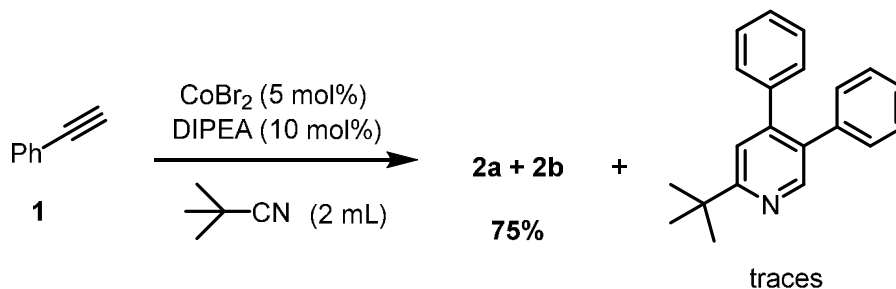
-Hexanes: 83% yield, 95% conversion

-Toluene: 30% yield, 40% conversion

*The solubility of CoBr₂, on our mmol scale according to procedure A, is not achieved if MeCN < than 0.25 mL (20 equiv) and no conversion occurred in those cases.

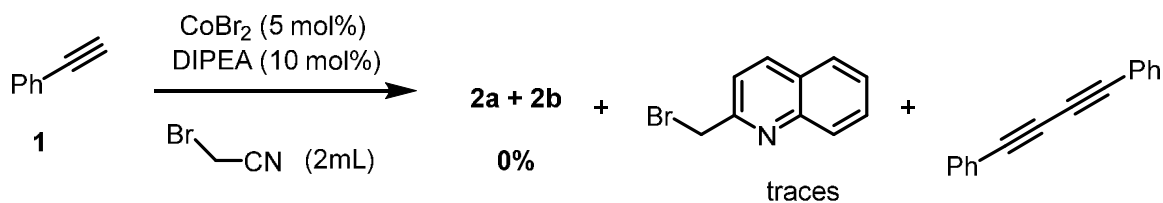
The following reactions were run in nitriles different from MeCN as solvent, in the same concentration.

a) Pivalonitrile (has no acidic α -hydrogen)



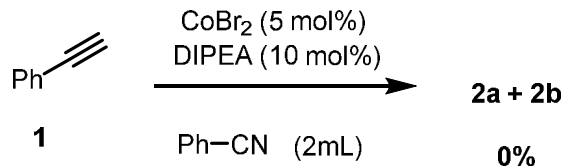
According to this experiment could be excluded the involvement of acidic α -hydrogen in the acetonitrile as part of the activation mechanism.

b) α -bromoacetonitrile (redox active nitrile)



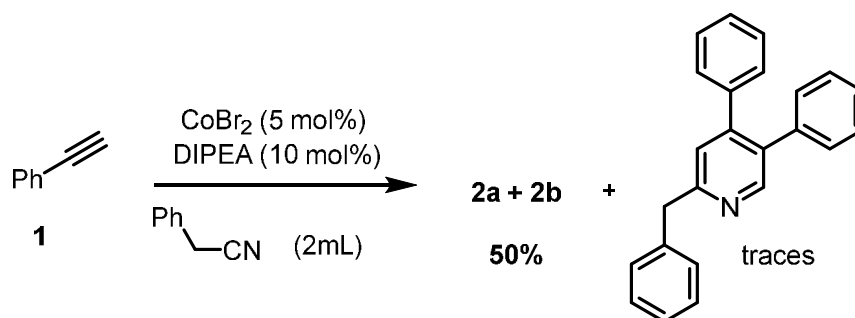
In this case the possible reduction of the bromo nitrile by Co(I) species is quenching the cyclotrimerization reaction.

c) Benzonitrile

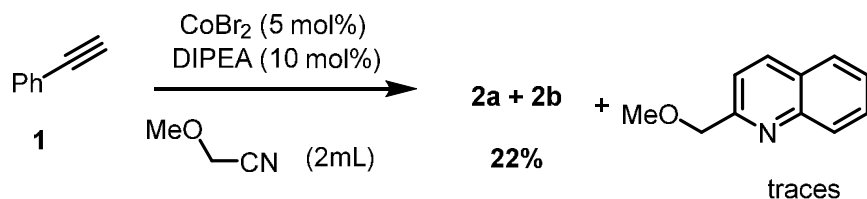


The reaction mixture is very poor soluble in benzonitrile.

d) Benzylcyanide



e) α -Methoxyacetonitrile

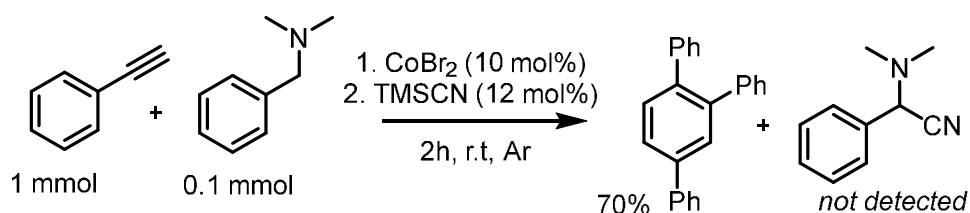


Attempt to Detect or Exclude the Presence of Amine Oxidation Byproducts (imine or aldehyde and amine after aqueous work-up):

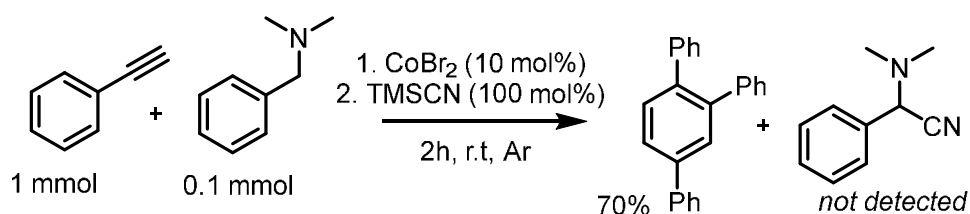
From big scale reactions and reaction run with higher molecular weight amines as NBu_3 or N,N -diethylbenzylamine no byproducts were observed (of a possible β -hydride elimination or SET oxidation) when the reaction mixtures were analyzed by GC-MS, headspace GC-MS or $^1\text{H-NMR}$.

Were also attempted trapping of in situ imine formation with TMS-cyanide.

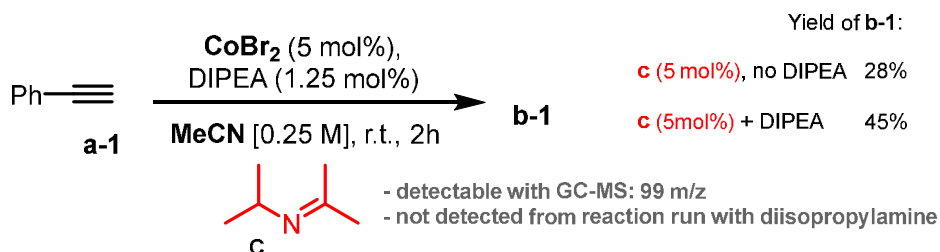
a)



b)

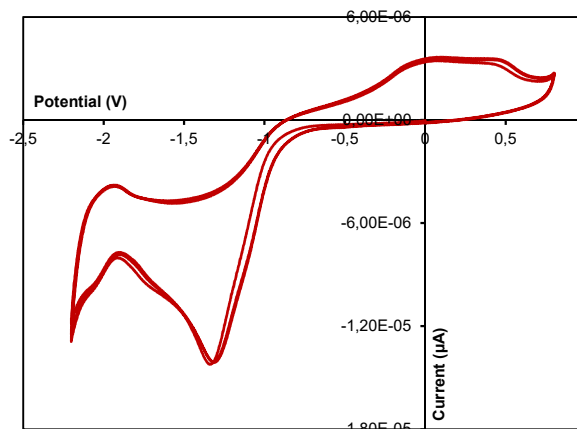


To exclude the possibility that the analytics and reaction analysis couldn't detect small amount of imine byproducts when present in the reaction mixture, N (isopropylidene)isopropylamine was synthesized and added into the reaction mixture.

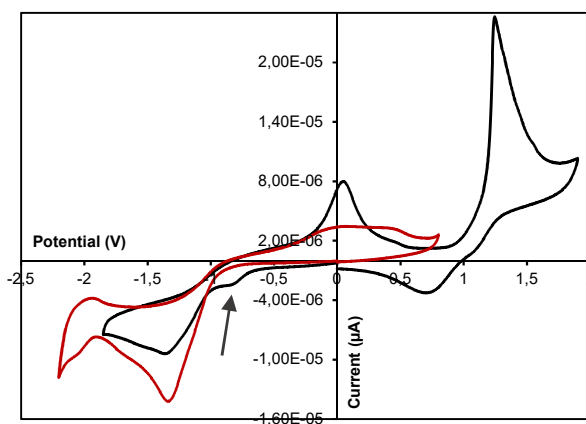


When exogenous imine is added to the reaction mixture in 5 mol% we were able to detect it from GC-MS. Moreover, the imine itself has a negative impact on the reaction outcome. This led us to exclude that such byproduct is produced in our reaction conditions.

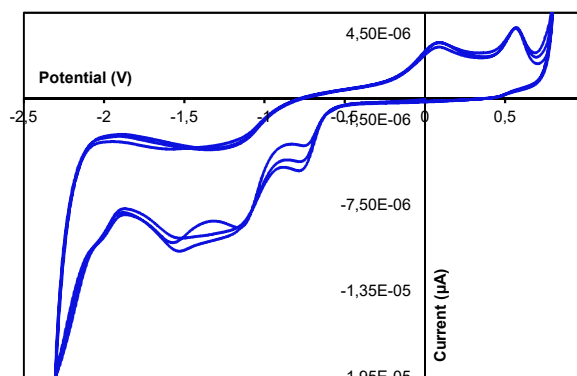
Cyclic Voltammetry



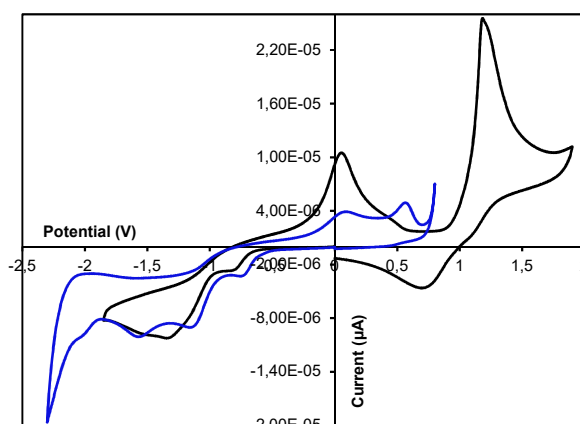
A) CV of an equimolar mixture of CoBr_2 and DIPEA (0.5 mM) in acetonitrile. New potential shifted to -1.33 V vs Ag/AgCl.



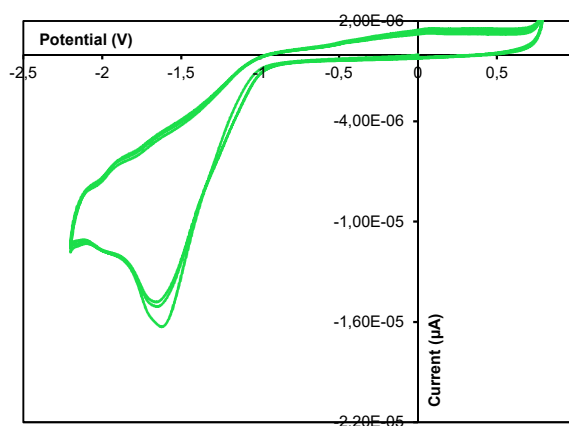
B) Comparison of A (in **red**) with a pure solution of CoBr_2 in acetonitrile in absence of DIPEA (in **black**). In presence of the amine the reduction peak at -0.75 V ca corresponding to the $\text{Co(II)}/\text{Co(I)}$ transition disappears either shifting towards more negative potentials in the zone of the $\text{Co(I)}/\text{Co(0)}$ transition or becoming too unstable for the CV detection or prior to measurement the Co is already reduced by amine.



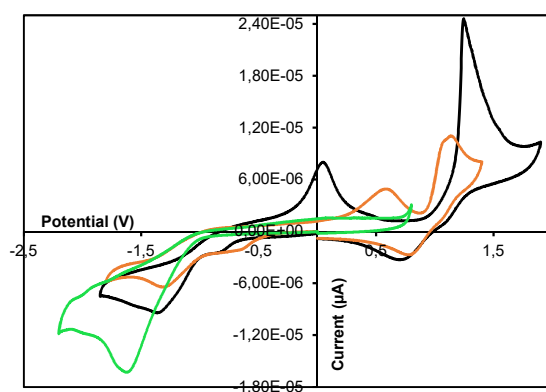
C) CV of an equimolar mixture of CoBr_2 and *N,N*-diethylaniline (a non-competent amine in the [2+2+2] reaction). It shows 2 peaks in the reduction.



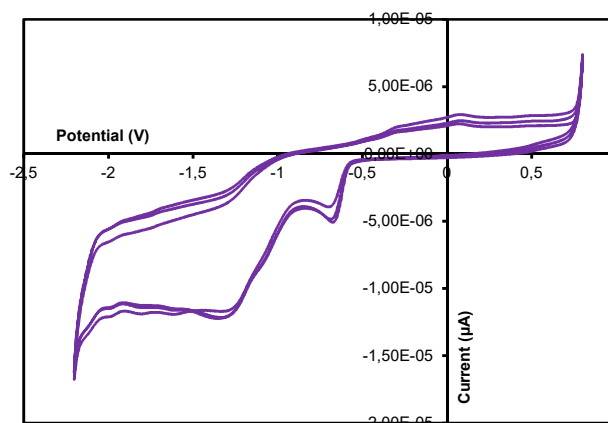
D) Comparison of C (in **blue**) with a pure solution of CoBr_2 in acetonitrile (in **black**). In this case the reduction events are very similar and the small peak reappears.



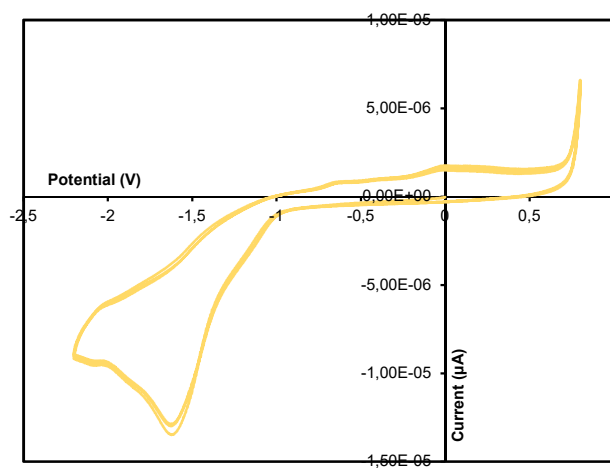
E) Phenylacetylene 10 mM in presence of DIPEA (0.5 equiv.) and CoBr_2 (0.5 equiv.) New potential shifted to -1.65 V vs Ag/AgCl.



F) Comparison of E (**green**) with a solution of pure CoBr_2 in acetonitrile (**black**) and a solution of only phenylacetylene and CoBr_2 in absence of DIPEA (**orange**)



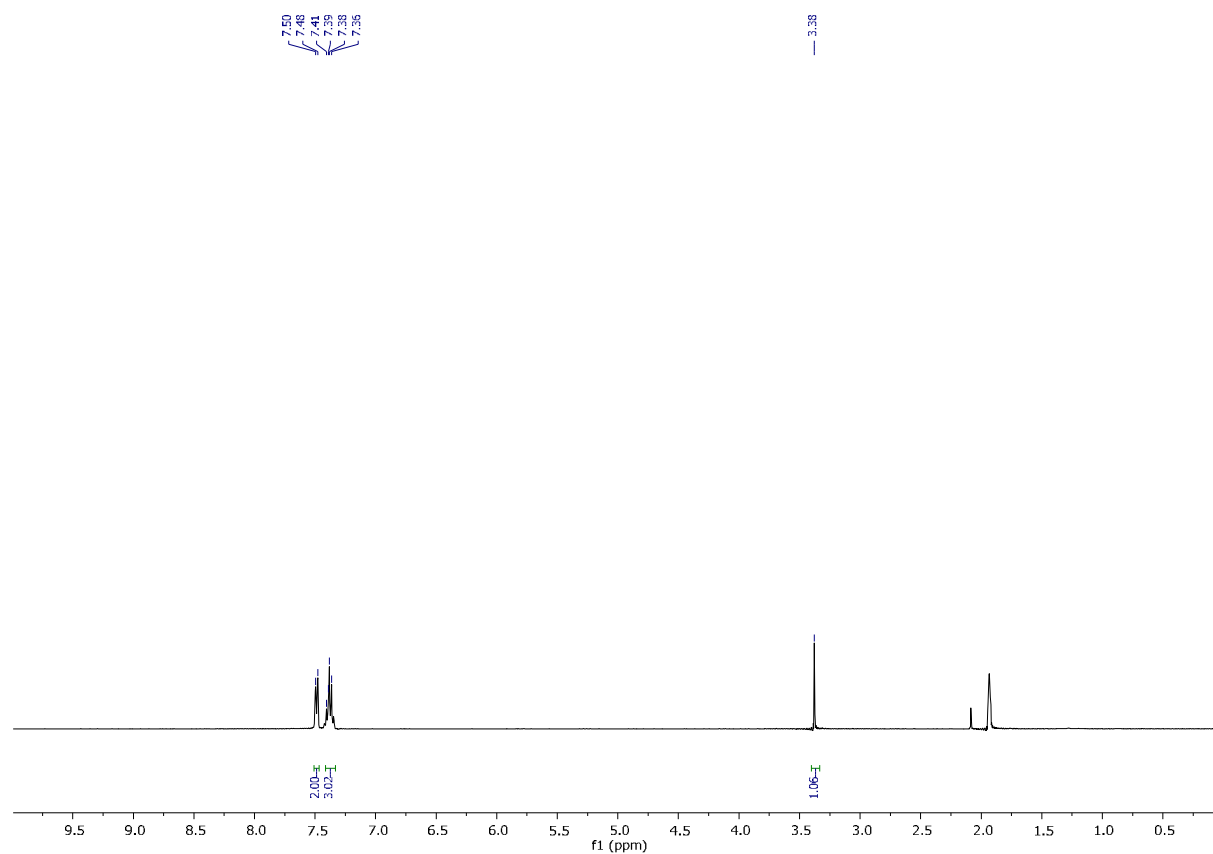
G) Phenylacetylene 10 mM in presence of *N,N*-diethylaniline (0.5 equiv.) and CoBr_2 (0.5 equiv.)



H) Propynylbenzene 10 mM in presence of DIPEA (0.5 equiv.) and CoBr_2 (0.5 equiv.)

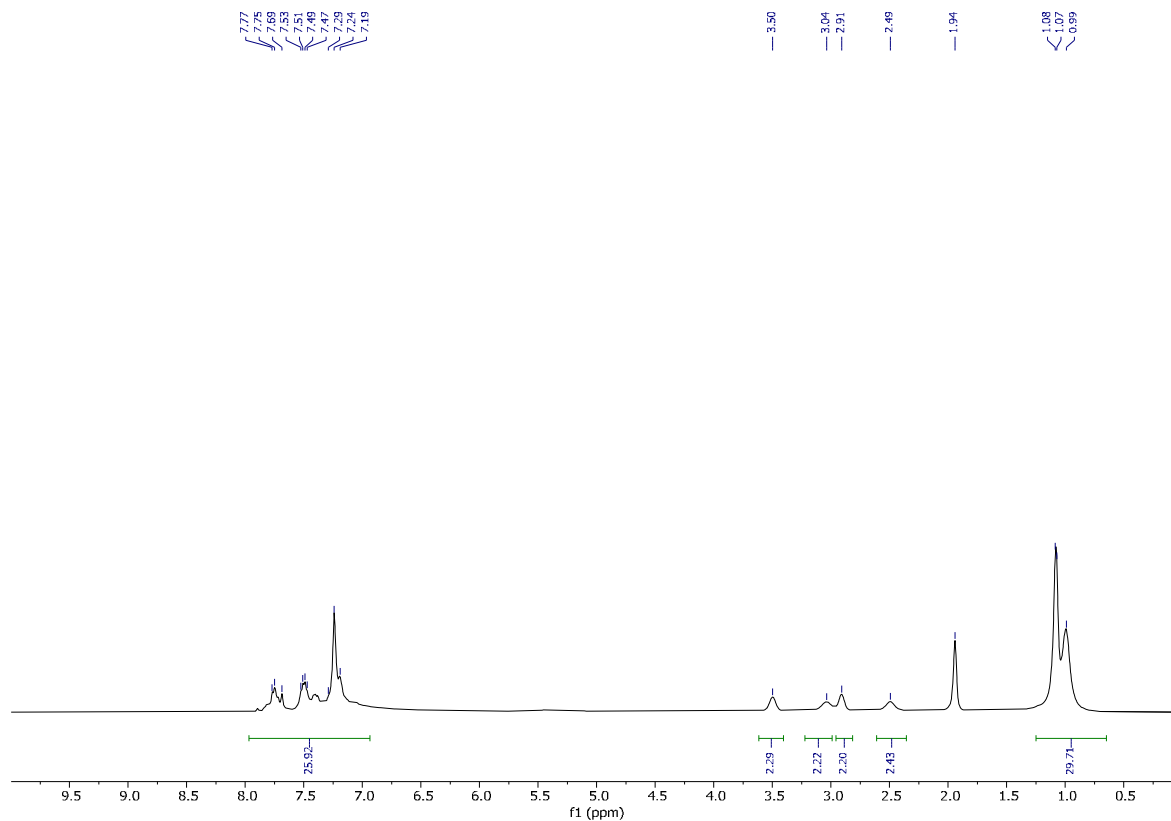
References for cyclic voltammetry studies on simple Co(II) salts in acetonitrile: a) Buriez, O., Labbé, E., Périchon, J. *Journal of Electroanalytical Chemistry* **2006**, 593, 99–104; b) Buriez, O., Seka, S., Périchon, J. *Chem. Eur. J.* **2003**, 9, 3597–3603; c) Polleux, L., Labbé, E., Buriez, O., Périchon, J. *Chem. Eur. J.* **2005**, 11, 4678–4686.

NMR Investigation on the Mechanism



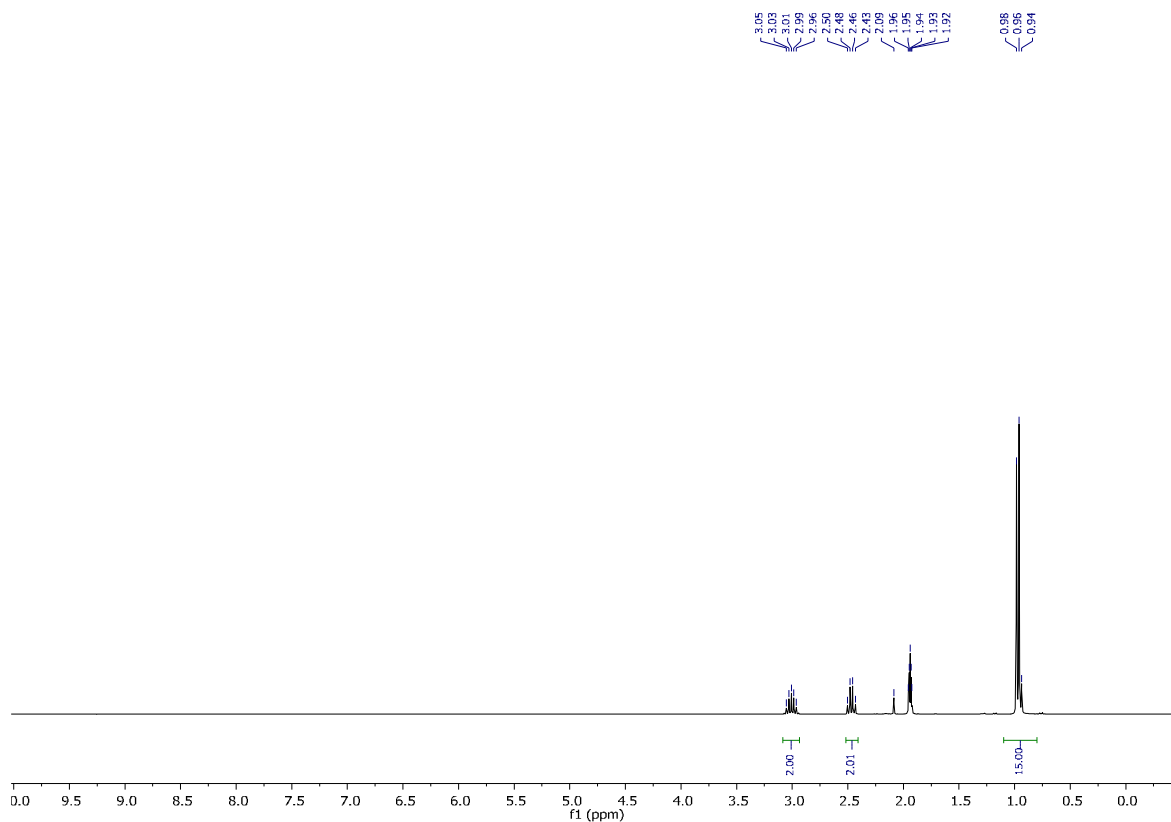
¹H NMR (400 MHz, CD₃CN) Phenylacetylene (100 μmol)/CoBr₂ (50 μmol).

No deviations from ¹H NMR of pure phenylacetylene in acetonitrile.

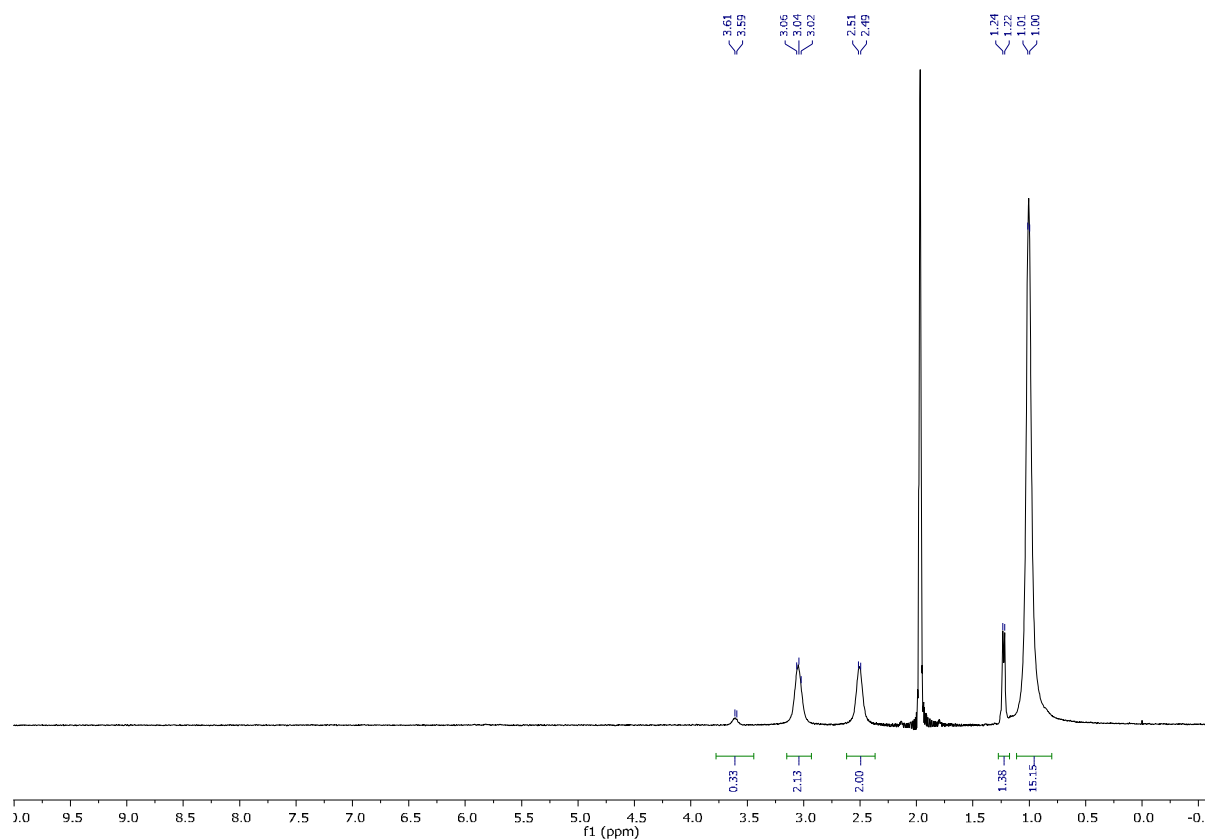


¹H NMR (400 MHz, CD₃CN) Phenylacetylene (0.15 mmol)/CoBr₂ (50 μmol)/DIPEA (25 μmol).

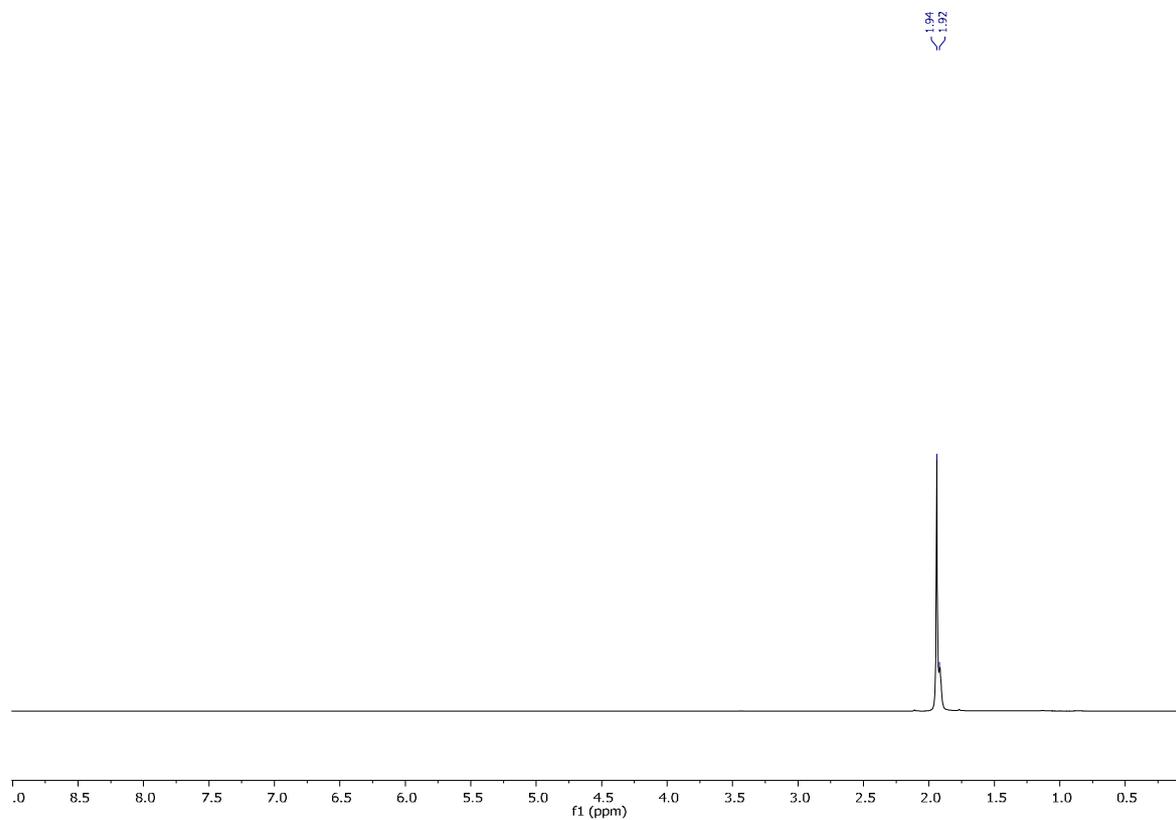
Full conversion of phenylacetylene, the DIPEA is divided in two species in a 1:1 ratio (one deshielded and one that has the signals of free DIPEA in acetonitrile).



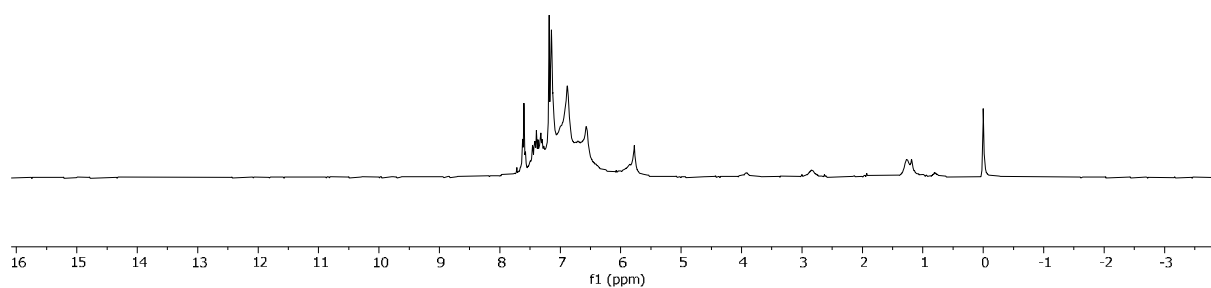
¹H NMR (400 MHz, CD₃CN) of DIPEA (100 μmol).



^1H NMR (400 MHz, CD_3CN) of DIPEA (100 μmol)/ CoBr_2 (50 μmol). A change of chemical shift for the methyl groups of DIPEA signals was observed after addition of CoBr_2 and the arising of two new signals at 3.60, 3.0 and 1.23 ppm respectively.



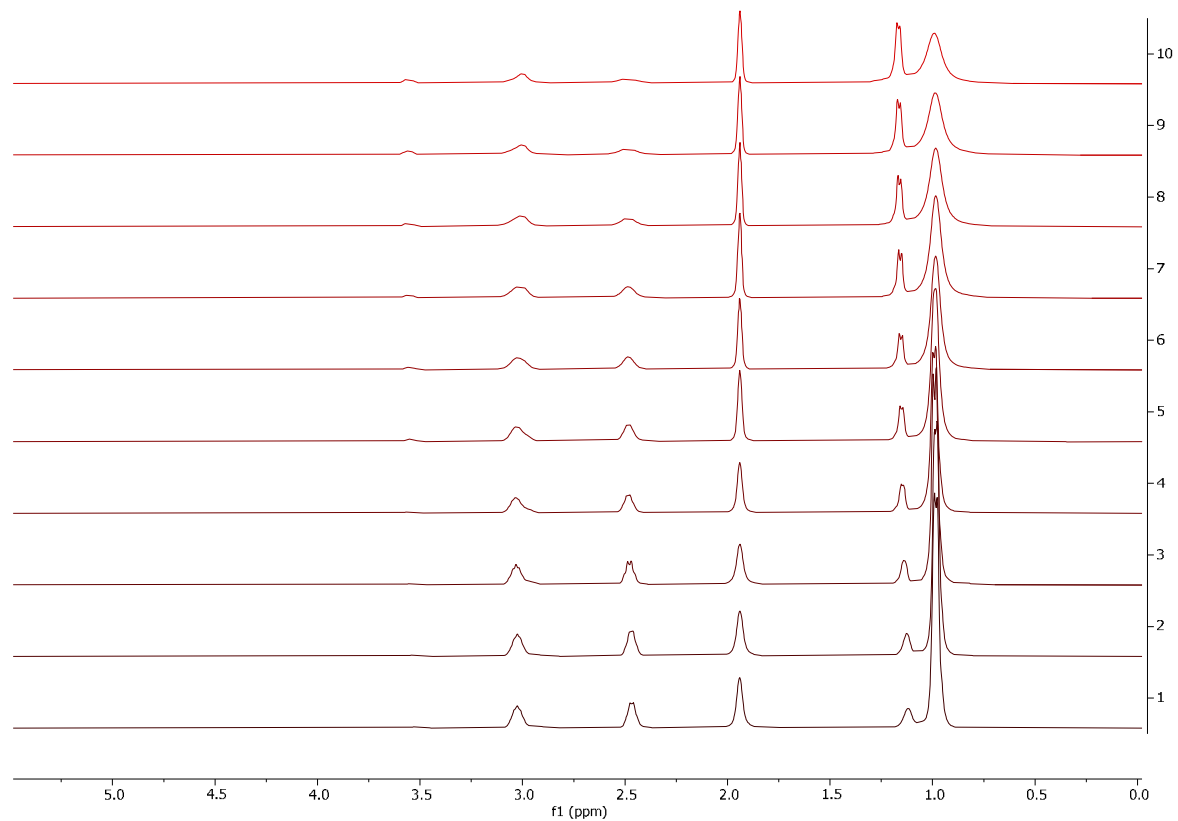
^1H NMR (400 MHz, CD_3CN) of $[\text{Co}(\text{MeCN})_6][\text{CoBr}_3\text{MeCN}]_2$.



¹H NMR (400 MHz, CDCl₃) of polyphenylacetylene (orange precipitate from the reaction mixture).

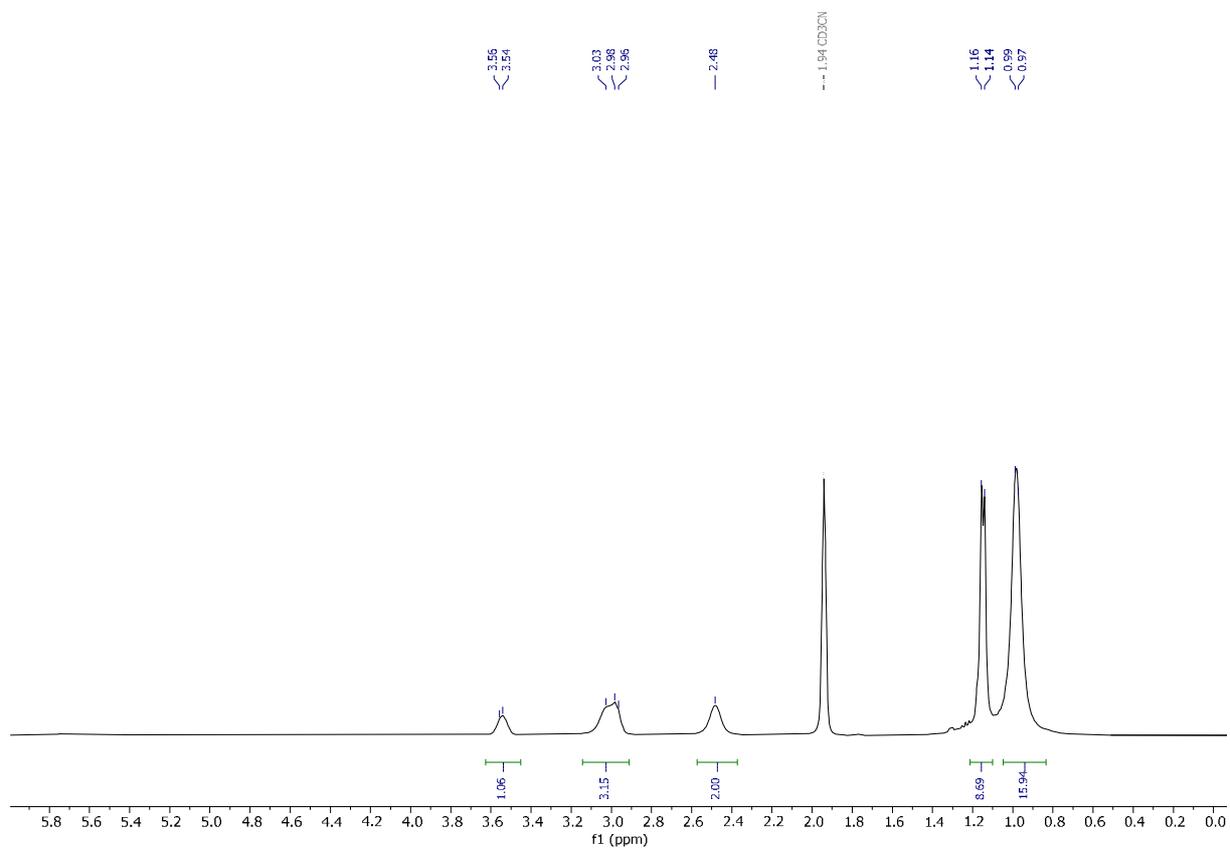
For comparison: K. Li, G. Wei; J. Darkwa, S. K. Pollack *Macromolecules* **2002**, *35*, 4573-4576

Temperature dependent NMR: A Young tube was charged with CoBr_2 (5.5 mg, 0.025 mmol) and dissolved in CD_3CN . The sample was frozen with liquid nitrogen and DIPEA (1 equiv.) was added. The spectra were acquired at increasing temperatures respectively from the bottom 243 K, 253 K, 263 K, 273 K, 283 K, 293 K, 303 K, 313 K, 323 K, 333 K.



^1H NMR (400 MHz, CD_3CN)

The temperature dependent NMR showed the equilibration of the two DIPEA species however no shift in ppm depending on the employed temperature were observed. According to the Curie's law no paramagnetic peaks could be detected. Moreover, the equilibration of the two species seem to depend on time and not on temperature.



¹H NMR (400 MHz, CD₃CN): same sample of the Temperature experiment above measured at r.t. after 2 h. The two species are in a ratio of 1:2.

Coordinated DIPEA: 3.55 ppm (m, 2H); 2.97 (m, 2H); 1.15 (m, 15H)

Free DIPEA: 2.98 ppm (m, 2H); 2.48 (s, 2H); 0.98 (s, 15H).

ATR-IR Investigations

The samples were assembled and recorded in an argon filled glovebox. The respective solutions were prepared immediately before the analysis, some drops of such solutions were directly poured on the ATR crystal surface and the spectra recorded.

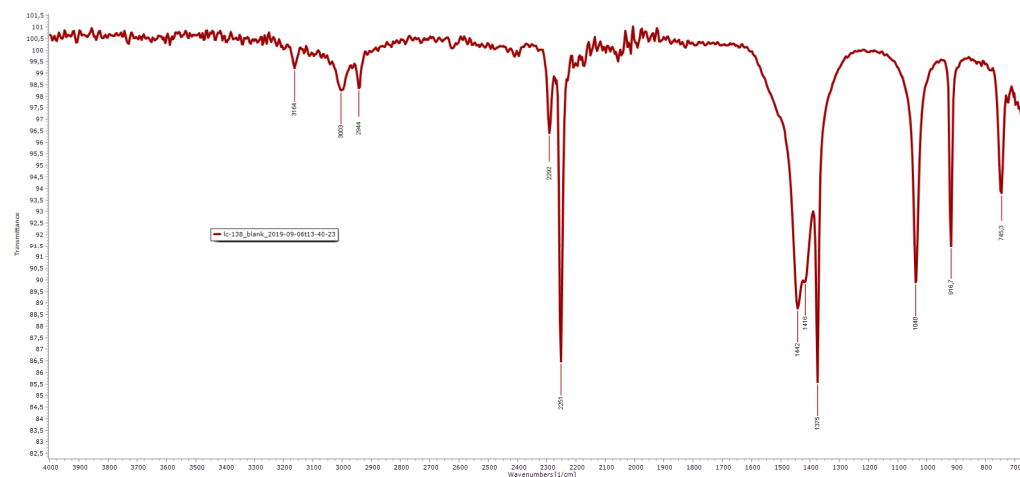


Figure 28. ATR-IR spectrum of pure acetonitrile. Characteristic stretching of free acetonitrile are at 2292 and 2251 cm^{-1} ; $\nu(\text{C}\equiv\text{N})$

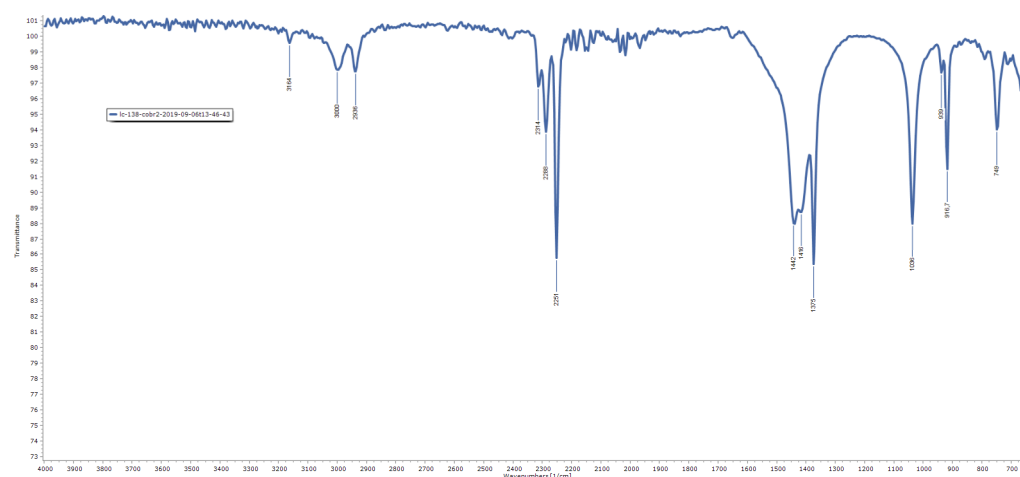


Figure 29. ATR-IR spectrum of CoBr_2 in acetonitrile. This spectrum shows the presence of both free acetonitrile (2251 cm^{-1}) and coordinated acetonitrile (2314 and 2288 cm^{-1}). The coordinated acetonitrile has higher wave numbers due to a lower π backbonding of both $\text{Co}(\text{MeCN})_6^{2+}$ ($\text{CoBr}_3\text{MeCN}^-$) into the nitrile.

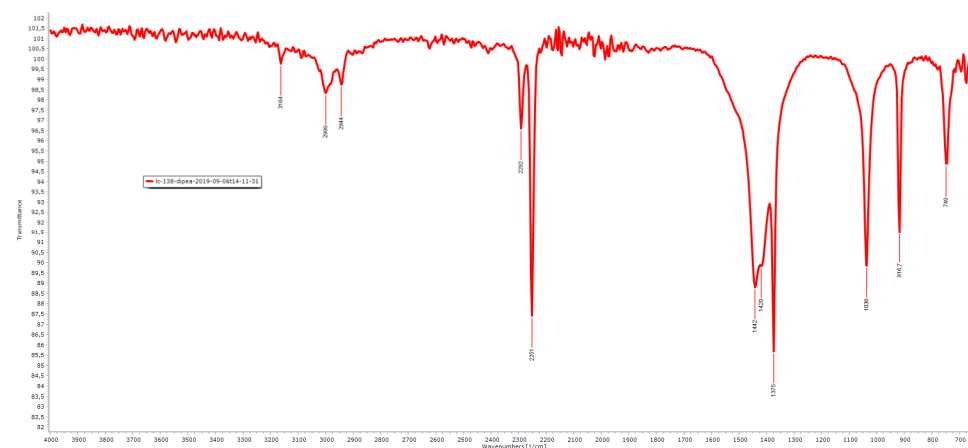


Figure 30. ATR-IR spectrum of a 1:1 mixture CoBr_2 and DIPEA in acetonitrile. There are no more the characteristic stretching of coordinated acetonitrile.

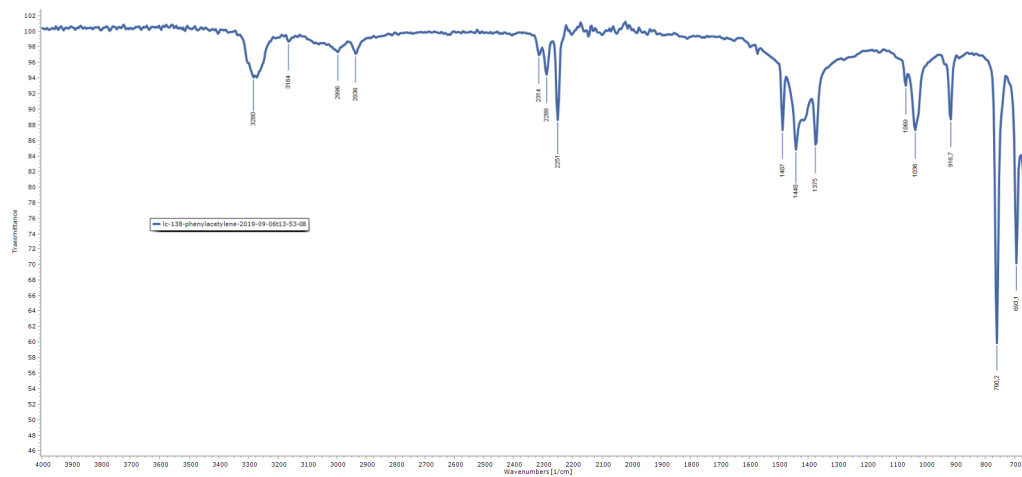
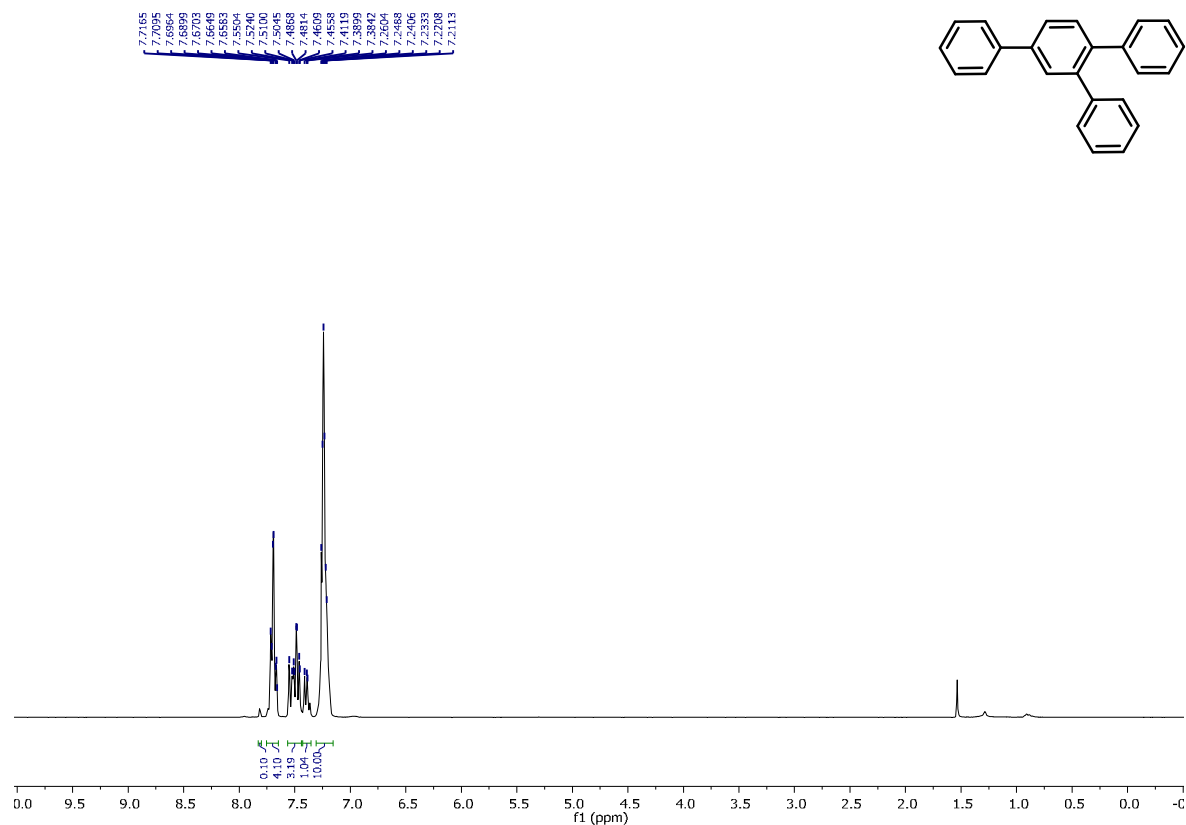


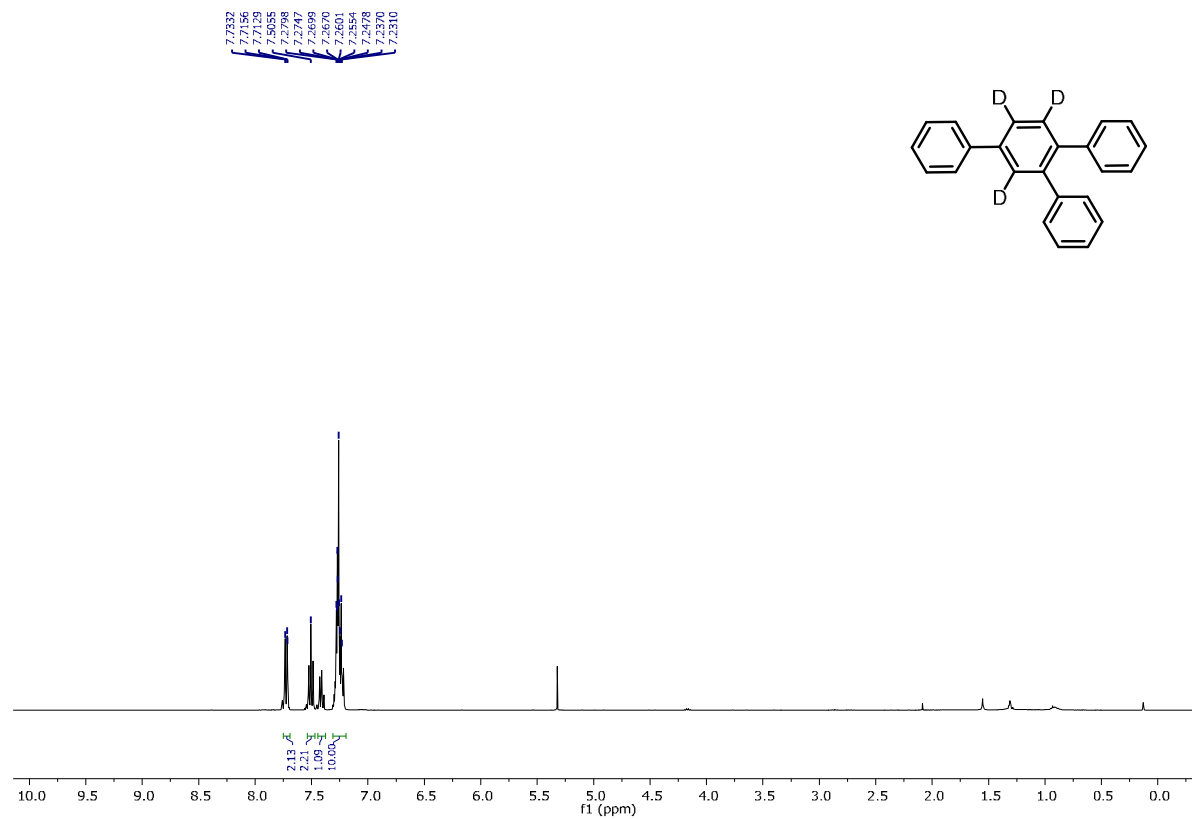
Figure 31. ATR-IR of a 1:1 mixture of CoBr_2 and phenylacetylene in acetonitrile. The coordination of acetonitrile is not affected and can be detected both coordinated and free acetonitrile.

For references on IR of $\text{Co}(\text{MeCN})_n\text{X}_2$ complexes: a) D. Stingham, A. L. Rüdiger, S. O. K. Giese, G. G. Nunes, J. F. Soares, D. L. Hughes, *Acta Cryst.* **2017**, C73, 104–114; b) Hijazi, A. K., Al Hmaideen, A., Syukri, S., Radhakrishnan, N., Herdtweck, E., Voit, B. & Kühn, F. E. *Eur. J. Inorg. Chem.*, **2008**, 2892–2898; c) Clarke, R. E., Ford, P. C. *Inorg. Chem.*, **1970**, 9, 227–235.

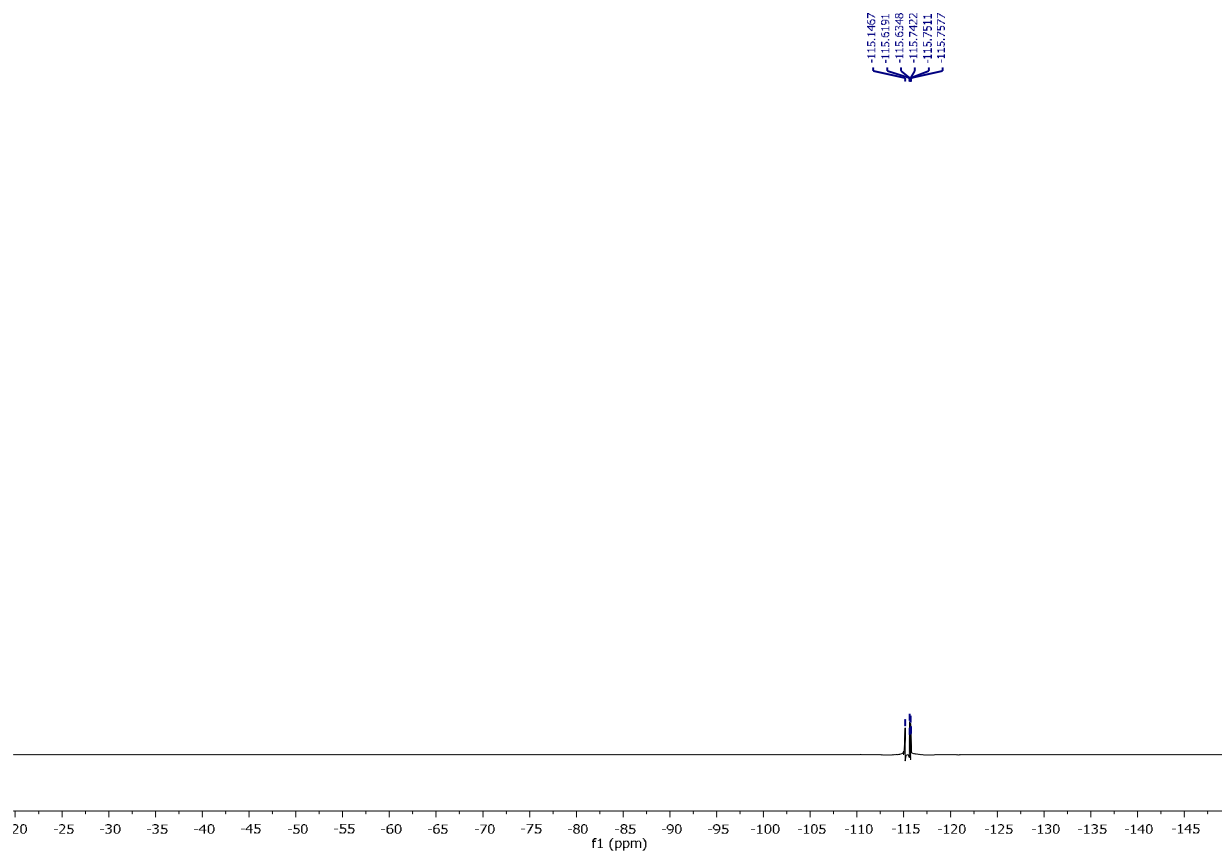
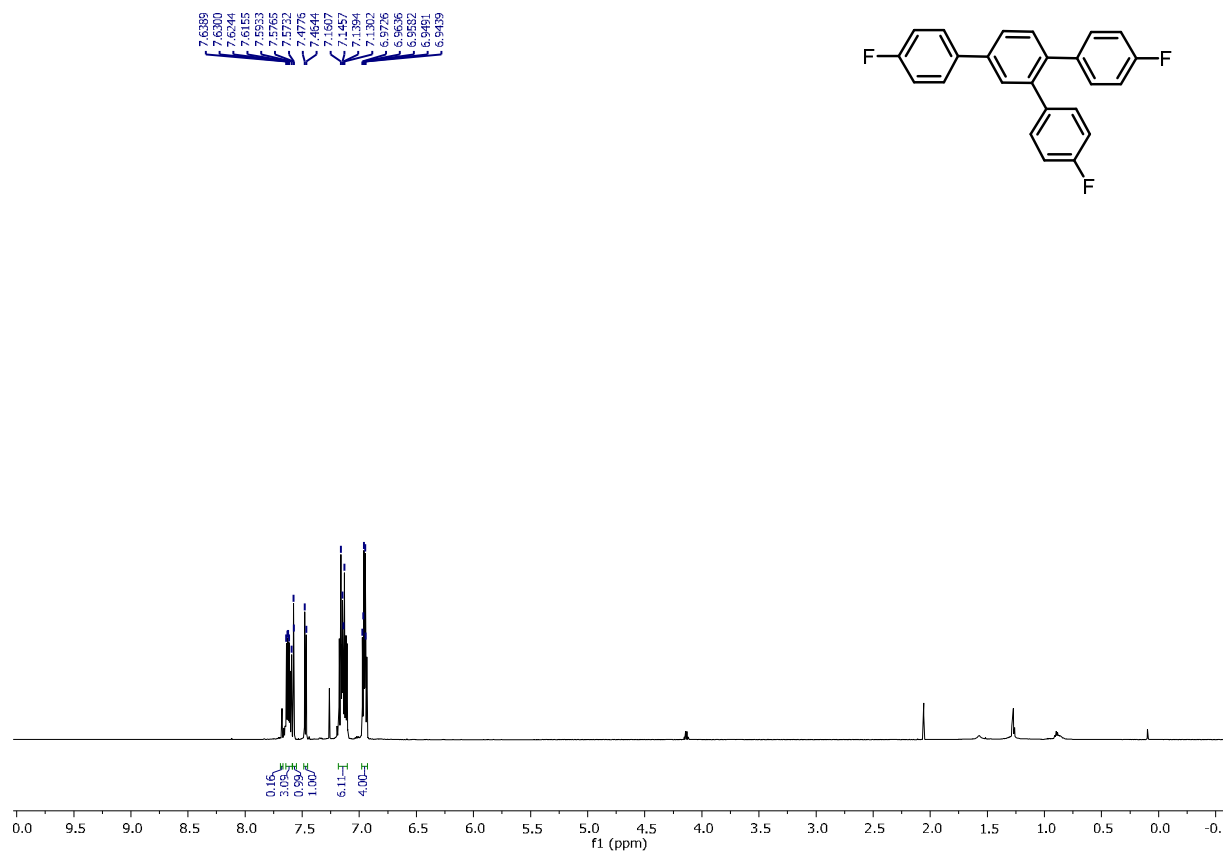
6.4.5 NMR of compounds

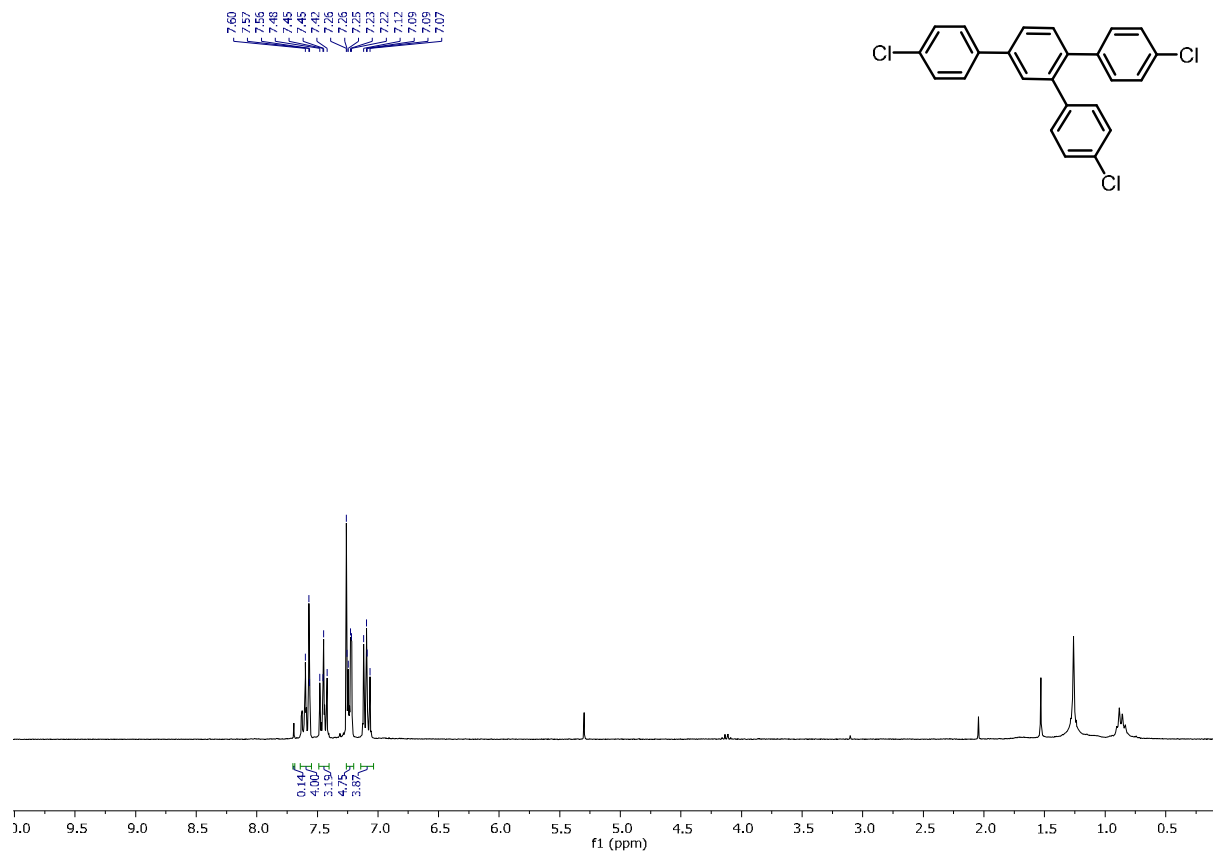


¹H NMR (400 MHz, CDCl₃) of 1,2,4-Triphenylbenzene (2)

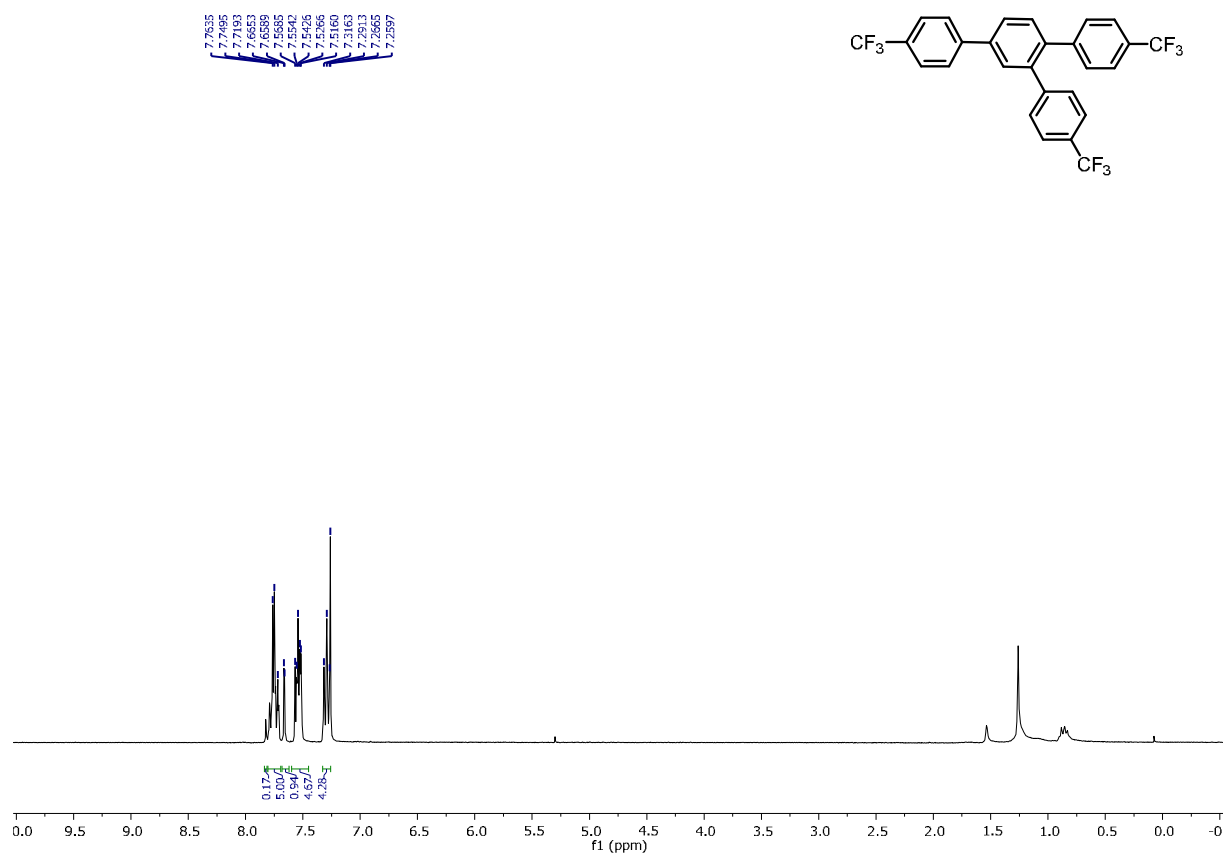


¹H NMR (400 MHz, CDCl₃) of 1,2,4-Triphenyl-3,5,6-trideuterobenzene (3)

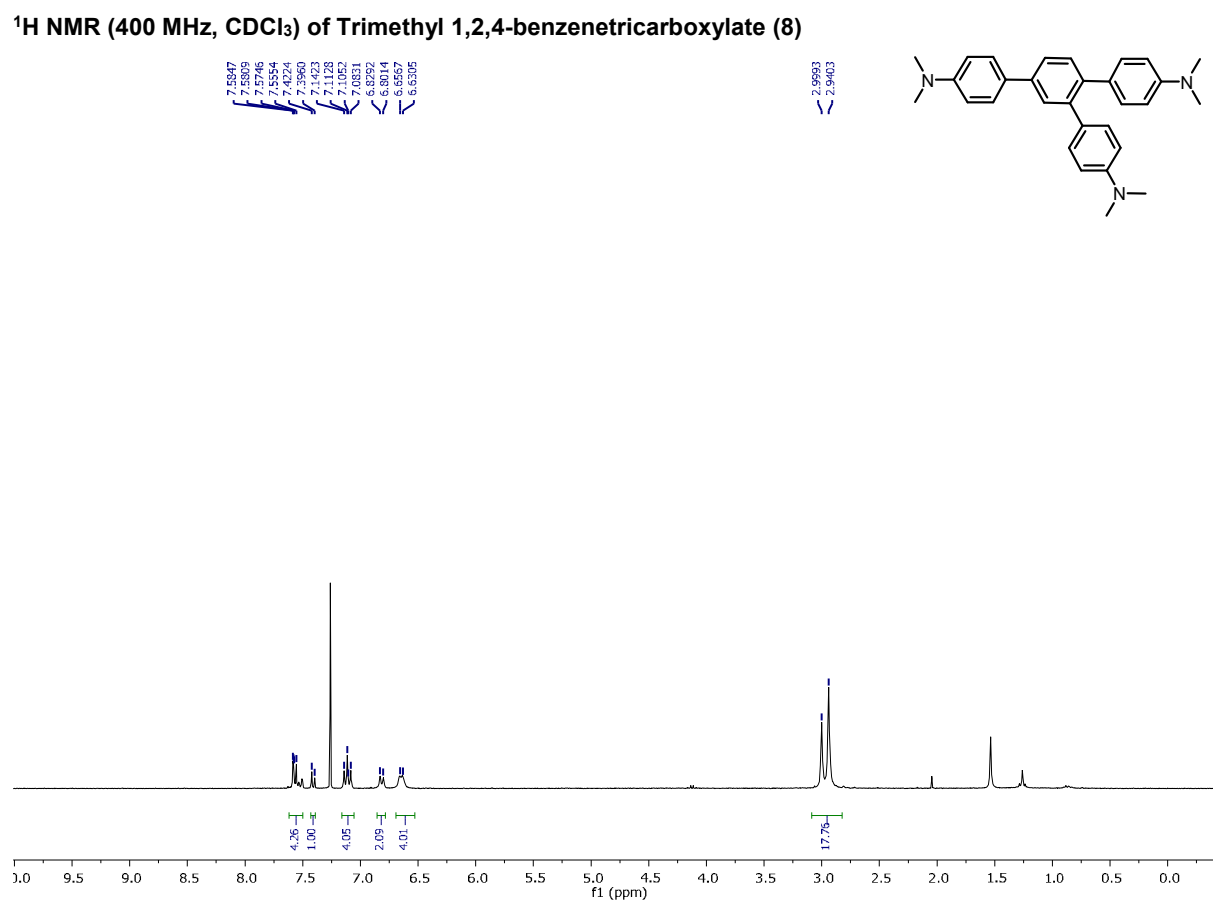
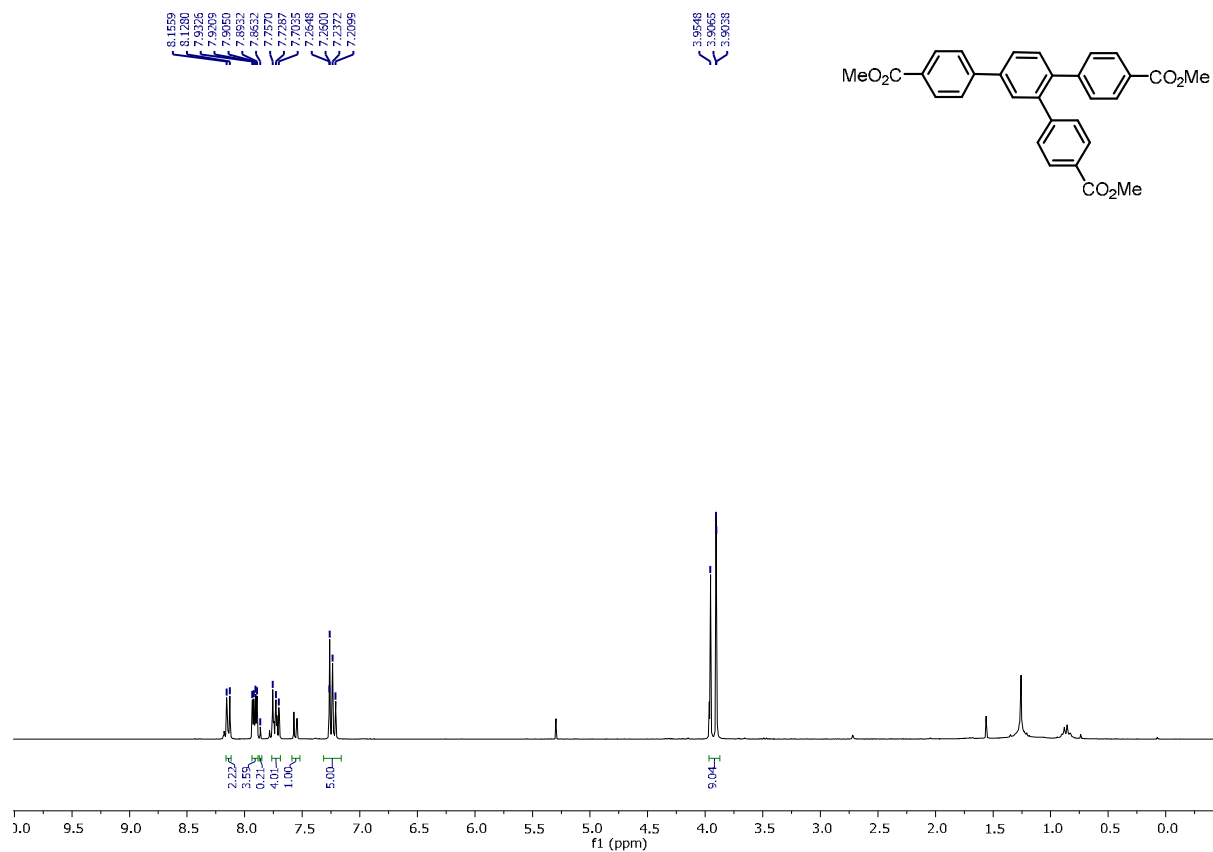


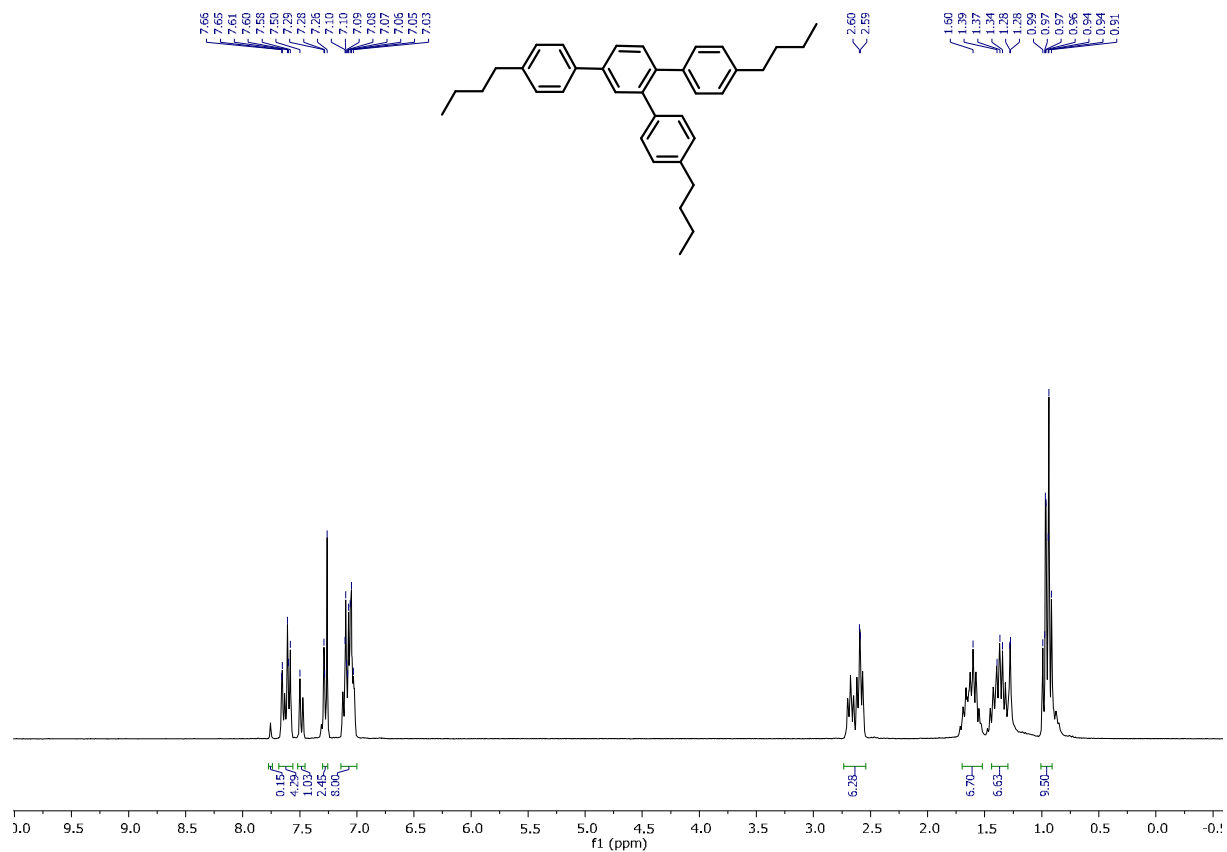


¹H NMR (400 MHz, CDCl₃) of 1,2,4-Tris(4-chlorophenyl)benzene (6)

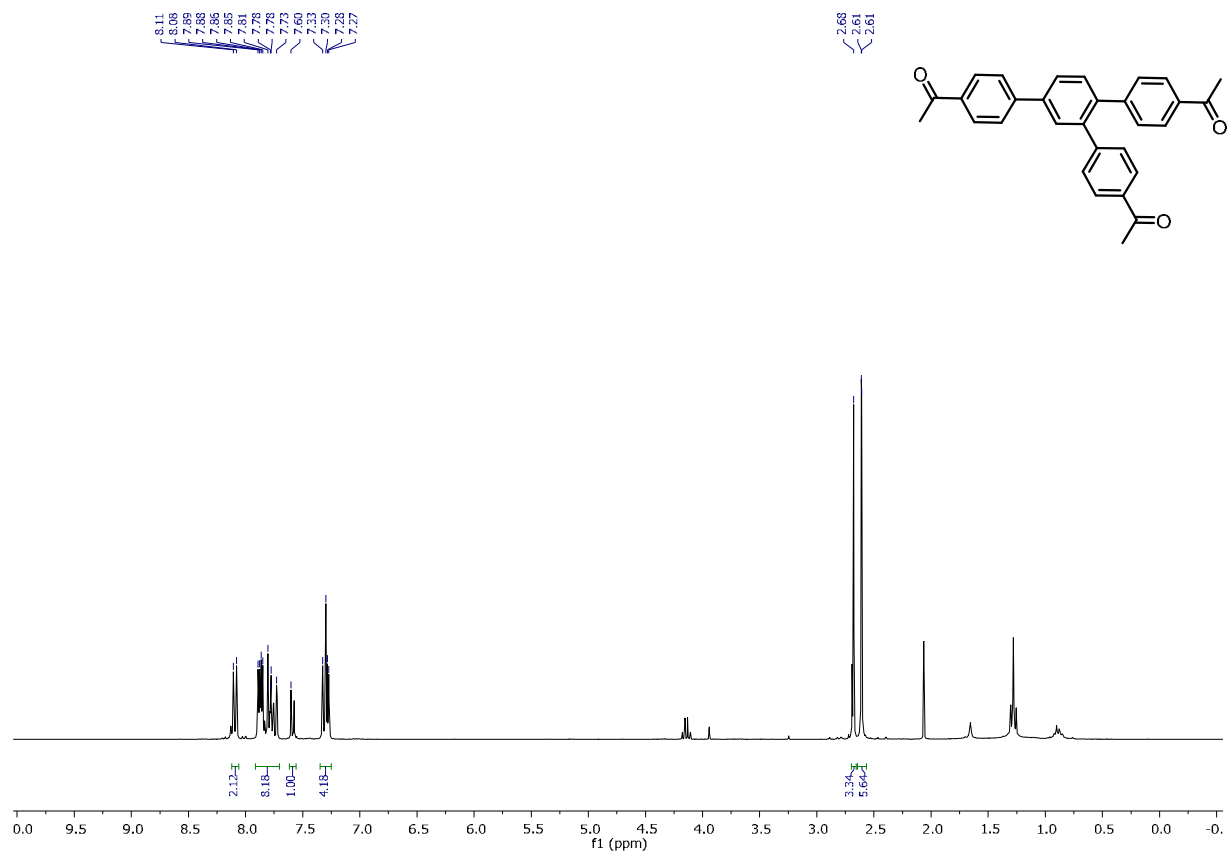


¹H NMR (400 MHz, CDCl₃) of 1,2,4-Tris(4-trifluoromethylphenyl)benzene (7)

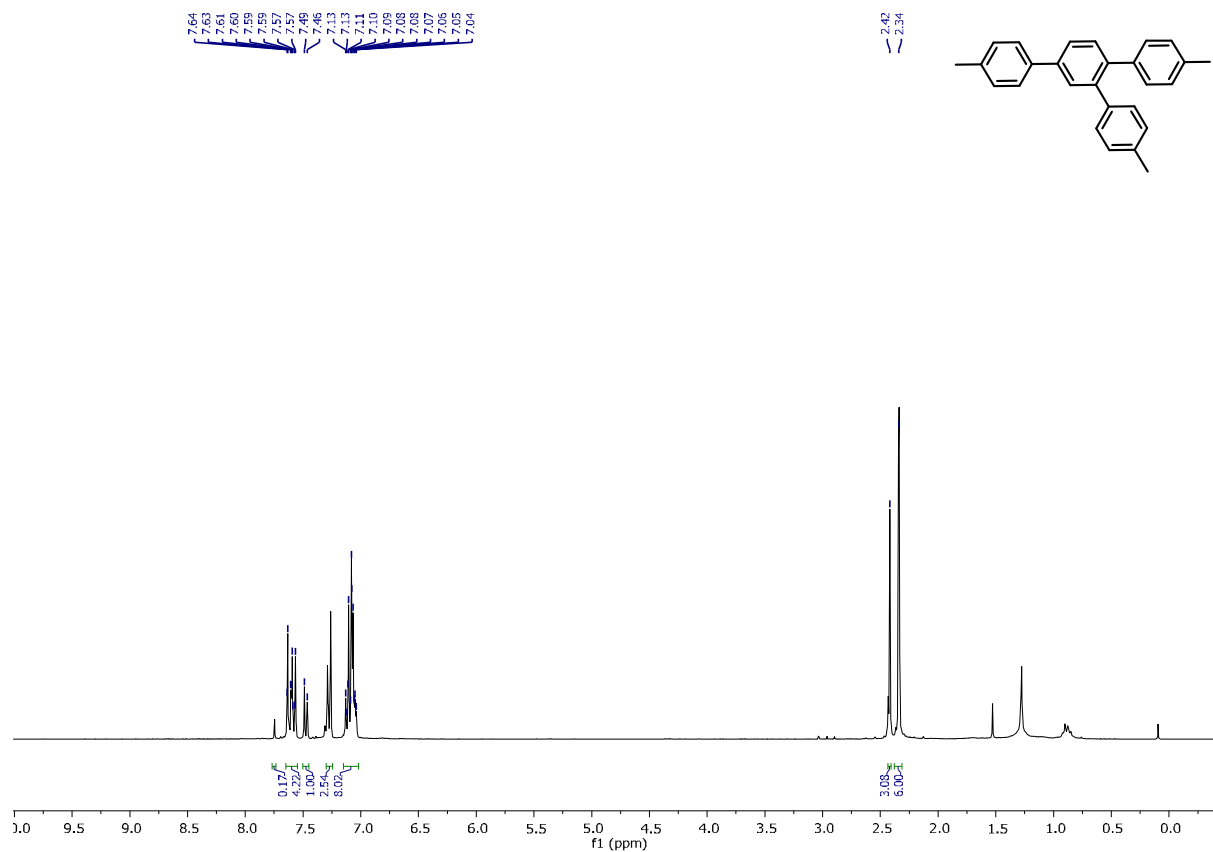




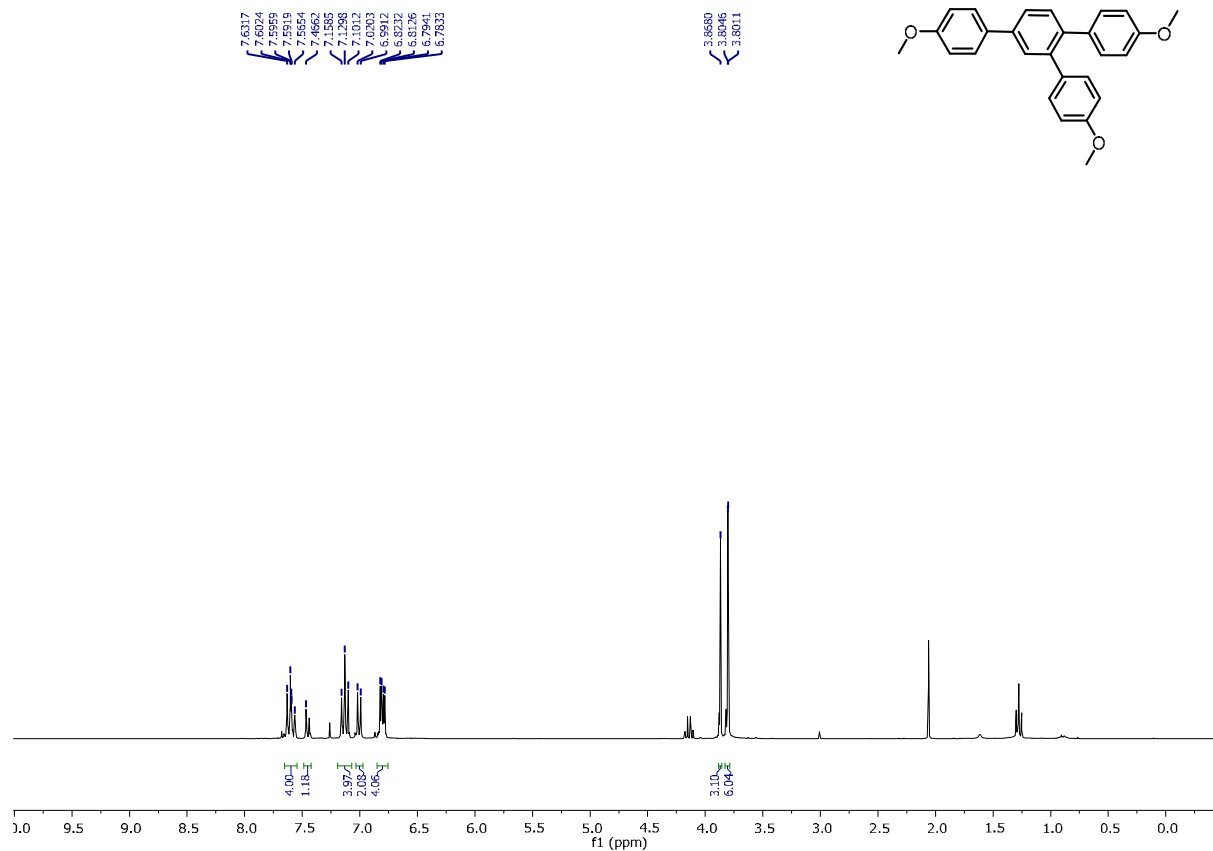
¹H NMR (400 MHz, CDCl₃) of 1,2,4-Tris(4-*n*-butylphenyl)benzene (10)



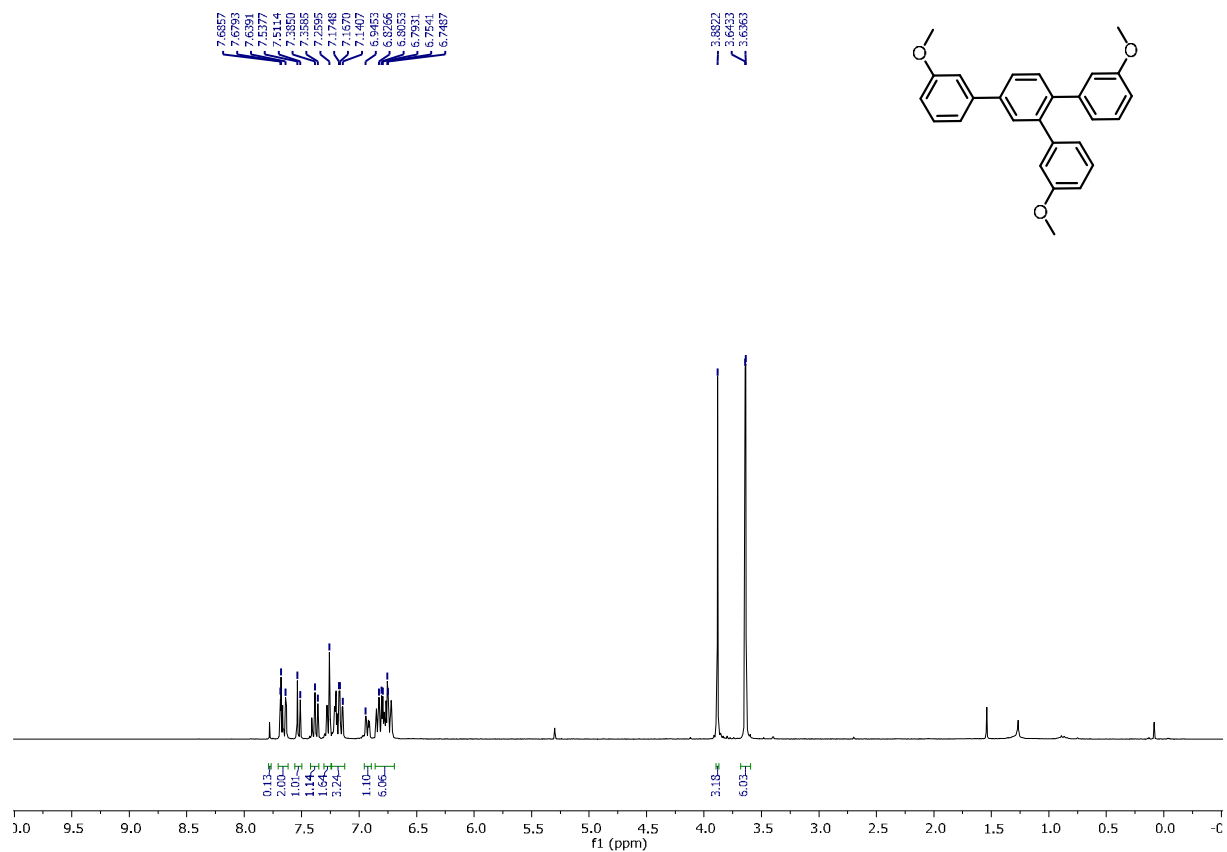
¹H NMR (400 MHz, CDCl₃) of 1,2,4-Tris(4-acetylphenyl)benzene (11)



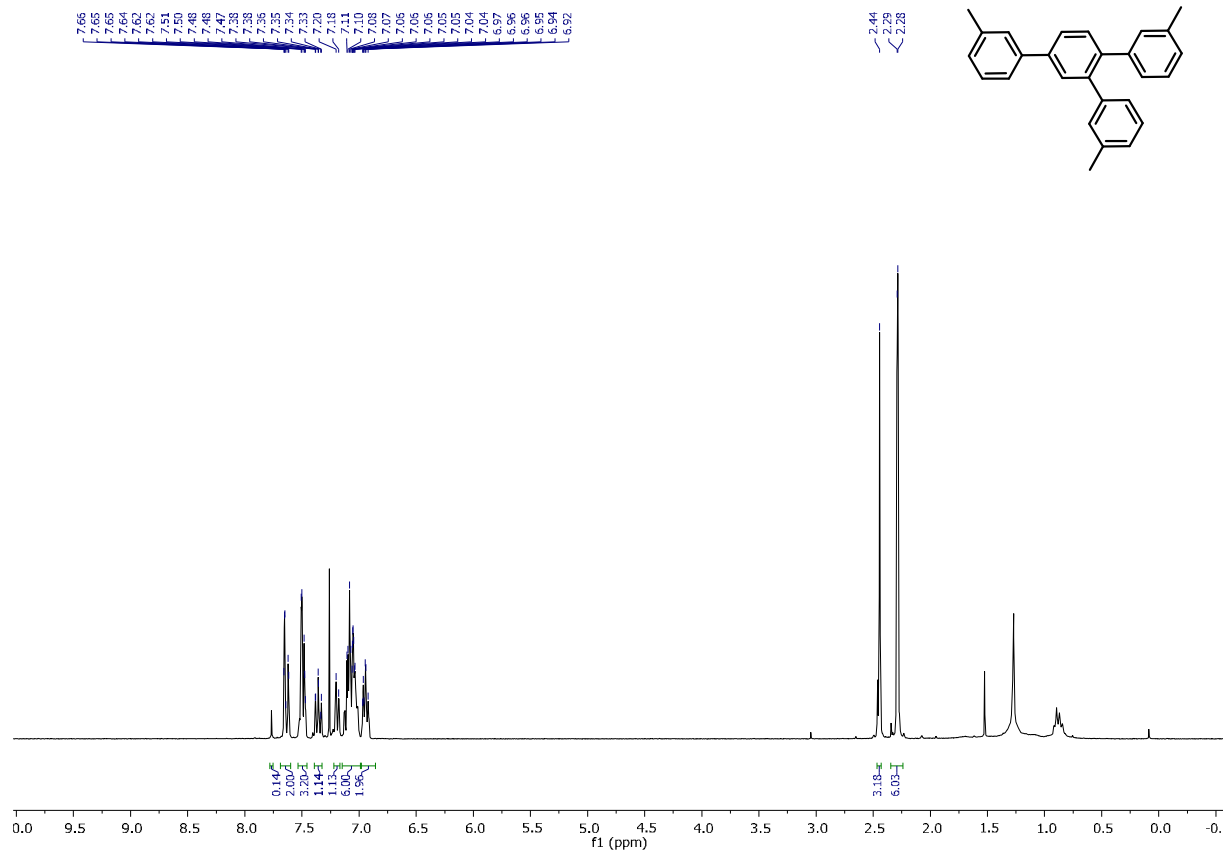
¹H NMR (400 MHz, CDCl₃) of 1,2,4-Tris(4-methylphenyl)benzene (12)



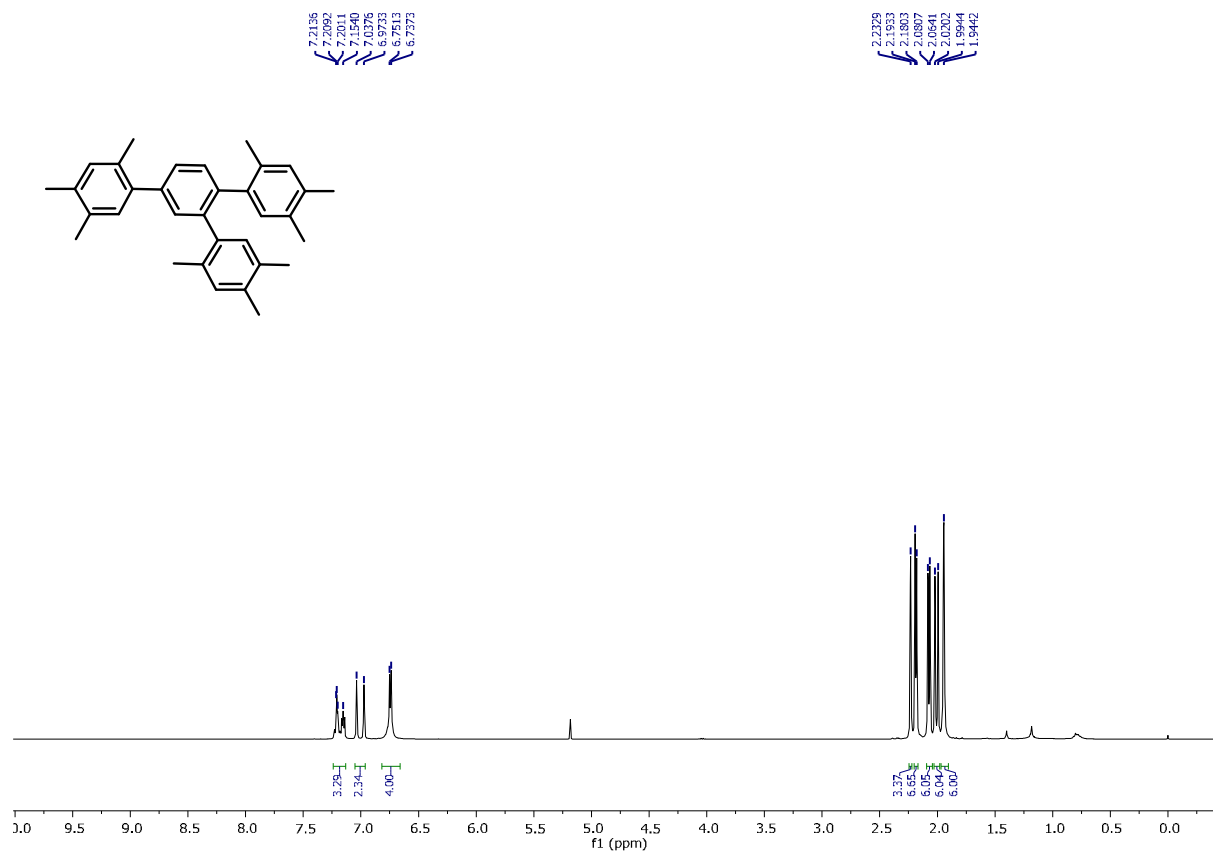
¹H NMR (400 MHz, CDCl₃) of 1,2,4-Tris(4-methoxyphenyl)benzene (13)



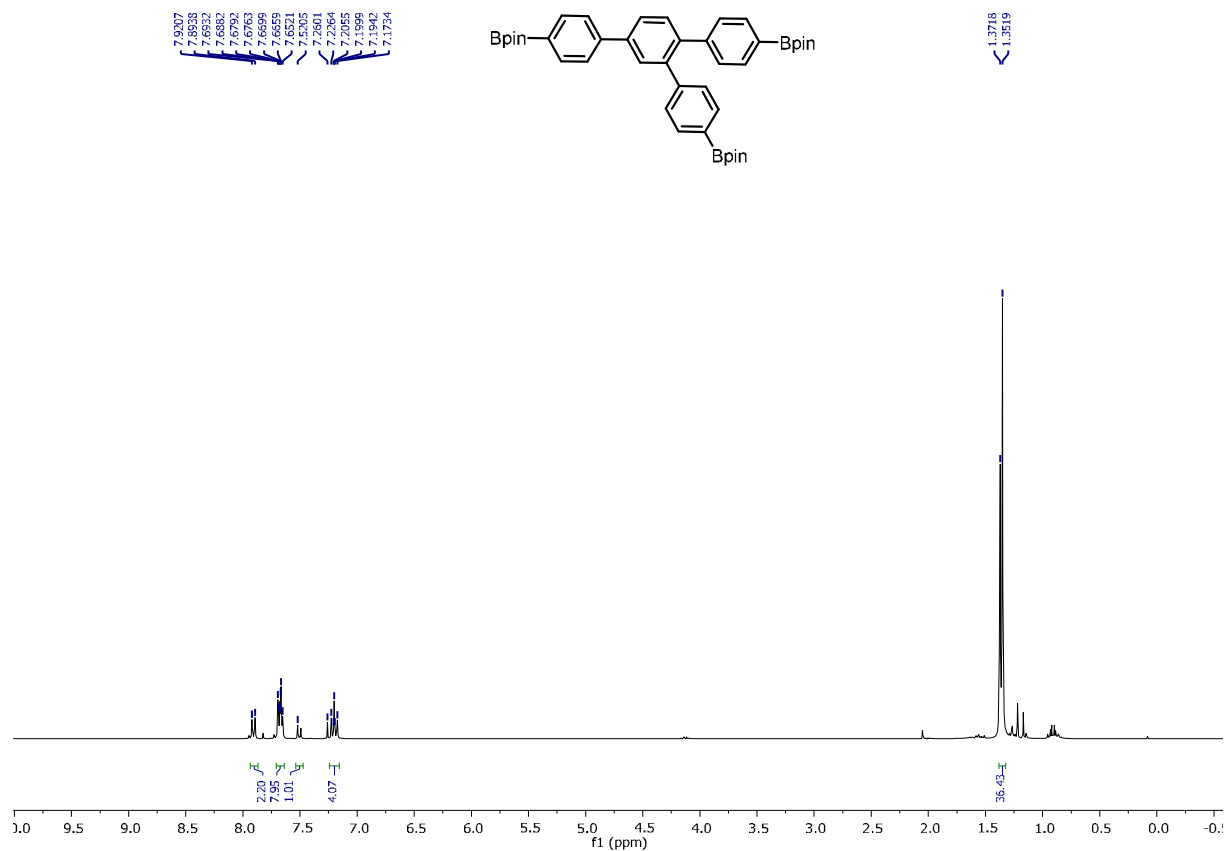
¹H NMR (400 MHz, CDCl₃) of 1,2,4-Tris(3-methoxyphenyl)benzene (14)



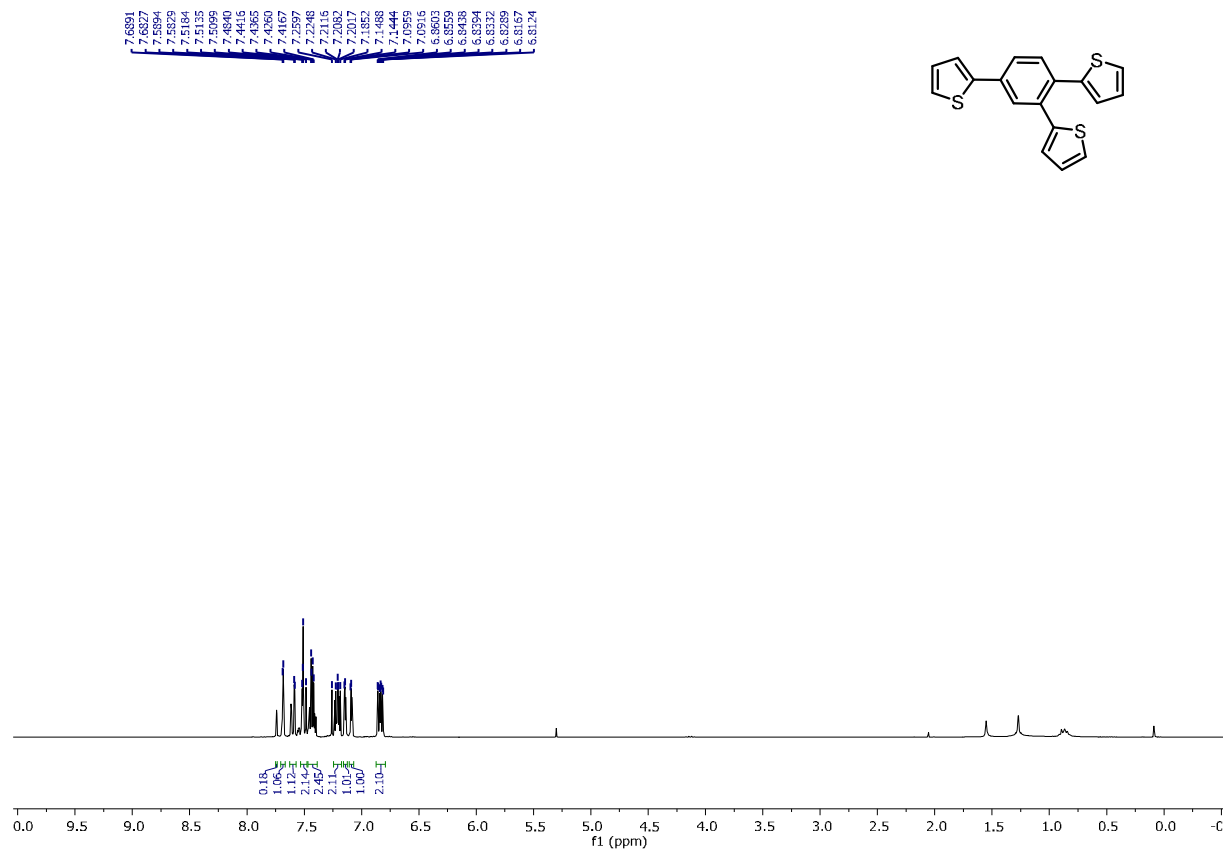
¹H NMR (400 MHz, CDCl₃) of 1,2,4-Tris(3-methylphenyl)benzene (15)



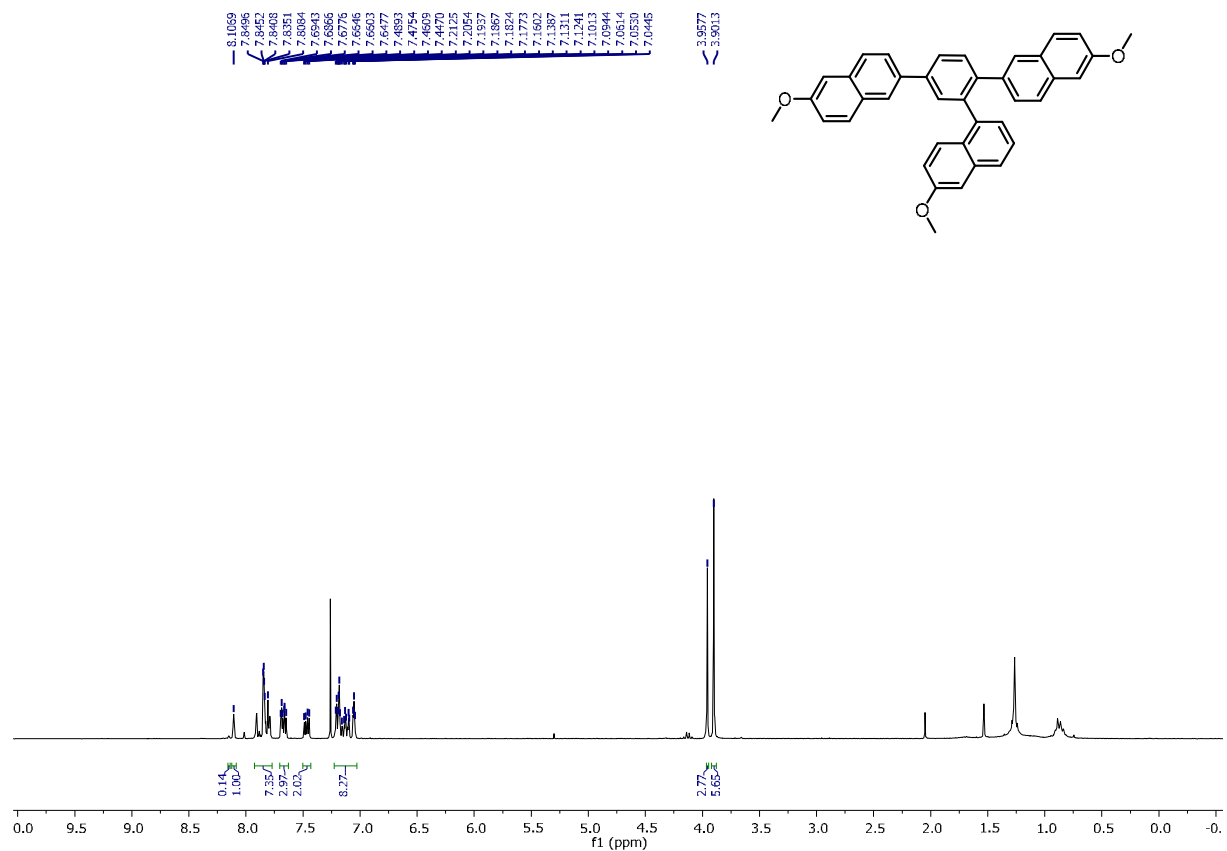
¹H NMR (400 MHz, CDCl₃) of 1,2,4-Tris-(2',4',5'-trimethylphenyl)benzene (18)



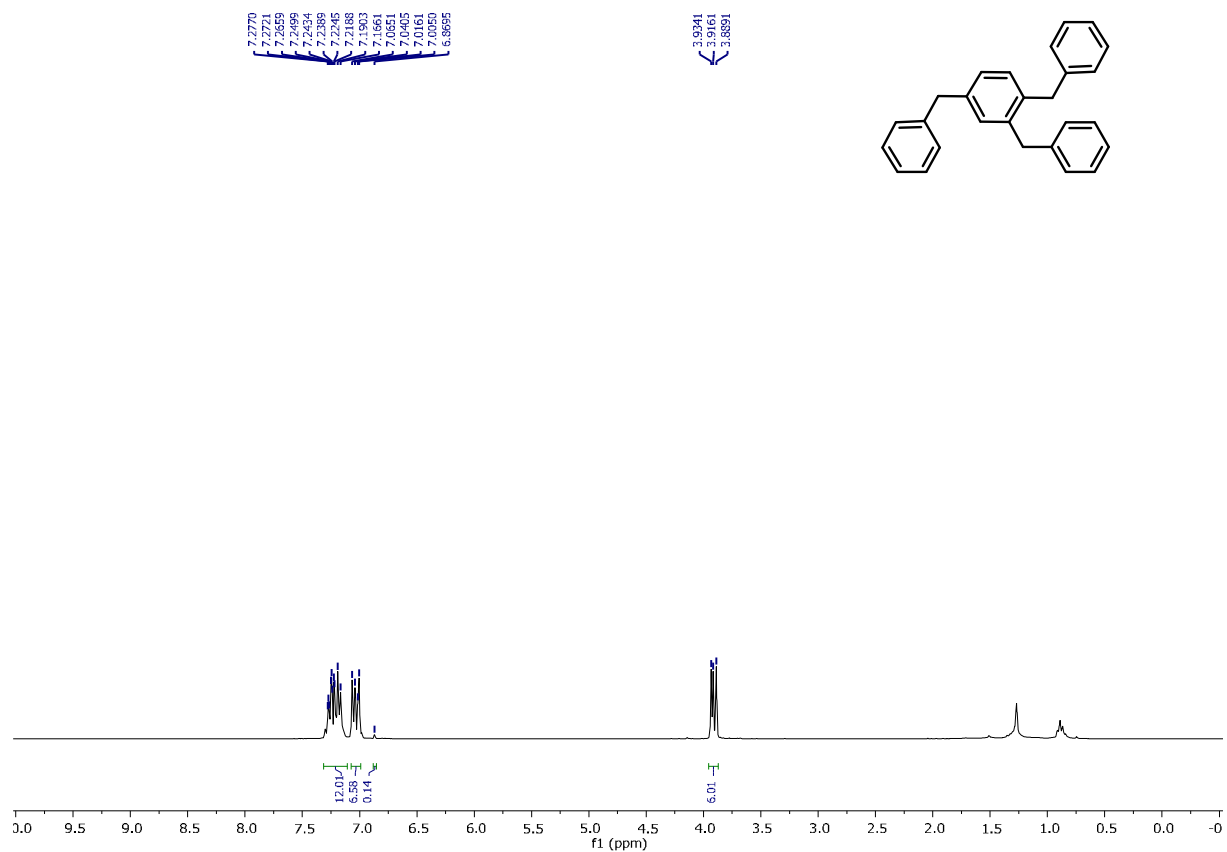
¹H NMR (400 MHz, CDCl₃) of 1,2,4-Tris(4-(pinacolato)boronylphenyl)benzene (19)



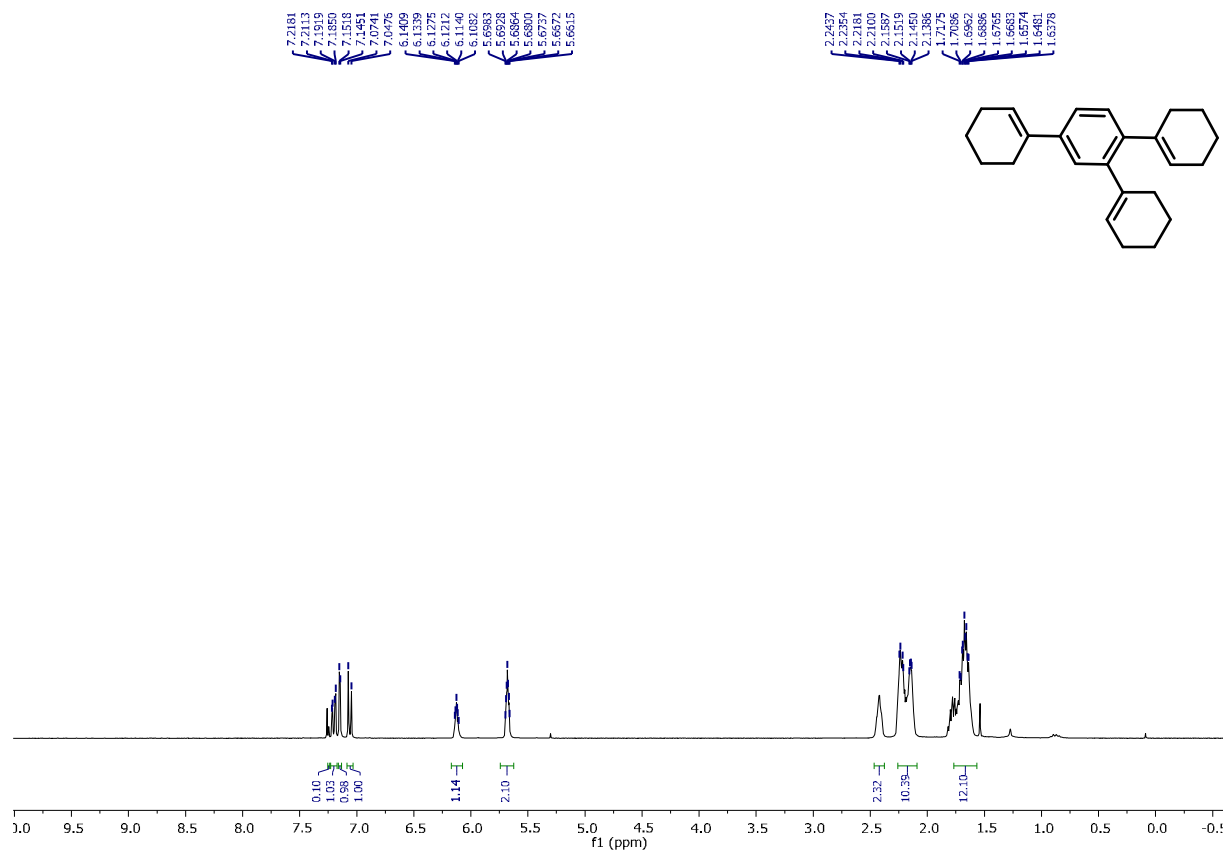
^1H NMR (400 MHz, CDCl_3) of 2,2',2''-(benzene-1,2,4-triyl)trithiophene (20)



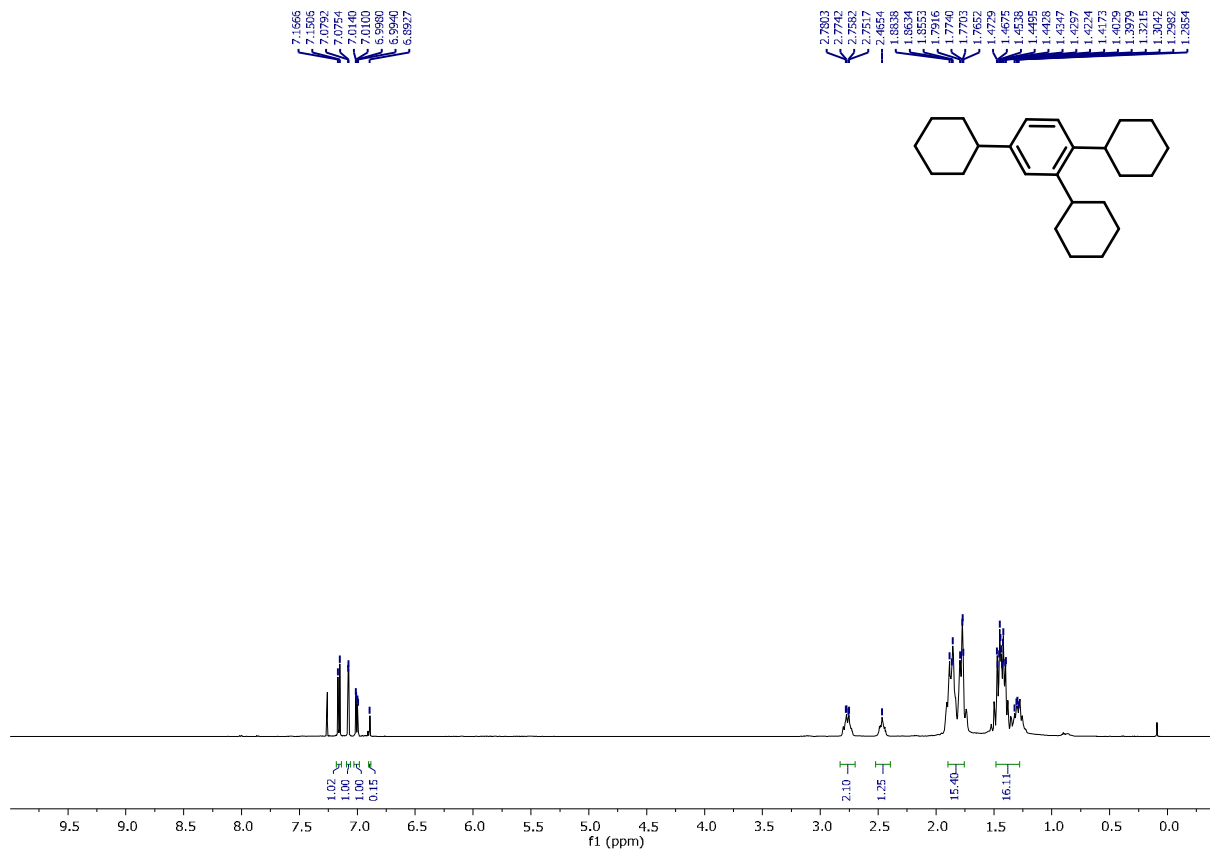
^1H NMR (400 MHz, CDCl_3) of 1,2,4-Tris-(6-methoxy-2-naphthyl)benzene (21)



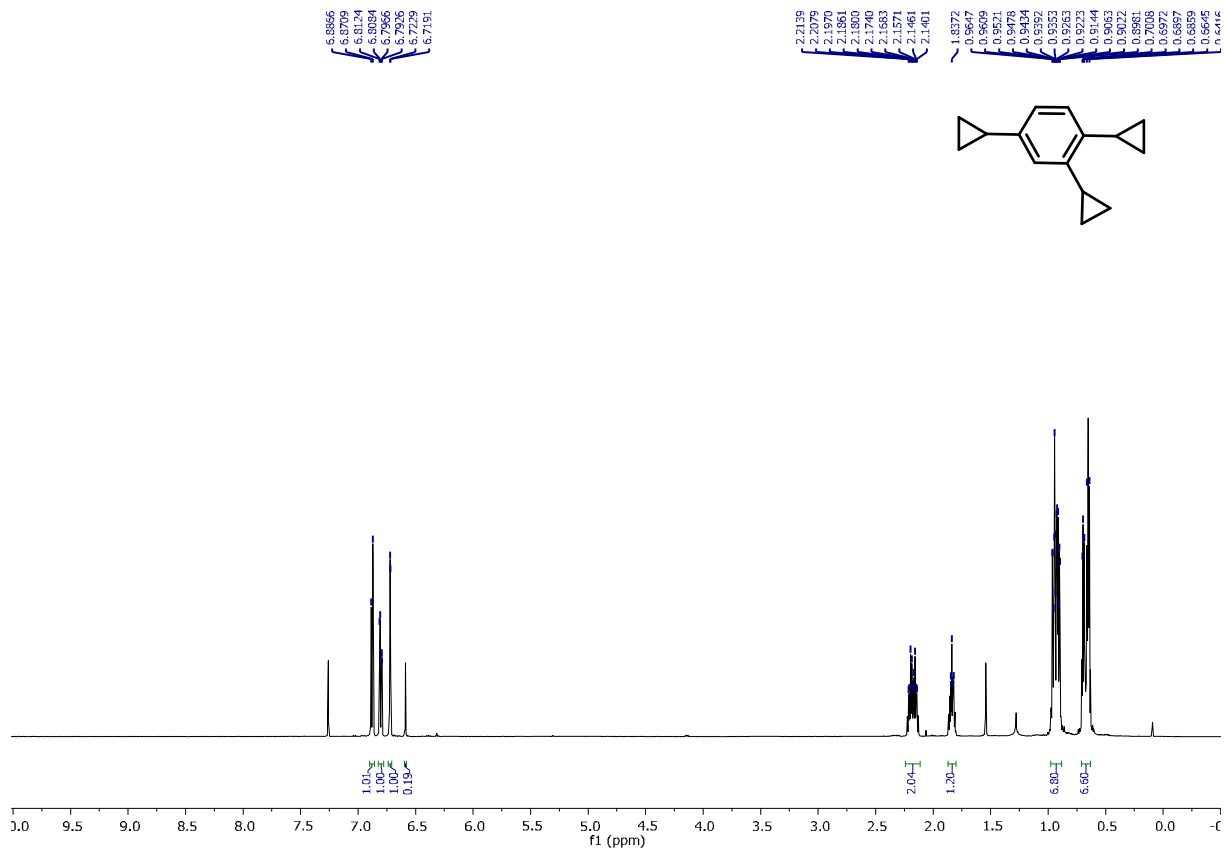
¹H NMR (400 MHz, CDCl₃) of 1,2,4-Tri-benzylbenzene (22)



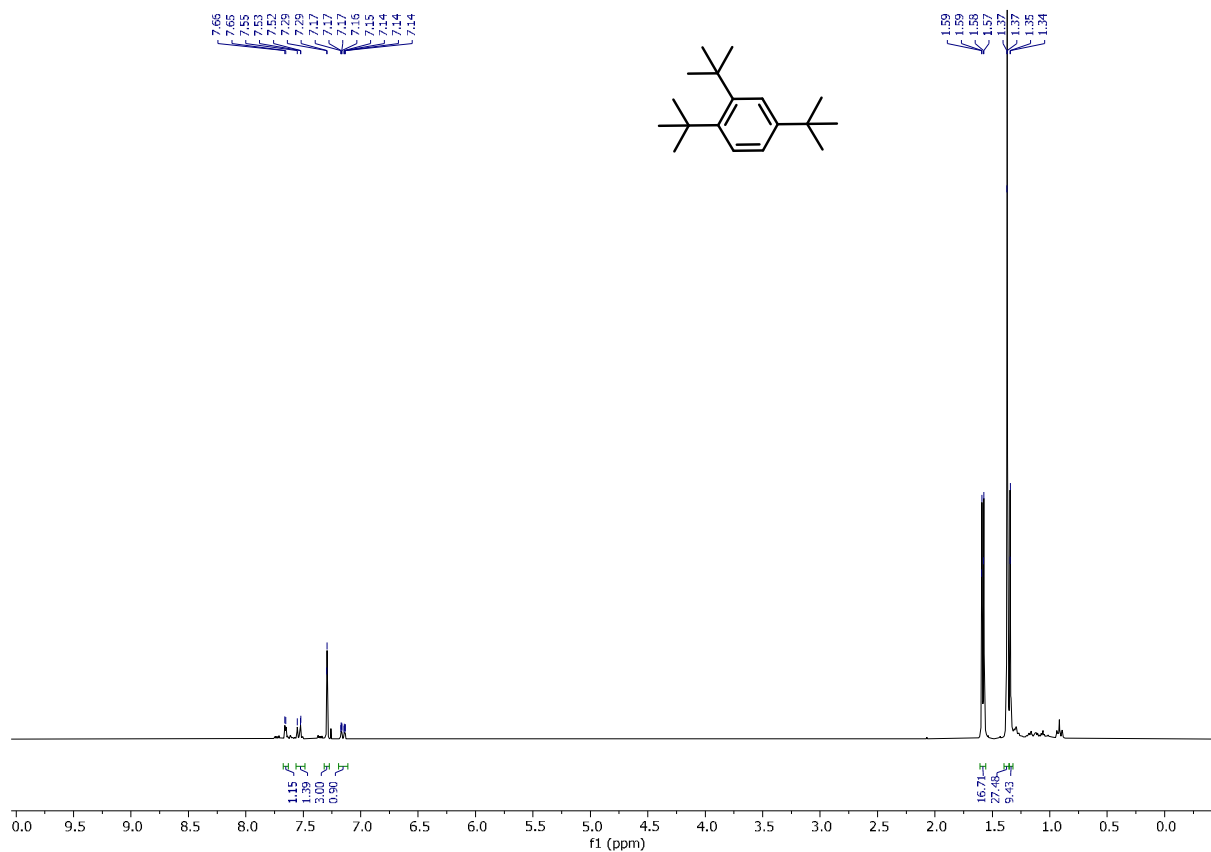
¹H NMR (400 MHz, CDCl₃) of 1,2,4-Tri(cyclohexen-1-yl)benzene (23)



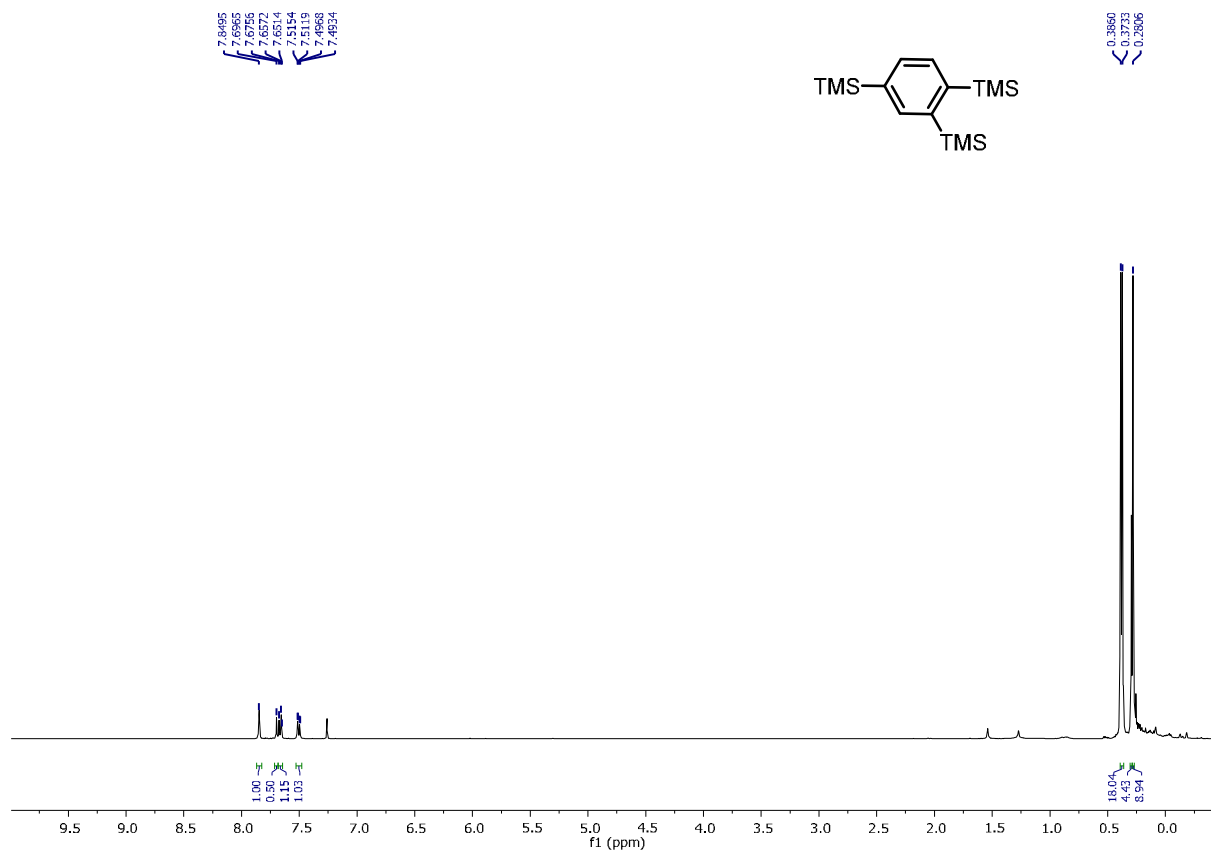
^1H NMR (400 MHz, CDCl_3) of 1,2,4-Tricyclohexylbenzene (24)



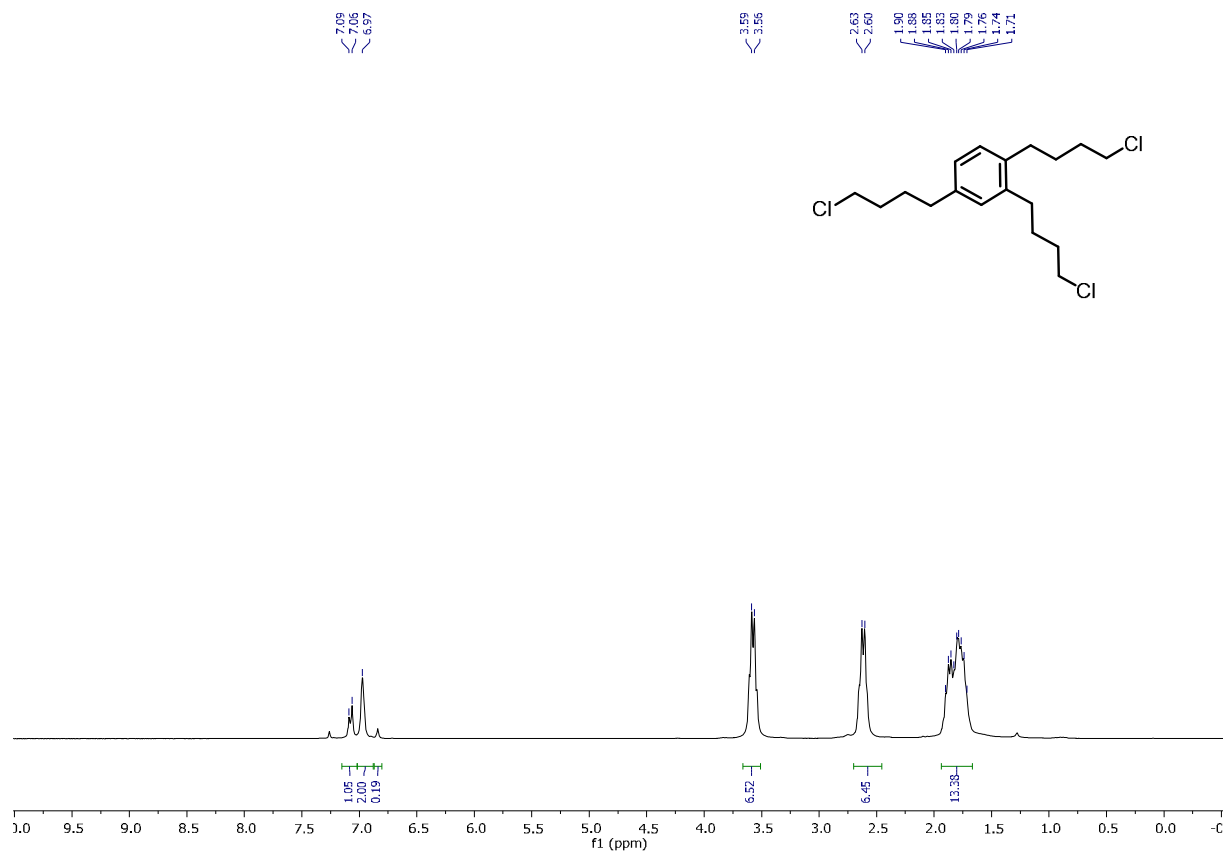
^1H NMR (400 MHz, CDCl_3) of 1,2,4-Tricyclopropylbenzene (25)



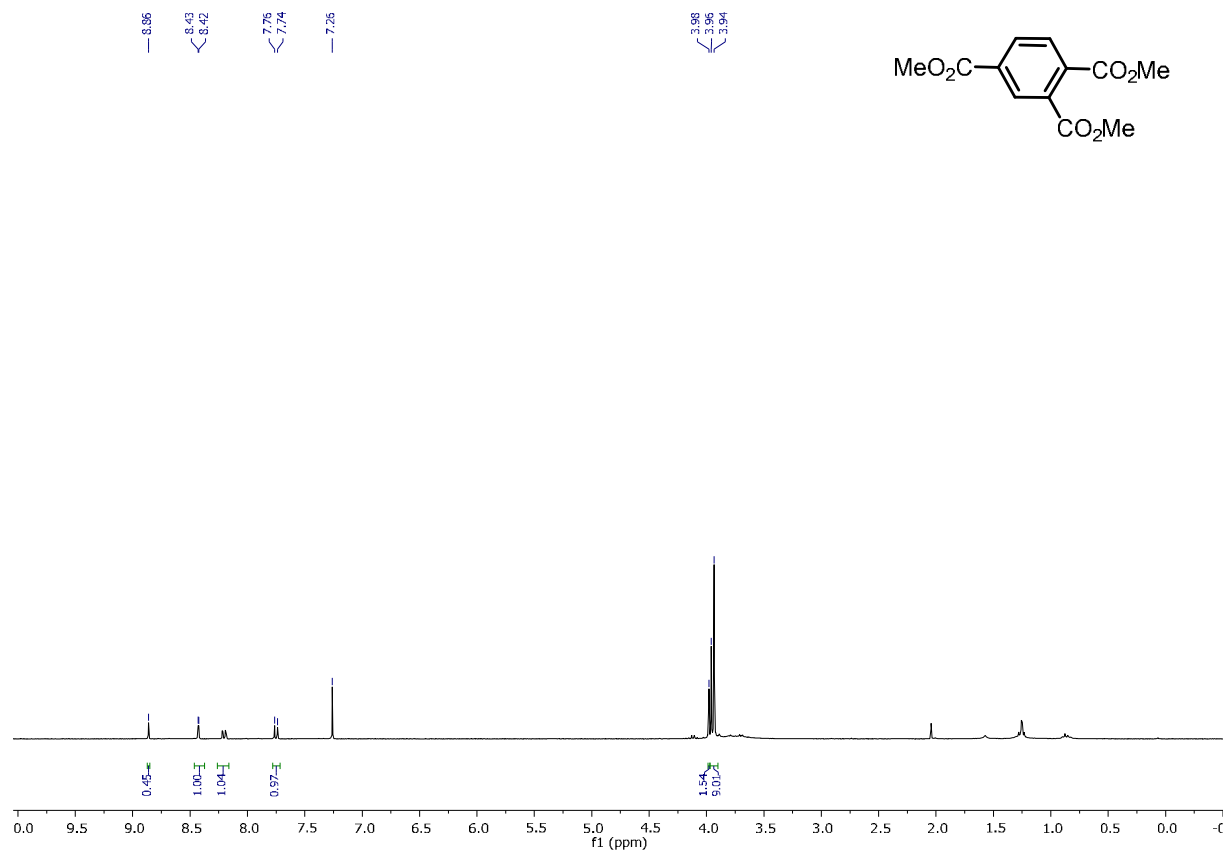
¹H NMR (400 MHz, CDCl₃) of 1,3,5- and 1,2,4-Tri-tert-butylbenzene 1:1 mixture (26)



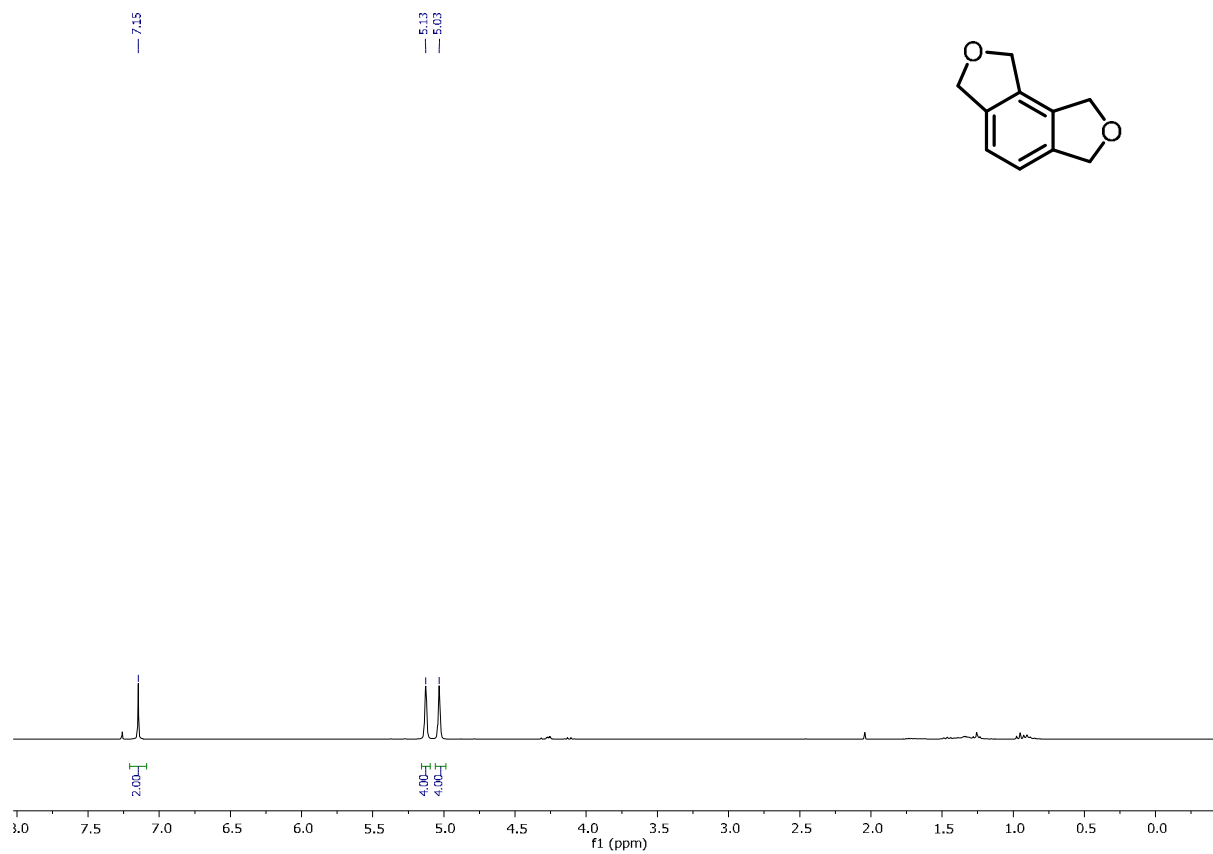
¹H NMR (400 MHz, CDCl₃) of 1,2,4-Tris(trimethylsilyl)benzene + 1,3,5-Tris(trimethylsilyl)benzene (27)



¹H NMR (400 MHz, CDCl₃) of 1,2,4-Tris(4-chlorobutyl)benzene (28)



¹H NMR (400 MHz, CDCl₃) of Trimethyl 1,2,4-benzenetricarboxylate (29)



6.5 References

1. Relevant review on the topic are reported: a) K. Tanaka, in *Transition-Metal-Mediated Aromatic Ring Construction*; John Wiley & Sons, Inc., **2013**; b) N. E. Schore, *Chem. Rev.* **1988**, *88*, 1081–1119; c) S. Saito, Y. Yamamoto, *Chem. Rev.* **2000**, *100*, 2901–2915. d)
2. G. M. Badger, G. E. Lewis, I. M. Napier, *J. Chem. Soc.* **1960**, 2825–2827.
3. W. Reppe, O. Schlichting, K. Klager, T. Toepel, *Justus Liebigs Ann. Chem.* **1948**, 560.
4. A. Roglans, A. Pla-Quintana, M. Solà, *Chem. Rev.* **2020**, DOI: 10.1021/acs.chemrev.0c00062; b) K. Yamamoto, H. Nagae, H. Tsurugi, K. Mashima, *Dalton Trans.*, **2016**, *45*, 17072–17081; c) N. Agenet, V. Gandon, K. P. C. Vollhardt, M. Malacria, C. Aubert, *J. Am. Chem. Soc.* **2007**, *129*, 28, 8860–8871; d) K. Kirchner, M. J. Calhorda, R. Schmidt, L. F. Veiros, *J. Am. Chem. Soc.* **2003**, *125*, 38, 11721–11729.
5. D. Brenna, M. Villa, T. N. Gieshoff, F. Fischer, M. Hapke, A. Jacobi von Wangelin, *Angew. Chem. Int. Ed.* **2017**, *56*, 8451–8454; *Angew. Chem.* **2017**, *129*, 8571–85746.
6. N. Neumeier, U. Chakraborty, D. Schaarschmidt, V. de la Pena O'Shea, R. Perez-Ruiz, A. Jacobi von Wangelin, *Angew. Chem. Int. Ed.* **2020**, *59*, 13473–13478; *Angew. Chem.* **2020**, *132*, 13575–13580.
7. a) K. P. C. Vollhardt, *Angew. Chem. Int. Ed. Engl.* **1984**, *23*, 539–556; b) V. Gandon, C. Aubert, M. Malacria, *Chem. Commun.* **2006**, 2209–2217; c) F. Montilla, T. Avilés, T. Casimiro, A. A. Ricardo, m. Nunes da Ponte, *J. Organomet. Chem.* **2001**, *631*, 13–118; d) A. W. Fatland, B. E. Eaton, *Org. Lett.* **2000**, *2* (20), 3131–3133.
8. Y. G. Budnikova, A. G. Kafiyatullina, Y. M. Kargin, O. G. Sinyashin, *Russ. Chem. Bull., Int. Ed.* **2003**, *52*, (7), 1423–1430.
9. a) H. Bönnerman, *Angew. Chem. Int. Ed. Engl.* **1978**, *17*, 505–515; b) G. Hilt, T. Vogler, W. Hess, F. Galbiati, *Chem. Commun.* **2005**, 1474–1475; c) G. Hilt, C. Hengst, W. Hess, *Eur. J.* **2008**, 2293–2297; d) S. M. Weber, G. Hilt, *Org. Lett.* **2019**, *21*, 4106–4110; e) L. Xu, R. Yu, Y. Wang, J. Chen, Z. Yang, *J. Org. Chem.* **2013**, *78*, 5744–5750.
10. a) K. E. Ruhl, T. Rovis, *J. Am. Chem. Soc.* **2016**, *138*, 15527–15530; b) B. D. Ravetz, K. E. Ruhl, T. Rovis, *ACS Catal.* **2018**, *8*, 5323–5327; c) J.-C. Grenier-Petel, S. K. Collins, *ACS Catal.* **2019**, *9*, 3213–3218; d) B. D. Ravetz, J. Y. Wang, K. E. Ruhl, T. Rovis, *ACS Catal.* **2019**, *9*, 200–204.
11. A. F. Khusnuriyalovaa, A. V. Sukhova, G. E. Bekmukhamedova, D. G. Yakhvarova, *Russ. J. Electrochem.* **2020**, *56*, 293–299.
12. a) G. Hilt, W. Hess, T. Vogler, C. Hengst, *J. Organomet. Chem.* **2005**, *690*, 5170–5181.
13. a) F. D. Lewis, T. I. Ho, *J. Am. Chem. Soc.* **1977**, *99*, 7991–7996; b) F. D. Lewis, T. I. Ho, T. I. *J. Am. Chem. Soc.* **1980**, *102*, 1751–1752; c) S. G. Cohen, A. Parola, G. H. Parsons, *Chem. Rev.* **1973**, *73*, 141–161; d) N. A. Romero, D. A. Nicewicz, *Chem. Rev.* **2016**, *116*, 10075–10166.
14. a) W. E. Hatfield, J. T. Yoke, *Inorg. Chem.* **1962**, *1*, 3, 463–470; b) H. M. Hilliard, D. D. Axtell, M. M. Gilbert, J. T. Yoke, *J. Inorg. Nucl. Chem.* **1969**, *31*, 2117–2121; c) L. M. Vallarino, V. L. Goedken, J. V. Quagliano, *Inorganica Chim. Acta*, **1978**, *29*, 125–130.
15. a) M. Kotora, F. Adámek, M. Hájek, *Catal. Lett.* **1993**, *18*, 345–348; b) Q. Li, W. Fan, D. Peng, B. Meng, S. Wang, R. Huang, S. Liu, S. Li, *ACS Catal.* **2020**, *10*, 4012–4018.
16. a) F. A. Cotton, L. M. Daniels, G. T. Jordan IV, C. A. Murillo, *Polyhedron* **1998**, *17*, 589–597; b) D. Stingham, A. L. Rüdiger, S. O. K. Giese, G. G. Nunes, J. F. Soares, D. L. Hughes, *Acta Cryst.* **2017**, *C73*, 104–114.
17. Such intermediates were detected in other works where Co(II)/terminal alkynes interaction were crucial for the *in situ* reduction. For examples see references 5 and 10-b.
18. N. Habadie, M. Dartiguenave, Y. Dartiguenave, J. F. Britten, A. L. Beauchamp, *Organometallics* **1989**, *8* (11), 2564–2569.
19. G. Wu, A. Jacobi von Wangelin, *Chem. Sci.* **2018**, *9*, 1795–1802.
20. X. Wang, J. Hu, J. Ren, T. Wu, J. Wu, F. Wu, *Tetrahedron* **2019**, *75* (50), 130715.
21. a) W. Liu, M. R. Hempstead, W. A. Nevin, M. Melnik, A. B. P. Lever, C. C. Leznoff, *J. Chem. Soc., Dalton Trans.* **1987**, 2511–2518; b) S. M. Socol, J. G. Verkade, *Inorg. Chem.* **1986**, *25* (15), 2658–2663.

7 Chapter 7: Appendix

7.1 List of abbreviations

Ac	acetyl	EI	electron impact
acac	acetylacetonate	equiv.	equivalent
Ar	aryl	ESI	electron spray ionization
ATRA	atom transfer radical addition	ET	energy transfer
BDE	bond dissociation energy	Et	ethyl
Bn	benzyl	eV	electron volt
bpy	2,2'-bipyridine	FID	flame ionization detector
CAN	ceric ammonium nitrate	GC	gas chromatography
CFL	compact fluorescent lightbulb	HAT	hydrogen atom transfer
Cy	cyclohexyl	hmde	Hexamethyldisilazide
CT	charge transfer	HOMO	highest occupied molecular orbital
CV	cyclic voltammetry	<i>i</i>Pr	<i>iso</i> -propyl
DCB	1,4-dicyanobenzene	ISC	intersystem crossing
DCM	dichloromethane	LED	light emitting diode
DCT	dibenzo[<i>a,e</i>]cyclooctatetraene	LUMO	lowest unoccupied molecular orbital
DEE	diethylether	Me	methyl
DFT	density functional theory	MS	mass spectrometry
DIBAL-H	diisobutylaluminium hydride	NMP	<i>N</i> -methylpyrrolidine
DMSO	dimethylsulfoxide	NMR	nuclear magnetic resonance
DMF	<i>N,N</i> -dimethylformamide	PET	photoinduced electron transfer
DOI	digital object identifier	Ph	phenyl

EA	ethylacetate		ppm	parts per million
R	substituent			
RT	room temperature			
SCE	standard calomel electrode			
SET	single electron transfer			
<i>t</i>-Bu	<i>tert</i> -buthyl			
TEA	triethylamine			
TEMPO	2,2,6,6-tetramethylpiperidine oxide	<i>N</i> -		
THF	tetrahydrofuran			
TLC	Thin layer chromatography			
TMS	trimethylsilyl			
TOF	turnover frequency			
UV	ultraviolet radiation			
Vis	visible radiation			

7.2 List of used chemicals

All used chemicals are listed in order of their CAS-number with their H- and P-phrases and GHS-symbol codes:

Chemical CAS Molecular formula	H-phrases P-phrases	GHS-symbols
Diethylether 60-29-7 C ₄ H ₁₀ O	H224 - H302 - H336 P210 - P261	GHS02, GHS07
Ethanol 64-17-5 C ₂ H ₆ O	H225 - H319 P210 - P280 - P305 + P351 + P338 - P337 + P313 - P403 + P235	GHS02, GHS07
Methanol 67-56-1 CH ₄ O	H225 - H301 + H311 + H331 - H370 P210 - P233 - P280 - P301 + P310 - P303 + P361 + P353 - P304 + P340 + P311	GHS02, GHS06, GHS08
2-Propanol 67-63-0 C ₃ H ₈ O	H225 - H319 - H336 P210 - P233 - P240 - P241 - P242 - P305 + P351 + P338	GHS02, GHS07
Acetone 67-64-1 C ₃ H ₆ O	H225 - H319 - H336 P210 - P233 - P240 - P241 - P242 - P305 + P351 + P338	GHS02, GHS07
<i>N,N</i> -Dimethylformamide 68-12-2 C ₃ H ₇ NO	H226 - H312 + H332 - H319 - H360D P210 - P280 - P303 + P361 + P353 - P304 + P340 + P312 - P305 + P351 + P338 - P308 + P313	GHS02, GHS07, GHS08
Diiodomethane 75-11-6 CH ₂ I ₂	H: 301+311 - 332- 315 - 319 - 335	GHS02, GHS06, GHS08, GHS09

	P: 280-302+352-305+351+338-308+310	
Acetonitrile 75-05-8 C ₂ H ₃ N	H225 - H302 + H312 - H319 - H331 P210 - P280 - P301 + P312 - P303 + P361 + P353 - P304 + P340 + P311 - P305 + P351 + P338	GHS02, GHS06
Dichloromethane 75-09-2 CH ₂ Cl ₂	H315 - H319 - H336 - H351 P201 - P202 - P261 - P302 + P352 - P305 + P351 + P338 - P308 + P313	GHS07, GHS08
Trimethylsilylchloride 75-77-4 C ₃ H ₉ SiCl	H225 - H301 + H331 - H312 - H314 P210 - P233 - P280 - P303 + P361 + P353 - P304 + P340 + P310 - P305 + P351 + P338	GHS02, GHS05, GHS06
Acetophenone 98-86-2 C ₈ H ₈ O	H302 - H319 P264 - P270 - P280 - P301 + P312 - P305 + P351 + P338 - P337 + P313	GHS07
Benzonitrile 100-47-0 C ₇ H ₅ N	H302 + H312 P264 - P270 - P280 - P301 + P312 - P302 + P352 + P312 - P362 + P364	GHS07
Diisopropylamine 108-18-9 C ₆ H ₁₅ N	H225 - H302 - H314 - H331 P210 - P280 - P303 + P361 + P353 - P304 + P340 + P310 - P305 + P351 + P338 - P403 + P233	GHS02, GHS05, GHS06
Aceticacid anhydride 108-24-7	H226 - H302 - H314 - H330	GHS02, GHS05, GHS06

C ₄ H ₆ O ₃	P210 - P280 - P301 + P312 - P303 + P361 + P353 - P304 + P340 + P310 - P305 + P351 + P338	
Toluene 108-88-3 C ₇ H ₈	H225 - H304 - H315 - H336 - H361d - H373 P210 - P240 - P301 + P310 + P330 - P302 + P352 - P314 - P403 + P233	GHS02, GHS07, GHS08
Pentane 109-66-0 C ₅ H ₁₂	H225 - H304 - H336 - H411 P210 - P273 - P301 + P310 + P331	GHS02, GHS07, GHS08, GHS09
1-Butyllithium (1.6 M in hexane) 109-72-8 C ₄ H ₉ Li	H225 - H250 - H261 - H304 - H314 - H336 - H361f - H373 - H411 P210 - P222 - P231 + P232 - P261 - P273 - P422	GHS02, GHS05, GHS07, GHS08, GHS09
Diethylamine 109-89-7 C ₄ H ₁₁ N	H225 - H302 + H332 - H311 - H314 - H335 P210 - P280 - P301 + P312 - P303 + P361 + P353 - P304 + P340 + P310 - P305 + P351 + P338	GHS02, GHS05, GHS06
Tetrahydrofuran 109-99-9 C ₄ H ₈ O	H225 - H302 - H319 - H335 - H336 - H351 P201 - P202 - P210 - P301 + P312 - P305 + P351 + P338 - P308 + P313	GHS02, GHS07, GHS08
Hexane 110-54-3 C ₆ H ₁₄	H225 - H304 - H315 - H336 - H361f - H373 - H411 P201 - P210 - P273 - P301 + P310 + P331 - P302 + P352 - P308 + P313	GHS02, GHS07, GHS08, GHS09

Triethylamine 121-44-8 C ₆ H ₁₅ N	H225 - H302 - H311 + H331 - H314 - H335 P210 - P280 - P301 + P330 + P331 - P303 + P361 + P353 - P304 + P340 + P311 - P305 + P351 + P338 + P310	GHS02, GHS05, GHS06
Trimethylphosphite 121-45-9 C ₃ H ₉ O ₃ P	H226 - H302 - H315 - H318 - H335 P261 - P280 - P305 + P351 + P338	GHS02, GHS05, GHS07
Ethylacetate 141-78-6 C ₄ H ₈ O ₂	H225 - H319 - H336P210 - P233 - P240 - P305 + P351 + P338 - P403 + P235	GHS02, GHS07
Sodiumhydrogencarbonat 144-55-8 NaHCO ₃	Not available/applicable	
Dibenzo[a,e]cyclooctatetraene 262-89-5 C ₁₆ H ₁₂	Not available/applicable	
Hydrazine (35 % in water) 302-01-2 H ₄ N ₂	H301 + H331 - H314 - H317 - H350 - H410 P201 - P261 - P273 - P280 - P301 + P310 + P330 - P305 + P351 + P338	GHS05, GHS06, GHS08, GHS09
Sodiumcarbonat 497-19-8 Na ₂ CO ₃	H319 P264 - P280 - P305 + P351 + P338 - P337 + P313	GHS07
Phenylacetylene 536-74-3 C ₈ H ₆	H226 - H304 - H315 - H319 P301 + P310 - P305 + P351 + P338 - P331	GHS02, GHS07, GHS08
<i>N</i> -Benzylideneaniline 538-51-2 C ₁₃ H ₁₁ N	H315 - H319 - H335 P302 + P352 - P305 + P351 + P338	GHS07

4-Iodo-aniline 540-37-4 C ₆ H ₆ IN	H302 - H315 - H319 - H335 P301 + P312 + P330 - P302 + P352 - P305 + P351 + P338	GHS07
Trimethylphosphine 594-09-2 C ₃ H ₉ P	H225 - H315 - H319 - H335 P210 - P302 + P352 - P305 + P351 + P338	GHS02, GHS07
Triphenylphosphine 603-35-0 C ₁₈ H ₁₅ P	H302 - H317 - H318 - H372 P280 - P301 + P312 + P330 - P302 + P352 - P305 + P351 + P338 + P310 - P314	GHS05, GHS07, GHS08
1-Octyne 629-05-0 C ₈ H ₁₄	H225 - H304 P210 - P301 + P310 - P331	GHS02, GHS08
Pentadecane 629-62-9 C ₁₅ H ₃₂	H304 P301 + P310 - P331	GHS08
3-Methyl-phenylacetylene 766-82-5 C ₉ H ₈	H226 - H304 - H315 - H319 - H335 P210 - P301 + P310 + P331 - P302 + P352 - P305 + P351 + P338	GHS07
4-Fluoro-phenylacetylene 766-98-3 C ₈ H ₅ F	H228 - H315 - H319 - H335 P210 - P240 - P241 - P261 - P302 + P352 - P305 + P351 + P338	GHS07
4-Methoxy-phenylacetylene 768-60-5 C ₉ H ₈ O	Not available/applicable	GHS02, GHS07, GHS08
Ammonium hydroxide 1336-21-6 H ₅ NO	H302 - H314 - H335 - H400 P261 - P273 - P280 - P301 + P312 - P303 + P361 +	

	P353 - P305 + P351 + P338	
Deuterated DMSO 2206-27-1 C ₂ D ₆ OS	Not available/applicable	
4-Ethynylbenzonitrile 3032-92-6 C ₉ H ₅ N	H315 - H319 - H335 P302 + P352 - P305 + P351 + P338	GHS02, GHS05, GHS07, GHS08
Iron-(II)-acetate 3094-87-9 FeO ₂ C ₄ H ₆	H315 - H319 - H335 P261 - P305 + P351 + P338	GHS05, GHS07
Magnesiumsulfate 7487-88-9 MgSO ₄	Not available/applicable	GHS07
Silicagel 7631-86-9 SiO ₂	Not available/applicable	GHS07
Sodium hydride 7646-69-7 NaH	H228 - H260 - H290 - H314 P210 - P231 + P232 - P260 - P280 - P303 + P361 + P353 - P305 + P351 + P338 + P310	GHS02, GHS07
Cobalt-(II)-chloride 7646-79-9 CoCl ₂	H302 - H317 - H334 - H341 - H350i - H360 - H410 P273 - P280 - P301 + P312 - P302 + P352 - P304 + P340 + P312 - P308 + P313	
Hydrochloricacid 7647-01-0 HCl	H290 - H314 - H335 P234 - P261 - P271 - P280 - P303 + P361 + P353 - P305 + P351 + P338	GHS02, GHS05
Sodium chloride 7647-14-5	Not available/applicable	GHS07

NaCl		
Sodiumsulfate 7757-82-6 Na ₂ SO ₄	Not available/applicable	GHS06, GHS08, GHS09
Iron-(II)-chloride 7758-94-3 FeCl ₂	H302 - H318 P264 - P270 - P280 - P301 + P312 - P305 + P351 + P338 - P501	GHS07, GHS08, GHS09
Cobalt-(II)-bromide 7789-43-7 CoBr ₂	H: 302-317-334- 341-350-410 P: 201-261-280- 284-304+340- 308+313	
4-Phenylpyridine <i>N</i> -oxide 1131-61-9 C ₁₁ H ₉ NO	Not available/applicable	
Hantzsch ester 1149-23-1 C ₁₃ H ₁₉ NO ₄	Not available/applicable	
Cobalt-(II)-acetylacetonate 14024-48-7 C ₁₀ H ₁₄ CoO ₄	H302 - H317 - H318 - H360F - H410 P201 - P273 - P280 - P301 + 312 + 330 - P305 + 351 + 338 + 310 - P308 + 313	GHS02, GHS07
Borane-tetrahydrofuran complex (1 M in THF) 14044-65-6 C ₄ H ₁₁ BO	H225 - H260 - H302 - H318 - H335 - H351 P201 - P210 - P231 + P232 - P280 - P305 + P351 + P338 + P310 - P308 + P313	GHS07
Eosin Y 17372-87-1 C ₂₀ H ₆ Br ₄ Na ₂ O ₅	H: 319 P: 260- 305+351+338	GHS07
Tris(bipyridine)ruthenium(II) chloride 50525-27-4 Ru(bpy) ₃ Cl ₂	Not available/applicable	
3-Ethynylaniline 54060-30-9	H226 - H315 - H319 - H335	GHS02, GHS05, GHS06, GHS08, GHS09

C ₈ H ₇ N	P210 - P302 + P352 - P305 + P351 + P338	
Cobalt-(II)-hexamethyldisilazide 93280-44-5 C ₂₄ H ₇₂ Co ₂ N ₄ Si ₈	H315 + H320 - H335 - H350 P231 - P280 - P305 + P351 + P338 - P403 + P233 - P422 - P501	
3DPAFIPN 2260543-73-3 C ₄₄ H ₃₀ FN ₅	Not available/applicable	

7.3 Summary

Aim of this thesis is the use of photoredox catalysis for the activation of small molecules and the development of new catalytic strategies.

In the beginning a short introduction to the field of photoredox catalysis is given. The basic theoretical background and the various definitions necessary to become familiar with the field are explained.

In the first chapter the synthesis of pyrazoles starting from cyclopropanols and diazonium salts under radiative conditions is reported. The development of a mild and fast reaction (20 min, r.t.) is discussed with a major focus on mechanistic aspects.

Main part of the thesis, in the chapters 3-4 and 5, deals with the chemistry of (4-substituted) Hantzsch esters. This old molecule has a well known history within classic thermal reactivity whereas acts as a potent hydride donor. What we present in the different chapters is the use of Hantzsch ester under photochemical conditions. In particular, in chapter 3 the chemistry of Hantzsch ester in its excited state is explored and employed in a powerful reduction protocol of *N*-oxides to *N*-arenes. In chapters 4 and 5 another kind of reactivity is presented: 4-substituted Hantzsch esters as radical precursors through photoredox activation. 4-carboxamido Hantzsch esters are synthesized and used for the carbamoylation of olefins and imines.

In the last part of the thesis a non-photoredox protocol is reported (chapter 6) whereas simple CoBr_2 salt is activated *in situ* by the use of stoichiometric aliphatic amines as DIPEA (*N,N*-diisopropyl ethylamine) for the cyclotrimerization of terminal alkynes.

7.4 Zusammenfassung

Ziel dieser Arbeit ist die Nutzung der Photoredoxkatalyse zur Aktivierung kleiner Moleküle und die Entwicklung neuer katalytischer Strategien.

Zu Beginn wird eine kurze Einführung in das Gebiet der Photoredoxkatalyse gegeben. Der grundlegende theoretische Hintergrund und die verschiedenen Definitionen, die zum Kennenlernen des Gebiets erforderlich sind, werden erläutert.

Im ersten Kapitel wird über die Synthese von Pyrazolen ausgehend von Cyclopropanolen und Diazoniumsalzen unter Strahlungsbedingungen berichtet. Die Entwicklung einer milden und schnellen Reaktion (20 min, r.t.) wird unter besonderer Berücksichtigung mechanistischer Aspekte diskutiert.

Der Hauptteil der Arbeit, in den Kapiteln 3-4 und 5, beschäftigt sich mit der Chemie von (4-substituierten) Hantzsch-Estern. Dieses alte Molekül hat eine bekannte Geschichte in der klassischen thermischen Reaktivität, während es als potenter Hydriddonor fungiert. Was wir in den verschiedenen Kapiteln vorstellen, ist die Verwendung von Hantzsch-Ester unter photochemischen Bedingungen. Insbesondere wird in Kapitel 3 die Chemie des Hantzsch-Esters im angeregten Zustand untersucht und in einem leistungsstarken Reduktionsprotokoll von *N*-Oxiden zu *N*-Arenen eingesetzt. In den Kapiteln 4 und 5 wird eine andere Art von Reaktivität vorgestellt: 4-substituierte Hantzsch-Ester als Radikalvorstufen durch Photoredoxaktivierung. 4-Carboxamido-Hantzsch-Ester werden synthetisiert und zur Carbamoylierung von Olefinen und Iminen verwendet.

Im letzten Teil der Arbeit wird ein Nicht-Photoredox-Protokoll beschrieben (Kapitel 6), während einfaches CoBr_2 -Salz *in situ* durch die Verwendung von unterstöchiometrischen aliphatischen Aminen als DIPEA (N,N-Diisopropylethylamin) für die Cyclotrimerisierung terminaler Alkine aktiviert wird.

7.5 Acknowledgements

In this last section I would like to thank all the people that I met and supported me in the last three years!

I thank you Axel, for giving me this opportunity to work in your group and explore new chemistry. I'm especially grateful for the large freedom in the selection of projects and their development that you gave me. Thank you for your mentorship, to teach me how to follow my own path, and to tackle science problems until are solved.

I would like to thank all the members from the AJvW group to share the lab and out of lab life: Sebastian, Patrick, Michael, Dieter, Christoph, Nils, Roderich, Robin, Jackie, Till, Mattis, Uttam, Pradip, Guojiao, Ursula, Javier, Ben. Thank you for teaching me how to drink and open a bottle of beer as a real German, I hope I didn't let you down! Thanks for the many dinners and evenings spent together and thanks for showing me new creative ways to use a funnel...Of course thank you also for the scientific discussions and lab life tricks. I thank Michael and Michal for working with me on my first project, thanks for the patience while I moved my first steps in the new lab. A special thanks goes to Andrey, Benrhard and Jenny, thanks for supporting me and dealing with me this whole time. These 3 years wouldn't have been the same without you!

Thanks also goes to all the students that crossed the lab in these years and worked with me on the different projects.

I'm extremely grateful to Mike and that our paths crossed here in Hamburg. Thanks for your motivation and support, for mentoring me on new projects and for the many scientific inputs.

Finally, I would like to thank my family. Grazie per esserci stati anche a distanza, per il vostro supporto su ogni mia decisione, per quanto difficile vi possa apparire. Grazie a delle mie vecchie amiche: Bianca, Elena e Chiara a quanto pare anche binari paralleli possono restare vicini. Grazie a te, che ancora una volta hai creduto in un sogno nel mio cassetto prima che ce lo mettessi, non vedo l'ora di vivere la prossima avventura, questa volta insieme.

7.6 Curriculum vitae

Luana Cardinale

September 2021

Ph.D student

Telephone: (039) 3385248735

University of Hamburg, Germany

Email: luana.cardinale@chemie.uni-hamburg.de

Summary

Synthetic organic chemist with experience in organocatalysis, photocatalysis and organometallic chemistry. Expertise in organic synthesis and hypothesis-driven reaction design with a background in analytical characterization and structure elucidation. Efficient, independent student who participated in productive collaborations on a variety of projects. Passionate about science and problem solving.

Education

University of Hamburg, Hamburg, Germany

2018–present

Ph.D. candidate, Organic Chemistry

University of Parma, Parma, Italy

2013–2018

M.Sc. in Chemistry and Pharmaceutical Technology – *Summa Cum Laude*

Research and Work Experience

University of Hamburg, Hamburg, Germany

2018–present

Graduate Student Researcher, Department of Chemistry

- Development of photocatalyst-free N–O bond photoreduction of nitroarenes and N-oxides.
- Development of aromatization-driven carbamoylation reactions via photoredox catalysis for the functionalization of C=C and C=N double bonds.
- Photocatalytic synthesis of aryl pyrazoles starting from arenediazonium salts.
- Study of simple amine-cobalt(II) complexes for the cyclotrimerization of terminal alkynes.

Advisor: Professor Axel Jacobi von Wangelin

University of Parma, Parma, Italy

2013–2018

Undergraduate Research Fellow,

- Synthesis of N-protected uracil derivatives for the investigation of organocatalytic [4+2] cycloadditions.
- Development of enantioselective synthesis of carbocycle-fused uracils via [4+2] cycloaddition.

Advisor: Professor Claudio Curti

“Stadio Tardini” Pharmacy, Parma, Italy.

2017–2018

- Internship as apprentice pharmacist.

Tutor: Sonia Mezzadri

University of Parma, Parma, Italy.

Summer semester 2016

- Librarian at the chemistry university library

Teaching Experience

University of Hamburg, Hamburg, DE

Mentor and supervisor of Bachelor thesis 2018-present

University of Hamburg, *Instructor*, Hamburg, DE

Organometallic Chemistry laboratory teaching assistant 2018-present

University of Parma, *Tutor*, Parma, IT

Tutorship for exercises in organic chemistry for first and second year undergraduate students 2017–2018

Proficiencies

Analytical Characterization: GC-MS and GC-FID Agilent (maintenance and repair), NMR, FT-IR, UV-Vis, HPLC, Cyclic Voltammetry.

Skills: Synthetic organic chemistry, chromatography, Schlenck technique, method development, catalysis, scripting, solvent purification system, glove box, Stern-Volmer analysis.

Publications

1. "Direct, Asymmetric Synthesis of Carbocycle-Fused Uracils via [4+2] cycloadditions: a Noncovalent Organocatalysis Approach" Marcantonio, E; Curti, C.; Battistini, L.; Sartori, A.; **Cardinale, L.**; Pelosi, G.; Zanardi, F. *Adv. Synth. Catal.* **2021**, *363*, 2625–2633.

2. "Aryl Pyrazoles from Photocatalytic Cycloadditions of Arenediazonium" **Cardinale, L.**; Neumeier, M.; Majek, M.; Jacobi von Wangelin, A. *Org. Lett.* **2020**, *22*, 18, 7219–7224.

3. "Photoredox-Catalyzed Addition of Carbamoyl Radicals to Olefins: A 1,4-Dihydropyridine Approach" **Cardinale, L.**; Konev, M. O.; Jacobi von Wangelin, A. *Chem. Eur. J.* **2020**, *26*, 8239–8243.

4. "Catalyst-Free N-Deoxygenation by Photoexcitation of Hantzsch Ester" Konev, M. O.; **Cardinale, L.**; Jacobi von Wangelin, A. *Org. Lett.* **2020**, *22*, 1316.

5. "Visible-Light-Mediated Synthesis of α -Amino Amides from 4-Amido-Hantzsch Esters and Imines" **Cardinale, L.**; Schmotz, M.-O. W. S.; Konev, M. O.; Jacobi von Wangelin, A. *Manuscript submitted*.

6. "The Latent Redox-Non-Innocent Behavior of Simple Amines Enables Reductant-Free Cobalt(II)-Catalyzed Cyclotrimerizations" **Cardinale, L.**; Schaarschmidt, D.; Jacobi von Wangelin, A. *Manuscript in preparation*.

Professional References

Prof. Axel Jacobi von Wangelin
University of Hamburg, Germany
Department of Inorganic and Synthetic Chemistry
Martin-Luther King Platz 6, 20146
(+49) 40 42838-2883
axel.jacobi@chemie.uni-hamburg.de

Prof. Claudio Curti
University of Parma, Italy
Department of Pharmacy
Parco Area delle Scienze 27, 43124
(+39) 0521 905006
claudio.curti@unipr.it

Prof. Franca Zanardi
University of Parma, Italy
Department of Pharmacy
Parco Area delle Scienze 27, 43124
(+39) 0521 905067
franca.zanardi@unipr.it

7.7 Eidesstattliche Erklärung

„Hiermit versichere ich an Eides statt, die vorliegende Dissertation selbst verfasst und keine anderen als die angegebenen Hilfsmittel benutzt zu haben. Die eingereichte schriftliche Fassung entspricht der auf dem elektronischen Speichermedium. Ich versichere, dass diese Dissertation nicht in einem früheren Promotionsverfahren eingereicht wurde.“

Datum, 15.09.2021

Unterschrift: 